Enhanced Strategies for Liquefaction Reconnaissance Mapping in Disaster-Affected Regions and Vulnerability Assessment of Buildings in Moderate-Seismicity Areas with Strong Site Amplification:

Supporting Informed Decision-Making for Improved Resilience

A dissertation submitted by

Christina Sanon

In partial fulfillment of the requirements for the degree of

Doctor of Philosophy

in

Civil and Environmental Engineering

TUFTS UNIVERSITY

May 2025

ADVISOR: Laurie G. Baise, Ph.D.

Abstract

Pre-disaster initiatives—including mitigation, prevention, and preparedness strategies—alongside post-disaster efforts focused on relief, recovery, and reconstruction, are fundamentally informed by predictive risk models that estimate potential damage and loss. The application of these models depends on the systematic transformation of diverse datasets into quantifiable, predictive metrics that enhance the understanding of regional vulnerabilities and support the formulation of targeted, evidence-based resilience strategies. This dissertation advances methodologies for both the geospatial documentation of earthquake-induced liquefaction and the assessment of building vulnerability in regions characterized by low-to-moderate seismicity and significant site amplification effects.

Chapter 1 introduces a standardized, remote sensing–based framework for post-earthquake reconnaissance mapping of liquefaction surface manifestations. The methodology integrates high-resolution satellite imagery with field-validated observations to produce polygon-based, labeled inventories containing both binary and categorical attributes (e.g., liquefaction type, confidence level, imagery source). These inventories—developed using data from the 2010 M7.0 Port-au-Prince (Haiti), 2011 M6.1 Christchurch (New Zealand), and 2021 M7.2 Nippes (Haiti) earthquakes—are intended to support the training of machine learning models for automated damage detection and are adaptable for broader applications across diverse natural hazards.

Chapter 2 addresses the limitations of seismic vulnerability assessment in Massachusetts by integrating high-resolution geotechnical and geological data, a comprehensive building inventory, and updated seismic hazard information from the U.S. Geological Survey. This chapter employs the FEMA HAZUS loss estimation framework to identify structural vulnerabilities—particularly in Unreinforced Masonry buildings—and emphasizes the importance of localized, mitigation-informed planning.

Chapter 3 extends the analysis presented in Chapter 2 by applying site-specific linear Ground Response Analysis (GRA) and comparing its results to conventional Vs_{30}-based amplification estimates. The results demonstrate that simplified proxies often underestimate ground motion amplification in areas with deep sedimentary layers and pronounced impedance contrasts. Consequently, many buildings are reclassified into higher Seismic Design Categories, underscoring the necessity of incorporating detailed site effects into seismic risk assessments to ensure accurate hazard representation and informed design guidelines.

Collectively, this dissertation advances the methodological toolkit for seismic risk assessment by integrating innovative data acquisition techniques, locally calibrated high-resolution geospatial and structural datasets, and

advanced analytical methodologies. These contributions enable the development of more accurate and actionable risk models and reinforce the empirical foundation for enhancing seismic resilience in data-limited, hazard-prone environments.

"I can do all things through Christ who strengthens me" — **Philippians 4:13**

To my family:

Without you, I would not be me.

Acknowledgements

First, I owe my deepest gratitude to my advisor, Dr. Laurie Baise, for your exceptional guidance and mentorship. Your expertise and insightful feedback have been invaluable in shaping both the direction and quality of my research. Your ability to offer constructive criticism while fostering an environment of intellectual curiosity and growth has played a pivotal role in my development as a scholar. During moments when I struggled to see the bigger picture or found myself mired in the details, I am especially grateful for your patience and understanding. You consistently challenged me to step back, think critically, and reassess my work from fresh perspectives. It became a running joke in the graduate office that you "dug me out of the rabbit hole," and I could not have asked for better guidance. Your commitment to my success has meant the world to me.

I am also deeply grateful to my dissertation committee members—Dr. Aggeliki Barberopoulou, Dr. Magaly Koch, and Dr. Babak Moaveni—for your invaluable contributions throughout this process. Your constructive comments, thoughtful critiques, and insightful suggestions shaped my research and broadened my approach. Each of you brought a unique perspective that challenged me to think more critically. Your expertise and attention to detail have not only enriched my academic journey at Tufts but also contributed significantly to my growth as a researcher. I feel incredibly fortunate to have had the opportunity to work with such a distinguished group of scholars.

This journey was not one I undertook alone, and I cannot take all the credit. To my family, words cannot fully capture how much your unwavering love, support, and encouragement have meant to me. To my parents, Denise, and Jean Earnst Sanon, thank you for always believing in me, even during moments of self-doubt. Your constant faith in me has been my guiding light. Mom, your love, and sacrifices have shaped me in ways I cannot fully articulate. You have always been my biggest cheerleader, offering not just words of encouragement, but the kind of love that fuels my spirit. I am endlessly thankful for your wisdom, the nurturing you have given me, and the countless ways you have shaped me into who I am today. I could not have made it this far without you. Papi, your quiet strength and dedication have been a constant source of inspiration. From your solid work ethic to the values of integrity you have instilled in me, I am forever grateful for the foundation you have provided. The lessons you have taught me, not just through words but through your actions, have shaped my approach to both my work and my personal life. And of course, my laundry was never undone (Ha!). I am deeply grateful to have such loving, dedicated, and inspiring parents.

To my sister, Barbara Sanon, thank you for being a constant source of support and understanding. Your patience, love, and empathy have been a grounding force during challenging times. You have always been there for

me, offering a listening ear, wise advice, and a sense of calm when I needed it most. I am fortunate to have you by my side. I love you long time.

To my grandmother, Eunomine Guerrier—the matriarch who laid the foundation for all that has followed—and to my aunts, uncles, and cherished cousins, who are in every sense like extended siblings: your pride in my accomplishments has been a continual source of motivation. Your unwavering support and deep sense of connection sustained me through difficult times. I love you all deeply, and I am profoundly grateful for the love and solidarity you have shown me throughout my life.

I would also like to acknowledge my friends, colleagues, and fellow students for their camaraderie and moral support. Special thanks to Catherine Knox for being a constant source of positivity (and for always knowing when a chai break was needed); to Elisa Jazan for your encouraging words and for offering me a place to stay when I needed it most; to Emre Uyeturk for your patience in listening to my endless reflections and rants, and for providing a judgment-free space to vent; and to Adel Asadi, who began this journey with me—though you left before me, your steadfast support never wavered. To my fellow Geohazards Group members—Marshall Pontrelli, Lekan Sodeinde, Ellie Meyer, Maggie Roberts, Hooman Shirzadi, Alex Chansky, Weiwei Zhan, and Sherry Nie (in no particular order); to the “liquefaction army” who made Chapter 1 possible; to everyone who shared the graduate office in Anderson Hall Room 311A—Jake Wessel, Abby Birnbaum, Ghazal Shabestanipour, and Januka Gyawali; and to the ever-spirited members of the Graduate Student Organization (GSO): thank you for the insightful conversations, thoughtful feedback, and the laughter that kept us going. I am so grateful to have walked this path in such good company.

A heartfelt thank you to the administrative staff—Laura Sacco (best hugger award!) and Debra McKnight—for your invaluable assistance and support. Your kindness and willingness to help behind the scenes made my experience much smoother, and I am deeply appreciative of all you did. Laura, your warmth, humor, and boundless positivity made every visit to the office something to look forward to. Your hugs could brighten even the most stressful days, and your genuine care reminded me that I was never alone in this journey. Debra, you get the "calm in the chaos" award—you knew just what to say and do on the day of my defense to ease my nerves and lift my spirit. Your thoughtfulness, your warm smile, and your quiet encouragement helped turn a nerve-wracking day into one I will always remember with gratitude and joy.

I am also grateful to all the teachers, professors, and mentors who have guided me throughout the years: Ann Herz at Westhill High School in Stamford, Connecticut, who encouraged me to "press send" on my graduate school

applications; Dr. Chris Letchford and Dr. Mohammed Alnaggar from my alma mater, Rensselaer Polytechnic Institute (RPI), who continued to offer support and encouragement throughout my academic journey; and the many professors I had the privilege of learning from at Tufts University—Dr. Lucy Jen, Dr. Jack Germain, Dr. Jon Lamontagne, and Dr. James (Jim) Kaklamanos (at Merrimack College)—whose wisdom and mentorship have been instrumental throughout this journey.

Finally, I wish to thank the organizations that provided financial and technical support: the National Geospatial-Intelligence Agency for funding the liquefaction project; the Massachusetts Division of Capital Asset Management and Maintenance (DCAMM) for much needed data, and the developers of R2D at the NHERI SimCenter for their vital technical assistance, especially Jinyan Zhao.

This is the part of the televised award shows where the music starts playing—so please forgive me if you are not named individually; blame the music on this page, not my heart. Please know that if you have ever supported my research, you, too, deserve my deepest thanks.

Malcolm Gladwell, journalist, and author, once said, "*Hold your values tightly, but your ideas loosely.*" This dissertation came into being as I worked to understand my life's purpose and how I want to contribute to the world. When I began this journey, I had no clear roadmap; over time, the path gradually revealed itself. This document represents a collection of ideas deeply intertwined with my core values—the culmination of years of hard work, perseverance, and growth. My journey is far from over, and my ideas will undoubtedly continue to evolve. However, I remain committed to serving others—to being a civil servant, in every sense (yes, pun intended!)—and to dedicating my life and career to making a meaningful difference.

This work is not the final word on the topics it addresses, nor is it meant to be. Rather, it is an open invitation—to debate, to challenge, to build upon, and to continue a conversation that I will never claim to have started, but on which I foolishly dared to opine. While my journey of refinement continues, this dissertation stands as a reflection of where I am today—and, for now, it is my proudest accomplishment. I am deeply grateful to all who have supported me in this labor of love. Though *I* did the laboring (mostly) happily, your encouragement and care made it possible.

Thank you for the love.

With gratitude,

Christina Sanon

Table of Contents

List of Figures

Introduction

Chapter 1 – Digitizing Earthquake-Induced Soil Liquefaction: *A Guide for Creating a Labeled Polygon-based Inventory of Surface Effects Using Remote Sensing Data*

Chapter 2 – Building Damage Assessment and Retrofitting Prioritization in Massachusetts Using a High-Resolution Site Characterization Map

Chapter 3 – Ground Response Analysis for Seismic Vulnerability Assessment: *Does detailed site characterization and ground response analysis change projected building damage estimates?*

Appendix B: Liquefaction Inventory Output Maps

Appendix C: Liquefaction Inventory Attribute Summaries

List of Tables

Introduction

Chapter 1 – Digitizing Earthquake-Induced Soil Liquefaction: *A Guide for Creating a Labeled Polygon-based Inventory of Surface Effects Using Remote Sensing Data*

Chapter 3 – Ground Response Analysis for Seismic Vulnerability Assessment: *Does detailed site characterization and ground response analysis change projected building damage estimates?*

Introduction

“There are years that ask questions and years that answer.”

— Zora Neale Hurston, Their Eyes Were Watching God

Urbanization has been a principal force in shaping modern human society, fundamentally altering settlement patterns, economic structures, and the spatial distribution of disaster risk. The transition from agrarian economies during the Industrial Revolution to increasingly service-oriented, post-industrial societies has been accompanied by accelerated urban growth. Between 1800 and 1910, the urban population in Europe increased from 10.9% to 32.8%, with comparable trends observed in Australia, Canada, New Zealand, and the United States (Estevez et al., 2016). This trend is projected to continue, with the United Nations forecasting a 32% increase in the global population between 2014 and 2050, predominantly concentrated in urban regions (Estevez et al., 2016). While urbanization fosters economic development and innovation, it concurrently intensifies exposure to natural hazards, particularly in contexts where infrastructure systems, governance structures, and resource management practices are insufficiently resilient.

Among natural hazards, seismic events—particularly earthquakes—pose a uniquely acute threat, characterized by their sudden onset wide-ranging effects, and potential for cascading, multi-dimensional impacts. Earthquakes not only damage the built environment but also expose latent systemic vulnerabilities within the social, economic, and infrastructural frameworks of affected regions. In response to such risks, Disaster Risk Reduction (DRR) frameworks underscore the imperative of integrating preparedness, mitigation, response, and recovery strategies to reduce disaster impacts and to strengthen resilience (Cui et al., 2018; Shaw, 2016). Although resilience has become a foundational principle within the field of disaster science—commonly defined as the capacity of systems to anticipate, absorb, adapt to, and recover from disruptive events—its operationalization remains methodologically complex and interdisciplinary (Foster, 2012; Bruneau et al., 2003; Koliou et al., 2018).

In the context of disasters, resilience is inherently multidimensional, encompassing the interrelated constructs of risk, vulnerability, susceptibility, and functionality. Risk is defined as the likelihood and potential consequence of hazardous events (Birkmann, 2007), while vulnerability encapsulates the susceptibility of social, economic, and infrastructural systems to harm, shaped by a complex interplay of historical, socio-economic, and governance factors (Adger, 2006). Susceptibility, more narrowly construed, pertains to the predisposition of specific structures or populations to sustain damage as a result of physical or material deficiencies (Fischer et al., 2016). Functionality refers to the capacity of critical systems to maintain or rapidly restore operational performance in the aftermath of disruption (Enderami et al., 2021). The integration of these dimensions is essential for a comprehensive assessment of seismic resilience and for the formulation of effective mitigation and recovery strategies.

Earthquake impacts manifest through primary (e.g., ground shaking, surface rupture), secondary (e.g., liquefaction, landslides), and tertiary (e.g., infrastructure collapse, public health crises) effects, each with distinct yet interconnected implications for recovery trajectories. Effective post-disaster data collection, encompassing both field reconnaissance and remote sensing methodologies, is critical to capturing these impacts, informing the development of evidence-based recovery strategies, and refining regulatory and engineering standards. In regions characterized by low-to-moderate seismicity, such as the Commonwealth of Massachusetts, the scarcity of localized seismic data presents a significant impediment to accurate seismic risk characterization. In particular, reliance on simplified amplification proxies such as Vs_{30} risks underestimating ground motion amplification in geologically complex settings, notably those characterized by deep sedimentary deposits and strong impedance contrasts (Baise et al., 2016).

Collectively, this dissertation advances the state of knowledge in seismic vulnerability and resilience assessment by integrating standardized remote sensing methodologies, high-resolution geotechnical characterization, and site-specific ground motion analyses. Through the application of these enhanced analytical frameworks, it seeks to address critical deficiencies in prevailing practice, particularly in regions where seismic hazards are historically underrecognized but where latent vulnerabilities may significantly exacerbate disaster impacts. By bridging post-disaster reconnaissance and localized vulnerability analysis, it contributes to the development of comprehensive, data-driven frameworks for seismic risk reduction and resilience enhancement. It affirms the principle that effective mitigation and preparedness efforts are predicated upon informed understanding of hazards and vulnerabilities, and that advancing knowledge is a prerequisite to advancing resilience outcomes in both high- and low-hazard regions confronting future seismic threats.

Enhanced Strategies for Liquefaction Reconnaissance Mapping in Disaster-Affected Regions

Earthquake reconnaissance data refers to the systematic collection of information following a seismic event to assess its impacts on the built environment, critical infrastructure systems, and the natural landscape. Such data are essential for characterizing earthquake phenomena, evaluating the extent and spatial distribution of damage, and informing future improvements in seismic design standards, construction practices, and emergency response planning. Reconnaissance activities are focused on documenting perishable evidence of earthquake impacts before it is altered or removed by recovery operations, environmental processes, or subsequent human activity. The timely and systematic

capture of these data enables the scientific and engineering communities to develop a comprehensive understanding of earthquake effects and to refine predictive models that underpin risk assessment and mitigation strategies.

Earthquake reconnaissance efforts span multiple disciplines and generate a wide range of critical data types, including:

- **Seismic data**: Epicenter location, magnitude, and focal depth recorded by seismic instrumentation networks.
- **Ground shaking data**: Peak ground acceleration (PGA) and spectral acceleration values at various periods captured through accelerometers and strong-motion networks.
- **Surface rupture and ground deformation**: Observations of fault surface ruptures, lateral spreading, and permanent ground displacements.
- **Geotechnical observations**: Documentation of ground failure mechanisms such as liquefaction, landslides, and ground settlement.
- **Structural damage assessments**: Evaluation of the performance of buildings, bridges, and lifeline infrastructure subjected to earthquake loading.
- **Lifeline system performance**: Assessment of disruptions to utilities, transportation networks, water supply systems, and communication infrastructure.
- **Social and economic impacts**: Data on casualties, displaced populations, and broader community disruptions.

These diverse datasets are obtained through a combination of seismic monitoring networks, remote sensing platforms (e.g., optical and radar satellite imagery), field-based reconnaissance missions, crowdsourced observations, and predictive hazard modeling frameworks.

Several coordinated organizations facilitate systematic post-earthquake reconnaissance efforts to ensure the timely, standardized, and comprehensive collection of high-value data.

The Geotechnical Extreme Events Reconnaissance (GEER) Association leads rapid response missions to document geotechnical and geological effects following significant natural and anthropogenic disasters. GEER's objectives include:

- Documenting geotechnical and related impacts of extreme events to advance research and professional practice.
- Employing innovative technologies for post-event reconnaissance.

- Enhancing the capabilities of individuals conducting reconnaissance.
- Training researchers and practitioners in effective field data collection methods.
- Coordinating multidisciplinary reconnaissance teams.
- Promoting standardization of measurements and reporting protocols.
- Disseminating timely and accessible post-event reports and datasets (Bray et al., 2018).

GEER findings are disseminated through web-based preliminary reports, peer-reviewed publications, curated data repositories, and technical seminars, ensuring that collected information is preserved and made widely available for future research and engineering applications.

Similarly, the Structural Extreme Events Reconnaissance (StEER) Network adopts a community-centered approach focused on documenting the performance of the built environment following natural hazard events (Kijewski-Correa et al., 2021). StEER operates under two complementary modalities:

- **Field Assessment Structural Teams (FASTs)**: Conduct in-situ field assessments to gather detailed observations of structural damage and lifeline system performance.
- **Virtual Assessment Structural Teams (VASTs)**: Remotely collect publicly available information and produce Preliminary Virtual Reconnaissance Reports (PVRRs) within days of an event.

Virtual reconnaissance enables the rapid capture of perishable data, provides broader spatial coverage than traditional field teams alone, supports strategic planning of field missions, and, where accessibility is constrained, can serve as a substitute for ground-based surveys.

The Earthquake Engineering Research Institute (EERI) established Virtual Earthquake Reconnaissance Teams (VERTs) in 2015 through its Learning from Earthquakes (LFE) program (Fischer and Hakhamaneshi, 2019). VERTs integrate satellite imagery analysis, crowdsourced data, social media mining, and remote sensing technologies to support rapid post-disaster data collection and synthesis. Their efforts complement those of GEER, StEER, and the DesignSafe cyberinfrastructure by expanding the spatial and temporal scope of reconnaissance activities.

The United Nations Satellite Centre (UNOSAT), operating under the auspices of the United Nations Institute for Training and Research (UNITAR), also provides satellite-based assessments for humanitarian mapping, disaster response, and recovery efforts. UNOSAT delivers rapid, high-resolution damage assessments derived from satellite imagery, supporting decision-making for international humanitarian operations (https://www.unitar.org).

In parallel, Volunteered Geographic Information (VGI) platforms have emerged as valuable tools for post-disaster mapping. The Humanitarian OpenStreetMap Team (HOT) mobilizes global volunteers to update spatial datasets in near real-time, providing critical information for damage assessment, resource allocation, and emergency response (Eckle and de Albuquerque, 2015). OpenStreetMap datasets, produced by HOT initiatives, have been instrumental in supporting disaster management efforts across a wide range of global contexts.

The work presented herein integrates a combination of reconnaissance datasets compiled by the Geotechnical Extreme Events Reconnaissance (GEER) Association, the Structural Extreme Events Reconnaissance (StEER) Network, and open-source imagery from platforms such as the MAXAR Open Data Program to support the development of liquefaction mapping methodologies.

Chapter 1 Overview

The first component of this dissertation addresses a critical and long-standing gap in post-earthquake reconnaissance: the absence of standardized, scalable methodologies for documenting the surface manifestations of earthquake-induced liquefaction. Liquefaction is a complex geotechnical phenomenon that originates in the subsurface as a consequence of elevated pore water pressures generated during seismic shaking, leading to a significant reduction in soil strength and stiffness. Although its genesis lies beneath the surface, liquefaction is visually identified through transient surface indicators such as sand boils, ground fissures, lateral spreading, and localized settlement. These features, while essential for diagnosing liquefaction activity, are ephemeral in nature—susceptible to environmental degradation, human disturbance, and rapid removal during emergency response and recovery operations.

The inherent challenge of detecting and characterizing a subsurface process based solely on its surface expressions necessitates a methodological framework that is both spatially rigorous and operationally efficient. Traditional field-based reconnaissance efforts, though capable of producing high-resolution observations, are frequently constrained by limited accessibility, time sensitivity, and resource availability. Moreover, the absence of standardized documentation protocols often results in inconsistent datasets, thereby limiting their applicability for comparative analysis, model validation, or integration into broader geospatial and computational frameworks.

To address these limitations, Chapter 1 introduces a remote sensing–based framework for the systematic mapping of liquefaction-induced surface features. The proposed methodology leverages high-resolution optical satellite imagery, supplemented by field-verified observations when available, to produce polygon-based, thematically labeled inventories. This framework is applied to three major seismic events: the 2010 M7.0 Port-au-Prince (Haiti),

2011 M6.1 Christchurch (New Zealand), and 2021 M7.2 Nippes (Haiti) earthquakes. These events were selected based on the availability of suitable imagery and documentation, as well as the prevalence of surface-level liquefaction features.

The resulting geospatial inventories are designed to support both immediate post-disaster impact assessments and the development of training datasets for automated damage detection models using computer vision techniques. By formalizing and operationalizing the liquefaction mapping process through remote sensing, this chapter advances a reproducible, scalable, and analytically robust methodology for documenting post-earthquake ground failure. In doing so, it contributes to the empirical foundation necessary for improving seismic risk models, informing resilience-oriented design strategies, and enhancing the technological infrastructure for future reconnaissance efforts.

Vulnerability Assessment of Buildings in Moderate-Seismicity Areas with Strong Site Amplification

The methodology shared between Chapters 2 and 3 is grounded in the distinctive geologic and seismic conditions of the Central and Eastern United States (CEUS), with a focused application in the Commonwealth of Massachusetts. This region, while generally classified as low-to-moderate in seismicity, is characterized by strong impedance contrasts and deep sedimentary deposits that amplify seismic ground motions in ways not fully captured by simplified modeling approaches. Recognizing these complexities, this research builds upon recent geotechnical mapping efforts (Mabee et al., 2023; Pontrelli et al., 2024) to incorporate high-resolution subsurface data into seismic risk assessment workflows.

To evaluate the vulnerability of Massachusetts' building stock, both analytical and real, this study aligns structural inventories with the 2020 NEHRP risk-targeted Maximum Considered Earthquake (MCEr) ground motions, integrating them within the Federal Emergency Management Agency's (FEMA) HAZUS loss estimation framework. This approach facilitates a standardized, data-driven analysis using HAZUS-informed capacity curves and fragility functions to estimate structural response to seismic excitation.

Chapters 2 and 3, while distinct in their specific focus, share a unified analytical foundation. Chapter 2 emphasizes the spatial distribution of seismic damage and the prioritization of retrofitting strategies using updated site classifications derived from geologic and geophysical data. Chapter 3 builds upon this foundation by replacing simplified amplification proxies with site-specific Ground Response Analysis (GRA), thereby refining the estimates of seismic demand and revealing the influence of local site effects on building performance.

The sections that follow outline the core datasets, modeling assumptions, and analytical workflows that support the comparative and complementary findings presented in both chapters. This joint methodological framework ensures internal consistency, reproducibility, and a coherent basis for integrated risk modeling and mitigation planning.

Regional Seismic Hazard Context in Massachusetts

Seismic activity in the Commonwealth of Massachusetts, while generally infrequent and moderate in magnitude, nonetheless poses a tangible risk to the built environment and public safety. The seismic hazard in this region arises from the broader geotectonic setting of the Central and Eastern United States (CEUS), where earthquakes typically originate from intraplate sources—tectonic activity occurring within the interior of a lithospheric plate rather than along active plate boundaries (Kafka, 2004; Kianiard et al., 2017; Ebel, 2025). These events are often associated with the reactivation of deeply buried fault systems and residual tectonic structures formed through ancient orogenic processes.

Massachusetts has experienced several historically significant earthquakes, most notably the 1727 Newburyport event (estimated M5.6) and the 1755 Cape Ann earthquake (estimated M6.3). The latter, centered approximately 32 kilometers offshore of Cape Ann, remains the most damaging seismic event in the state's recorded history. The Cape Ann earthquake produced widespread structural damage, particularly to masonry chimneys, foundation walls, and brick structures throughout Boston and surrounding municipalities. Contemporary reports indicate that nearly one-third of Boston's chimneys were destroyed, with significant urban disruption resulting from fallen masonry debris (Sorabella, 2006; Buell, 2020; Ebel, 2025).

Additional shaking in Massachusetts has originated from earthquakes centered in adjacent source zones, including the St. Lawrence Valley, the Laurentian Trough, central New Hampshire, Vermont, and southern Quebec. Among these, the 1925 M6.2 Charlevoix earthquake and the 1638 M6.5–7.0 Concord, New Hampshire earthquake were felt strongly throughout the Commonwealth, although no structural damage was reported (Ebel, 1996; Ebel, 2025).

To characterize seismic hazard across Massachusetts, **Figure 1** presents maps from the United States Geological Survey (USGS) that display Peak Ground Acceleration (PGA), 0.2-second spectral acceleration (S_a), and 1.0-second spectral acceleration for Site Class A conditions, which correspond to reference rock sites with a shear wave velocity (Vs_{30}) of 1500 m/s (Hashash et al., 2014). These maps are derived from the 2023 National Seismic Hazard Model (NSHM) uniform-hazard data release (Petersen et al., 2023), which estimates ground motions with a 2% probability of exceedance in 50 years—equivalent to a return period of approximately 2,475 years. This return

period is not arbitrary; rather, it represents a foundational benchmark in earthquake engineering and regulatory guidance and is widely adopted for the seismic design of critical infrastructure and land-use planning. It is particularly relevant for the development of risk-targeted ground motions used in building codes (e.g., ASCE 7 and NEHRP provisions), ensuring that structures are designed to withstand rare but potentially devastating seismic events. By integrating all credible seismic sources and ground motion prediction equations into a probabilistic framework, this uniform-hazard approach enables a consistent, long-term evaluation of seismic exposure across regions

Under Site Class A conditions, the uniform-hazard PGA values for Massachusetts range from 0.099g to 0.363g; the 0.2-second spectral acceleration ranges from 0.148g to 0.378g; and the 1.0-second spectral acceleration ranges from 0.050g to 0.083g. While the majority of the Commonwealth is subject to moderate seismic hazard, elevated levels of ground motion are observed in the northeastern region, particularly in Essex County and portions of Middlesex County. Although hard rock conditions in these areas generally attenuate seismic wave amplification, the presence of overlying soft sediments and glacial deposits in many locations can result in significant amplification effects—highlighting the importance of localized site characterization in seismic hazard assessments.

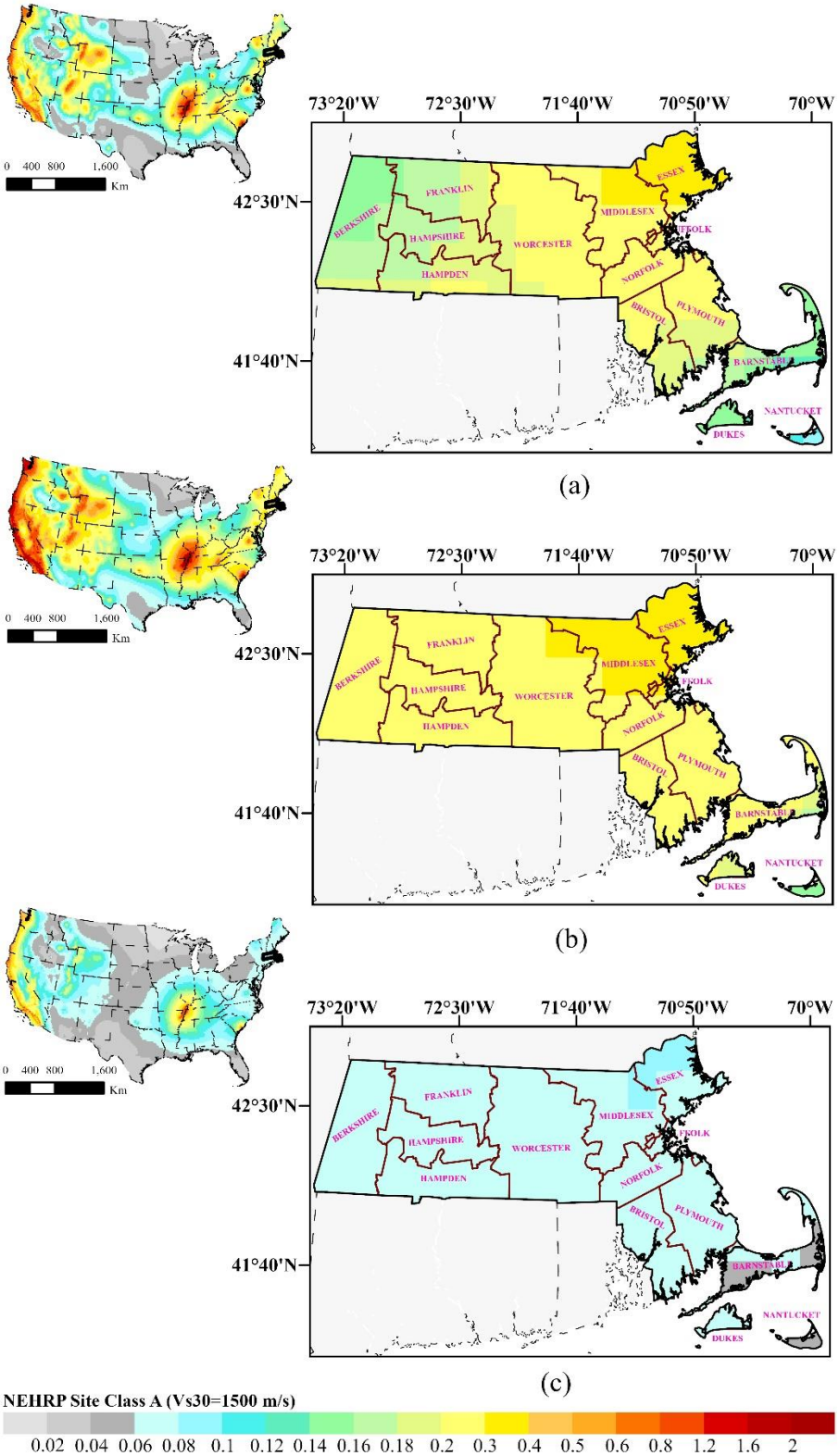

Figure 1: Uniform-hazard ground motion for a 2% probability of exceedance over 50 years, based on hark rock site conditions (Vs30 = 1500 m/s; Site Class A), derived from the 2023 National Seismic Hazard Model, showing the boundaries of the 14 counties in Massachusetts. (a) Peak Ground Acceleration (PGA) (g). (b) Short-period acceleration at 0.2 seconds. Long-period acceleration at 1 second.

Site Characterization

Site characterization constitutes a foundational component of seismic hazard assessment. The evaluation of local geologic and geotechnical conditions—including soil stratigraphy, bedrock depth, and topographic variability—provides critical insight into how seismic waves are modified as they propagate through the near-surface environment. These local site effects play a significant role in amplifying ground motions and elevating the risk of secondary hazards such as liquefaction, thereby influencing the vulnerability and performance of structures during seismic events.

In this study, high-resolution site characterization refers to the use of spatially granular data capable of capturing fine-scale geotechnical variability across the Commonwealth of Massachusetts. Such detail enables more accurate regional hazard modeling and supports building-specific vulnerability assessment through the application of FEMA's HAZUS fragility framework.

Microtremor horizontal-to-vertical spectral ratio (HVSR) data were used to generate a statewide depth-to-bedrock map and to develop surficial geologic unit–based power-law shear wave velocity (Vs) profiles (Pontrelli et al., 2024). The resulting depth-to-bedrock dataset (Mabee et al., 2023; see **Figure 2**) was integrated with a surficial geologic map of Massachusetts (Stone et al., 2018; Mabee et al., 2023; see **Figures 3 and 4**) to calculate the median distribution of time-averaged shear wave velocity to 30 meters (Vs_{30}) across the state (Pontrelli et al., 2024; **Figure 5**).

This geologically driven approach stands in contrast to two previously published Vs_{30} maps for Massachusetts: (1) the globally derived slope-based model by Wald and Allen (2007) and (2) the regionally developed geology-based Vs_{30} map for New England by Becker et al. (2011). Additionally, the fundamental site frequency (f_0) was estimated for sediment-over-bedrock regions using the mapped depth to bedrock and interpolated shear wave velocities, resulting in a median f_0 distribution map (Pontrelli et al., 2024; **Figure 6**).

The figures presented in this section emphasize four key geologic regions—(a) the Connecticut River Valley, (b) the Boston Basin, (c) Cape Cod, and (d) the North Shore—each of which exhibits notable heterogeneity in subsurface conditions and, consequently, in seismic site response characteristics.

Depth to Bedrock

The depth-to-bedrock map presented in **Figure 2** illustrates the spatial variability in the thickness of unconsolidated overburden across the Commonwealth of Massachusetts. This map was developed as part of a project funded by the Massachusetts Department of Transportation (MassDOT) Research Program, with the primary objective of compiling

and synthesizing borehole logs and geophysical data to produce a high-resolution subsurface dataset. The resulting map characterizes both the altitude of the bedrock surface and the overlying sediment thickness, offering valuable insights into geologic heterogeneity at the regional scale. The depth-to-bedrock values were calculated by subtracting interpolated bedrock surface elevations from topographic surface elevations, using digital elevation models at a spatial resolution of 100 meters (Mabee et al., 2023).

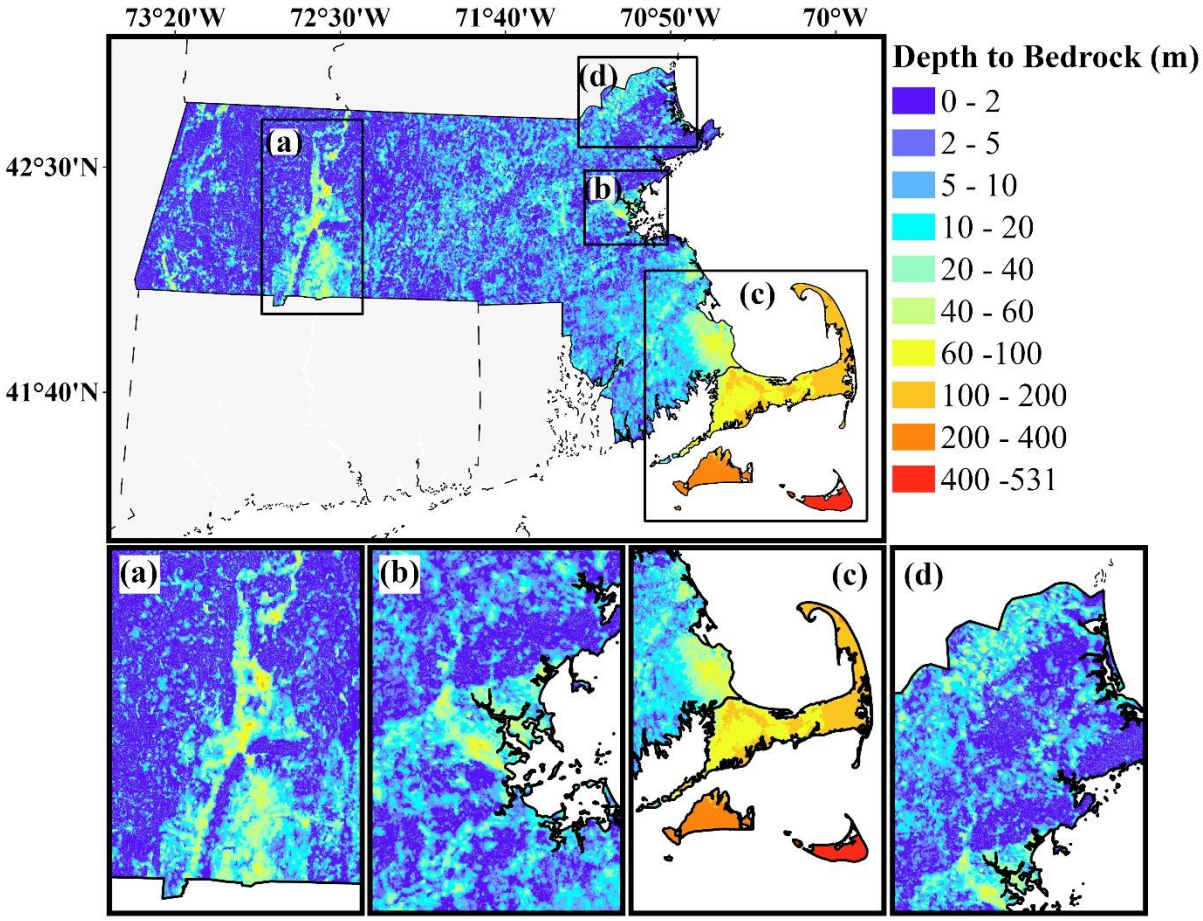

Figure 2: Depth to bedrock (Mabee et al., 2023). (a) Connecticut River Valley. (b) Boston Basin. (c) Cape Cod. (d) Massachusetts North Shore.

Shear Wave Velocity (Vs_{avg}) by Geologic Unit

The **Vs_{avg}** groupings shown in **Figure 4**—categorized as Low Velocity, Mid-Low Velocity, Mid-High Velocity, High Velocity, and Bedrock—are derived from the Massachusetts surficial geologic map, which delineates 23 distinct geologic units (Stone et al., 2018; see also **Figure 3**). These units were consolidated into five primary velocity groups based on shared mechanical characteristics and estimated relative shear wave velocities (Mabee et al., 2023). To refine these classifications, several researchers employed the horizontal-to-vertical spectral ratio (HVSR) method, a microtremor-based technique that estimates the fundamental resonance frequency of subsurface materials using

ambient seismic noise (Nakamura, 1989; Ibs-von Seht & Wohlenberg, 1999; Hayles et al., 2001; Yilar et al., 2017). Building on this approach, Pontrelli et al. (2023b) utilized the HVSR dataset compiled by Mabee et al. (2023), which comprises 1,342 fundamental frequency measurements across Massachusetts. This dataset was used to develop geology-based power law velocity profiles, modeling shear wave velocity gradients for each of the grouped surficial units, as illustrated in **Figure 4**.

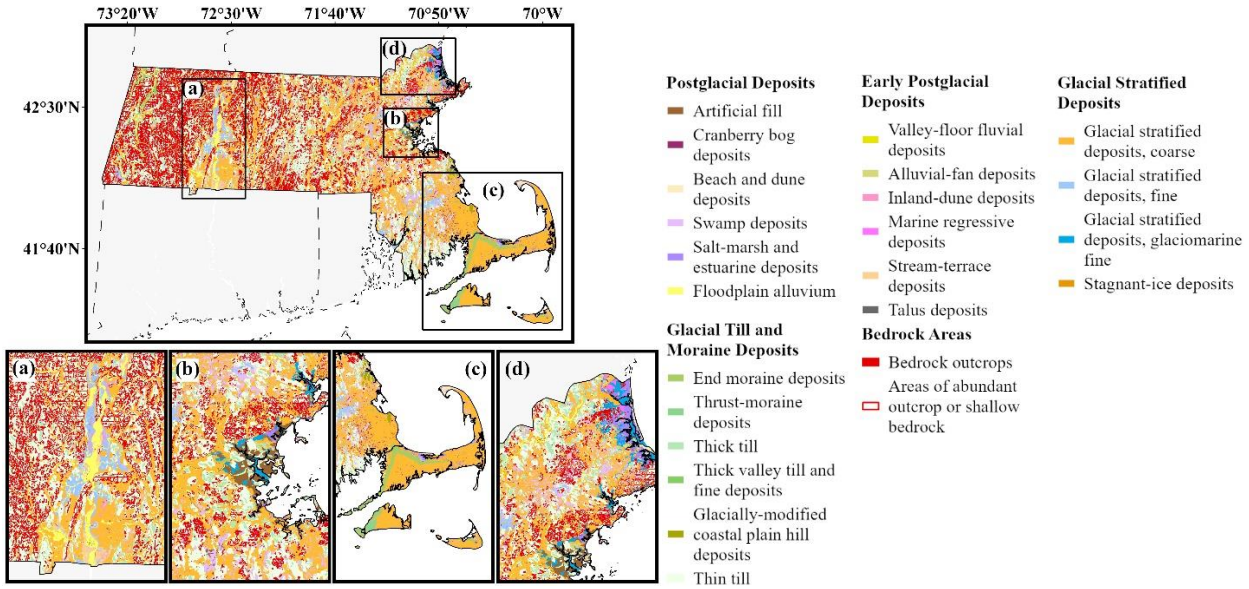

Figure 3: Surficial Geology (Stone et al., 2018). (a) Connecticut River Valley. (b) Boston Basin. (c) Cape Cod. (d) Massachusetts North Shore.

The relationship between subsurface stiffness and shear wave velocity is critical for assessing how seismic waves interact with geologic materials and subsequently affect the built environment. Low-velocity regions, which are typically composed of artificial fill, salt marsh, and swamp deposits, exhibit low stiffness and high compressibility, making them particularly susceptible to seismic wave amplification. Mid-low velocity regions, consisting of glacial stratified deposits, fine-grained glaciomarine materials, and similar sedimentary units, display moderate stiffness but retain a notable potential for amplification. Mid-high velocity areas, characterized by floodplain alluvium, alluvial-fan deposits, and coastal features such as beaches and dunes, offer improved resistance to seismic amplification due to increased material consolidation. High-velocity regions, including glacially modified coastal plain hill deposits, end moraine deposits, and till, are composed of dense, consolidated soils that are less prone to amplification effects. Bedrock regions, defined by surface-exposed or shallow bedrock outcrops, provide the greatest stiffness and the lowest susceptibility to seismic wave amplification.

Within Massachusetts, the Boston Basin and North Shore regions contain extensive areas mapped as Low and Mid-Low velocity groupings. The Boston Basin is largely underlain by artificial fill, while the North Shore features a combination of glacial stratified deposits, salt marsh, estuarine deposits, and swamp soils. Notably, the North Shore is estimated to experience the highest level of ground shaking in the state, as depicted in **Figure 1**, due to both its subsurface composition and regional seismic hazard characteristics.

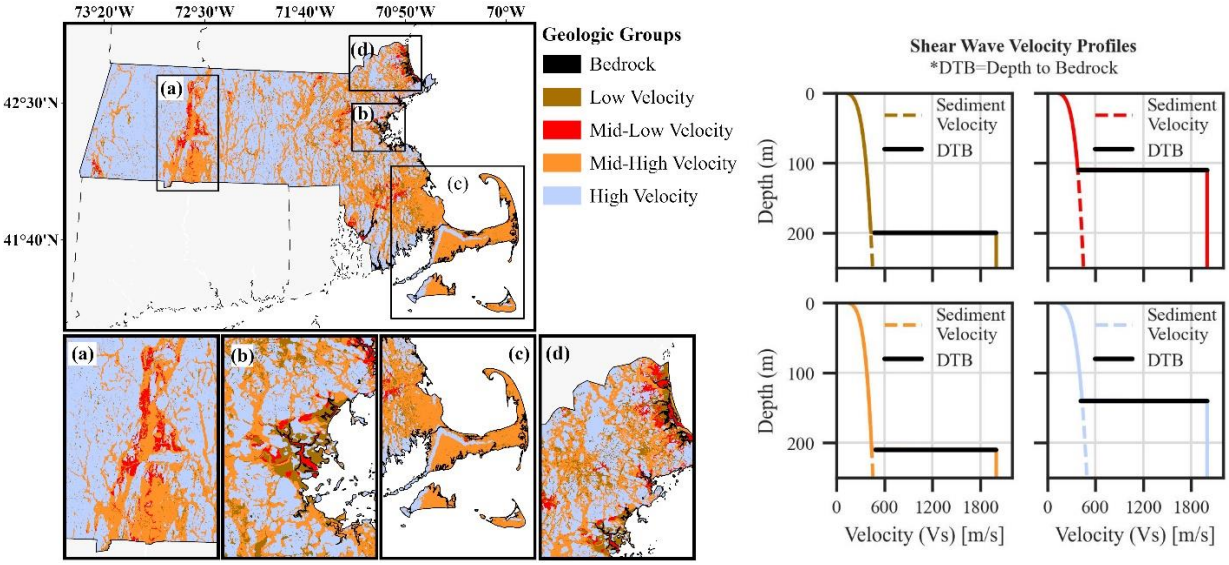

Figure 4: Geologic grouping for estimating shear wave velocity profiles and their respective estimated shear wave velocity profiles. (a) Connecticut River Valley. (b) Boston Basin. (c) Cape Cod. (d) Massachusetts North Shore.

The shear wave velocity (V_s) profiles are based on the following relationship:

$$V_s = 4\alpha z^{\beta+1} \qquad \text{(Equation 1)}$$

Where z is the depth-to-bedrock (**Figure 2**), and the geologic parameters (α and β), estimated from regression, can be found in **Table 1**, as provided by Pontrelli et al. (2024).

Table 1: Geologic parameters (α and β) used in the shear wave velocity (V_s) profile equation (Equation 1), derived from Pontrelli et al. (2024). These parameters correspond to the various surficial geologic units in Massachusetts and are used to model the shear wave velocity gradients based on depth-to-bedrock measurements.

Geologic Group	α	β
Low Velocity	33.51	-0.780
Mid-Low Velocity	35.40	-0.791
Mid-High Velocity	38.03	-0.801
High Velocity	35.85	-0.777

Time-averaged Shear Wave Velocity in the upper 30 meters (Vs_{30})

Figure 5 presents the 2020 NEHRP site classification map for Massachusetts, based on the median estimates of Vs_{30} at a spatial resolution of 100 meters. These Vs_{30} values—representing the time-averaged shear wave velocity over the upper 30 meters of the subsurface—were calculated for each surficial geologic unit using a layer-over-halfspace site response model, with shear wave velocity gradients informed by regional velocity profiles (as shown in **Figure 4**) and derived according to the methodology detailed in Pontrelli et al. (2023b). Vs_{30} is a key site parameter used for classifying seismic site conditions and for extracting design ground motions from the national seismic hazard maps developed by the United States Geological Survey (USGS).

The 2020 NEHRP site classes, summarized in **Table 1**, are assigned based on the median Vs_{30} value for each grid cell. In general, higher Vs_{30} values correspond to stiffer soils or bedrock conditions, which are associated with reduced seismic amplification, whereas lower Vs_{30} values are indicative of softer soils more susceptible to amplification effects. Across Massachusetts, the median Vs_{30} values derived for this dataset range from 223 m/s to 2500 m/s, corresponding to NEHRP 2020 site classes D through A, respectively. Notably, site classes DE and E—which represent very soft soils with extremely low shear wave velocities—are not observed within the mapped extent of this dataset.

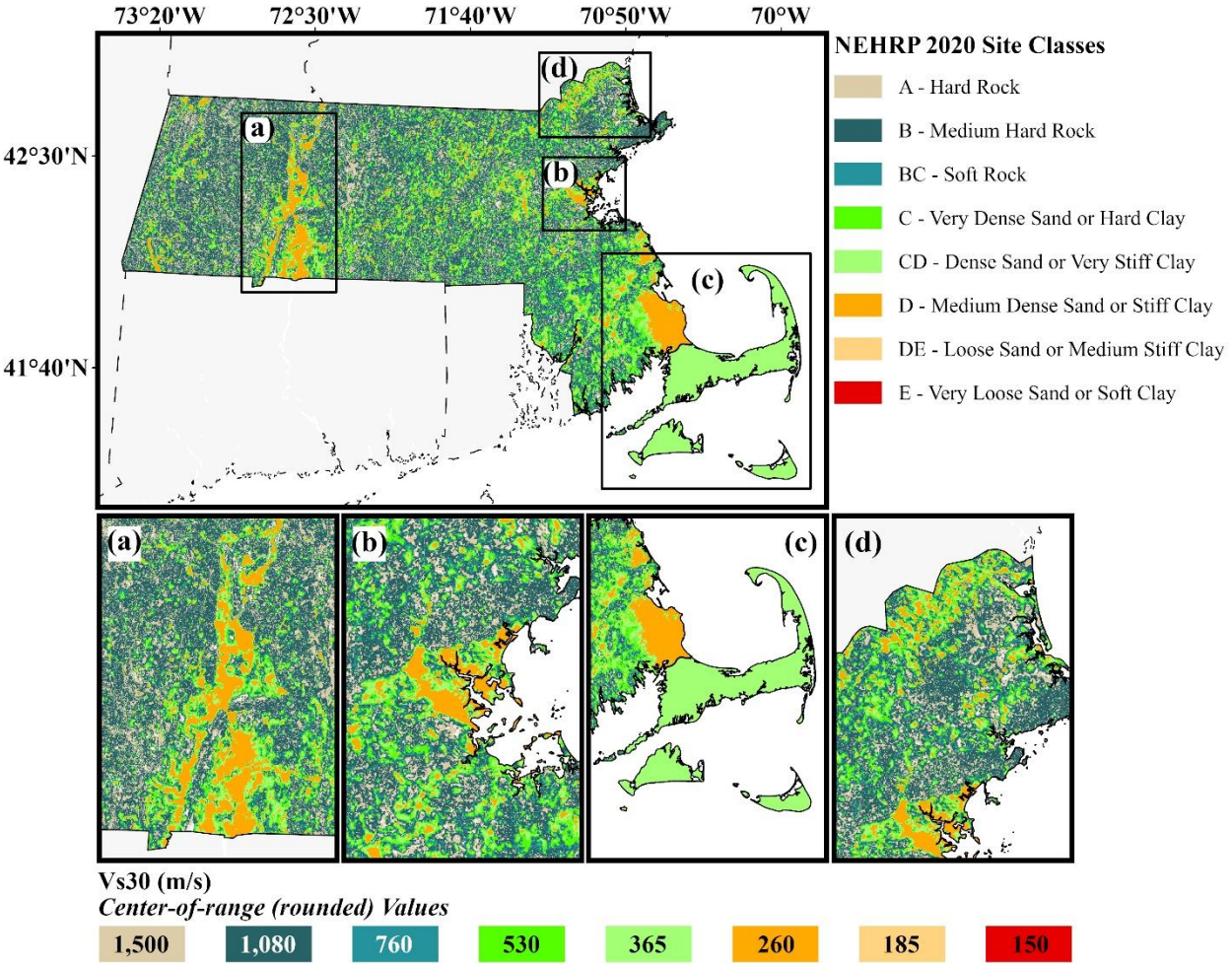

Figure 5: 2020 NEHRP Site Classification based on the median time-averaged shear wave velocity in the upper 30 meters (Vs_{30}) (Pontrelli et al., 2023b). (a) Connecticut River Valley. (b) Boston Basin. (c) Cape Cod. (d) Massachusetts North Shore.

Table 2: Site Classification (ASCE 7-22, Table 20.2-1)

Site Class	Vs_{30} Calculated Using Measured or Estimated Shear Wave Velocity Profile (ft/s)	Vs_{30} Calculated Using Measured or Estimated Shear Wave Velocity Profile (m/s)
A. Hard Rock	>5,000	>1,524
B. Medium hard rock	3,000 to ≤ 5,000	914.4 to ≤ 1,524
BC. Soft rock	2,100 to < 3,000	640.1 to < 914.4
C. Very dense sand or hard clay	1,450 to < 2,100	441.96 to < 640.1
CD. Dense sand or very stiff clay	1,000 to < 1,450	304.8 to < 441.96
D. Medium dense sand or stiff clay	700 to < 1,000	213.4 to < 304.8
DE. Loose sand or medium stiff clay	500 to < 700	152.4 to < 213.4
E. Very loose sand or soft clay	<500	<152.4

Fundamental Frequency (f_0)

Figure 6 presents the median distribution of the fundamental frequency (f_0) of soil profiles across Massachusetts, offering insights into the potential for site-specific resonance during seismic events. Similar to Vs30, the fundamental frequency is a key parameter in site characterization, reflecting the natural frequency of the soil column above bedrock. Higher f_0 values generally indicate stiffer or shallower soil profiles, whereas lower f_0 values are associated with softer or deeper sediments, which are more prone to amplifying long-period ground motions.

The f_0 map was generated by integrating the depth-to-bedrock data (**Figure 2**) with the geology-based shear wave velocity profiles (**Figure 4**), following the methodology outlined in Pontrelli et al. (2023a; 2023b). To ensure geophysical realism and consistency with observed spectral behavior, a frequency threshold was applied to mask anomalously high f_0 values associated with extremely shallow bedrock (typically less than 4 meters), which were not supported by field data. In areas where the sediment thickness fell below this threshold, the ground was assumed to behave as bedrock, and no f_0 value was assigned—these areas are displayed in white in **Figure 6**.

The applied threshold corresponds to the transition depth at which the median Vs_{30} value at a given pixel exceeds 760 m/s, delineating the boundary between NEHRP site class C and stiffer classes. This transition depth is not constant but varies spatially across geologic groupings and subregions. For example, in the Boston Basin, this threshold occurs at a depth of approximately 4.32 meters. The resulting f_0 map serves as a valuable tool for identifying regions where soil-structure resonance may exacerbate seismic demands on buildings, particularly those whose natural periods coincide with the site's fundamental frequency.

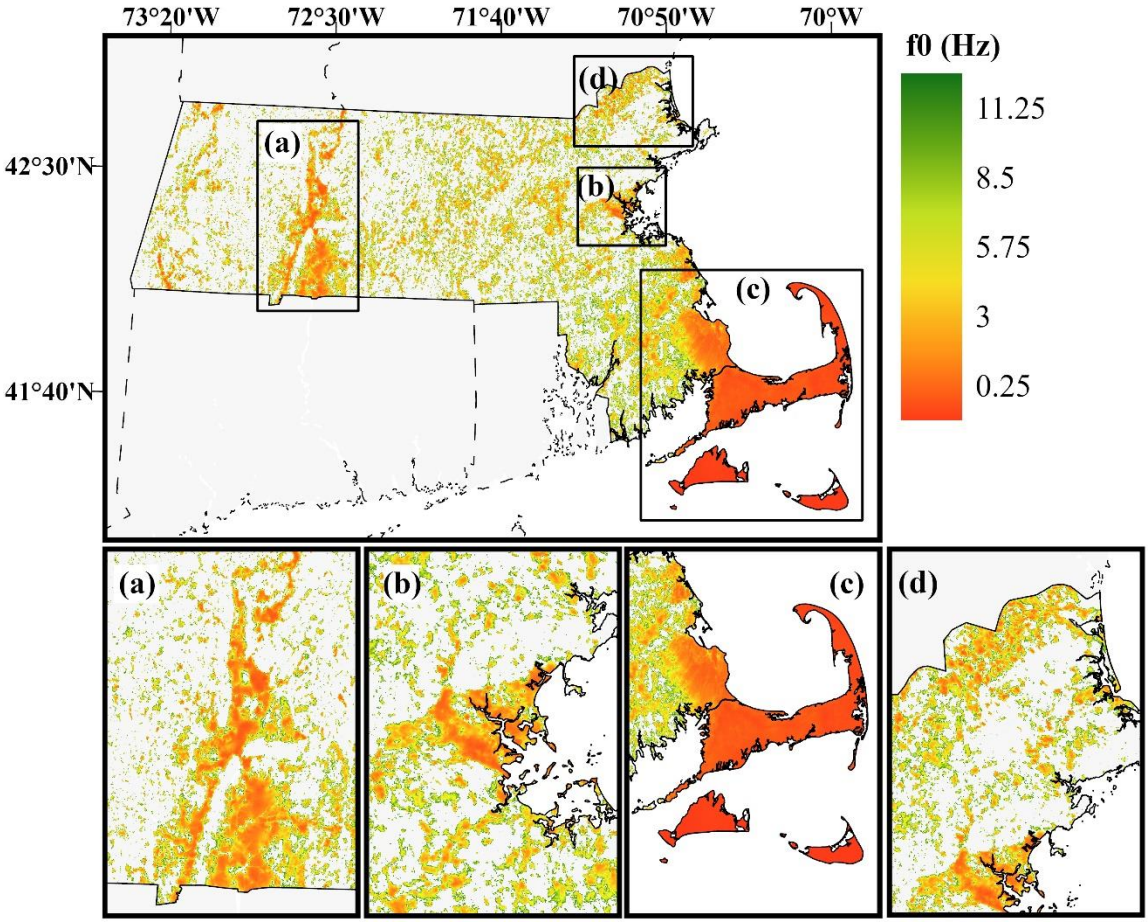

Figure 6: Fundamental frequency (f_0) (Pontrelli et al. 2023a, b). (a) Connecticut River Valley. (b) Boston Basin. (c) Cape Cod. (d) Massachusetts North Shore.

USGS Seismic Design Geodatabase

The National Seismic Hazard Model (NSHM), developed by the United States Geological Survey (USGS), serves as a foundational tool for assessing earthquake risk across the United States. It classifies regions by seismicity and estimates the potential levels of ground motion that buildings and infrastructure may experience during seismic events. The model integrates a broad range of data—including seismic source characteristics, historical earthquake records, and geological conditions—into a comprehensive probabilistic framework. The 2023 update (Petersen et al., 2023) incorporates significant advancements in seismic source modeling, fault rupture behavior, ground motion prediction, and probabilistic hazard assessment methodologies (Petersen et al., 2018).

In parallel, the USGS Seismic Design Geodatabase (Luco et al., 2021) provides gridded spectral acceleration values corresponding to the Maximum Considered Earthquake risk-targeted (MCE_r) ground motions. These values are calculated across 22 spectral periods (ranging from 0.0 to 10 seconds) and eight site classes, as defined by the

National Earthquake Hazards Reduction Program (NEHRP) (**Table 1**). The MCE_r values represent rare but plausible seismic events, defined as having a 2% probability of exceedance in 50 years (i.e., an annual exceedance probability of 0.0004), equivalent to a return period of approximately 2,475 years.

MCE_r ground motions are critical for designing structures to withstand extreme seismic demands, in accordance with ASCE 7 and the International Building Code (IBC). In contrast to uniform-hazard ground motion values, which estimate the probability of a certain level of shaking being exceeded, MCE_r values are risk-targeted and intended to ensure an acceptable collapse risk for a standardized fragility function (Spillatura et al., 2023). These values can be accessed through the USGS Geodatabase or the ASCE hazard tool, enabling engineers and planners to derive appropriate design spectra for site-specific applications.

This study adopts MCE_r ground motion values in place of scenario earthquakes to establish a conservative and code-consistent basis for assessing structural performance. This approach is particularly important in regions like Massachusetts, where seismicity is infrequent and risk communication may be challenged by a lack of recent damaging events. By anchoring the analysis in nationally recognized design criteria, the damage estimates produced here align with current structural engineering standards and minimize the likelihood of over- or underestimating risk.

The probability of damage for a given structure is calculated as the product of the probability of an earthquake occurring and the conditional probability that the structure exceeds a specific damage state given that event. For example, if the conditional probability of exceeding a damage state is 30% during an MCE_r event (with a 2% probability in 50 years), the annualized exceedance probability becomes approximately 0.0121%, or roughly 0.6% over 50 years.

Figure 7 outlines the methodology used to extract site-specific MCEr ground motion parameters from the USGS database using a high-resolution site characterization map, specifically the median Vs_{30} values developed for this study. The USGS geodatabase consists of a regular grid of ground motion values at 0.05° × 0.05° resolution. These values are interpolated into a raster surface, and each raster pixel is mapped to its corresponding site class based on Vs_{30}, enabling assignment of the appropriate ground motion values for that location.

This methodology was applied to extract the short-period (0.2s) and 1-second spectral acceleration values for each building location. These values form the two-period building design spectrum required for HAZUS-based fragility analyses and are adjusted for site class using NEHRP amplification factors.

The outputs are visualized in **Figure 8a**, which displays a mosaic of PGA_m (Maximum Considered Geometric Mean PGA) values adjusted for soil class (site effects). PGA_m is particularly relevant for geotechnical hazard evaluation, including liquefaction, lateral spreading, and seismic settlement, and is widely used in engineering code compliance. In contrast, **Figure 8b** presents the unadjusted MCE_G PGA, which reflects the geometric mean of the horizontal components of motion without risk-targeted modifications. Notably, the 0.0-second period spectral acceleration in the USGS geodatabase corresponds to this unadjusted PGA value. Areas with elevated PGA_m and MCE_G values—particularly in northeastern Massachusetts—are more likely to experience stronger shaking during a maximum considered earthquake, highlighting the importance of incorporating both site-specific and probabilistic ground motion data in regional hazard evaluations.

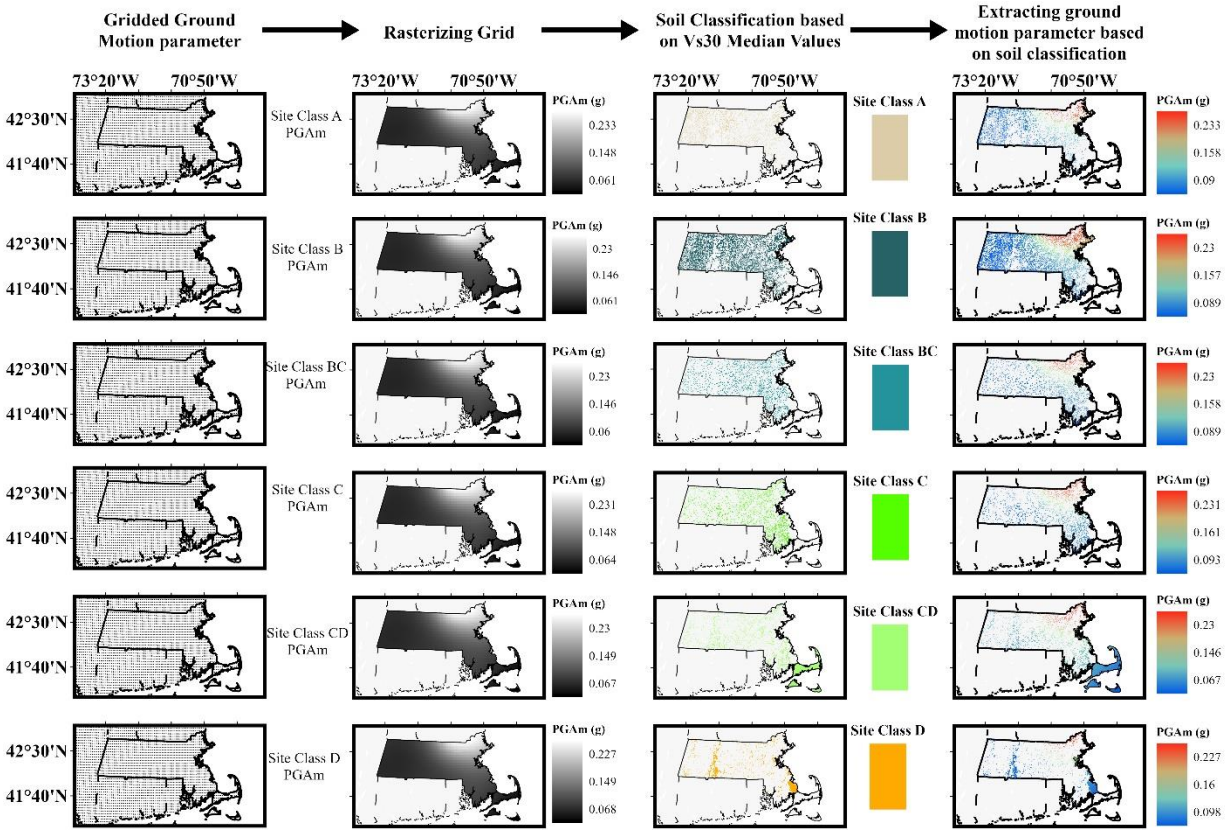

Figure 7: Workflow for extracting ground motion parameters from the USGS gridded design parameters, using site class determination based on the median estimate of Vs_{30} values map. This figure illustrates the process for extracting the Maximum Considered Geometric Mean (MCE_G) Peak Ground Acceleration adjusted to account for site class effects, PGA_m, ground motion parameter.

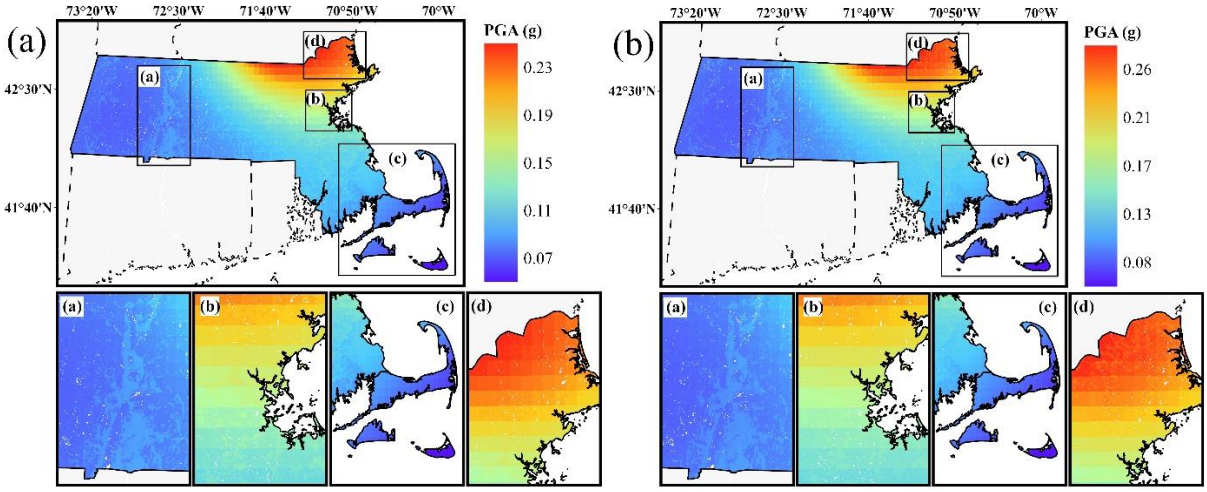

Figure 8: Mosaic maps of the Geometric mean Peak Ground Acceleration (PGA) for the state of Massachusetts based on the 2023 National Seismic Hazard Model (NSHM) data. (a) Maximum Considered Geometric Mean (MCEG) PGA adjusted for site class effects (PGAm). (b) Maximum Considered Earthquake (MCEG) PGA, representing the most severe shaking effects without adjustments for targeted risk. Insets: (a) Connecticut River Valley. (b) Boston Basin. (c) Cape Cod. (d) Massachusetts North Shore.

Fragility Analysis and Damage Estimation

The damage assessment workflow, illustrated in **Figure 9**, outlines the analytical process used to evaluate seismic vulnerability and conduct fragility-based analyses. The workflow begins with the characterization of the building stock, incorporating key attributes such as geographic location, year of construction, number of stories, and structural system. These attributes inform the assignment of appropriate HAZUS-defined building types and associated capacity parameters.

Subsequently, each building's location is used to assign a site class based on the median Vs_{30} estimates from the high-resolution site characterization map (see **Figure 5**), thereby capturing localized soil conditions that influence seismic amplification. With site class determined, risk-targeted Maximum Considered Earthquake (MCEr) spectral accelerations are extracted from the USGS seismic design geodatabase in accordance with the methodology described in **Figure 7**.

The spectral accelerations at the short-period and long-period values are then used to construct a 5%-damped elastic response spectrum for each building location. This response spectrum is integrated with HAZUS-defined capacity curves for each building type, enabling a quantitative assessment of structural performance under design-level seismic loading.

Finally, FEMA HAZUS fragility functions are applied to estimate the probability that a building will exceed each of four defined damage states—Slight, Moderate, Extensive, and Complete—conditional on the level of seismic

demand. This process facilitates the identification of at-risk structures within the regional building inventory and supports decision-making for seismic retrofitting, risk communication, and mitigation planning.

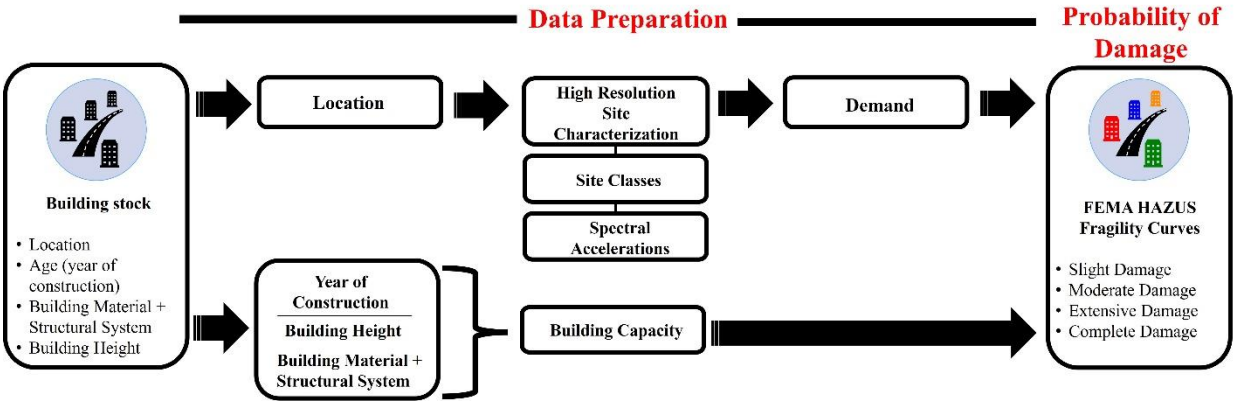

Figure 9: Damage State assessment workflow for seismic risk evaluation. The framework incorporates building stock characteristics, site-specific seismic hazard parameters, FEMA HAZUS fragility models to estimate damage probabilities.

HAZUS defines four primary damage state thresholds—Slight, Moderate, Extensive, and Complete—using fragility curves modeled as lognormal cumulative distribution functions. These curves integrate standardized building classification parameters with seismic performance metrics to estimate the probability of damage state exceedance as a function of ground motion intensity. The primary intensity measure is spectral displacement at the building's fundamental period, reflecting the peak structural response under seismic loading.

This peak response is determined by the intersection of the building's capacity curve and the seismic demand spectrum. The capacity curve characterizes the nonlinear relationship between lateral force and displacement for a given structure and is defined by two key points: the yield point, indicating the onset of inelastic behavior, and the ultimate point, representing the maximum capacity before failure mechanisms dominate. The demand spectrum is typically defined using a 5% damping ratio but is adjusted to account for effective damping and energy dissipation resulting from inelastic structural response.

Each HAZUS building classification, as cataloged in HAZUS 6.1 (see Table 5-1), is assigned a unique capacity curve and a suite of fragility curves for each damage state, reflecting both structural and non-structural performance under seismic loading (**Figure 10**). The probability of damage state exceedance is then computed by overlaying the MCEr-derived demand spectrum with the corresponding capacity curve and evaluating the fragility function at the resulting spectral displacement (**Figure 11**). Capacity curves are modeled using spline interpolation, following the procedures outlined by Porter (2009).

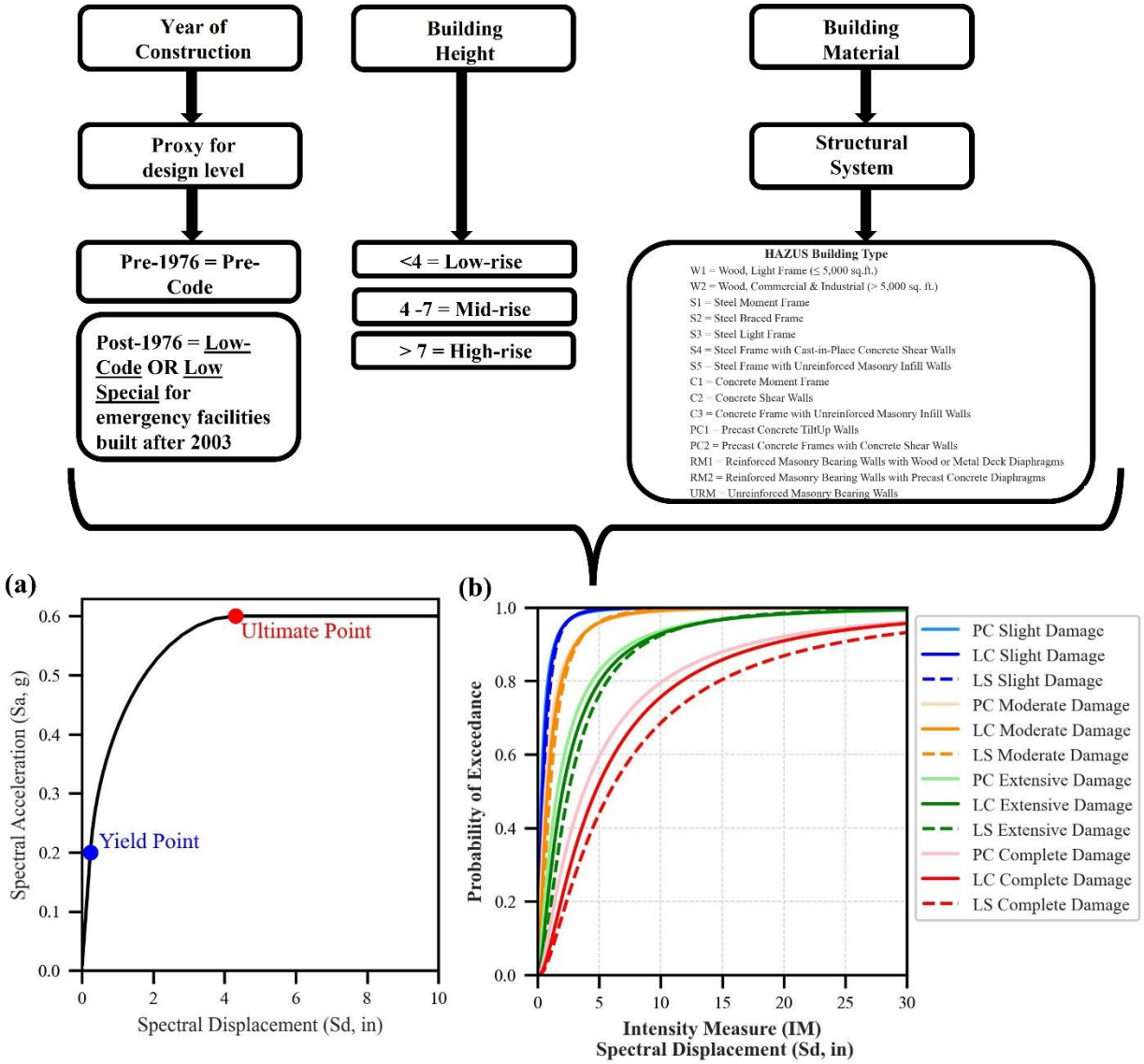

Figure 10: HAZUS workflow. (a) HAZUS method for defining a building's capacity curve. (b) HAZUS method for defining fragility curves. PC = Pre-Code; LC = Low-Code; LS = Low Special

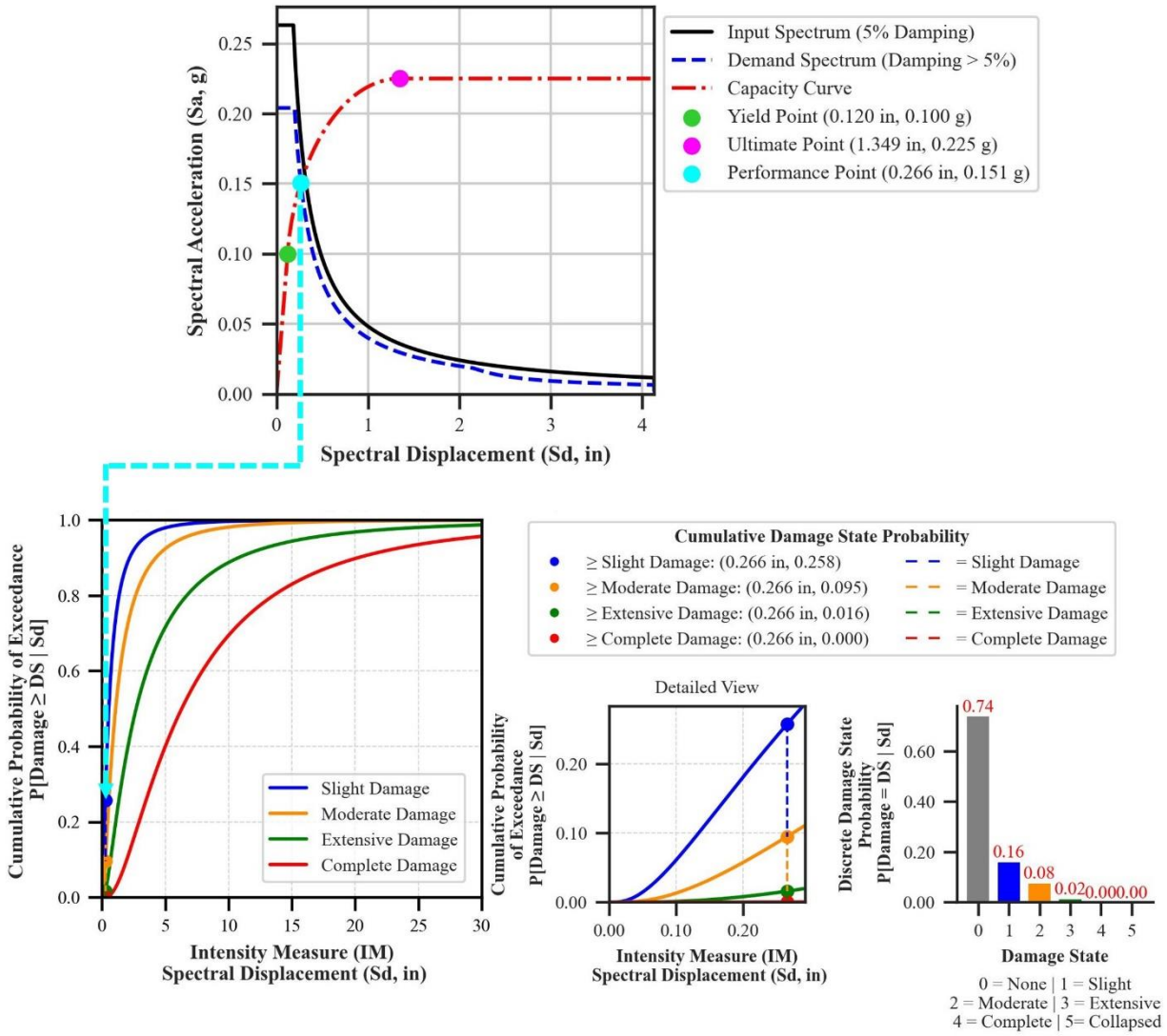

Figure 11: Sample damage state assessment, illustrating the process of estimating seismic damage probabilities using capacity, demand, and the peak building response for use with the fragility curves.

Chapter 2 Overview

Chapter 2 conducts a building-level seismic vulnerability assessment for the Commonwealth of Massachusetts by integrating a high-resolution site characterization map with a refined structural inventory to improve damage estimation and inform retrofitting prioritization. In regions such as Massachusetts—where seismicity is classified as low to moderate but subsurface conditions are complex—traditional loss models often lack the spatial granularity required to support localized risk mitigation. This chapter addresses that limitation by combining enhanced geotechnical and geological datasets with the Federal Emergency Management Agency's (FEMA) HAZUS loss estimation framework to evaluate potential seismic damage across a representative portfolio of buildings.

The analysis replaces the default HAZUS site classifications—typically based on generalized Vs30 values or broad geologic groupings—with a high-resolution site class map derived from state-specific geological and geophysical surveys. This enhancement improves the accuracy of ground motion amplification estimates used in the damage modeling process. The study relies on a proprietary, state-owned facility inventory, which provides detailed, building-specific information on occupancy type, construction material, number of stories, and construction era.

Using these high-resolution inputs, the HAZUS methodology quantifies the probability of structural damage under design-level ground motions. The assessment places particular emphasis on Unreinforced Masonry (URM) buildings, which are both seismically vulnerable and widely distributed across the state. The analysis produces a prioritized list of retrofit candidates based on structural characteristics and moderate damage exceedance probabilities.

The results demonstrate that integrating refined site classifications and detailed building data into the HAZUS framework significantly improves the spatial resolution of predicted damage outcomes. This approach reveals localized pockets of elevated risk that would likely remain obscured under default model assumptions. Additionally, the chapter analyzes variations in damage probability across structural typologies and occupancy classes to inform targeted mitigation strategies.

By aligning high-resolution geotechnical data with a proprietary structural inventory, Chapter 2 delivers a practical and scalable framework that enables state and local agencies to prioritize seismic retrofitting, allocate mitigation funding, and strengthen regional resilience planning. These findings lay the foundation for Chapter 3, which extends the analysis through site-specific Ground Response Analysis to further refine seismic demand and structural risk classification.

Chapter 3 Overview

Chapter 3 builds upon the findings of Chapter 2 by incorporating site-specific Ground Response Analysis (GRA) to enhance the characterization of seismic demand and its implications for building classification and damage estimation. While Chapter 2 employs high-resolution site classification to refine hazard inputs in the FEMA HAZUS framework, this chapter addresses the limitations of generalized amplification proxies—such as Vs_{30}—by modeling seismic wave propagation through stratified soil columns at each building site. This approach captures localized site effects with greater precision and reveals discrepancies between simplified and modeled ground motion estimates.

The analysis utilizes one-dimensional linear-equivalent site response modeling, applying NRATTLE-derived transfer functions to compute amplification factors across a portfolio of buildings. These transfer functions are

developed from site-specific geotechnical profiles that include shear-wave velocity, layer thickness, and soil classification data. By replacing default F_a and F_v amplification factors with those derived from GRA, the study recalculates spectral accelerations at each site and evaluates their influence on structural performance estimates.

The results are used to reassess building-level damage probabilities and Seismic Design Categories (SDCs), drawing comparisons between outcomes derived from Vs_{30}-based and GRA-based inputs. In many instances, buildings originally classified as lower-risk under Vs_{30} assumptions are reassigned to higher-risk categories, particularly in areas with deep sedimentary basins or pronounced impedance contrasts. This reclassification has significant implications for code compliance, retrofitting priorities, and regional hazard communication.

Chapter 3 also examines the spatial variability of site amplification across Massachusetts and quantifies the extent to which simplified methods may underrepresent seismic demand. By integrating GRA outputs with the HAZUS General Building Stock (GBS) inventory, the study highlights the impact of detailed ground motion modeling on damage estimation and mitigation planning at scale.

Overall, Chapter 3 demonstrates the value of incorporating localized site response into seismic risk assessments. The findings underscore the limitations of conventional proxies in geologically complex settings and support a more accurate, data-driven foundation for resilience planning. In doing so, this chapter reinforces the dissertation's broader argument: that improving the fidelity of site-specific inputs leads to more reliable risk models and ultimately to better-informed decisions for seismic design and disaster preparedness.

Chapter 1: Digitizing Earthquake-Induced Soil Liquefaction: *A Guide for Creating a Labeled Polygon-based Inventory of Surface Effects Using Remote Sensing Data*

"In God we trust; all others must bring data." — **W. Edwards Deming**

1.1 Significance of the Project

Accurate data collection serves as the backbone of informed decision-making in both pre-disaster planning and post-disaster response. In an increasingly data-driven world, the quality, resolution, and contextual relevance of the information gathered directly influence the effectiveness of mitigation strategies, emergency interventions, and long-term recovery efforts. High-quality data enables practitioners to move beyond generalized assumptions and instead make targeted, evidence-based decisions that reflect the specific vulnerabilities and capacities of affected communities. In the context of seismic risk, each data point—whether related to ground motion characteristics, structural typologies, or observed damage patterns—represents a critical component of the broader resilience framework. When systematically integrated, these data inform a comprehensive understanding of hazard exposure, structural performance, and community-level risk. Moreover, they support the refinement of predictive models, enhance the accuracy of loss estimation tools, and guide the development of building codes, land-use policies, and emergency preparedness plans.

Within this context, this chapter affirms the critical importance of high-quality, methodologically rigorous data collection to support the advancement of modern analytical tools, particularly computer vision algorithms for post-disaster damage assessment. The reliability and effectiveness of automated systems are inherently dependent on the structure, resolution, and consistency of the data on which they are trained. Inadequate, inconsistent, or poorly labeled datasets not only compromise model performance but may also lead to erroneous conclusions that hinder rather than support effective disaster response and recovery.

By advancing a standardized, remote sensing–based framework for the mapping of liquefaction surface manifestations, this research contributes to the development of geospatial datasets that are both scientifically robust and computationally tractable. The resulting inventories are designed to satisfy the dual demands of expert interpretability and machine-readiness, thereby facilitating the integration of emerging technologies—such as artificial intelligence and computer vision—into the domain of disaster reconnaissance and response.

More broadly, this work reflects a deliberate and forward-looking effort to align methodological innovation with technological advancement. Leveraging tools such as high-resolution satellite imagery, geospatial processing techniques, and automation-ready labeling strategies ensures that data products remain relevant, scalable, and adaptable within a rapidly evolving analytical landscape. In doing so, this project underscores that effective disaster risk reduction depends not simply on the availability of data, but on the collection of the *right* data, in the *right* way,

for the *right* purpose. It reinforces the principle that meaningful, technology-enabled decision-making is grounded in the systematic generation of reliable, high-value datasets tailored to the demands of both current and future applications.

1.2 Related Work

Previous studies have employed a variety of approaches to map and document ground failure phenomena, with a predominant emphasis on landslides. These inventories typically function not as standalone datasets, but as foundational components in broader analytical investigations. Consequently, post-disaster inventories are disseminated in diverse formats and exhibit varying degrees of accuracy and completeness, shaped by the specific scope, methodology, and objectives of each study. Although a substantial body of landslide inventories has been developed, comparable datasets for liquefaction-related ground failures remain relatively scarce. The methodology developed in this study draws primarily on the landslide inventory literature, while integrating key elements from existing liquefaction inventories and other image-based datasets designed to support computer vision applications.

1.2.1 Landslide Inventory and Databases

Traditional approaches to landslide mapping have historically relied on stereoscopic image interpretation, often supported by targeted field surveys (Guzzetti et al., 2012). These methods commonly utilize both pre- and post-event imagery (e.g., Sato et al., 2006), though some studies focus exclusively on post-event observations (e.g., Sekiguchi and Sato, 2006). Various remote sensing platforms have been employed to enhance mapping accuracy, including satellite imagery (e.g., Brown et al., 2011), aerial photography (e.g., Harp et al., 2011; Valkaniotis et al., 2018), or a combination of both (Fiorucci et al., 2011). In addition to image-based techniques, field validation plays a critical role in assessing the reliability of mapped features. Some researchers have conducted their own field investigations (e.g., Harp et al., 1981), while others have validated remote observations against field data collected by third parties (e.g., Martinez et al., 2021).

In recent years, the field has shifted toward more advanced methodologies that incorporate remote sensing change detection, deep learning algorithms, and Synthetic Aperture Radar (SAR) data processing. These innovations have substantially improved the capability to detect and map landslides across large areas with greater precision (e.g., Aimaiti et al., 2019; García-Rodríguez and Malpica, 2010; Li et al., 2016; Liv et al., 2020; Prakash et al., 2021; Singhroy et al., 1998). As these techniques evolve, they have also influenced the structure and content of landslide inventories, promoting greater consistency and comprehensiveness in how landslide events are cataloged.

Perera et al. (2022) propose that a comprehensive landslide inventory should comprise two principal components: a spatial component and an attribute component. The spatial component includes location and geometry (e.g., perimeter, area, volume), while the attribute component should, at minimum, capture the date of occurrence, landslide type, and associated impacts such as injuries or fatalities. Their web-based landslide inventory for Sri Lanka exemplifies this framework and includes fields such as EVENT ID, LOCATION, DATE, TIME, GEOMETRY (calculated using mapping software), TYPE OF LANDSLIDE, PRESENT CONDITION, LAND USE/COVER, and IMPACT. The classification system for "landslide type" is a simplified adaptation of the Cruden and Varnes (1996) taxonomy and includes categories such as landslide, mudslide, debris flow, rockfall, creep, other, and unknown.

Although landslide inventories differ in their level of detail, some large-scale databases have sought to standardize attributes across records. For instance, the National Landslide Database (NLD) of Great Britain, developed by the British Geological Survey (BGS), contains over 15,000 records (Foster et al., 2011) and includes more than 35 attributes per entry, covering parameters such as location, dimensions, movement type, trigger mechanism, slope characteristics, and observed damage. However, despite such efforts, not all records in large databases maintain complete attribute sets.

As methodologies for landslide mapping improve, increasing attention has been directed toward the completeness and accuracy of inventories. Completeness refers to the degree to which all landslides resulting from a given event are captured within a dataset. Incomplete inventories—those that omit smaller or less visible features—can limit the usefulness of the data for risk modeling and hazard assessment. Accuracy, on the other hand, concerns the reliability of the information recorded for each feature, including location, size, and type.

To address the inherent limitations of post-event mapping, many researchers employ thresholding—establishing a minimum detectable landslide size—to assess inventory completeness. For example, Huang and Lee (1999) reported that their inventory of landslides triggered by the 1998 M5.7 Jueili, Taiwan earthquake was 100% complete for features larger than 625 m^2. Görüm et al. (2014) applied a threshold of 890 m^2 to the 2002 M7.9 Denali, Alaska event and estimated that 80% of landslides exceeding this threshold were successfully captured. Similarly, Harp and colleagues employed thresholds of 10 m^2, 50 m^2, and 25 m^2 for the 1976 M7.5 Guatemala, 1980 M6.5 Mammoth Lakes, and 1994 M6.7 Northridge earthquakes, respectively (Harp et al., 1981; Harp et al., 1984; Harp and Jibson, 1995), with reported completeness rates increasing as thresholds increased (85%, 100%, and 90%, respectively).

Accuracy in landslide inventories is generally evaluated based on proximity of mapped features to actual locations, investigator expertise, and comparisons with ground-truth observations. While few inventories explicitly quantify these factors, their reliability is typically inferred through established best practices. Variables influencing mapping accuracy include the resolution of imagery, availability of ancillary data such as Digital Elevation Models (DEMs), interpretation techniques, and the level of experience of the interpreter. Carrara et al. (1992) demonstrated that inventory accuracy increases with both imagery resolution and analyst expertise.

Some studies have formally assessed inventory accuracy by comparing remotely mapped landslides with field-verified datasets. For instance, Rabby and Li (2019) achieved 88% accuracy in mapping landslides in the Bandarban District of Bangladesh by comparing Google Earth-based interpretations with field survey results. In their assessment, field data were treated as the accuracy benchmark, given that landslides were directly observed, geolocated via GPS, and measured on-site.

1.2.2 Liquefaction Inventories and Databases

Soil liquefaction is a complex phenomenon that garnered significant attention within the geotechnical engineering community following two landmark earthquakes in 1964: the M9.2 Good Friday earthquake in Anchorage, Alaska, and the M7.5 Niigata earthquake in Japan. Both events caused widespread liquefaction-induced damage, including slope failures, lateral spreading, and foundation collapses (Kramer, 2014). While not all soil types are susceptible to liquefaction, susceptibility can be assessed through historical case studies and geologic conditions. Field investigations following major earthquakes have proven essential in advancing the understanding of liquefaction behavior. These studies consistently demonstrate that locations with a history of liquefaction are more likely to experience recurrence if soil and groundwater conditions remain unchanged (Iwasaki, 1986; Wakamatsu, 2010). As such, liquefaction case histories serve as critical resources for identifying both specific sites and broader geological conditions that are vulnerable in future seismic events.

Building on this principle, Papathanassiou and Pavlides (2011) developed the DALO database—an open-access, point-based inventory documenting liquefaction occurrences from historical earthquakes throughout the Aegean region. The dataset spans several centuries, from the 16th century through the 2008 M6.5 Peloponnesus, Greece earthquake. Each entry includes the date, location, and a brief description of observed ground deformations. Select post-1950 entries are supplemented by photographic documentation. Similarly, Wakamatsu (2010) compiled a point-based GIS database of liquefaction sites in Japan, cataloging 16,500 liquefaction observations from 150

earthquake events occurring between 416 and 2008. Each record includes key attributes such as earthquake magnitude, epicenter location, focal depth, place names, and data sources.

Recent advancements in liquefaction mapping have expanded beyond historical case compilation to include remote sensing and machine learning techniques. These include change detection (e.g., Baik et al., 2019; Oommen et al., 2013; Ramakrishnan et al., 2006), object-based image classification (e.g., Morgenroth et al., 2016), and supervised classification methods, both semi-automated and fully automated (e.g., Middleton et al., 2020; Rashidian & Baise, 2018). Several studies have explored hybrid approaches to improve detection accuracy and spatial resolution (e.g., Papathanassiou et al., 2022).

Despite these advancements, a fundamental challenge persists--liquefaction originates below ground and may not always produce clear surface evidence. As a result, traditional liquefaction inventories have primarily relied on subsurface investigations to identify liquefiable soils and back-analyze ground failures. These inventories form the basis for widely used semi-empirical triggering models (e.g., Boulanger & Idriss, 2014; Seed & Idriss, 1970). The Next Generation Liquefaction (NGL) database (Brandenberg et al., 2020) exemplifies this approach by consolidating data on ground motion, in-situ testing, laboratory test results, and photographic evidence to support model development and research. However, acquiring detailed subsurface data is often cost-prohibitive or infeasible—especially in regions with uncertain susceptibility or limited investigation capacity.

Given these constraints, it is imperative to document visible surface manifestations of liquefaction whenever they occur. Such data offer vital insights into subsurface conditions and are particularly valuable when ground truth investigations are not possible. This study is motivated by the need to build accurate, geospatial liquefaction inventories that can support machine learning–based computer vision models for liquefaction prediction (e.g., Zhan et al., 2024; Zhu et al., 2017). Accordingly, the most relevant existing inventories are those that digitize surface-level manifestations from post-earthquake reconnaissance studies and official reports.

Field-based inventories typically rely on GPS to geolocate liquefaction features, with coordinate data often extracted from figure captions or maps in published reports. These datasets are commonly binary, indicating only whether liquefaction was observed at a given location. For example, Dashti et al. (2022), Morales-Velez & Pando (2020), and Rathje et al. (2010) provide simplified point inventories aggregated from field-identified surface effects. The GEER report on the 2020 M6.4 Puerto Rico earthquake illustrates this approach, including photos of sand boils

and ejecta observed at two locations—a tropical fruit farm and a commercial district known as "El Triángulo" in Guayanilla—mapped using only two representative points (Morales-Velez & Pando, 2020).

In contrast, the U.S. Geological Survey (USGS) produced a more comprehensive inventory for the same earthquake (Allstadt et al., 2021), comprising 43 labeled polygons for liquefaction and lateral spreading, 32 liquefaction occurrence points, and 81 non-occurrence points. The database includes several descriptive attributes, such as `TYPE`, `EJECTA`, `DISP` (displacement), `CERTAINTY`, and `COMMENTS`. These polygons represent approximated shapes of liquefaction features, based on the authors' "scientific judgment" and field observations. Notably, the USGS inventory integrates and acknowledges the original GEER points by digitizing polygons around them and referencing their source.

Another example is provided by Townsend et al. (2016), who developed the most detailed liquefaction inventory for the 2011 M6.1 Christchurch, New Zealand earthquake. This GIS-based dataset—hereafter referred to as the Townsend Polygons—was created using a combination of pre-event satellite imagery and very high-resolution (VHR) aerial photographs (1:1000 and 1:500). Liquefaction features were manually digitized as labeled polygons in ArcMap, bounded by roads but excluding the roadways themselves. The resulting database contains 13 attribute fields, including `FEATURE`, `EVIDENCE`, `ORIGINATOR`, `IMAGE`, `IMAGE_RES`, `SITE_VISIT`, `GNS_QA`, `GNSQA_NOTE`, `GNS_CERT`, `EXTERNAL_QA`, `CERTAINTY`, `local_img`, and `image_date`. While this inventory provides extensive spatial coverage of urban Christchurch, its broad polygon delineation—often encompassing entire city blocks—makes it less suitable for fine-grained computer vision applications focused on discrete surface features.

Both the USGS and Townsend datasets include detailed attribute schemes and incorporate measures of confidence in the data. In the USGS inventory, the `TYPE` attribute categorizes features into "Liquefaction Area" (e.g., sand boils, fissures, settlements), "Lateral Spread" (horizontal displacements near water), and "Settlement" (localized vertical deformation). The `CERTAINTY` field reflects two dimensions: (1) the confidence in accurate spatial representation and (2) the likelihood that the feature resulted from the earthquake. `CERTAINTY` values range from 1 (field-verified and confidently earthquake-induced) to 3 (identified through imagery alone without field verification).

In the Townsend inventory, the `FEATURE` attribute spans seven classes, including "Liquefaction," "Flooding – sediment," "Flooding – water," "Unknown," "Other," "Old flooding," and "Agricultural, anthropogenic." Certainty levels in this dataset were determined through a tiered quality assurance process. Initial classifications were made by

the originator, followed by internal QA review, and finally external review. Each step could reaffirm, modify, or downgrade the original classification based on field visits and interpretative consistency. Disagreements were resolved through reclassification or adjustments to the assigned certainty level.

1.2.3 Image-based Inventories for Computer Vision Applications

Several datasets have been specifically curated to support the development and evaluation of computer vision models in disaster response and object detection contexts. These datasets are distinguished by their high-quality annotations, standardized formats, and suitability for training and validating machine learning algorithms.

One prominent example is the xBD dataset, developed to facilitate automated assessment of building damage following natural disasters. The xBD dataset is a large-scale, polygon-based collection containing over 800,000 annotated building footprints (Gupta et al., 2019; Lam et al., 2018). It was created to advance artificial intelligence applications in humanitarian assistance and disaster recovery. The dataset features paired pre-disaster and post-disaster satellite imagery, provided in Red, Green, and Blue (RGB) format through the MAXAR/DigitalGlobe Open Data Program. To ensure high-fidelity damage labeling, imagery was selected based on a ground sample distance (GSD) of less than 0.8 meters.

The xBD dataset is partitioned into training, testing, and holdout sets using an 80-10-10 split, respectively. Specifically, the training set contains 18,336 image tiles and 632,222 annotated polygons; the test set includes 1,866 image tiles with 109,724 polygons; and the holdout set comprises 1,866 image tiles with 108,784 polygons. Importantly, the dataset encompasses both damaged and undamaged buildings, a distinction critical for developing machine learning models capable of discerning varying levels of structural damage. The xView2 Competition leveraged this dataset to challenge the artificial intelligence research community to develop models for automated damage detection from satellite imagery, thus promoting the refinement and benchmarking of AI-driven disaster response tools.

In a related domain, researchers at the Naval Information Warfare Center (NIWC) Pacific developed the BBCT (Barge, Cargo Ship, Container Ship, and Tanker) dataset in 2011 to support ship detection and classification tasks using satellite imagery (Rainey, 2019; Rainey et al., 2012). The BBCT dataset includes 200 grayscale examples for each of the four vessel categories, extracted from larger electro-optical satellite images using the RAPIER ship detection system. Each example was manually annotated with key vessel locations—specifically the bow, stern, port, and starboard points. To prepare the dataset for classification tasks, a standardized preprocessing sequence was

applied: each ship image was rotated so that all vessels faced the same orientation, cropped to maintain a maximum height-to-width ratio of 2:1, aligned, and resized to 300 × 150 pixels.

Together, datasets such as xBD and BBCT exemplify the importance of curated, high-quality annotated data for training robust and transferable machine learning models, particularly in the fields of disaster response and remote sensing object detection.

1.3 Method

Several key insights from the existing literature informed the development of the liquefaction inventories presented in this study, particularly regarding their applicability in computer vision–based damage detection. One of the most salient findings was the importance of including a well-defined and consistent set of inventory attributes. Although the level of detail varied across studies depending on the intended application, effective inventories consistently employed attributes that were clear, logically structured, and contextually relevant for analysis and decision-making. The literature demonstrated that increased attribute specificity is essential for training high-performing computer vision models and ensuring the inventory's interpretability and reliability in downstream analyses. At the same time, excessive attribute proliferation may introduce inconsistencies—especially given that not all earthquake events exhibit the same observable features. Consequently, selecting a set of core attributes applicable across a wide range of seismic events was necessary to support consistency, generalizability, and methodological rigor.

Commonly retained attributes included the date of occurrence, geographic location, feature type, extent of observed damage, and an indicator of certainty. The inclusion of a certainty metric was particularly valuable, as it enabled documentation of the confidence associated with each mapped feature, typically with respect to spatial accuracy and classification reliability. This concept of "confidence" is inherently tied to the broader metrics of accuracy and completeness, both of which are foundational to inventory quality.

Accuracy, as applied in the literature, generally referred to the thematic correctness of each entry—that is, the degree to which each mapped feature accurately reflects observed or verified ground conditions. Validation techniques included direct field verification and/or comparison with trusted ground-truth data sources. This validation process was especially useful for evaluating remote sensing–derived or machine learning–generated features, and it strengthened the interpretive validity of the final inventory products. The use of both pre- and post-event imagery was also identified as a best practice, enabling comparative analysis of seismic impacts, and enhancing the detection of subtle ground surface changes. Datasets containing high-resolution imagery, such as the xBD dataset (Gupta et al.,

2019; Lam et al., 2018), further improved the granularity of analysis, facilitating the identification of small-scale features and contributing to higher model accuracy.

Completeness, in contrast, was typically defined as the proportion of documented features relative to the total number of actual occurrences within a study area. Because the true number of liquefaction occurrences is rarely known with certainty (Guzzetti et al., 2012; Schmitt, 2017), many researchers adopted thresholding techniques to constrain the scope of mapping to detectable features above a defined spatial or visual threshold. This approach allowed for the creation of inventories that were as complete as reasonably possible while also maintaining practical data volumes and manageable processing demands.

To ensure compatibility with existing geospatial analysis tools and to support future research integration, many inventories were published in GIS-compatible formats. This design decision facilitates broad usability, supports integration into diverse workflows, and increases the long-term value of the datasets for hazard modeling, risk assessment, and machine learning applications.

Informed by these methodological precedents, the workflow implemented in this study—illustrated in **Figure 1**—comprised two primary components: (1) collecting and digitizing liquefaction occurrence data from post-earthquake reconnaissance reports and published sources for the purpose of ground-truthing, and (2) generating thematically labeled inventories for three major seismic events: the 2010 M7.0 earthquake in Port-au-Prince, Haiti; the 2011 M6.1 earthquake in Christchurch, New Zealand; and the 2021 M7.2 earthquake in Nippes, Haiti. The inventories were developed iteratively, with attribute selections refined over successive trials to balance specificity, applicability, and data consistency. While the final application of each inventory may vary depending on the needs of the end user, all inventories have been formatted for compatibility with geographic information systems (GIS) and are readily integrable into machine learning applications for automated damage detection and geospatial analysis.

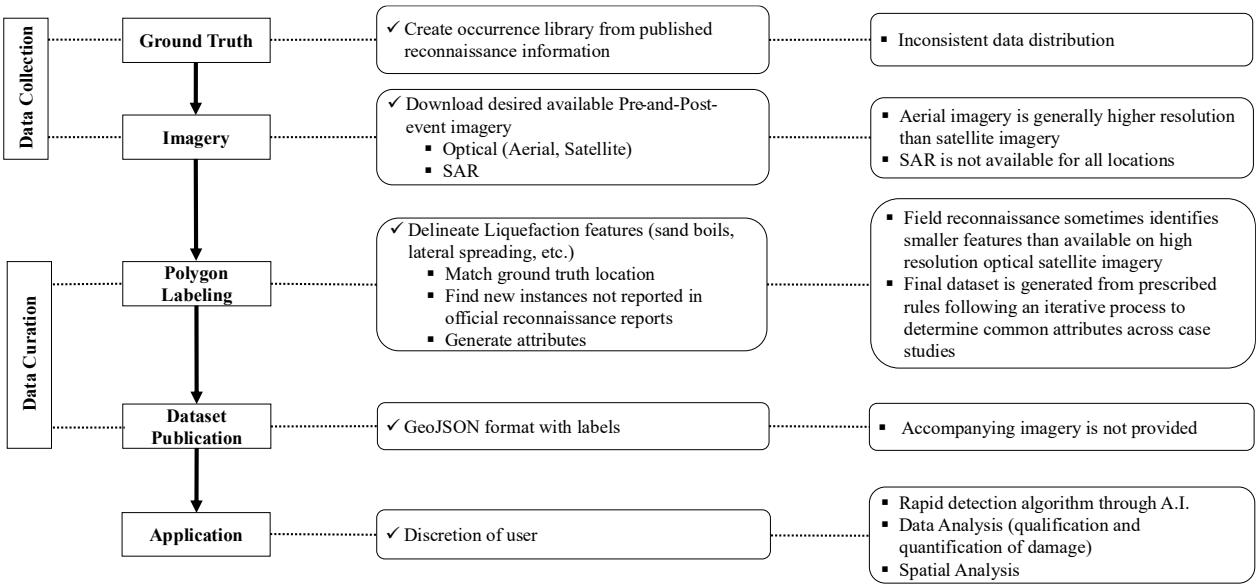

Figure 1: Workflow for Liquefaction Feature Mapping and Dataset Generation: This diagram outlines the process from data collection to application, including ground truth gathering, imagery acquisition, polygon labeling, and dataset publication. Key challenges and considerations at each stage, such as data inconsistency, resolution limitations, and reconnaissance constraints, are also highlighted.

1.3.1 Data Collection

Each event-specific inventory developed in this study was constructed using information extracted from post-earthquake reconnaissance reports, peer-reviewed studies, and freely available satellite imagery. Accurate interpretation of these sources required careful consideration of the authors' stated objectives, methodological approaches, and contextual assumptions. Understanding the intent and scope of each source was essential for evaluating the reliability and applicability of the reference data, as well as for recognizing its inherent limitations.

The digitization of liquefaction surface manifestations was guided by two core principles derived from best practices in ground-truth data utilization. First, ground-truth data were not assumed to be infallible; human error, interpretive subjectivity, and spatial uncertainty may be present in the original observations. Second, the data were not treated as exhaustive; none of the reference reports explicitly claimed to document all liquefaction occurrences associated with the respective seismic events. These guiding assumptions ensured that the digitization process remained both methodologically cautious and analytically transparent, acknowledging the potential for omissions or inaccuracies while maximizing the value of available empirical evidence

1.3.1.1 Ground Truth

Ground-truth data refer to information collected through direct field investigation following a seismic event. However, due to logistical constraints, accessibility challenges, and regional conditions, field investigations may not always be conducted immediately, may offer limited spatial coverage, or, in some cases, may not be feasible at all. In such instances, remote sensing methods are often employed to compile observational datasets that, although not conventionally classified as ground truth, are accepted by the relevant scientific community as reliable representations of event-induced effects based on prior knowledge and corroborative evidence. These remotely derived datasets are sometimes used to validate other remote methodologies, particularly in cases where traditional ground truth data are unavailable (e.g., Aimaiti et al., 2022).

Most existing liquefaction ground-truth inventories are point-based, recording the geographic coordinates of observed surface manifestations. For example, the GEER (Geotechnical Extreme Events Reconnaissance) reports used in this study to document the two Haiti earthquakes provide latitude and longitude coordinates for liquefaction occurrences (Dashti et al., 2022; Rathje et al., 2010). In both cases, a point represents the location of a documented ground failure, forming the basis for binary occurrence datasets (i.e., presence or absence of liquefaction). In contrast, polygon-based inventories—such as those produced for the Canterbury earthquake sequence (Townsend et al., 2016)—map broader regions affected by liquefaction. While this approach is effective for certain hazard mapping applications, it does not isolate individual surface features, making it less suitable for detailed feature extraction in computer vision applications.

The initial step in developing each case study inventory involved digitizing available liquefaction occurrences from reconnaissance reports or visualizing existing inventories where available. ArcGIS Pro was used to map the geographic coordinates extracted from post-earthquake reports for the 2010 and 2021 Haiti events and to visualize the polygonal liquefaction regions mapped for the 2011 Christchurch event.

The first ground-truth dataset pertains to the January 12, 2010, M7.0 earthquake that caused widespread damage in Port-au-Prince, Haiti. The city is situated on a coastal plain within the Cul-de-Sac basin, bounded by two mountain ranges, and is underlain by a combination of alluvial and marine-estuarine sediments, as well as reclaimed land deposits (Lambert et al., 1987). Liquefaction occurrences were concentrated near the North Wharf (Area B in **Figure 2**) and within the alluvial plains surrounding the city of Leogane, as shown in the bottom inset of **Figure 2**.

The 2010 Haiti liquefaction dataset includes 22 digitized points. Fourteen of these were extracted from coordinates provided in the official GEER reconnaissance report (Rathje et al., 2010), while the remaining eight were obtained from a complementary reconnaissance study by Olson et al. (2011). The GEER team conducted detailed field investigations, identifying and describing ground failure manifestations in the body of the report as well as within figure captions, which include both geographic coordinates and brief narrative descriptions of observed features. In contrast, the study by Olson and colleagues focused primarily on in-situ testing at selected sites, characterizing eight locations where liquefaction, lateral spreading, flow failure, and/or bearing capacity failures were observed. Their findings were intended to supplement existing case history databases, particularly for near-level ground liquefaction conditions.

Although the GEER and Olson datasets were digitized following a consistent protocol, the nature of the information they contain differs. The GEER data primarily capture individual surface manifestations, while the Olson data document broader site-level observations encompassing multiple features. Notably, the GEER points are spatially distributed across three of the eight sites investigated by the Olson team. In summary, the ground-truth dataset for the 2010 Haiti earthquake comprises eight confirmed liquefaction sites, with 14 discrete surface manifestation points distributed across three of these sites, as illustrated in **Figure 2**.

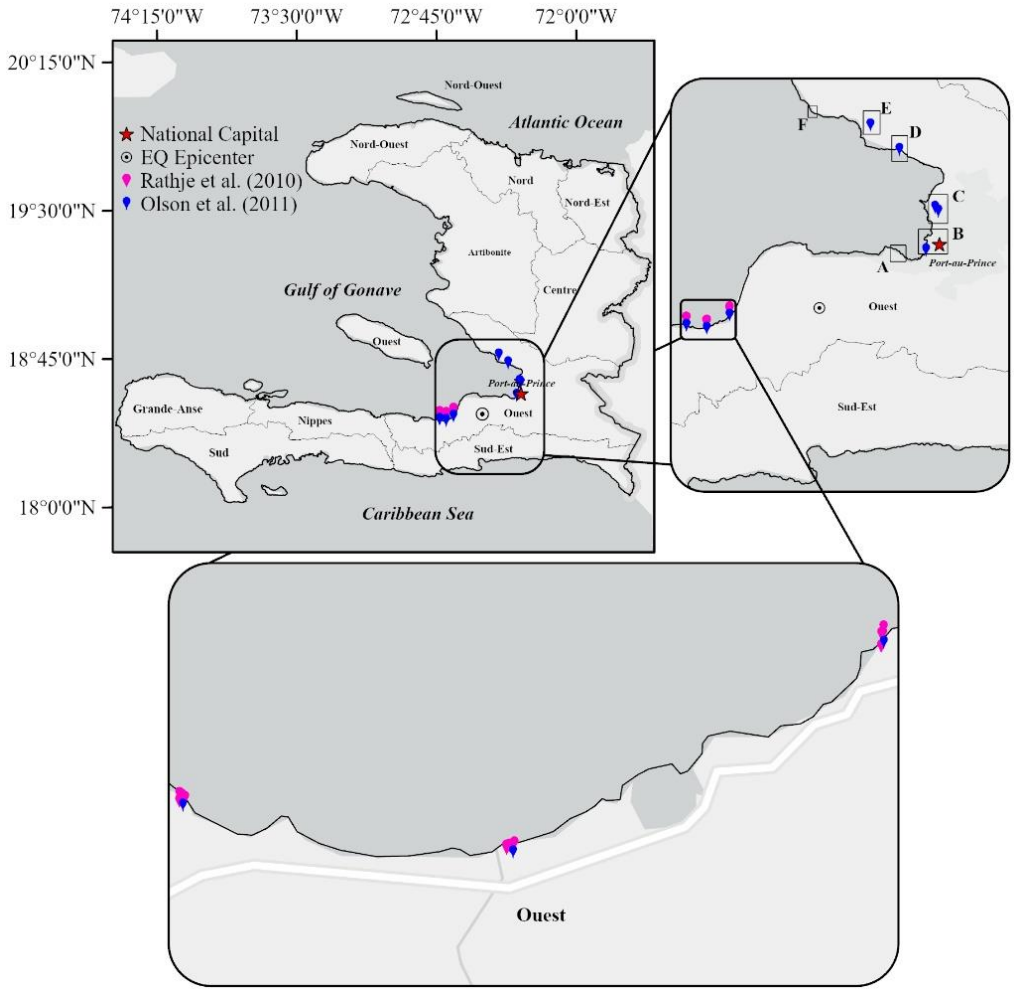

Figure 2: Ground truth point data of liquefaction occurrences from the 2010 M7.0 Haiti earthquake, digitized from available reconnaissance reports. Pink markers indicate liquefaction locations reported in the official GEER report (GEER-021) by Rathje et al. (2010), while blue markers represent locations documented in a reconnaissance study by Olson et al. (2011). Areas A–F in the top inset correspond to regions included in the inventory developed in this study, with Area B specifically highlighting liquefaction at the International Port of Port-au-Prince (North Wharf). The inset at the bottom shows regions near the city of Leogane, where widespread liquefaction was also observed.

The second set of ground-truth data used in this study was derived from the Townsend Polygons curated for the February 22, 2011, M6.1 Christchurch earthquake in New Zealand. The Christchurch event produced one of the most significant urban liquefaction occurrences ever recorded, with over 500,000 tons of liquefaction ejecta removed from streets and private properties (Villemure et al., 2012). The earthquake resulted in substantial infrastructural and societal impacts, including the abandonment of approximately 15,000 single-family homes and the demolition of numerous buildings within the Central Business District (CBD) (Chang et al., 2014; Rogers et al., 2014). In response to the extensive damage, the New Zealand government designated 602 hectares along the Avon River Corridor as a residential Red Zone, an area deemed beyond economic repair where residential redevelopment is prohibited (Huang,

2021; "History of the Ōtākaro Avon River Corridor"). This land is currently reserved for recreational use, ecological restoration, and the exploration of innovative land-use strategies.

The Townsend Polygons were created by digitizing surface deformation and ejecta features identified through a combination of ground-based photography and high-resolution satellite imagery. Visual detection methods were employed to map the spatial extent of liquefaction manifestations. To mitigate the inherent subjectivity of manual mapping, a comprehensive quality assurance protocol was implemented, including both internal and external reviews, supplemented by field verification where feasible. Despite these efforts, several limitations remain. In particular, the timing of data collection relative to post-earthquake cleanup operations led to the loss of some surface evidence, and as a result, not all mapped features could be field verified. Moreover, the digitization methodology differed between urban and rural contexts: in densely populated urban areas, mapping was performed at the parcel level, whereas individual features were delineated in less affected rural regions. Consequently, most roadways in Christchurch were excluded from the mapped dataset, and in some instances, entire parcels were classified as liquefaction-affected even though only a portion of the parcel exhibited visible surface effects. Additionally, discrete features were sometimes aggregated into larger polygons, potentially resulting in an overestimation of the affected area.

Nonetheless, the Townsend Polygons represent a comprehensive effort to capture the spatial distribution of liquefaction impacts in Christchurch, covering approximately 30% of the urban area. The mapped zones generally correspond to areas characterized by geotechnical and hydrological conditions favorable to liquefaction, as confirmed by independent studies.

To enhance the reliability and specificity of the dataset used for this study, the Townsend inventory was further refined by querying only those features labeled with the highest confidence level, “certain”, as illustrated in **Figure 3**. Following this refinement, the dataset included 3,923 polygons categorized as “Liquefaction,” 42 polygons classified as “Old Flooding,” 178 polygons representing “Flooding – Water,” 257 polygons denoting “Flooding – Sediment,” and 418 polygons categorized as “Unknown.” For the purposes of this analysis, only those polygons explicitly classified as “Liquefaction” were retained.

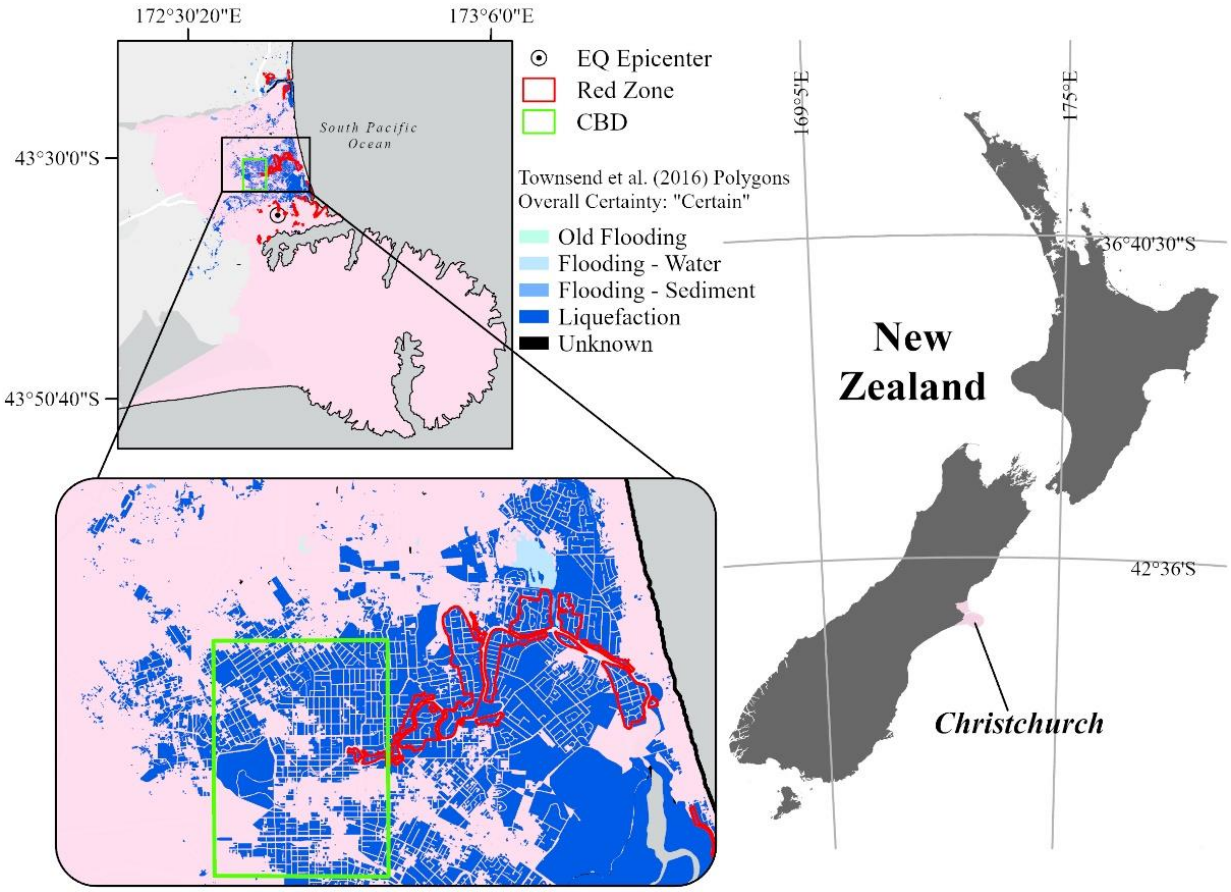

Figure 3: Ground truth data for the 2011 M6.1 Christchurch earthquake, as mapped by Townsend et al. (2016). The polygons represent areas classified with the highest certainty level ("certain"). The green box highlights the Central Business District (CBD), while the red outline delineates the residential Red Zone.

The third case study examines liquefaction induced by the M7.2 earthquake that struck Nippes, Haiti, on August 14, 2021—approximately 75 km west of the epicenter of the 2010 earthquake sequence in Port-au-Prince. Among the three events analyzed in this study, data collection for the 2021 earthquake resulted in the lowest resolution of information, primarily due to delays in field reconnaissance caused by the region's unstable political climate. Additionally, Tropical Storm Grace, which struck just two days after the mainshock, likely erased much of the surface evidence of liquefaction (Dashti et al. 2022).

Initial data collection was conducted remotely through crowdsourcing, incorporating reports from organizations such as USGS, USAID, CNIGS, CNSA, the UN, and the World Bank. This information was supplemented with satellite imagery and drone data collected by the World Bank. Later, local partners in affected areas carried out field reconnaissance, recording observations using StEER's Fulcrum phone application, which provided geolocated surface

effect data. However, sites documented in the GEER report using drone imagery were classified with lower certainty and categorized as “possible” liquefaction occurrences.

The complete ground truth point-based dataset, digitized from the GEER report, includes 84 documented ground failure occurrences, covering landslides, rockfalls, rockslides, slope failures, liquefaction, and two instances of liquefaction-induced building settlement. Of these 84 points, 18 specifically document liquefaction based on both field assessments and drone imagery, including the two cases of building settlement (**Figure 4**).

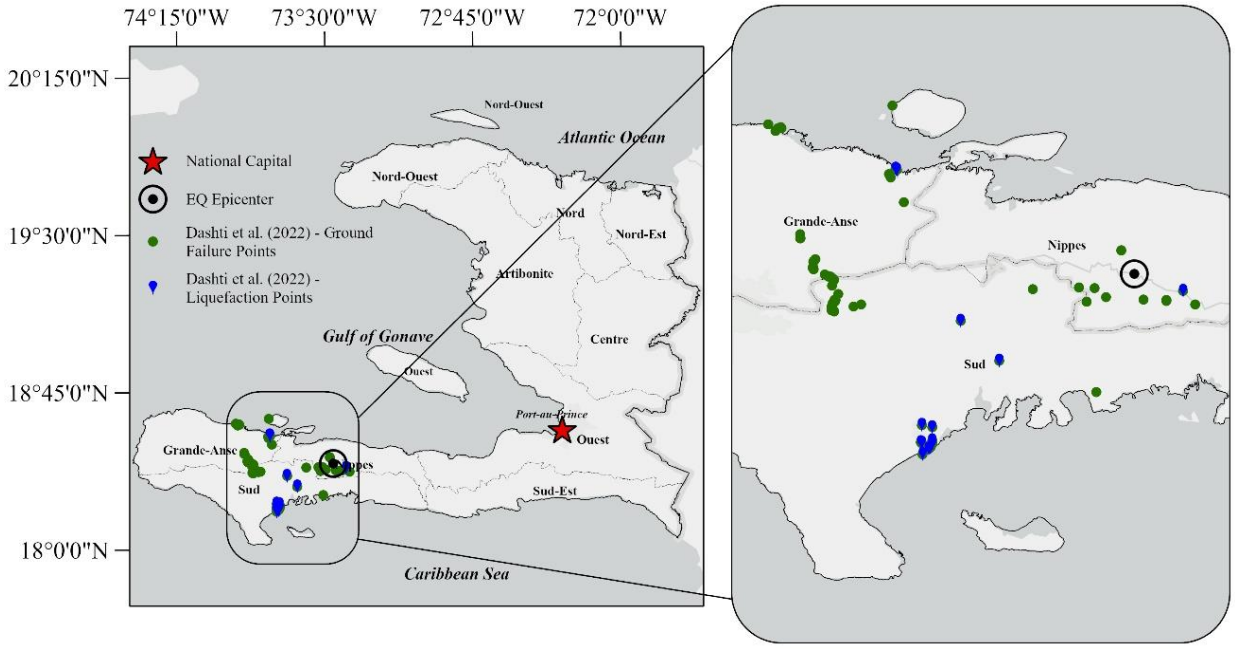

Figure 4: Ground truth data for the 2021 M7.2 Haiti earthquake digitized from GEER Report, GEER-073 (Dashti et al. 2022). Green points indicate all documented ground failure instances, while blue markers specifically denote the 18 identified liquefaction locations.

Table 1 provides a summary of the ground truth datasets mentioned above for the three earthquake events analyzed in this study. It outlines the key characteristics of each dataset, including the number of points or polygons, the sources of the data, the primary focus of the data collection, the methods used to acquire the data, and the limitations associated with each dataset. This table serves as a reference to understand the varying levels of completeness and certainty in the ground truth data used for validating the subsequent liquefaction inventories created for each event.

Table 1: Summary of ground truth datasets used in the creation of liquefaction inventories for the three earthquake events analyzed. The table includes details on the number of liquefaction points or polygons, data sources, focus of data collection, and any associated limitations for the 2010 Haiti (M7.0), 2011 Christchurch (M6.1), and 2021 Haiti (M7.2) events reconnaissance reports. These datasets were used to validate the accuracy and completeness of the liquefaction features mapped from satellite imagery and other remote sensing data.

Event	Ground Truth	Number of records	Mapping Methodology	Source	Mapping Focus	Limitations
M7.0 Port-au-Prince, Haiti (2010)	GEER-021	14 points	Field investigation	Rathje et al. (2010)	Surface manifestations	Some surface effects are aggregated in single points and others represent discrete manifestations
	Other	8 sites	Field investigation	Olson et al. (2011)	Subsurface investigations	Surface effects are aggregated in single points
M6.1 Christchurch, New Zealand (2011)	Townsend Polygons	3,923 polygons	Remote Sensing imagery	Townsend et al. (2016)	Surface liquefaction zones using parcel-mapping	Overrepresentation of spatial extent in some polygons
M7.2 Nippes, Haiti (2021)	GEER-073	84 total points; 18 specifically related to liquefaction	Remote through crowdsourcing and remote sensing data; field investigations by local partners and other Extreme Events Reconnaissance (EER) teams	Dashti et al. (2022)	Liquefaction, landslides, building settlement	Low data resolution; delayed reconnaissance; Tropical Storm Grace; uncertain data for some points

1.3.1.2 Imagery

Satellite and aerial imagery each offer distinct advantages for post-earthquake reconnaissance and remote sensing analysis. Satellite imagery typically provides broader spatial coverage at lower spatial resolution, with pixel sizes ranging from approximately 30 centimeters to several meters depending on the specific satellite platform. This wide-area coverage makes satellite imagery particularly valuable for monitoring large geographic regions, especially when rapid situational awareness is required. In contrast, aerial imagery—often acquired via manned aircraft or drones—typically achieves much higher spatial resolution, frequently reaching a few centimeters per pixel. This level of detail enables more precise identification of fine-scale surface features, making aerial imagery ideal for applications requiring localized, high-resolution observations. However, its availability is often limited by the need for targeted commissioning, logistical constraints, and cost considerations.

Both imagery types are subject to environmental limitations, including cloud cover and vegetation. Satellite data, especially optical imagery, are frequently affected by cloud interference, which can degrade image quality or render scenes unusable—particularly in regions with persistent or heavy cloud cover. Dense vegetation also presents a significant challenge, as it can obscure ground features and hinder the detection of liquefaction-related surface effects. While aerial platforms offer greater flexibility in terms of acquisition timing—enabling flights to be scheduled around favorable weather conditions—they remain susceptible to similar occlusion issues in densely vegetated areas or when flown at higher altitudes.

These limitations became particularly evident during the evaluation of the January 7, 2020, M6.4 earthquake in Puerto Rico. Initially, this event was considered a strong candidate for validating the mapping methodology developed in this study. The objective was to replicate and test the approach by digitizing liquefaction features based on the methodologies presented by Allstadt et al. (2021), and to compare the resulting dataset with their published polygon inventory. High-resolution pre- and post-event satellite imagery from the WorldView-3 sensor was obtained through the MAXAR Open Data Program. WorldView-3, which also supports the widely used xBD dataset, provides the highest commercially available spatial resolution for satellite imagery. However, in the open data program, only RGB bands were available, excluding the additional spectral bands typically used for enhanced feature discrimination.

Despite its high spatial fidelity, the utility of the WorldView-3 imagery in this context was limited. Vegetation, particularly in agricultural areas, significantly obscured liquefaction surface effects. For instance, one GEER-reported liquefaction occurrence was located within a mango plantation, where tree canopy coverage made detection of surface ejecta unfeasible (Morales-Vélez and Pando, 2020). In addition, the available WorldView-3 scene did not fully encompass the geographic extent of the mapped liquefaction features. Of the two key locations identified in the GEER report, only one was included in the available satellite tile, which captured 21 of the 32 GEER point locations and 24 of the 43 USGS polygons, as illustrated in **Figure 5a**.

To supplement this incomplete coverage, Sentinel-2 imagery was obtained from the USGS EarthExplorer data portal. Although Sentinel-2 imagery offers lower spatial resolution than WorldView-3, it provided full spatial coverage of the liquefaction features described in both the GEER and USGS reports (**Figure 5b**). However, the Sentinel-2 imagery was affected by widespread cloud cover, and the dense vegetation throughout the landscape further impeded the visual identification of relevant surface features.

Given these compounded challenges—including incomplete scene coverage, vegetation interference, and limited spectral resolution—a decision was made to forgo the manual digitization of new liquefaction features for this event. Instead, the published USGS attribute list was adopted as a reference model for informing the structure of the attribute schema used in this study. This allowed for general comparisons of feature types and spatial extents without introducing uncertainty through attempted re-digitization under suboptimal conditions.

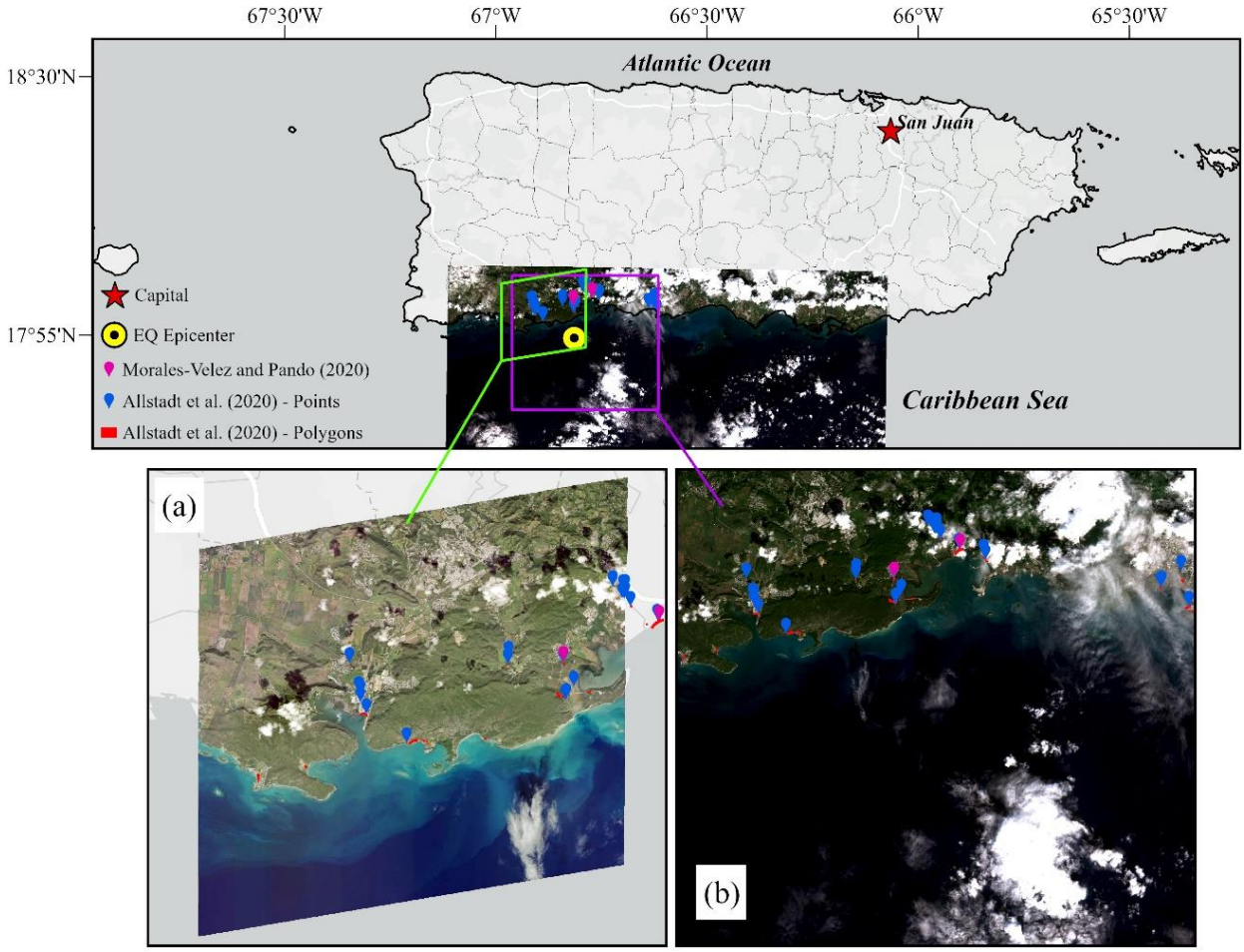

Figure 5: Comparison of satellite imagery used for detecting liquefaction features following the 2020 M6.4 earthquake in Puerto Rico. (a) Post-event WorldView-3 imagery (RGB) obtained from the MAXAR Open Data program. Despite the high resolution, vegetation in the tropical landscape significantly obstructed the detection of liquefaction features, particularly in areas such as the tropical fruit farm, as provided in GEER-066 (Morales-Velez and Pando, 2020). (b) Post-event Sentinel-2 imagery, sourced from the USGS Earth Explorer data portal, offering lower resolution than the WorldView-3 imagery. This image is affected by extensive cloud coverage, which, along with the vegetation, further complicated the accurate identification of liquefaction features.

Table 2 presents a summary of the satellite imagery utilized in this study. Given the transient nature of liquefaction surface manifestations, post-event imagery was selected to fall within a narrow temporal window—typically within a few days following the seismic event—to ensure accurate capture of perishable ground features. For pre-event

imagery, the general guideline was to select images acquired within the same calendar year as the event or, at most, within two years prior. This constraint was applied to minimize the risk of misinterpreting landscape changes unrelated to the earthquake.

All satellite imagery used for the 2010 and 2021 Haiti earthquakes was sourced from the MAXAR Open Data Program. Among overlapping image scenes (refer to **Figures 6 and 8**), the optimal image for mapping liquefaction features was selected based on two primary criteria: spatial resolution—defined by the Ground Sample Distance (GSD)—and cloud coverage. GSD refers to the physical ground distance between adjacent pixel centers in a remotely sensed image (Yang et al., 2024). Lower GSD values indicate higher spatial resolution, allowing finer detail to be resolved, while higher GSD values correspond to coarser resolution and reduced interpretability. For tasks involving the detection and delineation of liquefaction surface features, lower GSD (i.e., higher resolution) is typically preferred, as it enhances the precision and reliability of visual interpretation.

Although imagery from the WorldView satellite family (e.g., WorldView-2 and WorldView-3) already offers some of the highest commercially available resolutions, image quality can vary further based on acquisition conditions and GSD. Accordingly, preference was given to image scenes with minimal cloud coverage and the lowest GSD available. In contrast, while freely available sources such as Sentinel-2 offer broader coverage, their higher GSD makes them less suitable for detailed mapping applications.

For the 2010 Haiti earthquake, however, the post-event WorldView imagery did not provide complete coverage of the full reconnaissance area documented in the reference studies. As illustrated in **Figure 6**, one of the eight liquefaction sites surveyed by Olson et al. (2011)—which also contains five of the 14 GEER-identified surface manifestations—falls outside the available image extent. This limitation constrained the validation and spatial completeness of the resulting inventory, which was ultimately restricted to nine GEER points and seven of the Olson survey sites. As a result, the final liquefaction inventory for the 2010 event should be regarded as partial, reflecting only those ground-truth features located within the bounds of the available imagery scenes.

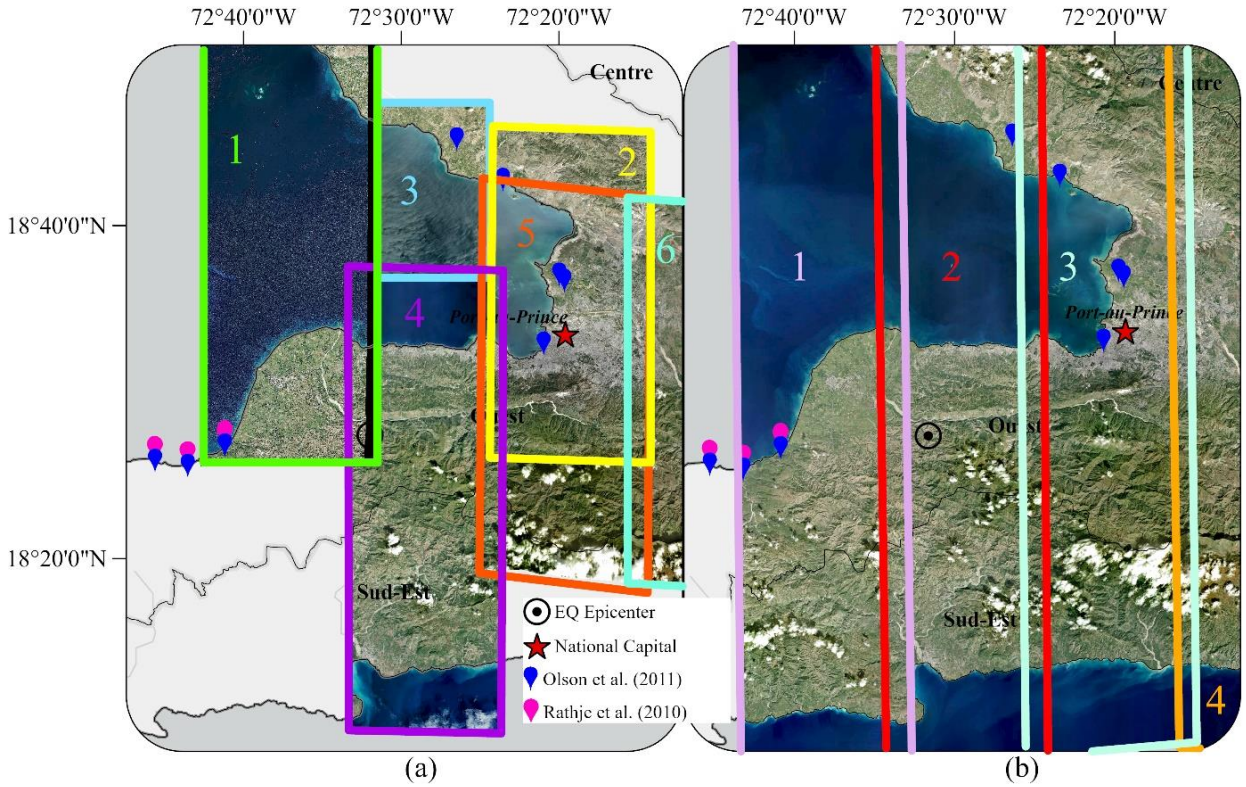

Figure 6: Satellite imagery for the 2010 M7.0 Haiti earthquake downloaded from MAXAR Open Data. The area shown corresponds to the same boundary as the top inset from **Figure 2**, encompassing all available ground truth data. (a) Pre-event imagery scenes. (b) Post-event imagery scenes. For resolution and acquisition dates, refer to **Table 2**.

For the digitization of the Christchurch liquefaction inventory, post-event aerial photographs acquired by NZ Aerial Mapping Ltd. for the Christchurch Response Centre (CRC) were utilized. These images were obtained from the LINZ Data Service and were provided as 1,785 ortho-rectified RGB GeoTIFF tiles, each with a spatial resolution of 10 centimeters. The high spatial resolution of the imagery made it well-suited for the identification and delineation of fine-scale surface features associated with liquefaction. Importantly, the Christchurch aerial imagery fully covered the geographic extent of the study area, offering comprehensive spatial coverage.

However, the combination of the widespread liquefaction damage across Christchurch and the extensive number of available aerial image tiles presented practical challenges. Given that the primary objective of this study is to develop training datasets for computer vision applications, utilizing the entire imagery set was neither necessary nor efficient. Therefore, a subset of 51 image tiles—representing approximately 2.8% of the total dataset—was selected for analysis, as illustrated in **Figure 7**. Tile selection prioritized areas surrounding the Central Business District (CBD), where significant liquefaction-induced damage to the built environment was observed, as well as

sections of the Avon River Corridor, now designated as part of the Red Zone for environmental restoration and innovative land-use initiatives.

As a result of this targeted selection strategy, the digitized inventory for the Christchurch event does not encompass all liquefaction features represented in the broader Townsend Polygon dataset. Accordingly, the dataset produced from this event is partial and should be interpreted as a focused, rather than comprehensive, representation of liquefaction surface manifestations within the study area.

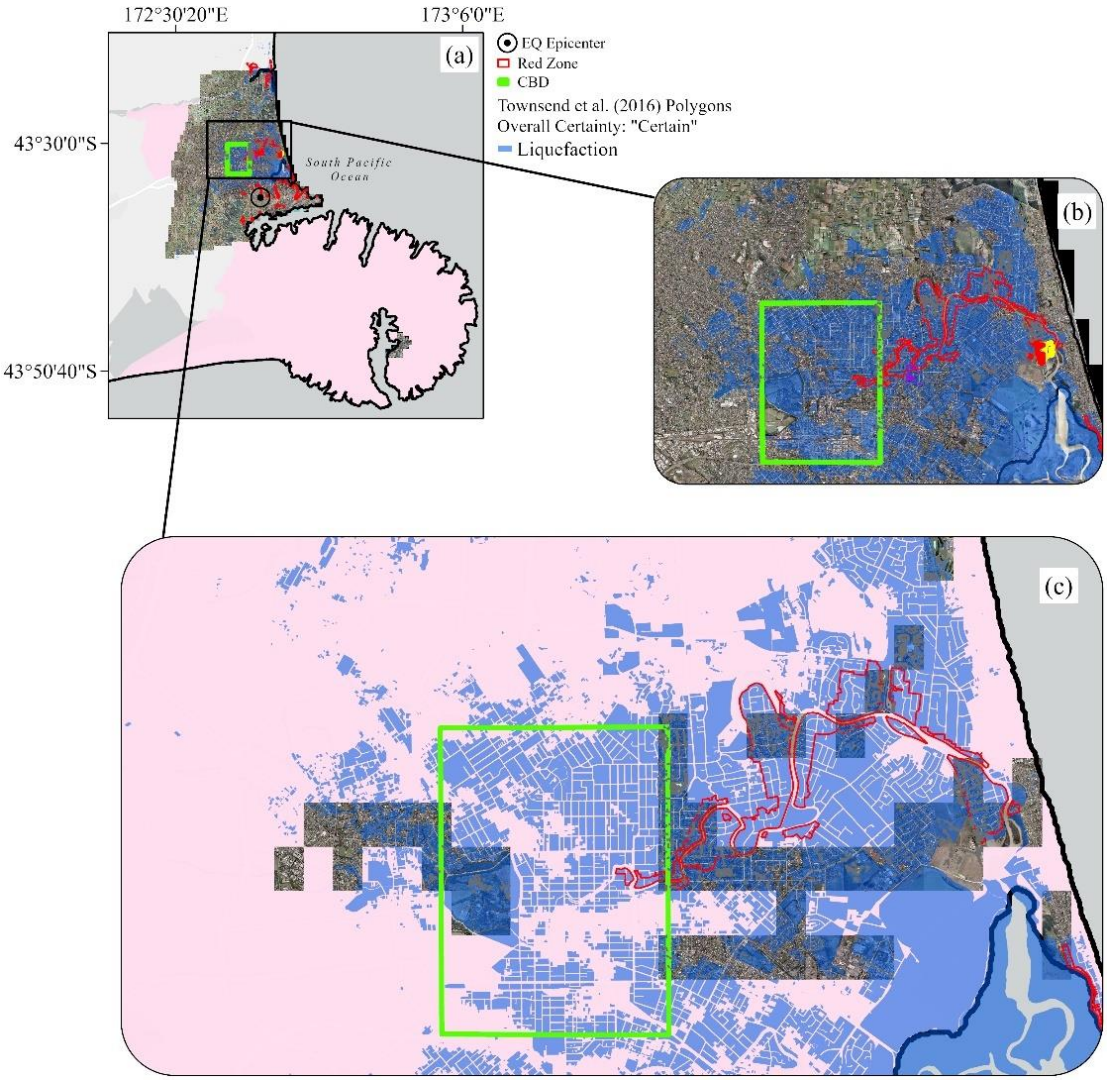

Figure 7: Post-event aerial imagery by NZ Aerial Mapping Ltd, downloaded from LINZ for the 2011 M6.1 Christchurch, New Zealand earthquake event. The blue polygons denote areas marked with an "overall certainty" label of “Certain.” The green box highlights the Central Business District (CBD), while the red outline indicates the residential Red Zone. (a) Total data area coverage. (b) Area of interest with all available imagery. (c) Area of interest showing only the image tiles used, as not all available images were employed in the development of the methodology in this study.

For the 2021 Haiti earthquake, high-resolution post-event satellite imagery from the WorldView platform was obtained through the MAXAR Open Data Program. While the imagery offers excellent spatial resolution suitable for detailed ground feature identification, its utility was significantly constrained by extensive cloud coverage, as illustrated in **Figure 8**. This environmental limitation impeded the comprehensive assessment of liquefaction manifestations across the full study area.

Despite these constraints, the available cloud-free imagery encompassed 11 of the 18 liquefaction observation points documented in the GEER reconnaissance report. As with the other case studies presented in this dissertation, the partial coverage of ground-truth locations necessitates the classification of the resulting inventory as incomplete. The dataset reflects only those features observable within the available imagery extent and should be interpreted accordingly with respect to its spatial limitations.

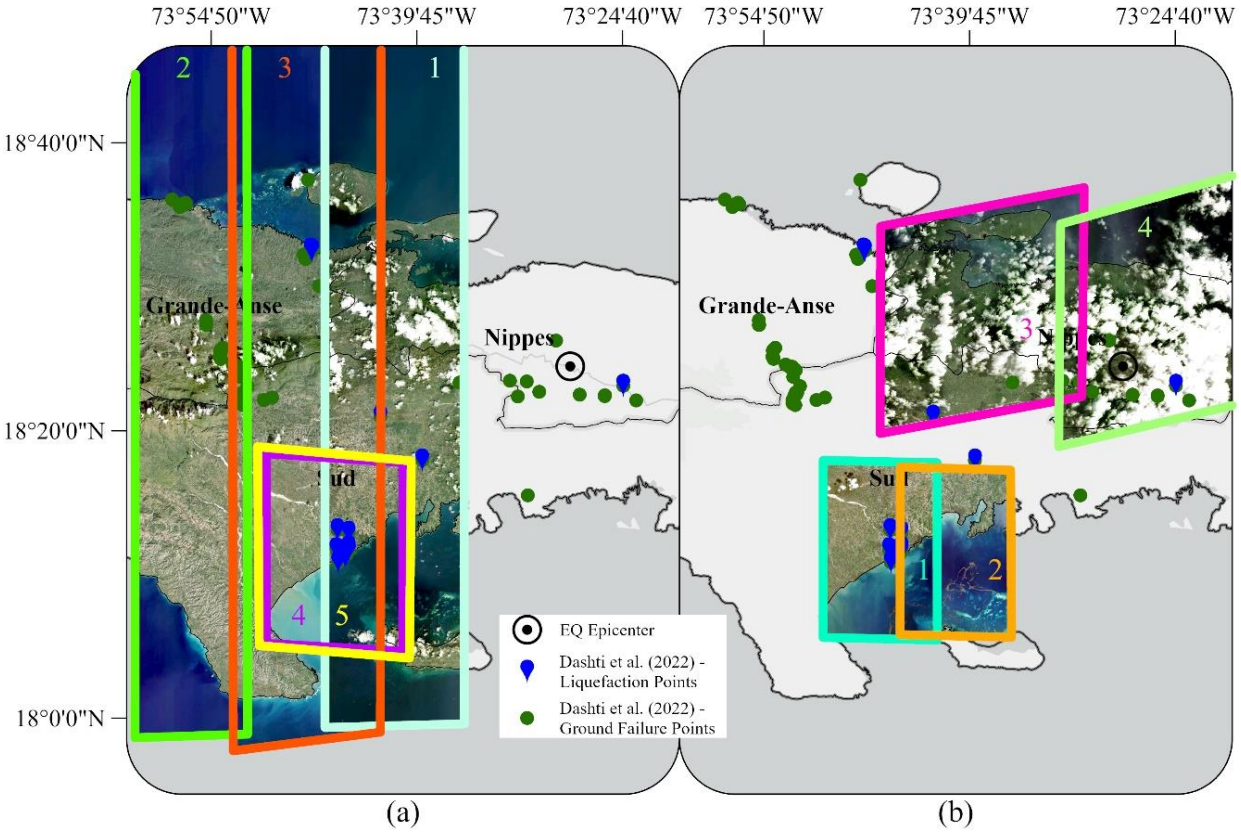

Figure 8: Satellite imagery for the 2021 M7.2 Haiti earthquake, downloaded from MAXAR Open Data. The area shown corresponds to the same boundary as the inset in Figure 4, covering all available ground truth data. However, the imagery scenes do not encompass all mapped liquefaction. (a) Pre-event imagery scenes. (b) Post-event imagery scenes. For resolution and acquisition dates, refer to **Table 2**.

Table 2: Summary of imagery used in the creation of the liquefaction inventories for the three earthquake events analyzed. The table provides details on the event, sensor type, image ID, acquisition date, spectral bands, resolution (maximum ground sample distance, GSD), format, text references, and data source for each imagery used in the study. All imagery is freely available.

Event	Sensor	Image ID	Date of Acquisition	Bands	Resolution (Max GSD)	Format	Text Reference	Source
M7.0 Port-au-Prince, Haiti (2010)	QB[1]-2	101001000793BC00*	1/15/2008	RGB	0.67 m	TIFF	Figure 6a1	MAXAR Open Data
	QB[1]-2	1010010009381800*	2/22/2009	RGB	0.65 m	TIFF	Figure 6a2	MAXAR Open Data
	QB[1]-2	101001000971FC00*	4/12/2009	RGB	0.61 m	TIFF	Figure 6a3	MAXAR Open Data
	WV[2]-2	103001000395D700*	12/13/2009	RGB	0.50 m	TIFF	Figure 6a4	MAXAR Open Data
	WV[2]-2	1030010003B16A00*	1/9/2010	RGB	0.56 m	TIFF	Figure 6a5	MAXAR Open Data
	WV[2]-2	1030010003BA7100*	1/9/2010	RGB	0.53 m	TIFF	Figure 6a6	MAXAR Open Data
	WV[2]-2	1030010003004400**	1/15/2010	RGB	0.51 m	TIFF	Figure 6b1	MAXAR Open Data
	WV[2]-2	1030010003A27E00**	1/15/2010	RGB	0.51 m	TIFF	Figure 6b2	MAXAR Open Data
	WV[2]-2	1030010003C29400**	1/15/2010	RGB	0.51 m	TIFF	Figure 6b3	MAXAR Open Data
	WV[2]-2	1030010003399600**	1/15/2010	RGB	0.50 m	TIFF	Figure 6b4	MAXAR Open Data
M6.1 Christchurch, New Zealand (2011)	Aerial	**	2/24/2011	RGB	0.1 m	GeoTIFF	Figure 7	LINZ Data Service
M6.4 Puerto Rico (2020)	S[3]-2B	L1C_T19QGV_A023102_20191124T150720*	11/24/2019	Multiband	10-m RGB	TIFF	Not referenced	USGS Earth Explorer
	WV[2]-3	103001008C7A2B00*	03/14/2019	RGB	0.47 m	TIFF	Not referenced	MAXAR Open Data
	WV[2]-3	103001008F51AB00*	03/14/2019	RGB	0.465 m	TIFF	Not referenced	MAXAR Open Data
	S[3]-2B	L1C_T19QGV_A014837_20200108T150715**	01/08/2020	Multiband	10-m RGB	TIFF	Figure 5a	USGS Earth Explorer
	WV[2]-3	1040010055B93D00**	01/08/2020	RGB	0.45 m	TIFF	Figure 5b	MAXAR Open Data
M7.2 Nippes, Haiti (2021)	WV[2]-2	10300100A450A500*	4/5/2020	RGB	0.50 m	TIFF	Figure 8a1	MAXAR Open Data
	WV[2]-3	1040010063636500*	12/17/2020	RGB	0.36 m	TIFF	Figure 8a2	MAXAR Open Data
	WV[2]-2	10300100B4C41A00*	2/27/2021	RGB	0.57 m	TIFF	Figure 8a3	MAXAR Open Data
	GE[4]-1	1050010024A51F00*	5/31/2021	RGB	0.51 m	TIFF	Figure 8a4	MAXAR Open Data
	WV[2]-2	10300100C1BBC200*	7/13/2021	RGB	0.56 m	TIFF	Figure 8a5	MAXAR Open Data
	WV[2]-3	104001006CA11700**	8/15/2021	RGB	0.37 m	TIFF	Figure 8b1	MAXAR Open Data
	WV[2]-3	104001006C9FC800**	8/15/2021	RGB	0.35 m	TIFF	Figure 8b2	MAXAR Open Data
	WV[2]-3	104001006CA68300**	8/16/2021	RGB	0.54 m	TIFF	Figure 8b3	MAXAR Open Data
	WV[2]-3	104001006B278A00**	8/16/2021	RGB	0.60 m	TIFF	Figure 8b4	MAXAR Open Data

1 Quickbird
2 WorldView
3 Sentinel
4 GeoEye
* Pre-event
** Post-event

1.3.2 Inventory Curation

To develop the digital, image-based liquefaction inventories presented in this study, individual surface manifestations were manually delineated as polygons. Each polygon represents a discrete liquefaction feature, mapped through detailed visual interpretation of high-resolution imagery. This process was guided by documented observations from the literature, field investigation photographs, and other authoritative sources that provided examples of recognizable surface effects, such as sand boils, lateral spreading, and ground fissures.

Following initial digitization, the delineated features were validated against corresponding occurrence points or polygon datasets from the available ground-truth sources associated with each case study. To ensure consistency across all three events, a standardized attribute schema was applied uniformly. The specific feature labels were finalized through several iterative refinement cycles conducted during the analysis of each case study. This iterative process ensured that a consistent and interpretable classification system was used to describe similar surface features across different geographic and geologic contexts, thereby enhancing both intra- and inter-event comparability.

1.3.2.1 Polygons

Each labeled polygon representing a liquefaction surface manifestation was manually delineated using high-resolution imagery and constructed with relatively simple geometric shapes to enhance the accuracy and interpretability of the mapped features. Simplified geometries were intentionally employed to closely reflect the visible boundaries of surface effects while minimizing the potential for overfitting or artificial precision that could arise from more complex polygon structures.

Figure 9 illustrates the general procedure used to delineate liquefaction surface manifestations, using an example from the 2011 M6.1 Christchurch earthquake. In this example, a surface feature documented in the Townsend ground-truth polygon dataset is paired with corresponding post-event aerial imagery to demonstrate the typical workflow and visual cues used to define polygon boundaries.

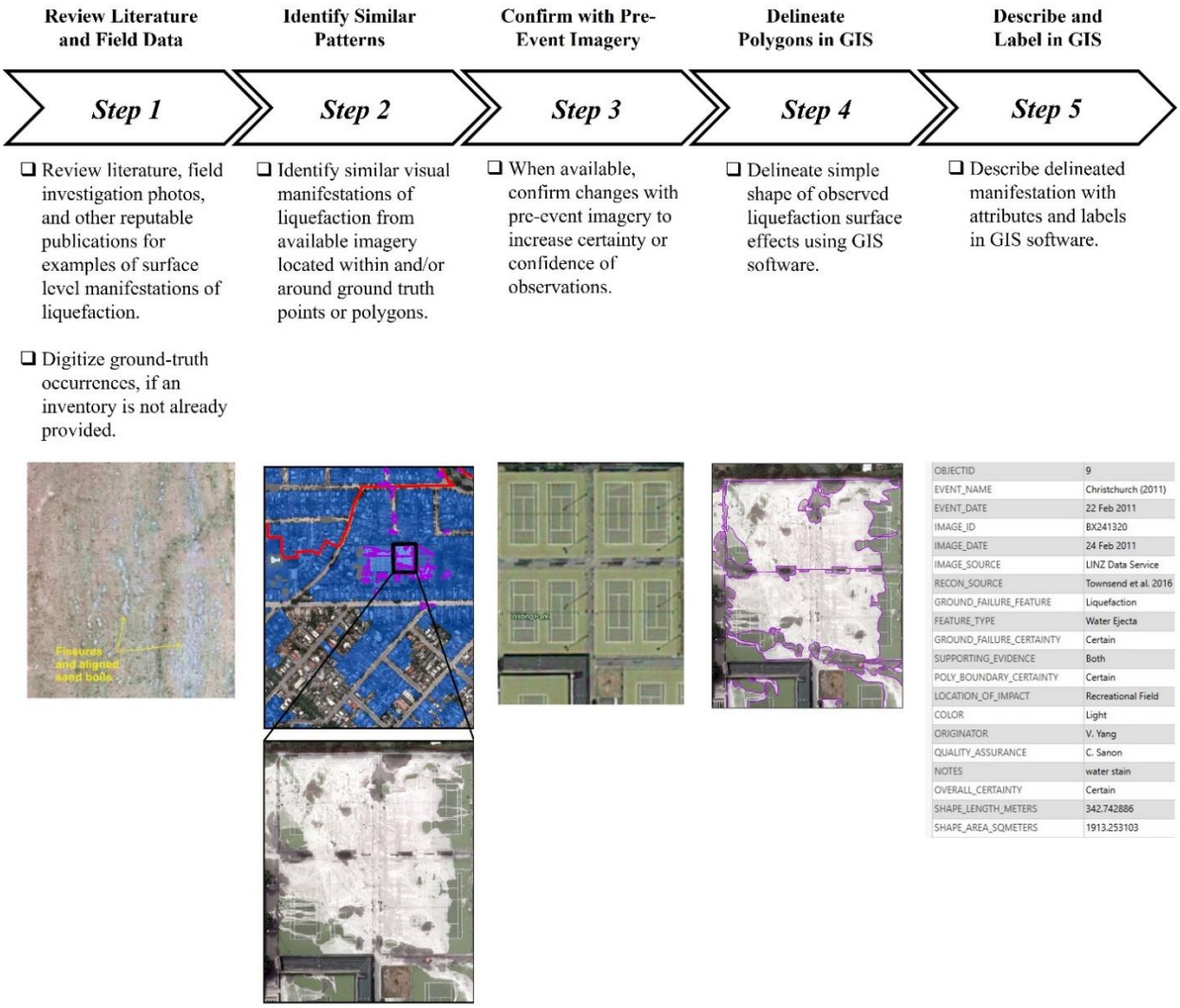

Figure 9: Generalized steps for digitizing manifestations of earthquake-induced liquefaction from imagery and ground truth data. Step 1: Fissures and aligned sand boils from the Christchurch 2011 earthquake event. Picture by courtesy of **Figure 7** in Townsend et al. (2016). Step 2: IMAGE_ID: BX241320 with (blue polygons) and without Townsend Polygons. Step 3: Pre-event image - Google Earth Historical Imagery GeoEye taken on 2/7/2011. Step 4: Polygons (purple outline) delineating liquefaction manifestation from IMAGE_ID: BX241320 for the Christchurch 2011 earthquake event. Step 5: Sample attribute table.

1.3.2.2 Labels and Attributes

The development of the attribute schema for this study was informed by a comprehensive review of existing liquefaction and ground failure inventories. Each attribute was assigned a predefined set of domain values aligned with terminology and classification standards commonly used in the liquefaction research community. In contrast to other databases that may have incomplete attribute fields across multiple event records, the inventories developed here were designed to ensure that each event entry was fully populated. To achieve this, the final set of domain values was refined through multiple iterations, with the goal of capturing commonalities across case studies while maintaining

clarity and consistency. Attribute values were specified directly within the GIS platform's attribute table. Full details of the schema are presented in **Table 3**.

Consistent with the recommendations by Perera et al. (2021) for landslide inventory development—which emphasize the inclusion of both spatial geometry and descriptive characteristics—each liquefaction feature in this study includes both geometric and semantic attributes. The spatial attribute fields include `EVENT_NAME`, `LOCATION_OF_IMPACT`, `SHAPE_LENGTH_METERS`, and `SHAPE_AREA_SQMETERS`. While many other hazard databases use `EVENT_ID` to represent unique events, the field `EVENT_NAME` was used here to provide more descriptive and case-specific identifiers, facilitating independent querying of individual case studies. The `LOCATION_OF_IMPACT` field serves a dual role, indicating both the physical environment and the type of infrastructure affected. This field distinguishes, for example, between sand boils occurring in residential yards—where impacts are minimal—and those affecting roads, where transportation functionality may be compromised.

Feature geometry measurements, including polygon perimeter and area, were calculated within the GIS environment. Unlike conventional Euclidean calculations, these values reflect geodesic measurements to account for Earth's curvature, ensuring greater accuracy across geographically dispersed datasets. The corresponding fields, `SHAPE_LENGTH_METERS` and `SHAPE_AREA_SQMETERS`, store these values explicitly, with units indicated for transparency. These geometric attributes—along with `LOCATION_OF_IMPACT`—support quantification of the physical extent and potential consequences of liquefaction-induced ground deformation. Larger or more spatially concentrated features (e.g., extensive lateral spreading or high-volume ejecta) may indicate more severe damage and are important for assessing zonal impacts, informing repair prioritization, and estimating response and recovery needs.

The remaining attributes fall into two broad categories: imagery-specific and feature-specific. Imagery-specific attributes include `IMAGE_ID`, `IMAGE_DATE`, and `IMAGE_SOURCE`. These fields respectively record the unique identifier of the imagery tile used, the date of acquisition, and the image provider (e.g., MAXAR, LINZ). This metadata supports reproducibility and transparency in visual interpretation.

Feature-specific attributes capture the nature, interpretation, and verification status of each digitized liquefaction manifestation. These include:

- `OBJECT_ID`: A system-generated unique identifier for each row in the attribute table, with each case study beginning from 1.
- `SHAPE`: A system-generated field indicating the geometry type (i.e., polygon).

- EVENT_DATE: The date of the earthquake event, equivalent to the "movement date" field in landslide inventories. In sequences involving multiple seismic events, this field reflects only the mainshock date, with the IMAGE_DATE field providing additional temporal resolution.
- RECON_SOURCE: The source of ground-truth data used to support digitization. For the 2010 Haiti case study, multiple sources were used (RECON_SOURCE1, RECON_SOURCE2) to reference both the GEER (Rathje et al., 2010) and Olson et al. (2011) reports.
- GROUND_FAILURE_FEATURE: A general descriptor indicating the inventory's purpose (e.g., "Liquefaction").
- FEATURE_TYPE: The specific surface manifestation observed. Four domain values are defined: "Lateral Spreading," "Sand Ejecta," "Water Ejecta," and "Other." These were derived from visual signatures in imagery (see **Figure 10a**). For instance:
    - "Lateral Spreading" features typically include visible cracks or displaced shoreline boundaries.
    - "Sand Ejecta" refers to sediment expelled to the surface.
    - "Water Ejecta" refers to water stains, streaks, or pooling.
    - "Other" captures ambiguous or undocumented manifestations.

The level of confidence in each feature's classification is recorded in:

- GROUND_FAILURE_CERTAINTY: Values include "Certain," "Probable," and "Uncertain," reflecting the confidence level in identifying the feature as a liquefaction manifestation.
- SUPPORTING_EVIDENCE: Specifies whether the classification was supported by field evidence, visual analysis, or both.
- POLY_BOUNDARY_CERTAINTY: Reflects confidence in the polygon's shape accuracy, with options "Certain" or "Uncertain."
- OVERALL_CERTAINTY: A synthesis of all other certainty fields, determined after a quality assurance review (see Section 3.2.3).

Additional descriptive attributes include:

- COLOR: Captures visual properties of the surface feature, based on tone and saturation. The following domain values are defined: "Dark" (typically moist, dark-gray sand), "Light" (dry or bleached appearance), and "Other" (see **Figure 10b**).
- ORIGINATOR: Name or initials of the individual who digitized the feature.
- QUALITY_ASSURANCE: Name or initials of the individual who reviewed the feature during QA procedures.
- NOTES: An open text field for miscellaneous observations or explanatory remarks, populated by either the originator or the reviewer.

The LOCATION_OF_IMPACT domain values were finalized after all three case studies were completed to ensure consistency. While the list is not exhaustive, it provides a standardized structure for future adaptation across additional events or other ground failure types.

Table 3: List of attributes used in the liquefaction inventory, including predefined domain values for each attribute. The table outlines both spatial and feature-specific attributes, with explanations for their purpose in mapping and analyzing liquefaction effects. These attributes are designed to standardize the inventory across multiple events and ensure consistency in data collection and analysis.

#	Attribute Field	Domain Value Field	Description
1	OBJECTID	-	Autogenerated by GIS Software
2	SHAPE	Polygon	Autogenerated by GIS Software
3	EVENT_NAME	1. Haiti (2010) 2. Christchurch (2011) 3. Haiti (2021)	Earthquake Event
4	EVENT_DATE	1. 12 Jan 2010 2. 22 Feb 2011 3. 14 Aug 2021	Date of earthquake occurrence (Main Shock)
5	IMAGE_ID	Varies by imagery tile Input appropriate post-event image ID	As provided by image source
6	IMAGE_DATE	Varies by best imagery used to digitize the specific feature	Date of post-event imagery acquisition by image provider
7	IMAGE_SOURCE	1. Maxar Open Data Program 2. LINZ Data Service	Imagery provider
8	RECON_SOURCE	Varies by event Input appropriate source material	Source (s) of ground truth
9	GROUND_FAILURE_FEATURE	Liquefaction	Earthquake-induce secondary effect

10	FEATURE_TYPE	1. Lateral Spreading 2. Sand Ejecta 3. Water Ejecta 4. Other	Description of feature delineated
11	GROUND_FAILURE_CERTAINTY	1. Certain 2. Uncertain 3. Probable	As determined by originator based on ground truth data
12	SUPPORTING_EVIDENCE	1. Digitized from points or polygons provided in reconnaissance study 2. Visual interpretation of ground failure occurrence 3. Both	Reason for digitizing feature
13	POLY_BOUNDARY_CERTAINTY	1. Certain 2. Uncertain	As determined by originator
14	LOCATION_OF_IMPACT	1. Driveway 2. Free Field 3. Parking Lot 4. Recreational Field 5. Road 6. Seaport 7. Sidewalk 8. Miscellaneous Coastline 9. Other	Physical place where feature is found and mapped
15	COLOR	1. Dark 2. Light 3. Other	General hue of feature
16	ORIGINATOR	-	Person digitizing feature
	QUALITY_ASSURANCE	-	Person validating polygons
17	NOTES	-	Miscellaneous details at the discretion of the originator or QA person
18	OVERALL_CERTAINTY	1. Certain 2. Uncertain 3. Probable	As determined from QA review by combining ground failure certainty and polygon certainty
19	SHAPE_LENGTH_METERS	-	Geodesic measurement calculated in GIS Software
20	SHAPE_AREA_SQMETERS	-	Geodesic measurement calculated in GIS Software

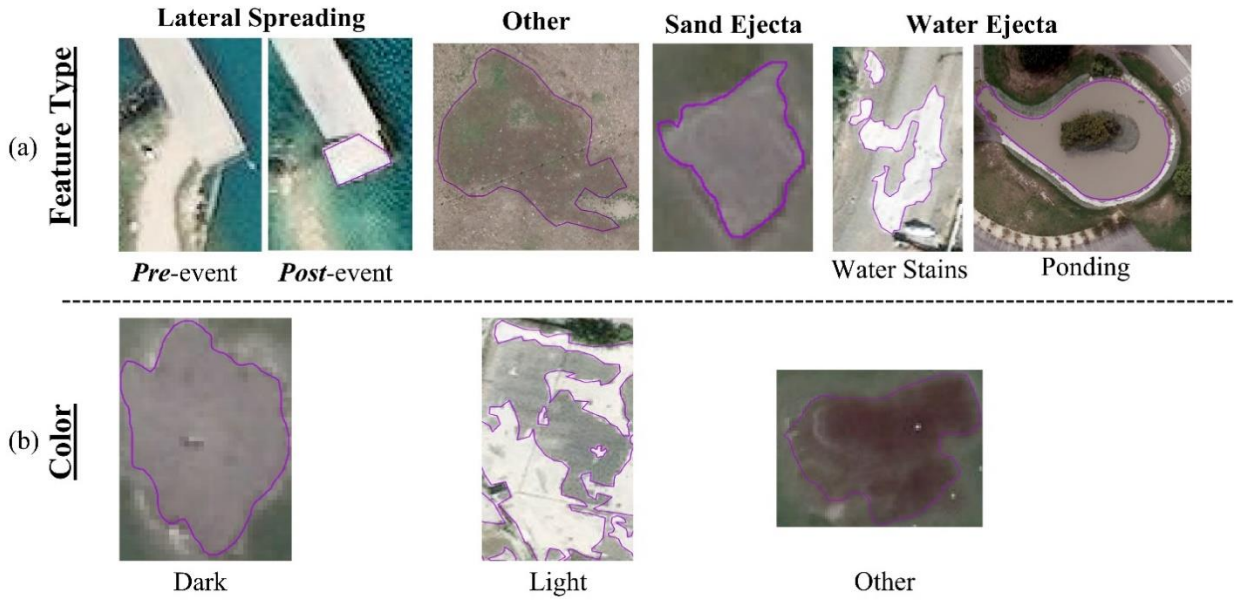

Figure 10: Classification of liquefaction feature types and color attributes. (a) Feature types are based on visual characteristics, such as lateral movement identified from comparing pre- and post-event images or the accumulation of sediment or water. (b) Color attributes based on the typical visual appearance of liquefaction features observed in the case studies.

1.3.2.3 Dataset Publication

Each case study inventory developed in this research is available for download in the form of a shapefile (`.shp`), a widely supported format compatible with most Geographic Information System (GIS) software platforms. To facilitate broader usability, particularly for web-based mapping applications and computer vision workflows, a sample script for converting the shapefile into the GeoJSON (`.json`) format is provided in **Appendix A**. GeoJSON is commonly used in web development and machine learning environments due to its lightweight, human-readable structure and compatibility with modern geospatial libraries.

While the high-resolution imagery used for digitizing liquefaction surface manifestations is not publicly distributed alongside the shapefiles due to licensing restrictions and proprietary access agreements, complete metadata regarding the source, acquisition date, and provider of each image is embedded within the attribute table of each polygon feature. This enables end users to independently obtain the corresponding imagery, subject to availability and access permissions, and align it with the digitized polygon data for visualization, training, or further analysis.

This distribution model aligns with best practices established by large-scale computer vision challenges, such as the xView competition, which similarly provide annotated geospatial data separately from imagery while maintaining interoperability. The format and structure of the provided inventories are designed to support flexible

integration into downstream applications for disaster impact assessment, hazard mapping, and automated feature detection.

1.4 Discussion

Inventories derived from remote sensing imagery are inherently subject to various forms of uncertainty, stemming from both technical and contextual factors. These ambiguities arise due to sensor limitations, atmospheric interference, temporal variability across the study area, and the inherent complexity of the landscape. Additionally, image processing techniques employed by data providers—such as radiometric corrections, orthorectification, or compression—may introduce further distortions or inconsistencies. Beyond the imagery itself, the reliability and completeness of ground-truth or validation datasets, as well as the experience and interpretive judgment of the investigators, contribute significantly to the overall accuracy and consistency of the digitized features.

The temporal proximity between image acquisition and the seismic event is particularly critical for the accurate detection of transient phenomena such as liquefaction. Imagery acquired before or during an earthquake may fail to capture post-event changes such as surface ejecta, ground deformation, or flooding, thereby limiting the ability to accurately map event-specific surface manifestations. Conversely, imagery captured during emergency response or cleanup operations may reflect altered conditions that obscure or erase critical surface evidence.

This limitation was particularly evident in the Christchurch case study. Although the post-event aerial imagery was of exceptionally high spatial resolution, it was acquired after significant cleanup efforts had already commenced. Consequently, many liquefaction features had been removed or altered, and thus no longer reflected their original form or spatial extent. As a result, several features were omitted from the inventory due to insufficient visual evidence or reduced interpretability (see **Figure 11**).

This observation underscores a broader methodological implication: in remote sensing–based disaster mapping, both the surface features and the imagery used to capture them should be regarded as perishable data. The timing of image acquisition plays a critical role in determining the accuracy, completeness, and reliability of the resulting inventory. Accordingly, future methodologies should explicitly account for this temporal sensitivity when designing workflows for the documentation of post-disaster surface effects.

(a) (b) (c)

Figure 11: Cleanup efforts following the 2011 Christchurch event. (a) Volunteers from Canterbury University clean up liquefaction ejecta on February 24, 2011 - the date of imagery acquisition for the data used in developing the liquefaction image inventory (https://www.theatlantic.com/photo/2011/02/new-zealand-earthquake-search-rescue-and-repair/100016/). (b) Excavator truck, with bucket arm to remove ejecta, seen in the aerial imagery by LINZ (IMAGE_ID: BX241228) captured on February 24, 2011. (c) Dump trucks carrying ejecta from the roads, as seen in seen in the aerial imagery by LINZ (IMAGE_ID: BX241118), captured on February 24, 2011.

Additional limitations emerged from the reliance on accurate and precise ground truth information, which served as the foundation for validating and contextualizing the digitized features. In several instances across the case studies, discrepancies were identified that affected the usability of certain ground truth records. For example, some ground truth points were geolocated in oceanic regions, likely due to coordinate entry errors or imprecise georeferencing, thereby disqualifying them from use in surface feature mapping. In other cases, the reported ground truth points did not spatially align with the features described in the associated reconnaissance reports, necessitating interpretive judgment or extrapolation by the investigator.

This challenge was particularly evident in the 2010 Haiti inventory, where the number of mapped features exceeded the number of ground truth points. This discrepancy was partly attributable to the nature of the ground truth data itself—some points represented generalized site-level observations rather than discrete, georeferenced surface features. As a result, multiple surface manifestations were mapped within a single site-level reference point, introducing variability in the spatial density and granularity of the resulting inventory.

Further complications arose from spatial misalignment due to variations in satellite sensor viewing angles and acquisition geometry. **Figure 12** illustrates this issue using the pre- and post-event imagery from the 2021 M7.2 Haiti earthquake. The red polygon remains fixed, yet the underlying imagery appears slightly shifted, highlighting inconsistencies in building positions and shadow orientations. These misalignments are likely the result of differences in satellite viewing angles or sun azimuth during image capture. Even minimal spatial displacements of this kind can

introduce distortions in visual interpretation, complicating feature identification and reducing confidence in the accuracy of polygon delineation and classification.

Taken together, these limitations underscore the importance of applying careful quality control measures, exercising interpretive caution, and acknowledging the potential for uncertainty when digitizing event-driven features based on remote sensing and supporting ground-truth data.

Figure 12: Misalignment of pre- and post-event satellite imagery for the 2021 M7.2 Haiti earthquake. The images were slightly misaligned, as indicated by the red marker. (a) Pre-event imagery (IMAGE_ID: 10300100B4C41A00). (b) Post-event imagery (IMAGE_ID: 104001006CA11700).

Discrepancies also arose between features documented in post-earthquake reconnaissance reports and those that could be visually identified using the available satellite imagery. In some cases, ground failures described in authoritative sources were not discernible in the imagery, due to factors such as spatial resolution, image quality, or environmental obstructions. **Figure 13** presents an illustrative example from the 2021 M7.2 Nippes, Haiti earthquake, where surface cracking—potentially indicative of lateral spreading near a river—was reported in GEER Report No. 073 (Dashti et al., 2022) and further supported by OpenStreetMap annotations. Despite this corroborating documentation, the feature

could not be detected through visual inspection of the post-event satellite imagery, likely due to insufficient resolution or obscuring vegetation. As a result, the feature was excluded from the final inventory.

This example highlights a broader limitation in remote sensing–based mapping workflows: not all ground-verified features can be captured using satellite imagery alone, particularly when features are subtle, degraded, or spatially ambiguous. Such cases underscore the need for caution when interpreting omissions in remotely sensed inventories and reaffirm the importance of integrating diverse data sources to improve completeness and confidence in mapped outputs.

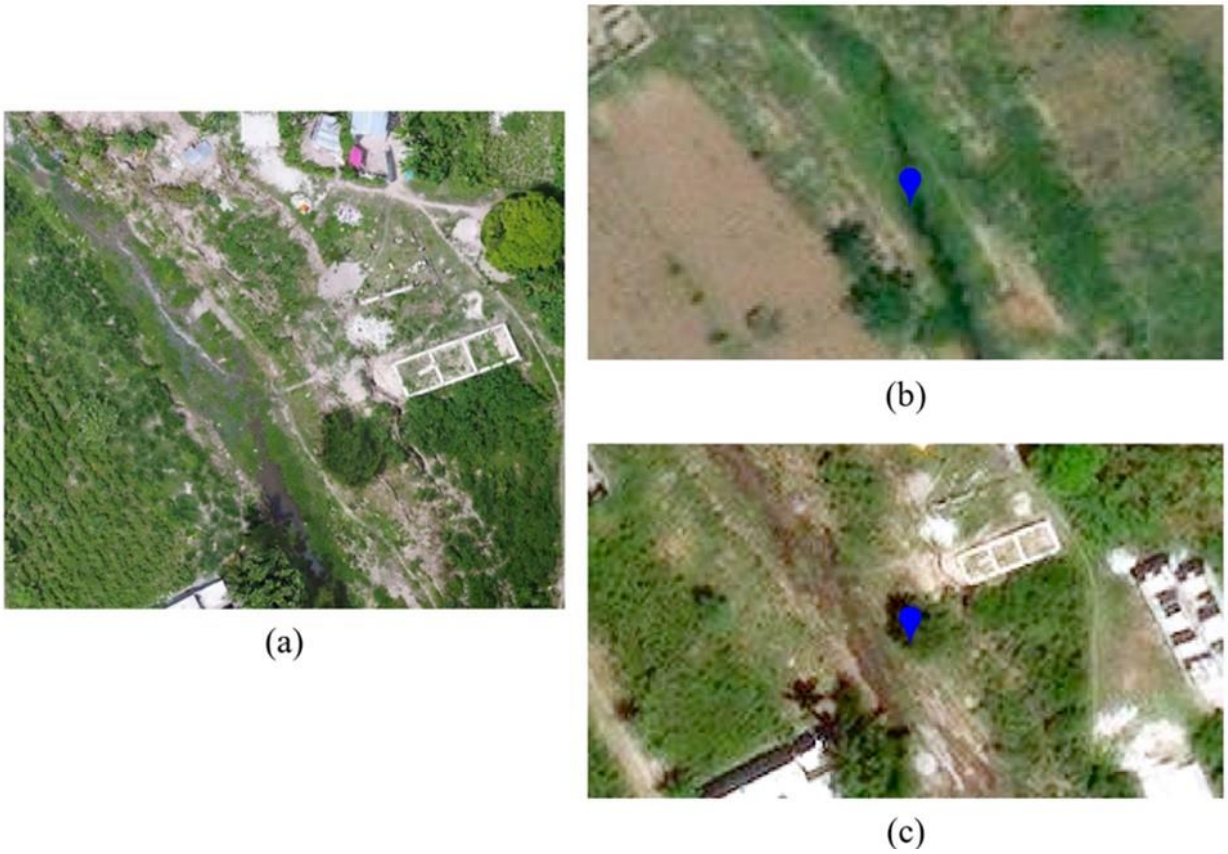

Figure 13: Discrepancy between the reconnaissance report and satellite imagery for lateral spreading near a river during the 2021 M7.2 Haiti earthquake (Dashti et al. 2022). (a) Cracking associated with potential lateral spreading, as documented in the GEER report, based on their remote detection using OpenStreetMap. (b) Pre-event satellite imagery used to visually detect changes, as indicated in the GEER report (IMAGE_ID: 10300100A450A500). (c) Post-event satellite imagery where the lateral spreading feature is not clearly visible, leading to its exclusion from the final inventory (IMAGE_ID: 104001006CA11700).

In **Figure 14a**, adapted from the GEER-021 report for the 2010 M7.0 Port-au-Prince, Haiti earthquake (Rathje et al., 2010), lateral spreading at the International Port of Port-au-Prince is clearly visible in the ground-truth photograph. The image captures extensive ground cracking and displacement along the waterfront, providing strong visual

evidence of liquefaction-induced lateral movement. However, as shown in **Figure 14b**, the corresponding satellite imagery does not clearly depict these features, likely due to limitations in spatial resolution, image angle, or visual contrast between disturbed and undisturbed areas.

To reconcile these differences, **Figure 14c** presents the digitized interpretation of the lateral spreading area, shown in blue. This outline represents the most accurate approximation of the feature based on available imagery and supporting ground-truth documentation. Through this interpretive process, six discrete features were identified and delineated, each corresponding to ground fragments likely resulting from liquefaction-induced cracking and deformation. This example illustrates both the value of ground-truth photography for contextualizing satellite data and the challenges inherent in identifying subtle deformation features through remote sensing alone.

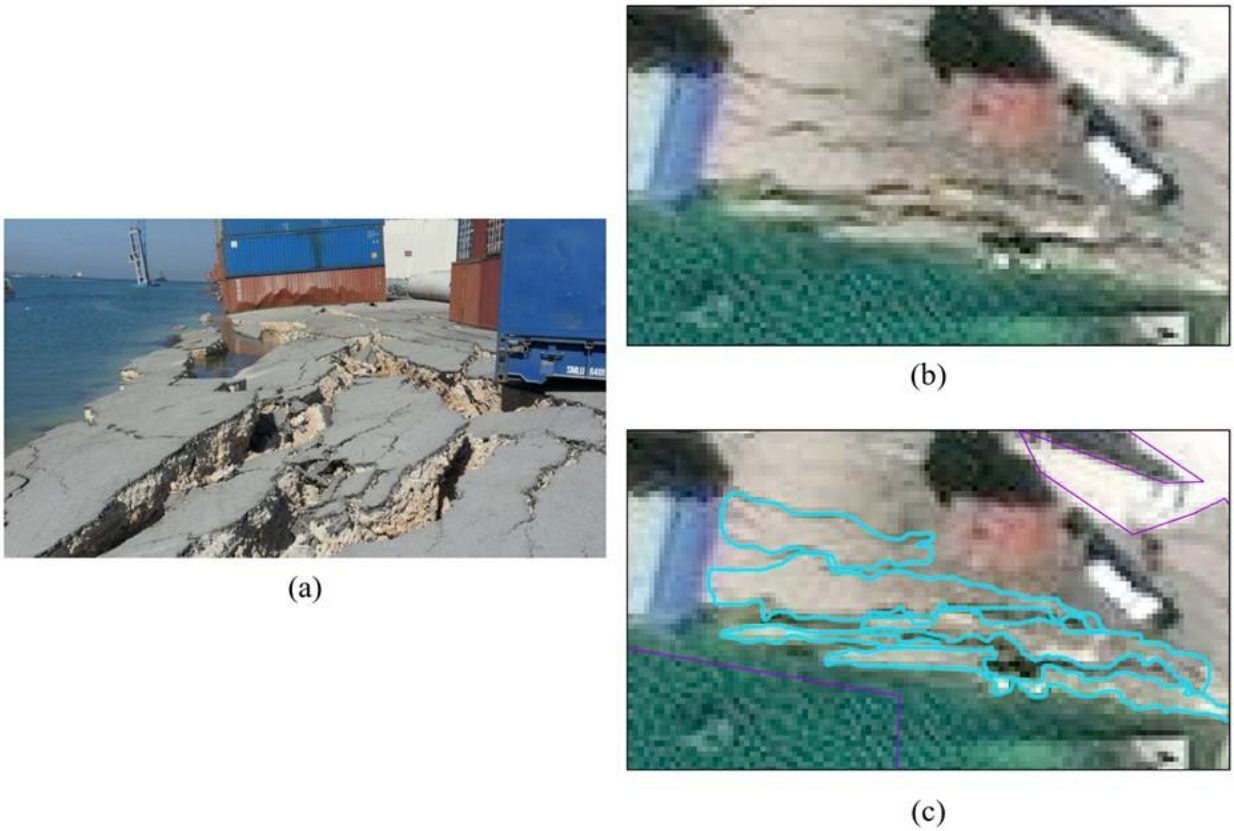

Figure 14: Comparison of ground truth and satellite imagery for lateral spreading at the International Port of Port-au-Prince during the 2010 M7.0 Haiti earthquake (Rathje et al. 2010). (a) Ground truth photo, courtesy of the GEER-021, showing clear evidence of lateral spreading. (b) Satellite imagery where the lateral spreading is not clearly visible due to limitations in satellite resolution (IMAGE_ID: 1030010003C29400). (c) The blue outline represents best attempt to document the lateral spreading, resulting in the identification of six features corresponding to the fragments caused by the separation of the ground (IMAGE_ID: 1030010003C29400).

In addition to the limitations previously mentioned, time constraints and the sheer volume of data—particularly in the Christchurch case study—led to the decision to digitize only those features with well-defined boundaries within an

image tile or imagery strip, as well as features that appeared to retain their original form at the time of image acquisition. As a result, many features were intentionally excluded from the inventories. While having lots of data is generally beneficial, the volume can sometimes become overwhelming, requiring a trade-off between data quantity, time, and the completeness of the final inventory. This highlights the need for more efficient methods, such as computer vision, to process large datasets effectively.

For a detailed summary of the factors influencing the use of remote sensing data and their impact on the accuracy and reliability of the results, refer to **Table 4**.

Table 4: Summary of the key factors contributing to ambiguities in remote sensing methodologies, highlighting their role in the feature identification process and their influence on the accuracy and reliability of results in inventory development.

Factor	Impact on Analysis	Explanation	Inventory Impacted
Sensor Limitations	Image Resolution	Imagery with lower resolution, such as imagery acquired from Sentinel or more commonly Landsat, can impact the visual detection of small-scale features like cracks or shallow depressions in the ground.	2021 Haiti
	Image Viewing Angle	Differences in viewing angles might result in slight misalignments, leading to spatial inaccuracies in the analysis.	
Temporal Variations	Seasonal & Environmental Changes	Satellite imagery captured in the spring may display dense vegetation, which could obscure the detection of certain features.	2020 Puerto Rico 2021 Haiti
Atmospheric Conditions	Cloud Coverage	A satellite image captured during overcast conditions may obscure important surface features.	2020 Puerto Rico 2021 Haiti
Complexity of the Study Area	Imposed Time Constraint	In areas with widespread conditions of interest, only a subset of the available data can be processed within a reasonable timeframe, i.e., not all features can be fully examined or classified. Certain areas may be underrepresented or excluded from the analysis, leading to gaps in the inventory.	2011 Christchurch
Image Processing Techniques	Image Calibration	Different methods of radiometric calibration can result in varying levels of brightness and contrast in the imagery, impacting feature detection accuracy.	Indirect impact
Data Availability and Selection	Completeness and Data Exclusion	Lack of field validation data for a specific region may lead to misclassification of features.	2010 Haiti 2021 Haiti
Investigators	Analyst Expertise	An investigator with less experience in GIS may delineate a feature with lower accuracy, or someone unfamiliar with a phenomenon like liquefaction might misclassify or mislabel a feature.	All
Image Acquisition	Project timing	Imagery captured during or after emergency cleanup efforts may not accurately represent the original features, as some features may have been removed or altered.	2011 Christchurch
	Sun Positioning	Variations in the sun's position between pre- and post-event images may lead to differences in shadow length and direction, making it difficult to accurately compare the two images or interpret features consistently.	Haiti 2021

1.4.1 Quality Assurance

Quality assurance (QA) is essential for ensuring the accuracy, reliability, and internal consistency of geospatial data derived from remote sensing imagery. In this study, a comprehensive QA framework was implemented to minimize

interpretive errors and maintain high standards of methodological rigor throughout the digitization process. The QA process encompassed two principal components: (1) data validation through ground truthing and documentation, and (2) consistency enforcement through centralized review and interpretation normalization.

1. Data Validation and Ground Truthing

To ensure the validity of feature classifications and interpretations derived from imagery, ground-truth data served as a primary reference. These validation data were sourced from post-earthquake reconnaissance reports, which were largely informed by direct field observations. When discrepancies emerged between the imagery-based interpretations and the reported ground-truth data, additional reviews were conducted to investigate potential causes. These reviews considered several factors, including imagery resolution, acquisition timing, vegetation or urban obstructions, and positional misalignments.

If a plausible explanation for the discrepancy—such as temporal misalignment or degraded image quality—could not be identified, the conflicting feature or ground-truth point was excluded from the final inventory. To further promote transparency and traceability in the digitization workflow, a `NOTES` field was included in the attribute schema. This field captured the rationale for including each digitized feature, offering qualitative insights into decision-making—particularly in cases of ambiguity or conflicting evidence. This documentation practice enhanced accountability and supported *post hoc* review of inventory entries.

2. Consistency in Interpretation

To ensure interpretive consistency across multiple case studies, a single investigator was assigned to standardize the classification and labeling process across all events. This centralized QA approach minimized subjective variability that could otherwise arise from individual mapping styles, especially when delineating features with complex or subtle boundaries. Centralizing the review process also mitigated potential discrepancies in feature geometry or labeling, which could lead to systematic overestimation or underestimation of surface effects.

An illustrative example of this QA approach is presented in **Figure 15**. The tile shown was independently digitized by two originators: Originator A mapped 49 features, while Originator B identified 44. Upon review, a reconciled version of the tile was created by synthesizing the two interpretations. This review led to the identification of new features, refinement of existing geometries, and in some cases, the exclusion of ambiguously mapped polygons. The final QA-approved inventory for the tile included 80 features—some newly introduced, while others were redrawn

for greater precision or subdivided into more accurate representations. Polygons with overly complex geometries or questionable provenance were removed to preserve interpretive clarity and dataset integrity.

This rigorous QA process was particularly crucial for the Christchurch 2011 inventory, where cleanup efforts had already begun at the time of image acquisition. In such contexts, the visual evidence of liquefaction was often degraded or altered, requiring additional scrutiny and conservative decision-making during feature inclusion. The QA framework implemented in this study thus served not only as a mechanism for quality control but also as a methodological safeguard to enhance the interpretive robustness of the final inventories.

Figure 15: Comparison of feature delineation by two originators for a single imagery tile. Originator A initially mapped 49 features, while Originator B mapped 44 features. After a thorough review and standardization process, the final inventory included 80 features—primarily consisting of redrawn features, separated smaller features, and a few newly identified ones.

1.4.2 Completeness

The completeness of the liquefaction feature inventories developed in this study is subject to several critical limitations. First and foremost, features included in the final datasets were constrained by time, personnel resources, and interpretability. Only those manifestations that were well-defined, visually discernible, and bounded with reasonable confidence were retained. Features exhibiting ambiguous geometry or uncertain classification were deliberately omitted following final quality assurance review. This decision reflects a prioritization of accuracy and consistency over exhaustive coverage, acknowledging that a fully comprehensive inventory would require substantially greater time, imagery processing capacity, and human resources.

The inherent incompleteness of these inventories was further compounded by limitations in both imagery availability and ground truth data quality, as discussed in preceding sections. In particular, spatial gaps in image

coverage, cloud obstructions, vegetation interference, and inconsistencies in ground truth coordinates contributed to an underrepresentation of actual liquefaction occurrences. In areas lacking high-confidence ground truth points, or where satellite imagery failed to adequately capture surface manifestations, features may have gone undetected or unverified.

An important methodological question arises from these limitations: how incomplete is incomplete? To explore this, a relative comparison was made between the Haiti inventories and the published USGS liquefaction polygon dataset for the 2020 M6.4 Puerto Rico earthquake. Given comparable tectonic settings, similar urban development patterns, and shared challenges in post-event data acquisition across these regions, the comparison offers a contextually relevant baseline for assessing relative feature density and spatial coverage.

The USGS dataset for Puerto Rico includes 43 liquefaction polygons totaling 0.15 km² in area. By comparison, the 2010 Haiti inventory comprises 91 polygons (0.04 km² total area), while the 2021 Haiti inventory includes 11 polygons (0.01 km²). These totals produce a relative coverage ratio of approximately 2:1 (Haiti 2010 to Puerto Rico) and 1:4 (Haiti 2021 to Puerto Rico), suggesting both event-specific variation and disparities in data resolution.

However, these ratios are inherently misleading as indicators of completeness. In the 2010 Haiti dataset, for instance, features such as lateral spreading were often delineated as fragmented ground displacements—resulting in the same phenomenon being represented by multiple polygons. This form of double-counting inflates the polygon count and artificially elevates the perceived completeness of the dataset. Thus, polygon counts alone are a flawed metric for inventory completeness, particularly when feature type and delineation style vary across datasets.

Moreover, the spatial extent of digitized features captures only a fraction of the total liquefaction hazard zone. According to USGS estimates based on the Zhu et al. (2017) probabilistic liquefaction model, the 2010 M7.0 Haiti earthquake affected an area of over 100 km², while the 2021 M7.2 Haiti event produced a similarly broad hazard footprint. In contrast, the Puerto Rico earthquake affected an estimated 10 km². When comparing digitized coverage against these hazard areas, the coverage rates are as follows:

- Puerto Rico: 0.15 km² / 10 km² = 1.5% coverage
- Haiti 2010: 0.04 km² / 100 km² = 0.04% coverage
- Haiti 2021: 0.01 km² / 100 km² = 0.01% coverage

These values highlight the substantial underrepresentation inherent in image-based inventories, even under favorable conditions. For Christchurch, this limitation is even more pronounced: only 51 out of 1,785 available

imagery tiles (2.8%) were used for digitization, further emphasizing the methodological constraint on inventory completeness due to resource limitations and targeted tile selection.

In summary, while polygon count and total area provide a rough estimate of inventory density, they are insufficient—and potentially misleading—as standalone measures of completeness. Fragmented representations of continuous phenomena, such as lateral spreading, distort the relationship between feature count and actual surface impact. Furthermore, meaningful completeness assessments must account for the spatiotemporal variability of image quality, the limitations of supporting ground truth data, and the probabilistic nature of liquefaction modeling itself. As such, the inventories presented here should be interpreted as representative, rather than exhaustive, visualizations of liquefaction effects in each case study.

1.4.3 Accuracy

Achieving a consistent and interpretable liquefaction inventory required addressing several challenges associated with the accurate interpretation of ground-truth data and the selection of appropriate remote sensing imagery. A critical component of this process involved establishing a standardized definition for what constitutes a visible surface manifestation of liquefaction, grounded in the visual analysis of post-event imagery. Liquefaction-induced surface effects are inherently heterogeneous in terms of size, shape, texture, and coloration, making it difficult to develop a universally applicable classification framework—particularly for subtle or spatially diffuse phenomena, such as level-ground liquefaction.

Liquefaction surface manifestations may include but are not limited to: lateral and vertical ground displacements, bearing capacity failures, sand boils or “volcanoes,” sediment ejecta, and mixtures of expelled water and soil. These effects can result in damage such as fissuring of pavements, structural tilting or settlement, foundation collapse, uplift of underground infrastructure, and bridge failures. However, not all these manifestations are readily visible or distinguishable from satellite or aerial imagery, particularly when subtle, obscured by vegetation, or degraded over time.

To preserve consistency and ensure that only features aligned with the study’s operational definition were included, certain categories of damage—such as general road fissures or structural settlement—were excluded from the inventories unless they were directly associated with clearly interpretable liquefaction-related signatures. For the purpose of this study, *visible liquefaction* was defined as any observable evidence of wetness, fragmented or displaced ground (e.g., lateral spreading), or sediment ejecta. For example, lateral spreading was inferred from missing land

segments or shoreline shifts observed via visual change detection between pre- and post-event imagery. Similarly, features such as slurry deposits, localized ponding, or residual stains—particularly when corroborated by ground-truth data—were classified under the label "Water Ejecta."

To evaluate the confidence and reliability of each digitized feature, four core attributes were assigned to every polygon in the inventory:

- `SUPPORTING_EVIDENCE`: This attribute records the source of validation for each feature, including direct reference to ground-truth data or corroborating evidence from published field reconnaissance reports and technical literature. It distinguishes features identified solely through visual analysis from those confirmed by field observations.
- `GROUND_FAILURE_CERTAINTY`: This field captures the level of confidence in the classification of the feature as a liquefaction manifestation. It is based on the investigator's judgment, informed by visual cues in the imagery and contextual knowledge. This attribute is especially critical given the subjective nature of visual interpretation in cases with limited ground verification.
- `POLY_BOUNDARY_CERTAINTY`: This attribute assesses the degree of confidence in the spatial delineation of each polygon. It is used to highlight cases where the edges of a feature may be indistinct or ambiguous due to image resolution, overlapping ground effects, or post-event modifications.
- `OVERALL_CERTAINTY`: This composite attribute synthesizes both the classification confidence and boundary delineation confidence into a single holistic score. It provides an overarching assessment of each feature's reliability and is used to inform filtering or weighting procedures in subsequent analyses (see **Table 5** for domain values and definitions).

By incorporating these attributes into the classification workflow, the study ensures a systematic and reproducible approach to feature interpretation, allowing for consistent classification across different investigators and case studies. The use of standardized domain values further enhances the interoperability of the inventories, enabling future integration into automated detection workflows and cross-event comparative analyses.

Table 5: Certainty attributes used to assess the accuracy of each case study inventory. This table presents the relationships between two key attributes used to evaluate the reliability and certainty of the liquefaction features identified in the inventory: Ground Failure Certainty and Polygon Certainty.

Ground Failure Certainty	Polygon Certainty	Overall Certainty
Certain	Certain	**Certain**
Certain	Uncertain	**Probable**
Uncertain	Certain	**Uncertain**
Uncertain	Uncertain	**Uncertain**
Probable	Certain	**Probable**
Probable	Uncertain	**Uncertain**

Although existing literature frequently advocates for the establishment of a minimum mapping threshold to enhance inventory completeness and reliability, no consistent or event-agnostic threshold was implemented in this study. This decision was not an oversight, but rather a deliberate methodological choice informed by the inherent heterogeneity of liquefaction manifestations across the three case study regions. Each seismic event produced distinctly different surface expressions of liquefaction—ranging in size, morphology, and visual clarity—which posed significant challenges to the adoption of a standardized size-based exclusion criterion. These challenges are further compounded by the context-specific nature of liquefaction processes, which depend on localized subsurface conditions, built environment interactions, and the timing and intensity of post-event imagery acquisition.

As illustrated in **Figure 16**, the wide variability in mapped feature areas across the three inventories—and in comparison to the U.S. Geological Survey's (USGS) inventory for the 2020 M6.4 Puerto Rico earthquake—highlights the difficulty in applying a consistent minimum-size threshold. The boxplots in **Figure 16** demonstrate a substantial range of feature sizes, underscoring both inter-event variability and intra-inventory dispersion. This variability reflects not only genuine differences in liquefaction characteristics but also methodological influences, such as the resolution of the imagery used and the subjective precision applied during manual polygon delineation.

In high-resolution imagery, such as that used for the Christchurch inventory, smaller features could be identified and delineated with relatively high spatial precision, resulting in a greater number of compact polygons. In contrast, lower-resolution imagery—as encountered in portions of the 2021 Haiti dataset—often necessitated the aggregation of diffuse or visually ambiguous features into larger, more generalized polygons. Consequently, feature size became more reflective of image resolution and mapping fidelity than of actual physical dimensions of the phenomena, making the application of a rigid threshold methodologically inappropriate.

Given these constraints, the methodological focus of the study shifted toward standardizing the classification process and clearly defining the visual and contextual attributes that characterized mappable liquefaction features.

Rather than exclude features based on size alone, the study relied on qualitative and interpretive confidence measures to assess reliability. The attributes `SUPPORTING_EVIDENCE`, `GROUND_FAILURE_CERTAINTY`, `POLY_BOUNDARY_CERTAINTY`, and `OVERALL_CERTAINTY` collectively served to document the rationale for feature inclusion and the confidence in their delineation. This approach preserved transparency and accountability in the inventory development process, while acknowledging the methodological limitations imposed by spatial resolution and interpretive subjectivity.

While no formal size threshold was applied, the integrity of the inventories was maintained through standardized digitization protocols and the systematic use of interpretive confidence metrics. This approach allowed for greater flexibility across diverse case study conditions while ensuring that mapped features met minimum standards for visual and contextual reliability.

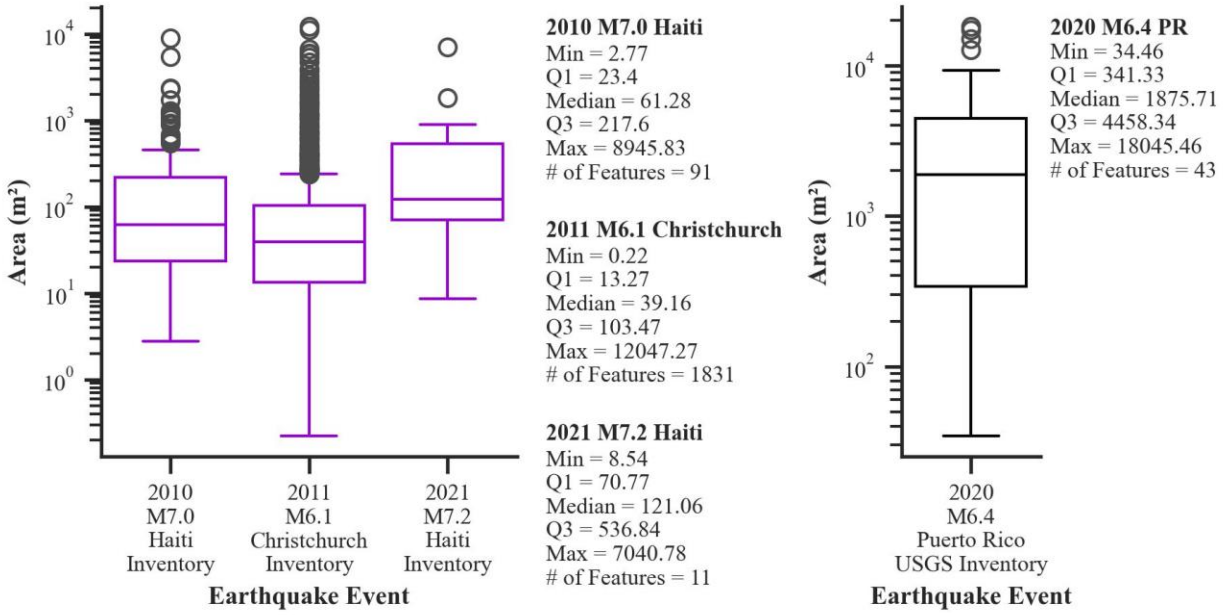

Figure 16: Distribution of liquefaction feature areas for the 2010 M7.0 Port-au-Prince, Haiti; 2011 M6.1 Christchurch, New Zealand; 2021 M7.2 Nippes, Haiti earthquakes; and 2020 M6.4 Puerto Rico included for comparative purposes.

Figure 17 presents the distribution of liquefaction features by Overall Certainty classification for the three inventories developed in this study, alongside the USGS inventory for the 2020 M6.4 Puerto Rico earthquake. The purpose of this comparison is to assess the level of interpretive confidence associated with each inventory and to contextualize the impact of data quality, imagery resolution, and ground-truth availability on classification reliability.

For the Puerto Rico dataset, certainty classifications follow the USGS schema: a value of "1" denotes the highest level of confidence, corresponding to features that were field verified at well-documented locations and

strongly attributed to liquefaction. A value of "2" indicates moderate certainty, assigned to field-verified features with ambiguous origins or uncertain linkage to liquefaction processes. A value of "3" reflects the lowest certainty level, reserved for features identified solely through satellite imagery in the absence of field verification.

As illustrated in the figure, the Christchurch inventory exhibits the highest proportion of features classified as "Certain," with 82.1% of the digitized features falling into this category. Similarly, the Puerto Rico inventory shows a high level of classification confidence, with 81.4% of features assigned a certainty value of "1." These two inventories—while developed using different classification systems—are comparable in terms of the overall proportion of high-certainty features. This similarity reflects the robust field documentation available for both events, as well as the availability of high-resolution imagery that facilitated confident visual interpretation.

In contrast, the 2021 Haiti inventory demonstrates the highest level of classification uncertainty, with 81.8% of features (9 out of 11) categorized as "Uncertain." This elevated uncertainty is attributable to multiple factors, including sparse ground-truth data, limited post-event field reconnaissance, and the presence of cloud cover and vegetation that impaired visibility in satellite imagery. The lack of high-quality, validated reference points and the reliance on lower-resolution or obstructed imagery substantially limited the confidence with which features could be delineated and attributed to liquefaction.

These differences underscore the critical role of supporting data—particularly field verification—in establishing interpretive confidence in remotely sensed liquefaction inventories. While standardized classification frameworks and consistent digitization protocols were applied across all case studies, the reliability of the resulting inventories ultimately reflects the quality of the underlying data inputs and environmental conditions during image acquisition.

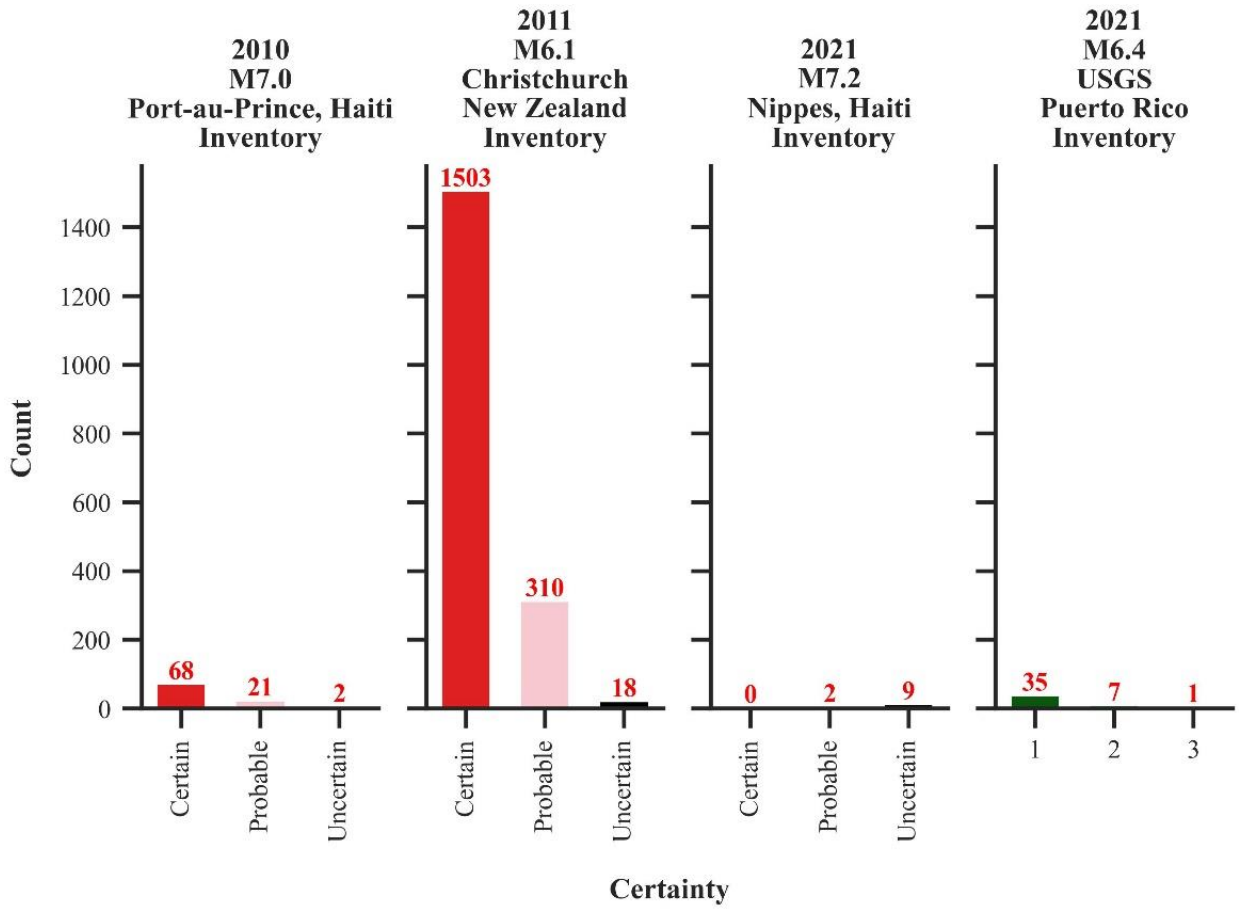

Figure 17: Distribution of liquefaction feature counts categorized by "Overall Certainty" for the inventories developed for the 2010 M7.0 Earthquake in Port-au-Prince, Haiti, the 2011 M6.1 Earthquake in Christchurch, New Zealand and the 2021 M7.2 Earthquake in Nippes, Haiti along with the Certainty classification for the 2021 M6.4 Puerto Rico earthquake inventory, as defined by the USGS. For the Puerto Rico inventory, a "1" denotes the highest certainty, assigned to features that were field-verified at well-known locations and are highly likely to be related to liquefaction; a "2" represents features that were field-verified but may or may not be associated with liquefaction; and a "3" indicates the lowest certainty, assigned to features mapped using satellite imagery without field verification.

1.5 Inventory Summary

This section synthesizes the key characteristics of liquefaction features documented across the three case studies, with emphasis on the relationship between ground truth data availability, image resolution, and the resulting inventory content. **Table 6** presents a comparative overview of the digitized features for the 2010 M7.0 Haiti, 2011 M6.1 Christchurch, and 2021 M7.2 Haiti earthquakes. The table categorizes features by type, supporting evidence, color classification, location of impact, and overall certainty. Supplementary visual materials—including representative feature maps and summary graphics—are provided in **Appendix B** and **Appendix C**, respectively.

The scope and completeness of each inventory were strongly influenced by the availability of high-resolution imagery, the extent of post-event field reconnaissance, and the quality of ground truth documentation. Among the

three events, the 2011 Christchurch earthquake inventory is the most comprehensive, comprising 1,831 liquefaction features, due to the availability of detailed reconnaissance data and high-resolution post-event aerial imagery. In contrast, the inventories for the 2010 and 2021 Haiti events include 91 and 11 features, respectively—reflecting more limited data access and less favorable imaging conditions.

The distribution of liquefaction feature types varied substantially across the events. In Christchurch, sand ejecta was the most frequently observed manifestation, comprising 1,275 of the total features. The 2010 Haiti inventory was dominated by water ejecta (64 instances), while the 2021 Haiti inventory contained relatively few instances of any feature type. These differences suggest both variation in the physical expression of liquefaction and disparities in observational capacity across the study areas. The Christchurch event, in particular, exhibited more spatially extensive liquefaction, especially in urban and peri-urban zones.

Patterns in the supporting evidence attribute further reinforce the relationship between data availability and inventory completeness. Christchurch recorded the highest number of features documented using both ground truth observations and image-based interpretation, while 64% of features in the 2021 Haiti inventory (7 out of 11) were classified as image-based only. This reflects either the absence of reliable ground-truth data or spatial misalignment between the imagery and documented observations. The designation “Both” was applied when features were supported by both field validation and visually discernible indicators in the imagery. Christchurch had the highest absolute and proportional count of features in this category, underscoring the robustness of its documentation process.

The color classification of liquefied deposits varied by event, primarily influenced by the timing of image acquisition and site-specific soil conditions. The Christchurch dataset was dominated by dark-colored sediments (1,084 instances), likely due to the high moisture content of recently ejected material captured just two days post-event. In contrast, the 2010 Haiti inventory exhibited a more balanced distribution between light and dark-colored deposits, suggesting greater variability in sediment exposure, drying, or imaging conditions.

The location of impact categories reveal further differences in the spatial extent and infrastructural consequences of liquefaction. In Christchurch, liquefaction was observed in diverse settings, with features documented on roads (584 instances), open fields (444), and driveways (249), reflecting widespread disruption in residential and transportation networks. By comparison, the 2010 Haiti inventory was concentrated at seaport locations (75 instances), while the 2021 Haiti inventory recorded only isolated occurrences with minimal infrastructural overlap. These findings

suggest a greater degree of urban exposure and damage potential in Christchurch relative to the Haitian case studies, although they may also reflect the differing scope of field investigations and imaging coverage.

Lastly, the overall certainty metric highlights the relative confidence in feature classification across events. Christchurch contained the highest number of features labeled as certain (1,503 instances), with an additional 310 features designated as probable. In contrast, the 2010 Haiti inventory included 68 certain and 20 probable classifications, while the 2021 Haiti inventory included only 6 certain and 2 probable features. These patterns reinforce the conclusion that the Christchurch inventory was both the most comprehensive and the most rigorously validated, benefiting from timely field verification and superior imagery quality.

Table 6: Comparative overview of liquefaction features documented for the 2010 M7.0 Haiti Earthquake, 2011 M6.1 Christchurch Earthquake, and 2021 M7.2 Haiti Earthquake.

		2010 Haiti	2011 Christchurch	2021 Haiti
Feature Type	Lateral Spreading	26	6	8
	Sand Ejecta	0	1,275	0
	Water Ejecta	64	282	3
	Other	1	268	0
Supporting Evidence	Digitized from points or polygons provided in reconnaissance study	2	8	4
	Visual interpretation of liquefaction ground failure occurrence	7	703	7
	Both	82	1,120	0
Color	Dark	0	1,084	0
	Light	64	171	1
	Other	27	576	10
Location of Impact	Driveway	0	249	0
	Free Field	8	444	2
	Parking Lot	0	69	0
	Recreational Field	0	357	0
	Road	0	584	0
	Seaport	75	0	0
	Sidewalk	0	72	0
	Miscellaneous Coastline	8	0	6
	Other	0	56	3
Overall Certainty	Certain	68	1,503	0
	Uncertain	2	18	9
	Probable	21	310	2

1.5.1 Inventory Application

Libraries and geospatial datasets developed in the aftermath of disasters play a critical role in characterizing event impacts, guiding emergency response, and informing both policy and infrastructure resilience planning. The completeness and accuracy of such datasets are paramount, as they underpin evidence-based decision-making, support

analytical research, and provide training data for the development of predictive models. In the context of this study, the event-specific liquefaction inventories were designed not only as static post-disaster records, but also as foundational datasets for the advancement of machine learning methodologies—particularly those using computer vision to enhance and automate reconnaissance workflows.

The integration of computer vision in disaster reconnaissance holds the potential to significantly expand and refine post-event datasets. While the application of these inventories remains at the discretion of the end user, the following section outlines practical pathways for leveraging the developed shapefiles and associated imagery in semi-supervised image classification workflows. These computer vision techniques offer a pathway to scale post-disaster mapping beyond the limits of manual digitization, particularly when integrated with the structured, polygon-based inventories developed in this study. Whether used for quality control, inventory completion, or future disaster response training, these tools hold promise for expanding the role of remote sensing and machine learning in geotechnical hazard assessment.

1. Image classification and Object Detection

All computer vision methodologies, regardless of complexity, require a labeled training set to initiate the model-building process. The inventories developed here provide such a foundation, offering binary-labeled polygons representing documented liquefaction occurrences. These shapefiles, paired with the associated satellite or aerial imagery, allow users to generate labeled image tiles suitable for model training and testing. If desired, users may manually expand the training set by delineating additional features, following the methodology described in this study and demonstrated by Asadi et al. (2023).

Image classification is the most fundamental approach, wherein an entire image is assigned to a predefined category based on its visual properties (Hafiz and Bhat, 2020; Hoeser and Kuenzer, 2020). For example, users could train a model to distinguish between images containing liquefaction features and those that do not. However, this method provides only image-level labels, making it better suited for detecting global or qualitative properties—such as overall image clarity—rather than specific object locations (**Figure 18a**).

In contrast, object detection techniques provide more spatially explicit outputs by identifying and localizing specific objects within an image. These algorithms detect and return bounding boxes around regions of interest—in this case, liquefaction features (Gu et al., 2022; Hoeser and Kuenzer, 2020). While this method offers actionable

location data (**Figure 18b**), bounding boxes do not precisely delineate object boundaries, and therefore cannot be reliably used to estimate feature areas—a critical parameter for geospatial hazard assessments.

2. Image Segmentation

Image segmentation methods address the limitations of classification and object detection by offering pixel-level delineation of features. In semantic segmentation, each pixel in an image is assigned a class label, producing more detailed spatial representations of liquefaction features. When applied to this study's inventory, semantic segmentation would identify all pixels associated with liquefaction, regardless of subtle within-class variations such as material color or shape (Gu et al., 2022). For example, both dark and light ejecta would be grouped under a single "liquefaction" label (**Figure 18c**).

A more advanced variant, instance segmentation, combines the benefits of object detection and semantic segmentation. This technique not only delineates each pixel belonging to a liquefaction feature but also distinguishes between separate instances of similar features (Gu et al., 2022; Hafiz and Bhat, 2020). In the context of this research, instance segmentation enables more granular mapping by distinguishing between individual liquefaction features and separating them from adjacent structures or background elements, such as vegetation or buildings **(Figure 18d**). Unlike semantic segmentation, which aggregates all similar features into a single class, instance segmentation treats each occurrence independently, allowing for precise area estimation, typological classification, and spatial distribution analysis.

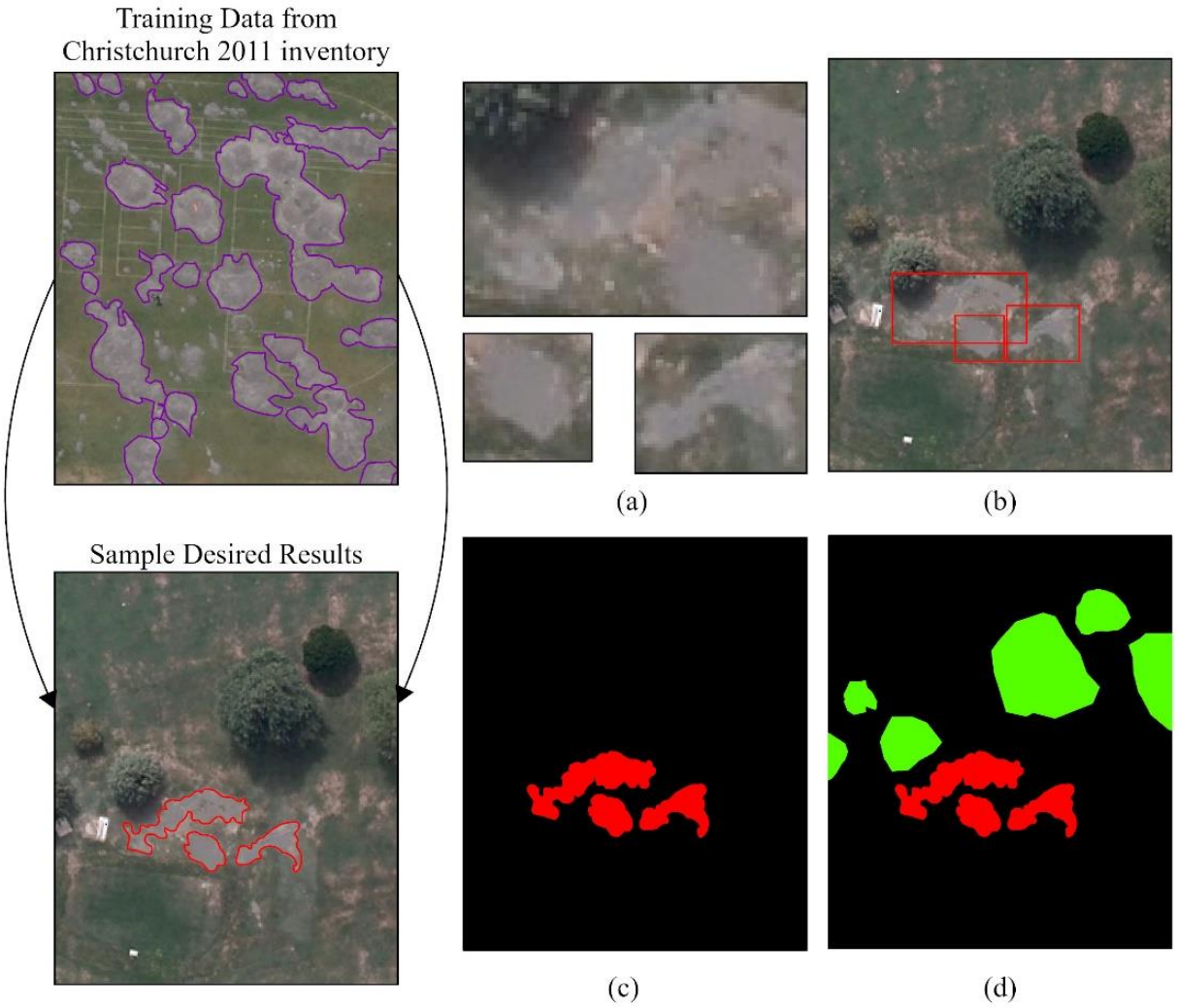

Figure 18: Examples of different image analysis techniques for liquefaction detection. (a) Image classification: liquefaction manifestations are identified based on a training dataset. (b) Object detection: bounding boxes are used to outline liquefaction features. (c) Semantic image segmentation: individual pixels belonging to liquefaction features are categorized and localized within the image. (d) Instance segmentation: unique liquefaction features are differentiated with pixel-level precision, offering a detailed and granular understanding of each feature. These techniques can enhance the accuracy and completeness of the event inventories by providing varying levels of detail in detecting and delineating liquefaction features.

1.6 Conclusion

Following an earthquake, the systematic documentation and dissemination of lessons learned are essential for advancing both engineering practice and geohazard research. Inventories of observed impacts serve a critical role in understanding ground failure mechanisms, supporting the development of predictive models, and informing disaster risk reduction strategies. Among secondary seismic hazards, earthquake-induced liquefaction remains a particularly consequential phenomenon due to its potential to cause widespread damage to lifelines, infrastructure, and the built

environment. Comprehensive inventories of liquefaction manifestations not only enable regional risk assessments but also contribute to the global understanding of liquefaction processes and their consequences.

This study developed and tested a standardized methodology for creating spatially accurate, polygon-based inventories of liquefaction surface manifestations using high-resolution imagery and validated ground truth data. The approach was designed to be both scalable and adaptable across diverse geologic, geographic, and data-availability contexts. Three significant earthquake events were selected as case studies to evaluate the method's applicability and robustness: the 2010 M7.0 Port-au-Prince, Haiti earthquake; the 2011 M6.1 Christchurch, New Zealand earthquake; and the 2021 M7.2 Nippes, Haiti earthquake. These events were chosen to reflect a range of seismic environments, imagery types, and levels of ground truth documentation.

It is important to emphasize that the resulting inventories are not intended to be exhaustive. Their incompleteness reflects known limitations associated with data availability, image resolution, ground access, and the transient nature of surface effects. However, this limitation simultaneously highlights the potential for future refinement—through additional field surveys, integration of higher-resolution or multispectral imagery, and the application of advanced machine learning models. In regions where ground truth data are sparse, inventories such as those developed in this study can serve as a foundation for gap-filling and model training.

The methodology emphasized the use of near real-time post-event imagery—acquired shortly after each earthquake—to capture perishable surface features before degradation or cleanup activities altered their appearance. Pre-event imagery was used as a baseline for change detection and contextual analysis. Ground truth data were primarily sourced from reputable reconnaissance reports, including those published by the Geotechnical Extreme Events Reconnaissance (GEER) Association and the U.S. Geological Survey (USGS). Where available, these datasets provided essential verification of visually identified liquefaction features.

The study also required a deliberate and context-specific operational definition of visible liquefaction. While liquefaction is fundamentally a subsurface process, surface manifestations such as lateral spreading, sand boils, and sediment ejecta were prioritized for inclusion. In certain cases—particularly in regions with dense vegetation or limited resolution—indirect indicators such as water stains, ponding, and anomalous sediment deposits were also mapped under a broadened definition of visible liquefaction.

Despite challenges related to inconsistent image quality, limited spatial coverage, and the manual nature of the digitization process, this research generated important methodological insights. These lessons inform the following set of recommendations for future liquefaction inventory development:

- **Use Polygon-Based Mapping of Individual Surface Features**

  Rationale: Polygon geometries provide precise spatial boundaries, offering greater fidelity than point data and avoiding overgeneralization associated with region-wide shapefiles.

- **Incorporate Binary and Categorical Labels for Each Feature**

  Rationale: Binary labels (e.g., occurrence/non-occurrence) enable rapid classification, while categorical labels (e.g., sand ejecta, lateral spreading) allow for nuanced analysis. Bibliographic metadata improves traceability.

- **Prioritize Near Real-Time Post-Event Imagery Acquisition**

  Rationale: Surface manifestations of liquefaction are ephemeral. Early imagery acquisition preserves the spatial accuracy of features prior to environmental alteration or anthropogenic disturbance.

- **Ensure Imagery Coverage of the Entire Impacted Region**

  Rationale: Comprehensive spatial coverage minimizes geographic bias and ensures that unmapped features are not erroneously excluded due to limited image availability.

- **Use Very High-Resolution Imagery (Preferred <2m GSD)**

  Rationale: High-resolution data is critical for identifying and delineating small-scale liquefaction features that may be invisible in lower-resolution datasets.

- **Leverage Pre-Event Imagery for Contextual and Comparative Analysis**

  Rationale: Pre-event imagery supports change detection and improves feature validation in areas lacking ground truth data.

- **Distribute Inventories in Transferable, GIS-Compatible Formats**

  Rationale: Shapefiles and GeoJSONs promote accessibility, interoperability, and integration into risk models, decision-support tools, and computer vision workflows.

These recommendations, drawn directly from the implementation and evaluation of the proposed methodology, establish a framework for future liquefaction inventories that emphasizes accuracy, scalability, and data transparency.

By contributing standardized inventories and clear methodological guidance, this work supports broader efforts to enhance post-disaster data collection and inform more resilient engineering, planning, and policy decisions.

1.7 Data and Resources

All images and ground truth data used in this study are publicly accessible and have been properly cited in accordance with the relevant sources.

1.8 Project Acknowledgements

Many thanks to K. Boylan, J. Cornelius, S. Flower, L. Schwartz, and V. Yang for their involvement in helping to digitize the inventories for the 2010 M7.0 Port-au-Prince, Haiti and 2011 M6.1 Christchurch, New Zealand earthquakes.

Chapter 2: Building Damage Assessment and Retrofitting Prioritization in Massachusetts Using a High-Resolution Site Characterization Map

"An ounce of prevention is worth a pound of cure." — **Benjamin Franklin**

2.1 Significance of the Project

Mitigation serves as a cornerstone of disaster risk reduction by proactively addressing vulnerabilities and limiting the cascading consequences of natural hazards (Bullock et al., 2018; FEMA, 2024; UNDRR, 2015). Mitigation strategies encompass structural retrofitting, land-use planning, adoption and enforcement of up-to-date building codes, and ongoing public education initiatives (Burby & May, 1999; Musacchio et al., 2015; Zhang et al., 2021). These interventions not only reduce the likelihood of structural damage and casualties but also facilitate the rapid restoration of essential infrastructure systems following an event (D'Agostino et al., 2018; Salam & Khan, 2020).

Although Massachusetts is not commonly associated with high seismic hazard, its vulnerability is amplified by a confluence of aging infrastructure, limited adoption of seismic design standards in older construction, and pronounced geologic heterogeneity. Notably, the state exhibits strong impedance contrasts—particularly in urbanized regions such as Boston—where soft, shallow sediments overlie dense bedrock (Baise et al., 2016; Pontrelli et al., 2024). These conditions can lead to ground motion amplification by up to a factor of 10 (Baise et al., 2016), with potential for resonance effects that further elevate the risk of structural damage when seismic wave frequencies align with the natural frequency of buildings.

Traditional loss estimation models, particularly in regions of low-to-moderate seismicity, often rely on coarse geologic classification schemes and generalized assumptions about building stock. These simplifications can obscure localized risk concentrations, impeding the formulation of effective mitigation strategies. This chapter addresses these limitations by integrating a high-resolution site characterization map with a detailed inventory of state-owned buildings. The alignment of localized geotechnical data with nationally standardized modeling tools such as FEMA's HAZUS loss estimation framework enables a more granular and spatially explicit assessment of seismic risk.

The significance of this work lies in its practical applicability to real-world mitigation planning. By providing decision-makers with enhanced insight into the spatial distribution of risk and the vulnerability of critical structures, the analysis facilitates the prioritization of seismic retrofitting investments. This is particularly relevant in Massachusetts, where the combination of aging infrastructure and complex subsurface conditions warrants proactive risk reduction, despite the infrequency of major earthquakes.

Furthermore, the methodology presented herein offers a transferable model for other data-limited jurisdictions within the Central and Eastern United States (CEUS). It demonstrates how high-resolution geotechnical datasets and disaggregated structural inventories can be operationalized within standardized loss estimation tools to support risk-

informed decision-making. In doing so, this work contributes to broader efforts in enhancing seismic resilience and ensuring the long-term safety and functionality of the built environment.

2.2 Building Inventory

This analysis focuses on a curated subset of state-owned buildings in Massachusetts. While the findings may not fully represent the broader distribution of structures statewide, the methodology presented offers a scalable framework for earthquake hazard, vulnerability, and risk assessments. The results aim to inform targeted mitigation strategies, guide resource allocation, and enhance resilience—particularly in regions where local site conditions amplify seismic ground motions for this specific building portfolio.

The analyzed inventory comprises 2,676 state-owned buildings with diverse functional classifications (**Figure 1a**), spanning construction dates from 1658 to 2024. Although not exhaustive of all state-owned facilities, the dataset includes buildings from all 14 Massachusetts counties (**Figure 1b**) and captures the full range of soil conditions as defined by the median estimates of Vs_{30} (**Figure 1c**). Low-rise buildings dominate the inventory, accounting for approximately 91% of all structures (**Figure 1d**).

Buildings were categorized by primary lateral load-resisting system using FEMA HAZUS definitions. All HAZUS building types are represented except for Mobile Homes, with wood light-frame construction (W1) constituting the largest share at 38.3% (**Figure 1e**). Construction year was used to determine seismic design vintage, following HAZUS conventions for Uniform Building Code (UBC) Seismic Zone 2a: buildings constructed prior to 1976 are classified as pre-code (PC), those between 1976 and 2003 as low-code (LC), and those constructed after 2003 as low-special (LS) if they meet essential facility criteria.

The inventory includes 1,256 commercial buildings, 285 educational facilities, and 197 government buildings. Of these, 15 are COM6 (hospitals), 27 are EDU1 (K–12 schools), 258 are EDU2 (higher education), and 39 are GOV2 (emergency services), including 32 police stations and 7 fire stations. Pre-code buildings represent 69% of the total inventory, while only five essential facilities were built after 2003 (**Figure 1f**).

Building use and occupancy are classified per the International Building Code (IBC), which assigns structures to one of four Risk Categories (I–IV) based on societal importance and consequences of failure. Risk Category IV is reserved for critical infrastructure and life-safety facilities. In this study, all COM6, EDU1, EDU2, and GOV2 buildings are conservatively assigned to Risk Category IV.

Risk category assignments influence the Seismic Design Category (SDC), which integrates local seismic hazard with occupancy importance. SDCs are derived from the short-period (SDS) and 1-second (SD1) spectral response accelerations obtained from MCE_r ground motion parameters. Essential facilities with elevated risk categories are typically assigned more stringent SDCs to ensure performance during and after seismic events.

Figure 1g summarizes the intersection of Risk Category and SDC for the inventory. Most buildings (41.1%) fall within Risk Category II and 60% are in SDC A, reflecting relatively low seismic hazard. However, a subset of 195 buildings (7.3%)—classified as Risk Category IV and SDC C—represents essential facilities subject to moderate seismic hazard, necessitating heightened design considerations to ensure post-event functionality.

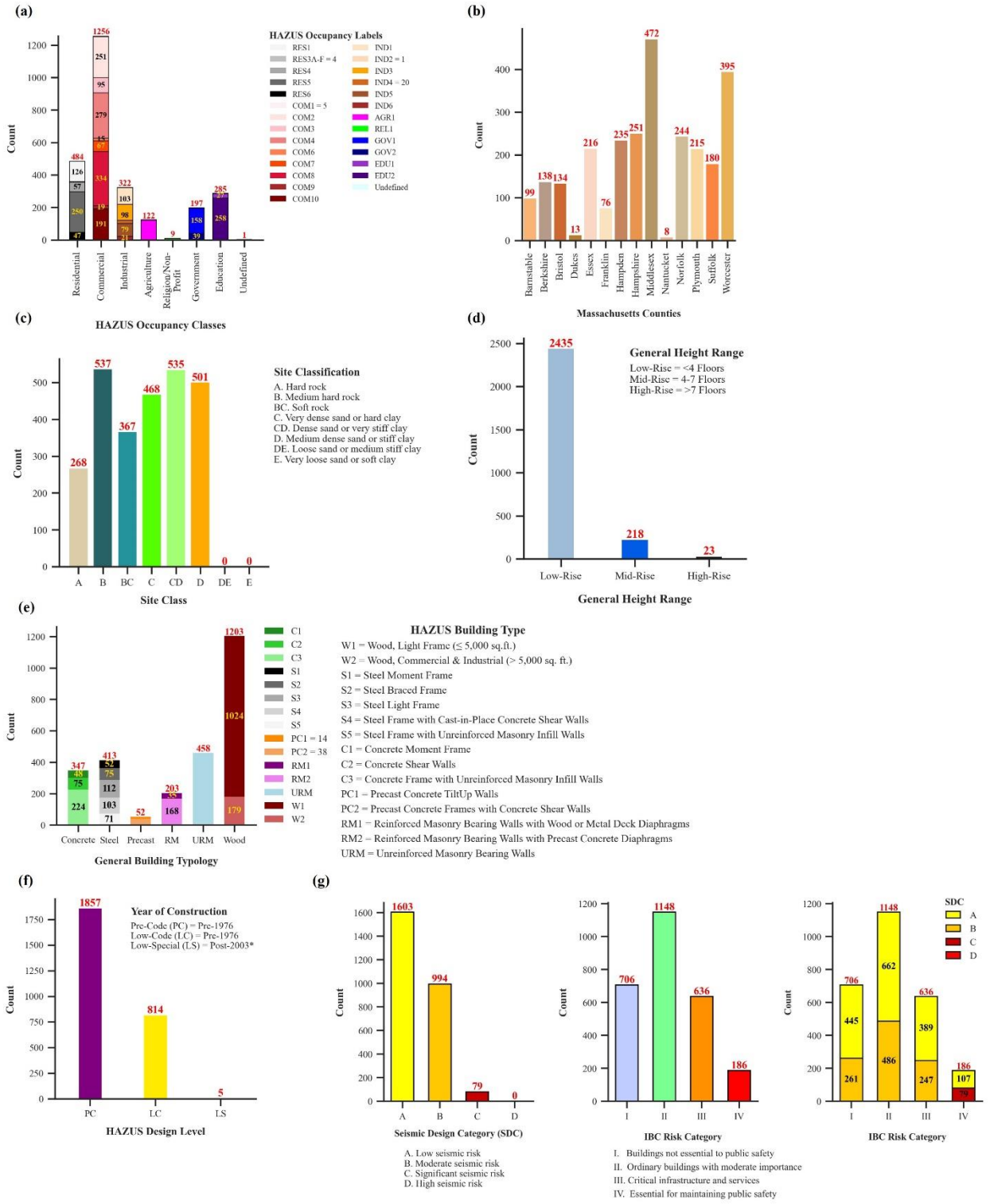

Figure 1: Summary of building inventory content. (a) Distribution of buildings by HAZUS Occupancy Classes. (b) Distribution of buildings across the 14 counties in Massachusetts. (c) Distribution of buildings by site classes. (d) Distribution of buildings by building height, generalized per FEMA HAZUS 6.1. (e) Distribution of buildings by construction material and structural system. (f) Distribution of buildings by design level, as determined from the year of construction. (g) Distribution of buildings by Risk Category and Seismic Design Category.

2.3 Summary of Fragility Analysis and Damage Estimation Methodology

This analysis evaluates the seismic vulnerability of 2,676 state-owned buildings across Massachusetts by integrating a high-resolution geotechnical and structural dataset. The building inventory includes critical structural and occupancy attributes—such as geographic location, occupancy classification, number of stories, construction material, and year of construction—which are used to assign each structure a FEMA HAZUS-defined structural typology.

Each building is spatially associated with a site class derived from a 100-meter resolution map of median Vs_{30} values. This map incorporates locally calibrated geologic and geophysical data, including surficial geologic units, horizontal-to-vertical spectral ratio (HVSR) measurements, and depth-to-bedrock information. For each site class, short-period (S_{ms}) and 1-second (S_{m1}) spectral acceleration values are extracted from the 2023 U.S. Geological Survey (USGS) National Seismic Hazard Model (NSHM), using risk-targeted Maximum Considered Earthquake (MCE_r) parameters.

A 5%-damped response spectrum is then generated for each building based on its site classification and the corresponding MCE_r ground motion values, with reductions applied to account for energy dissipation and hysteretic behavior. This spectrum is integrated with HAZUS-defined capacity curves—parameterized by building type, height classification, and seismic code level—to determine the spectral displacement at the intersection of seismic demand and structural capacity. Finally, HAZUS fragility functions—lognormal probability distributions calibrated to each structural typology—are applied to estimate the probability of exceeding four defined damage states: Slight, Moderate, Extensive, and Complete.

2.4 Results and Discussion

The analysis focuses on the probability of exceeding the moderate damage state, which serves as a critical threshold for assessing structural vulnerability under seismic loading. These estimated probabilities enable the prioritization of buildings based on their relative susceptibility to significant damage during a design-level seismic event. Although the assessment incorporates resonance effects—capturing the amplification of seismic forces due to alignment between structural and site natural frequencies—these effects are treated as a secondary differentiator. They are used to distinguish between buildings with otherwise similar damage probabilities. Further refinement of the resonance analysis is recommended to enhance its accuracy and integration within the overall vulnerability framework.

2.4.1 Describing the Cumulative Probability of Exceedance

The results presented in this section are based on the cumulative probability of exceeding the moderate damage state, which is widely regarded as a critical threshold in seismic performance assessments. At this level, a building's structural integrity may be compromised, though the facility may still remain operational. Exceedance of this threshold often marks a transition from functional continuity to significant disruption, with corresponding increases in required repair efforts and uncertainty regarding the building's role in post-earthquake recovery. As such, identifying and prioritizing buildings with a higher likelihood of reaching or surpassing the moderate damage state supports more focused and effective mitigation planning—particularly when compounded by additional risk factors such as structural resonance.

To enhance interpretability and support decision-making, the cumulative probabilities of moderate damage were stratified into three categories: low, moderate, and high risk. The low category is defined as a probability of 10% or less, with the 10% threshold selected based on the central tendency of the inventory's distribution of moderate damage exceedance probabilities. The moderate category corresponds to probabilities between 10% and 30%, while the high category includes values greater than 30%. The distribution of buildings across these risk levels is shown in **Figure 2**. Given the design-level ground motion has a 2% probability of occurrence in 50 years, the equivalent annualized probabilities are approximately 0.004% for 10% exceedance and 0.012% for 30% exceedance. Accordingly, the low, moderate, and high classifications correspond to annualized probabilities of less than 0.004%, between 0.004% and 0.012%, and greater than 0.012%, respectively.

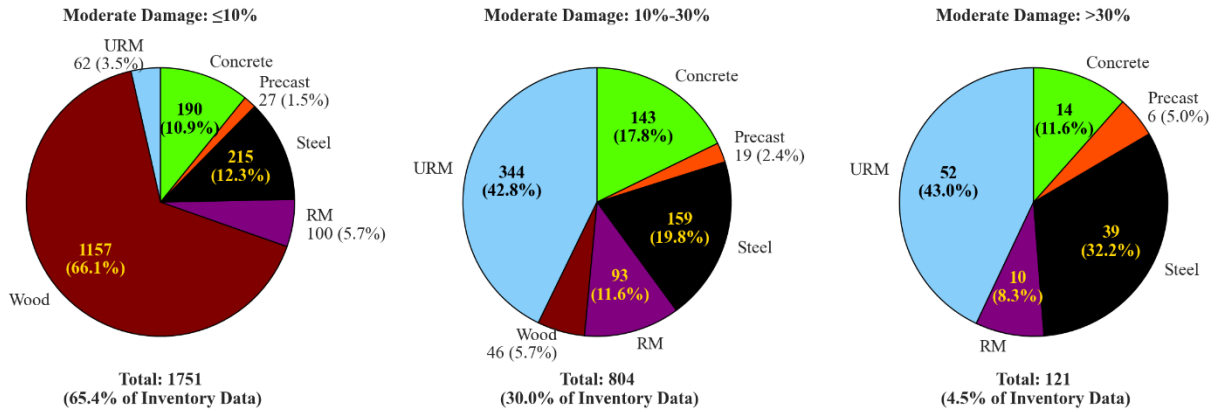

Figure 2: Distribution of Moderate Damage state threshold by building material.

As shown in **Figure 2**, 121 buildings—comprising 4.5% of the total inventory—fall into the high category for the cumulative probability of exceeding the moderate damage state. This category is predominantly composed of

Unreinforced Masonry (URM) buildings, which represent 43% of the high-risk group. URM structures also constitute 42.8% of the buildings in the moderate damage category. Collectively, these two categories encompass 396 of the 458 URM buildings in the inventory, underscoring the heightened seismic vulnerability of this structural typology.

While steel buildings are generally considered to have greater seismic resistance, a notable proportion of them are also classified in the high damage probability category (**Figure 2**). As detailed in **Figure 4**, among the 39 steel buildings in this category, 23 are classified as S3, 9 as S4L, and 7 as S5L. It is important to highlight that S5 structures—those with unreinforced masonry infill walls—are no longer permitted under current building code provisions, a restriction that also applies to C3 structures. The inventory includes 224 C3 buildings. Within the high-risk group, the majority of concrete buildings (9 structures) are low-rise C3L types.

Comparative analysis of building performance using capacity curves, shown in **Figure 3a**, reveals that certain steel structures—particularly S3 and S4L—exhibit lower lateral force resistance than other steel types. As illustrated in **Figures 3b and 3c**, fragility curves for S3 structures at Low-Code and Pre-Code design levels resemble those of URML buildings. For equivalent peak building responses beyond the capacity–demand intersection point (indicated in red), S3 buildings have a higher probability of exceeding the moderate damage threshold. Similarly, C3L buildings demonstrate greater exceedance probabilities than URMM structures prior to their intersection point (marked in purple).

According to the HAZUS 6.1 manual, building response is modeled as linear up to the yield point, transitioning to nonlinear (plastic) behavior between the yield and ultimate points. Beyond the ultimate point, the structure is assumed to enter a fully plastic state, maintaining constant strength through permanent deformation. Among the structural systems analyzed, W1 buildings display the most gradual transition and the broadest range between control points, indicating superior ductility and energy dissipation capacity. No wood structures were classified in the high damage category, suggesting that none exhibited a cumulative probability greater than 30% of exceeding the moderate damage state (**Figures 2 and 4**). In contrast, S3 and S4L buildings, characterized by lower strength and reduced deformation capacity, are more susceptible to significant damage under seismic loading.

As shown in **Figure 5**, the largest peak building responses were recorded for an S4L structure, followed by an S3 building. However, it is important to note that these responses are also influenced by site-specific ground motion parameters, as previously discussed.

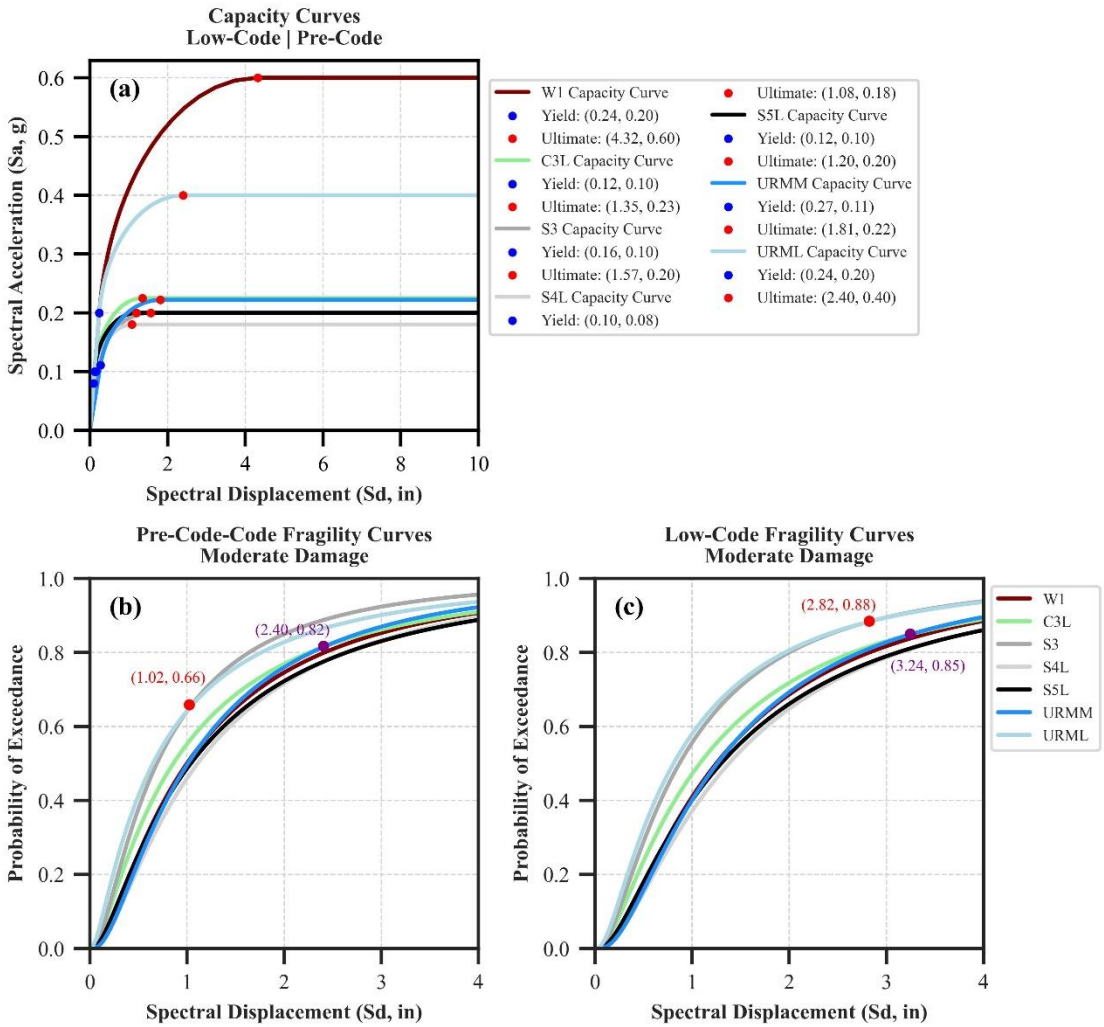

Figure 3: Comparison curves for selected building types: W1, C3L, S3, S4L, S5L, URMM, and URML. (a) Capacity Curves. (b) Fragility curve for Pre-Code design level. (c) Fragility curves for Low-Code design level.

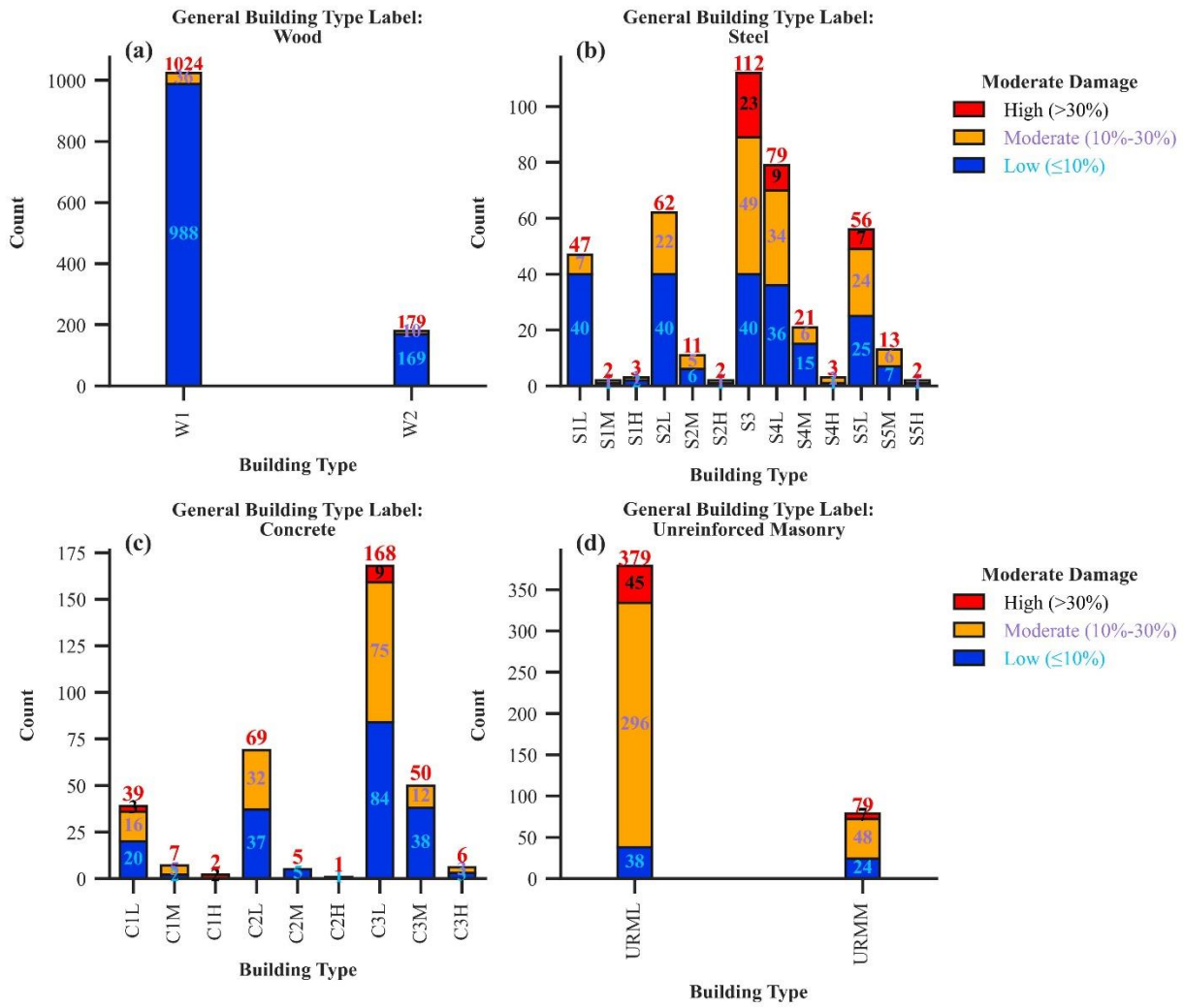

Figure 4: Distribution of select building materials within the Moderate Damage categories: (a) Wood; (b) Steel; (c) Concrete; and (d) URM. See Figure 1e for a definition of the HAZUS structural types.

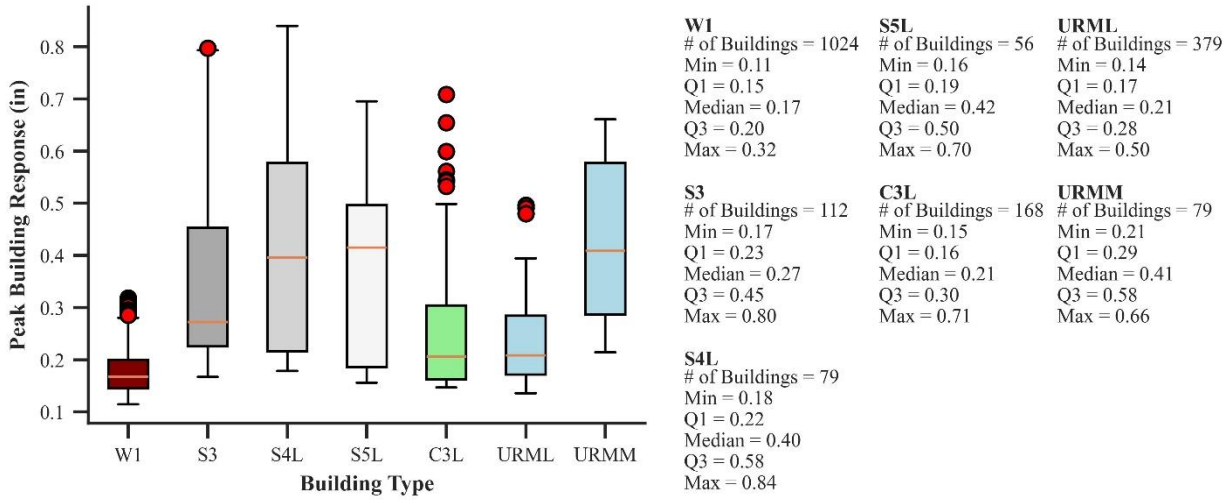

Figure 5: Boxplots of the peak building response for the selected building types: W1, S3, S4L, S5L, C3L, URML, URMM.

2.4.2 Secondary Effects

In addition to the primary effects of seismic events, secondary phenomena—particularly resonance effects—can substantially influence structural performance and overall seismic risk. These effects emerge from dynamic interactions between seismic ground motions and the natural frequencies of soil layers and structures. When the dominant frequency of ground motion closely aligns with a building's fundamental period, resonance may occur, resulting in amplified structural vibrations and elevated damage potential.

Resonance plays a critical role in seismic hazard assessments, especially in regions with significant impedance contrasts—sharp differences in seismic wave velocity between geologic layers. This condition is prevalent in many areas of Massachusetts, where soft, unconsolidated sediments frequently overlie stiff bedrock. The resulting velocity discontinuities alter wave propagation behavior, leading to amplification of ground motions at the surface. These localized amplifications can intensify structural demand and increase the probability of damage, even in regions traditionally classified as low-to-moderate seismic hazard zones. As such, the inclusion of resonance effects is essential for accurately evaluating seismic vulnerability and informing mitigation strategies in geologically complex environments.

2.4.2.1 Likelihood of Resonance

Resonance studies typically rely on computational modeling techniques or instrumentation-based methods to characterize the dynamic properties of buildings. These approaches often involve detailed architectural and structural information to determine natural frequencies and vibration modes (Trifunac et al., 2001a; 2001b; Doebling et al.,

1998; Li & Jirsa, 1998). As this study did not employ either of these techniques, building fundamental frequencies were estimated empirically using the relationship specified in ASCE 7-22 Table 12.8-2, which expresses the fundamental period as a function of building height (**Figure 6**). For each structural classification, this period was then converted to natural frequency by taking its inverse.

To assess the potential for soil-structure resonance, the estimated building frequencies were compared against the fundamental frequency of the underlying soil (f_0), derived from the spatial distribution of HVSR-based measurements (see Site Characterization). Resonance was considered likely where the building's estimated natural frequency approximated or matched the soil's f_0 at the same location.

This approach is consistent with methodologies applied in previous resonance studies. For example, Gosar et al. (2009) used the HVSR method to estimate both the building and free-field natural frequencies, identifying resonance where the two values closely aligned. Pinzón et al. (2019) employed a similar methodology in Barcelona, mapping soil periods and comparing them with building periods estimated from an empirical height-to-period relationship specified in the Eurocode. Tallini et al. (2020) also utilized this comparison-based approach to delineate resonance-prone zones in Central Italy. The methodology adopted in this study aligns with these established approaches, offering a practical proxy for resonance assessment in the absence of structure-specific dynamic data.

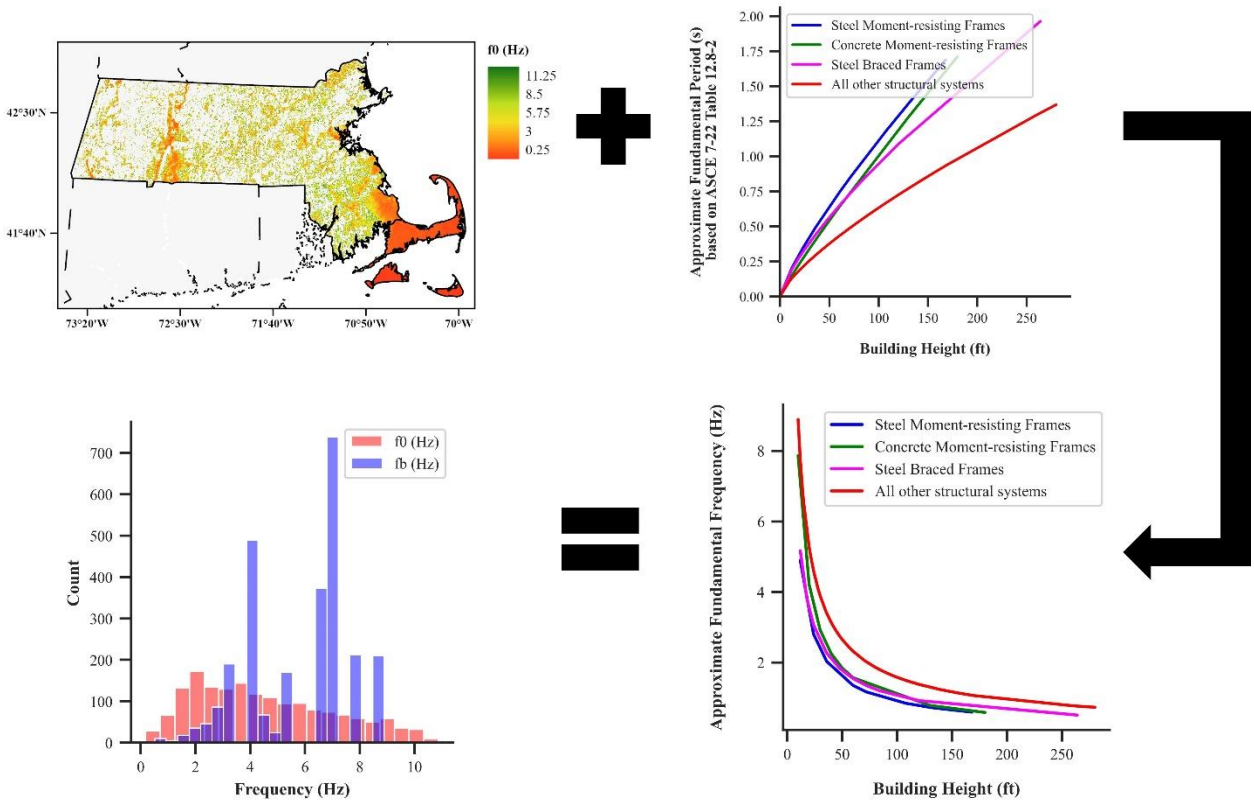

Figure 6: The natural frequency of the buildings was calculated using the inverse relationship between period and frequency, with the period determined from the approximate fundamental period equation in ASCE 7-22 Table 12.8-2. The percentage difference between the building frequency (f_b) and the natural frequency of the soil (f_0) at the site were compared to determine likelihood of resonance.

In this study, buildings were classified into three resonance likelihood categories based on the percentage difference between the estimated fundamental frequency of the structure and the underlying soil frequency (f_0). These categories are defined as follows: High likelihood (0–15% frequency difference), Moderate likelihood (15–25%), and Low likelihood (>25%), as shown in **Figure 7**. This classification follows the thresholds proposed by Gosar (2010), who identified ±15% as the critical range for potential soil-structure resonance, with increasing divergence indicating a reduced likelihood of resonance effects.

The distribution of buildings across these categories generally reflects the underlying distribution of structural typologies within the inventory rather than indicating systematic susceptibility tied to specific structural systems. While unreinforced masonry and certain steel frame buildings are represented across all categories, most structures fall within the Low resonance likelihood range, suggesting limited frequency overlap with site conditions. Nonetheless, given the pronounced impedance contrasts and resonance-prone soil profiles in regions such as the Boston Basin and the North Shore, the potential for resonance remains a relevant concern. Its possible presence in

structurally vulnerable buildings—particularly those with higher cumulative damage probabilities—warrants continued investigation and may inform targeted risk mitigation strategies.

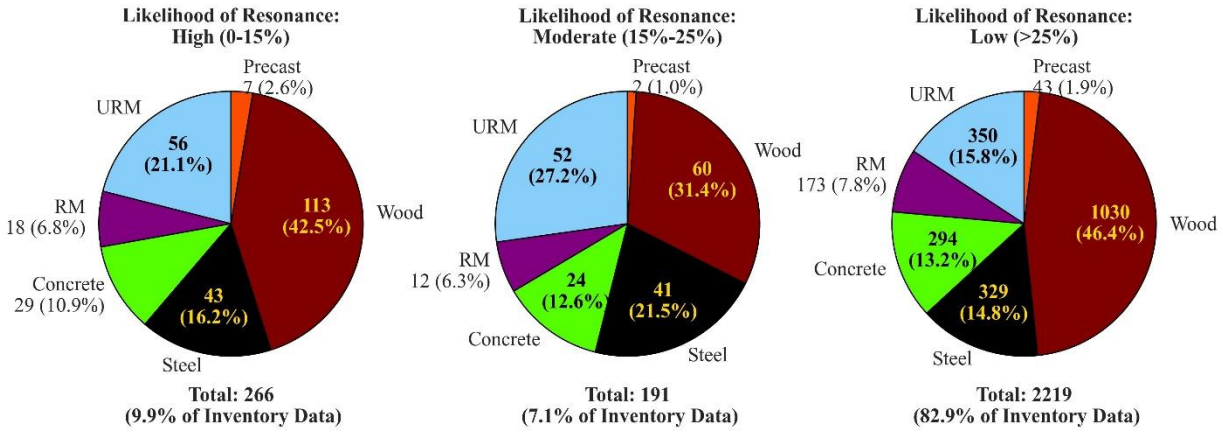

Figure 7: Distribution of likelihood of resonance by building material type.

The natural frequency of a building is primarily governed by its mass, height, and structural stiffness. Since a building's period is directly proportional to its height and inversely proportional to its natural frequency, taller structures typically exhibit lower natural frequencies and are therefore more susceptible to resonance with low-frequency seismic waves. Conversely, shorter buildings, which possess higher natural frequencies, are more sensitive to higher-frequency shaking. This general relationship is reflected in the trends shown in Figure 8.

Seismic wave behavior is further modulated by local site conditions. Buildings located on softer soils—particularly those classified as Site Classes C through E—are more prone to resonance effects due to the amplification of long-period seismic waves and the lower fundamental site frequencies (f_0) associated with these soil profiles. Taller buildings are especially vulnerable at such sites, as their lower structural frequencies are more likely to coincide with the site's natural frequency, amplifying seismic demand. In contrast, buildings on stiffer soils (e.g., Site Classes A and B) are less likely to experience resonance; any such effects are typically limited to short-period structures, such as low-rise buildings.

Within the inventory, 241 buildings are classified as mid- or high-rise. Of these, 131 are located on Site Classes CD and D, which exhibit higher susceptibility to amplification effects. Among this group, 23 buildings meet the criteria for a high likelihood of resonance, and another 23 exhibit a moderate likelihood. Additionally, 243 low-rise buildings located on soil classes with elevated f_0 values—primarily BC and C, as well as some within CD and D—also fall into the high resonance likelihood category.

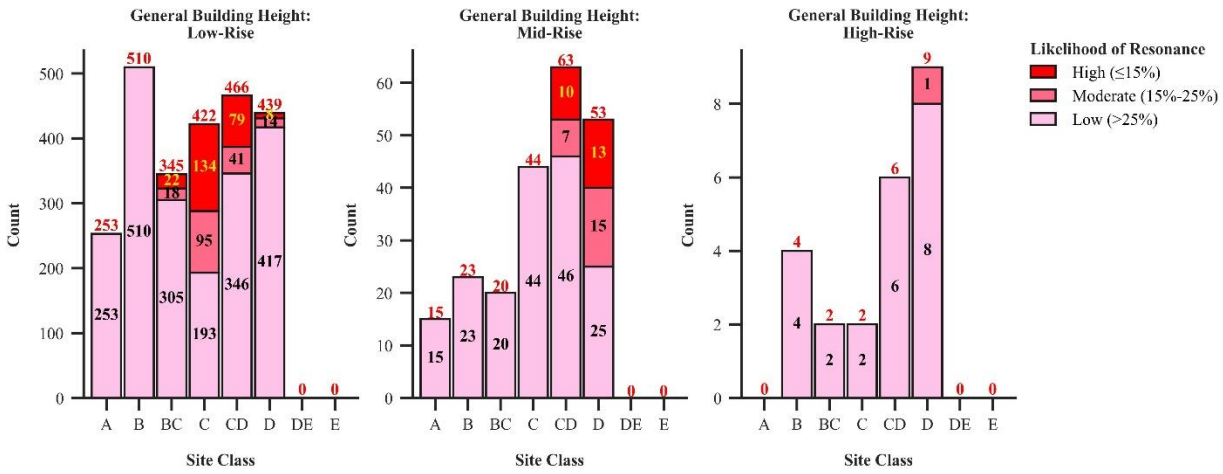

Figure 8: Likelihood of resonance across building general height, as determined by FEMA HAZUS, and soil site classes.

2.4.3 Prioritizing Buildings at Risk

In data analysis and statistical modeling, the identification of local maxima plays a pivotal role in characterizing distributional properties, particularly in the context of density estimation and clustering. A local maximum is defined as a point that exceeds the values of its immediate neighbors, although it may not represent the global peak of the dataset or function. These points often correspond to modes—areas of high data concentration—and serve as indicators of underlying distributional structure or clustering behavior (Silverman et al., 1996).

The occurrence of multiple local maxima signifies a multimodal distribution, which may suggest the presence of distinct subpopulations or heterogeneous underlying processes (Hartigan, 1975). This insight is particularly valuable for segmenting datasets into meaningful analytical groups, identifying systematic differences across subgroups, or uncovering latent variables that drive observed variability. Furthermore, regions characterized by relatively sparse data between peaks may represent outlier behavior or anomalous conditions, making local maxima a useful diagnostic in anomaly detection and robustness analysis (Hastie et al., 2001). Recognizing and interpreting local maxima enhances the accuracy and interpretability of statistical models and supports the generation of more reliable, data-driven conclusions.

In the context of seismic damage and risk assessment, identifying local maxima in damage exceedance probabilities facilitates the detection of structurally or contextually similar building clusters. These groupings reflect commonalities in vulnerability, whether related to construction typology, geotechnical conditions, or design era. Understanding these clusters is essential for informing policy and planning decisions, particularly those related to seismic retrofitting, hazard mitigation, and the prioritization of limited resources. Targeting interventions at buildings

within the higher-risk clusters identified through this process can improve both the efficiency and effectiveness of risk-reduction strategies.

The density plot shown in **Figure 9** depicts the distribution of cumulative moderate damage state exceedance probabilities across the 2,676-building inventory evaluated in this study. The distribution displays three distinct local maxima, indicating a multimodal pattern. The primary mode, located at approximately 3.57%, suggests that the majority of buildings exhibit relatively low vulnerability. Secondary peaks at approximately 29.46% and 46.17% reveal subpopulations of buildings with substantially higher probabilities of exceeding the moderate damage threshold. These peaks may correspond to specific structural types or site conditions that elevate seismic risk.

The 90th percentile threshold, calculated at 24.04%, delineates the upper decile of risk, meaning that 2,408 buildings have cumulative probabilities below this value. The remaining 268 buildings—approximately 10% of the inventory—exceed this threshold and are thus considered at elevated risk. This probability of exceedance corresponds to an annualized risk of approximately 0.00996%, assuming an earthquake hazard with a 2% probability of occurrence within a 50-year period. This stratification offers a quantitative basis for prioritizing buildings for mitigation, further study, or retrofitting interventions.

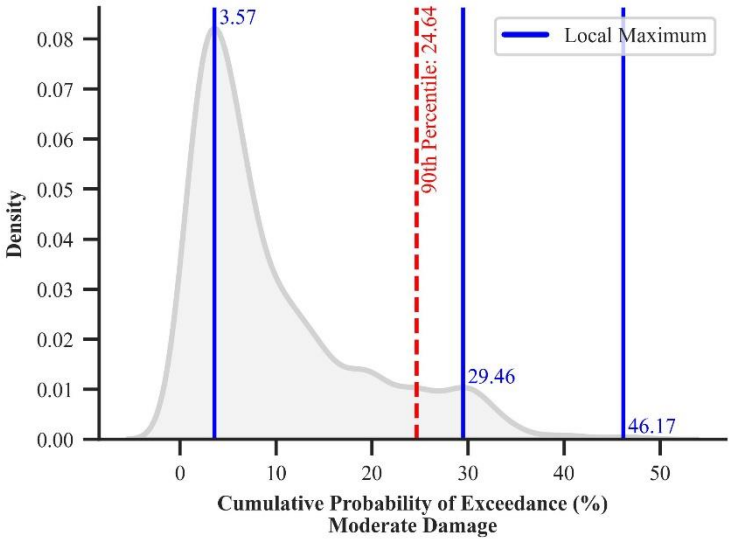

Figure 9: Probability density function of the cumulative probability of exceedance for moderate damage. The distribution exhibits three local maxima (blue lines) at approximately 3.57%, 29.46%, and 46.17%, indicating varying clusters among the buildings. The 90th percentile threshold (red dashed line) at 24.04% marks the point where 90% of the buildings have a lower probability of exceeding moderate damage, indicating that a small subset of structures faces a higher risk.

Based on the local maxima identified in the cumulative moderate damage exceedance probability distribution, **Figure 10b** segments the building inventory into five discrete categories. This segmentation facilitates a more granular and

targeted assessment of structural vulnerability. In the figure, black boxplots represent buildings below the 90th percentile threshold (24.04%), while red boxplots highlight those above this threshold, indicating elevated damage potential.

The overall distribution exhibits a pronounced right-skew, with the majority of buildings concentrated in lower probability ranges and a smaller subset exhibiting markedly higher vulnerability. Segment 1 (0.10%–3.57%) includes 765 buildings (28.6% of the inventory), with a median exceedance probability of 2.16%, suggesting comparatively low seismic susceptibility. Segment 2, spanning probabilities from 3.57% to 24.64%, contains the largest share of buildings (1,643 or 61.4%), with a median probability of 7.96%. Although this segment includes buildings with elevated risk, most remain well below the damage exceedance threshold used to define the upper decile.

A marked inflection occurs at the 90th percentile (24.64%), indicating the transition into the highest-risk categories. Segment 3 (24.64%–29.46%) consists of 137 buildings (5.1%), with a median exceedance probability of 26.80%. Segment 4 (29.46%–46.17%) includes 127 buildings and exhibits a higher median probability of 31.86%, representing structures with substantially increased vulnerability. Segment 5, encompassing the extreme upper tail of the distribution, comprises just four buildings with probabilities ranging from 46.17% to 48.34%. These structures exhibit the highest estimated damage probabilities in the inventory and are classified as statistical outliers.

This segmentation underscores that while most buildings have relatively low probabilities of exceeding the moderate damage state, a small subset exhibits significantly higher risk. The steep decline in the number of buildings beyond the 90th percentile reflects a heavily skewed distribution, where extreme vulnerability is rare but of high consequence for risk mitigation planning. Segments 4 and 5 are considered statistical outliers based on the Interquartile Range (IQR) method (**Figure 10a**), encompassing 134 buildings. An additional three buildings in Segment 3 also meet the outlier criterion.

Figures 11 through 13 provide further breakdowns of the top decile (268 buildings), summarizing key structural, occupancy, and hazard attributes. These visualizations support a clearer understanding of the physical and functional characteristics associated with elevated seismic risk and help inform strategic prioritization of mitigation actions.

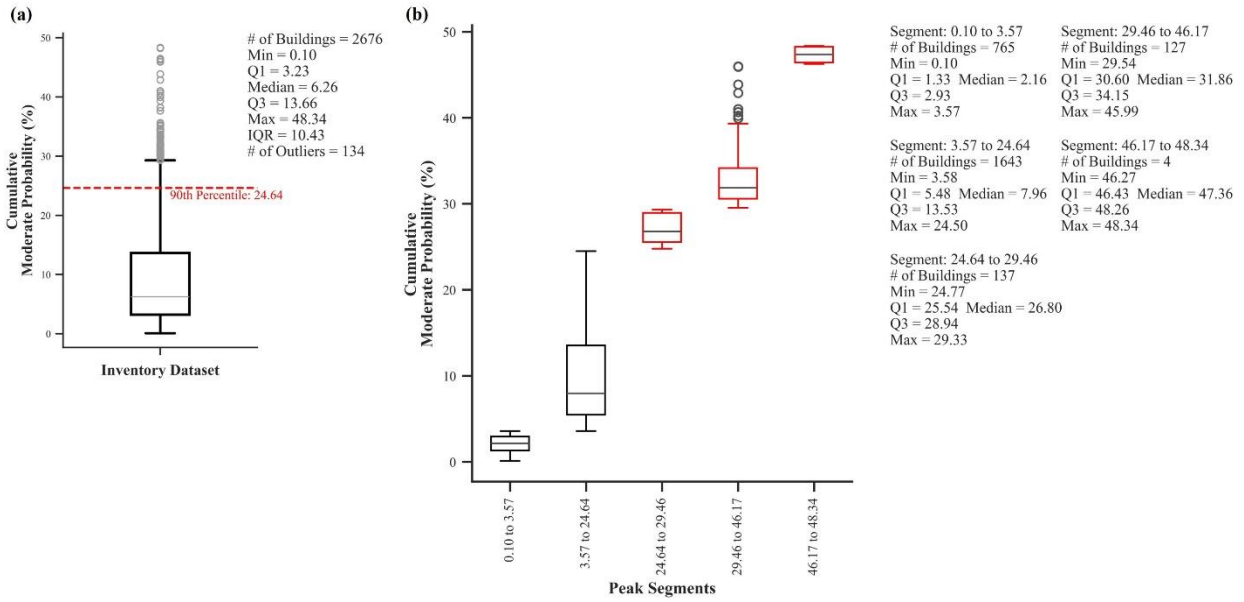

Figure 10: Box plot of cumulative probability of moderate damage (a) Inventory dataset. (b) across different peak segments. The black boxplots in (b) represent buildings with probabilities below the 90th percentile threshold (24.04%), while the red box plots indicate buildings exceeding this threshold, signifying higher probabilities. The increasing trend in probability across segments reflects the varying levels of heightened risk.

Figure 11 provides a detailed classification of buildings within the top decile of cumulative moderate damage probability, organized by key inventory attributes: (a) General Building Height, (b) HAZUS Design Level, and (c) General Building Typology. These attributes are shown across Segments 3, 4, and 5, which represent ascending levels of structural vulnerability.

In panel (a), low-rise buildings constitute the majority across all three segments. Segments 3 and 4 contain over 115 low-rise buildings each, while Segment 5—representing the most extreme risk category—includes only three. Mid-rise buildings are less frequent, with 22 in Segment 3, 9 in Segment 4, and one in Segment 5. High-rise buildings are nearly absent, with only two present in Segment 4, underscoring the predominance of low-rise construction within the most vulnerable subset.

Panel (b) highlights that most buildings in the top 10% fall under the Pre-Code (PC) category: 108 in Segment 3, 116 in Segment 4, and 2 in Segment 5. The Low-Code (LC) category is less represented, with 29 buildings in Segment 3, 11 in Segment 4, and 2 in Segment 5. Notably, the Low-Special (LS) category—typically representing essential facilities built to more stringent standards—is entirely absent from the top 10%, indicating that newer, code-compliant buildings are less vulnerable.

In panel (c), variation in structural typology is evident. No Wood buildings appear in the highest-risk segments, consistent with earlier findings regarding their strong performance. Steel buildings are present in all segments: 31 in

Segment 3, 36 in Segment 4, and 4 in Segment 5. Concrete buildings appear in Segment 3 (23) and Segment 4 (19), while Precast structures are limited in occurrence—five in Segment 3 and six in Segment 4. Reinforced Masonry (RM) buildings are moderately represented, with 19 and 11 in Segments 3 and 4, respectively. Unreinforced Masonry (URM) structures are particularly prominent, comprising 59 buildings in Segment 3 and 55 in Segment 4.

Although S3 Steel buildings are widely distributed across the high-risk segments, URM buildings are more disproportionately represented. Specifically, 114 out of the 458 URM buildings (approximately 25%) appear within the 90th percentile, compared to 71 out of 413 Steel buildings (approximately 17%). This overrepresentation indicates that URMs are the most seismically vulnerable typology in the inventory, both in terms of frequency and concentration within the highest-risk categories. These findings reinforce the need for targeted mitigation and retrofitting strategies focused on URM structures in regions with amplified seismic hazard.

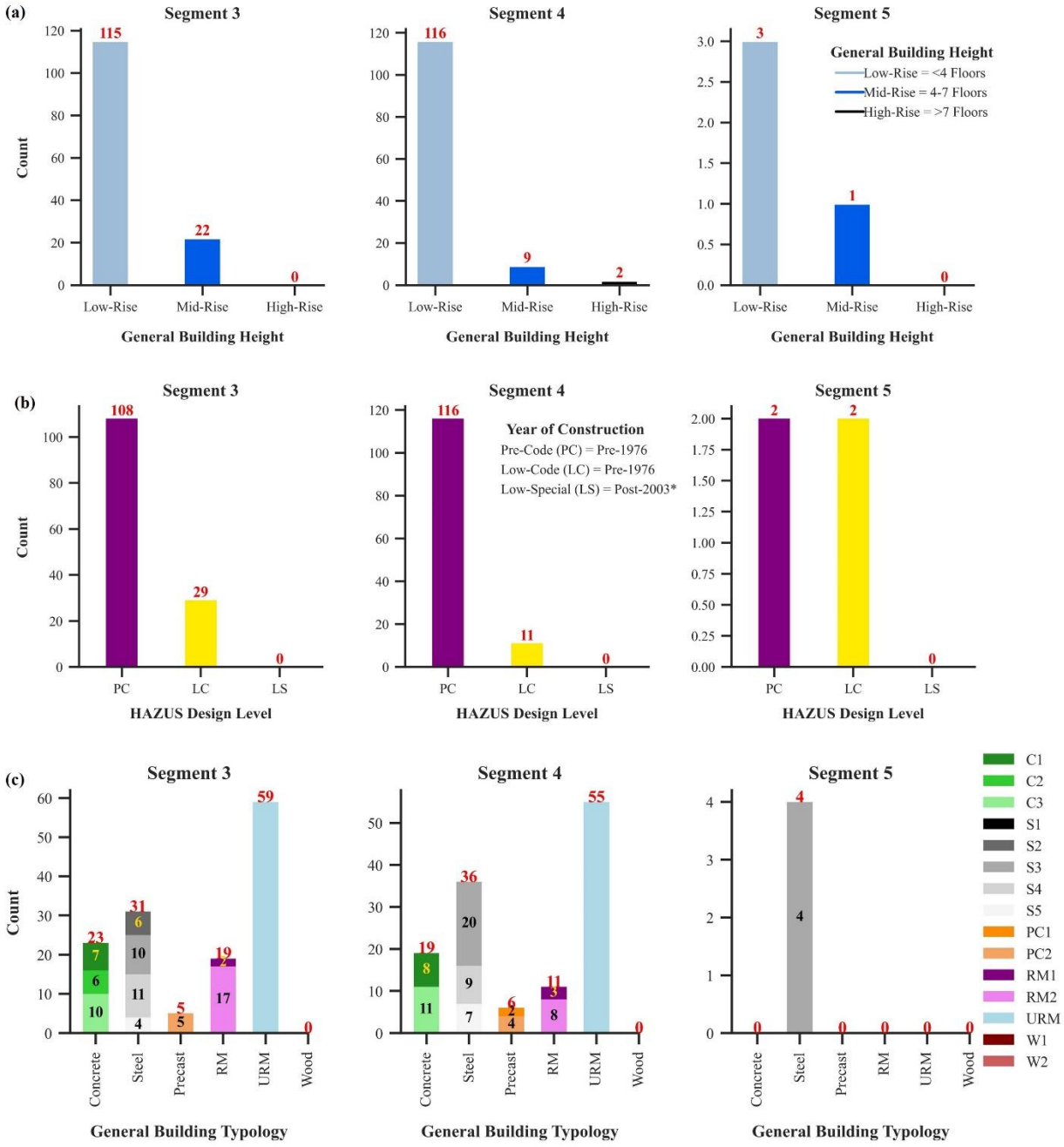

Figure 11: Distribution of buildings within the top 10% of damage probability, categorized by key structural attributes. (a) General building Height. (b) Design Level. (c) General Building Typology.

Figure 12 presents site characterization data for buildings in Segments 3, 4, and 5, highlighting geotechnical factors influencing seismic vulnerability. Panel (a) shows that Site Classes CD (dense sand or very stiff clay) and D (medium dense sand or stiff clay) dominate across all segments. Segment 3 includes 86 buildings in Site Class D, 50 in CD, and one in C. Segment 4 similarly comprises 72 buildings in D and 55 in CD. All four buildings in Segment 5 fall exclusively within Site Class D.

Panel (b) illustrates resonance likelihood. In Segments 3 and 4, most buildings fall in the low-likelihood category (>25%), with 112 and 97 buildings, respectively. A smaller proportion exhibits higher resonance potential: 10 buildings in Segment 3 and 18 in Segment 4 fall within the high-likelihood range (0–15%), while 15 and 12 fall in the moderate range (15–25%). All buildings in Segment 5 are classified as low likelihood.

These results indicate that while soft to moderately stiff soil conditions are common among high-risk buildings, resonance effects are not uniformly present. This suggests either limitations in the resonance screening methodology or the need for more detailed ground response modeling to fully capture the interaction between site conditions and structural performance.

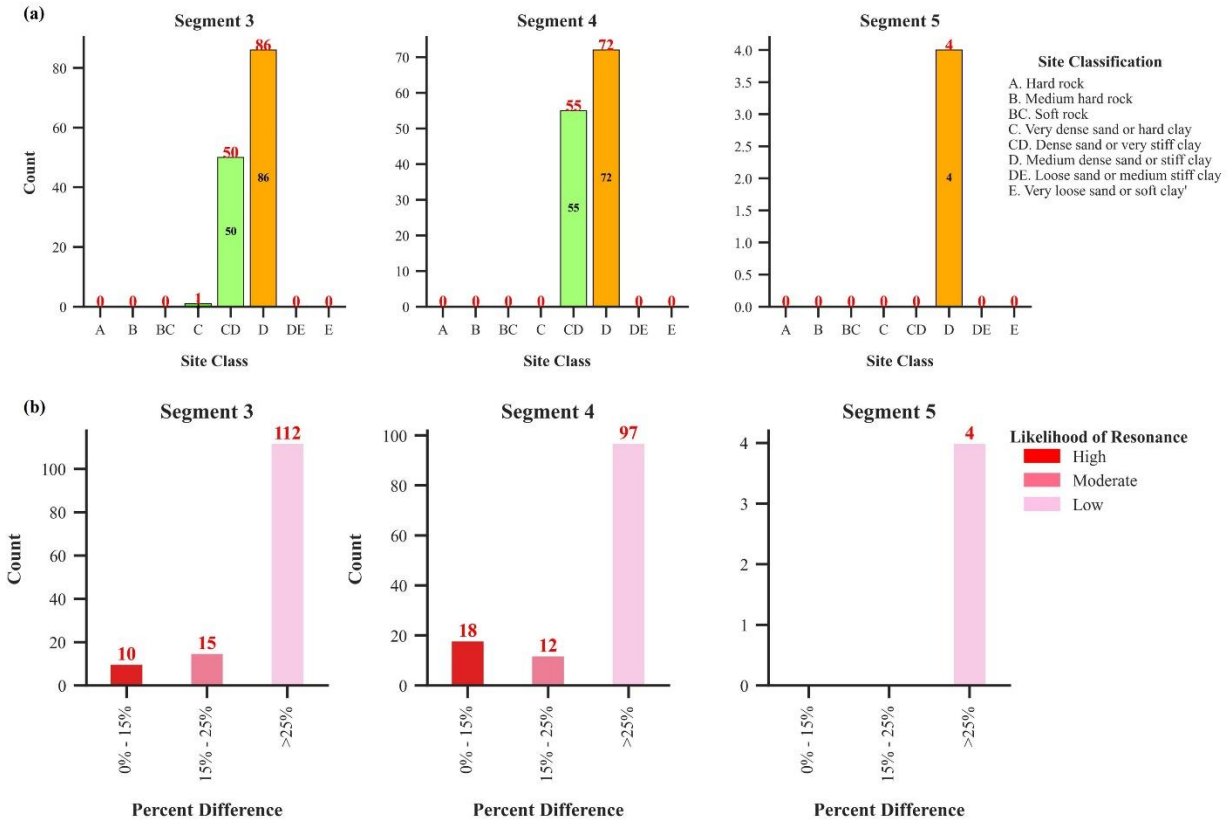

Figure 12: Distribution of site classifications and resonance likelihood in the 90th percentile. (a) Site classification of buildings in Segments 3, 4, and 5, showing a predominance of CD (dense sand or very stiff clay) and D (medium dense sand or stiff clay) categories. (b) Resonance likelihood distribution, where most buildings exhibit low likelihood (>25%).

Figure 13 presents a summary of building inventory characteristics across Segments 3, 4, and 5, disaggregated by HAZUS occupancy classification, IBC Risk Category, and geographic distribution by Massachusetts county.

Panel (a) illustrates the distribution of buildings by occupancy class. Commercial buildings represent the predominant class in both Segment 3 (64 buildings) and Segment 4 (58 buildings). In contrast, Segment 5 includes only a limited number of buildings, with no single occupancy class exceeding two structures.

Panel (b) shows the distribution of buildings by IBC Risk Category. Segments 3 and 4 are primarily composed of Risk Category II buildings (58 and 53 structures, respectively), followed by Risk Category III (20 and 26 structures, respectively) and Risk Category I (18 and 19 structures, respectively). Segment 5 contains four buildings, distributed as follows: one each in Risk Categories I and II, and two in Risk Category IV. Color coding in the panel further indicates that most buildings are classified as Seismic Design Category (SDC) B, though a notable proportion falls within SDC C—particularly in Segment 3 (40 buildings) and Segment 4 (29 buildings), with two SDC C buildings also present in Segment 5.

Panel (c) displays the county-level distribution of buildings across Massachusetts. Middlesex County contains the largest share in both Segment 3 (33 buildings) and Segment 4 (55 buildings). Segment 5 comprises four buildings in total, two of which are located in Essex County—a region identified as having the highest expected seismic shaking intensity in the state.

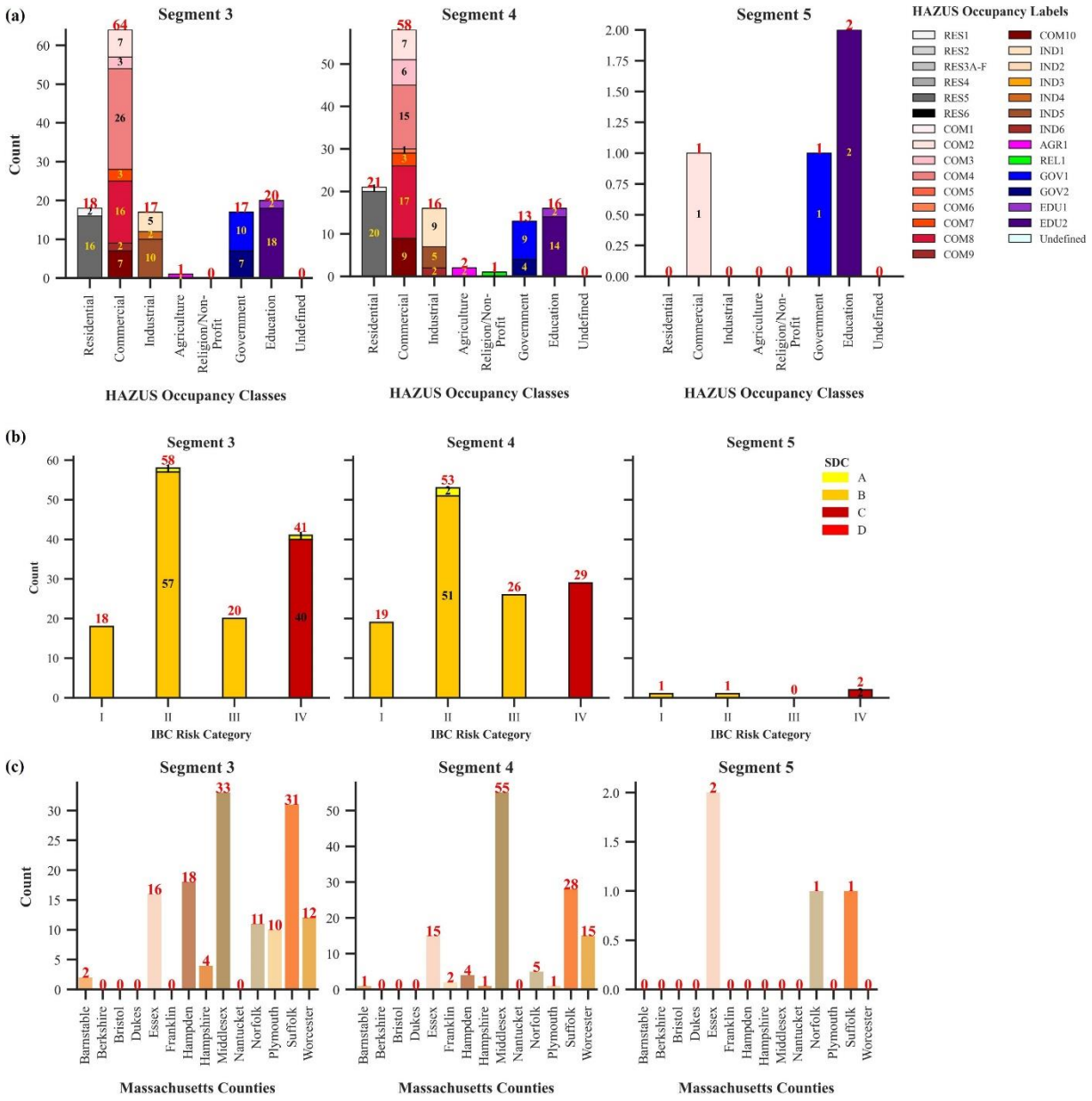

Figure 13: Essential buildings in Risk Category IV and Seismic Design Category C. (a) General Building Typology. (b) HAZUS Occupancy Class. (c) Massachusetts Counties.

The integrated analysis presented in **Figures 11 through 13** identifies the buildings most vulnerable to seismic damage as predominantly low-rise structures constructed prior to the adoption of modern seismic codes (Pre-Code), with commercial occupancy and unreinforced masonry (URM) construction. These buildings are primarily concentrated in Segments 3 and 4, which represent the 90th percentile range for moderate damage exceedance probabilities—ranging from 24.64% to 46.17%—and are commonly located in areas underlain by Site Classes CD and D, which are known to amplify seismic ground motions. Additionally, many of these structures fall within IBC

Risk Categories II and III, with significant concentrations in Middlesex and Suffolk Counties. While adverse soil conditions contribute to seismic amplification, the findings indicate that structural characteristics—particularly construction material, code level, and building height—are the primary determinants of seismic vulnerability in this dataset. Notably, the role of site resonance appears secondary to these structural factors in influencing damage probability outcomes.

Given these findings, retrofitting efforts should prioritize low-rise URM buildings, particularly those with essential functions. Special attention should be directed toward buildings classified as Risk Category IV and located in Seismic Design Category C areas, due to their critical roles in emergency response and post-disaster recovery. These results are synthesized in Figure 14, which presents a retrofitting prioritization framework. The proposed ranking begins with Segment 5, followed by Segment 4, and then Segment 3, with structures ordered within each segment by descending probability of moderate damage exceedance.

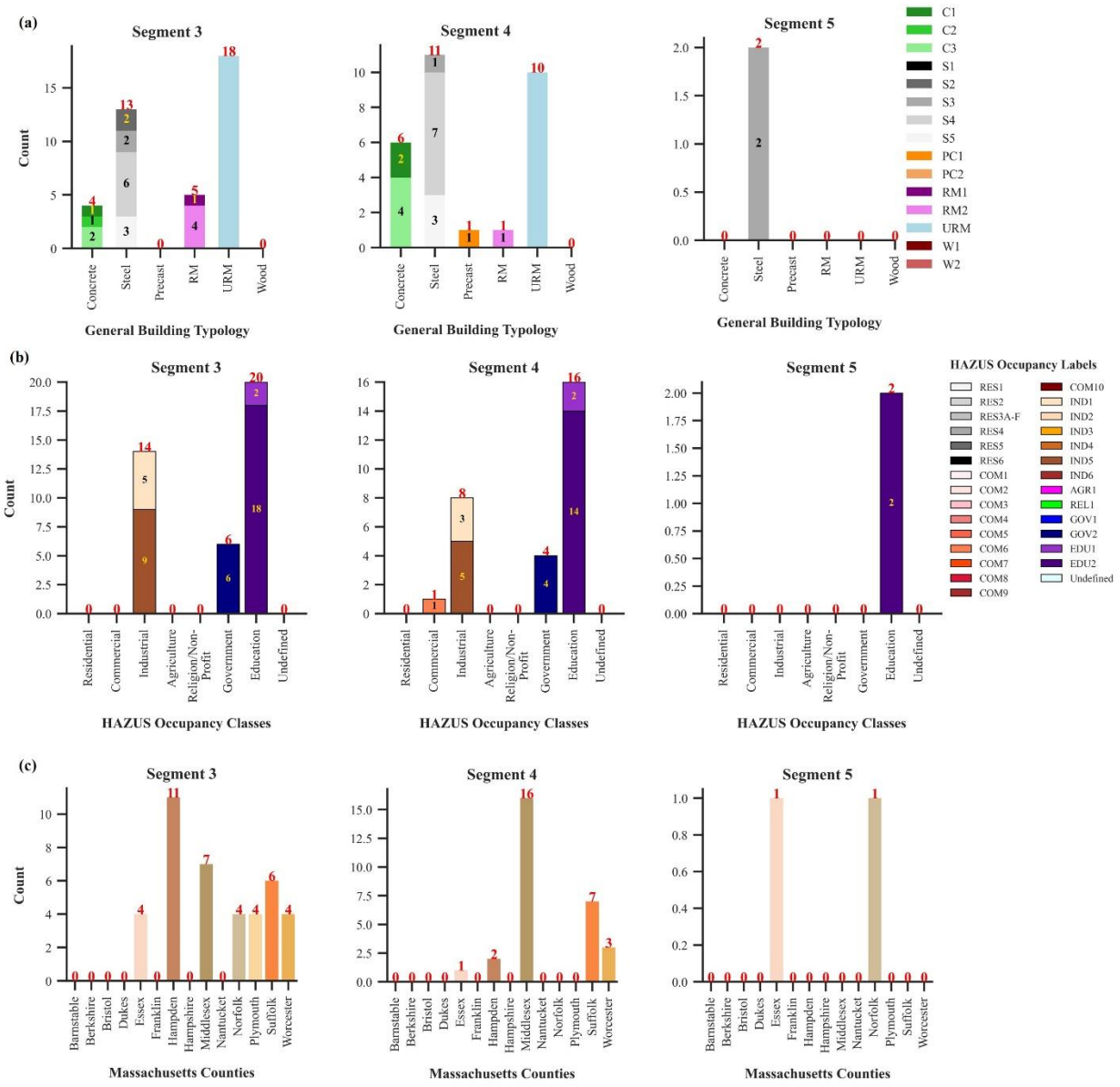

Figure 14: Essential buildings in Risk Category IV and Seismic Design Category C. (a) General Building Typology. (b) HAZUS Occupancy Class. (c) Massachusetts Counties.

2.5 Limitations

As with any research effort, certain limitations constrain the scope, accuracy, and generalizability of the results. This section outlines key limitations associated with the building inventory, analytical methods, and broader contextual assumptions. While these limitations do not invalidate the findings, they highlight areas where additional research and refinement are warranted to enhance the robustness and applicability of the conclusions.

2.5.1 Building Inventory Constraints

The building dataset used in this analysis represents only a subset of state-owned structures and does not reflect the full range of building types, geographic locations, or occupancy classes across the Commonwealth of Massachusetts. For example, while 32 police stations are included in this study, the Massachusetts GIS database reports over 400 such facilities statewide. Similarly, the National Structures Inventory (NSI) records 956 hospitals and 2,459 schools in Massachusetts, whereas this analysis includes only 15 COM6 (hospital) and 285 EDU1/EDU2 (school) buildings. As such, the conclusions drawn from this analysis pertain specifically to the analyzed sample and may not be fully generalizable to the entire state building stock.

Nevertheless, the insights derived from this subset are consistent with findings in other seismic vulnerability studies. The identification of Unreinforced Masonry (URM) structures as highly vulnerable is well established; however, the results also indicate that certain Steel Moment Frame (S3) buildings exhibit comparable risk profiles. This highlights the importance of avoiding assumptions about typological performance and underscores the need for continued vulnerability assessments and targeted seismic mitigation strategies. While the analysis is limited in its representativeness, the methodology and observed trends can be applied to similar buildings or regions within the state, supporting more localized assessments of seismic risk.

2.5.2 Limitations of the HAZUS Framework

The FEMA HAZUS methodology, while widely used for seismic loss estimation, introduces inherent limitations due to its generalized structure classifications and reliance on predefined fragility functions. HAZUS assigns buildings to broad typological categories—such as Wood Frame or Steel Frame structures—based on basic structural characteristics. However, these categories do not capture important nuances in construction quality, material variability, or design differences that can significantly influence a building's seismic performance.

For example, two buildings of the same HAZUS typology may differ substantially in detailing, retrofitting status, or structural configuration, yet HAZUS treats them as having identical seismic response properties. In addition, fragility curves within the HAZUS framework are developed from empirical and expert-judgment-based data, often rooted in regions with higher seismicity and historical earthquake records. Their application in low-to-moderate seismic zones, such as Massachusetts, may therefore yield oversimplified or uncertain results. The integration of high-resolution site classification data in this study helps address some of these deficiencies by refining ground motion

inputs; however, further adaptation of fragility functions for local structural performance characteristics remains necessary to enhance predictive accuracy.

2.5.3 Implications for Future Work

Seismic hazard mitigation in moderate seismicity regions such as the Central and Eastern United States (CEUS) presents distinct challenges. In these regions, earthquake ground motions attenuate more gradually with distance, resulting in broader zones of potential impact even for moderate-magnitude events (Kianiard et al., 2017). Coupled with the relatively infrequent occurrence of damaging earthquakes, this attenuation behavior contributes to both physical vulnerability and reduced preparedness at the community level.

Moreover, site effects—including strong impedance contrasts between shallow soils and rigid bedrock—can significantly amplify seismic ground motions (Baise et al., 2016; Nordenson and Bell, 2000). These localized amplification effects are particularly relevant in areas underlain by glacial sediments or coastal deposits, such as those observed in Massachusetts. Despite efforts in this study to incorporate high-resolution geotechnical data, the current analysis does not fully resolve amplification effects associated with resonance or localized variations in soil conditions.

Future work should build on these findings by refining the treatment of site effects, particularly in regions identified as exhibiting elevated amplification or resonance potential. A reanalysis incorporating updated soil response models, expanded building inventories, and locally calibrated fragility functions would improve the predictive resolution of damage estimates. Additionally, more detailed investigation of building-specific resonance—especially for mid- and high-rise structures in high-amplification zones—could better inform retrofitting prioritization and emergency planning strategies. Continued refinement of site-response modeling and the integration of structural monitoring data will be critical for advancing earthquake resilience planning in data-limited, moderate-hazard regions.

2.6 Conclusion

This chapter presents a comprehensive, data-driven evaluation of seismic vulnerability across Massachusetts, with a particular emphasis on identifying and prioritizing buildings most likely to sustain moderate structural damage during an earthquake. The analysis integrates high-resolution geotechnical and geological data, an extensive state-owned building inventory, and risk-targeted ground motion parameters derived from the 2023 USGS National Seismic Hazard Model. Using FEMA's HAZUS loss estimation framework, the study applies standardized capacity curves and fragility functions to estimate the probability of damage exceedance for each structure. Statistical techniques—

including local maxima analysis—were employed to characterize the distribution of risk, revealing a multimodal pattern that delineates distinct clusters of seismic vulnerability.

The most vulnerable buildings were found to be predominantly low-rise, pre-code Unreinforced Masonry (URM) structures and commercial facilities located primarily in Middlesex and Suffolk counties. These buildings are commonly on Site Classes CD and D, which are associated with increased seismic amplification. While structural resonance was evaluated, it was not found to be a dominant driver of vulnerability in the dataset. Within the 90^{th} percentile of moderate damage exceedance, URM and light-frame Steel buildings are prominently represented. Notably, 25% of all URM structures fall within this high-risk category, compared to 17% Steel buildings, predominantly light frame—underscoring the heightened and more consistent risk associated with URM typologies. Although the highest individual damage probabilities were associated with certain light-frame Steel buildings, URMs exhibit broader and more systemic vulnerability across the inventory.

Based on the segmentation of damage probabilities, a tiered retrofitting prioritization strategy is proposed. Buildings in Segment 5, which exhibit the highest probabilities of moderate damage exceedance, should receive immediate attention. Segments 4 and 3, followed by 2 then 1, should be addressed in subsequent phases, in descending order of damage probabilities. Special consideration should also be given to facilities classified as IBC Risk Category IV and Seismic Design Category C, due to their essential role in emergency response and recovery. A total of 71 such buildings were identified in the analysis.

In summary, this chapter demonstrates the value of high-resolution site characterization and structural data in enabling localized, actionable seismic risk assessments. The findings support the development of targeted mitigation strategies, which are essential for enhancing the resilience of Massachusetts' built environment. By identifying the most at-risk buildings and prioritizing retrofitting investments accordingly, the state can better prepare for future seismic events and reduce the likelihood of catastrophic structural failures.

2.7 Data and Resources

The building inventory used in this study is proprietary, and access to this data is restricted due to proprietary rights and cannot be shared publicly. Ground motion data used in the analysis were sourced from the United States Geological Survey (USGS) Seismic Design Geodatabase for the 2020 NEHRP recommended seismic provisions and 2022 ASCE/SEI 7 standard by Luco et al. (2021) and are publicly available. The depth-to-bedrock map was obtained

from MassGIS (Massachusetts Bureau of Geographic Information) and is also publicly available. All other data and resources referenced in this article are cited accordingly and are integral to the analyses and findings presented.

2.8 Project Acknowledgments

Many thanks to the Massachusetts Division of Capital Asset Management & Maintenance (DCAMM) for providing the building inventory used in this study. Their assistance in granting access to their data was instrumental in conducting the analysis.

Chapter 3: Ground Response Analysis for Seismic Vulnerability Assessment: *Does detailed site characterization and ground response analysis change projected building damage estimates?*

"Do the best you can until you know better. Then, when you know better, do better."— **Maya Angelou**

3.1 Significance of the Project

Seismic hazard assessments are essential for understanding the risks posed by earthquakes to buildings, infrastructure, and communities—especially in regions that are not typically associated with frequent or high-magnitude seismic events. In the Central and Eastern United States (CEUS), including Massachusetts, seismicity is infrequent but not insignificant. The region's vulnerability is often amplified by site-specific geologic conditions, such as deep sedimentary layers and sharp impedance contrasts, which can intensify ground shaking even during low-magnitude earthquakes (Perkins, 2024; Kianiard et al., 2017; Pratt et al., 2017). These localized effects are frequently overlooked in conventional seismic hazard models that rely on simplified site proxies like Vs_{30}—the time-averaged shear-wave velocity over the upper 30 meters of the subsurface.

While Vs_{30} has been widely adopted for its simplicity and compatibility with building codes and national seismic hazard maps (Boore et al., 2011; Borcherdt, 1994), it offers only a generalized approximation of site amplification. It does not account for deeper stratigraphy, abrupt changes in material properties, or frequency-dependent amplification—factors that are especially critical in geologically complex regions like Massachusetts (Pontrelli et al., 2023; Pyke, 2020; Lee & Trifunac, 2010). As a result, hazard estimates and building damage projections derived from Vs_{30} alone may underrepresent or mischaracterize actual seismic risks (Tilashalski et al., 2015; Wald & Mori, 2000).

This chapter addresses these limitations by employing linear one-dimensional Ground Response Analysis (GRA) to explicitly model the propagation of seismic waves through stratified geologic media. The method incorporates high-resolution inputs—including depth to bedrock, geologic unit-based velocity profiles, and impedance contrasts—to simulate how seismic energy is amplified or attenuated at the surface (Baise et al., 2016; Haji-Soltani & Pezeshk, 2017). As demonstrated in previous studies, impedance contrasts between soft sediments and underlying bedrock in areas like the Boston Basin can result in amplification factors exceeding 10 at frequencies corresponding to the depth of sedimentary layers (Baise et al., 2016). Such site effects are not captured by Vs_{30}-based models but are critical to accurate damage prediction.

Using Massachusetts as a case study, this chapter evaluates how the use of GRA alters projections of spectral acceleration, Seismic Design Category (SDC) classifications, and building damage probabilities relative to those derived from Vs_{30}-based site amplification. The analysis applies FEMA HAZUS fragility functions to estimate

cumulative exceedance probabilities for the moderate damage state, allowing for a direct comparison between the two methods across a shared inventory of state-owned buildings.

In addition to comparing ground motion modeling techniques, this chapter also examines how the granularity of exposure data influences seismic risk assessments. Specifically, it contrasts results derived from the HAZUS General Building Stock (GBS)—which provides a generalized representation of regional building typologies—with those based on a refined state-owned inventory containing facility-specific attributes. The dual comparison—between amplification models (Vs_{30} vs. GRA) and inventory resolution (generalized vs. specific)—highlights the sensitivity of seismic vulnerability assessments to both hazard characterization and exposure detail.

The significance of this work lies in its potential to inform more accurate and locally responsive hazard mitigation strategies. In regions like Massachusetts—where relatively infrequent but potentially damaging earthquakes interact with complex geologic conditions—simplified proxies may obscure localized risks that are critical for informed decision-making. The findings of this study provide empirical evidence to support the adoption of refined site characterization methods in seismic vulnerability assessments, particularly for critical infrastructure and essential facilities.

Moreover, the analytical framework used here is scalable and transferable to other regions within the CEUS, where site amplification effects are often underrepresented in national models. As such, this chapter contributes not only to state-specific hazard preparedness but also to the broader effort to improve regional seismic resilience through enhanced modeling practices and data-driven infrastructure planning.

3.2 Building Inventory

The HAZUS National Database serves as a foundational resource for hazard risk assessment, offering a comprehensive suite of spatial and non-spatial datasets to support evaluations of natural hazard impacts. It includes detailed information on the General Building Stock (GBS), demographic characteristics, essential facilities, transportation infrastructure, and utility systems. These datasets enable the estimation of exposure for buildings, populations, and lifelines, providing critical inputs for loss modeling and emergency planning. Each dataset is accompanied by a data dictionary that defines spatial layers and tabular attributes. HAZUS building inventories are compiled from a combination of local sources—such as tax assessor records, census data, and regional building databases—and are supplemented by remote sensing techniques. Structural typologies are generally assigned based on land use,

geographic location, and prevailing construction practices in each region (HAZUS inventory Technical Manual – HAZUS 6.0).

This chapter focuses on the "care facilities" subset of the HAZUS GBS, which includes hospital buildings. These facilities are essential for maintaining public health and safety and play a critical role in post-disaster response and recovery. Assessing their seismic vulnerability is therefore vital for informing retrofitting priorities, structural strengthening efforts, and continuity-of-operations planning.

The dataset analyzed comprises 160 care facilities across the Commonwealth of Massachusetts (**Figure 1**). Of these, 142 are classified as pre-code buildings, constructed prior to the adoption of the state's seismic design provisions in 1976. The majority—138 buildings—are identified as Low-Rise Unreinforced Masonry (URML), while the remaining 22 are classified as low-rise Reinforced Masonry (RM) structures with wood or metal deck diaphragms. Most facilities are located on Site Class D soils, which are prone to seismic amplification. Geographically, Suffolk and Middlesex counties contain the highest concentrations, with 28 facilities each. The dataset primarily represents mid-sized hospitals, defined as having capacities between 50 and 150 beds.

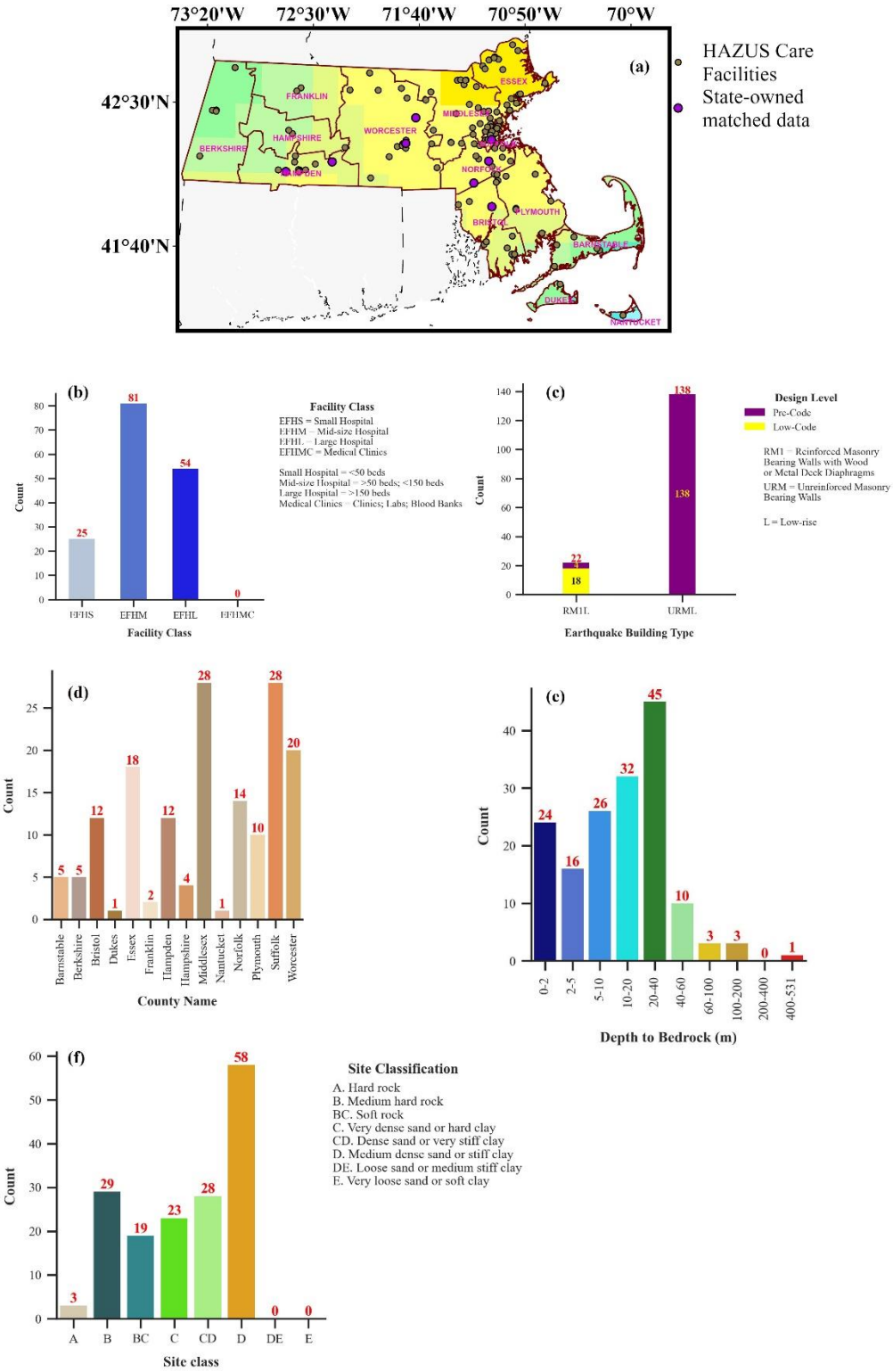

Figure 1: HAZUS General Building Stock (GBS) Care facilities. (a) Spatial distribution plotted on the Peak Ground Acceleration (PGA) (g) from the Uniform-hazard ground motion for a 2% probability of exceedance over 50 years, based on hark rock site conditions (Vs_{30} = 1500 m/s; Site Class A). (b) Distribution by facility class. (c) Distribution by design level per building type. (d) Distribution by Counties. (e) Distribution by depth to bedrock range. (f) Distribution by Site class.

The HAZUS-based hospital inventory evaluated in this chapter differs substantially from the refined state-owned building dataset used in Chapter 2. While the latter encompasses a broad cross-section of facilities with detailed structural attributes, the HAZUS GBS provides a generalized representation of infrastructure based on standardized typologies and aggregated regional assumptions. In particular, HAZUS assigns structural classifications using land use data and census-derived occupancy types, rather than facility-specific engineering records. Consequently, the care facilities dataset in HAZUS reflects a uniform building typology—primarily low-rise URMs—whereas the state-owned inventory includes a wider range of structural systems and design vintages.

This contrast offers a valuable opportunity to examine how the resolution of exposure data influences projected seismic damage. By comparing results derived from both Vs_{30}-based and site-specific Ground Response Analysis (GRA), across generalized and asset-specific building inventories, this chapter evaluates the sensitivity of seismic vulnerability assessments to both hazard inputs and exposure data quality. The findings offer insight into the limitations of generalized models and underscore the benefits of refined, site-specific characterization in enhancing the accuracy of seismic risk projections.

3.3 Methodology

This section outlines the methodology used to assess seismic vulnerability and estimate potential building damage for a set of buildings in Massachusetts. The approach integrates seismic hazard parameters, two alternative site characterization techniques, and standardized fragility models to evaluate structural performance. Specifically, the analysis compares results derived from linear one-dimensional Ground Response Analysis (GRA) with those obtained using the traditional Vs_{30}-based amplification method. This comparative framework is designed to quantify how differences in site response modeling influence damage projections, offering insights into the implications of using detailed versus simplified site characterization approaches in seismic risk assessments.

3.3.1 Linear SH1D Ground Response Analysis (GRA)

The Linear SH1D Ground Response Analysis (GRA) provides a site-specific approach to modeling seismic wave amplification by accounting for subsurface stratigraphy and material properties at each building location. Unlike simplified proxies such as Vs_{30}, which provide average shear-wave velocities over a fixed depth, the SH1D method explicitly models the propagation of seismic waves through vertically layered soil profiles. This allows for the resolution of localized amplification effects driven by impedance contrasts between geologic layers.

For each site, the subsurface profile is defined by a sequence of soil layers characterized by thickness, shear-wave velocity (V_s), and density. These shear-wave velocity profiles were developed from geologic unit–based power-law models (Equation 1), truncated at the mapped depth to bedrock, and assigned a fixed bedrock velocity of 2000 m/s. As a result of the modeled profiles, NEHRP Site Classes DE and E are not present in this analysis.

Ground response simulations were conducted using the NRATTLE code—originally developed in R by C. Mueller and modified by R. Herrmann—translated into Python for this study. The program implements the Thomson-Haskell matrix method (Thomson, 1950; Haskell, 1953) to solve 1D linear wave propagation in layered media. The model computes transfer functions that describe the modification of input motions (assumed at rock outcrop) as they propagate through the overlying soil column, resulting in surface-level ground motions. Rock reference motions (Site Class A) were used as input to maintain consistency with USGS-defined bedrock spectra.

A representative model output is shown in **Figure 2** for one of eight matched structures from the state-owned building inventory. The analysis yields two key parameters used in seismic design: the short-period amplification factor (F_a) and the long-period amplification factor (F_v). These factors are derived from the computed response spectra and quantify the frequency-dependent amplification effects at each site.

- F_a reflects the amplification of short-period (high-frequency) motions, typically within the 0.1–0.5 second range. These motions are most relevant for low-rise buildings, which are particularly sensitive to higher-frequency shaking. A higher F_a value indicates greater amplification of these short-period components, which can increase non-structural damage and demand in stiff structural systems.
- F_v captures the amplification of long-period (low-frequency) motions, within the 0.5–1.5 second range. These components primarily affect taller, more flexible buildings. High F_v values suggest increased amplification of these lower-frequency waves, potentially inducing greater lateral displacements and demand in mid- to high-rise structures.

Together, F_a and F_v provide a frequency-specific characterization of site effects, enhancing the resolution of seismic hazard assessments and enabling structure-specific risk evaluations. These factors directly influence the generation of site-specific design spectra and are integrated into the fragility analysis framework described in Section 3.3.3.

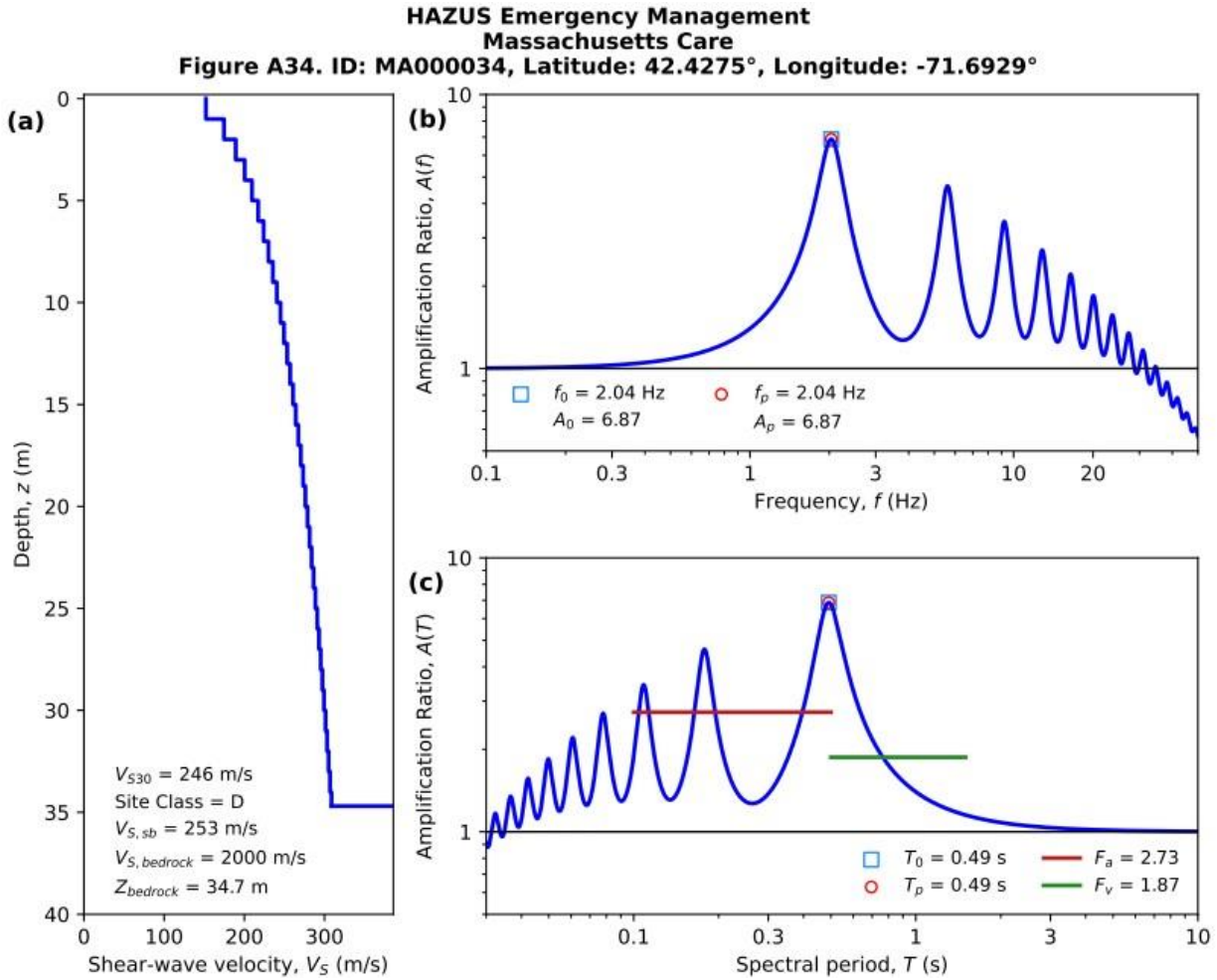

Figure 2: Sample 1D GRA output. F_a and F_v were used to amplify the short-period and long-period seismic ground motions.

3.3.2 Summary of Vs_{30} Amplification and the USGS Seismic Design Geodatabase

The Vs_{30}-based amplification method follows a simplified approach to estimating local ground motion effects using the time-averaged shear-wave velocity over the upper 30 meters of the subsurface (Vs_{30}). Each building is assigned a site class based on a 100-meter resolution Vs_{30} map derived from local geologic and geophysical datasets, including surficial geologic units and empirical velocity profiles. These site classes are used to access spectral acceleration values from the 2023 U.S. Geological Survey (USGS) Seismic Design Geodatabase.

This geodatabase contains gridded, risk-targeted Maximum Considered Earthquake (MCE_r) spectral response accelerations for 22 periods and across eight NEHRP site classes. The extracted values represent shaking intensities with a 2% probability of exceedance over 50 years and are consistent with design parameters used in ASCE 7 and FEMA standards. Short-period and long-period spectral acceleration values—S_{ms} and S_{m1}—are interpolated for each

site class and applied to generate building-specific 5%-damped response spectra. These spectra represent seismic demand curves used to evaluate structural performance under design-level shaking.

3.3.3 Summary of Fragility Analysis and Damage Estimation Methodology

The fragility analysis and damage estimation methodology are rooted in the HAZUS-MH framework developed by FEMA for national-scale loss estimation. For each building in the inventory, the seismic demand—represented by the 5%-damped response spectrum generated from either the Vs_{30} or GRA input—is compared to the structure's capacity, defined by a bilinear capacity curve. These capacity curves are parameterized by building type, code level (Pre-Code, Low-Code, or Low-Special), and building height.

The point of intersection between the capacity curve and the response spectrum determines the building's peak spectral displacement during shaking. This displacement is then used as the input for a set of lognormal fragility functions, which define the probability of exceeding four progressive damage states: Slight, Moderate, Extensive, and Complete. These fragility functions are calibrated for each building type using structural performance data, empirical observations, and expert judgment, and they incorporate both structural and non-structural damage components.

In this analysis, emphasis is placed on the moderate damage state exceedance probability, which serves as a key indicator of compromised functionality and potential need for repair. Probabilities are calculated cumulatively for each structure, enabling comparative evaluation across hazard input types (Vs_{30} vs. GRA) and exposure datasets (generalized vs. specific).

3.4 Results and Discussion

After applying the two site characterization methodologies—Vs_{30}-based amplification and one-dimensional Ground Response Analysis (GRA)—building damage estimates were calculated by integrating the modified seismic input parameters with the FEMA HAZUS fragility functions. This approach enables the evaluation of how differences in site response modeling influence projected damage outcomes across the building inventory. A comparative analysis was conducted to quantify the impacts of each method on structural vulnerability estimates. By contrasting simplified, proxy-based amplification (Vs_{30}) with site-specific ground response modeling (GRA), the analysis identifies the strengths and limitations of each approach. This evaluation provides critical insight into the role of local geotechnical conditions in shaping seismic risk assessments and supports more informed decision-making for hazard mitigation and infrastructure resilience at the regional scale.

3.4.1 Site Amplification Method Comparison

This section presents a comparative analysis of two site response approaches: Vs_{30}-based amplification and linear one-dimensional Ground Response Analysis (GRA). The comparison examines how each method influences spectral demand estimates and resulting structural performance across a range of buildings and site classes. The analysis is framed around cumulative probabilities of exceeding the moderate damage state, as defined by HAZUS fragility functions, to assess building susceptibility under each amplification approach. Key differences are highlighted in terms of average percent changes and the distribution of damage estimates, with particular emphasis on the variability captured by site-specific modeling versus generalized proxies.

Figure 3 illustrates the distribution of cumulative moderate damage exceedance probabilities for both approaches. The Vs_{30}-based method yields a narrower distribution, with probabilities clustering around the mean value of 20.52% and a maximum of 44.23%. In contrast, the 1D GRA method produces a wider distribution, with a notably higher maximum exceedance probability of 61.98%, reflecting a greater potential for localized amplification and elevated damage. This broader variability suggests that GRA more accurately captures the heterogeneity of subsurface conditions.

While the maximum probability is higher for GRA, the 90^{th} percentile value is lower (29.48% vs. 30.58%), indicating that extreme responses are limited to a smaller number of sites. The Vs_{30}-based method, by comparison, shows a broader spread of moderately high exceedance values, likely due to the uniformity of its empirical assumptions across diverse site conditions. These findings suggest that Vs_{30}-based amplification may overgeneralize ground motion effects, leading to inflated damage predictions across a wider portion of the inventory. In contrast, GRA yields a more refined and spatially differentiated assessment, with most buildings exhibiting moderate risk but select locations showing significantly elevated vulnerability due to site-specific amplification characteristics.

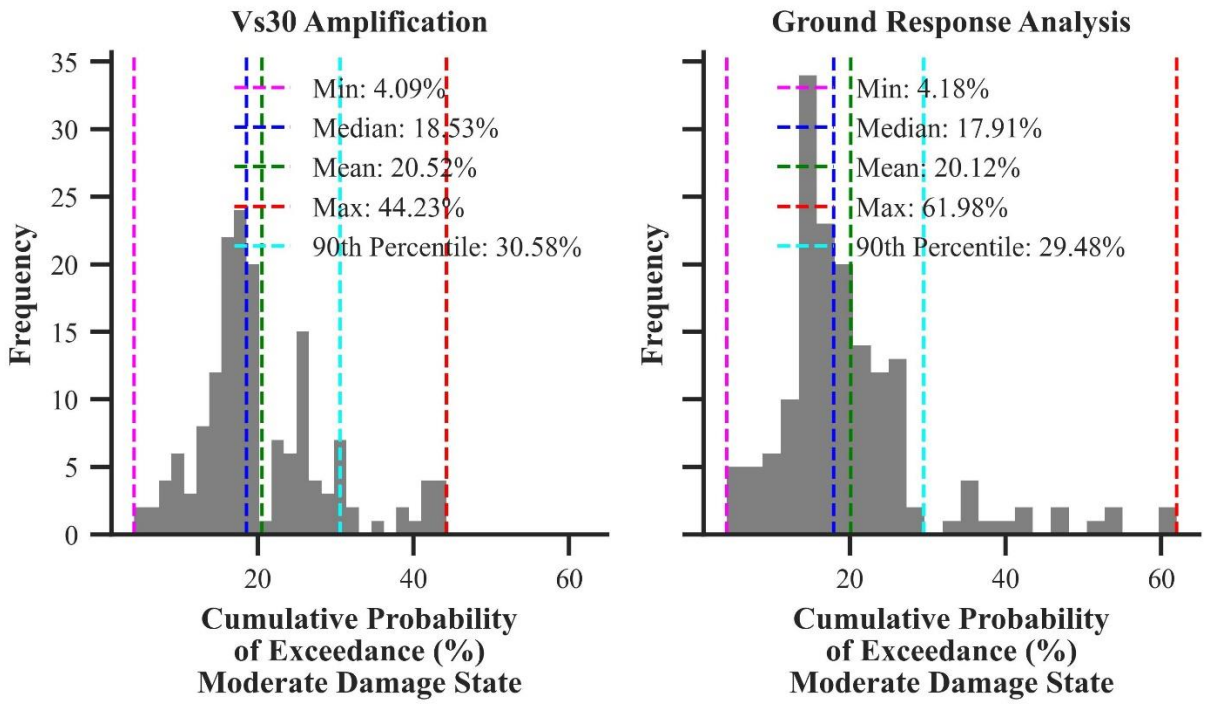

Figure 3: Histogram comparison of the two amplification methods: Vs30-based amplification and Ground Response Analysis (GRA).

Figure 4 supports the preceding observations by illustrating the average percent change in ground motion parameters, under moderate damage probability conditions, across different site classes when comparing Vs_{30}-based amplification to 1D Ground Response Analysis (GRA). Site Classes B through CD exhibit negative percent changes, with the most substantial decrease observed in Site Class CD (−24.83%). This trend indicates that the 1D GRA method generally predicts lower amplification levels than the Vs_{30}-based method for relatively stiff soil profiles. These reductions suggest that Vs_{30}-based amplification may overestimate ground motion effects in these site classes due to its inability to account for detailed subsurface stratigraphy or frequency-dependent damping characteristics.

In contrast, Site Class D shows a marked positive percent change (+22.05%), demonstrating that the 1D analysis estimates significantly higher amplification than the Vs_{30}-based method in softer soil conditions. This increase is likely attributable to GRA's capacity to model resonance effects and impedance contrasts, which are prevalent in soft, deep soil profiles and are typically neglected in simplified Vs_{30}-based approximations.

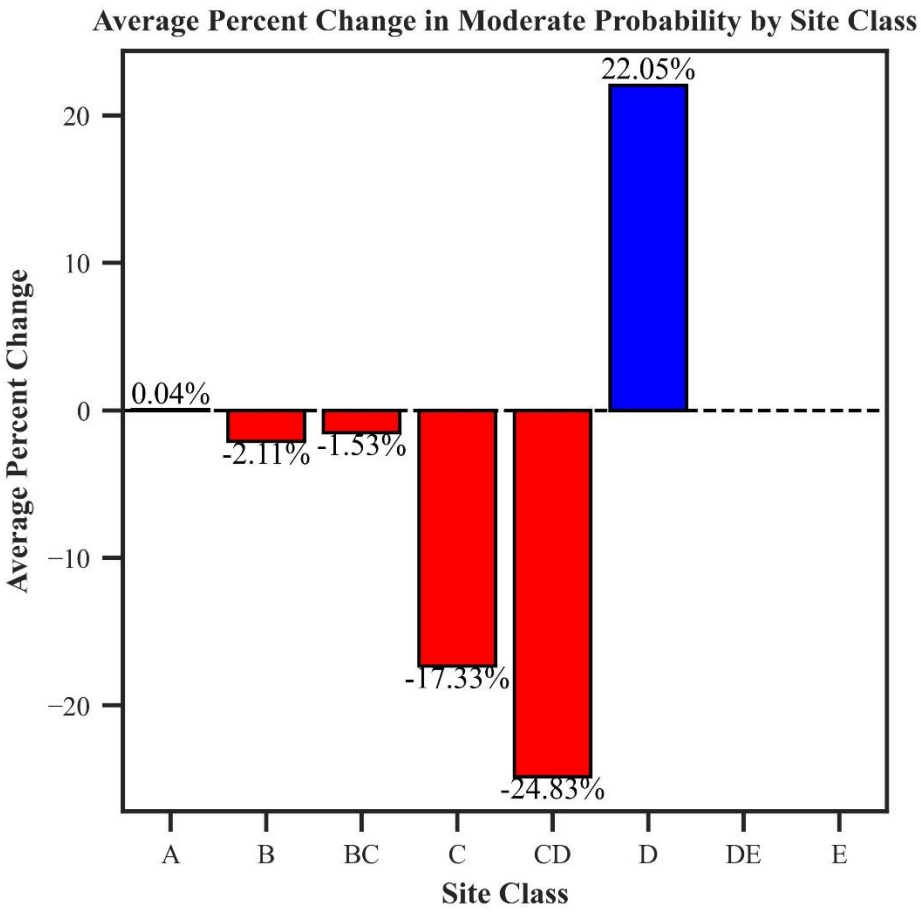

Figure 4: Average percent difference change calculated for the two amplification methods: Vs_{30}-based amplification and Ground Response Analysis (GRA).

To better understand how these subsurface characteristics translate into differing seismic demands, **Figure 5** provides a direct comparison of GRA-derived demand spectra and transfer functions for two representative Site Class D buildings, illustrating how soil depth and stiffness fundamentally shape the frequency content and amplitude of surface ground motion. The shape of the demand spectra in **Figure 5** reflects the critical influence of site-specific soil conditions on seismic wave amplification and the resulting structural response. Although both buildings (MA000064 and MA000066) are situated on Site Class D soils, their contrasting subsurface conditions produce markedly different demand spectra. MA000064, shown in the upper panel, is underlain by a relatively shallow soil column (~23.9 m to bedrock) with stiffer material properties, resulting in a higher average shear-wave velocity and a fundamental frequency of 2.75 Hz. This configuration yields a sharp, narrow amplification peak in the transfer function, which is reflected in the steep and narrow GRA demand spectrum. Despite a higher F_a value, the site exhibits significant amplification over a limited range of short periods, with spectral acceleration decaying rapidly beyond the peak. This

spectral shape poses the greatest hazard to low-rise, stiff structures—such as unreinforced masonry buildings or short-span steel frames—whose fundamental periods are more likely to align with the site's short-period amplification range. In contrast, MA000066, shown in the lower panel, overlies a much deeper and softer soil column (~47.6 m), with a lower fundamental frequency of 1.62 Hz and a higher F_v value. This site condition facilitates the amplification of longer-period seismic waves and results in a broader, flatter transfer function. Consequently, the GRA demand spectrum for MA000066 is substantially wider, with sustained spectral acceleration over a larger range of displacements. This spectral shape presents an elevated risk to mid- to high-rise structures or buildings with flexible frames, which may resonate within the long-period range captured by the broader spectrum. This broader response is not merely a product of scaling via F_a and F_v, but rather a reflection of physical resonance effects captured by the full 1D wave propagation model, emphasizing the importance of detailed ground response analysis in accurately characterizing structural vulnerability across a spectrum of building types.

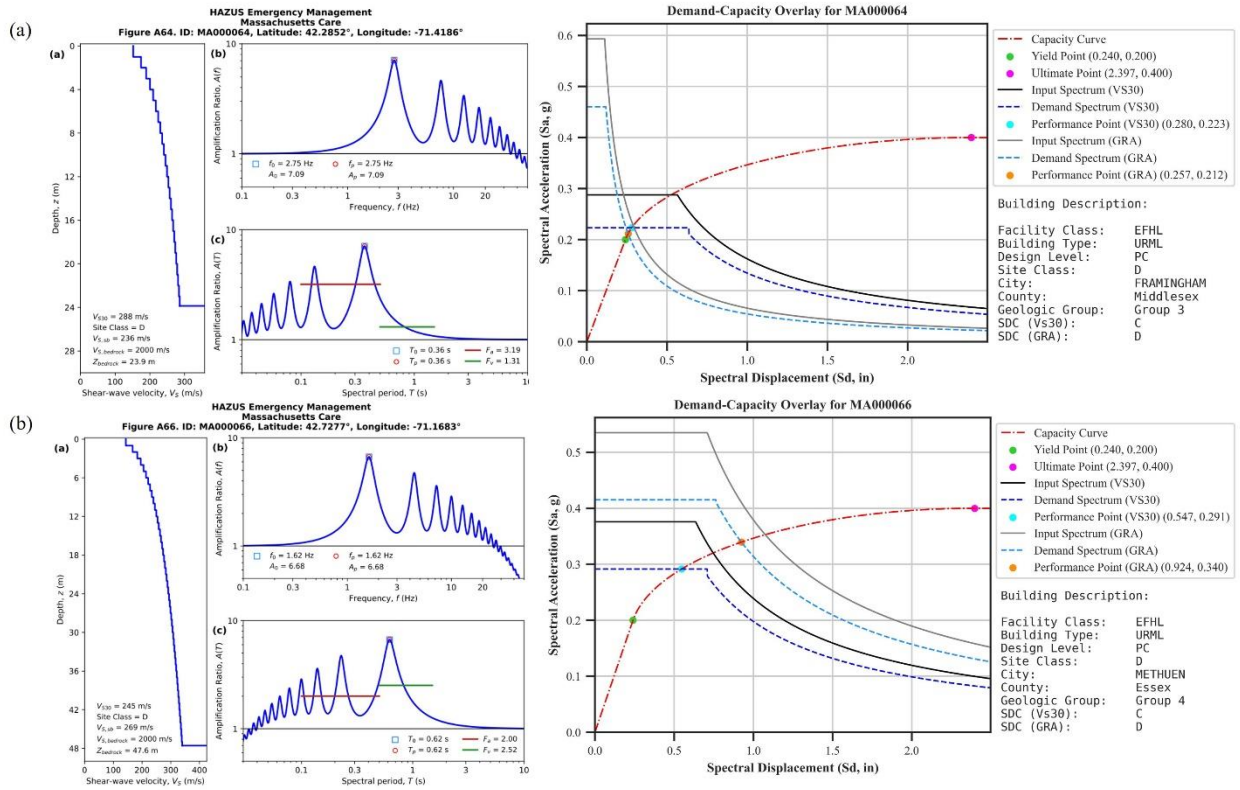

Figure 5: Comparison of GRA-derived demand spectra and transfer functions for two Site Class D buildings with differing subsurface profiles: (a) MA000064, underlain by a shallow (~23.9 m) stiff soil column, and (b) MA000066, underlain by a deeper (~47.6 m) soft soil column.

Building on the previous comparison of Site Class D profiles—where depth to bedrock and soil stiffness were shown to significantly shape spectral response—it is instructive to evaluate how these effects manifest across a broader range

of site classifications. **Figure 6** presents demand-capacity overlays for five buildings situated on sites ranging from Site Class A to CD. Although all profiles have depths to bedrock less than 30 meters—the threshold conventionally used in Vs_{30}-based site amplification—the figure reveals substantial variability in demand spectrum shapes and performance point locations. These variations underscore the influence of even modest changes in soil stratigraphy and mechanical properties on seismic demand and structural performance.

The two buildings located on Site Classes A and B (MA000123 and MA000105) are underlain by shallow, stiff soil columns with bedrock depths less than 10 meters. For these sites, the Vs_{30}-based and GRA-derived demand spectra are nearly indistinguishable, indicating minimal site amplification and limited dynamic response. This result aligns with expectations for hard rock conditions, where resonance effects and impedance contrasts are negligible. Accordingly, **Figure 4** demonstrates that the estimated moderate damage probabilities generally differ minimally between the two amplification methods for these site classes.

In contrast, the buildings situated on softer Site Classes BC, C, and CD exhibit greater divergence between the Vs_{30}-based and GRA spectra, accompanied by more pronounced differences in estimated damage probabilities. These discrepancies are especially evident in the widening of the Vs_{30}-derived demand curves, which suggests that the simplified method may overgeneralize amplification in sites with intermediate stiffness. Notably, MA000135—classified as Site Class CD and characterized by the deepest soil column in the group (20.7 meters)—exhibits the broadest Vs_{30}-based demand spectrum. This spectral broadening likely reflects the influence of more compressible soils with lower shear-wave velocities, which prolong the amplification window and reduce effective damping.

Across the sites underlain by softer soils—particularly those classified as BC, C, and CD—a consistent trend emerges in the comparative spectral behavior between Vs_{30}-based and GRA-derived demand curves. As depth to bedrock increases within these soil classes, the Vs_{30}-based spectra tend to widen, reflecting a broader period range of predicted amplification. This broadening occurs because Vs_{30}, as a single-value proxy, lacks the resolution to capture resonance phenomena tied to specific subsurface conditions and instead distributes amplification more diffusely across the spectrum. In contrast, the GRA-derived spectra become increasingly narrow and focused with increasing soil depth. This narrowing indicates that one-dimensional ground response modeling more precisely isolates frequency bands where amplification is physically supported by the dynamic properties of the soil profile. Rather than implying uniform amplification across an extended period range, GRA localizes seismic demand around discrete resonant frequencies governed by impedance contrasts and stratigraphic layering. This divergence highlights the tendency of

Vs_{30}-based methods to overgeneralize site effects, while GRA provides a more constrained and physically realistic representation of seismic amplification in stratified, compressible soils.

However, this trend is not immediately apparent in the Site Class D profiles shown in **Figure 5**. Specifically, the broader GRA spectrum observed for MA000066 may seem to contradict the pattern of narrowing seen in shallower soft soil sites. This divergence can be attributed to the increased depth and complexity of the subsurface profile at this location. While softer soil sites with bedrock depths under 30 meters tend to exhibit narrowly peaked GRA spectra due to well-defined fundamental modes, the ~47.6-meter profile at MA000066 supports a wider range of vibrational modes. The greater depth and lower stiffness of the soil column allow for the amplification of a broader frequency range, resulting in a wider GRA spectrum. Rather than contradicting the trend, this represents a logical extension of it—where deeper, softer profiles introduce more distributed resonance effects. The 1D GRA method captures this behavior by resolving multiple overlapping amplification bands, particularly at longer periods where energy trapping and impedance contrasts are more pronounced. This observation reinforces the value of GRA in capturing both sharply defined and broadly distributed amplification phenomena, depending on the specific subsurface conditions.

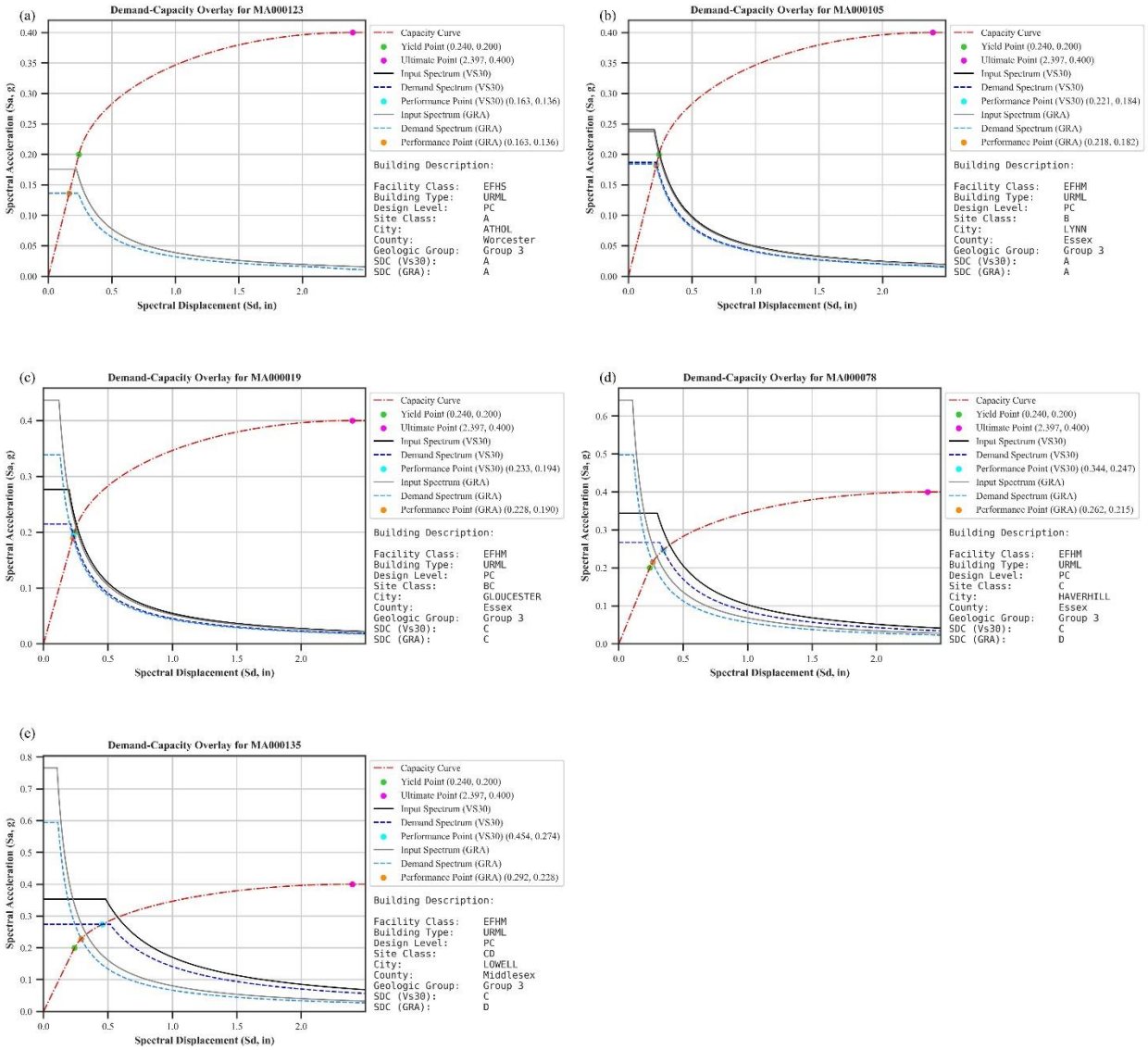

Figure 6: Demand-capacity overlays for five buildings located on sites with depth to bedrock less than 30 meters, spanning Site Classes A through CD. (a) Site Class A. (b) Site Class B. (c) Site Class BC. (d) Site Class C. (e) Site Class CD.

The observed patterns are further illustrated in the spatial distribution of moderate damage exceedance probabilities shown in **Figures 7 and 8**, depicting GRA and Vs_{30} amplification, respectively. In particular, inset (b), which focuses on the Boston Basin, reveals a marked difference between the GRA- and Vs_{30}-based estimates. Under GRA, the Basin exhibits a concentrated cluster of high-probability exceedance values (magenta and red markers), reflecting strong localized amplification associated with the basin's deep, low-velocity sedimentary fill. The GRA approach effectively resolves this spatial heterogeneity by modeling wave propagation through the entire soil column, including the resonance and impedance contrast effects that dominate in such geologic settings. In contrast, the Vs_{30}-based map

displays a more diffuse and attenuated hazard pattern across the same region. While it identifies general susceptibility, it fails to capture the concentrated amplification seen under GRA—an expected outcome, as Vs_{30} averages shear-wave velocity over only the upper 30 meters and lacks sensitivity to deeper stratigraphy and frequency-dependent amplification. The comparison reinforces the earlier observation: deeper, softer sites such as those found in the Boston Basin support multiple vibrational modes, resulting in broader amplification spectra and more severe structural demand. By capturing these nuances, GRA offers a more accurate spatial representation of seismic hazard in complex geologic environments, where simplified proxies like Vs_{30} may underrepresent localized risk.

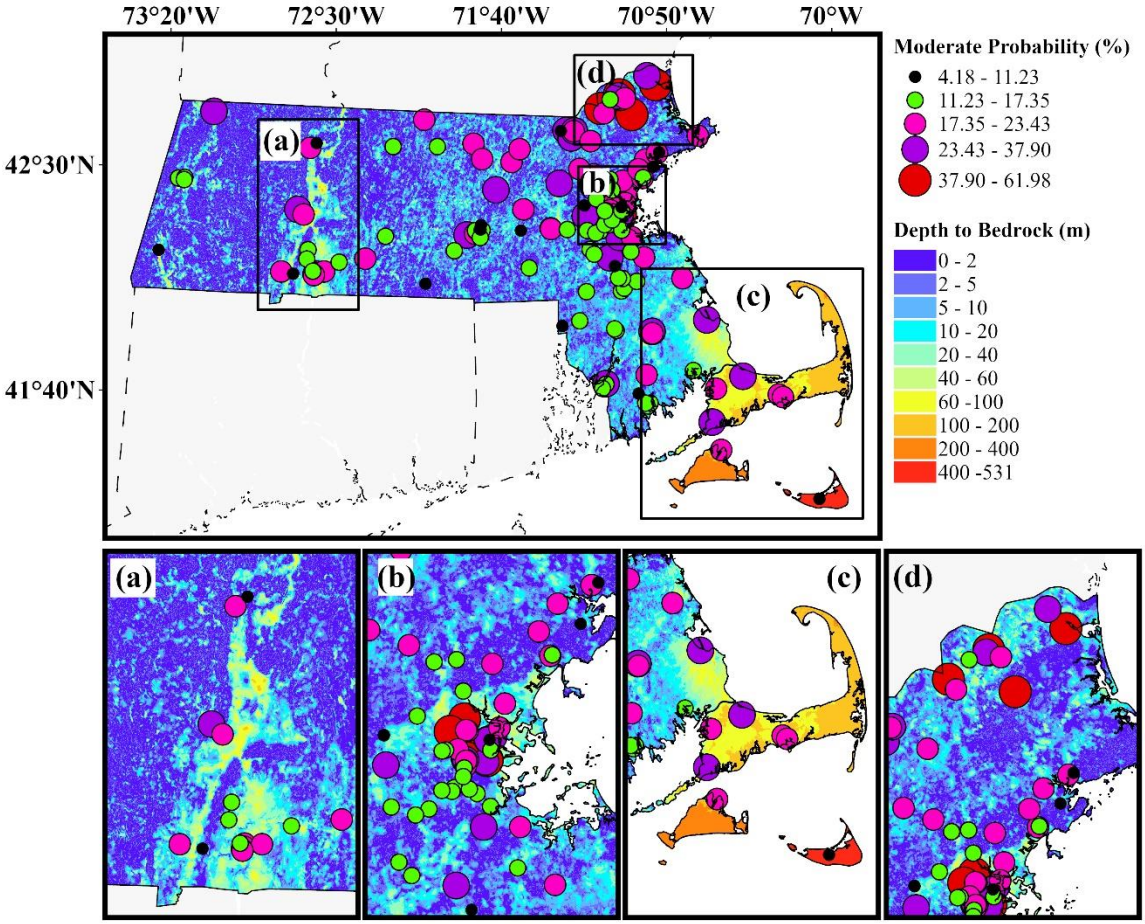

Figure 7: Spatial distribution of cumulative moderate damage exceedance probabilities derived from 1D Ground Response Analysis (GRA). Circles represent 160 state-owned facilities plotted over a statewide map of depth to bedrock. Marker size is scaled by exceedance probability, and color reflects probability bins ranging from 4.18% to 61.98%. (a) Connecticut River Valley. (b) Boston Basin. (c) Cape Cod. (d) Massachusetts North Shore.

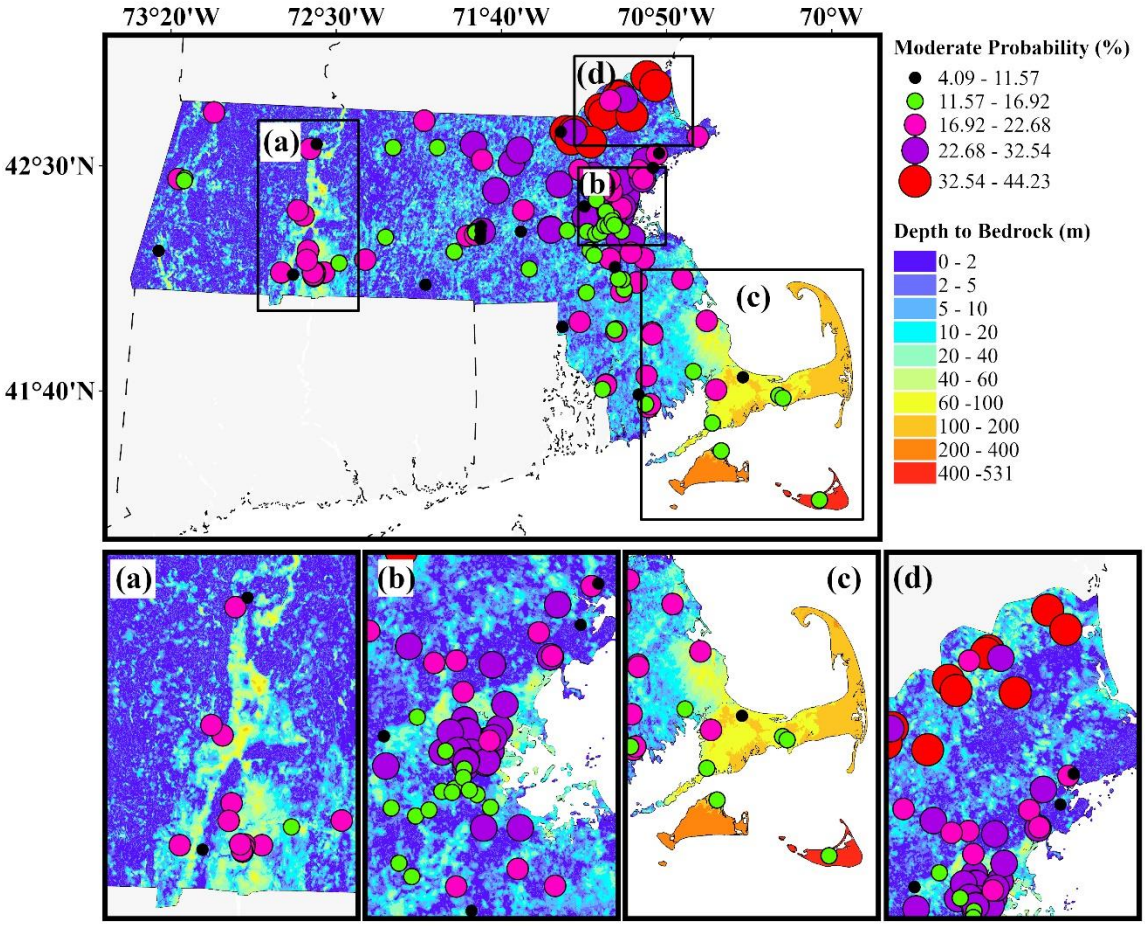

Figure 8: Spatial distribution of cumulative moderate damage exceedance probabilities derived from Vs30-based amplification. Circles represent the same 160 state-owned facilities overlaid on depth to bedrock, with marker size and color corresponding to exceedance probability bins (4.09% to 44.23%). (a) Connecticut River Valley. (b) Boston Basin. (c) Cape Cod. (d) Massachusetts North Shore.

3.4.2 High-Risk Building Identification Based on 90th Percentile Damage Probabilities

Given the GBS of 160 buildings, the top 10%—representing the 90th percentile—corresponds to 16 buildings with the highest cumulative probabilities of exceeding the moderate damage state. As illustrated in **Figure 9**, both the Vs_{30}-based and GRA-based approaches identify 16 high-risk buildings; however, their geospatial and geotechnical distributions differ notably. Under the GRA approach, all high-risk buildings are exclusively located on Site Class D. In contrast, the Vs_{30}-based method identifies buildings across both Site Classes CD and D. This divergence highlights the enhanced ability of GRA to capture localized site effects, owing to its explicit modeling of subsurface stratigraphy and dynamic wave propagation.

Panel (c) further underscores the influence of depth to bedrock on seismic amplification. The buildings identified as high-risk under the GRA framework are associated with significantly deeper soil profiles, ranging from

approximately 20 to 200 meters. Conversely, buildings identified under the Vs_{30} approach generally overlie shallower deposits (10–60 meters). This distinction emphasizes the heightened sensitivity of GRA to deep, soft-soil conditions that promote resonance and long-period wave amplification—features that the Vs_{30} proxy may fail to capture due to its limited depth resolution and reliance on surface conditions.

Finally, panel (d) shows that the spatial distribution of the highest-risk buildings aligns with areas expected to experience elevated seismic shaking, particularly in Suffolk, Essex, and Middlesex counties. These regions correspond with zones of higher peak ground acceleration (PGA) identified in the seismic hazard maps (see Introduction section), reinforcing the credibility of the damage estimates derived through the GRA method.

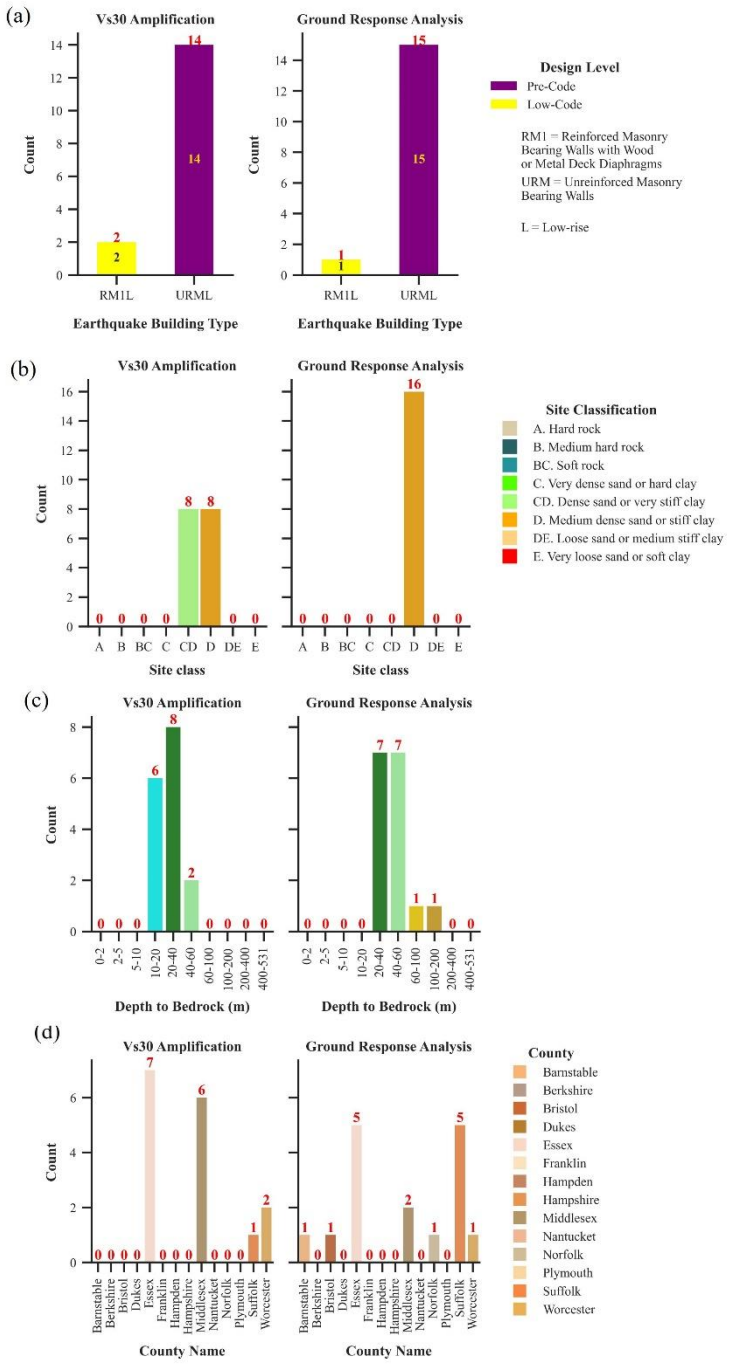

Figure 9: Comparison of the top 10% (90th percentile) most amplified buildings based on Vs30-based amplification and Ground Response Analysis (GRA) methods across (a) earthquake building types and design levels, (b) site classifications, (c) Depth to bedrock range, and (d) County distributions.

3.4.3 Inventory Sensitivity Assessment

To facilitate a preliminary comparison of seismic vulnerability outcomes between a localized facility-level inventory and a generalized national dataset, a matched subset was constructed by cross-referencing state-owned buildings with

the default entries in the HAZUS General Building Stock (GBS) database. Of the 15 state-owned care facilities initially analyzed, only eight could be reliably matched to corresponding GBS records, primarily due to inconsistencies in geographic referencing and resolution between the two datasets.

As presented in **Figure 10**, this matched dataset enables a direct comparison of structural typologies and seismic performance estimates across both inventories. Although the sample size is limited, it offers valuable insight into the implications of data resolution, classification assumptions, and exposure modeling practices. Importantly, only two of the state-owned buildings in this matched set are classified as Unreinforced Masonry (URM), in contrast to the predominance of URM typologies in the GBS hospital dataset. Given that HAZUS fragility functions are highly sensitive to structural system, material properties, and design level, this divergence in building typology underscores the limitations of generalized exposure models when applied to site-specific or asset-specific risk assessments. The comparison highlights how inventory resolution and typological accuracy can significantly influence projected damage outcomes, thereby affecting the prioritization of seismic mitigation measures.

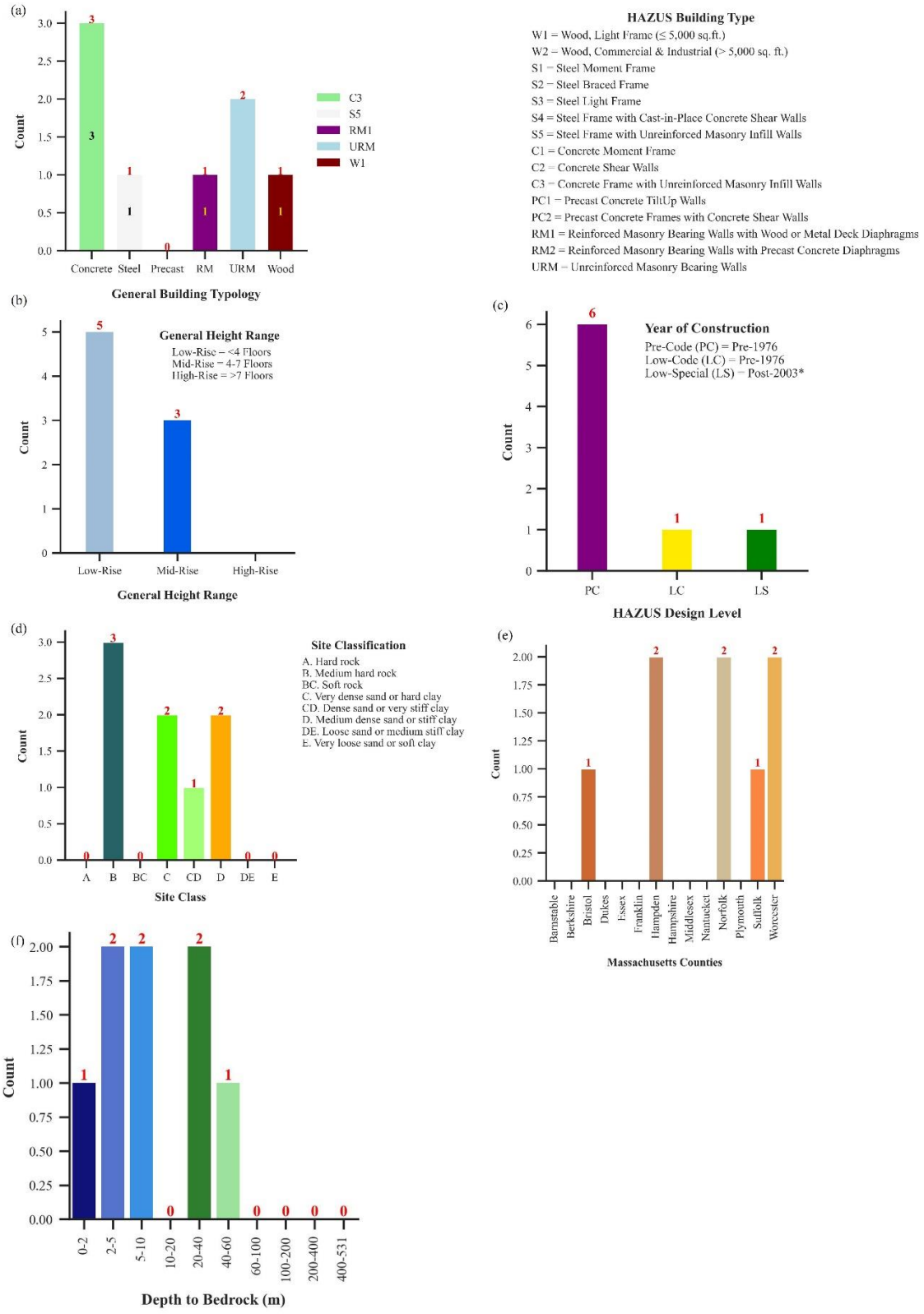

Figure 10: State-owned care facilities with matching GBS matching location. (a) general Building Typology. (b) General building height. (c) HAZUS Design Level. (d) Site Classes. (e) County Locations. (f) Depth to bedrock. The building characteristics are more specific than those used in the GBS.

Figure 11 presents the cumulative probability of exceedance for the moderate damage state based on Vs_{30}-derived site amplification. Across the matched dataset, the HAZUS General Building Stock (GBS) consistently yields higher exceedance probabilities than the state-owned building inventory. The median probability of moderate damage exceedance for the HAZUS GBS is 16.37%, notably higher than the 11.23% median observed for the state-owned structures. Both inventories contain statistical outliers, with the maximum values reaching 31.41% for the state-owned dataset and 26.69% for the HAZUS GBS.

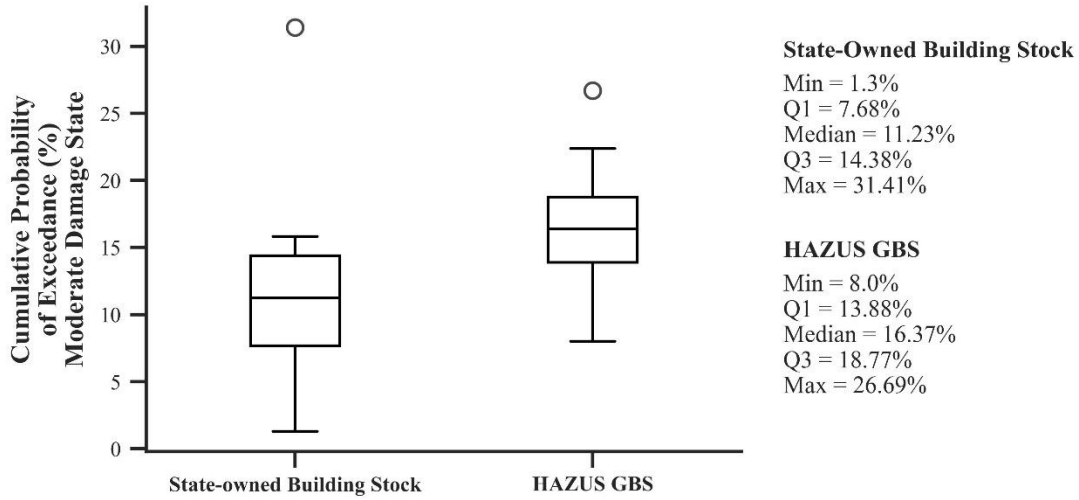

Figure 11: Comparison of Cumulative Probability of Exceedance (%) for Moderate Damage State Using Vs30-Based Amplification.

Figure 12 illustrates the same comparison using ground motion estimates derived from site-specific GRA. Under this approach, the disparity in estimated damage probabilities becomes even more pronounced. The median exceedance probability for the HAZUS GBS remains elevated at 15.27%—nearly twice that of the state-owned inventory, which declines to 7.92%. Additionally, the maximum exceedance value for the HAZUS dataset increases substantially to 37.9%, compared to 25.55% for the state-owned buildings. These findings suggest that site-specific ground response modeling amplifies differences in projected seismic performance, particularly highlighting the influence of structural typology and inventory granularity. The more conservative fragility assumptions applied to generalized HAZUS building types, particularly the predominance of URM classifications, likely contribute to the consistently higher damage probabilities in the GBS across both amplification methodologies.

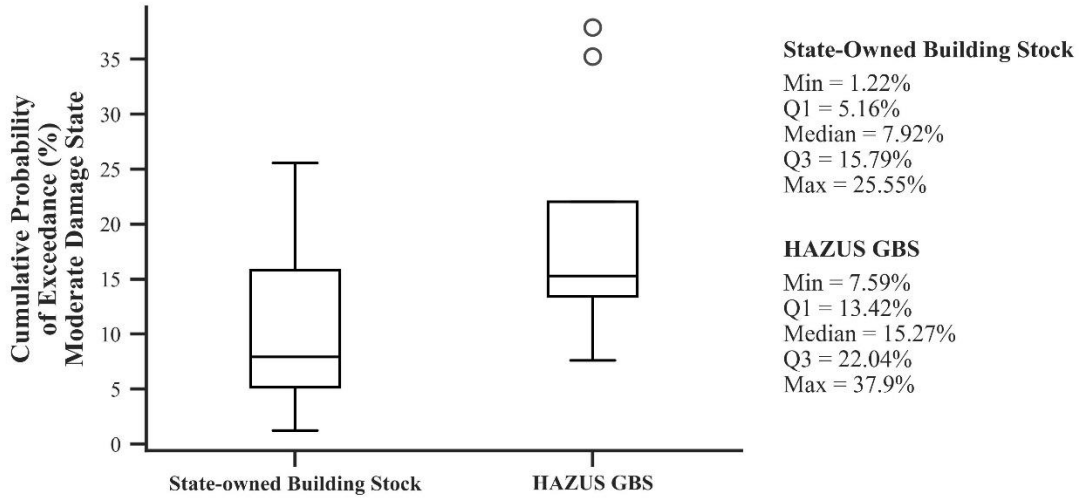

Figure 12: Comparison of Cumulative Probability of Exceedance (%) for Moderate Damage State Using Ground Response Analysis.

3.5 Implications

This section evaluates the broader implications of adopting Vs_{30}-based versus Ground Response Analysis (GRA)-based methods for characterizing site amplification, with particular focus on resonance effects and their influence on Seismic Design Category (SDC) classification. While the Vs_{30} approach provides a simplified, empirically-derived estimate of site effects, it lacks sensitivity to resonance phenomena associated with deeper, stratified, or highly variable subsurface conditions. As demonstrated in this study, the GRA method—by explicitly modeling shear-wave propagation through site-specific velocity profiles—captures complex amplification patterns that may not be reflected in Vs_{30}-based approximations.

These differences are not trivial. GRA-derived spectra frequently indicate elevated ground motions, especially at longer periods, which can influence the assignment of SDC classifications. This shift has direct design implications, as higher SDCs correspond to more stringent structural requirements under prevailing building codes. Consequently, buildings situated on soft, thick, or impedance-contrasting soil profiles may be under-classified when Vs_{30} is used alone, leading to underestimation of seismic demand in design.

However, the interpretation of these amplification effects must be contextualized within the characteristics of the building inventory under study. The HAZUS General Building Stock (GBS), which is used in this analysis, predominantly consists of low-rise structures. These buildings are generally governed by short-period response and are therefore less affected by long-period amplification that GRA tends to highlight. This introduces a potential mismatch: while GRA improves the resolution of site effects, the simplified structural models in HAZUS may not

fully reflect how these effects translate into vulnerability, especially for buildings whose dynamic response lies outside the amplified frequency band. As such, future work should explore the interaction between improved site response modeling and more detailed structural modeling to better align hazard inputs with realistic building behavior.

3.5.1 Soil-Structure Resonance

The comparison between GRA and Vs_{30}-based methods reveals fundamental differences in how each approach accounts for potential resonance phenomena driven by local site conditions. As shown in **Figure 9c**, the GRA method consistently predicts greater spectral amplification at sites underlain by deeper soil columns. These deeper deposits are associated with lower fundamental soil frequencies, which in turn increase the potential for resonance with long-period components of ground motion. This effect is particularly relevant for mid- to high-rise buildings, whose natural periods may coincide with these amplified frequency bands, thereby intensifying dynamic structural response through resonance.

This relationship is well-supported by empirical period-height models such as:

$$T = C_h h^x \qquad \text{(Equation 1)}$$

where T is the fundamental period and h is the building height (ASCE 7-22) (**Figure 13**). For example, typical moment-resisting frames exceeding 10 stories can exhibit fundamental periods between 1.0 and 2.5 seconds—overlapping with the long-period amplification observed in deeper soil sites. However, a critical limitation of this study is the reliance on the HAZUS General Building Stock (GBS), which is dominated by low-rise structures (generally 1 to 3 stories). These buildings tend to have shorter natural periods, typically below 0.5 seconds, making them more responsive to high-frequency shaking. Consequently, while GRA successfully captures site-specific resonance potential, its full implications for structural damage may be muted in this analysis due to the limited resonance sensitivity of the building stock under consideration.

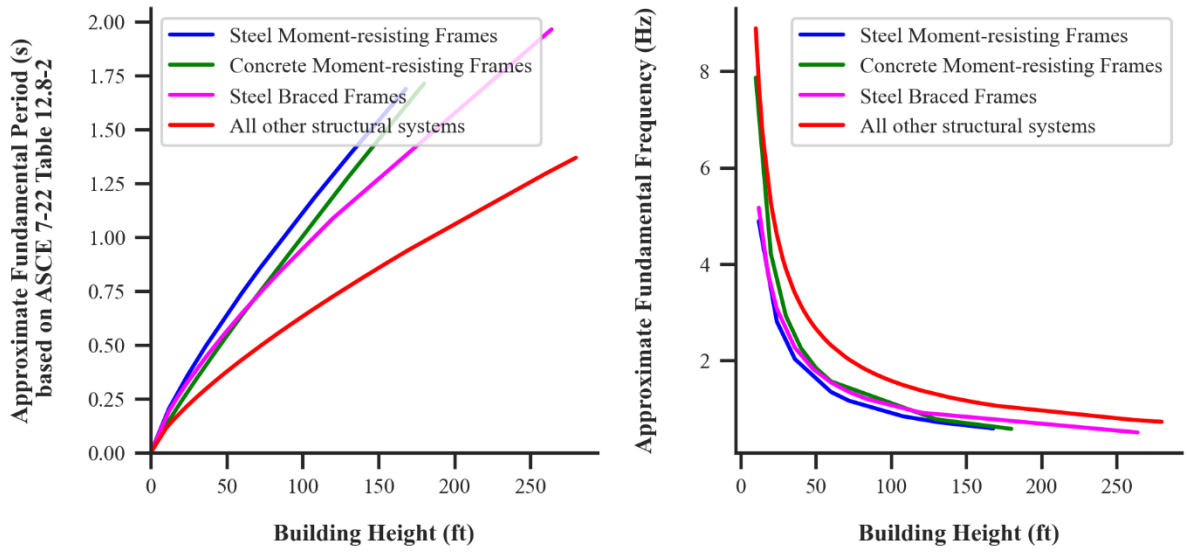

Figure 13: Relationship between building height and approximate fundamental period, as estimated using empirical formulas from ASCE 7-22 Table 12.8-2, and the corresponding natural frequency. The derived frequencies illustrate how structural period scales with height, highlighting the potential for resonance with long-period ground motions on deep or soft soil sites.

This disconnect between the modeled site response and the characteristics of the building inventory carries two critical implications. First, there is a risk of undetected vulnerability in unrepresented building types. The most pronounced resonance-driven amplification effects—especially those associated with deeper, softer soil profiles—are likely to pose heightened risk to mid- and high-rise buildings, which are largely absent from the current dataset. Second, seismic risk may be systematically underestimated due to the dominance of low-rise structures in the HAZUS General Building Stock. These buildings are primarily sensitive to short-period ground motions, potentially obscuring the significance of long-period amplification that would be more impactful for taller structures.

Accordingly, while GRA provides a higher-resolution, physics-based framework for modeling site-specific amplification—including the capacity to capture resonance phenomena—its full utility is constrained by the representativeness of the building inventory. Future vulnerability assessments should consider incorporating a broader spectrum of building typologies, particularly incorporating structural height, to evaluate the interaction more accurately between localized ground motion characteristics and dynamic building response.

3.5.2 Seismic Design Category Classification

Beyond soil-structure resonance effects, the differences between GRA- and Vs_{30}-based amplification methods have significant implications for Seismic Design Category (SDC) classification. In seismic design practice, localized site conditions are addressed by adjusting mapped spectral accelerations—S_s (short-period) and S_1 (long-period)—using

site-specific amplification factors, F_a and F_v. These coefficients, defined in seismic design standards such as ASCE 7, are functions of both site classification and regional hazard level. Their role is to modify ground motion parameters to reflect the influence of soil-induced amplification or attenuation, providing a simplified representation of complex site response behavior within code-based design frameworks.

For a given site, the short-period spectral acceleration (S_s) is amplified using F_a to produce the mapped short-period value:

$$S_{MS} = F_a * S_s \qquad \text{(Equation 2)}$$

Similarly, the long-period spectral acceleration (S_1) is amplified using F_v to obtain the mapped long-period value:

$$S_{M1} = F_v * S_1 \qquad \text{(Equation 3)}$$

These mapped values are then scaled by a factor of 2/3—per ASCE 7 provisions—to derive the design-level spectral accelerations:

$$S_{DS} = \frac{2}{3} * F_a * S_s \qquad \text{(Equation 4)}$$
$$S_{D1} = \frac{2}{3} * F_v * S_1 \qquad \text{(Equation 5)}$$

These parameters, S_{ds} and S_{d1}, are used to determine the Seismic Design Category (SDC), with the more severe value controlling the classification, as outlined in **Tables 2 and 3**. The resulting SDC is further informed by the building's assigned Risk Category, based on its use and occupancy (e.g., essential facilities fall under Risk Category IV, per **Table 1**). In this study, all buildings are assumed to belong to Risk Category IV, reflecting their emergency management functions and the heightened performance expectations that accompany this classification.

The SDC designation governs the level of seismic detailing, ductility, and lateral force-resistance requirements in structural design. Sites underlain by soft or deep soil conditions—typically corresponding to Site Classes D and E—tend to exhibit larger amplification factors (F_a and F_v) relative to stiffer soils or rock (Site Classes A or B). This results in higher mapped and design spectral accelerations, particularly in the long-period range, where amplification effects are often intensified by resonance and impedance contrasts between stratified soil layers and underlying bedrock.

Table 1: Risk Categories (ASCE 7, Table 1.5-1)

Risk Category	Definition	Examples
I	Buildings that represent a low hazard to human life in the event of failure.	Agricultural buildings, certain storage facilities.
II	Buildings that are not classified in Risk Categories I, III, or IV. They have a normal hazard level for human life.	Most commercial and residential buildings.
III	Buildings that pose a substantial hazard to human life in the event of failure, including those with high occupancy or essential facilities.	Assembly occupancies, schools, and certain hospitals.
IV	Essential facilities that are critical for emergency response and recovery, designed to remain operational after a seismic event.	Fire stations, police stations, critical emergency structures.

Table 2: Seismic Design Category Based on Short-Period Response Acceleration Parameter (ASCE 7-22, Table 11.6-1).

	Risk Category	
Values of S_{DS}	**I or II or III**	**IV**
$S_{DS} < 0.167$	A	A
$0.167 \leq S_{DS} < 0.33$	B	C
$0.33 \leq S_{DS} < 0.50$	C	D
$0.50 \leq S_{DS}$	D	D

Table 3: Seismic Design Category Based on 1-s Response Acceleration Parameter (ASCE 7-22, Table 11.6-2).

	Risk Category	
Values of S_{D1}	**I or II or III**	**IV**
$S_{D1} < 0.067$	A	A
$0.067 \leq S_{D1} < 0.133$	B	C
$0.133 \leq S_{D1} < 0.20$	C	D
$0.20 \leq S_{D1}$	D	

Although amplification factors F_a and F_v are standard factors in seismic design, they are simplified, empirically derived coefficients based solely on Vs_{30} and do not fully capture the complexity of site-specific conditions. In contrast, GRA offers a more detailed, physics-based approach by modeling seismic wave propagation through stratified soil profiles. This often results in higher and more realistic estimates of mapped spectral accelerations (S_{ms} and S_{m1}) than those obtained using Vs_{30}-based approximations.

As shown in **Figures 14 and 15**, these differences have direct implications for Seismic Design Category (SDC) classification. Vs_{30}-based amplification frequently yields lower design spectral values (S_{ds} and S_{d1}), placing buildings into lower SDCs—such as Category C—potentially underestimating seismic demand. GRA-derived values, however, often result in upward reclassification. For example, of the 96 buildings initially assigned to SDC C using Vs_{30}, 50

buildings (52%) were reclassified to SDC D when GRA inputs were used. Similarly, 28 buildings moved from SDC A to C, representing a significant shift in design requirements. Within the subset of buildings in the 90th percentile of moderate damage probability, half of those originally classified as SDC C were reassigned to SDC D based on GRA results (**Figure 16**). These reclassifications represent meaningful increases in required seismic design stringency, reinforcing the limitations of simplified site factors and the importance of incorporating detailed ground response modeling, particularly in regions with complex or amplification-prone soils.

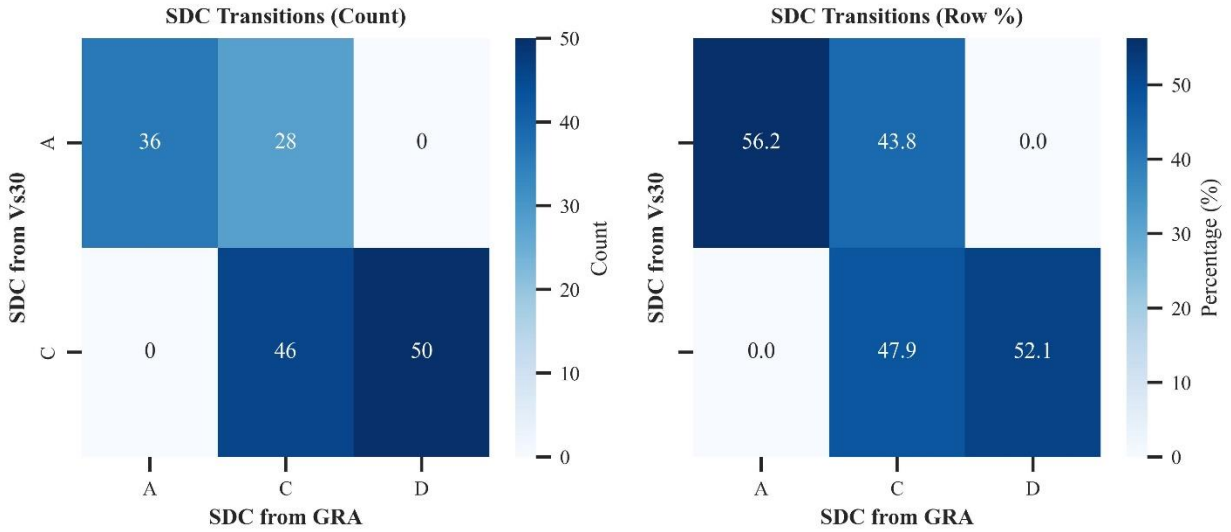

Figure 14: Comparison of Seismic Design Category (SDC) classifications based on Vs30-based amplification versus Ground Response Analysis (GRA). The left heatmap shows the number of buildings transitioning between SDCs (A, C, D), while the right heatmap expresses these transitions as row-wise percentages. Notably, 52.1% of buildings originally classified as SDC C under the Vs30 approach are reclassified as SDC D using GRA, indicating that simplified site factors may underestimate seismic design demands for a significant portion of the building stock.

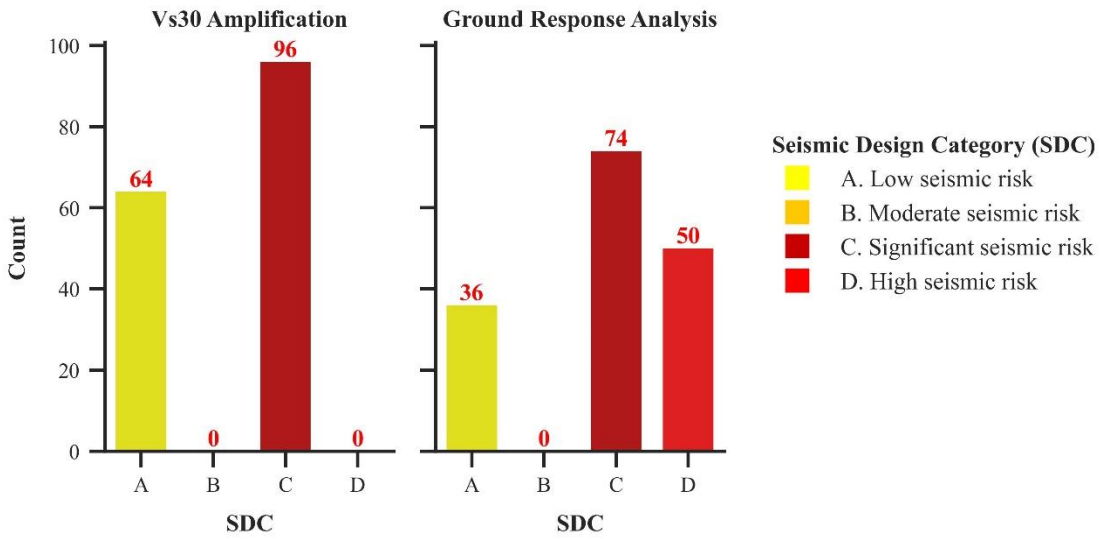

Figure 15: Comparison of Seismic Design Category (SDC) distributions based on Vs30-based amplification (left) and Ground Response Analysis (GRA) (right). Vs30-based estimates classify most buildings into SDC C (significant seismic risk) and SDC A (low risk), with no structures assigned to the highest-risk category (SDC D). In contrast, GRA reveals a substantial increase in buildings classified as SDC D (high seismic risk), reflecting more pronounced site-specific amplification effects. Notably, 50 buildings—absent from the D category under Vs30—were reclassified into SDC D using GRA, underscoring the limitations of simplified site characterization in capturing critical seismic design demands.

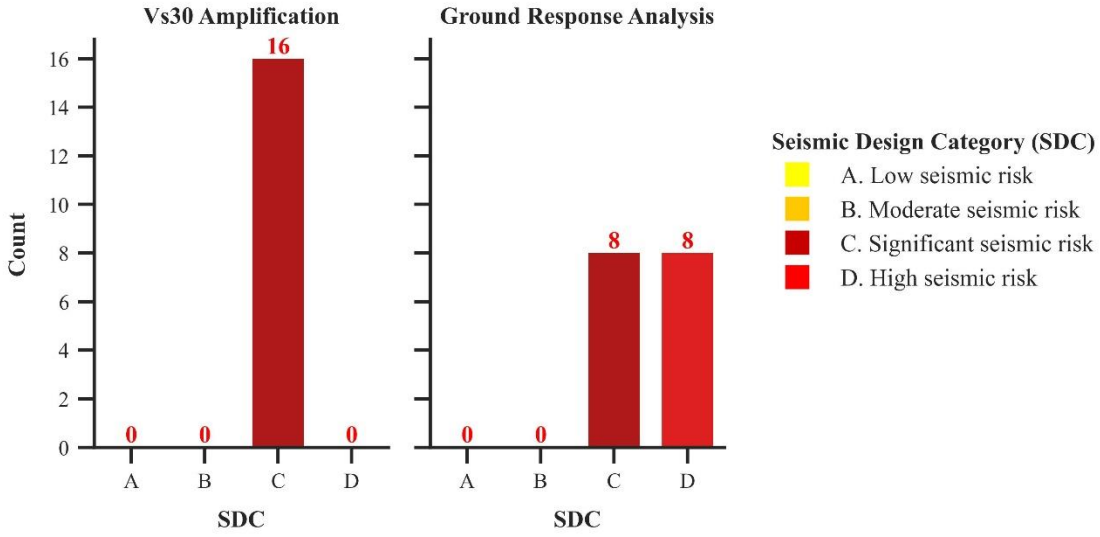

Figure 16: Seismic Design Category (SDC) classification for the buildings in the 90th percentile of cumulative moderate damage probabilities of exceedance based on Vs30 amplification (left) and Ground Response Analysis (GRA) (right). All 16 buildings are initially classified as SDC C using Vs30-based site coefficients, suggesting significant but not high seismic risk. However, GRA results reveal that 8 of these buildings (50%) warrant reclassification to SDC D, reflecting elevated site-specific amplification. This shift highlights how simplified Vs30-based methods may underestimate seismic demand under higher-intensity shaking, particularly for structures situated on soft or deep soil profiles.

3.6 Conclusion

This study underscores the critical importance of accurate site characterization in seismic vulnerability assessments, particularly in regions like the Central and Eastern United States (CEUS), where soft soils, deep sediment layers, and strong impedance contrasts are prevalent. Traditional seismic hazard models and building codes typically rely on Vs_{30} as a proxy for site amplification. While Vs_{30}-based methods offer simplicity and widespread applicability, they fail to capture the effects of deeper stratigraphy, site-specific impedance contrasts, and frequency-dependent amplification—factors that significantly influence ground motion intensity and structural response.

By integrating high-resolution geotechnical datasets—including shear-wave velocity profiles and depth-to-bedrock maps—this study applied both Vs_{30}-based amplification and linear one-dimensional Ground Response Analysis (GRA) to evaluate seismic performance using FEMA HAZUS-informed fragility functions. The results demonstrate that Vs_{30}-based methods tend to produce smoother, generalized estimates that are less sensitive to localized geologic variability. In contrast, GRA captures a broader spectrum of site-specific responses, yielding higher peak spectral accelerations and moderate damage exceedance probabilities at sites characterized by strong amplification.

Quantitatively, the GRA approach produced a maximum moderate damage exceedance probability of 61.98%, compared to 44.23% for Vs_{30}—highlighting GRA's ability to reflect extreme site effects. The 90th percentile exceedance probability was slightly lower for GRA (29.48%) than for Vs_{30} (30.58%), indicating that while GRA better identifies outlier risks, it offers more restrained estimates across most sites. This distinction is crucial for policy and design, as it reveals that Vs_{30}-based methods may overgeneralize hazard, potentially leading to both overdesign in low-risk settings and underdesign in high-risk ones.

These amplification patterns have direct implications for Seismic Design Category (SDC) classification. The use of F_a and F_v—empirical multipliers based on Vs_{30}—often underrepresents actual site amplification, particularly at longer periods associated with soft soil response. GRA, by simulating wave propagation through layered soils, captures the effects of stratification and impedance contrast, resulting in higher S_{ms} and S_{m1} values and, consequently, higher SDCs. Of the 96 buildings originally classified as SDC C using Vs_{30}, over half (52%) were reclassified as SDC D using GRA. A similar trend was observed within the highest-risk subset: 50% of buildings in the 90^{th} percentile group shifted from SDC C to D. These changes carry substantial design implications, necessitating stricter lateral force-resisting systems, enhanced ductility, and improved anchorage provisions.

Additionally, the study compared generalized HAZUS General Building Stock (GBS) with a refined dataset of state-owned facilities. The state-owned buildings consistently exhibited lower exceedance probabilities, owing to both improved structural characteristics and more accurate representation of local site conditions. This contrast highlights the limitations of relying solely on generalized national inventories, which may misrepresent actual risk and result in conservative or misaligned design strategies.

Thus, while V_{S30} remains a useful and accessible proxy, this study emphasizes that it should not be the sole amplification method in geologically complex regions. Incorporating GRA into hazard assessment workflows provides a more precise understanding of site amplification effects, enabling more accurate damage estimation and informed seismic design. As seismic design standards and hazard mapping continue to evolve—especially in low- to moderate-seismicity regions—adopting regionally calibrated, physics-based methods will be critical to enhancing infrastructure resilience and supporting evidence-based mitigation planning.

3.7 Data and Resources

The state-owned building inventory used in this study is proprietary, and access to this data is restricted due to proprietary rights and cannot be shared publicly. Ground motion data used in the analysis were sourced from the United States Geological Survey (USGS) Seismic Design Geodatabase for the 2020 NEHRP recommended seismic provisions and 2022 ASCE/SEI 7 standard by Luco et al. (2021) and are publicly available. The depth-to-bedrock map was obtained from MassGIS (Massachusetts Bureau of Geographic Information) and is also publicly available. All other data and resources referenced in this article are freely available and are cited accordingly.

3.8 Project Acknowledgements

Many thanks to the Massachusetts Division of Capital Asset Management & Maintenance (DCAMM) for providing the state-owned building inventory used in this study. Their assistance in granting access to their data was instrumental in conducting the analysis.

Conclusion

“What we call the beginning is often the end. And to make an end is to make a beginning. The end is where we start from.” — **T.S. Eliot**

While earthquakes are natural phenomena, the extent of devastation they cause is often shaped by human choices—particularly decisions around preparedness, data use, and investment in resilience. This dissertation underscores the critical importance of integrating high-resolution data, geotechnical insight, and localized analysis into seismic risk assessment practices. Across its chapters, the work presents a progression of methodologies aimed at bridging the gap between national-scale hazard models and site- or asset-specific realities.

Chapter 1 established a standardized approach for post-earthquake liquefaction mapping, demonstrating how remote sensing and geospatial analytics can improve the speed and accuracy of ground failure assessments. Chapter 2 examined how high-resolution geotechnical data, combined with refined structural inventories, can produce more nuanced evaluations of building vulnerability in low-to-moderate seismicity regions—revealing the hidden risks posed by simplified assumptions. Chapter 3 extended this work by comparing traditional Vs_{30}-based site amplification methods with site-specific ground response analysis, showing how detailed subsurface modeling can significantly alter projected damage estimates and Seismic Design Category classifications.

Together, these contributions promote a more informed, data-driven approach to seismic risk mitigation—one that enables engineers, planners, and policymakers to prioritize interventions where they are most needed. Rather than treating earthquake resilience as reactive or prescriptive, this dissertation advocates for anticipatory strategies grounded in empirical evidence and local conditions. In doing so, it highlights the need for adaptable frameworks that evolve with our understanding of both built and natural environments.

Ultimately, the goal of this body of work is not only to improve the technical accuracy of hazard assessments, but also to support the broader imperative of community resilience. By equipping decision-makers with better tools and more actionable insights, the work contributes to a future where seismic safety is not left to chance—but instead, is the outcome of deliberate, informed, and equitable planning.

Chapter 1 Summary of Contributions

Through the creation of polygon-based inventories across three diverse seismic events, this research provides both practical tools and methodological ingenuity for scientific inquiry and applied hazard mitigation. The contributions outlined below reflect the broader implications of this work and its value to the fields of earthquake engineering, geospatial analysis, and disaster risk reduction:

- **Standardized methodologies enable scalability and reproducibility**: The digitization protocol developed in this study—grounded in clearly defined attribute fields, metadata standards, and quality assurance

procedures—demonstrates that liquefaction surface inventories can be systematically produced across a range of geologic and geographic contexts. This approach supports future inventory expansion, cross-event comparison, and methodological replication.

- **Imagery resolution and acquisition timing are critical to inventory accuracy**: The quality and completeness of each inventory were strongly dependent on the availability of very high-resolution, cloud-free imagery acquired shortly after the seismic event. Timely image capture was essential for detecting perishable surface manifestations and producing detailed, spatially reliable maps.
- **Ground truth data strengthens interpretive reliability**: Confidence in feature classification was highest in inventories that incorporated validated field data. In contrast, areas with sparse or ambiguous ground truth exhibited greater uncertainty. This reinforces the importance of integrating reconnaissance findings into remote sensing workflows to improve inventory reliability.
- **Polygon-based mapping enhances spatial precision**: Representing liquefaction features as polygons—rather than points or broad zones—enabled detailed measurement of extent, geometry, and spatial distribution. This level of granularity is vital for quantitative hazard modeling, infrastructure impact analysis, and pixel-level training of machine learning models.
- **Inventories serve dual functions as scientific records and training datasets**: Beyond their value as geospatial documentation tools, the inventories generated here are well-suited for use in supervised learning applications. Their structured format and high spatial fidelity support the development of semi-automated and fully automated post-disaster damage detection models.
- **Methodological adaptability facilitates use in data-scarce regions**: The reliance on publicly available or commercial remote sensing data—combined with a standardized, metadata-rich framework—makes this methodology transferable to contexts with limited field reconnaissance capacity, thereby addressing persistent data access disparities in global risk modeling.
- **High-quality data is foundational to resilience-building**: The findings of this study affirm that timely, interpretable, and well-structured data are essential to the development of effective risk models, seismic design guidance, and disaster response strategies. These inventories contribute to both retrospective damage assessments and forward-looking planning efforts aimed at reducing vulnerability to future earthquakes.

These contributions collectively underscore the methodological rigor, technical applicability, and broader significance of the study. They reinforce the guiding principle that advancing resilience begins with advancing the quality, accessibility, and usability of post-disaster data.

Chapter 2 Summary of Contributions

Chapter 2 presents a regionally tailored seismic vulnerability assessment for the Commonwealth of Massachusetts, advancing methodologies for hazard analysis and risk-informed decision-making in low-to-moderate seismicity zones. This chapter contributes a scalable and transferable framework that responds to the unique geologic, structural, and regulatory characteristics of the Central and Eastern United States (CEUS), where seismic hazard is often underestimated due to infrequent large events and generalized modeling inputs.

Key contributions include:

- **Regional Integration of High-Resolution Site Characterization Data**: By leveraging a 100-meter resolution Vs_{30} map developed from locally calibrated geologic, geophysical, and microtremor data, the analysis captures amplification effects tied to site-specific conditions—such as impedance contrasts—commonly found across CEUS states. This approach improves upon national-scale models that often obscure localized risk patterns.
- **Use of Updated Seismic Design Ground Motions**: Incorporating 2023 USGS MCE_r values enables a regionally relevant application of the latest hazard information, ensuring consistency with modern code-based design practices and facilitating the identification of structures potentially under-designed for current seismic expectations.
- **Building-Level Vulnerability Characterization**: The study evaluates 2,676 state-owned buildings using FEMA HAZUS capacity and fragility curves, assigning damage probabilities based on structural system, height, code level, and occupancy class. The application of this method to a real, heterogeneous inventory—rather than synthetic proxies—strengthens its practical utility.
- **Multimodal Risk Segmentation and Statistical Prioritization**: By applying local maxima analysis to the distribution of damage probabilities, the chapter introduces a replicable technique for segmenting risk across building portfolios. This allows for prioritization of retrofitting actions based on both absolute vulnerability and structural function, supporting effective mitigation planning at the regional scale.

- **Regionally Scalable Retrofitting Strategy**: The prioritization framework—centered on the interaction between structural fragility, site class, and seismic demand—is directly transferable to other CEUS jurisdictions with similar geologic variability and legacy infrastructure. It provides a data-driven model for allocating limited retrofit resources to maximize resilience impact.
- **Practical Bridge Between Geotechnical and Structural Risk Assessment**: By aligning high-resolution subsurface data with standardized loss estimation tools, the study bridges the gap between geotechnical site effects and structural damage modeling in CEUS contexts, where such integration is often limited due to data scarcity or methodological inertia.

Overall, Chapter 2 underscores the critical importance of regional specificity in seismic vulnerability assessment. It offers a rigorous, reproducible methodology that enhances the accuracy and relevance of risk modeling in CEUS states—supporting more informed mitigation policy, infrastructure investment, and disaster preparedness planning across a historically under-characterized seismic landscape.

Chapter 3 Summary of Contributions

This chapter advances seismic risk assessment practices by quantifying the effects of site-specific ground response modeling on predicted building damage, spectral amplification, and seismic design classification. The analysis demonstrates that Ground Response Analysis (GRA), when informed by detailed subsurface geotechnical data, can meaningfully alter damage projections compared to traditional Vs_{30}-based methods. By applying both amplification approaches to a shared building inventory, this study isolates the influence of local soil behavior—captured through GRA—on spectral response and damage probability.

Key contributions of this chapter include:

- **Demonstrated divergence between simplified and physics-based site amplification methods**: GRA was shown to produce higher maximum damage exceedance probabilities and more varied spectral response shapes, particularly for buildings located on deeper, softer soil profiles. This highlights the limitations of relying solely on Vs_{30}-based amplification in geologically complex regions.
- **Identification of SDC reclassification trends**: More than 50% of buildings originally placed in Seismic Design Category (SDC) C using Vs_{30}-derived coefficients were reclassified to SDC D under GRA, reflecting the upward shift in seismic demand captured by detailed site response modeling. Similarly, 44% shifted from

SDC A to SDC C. This shift has direct implications for code compliance and design-level detailing requirements.

- **Characterization of spectral shape variability**: The chapter explores how resonance effects—amplification tied to specific frequency bands—are more accurately captured using GRA. This spectral localization is especially important for mid- and high-rise structures whose dynamic periods align with soil site frequencies.
- **Comparison of generalized versus asset-specific building data**: A side-by-side comparison of the HAZUS General Building Stock (GBS) and a state-owned building inventory revealed significant differences in damage predictions and structural classifications. The HAZUS dataset, while useful for regional screening, overrepresented vulnerable typologies such as URM and failed to reflect improvements present in actual facilities.
- **Implications for seismic mitigation and design policy**: The findings support the integration of GRA into standard seismic evaluation workflows, especially in the Central and Eastern U.S., where traditional proxies may not capture key subsurface variability. The results also emphasize the importance of inventory resolution, as generalized exposure datasets may lead to misinformed vulnerability estimates.

Through this comparative framework, the chapter contributes a regionally calibrated, data-informed approach to improving seismic risk accuracy, hazard communication, and design-level decision-making.

References

Introduction

Adger, W. N. (2006). Vulnerability. *Global Environmental Change*, *16*(3), 268–281. https://doi.org/10.1016/j.gloenvcha.2006.02.006

American Society of Civil Engineers. (2022). *Minimum design loads and associated criteria for buildings and other structures (ASCE/SEI 7-22)*.

Baise, L. G., Kaklamanos, J., Berry, B. M., & Thompson, E. M. (2016). Soil amplification with a strong impedance contrast: Boston, Massachusetts. *Engineering Geology*, *202*, 1–13. https://doi.org/10.1016/j.enggeo.2015.12.016

Becker, L. R., Fratto, E. S., Patriarco, S. P., Marvinney, R. G., Mabee, S. B., & Thomas, M. A. (2011). (tech.). *Utilizing the Surficial Geology of the Northeast United States to Improve NEHRP Site Effect Classifications in HAZUS-MH: Collaborative Research with NESEC and the NESEC State Geologists*. U.S. Geological Survey National Earthquake Hazard Reduction Program Award No. G10AP00014.

Birkmann, J. (2007). Risk and vulnerability indicators at different scales:applicability, usefulness and policy implications. *Environmental Hazards*, *7*(1), 20–31. https://doi.org/10.1016/j.envhaz.2007.04.002

Bray, J. D., Frost, J. D., Rathje, E. M., & Garcia, F. E. (2018). Turning disaster into knowledge in geotechnical earthquake engineering. *Geotechnical Earthquake Engineering and Soil Dynamics V*. https://doi.org/10.1061/9780784481462.018

Bruneau, M., Chang, S. E., Eguchi, R. T., Lee, G. C., O'Rourke, T. D., Reinhorn, A. M., Shinozuka, M., Tierney, K., Wallace, W. A., & von Winterfeldt, D. (2003). A framework to quantitatively assess and enhance the seismic resilience of Communities. *Earthquake Spectra*, *19*(4), 733–752. https://doi.org/10.1193/1.1623497

Buell, S. (2020). Back-to-back earthquakes are a reminder: massachusetts is on shaky ground. *Boston Magazine*. Retrieved from https://www.bostonmagazine.com/news/2020/11/24/massachusetts-earthquakes/

Cui, K., Han, Z., & Wang, D. (2018). Resilience of an earthquake-stricken rural community in Southwest China: Correlation with disaster risk reduction efforts. *International Journal of Environmental Research and Public Health*, *15*(3), 407. https://doi.org/10.3390/ijerph15030407

Ebel, J. (2025). *Massachusetts earthquakes*. Northeast States Emergency Consortium. https://nesec.org/massachusetts-earthquakes/

Ebel, J. E. (1996). The seventeenth century seismicity of Northeastern North America. *Seismological Research Letters*, *67*(3), 51–68. https://doi.org/10.1785/gssrl.67.3.51

Eckle, M., & de Albuquerque, J. P. (2015). ISCRAM Conference. In *Quality Assessment of Remote Mapping in OpenStreetMap for Disaster Management Purposes*. Kristiansand.

Enderami, S. A., Sutley, E. J., & Hofmeyer, S. L. (2021). Defining organizational functionality for evaluation of post-disaster community resilience. *Sustainable and Resilient Infrastructure*, *7*(5), 606–623. https://doi.org/10.1080/23789689.2021.1980300

Estevez, E., Lopes, N., & Janowski, T. (2016). (tech.). *Smart Sustainable Cities: Reconnaissance Study*. United Nations University Operating Unit on Policy-Driven Electronic Governance.

Federal Emergency Management Agency (FEMA), & National Institute of Building Sciences (NIBS) . (2022, July). *Hazus Earthquake Model Technical Manual*. HAZUS 6.1.

Fischer, E. C., & Hakhamaneshi, M. (2019). The new paradigm of Post-Disaster Reconnaissance: Using virtual methods to enhance systematic in-field data collection. *GEOSTRATA Magazine*, *23*(3), 60–65. https://doi.org/10.1061/geosek.0000142

Fischer, K., Häring, I., Riedel, W., Vogelbacher, G., & Hiermaier, S. (2016). Susceptibility, vulnerability, and averaged risk analysis for resilience enhancement of urban areas. *International Journal of Protective Structures*, *7*(1), 45–76. https://doi.org/10.1177/2041419615622727

Foster, K. A. (2012). In search of regional resilience - Urban and regional policy and its effects: Building resilient regions. *Brookings Institution Press* , *4*, 24–59.

Hashash, Y. M., Kottke, A. R., Stewart, J. P., Campbell, K. W., Kim, B., Moss, C., Nikolaou, S., Rathje, E. M., & Silva, W. J. (2014). Reference rock site condition for Central and eastern North America. *Bulletin of the Seismological Society of America*, *104*(2), 684–701. https://doi.org/10.1785/0120130132

Hayles, K. E., Ebel, J. E., & Urzua, A. (2001). Microtremor Measurements to Obtain Resonant Frequencies & Ground Shaking Amplification for Soil Sites in Boston. *Civil Engineering Practice*, *16*(2), 17–36.

Ibs-von Seht, M., & Wohlenberg, J. (1999). Microtremor measurements used to map thickness of soft sediments. *Bulletin of the Seismological Society of America*, *89*(1), 250–259. https://doi.org/10.1785/bssa0890010250

Kijewski-Correa, T., Roueche, D. B., Mosalam, K. M., Prevatt, D. O., & Robertson, I. (2021). Steer: A community-centered approach to assessing the performance of the built environment after natural hazard events. *Frontiers in Built Environment*, *7*. https://doi.org/10.3389/fbuil.2021.636197

Kafka, A. L. (2004). Why Does the Earth Quake in New England? The Science of Unexpected Earthquakes. http://aki.bc.edu/why_quakes.html

Kianiard, E., O'Donnell, A., & Lai, T. (2017). 16th World Conference on Earthquake. In *Evaluation Of Shake And Liquefaction Damages Due To Earthquake Scenarios In Boston, Massachusetts*. Santiago.

Koliou, M., van de Lindt, J. W., McAllister, T. P., Ellingwood, B. R., Dillard, M., & Cutler, H. (2018). State of the research in community resilience: Progress and challenges. *Sustainable and Resilient Infrastructure*, *5*(3), 131–151. https://doi.org/10.1080/23789689.2017.1418547

Luco, N., Rezaeian , S., Rukstales , K. S., Powers, P. M., Shumway, A. M., Martinez, E. M., & Smoczyk, G. M. (2021). Gridded earthquake ground motions for the 2020 NEHRP recommended seismic provisions and 2022 ASCE/SEI 7 standard. *(US Geological Survey Data Release)*. https://doi.org/https://doi.org/10.5066/P9I0R4O6

Mabee, S. B., Duncan, C. C., Clement, W. P., & Pontrelli, M. A. (2023). *Massachusetts Depth to Bedrock Project*. MassDOT Office of Transportation Planning, Research and Technology Transfer Section, Research Report, 173 p.

Nakamura, Y. (1989). (rep.). *Method for dynamic characteristics estimation of subsurface using microtremor on the ground surface* (1st ed., Vol. 30, pp. 25–33). Japan: Quarterly Report of RTRI (Railway Technical Research Institute).

Petersen, M. D., Shumway, A. M., Powers, P. M., Field, E. H., Moschetti, M. P., Jaiswal, K. S., Milner, K. R., Rezaeian, S., Frankel, A. D., Llenos, A. L., Michael, A. J., Altekruse, J. M., Ahdi, S. K., Withers, K. B., Mueller, C. S., Zeng, Y., Chase, R. E., Salditch, L. M., Luco, N., … Witter, R. C. (2023). The 2023 US 50-state national seismic hazard model: Overview and implications. *Earthquake Spectra*, *40*(1), 5–88. https://doi.org/10.1177/87552930231215428

Petersen, M. D., Shumway, A. M., Powers, P. M., Field, E. H., Moschetti, M. P., Jaiswal, K. S., Milner, K. R., Rezaeian, S., Frankel, A. D., Llenos, A. L., Michael, A. J., Altekruse, J. M., Ahdi, S. K., Withers, K. B., Mueller, C. S., Zeng, Y., Chase, R. E., Salditch, L. M., Luco, N., … Witter, R. C. (2023). The 2023 US 50-state national seismic hazard model: Overview and implications. *Earthquake Spectra*, *40*(1), 5–88. https://doi.org/10.1177/87552930231215428

Pontrelli, M., Baise, L. G., Ebel, J. E., & Mabee, S. (2024). *Maps of Distributional Parameters of F0 for Massachusetts, USA Derived from a High-Resolution Continuous Depth-to-Bedrock Map*.

Pontrelli, M., Baise, L., & Ebel, J. (2023a). Regional-scale site characterization mapping in high impedance environments using soil fundamental resonance (F0): New England, USA. *Engineering Geology*, *315*, 107043. https://doi.org/10.1016/j.enggeo.2023.107043

Pontrelli, M., Baise, L., & Ebel, J. (2023b). *Mapping Fundamental Frequency (F0) as a Site Response Parameter Using a Multi-Scale Approach with State-Level Surficial Geologic Maps and Local Sedimentary Deposit Information*. https://doi.org/10.2139/ssrn.4435102

Porter, K. (2009). Cracking an open safe: Hazus vulnerability functions in terms of structure-independent spectral acceleration. *Earthquake Spectra*, *25*(2), 361–378. https://doi.org/10.1193/1.3106680

Rathje, E. M., & Franke, K. (2016). Remote Sensing for geotechnical earthquake reconnaissance. *Soil Dynamics and Earthquake Engineering*, *91*, 304–316. https://doi.org/10.1016/j.soildyn.2016.09.016

Shaw, R. (2016). Community-based Disaster Risk Reduction. *Oxford Research Encyclopedia of Natural Hazard Science*. https://doi.org/10.1093/acrefore/9780199389407.013.47

Sorabella, S. (2006). *Ground Motion Selection For Boston, Massachusetts* (thesis).

Spillatura, A., Vamvatsikos, D., Kohrangi, M., & Bazzurro, P. (2023). Harmonizing seismic performance via risk targeted Spectra: State of the art, Dependencies, and implementation proposals. *Earthquake Engineering & Structural Dynamics*, *52*(13), 4277–4299. https://doi.org/10.1002/eqe.3941

Stone, J. R., DiGiacomo-Cohen, M. L., Stone, B. D., & Mabee, S. B. (2018). Surficial materials of Massachusetts—a 1:24,000-scale geologic Map Database. *Scientific Investigations Map*. https://doi.org/10.3133/sim3402

United Nations Satellite Centre UNOSAT | unitar. (n.d.). https://unitar.org/sustainable-development-goals/united-nations-satellite-centre-UNOSAT

Wald, D. J., & Allen, T. I. (2007). Topographic slope as a proxy for seismic site conditions and amplification. *Bulletin of the Seismological Society of America*, *97*(5), 1379–1395. https://doi.org/10.1785/0120060267

Yilar, E., Baise, L. G., & Ebel, J. E. (2017). Using H/V measurements to determine depth to bedrock and VS30 in Boston, Massachusetts. *Engineering Geology*, *217*, 12–22. https://doi.org/10.1016/j.enggeo.2016.12.002

Chapter 1 – Digitizing Earthquake-Induced Soil Liquefaction: *A Guide for Creating a Labeled Polygon-based Inventory of Surface Effects Using Remote Sensing Data*

Aimaiti, Y., Liu, W., Yamazaki, F., & Maruyama, Y. (2019). Earthquake-induced landslide mapping for the 2018 Hokkaido Eastern Iburi earthquake using palsar-2 data. *Remote Sensing*, *11*(20), 2351. https://doi.org/10.3390/rs11202351

Aimaiti, Y., Sanon, C., Koch, M., Baise, L. G., & Moaveni, B. (2022). War related building damage assessment in Kyiv, Ukraine, using sentinel-1 radar and sentinel-2 optical images. *Remote Sensing*, *14*(24), 6239. https://doi.org/10.3390/rs14246239

Al Shafian, S., & Hu, D. (2024). Integrating machine learning and remote sensing in disaster management: A decadal review of post-disaster building damage assessment. *Buildings*, *14*(8), 2344. https://doi.org/10.3390/buildings14082344

Allstadt, K. E., Thompson, E. M., Jibson, R. W., Wald, D. J., Hearne, M., Hunter, E. J., Fee, J., Schovanec, H., Slosky, D., & Haynie, K. L. (2021). The US Geological Survey Ground Failure Product: Near-real-time estimates of earthquake-triggered landslides and liquefaction. *Earthquake Spectra*, *38*(1), 5–36. https://doi.org/10.1177/87552930211032685

Asadi, A., Baise, L. G., Sanon, C., Koch, M., Chatterjee, S., & Moaveni, B. (2023). Semi-supervised Learning method for the augmentation of an incomplete image-based inventory of earthquake-induced soil liquefaction surface effects. Remote Sensing, 15(19), 4883. https://doi.org/10.3390/rs15194883

Baik, H., Son, Y.-S., & Kim, K.-E. (2019). Detection of liquefaction phenomena from the 2017 Pohang (Korea) earthquake using remote sensing data. *Remote Sensing*, *11*(18), 2184. https://doi.org/10.3390/rs11182184

Baise, L. G., & Rashidian, V. (2018). A geospatial approach to liquefaction assessment for rapid response and loss estimation. *Geotechnical Earthquake Engineering and Soil Dynamics V*. https://doi.org/10.1061/9780784481462.001

Bello, O. M., & Aina, Y. A. (2014). Satellite Remote Sensing as a tool in disaster management and sustainable development: Towards a synergistic approach. *Procedia - Social and Behavioral Sciences*, *120*, 365–373. https://doi.org/10.1016/j.sbspro.2014.02.114

Bird, J. F., & Bommer, J. J. (2004). Earthquake losses due to ground failure. *Engineering Geology*, *75*(2), 147–179. https://doi.org/10.1016/j.enggeo.2004.05.006

Boccardo, P., & Giulio Tonolo, F. (2014). Remote Sensing Role in emergency mapping for disaster response. *Engineering Geology for Society and Territory - Volume 5*, 17–24. https://doi.org/10.1007/978-3-319-09048-1_3

Booth, E., Saito, K., Spence, R., Madabhushi, G., & Eguchi, R. T. (2011). Validating assessments of seismic damage made from remote sensing. *Earthquake Spectra*, *27*(1_suppl1), 157–177. https://doi.org/10.1193/1.3632109

Boulanger, R. W., & Idriss, I. M. (2014). (rep.). *CPT and SPT Based Liquefaction Triggering Procedures*. Davis, CA: Univ. of California, Davis.

Brandenberg, S. J., Zimmaro, P., Stewart, J. P., Kwak, D. Y., Franke, K. W., Moss, R. E., Çetin, K. Ö., Can, G., Ilgac, M., Stamatakos, J., Weaver, T., & Kramer, S. L. (2020). Next-generation liquefaction database. *Earthquake Spectra*, *36*(2), 939–959. https://doi.org/10.1177/8755293020902477

Bray, J. D., Frost, J. D., Rathje, E. M., & Garcia, F. E. (2019). Recent advances in geotechnical post-earthquake reconnaissance. *Frontiers in Built Environment*, *5*(5). https://doi.org/10.3389/fbuil.2019.00005

Brown, D., Saito, K., Liu, M., Spence, R., So, E., & Ramage, M. (2011). The use of remotely sensed data and ground survey tools to assess damage and monitor early recovery following the 12.5.2008 wenchuan earthquake in China. *Bulletin of Earthquake Engineering*, *10*(3), 741–764. https://doi.org/10.1007/s10518-011-9318-7

Carrara, A., Cardinali, M., & Guzzetti, F. (1992). Uncertainty in assessing landslide hazard and risk. *ITC Journal*, *2*, 172–183.

Chang, S. E., Taylor, J. E., Elwood, K. J., Seville, E., Brunsdon, D., & Gartner, M. (2014). Urban disaster recovery in Christchurch: The Central Business District Cordon and other critical decisions. *Earthquake Spectra*, *30*(1), 513–532. https://doi.org/10.1193/022413eqs050m

Chansky, A., Baise, L. G., & Moaveni, B. (2023). National liquefaction loss database and event-level fragility functions. *Earthquake Spectra*. https://doi.org/10.1177/87552930231194550

Daniell, J. E., Schaefer, A. M., & Wenzel, F. (2017). Losses associated with secondary effects in earthquakes. *Frontiers in Built Environment*, *3*. https://doi.org/10.3389/fbuil.2017.00030

Dashti, S., & Ganapati, N. E. (Eds.). (2022). Reconnaissance following the august 14, 2021 Haiti earthquake: perspectives from geotechnical engineering and social/political sciences. *Geotechnical Extreme Events Reconnaissance (GEER) Report No. 073*. https://doi.org/10.18118/G60090

Dell'Oro, L. (2017). Overview of UNITAR-UNOSAT and GDACS Satellite Mapping Coordination System. https://appliedsciences.nasa.gov/sites/default/files/2020-11/gdacspart1bv2.pdf

Denis, G., de Boissezon, H., Hosford, S., Pasco, X., Montfort, B., & Ranera, F. (2016). The evolution of Earth Observation satellites in Europe and its impact on the performance of emergency response services. *Acta Astronautica*, *127*, 619–633. https://doi.org/10.1016/j.actaastro.2016.06.012

Federal Emergency Management Agency - FEMA. (2000). Hazus 99 estimated annualized earthquake losses for the United States. http://www.disastersrus.org/emtools/earthquakes/FEMA366.pdf

Federal Emergency Management Agency - FEMA. (2016). Damage assessment manual. https://www.fema.gov/sites/default/files/2020-07/fema_damage-assessment-manual_4-5-2016.pdf

Ferreira, B., Silva, R. G., & Iten, M. (2022). Earth observation satellite imagery information-based decision support using machine learning. *Remote Sensing*, *14*(15), 3776. https://doi.org/10.3390/rs14153776

Fiorucci, F., Cardinali, M., Carlà, R., Rossi, M., Mondini, A. C., Santurri, L., Ardizzone, F., & Guzzetti, F. (2011). Seasonal landslide mapping and estimation of landslide mobilization rates using aerial and satellite images. *Geomorphology*, *129*(1–2), 59–70. https://doi.org/10.1016/j.geomorph.2011.01.013

Foster, C., Pennington, C. V., Culshaw, M. G., & Lawrie, K. (2011). The National Landslide Database of Great Britain: Development, evolution and applications. *Environmental Earth Sciences*, *66*(3), 941–953. https://doi.org/10.1007/s12665-011-1304-5

García-Rodríguez, M. J., & Malpica, J. A. (2010). Assessment of earthquake-triggered landslide susceptibility in El Salvador based on an artificial neural network model. *Natural Hazards and Earth System Sciences*, *10*(6), 1307–1315. https://doi.org/10.5194/nhess-10-1307-2010

Ghosh Mondal, T., Jahanshahi, M. R., Wu, R., & Wu, Z. Y. (2020). Deep learning-based multi-class damage detection for Autonomous Post-Disaster Reconnaissance. *Structural Control and Health Monitoring*, *27*(4). https://doi.org/10.1002/stc.2507

Gu, W., Bai, S., & Kong, L. (2022). A review on 2D instance segmentation based on Deep Neural Networks. *Image and Vision Computing*, *120*, 104401. https://doi.org/10.1016/j.imavis.2022.104401

Gupta, R., Hosfelt, R., Sajeev, S., Patel, N., Goodman, B., Doshi, J., Heim, E., Choset, H., & Gaston, M. (2019). *XBD: A dataset for assessing building damage from satellite imagery*. arXiv.org. https://arxiv.org/abs/1911.09296

Guzzetti, F., Mondini, A. C., Cardinali, M., Fiorucci, F., Santangelo, M., & Chang, K.-T. (2012). Landslide inventory maps: New tools for an old problem. *Earth-Science Reviews*, *112*(1–2), 42–66. https://doi.org/10.1016/j.earscirev.2012.02.001

Hafiz, A. M., & Bhat, G. M. (2020). A survey on instance segmentation: State of the art. *International Journal of Multimedia Information Retrieval*, *9*(3), 171–189. https://doi.org/10.1007/s13735-020-00195-x

Harp, E. L., & Jibson, R. W. (1995). Inventory of landslides triggered by the 1994 Northridge, California earthquake. *Open-File Report*. https://doi.org/10.3133/ofr95213

Harp, E. L., Keefer, D. K., Sato, H. P., & Yagi, H. (2011). Landslide inventories: The Essential Part of seismic landslide hazard analyses. *Engineering Geology*, *122*(1–2), 9–21. https://doi.org/10.1016/j.enggeo.2010.06.013

Harp, E. L., Tanaka, K., Sarmiento, J., & Keefer, D. K. (1984). Landslides from the May 25-27, 1980, Mammoth Lakes, California, earthquake sequence. *USGS*. https://doi.org/10.3133/i1612

Harp, E. L., Wilson, R. C., & Wieczorek, G. F. (1981). Landslides from the February 4, 1976, Guatemala earthquake. *Professional Paper*. https://doi.org/10.3133/pp1204a

History of the ōtākaro Avon River Corridor. Christchurch City Council. (n.d.). https://ccc.govt.nz/parks-and-gardens/regenerationareas/otakaro-avon-river-corridor/history-and-background/

Hoeser, T., & Kuenzer, C. (2020). Object detection and image segmentation with deep learning on earth observation data: A review-part I: Evolution and recent trends. *Remote Sensing*, *12*(10), 1667. https://doi.org/10.3390/rs12101667

Huang, T. F., & Lee, C.-T. (1999). *1999, Landslides Triggered by Jueili Earthquake: U.S. Geological Survey Data Release*. https://doi.org/https://doi.org/10.5066/P96GI03H

Huang, Y. (2021). Salience of hazard disclosure and house prices: Evidence from Christchurch, New Zealand. *Regional Science and Urban Economics*, *88*, 103679. https://doi.org/10.1016/j.regsciurbeco.2021.103679

Huyck, C., Verrucci, E., & Bevington, J. (2014). Chapter 1 - Remote Sensing for Disaster Response: A Rapid, Image-Based Perspective. In M. Wyss & J. F. Shroder (Eds.), *Earthquake hazard, risk, and disasters* (pp. 1–24). essay, Elsevier/Academic Press.

Iwasaki, T. (1986). Soil liquefaction studies in Japan: State-of-the-art. *Soil Dynamics and Earthquake Engineering*, *5*(1), 2–68. https://doi.org/10.1016/0267-7261(86)90024-2

Keefer, D. K. (1984). Landslides caused by earthquakes. *Geological Society of America Bulletin*, *95*(4), 406. https://doi.org/10.1130/0016-7606(1984)95<406:lcbe>2.0.co;2

Kirschbaum, D., Stanley, T., & Zhou, Y. (2015). Spatial and temporal analysis of a global landslide catalog. *Geomorphology*, *249*, 4–15. https://doi.org/10.1016/j.geomorph.2015.03.016

Kramer, S. L. (2014). Chapter 9 - Liquefaction. In *Geotechnical earthquake engineering*. essay, Prentice Hall.

Lam, D., Kuzma, R., McGee, K., Dooley, S., Laielli, M., Klaric, M., Bulatov, Y., & McCord, B. (2018). *XView: Objects in context in overhead imagery*. arXiv.org. https://arxiv.org/abs/1802.07856

Lambert, M., Gaudin, J., & Cohen, R. (1987). Geologic Map of Haiti, South-East Region: Port-au-Prince. *Centre d'Etudes et de Realisations Cartographiques Geographiques (CERCG), National Center for Scientific Research (CNRS), Paris, France*.

Li, Z., Shi, W., Myint, S. W., Lu, P., & Wang, Q. (2016). Semi-automated landslide inventory mapping from bitemporal aerial photographs using change detection and level set method. *Remote Sensing of Environment*, *175*, 215–230. https://doi.org/10.1016/j.rse.2016.01.003

Manunta, P., & Coulson, S. (2024). *Satellite Earth Observation Assets and solutions.* ADB Sustainable Development Working Paper Series. https://www.adb.org/sites/default/files/publication/1010481/sdwp-099-satellite-earth-observation-assets-solutions.pdf

Marano, K. D., Wald, D. J., & Allen, T. I. (2009). Global earthquake casualties due to secondary effects: A quantitative analysis for improving rapid loss analyses. *Natural Hazards*, *52*(2), 319–328. https://doi.org/10.1007/s11069-009-9372-5

Martinez, S. N., Schaefer, L. N., Allstadt, K. E., & Thompson, E. M. (2021). Evaluation of remote mapping techniques for earthquake-triggered landslide inventories in an urban subarctic environment: A case study of the 2018 anchorage, Alaska earthquake. *Frontiers in Earth Science*, *9*. https://doi.org/10.3389/feart.2021.673137

Mavroulis, S., Diakakis, M., Kranis, H., Vassilakis, E., Kapetanidis, V., Spingos, I., Kaviris, G., Skourtsos, E., Voulgaris, N., & Lekkas, E. (2022). Inventory of historical and recent earthquake-triggered landslides and assessment of related susceptibility by GIS-based analytic hierarchy process: The case of Cephalonia (ionian islands, Western Greece). *Applied Sciences*, *12*(6), 2895. https://doi.org/10.3390/app12062895

Middleton, M., Heikkonen, J., Nevalainen, P., Hyvönen, E., & Sutinen, R. (2020). Machine learning-based mapping of micro-topographic earthquake-induced Paleo-pulju moraines and liquefaction spreads from a digital elevation model acquired through Laser Scanning. *Geomorphology*, *358*, 107099. https://doi.org/10.1016/j.geomorph.2020.107099

Morales-Velez, A. C., & Pando, M. (2020). Geotechnical Reconnaissance of the January 7, 2020 M6.4 Southwest Puerto Rico Earthquake and Associated Seismic Sequence. *Geotechnical Extreme Event Reconnaissance Association GEER-066.* https://doi.org/10.18118/G66Q2F

Morgenroth, J., Hughes, M. W., & Cubrinovski, M. (2016). Object-based image analysis for mapping earthquake-induced liquefaction ejecta in Christchurch, New Zealand. *Natural Hazards*, *82*(2), 763–775. https://doi.org/10.1007/s11069-016-2217-0

Nowicki Jessee, M. A., Hamburger, M. W., Allstadt, K., Wald, D. J., Robeson, S. M., Tanyas, H., Hearne, M., & Thompson, E. M. (2018). A global empirical model for near-real-time assessment of seismically induced landslides. *Journal of Geophysical Research: Earth Surface*, *123*(8), 1835–1859. https://doi.org/10.1029/2017jf004494

Olson, S. M., Green, R. A., Lasley, S., Martin, N., Cox, B. R., Rathje, E., Bachhuber, J., & French, J. (2011). Documenting liquefaction and lateral spreading triggered by the 12 January 2010 Haiti earthquake. *Earthquake Spectra*, *27*(1_suppl1), 93–116. https://doi.org/10.1193/1.3639270

Oommen, T., Baise, L. G., Gens, R., Prakash, A., & Gupta, R. P. (2013). Documenting earthquake-induced liquefaction using satellite remote sensing image transformations. *Environmental & Engineering Geoscience*, *19*(4), 303–318. https://doi.org/10.2113/gseegeosci.19.4.303

Papathanassiou, G., & Pavlides, Sp. (2011). GIS-based database of historical liquefaction occurrences in the broader Aegean region, Dalo v1.0. *Quaternary International*, *242*(1), 115–125. https://doi.org/10.1016/j.quaint.2011.03.049

Papathanassiou, George, Valkaniotis, S., Ganas, A., Stampolidis, A., Rapti, D., & Caputo, R. (2022). Floodplain evolution and its influence on liquefaction clustering: The case study of March 2021 Thessaly, Greece, seismic sequence. *Engineering Geology*, *298*, 106542. https://doi.org/10.1016/j.enggeo.2022.106542

Perera, E. N., Gunaratne, A. M. C. T., & Samarasinghe, S. B. D. (2022). Participatory landslide inventory (PLI): An online tool for the development of a landslide inventory. *Complexity*, *2022*, 1–10. https://doi.org/10.1155/2022/2659203

Prakash, N., Manconi, A., & Loew, S. (2021). A new strategy to map landslides with a generalized convolutional neural network. *Scientific Reports*, *11*(1). https://doi.org/10.1038/s41598-021-89015-8

Rabby, Y. W., & Li, Y. (2019). Landslide inventory (2001-2017) of Chittagong hilly areas, Bangladesh. *Data*, *5*(1). https://doi.org/10.20944/preprints201911.0269.v1

Rainey, K. (2019). Building an operationally relevant dataset from satellite imagery. *IGARSS 2019 - 2019 IEEE International Geoscience and Remote Sensing Symposium*. https://doi.org/10.1109/igarss.2019.8900177

Rainey, K., Parameswaran, S., Harguess, J., & Stastny, J. (2012). Vessel classification in overhead satellite imagery using learned dictionaries. *SPIE Proceedings*. https://doi.org/10.1117/12.928875

Ramakrishnan, D., Mohanty, K. K., Nayak, S. R., & Chandran, R. V. (2006). Mapping the liquefaction induced soil moisture changes using remote sensing technique: An attempt to map the earthquake induced liquefaction around Bhuj, Gujarat, India. *Geotechnical and Geological Engineering*, *24*(6), 1581–1602. https://doi.org/10.1007/s10706-005-3811-1

Rashidian, V., & Baise, L. G. (2018). Rapid liquefaction detection using remote sensing techniques: 2011 Christchurch earthquake. *Geotechnical Earthquake Engineering and Soil Dynamics V*. https://doi.org/10.1061/9780784481455.046

Rathje, E. M., & Adams, B. J. (2008). The role of remote sensing in earthquake science and engineering: Opportunities and challenges. *Earthquake Spectra*, *24*(2), 471–492. https://doi.org/10.1193/1.2923922

Rathje, E. M., & Franke, K. (2016). Remote Sensing for geotechnical earthquake reconnaissance. *Soil Dynamics and Earthquake Engineering*, *91*, 304–316. https://doi.org/10.1016/j.soildyn.2016.09.016

Rathje, E. M., Bachhuber, J., Cox, B., French, J., Green, R., Olson, S., Rix, G., Wells, D., & Suncar, O. (2010). Geotechnical Engineering Reconnaissance of the 2010 Haiti Earthquake. *Geotechnical Extreme Events Reconnaissance (GEER) Report No. 021*. https://doi.org/10.18118/G6SG6T

Rogers, N., Williams, K., Jacka, M., Wallace, S., & Leeves, J. (2014). Geotechnical aspects of Disaster Recovery Planning in residential Christchurch and surrounding districts affected by liquefaction. *Earthquake Spectra*, *30*(1), 493–512. https://doi.org/10.1193/021513eqs029m

Sato, H. P., Hasegawa, H., Fujiwara, S., Tobita, M., Koarai, M., Une, H., & Iwahashi, J. (2006). Interpretation of landslide distribution triggered by the 2005 northern Pakistan earthquake using spot 5 imagery. *Landslides*, *4*(2), 113–122. https://doi.org/10.1007/s10346-006-0069-5

Schmitt, R. G., Tanyas, H., Nowicki Jessee, M. A., Zhu, J., Biegel, K. M., Allstadt, K. E., Jibson, R. W., Thompson, E. M., van Westen, C. J., Sato, H. P., Wald, D. J., Godt, J. W., Gorum, T., Xu, C., Rathje, E. M., & Knudsen, K. L. (2017). An open repository of earthquake-triggered ground-failure inventories. *Data Series*. https://doi.org/10.3133/ds1064

Seed, H. B., & Idriss, I. M. (1970). (rep.). *Soil Moduli and Damping Factors for Dynamic Response Analyses*. Berkeley, CA: National Technical Reports Library.

Sekiguchi, T., & Sato, H. P. (2006). Feature and distribution of landslides induced by the Mid Niigata Prefecture earthquake in 2004, Japan. *Journal of the Japan Landslide Society*, *43*(3), 142–154. https://doi.org/10.3313/jls.43.142

Singhroy, V., Mattar, K. E., & Gray, A. L. (1998). Landslide characterisation in Canada using interferometric SAR and combined SAR and TM Images. *Advances in Space Research*, *21*(3), 465–476. https://doi.org/10.1016/s0273-1177(97)00882-x

Thenkabail, P. S., & Kerle, N. (2015). Disasters: Risk Assessment, Management, and Post-Disaster Studies Using Remote Sensing. In *Remote Sensing of Water Resources, disasters, and urban studies* (pp. 455–477). essay, Taylor & Francis.

Townsend, D., Lee, J., Strong, D., Jongens, R., Smith Lyttle, B., Ashraf, S., Rosser, B., Perrin, N., Lyttle, K., Cubrinovski, M., Taylor, M., Hughes, M., Wilson, T., Almond, P., Jacka, M., McCahon, I., & Christensen, S. (2016). Mapping surface liquefaction caused by the September 2010 and February 2011 Canterbury earthquakes: A Digital Dataset. *New Zealand Journal of Geology and Geophysics*, *59*(4), 496–513. https://doi.org/10.1080/00288306.2016.1182929

Valkaniotis, S., Papathanassiou, G., & Ganas, A. (2018). Mapping an earthquake-induced landslide based on UAV imagery; Case study of the 2015 Okeanos landslide, Lefkada, Greece. *Engineering Geology*, *245*, 141–152. https://doi.org/10.1016/j.enggeo.2018.08.010

Wakamatsu, K. (2010). *Development of GIS Database for Historic Liquefaction Sites in Japan, 416 ─2008.* University of Tokyo Press, Tokyo Japan.

Wang, P., Fan, E., & Wang, P. (2021). Comparative analysis of image classification algorithms based on traditional machine learning and Deep Learning. *Pattern Recognition Letters*, *141*, 61–67. https://doi.org/10.1016/j.patrec.2020.07.042

Westrope, C., Banick, R., & Levine, M. (2014). Groundtruthing OpenStreetMap Building Damage Assessment. *Procedia Engineering*, *78*, 29–39. https://doi.org/10.1016/j.proeng.2014.07.035

Whitworth, M. R., Giardina, G., Penney, C., Di Sarno, L., Adams, K., Kijewski-Correa, T., Black, J., Foroughnia, F., Macchiarulo, V., Milillo, P., Ojaghi, M., Orfeo, A., Pugliese, F., Dönmez, K., Aktas, Y. D., & Macabuag, J. (2022). Lessons for remote post-earthquake reconnaissance from the 14 August 2021 Haiti earthquake. *Frontiers in Built Environment*, *8*. https://doi.org/10.3389/fbuil.2022.873212

Yang, Y., Wang, C., Cai, Z., Song, P., Huang, G., Cheng, M., & Zang, Y. (2024). Gsddet: Ground sample distance-guided object detection for remote sensing images. *IEEE Transactions on Geoscience and Remote Sensing*, *62*, 1–12. https://doi.org/10.1109/tgrs.2023.3309838

Youd, T. L. (1973). Liquefaction, flow, and associated ground failure. *Circular*. https://doi.org/10.3133/cir688

Zhu, J., Baise, L. G., & Thompson, E. M. (2017). An updated geospatial liquefaction model for Global Application. *Bulletin of the Seismological Society of America*, *107*(3), 1365–1385. https://doi.org/10.1785/0120160198

Chapter 2 – Building Damage Assessment and Retrofitting Prioritization in Massachusetts Using a High-Resolution Site Characterization Map

American Society of Civil Engineers. (2022). *Minimum design loads and associated criteria for buildings and other structures (ASCE/SEI 7-22).*

Baise, L. G., Kaklamanos, J., Berry, B. M., & Thompson, E. M. (2016). Soil amplification with a strong impedance contrast: Boston, Massachusetts. *Engineering Geology*, *202*, 1–13. https://doi.org/10.1016/j.enggeo.2015.12.016

Becker, L. R., Fratto, E. S., Patriarco, S. P., Marvinney, R. G., Mabee, S. B., & Thomas, M. A. (2011). (tech.). *Utilizing the Surficial Geology of the Northeast United States to Improve NEHRP Site Effect*

Classifications in HAZUS-MH: Collaborative Research with NESEC and the NESEC State Geologists. U.S. Geological Survey National Earthquake Hazard Reduction Program Award No. G10AP00014.

Buell, S. (2020). Back-to-back earthquakes are a reminder: massachusetts is on shaky ground. *Boston Magazine*. Retrieved from https://www.bostonmagazine.com/news/2020/11/24/massachusetts-earthquakes/

Bullock, J. A., Haddow, G. D., & Coppola, D. P. (2018). Mitigation, prevention, and Preparedness. *Homeland Security*, 291–322. https://doi.org/10.1016/b978-0-12-804465-0.00010-8

Burby, R. J., & May, P. J. (1999). Making building codes an effective tool for earthquake hazard mitigation. *Environmental Hazards*, *1*(1), 27–37. https://doi.org/10.3763/ehaz.1999.0104

Chen, T.-L., & Chang, H.-S. (2018). The effects of zoning regulations along fault zone areas on land development and property values after the 921 chi-chi earthquake in Taiwan. *Sustainability*, *10*(4), 1175. https://doi.org/10.3390/su10041175

Department of Homeland Security (DHS). (2015). *DHS Resilience Framework: Providing a Roadmap for the Department in Operational Resilience and Readiness*.

Doebling, S. W., Farrar, C. R., & Prime, M. B. (1998). A summary review of vibration-based damage identification methods. *The Shock and Vibration Digest*, *30*(2), 91–105. https://doi.org/10.1177/058310249803000201

D'Agostino, G., Di Pietro, A., Giovinazzi, S., Porta, L. L., Pollino, M., Rosato, V., & Tofani, A. (2018). Earthquake simulation on urban areas: Improving contingency plans by Damage Assessment. *Lecture Notes in Computer Science*, 72–83. https://doi.org/10.1007/978-3-030-05849-4_6

Ebel, J. (2025). *Massachusetts earthquakes*. Northeast States Emergency Consortium. https://nesec.org/massachusetts-earthquakes/

Ebel, J. E. (1996). The seventeenth century seismicity of Northeastern North America. *Seismological Research Letters*, *67*(3), 51–68. https://doi.org/10.1785/gssrl.67.3.51

Ergünay, O., & Gülkan, P. (1993). Land-use planning as instrument of earthquake hazard mitigation. *Comprehensive Approach to Earthquake Disaster Mitigation*, 235–277. https://doi.org/10.1007/978-3-322-85461-2_13

Federal Emergency Management Agency (FEMA), & National Institute of Building Sciences (NIBS) . (2022, July). *Hazus Earthquake Model Technical Manual*. HAZUS 6.1.

Gosar, A. (2010). Site effects and soil-structure resonance study in the Kobarid Basin (NW slovenia) using microtremors. *Natural Hazards and Earth System Sciences*, *10*(4), 761–772. https://doi.org/10.5194/nhess-10-761-2010

Gosar, Andrej, Rošer, J., Šket Motnikar, B., & Zupančič, P. (2009). Microtremor study of site effects and soil-structure resonance in the city of Ljubljana (Central Slovenia). *Bulletin of Earthquake Engineering*, *8*(3), 571–592. https://doi.org/10.1007/s10518-009-9113-x

Grant, D. N., Bommer, J. J., Pinho, R., Calvi, G. M., Goretti, A., & Meroni, F. (2007). A prioritization scheme for seismic intervention in school buildings in Italy. *Earthquake Spectra*, *23*(2), 291–314. https://doi.org/10.1193/1.2722784

Hartigan, J. A. (1975). *Clustering algorithms*. John Wiley & Sons.

Hashash, Y. M., Kottke, A. R., Stewart, J. P., Campbell, K. W., Kim, B., Moss, C., Nikolaou, S., Rathje, E. M., & Silva, W. J. (2014). Reference rock site condition for Central and eastern North America. *Bulletin of the Seismological Society of America*, *104*(2), 684–701. https://doi.org/10.1785/0120130132

Hastie, T., Tibshirani, R., & Friedman, J. H. (2001). *The elements of statistical learning data mining, Inference, and prediction*. Springer New York.

Hayles, K. E., Ebel, J. E., & Urzua, A. (2001). Microtremor Measurements to Obtain Resonant Frequencies & Ground Shaking Amplification for Soil Sites in Boston. *Civil Engineering Practice*, *16*(2), 17–36.

Ibs-von Seht, M., & Wohlenberg, J. (1999). Microtremor measurements used to map thickness of soft sediments. *Bulletin of the Seismological Society of America*, *89*(1), 250–259. https://doi.org/10.1785/bssa0890010250

Intergovernmental Panel on Climate Change (IPCC). (2014). *Adaptation to Climate Change - Guidelines on Vulnerability, Impacts and Risk Assessment*. https://doi.org/10.3403/30361479

Kafka, A. L. (2004). Why Does the Earth Quake in New England? The Science of Unexpected Earthquakes. http://aki.bc.edu/why_quakes.html

Kianiard, E., O'Donnell, A., & Lai, T. (2017). 16th World Conference on Earthquake. In *Evaluation Of Shake And Liquefaction Damages Due To Earthquake Scenarios In Boston, Massachusetts*. Santiago.

Li, Y. R., & Jirsa, J. O. (1998). Nonlinear analyses of an instrumented structure damaged in the 1994 Northridge earthquake. *Earthquake Spectra*, *14*(2), 265–283. https://doi.org/10.1193/1.1585999

Luco, N., Rezaeian , S., Rukstales , K. S., Powers, P. M., Shumway, A. M., Martinez, E. M., & Smoczyk, G. M. (2021). Gridded earthquake ground motions for the 2020 NEHRP recommended seismic provisions and 2022 ASCE/SEI 7 standard. *(US Geological Survey Data Release)*. https://doi.org/https://doi.org/10.5066/P9I0R4O6

Luft, R. W., & Simpson, H. (1979). *Journal of the Boston Society Of Civil Engineers Section*, *66*(2), 67–87.

Mabee, S. B., Duncan, C. C., Clement, W. P., & Pontrelli, M. A. (2023). *Massachusetts Depth to Bedrock Project*. MassDOT Office of Transportation Planning, Research and Technology Transfer Section, Research Report, 173 p.

Musacchio, G., Falsaperla, S., Bernhardsdóttir, A. E., Ferreira, M. A., Sousa, M. L., Carvalho, A., & Zonno, G. (2015). Education: Can a bottom-up strategy help for earthquake disaster prevention? *Bulletin of Earthquake Engineering*, *14*(7), 2069–2086. https://doi.org/10.1007/s10518-015-9779-1

Nakamura, Y. (1989). (rep.). *Method for dynamic characteristics estimation of subsurface using microtremor on the ground surface* (1st ed., Vol. 30, pp. 25–33). Japan: Quarterly Report of RTRI (Railway Technical Research Institute).

Nordenson, G. J., & Bell, G. R. (2000). Seismic Design Requirements for regions of moderate seismicity. *Earthquake Spectra*, *16*(1), 205–225. https://doi.org/10.1193/1.1586091

Petersen, M. D., Shumway, A. M., Powers, P. M., Field, E. H., Moschetti, M. P., Jaiswal, K. S., Milner, K. R., Rezaeian, S., Frankel, A. D., Llenos, A. L., Michael, A. J., Altekruse, J. M., Ahdi, S. K., Withers, K. B., Mueller, C. S., Zeng, Y., Chase, R. E., Salditch, L. M., Luco, N., … Witter, R. C. (2023). The 2023 US 50-state national seismic hazard model: Overview and implications. *Earthquake Spectra*, *40*(1), 5–88. https://doi.org/10.1177/87552930231215428

Petersen, M. D., Shumway, A. M., Powers, P. M., Mueller, C. S., Moschetti, M. P., Frankel, A. D., Rezaeian, S., McNamara, D. E., Luco, N., Boyd, O. S., Rukstales, K. S., Jaiswal, K. S., Thompson, E. M., Hoover, S. M.,

Clayton, B. S., Field, E. H., & Zeng, Y. (2019). The 2018 update of the US National Seismic Hazard Model: Overview of model and implications. *Earthquake Spectra*, *36*(1), 5–41. https://doi.org/10.1177/8755293019878199

Pinzón, L. A., Pujades, L. G., Macau, A., & Figueras, S. (2019). Increased seismic hazard in Barcelona (Spain) due to soil-building resonance effects. *Soil Dynamics and Earthquake Engineering*, *117*, 245–250. https://doi.org/10.1016/j.soildyn.2018.11.022

Ploeger, S. K., Atkinson, G. M., & Samson, C. (2009). Applying the Hazus-MH software tool to assess seismic risk in downtown Ottawa, Canada. *Natural Hazards*, *53*(1), 1–20. https://doi.org/10.1007/s11069-009-9408-x

Pontrelli, M., Baise, L. G., Ebel, J. E., & Mabee, S. (2024). *Maps of Distributional Parameters of F0 for Massachusetts, USA Derived from a High-Resolution Continuous Depth-to-Bedrock Map*.

Pontrelli, M., Baise, L., & Ebel, J. (2023a). Regional-scale site characterization mapping in high impedance environments using soil fundamental resonance (F0): New England, USA. *Engineering Geology*, *315*, 107043. https://doi.org/10.1016/j.enggeo.2023.107043

Pontrelli, M., Baise, L., & Ebel, J. (2023b). *Mapping Fundamental Frequency (F0) as a Site Response Parameter Using a Multi-Scale Approach with State-Level Surficial Geologic Maps and Local Sedimentary Deposit Information*. https://doi.org/10.2139/ssrn.4435102

Porter, K. (2009). Cracking an open safe: Hazus vulnerability functions in terms of structure-independent spectral acceleration. *Earthquake Spectra*, *25*(2), 361–378. https://doi.org/10.1193/1.3106680

Salam, M. A., & Khan, S. A. (2020). Lessons from the Humanitarian Disaster Logistics Management. *Benchmarking: An International Journal*, *27*(4), 1455–1473. https://doi.org/10.1108/bij-04-2019-0165

Silverman, B., Cox, D. R., & Hinkley, D. V. (1996). *Density Estimation for statistics and data analysis*. Chapman & Hall.

Sorabella, S. (2006). *Ground Motion Selection For Boston, Massachusetts* (thesis).

Spillatura, A., Vamvatsikos, D., Kohrangi, M., & Bazzurro, P. (2023). Harmonizing seismic performance via risk targeted Spectra: State of the art, Dependencies, and implementation proposals. *Earthquake Engineering & Structural Dynamics*, *52*(13), 4277–4299. https://doi.org/10.1002/eqe.3941

Stone, J. R., DiGiacomo-Cohen, M. L., Stone, B. D., & Mabee, S. B. (2018). Surficial materials of Massachusetts—a 1:24,000-scale geologic Map Database. *Scientific Investigations Map*. https://doi.org/10.3133/sim3402

Tallini, M., Lo Sardo, L., & Spadi, M. (2020). Seismic site characterisation of red soil and soil-building resonance effects in l'aquila downtown (Central Italy). *Bulletin of Engineering Geology and the Environment*, *79*(8), 4021–4034. https://doi.org/10.1007/s10064-020-01795-x

Trifunac, M. D., Ivanović, S. S., & Todorovska, M. I. (2001a). Apparent periods of a building. I: Fourier analysis. *Journal of Structural Engineering*, *127*(5), 517–526. https://doi.org/10.1061/(asce)0733-9445(2001)127:5(517)

Trifunac, M. D., Ivanović, S. S., & Todorovska, M. I. (2001b). Apparent periods of a building. II: Time-frequency analysis. *Journal of Structural Engineering*, *127*(5), 527–537. https://doi.org/10.1061/(asce)0733-9445(2001)127:5(527)

United Nations Office for Disaster Risk Reduction (UNDRR). (2015). Sendai Framework for Disaster Risk Reduction 2015-2030. *Human Rights Documents Online*. https://doi.org/10.1163/2210-7975_hrd-9813-2015016

USGS National Earthquake Information Center, PDE. (2009). *M 5.9 - The 1755 Cape Ann, Massachusetts Earthquake*. Earthquake hazards program. https://earthquake.usgs.gov/earthquakes/eventpage/ushis7/region-info

Wald, D. J., & Allen, T. I. (2007). Topographic slope as a proxy for seismic site conditions and amplification. *Bulletin of the Seismological Society of America*, *97*(5), 1379–1395. https://doi.org/10.1785/0120060267

Yilar, E., Baise, L. G., & Ebel, J. E. (2017). Using H/V measurements to determine depth to bedrock and VS30 in Boston, Massachusetts. *Engineering Geology*, *217*, 12–22. https://doi.org/10.1016/j.enggeo.2016.12.002

Chapter 3 – Ground Response Analysis for Seismic Vulnerability Assessment: *Does detailed site characterization and ground response analysis change projected building damage estimates?*

American Society of Civil Engineers. (2022). *Minimum design loads and associated criteria for buildings and other structures (ASCE/SEI 7-22).*

Anastasiadis, A., & Riga, E. (2013). Site classification and spectral amplification for seismic code provisions. *Geotechnical, Geological and Earthquake Engineering*, 23–72. https://doi.org/10.1007/978-3-319-03182-8_2

Baise, L. G., Kaklamanos, J., Berry, B. M., & Thompson, E. M. (2016). Soil amplification with a strong impedance contrast: Boston, Massachusetts. *Engineering Geology*, *202*, 1–13. https://doi.org/10.1016/j.enggeo.2015.12.016

Boore, D. M. (2005). SMSIM – Fortran programs for simulating ground motions from earthquakes: Version 2.3 – A revision of OFR 96-80-A, U.S. Geol. Surv. Open-File Rept. 2008–1128, 55 pp.

Boore, D. M., Thompson, E. M., & Cadet, H. (2011). Regional correlations of VS30 and velocities averaged over depths less than and greater than 30 meters. *Bulletin of the Seismological Society of America*, *101*(6), 3046–3059. https://doi.org/10.1785/0120110071

Boore, David M. (2015). Determining generic velocity and density models for crustal amplification calculations, with an update of the generic site amplification for. *Bulletin of the Seismological Society of America*, *106*(1), 313–317. https://doi.org/10.1785/0120150229

Boore, David M., & Joyner, W. B. (1997). Site amplifications for Generic Rock Sites. *Bulletin of the Seismological Society of America*, *87*(2), 327–341. https://doi.org/10.1785/bssa0870020327

Boore, David M. (2004). Can site response be predicted? *Journal of Earthquake Engineering*, *8*(sup001), 1–41. https://doi.org/10.1080/13632460409350520

Borcherdt, R. D. (1994). Estimates of site-dependent response spectra for Design (methodology and justification). *Earthquake Spectra*, *10*(4), 617–653. https://doi.org/10.1193/1.1585791

Borcherdt, R. D., & Glassmoyer, G. (1992). On the characteristics of local geology and their influence on ground motions generated by the Loma Prieta earthquake in the San Francisco Bay Region, California. *Bulletin of the Seismological Society of America*, *82*(2), 603–641. https://doi.org/10.1785/bssa0820020603

Buell, S. (2020). Back-to-back earthquakes are a reminder: massachusetts is on shaky ground. *Boston Magazine*. Retrieved from https://www.bostonmagazine.com/news/2020/11/24/massachusetts-earthquakes/.

Campbell, K. W. (2009). Estimates of shear-wave Q and 0 for unconsolidated and semiconsolidated sediments in eastern North America. *Bulletin of the Seismological Society of America*, *99*(4), 2365–2392. https://doi.org/10.1785/0120080116

Castellaro, S., Mulargia, F., & Rossi, P. L. (2008). VS30: Proxy for seismic amplification? *Seismological Research Letters*, *79*(4), 540–543. https://doi.org/10.1785/gssrl.79.4.540

Dobry, R., Borcherdt, R. D., Crouse, C. B., Idriss, I. M., Joyner, W. B., Martin, G. R., Power, M. S., Rinne, E. E., & Seed, R. B. (2000). New site coefficients and site classification system used in recent building seismic code provisions. *Earthquake Spectra*, *16*(1), 41–67. https://doi.org/10.1193/1.1586082

Dobry, Ricardo & Iai, Susumu. (2000). Recent developments in the understanding of earthquake site response and associated seismic code implementation. Proceedings, GeoEng2000, International Conference on Geotechnical & Geological Engineering. 1.

Ebel, J. (2025). *Massachusetts earthquakes*. Northeast States Emergency Consortium. https://nesec.org/massachusetts-earthquakes/

Ebel, J. E. (1996). The seventeenth century seismicity of Northeastern North America. *Seismological Research Letters*, *67*(3), 51–68. https://doi.org/10.1785/gssrl.67.3.51

Federal Emergency Management Agency (FEMA), & National Institute of Building Sciences (NIBS). (2024, July). *Hazus Earthquake Model Technical Manual*. HAZUS 6.1.

Federal Emergency Management Agency (FEMA), & National Institute of Building Sciences (NIBS). (2022, November). *Hazus Inventory Technical Manual*. HAZUS 6.0

Gallipoli, M. R., & Mucciarelli, M. (2009). Comparison of site classification from VS30, VS10, and HVSR in Italy. *Bulletin of the Seismological Society of America*, *99*(1), 340–351. https://doi.org/10.1785/0120080083

Haji-Soltani, A., & Pezeshk, S. (2017). A comparison of different approaches to incorporate site effects into psha: A case study for a Liquefied Natural Gas Tank. *Bulletin of the Seismological Society of America*, *107*(6), 2927–2947. https://doi.org/10.1785/0120170026

Hashash, Y. M., Kottke, A. R., Stewart, J. P., Campbell, K. W., Kim, B., Moss, C., Nikolaou, S., Rathje, E. M., & Silva, W. J. (2014). Reference rock site condition for Central and eastern North America. *Bulletin of the Seismological Society of America*, *104*(2), 684–701. https://doi.org/10.1785/0120130132

Haskell, N. A. (1953). The dispersion of surface waves on multilayered media*. *Bulletin of the Seismological Society of America*, *43*(1), 17–34. https://doi.org/10.1785/bssa0430010017

Heath, D. C., Wald, D. J., Worden, C. B., Thompson, E. M., & Smoczyk, G. M. (2020). A global hybrid *Vs*₃₀ map with a topographic slope–based default and regional map insets. *Earthquake Spectra*, *36*(3), 1570–1584. https://doi.org/10.1177/8755293020911137

Ibs-von Seht, M., & Wohlenberg, J. (1999). Microtremor measurements used to map thickness of soft sediments. *Bulletin of the Seismological Society of America*, *89*(1), 250–259. https://doi.org/10.1785/bssa0890010250

Kafka, A. L. (2004). Why Does the Earth Quake in New England? The Science of Unexpected Earthquakes. http://aki.bc.edu/why_quakes.html

Kaklamanos, J., Baise, L. G., Thompson, E. M., & Dorfmann, L. (2015). Comparison of 1D linear, equivalent-linear, and nonlinear site response models at six KiK-net validation sites. *Soil Dynamics and Earthquake Engineering*, *69*, 207–219. https://doi.org/10.1016/j.soildyn.2014.10.016

Kianiard, E., O'Donnell, A., & Lai, T. (2017). 16th World Conference on Earthquake. In Evaluation Of Shake And Liquefaction Damages Due To Earthquake Scenarios In Boston, Massachusetts. Santiago.

Kianiard, E., O'Donnell, A., & Lai, T. (2017). 16th World Conference on Earthquake. In *Evaluation Of Shake And Liquefaction Damages Due To Earthquake Scenarios In Boston, Massachusetts*. Santiago.

Kramer, S. L. (2014). *Geotechnical earthquake engineering*. Prentice Hall.

Lee, V. W., & Trifunac, M. D. (2010). Should average shear-wave velocity in the top 30m of soil be used to describe seismic amplification? *Soil Dynamics and Earthquake Engineering*, *30*(11), 1250–1258. https://doi.org/10.1016/j.soildyn.2010.05.007

Lermo, J., & Chávez-García, F. J. (1993). Site effect evaluation using spectral ratios with only one station. *Bulletin of the Seismological Society of America*, *83*(5), 1574–1594. https://doi.org/10.1785/bssa0830051574

Luco, N., Rezaeian , S., Rukstales , K. S., Powers, P. M., Shumway, A. M., Martinez, E. M., & Smoczyk, G. M. (2021). Gridded earthquake ground motions for the 2020 NEHRP recommended seismic provisions and 2022 ASCE/SEI 7 standard. *(US Geological Survey Data Release)*. https://doi.org/https://doi.org/10.5066/P9I0R4O6

Luft, R. W., & Simpson, H. (1979). *Journal of the Boston Society Of Civil Engineers Section*, *66*(2), 67–87.

Luzi, L., Puglia, R., Pacor, F., Gallipoli, M. R., Bindi, D., & Mucciarelli, M. (2011). Proposal for a soil classification based on parameters alternative or complementary to vs,30. *Bulletin of Earthquake Engineering*, *9*(6), 1877–1898. https://doi.org/10.1007/s10518-011-9274-2

Mabee, S. B. (2022). A Data Set of Depth to Bedrock Describers in Dill Holes and Geophysical Surveys for Massachusetts. *In Review*.

Mabee, S. B., Duncan, C. C., Clement, W. P., & Pontrelli, M. A. (2023). *Massachusetts Depth to Bedrock Project*. MassDOT Office of Transportation Planning, Research and Technology Transfer Section, Research Report, 173 p.

Nakamura, Y. (1989). (rep.). *Method for dynamic characteristics estimation of subsurface using microtremor on the ground surface* (1st ed., Vol. 30, pp. 25–33). Japan: Quarterly Report of RTRI (Railway Technical Research Institute).

Nordenson, G. J., & Bell, G. R. (2000). Seismic Design Requirements for regions of moderate seismicity. *Earthquake Spectra*, *16*(1), 205–225. https://doi.org/10.1193/1.1586091

Perkins, S. (2024). *Seismic risk in eastern U.S. may be higher than previously thought*. Scientific American. https://www.scientificamerican.com/article/seismic-risk-in-eastern-us-may-be-higher-than-previously-thought/

Petersen, M. D., Shumway, A. M., Powers, P. M., Field, E. H., Moschetti, M. P., Jaiswal, K. S., Milner, K. R., Rezaeian, S., Frankel, A. D., Llenos, A. L., Michael, A. J., Altekruse, J. M., Ahdi, S. K., Withers, K. B., Mueller, C. S., Zeng, Y., Chase, R. E., Salditch, L. M., Luco, N., … Witter, R. C. (2023). The 2023 US 50-state national seismic hazard model: Overview and implications. *Earthquake Spectra*, *40*(1), 5–88. https://doi.org/10.1177/87552930231215428

Petersen, M. D., Shumway, A. M., Powers, P. M., Mueller, C. S., Moschetti, M. P., Frankel, A. D., Rezaeian, S., McNamara, D. E., Luco, N., Boyd, O. S., Rukstales, K. S., Jaiswal, K. S., Thompson, E. M., Hoover, S. M., Clayton, B. S., Field, E. H., & Zeng, Y. (2019). The 2018 update of the US National Seismic Hazard Model: Overview of model and implications. *Earthquake Spectra*, *36*(1), 5–41. https://doi.org/10.1177/8755293019878199

Pontrelli, M., Baise, L. G., Ebel, J. E., & Mabee, S. (2024). *Maps of Distributional Parameters of F0 for Massachusetts, USA Derived from a High-Resolution Continuous Depth-to-Bedrock Map*.

Pontrelli, M., Baise, L., & Ebel, J. (2023a). Regional-scale site characterization mapping in high impedance environments using soil fundamental resonance (F): New England, USA. *Engineering Geology*, *315*, 107043. https://doi.org/10.1016/j.enggeo.2023.107043

Pontrelli, M., Baise, L., & Ebel, J. (2023b). Regional-scale site characterization mapping in high impedance environments using soil fundamental resonance (F0): New England, USA. *Engineering Geology*, *315*, 107043. https://doi.org/10.1016/j.enggeo.2023.107043

Pontrelli, M., Baise, L., & Ebel, J. (2023c). *Mapping Fundamental Frequency (F0) as a Site Response Parameter Using a Multi-Scale Approach with State-Level Surficial Geologic Maps and Local Sedimentary Deposit Information*. https://doi.org/10.2139/ssrn.4435102

Porter, K. (2009). Cracking an open safe: Hazus vulnerability functions in terms of structure-independent spectral acceleration. *Earthquake Spectra*, *25*(2), 361–378. https://doi.org/10.1193/1.3106680

Pratt, T. L., Horton, J. W., Muñoz, J., Hough, S. E., Chapman, M. C., & Olgun, C. G. (2017). Amplification of earthquake ground motions in Washington, DC, and implications for hazard assessments in Central and eastern North America. *Geophysical Research Letters*, *44*(24). https://doi.org/10.1002/2017gl075517

Pyke, Robert. (2020). Limitations of Vs30 for characterizing sites for ground motion studies and guidance on the conduct of nonlinear site response analyses.

Rathje, E. M., Kottke, A. R., & Trent, W. L. (2010). Influence of input motion and site property variabilities on seismic site response analysis. *Journal of Geotechnical and Geoenvironmental Engineering*, *136*(4), 607–619. https://doi.org/10.1061/(asce)gt.1943-5606.0000255

Sorabella, S. (2006). *Ground Motion Selection For Boston, Massachusetts* (thesis).

Thomson, W. T. (1950). Transmission of elastic waves through a stratified solid medium. *Journal of Applied Physics*, *21*(2), 89–93. https://doi.org/10.1063/1.1699629

Tilashalski, M., Guney Olgun, C., Rodriguez-Marek, A., Godfrey, E. A., Chapman, M. C., Shamsalsadati, S., & Eddy, M. A. (2015). Regional geology and seismic site amplification in the Washington, DC, Metropolitan Area. *IFCEE 2015*, 1278–1287. https://doi.org/10.1061/9780784479087.115

Tuttle, M., & Seeber, L. (1991). Historic and prehistoric earthquake-induced liquefaction in Newbury, Massachusetts. *Geology*, *19*(6), 594. https://doi.org/10.1130/0091-7613(1991)019<0594:hapeil>2.3.co;2

USGS Earthquake Hazards Program. (2024). *Why should people in the Eastern United States be concerned about earthquakes?*. USGS. https://www.usgs.gov/faqs/why-should-people-eastern-united-states-be-concerned-about-earthquakes

USGS National Earthquake Information Center, PDE. (2009). *M 5.9 - The 1755 Cape Ann, Massachusetts Earthquake*. Earthquake hazards program. https://earthquake.usgs.gov/earthquakes/eventpage/ushis7/region-info

Wald, D. J., & Allen, T. I. (2007). Topographic slope as a proxy for seismic site conditions and amplification. *Bulletin of the Seismological Society of America*, *97*(5), 1379–1395. https://doi.org/10.1785/0120060267

Wald, L. A., & Mori, J. (2000). Evaluation of methods for estimating linear site-response amplifications in the Los Angeles region. *Bulletin of the Seismological Society of America*, *90*(6B). https://doi.org/10.1785/0119970170

Yilar, E., Baise, L. G., & Ebel, J. E. (2017). Using H/V measurements to determine depth to bedrock and VS30 in Boston, Massachusetts. *Engineering Geology*, *217*, 12–22. https://doi.org/10.1016/j.enggeo.2016.12.002

Zalachoris, G., & Rathje, E. M. (2015). Evaluation of one-dimensional site response techniques using borehole arrays. *Journal of Geotechnical and Geoenvironmental Engineering*, *141*(12). https://doi.org/10.1061/(asce)gt.1943-5606.0001366

Appendix A: Code for Converting (.shp) to (.GeoJSON)

```
# Import necessary libraries
import geopandas as gpd

# Load the shapefile into a GeoDataFrame
shapefile_path = 'path_to_your_shapefile.shp'  # Update this with your shapefile's path
gdf = gpd.read_file(shapefile_path)

# Convert to GeoJSON and save
geojson_path = 'output_path.geojson'  # Specify the output path for the GeoJSON file
gdf.to_file(geojson_path, driver='GeoJSON')

print(f"Conversion successful! GeoJSON saved at: {geojson_path}")
```

Appendix B: Liquefaction Inventory Output Maps

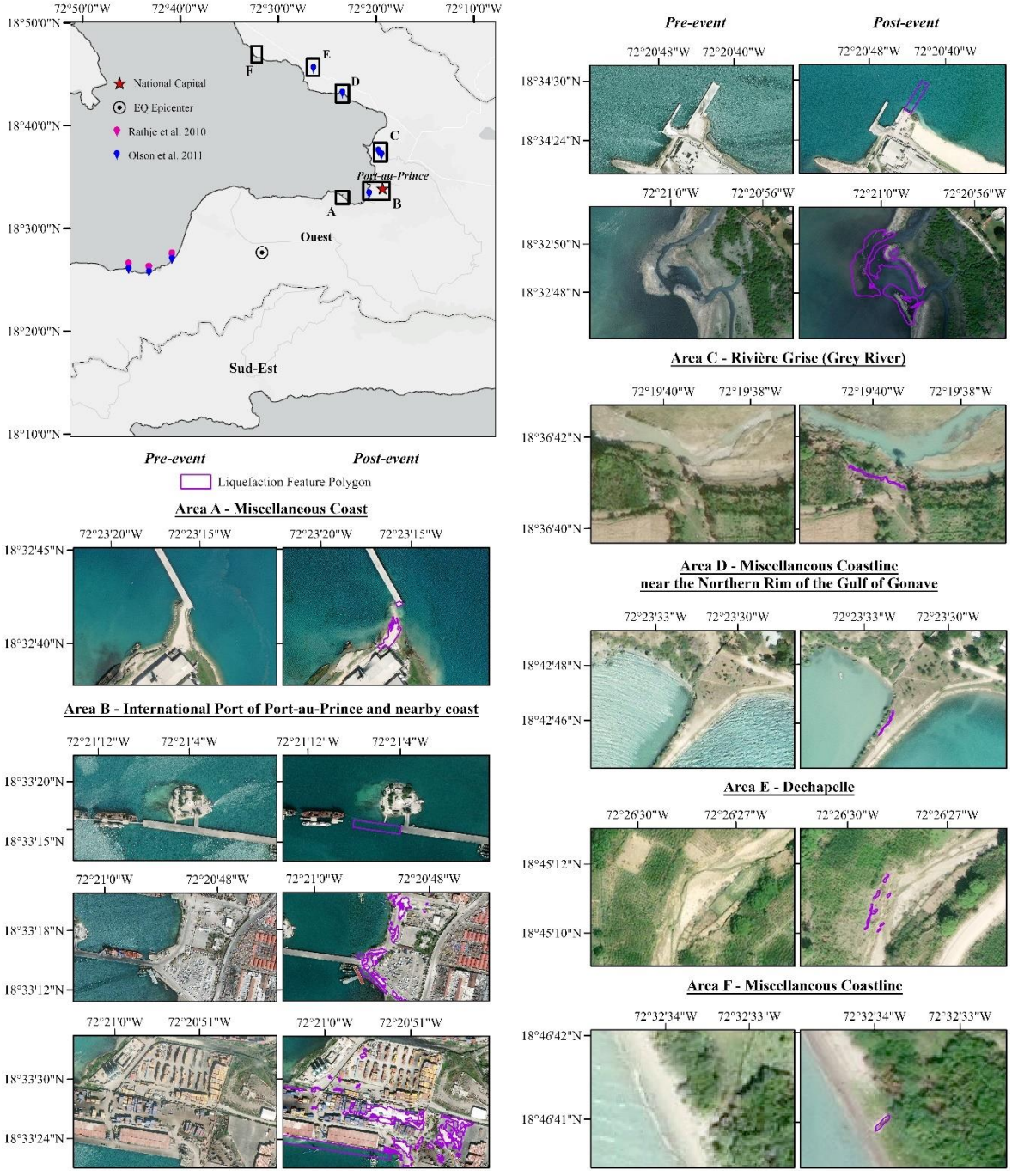

Figure B1: Maps Displaying Digitized Liquefaction Features Across the Study Area for the 2010 M7.0 Earthquake Event in Port-au-Prince, Haiti. This figure presents a series of maps illustrating the spatial extent of liquefaction features identified through field observations and geotechnical analysis in the aftermath of the 2010 M7.0 earthquake in Port-au-Prince, Haiti. Each map represents a specific location within the study area and is labeled accordingly. The maps show manifestations of liquefaction phenomena, such as sand boils and sand ejecta, which have been digitized in purple. The polygons are overlaid on post-event satellite imagery and compared with pre-event imagery allowing for a visual comparison of the landscape before and after the earthquake.

Figure B2: Maps Displaying Digitized Liquefaction Features Across the Study Area for the 2011 M6.1 Earthquake Event in Christchurch, New Zealand. This figure presents a series of maps that illustrate the spatial extent of liquefaction features identified through field observations and remote mapping in the aftermath of the 2011 M6.1 earthquake in Christchurch, New Zealand. Each map corresponds to a specific location within the study area and is labeled accordingly. The maps depict the distribution of liquefaction-induced phenomena, such as sand boils and sand ejecta, which have been digitized in purple. The digitized features are overlaid on post-event aerial imagery to show the relationship between the mapped liquefaction areas observed after the earthquake. Additionally, the maps include a comparison with ground truth polygons for a visual comparison of the two datasets.

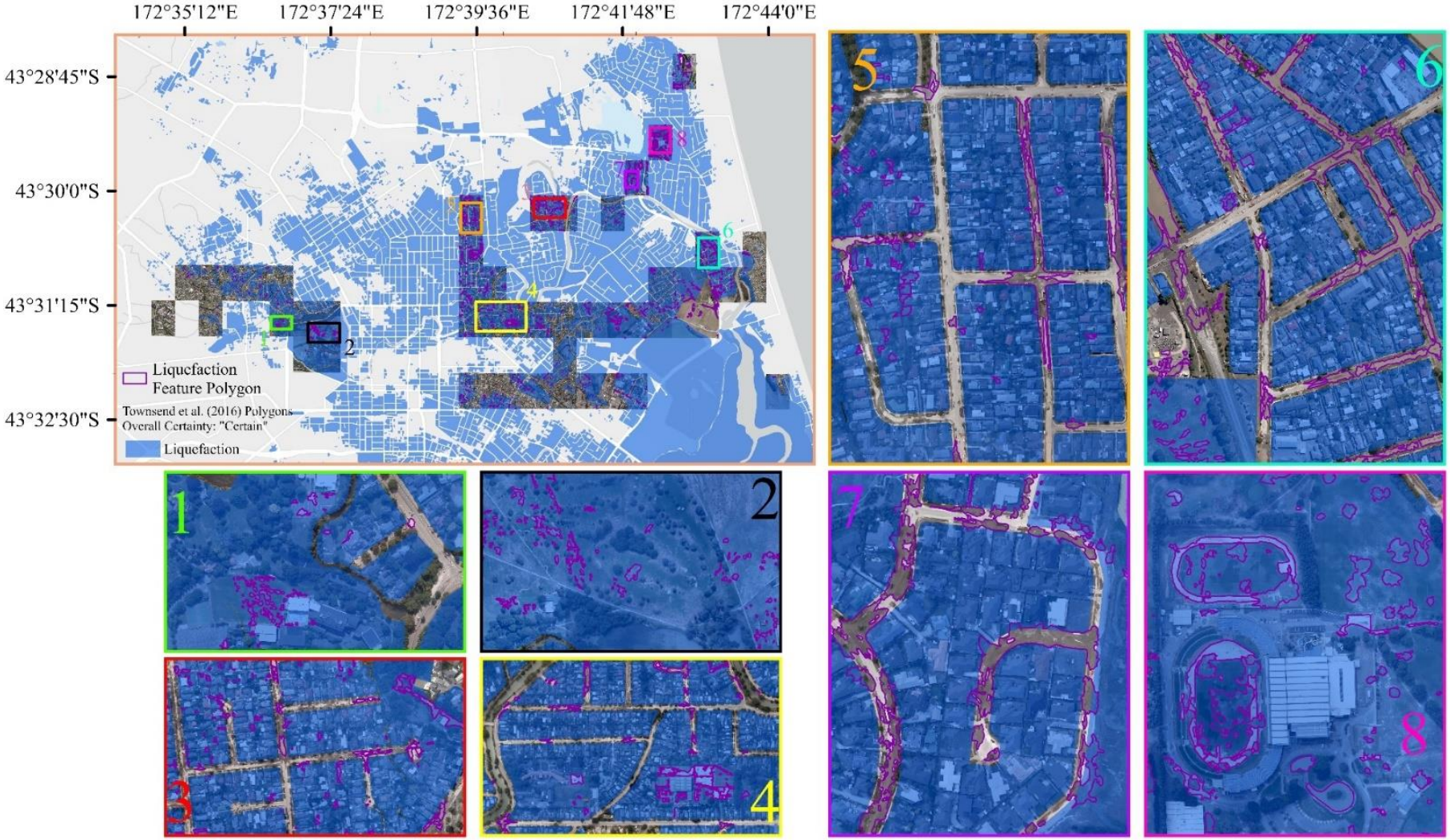

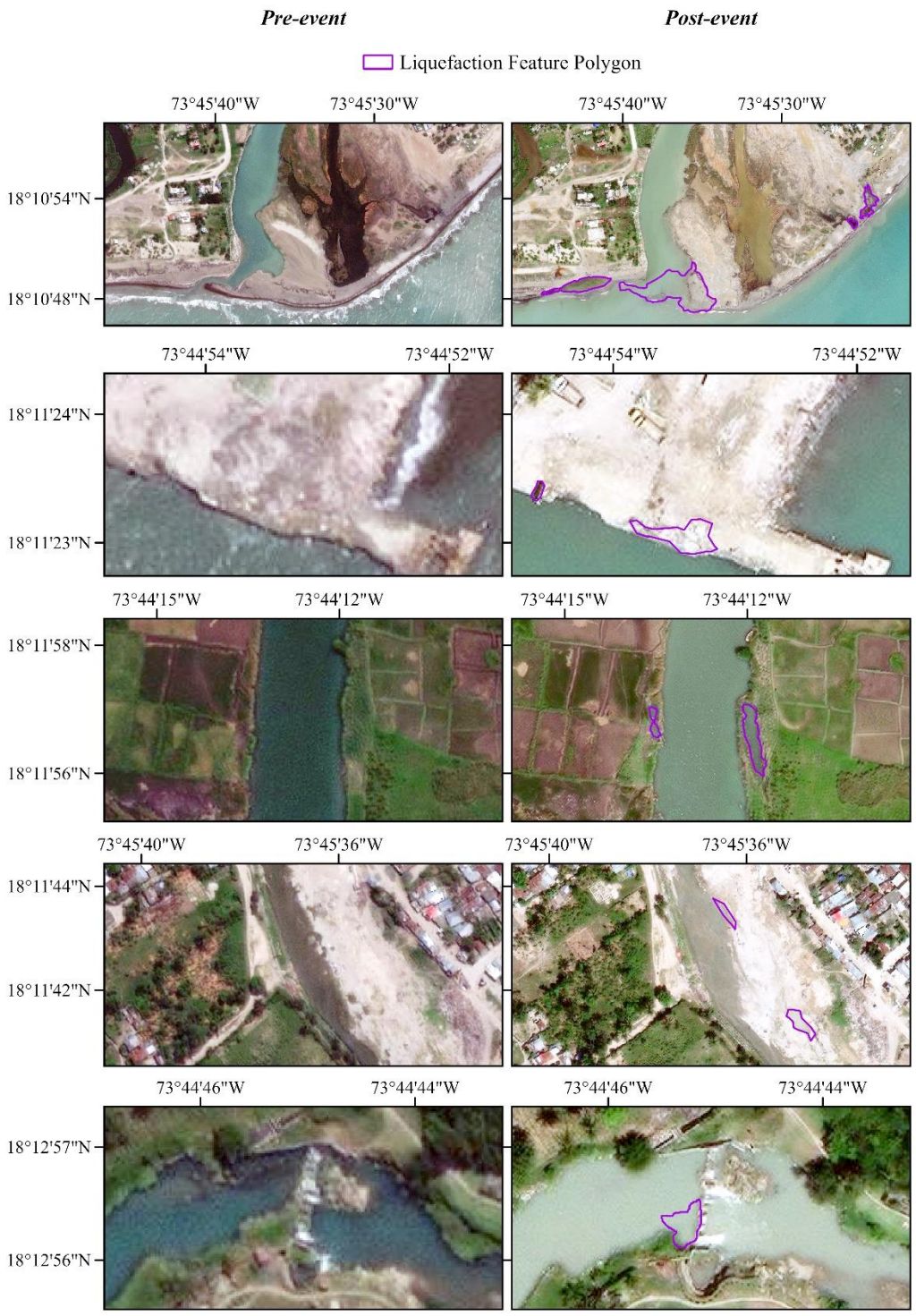

Figure B3: Maps Displaying Digitized Liquefaction Features Across the Study Area for the 2021 M7.2 Earthquake Event in Nippes, Haiti. This figure presents a series of maps illustrating the spatial extent of liquefaction features identified through field observations, crowdsourcing, and remote detection in the aftermath of the 2021 M7.2 earthquake in Nippes, Haiti. Each map represents a specific location within the study area. The maps show the features, which have been digitized in purple to highlight discrete manifestations of liquefaction phenomena, such as sand boils and sand ejecta. The polygons are overlaid on post-event satellite imagery and compared with pre-event imagery allowing for a visual comparison of the landscape before and after the earthquake.

Appendix C: Liquefaction Inventory Attribute Summaries

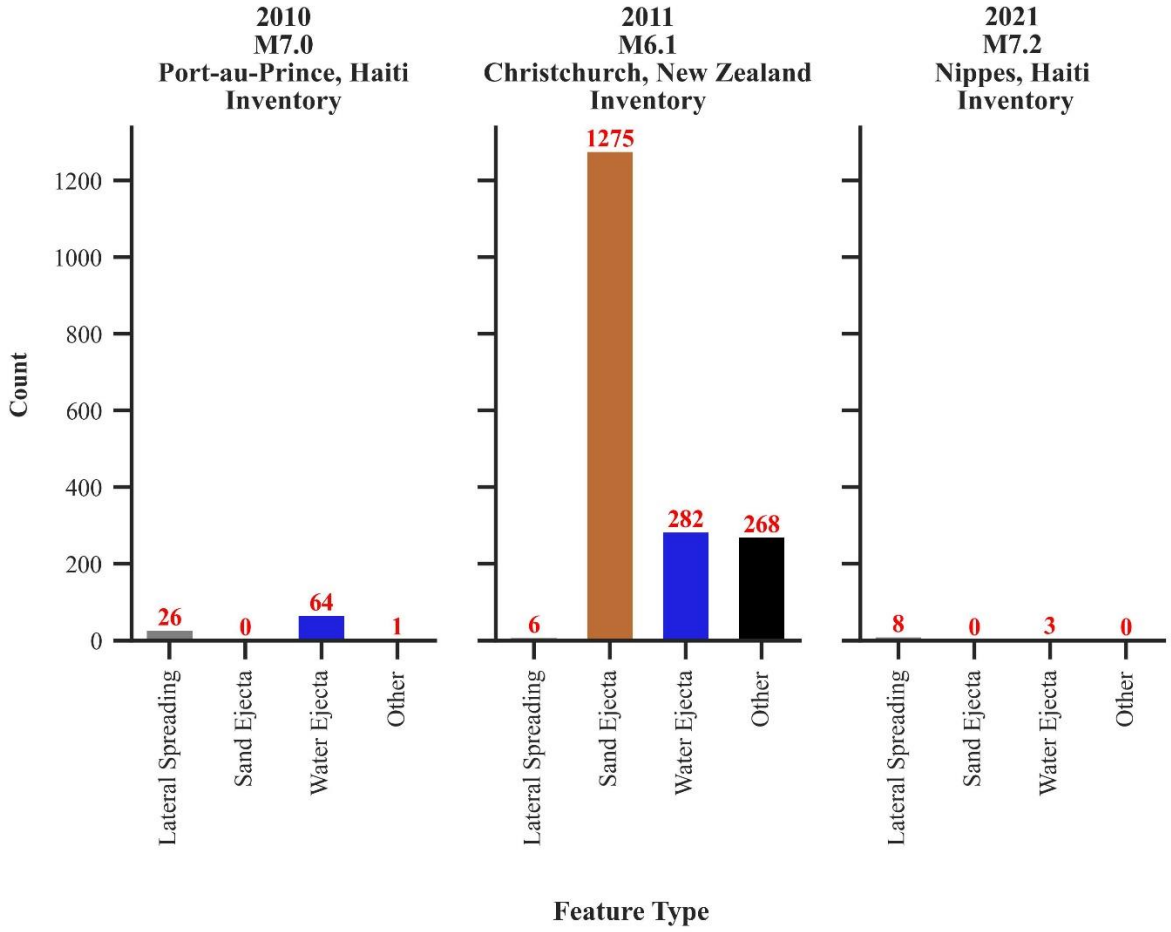

Figure C1: Summary of Liquefaction Feature Types Digitized for the Creation of Inventories for the 2010 M7.0 Earthquake in Port-au-Prince, Haiti; the 2011 M6.1 Earthquake in Christchurch, New Zealand; and the 2021 M7.2 Earthquake in Nippes, Haiti. This figure presents a comparative overview of the different liquefaction feature types observed and digitized for the three earthquake events, highlighting the variations in feature types that could be observed.

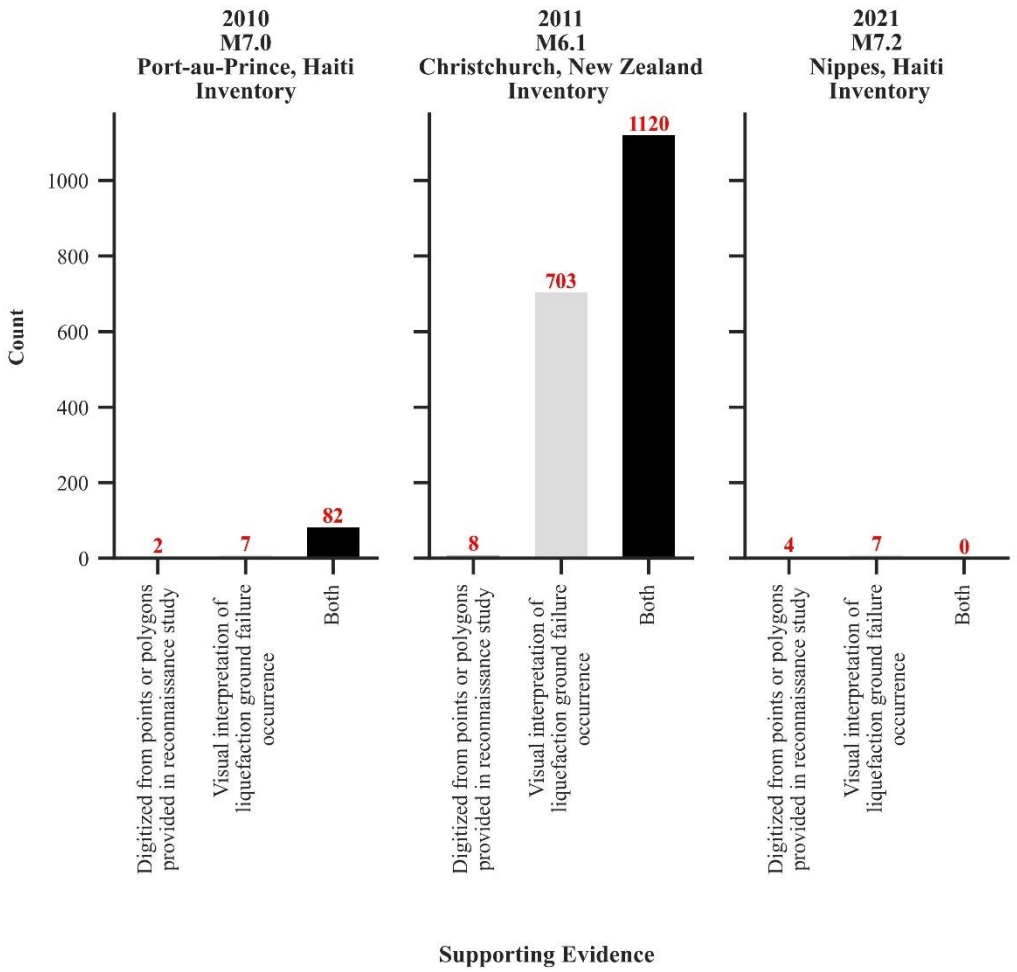

Figure C2: Summary of the Supporting Evidence Attribute Used in the Creation of Inventories for the 2010 M7.0 Earthquake in Port-au-Prince, Haiti; the 2011 M6.1 Earthquake in Christchurch, New Zealand; and the 2021 M7.2 Earthquake in Nippes, Haiti. This figure summarizes the various forms of supporting evidence that were utilized to verify and refine the identification of liquefaction features across the three events. The comparison highlights the diversity and availability of supporting evidence for each earthquake, providing insights into how different types of ground truth data contributed to the accuracy and completeness of the inventories.

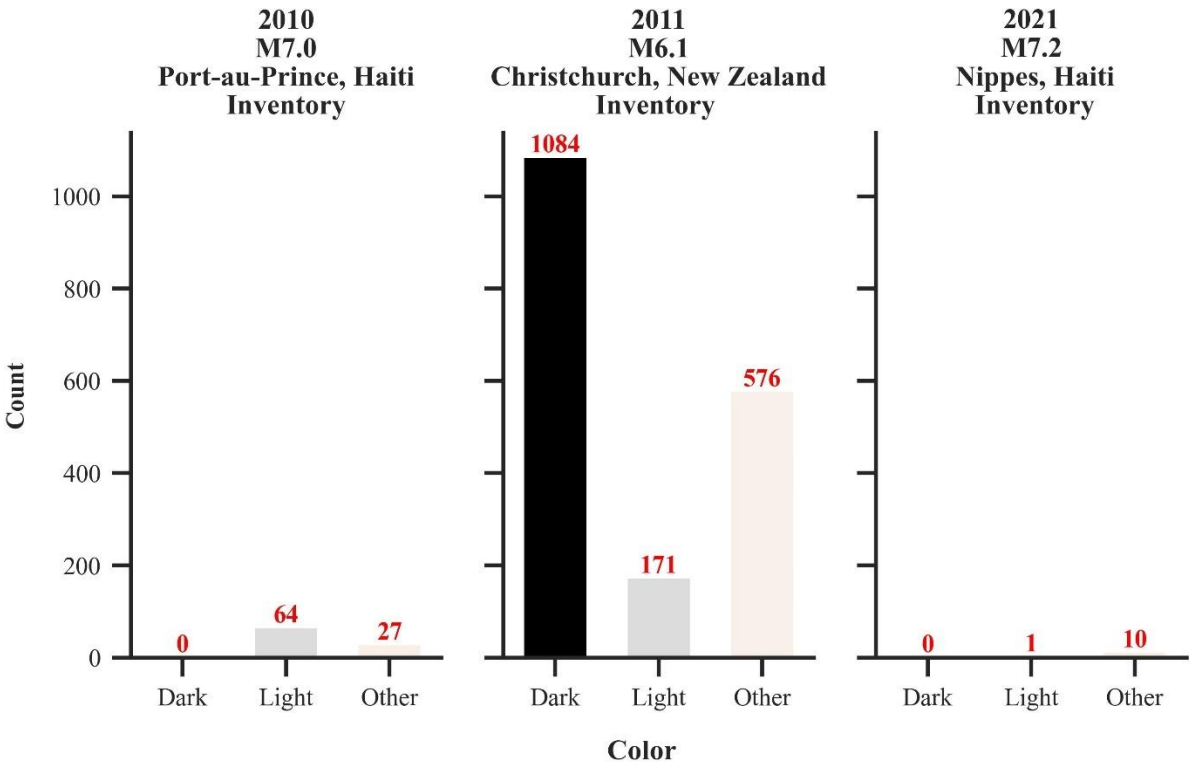

Figure C3: Summary of the Color Attribute Used in the Creation of Inventories for the 2010 M7.0 Earthquake in Port-au-Prince, Haiti; the 2011 M6.1 Earthquake in Christchurch, New Zealand; and the 2021 M7.2 Earthquake in Nippes, Haiti. This figure provides an overview of the color attribute used to distinguish liquefaction in the digitized inventories for the three earthquake events. The graph illustrates the distribution of the color attribute, demonstrating how the visual distinction supports the classification and analysis of liquefaction manifestations.

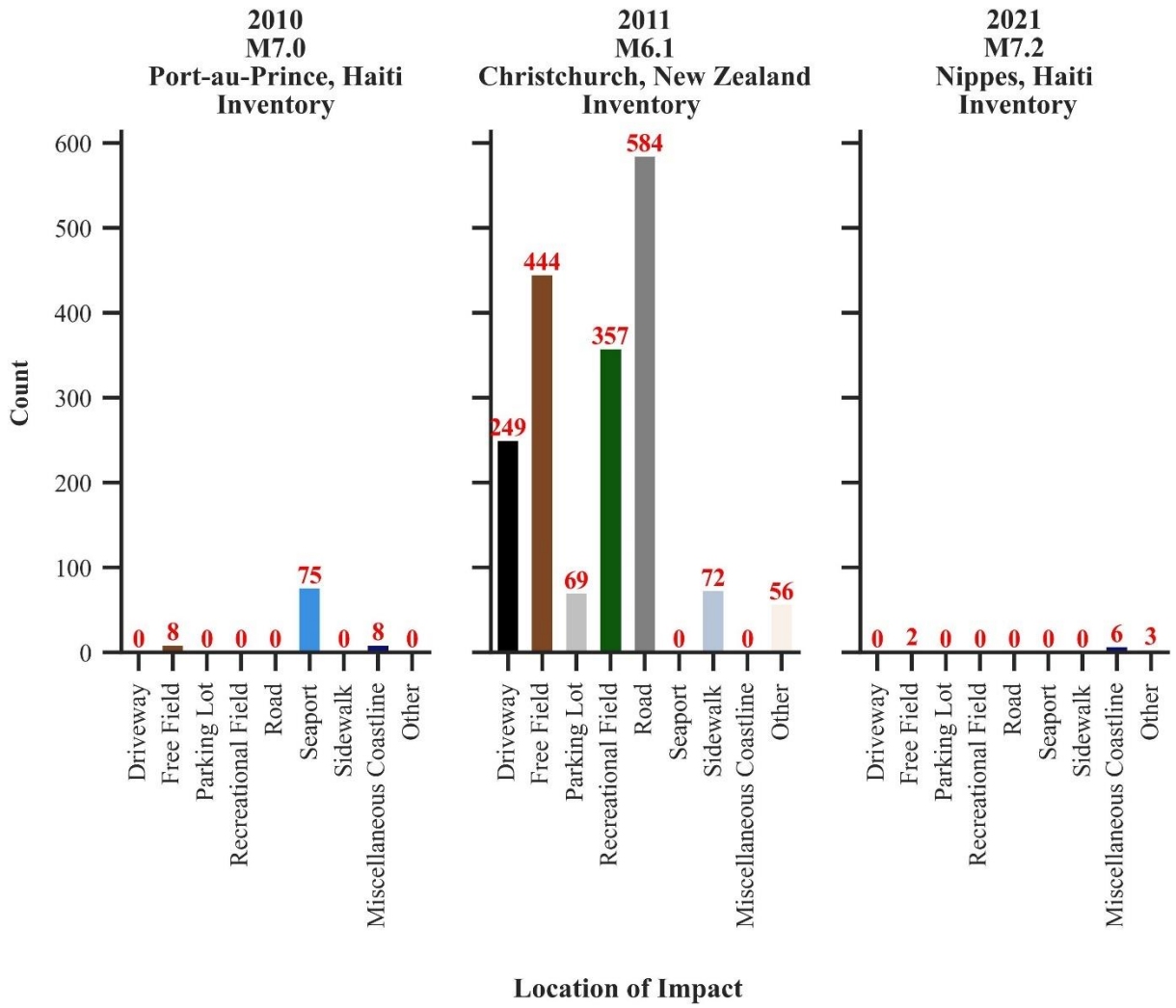

Figure C4: Summary of the Location of Impact Attribute Used in the Creation of Inventories for the 2010 M7.0 Earthquake in Port-au-Prince, Haiti; the 2011 M6.1 Earthquake in Christchurch, New Zealand; and the 2021 M7.2 Earthquake in Nippes, Haiti. This figure provides a comparative overview of the "Location of Impact" attribute used to record the spatial distribution of liquefaction features in the digitized inventories for the three earthquake events. The graph illustrates how the location of each liquefaction feature was geographically mapped within the study areas, highlighting the areas most affected by liquefaction. It demonstrates the variability in the spatial distribution of impact across the three events, reflecting potential societal losses and the extent of damage in the different regions.

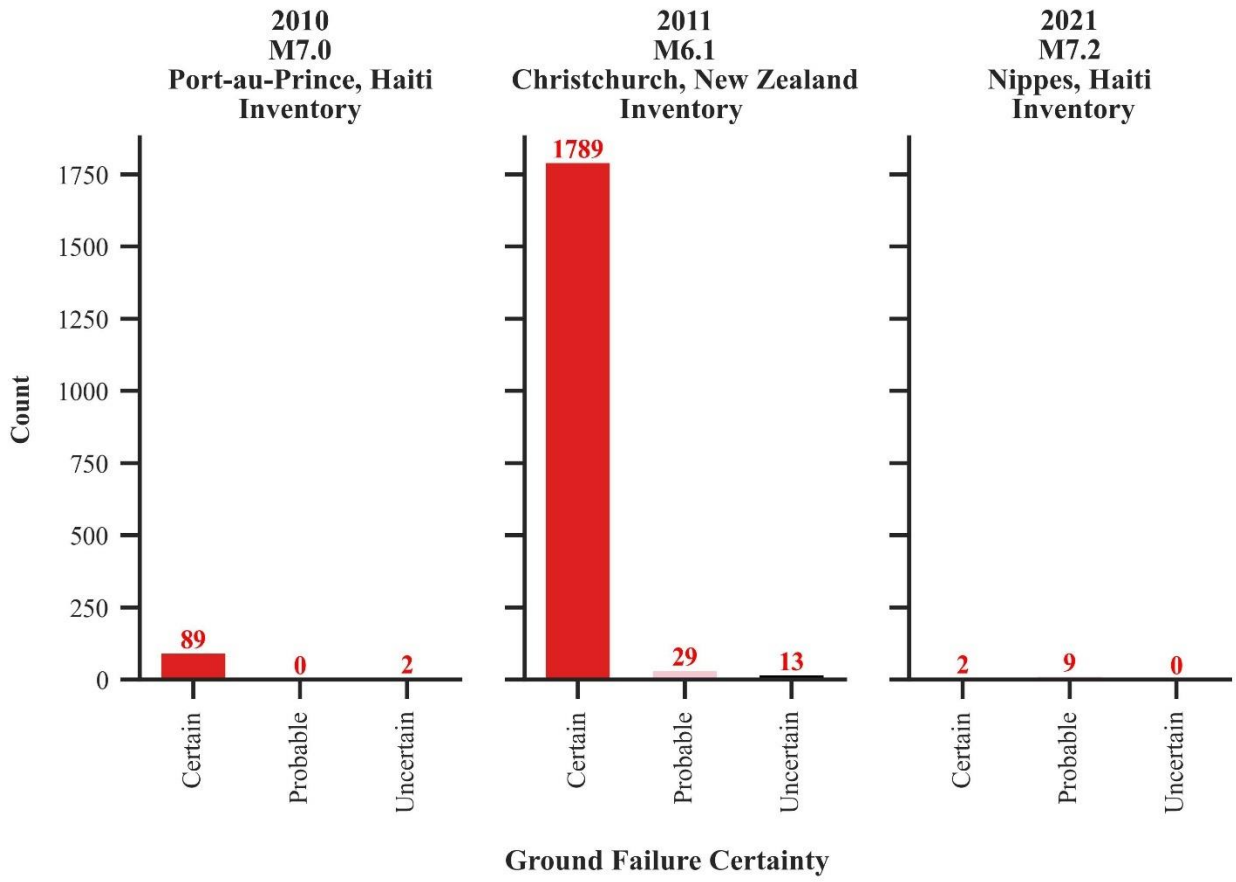

Figure C5: Summary of the "Ground Failure Certainty" Attribute Used in the Creation of Inventories for the 2010 M7.0 Earthquake in Port-au-Prince, Haiti; the 2011 M6.1 Earthquake in Christchurch, New Zealand; and the 2021 M7.2 Earthquake in Nippes, Haiti. This figure provides an overview of the "Ground Failure Certainty" attribute used to assess the confidence in the identification of liquefaction features in the digitized inventories for the three earthquake events. The graph illustrates the distribution of certainty levels assigned to each liquefaction feature, based on the quality of supporting data such as field observations, remote sensing imagery, and geotechnical reports. The certainty levels reflect the confidence in the occurrence of liquefaction phenomena at specific locations, with higher certainty associated with more reliable data sources. This attribute helps in evaluating the reliability of the liquefaction inventories and potential use in further analysis.

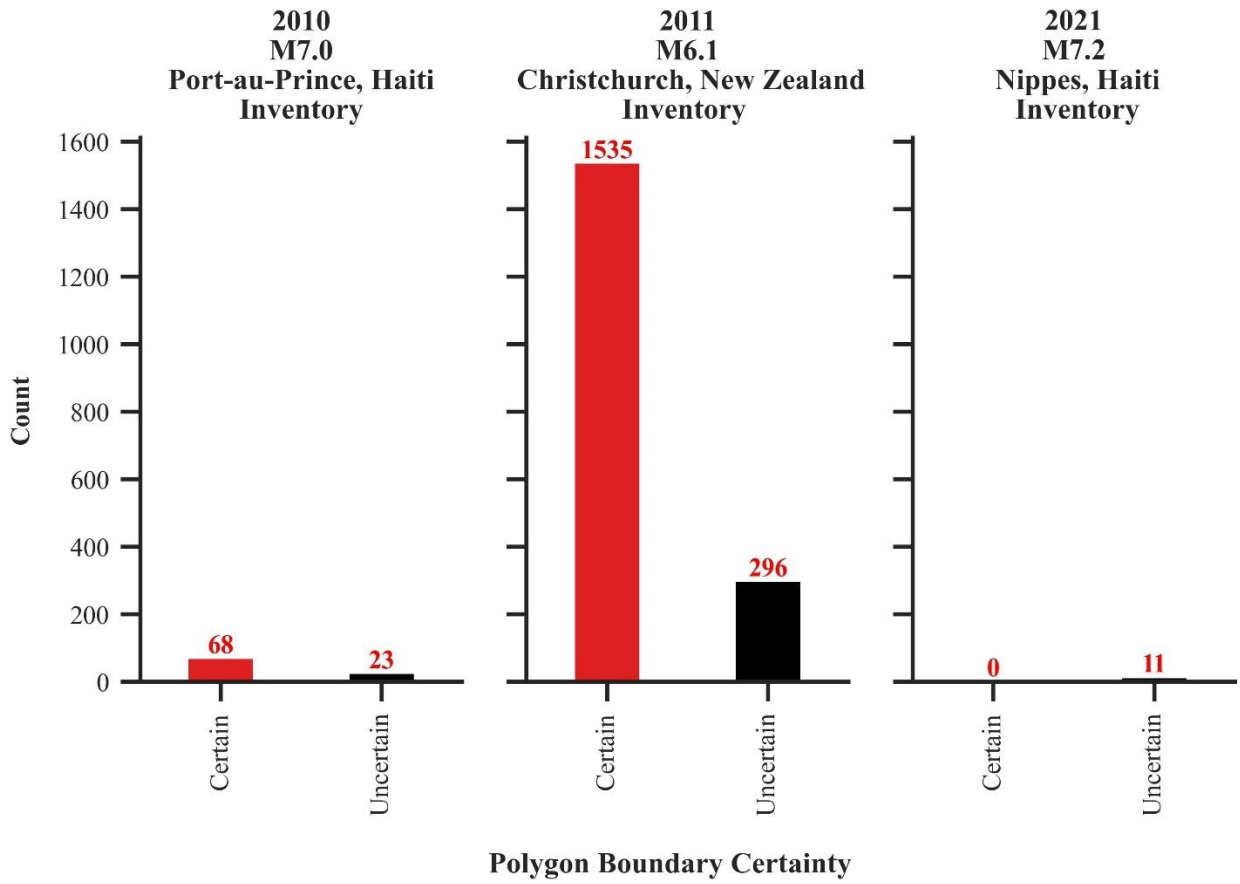

Figure C6: Summary of the "Polygon Boundary Certainty" Attribute Used in the Creation of Inventories for the 2010 M7.0 Earthquake in Port-au-Prince, Haiti; the 2011 M6.1 Earthquake in Christchurch, New Zealand; and the 2021 M7.2 Earthquake in Nippes, Haiti. This figure summarizes the "Polygon Boundary Certainty" attribute, which indicates the confidence in the delineation of liquefaction feature boundaries in the digitized inventories. The graph shows the distribution of certainty levels assigned to the accuracy of polygon boundaries, reflecting the precision with which liquefaction features were mapped. These certainty levels take into account factors such as the resolution of the imagery used, the availability of ground truth data, and the clarity of feature identification. This attribute provides insights into the reliability of feature boundaries and the potential for errors in feature classification and extent.

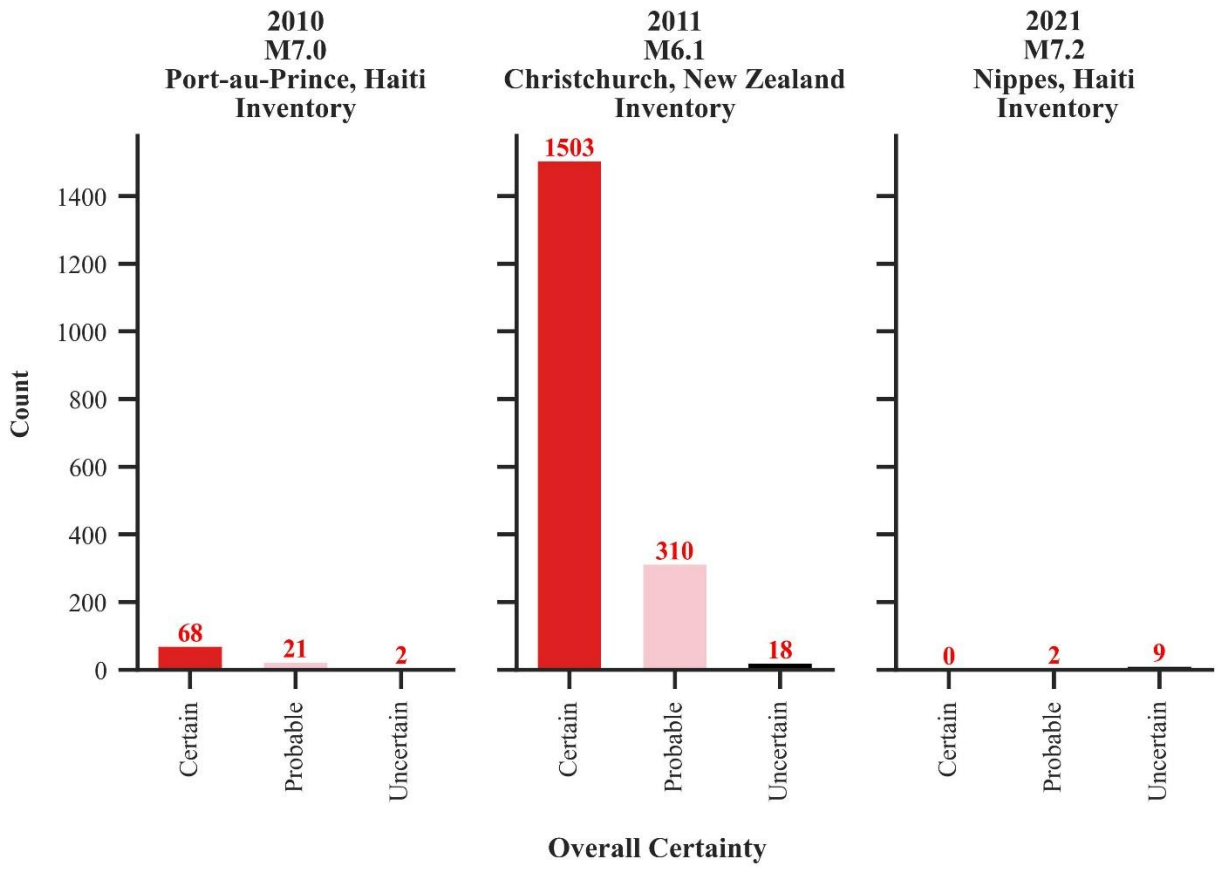

Figure C7: Summary of the "Overall Certainty" Attribute Used in the Creation of Inventories for the 2010 M7.0 Earthquake in Port-au-Prince, Haiti; the 2011 M6.1 Earthquake in Christchurch, New Zealand; and the 2021 M7.2 Earthquake in Nippes, Haiti. This figure presents the "Overall Certainty" attribute, which combines both "Ground Failure Certainty" and "Polygon Boundary Certainty" to provide an overall confidence level in the digitized liquefaction inventory for each earthquake event. The graph illustrates the distribution of overall certainty levels assigned to each liquefaction feature, taking into account both the reliability of the feature's occurrence (ground failure certainty) and the precision of its boundary delineation (polygon boundary certainty). Features with higher certainty are based on robust ground truth data and precise mapping, while lower certainty reflects areas where data limitations or mapping challenges occurred. This combined measure offers a comprehensive view of the confidence in the inventory, guiding its potential application in further studies or hazard assessments.

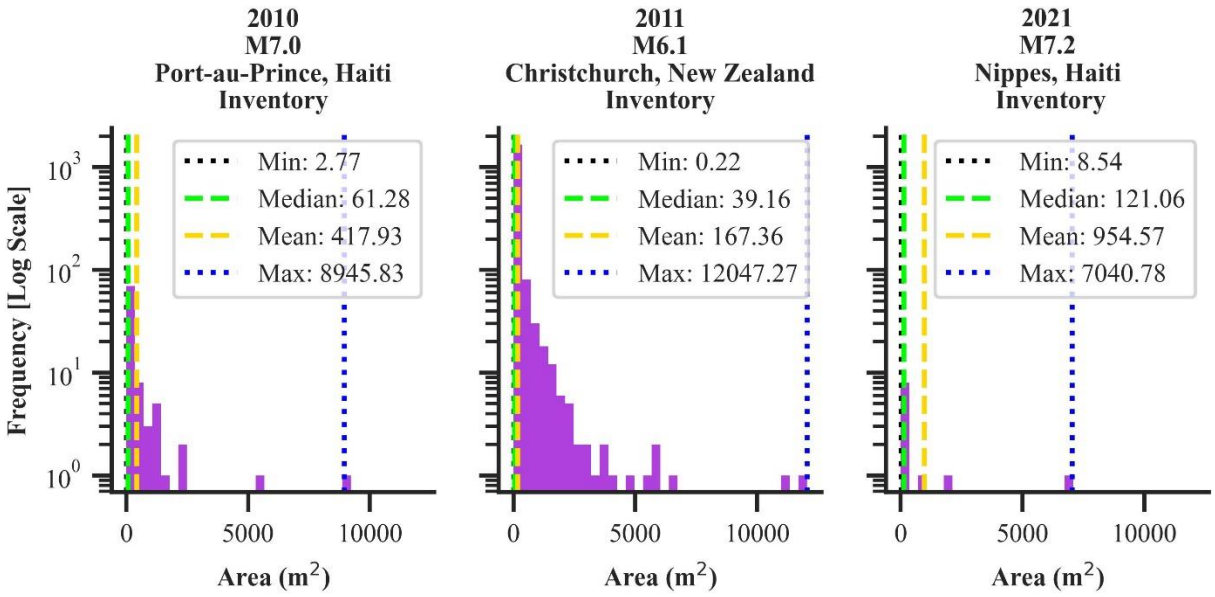

Figure C8: Histogram Depicting Liquefaction Feature Sizes Across the 2010 M7.0 Earthquake in Port-au-Prince, Haiti; the 2011 M6.1 Earthquake in Christchurch, New Zealand; and the 2021 M7.2 Earthquake in Nippes, Haiti. This figure presents histograms illustrating the distribution of liquefaction feature sizes observed across the three earthquake events. The data highlights the relationship between the quality of ground truth data and imagery with the precision of feature delineation. Better-quality ground truth data and clearer imagery resulted in smaller, more distinct liquefaction features, while poorer data led to larger, less defined features. The histograms offer insight into how data quality influenced the accuracy of liquefaction feature classification and size estimation, underscoring the importance of high-resolution imagery and robust ground truth in creating precise inventories.

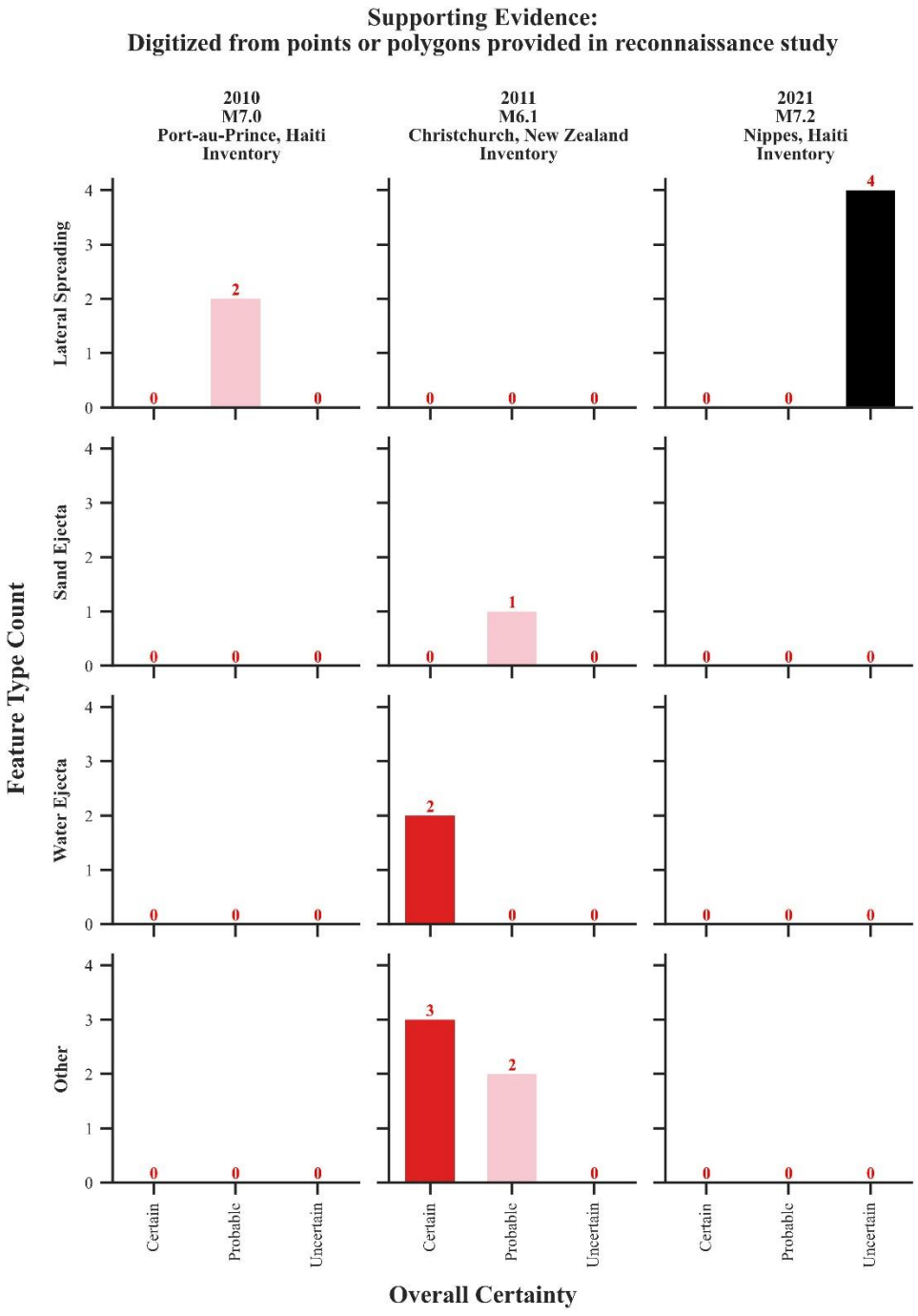

Figure C9: Combined Liquefaction Feature Type and Overall Certainty for Features Digitized from Points or Polygons Provided in Reconnaissance Study for the 2010 M7.0 Earthquake in Port-au-Prince, Haiti; the 2011 M6.1 Earthquake in Christchurch, New Zealand; and the 2021 M7.2 Earthquake in Nippes, Haiti. This figure assesses the overall certainty by feature type, specifically for liquefaction features digitized from points or polygons provided in reconnaissance reports or ground truth data. It highlights how different feature types are associated with varying levels of certainty, reflecting the accuracy and reliability of the data used for feature identification. The visualization offers insights into how the quality of reconnaissance study data influences the confidence in the classification and mapping of specific liquefaction features across the three earthquake events.

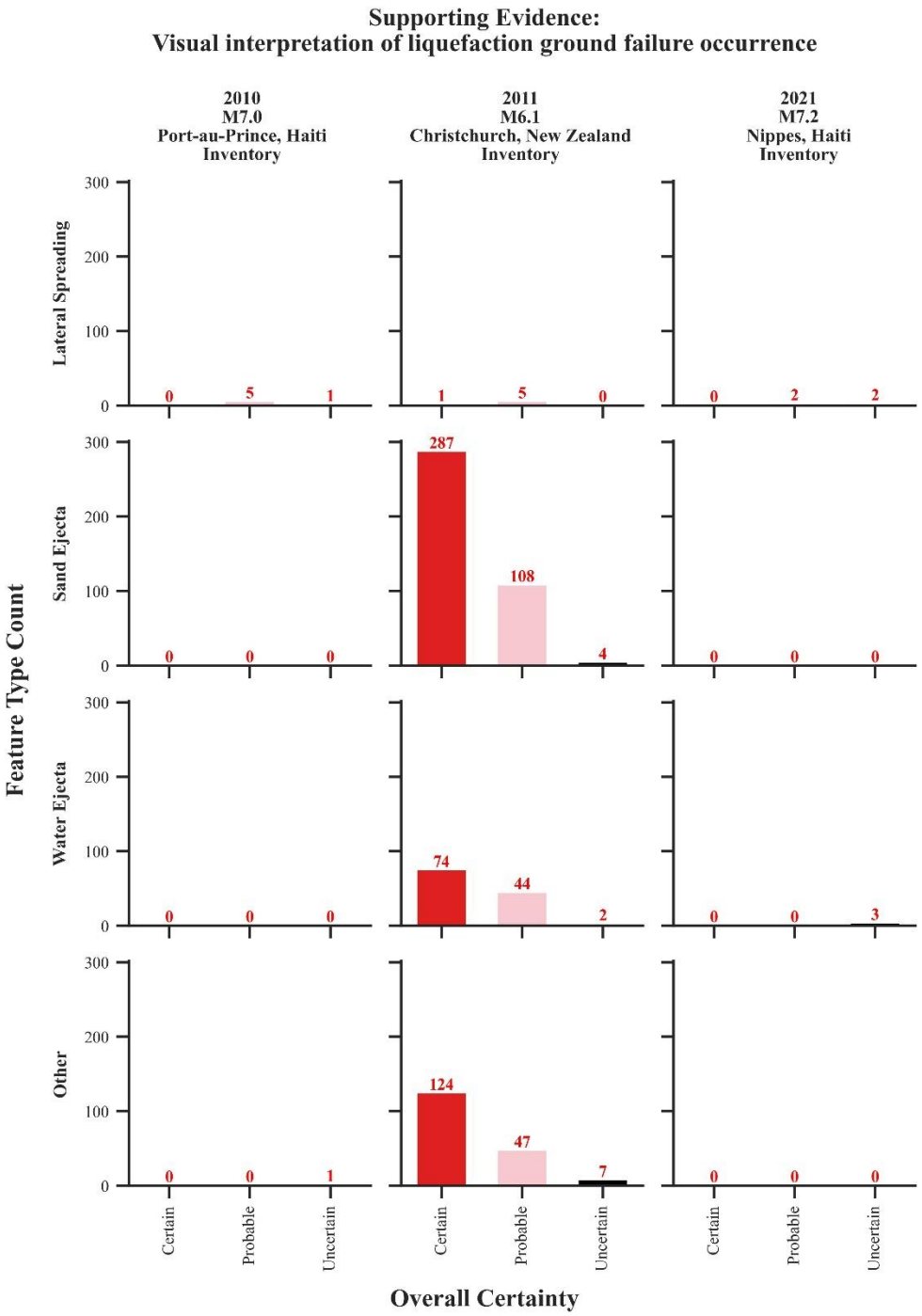

Figure C10: Combined Liquefaction Feature Type and Overall Certainty for Features Digitized Using Visual Interpretation for the 2010 M7.0 Earthquake in Port-au-Prince, Haiti; the 2011 M6.1 Earthquake in Christchurch, New Zealand; and the 2021 M7.2 Earthquake in Nippes, Haiti. This figure combines liquefaction feature types and overall certainty for features digitized through visual interpretation alone. The graph highlights the confidence in feature identification and delineation when relying solely on visual analysis, reflecting challenges such as image clarity and interpretive subjectivity. This visualization provides insights into how the use of visual interpretation influences the accuracy and confidence of liquefaction feature classification across the three events.

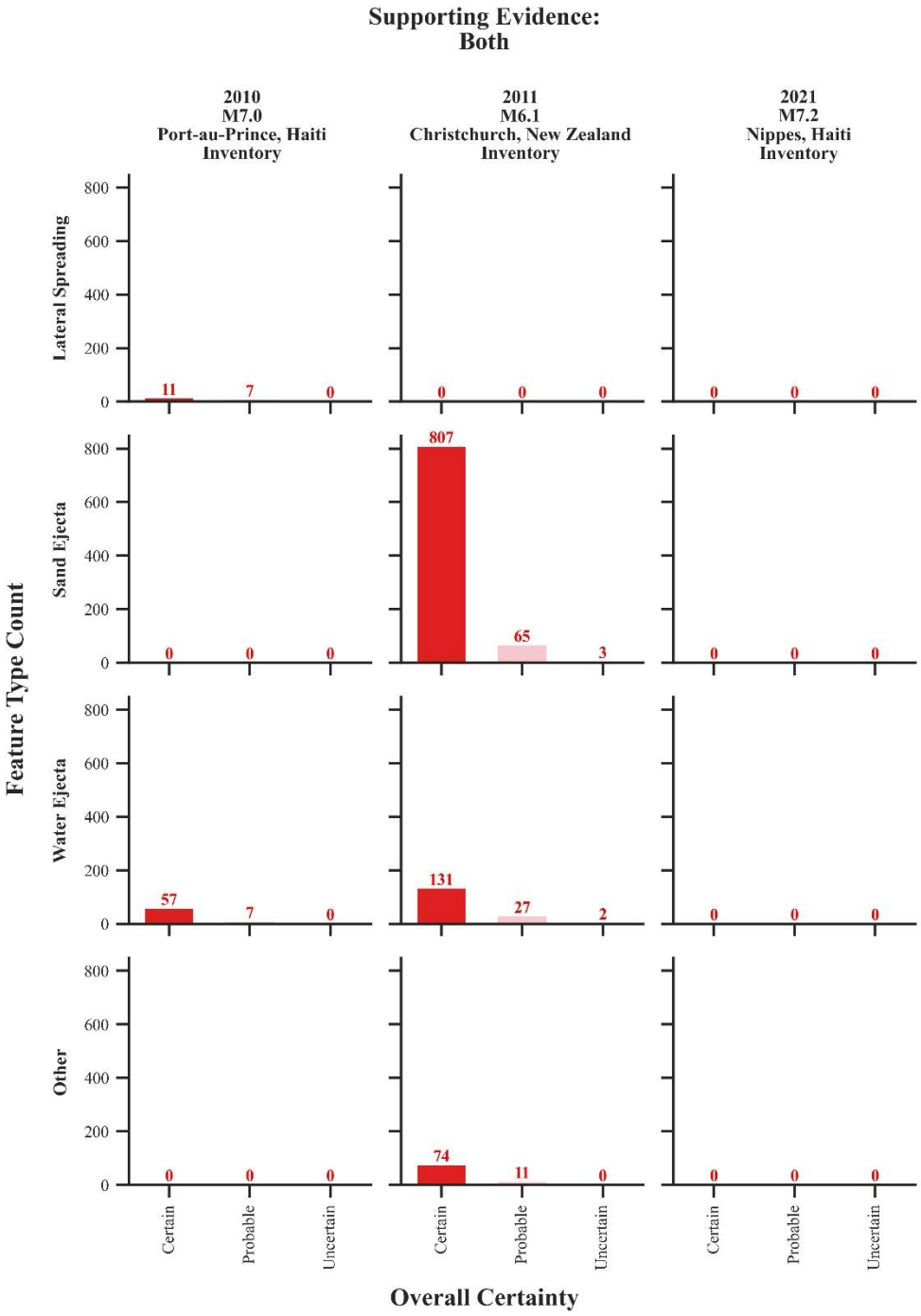

Figure C11: Combined Liquefaction Feature Type and Overall Certainty for Features Digitized from Points or Polygons from Reconnaissance Reports and Visually Easy to Detect for the 2010 M7.0 Earthquake in Port-au-Prince, Haiti; the 2011 M6.1 Earthquake in Christchurch, New Zealand; and the 2021 M7.2 Earthquake in Nippes, Haiti. This figure combines liquefaction feature types and overall certainty for features digitized from points or polygons provided in reconnaissance reports that were visually easy to detect. It demonstrates how feature types correspond to varying levels of certainty, with features that were clearly visible in imagery showing higher confidence in identification and delineation. The graph reflects the reliability of features identified through both reconnaissance data and clear visual interpretation, highlighting how ease of detection improves the accuracy of mapping and certainty across the three earthquake events.

Appendix D: Linear SH1D Maps of Parameters – GBS Care Facilities

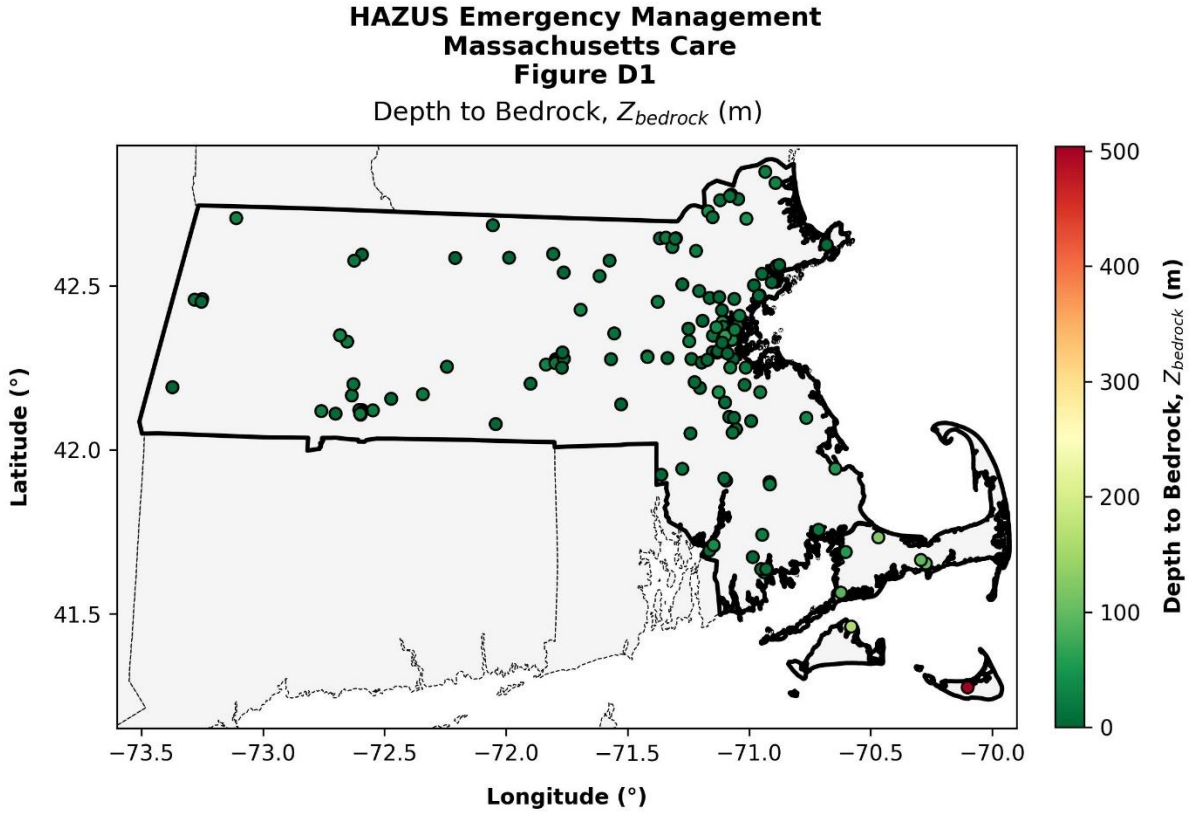

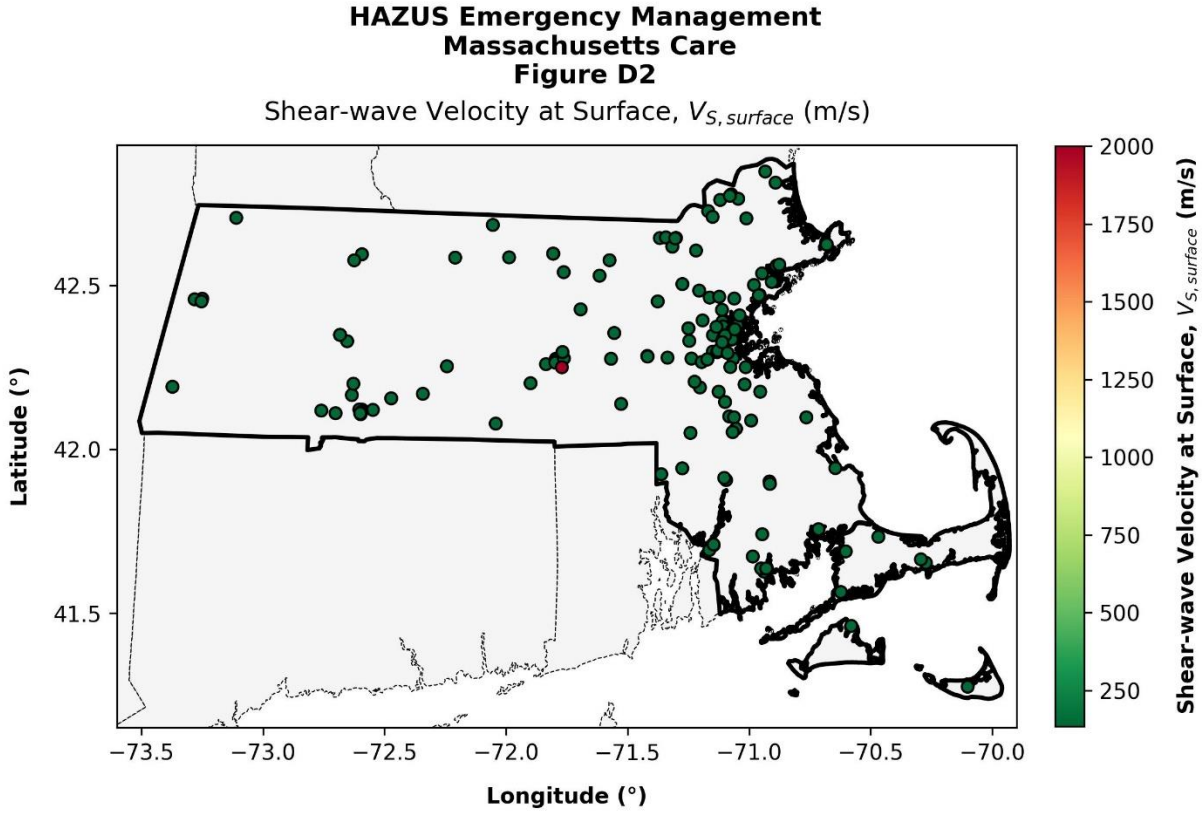
HAZUS Emergency Management
Massachusetts Care
Figure D2
Shear-wave Velocity at Surface, $V_{S,surface}$ (m/s)
Latitude (°)
42.5
42.0
41.5
−73.5
−73.0
−72.5
−72.0
−71.5
−71.0
−70.5
−70.0
Longitude (°)
2000
1750
1500
1250
1000
750
500
250
Shear-wave Velocity at Surface, $V_{S,surface}$ (m/s)

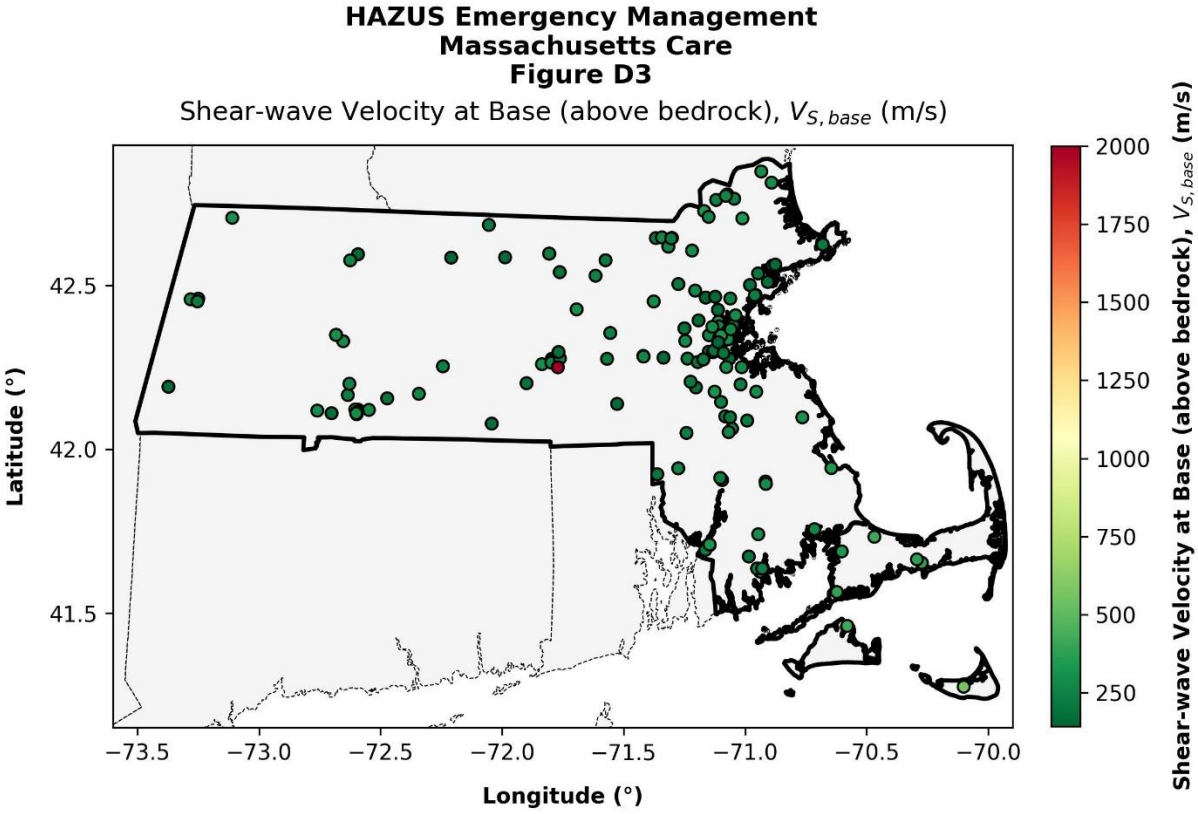
HAZUS Emergency Management
Massachusetts Care
Figure D3
Shear-wave Velocity at Base (above bedrock), $V_{S,base}$ (m/s)
Latitude (°)
42.5
42.0
41.5
−73.5
−73.0
−72.5
−72.0
−71.5
−71.0
−70.5
−70.0
Longitude (°)
2000
1750
1500
1250
1000
750
500
250
Shear-wave Velocity at Base (above bedrock), $V_{S,base}$ (m/s)

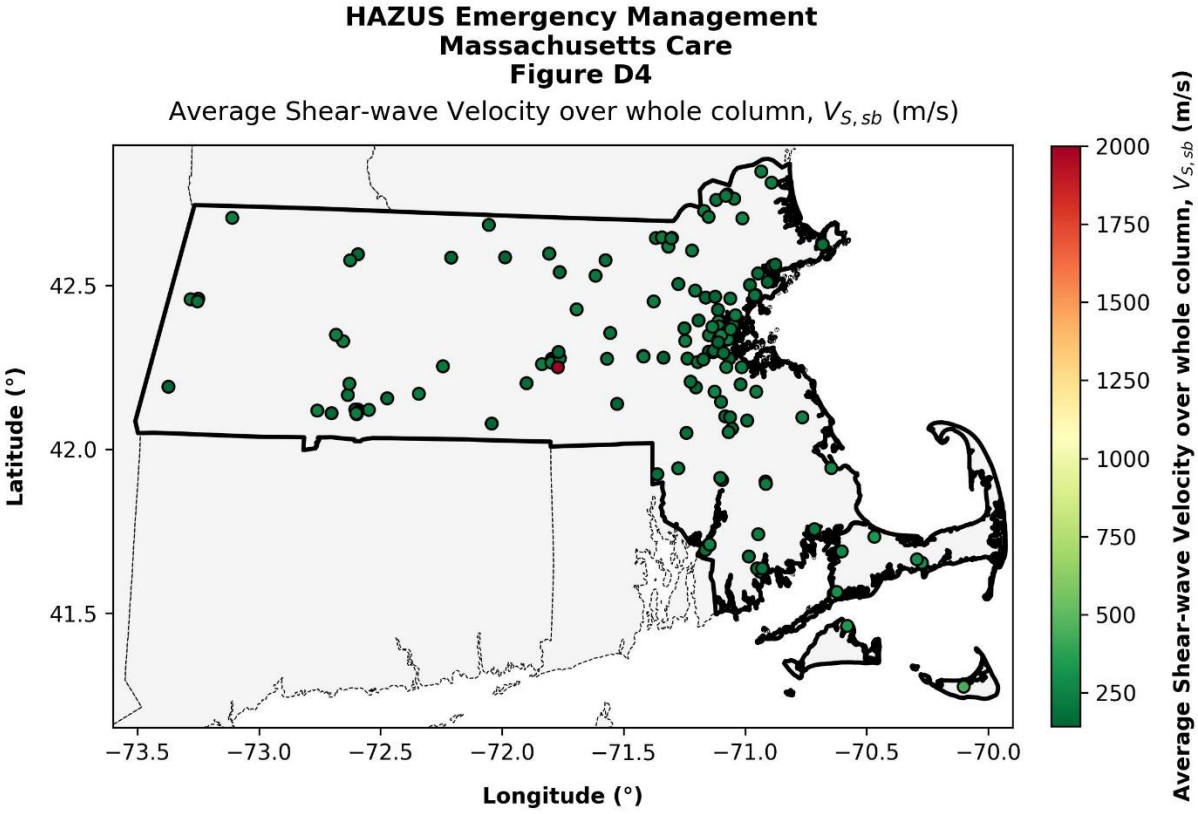
HAZUS Emergency Management
Massachusetts Care
Figure D4
Average Shear-wave Velocity over whole column, $V_{S,sb}$ (m/s)
Latitude (°)
42.5
42.0
41.5
−73.5
−73.0
−72.5
−72.0
−71.5
−71.0
−70.5
−70.0
Longitude (°)
2000
1750
1500
1250
1000
750
500
250
Average Shear-wave Velocity over whole column, $V_{S,sb}$ (m/s)

HAZUS Emergency Management
Massachusetts Care
Figure D5

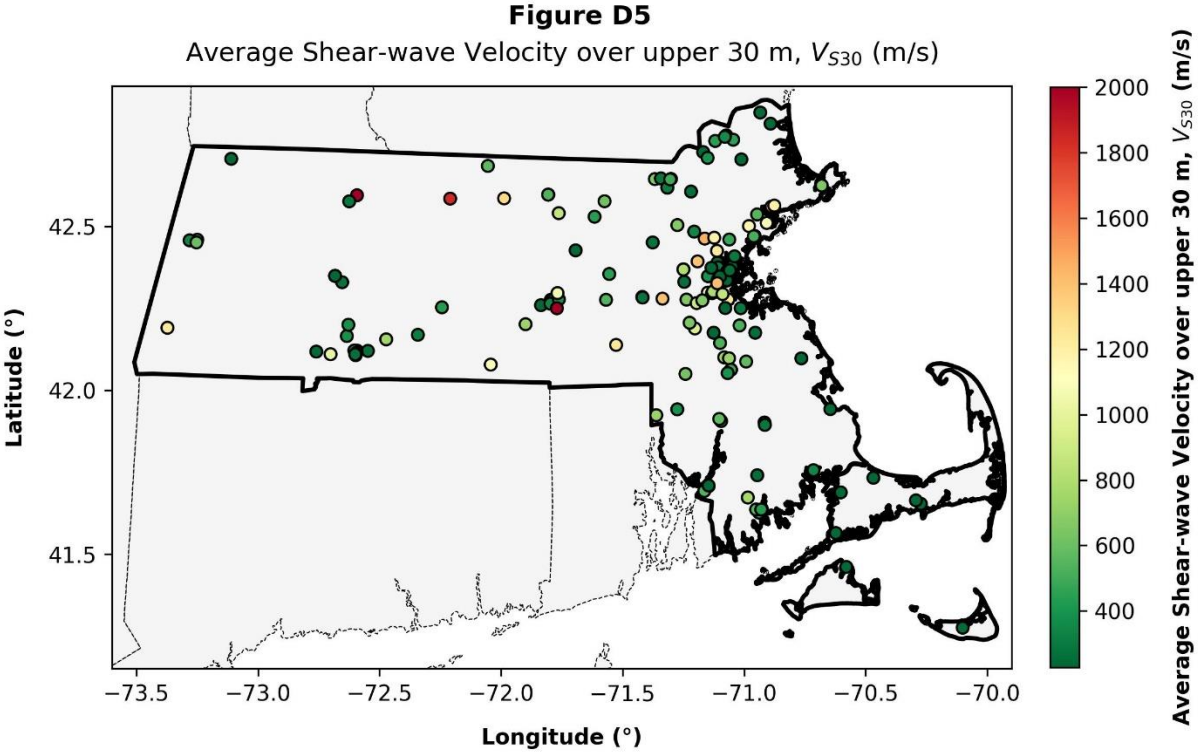

HAZUS Emergency Management
Massachusetts Care
Figure D6

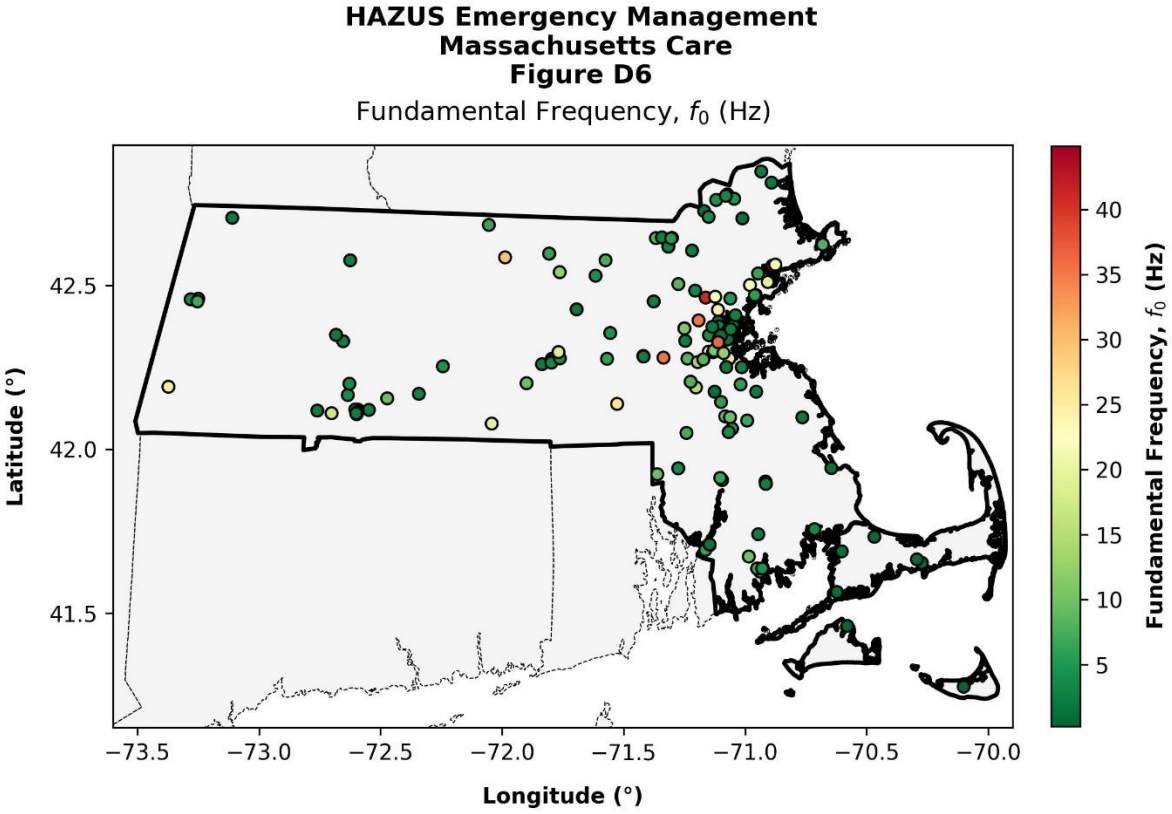

HAZUS Emergency Management
Massachusetts Care
Figure D7

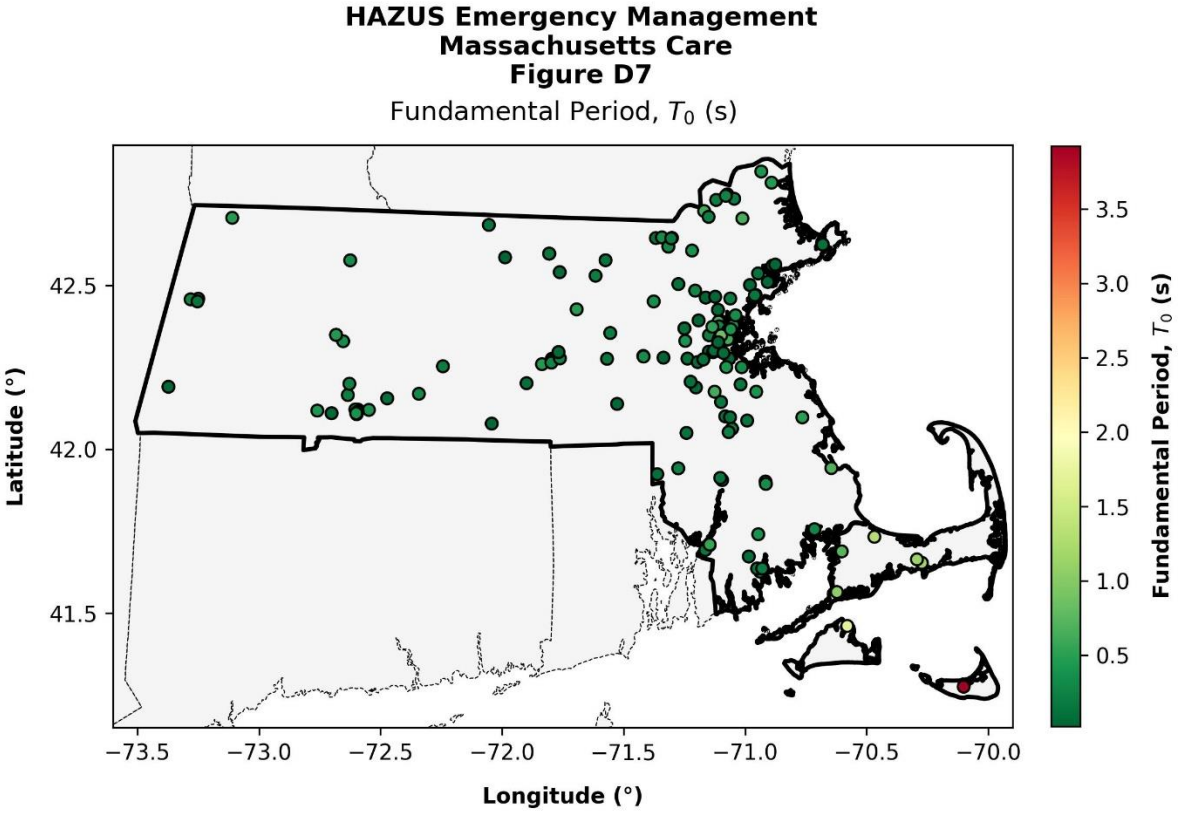

HAZUS Emergency Management
Massachusetts Care
Figure D8

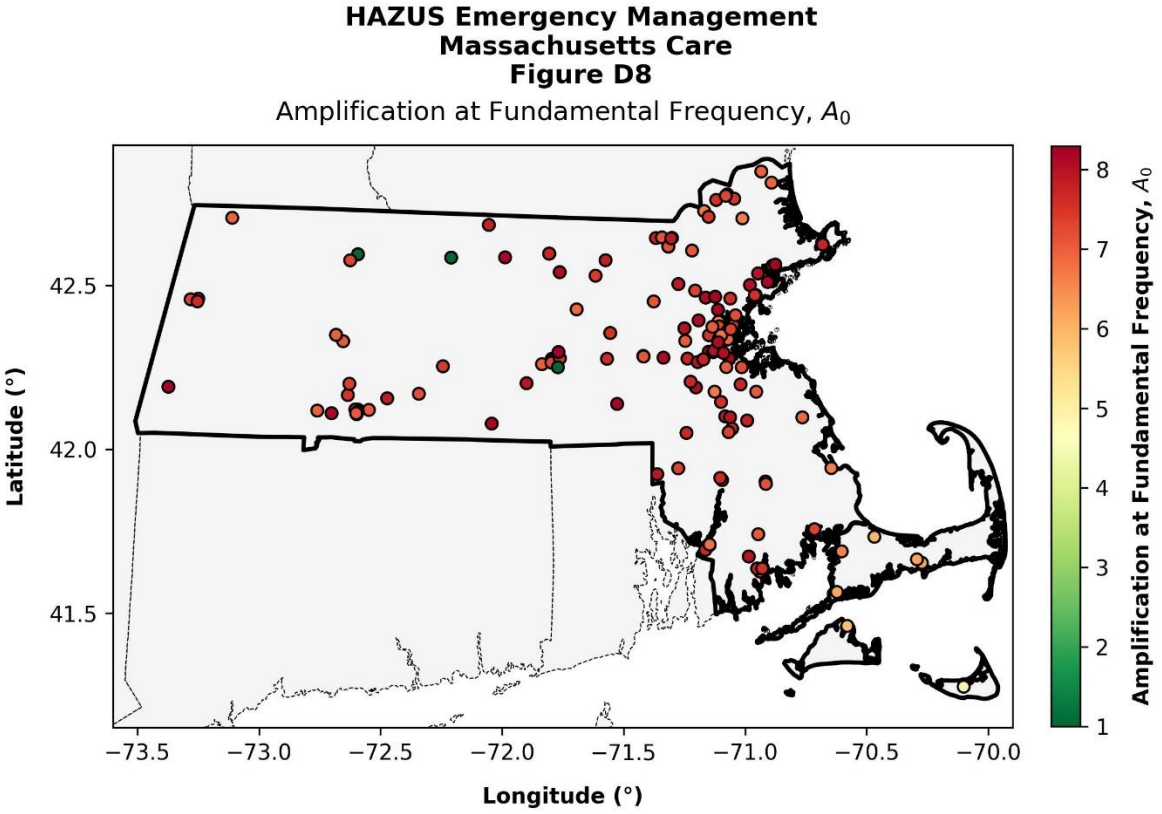

HAZUS Emergency Management
Massachusetts Care
Figure D9

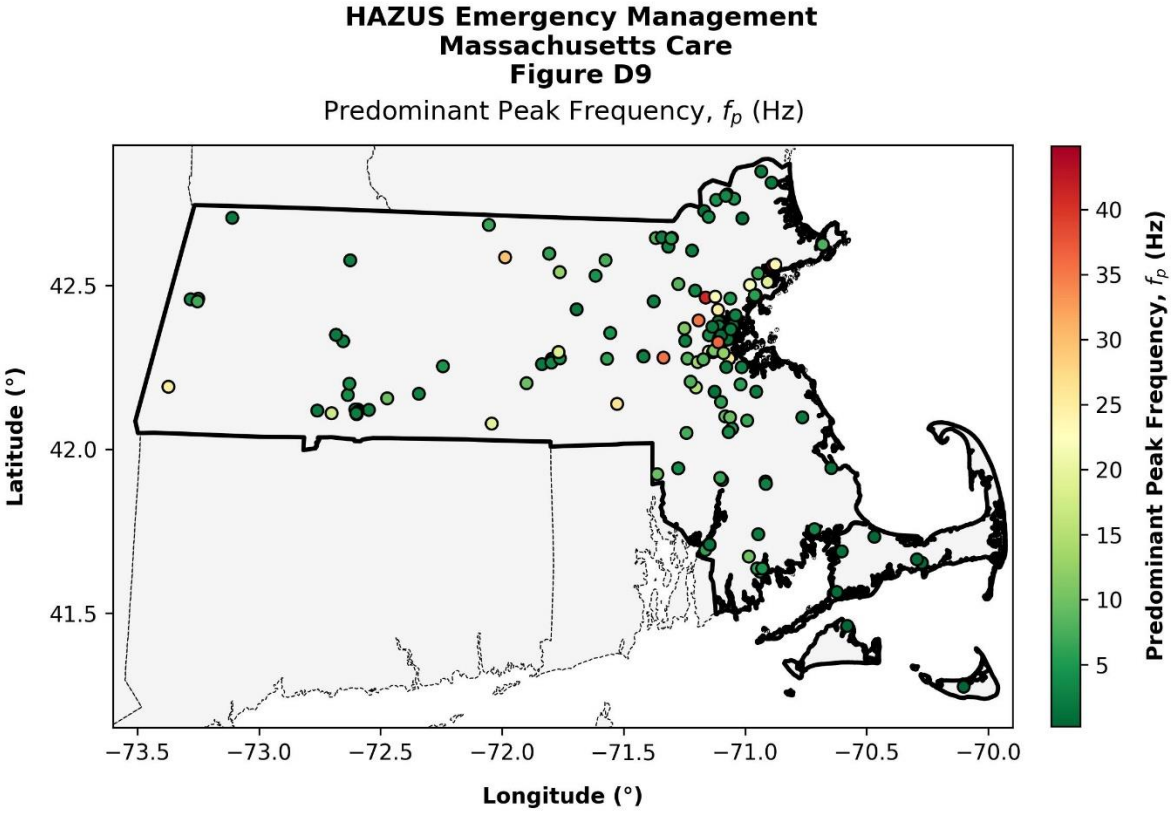

HAZUS Emergency Management
Massachusetts Care
Figure D10

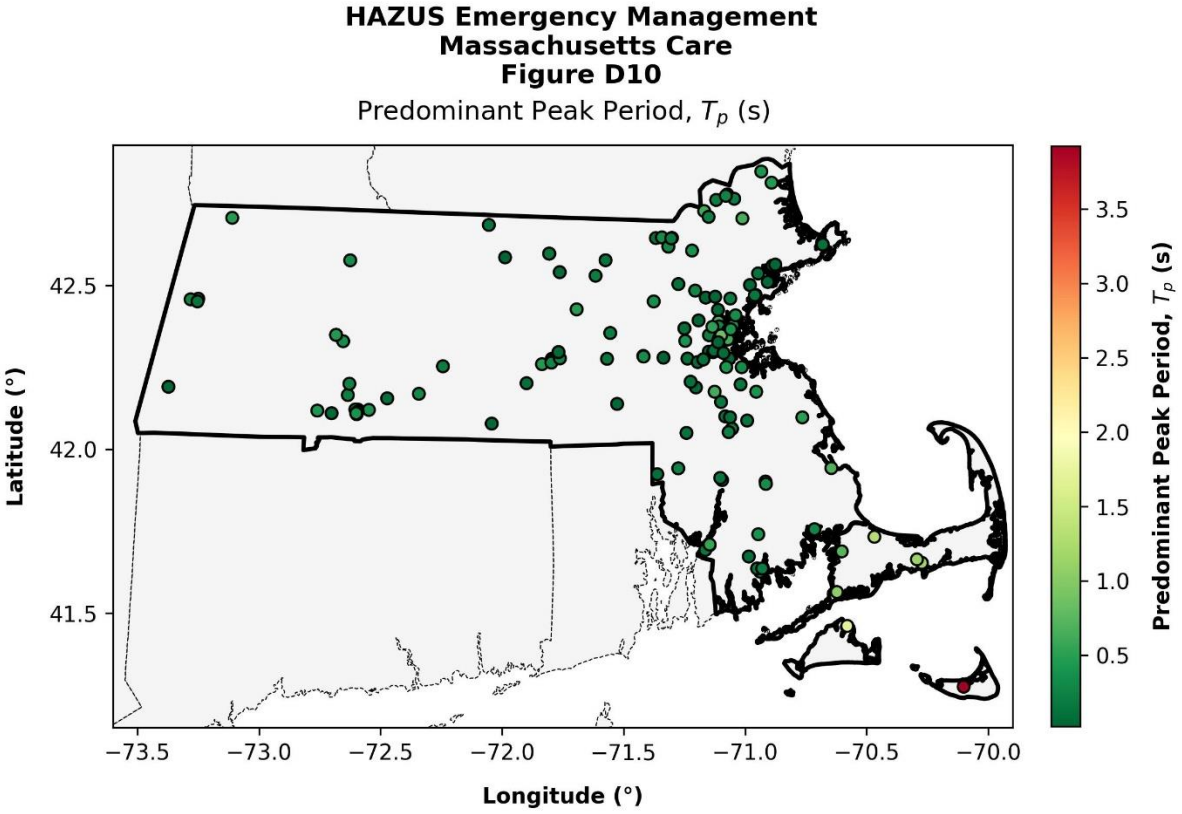

HAZUS Emergency Management
Massachusetts Care
Figure D11

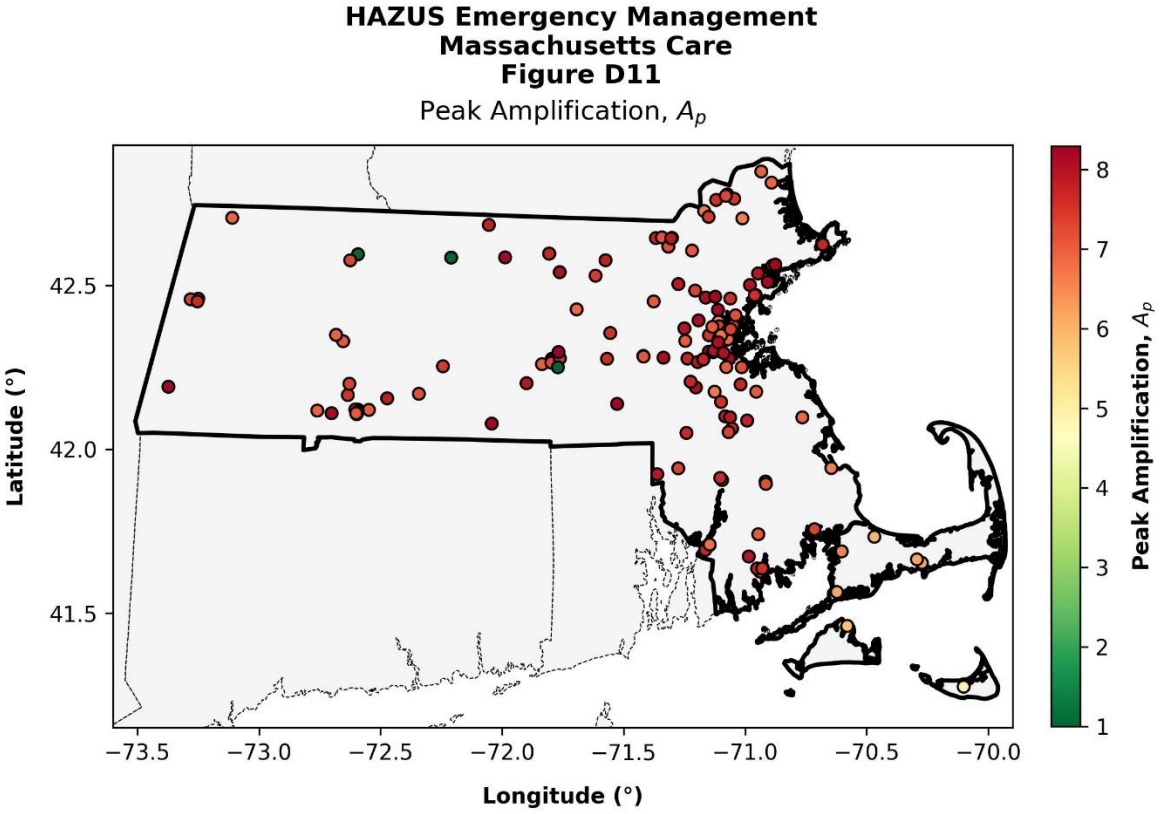

HAZUS Emergency Management
Massachusetts Care
Figure D12

Mean Short-period Amplification Ratio (0.1-0.5 s), F_a

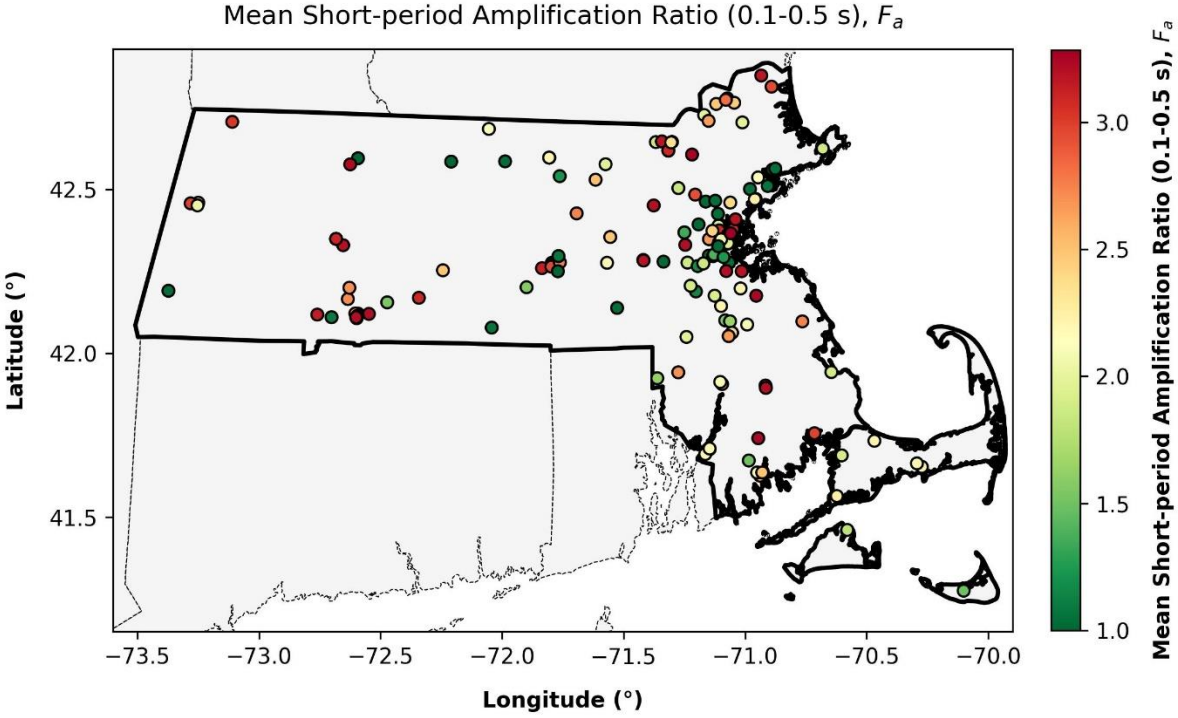

HAZUS Emergency Management
Massachusetts Care
Figure D13

Mean Intermediate-period Amplification Ratio (0.5-1.5 s), F_v

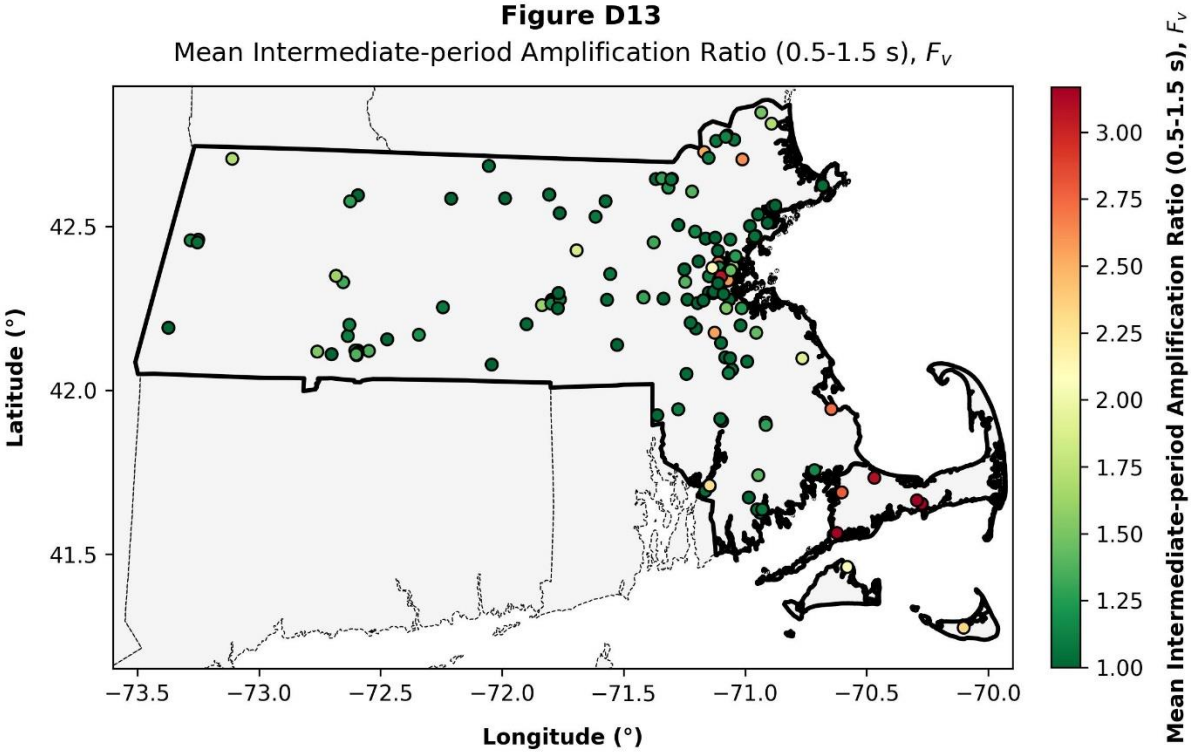

Appendix E: Linear SH1D Transfer Function Plots – GBS Care Facilities

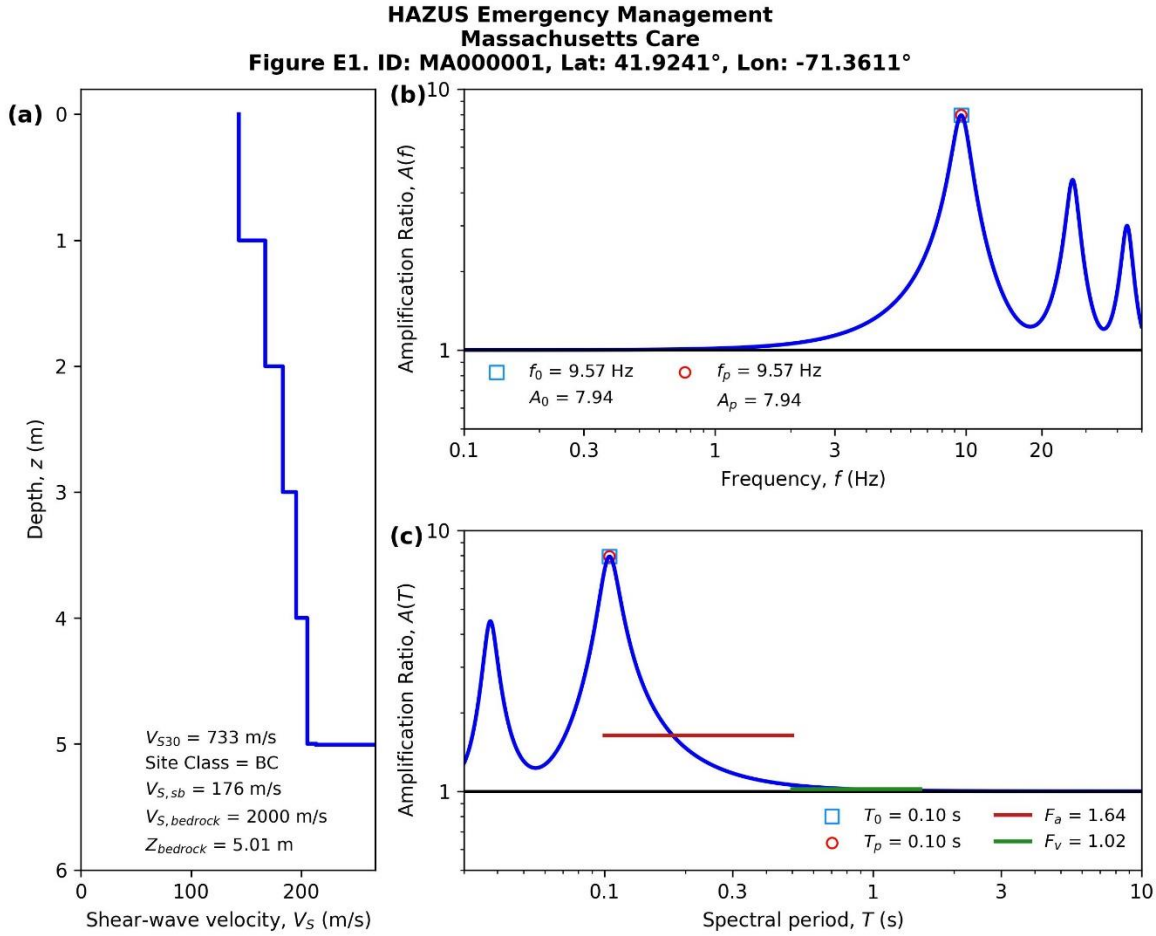

HAZUS Emergency Management
Massachusetts Care
Figure E2. ID: MA000002, Lat: 42.3508°, Lon: -71.1212°

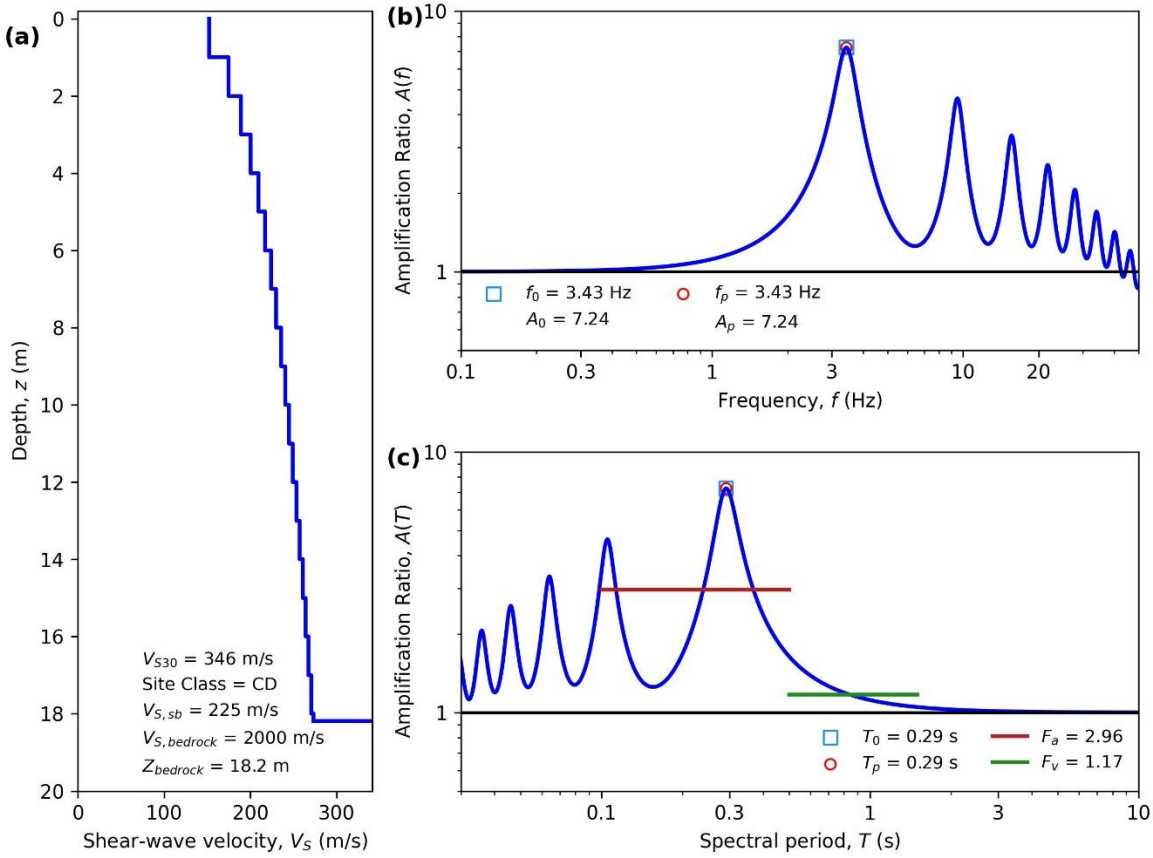

HAZUS Emergency Management
Massachusetts Care
Figure E3. ID: MA000003, Lat: 42.3631°, Lon: -71.0663°

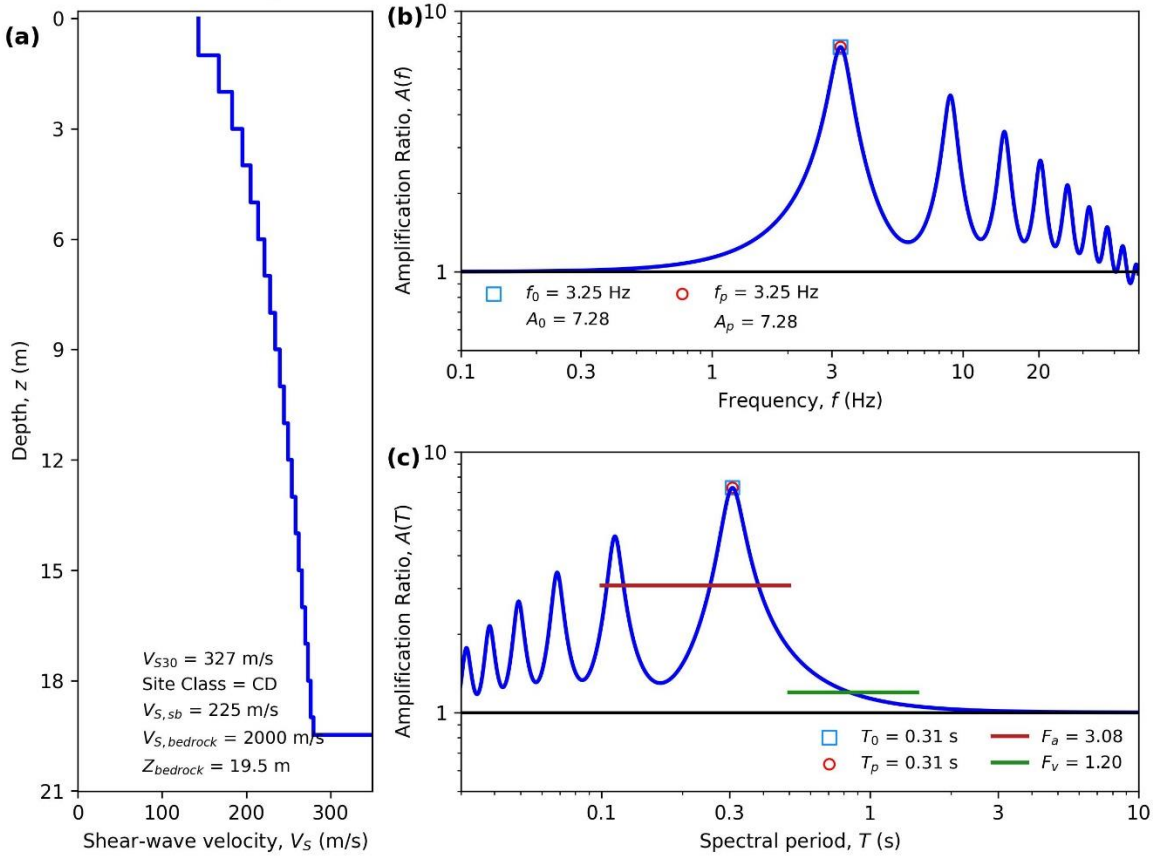

HAZUS Emergency Management
Massachusetts Care
Figure E4. ID: MA000004, Lat: 42.3785°, Lon: -71.0491°

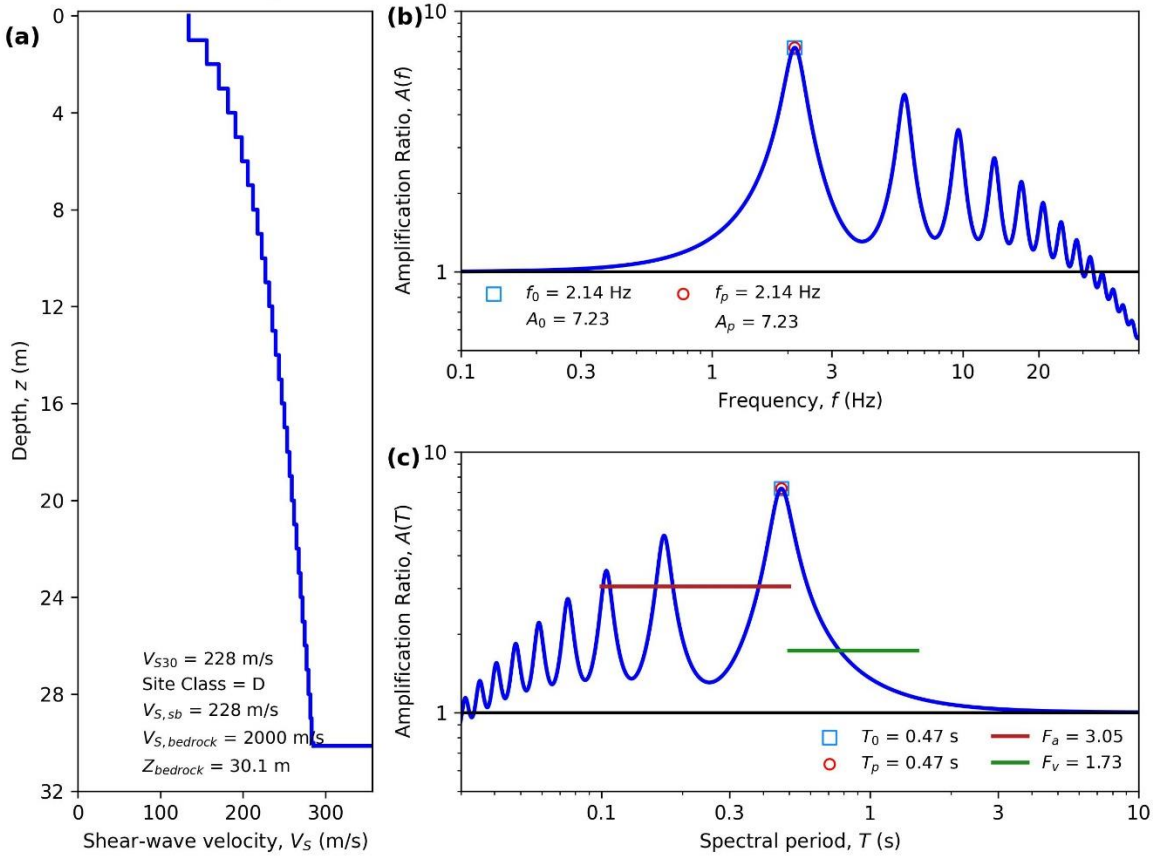

HAZUS Emergency Management
Massachusetts Care
Figure E5. ID: MA000005, Lat: 41.7075°, Lon: -71.1457°

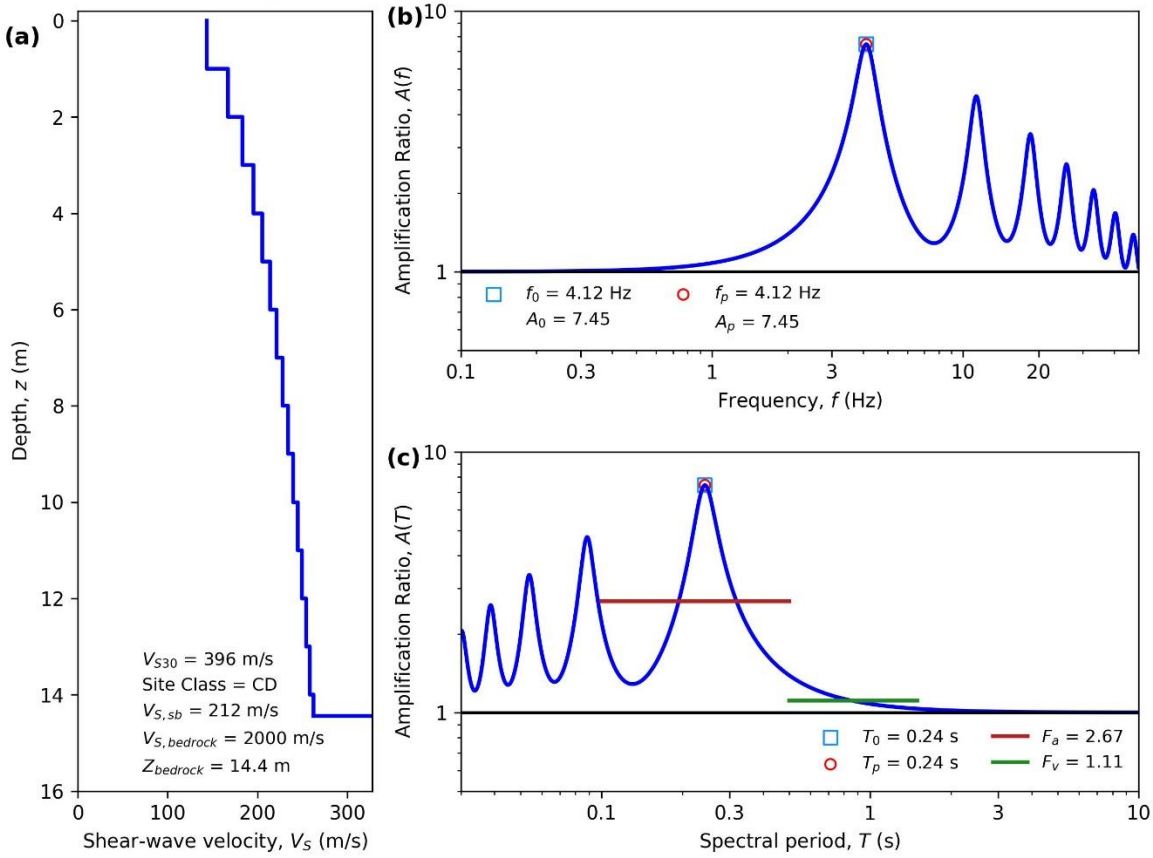

HAZUS Emergency Management
Massachusetts Care
Figure E6. ID: MA000006, Lat: 42.4716°, Lon: -70.9568°

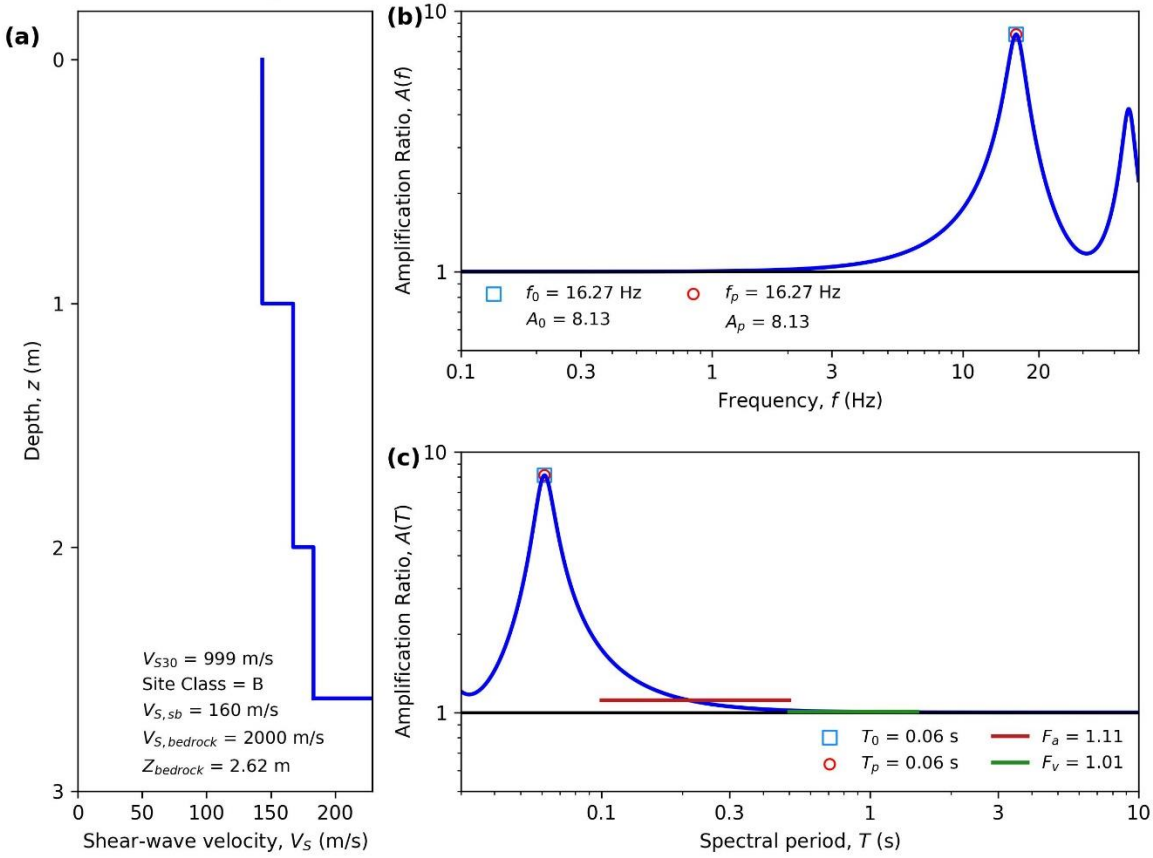

HAZUS Emergency Management
Massachusetts Care
Figure E7. ID: MA000007, Lat: 42.1558°, Lon: -72.4721°

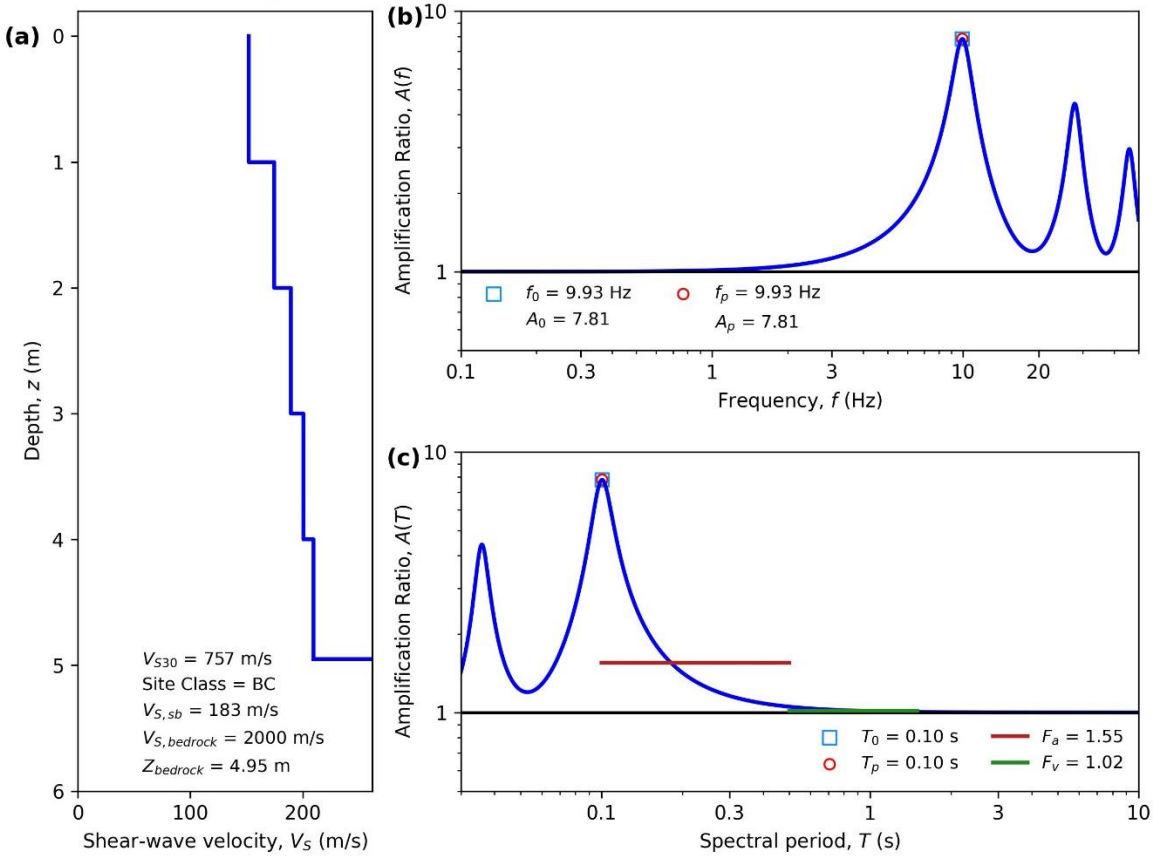

HAZUS Emergency Management
Massachusetts Care
Figure E8. ID: MA000008, Lat: 42.2771°, Lon: -71.2369°

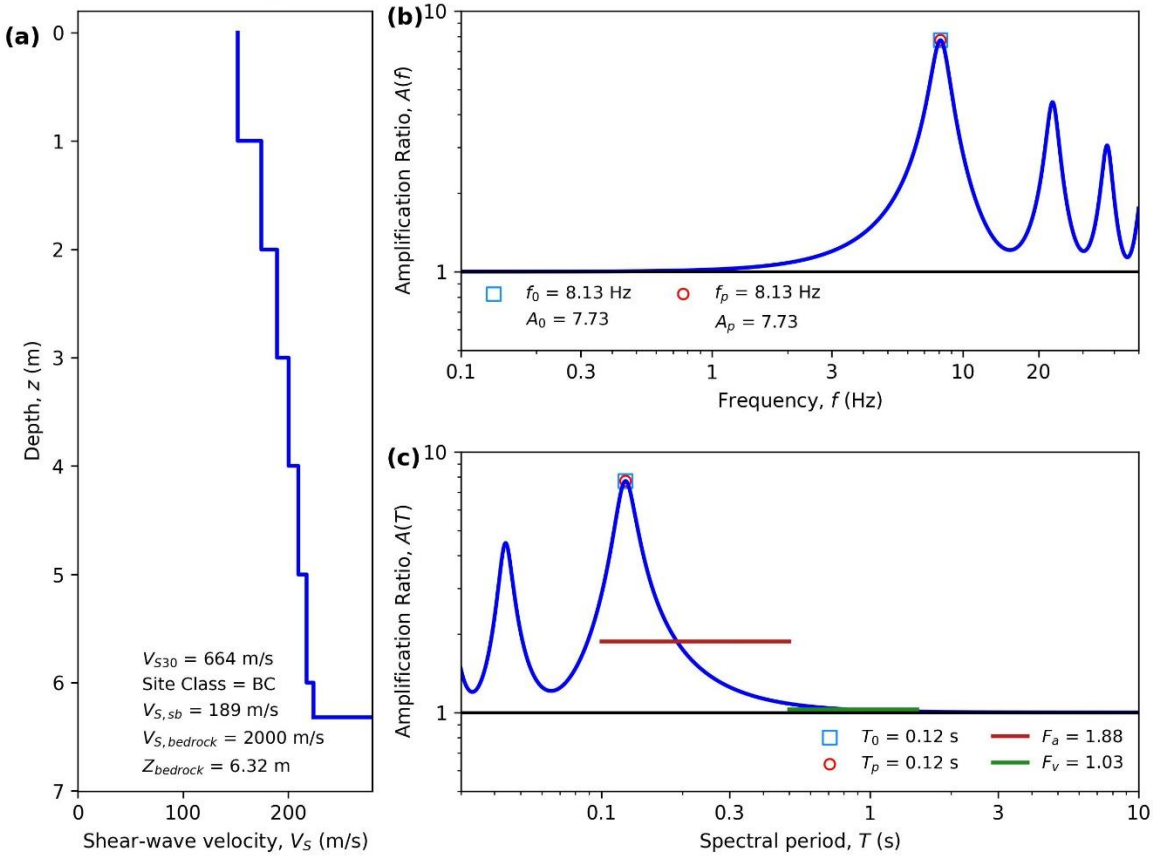

HAZUS Emergency Management
Massachusetts Care
Figure E9. ID: MA000009, Lat: 41.7407°, Lon: -70.9458°

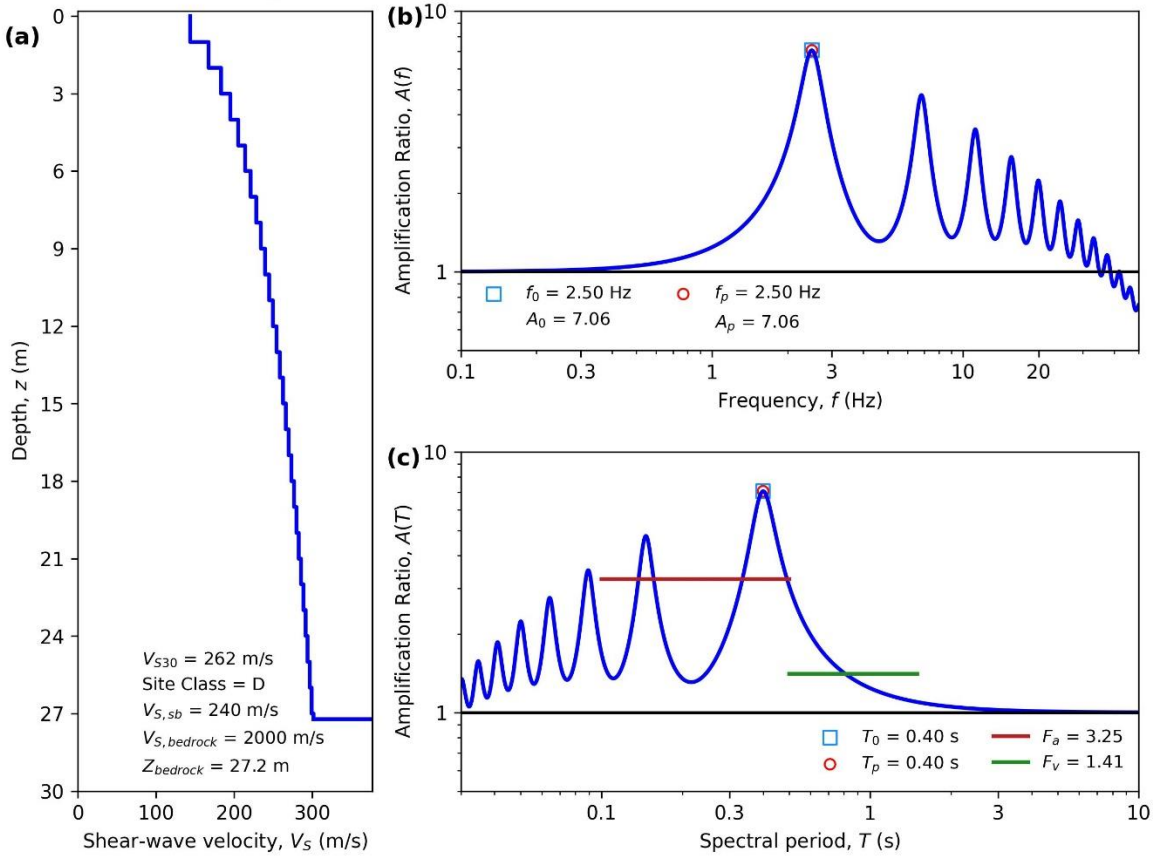

HAZUS Emergency Management
Massachusetts Care
Figure E10. ID: MA000010, Lat: 42.1890°, Lon: -71.2021°

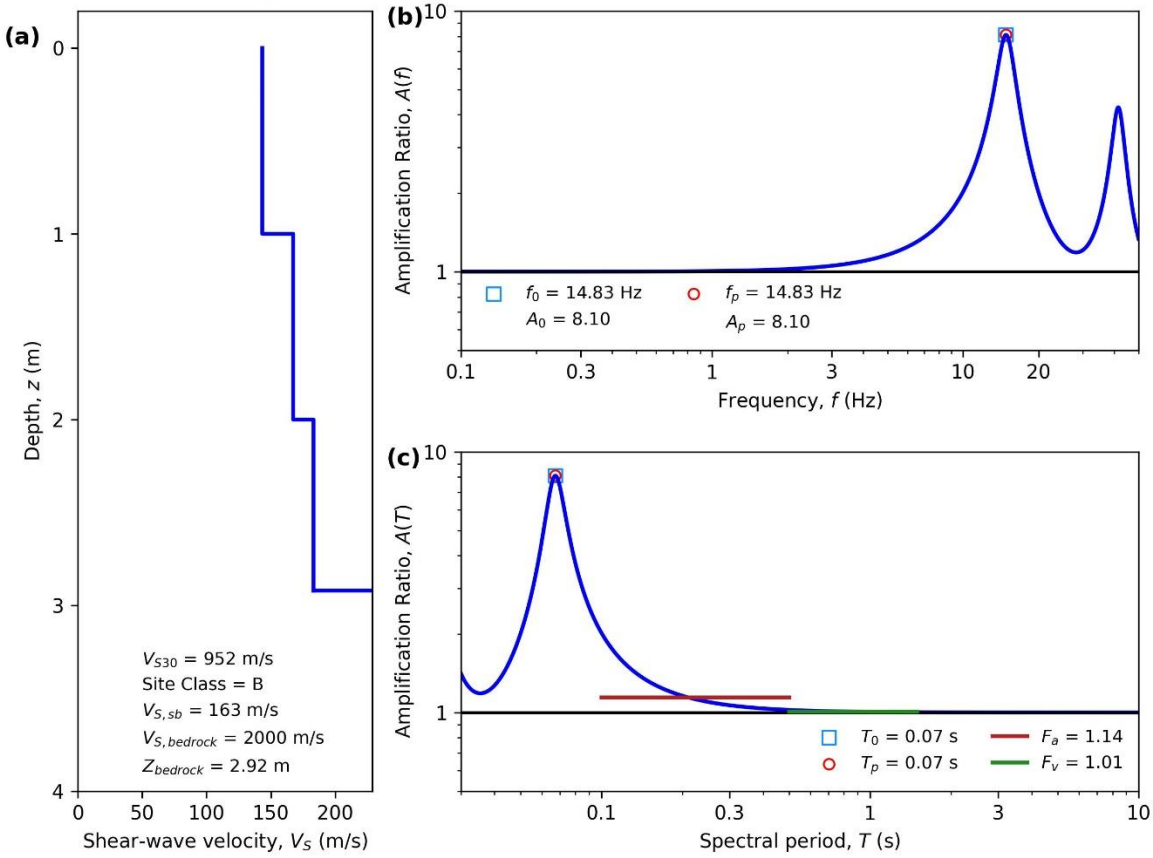

HAZUS Emergency Management
Massachusetts Care
Figure E11. ID: MA000011, Lat: 41.7330°, Lon: -70.4681°

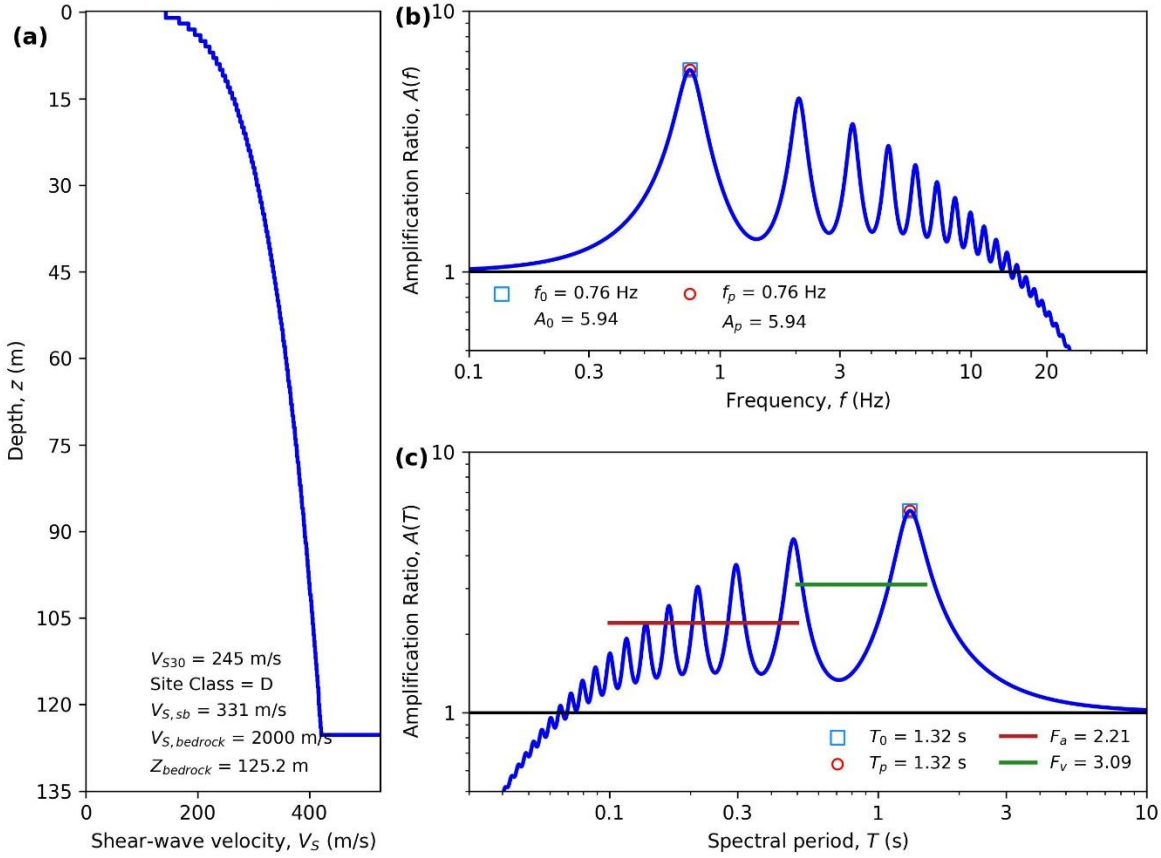

HAZUS Emergency Management
Massachusetts Care
Figure E12. ID: MA000012, Lat: 42.3900°, Lon: -71.1094°

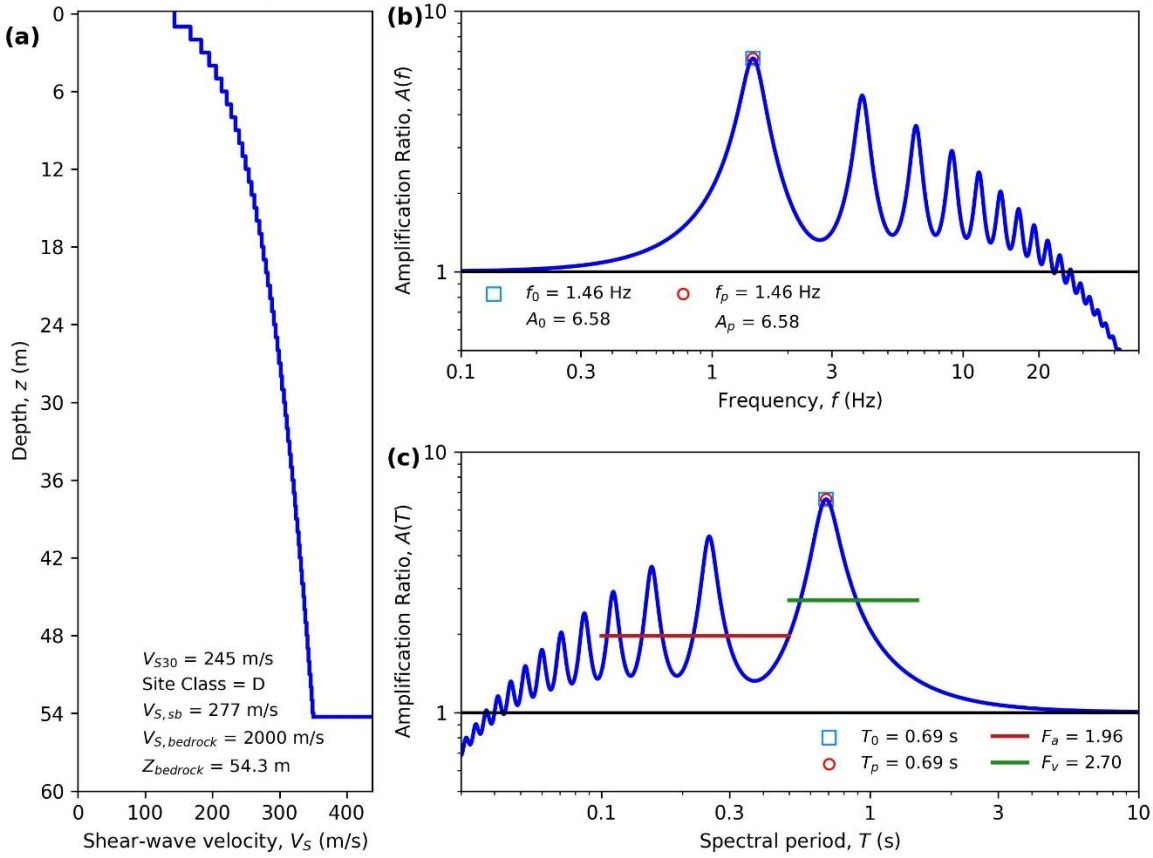

HAZUS Emergency Management
Massachusetts Care
Figure E13. ID: MA000013, Lat: 42.1213°, Lon: -72.5924°

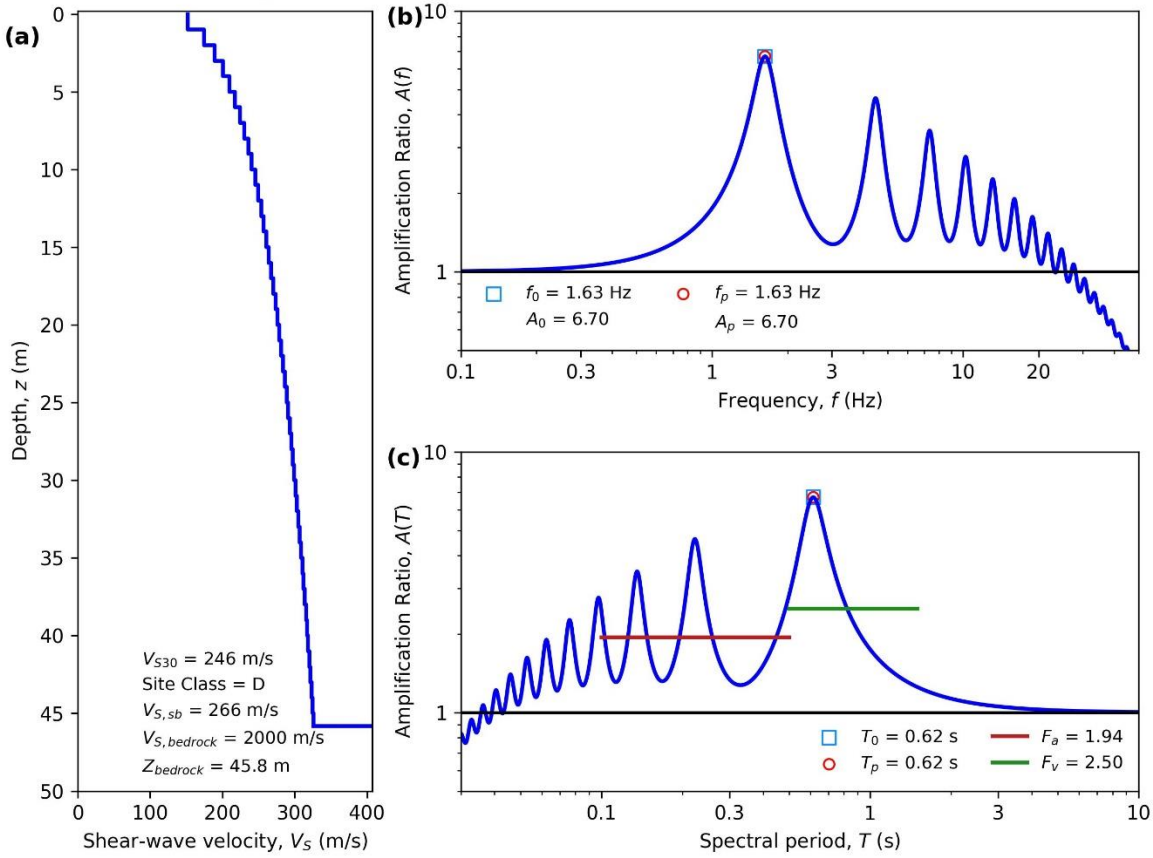

HAZUS Emergency Management
Massachusetts Care
Figure E14. ID: MA000014, Lat: 42.2764°, Lon: -71.7949°

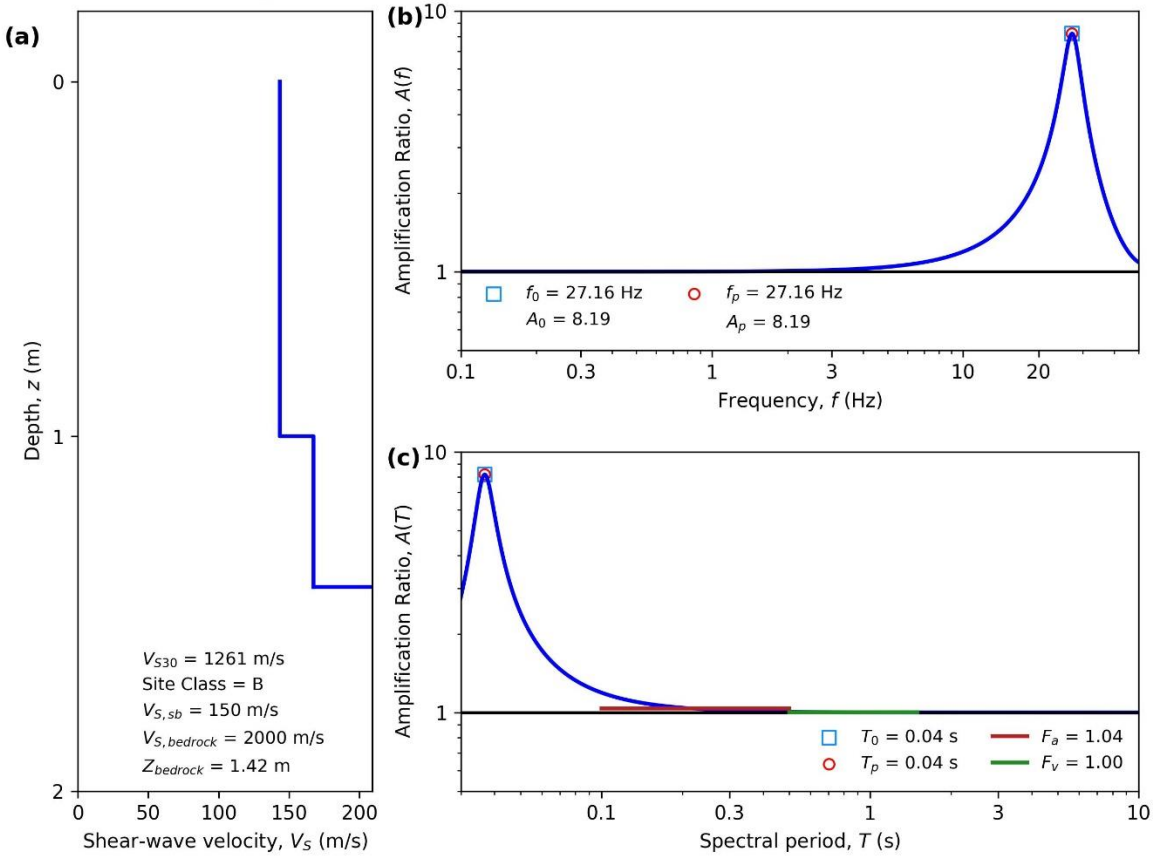

HAZUS Emergency Management
Massachusetts Care
Figure E15. ID: MA000015, Lat: 42.5047°, Lon: -71.2744°

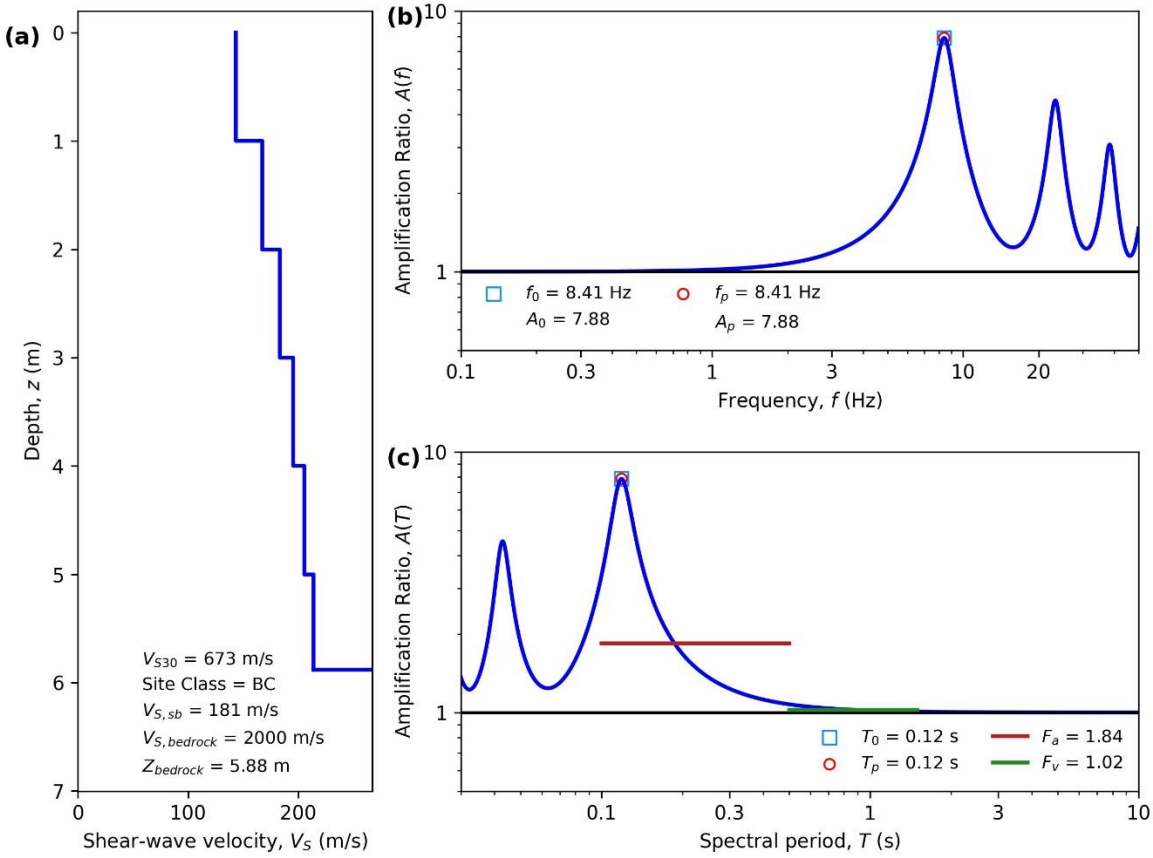

HAZUS Emergency Management
Massachusetts Care
Figure E16. ID: MA000016, Lat: 42.8484°, Lon: -70.9334°

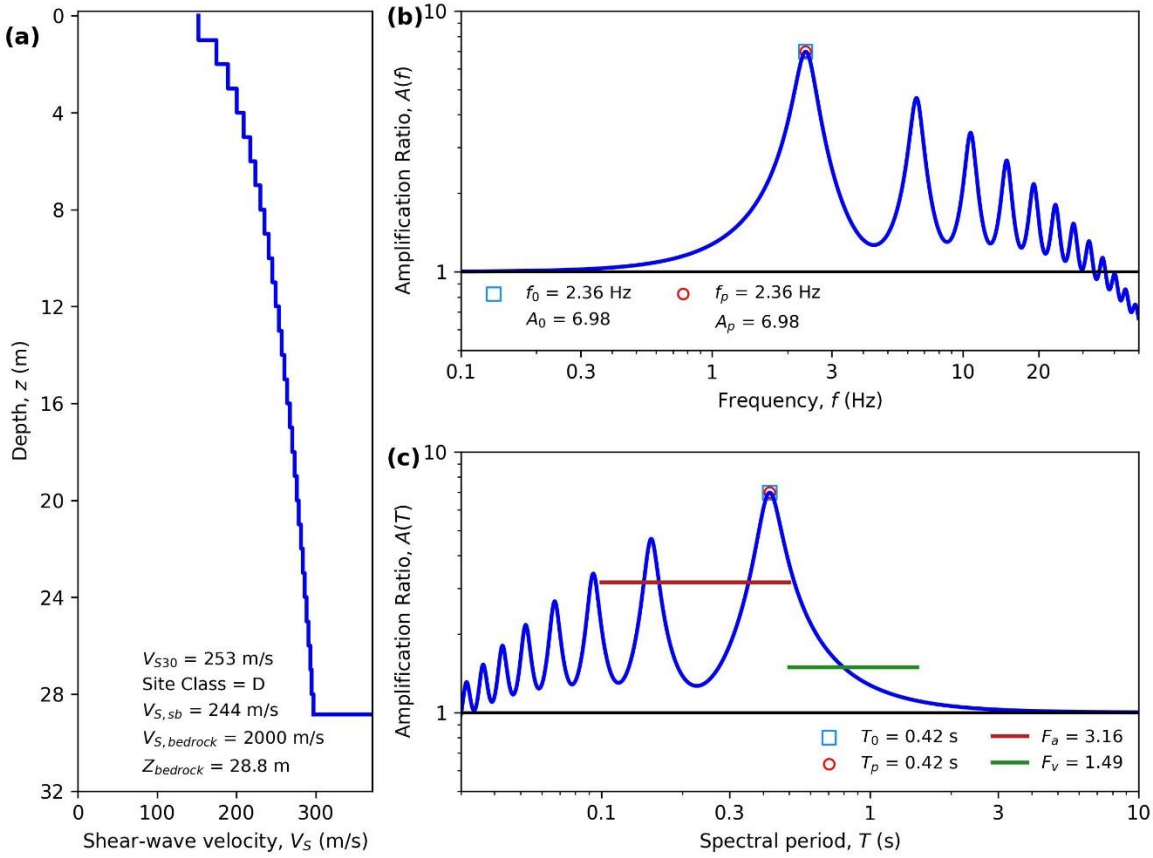

HAZUS Emergency Management
Massachusetts Care
Figure E17. ID: MA000017, Lat: 42.3379°, Lon: -71.1092°

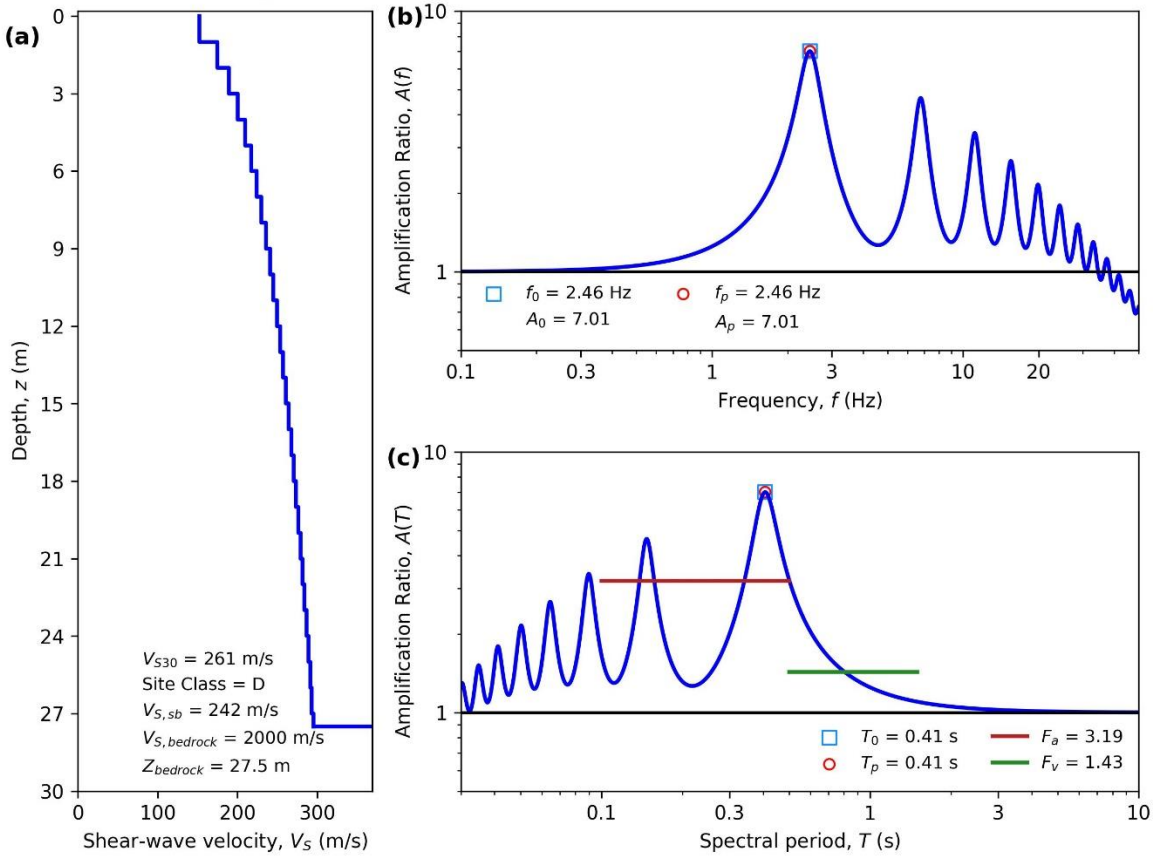

HAZUS Emergency Management
Massachusetts Care
Figure E18. ID: MA000018, Lat: 42.3158°, Lon: -71.1123°

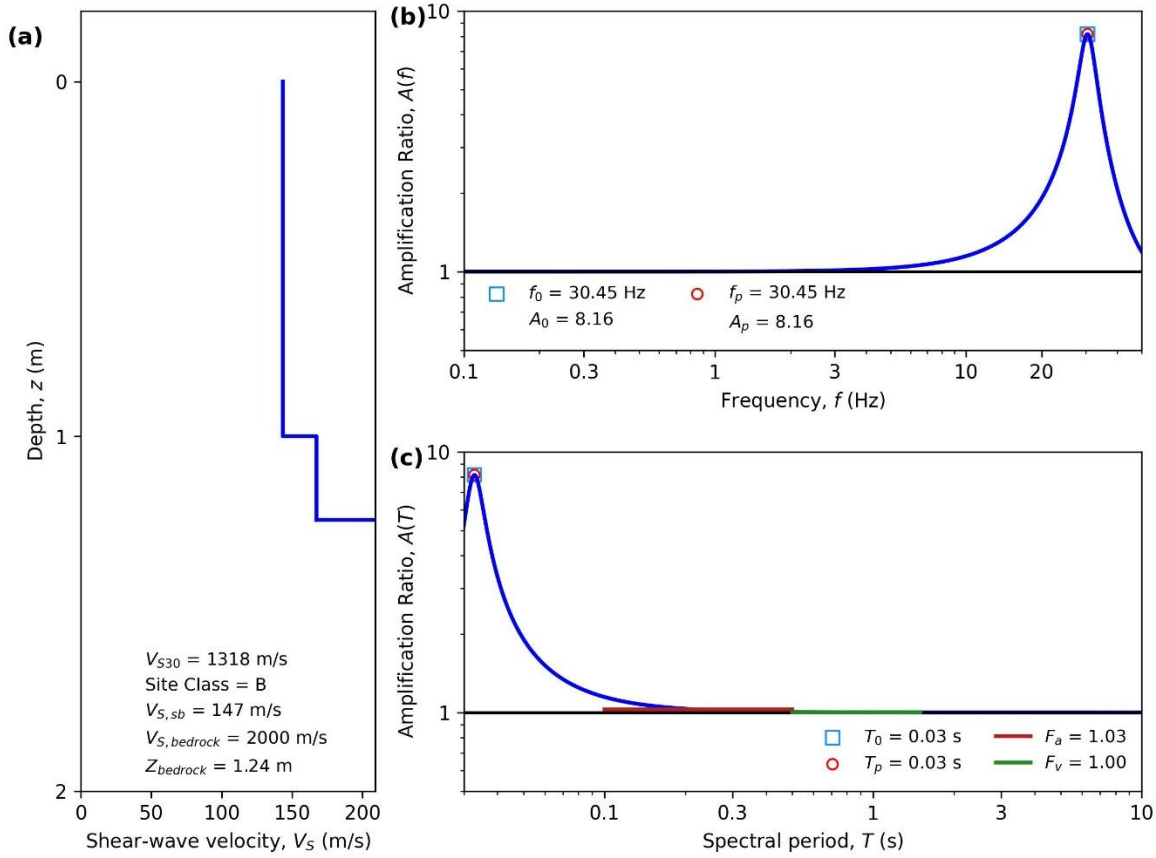

HAZUS Emergency Management
Massachusetts Care
Figure E19. ID: MA000019, Lat: 42.6255°, Lon: -70.6806°

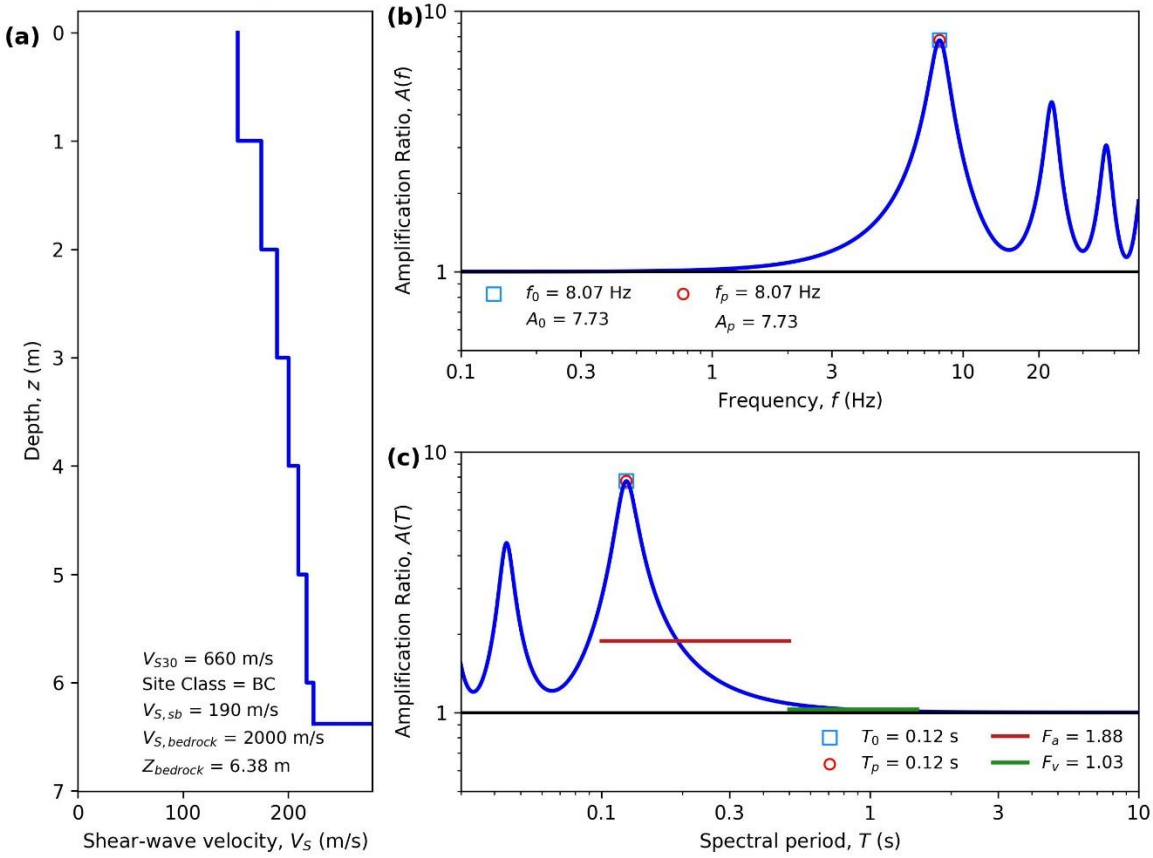

HAZUS Emergency Management
Massachusetts Care
Figure E20. ID: MA000020, Lat: 42.2019°, Lon: -71.8988°

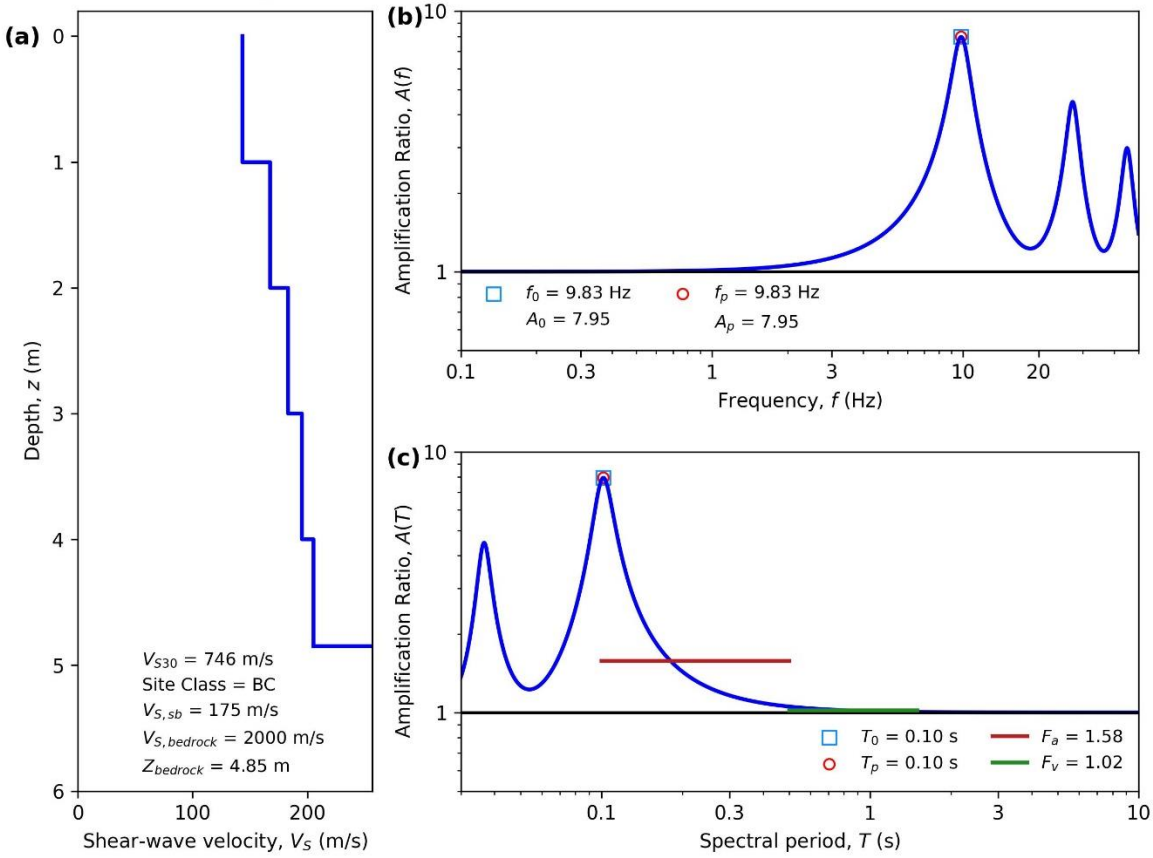

HAZUS Emergency Management
Massachusetts Care
Figure E21. ID: MA000021, Lat: 42.2797°, Lon: -71.7691°

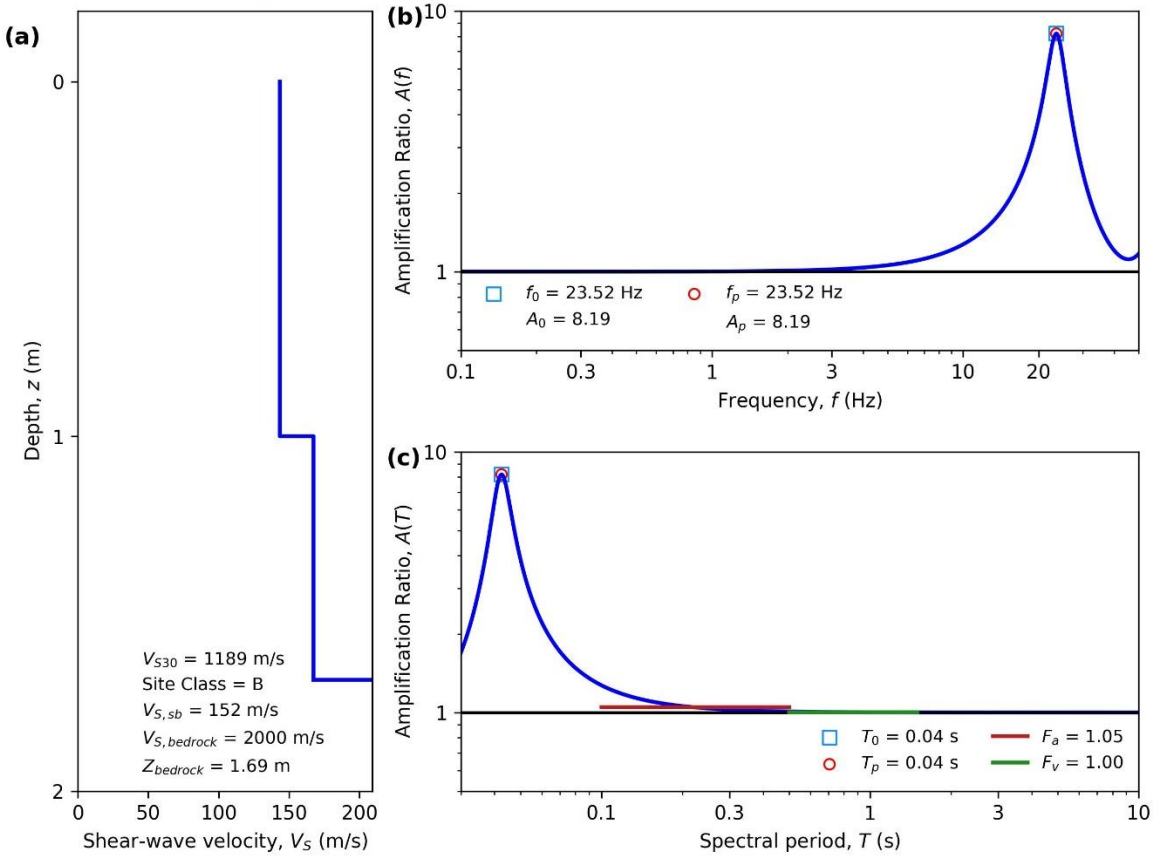

HAZUS Emergency Management
Massachusetts Care
Figure E22. ID: MA000022, Lat: 42.2983°, Lon: -71.1493°

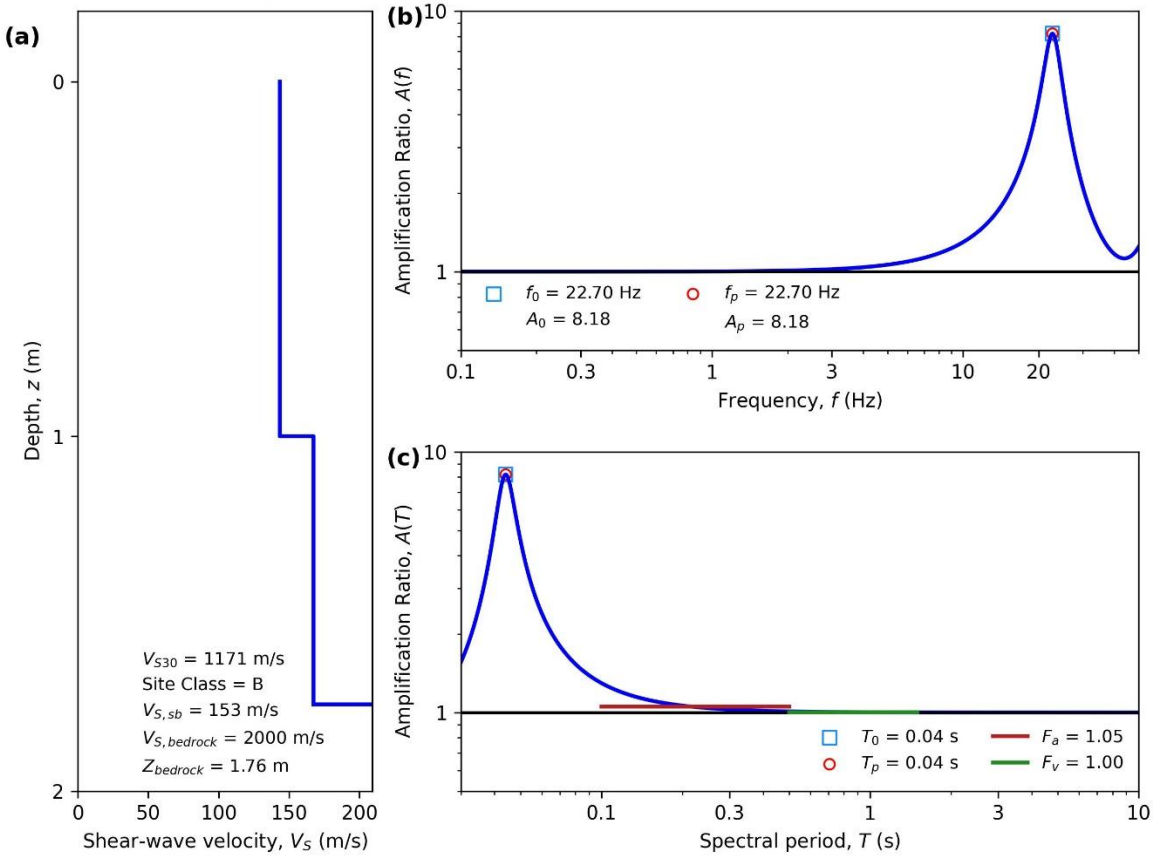

HAZUS Emergency Management
Massachusetts Care
Figure E23. ID: MA000023, Lat: 42.2968°, Lon: -71.1318°

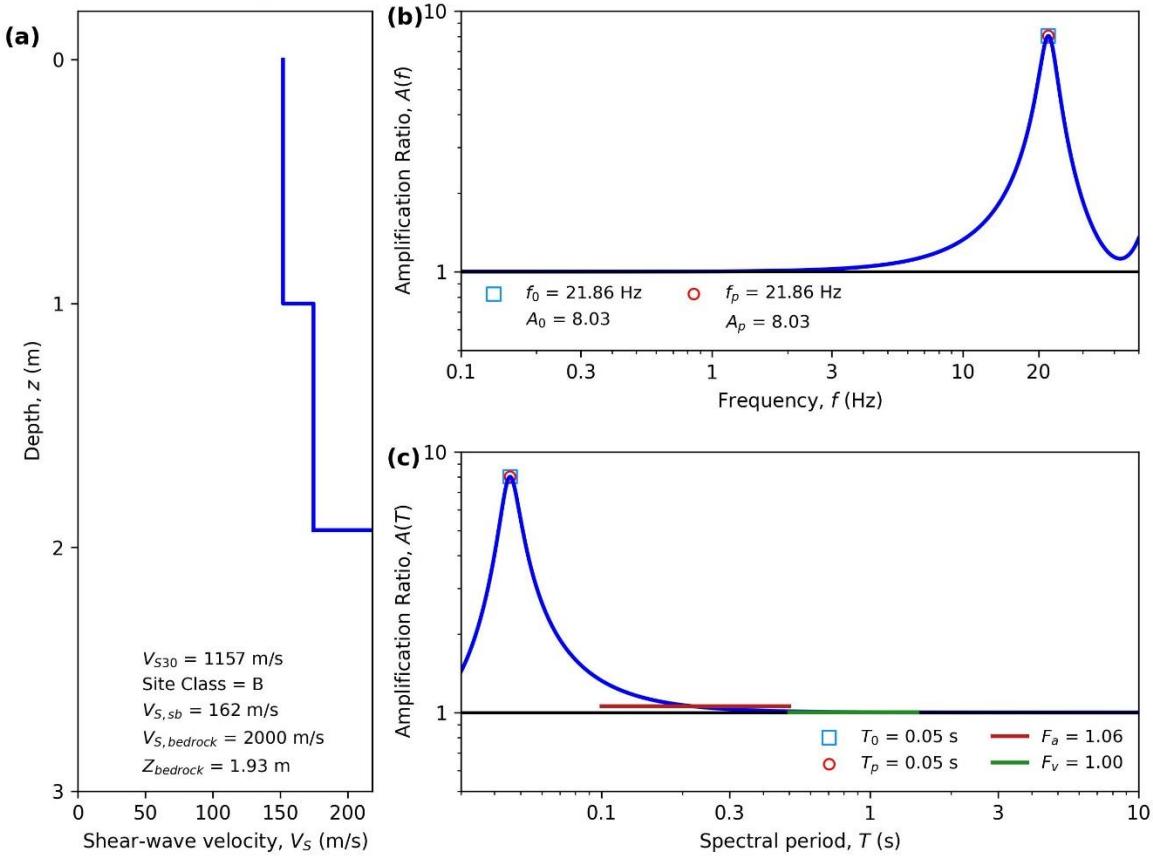

HAZUS Emergency Management
Massachusetts Care
Figure E24. ID: MA000024, Lat: 42.2996°, Lon: -71.1017°

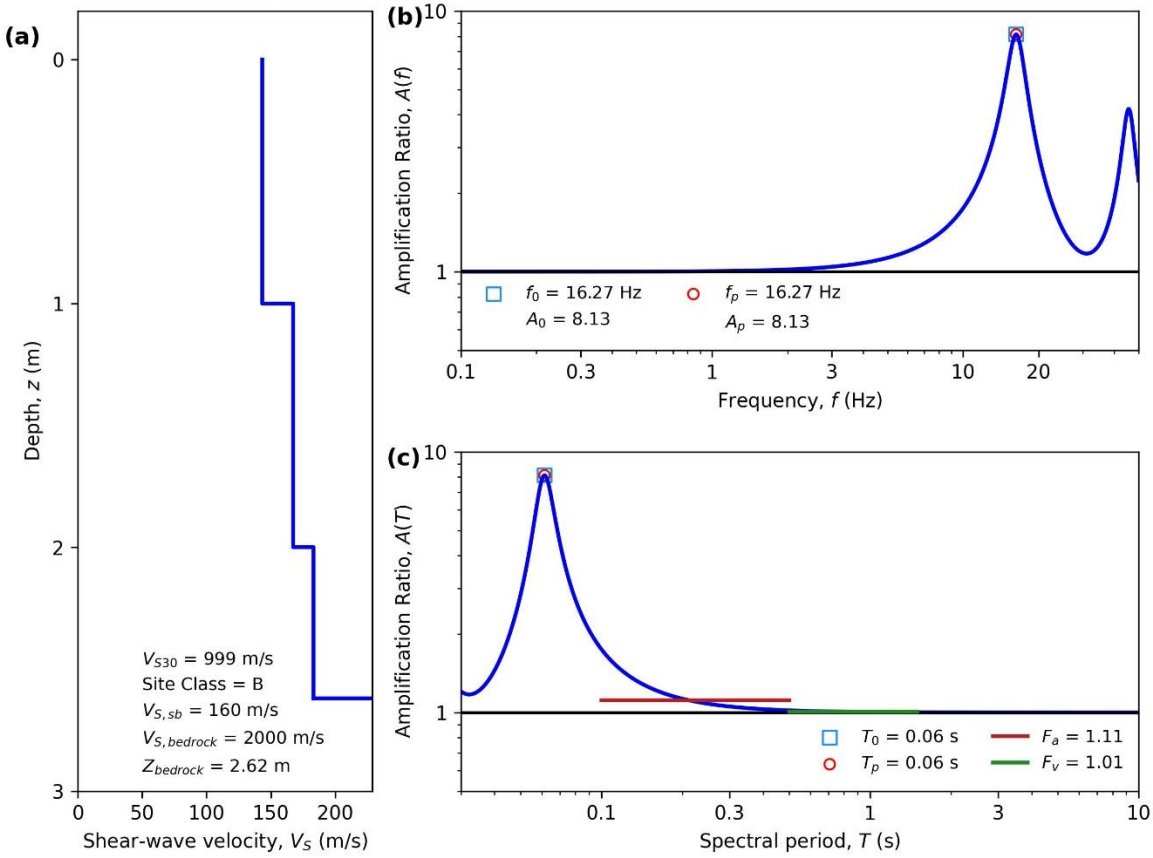

HAZUS Emergency Management
Massachusetts Care
Figure E25. ID: MA000025, Lat: 42.2665°, Lon: -71.1950°

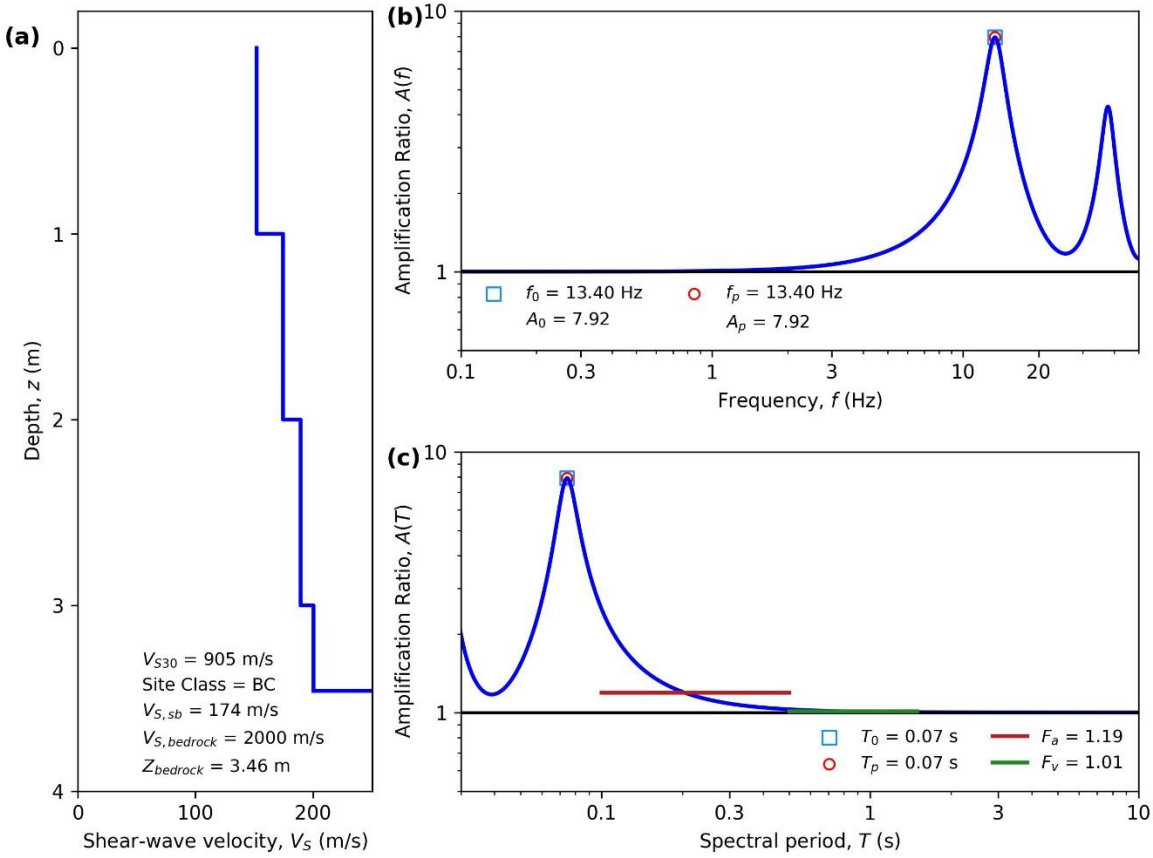

HAZUS Emergency Management
Massachusetts Care
Figure E26. ID: MA000026, Lat: 42.0976°, Lon: -70.7645°

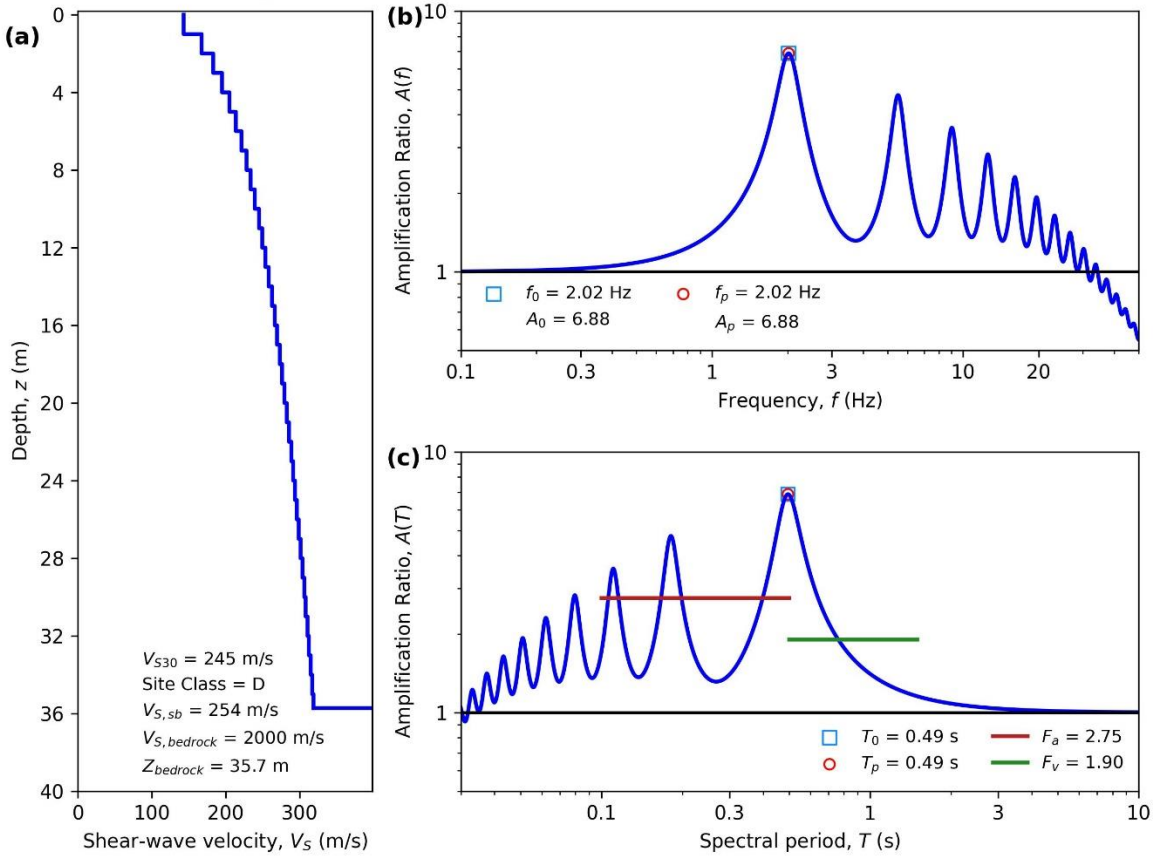

HAZUS Emergency Management
Massachusetts Care
Figure E27. ID: MA000027, Lat: 42.3696°, Lon: -71.2493°

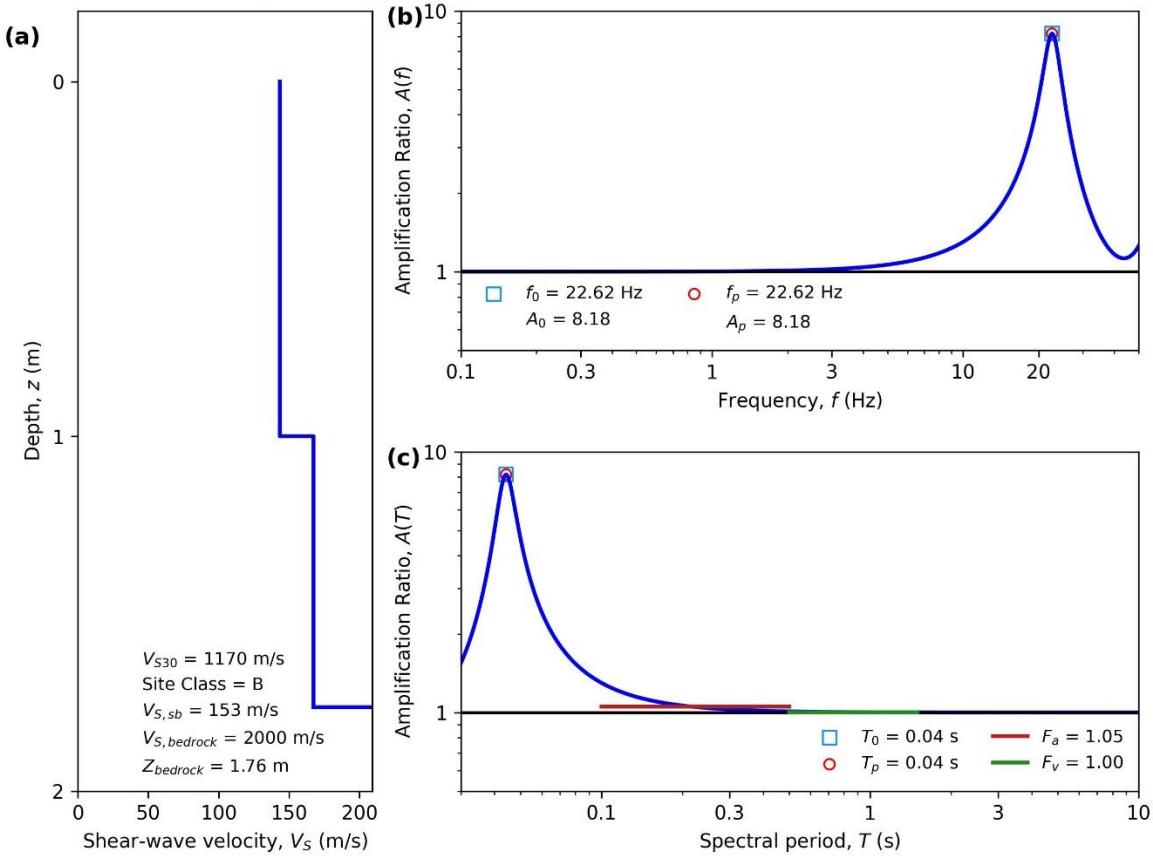

HAZUS Emergency Management
Massachusetts Care
Figure E28. ID: MA000028, Lat: 42.1446°, Lon: -71.0988°

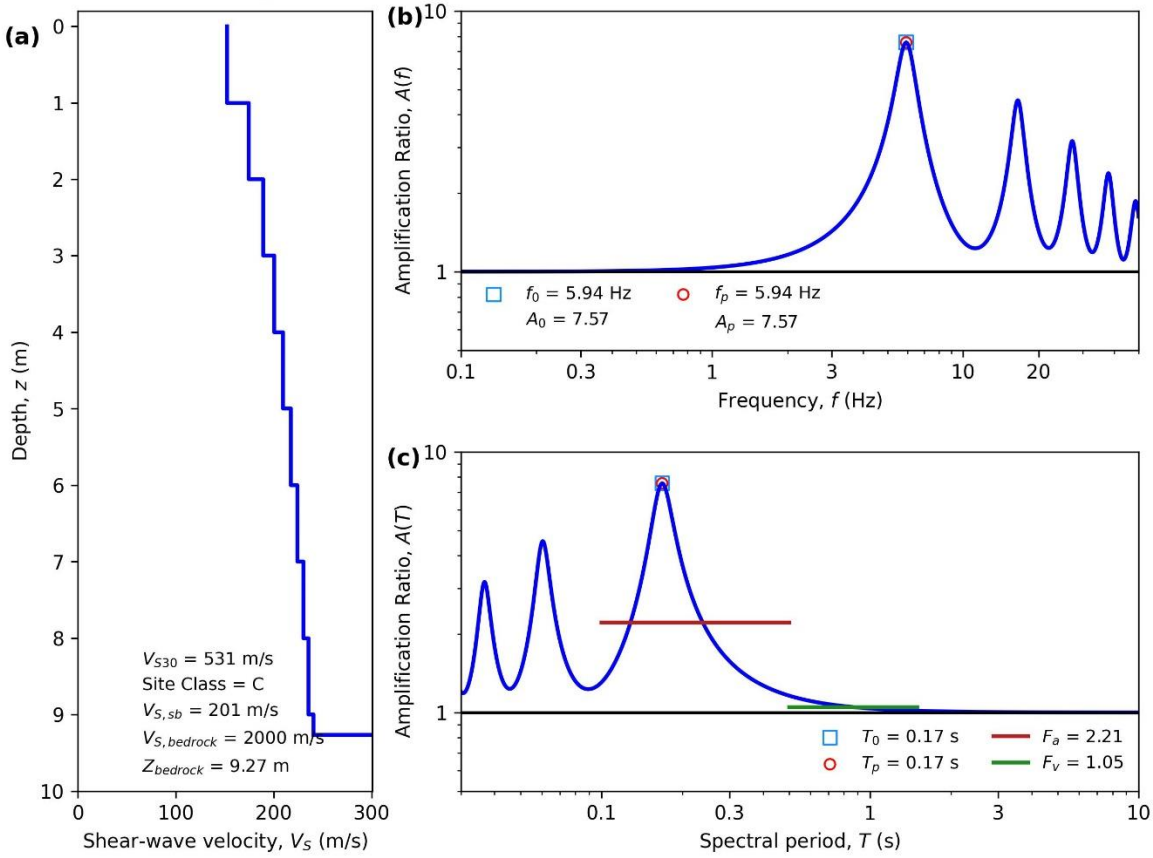

HAZUS Emergency Management
Massachusetts Care
Figure E29. ID: MA000029, Lat: 41.4608°, Lon: -70.5798°

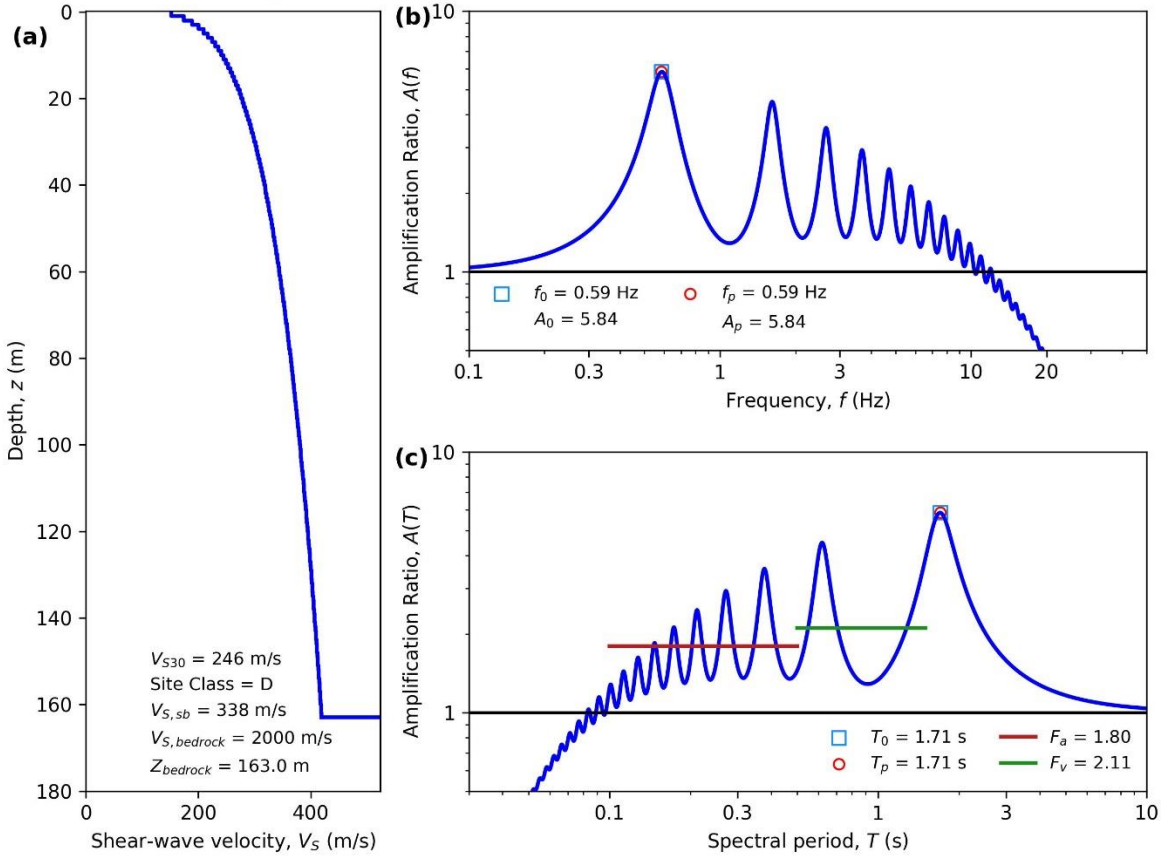

HAZUS Emergency Management
Massachusetts Care
Figure E30. ID: MA000030, Lat: 41.6264°, Lon: -70.9384°

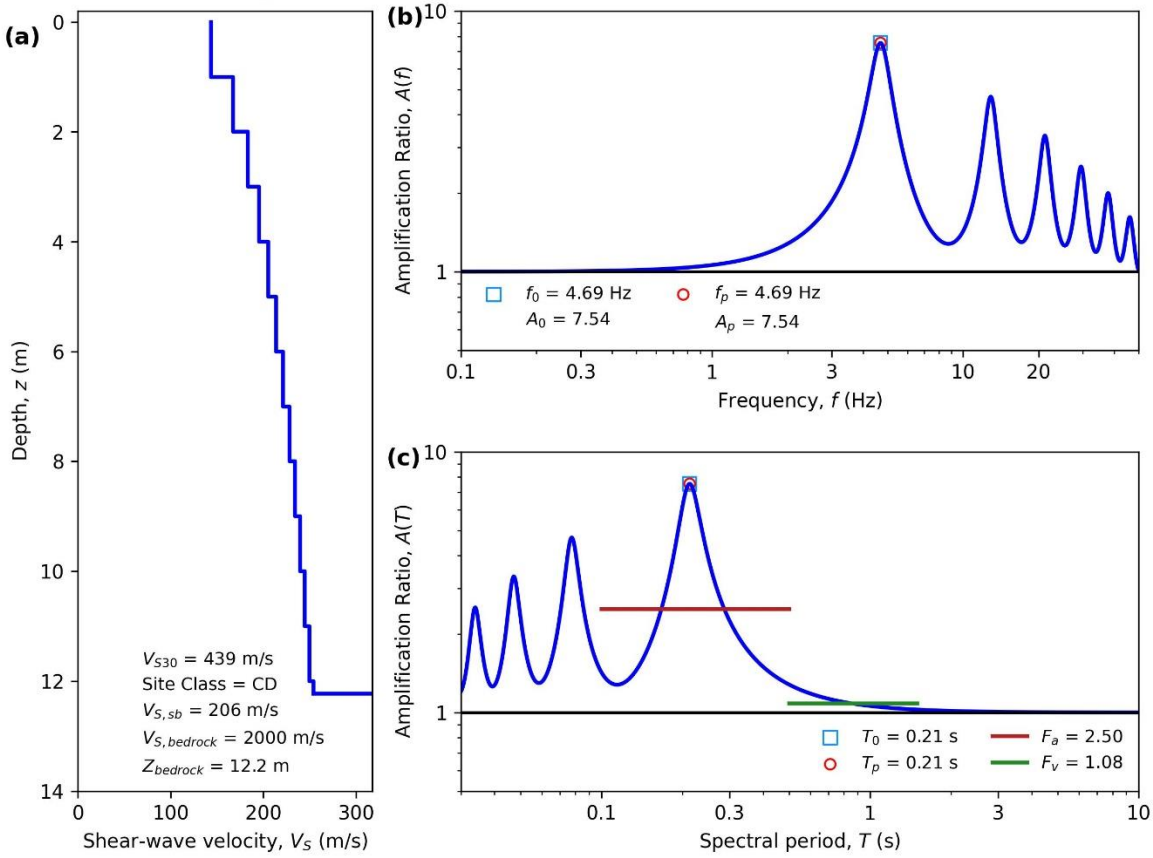

HAZUS Emergency Management
Massachusetts Care
Figure E31. ID: MA000031, Lat: 42.4600°, Lon: -73.2492°

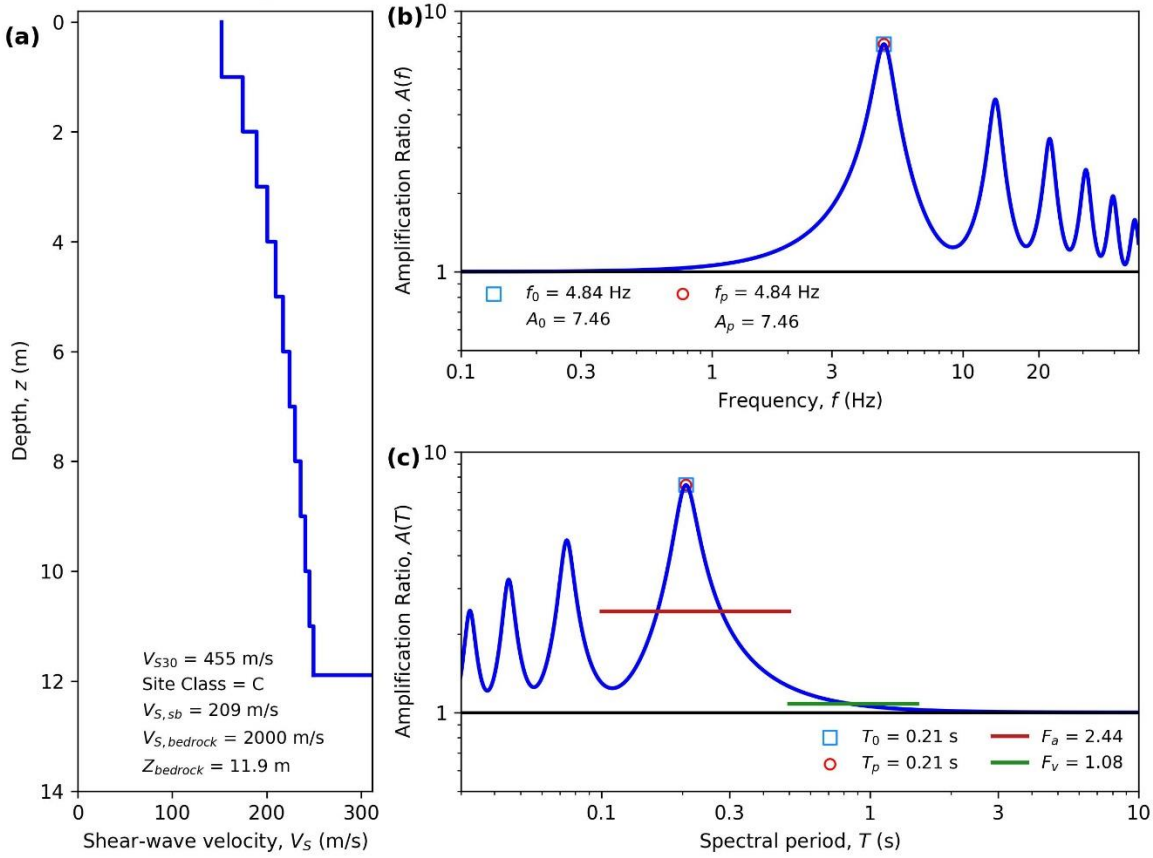

HAZUS Emergency Management
Massachusetts Care
Figure E32. ID: MA000032, Lat: 41.6534°, Lon: -70.2729°

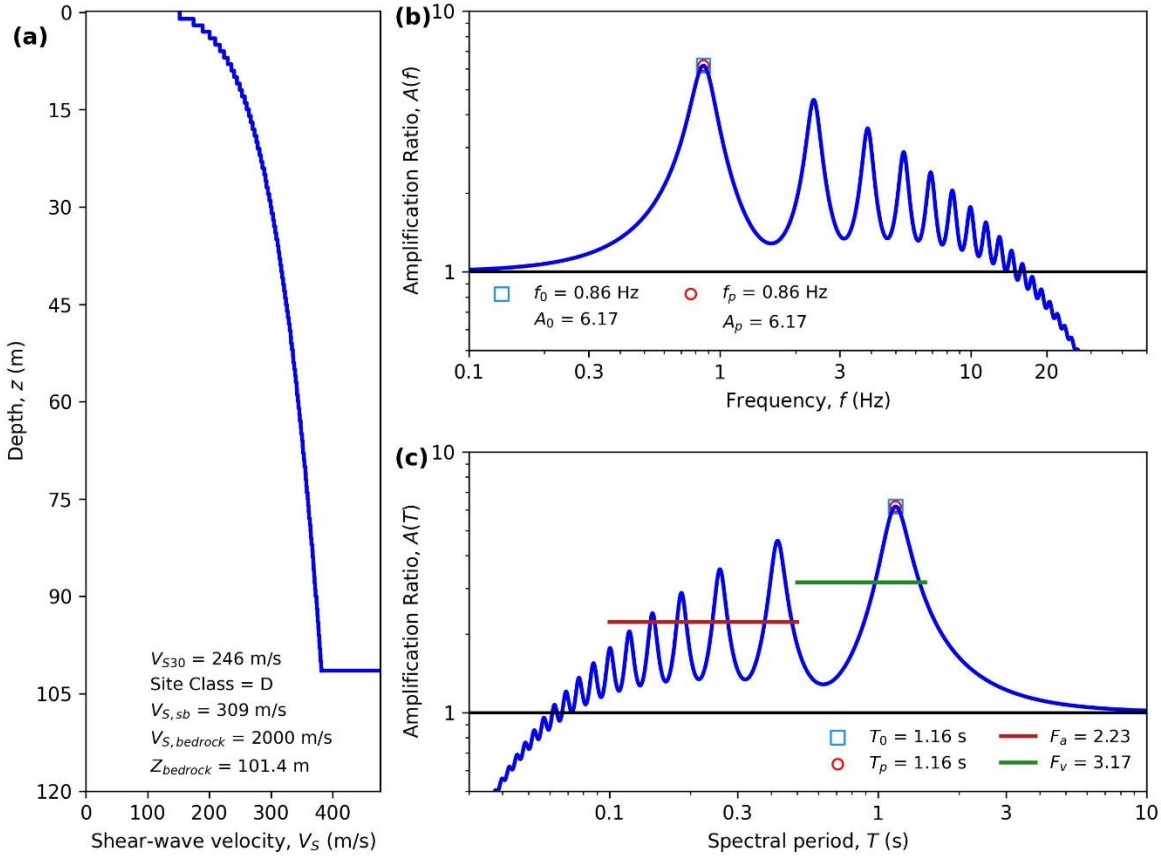

HAZUS Emergency Management
Massachusetts Care
Figure E33. ID: MA000033, Lat: 42.2775°, Lon: -71.0654°

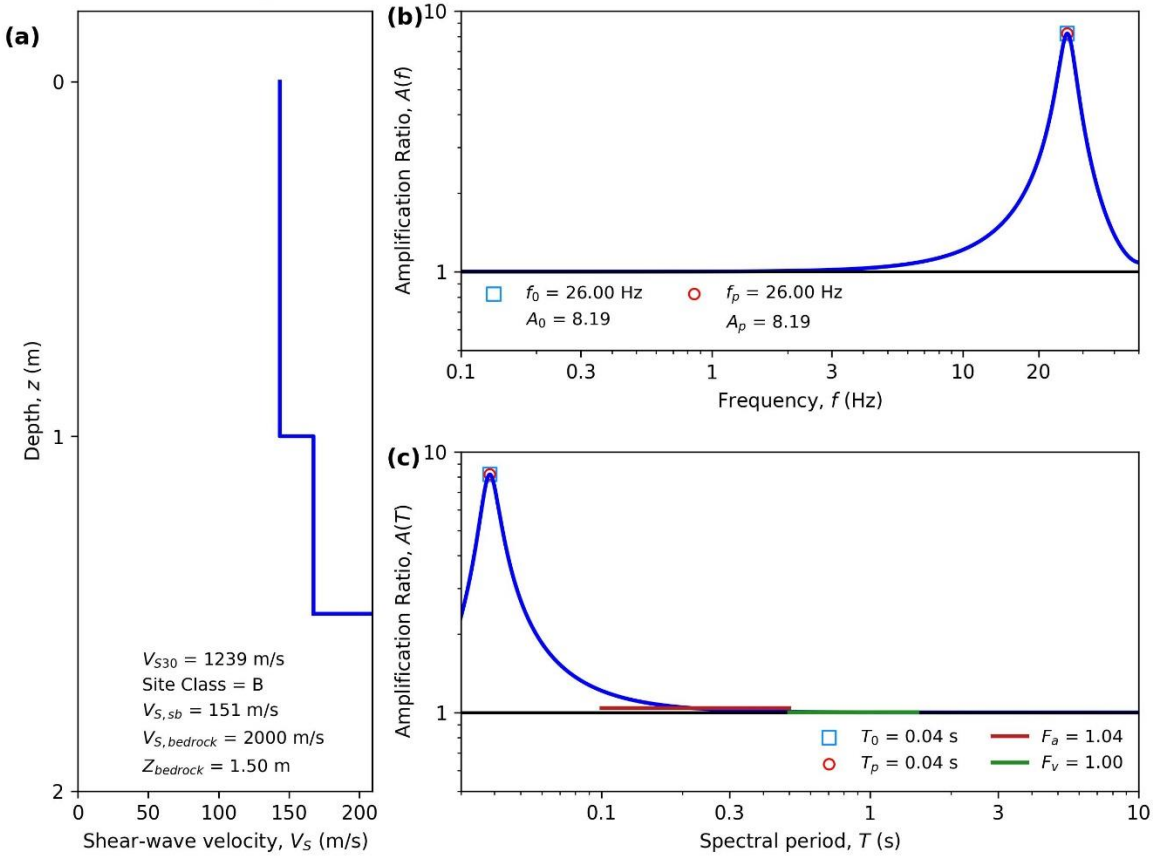

HAZUS Emergency Management
Massachusetts Care
Figure E34. ID: MA000034, Lat: 42.4275°, Lon: -71.6929°

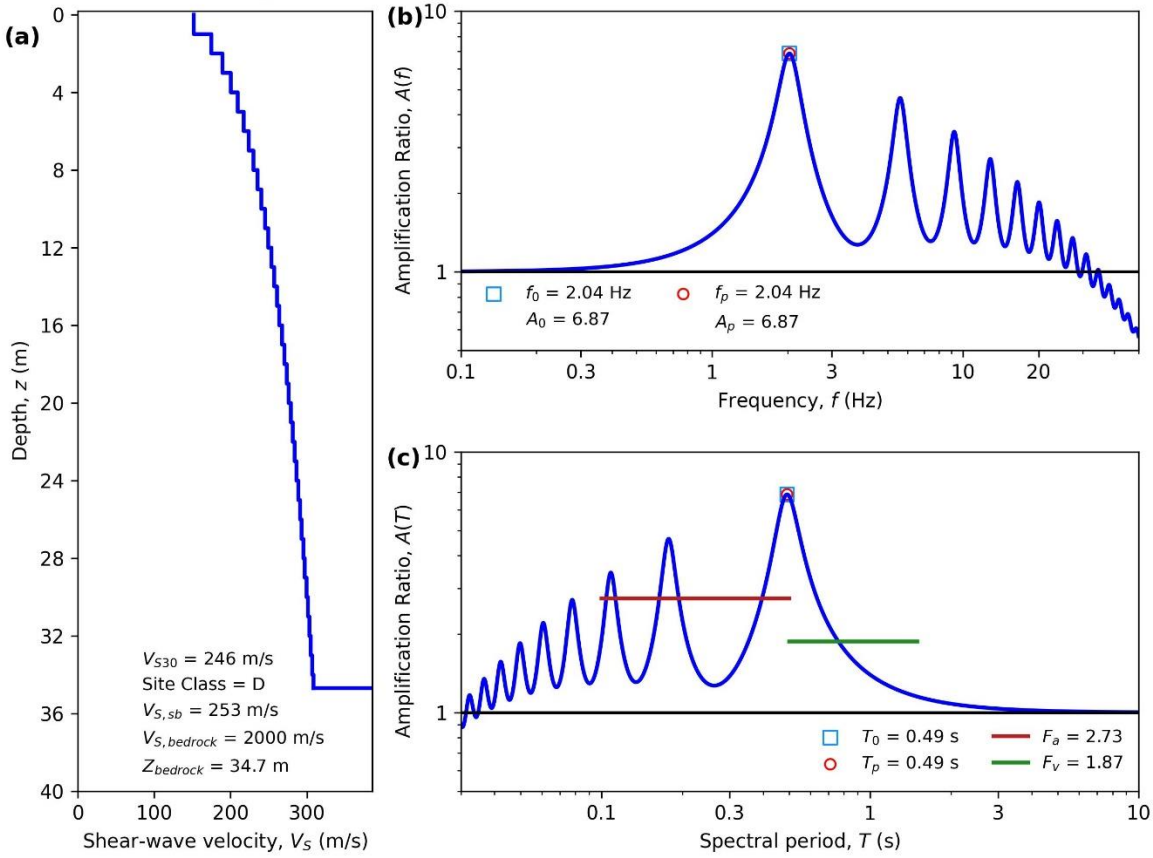

HAZUS Emergency Management
Massachusetts Care
Figure E35. ID: MA000035, Lat: 42.5863°, Lon: -71.9871°

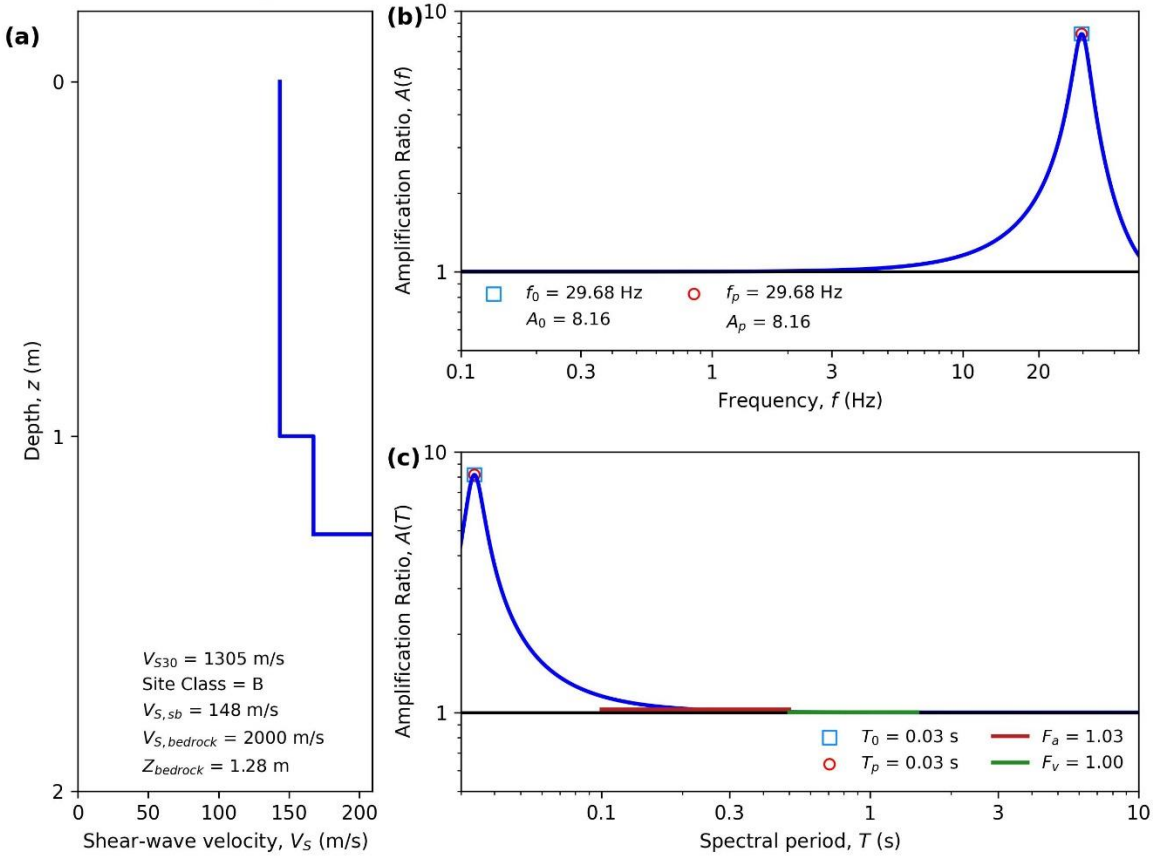

HAZUS Emergency Management
Massachusetts Care
Figure E36. ID: MA000036, Lat: 42.2729°, Lon: -71.7923°

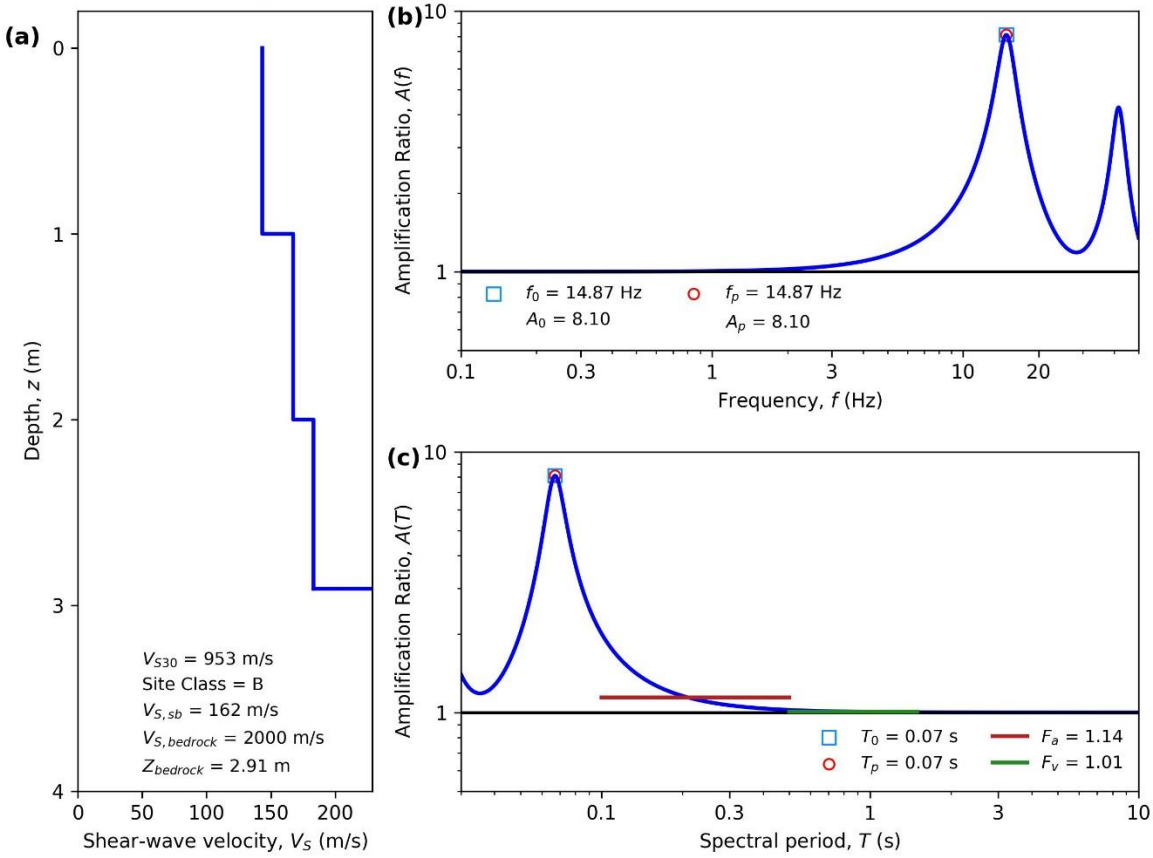

HAZUS Emergency Management
Massachusetts Care
Figure E37. ID: MA000037, Lat: 42.6457°, Lon: -71.3008°

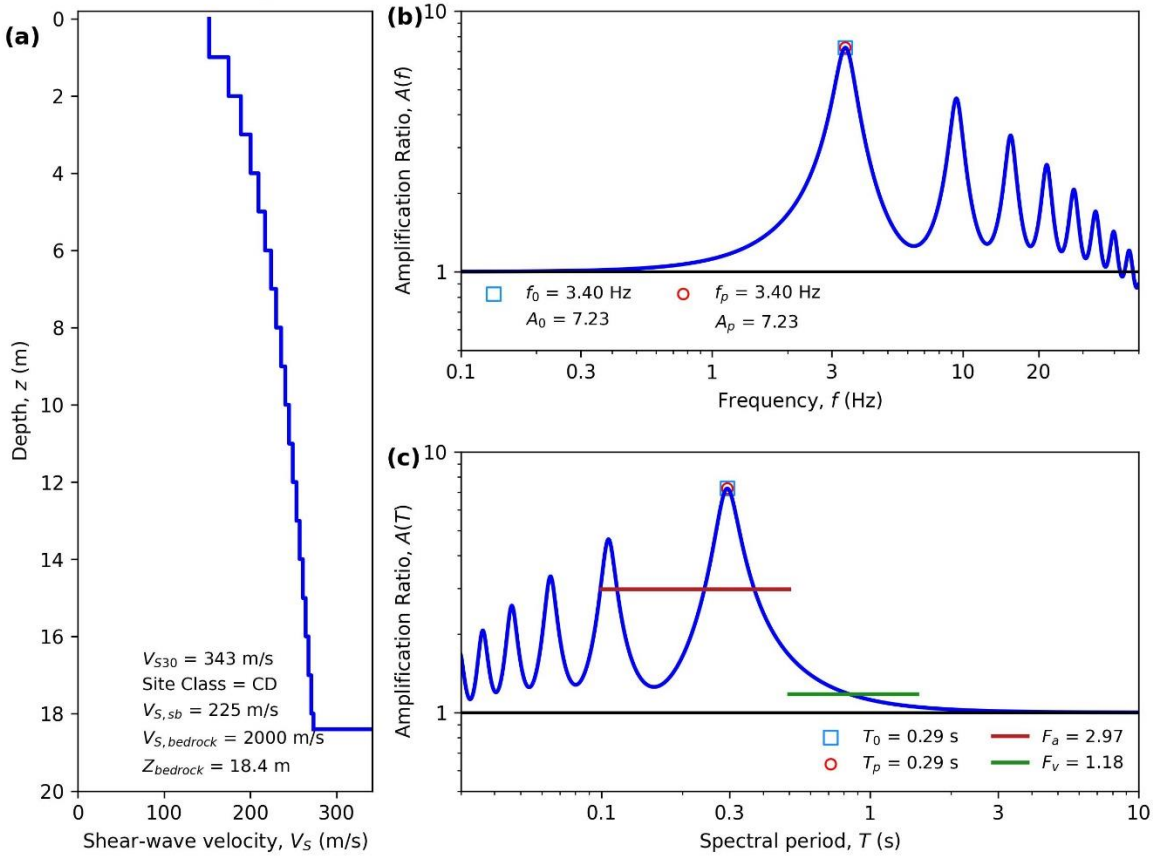

HAZUS Emergency Management
Massachusetts Care
Figure E38. ID: MA000038, Lat: 42.3312°, Lon: -71.2460°

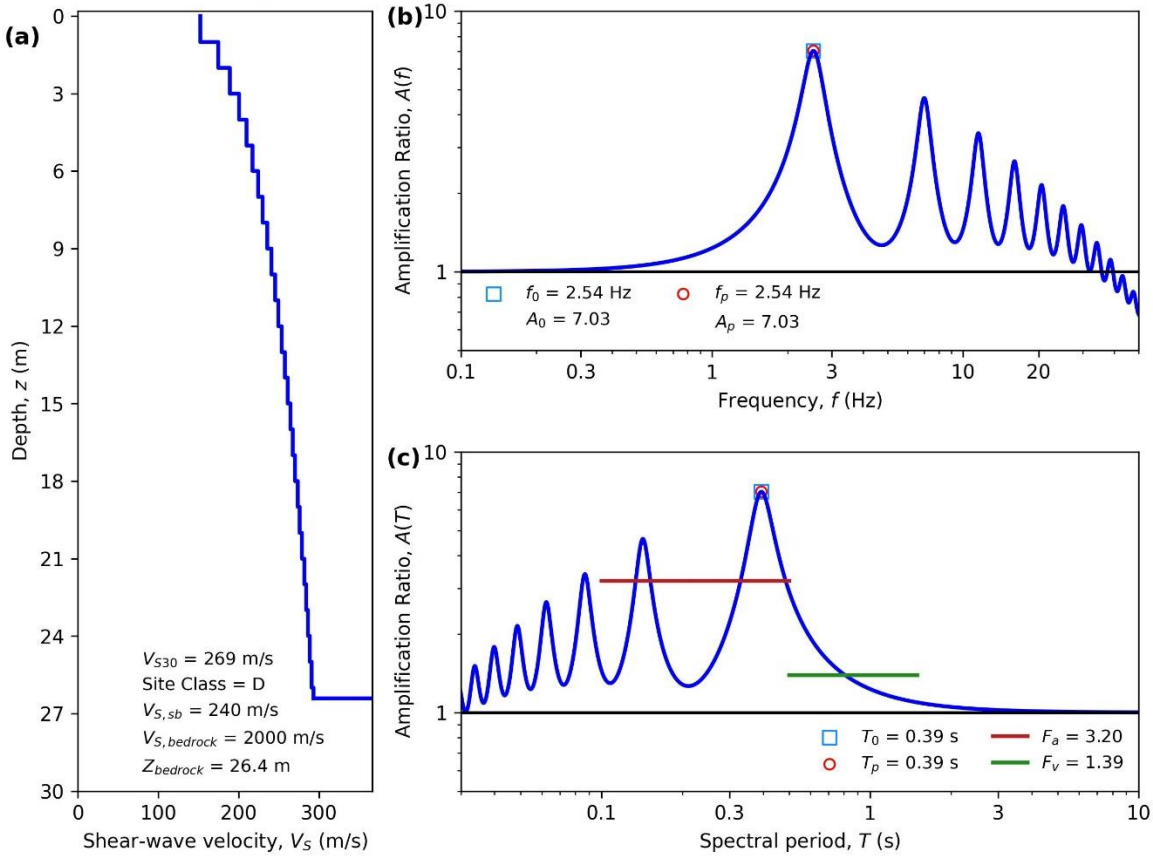

HAZUS Emergency Management
Massachusetts Care
Figure E39. ID: MA000039, Lat: 42.3745°, Lon: -71.1041°

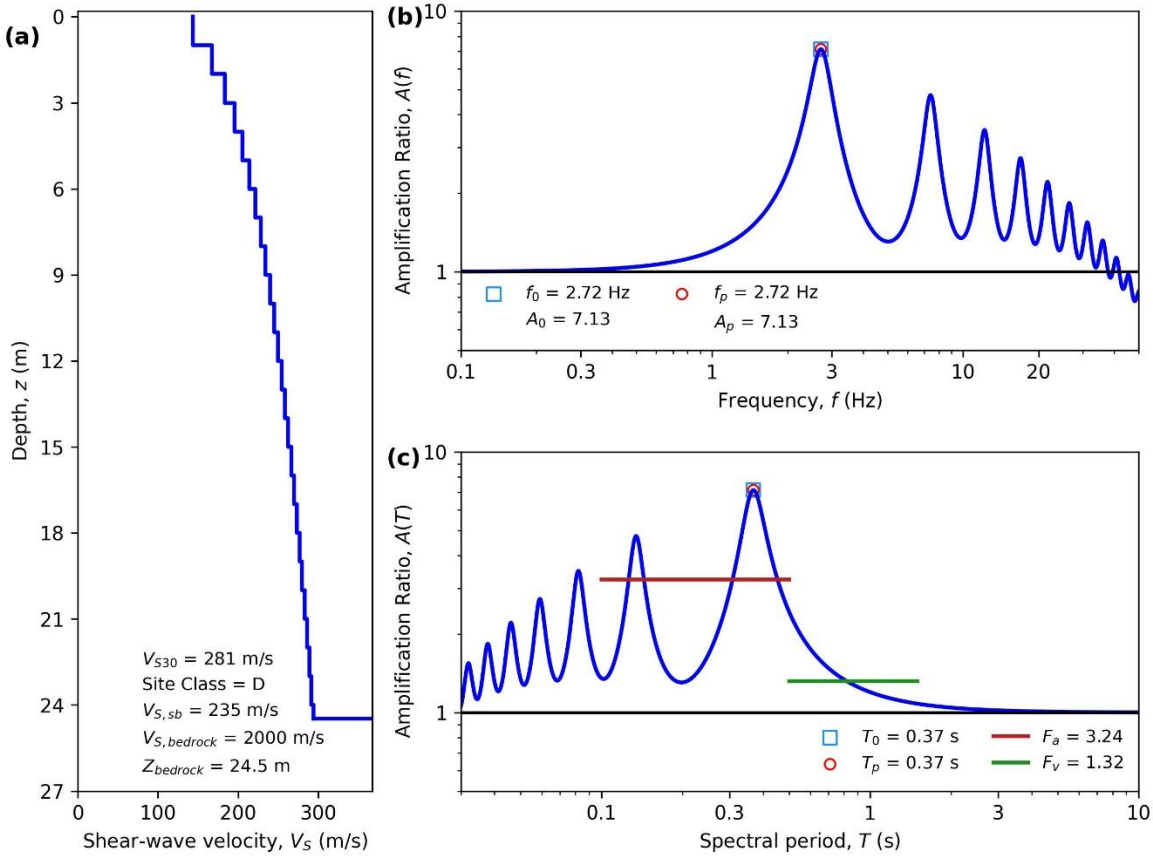

HAZUS Emergency Management
Massachusetts Care
Figure E40. ID: MA000040, Lat: 42.4093°, Lon: -71.0394°

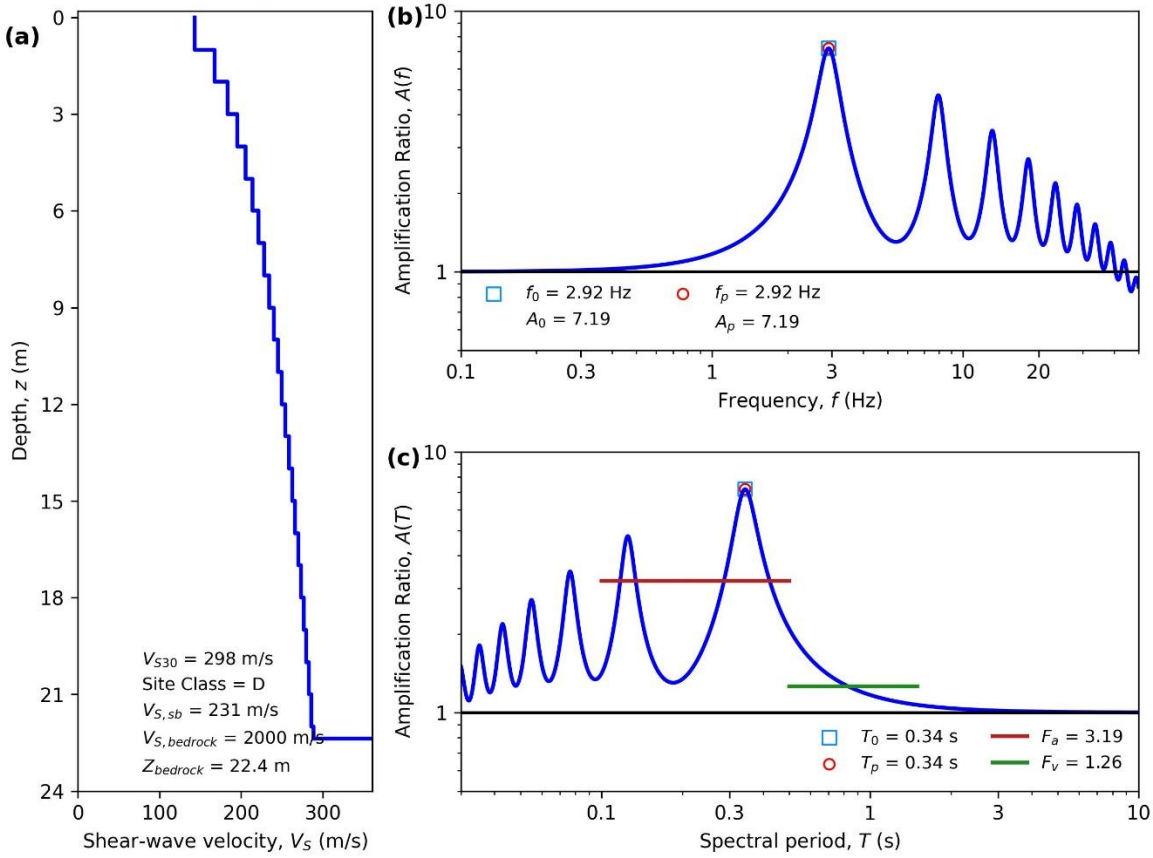

HAZUS Emergency Management
Massachusetts Care
Figure E41. ID: MA000041, Lat: 42.1659°, Lon: -72.6340°

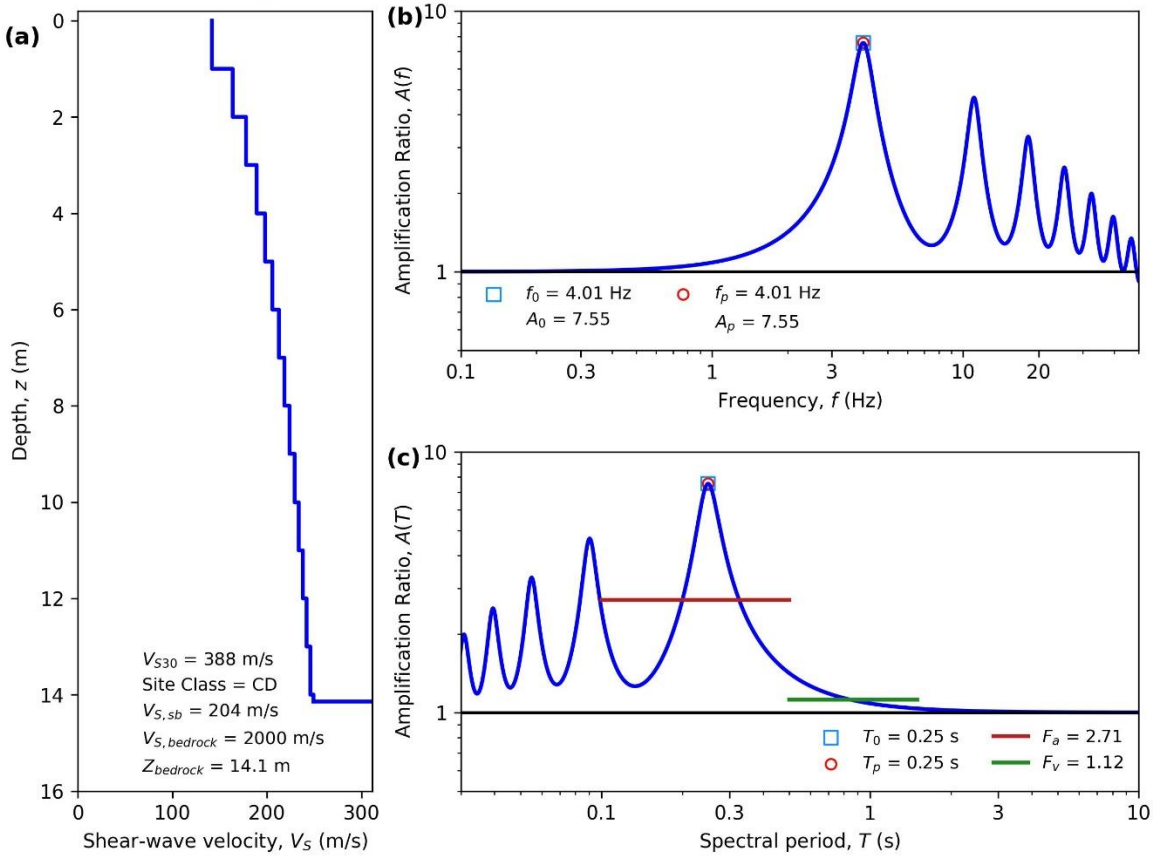

HAZUS Emergency Management
Massachusetts Care
Figure E42. ID: MA000042, Lat: 42.1217°, Lon: -72.6032°

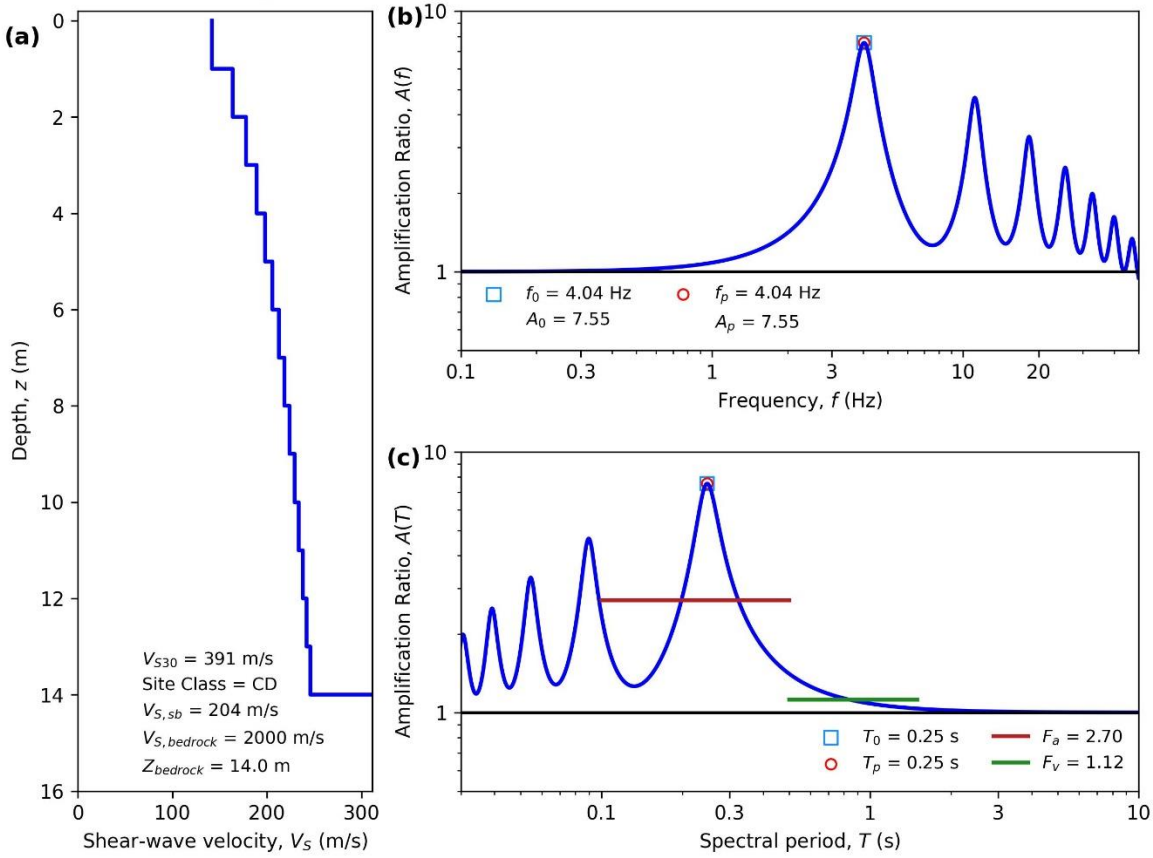

HAZUS Emergency Management
Massachusetts Care
Figure E43. ID: MA000043, Lat: 42.3495°, Lon: -72.6824°

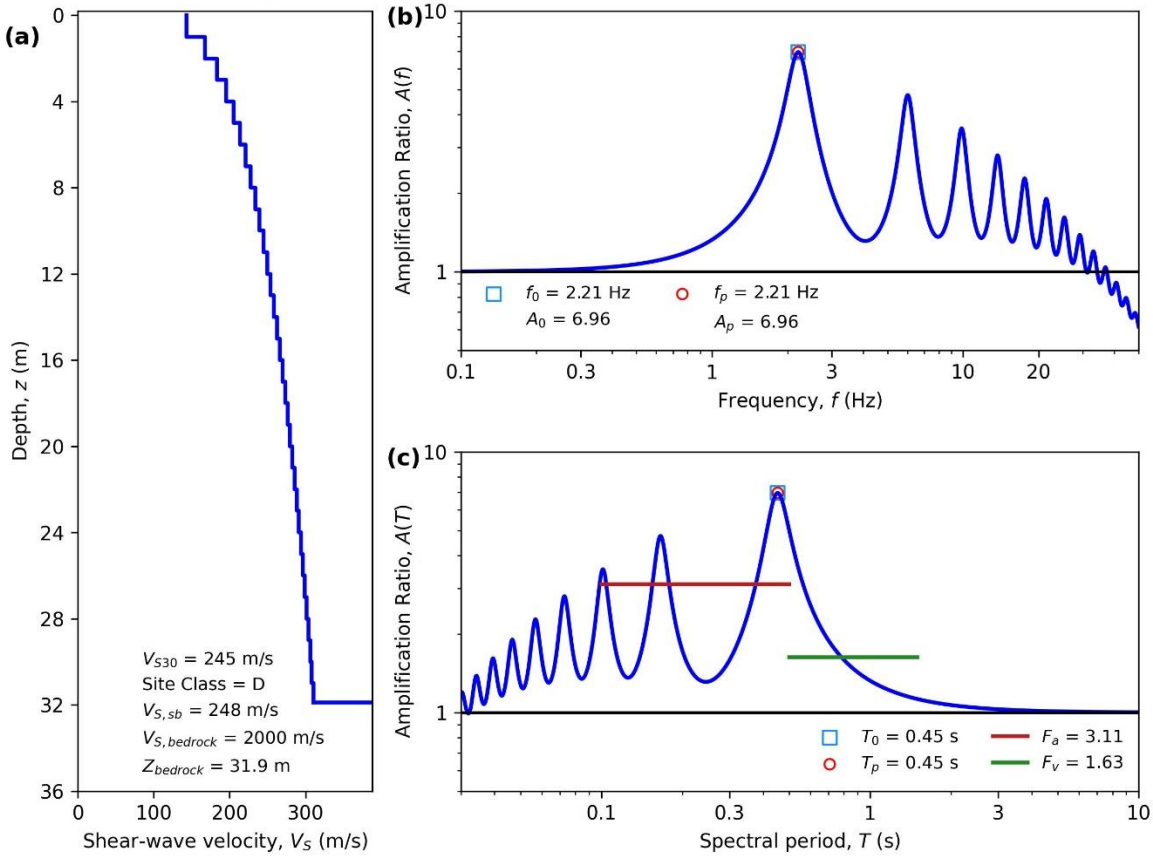

HAZUS Emergency Management
Massachusetts Care
Figure E44. ID: MA000044, Lat: 42.0630°, Lon: -71.0539°

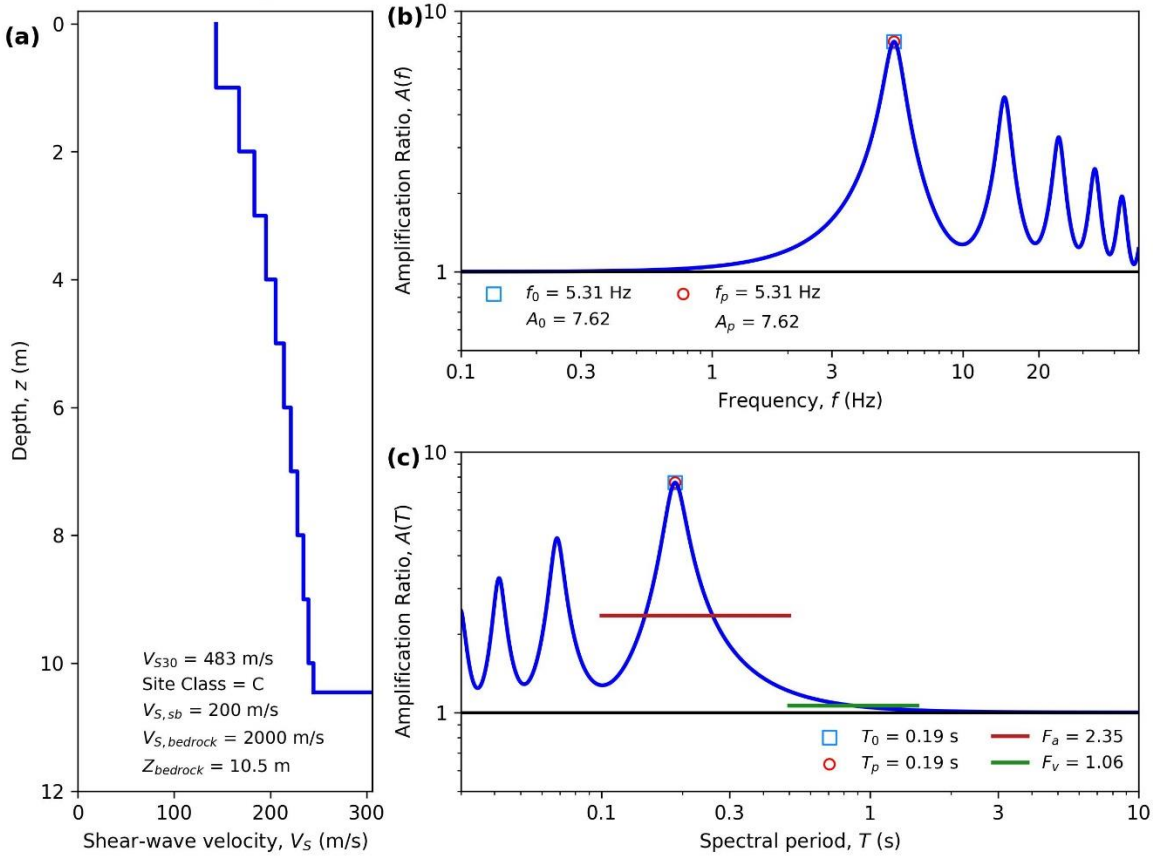

HAZUS Emergency Management
Massachusetts Care
Figure E45. ID: MA000045, Lat: 42.3500°, Lon: -71.1426°

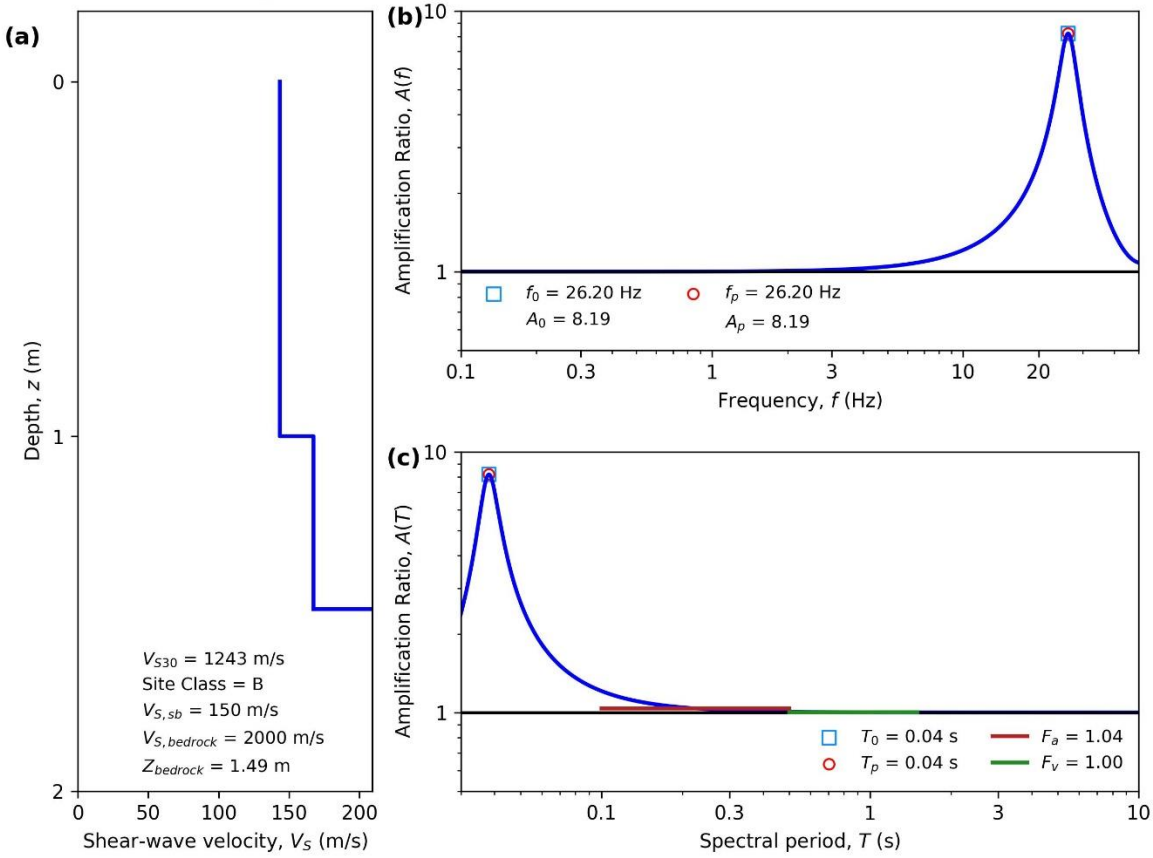

HAZUS Emergency Management
Massachusetts Care
Figure E46. ID: MA000046, Lat: 42.3753°, Lon: -71.1069°

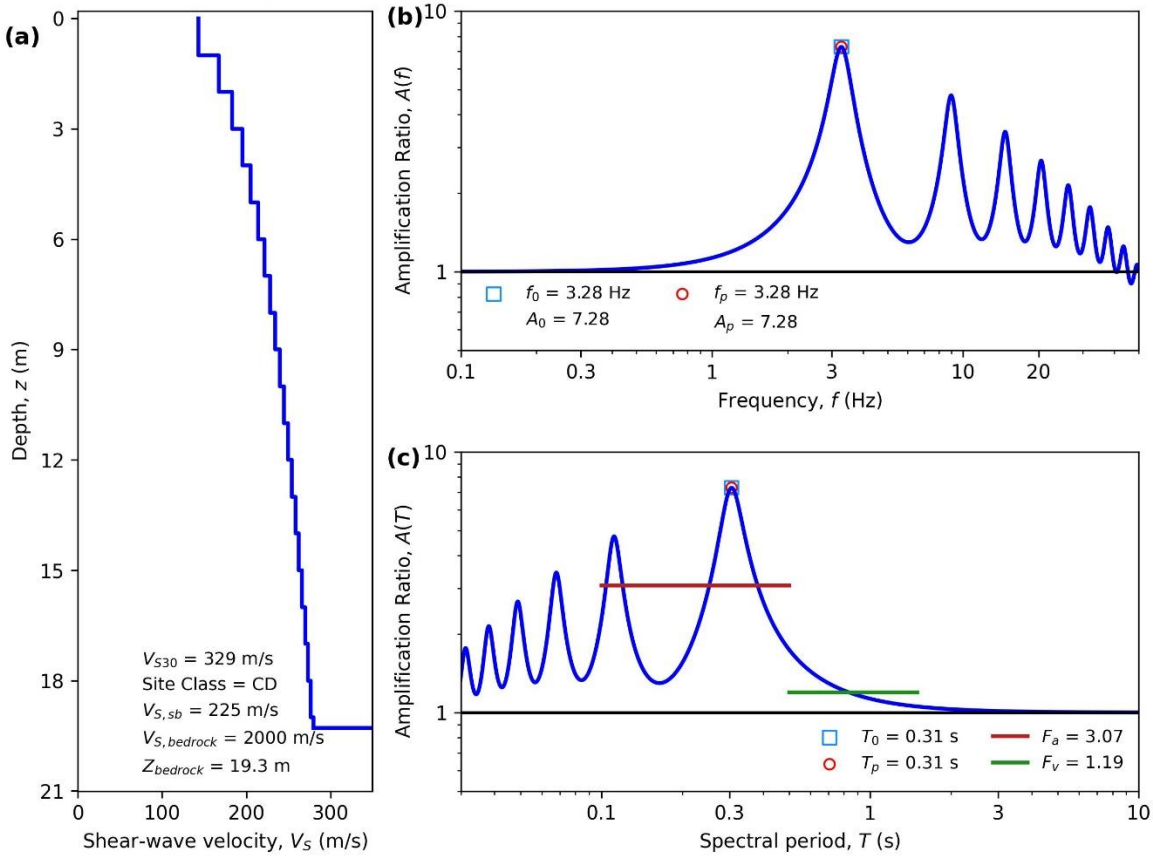

HAZUS Emergency Management
Massachusetts Care
Figure E47. ID: MA000047, Lat: 42.1104°, Lon: -72.7009°

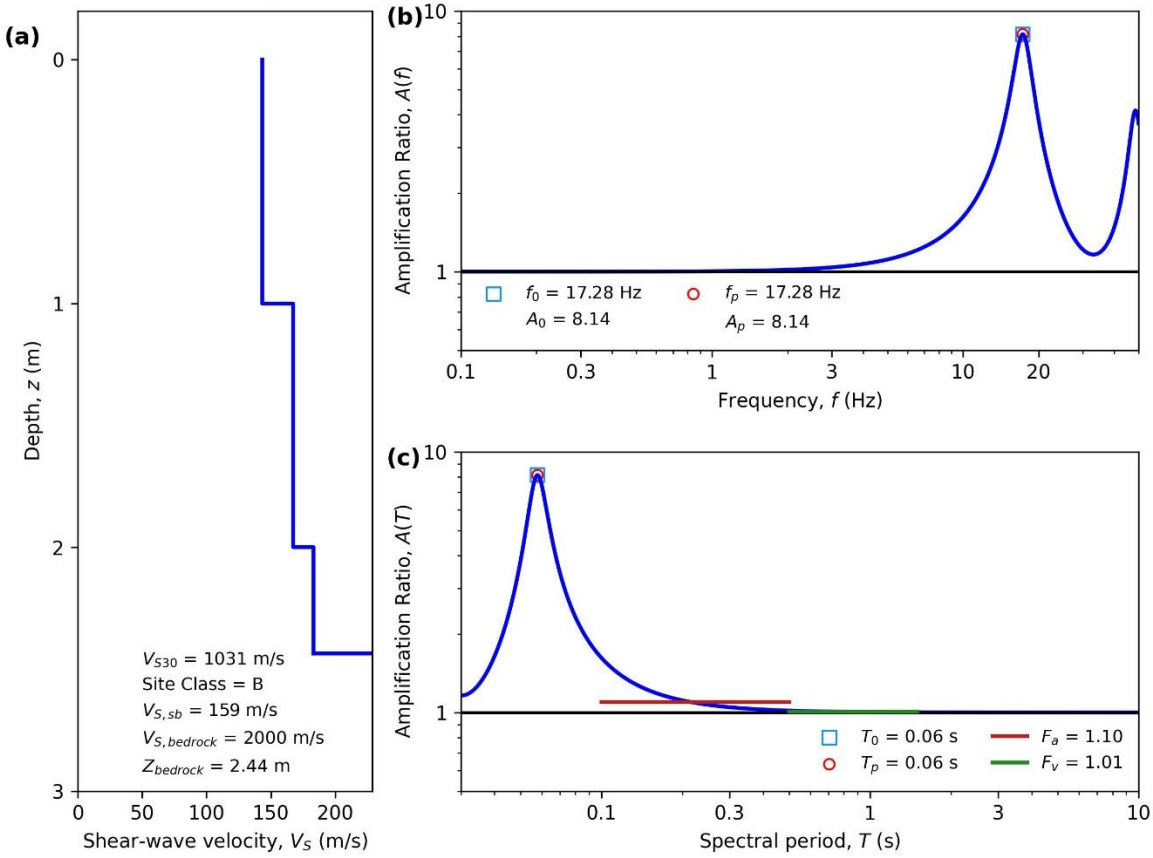

HAZUS Emergency Management
Massachusetts Care
Figure E48. ID: MA000048, Lat: 42.3937°, Lon: -71.1913°

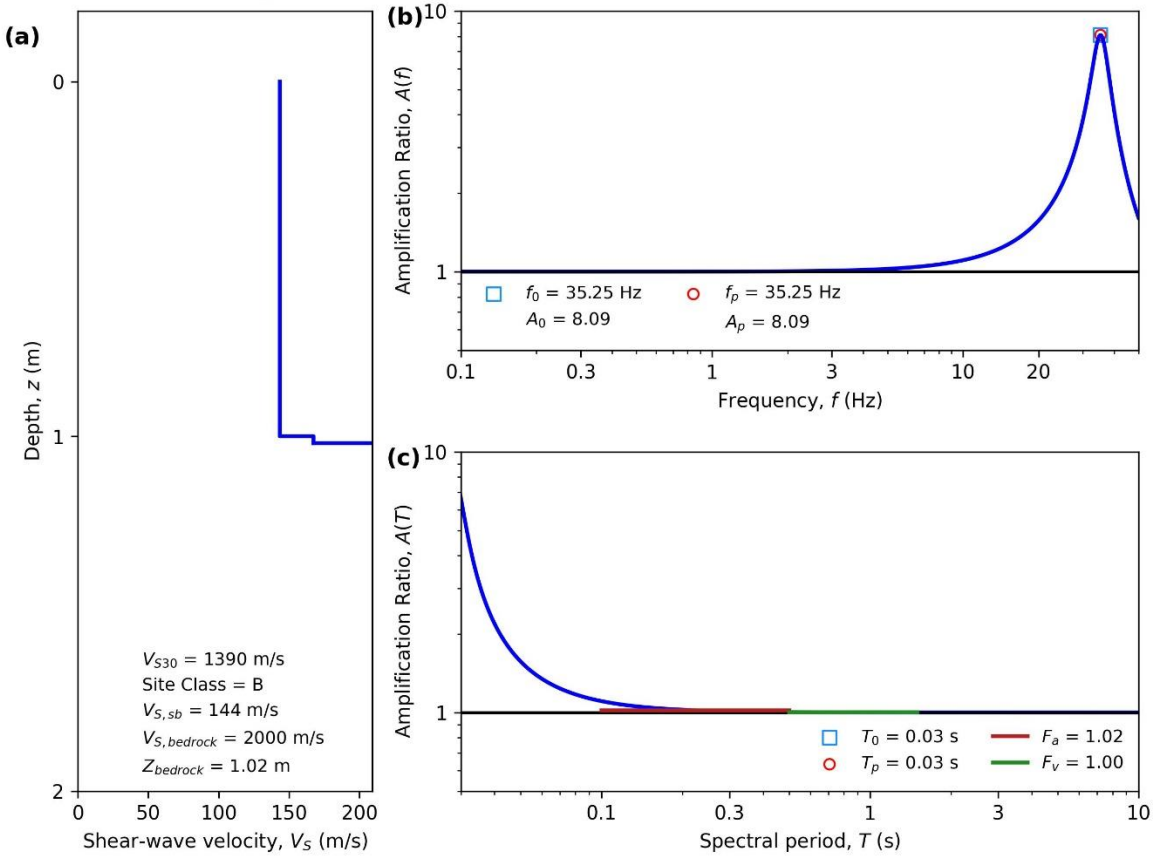

HAZUS Emergency Management
Massachusetts Care
Figure E49. ID: MA000049, Lat: 42.1760°, Lon: -71.1253°

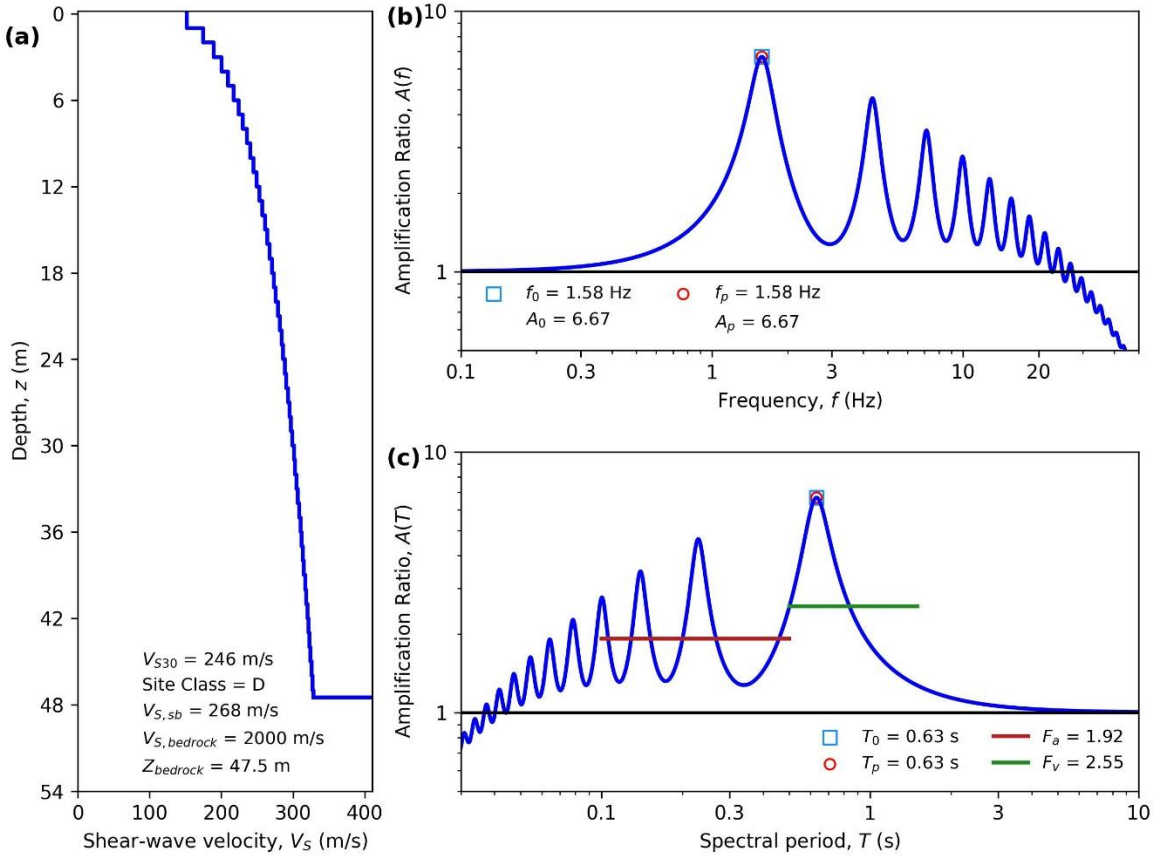

HAZUS Emergency Management
Massachusetts Care
Figure E50. ID: MA000050, Lat: 41.9420°, Lon: -71.2748°

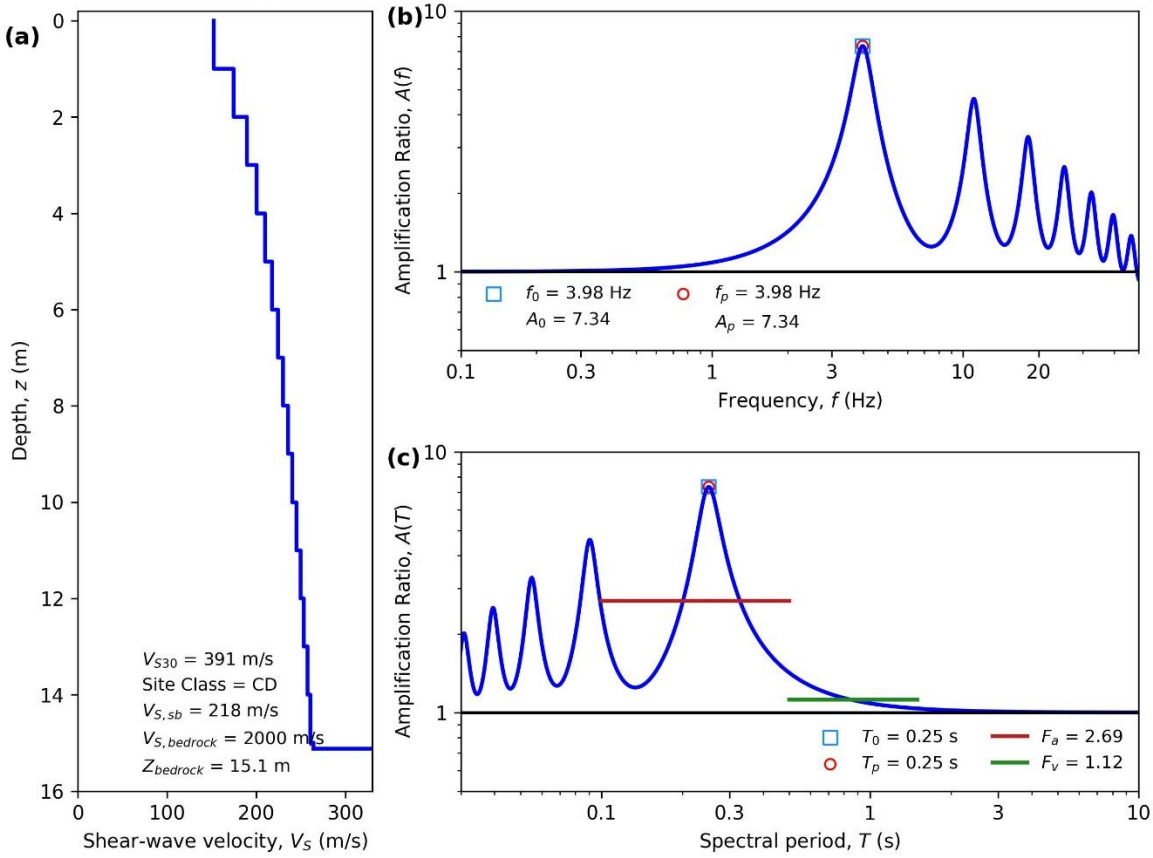

HAZUS Emergency Management
Massachusetts Care
Figure E51. ID: MA000051, Lat: 41.9062°, Lon: -71.0945°

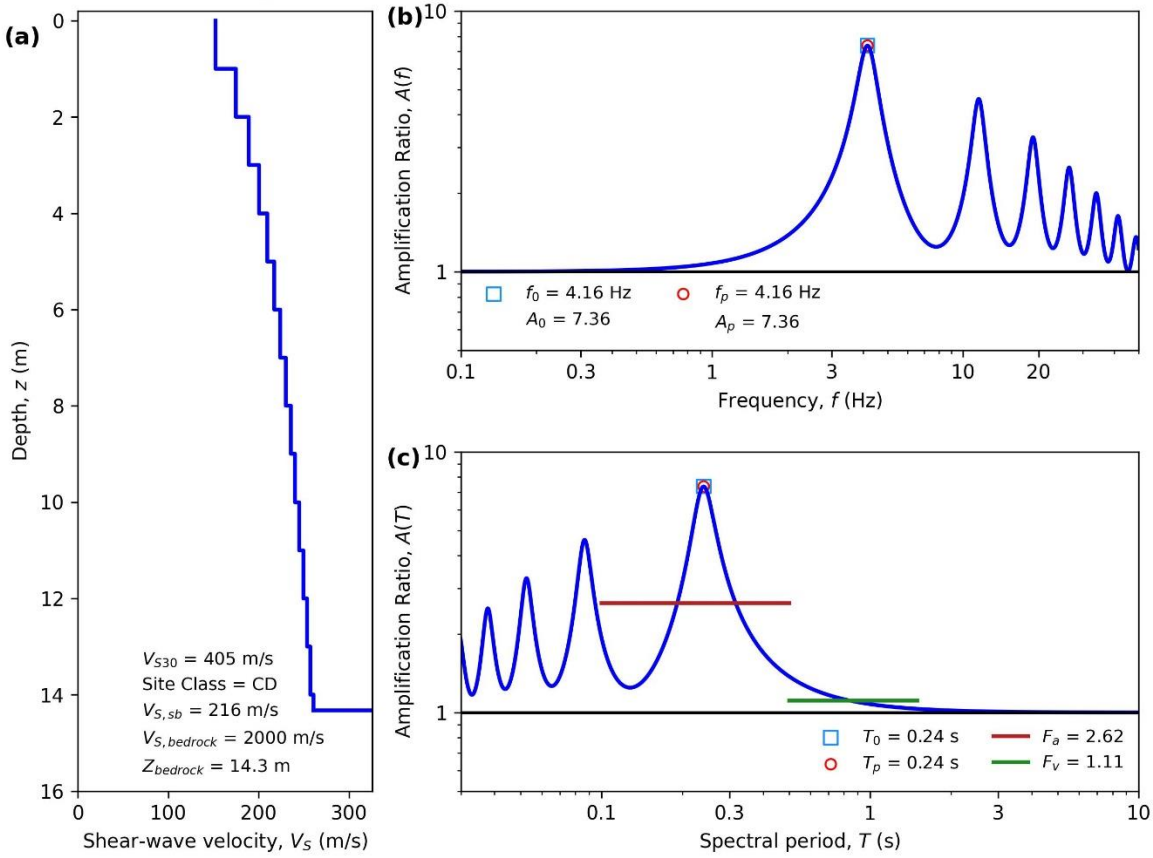

HAZUS Emergency Management
Massachusetts Care
Figure E52. ID: MA000052, Lat: 41.6926°, Lon: -71.1637°

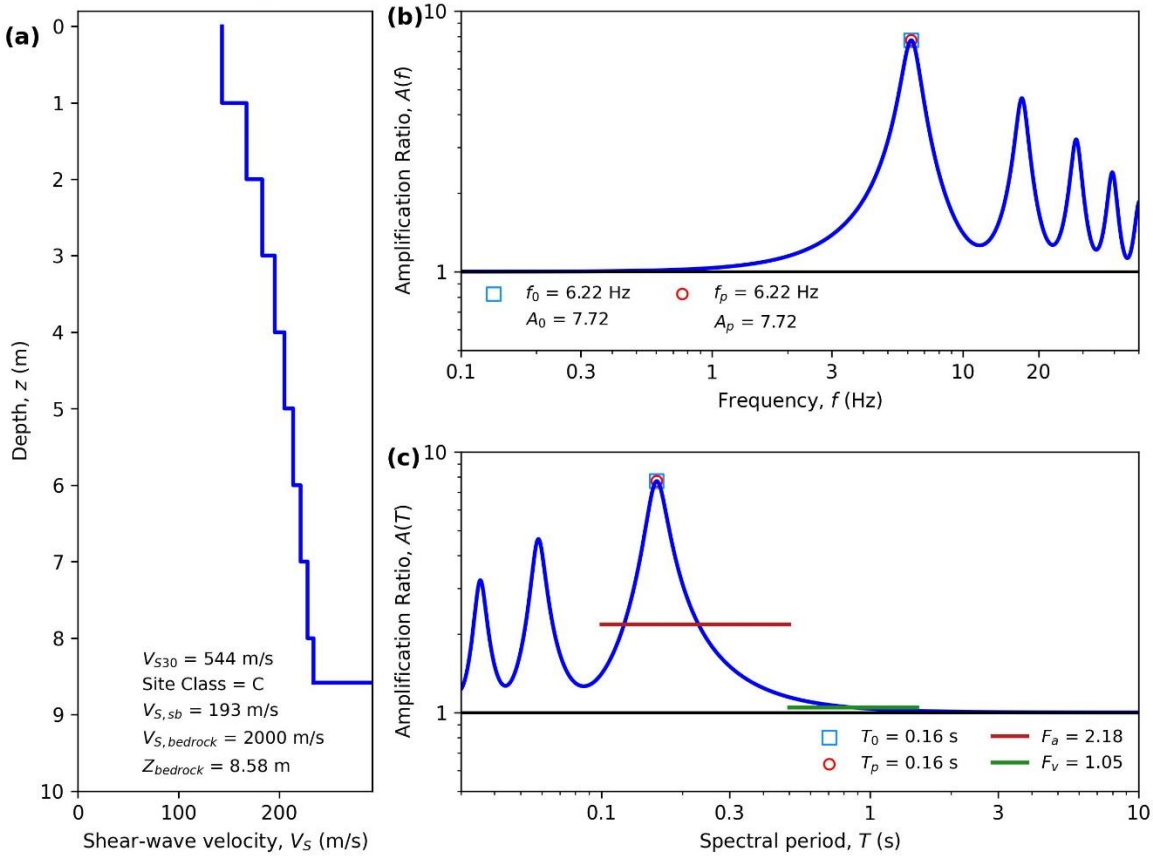

HAZUS Emergency Management
Massachusetts Care
Figure E53. ID: MA000053, Lat: 42.1911°, Lon: -73.3719°

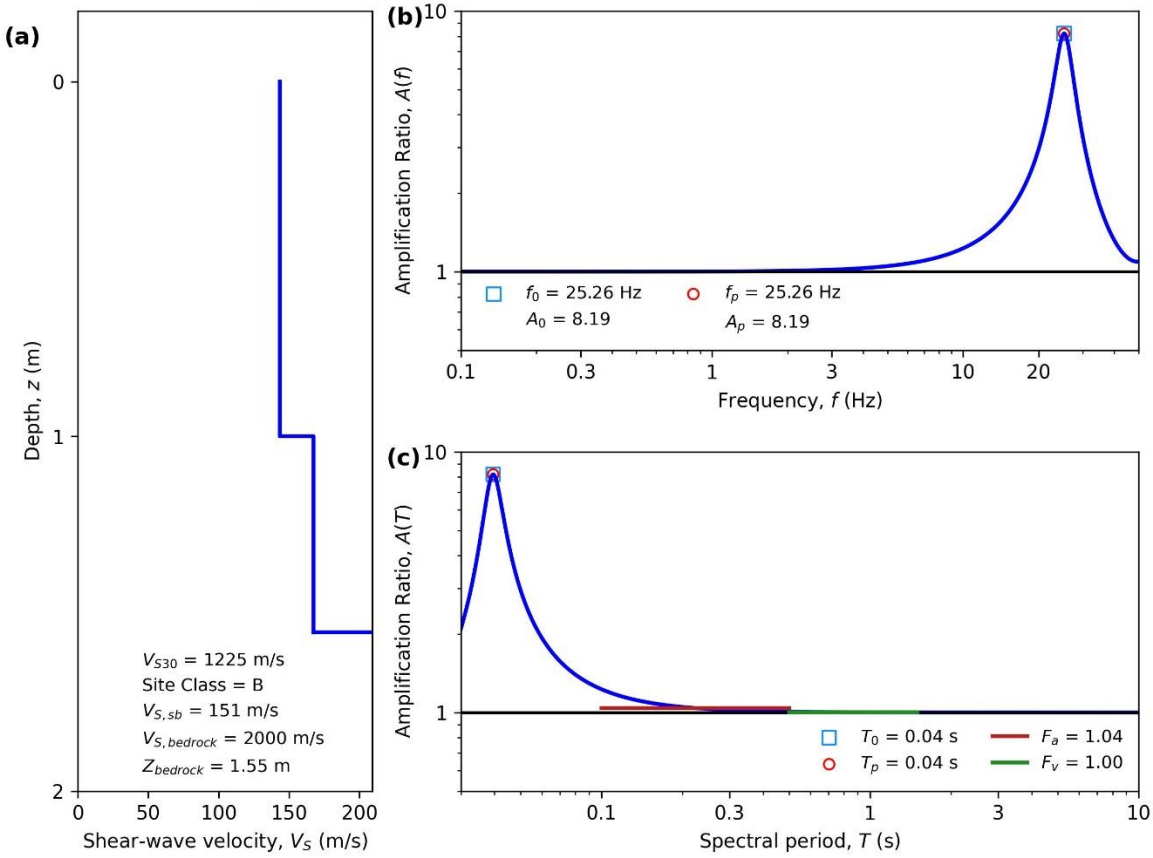

HAZUS Emergency Management
Massachusetts Care
Figure E54. ID: MA000054, Lat: 41.5642°, Lon: -70.6223°

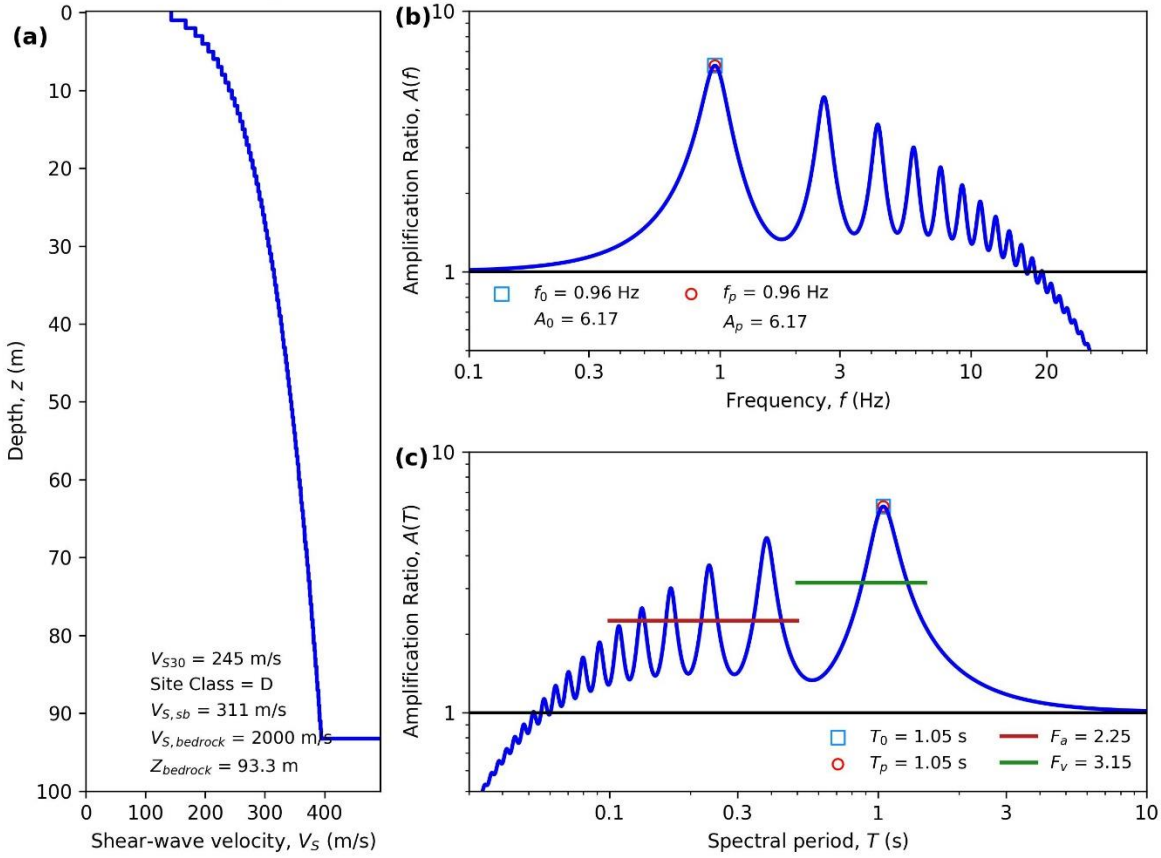

HAZUS Emergency Management
Massachusetts Care
Figure E55. ID: MA000055, Lat: 41.2752°, Lon: -70.1008°

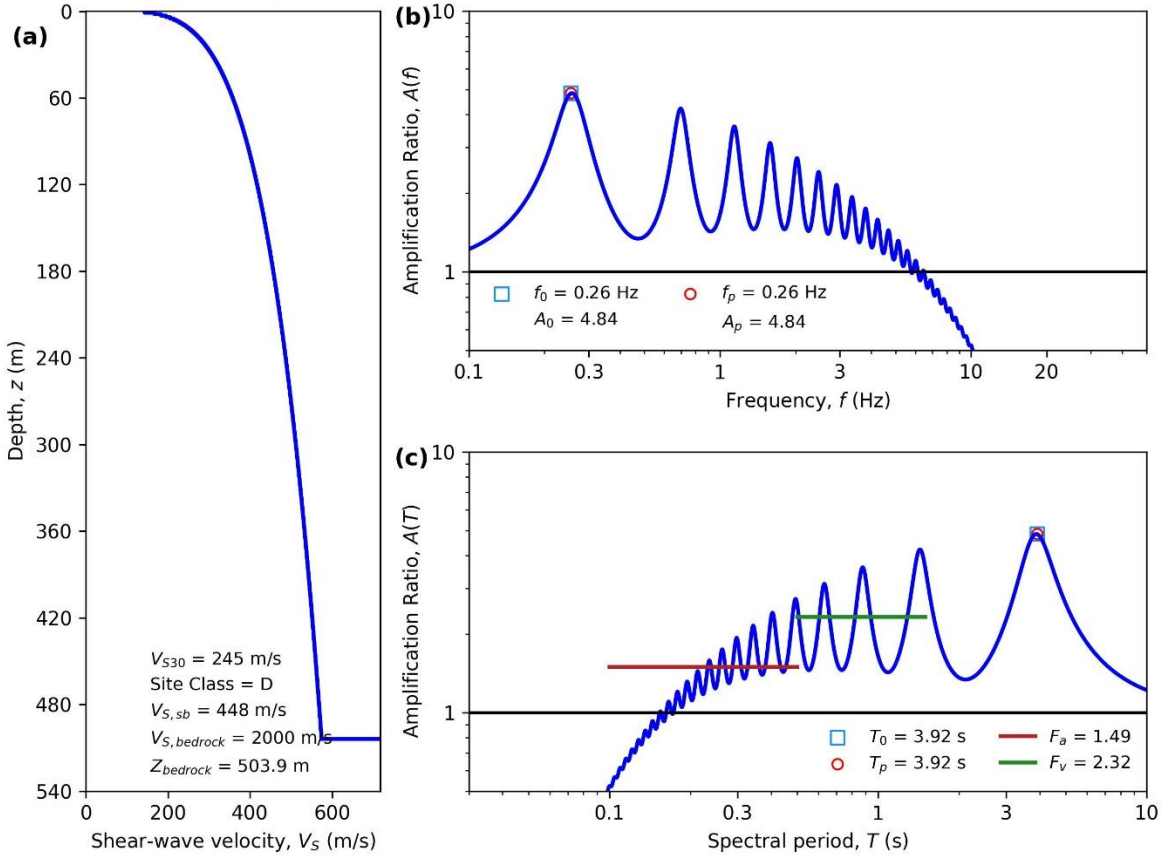

HAZUS Emergency Management
Massachusetts Care
Figure E56. ID: MA000056, Lat: 42.3395°, Lon: -71.1051°

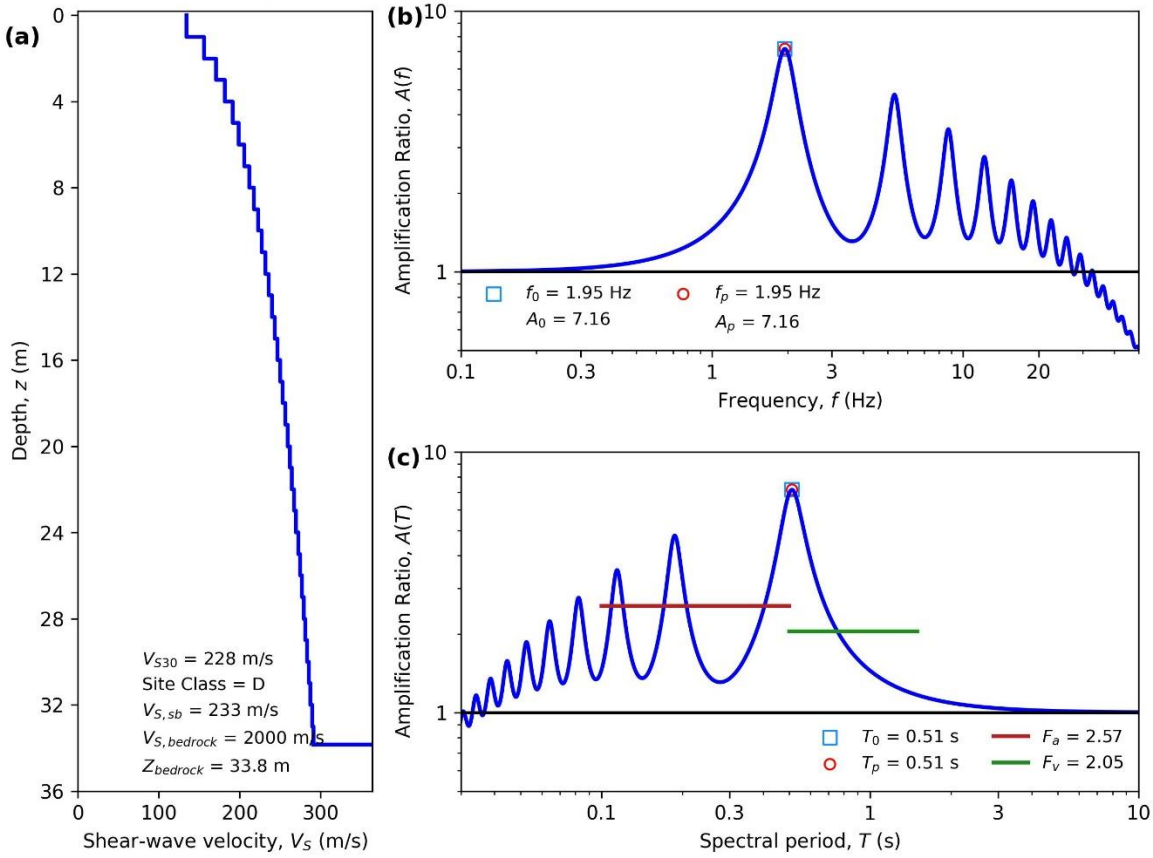

HAZUS Emergency Management
Massachusetts Care
Figure E57. ID: MA000057, Lat: 42.3347°, Lon: -71.0732°

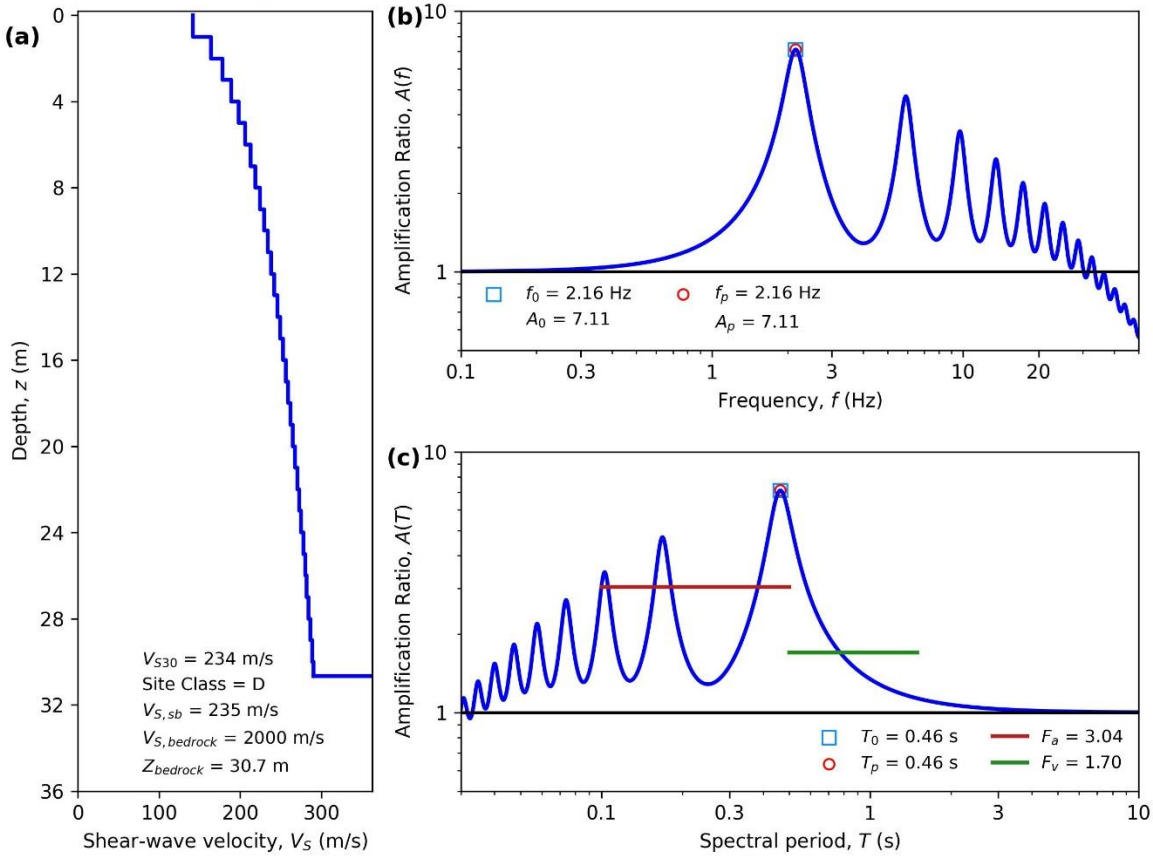

HAZUS Emergency Management
Massachusetts Care
Figure E58. ID: MA000058, Lat: 42.3629°, Lon: -71.0701°

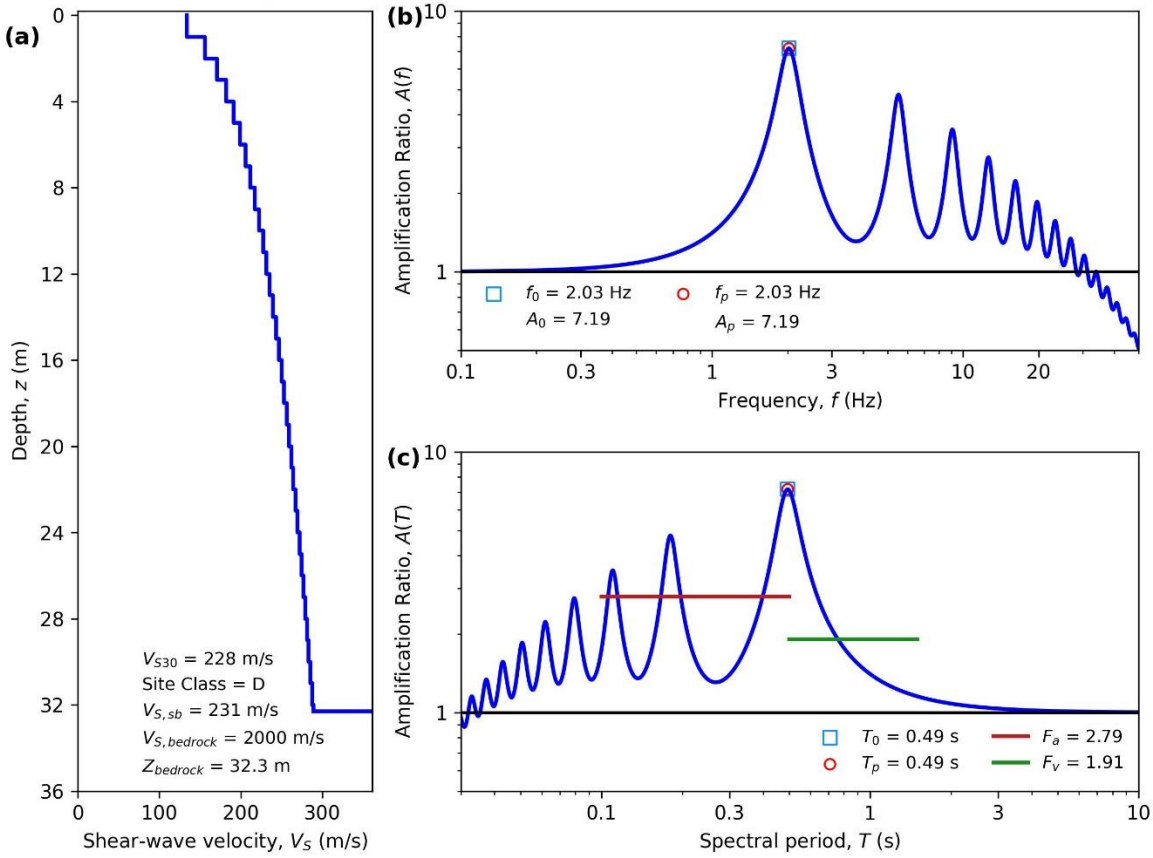

HAZUS Emergency Management
Massachusetts Care
Figure E59. ID: MA000059, Lat: 42.3372°, Lon: -71.1064°

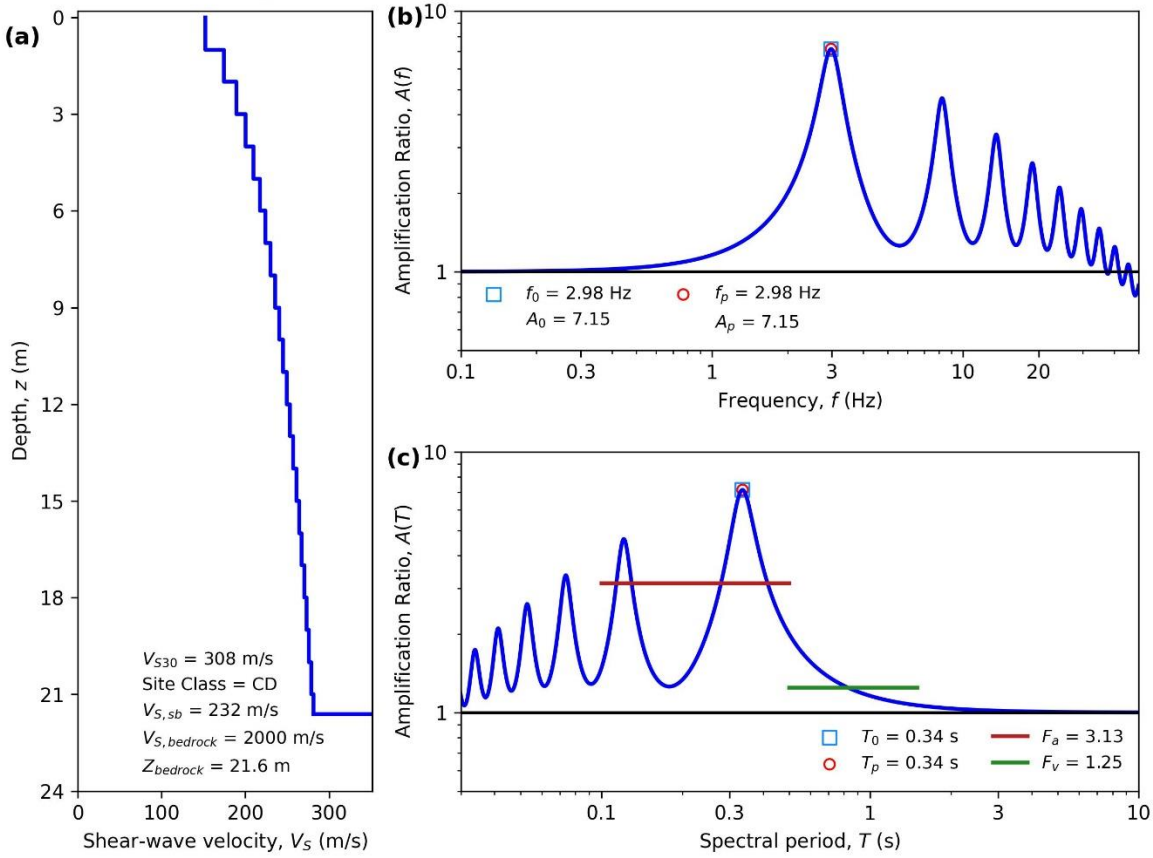

HAZUS Emergency Management
Massachusetts Care
Figure E60. ID: MA000060, Lat: 42.5976°, Lon: -71.8054°

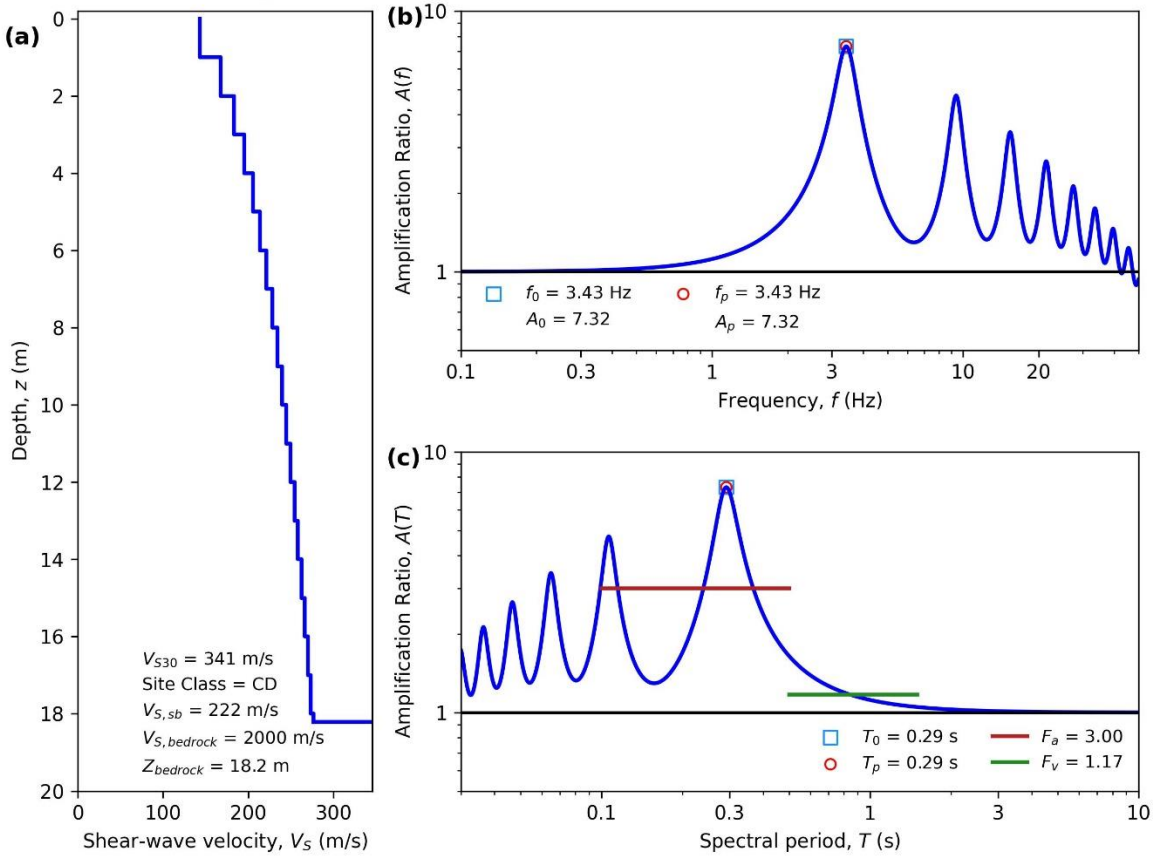

HAZUS Emergency Management
Massachusetts Care
Figure E61. ID: MA000061, Lat: 42.5411°, Lon: -71.7624°

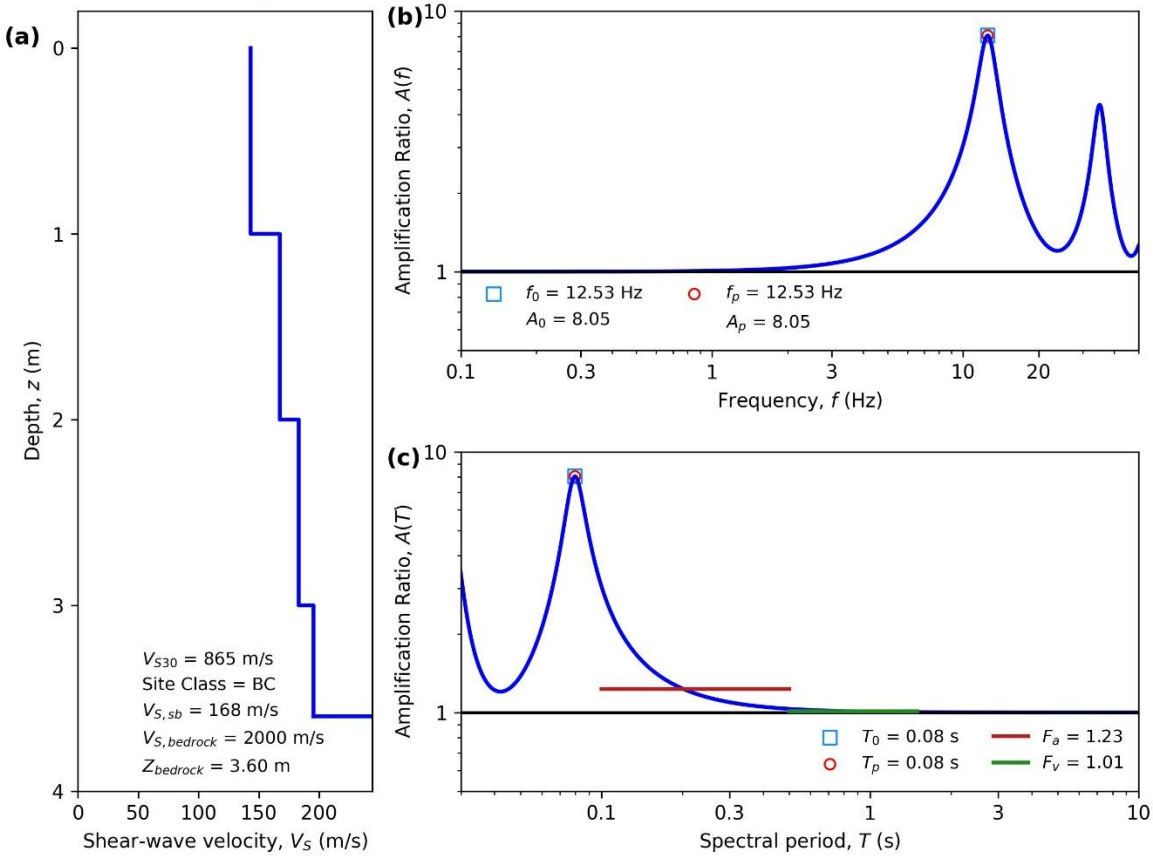

HAZUS Emergency Management
Massachusetts Care
Figure E62. ID: MA000062, Lat: 42.4605°, Lon: -71.0609°

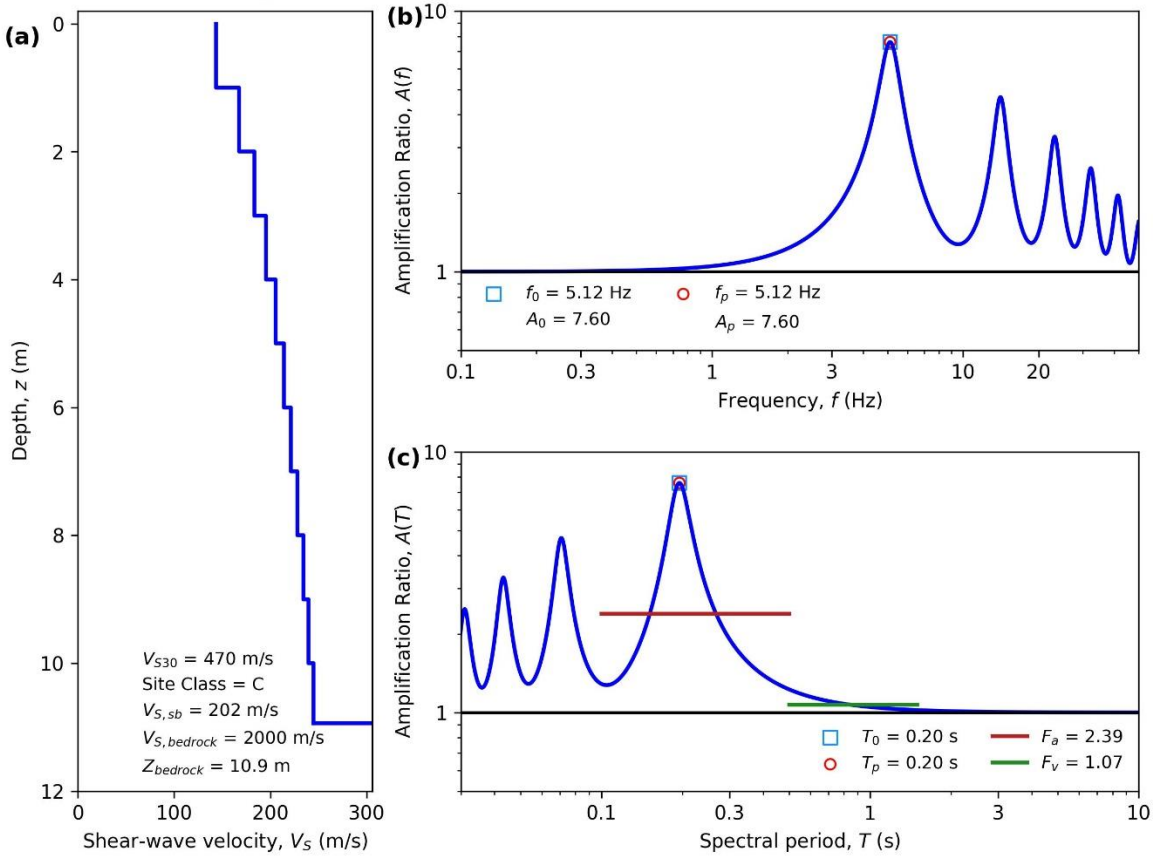

HAZUS Emergency Management
Massachusetts Care
Figure E63. ID: MA000063, Lat: 42.3553°, Lon: -71.5546°

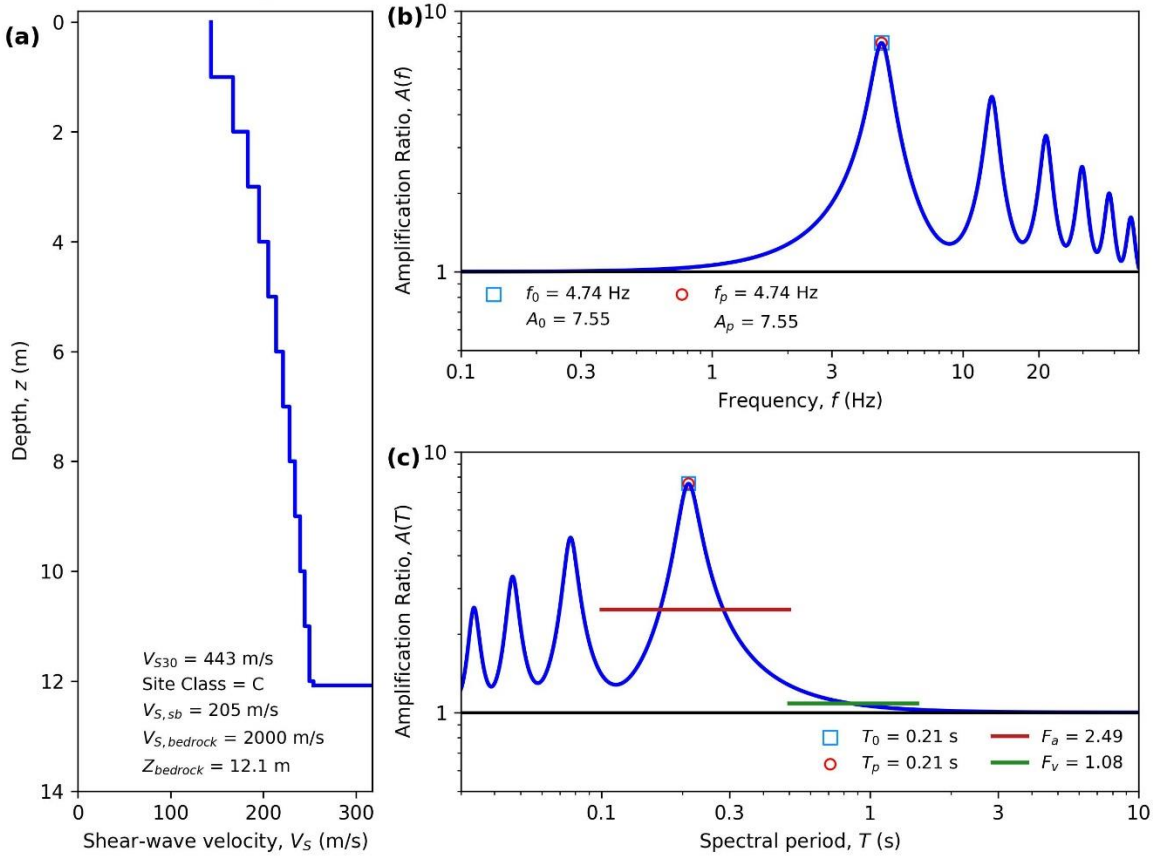

HAZUS Emergency Management
Massachusetts Care
Figure E64. ID: MA000064, Lat: 42.2852°, Lon: -71.4186°

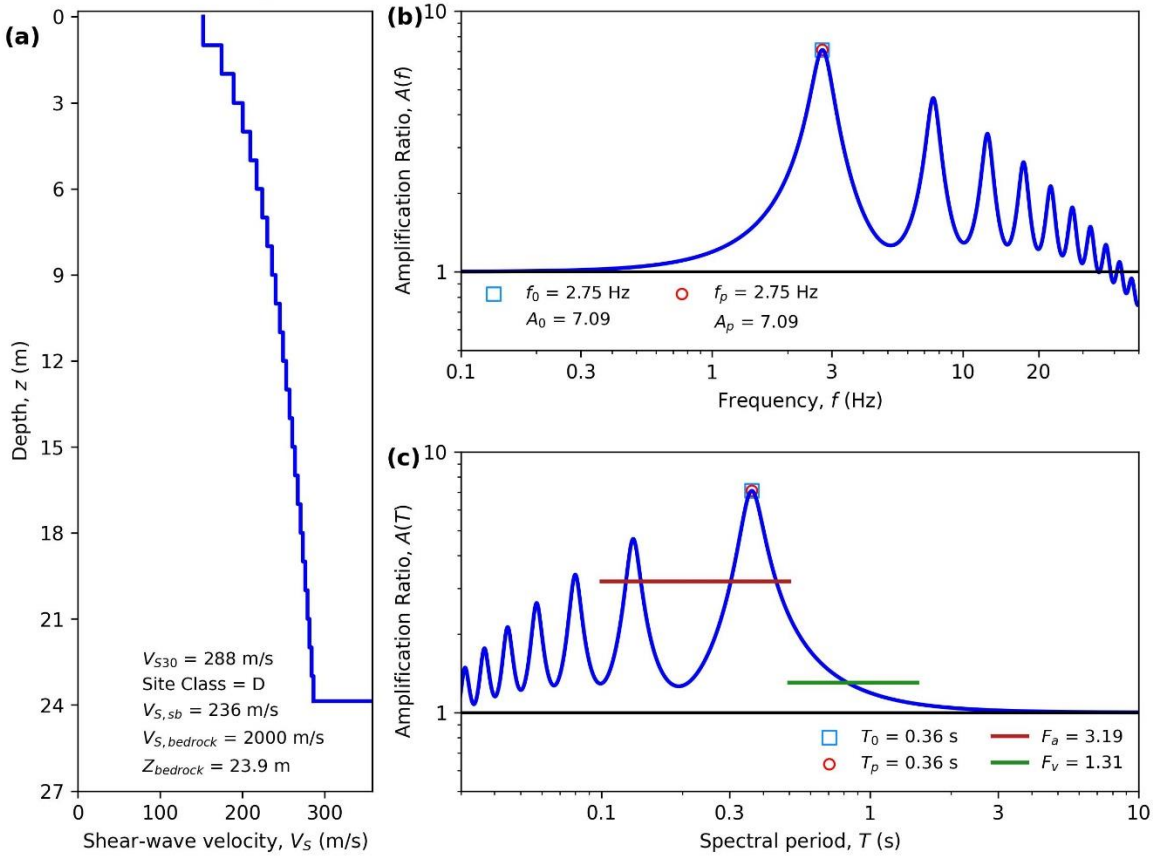

HAZUS Emergency Management
Massachusetts Care
Figure E65. ID: MA000065, Lat: 42.2536°, Lon: -72.2428°

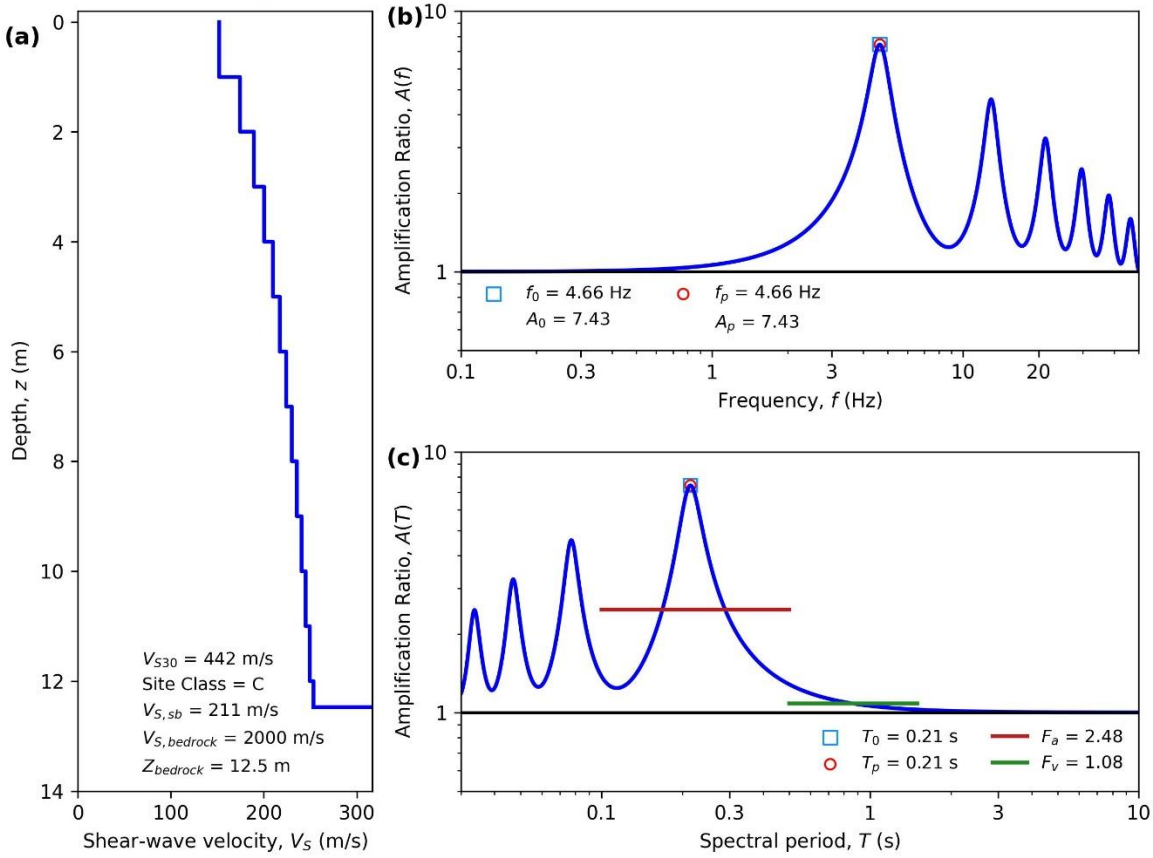

HAZUS Emergency Management
Massachusetts Care
Figure E66. ID: MA000066, Lat: 42.7277°, Lon: -71.1683°

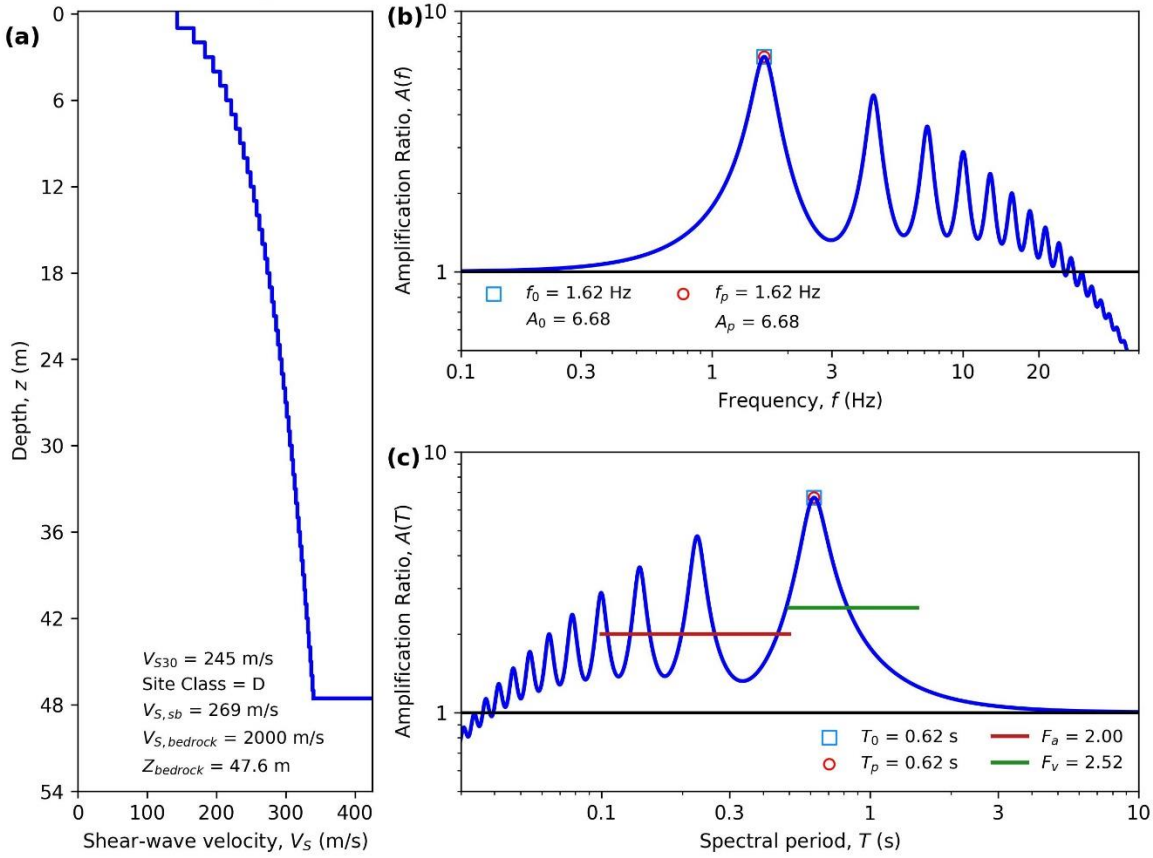

HAZUS Emergency Management
Massachusetts Care
Figure E67. ID: MA000067, Lat: 41.9017°, Lon: -70.9160°

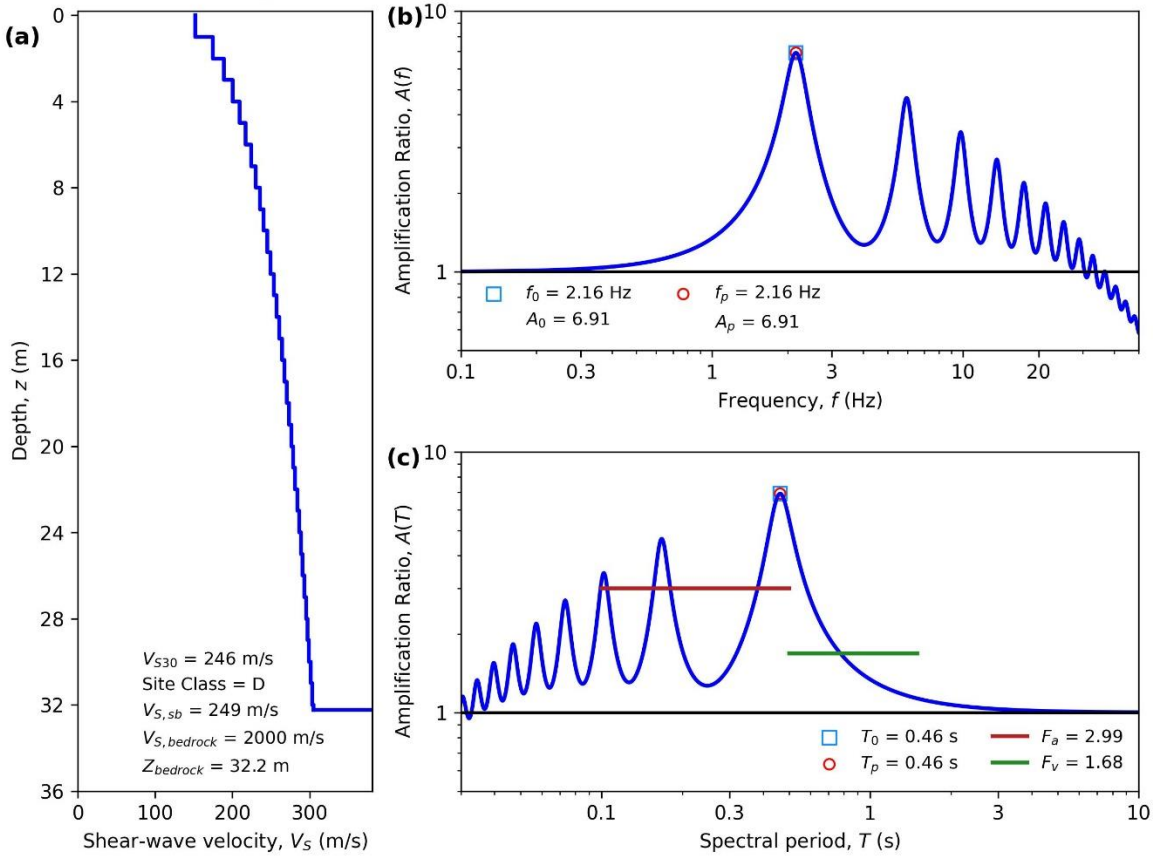

HAZUS Emergency Management
Massachusetts Care
Figure E68. ID: MA000068, Lat: 42.7785°, Lon: -71.0732°

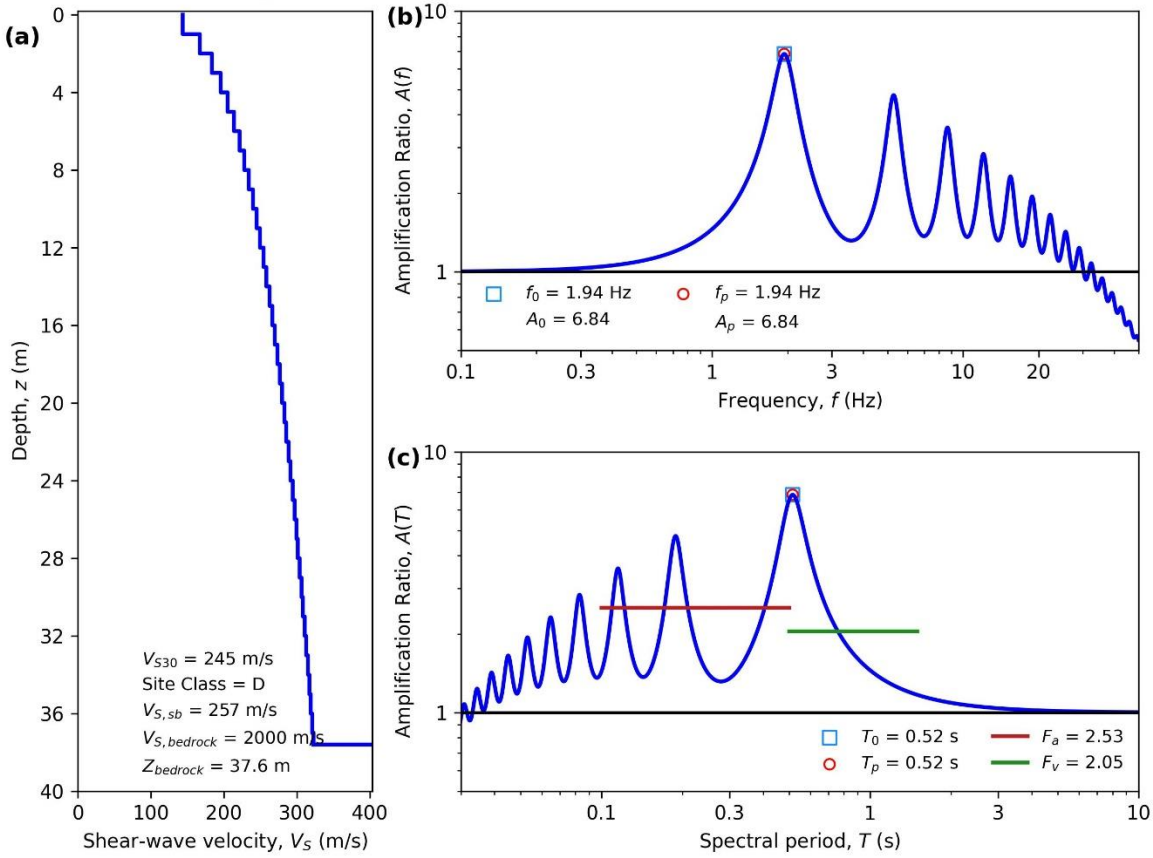

HAZUS Emergency Management
Massachusetts Care
Figure E69. ID: MA000069, Lat: 42.1205°, Lon: -72.5474°

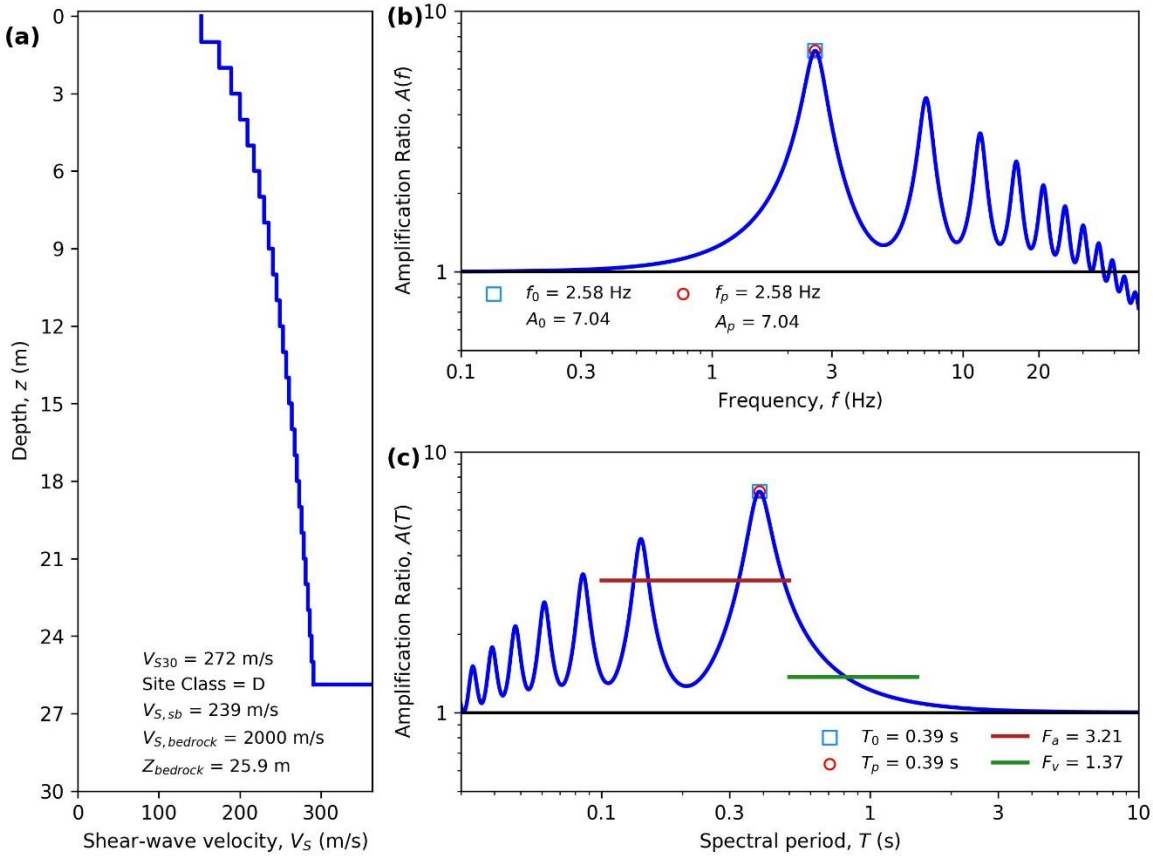

HAZUS Emergency Management
Massachusetts Care
Figure E70. ID: MA000070, Lat: 42.4634°, Lon: -71.1619°

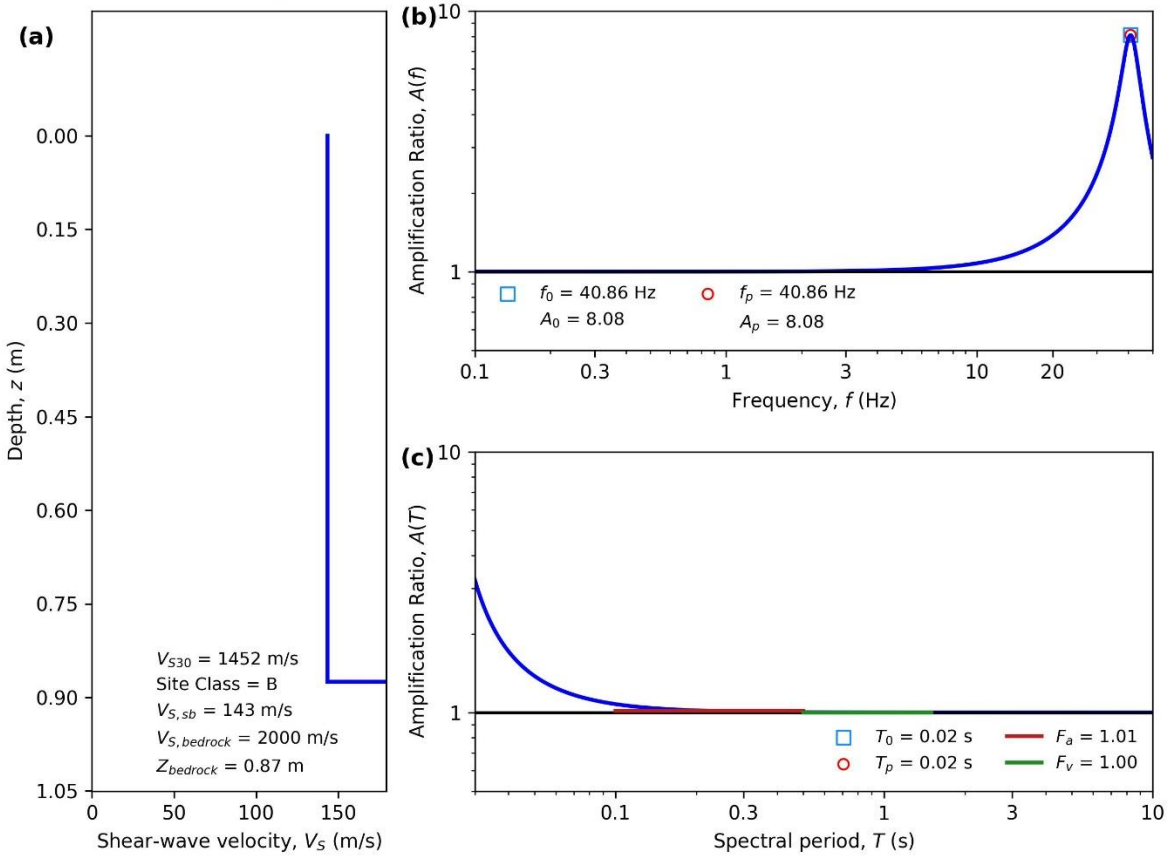

HAZUS Emergency Management
Massachusetts Care
Figure E71. ID: MA000071, Lat: 42.2513°, Lon: -71.0772°

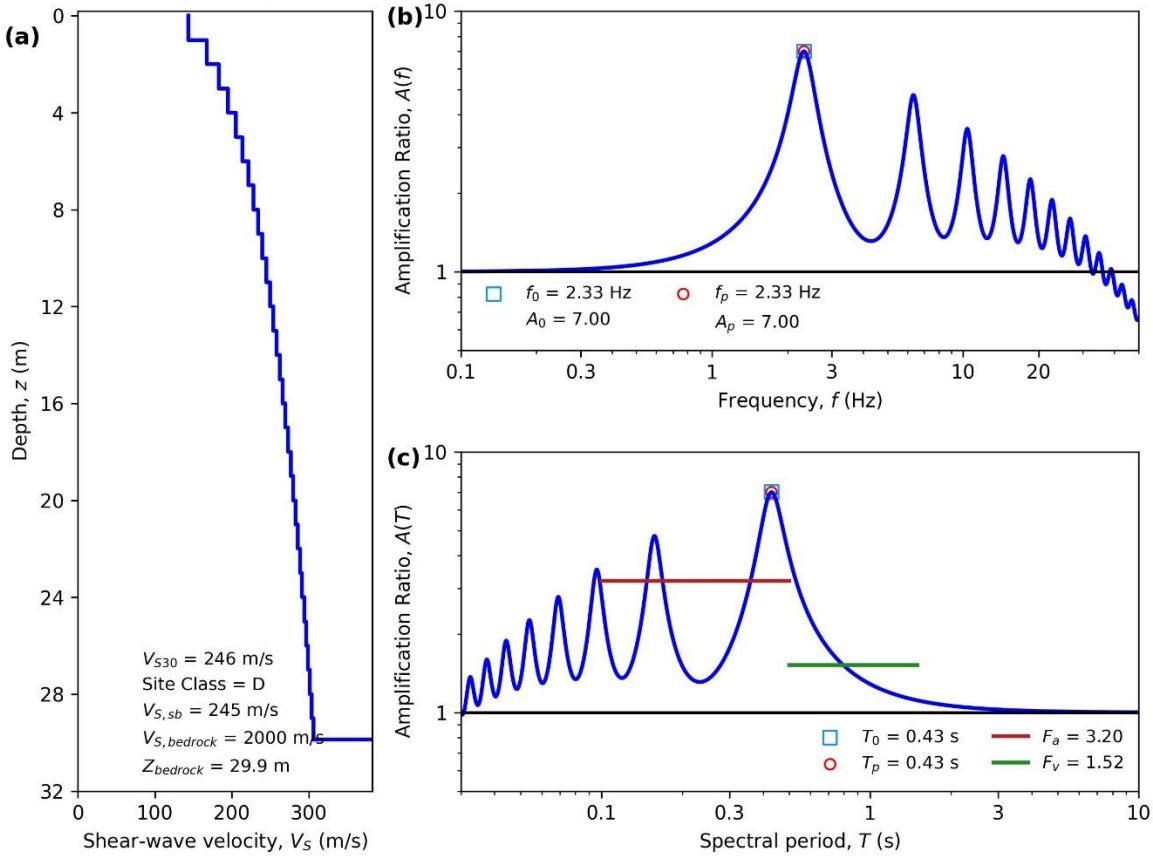

HAZUS Emergency Management
Massachusetts Care
Figure E72. ID: MA000072, Lat: 42.5372°, Lon: -70.9464°

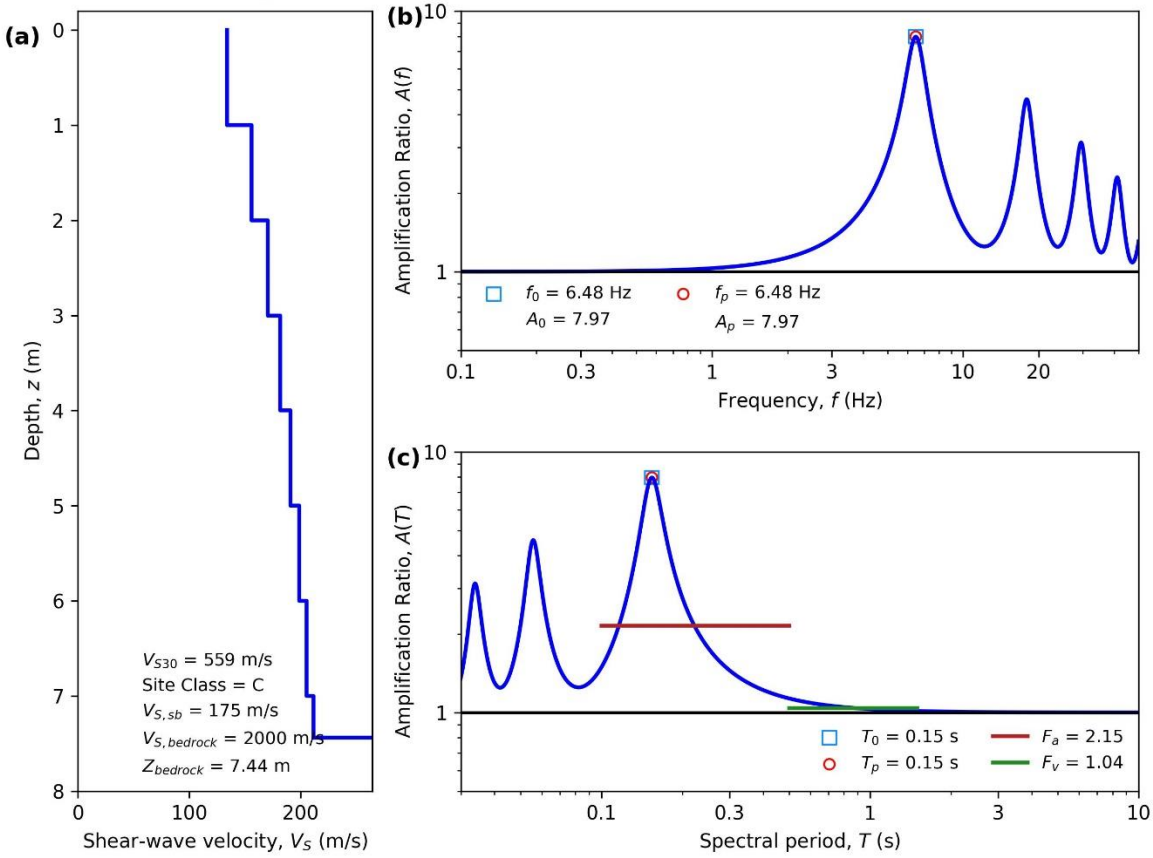

HAZUS Emergency Management
Massachusetts Care
Figure E73. ID: MA000073, Lat: 42.0786°, Lon: -72.0421°

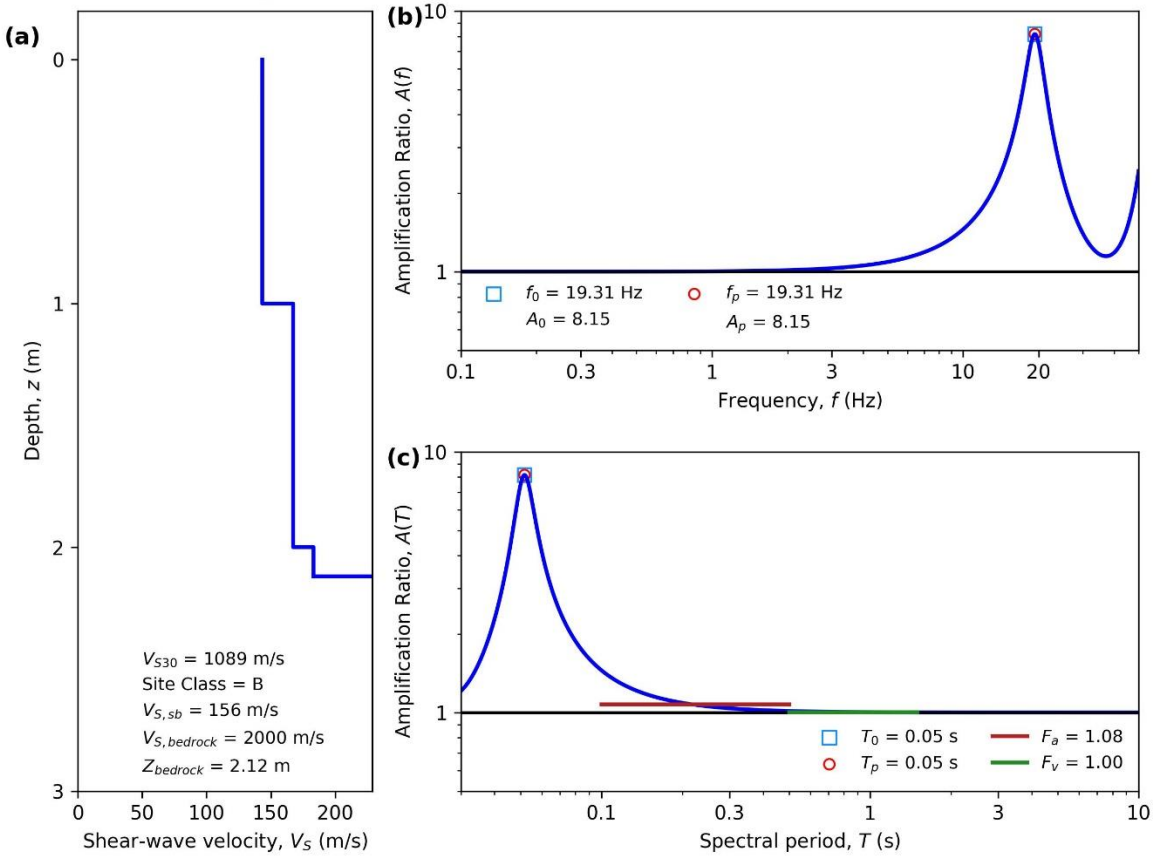

HAZUS Emergency Management
Massachusetts Care
Figure E74. ID: MA000074, Lat: 42.3302°, Lon: -72.6532°

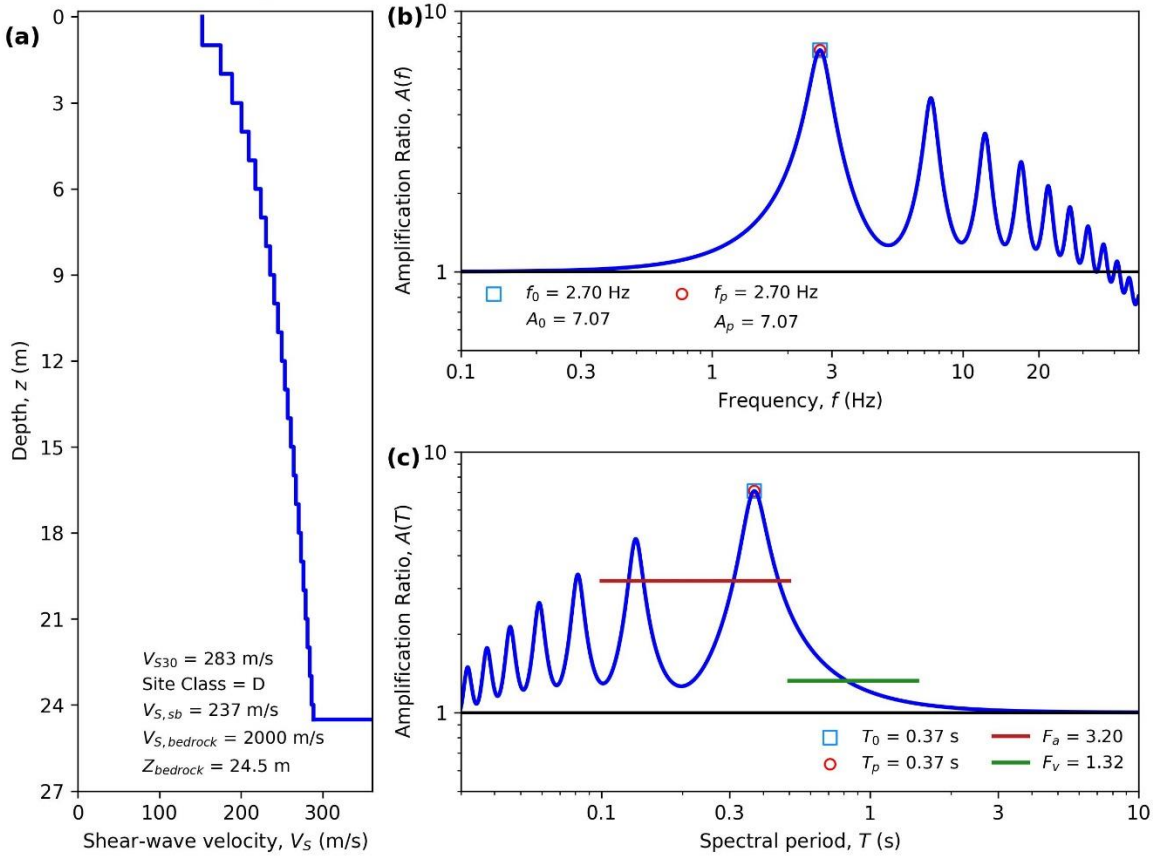

HAZUS Emergency Management
Massachusetts Care
Figure E75. ID: MA000075, Lat: 41.7561°, Lon: -70.7144°

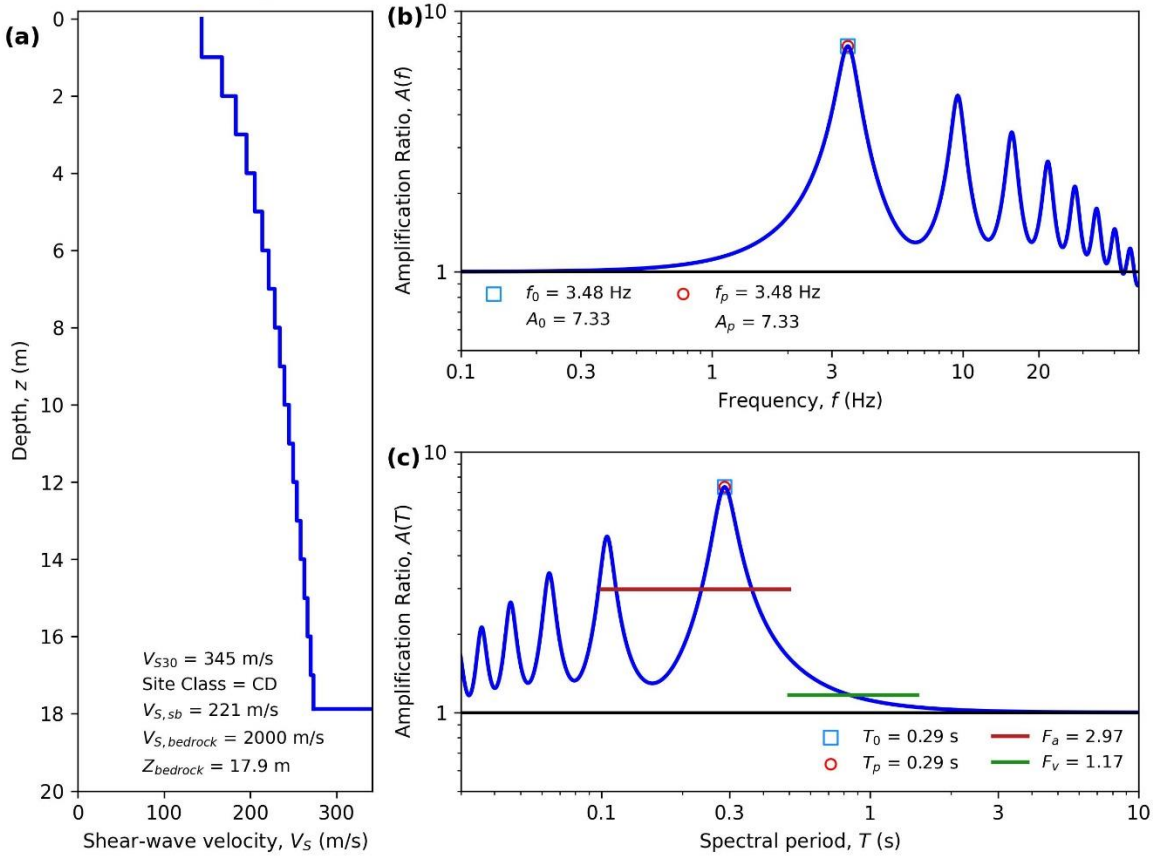

HAZUS Emergency Management
Massachusetts Care
Figure E76. ID: MA000076, Lat: 41.9428°, Lon: -70.6451°

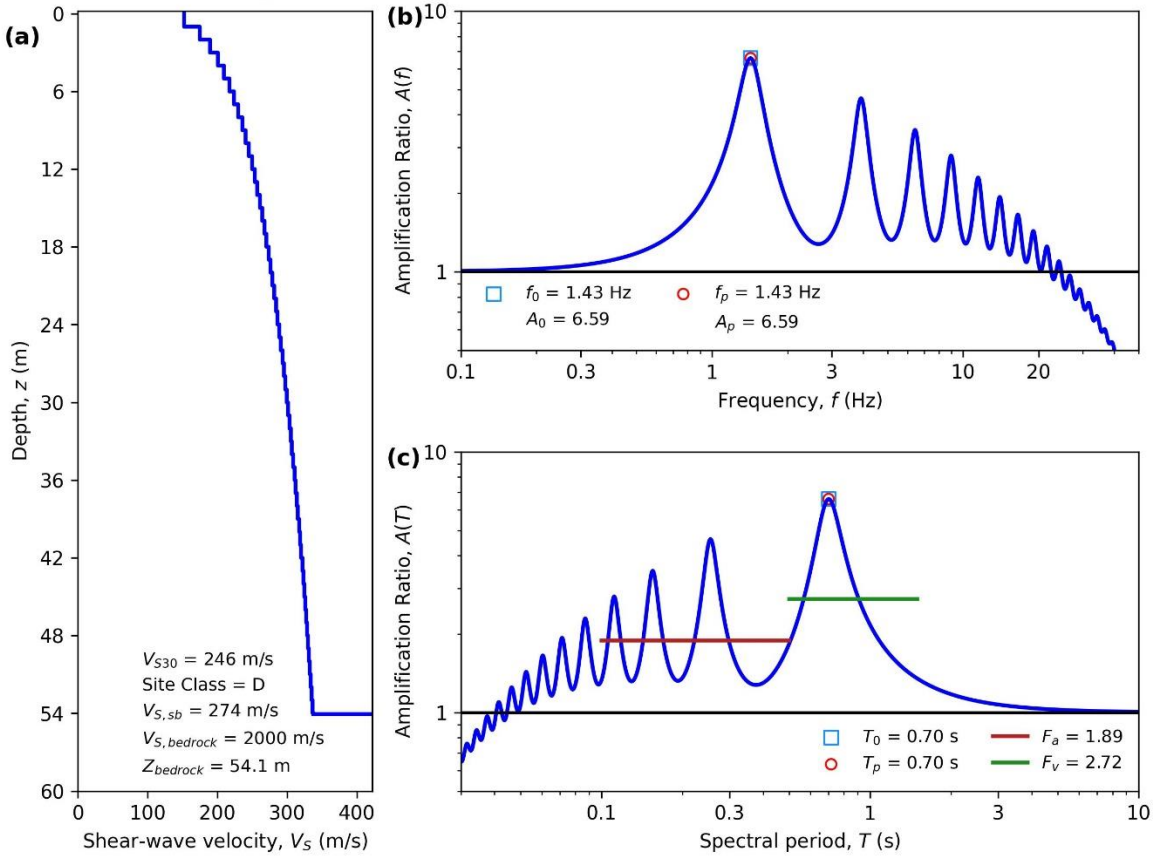

HAZUS Emergency Management
Massachusetts Care
Figure E77. ID: MA000077, Lat: 42.3297°, Lon: -71.1077°

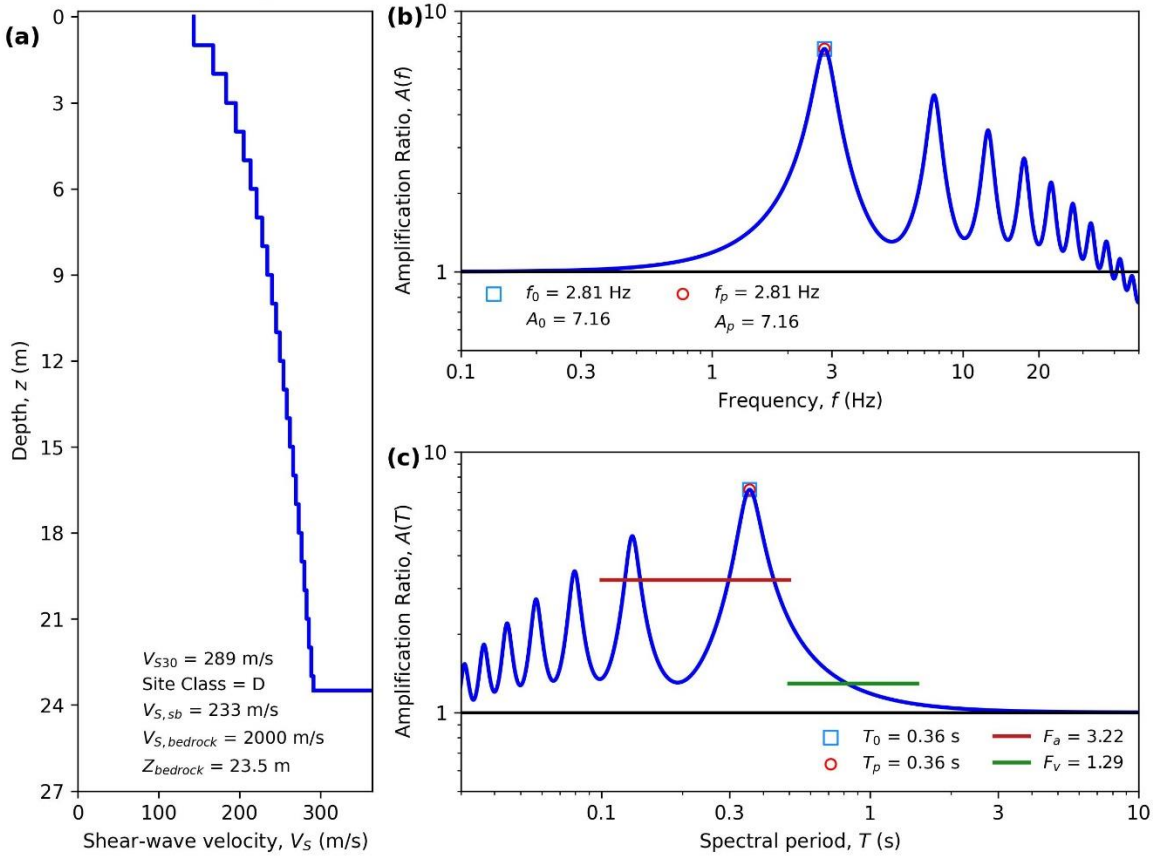

HAZUS Emergency Management
Massachusetts Care
Figure E78. ID: MA000078, Lat: 42.7653°, Lon: -71.0448°

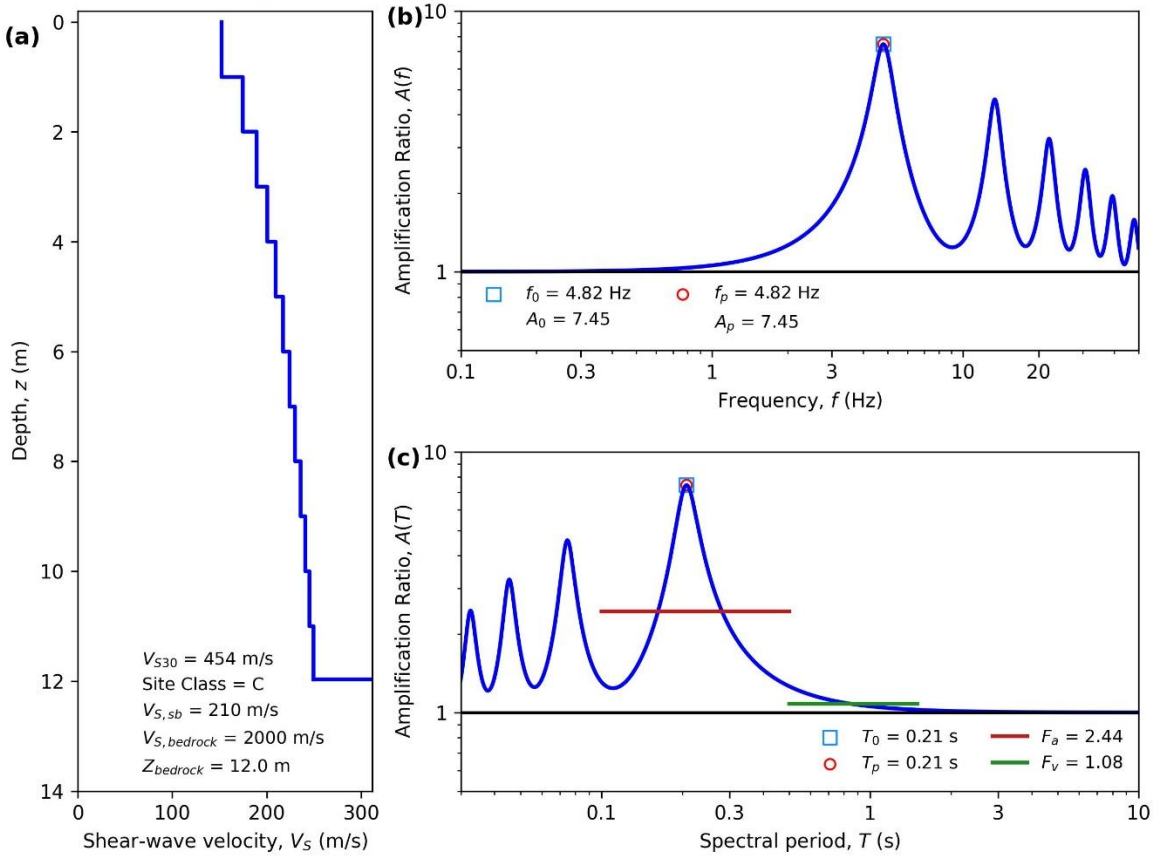

HAZUS Emergency Management
Massachusetts Care
Figure E79. ID: MA000079, Lat: 42.3626°, Lon: -71.0693°

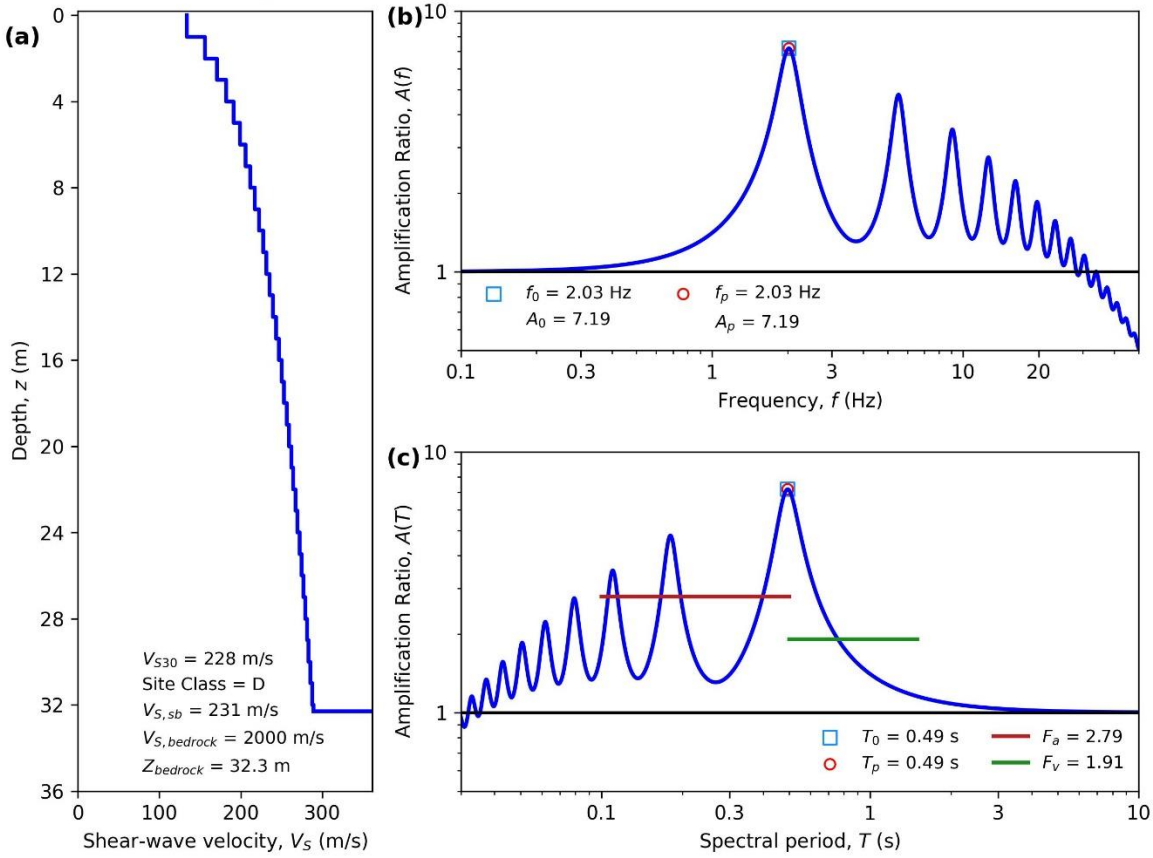

HAZUS Emergency Management
Massachusetts Care
Figure E80. ID: MA000080, Lat: 42.3691°, Lon: -71.2496°

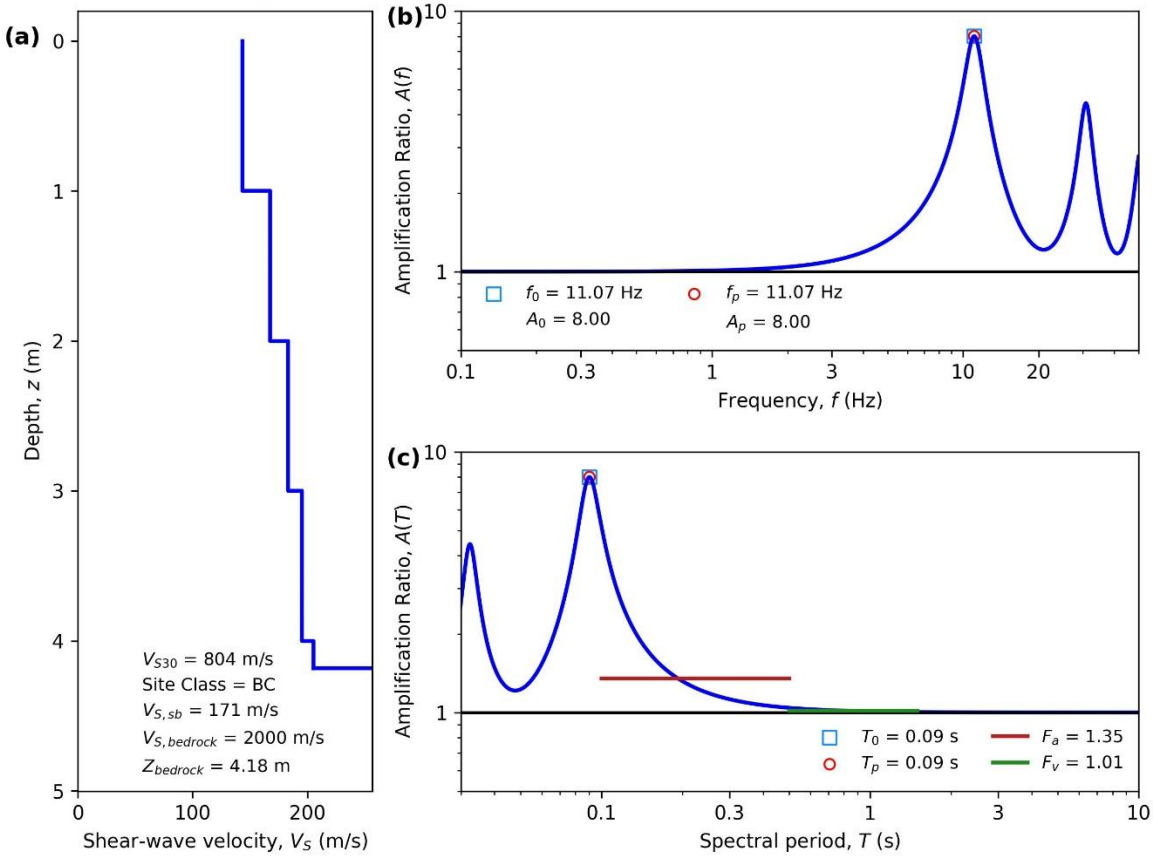

HAZUS Emergency Management
Massachusetts Care
Figure E81. ID: MA000081, Lat: 42.1007°, Lon: -71.0816°

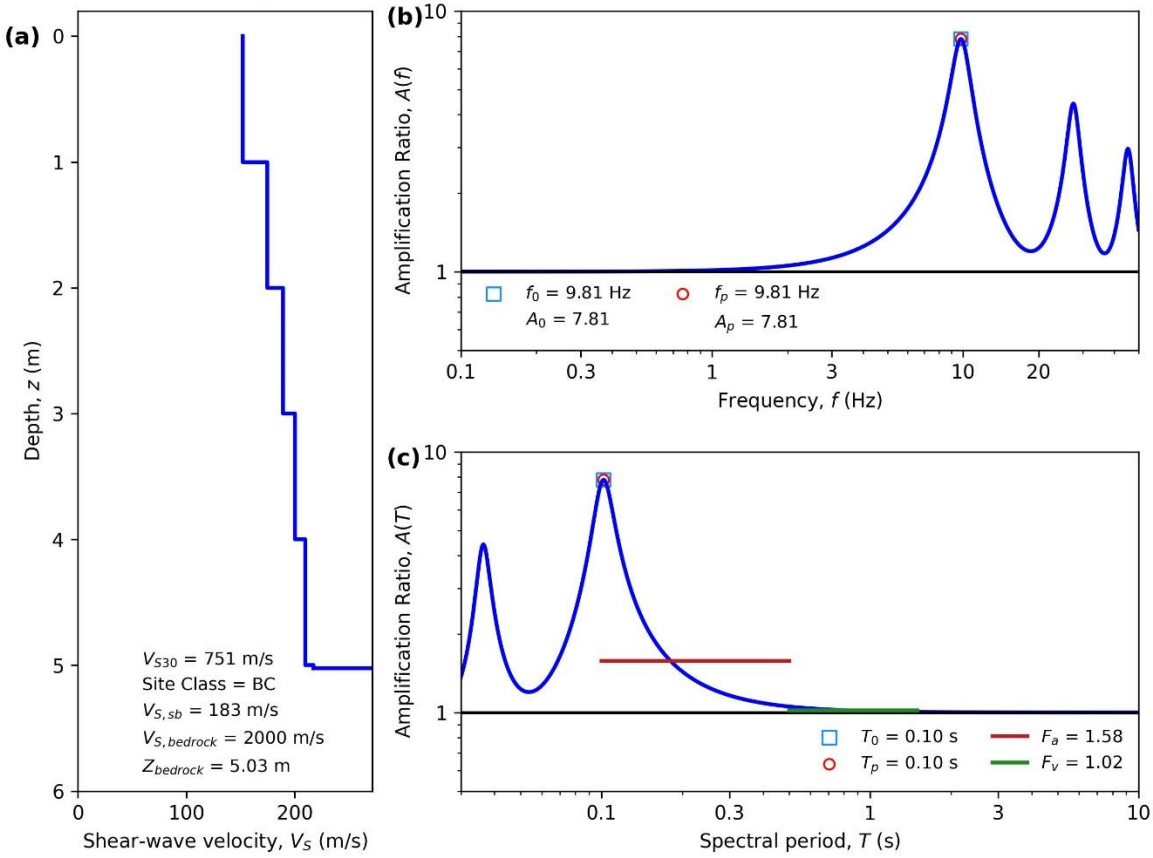

HAZUS Emergency Management
Massachusetts Care
Figure E82. ID: MA000082, Lat: 42.6452°, Lon: -71.3669°

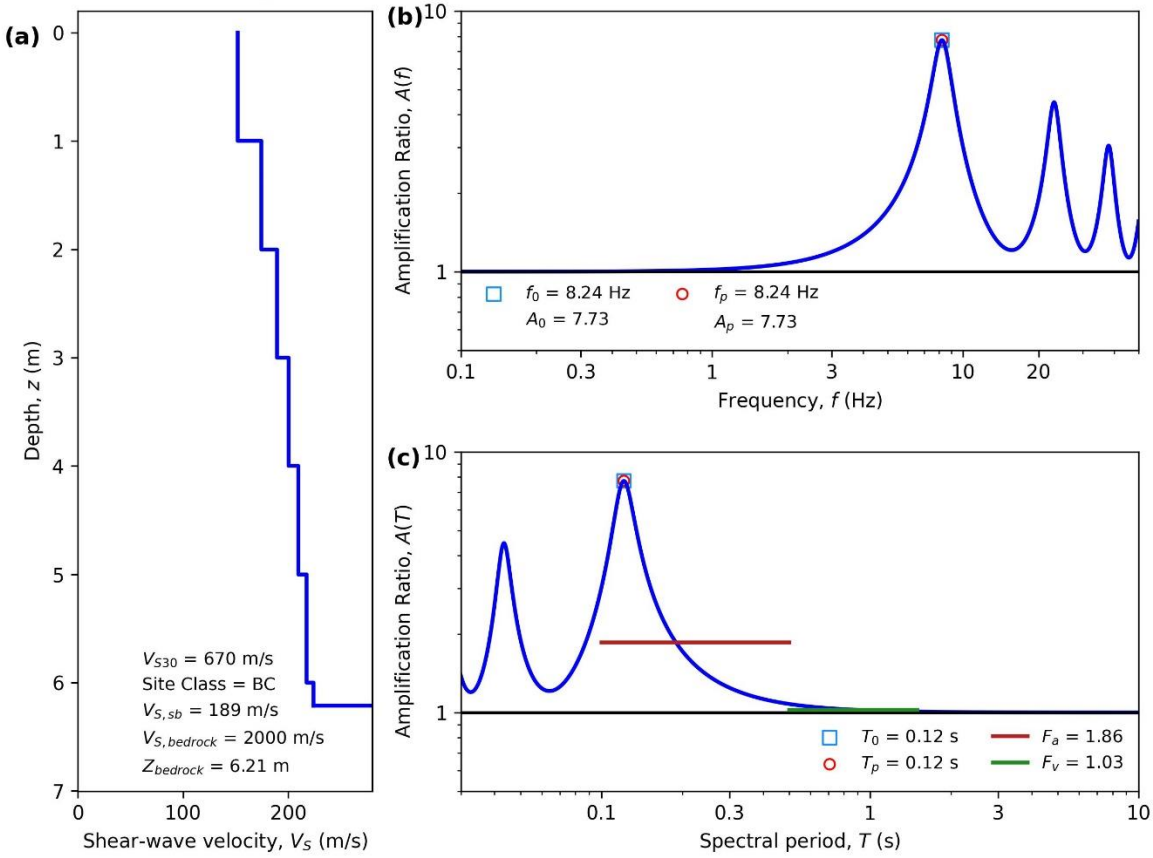

HAZUS Emergency Management
Massachusetts Care
Figure E83. ID: MA000083, Lat: 42.5610°, Lon: -70.8872°

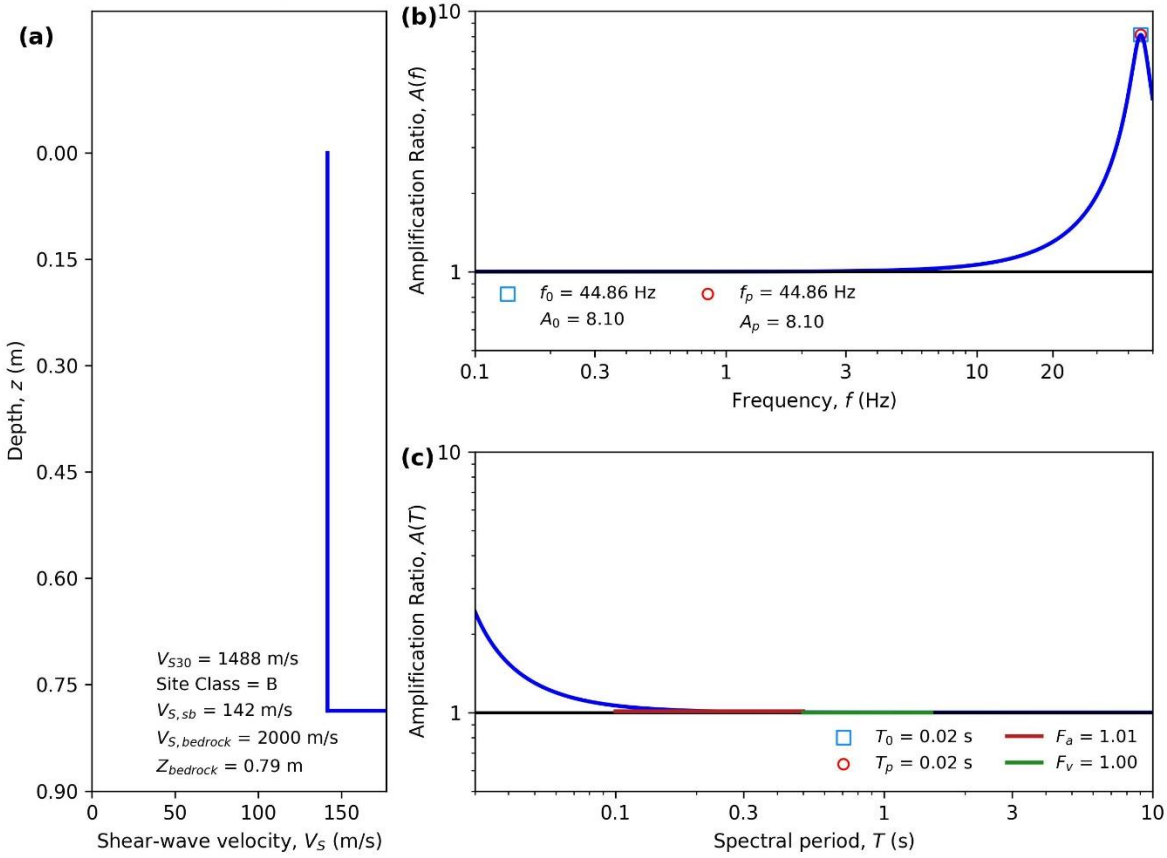

HAZUS Emergency Management
Massachusetts Care
Figure E84. ID: MA000084, Lat: 41.6727°, Lon: -70.9847°

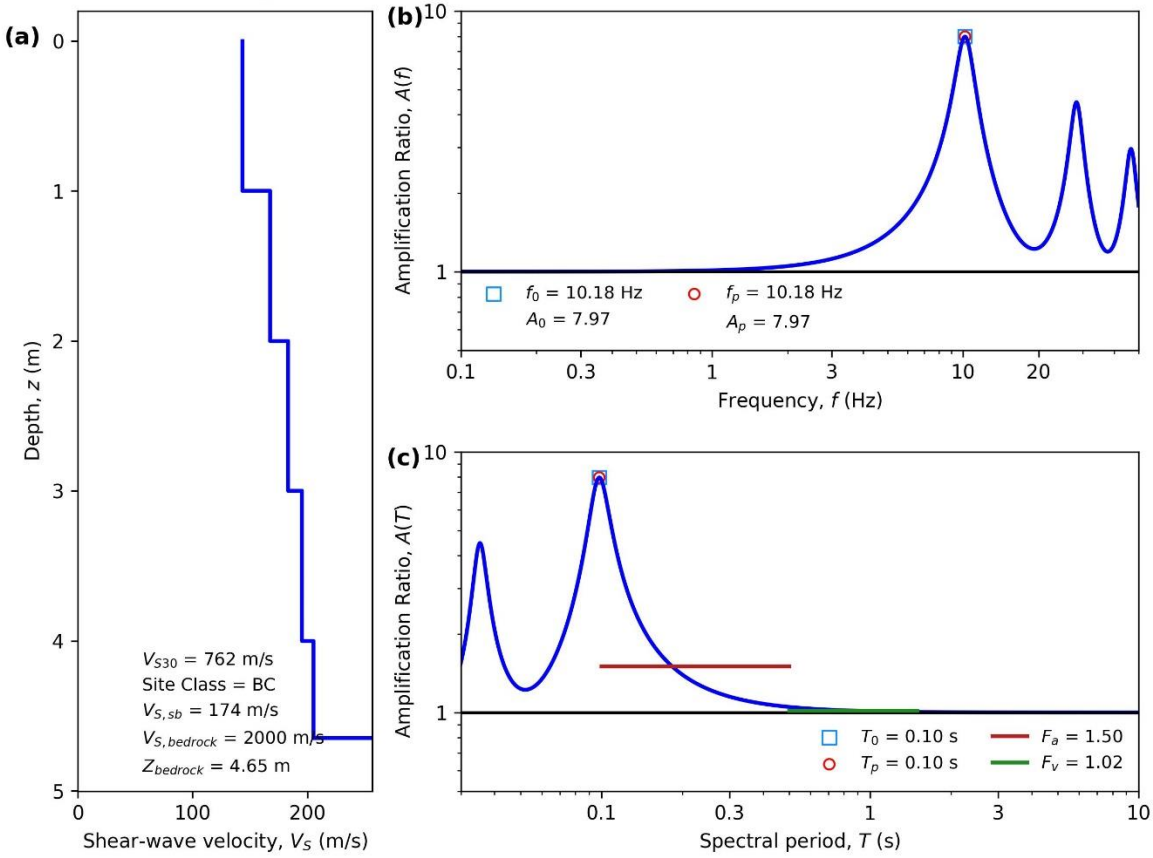

HAZUS Emergency Management
Massachusetts Care
Figure E85. ID: MA000085, Lat: 42.3487°, Lon: -71.1485°

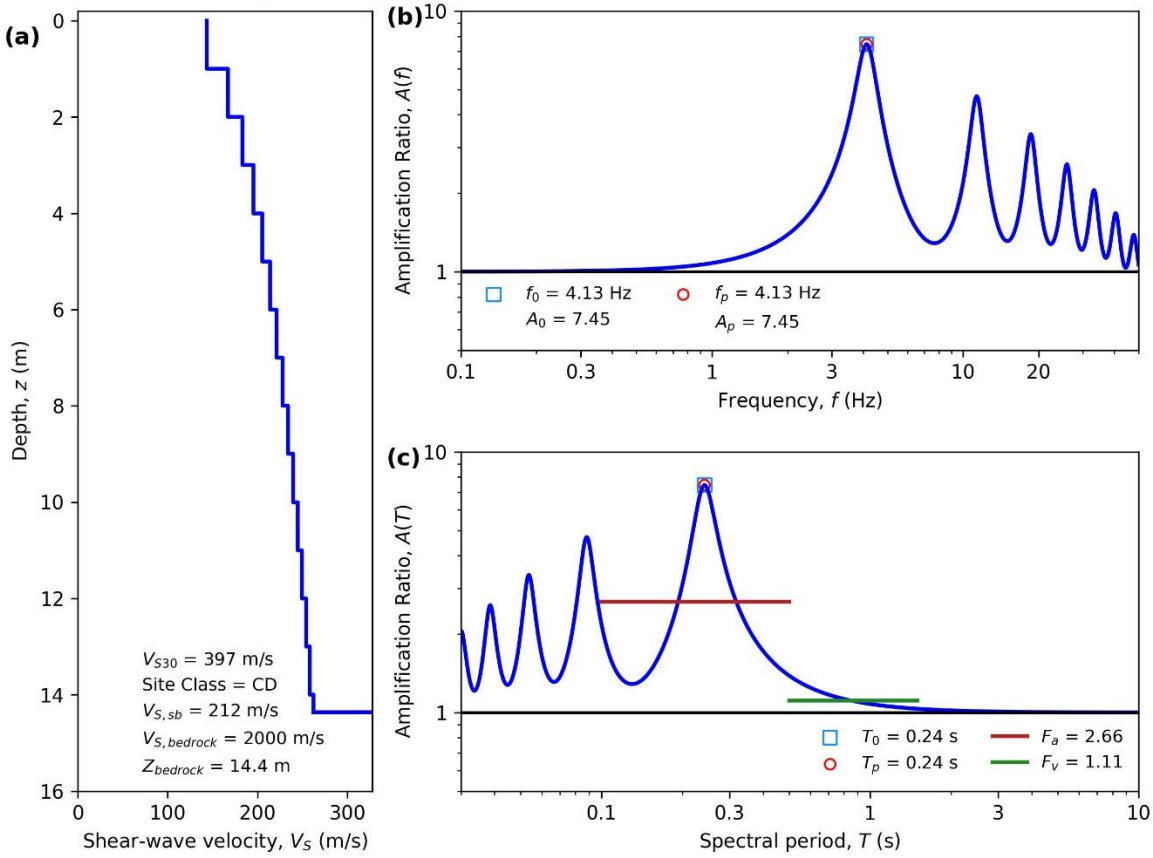

HAZUS Emergency Management
Massachusetts Care
Figure E86. ID: MA000086, Lat: 42.3496°, Lon: -72.6824°

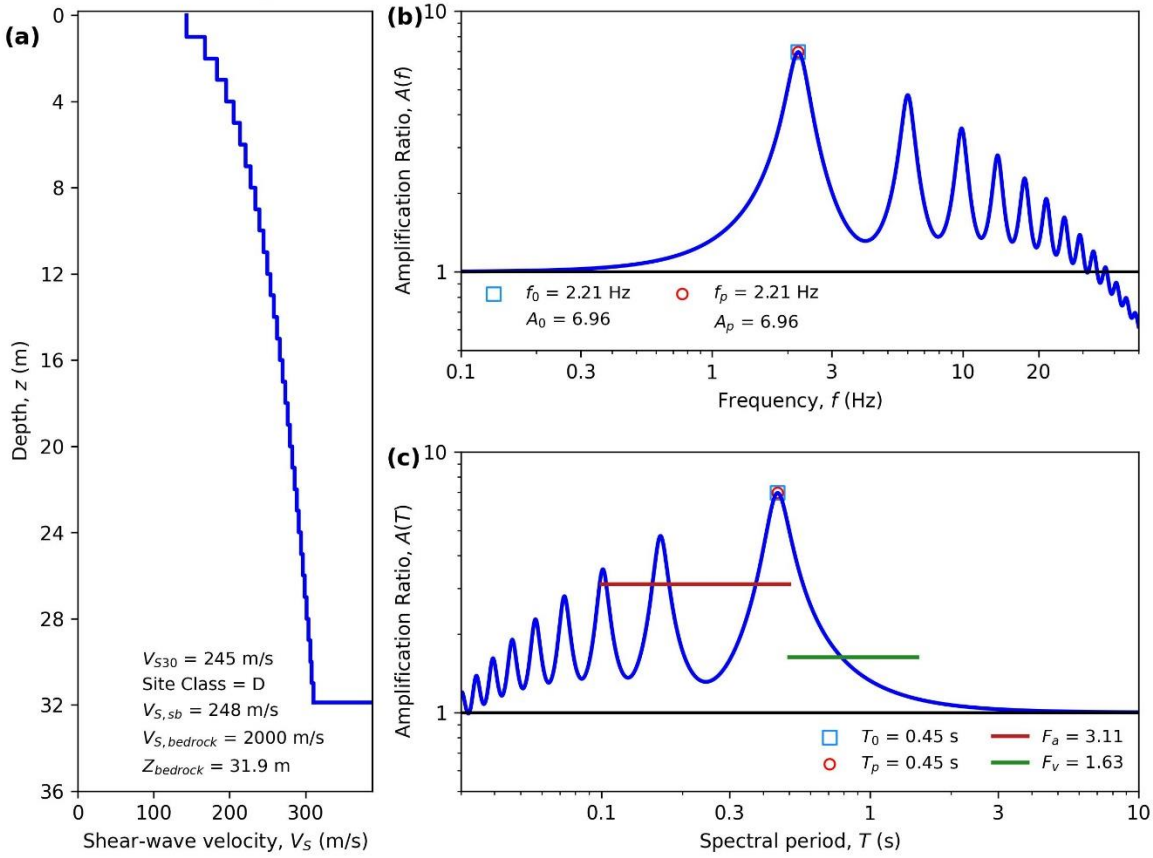

HAZUS Emergency Management
Massachusetts Care
Figure E87. ID: MA000087, Lat: 42.6472°, Lon: -71.3421°

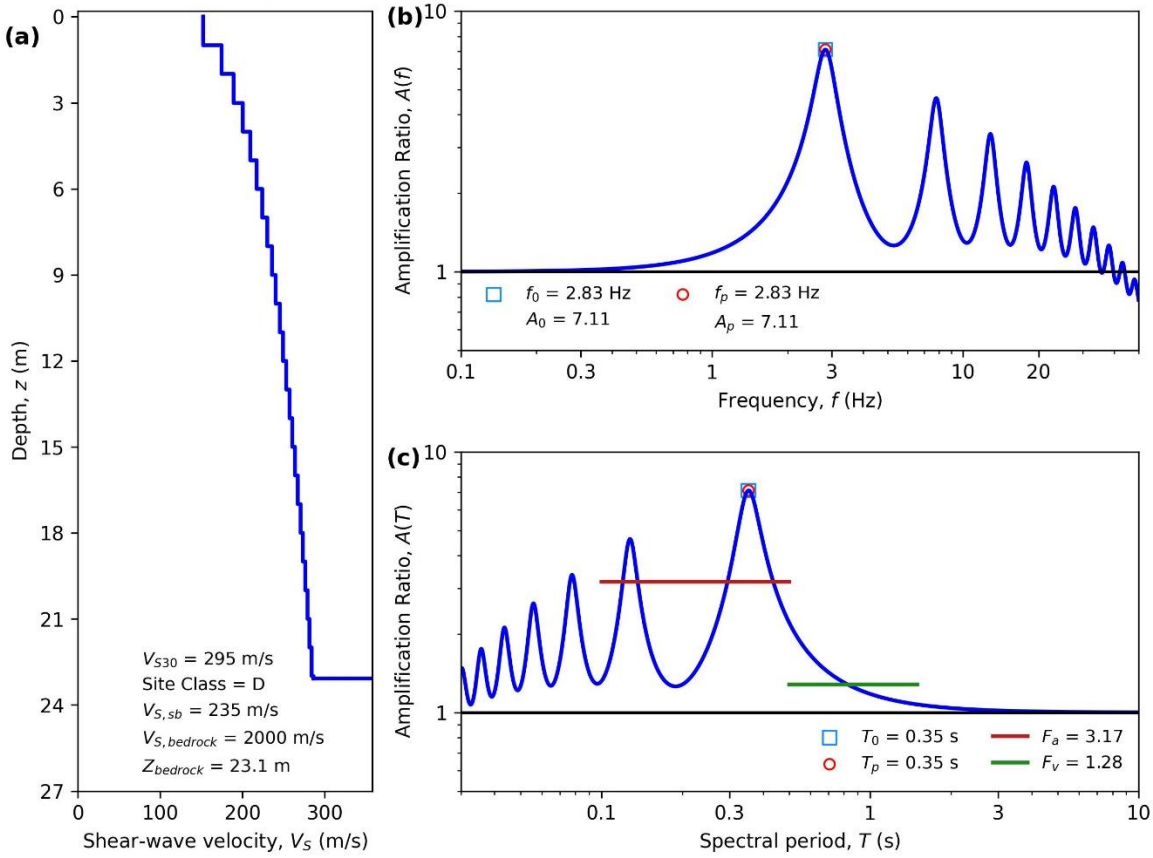

HAZUS Emergency Management
Massachusetts Care
Figure E88. ID: MA000088, Lat: 41.9127°, Lon: -71.1022°

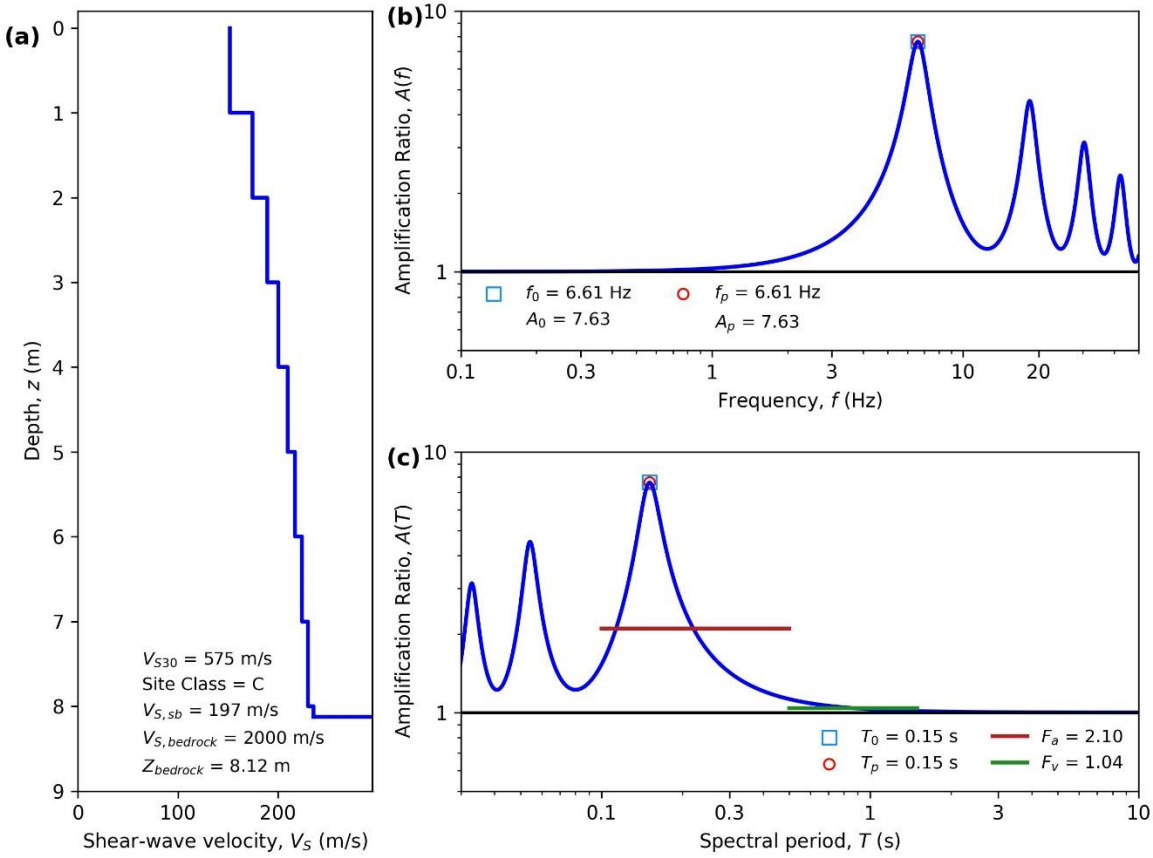

HAZUS Emergency Management
Massachusetts Care
Figure E89. ID: MA000089, Lat: 42.6071°, Lon: -71.2182°

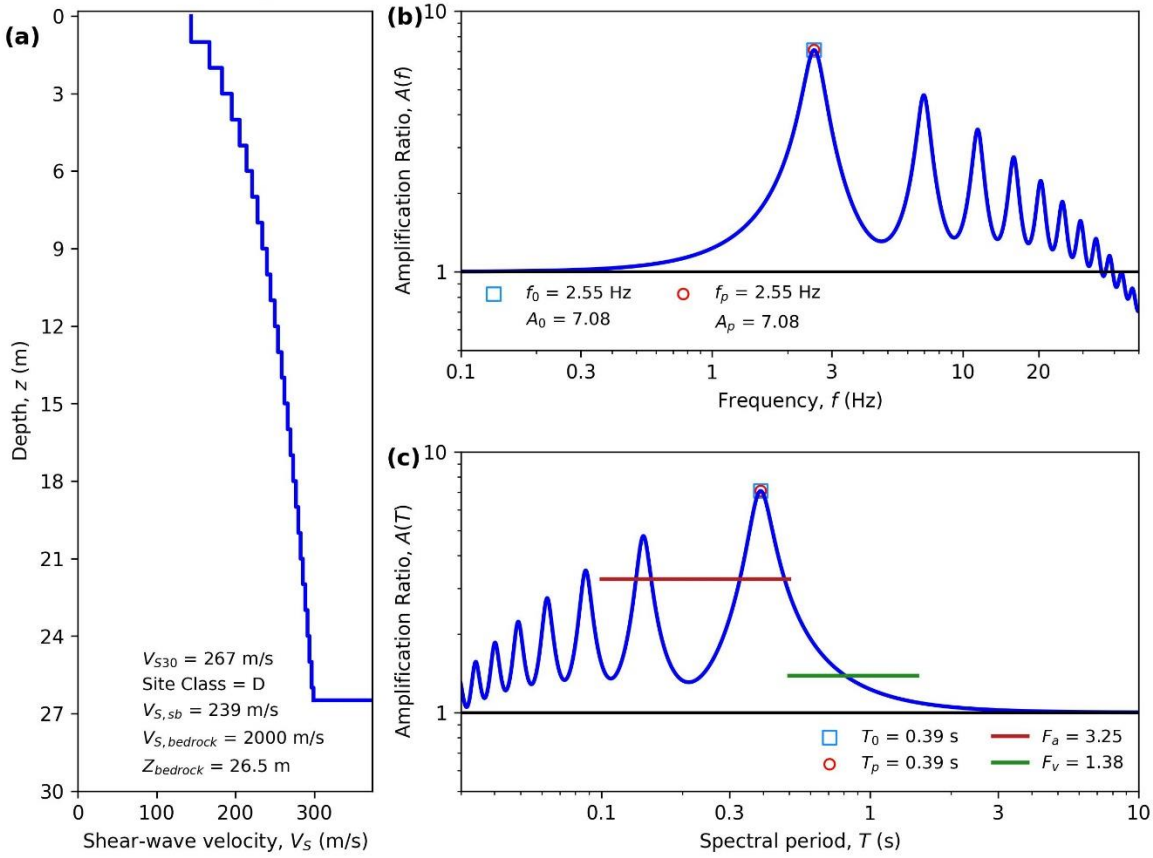

HAZUS Emergency Management
Massachusetts Care
Figure E90. ID: MA000090, Lat: 42.5641°, Lon: -70.8757°

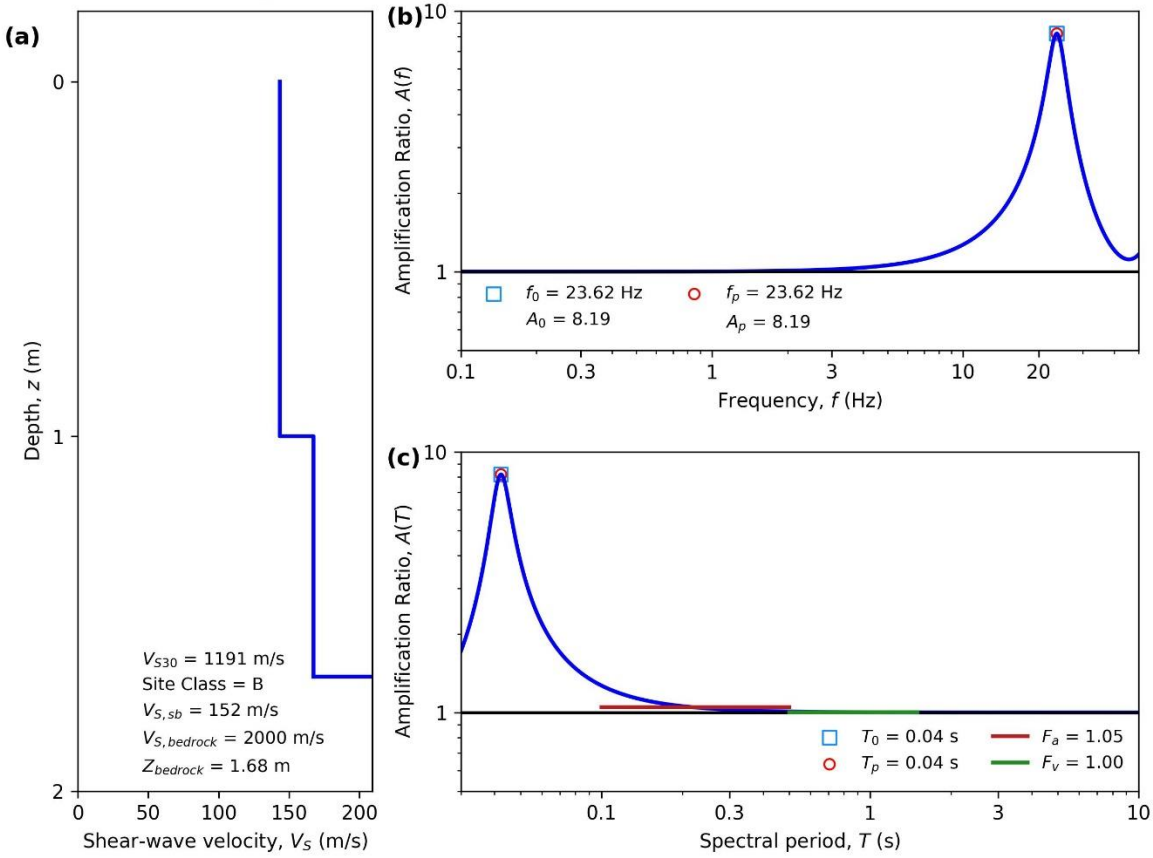

HAZUS Emergency Management
Massachusetts Care
Figure E91. ID: MA000091, Lat: 42.5111°, Lon: -70.9068°

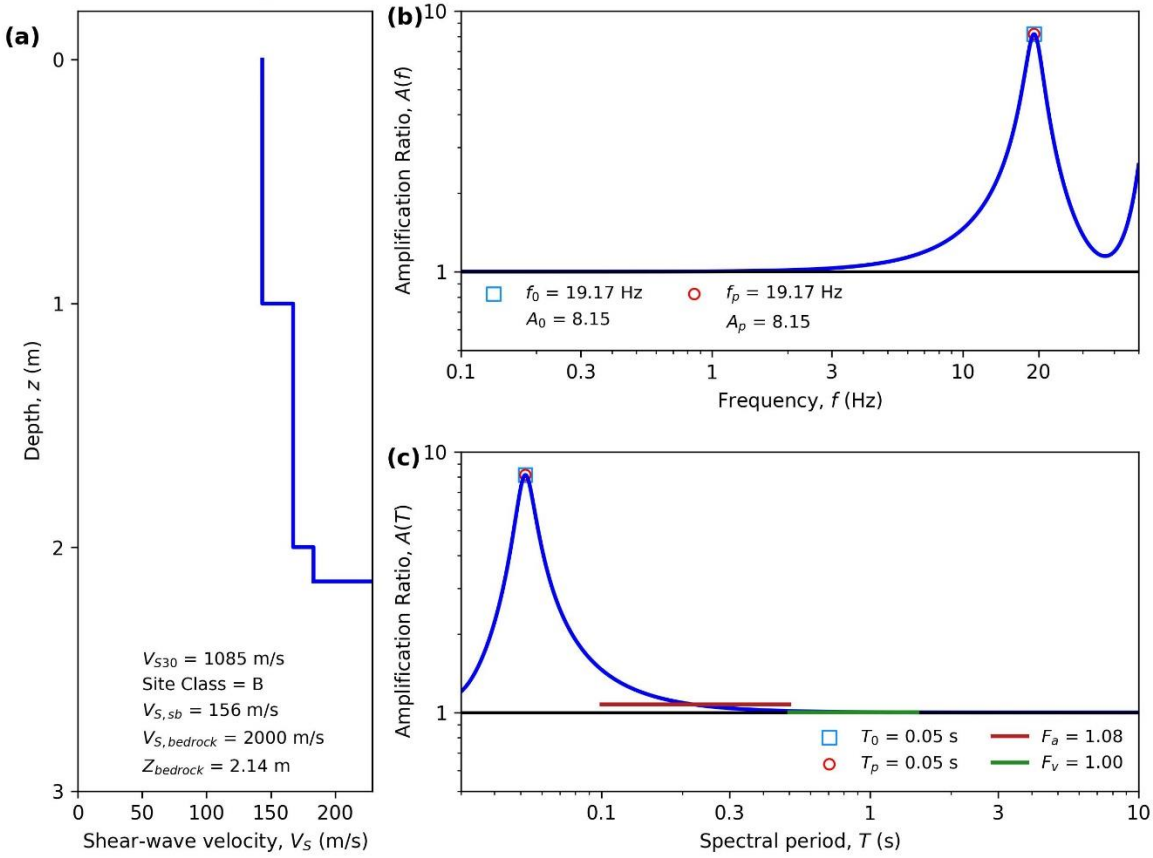

HAZUS Emergency Management
Massachusetts Care
Figure E92. ID: MA000092, Lat: 42.4259°, Lon: -71.1114°

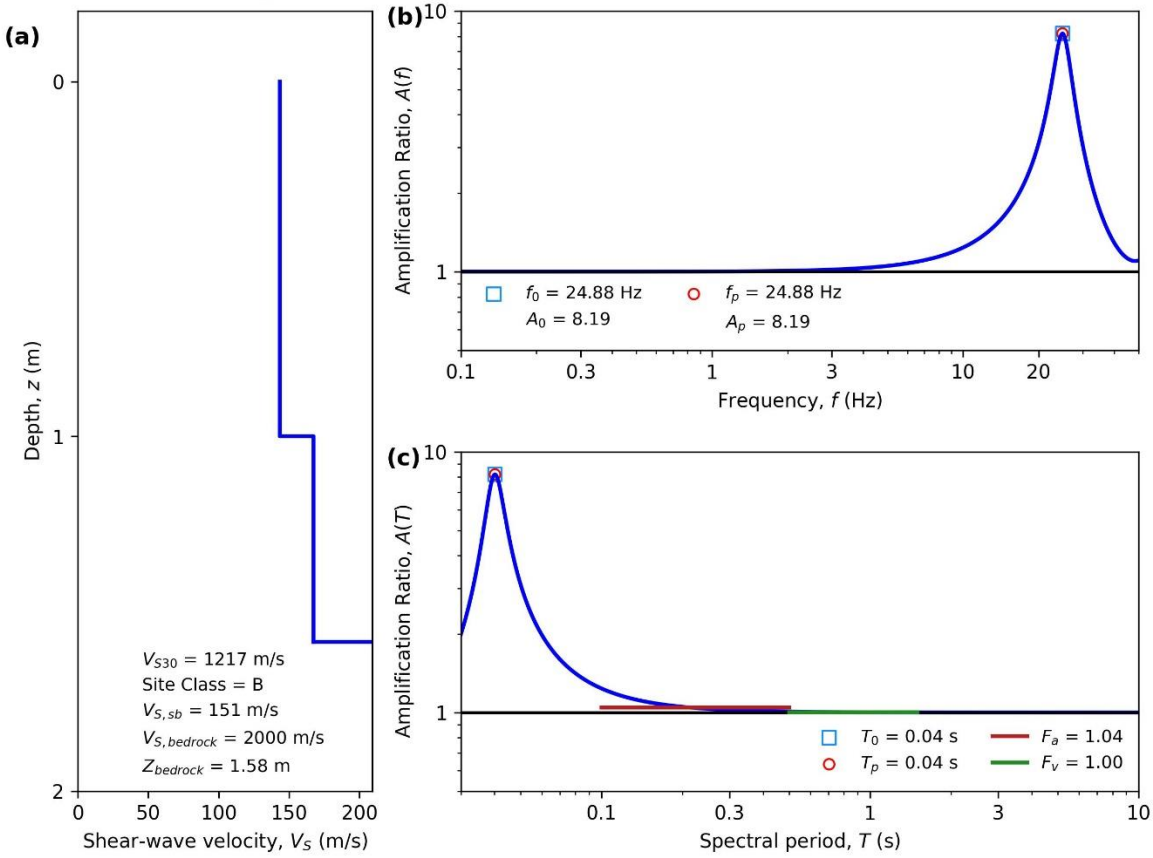

HAZUS Emergency Management
Massachusetts Care
Figure E93. ID: MA000093, Lat: 42.2746°, Lon: -71.1717°

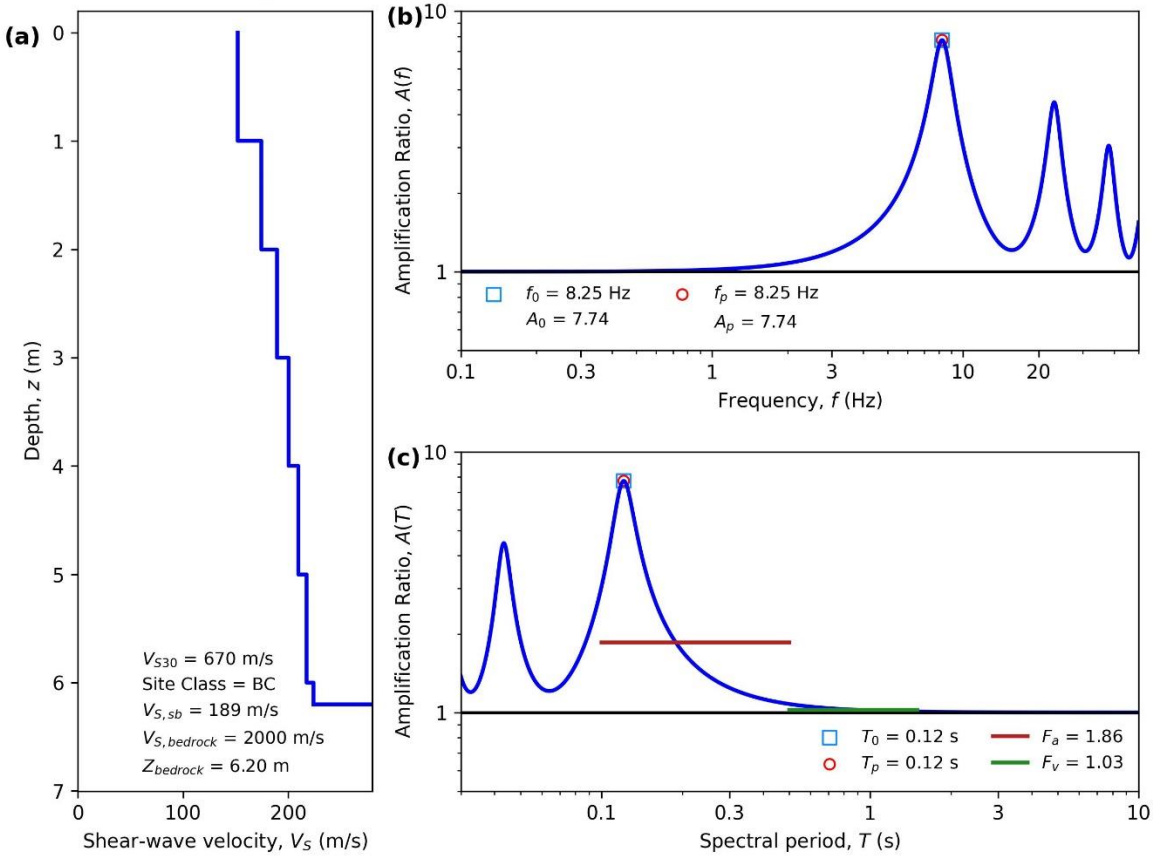

HAZUS Emergency Management
Massachusetts Care
Figure E94. ID: MA000094, Lat: 42.7052°, Lon: -71.0111°

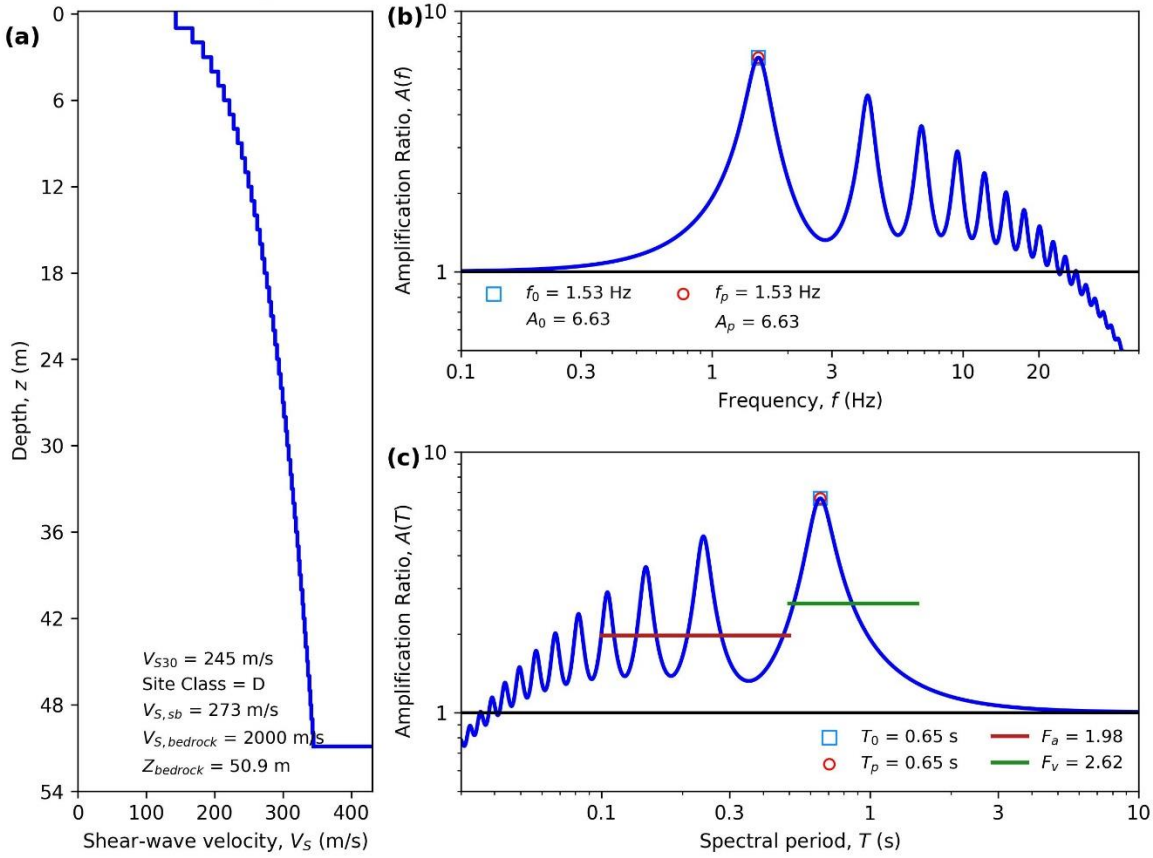

HAZUS Emergency Management
Massachusetts Care
Figure E95. ID: MA000095, Lat: 42.3270°, Lon: -71.1103°

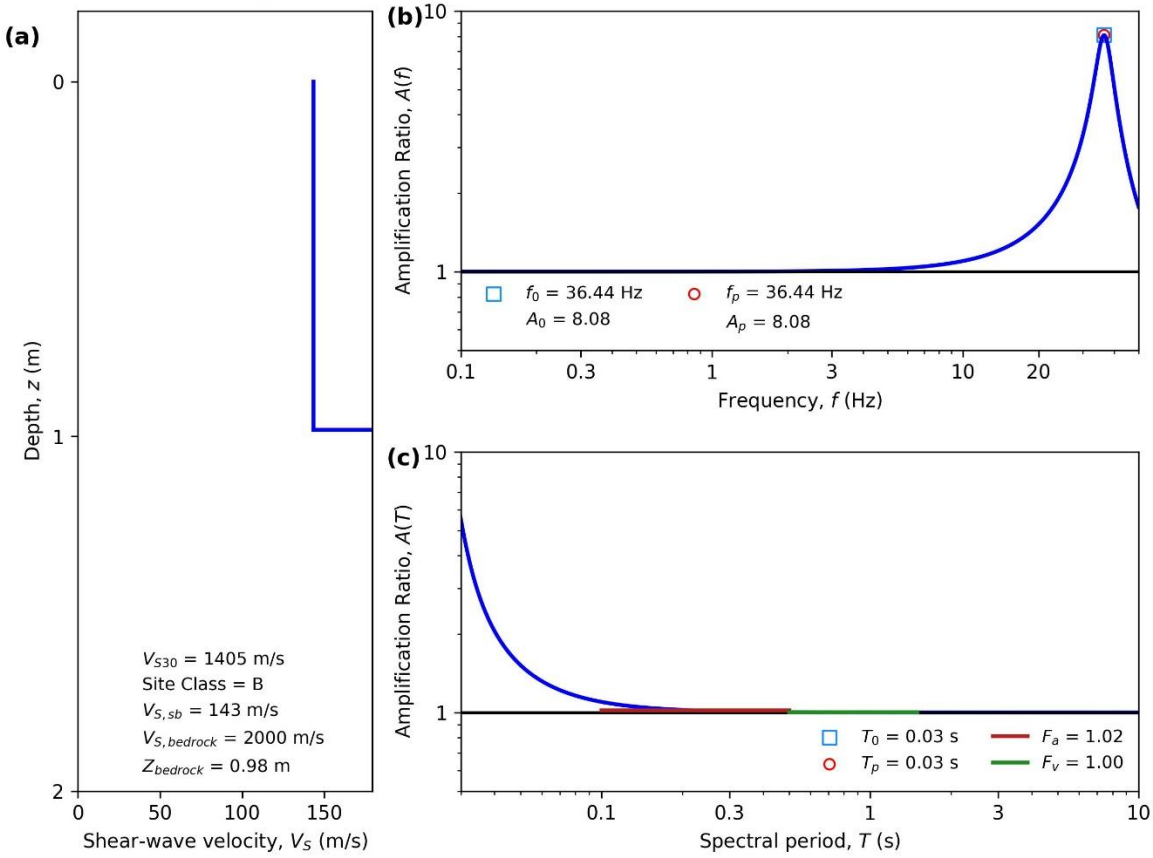

HAZUS Emergency Management
Massachusetts Care
Figure E96. ID: MA000096, Lat: 41.8944°, Lon: -70.9145°

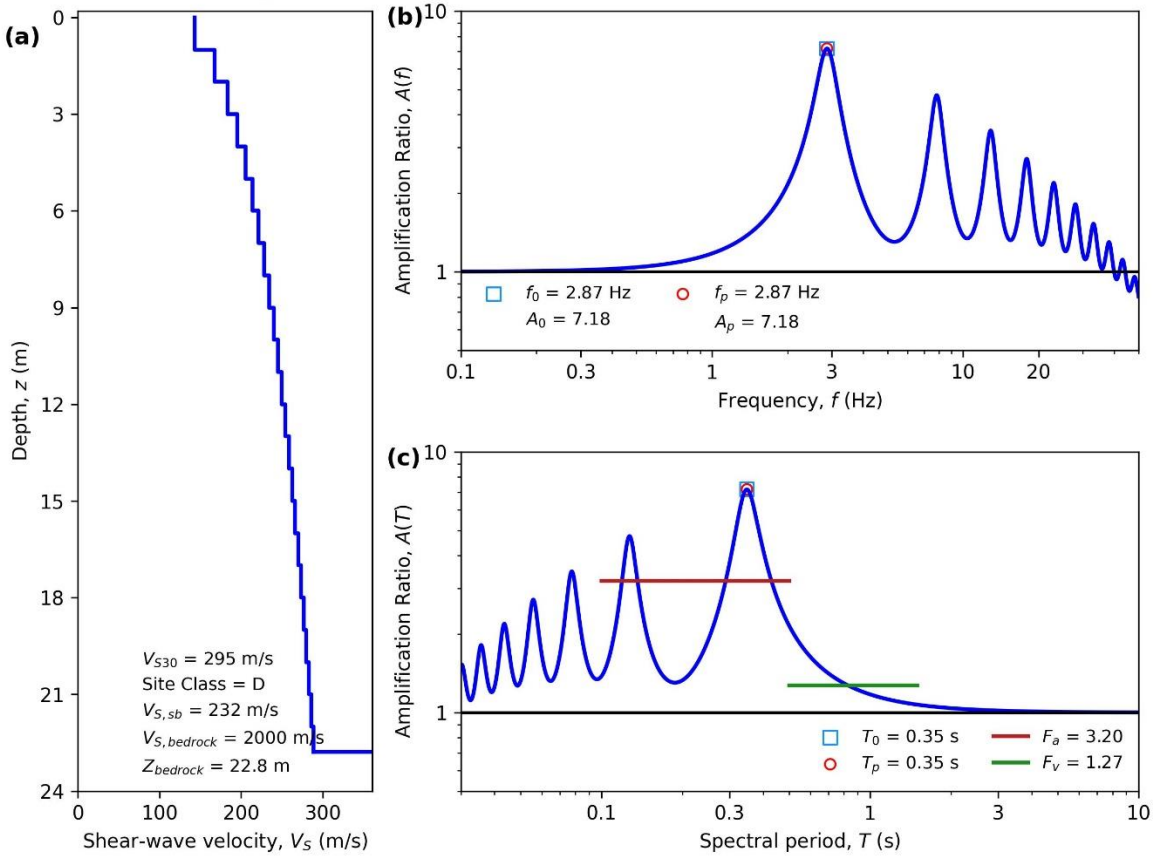

HAZUS Emergency Management
Massachusetts Care
Figure E97. ID: MA000097, Lat: 42.2765°, Lon: -71.5678°

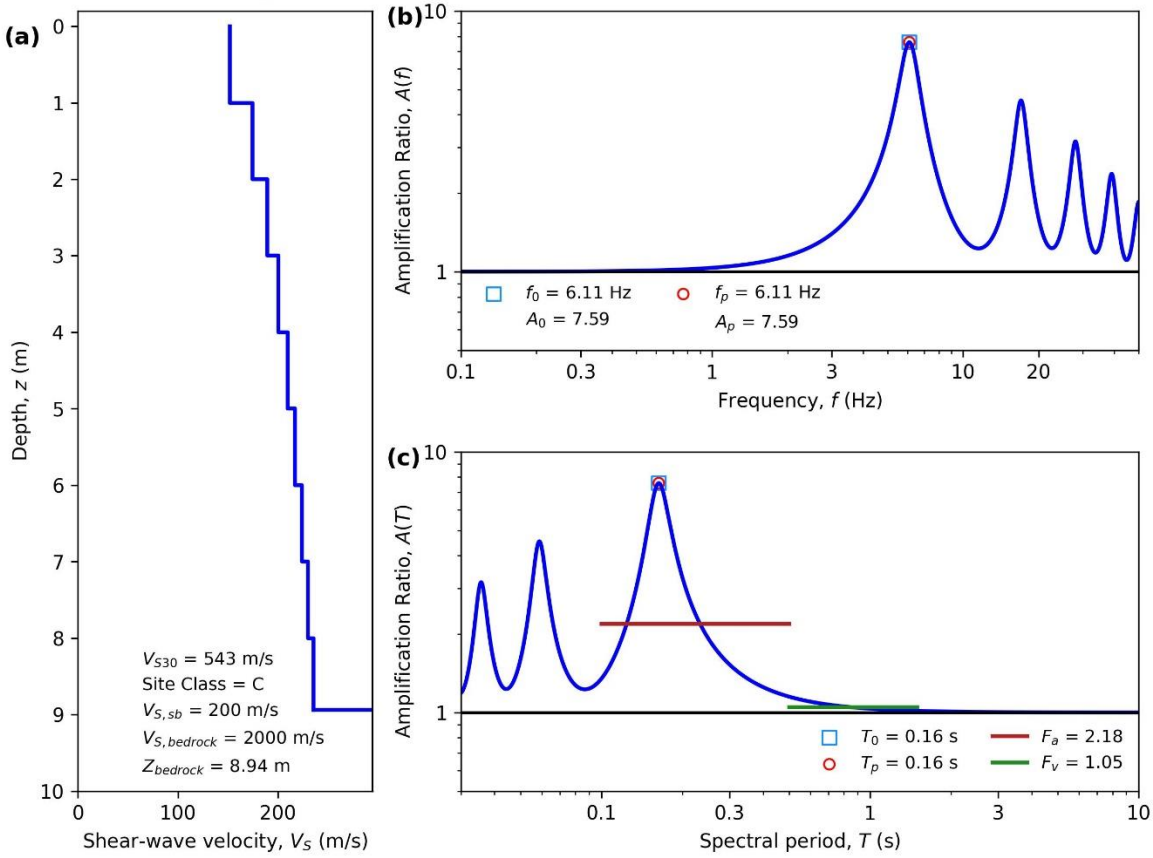

HAZUS Emergency Management
Massachusetts Care
Figure E98. ID: MA000098, Lat: 42.1981°, Lon: -71.0185°

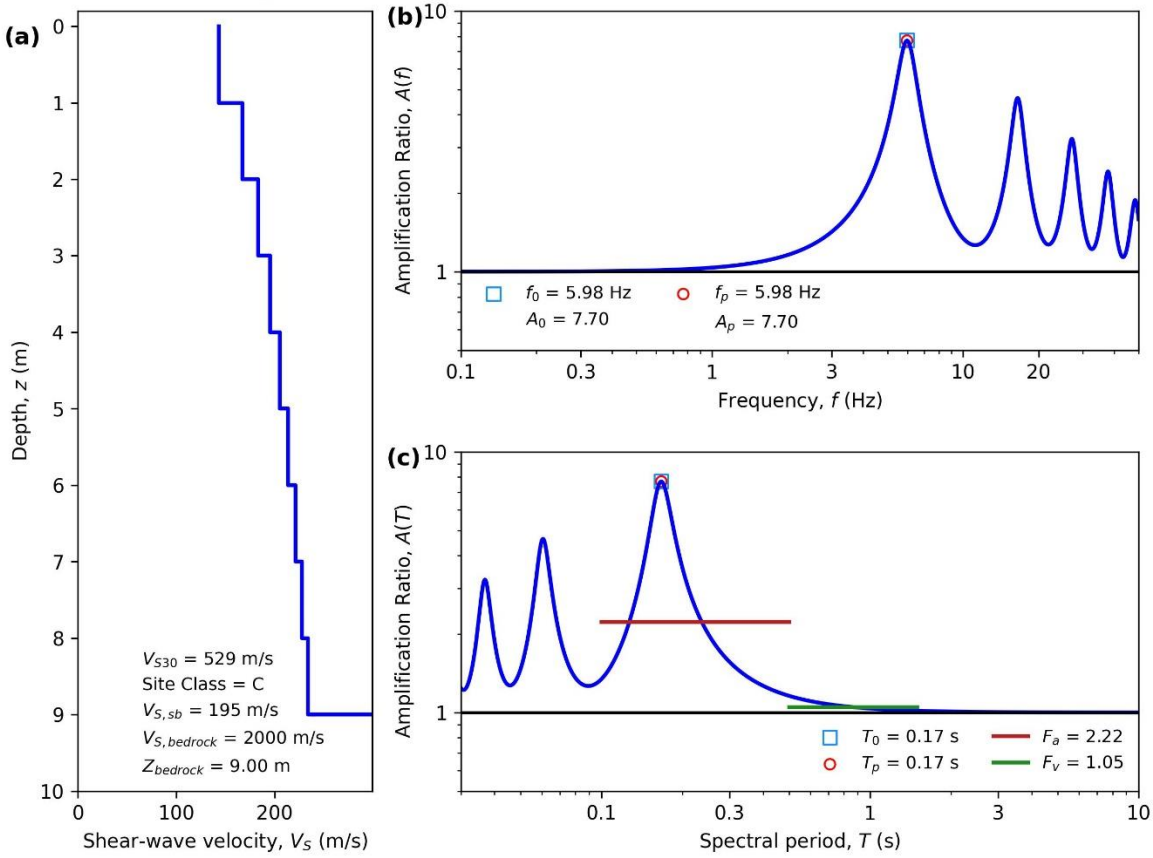

HAZUS Emergency Management
Massachusetts Care
Figure E99. ID: MA000099, Lat: 42.0879°, Lon: -70.9915°

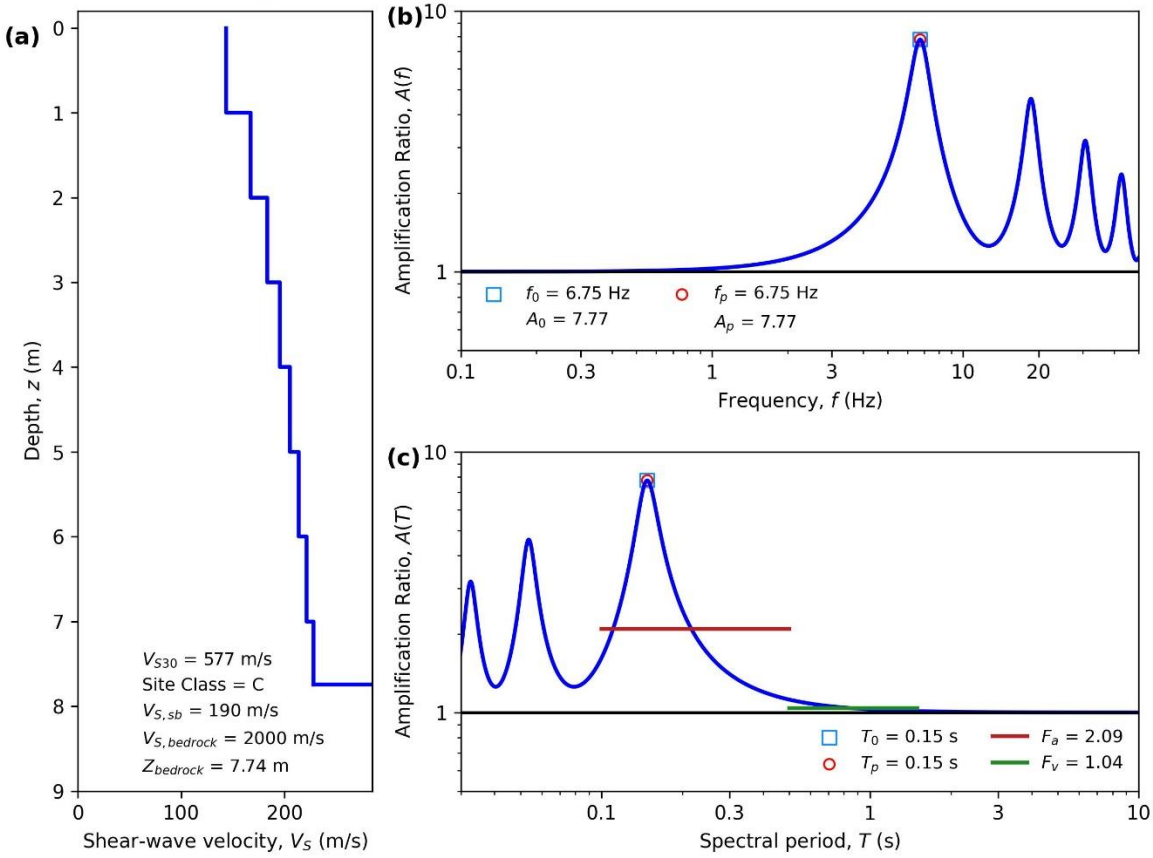

HAZUS Emergency Management
Massachusetts Care
Figure E100. ID: MA000100, Lat: 42.0501°, Lon: -71.2411°

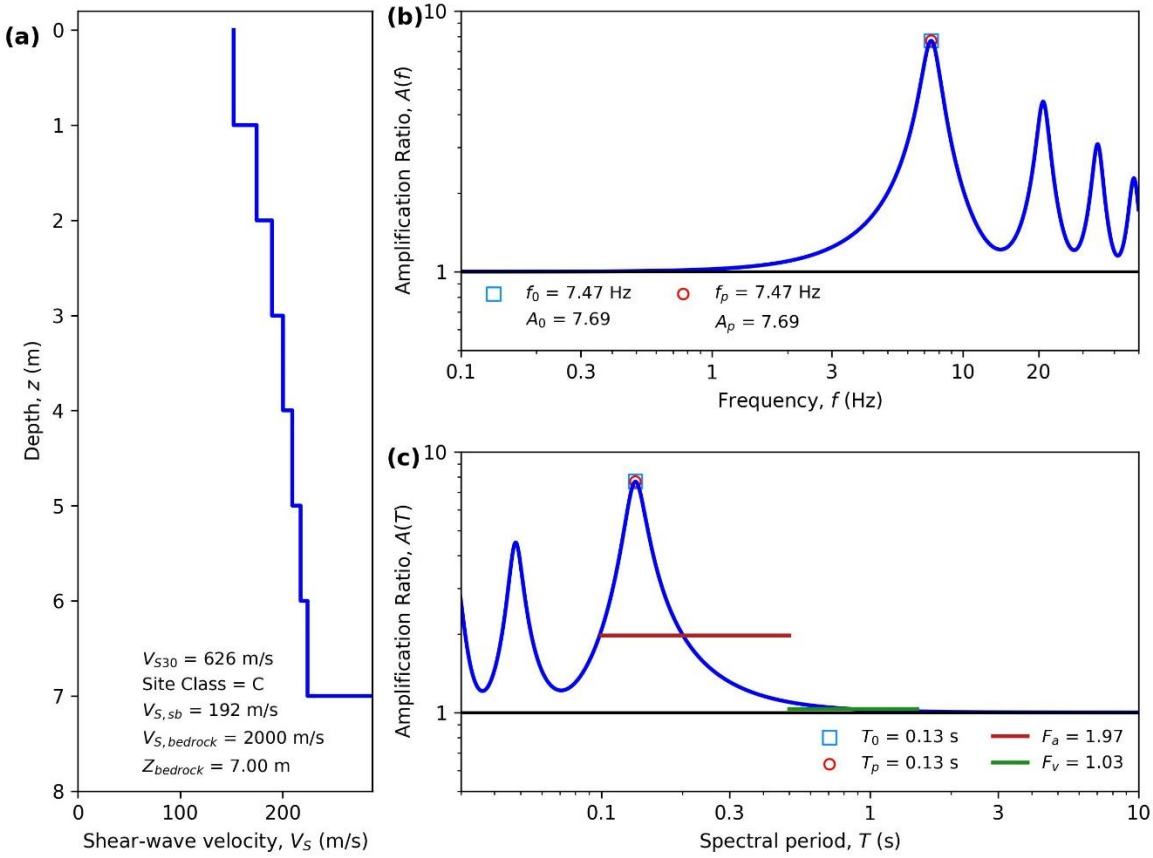

HAZUS Emergency Management
Massachusetts Care
Figure E101. ID: MA000101, Lat: 42.7616°, Lon: -71.1189°

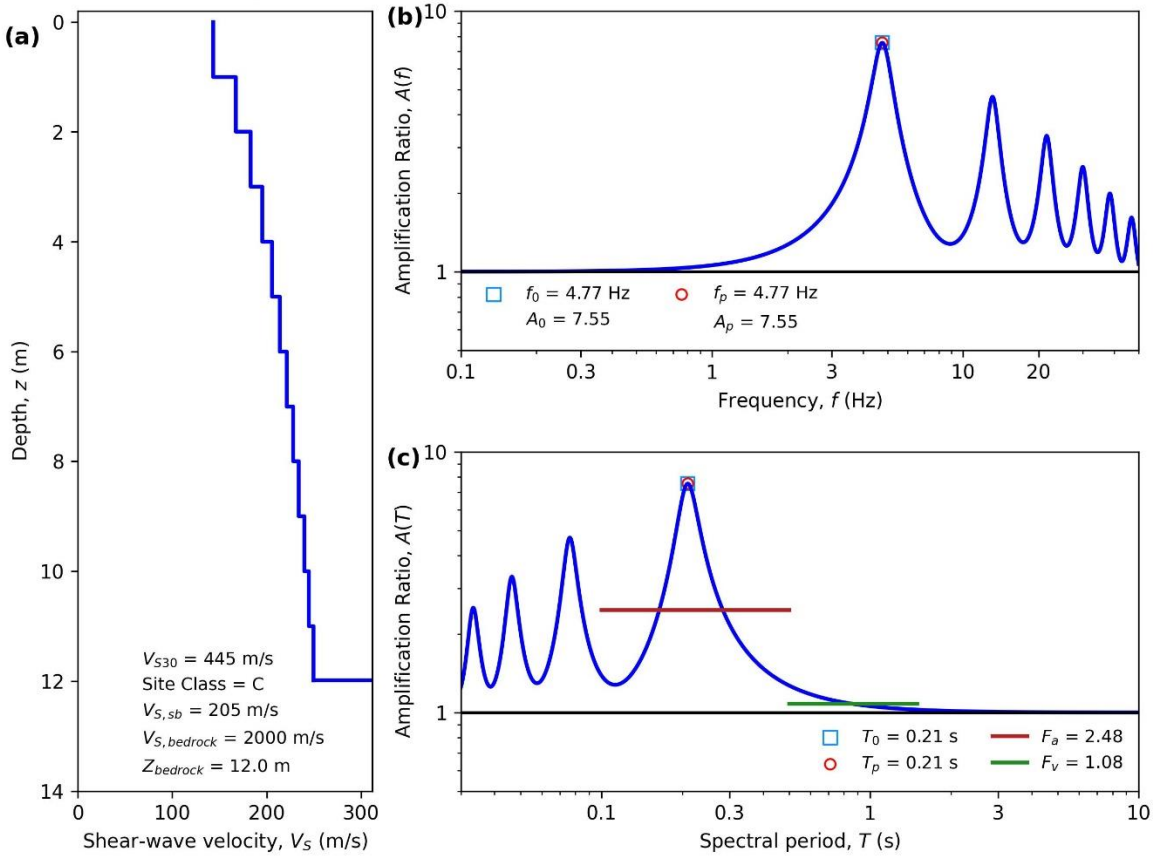

HAZUS Emergency Management
Massachusetts Care
Figure E102. ID: MA000102, Lat: 42.0979°, Lon: -71.0619°

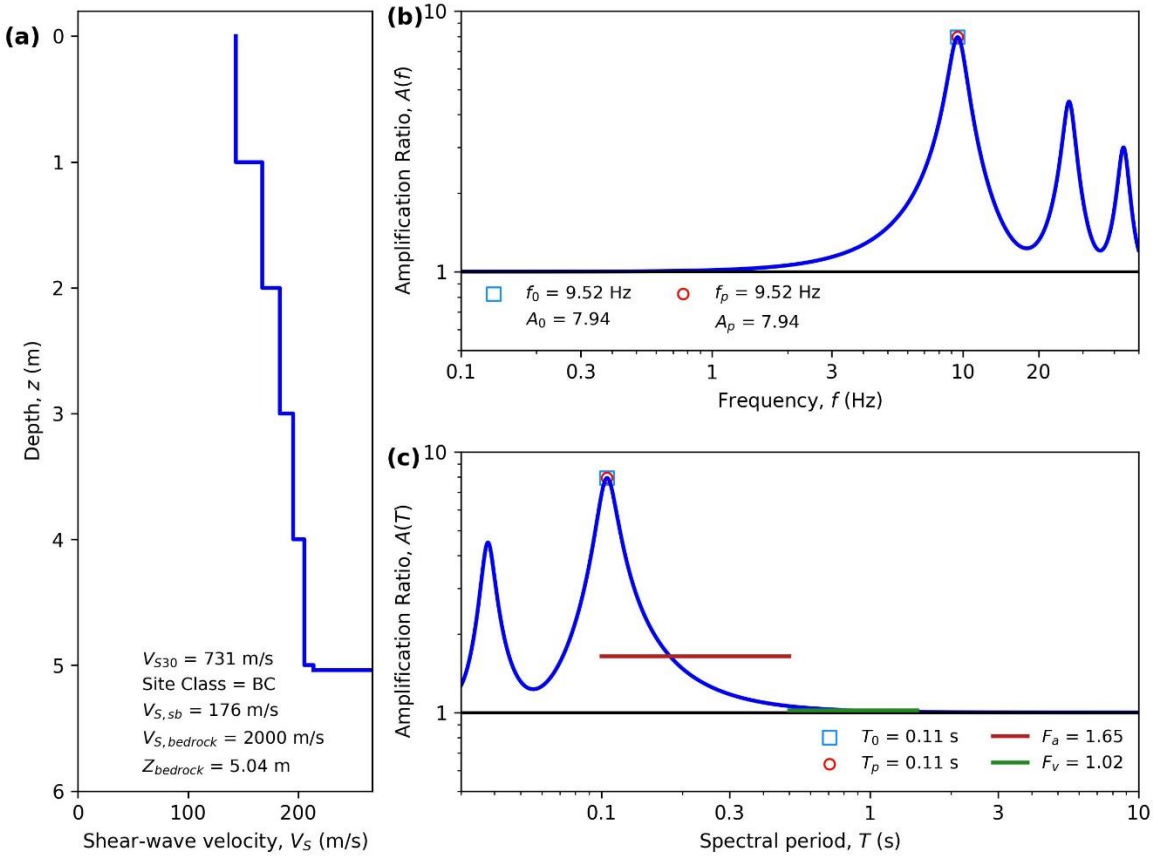

HAZUS Emergency Management
Massachusetts Care
Figure E103. ID: MA000103, Lat: 42.2065°, Lon: -71.2241°

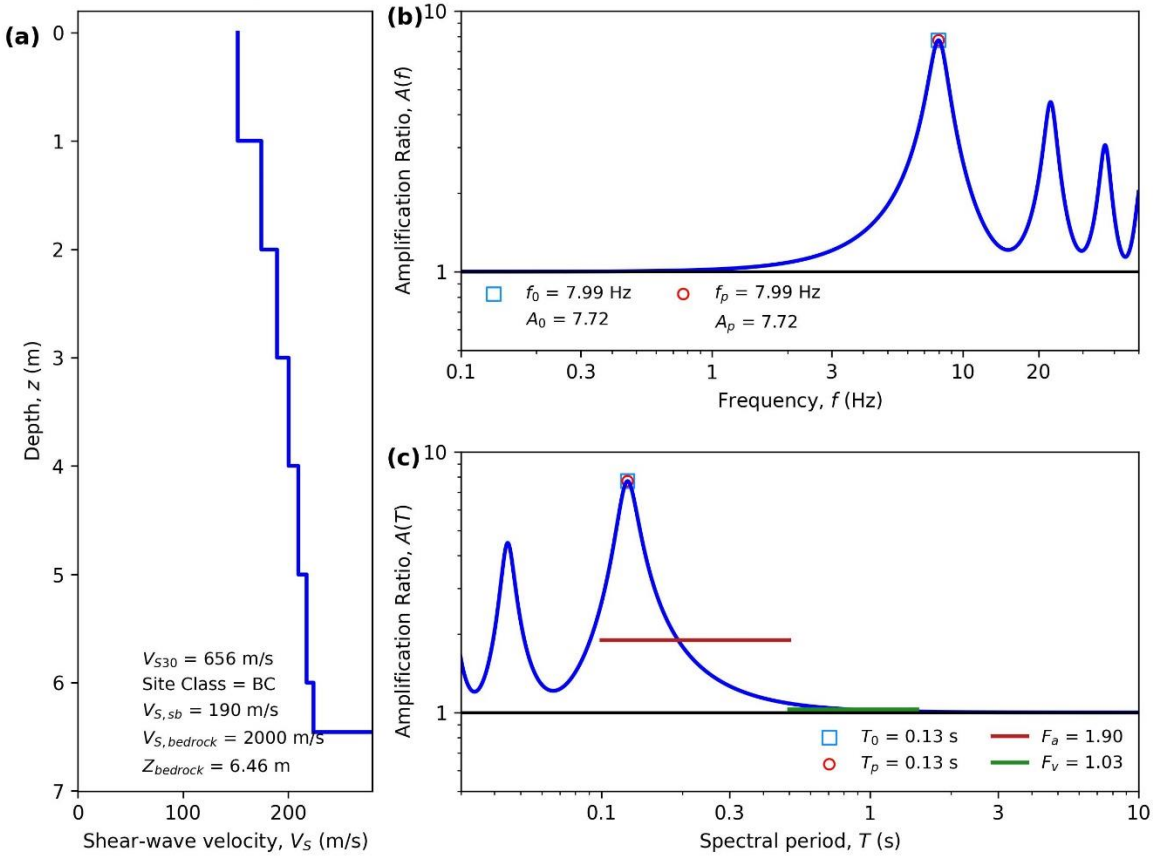

HAZUS Emergency Management
Massachusetts Care
Figure E104. ID: MA000104, Lat: 42.2601°, Lon: -71.8354°

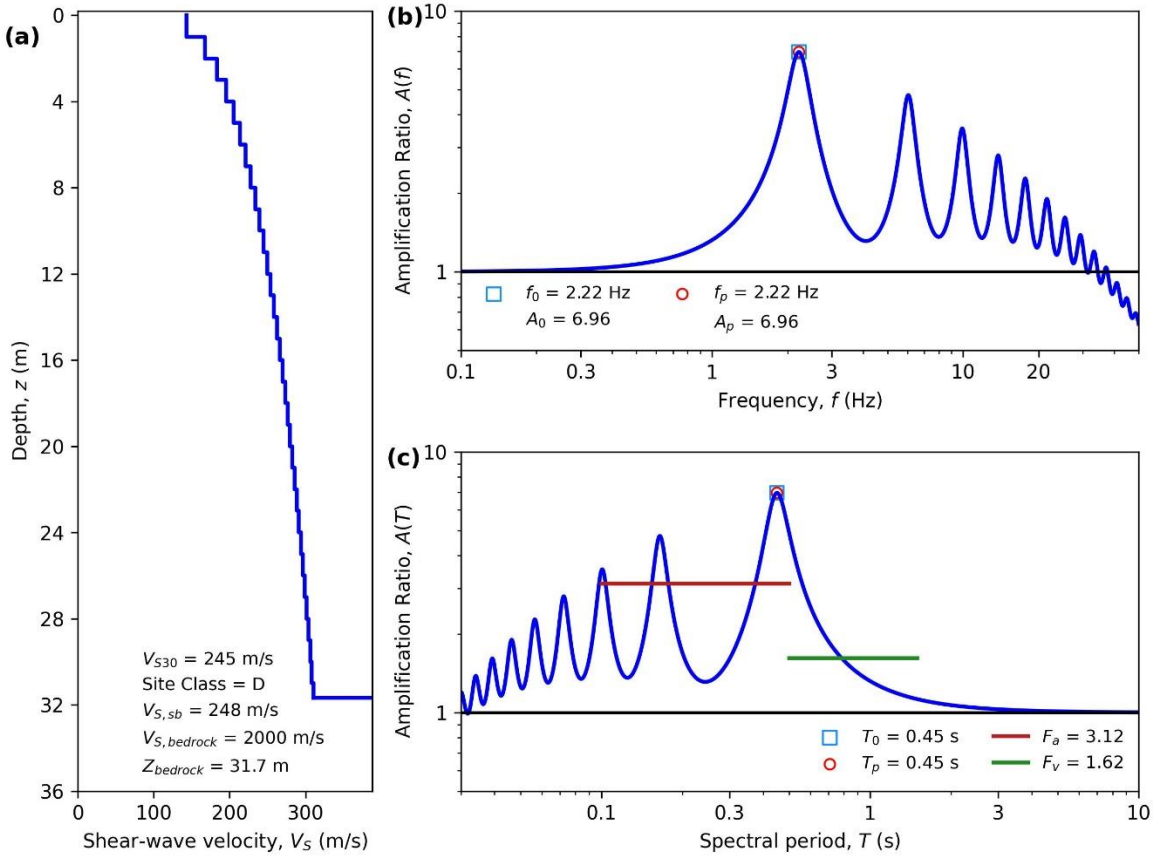

HAZUS Emergency Management
Massachusetts Care
Figure E105. ID: MA000105, Lat: 42.5018°, Lon: -70.9799°

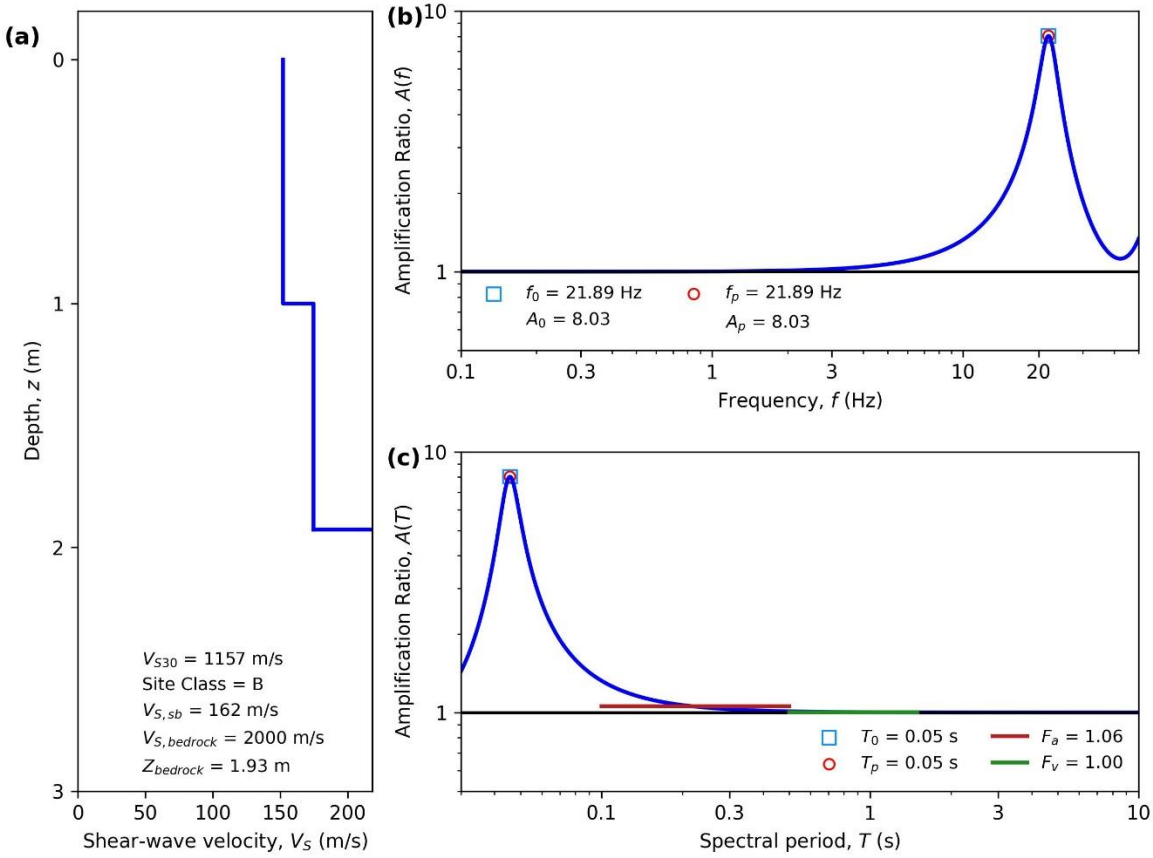

HAZUS Emergency Management
Massachusetts Care
Figure E106. ID: MA000106, Lat: 42.4581°, Lon: -73.2807°

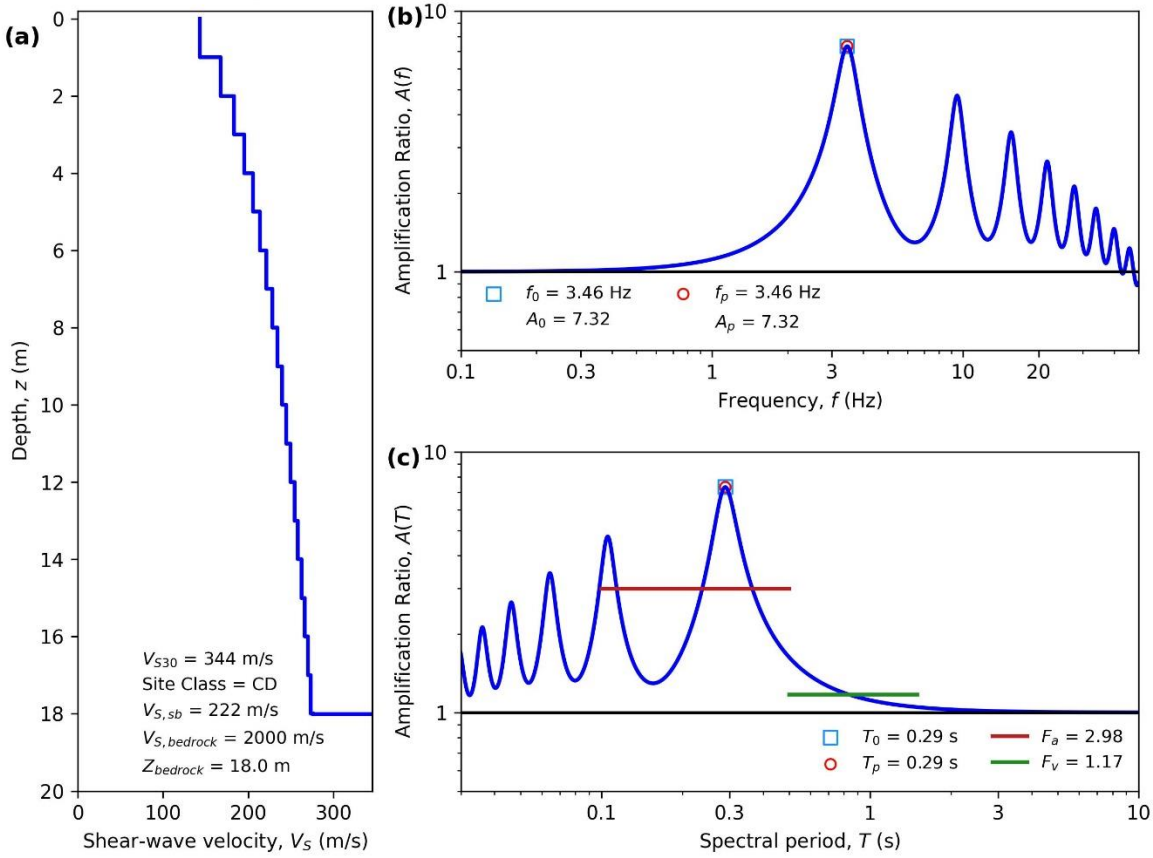

HAZUS Emergency Management
Massachusetts Care
Figure E107. ID: MA000107, Lat: 42.3376°, Lon: -71.1082°

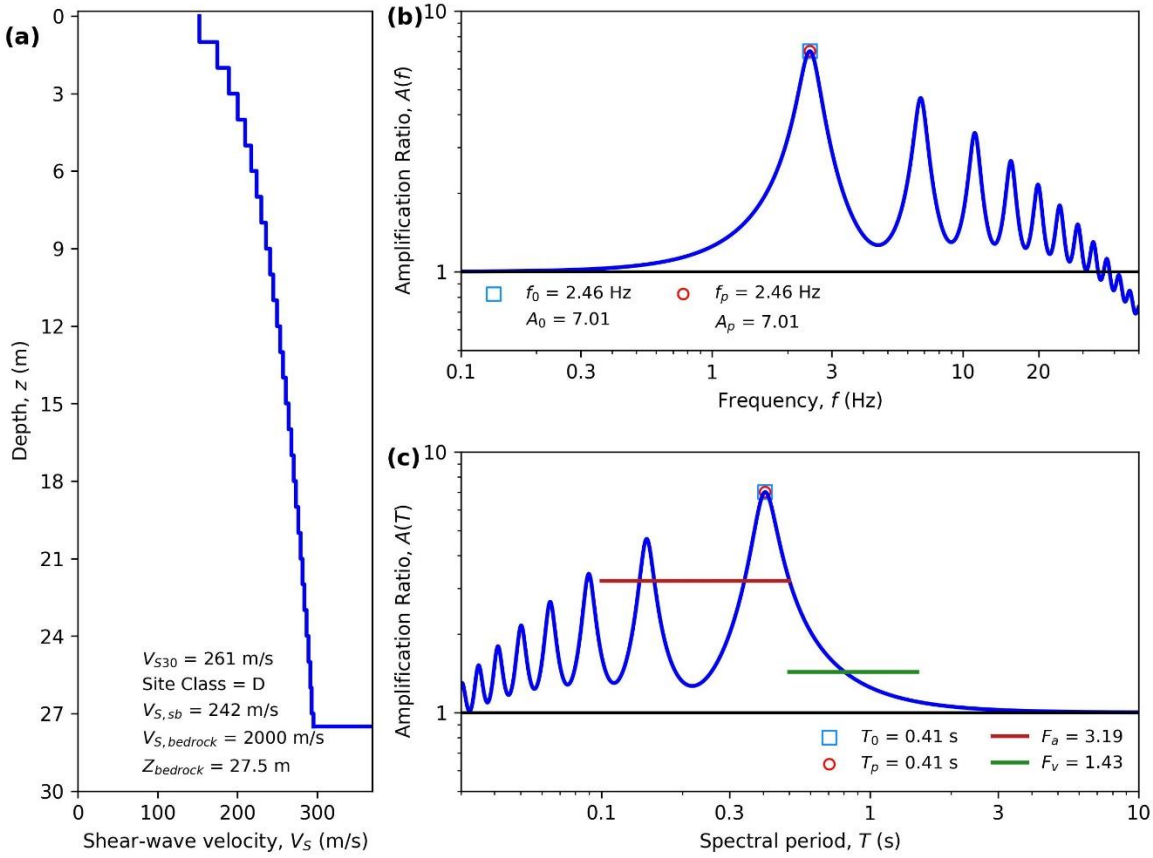

HAZUS Emergency Management
Massachusetts Care
Figure E108. ID: MA000108, Lat: 42.3015°, Lon: -71.1283°

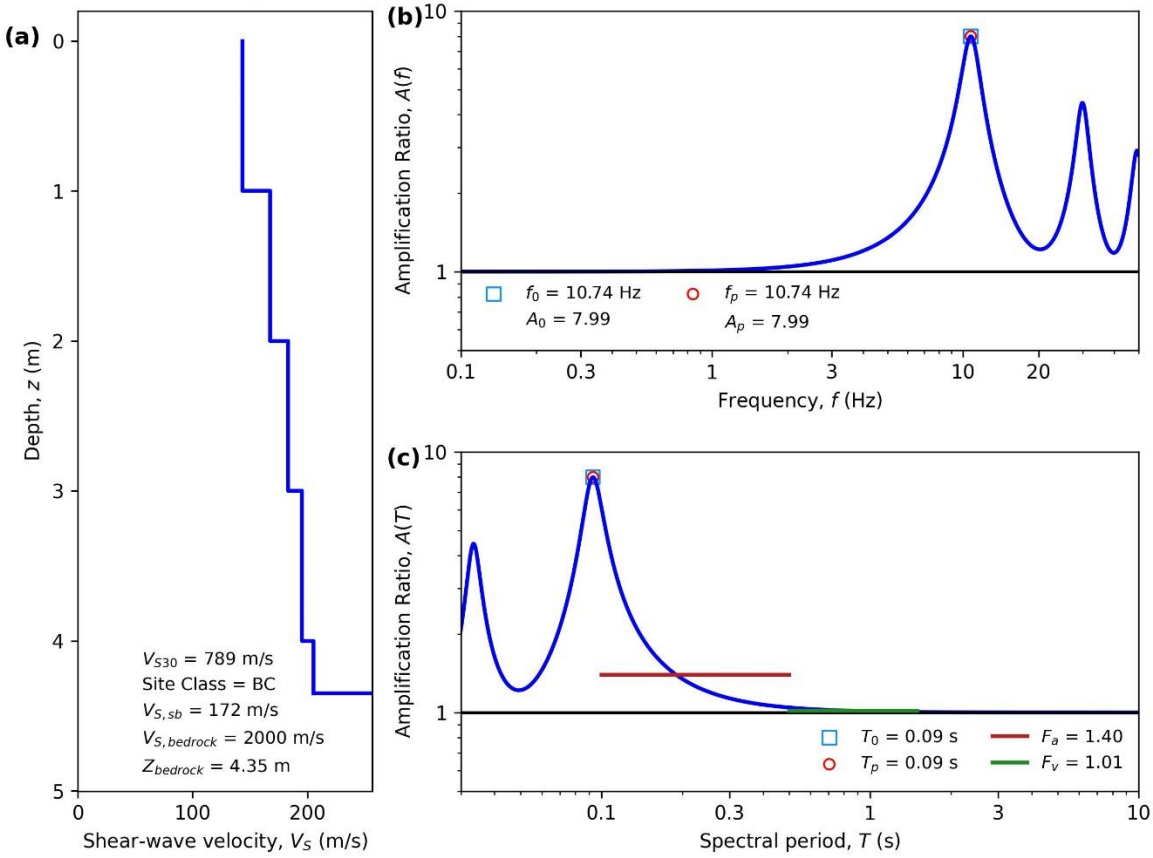

HAZUS Emergency Management
Massachusetts Care
Figure E109. ID: MA000109, Lat: 42.1388°, Lon: -71.5264°

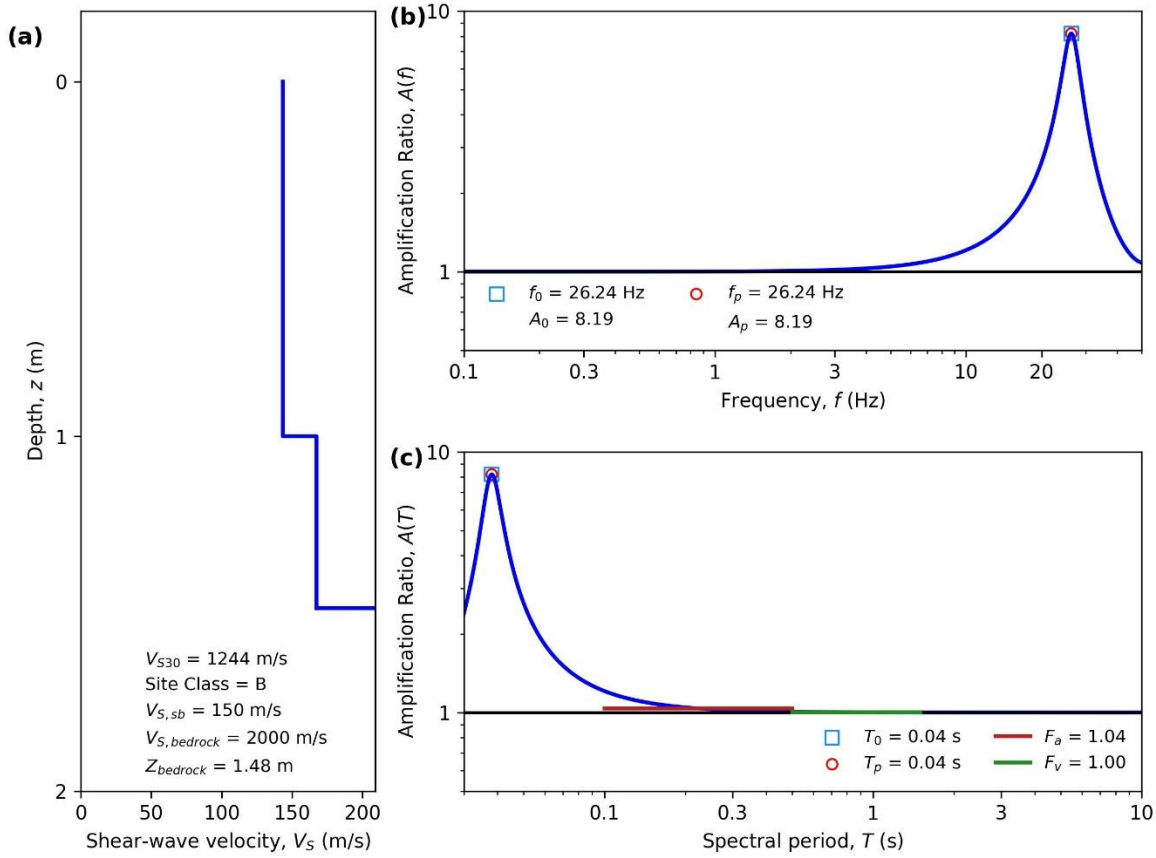

HAZUS Emergency Management
Massachusetts Care
Figure E110. ID: MA000110, Lat: 42.2648°, Lon: -71.7967°

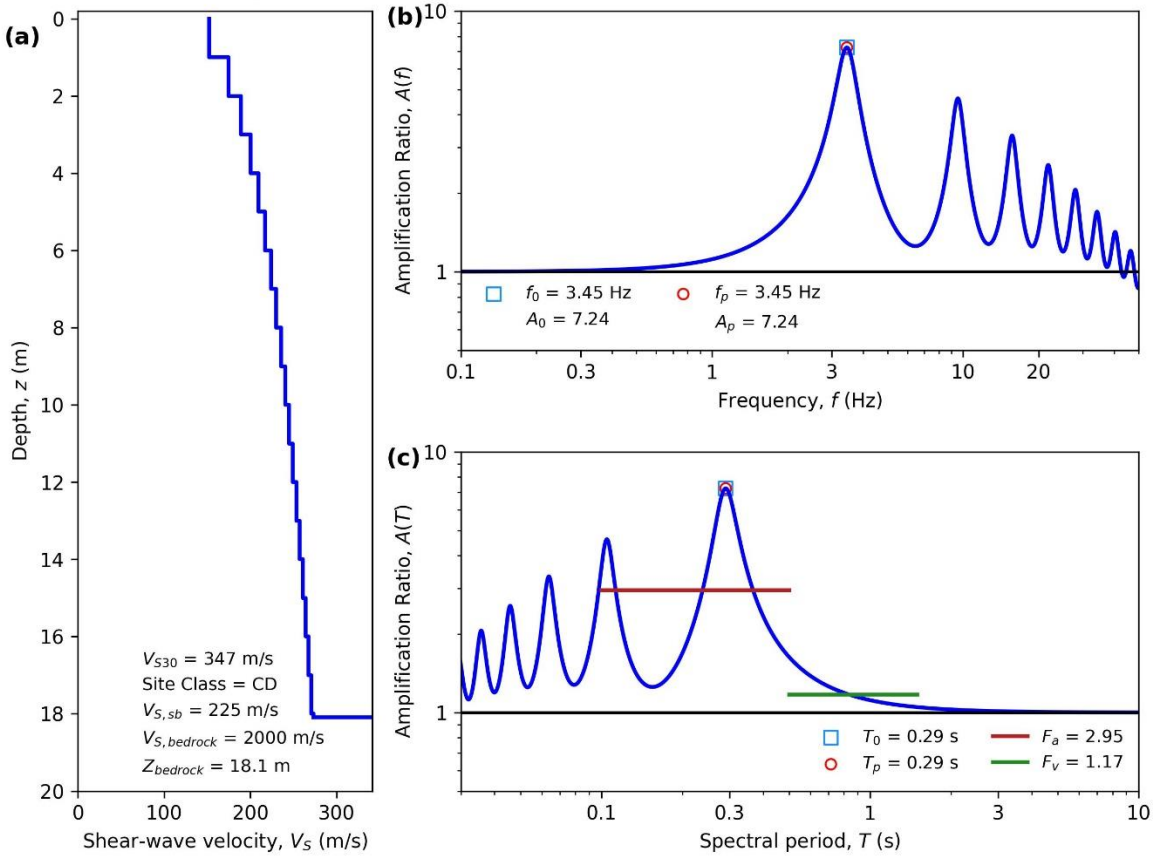

HAZUS Emergency Management
Massachusetts Care
Figure E111. ID: MA000111, Lat: 42.5775°, Lon: -71.5739°

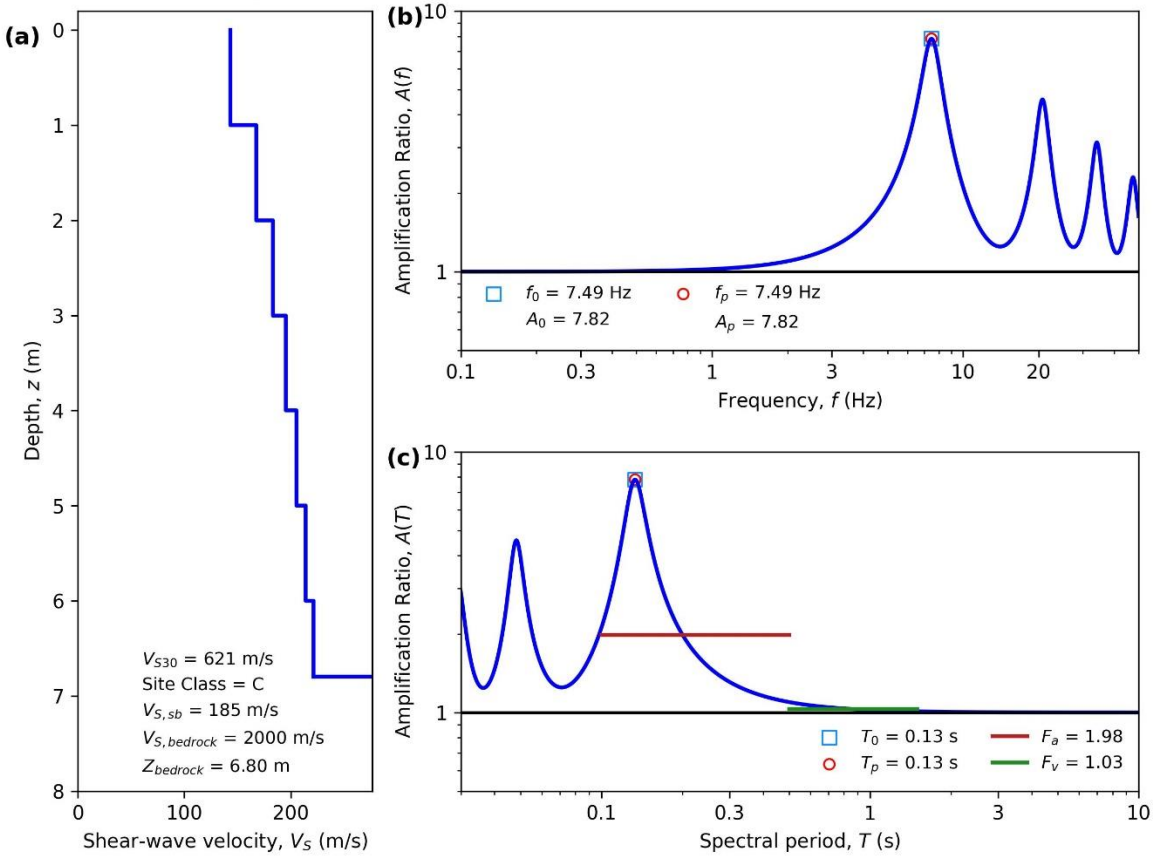

HAZUS Emergency Management
Massachusetts Care
Figure E112. ID: MA000112, Lat: 42.3741°, Lon: -71.1343°

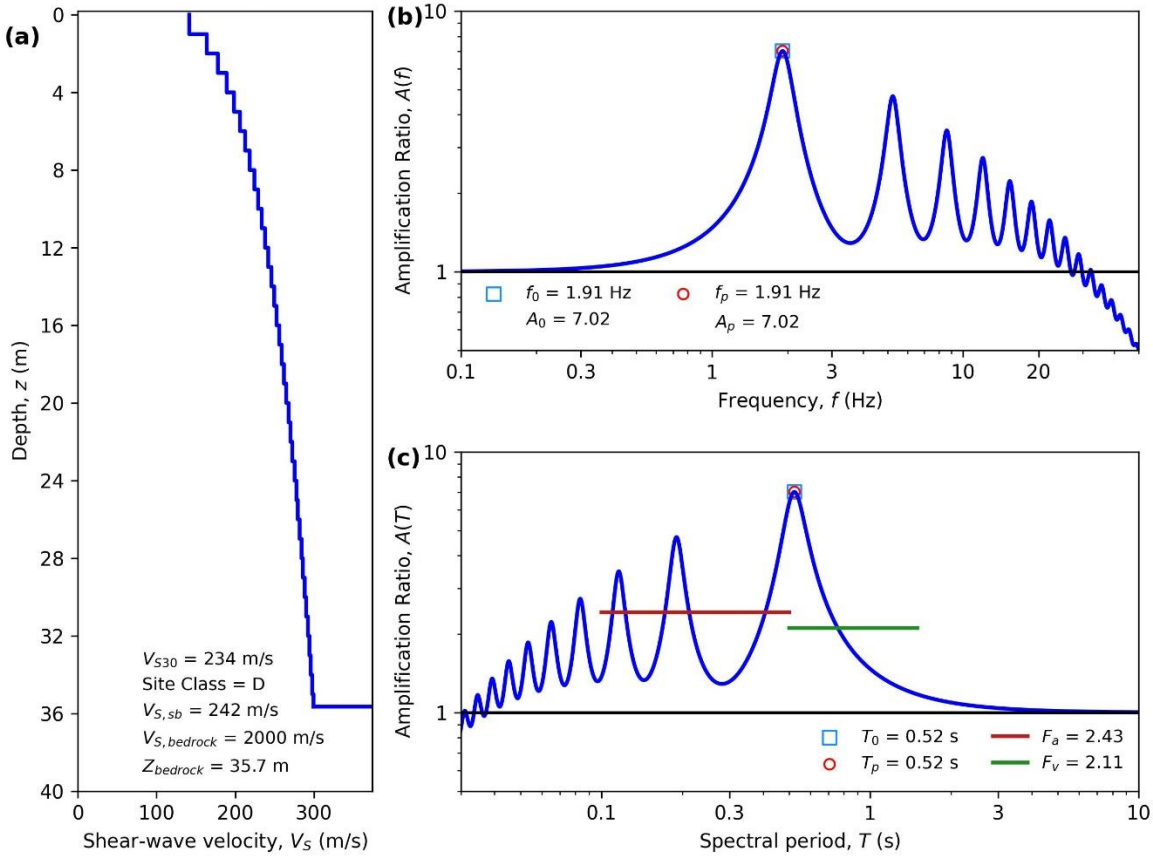

HAZUS Emergency Management
Massachusetts Care
Figure E113. ID: MA000113, Lat: 42.2003°, Lon: -72.6276°

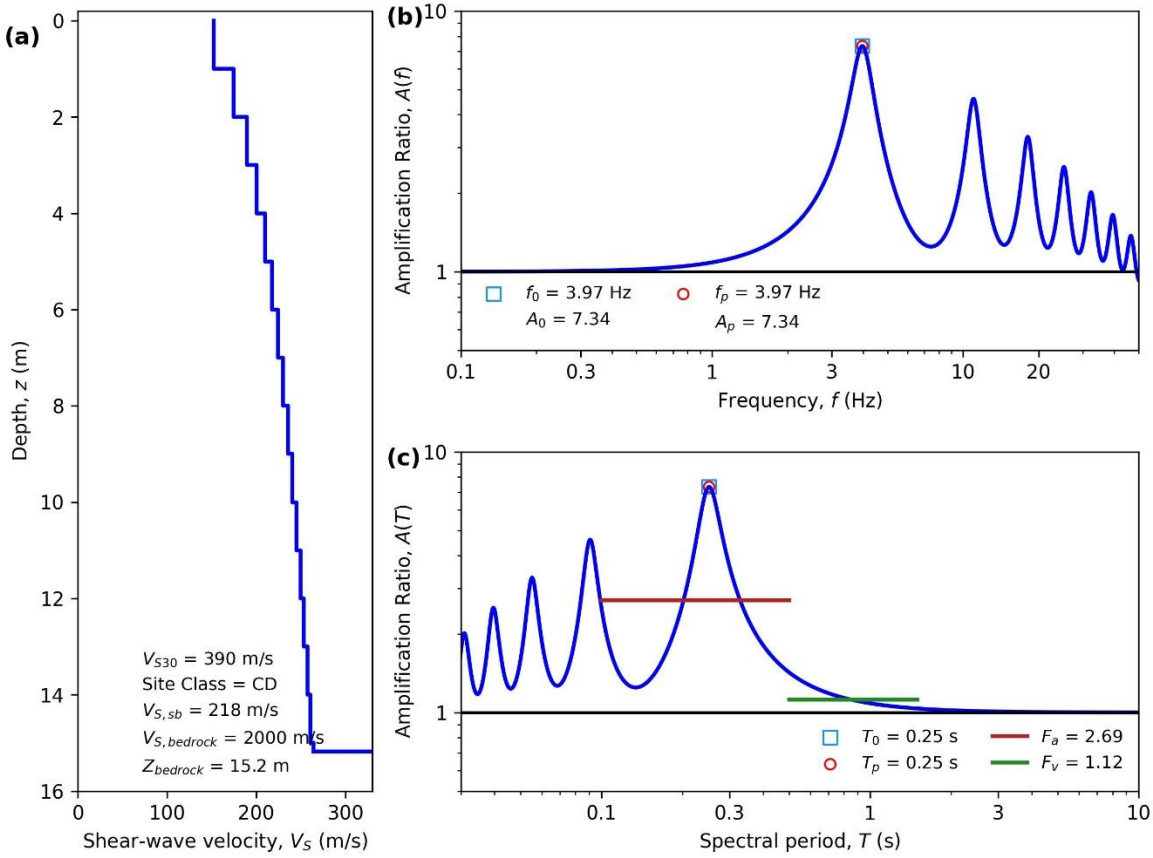

HAZUS Emergency Management
Massachusetts Care
Figure E114. ID: MA000114, Lat: 42.1183°, Lon: -72.7596°

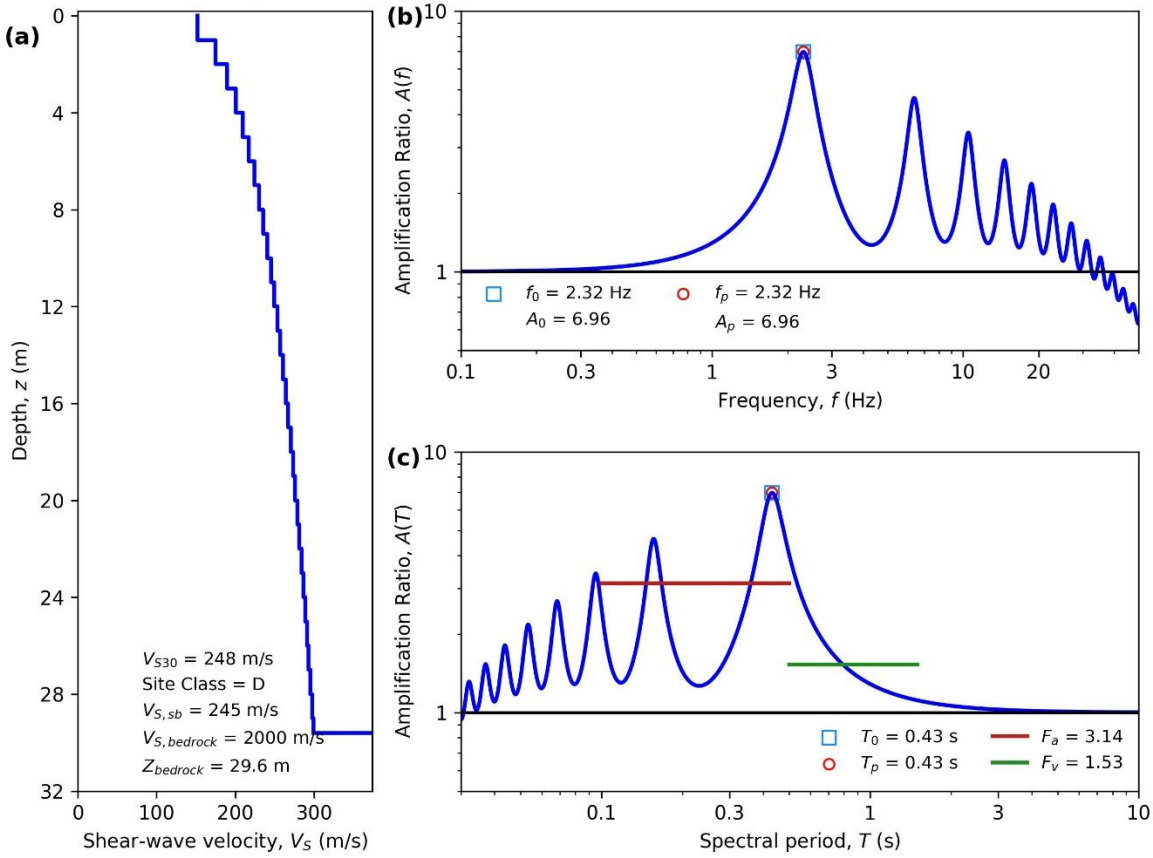

HAZUS Emergency Management
Massachusetts Care
Figure E115. ID: MA000115, Lat: 42.1760°, Lon: -70.9541°

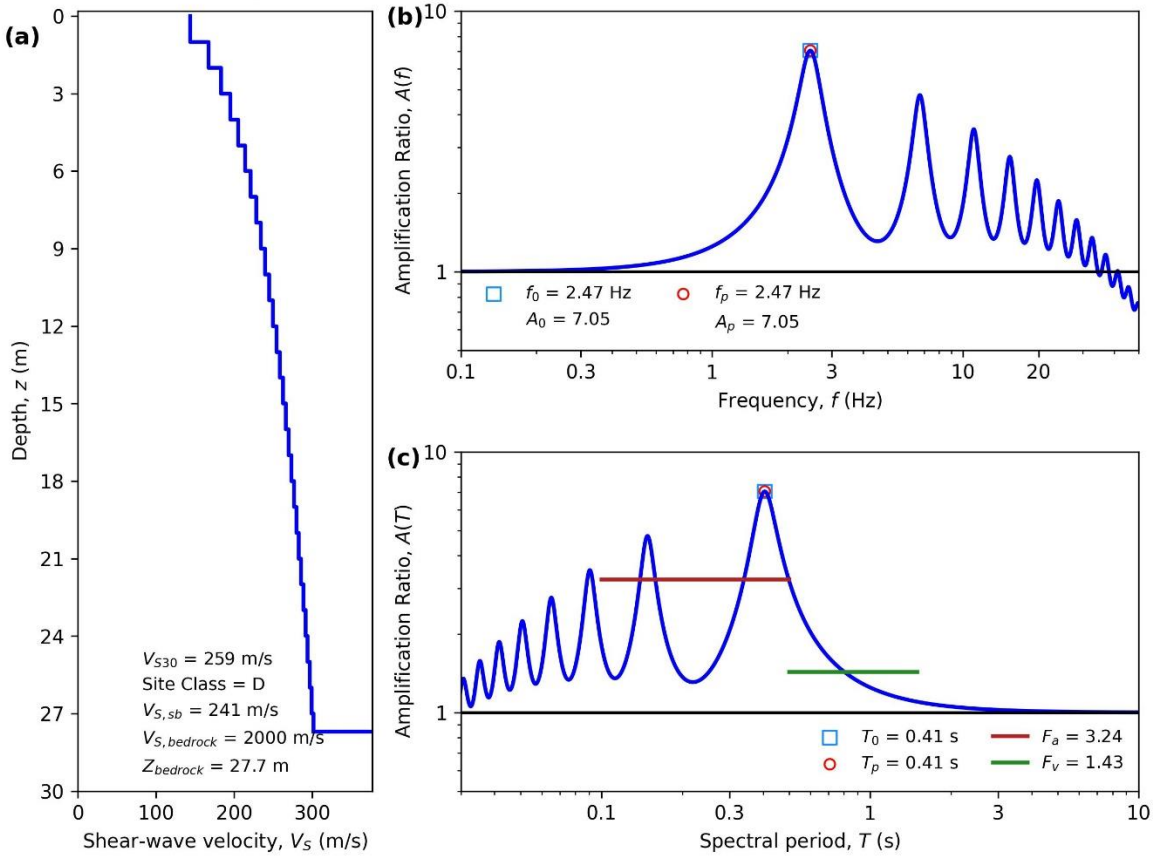

HAZUS Emergency Management
Massachusetts Care
Figure E116. ID: MA000116, Lat: 41.7094°, Lon: -71.1460°

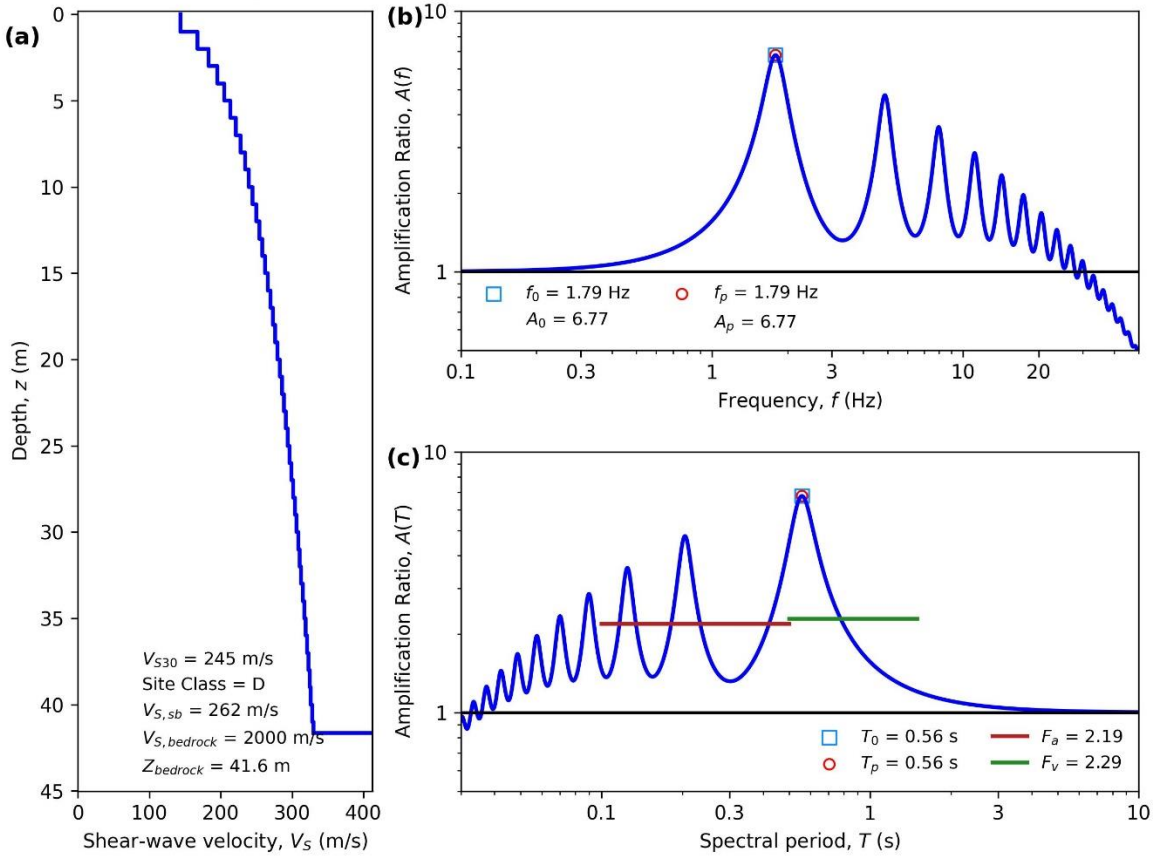

HAZUS Emergency Management
Massachusetts Care
Figure E117. ID: MA000117, Lat: 42.7071°, Lon: -73.1095°

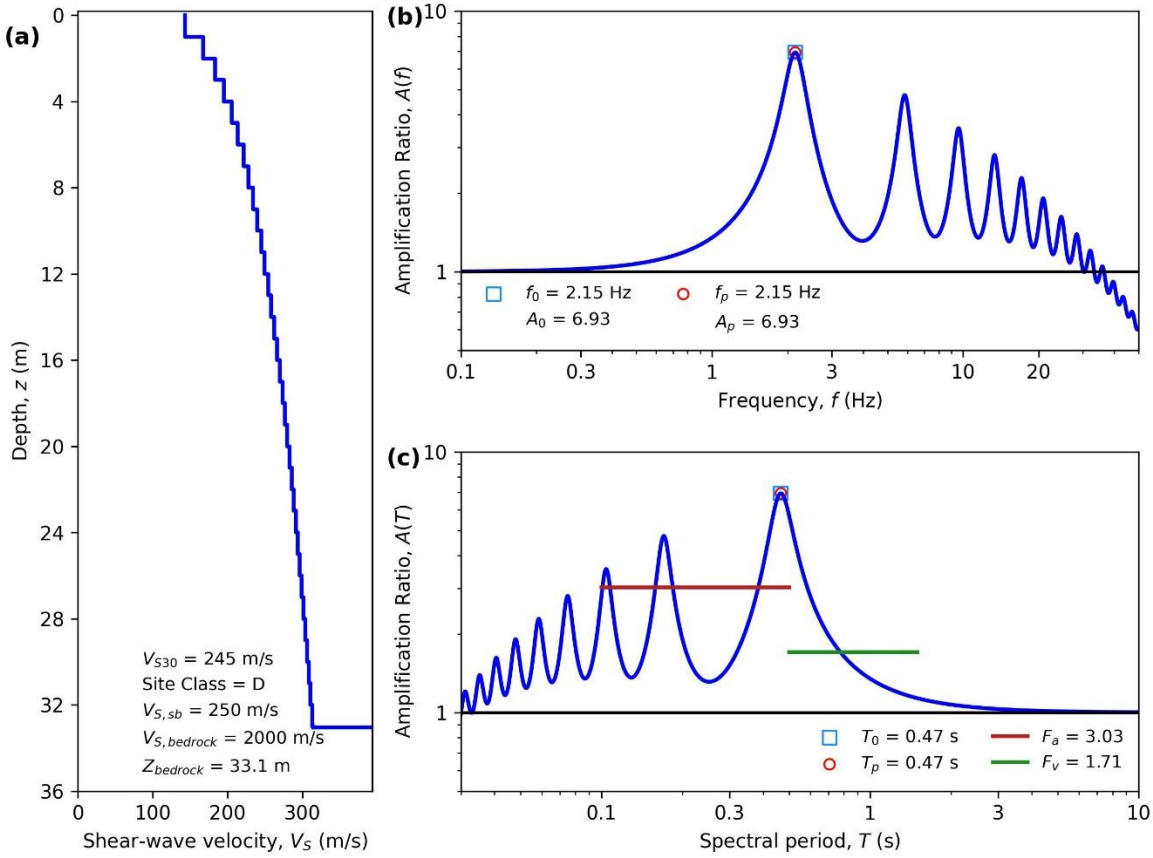

HAZUS Emergency Management
Massachusetts Care
Figure E118. ID: MA000118, Lat: 42.8144°, Lon: -70.8911°

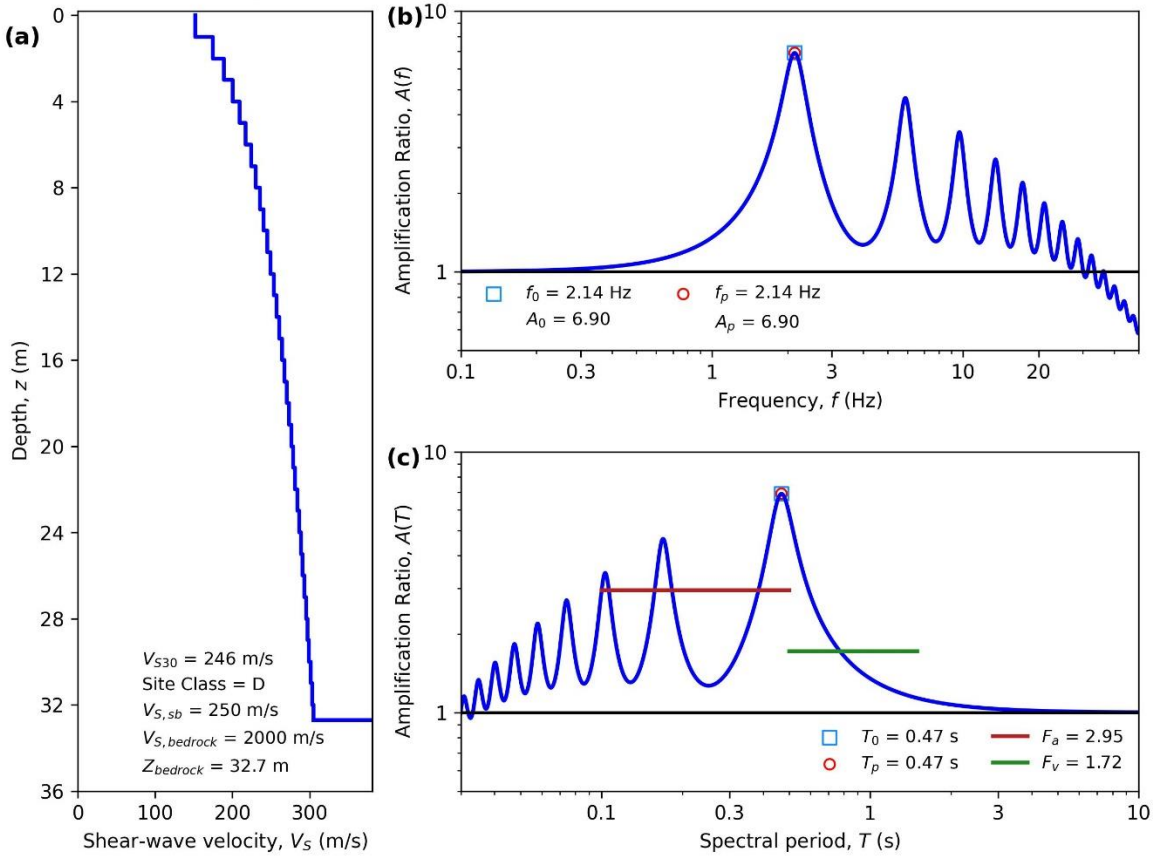

HAZUS Emergency Management
Massachusetts Care
Figure E119. ID: MA000119, Lat: 42.7100°, Lon: -71.1501°

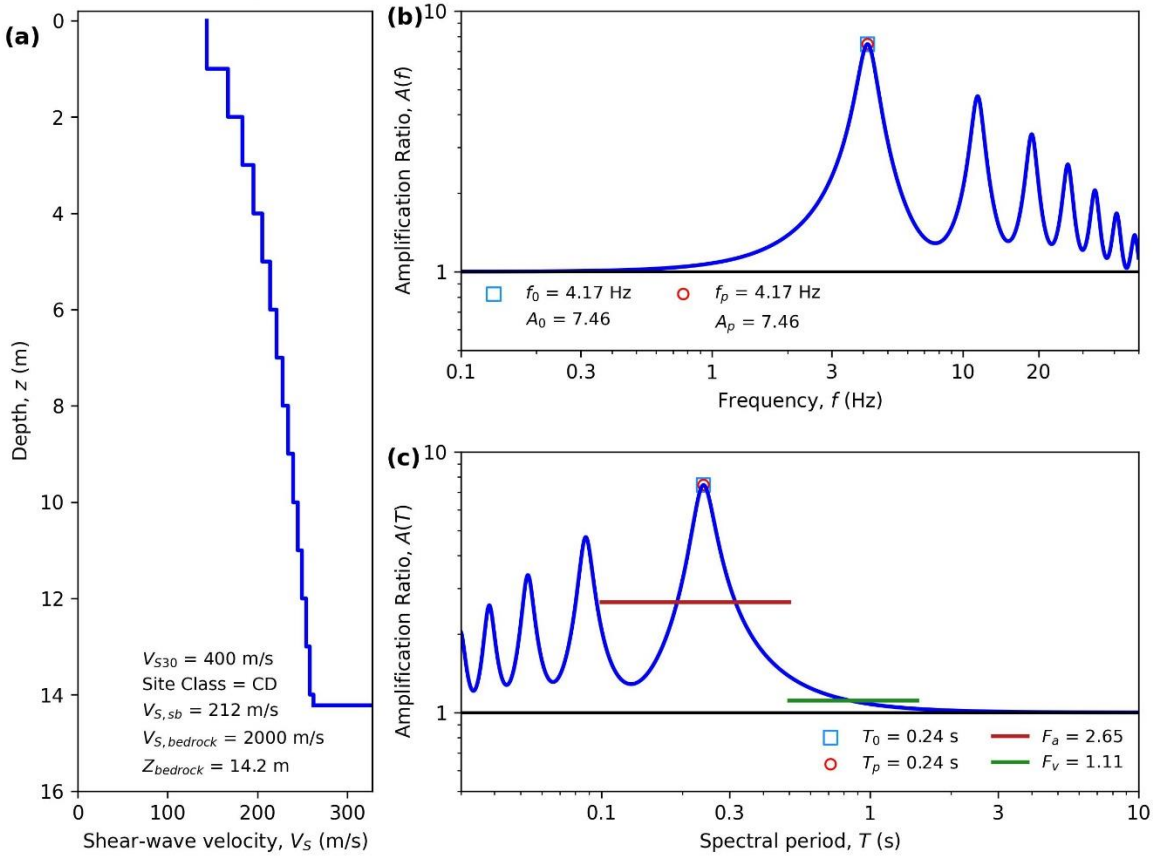

HAZUS Emergency Management
Massachusetts Care
Figure E120. ID: MA000120, Lat: 42.3499°, Lon: -71.0640°

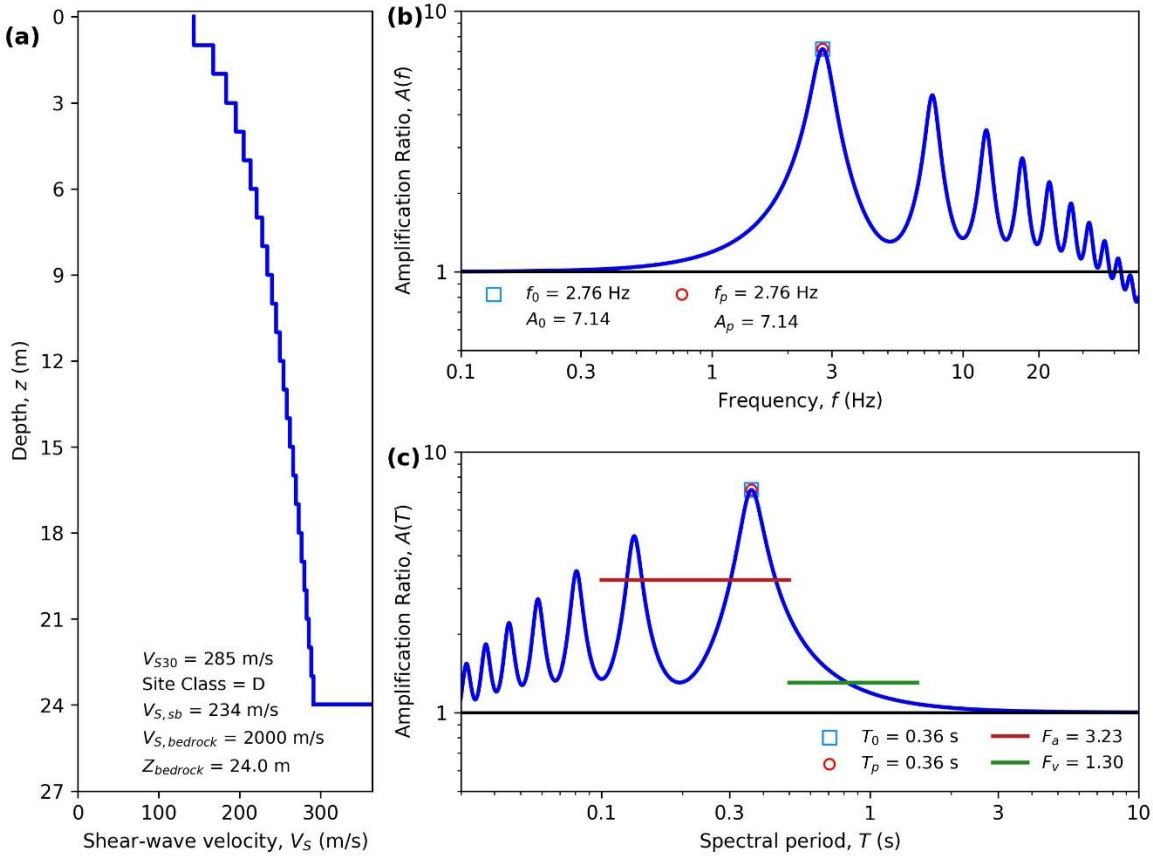

HAZUS Emergency Management
Massachusetts Care
Figure E121. ID: MA000121, Lat: 42.3370°, Lon: -71.0706°

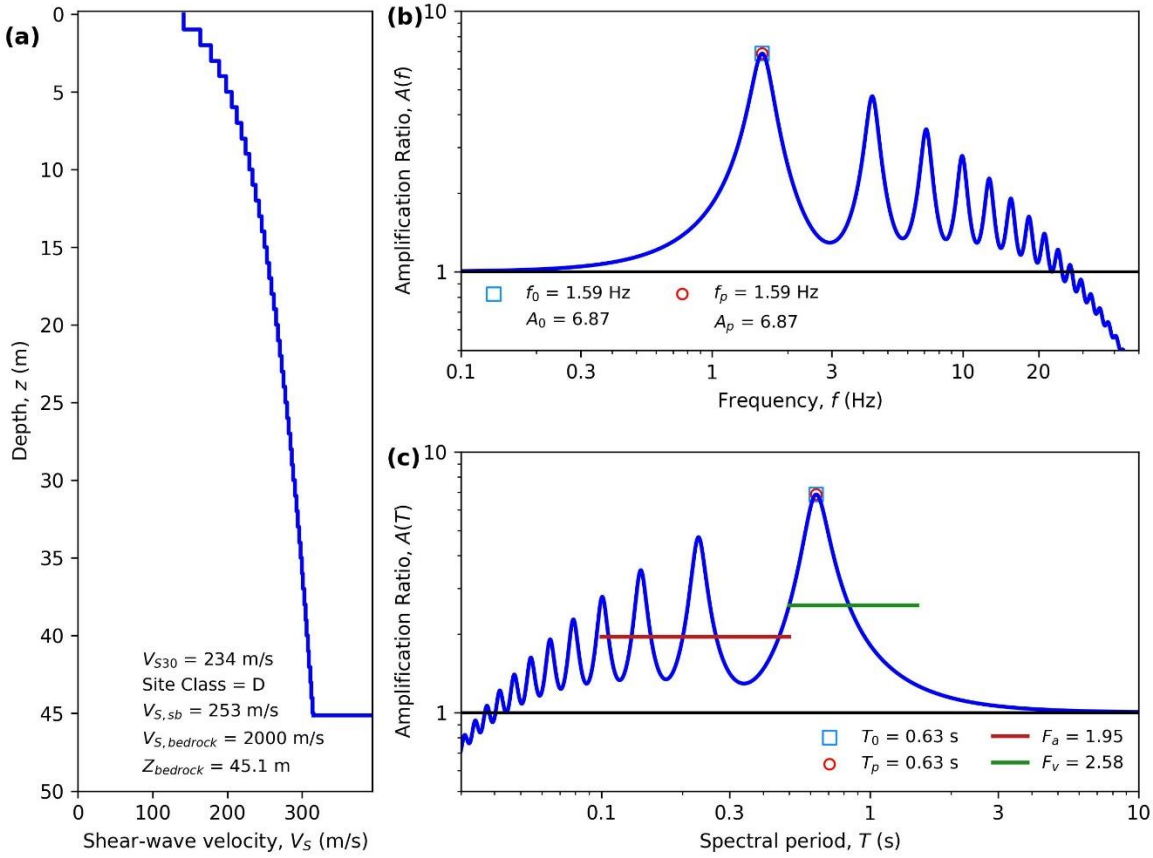

HAZUS Emergency Management
Massachusetts Care
Figure E122. ID: MA000122, Lat: 42.3359°, Lon: -71.1068°

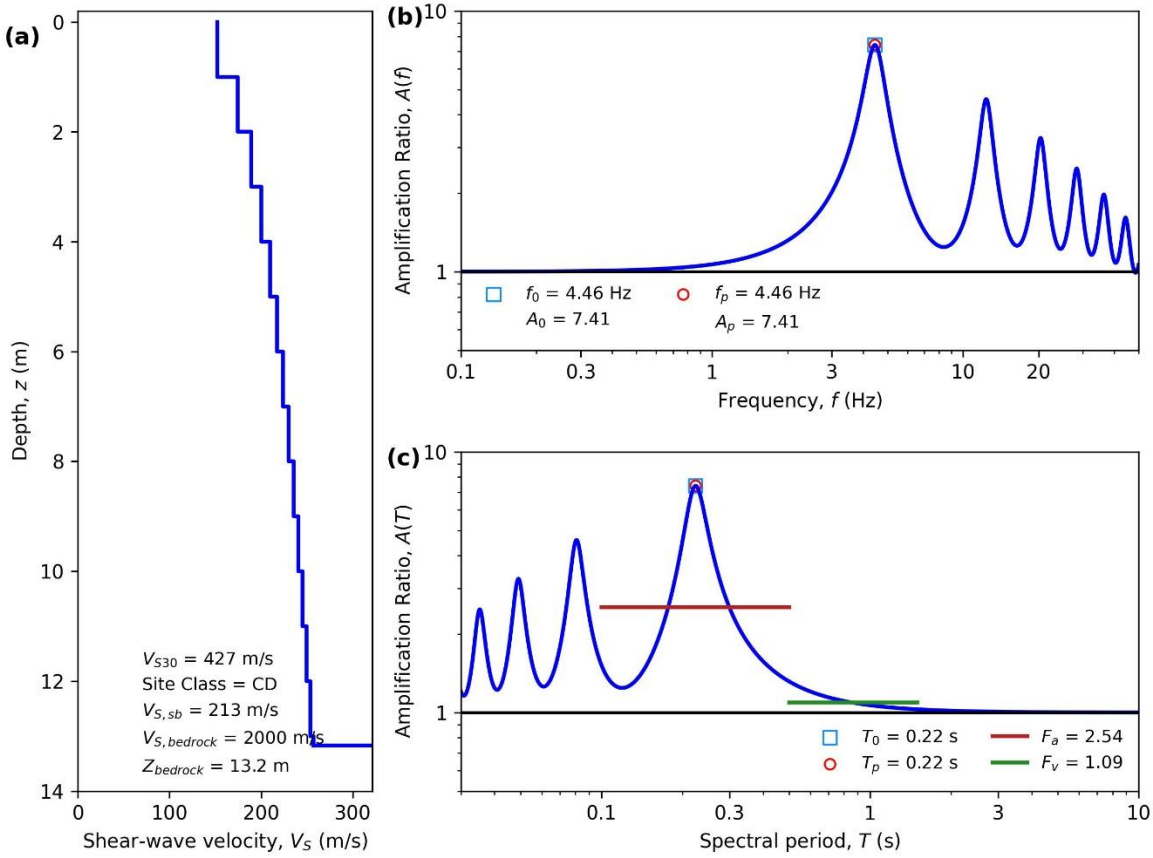

HAZUS Emergency Management
Massachusetts Care
Figure E123. ID: MA000123, Lat: 42.5855°, Lon: -72.2089°

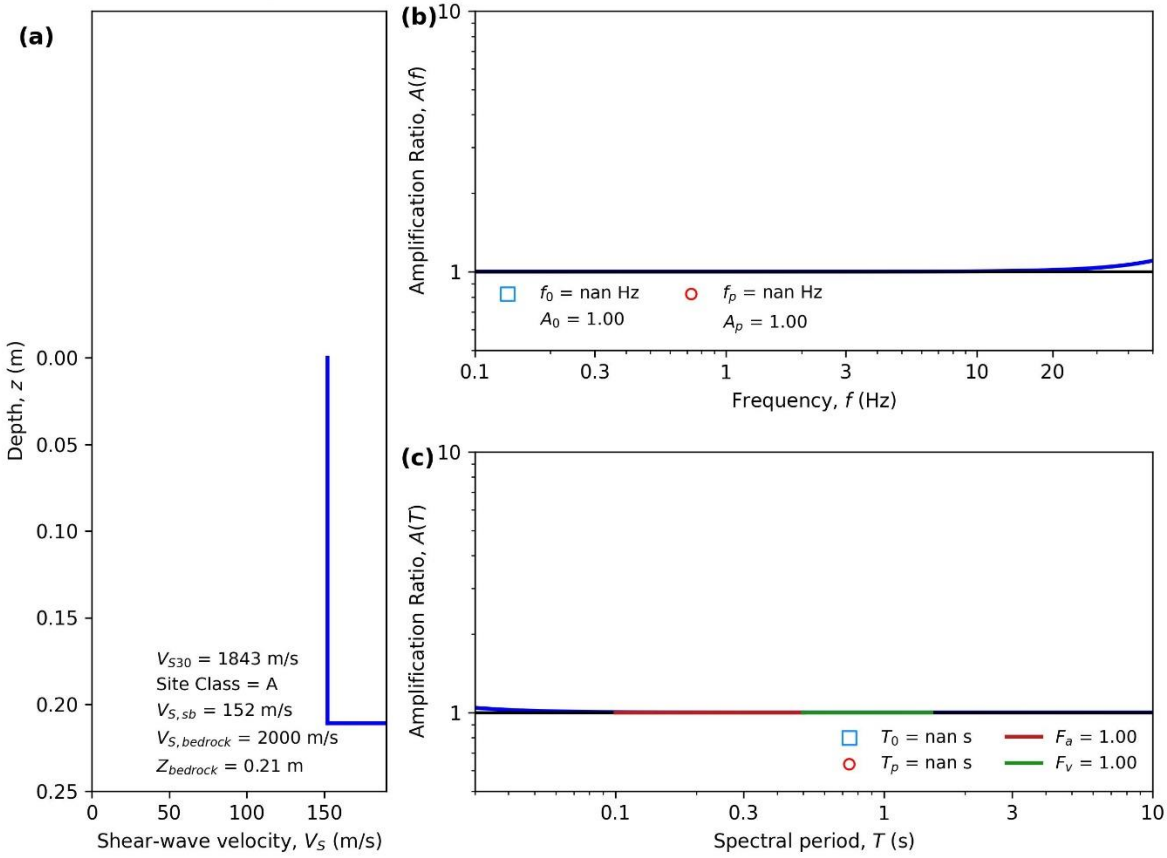

HAZUS Emergency Management
Massachusetts Care
Figure E124. ID: MA000124, Lat: 42.2778°, Lon: -71.7617°

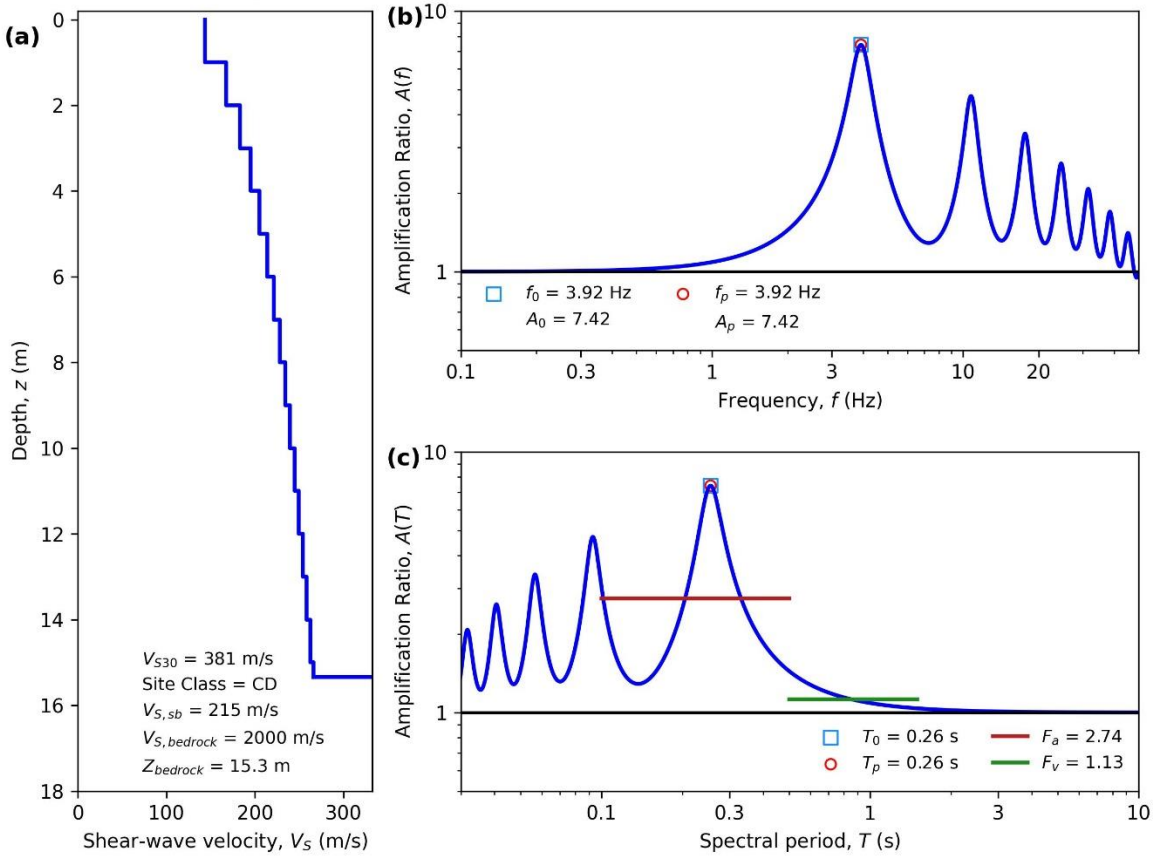

HAZUS Emergency Management
Massachusetts Care
Figure E125. ID: MA000125, Lat: 42.4517°, Lon: -71.3758°

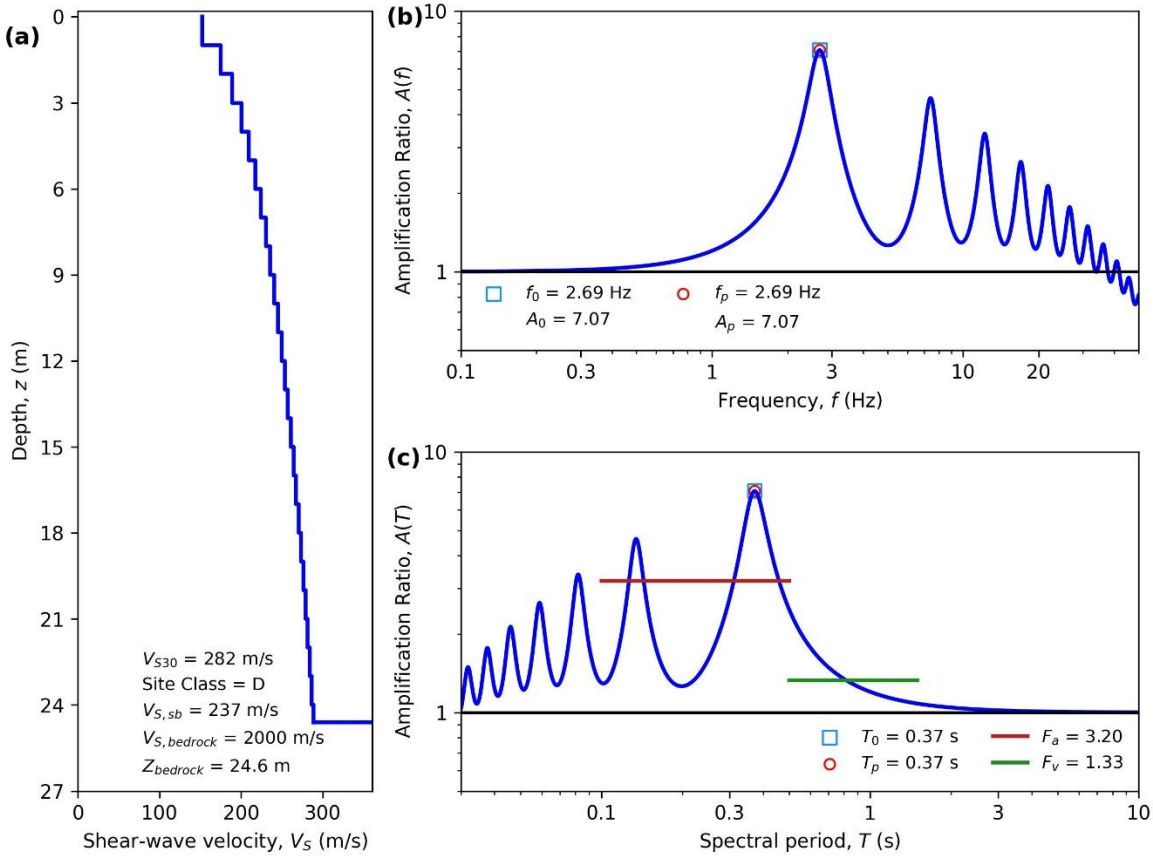

HAZUS Emergency Management
Massachusetts Care
Figure E126. ID: MA000126, Lat: 42.2800°, Lon: -71.3356°

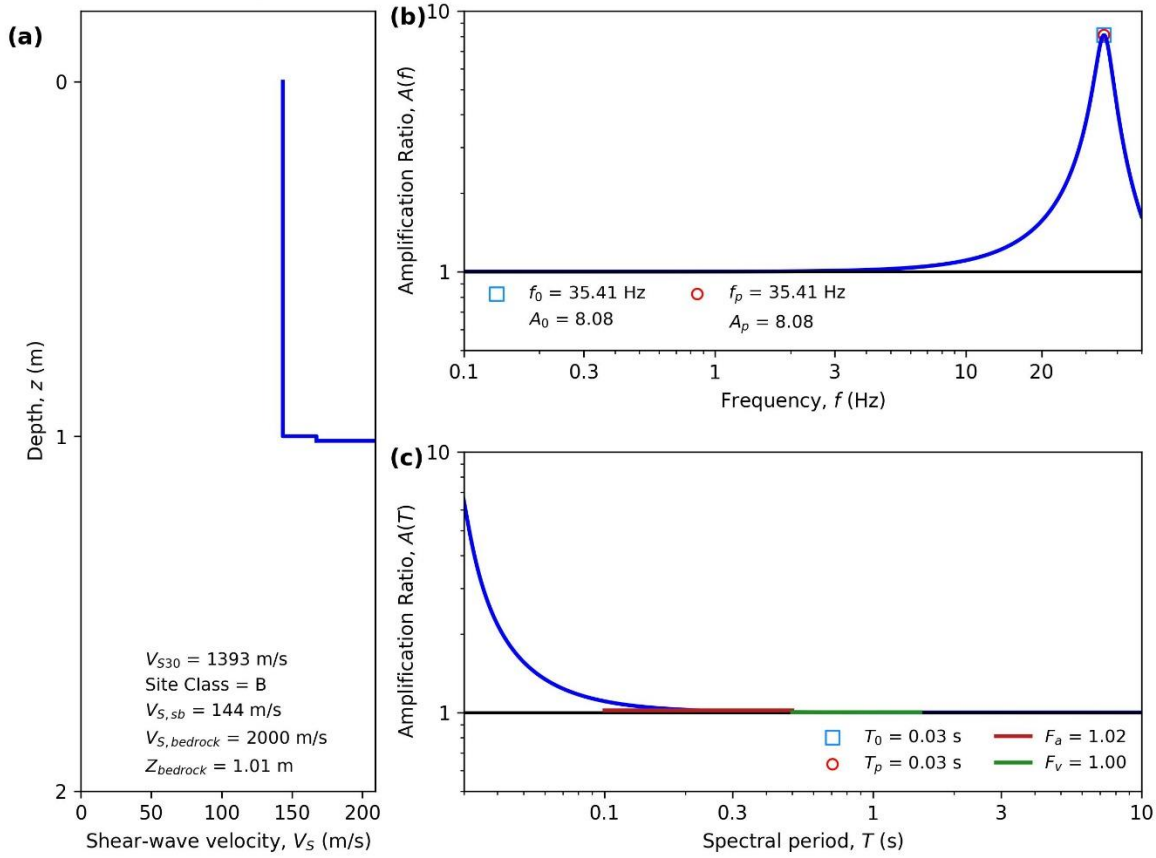

HAZUS Emergency Management
Massachusetts Care
Figure E127. ID: MA000127, Lat: 42.4660°, Lon: -71.1228°

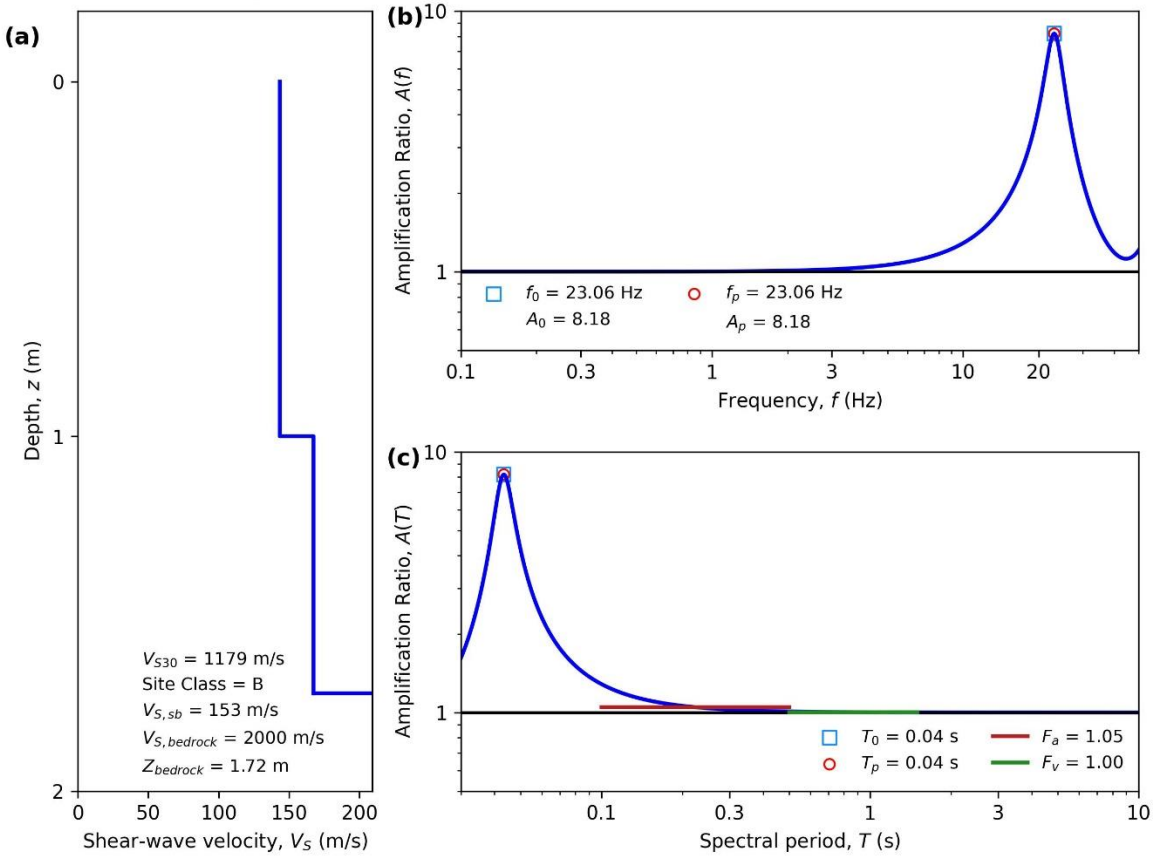

HAZUS Emergency Management
Massachusetts Care
Figure E128. ID: MA000128, Lat: 42.5957°, Lon: -72.5923°

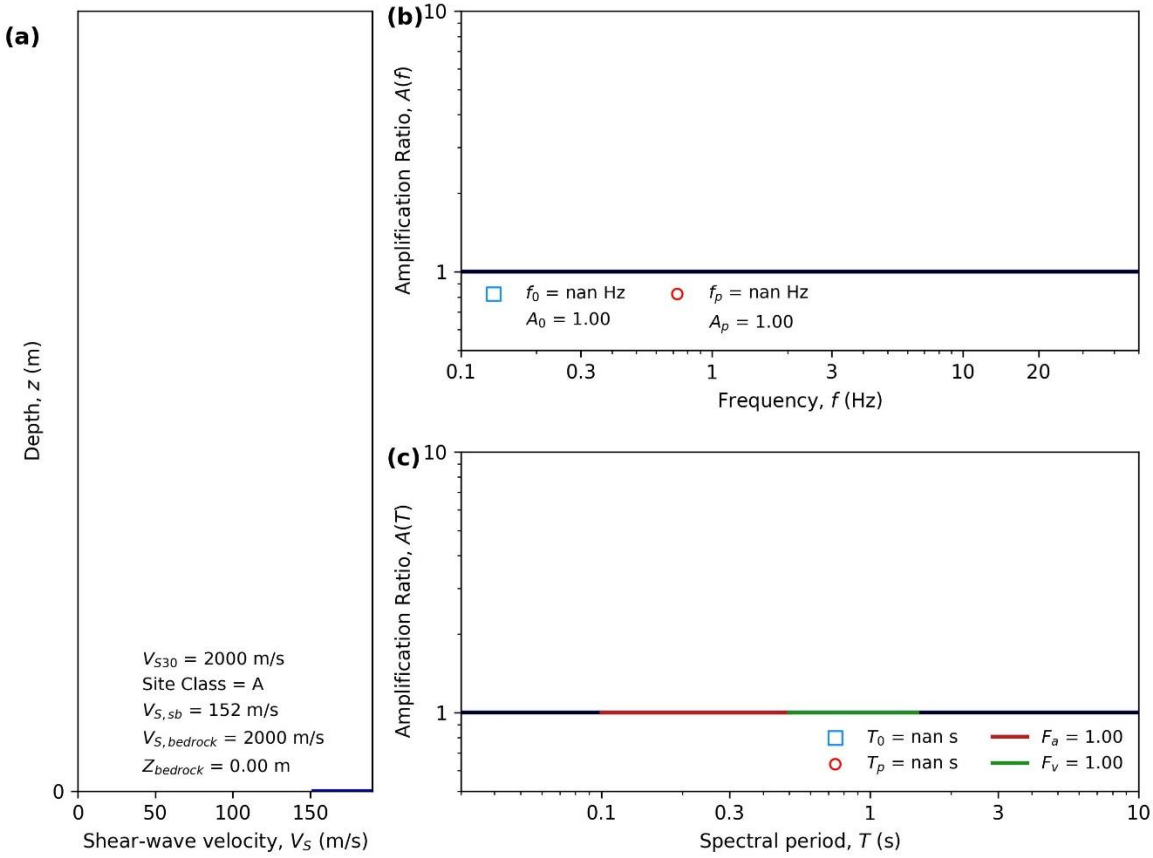

HAZUS Emergency Management
Massachusetts Care
Figure E129. ID: MA000129, Lat: 42.1151°, Lon: -72.5933°

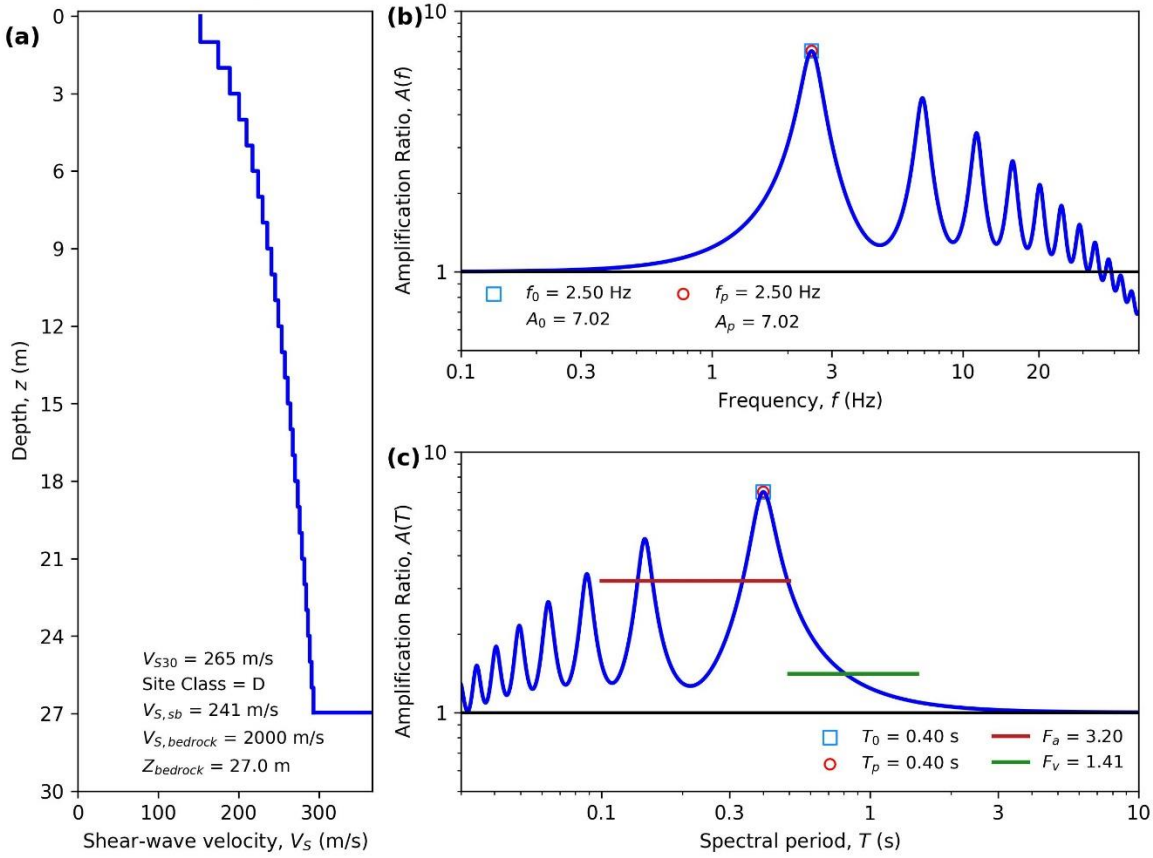

HAZUS Emergency Management
Massachusetts Care
Figure E130. ID: MA000130, Lat: 42.1696°, Lon: -72.3418°

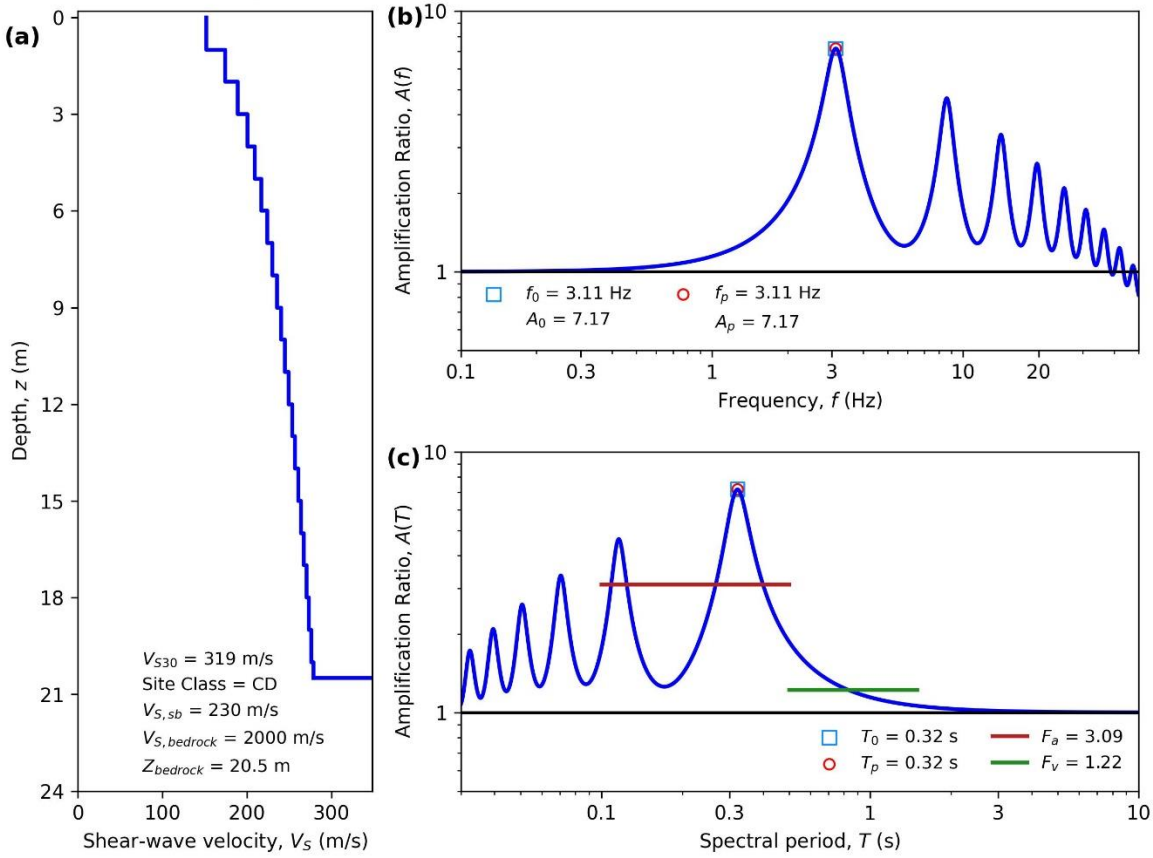

HAZUS Emergency Management
Massachusetts Care
Figure E131. ID: MA000131, Lat: 42.4847°, Lon: -71.2053°

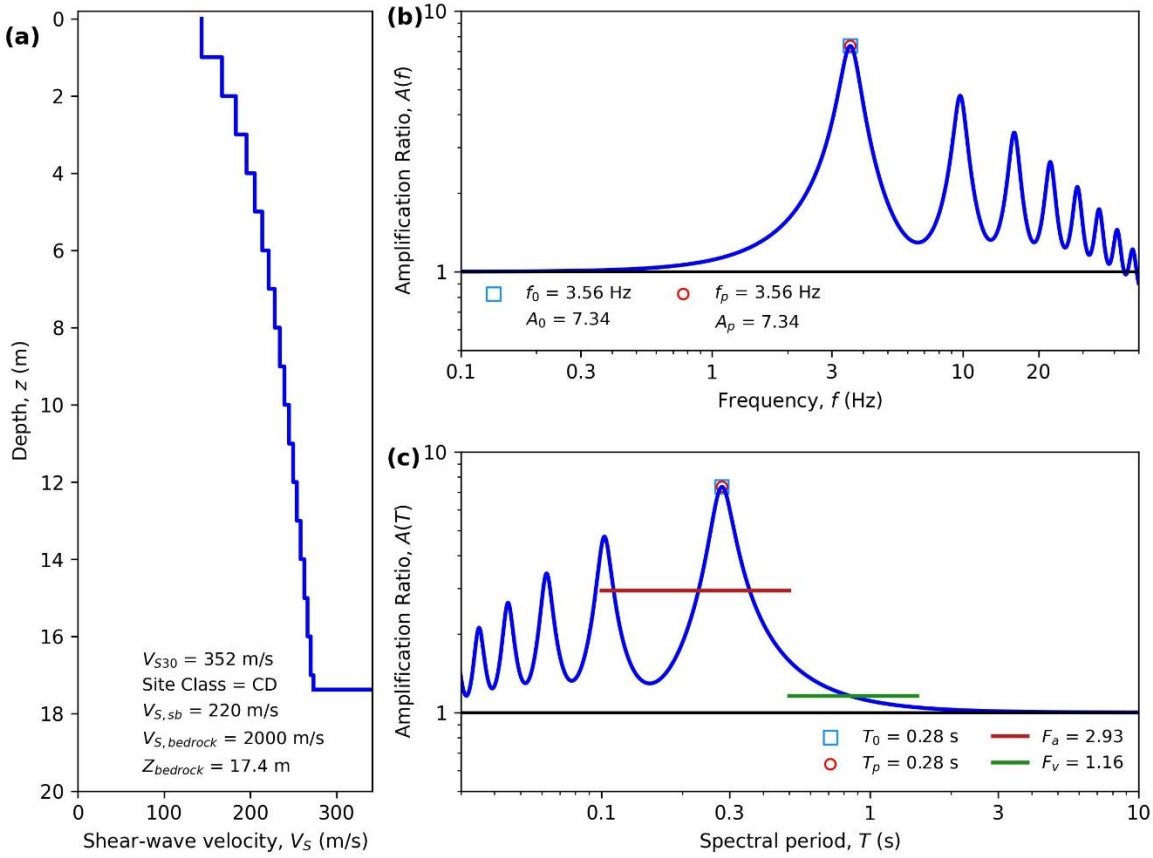

HAZUS Emergency Management
Massachusetts Care
Figure E132. ID: MA000132, Lat: 41.6884°, Lon: -70.6024°

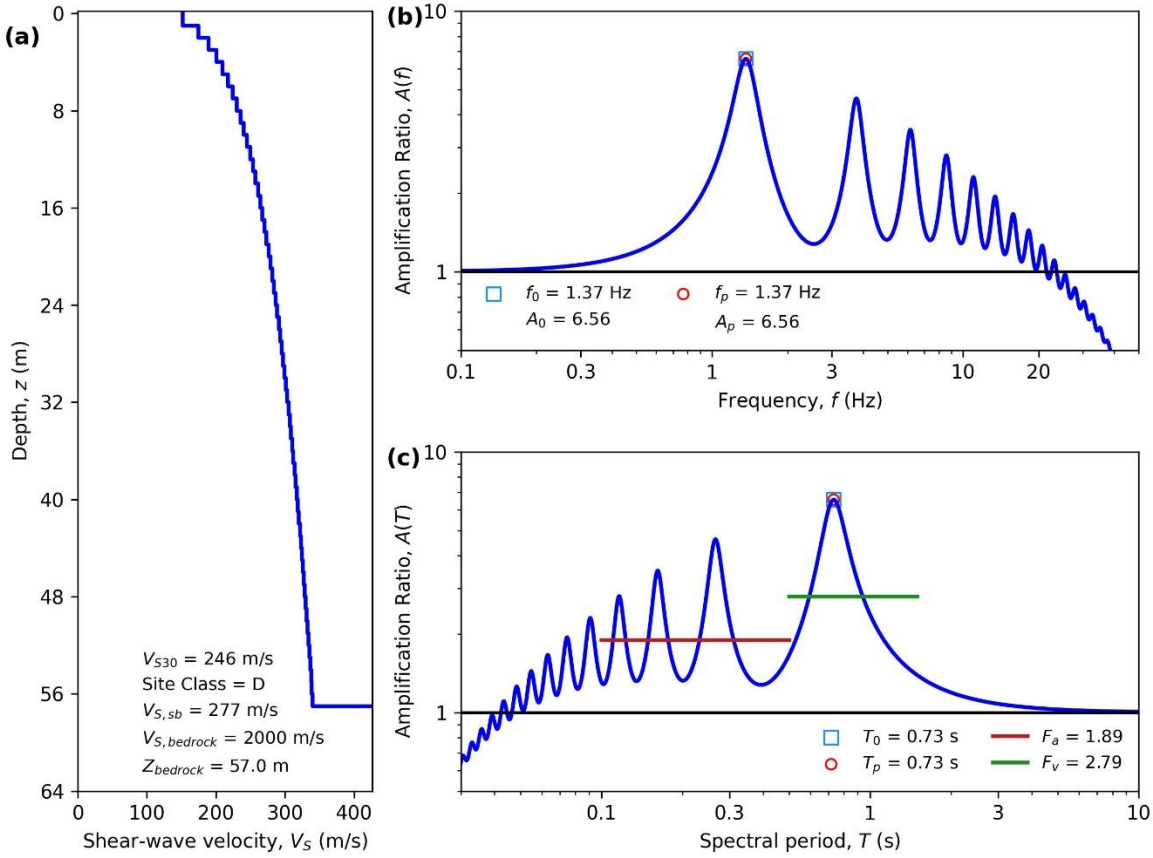

HAZUS Emergency Management
Massachusetts Care
Figure E133. ID: MA000133, Lat: 42.3363°, Lon: -71.0707°

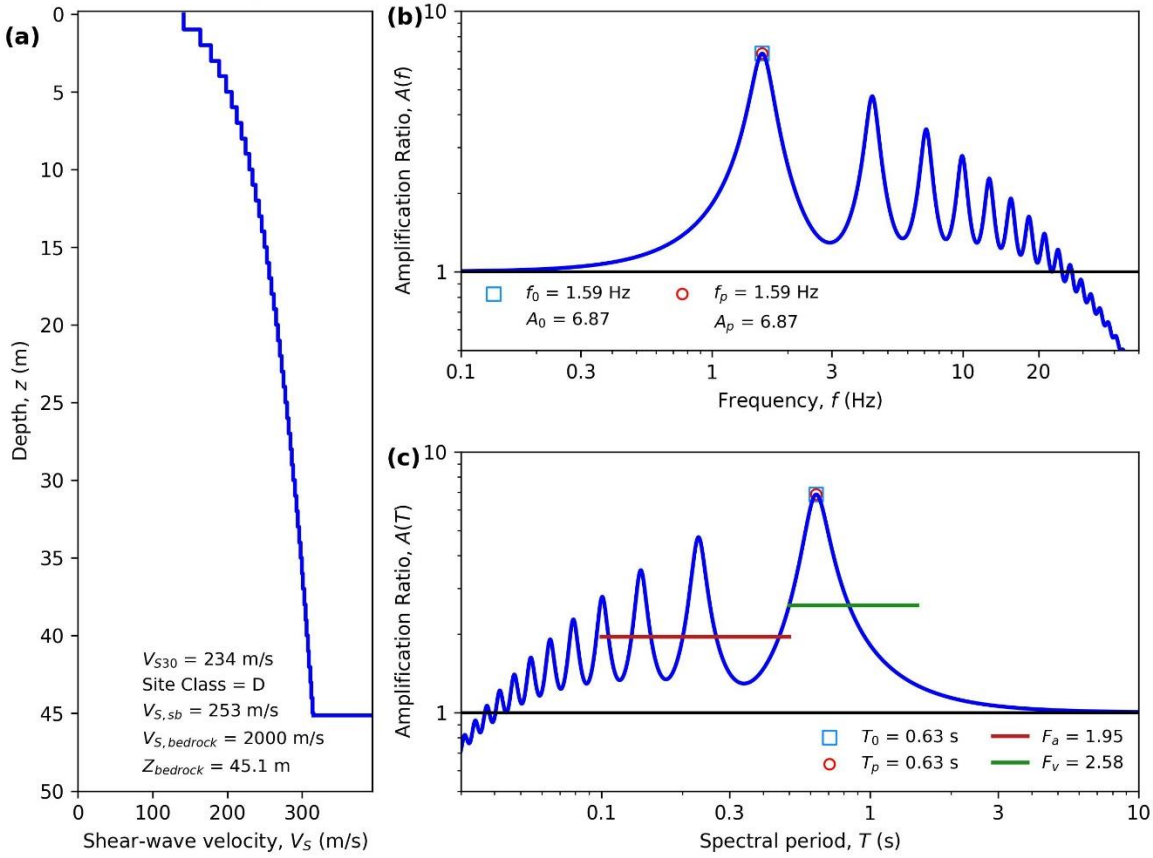

HAZUS Emergency Management
Massachusetts Care
Figure E134. ID: MA000134, Lat: 42.5303°, Lon: -71.6150°

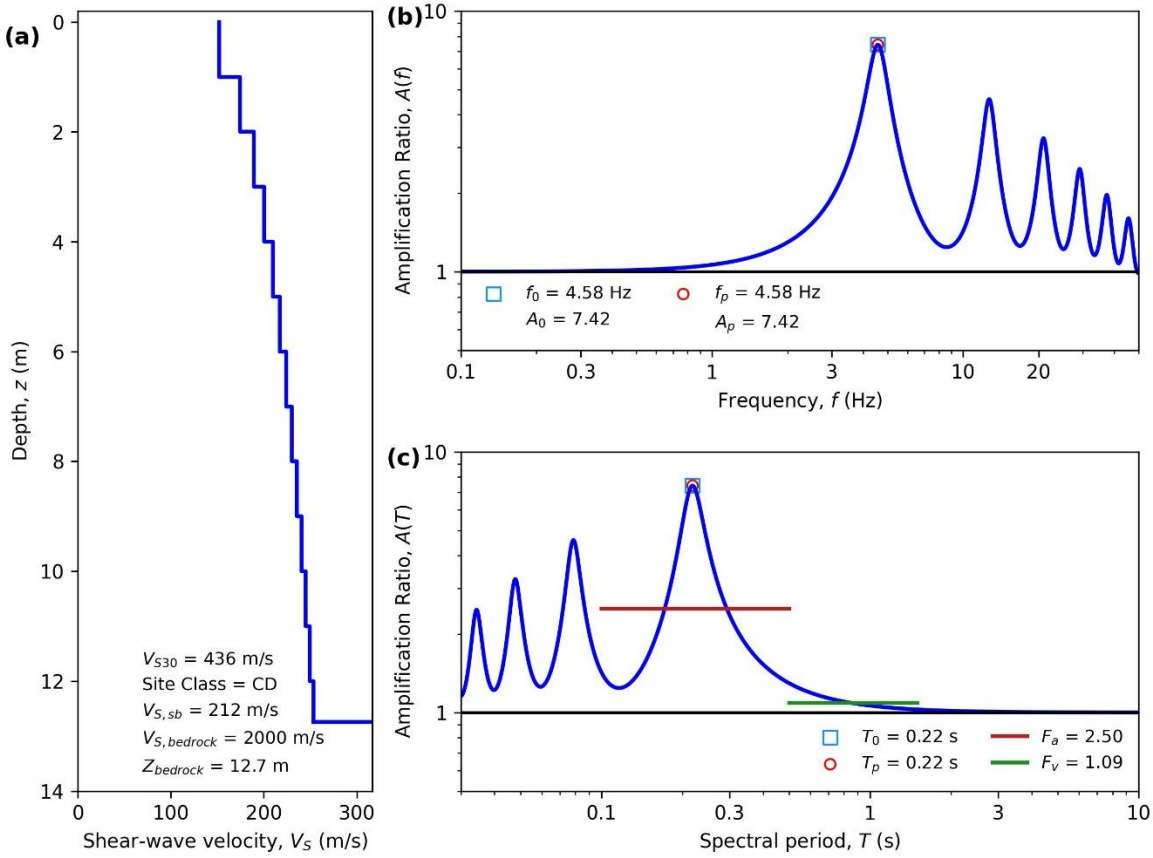

HAZUS Emergency Management
Massachusetts Care
Figure E135. ID: MA000135, Lat: 42.6191°, Lon: -71.3154°

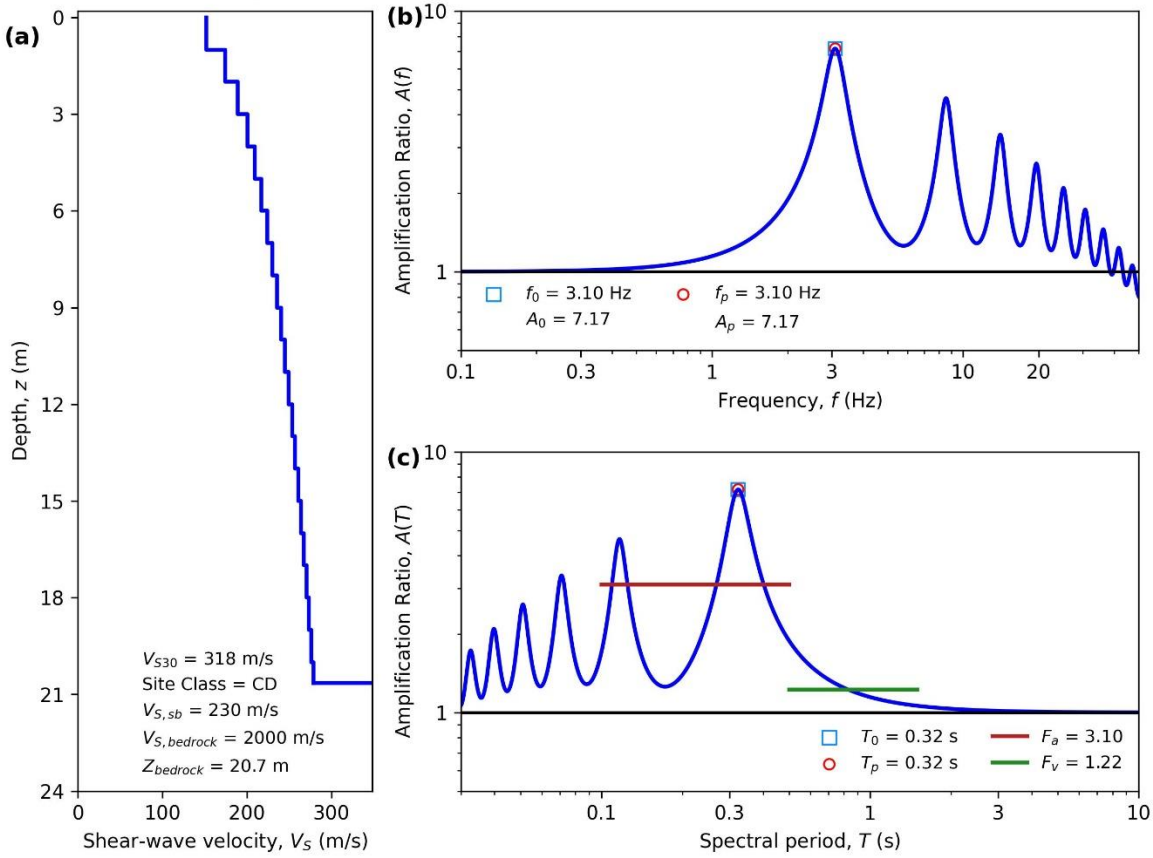

HAZUS Emergency Management
Massachusetts Care
Figure E136. ID: MA000136, Lat: 42.0630°, Lon: -71.0539°

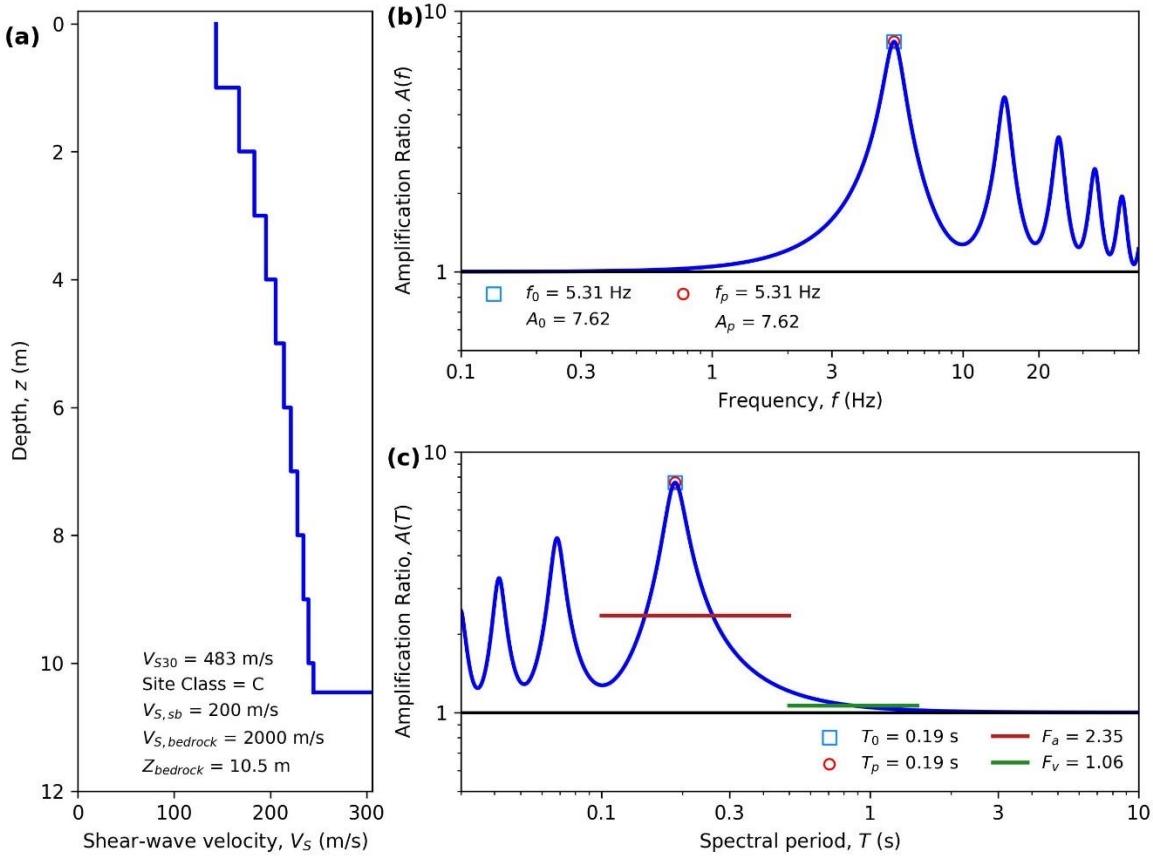

HAZUS Emergency Management
Massachusetts Care
Figure E137. ID: MA000137, Lat: 42.3482°, Lon: -71.0985°

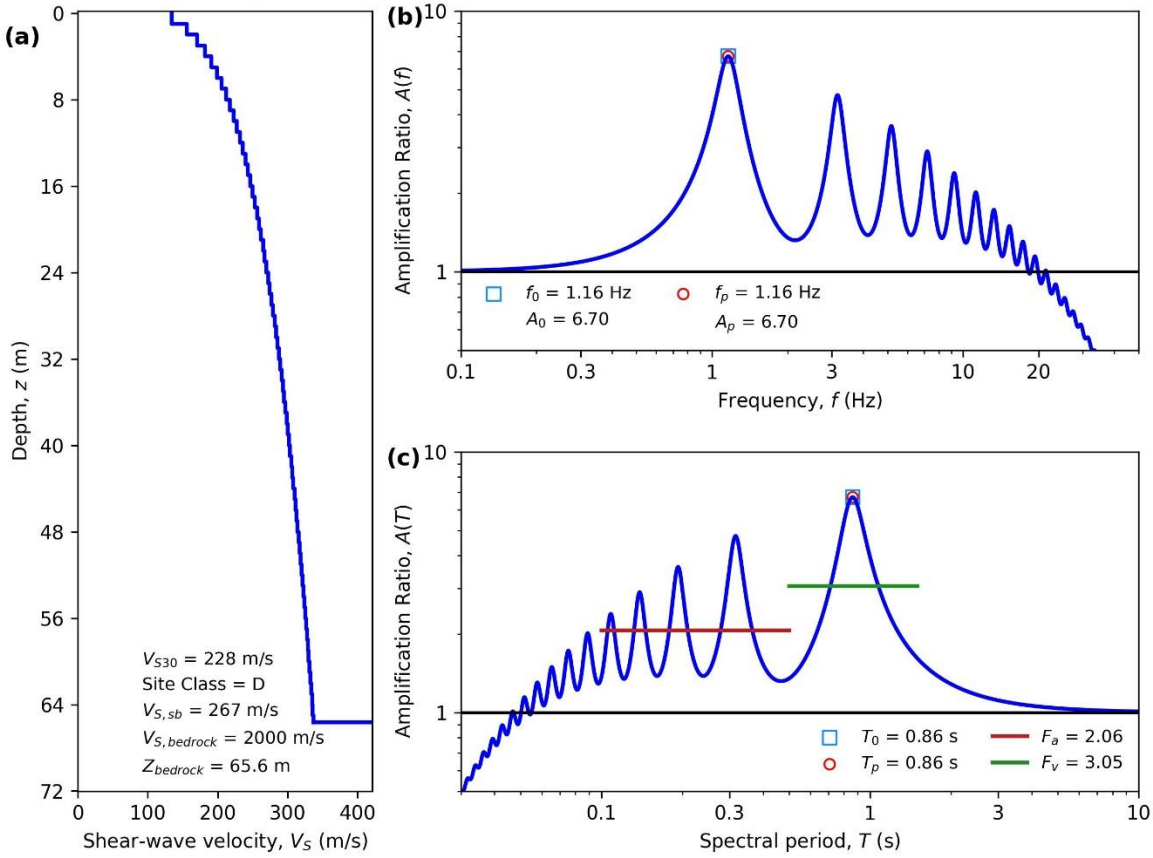

HAZUS Emergency Management
Massachusetts Care
Figure E138. ID: MA000138, Lat: 42.2746°, Lon: -71.1717°

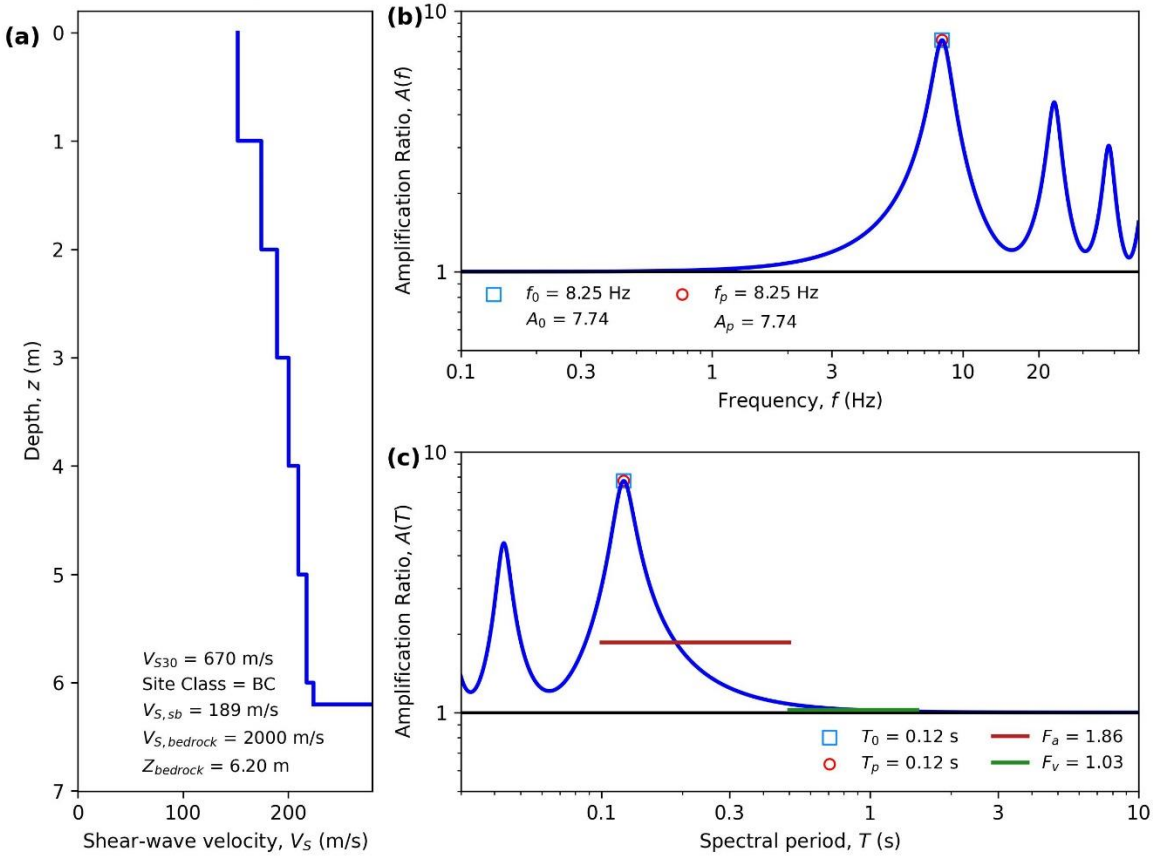

HAZUS Emergency Management
Massachusetts Care
Figure E139. ID: MA000139, Lat: 42.2834°, Lon: -71.4176°

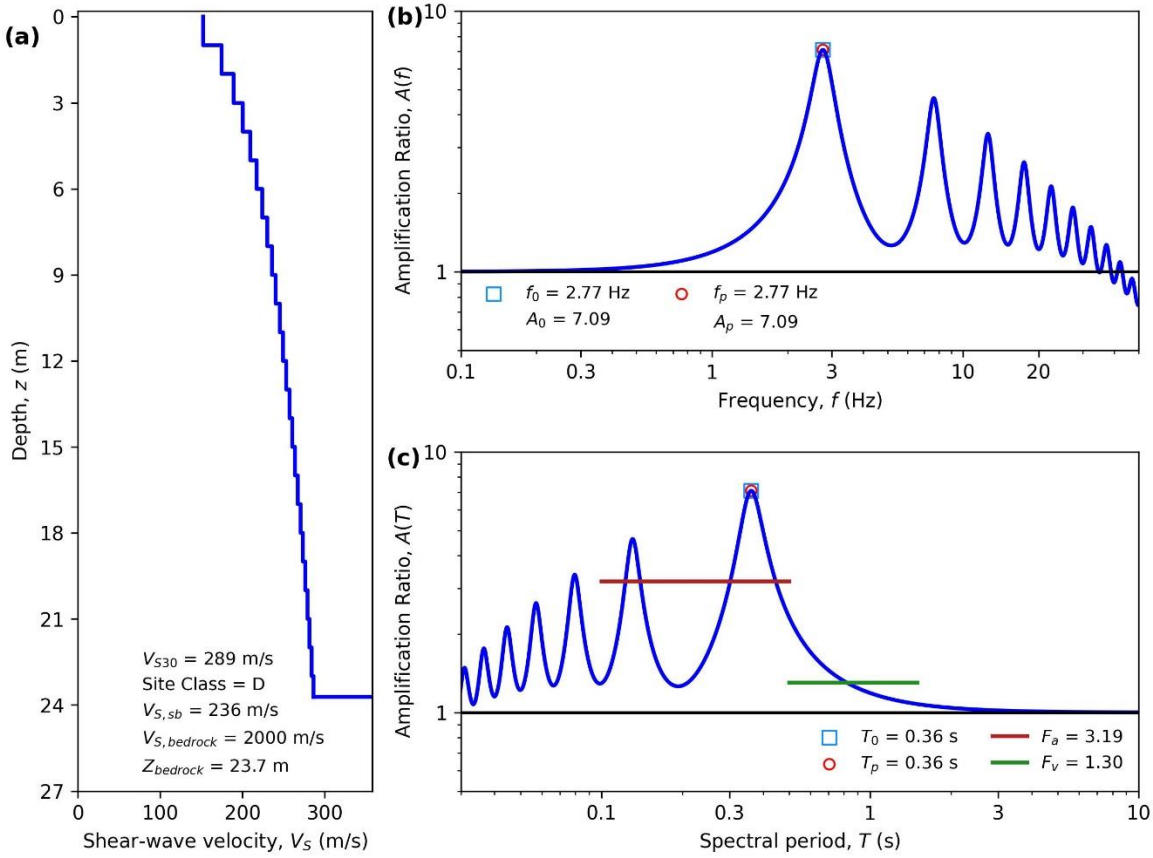

HAZUS Emergency Management
Massachusetts Care
Figure E140. ID: MA000140, Lat: 42.3665°, Lon: -71.0590°

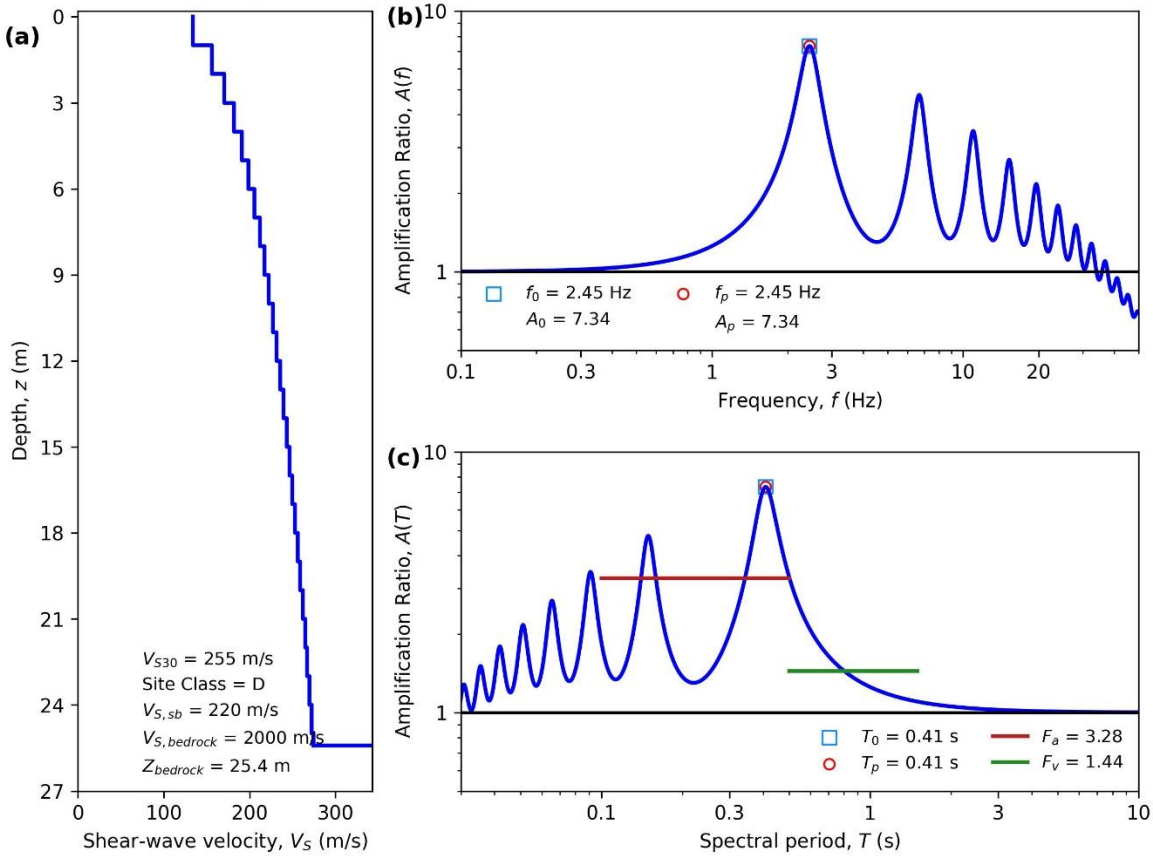

HAZUS Emergency Management
Massachusetts Care
Figure E141. ID: MA000141, Lat: 42.3270°, Lon: -71.1103°

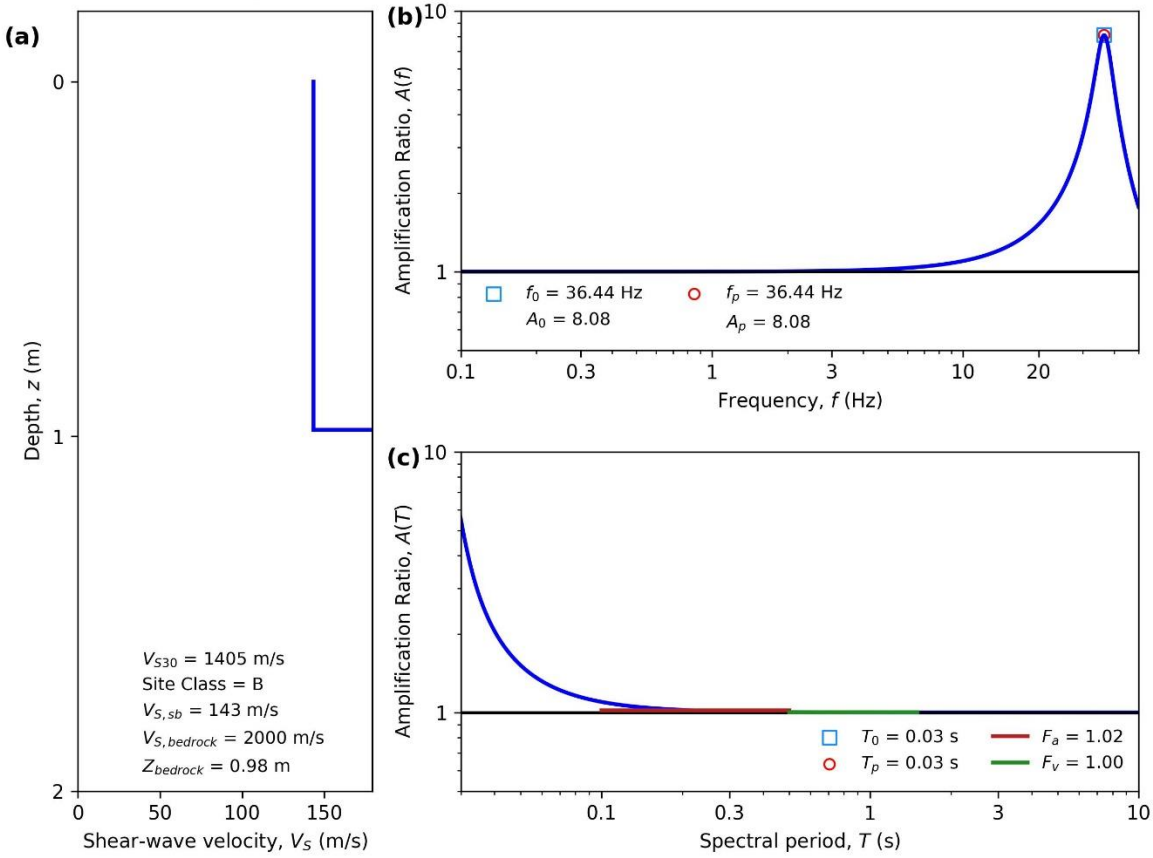

HAZUS Emergency Management
Massachusetts Care
Figure E142. ID: MA000142, Lat: 42.2941°, Lon: -71.0885°

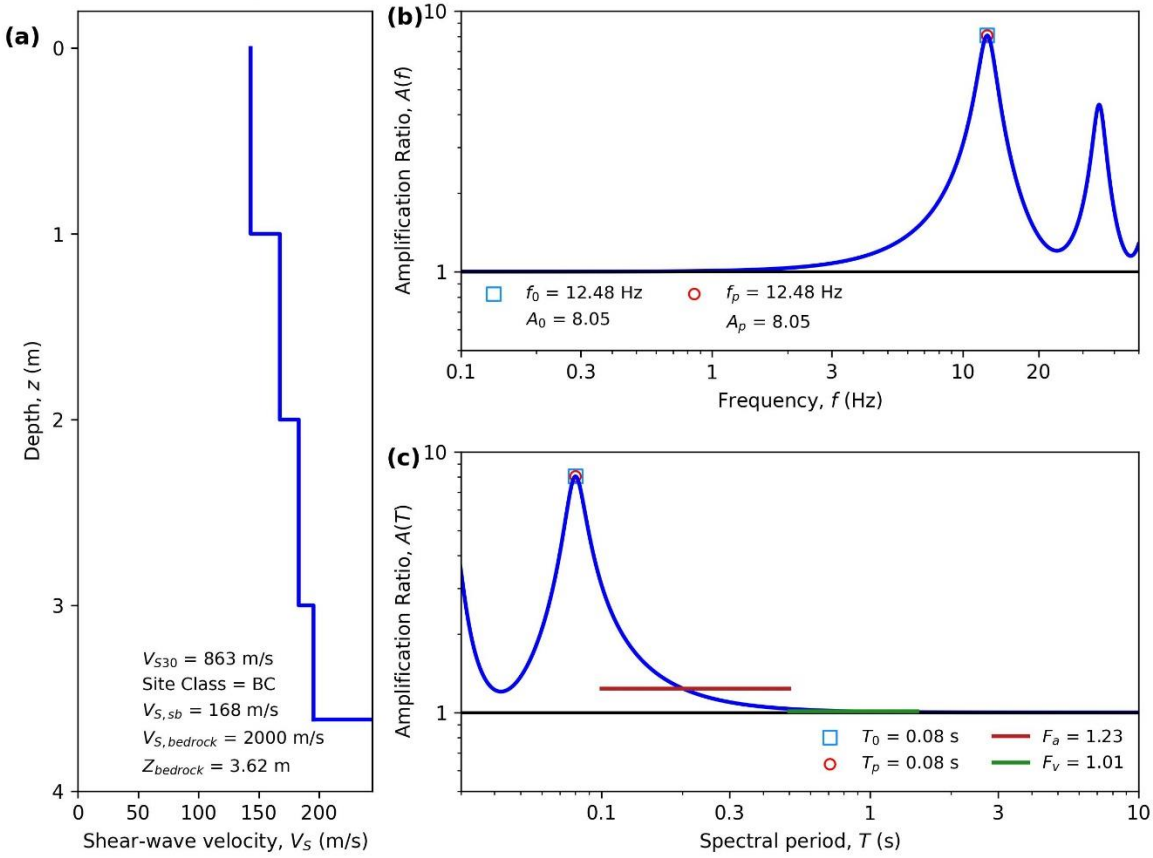

HAZUS Emergency Management
Massachusetts Care
Figure E143. ID: MA000143, Lat: 42.6192°, Lon: -71.3156°

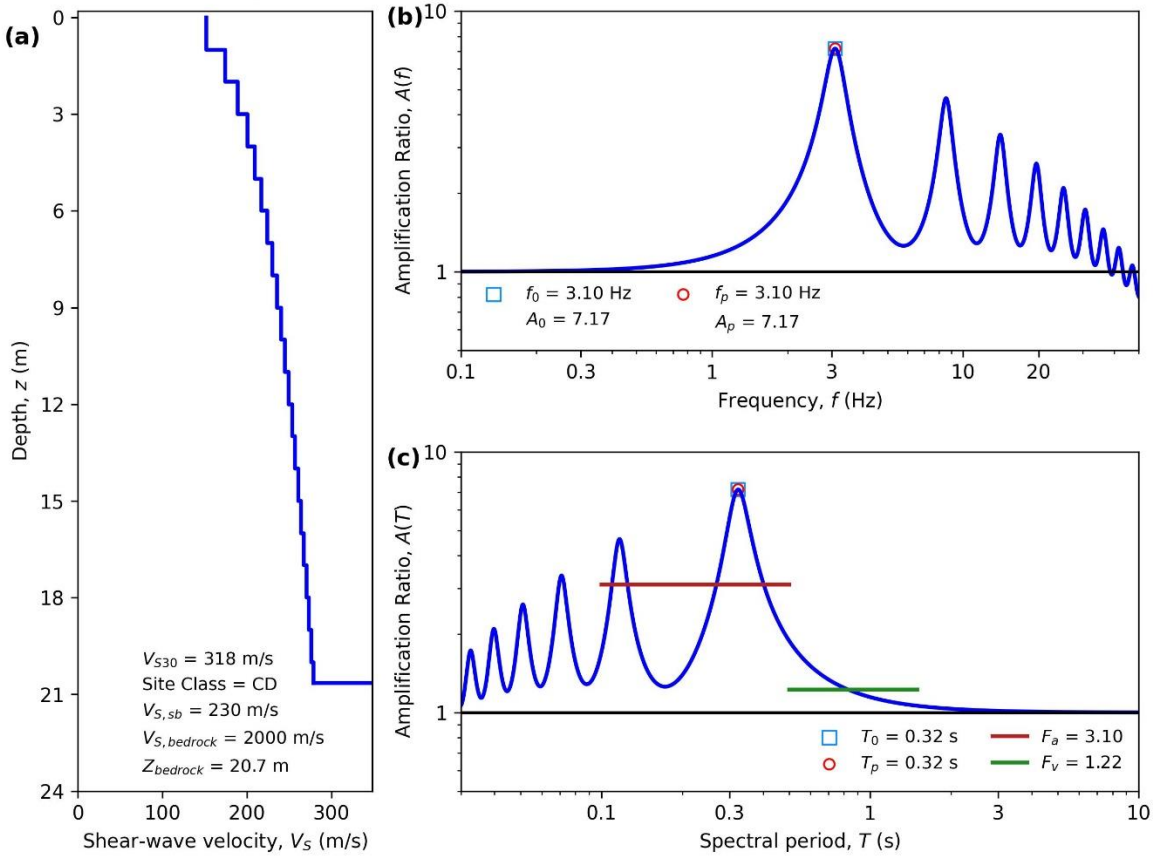

HAZUS Emergency Management
Massachusetts Care
Figure E144. ID: MA000144, Lat: 42.5977°, Lon: -71.8060°

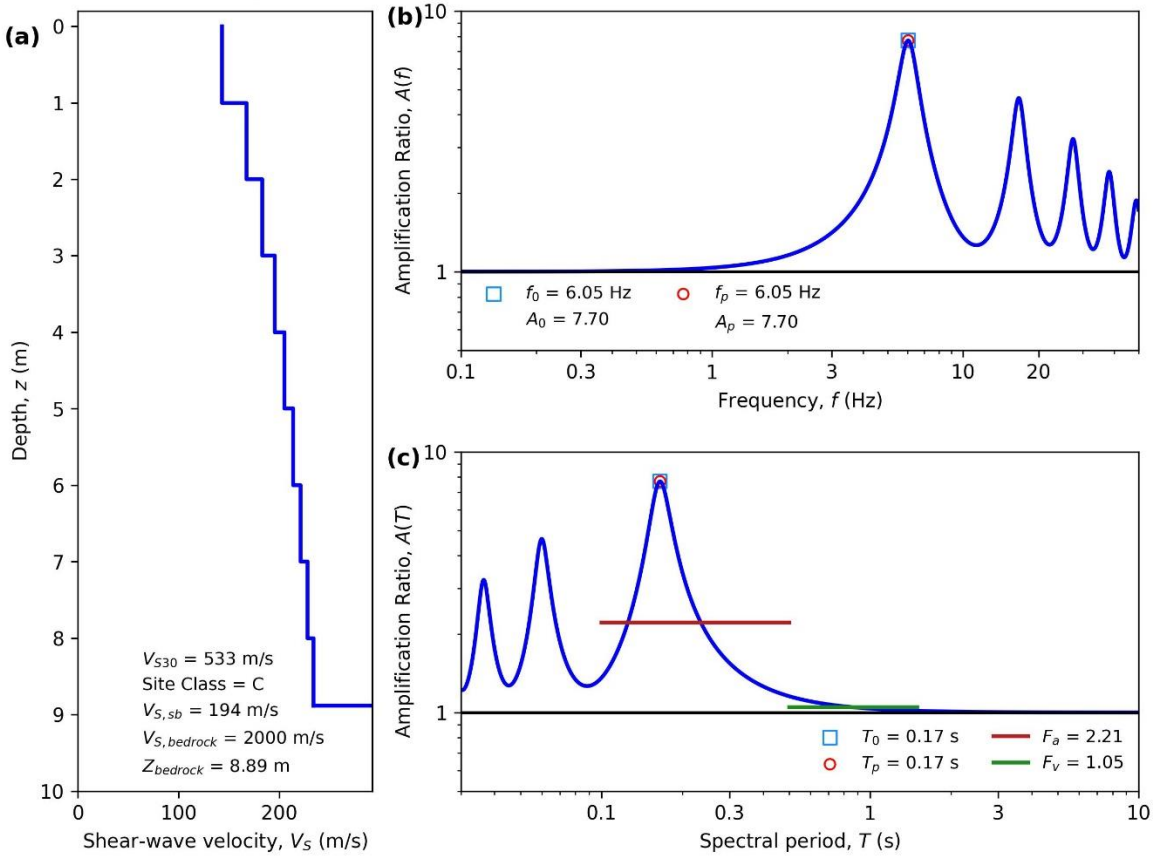

HAZUS Emergency Management
Massachusetts Care
Figure E145. ID: MA000145, Lat: 42.2507°, Lon: -71.7700°

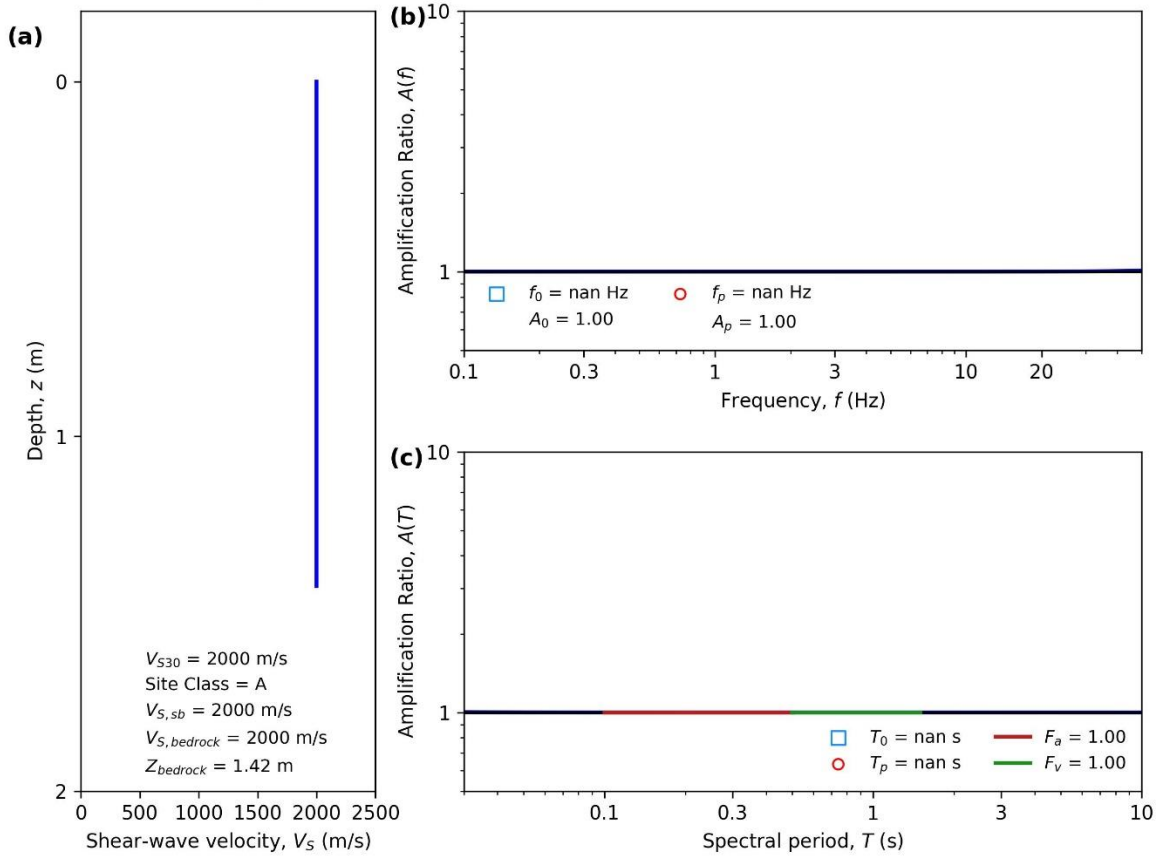

HAZUS Emergency Management
Massachusetts Care
Figure E146. ID: MA000146, Lat: 42.6442°, Lon: -71.3039°

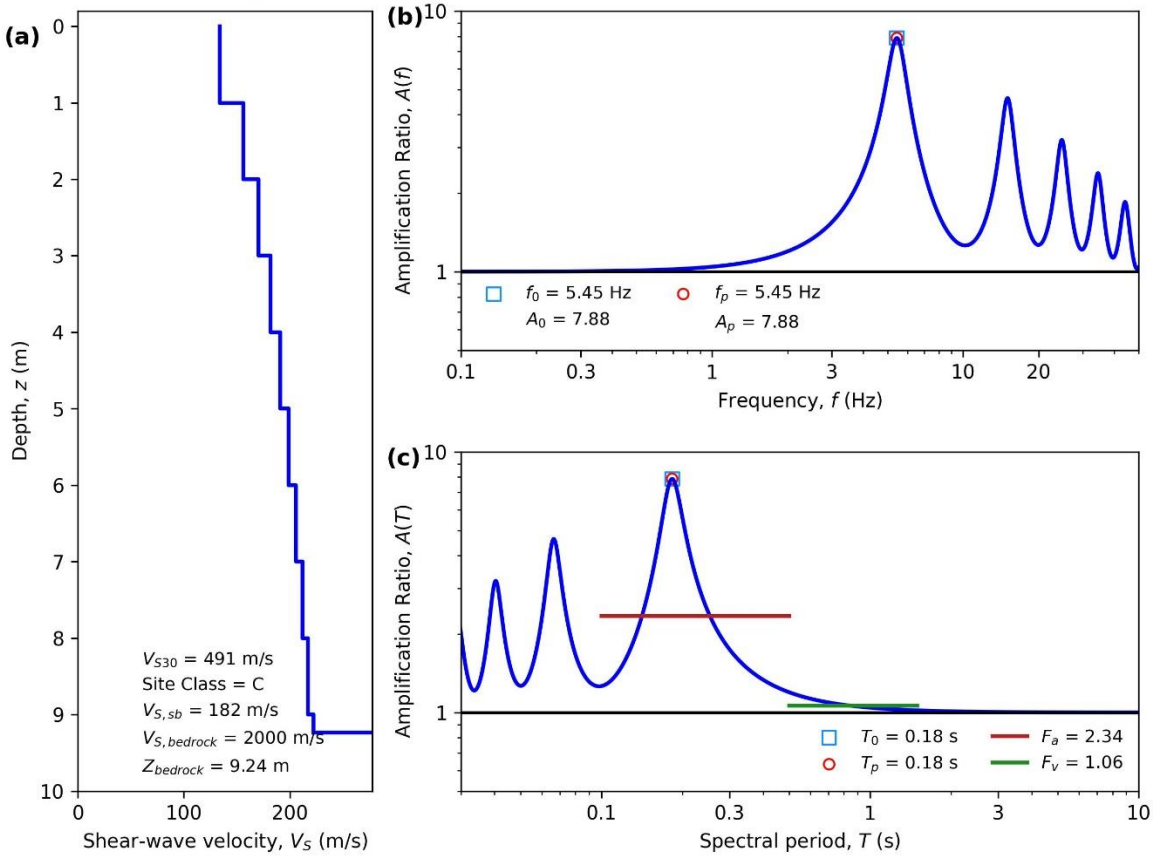

HAZUS Emergency Management
Massachusetts Care
Figure E147. ID: MA000147, Lat: 41.6361°, Lon: -70.9506°

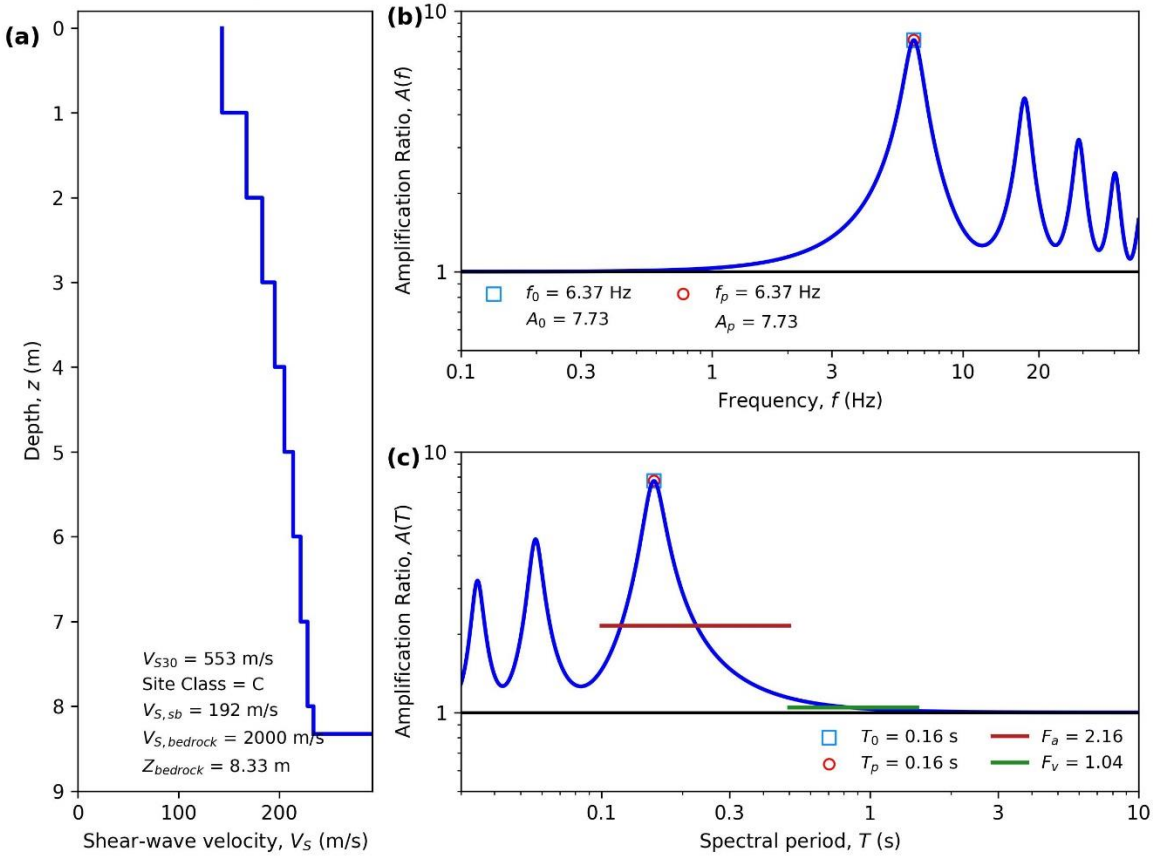

HAZUS Emergency Management
Massachusetts Care
Figure E148. ID: MA000148, Lat: 42.6853°, Lon: -72.0539°

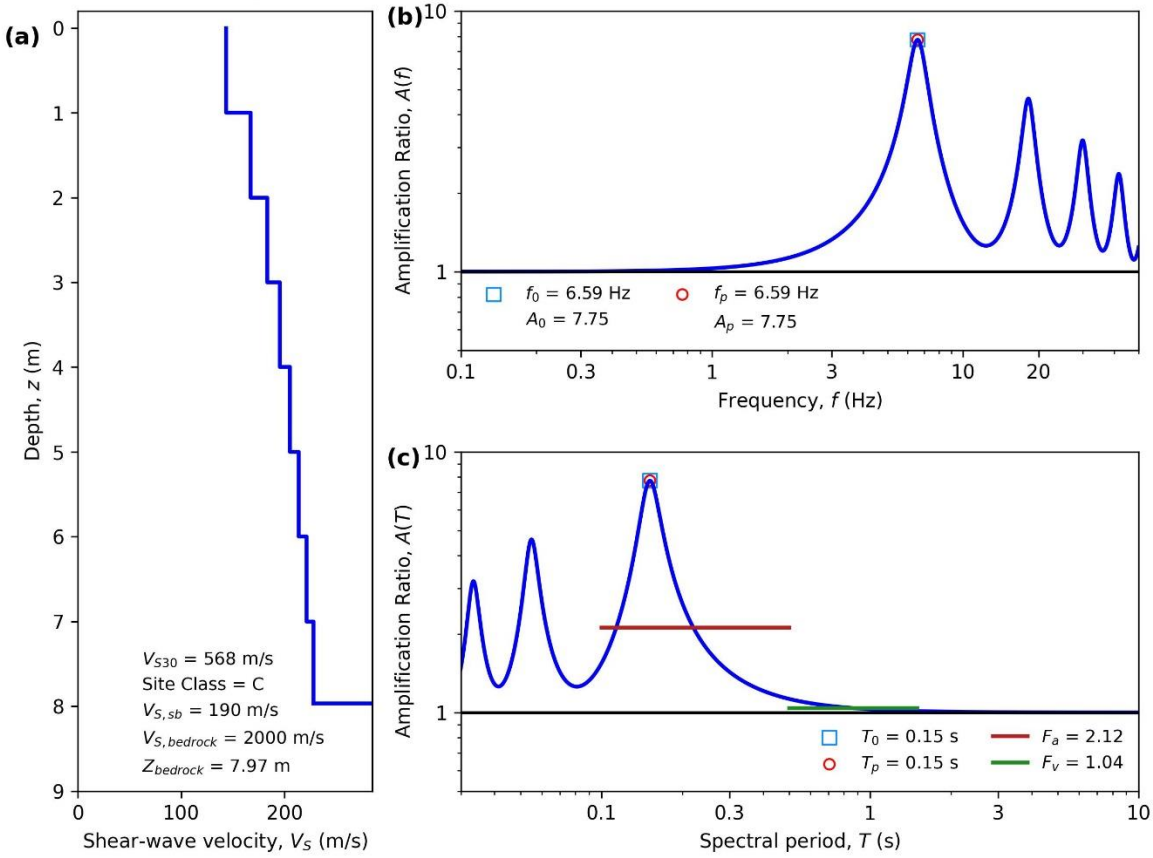

HAZUS Emergency Management
Massachusetts Care
Figure E149. ID: MA000149, Lat: 42.2971°, Lon: -71.7674°

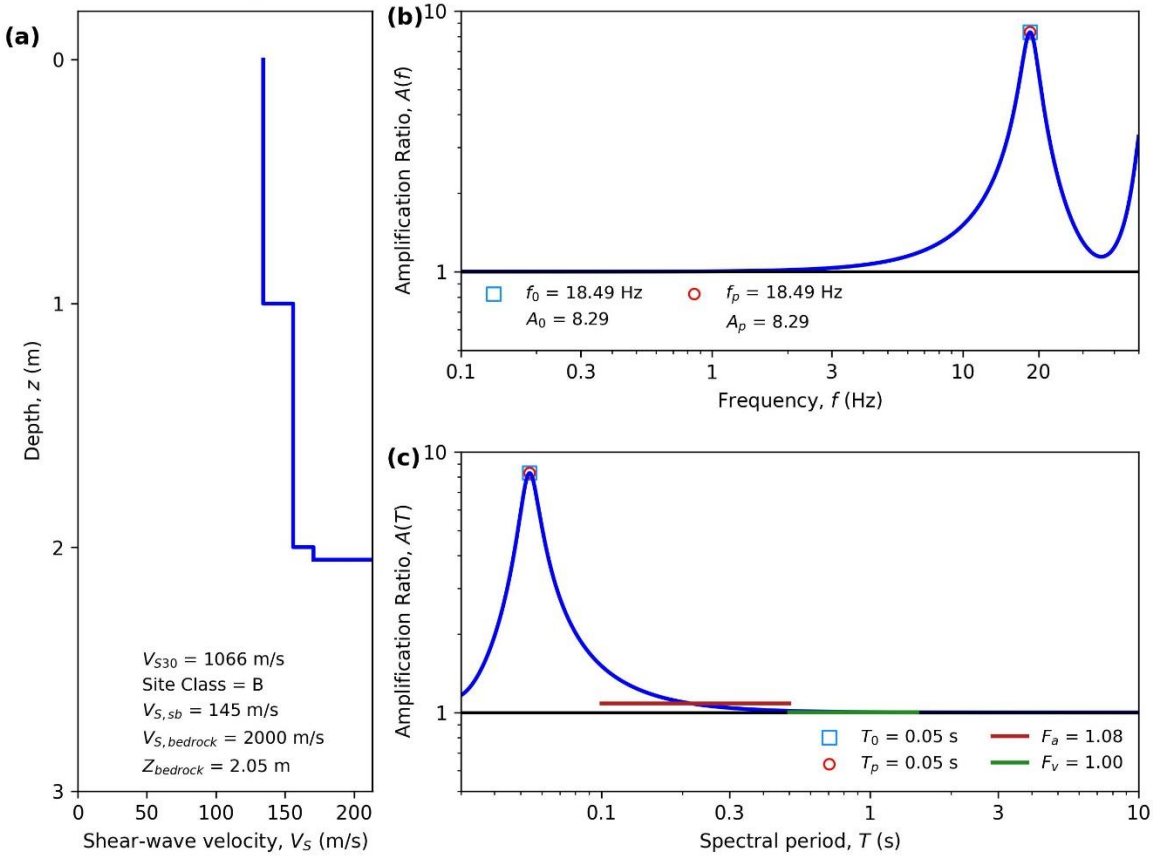

HAZUS Emergency Management
Massachusetts Care
Figure E150. ID: MA000150, Lat: 41.6362°, Lon: -70.9294°

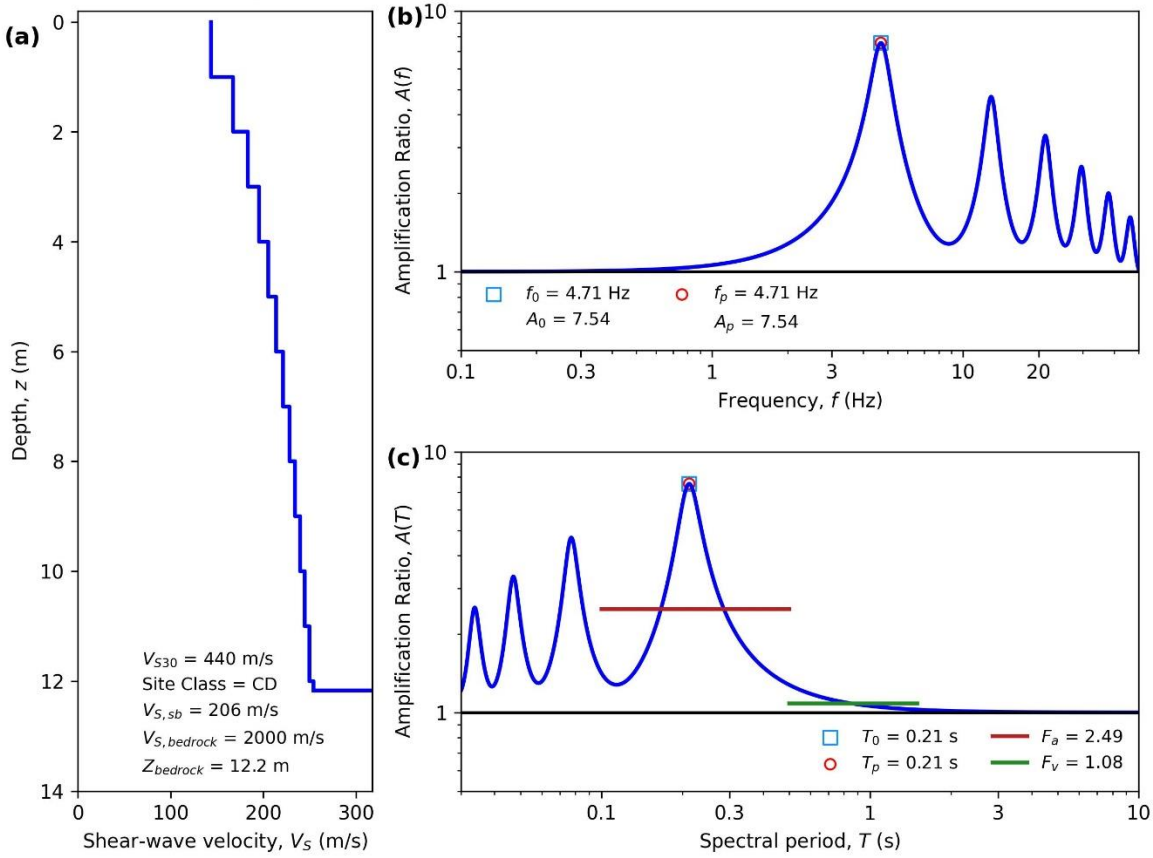

HAZUS Emergency Management
Massachusetts Care
Figure E151. ID: MA000151, Lat: 42.5772°, Lon: -72.6242°

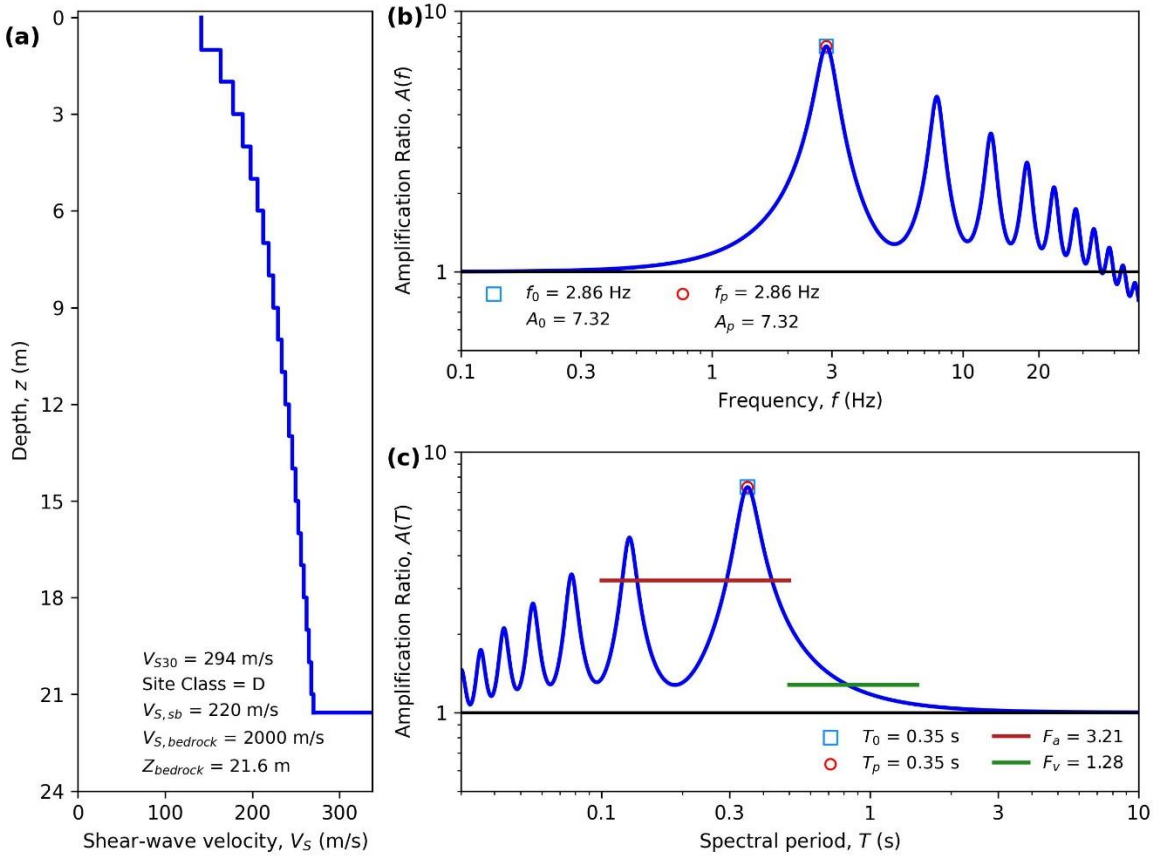

HAZUS Emergency Management
Massachusetts Care
Figure E152. ID: MA000152, Lat: 42.1073°, Lon: -72.5976°

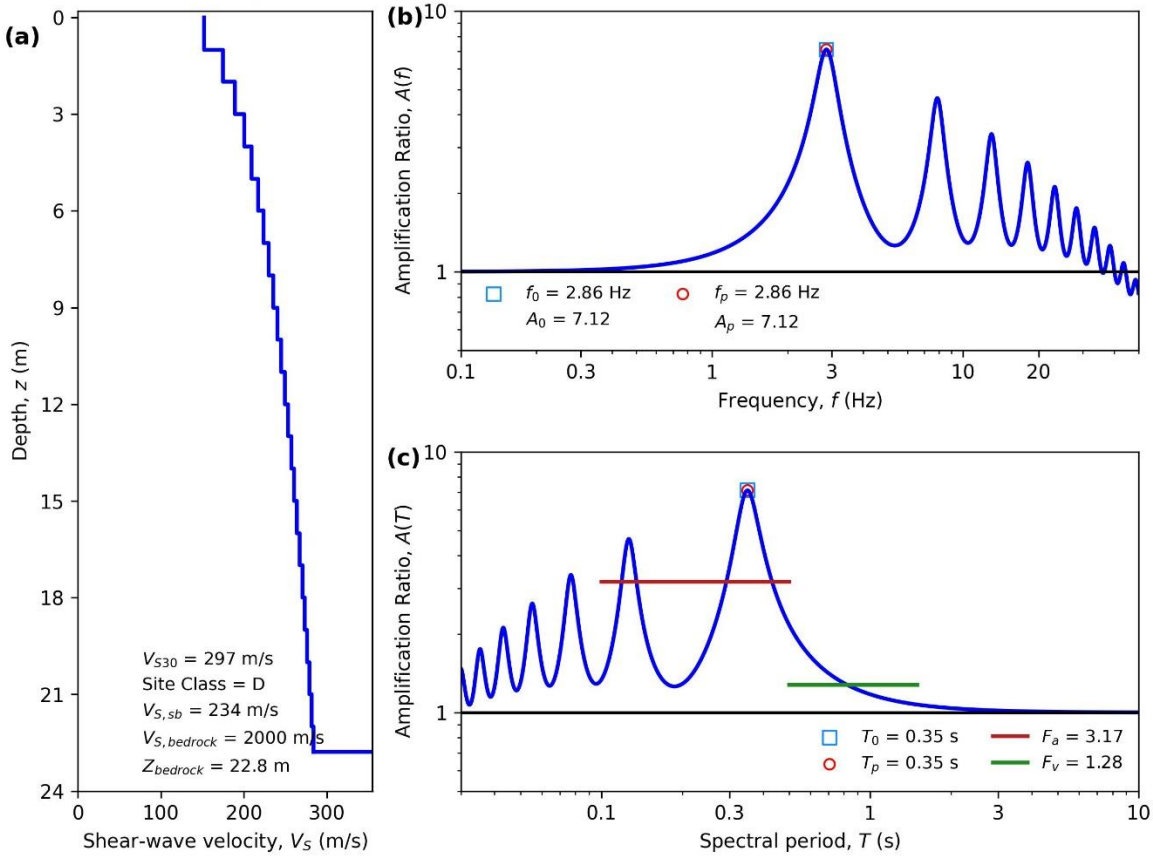

HAZUS Emergency Management
Massachusetts Care
Figure E153. ID: MA000153, Lat: 42.4518°, Lon: -73.2525°

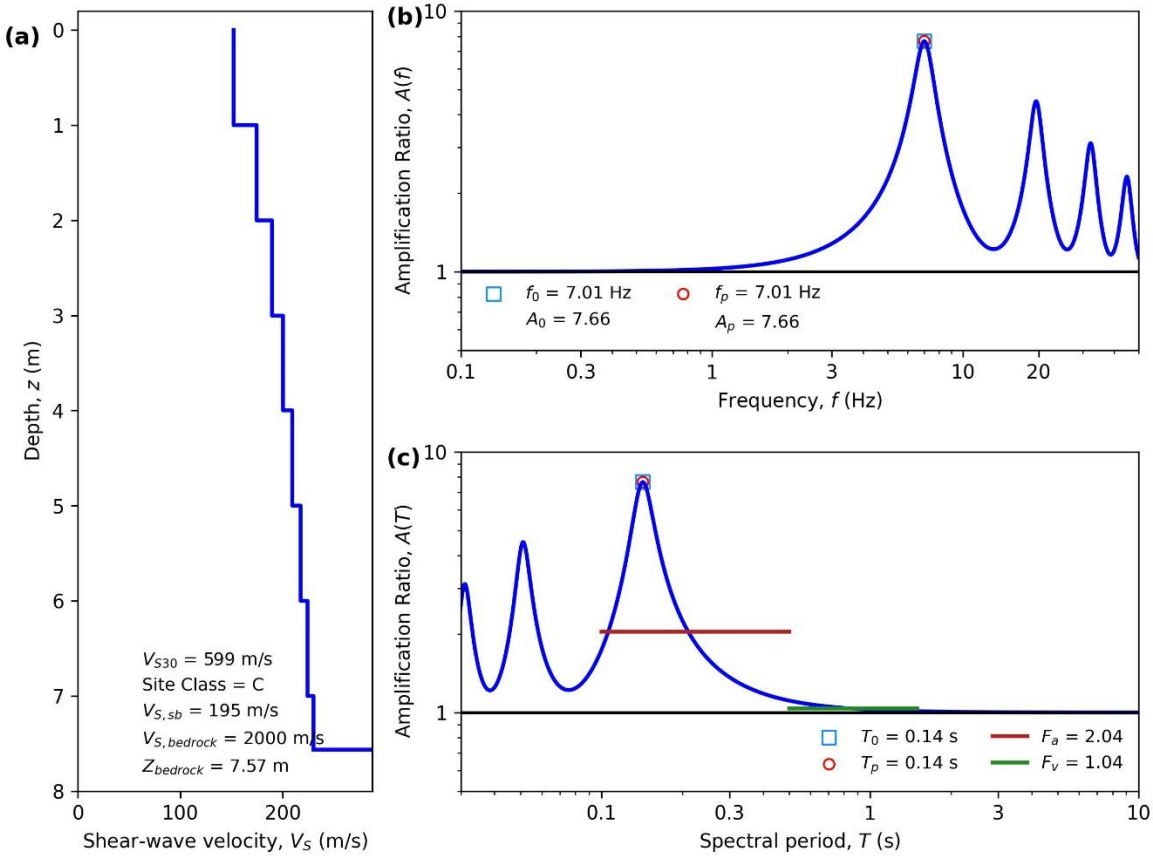

HAZUS Emergency Management
Massachusetts Care
Figure E154. ID: MA000154, Lat: 42.0526°, Lon: -71.0675°

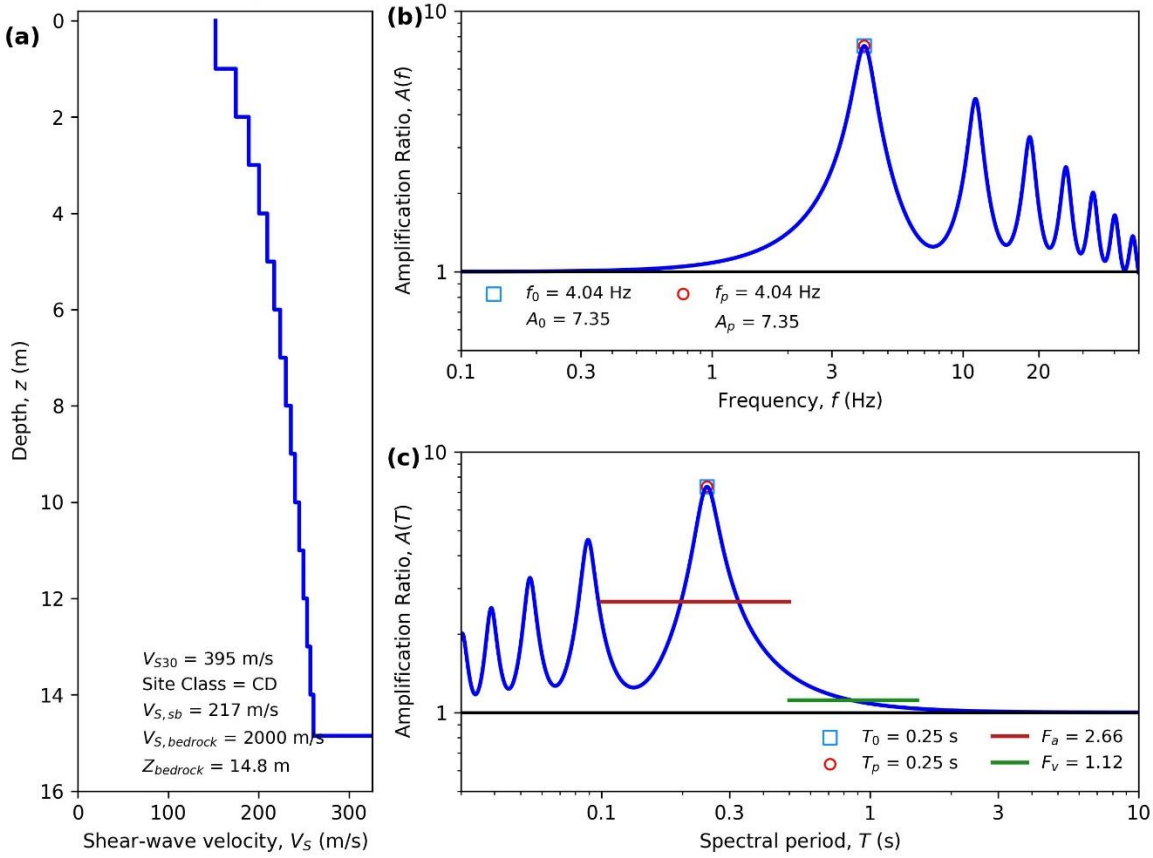

HAZUS Emergency Management
Massachusetts Care
Figure E155. ID: MA000155, Lat: 42.7743°, Lon: -71.0792°

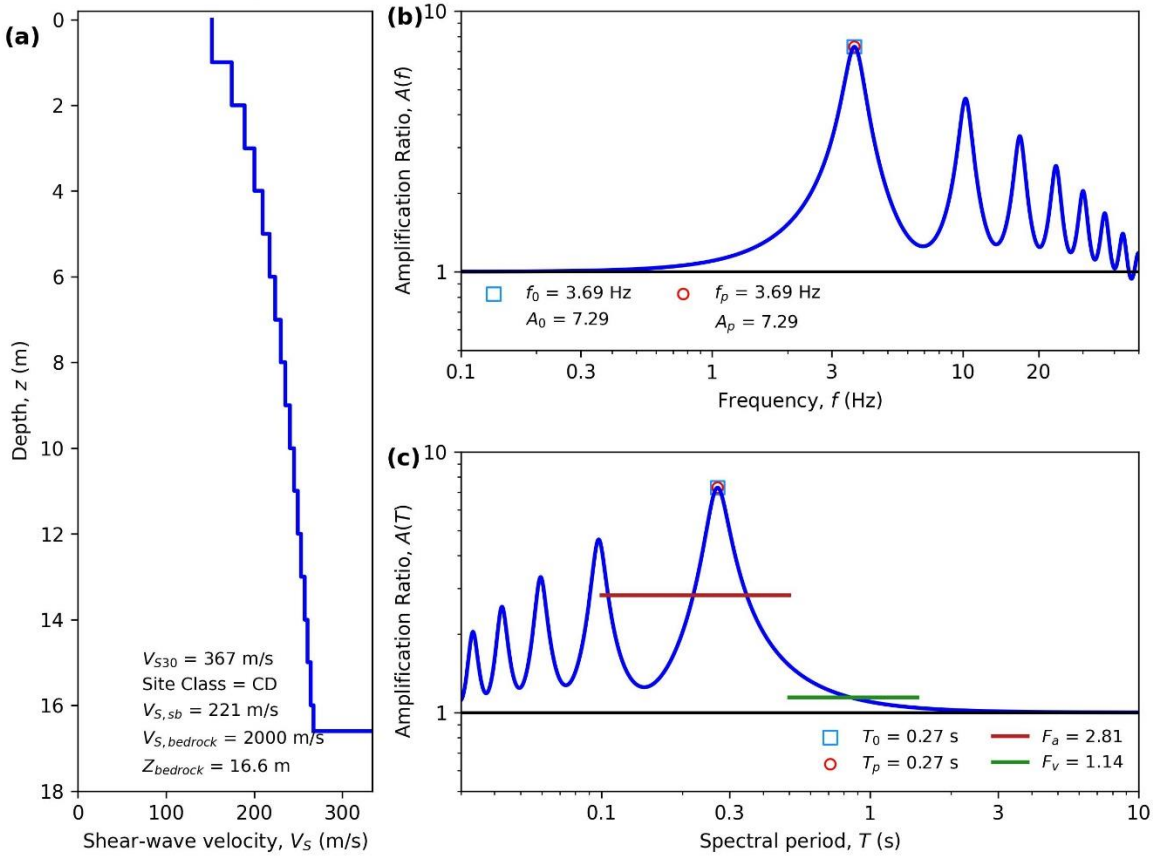

HAZUS Emergency Management
Massachusetts Care
Figure E156. ID: MA000156, Lat: 42.1101°, Lon: -72.5996°

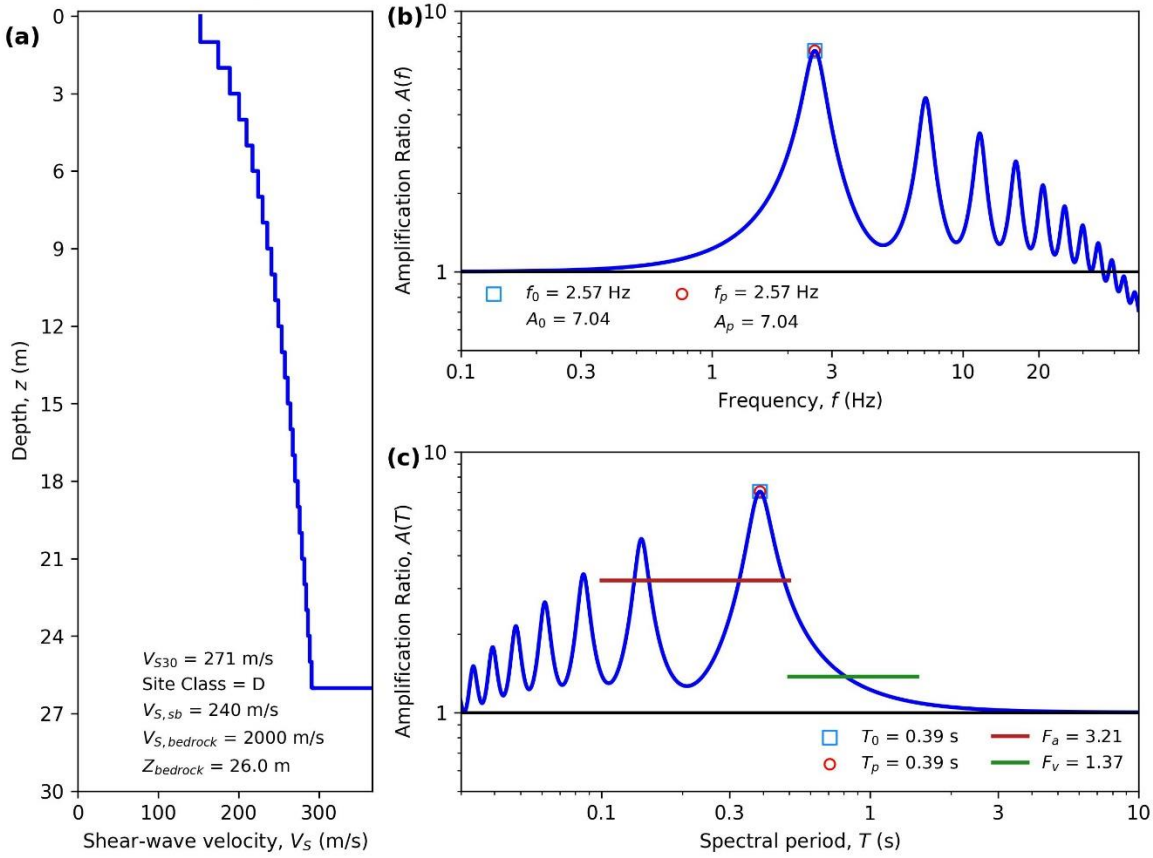

HAZUS Emergency Management
Massachusetts Care
Figure E157. ID: MA000157, Lat: 42.4705°, Lon: -70.9600°

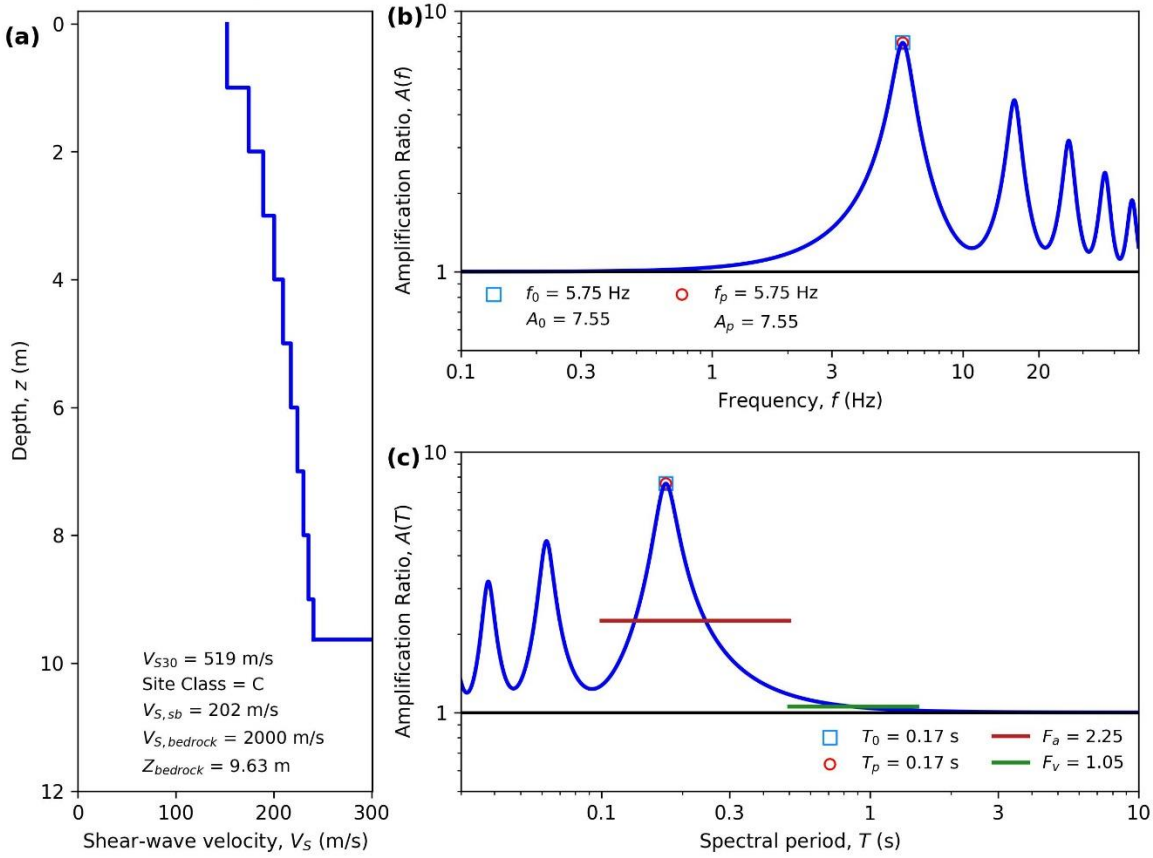

HAZUS Emergency Management
Massachusetts Care
Figure E158. ID: MA000158, Lat: 42.6255°, Lon: -70.6806°

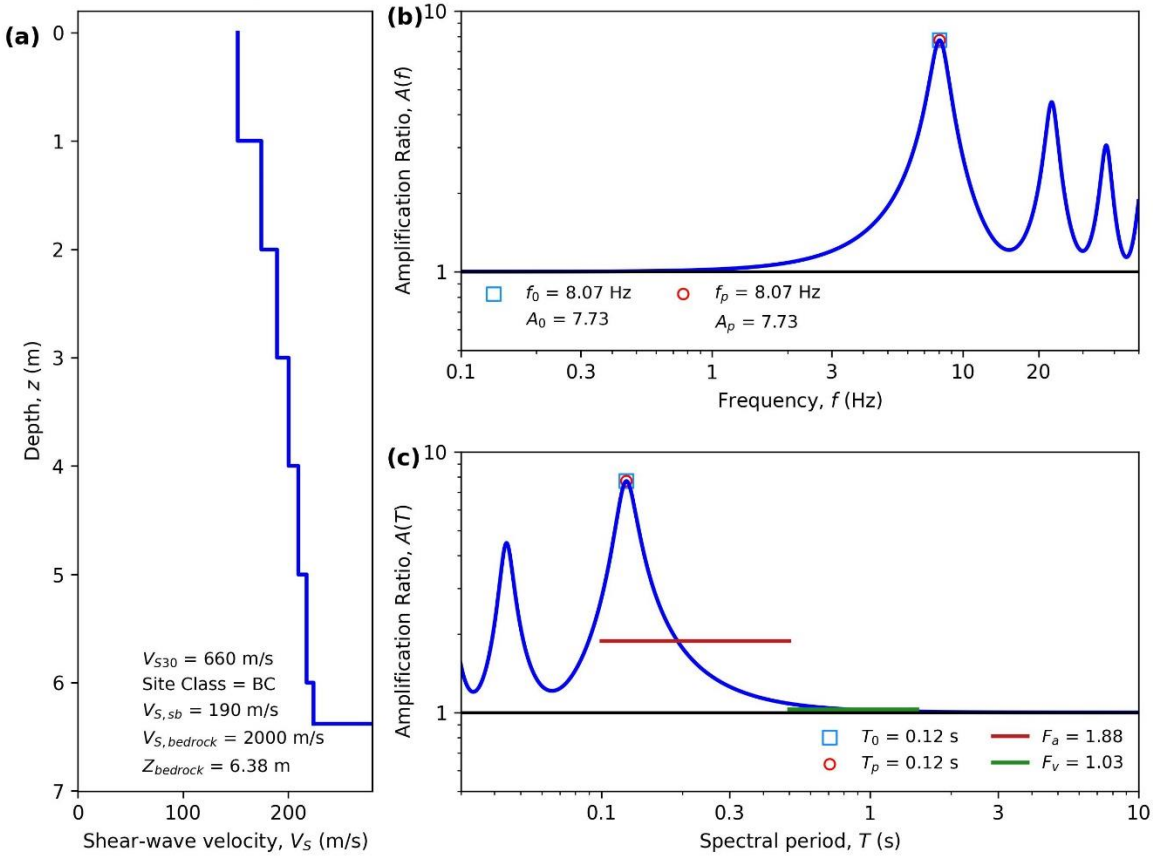

HAZUS Emergency Management
Massachusetts Care
Figure E159. ID: MA000159, Lat: 41.6640°, Lon: -70.2931°

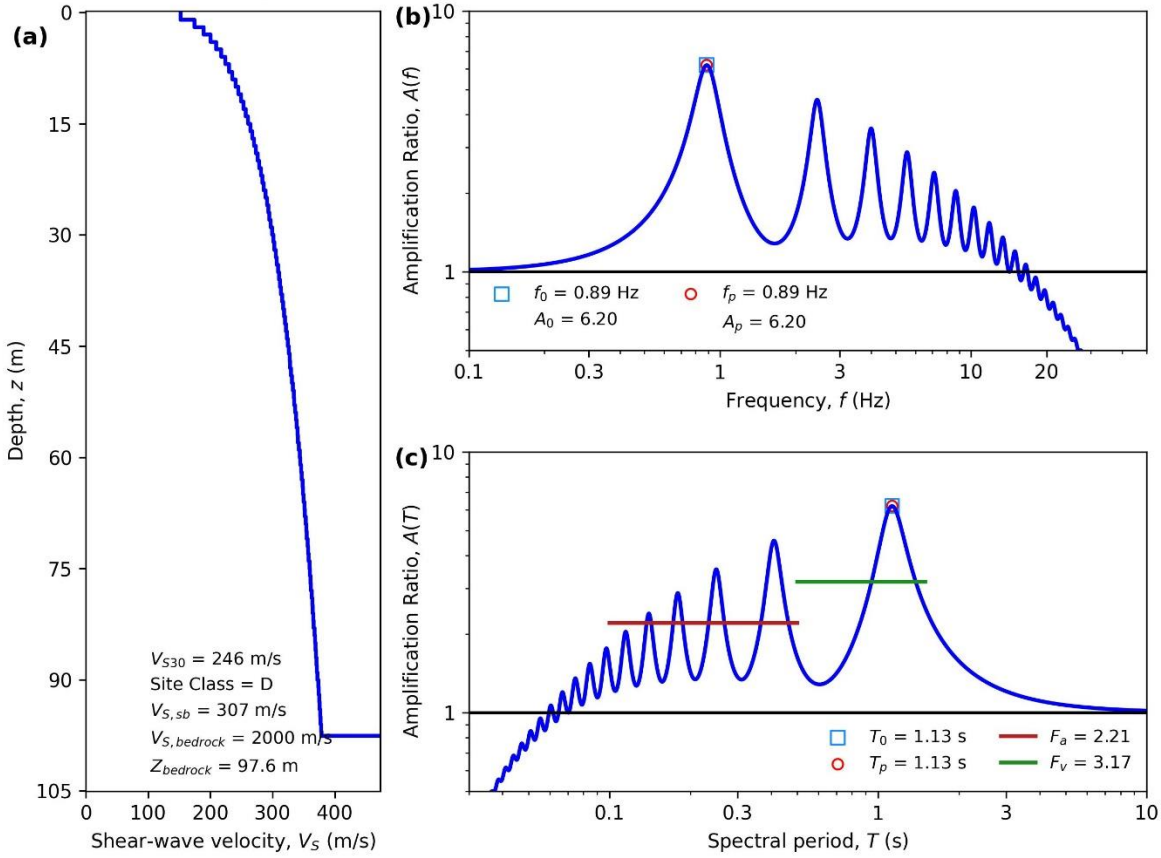

HAZUS Emergency Management
Massachusetts Care
Figure E160. ID: MA000160, Lat: 42.2509°, Lon: -71.0138°

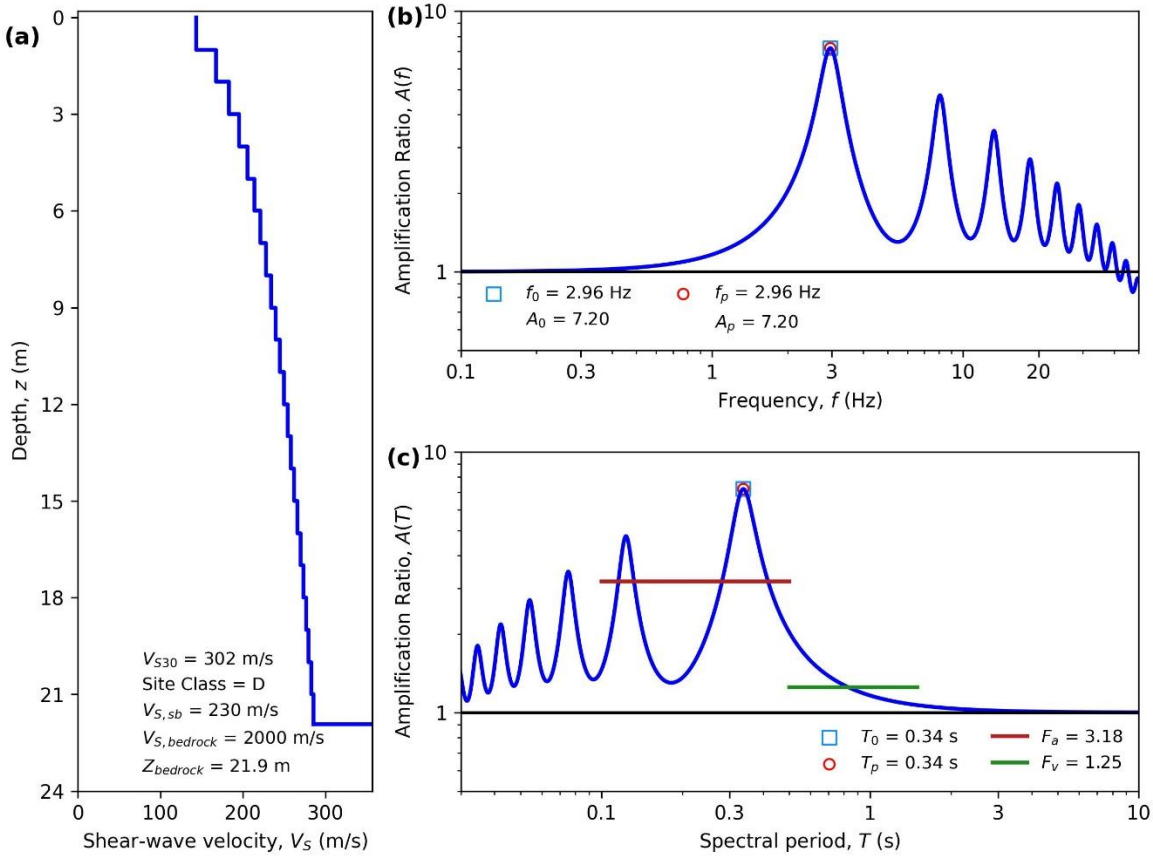

Appendix F: HAZUS GRA Fragility Output – GBS Care Facilities

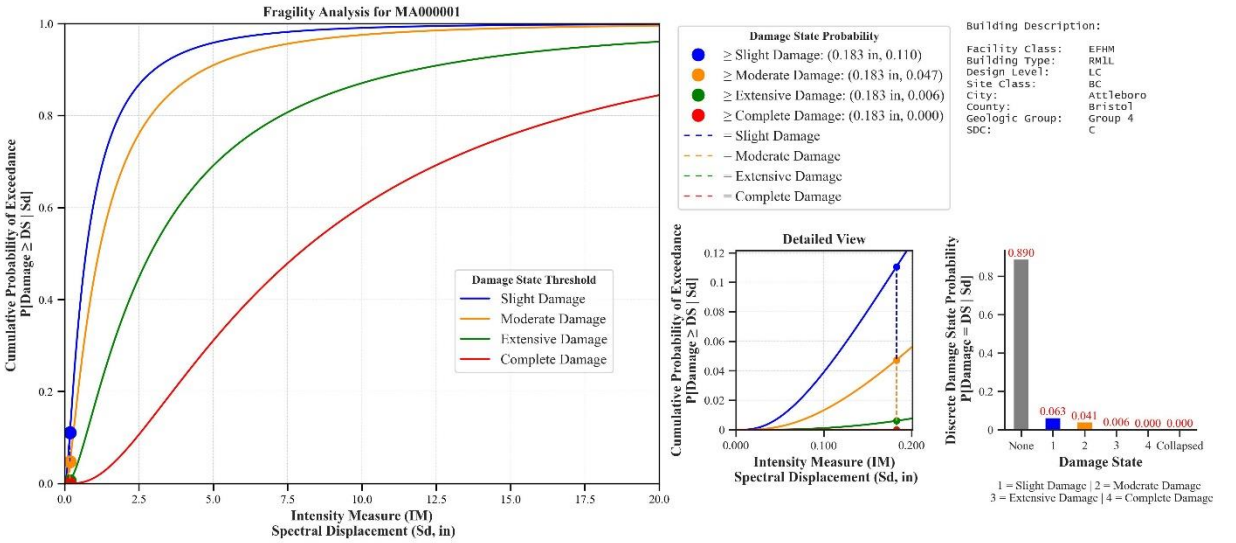
Fragility Analysis for MA000001
Cumulative Probability of Exceedance P[Damage ≥ DS | Sd]
Intensity Measure (IM) Spectral Displacement (Sd, in)
Damage State Threshold
Slight Damage
Moderate Damage
Extensive Damage
Complete Damage
Damage State Probability
≥ Slight Damage: (0.183 in, 0.110)
≥ Moderate Damage: (0.183 in, 0.047)
≥ Extensive Damage: (0.183 in, 0.006)
≥ Complete Damage: (0.183 in, 0.000)
Building Description:
Facility Class: EFHM
Building Type: RM1L
Design Level: LC
Site Class: BC
City: Attleboro
County: Bristol
Geologic Group: Group 4
SDC: C
Detailed View
Discrete Damage State Probability P[Damage = DS | Sd]
0.890
0.063
0.041
0.006
0.000
0.000
None
Collapsed
Damage State
1 = Slight Damage | 2 = Moderate Damage
3 = Extensive Damage | 4 = Complete Damage

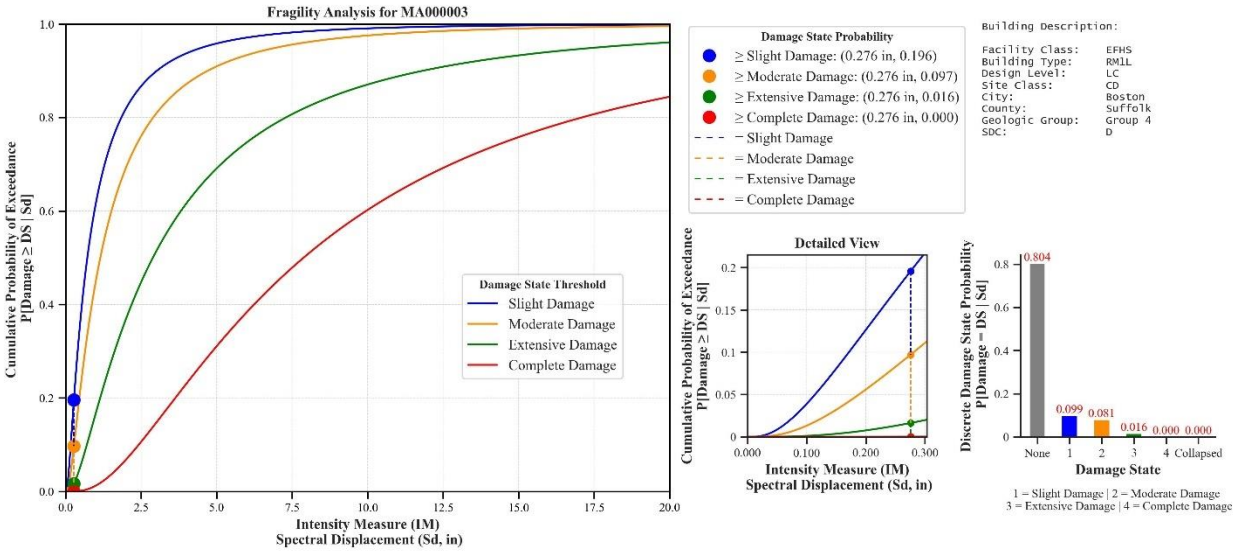
Fragility Analysis for MA000003
Cumulative Probability of Exceedance P[Damage ≥ DS | Sd]
Intensity Measure (IM) Spectral Displacement (Sd, in)
Damage State Threshold
Slight Damage
Moderate Damage
Extensive Damage
Complete Damage
Damage State Probability
≥ Slight Damage: (0.276 in, 0.196)
≥ Moderate Damage: (0.276 in, 0.097)
≥ Extensive Damage: (0.276 in, 0.016)
≥ Complete Damage: (0.276 in, 0.000)
Building Description:
Facility Class: EFHS
Building Type: RM1L
Design Level: LC
Site Class: CD
City: Boston
County: Suffolk
Geologic Group: Group 4
SDC: D
Detailed View
Discrete Damage State Probability P[Damage = DS | Sd]
0.804
0.099
0.081
0.016
0.000
0.000
None
Collapsed
Damage State
1 = Slight Damage | 2 = Moderate Damage
3 = Extensive Damage | 4 = Complete Damage

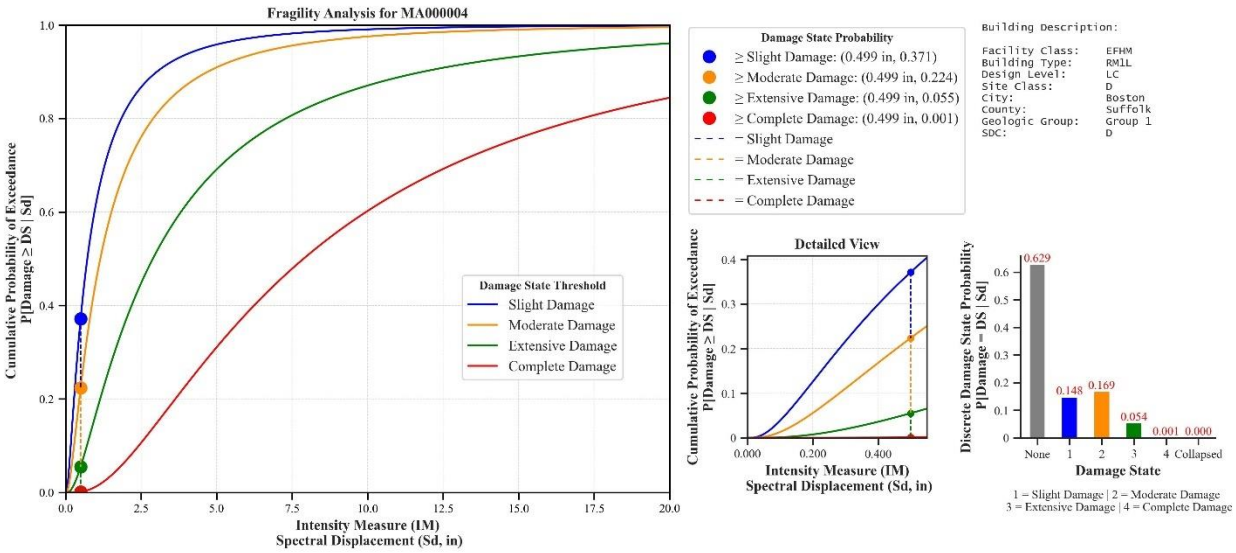
Fragility Analysis for MA000004
Cumulative Probability of Exceedance P[Damage ≥ DS | Sd]
Intensity Measure (IM) Spectral Displacement (Sd, in)
Damage State Threshold
Slight Damage
Moderate Damage
Extensive Damage
Complete Damage
Damage State Probability
≥ Slight Damage: (0.499 in, 0.371)
≥ Moderate Damage: (0.499 in, 0.224)
≥ Extensive Damage: (0.499 in, 0.055)
≥ Complete Damage: (0.499 in, 0.001)
Building Description:
Facility Class: EFHM
Building Type: RM1L
Design Level: LC
Site Class: D
City: Boston
County: Suffolk
Geologic Group: Group 1
SDC: D
Detailed View
Discrete Damage State Probability P[Damage = DS | Sd]
0.629
0.148
0.169
0.054
0.001
0.000
None
Collapsed
Damage State
1 = Slight Damage | 2 = Moderate Damage
3 = Extensive Damage | 4 = Complete Damage

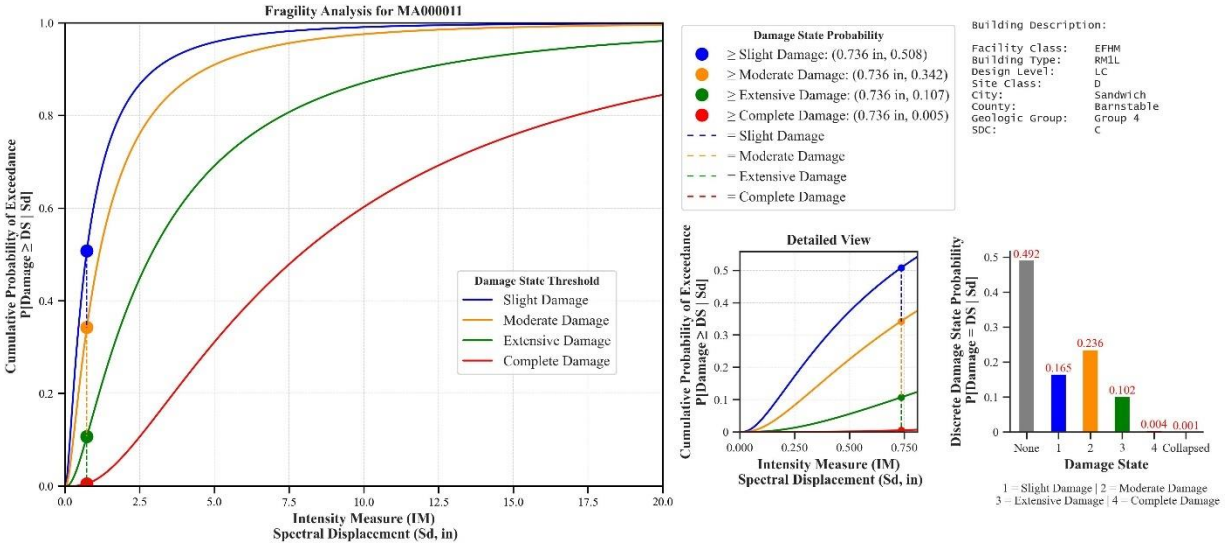
Fragility Analysis for MA000011
Cumulative Probability of Exceedance P[Damage ≥ DS | Sd]
Intensity Measure (IM) Spectral Displacement (Sd, in)
Damage State Threshold
Slight Damage
Moderate Damage
Extensive Damage
Complete Damage
Damage State Probability
≥ Slight Damage: (0.736 in, 0.508)
≥ Moderate Damage: (0.736 in, 0.342)
≥ Extensive Damage: (0.736 in, 0.107)
≥ Complete Damage: (0.736 in, 0.005)
= Slight Damage
= Moderate Damage
= Extensive Damage
= Complete Damage
Detailed View
Building Description:
Facility Class: EFHM
Building Type: RM1L
Design Level: LC
Site Class: D
City: Sandwich
County: Barnstable
Geologic Group: Group 4
SDC: C
Discrete Damage State Probability P[Damage = DS | Sd]
0.492
0.165
0.236
0.102
0.004
0.001
None
1
2
3
4 Collapsed
Damage State
1 = Slight Damage | 2 = Moderate Damage
3 = Extensive Damage | 4 = Complete Damage

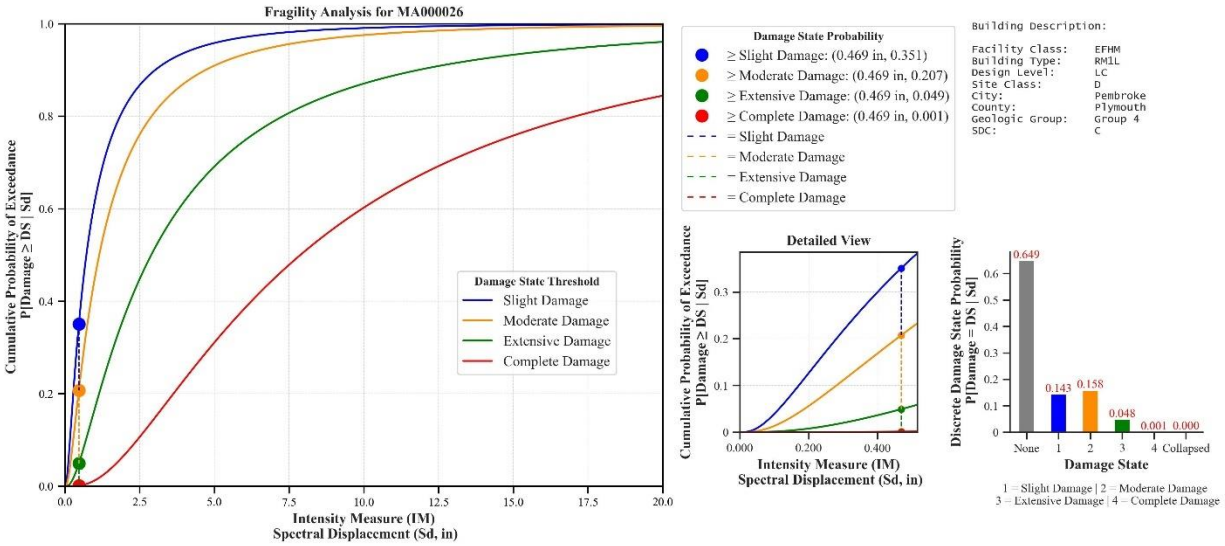
Fragility Analysis for MA000026
Cumulative Probability of Exceedance P[Damage ≥ DS | Sd]
Intensity Measure (IM) Spectral Displacement (Sd, in)
Damage State Threshold
Slight Damage
Moderate Damage
Extensive Damage
Complete Damage
Damage State Probability
≥ Slight Damage: (0.469 in, 0.351)
≥ Moderate Damage: (0.469 in, 0.207)
≥ Extensive Damage: (0.469 in, 0.049)
≥ Complete Damage: (0.469 in, 0.001)
= Slight Damage
= Moderate Damage
= Extensive Damage
= Complete Damage
Detailed View
Building Description:
Facility Class: EFHM
Building Type: RM1L
Design Level: LC
Site Class: D
City: Pembroke
County: Plymouth
Geologic Group: Group 4
SDC: C
Discrete Damage State Probability P[Damage = DS | Sd]
0.649
0.143
0.158
0.048
0.001
0.000
None
1
2
3
4 Collapsed
Damage State
1 = Slight Damage | 2 = Moderate Damage
3 = Extensive Damage | 4 = Complete Damage

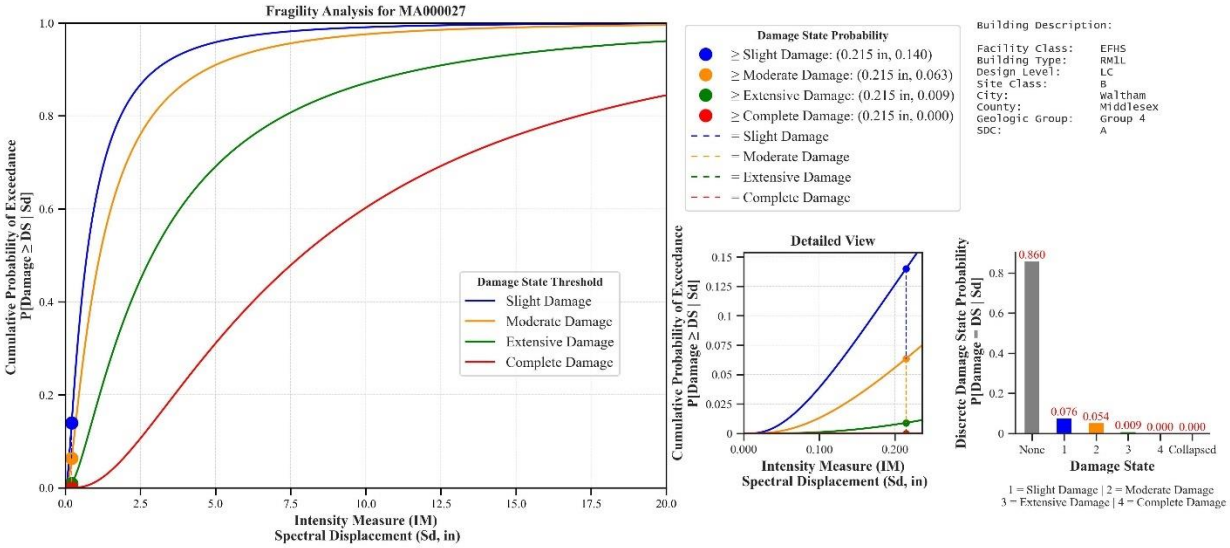
Fragility Analysis for MA000027
Cumulative Probability of Exceedance P[Damage ≥ DS | Sd]
Intensity Measure (IM) Spectral Displacement (Sd, in)
Damage State Threshold
Slight Damage
Moderate Damage
Extensive Damage
Complete Damage
Damage State Probability
≥ Slight Damage: (0.215 in, 0.140)
≥ Moderate Damage: (0.215 in, 0.063)
≥ Extensive Damage: (0.215 in, 0.009)
≥ Complete Damage: (0.215 in, 0.000)
= Slight Damage
= Moderate Damage
= Extensive Damage
= Complete Damage
Detailed View
Building Description:
Facility Class: EFHS
Building Type: RM1L
Design Level: LC
Site Class: B
City: Waltham
County: Middlesex
Geologic Group: Group 4
SDC: A
Discrete Damage State Probability P[Damage = DS | Sd]
0.860
0.076
0.054
0.009
0.000
0.000
None
1
2
3
4 Collapsed
Damage State
1 = Slight Damage | 2 = Moderate Damage
3 = Extensive Damage | 4 = Complete Damage

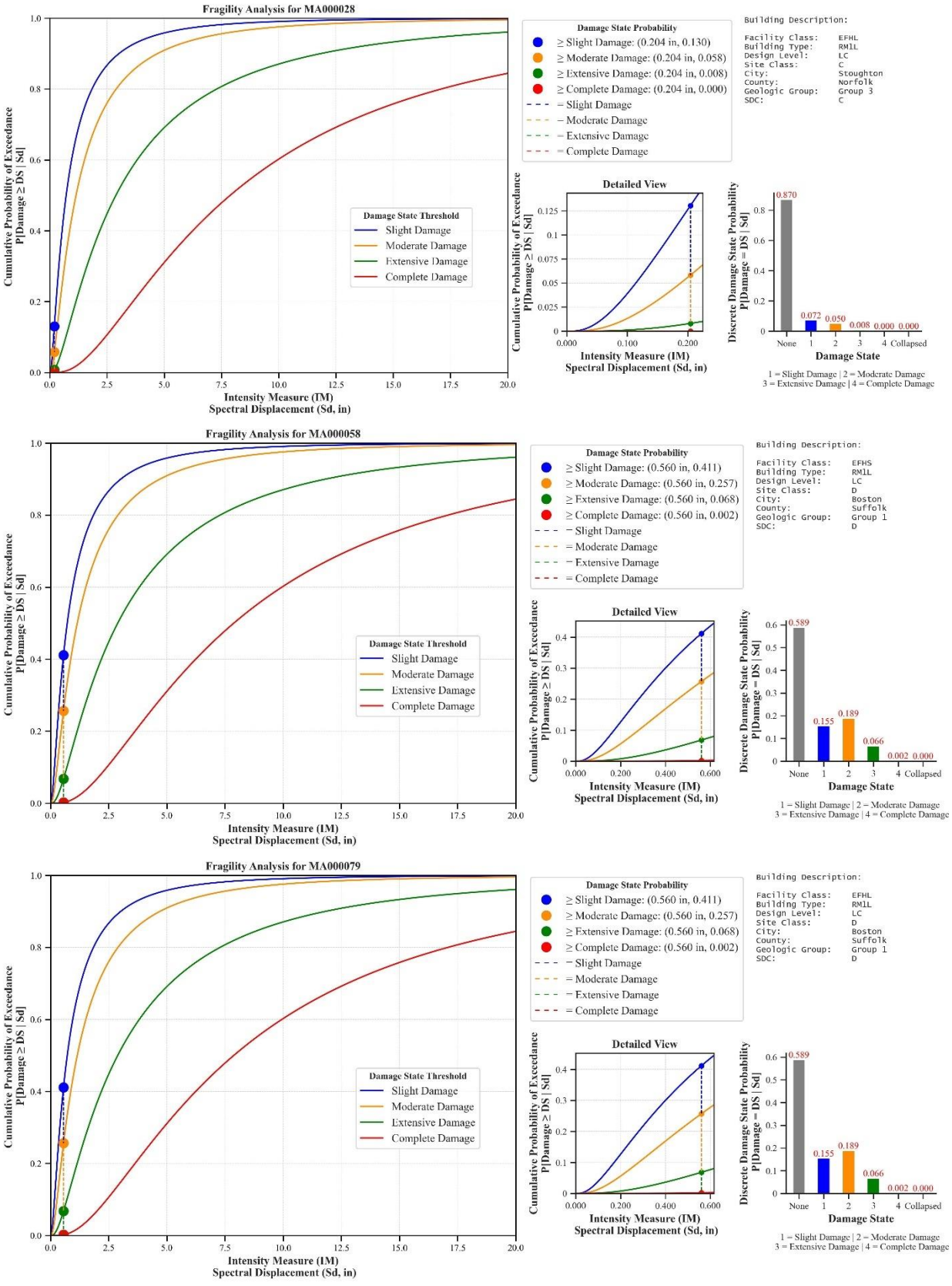
Fragility Analysis for MA000028
Damage State Threshold
Slight Damage
Moderate Damage
Extensive Damage
Complete Damage
Cumulative Probability of Exceedance
P[Damage ≥ DS | Sd]
Intensity Measure (IM)
Spectral Displacement (Sd, in)
Damage State Probability
≥ Slight Damage: (0.204 in, 0.130)
≥ Moderate Damage: (0.204 in, 0.058)
≥ Extensive Damage: (0.204 in, 0.008)
≥ Complete Damage: (0.204 in, 0.000)
Building Description:
Facility Class: EFHL
Building Type: RM1L
Design Level: LC
Site Class: C
City: Stoughton
County: Norfolk
Geologic Group: Group 3
SDC: C
Detailed View
Discrete Damage State Probability
P[Damage = DS | Sd]
0.870
0.072
0.050
0.008
0.000
0.000
None
Collapsed
Damage State
1 = Slight Damage | 2 = Moderate Damage
3 = Extensive Damage | 4 = Complete Damage
Fragility Analysis for MA000058
Damage State Threshold
Slight Damage
Moderate Damage
Extensive Damage
Complete Damage
Cumulative Probability of Exceedance
P[Damage ≥ DS | Sd]
Intensity Measure (IM)
Spectral Displacement (Sd, in)
Damage State Probability
≥ Slight Damage: (0.560 in, 0.411)
≥ Moderate Damage: (0.560 in, 0.257)
≥ Extensive Damage: (0.560 in, 0.068)
≥ Complete Damage: (0.560 in, 0.002)
Building Description:
Facility Class: EFHS
Building Type: RM1L
Design Level: LC
Site Class: D
City: Boston
County: Suffolk
Geologic Group: Group 1
SDC: D
Dctailed View
Discrete Damage State Probability
P[Damage = DS | Sd]
0.589
0.155
0.189
0.066
0.002
0.000
None
Collapsed
Damage State
1 = Slight Damage | 2 = Moderate Damage
3 = Extensive Damage | 4 = Complete Damage
Fragility Analysis for MA000079
Damage State Threshold
Slight Damage
Moderate Damage
Extensive Damage
Complete Damage
Cumulative Probability of Exceedance
P[Damage ≥ DS | Sd]
Intensity Measure (IM)
Spectral Displacement (Sd, in)
Damage State Probability
≥ Slight Damage: (0.560 in, 0.411)
≥ Moderate Damage: (0.560 in, 0.257)
≥ Extensive Damage: (0.560 in, 0.068)
≥ Complete Damage: (0.560 in, 0.002)
Building Description:
Facility Class: EFHL
Building Type: RM1L
Design Level: LC
Site Class: D
City: Boston
County: Suffolk
Geologic Group: Group 1
SDC: D
Dctailed View
Discrete Damage State Probability
P[Damage = DS | Sd]
0.589
0.155
0.189
0.066
0.002
0.000
None
Collapsed
Damage State
1 = Slight Damage | 2 = Moderate Damage
3 = Extensive Damage | 4 = Complete Damage

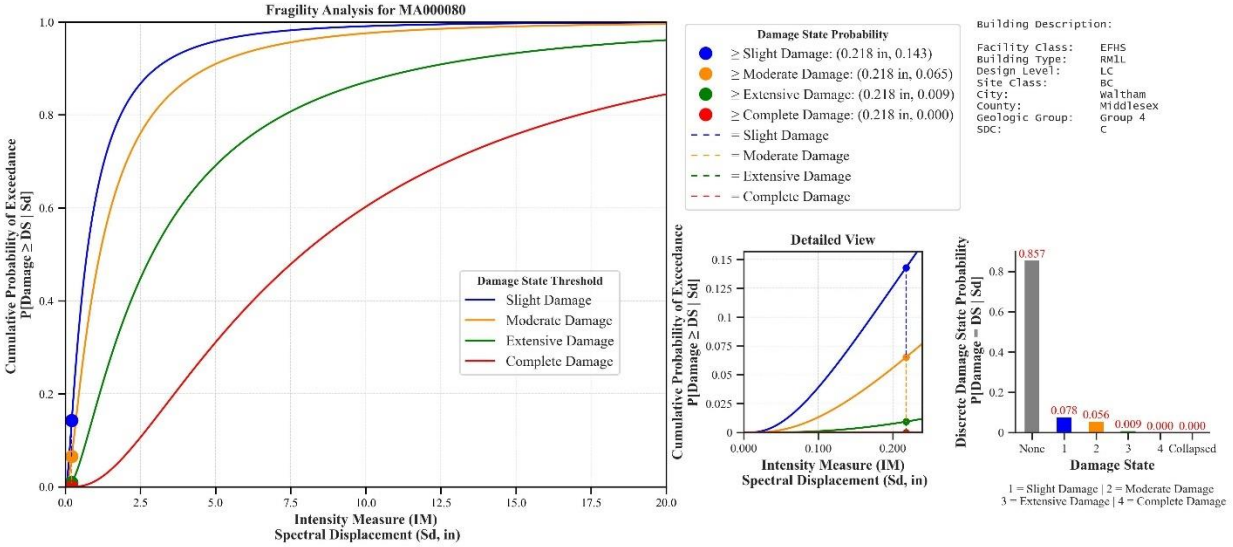
Fragility Analysis for MA000080
Cumulative Probability of Exceedance P[Damage ≥ DS | Sd]
Intensity Measure (IM) Spectral Displacement (Sd, in)
Damage State Threshold
Slight Damage
Moderate Damage
Extensive Damage
Complete Damage
Damage State Probability
≥ Slight Damage: (0.218 in, 0.143)
≥ Moderate Damage: (0.218 in, 0.065)
≥ Extensive Damage: (0.218 in, 0.009)
≥ Complete Damage: (0.218 in, 0.000)
= Slight Damage
= Moderate Damage
= Extensive Damage
= Complete Damage
Building Description:
Facility Class: EFHS
Building Type: RM1L
Design Level: LC
Site Class: BC
City: Waltham
County: Middlesex
Geologic Group: Group 4
SDC: C
Detailed View
Discrete Damage State Probability P[Damage = DS | Sd]
0.857
0.078
0.056
0.009
0.000
0.000
None
Collapsed
Damage State
1 = Slight Damage | 2 = Moderate Damage
3 = Extensive Damage | 4 = Complete Damage

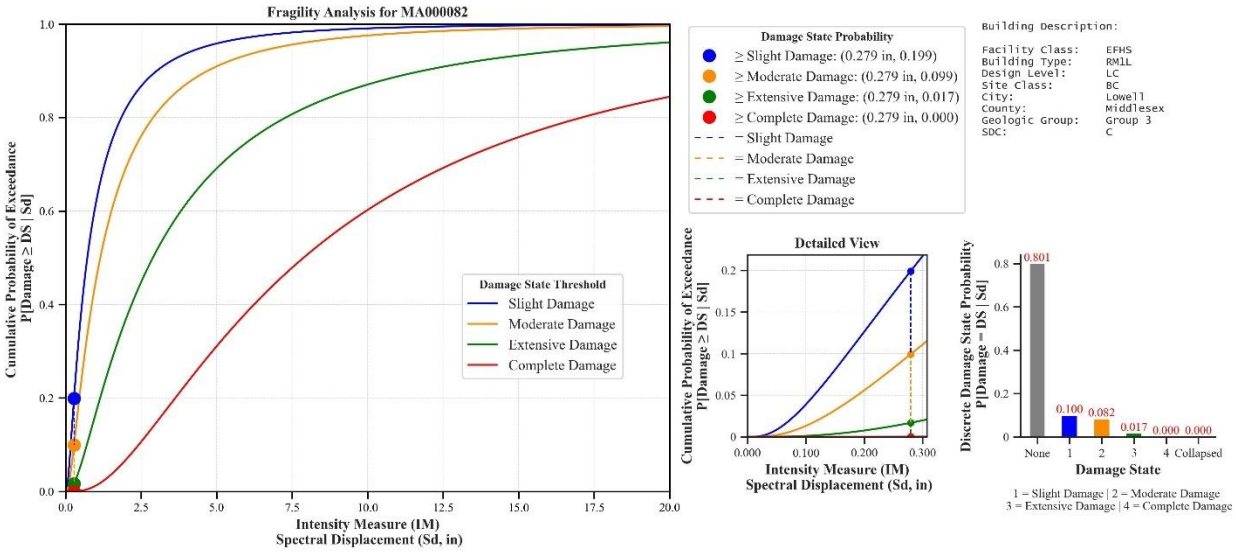
Fragility Analysis for MA000082
Cumulative Probability of Exceedance P[Damage ≥ DS | Sd]
Intensity Measure (IM) Spectral Displacement (Sd, in)
Damage State Threshold
Slight Damage
Moderate Damage
Extensive Damage
Complete Damage
Damage State Probability
≥ Slight Damage: (0.279 in, 0.199)
≥ Moderate Damage: (0.279 in, 0.099)
≥ Extensive Damage: (0.279 in, 0.017)
≥ Complete Damage: (0.279 in, 0.000)
= Slight Damage
= Moderate Damage
= Extensive Damage
= Complete Damage
Building Description:
Facility Class: EFHS
Building Type: RM1L
Design Level: LC
Site Class: BC
City: Lowell
County: Middlesex
Geologic Group: Group 3
SDC: C
Detailed View
Discrete Damage State Probability P[Damage = DS | Sd]
0.801
0.100
0.082
0.017
0.000
0.000
None
Collapsed
Damage State
1 = Slight Damage | 2 = Moderate Damage
3 = Extensive Damage | 4 = Complete Damage

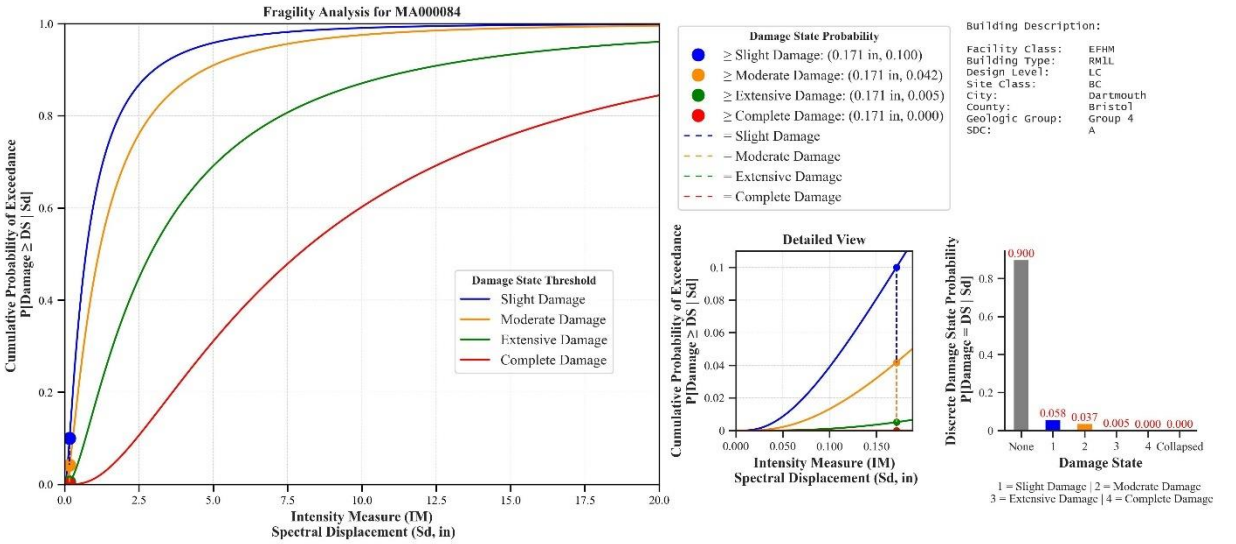
Fragility Analysis for MA000084
Cumulative Probability of Exceedance P[Damage ≥ DS | Sd]
Intensity Measure (IM) Spectral Displacement (Sd, in)
Damage State Threshold
Slight Damage
Moderate Damage
Extensive Damage
Complete Damage
Damage State Probability
≥ Slight Damage: (0.171 in, 0.100)
≥ Moderate Damage: (0.171 in, 0.042)
≥ Extensive Damage: (0.171 in, 0.005)
≥ Complete Damage: (0.171 in, 0.000)
= Slight Damage
= Moderate Damage
= Extensive Damage
= Complete Damage
Building Description:
Facility Class: EFHM
Building Type: RM1L
Design Level: LC
Site Class: BC
City: Dartmouth
County: Bristol
Geologic Group: Group 4
SDC: A
Detailed View
Discrete Damage State Probability P[Damage = DS | Sd]
0.900
0.058
0.037
0.005
0.000
0.000
None
Collapsed
Damage State
1 = Slight Damage | 2 = Moderate Damage
3 = Extensive Damage | 4 = Complete Damage

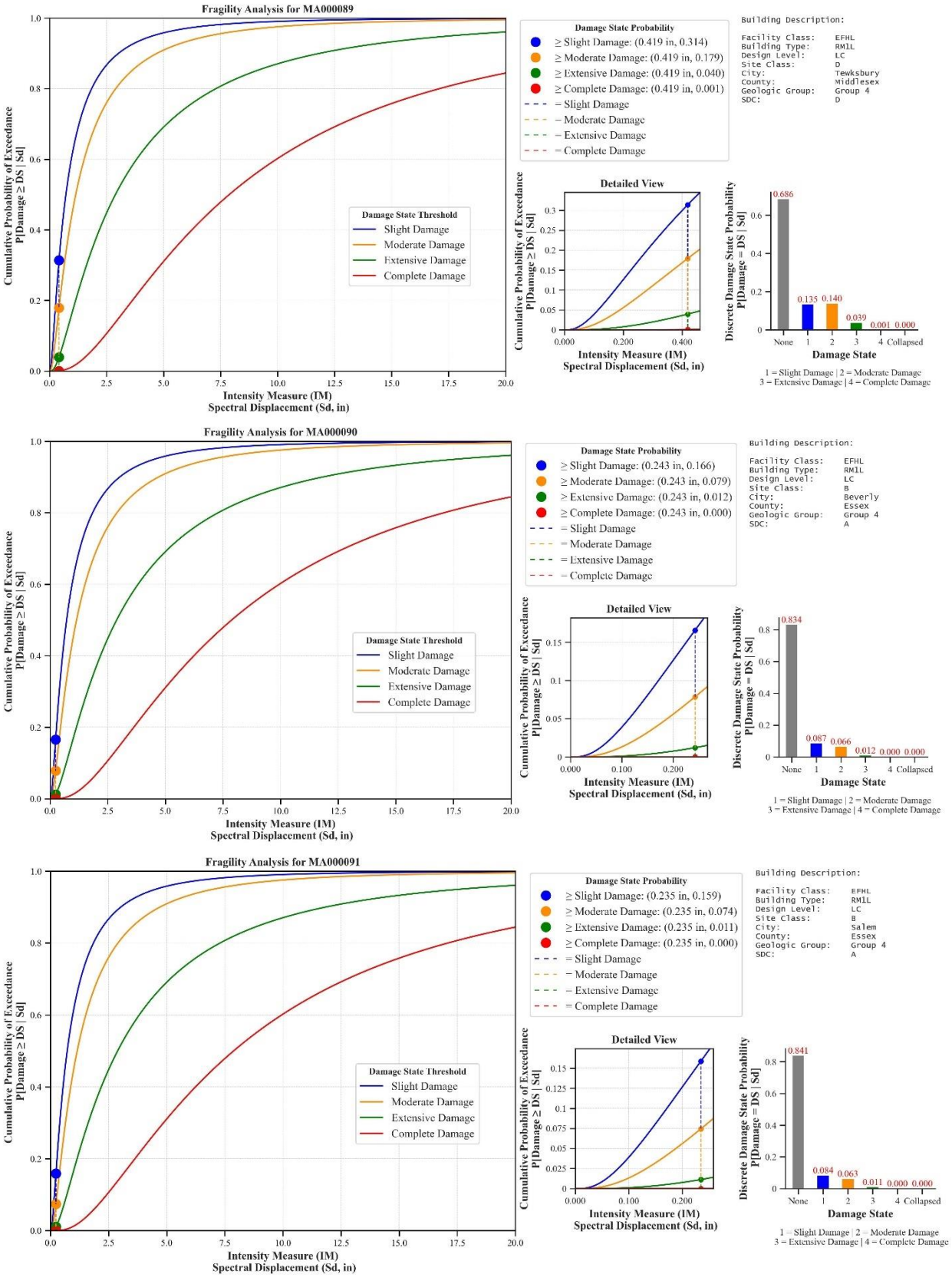
Fragility Analysis for MA000089
Cumulative Probability of Exceedance P[Damage ≥ DS | Sd]
Intensity Measure (IM) Spectral Displacement (Sd, in)
Damage State Threshold
Slight Damage
Moderate Damage
Extensive Damage
Complete Damage
Damage State Probability
≥ Slight Damage: (0.419 in, 0.314)
≥ Moderate Damage: (0.419 in, 0.179)
≥ Extensive Damage: (0.419 in, 0.040)
≥ Complete Damage: (0.419 in, 0.001)
= Slight Damage
= Moderate Damage
= Extensive Damage
= Complete Damage
Building Description:
Facility Class: EFHL
Building Type: RM1L
Design Level: LC
Site Class: D
City: Tewksbury
County: Middlesex
Geologic Group: Group 4
SDC: D
Detailed View
Discrete Damage State Probability P[Damage = DS | Sd]
0.686
0.135
0.140
0.039
0.001
0.000
None
1
2
3
4
Collapsed
Damage State
1 = Slight Damage | 2 = Moderate Damage
3 = Extensive Damage | 4 = Complete Damage
Fragility Analysis for MA000090
Damage State Probability
≥ Slight Damage: (0.243 in, 0.166)
≥ Moderate Damage: (0.243 in, 0.079)
≥ Extensive Damage: (0.243 in, 0.012)
≥ Complete Damage: (0.243 in, 0.000)
Building Description:
Facility Class: EFHL
Building Type: RM1L
Design Level: LC
Site Class: B
City: Beverly
County: Essex
Geologic Group: Group 4
SDC: A
0.834
0.087
0.066
0.012
0.000
0.000
Fragility Analysis for MA000091
Damage State Probability
≥ Slight Damage: (0.235 in, 0.159)
≥ Moderate Damage: (0.235 in, 0.074)
≥ Extensive Damage: (0.235 in, 0.011)
≥ Complete Damage: (0.235 in, 0.000)
Building Description:
Facility Class: EFHL
Building Type: RM1L
Design Level: LC
Site Class: B
City: Salem
County: Essex
Geologic Group: Group 4
SDC: A
0.841
0.084
0.063
0.011
0.000
0.000

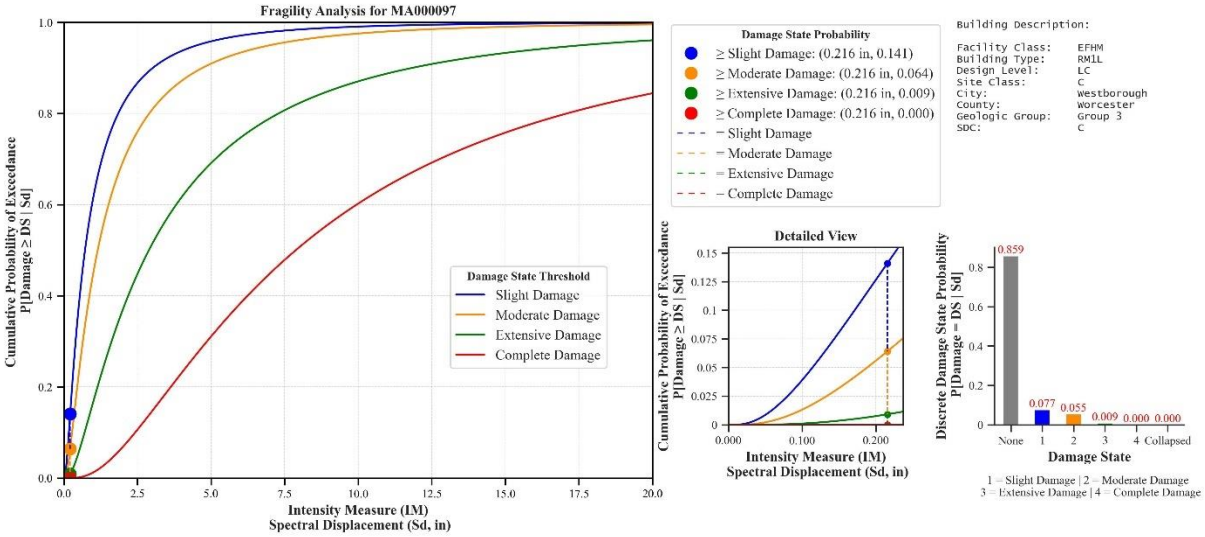
Fragility Analysis for MA000097
Damage State Probability
≥ Slight Damage: (0.216 in, 0.141)
≥ Moderate Damage: (0.216 in, 0.064)
≥ Extensive Damage: (0.216 in, 0.009)
≥ Complete Damage: (0.216 in, 0.000)
– Slight Damage
– Moderate Damage
– Extensive Damage
– Complete Damage
Building Description:
Facility Class: EFHM
Building Type: RM1L
Design Level: LC
Site Class: C
City: Westborough
County: Worcester
Geologic Group: Group 3
SDC: C
Damage State Threshold
Slight Damage
Moderate Damage
Extensive Damage
Complete Damage
Cumulative Probability of Exceedance P[Damage ≥ DS | Sd]
Intensity Measure (IM) Spectral Displacement (Sd, in)
Detailed View
Discrete Damage State Probability P[Damage = DS | Sd]
0.859
0.077
0.055
0.009
0.000
0.000
None 1 2 3 4 Collapsed
Damage State
1 = Slight Damage | 2 = Moderate Damage
3 = Extensive Damage | 4 = Complete Damage

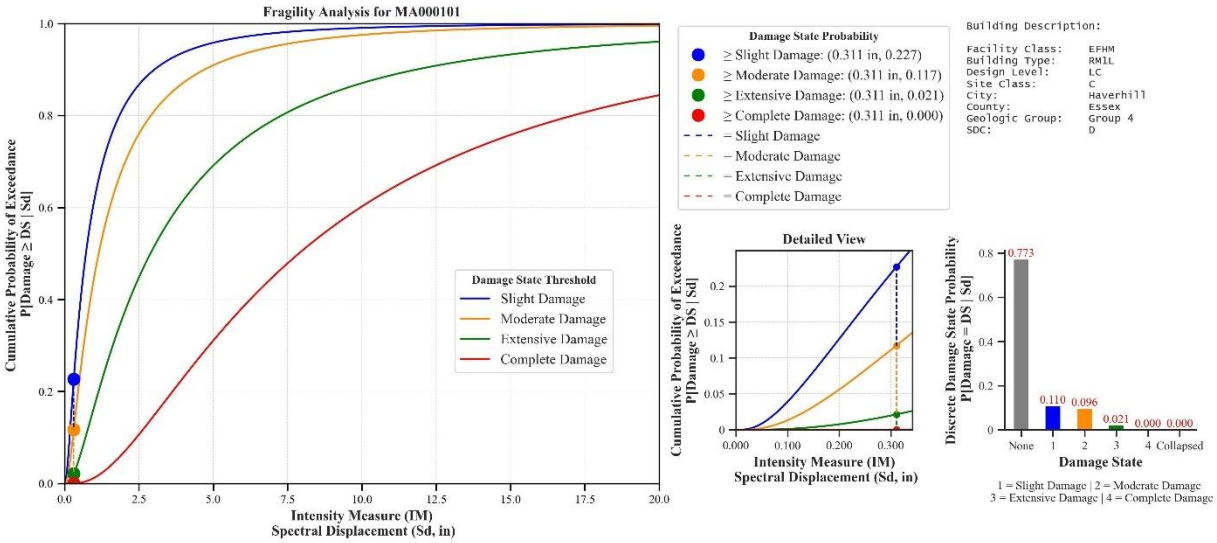
Fragility Analysis for MA000101
Damage State Probability
≥ Slight Damage: (0.311 in, 0.227)
≥ Moderate Damage: (0.311 in, 0.117)
≥ Extensive Damage: (0.311 in, 0.021)
≥ Complete Damage: (0.311 in, 0.000)
– Slight Damage
– Moderate Damage
– Extensive Damage
– Complete Damage
Building Description:
Facility Class: EFHM
Building Type: RM1L
Design Level: LC
Site Class: C
City: Haverhill
County: Essex
Geologic Group: Group 4
SDC: D
Damage State Threshold
Slight Damage
Moderate Damage
Extensive Damage
Complete Damage
Cumulative Probability of Exceedance P[Damage ≥ DS | Sd]
Intensity Measure (IM) Spectral Displacement (Sd, in)
Detailed View
Discrete Damage State Probability P[Damage = DS | Sd]
0.773
0.110
0.096
0.021
0.000
0.000
None 1 2 3 4 Collapsed
Damage State
1 = Slight Damage | 2 = Moderate Damage
3 = Extensive Damage | 4 = Complete Damage

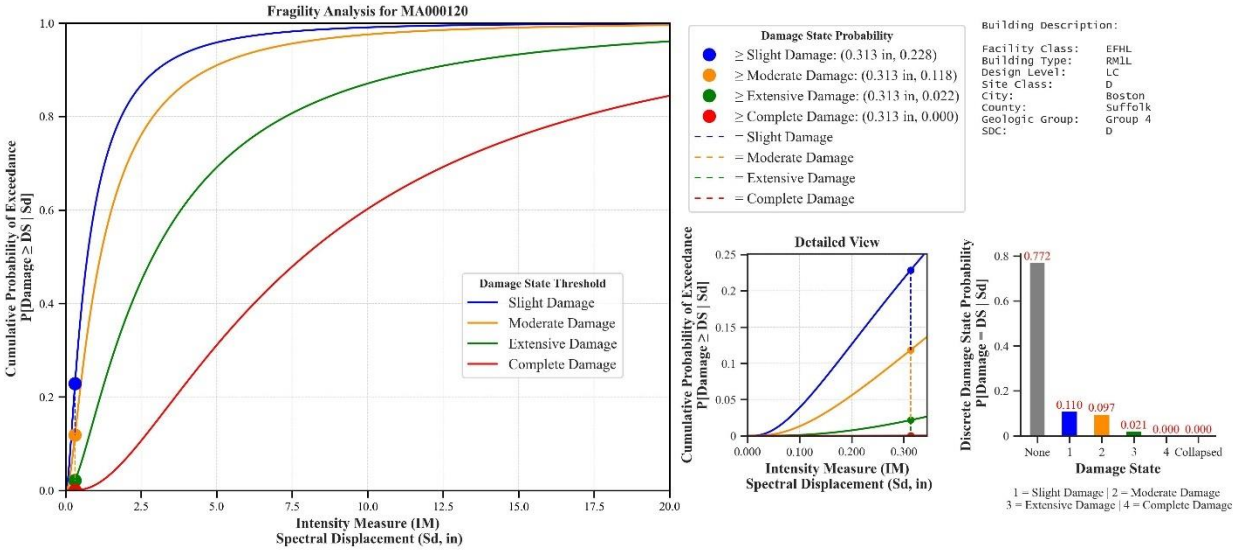
Fragility Analysis for MA000120
Damage State Probability
≥ Slight Damage: (0.313 in, 0.228)
≥ Moderate Damage: (0.313 in, 0.118)
≥ Extensive Damage: (0.313 in, 0.022)
≥ Complete Damage: (0.313 in, 0.000)
– Slight Damage
– Moderate Damage
– Extensive Damage
– Complete Damage
Building Description:
Facility Class: EFHL
Building Type: RM1L
Design Level: LC
Site Class: D
City: Boston
County: Suffolk
Geologic Group: Group 4
SDC: D
Damage State Threshold
Slight Damage
Moderate Damage
Extensive Damage
Complete Damage
Cumulative Probability of Exceedance P[Damage ≥ DS | Sd]
Intensity Measure (IM) Spectral Displacement (Sd, in)
Detailed View
Discrete Damage State Probability P[Damage = DS | Sd]
0.772
0.110
0.097
0.021
0.000
0.000
None 1 2 3 4 Collapsed
Damage State
1 = Slight Damage | 2 = Moderate Damage
3 = Extensive Damage | 4 = Complete Damage

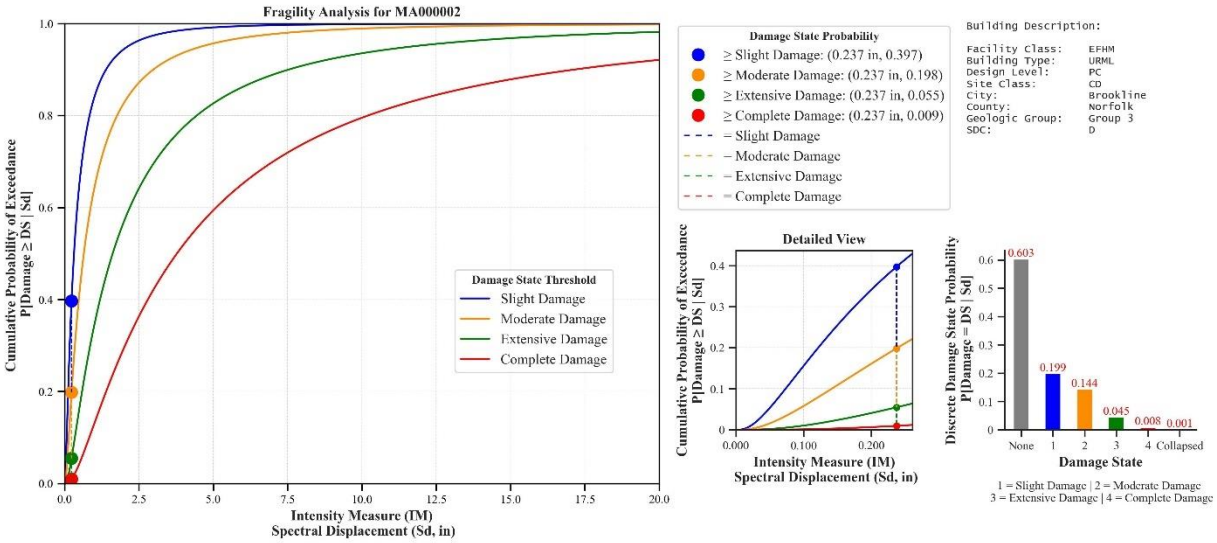
Fragility Analysis for MA000002
Cumulative Probability of Exceedance P[Damage ≥ DS | Sd]
Intensity Measure (IM) Spectral Displacement (Sd, in)
Damage State Threshold
Slight Damage
Moderate Damage
Extensive Damage
Complete Damage
Damage State Probability
≥ Slight Damage: (0.237 in, 0.397)
≥ Moderate Damage: (0.237 in, 0.198)
≥ Extensive Damage: (0.237 in, 0.055)
≥ Complete Damage: (0.237 in, 0.009)
Building Description:
Facility Class: EFHM
Building Type: URML
Design Level: PC
Site Class: CD
City: Brookline
County: Norfolk
Geologic Group: Group 3
SDC: D
Detailed View
Discrete Damage State Probability P[Damage = DS | Sd]
0.603
0.199
0.144
0.045
0.008
0.001
None
Collapsed
Damage State
1 = Slight Damage | 2 = Moderate Damage
3 = Extensive Damage | 4 = Complete Damage

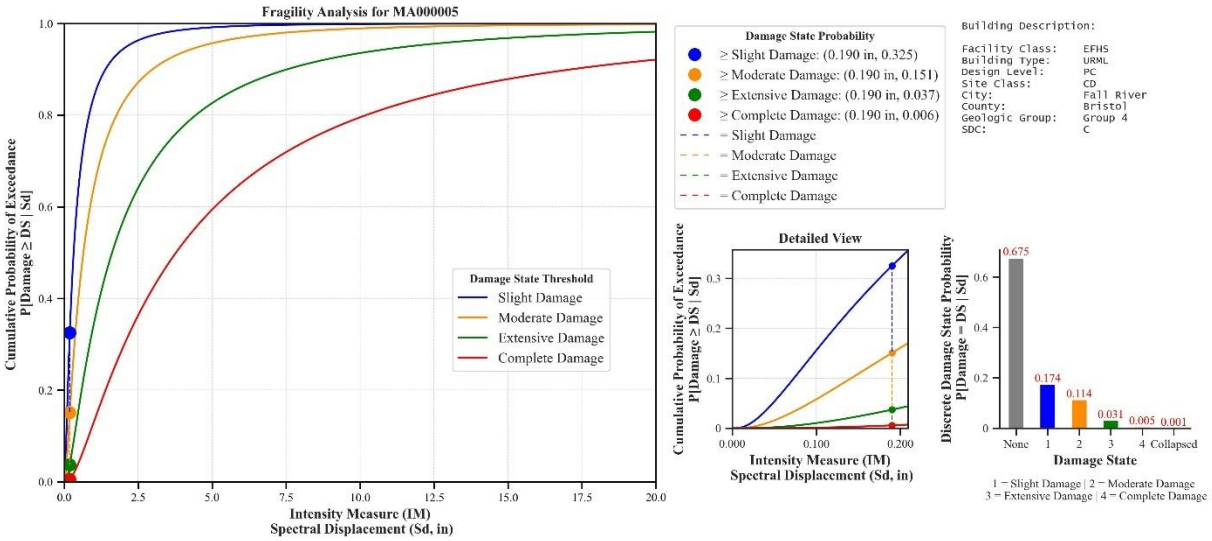
Fragility Analysis for MA000005
Cumulative Probability of Exceedance P[Damage ≥ DS | Sd]
Intensity Measure (IM) Spectral Displacement (Sd, in)
Damage State Threshold
Slight Damage
Moderate Damage
Extensive Damage
Complete Damage
Damage State Probability
≥ Slight Damage: (0.190 in, 0.325)
≥ Moderate Damage: (0.190 in, 0.151)
≥ Extensive Damage: (0.190 in, 0.037)
≥ Complete Damage: (0.190 in, 0.006)
Building Description:
Facility Class: EFHS
Building Type: URML
Design Level: PC
Site Class: CD
City: Fall River
County: Bristol
Geologic Group: Group 4
SDC: C
Detailed View
Discrete Damage State Probability P[Damage = DS | Sd]
0.675
0.174
0.114
0.031
0.005
0.001
None
Collapsed
Damage State
1 = Slight Damage | 2 = Moderate Damage
3 = Extensive Damage | 4 = Complete Damage

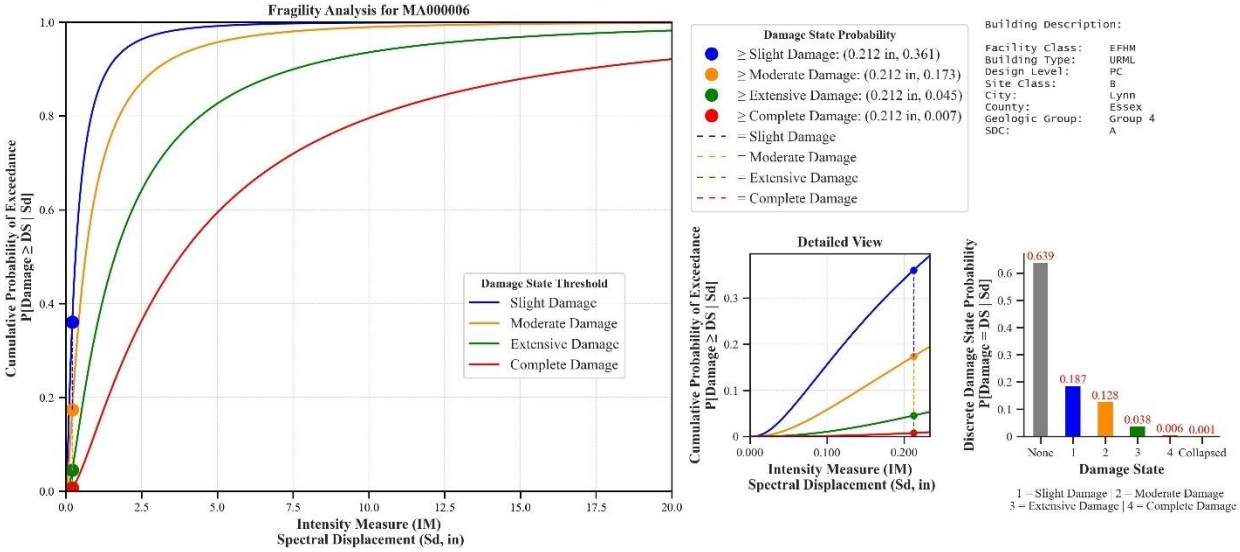
Fragility Analysis for MA000006
Cumulative Probability of Exceedance P[Damage ≥ DS | Sd]
Intensity Measure (IM) Spectral Displacement (Sd, in)
Damage State Threshold
Slight Damage
Moderate Damage
Extensive Damage
Complete Damage
Damage State Probability
≥ Slight Damage: (0.212 in, 0.361)
≥ Moderate Damage: (0.212 in, 0.173)
≥ Extensive Damage: (0.212 in, 0.045)
≥ Complete Damage: (0.212 in, 0.007)
Building Description:
Facility Class: EFHM
Building Type: URML
Design Level: PC
Site Class: B
City: Lynn
County: Essex
Geologic Group: Group 4
SDC: A
Detailed View
Discrete Damage State Probability P[Damage = DS | Sd]
0.639
0.187
0.128
0.038
0.006
0.001
None
Collapsed
Damage State
1 = Slight Damage | 2 = Moderate Damage
3 = Extensive Damage | 4 = Complete Damage

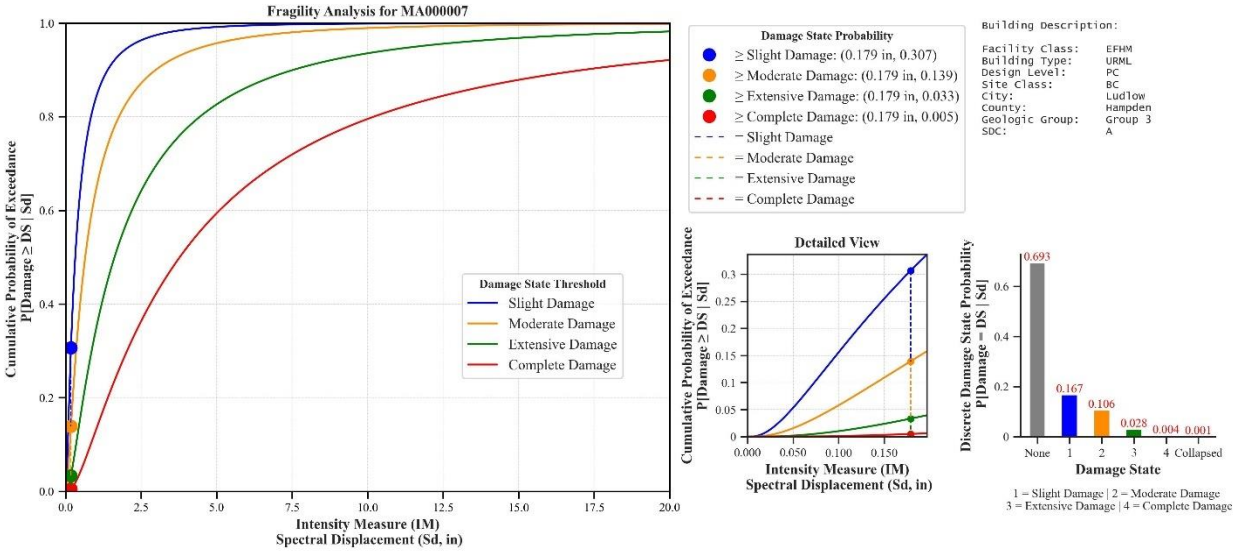
Fragility Analysis for MA000007
Cumulative Probability of Exceedance
P[Damage ≥ DS | Sd]
Intensity Measure (IM)
Spectral Displacement (Sd, in)
Damage State Threshold
Slight Damage
Moderate Damage
Extensive Damage
Complete Damage
Damage State Probability
≥ Slight Damage: (0.179 in, 0.307)
≥ Moderate Damage: (0.179 in, 0.139)
≥ Extensive Damage: (0.179 in, 0.033)
≥ Complete Damage: (0.179 in, 0.005)
= Slight Damage
= Moderate Damage
= Extensive Damage
= Complete Damage
Detailed View
Building Description:
Facility Class: EFHM
Building Type: URML
Design Level: PC
Site Class: BC
City: Ludlow
County: Hampden
Geologic Group: Group 3
SDC: A
Discrete Damage State Probability
P[Damage = DS | Sd]
0.693
0.167
0.106
0.028
0.004
0.001
None
1
2
3
4 Collapsed
Damage State
1 = Slight Damage | 2 = Moderate Damage
3 = Extensive Damage | 4 = Complete Damage

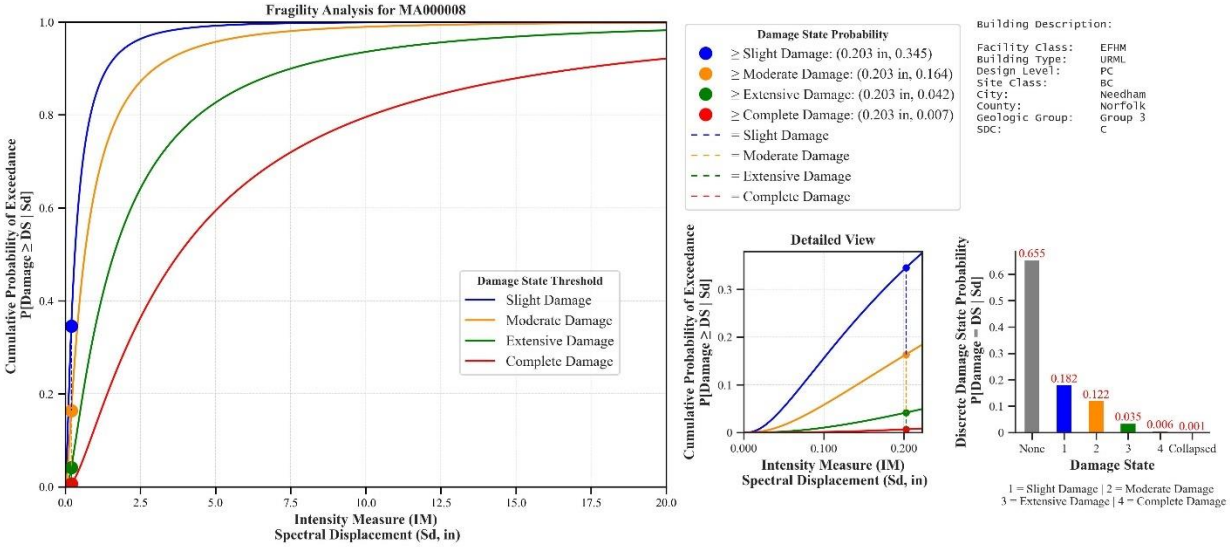
Fragility Analysis for MA000008
Cumulative Probability of Exceedance
P[Damage ≥ DS | Sd]
Intensity Measure (IM)
Spectral Displacement (Sd, in)
Damage State Threshold
Slight Damage
Moderate Damage
Extensive Damage
Complete Damage
Damage State Probability
≥ Slight Damage: (0.203 in, 0.345)
≥ Moderate Damage: (0.203 in, 0.164)
≥ Extensive Damage: (0.203 in, 0.042)
≥ Complete Damage: (0.203 in, 0.007)
= Slight Damage
= Moderate Damage
= Extensive Damage
= Complete Damage
Detailed View
Building Description:
Facility Class: EFHM
Building Type: URML
Design Level: PC
Site Class: BC
City: Needham
County: Norfolk
Geologic Group: Group 3
SDC: C
Discrete Damage State Probability
P[Damage = DS | Sd]
0.655
0.182
0.122
0.035
0.006
0.001
None
1
2
3
4 Collapsed
Damage State
1 = Slight Damage | 2 = Moderate Damage
3 = Extensive Damage | 4 = Complete Damage

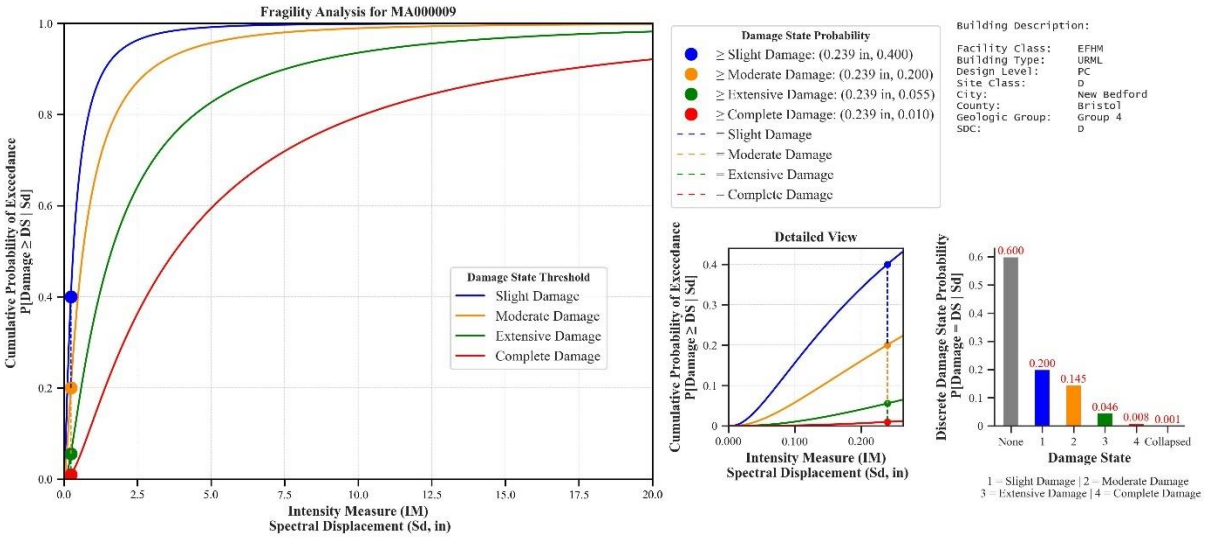
Fragility Analysis for MA000009
Cumulative Probability of Exceedance
P[Damage ≥ DS | Sd]
Intensity Measure (IM)
Spectral Displacement (Sd, in)
Damage State Threshold
Slight Damage
Moderate Damage
Extensive Damage
Complete Damage
Damage State Probability
≥ Slight Damage: (0.239 in, 0.400)
≥ Moderate Damage: (0.239 in, 0.200)
≥ Extensive Damage: (0.239 in, 0.055)
≥ Complete Damage: (0.239 in, 0.010)
= Slight Damage
= Moderate Damage
= Extensive Damage
= Complete Damage
Detailed View
Building Description:
Facility Class: EFHM
Building Type: URML
Design Level: PC
Site Class: D
City: New Bedford
County: Bristol
Geologic Group: Group 4
SDC: D
Discrete Damage State Probability
P[Damage = DS | Sd]
0.600
0.200
0.145
0.046
0.008
0.001
None
1
2
3
4 Collapsed
Damage State
1 = Slight Damage | 2 = Moderate Damage
3 = Extensive Damage | 4 = Complete Damage

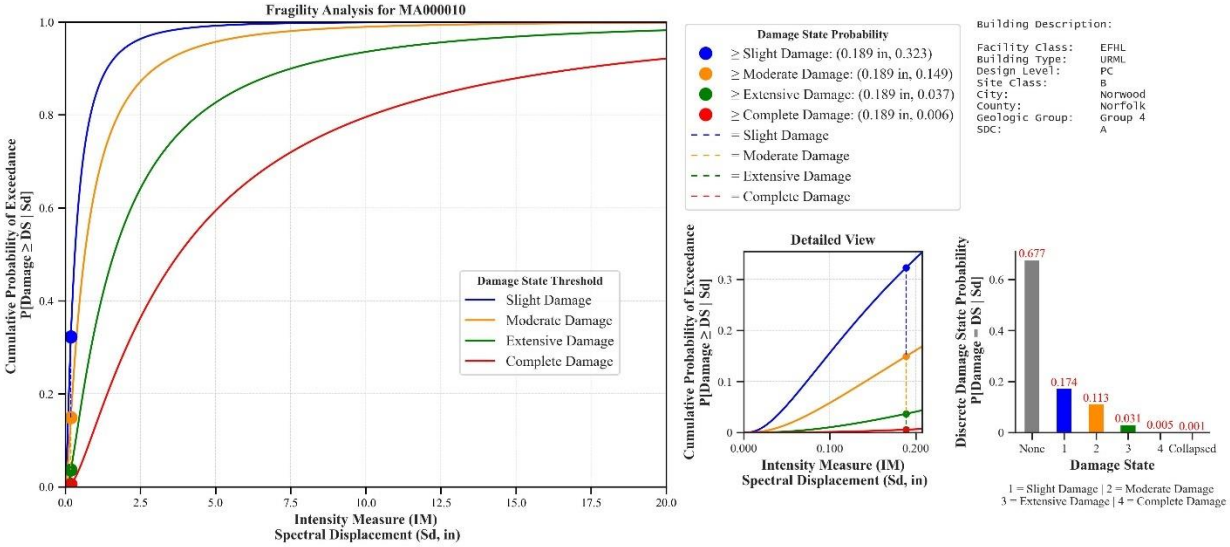
Fragility Analysis for MA000010
Cumulative Probability of Exceedance P[Damage ≥ DS | Sd]
Intensity Measure (IM) Spectral Displacement (Sd, in)
Damage State Threshold
Slight Damage
Moderate Damage
Extensive Damage
Complete Damage
Damage State Probability
≥ Slight Damage: (0.189 in, 0.323)
≥ Moderate Damage: (0.189 in, 0.149)
≥ Extensive Damage: (0.189 in, 0.037)
≥ Complete Damage: (0.189 in, 0.006)
Building Description:
Facility Class: EFHL
Building Type: URML
Design Level: PC
Site Class: B
City: Norwood
County: Norfolk
Geologic Group: Group 4
SDC: A
Detailed View
Discrete Damage State Probability P[Damage = DS | Sd]
0.677
0.174
0.113
0.031
0.005
0.001
None
Collapsed
Damage State
1 = Slight Damage | 2 = Moderate Damage
3 = Extensive Damage | 4 = Complete Damage

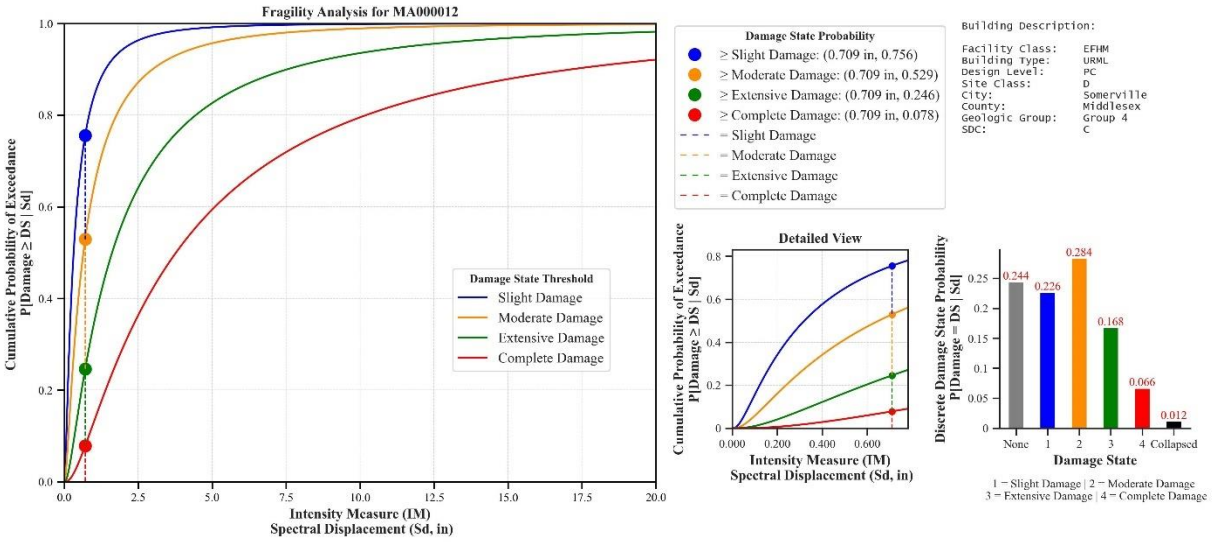
Fragility Analysis for MA000012
Cumulative Probability of Exceedance P[Damage ≥ DS | Sd]
Intensity Measure (IM) Spectral Displacement (Sd, in)
Damage State Threshold
Slight Damage
Moderate Damage
Extensive Damage
Complete Damage
Damage State Probability
≥ Slight Damage: (0.709 in, 0.756)
≥ Moderate Damage: (0.709 in, 0.529)
≥ Extensive Damage: (0.709 in, 0.246)
≥ Complete Damage: (0.709 in, 0.078)
Building Description:
Facility Class: EFHM
Building Type: URML
Design Level: PC
Site Class: D
City: Somerville
County: Middlesex
Geologic Group: Group 4
SDC: C
Detailed View
Discrete Damage State Probability P[Damage = DS | Sd]
0.244
0.226
0.284
0.168
0.066
0.012
None
Collapsed
Damage State
1 = Slight Damage | 2 = Moderate Damage
3 = Extensive Damage | 4 = Complete Damage

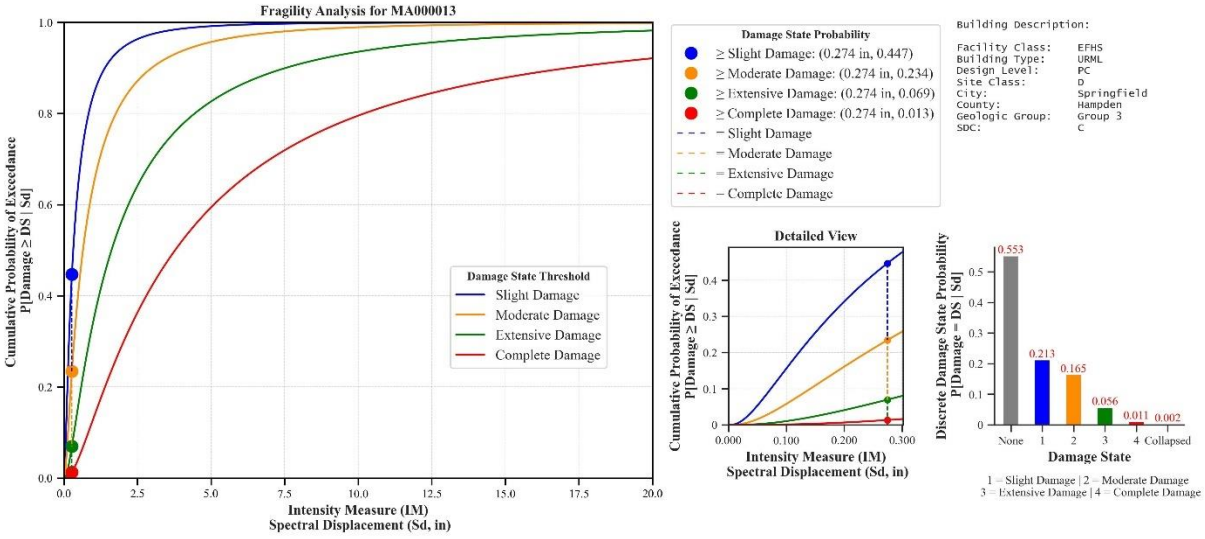
Fragility Analysis for MA000013
Cumulative Probability of Exceedance P[Damage ≥ DS | Sd]
Intensity Measure (IM) Spectral Displacement (Sd, in)
Damage State Threshold
Slight Damage
Moderate Damage
Extensive Damage
Complete Damage
Damage State Probability
≥ Slight Damage: (0.274 in, 0.447)
≥ Moderate Damage: (0.274 in, 0.234)
≥ Extensive Damage: (0.274 in, 0.069)
≥ Complete Damage: (0.274 in, 0.013)
Building Description:
Facility Class: EFHS
Building Type: URML
Design Level: PC
Site Class: D
City: Springfield
County: Hampden
Geologic Group: Group 3
SDC: C
Detailed View
Discrete Damage State Probability P[Damage = DS | Sd]
0.553
0.213
0.165
0.056
0.011
0.002
None
Collapsed
Damage State
1 = Slight Damage | 2 = Moderate Damage
3 = Extensive Damage | 4 = Complete Damage

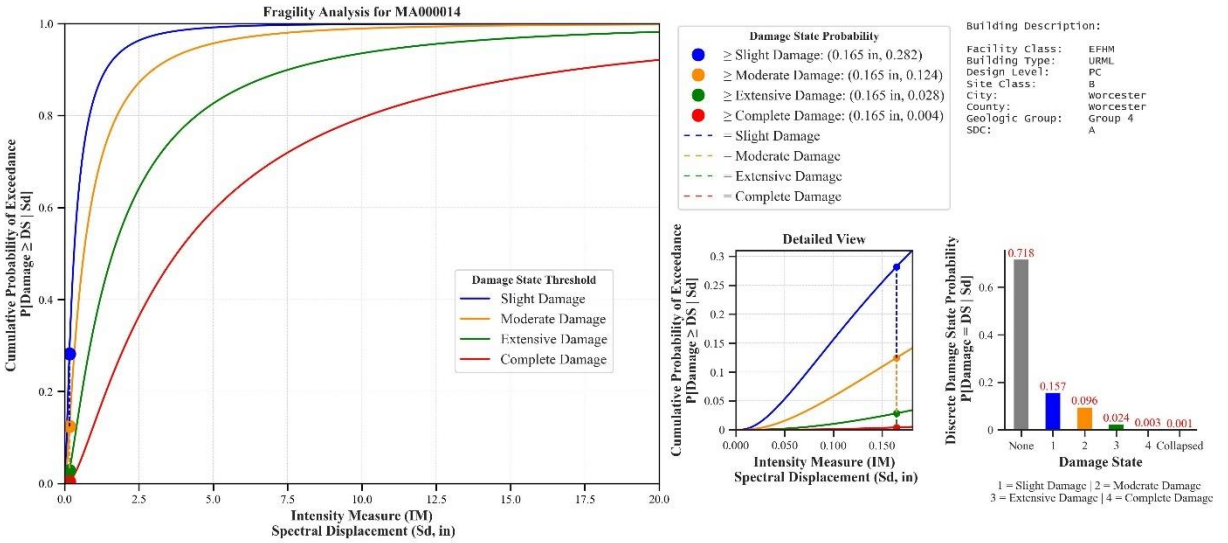
Fragility Analysis for MA000014
Cumulative Probability of Exceedance P[Damage ≥ DS | Sd]
Intensity Measure (IM) Spectral Displacement (Sd, in)
Damage State Threshold
Slight Damage
Moderate Damage
Extensive Damage
Complete Damage
Damage State Probability
≥ Slight Damage: (0.165 in, 0.282)
≥ Moderate Damage: (0.165 in, 0.124)
≥ Extensive Damage: (0.165 in, 0.028)
≥ Complete Damage: (0.165 in, 0.004)
= Slight Damage
= Moderate Damage
= Extensive Damage
= Complete Damage
Detailed View
Discrete Damage State Probability P[Damage = DS | Sd]
0.718
0.157
0.096
0.024
0.003
0.001
None
1
2
3
4
Collapsed
Damage State
1 = Slight Damage | 2 = Moderate Damage
3 = Extensive Damage | 4 = Complete Damage
Building Description:
Facility Class: EFHM
Building Type: URML
Design Level: PC
Site Class: B
City: Worcester
County: Worcester
Geologic Group: Group 4
SDC: A

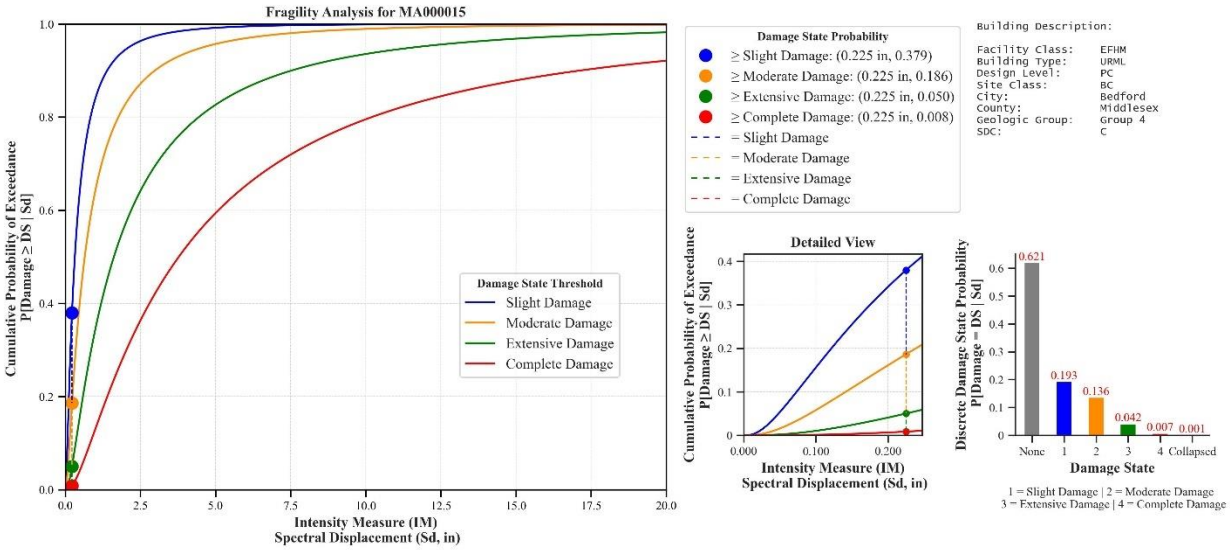
Fragility Analysis for MA000015
Cumulative Probability of Exceedance P[Damage ≥ DS | Sd]
Intensity Measure (IM) Spectral Displacement (Sd, in)
Damage State Threshold
Slight Damage
Moderate Damage
Extensive Damage
Complete Damage
Damage State Probability
≥ Slight Damage: (0.225 in, 0.379)
≥ Moderate Damage: (0.225 in, 0.186)
≥ Extensive Damage: (0.225 in, 0.050)
≥ Complete Damage: (0.225 in, 0.008)
= Slight Damage
= Moderate Damage
= Extensive Damage
= Complete Damage
Detailed View
Discrete Damage State Probability P[Damage = DS | Sd]
0.621
0.193
0.136
0.042
0.007
0.001
None
1
2
3
4
Collapsed
Damage State
1 = Slight Damage | 2 = Moderate Damage
3 = Extensive Damage | 4 = Complete Damage
Building Description:
Facility Class: EFHM
Building Type: URML
Design Level: PC
Site Class: BC
City: Bedford
County: Middlesex
Geologic Group: Group 4
SDC: C

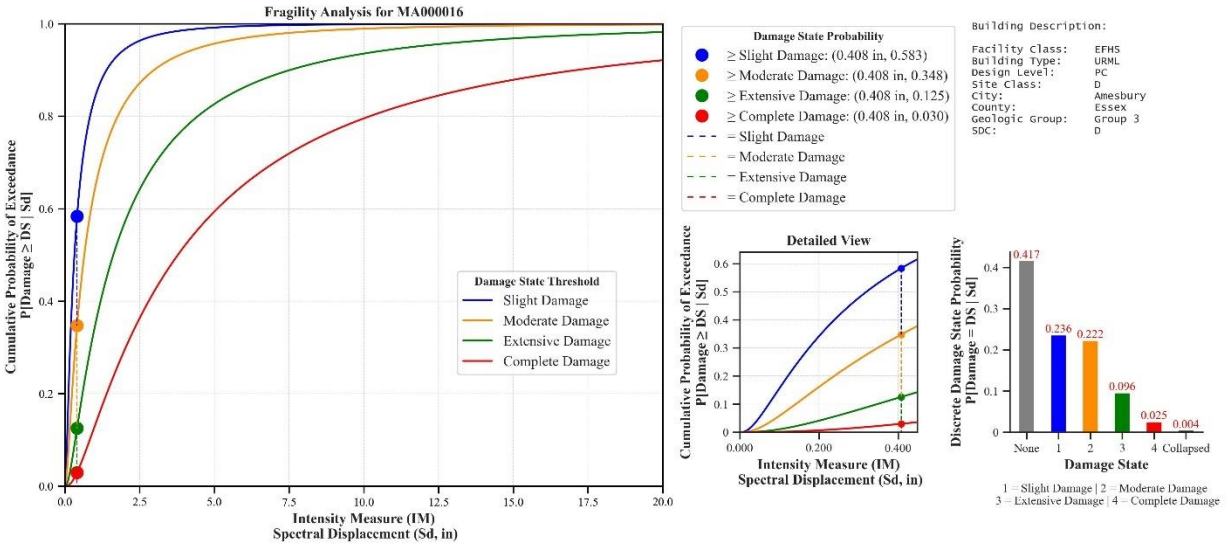
Fragility Analysis for MA000016
Cumulative Probability of Exceedance P[Damage ≥ DS | Sd]
Intensity Measure (IM) Spectral Displacement (Sd, in)
Damage State Threshold
Slight Damage
Moderate Damage
Extensive Damage
Complete Damage
Damage State Probability
≥ Slight Damage: (0.408 in, 0.583)
≥ Moderate Damage: (0.408 in, 0.348)
≥ Extensive Damage: (0.408 in, 0.125)
≥ Complete Damage: (0.408 in, 0.030)
= Slight Damage
= Moderate Damage
= Extensive Damage
= Complete Damage
Detailed View
Discrete Damage State Probability P[Damage = DS | Sd]
0.417
0.236
0.222
0.096
0.025
0.004
None
1
2
3
4
Collapsed
Damage State
1 = Slight Damage | 2 = Moderate Damage
3 = Extensive Damage | 4 = Complete Damage
Building Description:
Facility Class: EFHS
Building Type: URML
Design Level: PC
Site Class: D
City: Amesbury
County: Essex
Geologic Group: Group 3
SDC: D

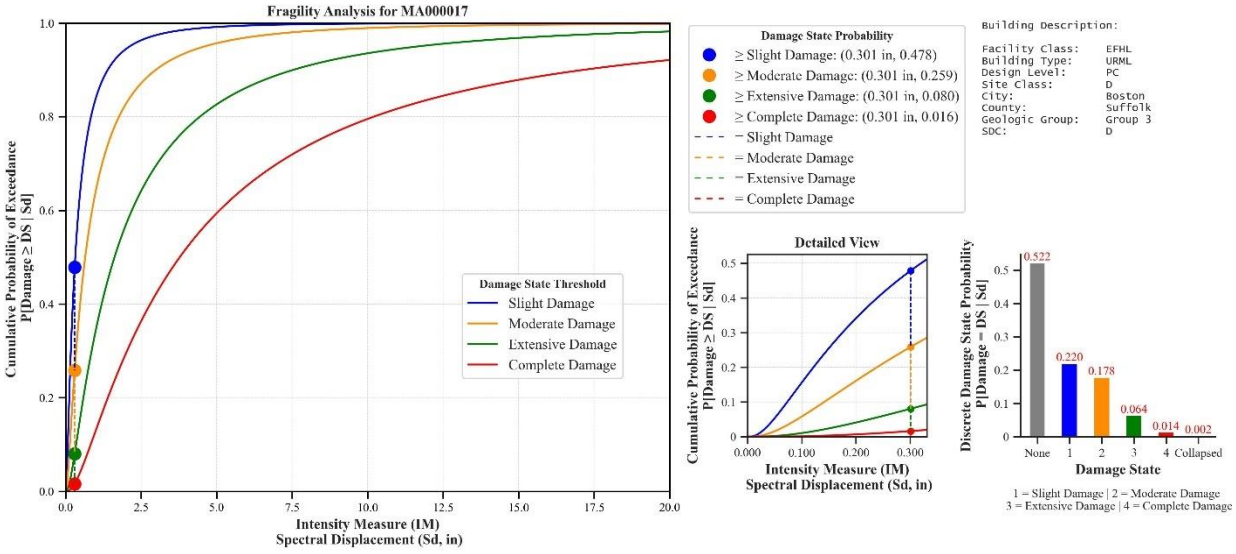
Fragility Analysis for MA000017
Cumulative Probability of Exceedance P[Damage ≥ DS | Sd]
Intensity Measure (IM) Spectral Displacement (Sd, in)
Damage State Threshold
Slight Damage
Moderate Damage
Extensive Damage
Complete Damage
Damage State Probability
≥ Slight Damage: (0.301 in, 0.478)
≥ Moderate Damage: (0.301 in, 0.259)
≥ Extensive Damage: (0.301 in, 0.080)
≥ Complete Damage: (0.301 in, 0.016)
Detailed View
Discrete Damage State Probability P[Damage = DS | Sd]
0.522
0.220
0.178
0.064
0.014
0.002
None 1 2 3 4 Collapsed
Damage State
1 = Slight Damage | 2 = Moderate Damage
3 = Extensive Damage | 4 = Complete Damage
Building Description:
Facility Class: EFHL
Building Type: URML
Design Level: PC
Site Class: D
City: Boston
County: Suffolk
Geologic Group: Group 3
SDC: D

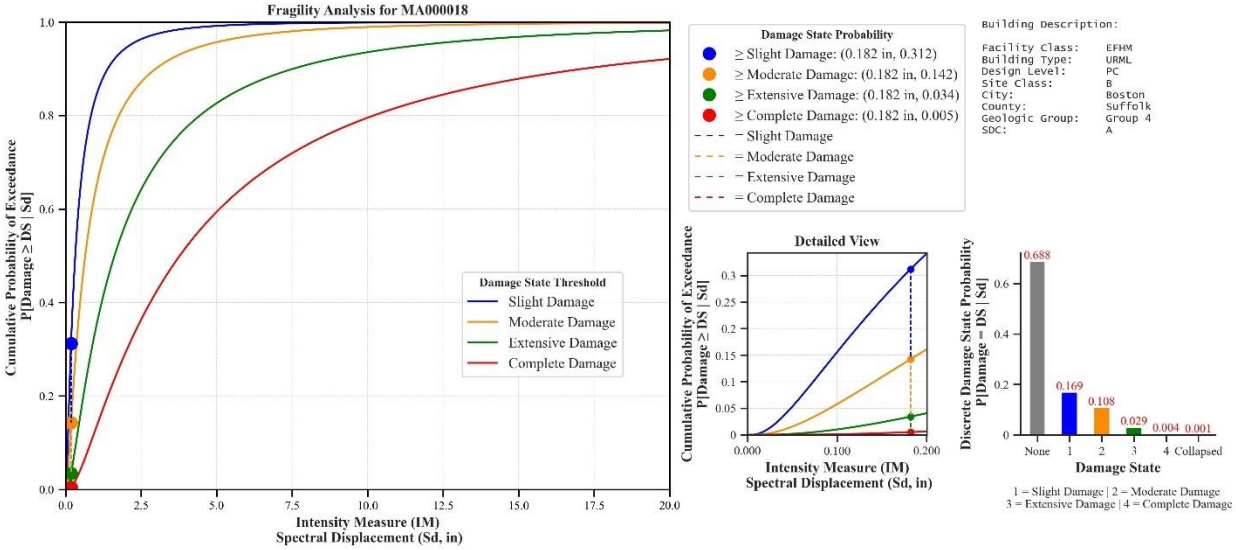
Fragility Analysis for MA000018
Cumulative Probability of Exceedance P[Damage ≥ DS | Sd]
Intensity Measure (IM) Spectral Displacement (Sd, in)
Damage State Threshold
Slight Damage
Moderate Damage
Extensive Damage
Complete Damage
Damage State Probability
≥ Slight Damage: (0.182 in, 0.312)
≥ Moderate Damage: (0.182 in, 0.142)
≥ Extensive Damage: (0.182 in, 0.034)
≥ Complete Damage: (0.182 in, 0.005)
Detailed View
Discrete Damage State Probability P[Damage = DS | Sd]
0.688
0.169
0.108
0.029
0.004
0.001
None 1 2 3 4 Collapsed
Damage State
1 = Slight Damage | 2 = Moderate Damage
3 = Extensive Damage | 4 = Complete Damage
Building Description:
Facility Class: EFHM
Building Type: URML
Design Level: PC
Site Class: B
City: Boston
County: Suffolk
Geologic Group: Group 4
SDC: A

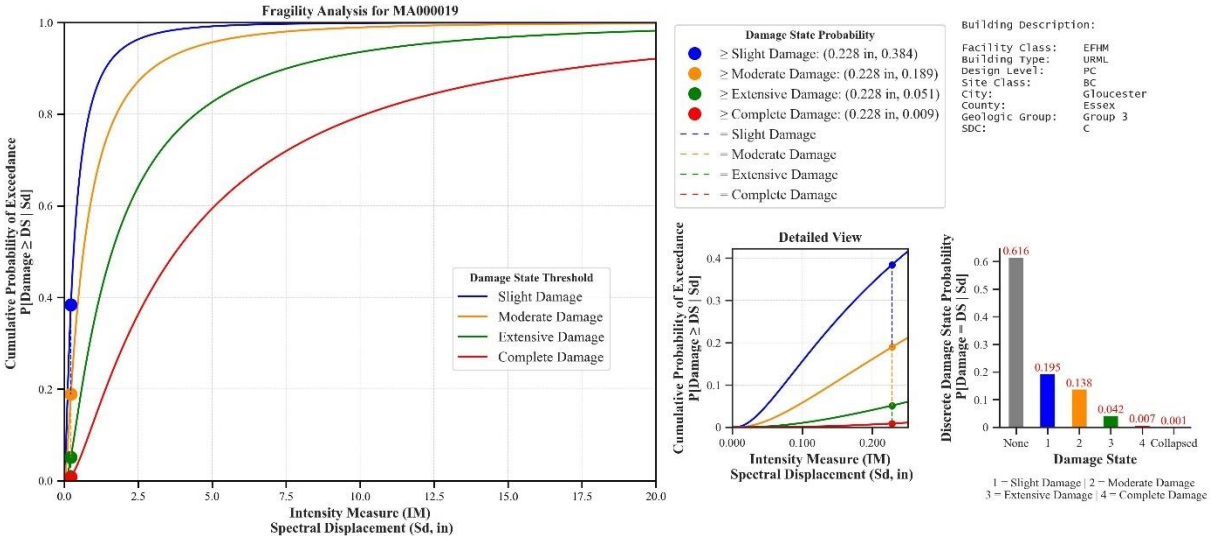
Fragility Analysis for MA000019
Cumulative Probability of Exceedance P[Damage ≥ DS | Sd]
Intensity Measure (IM) Spectral Displacement (Sd, in)
Damage State Threshold
Slight Damage
Moderate Damage
Extensive Damage
Complete Damage
Damage State Probability
≥ Slight Damage: (0.228 in, 0.384)
≥ Moderate Damage: (0.228 in, 0.189)
≥ Extensive Damage: (0.228 in, 0.051)
≥ Complete Damage: (0.228 in, 0.009)
Detailed View
Discrete Damage State Probability P[Damage = DS | Sd]
0.616
0.195
0.138
0.042
0.007
0.001
None 1 2 3 4 Collapsed
Damage State
1 = Slight Damage | 2 = Moderate Damage
3 = Extensive Damage | 4 = Complete Damage
Building Description:
Facility Class: EFHM
Building Type: URML
Design Level: PC
Site Class: BC
City: Gloucester
County: Essex
Geologic Group: Group 3
SDC: C

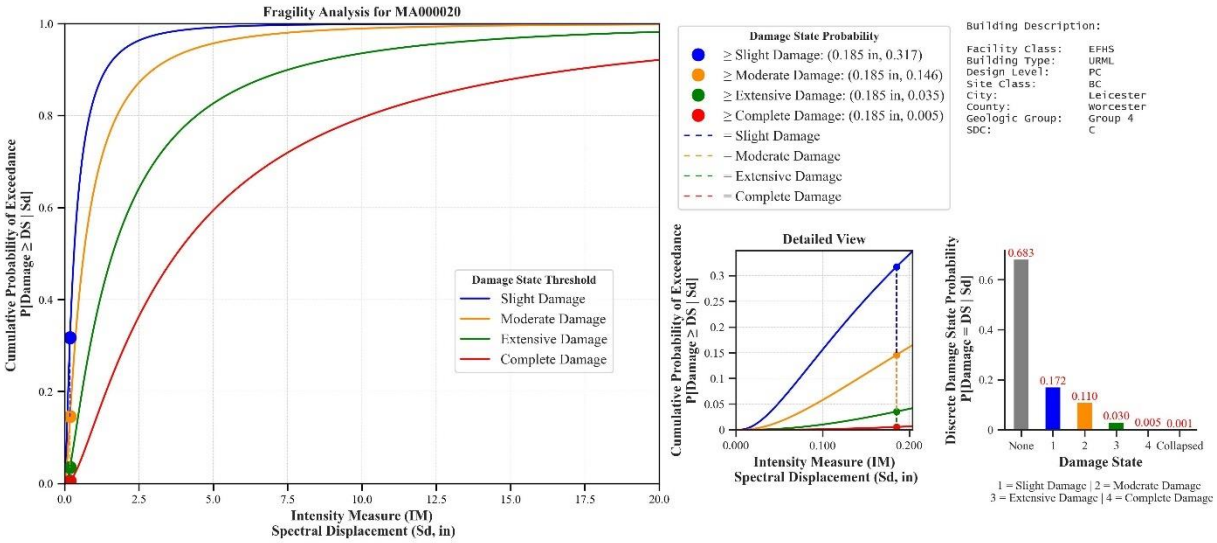
Fragility Analysis for MA000020
Cumulative Probability of Exceedance P[Damage ≥ DS | Sd]
Intensity Measure (IM) Spectral Displacement (Sd, in)
Damage State Threshold
Slight Damage
Moderate Damage
Extensive Damage
Complete Damage
Damage State Probability
≥ Slight Damage: (0.185 in, 0.317)
≥ Moderate Damage: (0.185 in, 0.146)
≥ Extensive Damage: (0.185 in, 0.035)
≥ Complete Damage: (0.185 in, 0.005)
= Slight Damage
= Moderate Damage
= Extensive Damage
= Complete Damage
Detailed View
Building Description:
Facility Class: EFHS
Building Type: URML
Design Level: PC
Site Class: BC
City: Leicester
County: Worcester
Geologic Group: Group 4
SDC: C
Discrete Damage State Probability P[Damage = DS | Sd]
0.683
0.172
0.110
0.030
0.005
0.001
None
Collapsed
Damage State
1 = Slight Damage | 2 = Moderate Damage
3 = Extensive Damage | 4 = Complete Damage

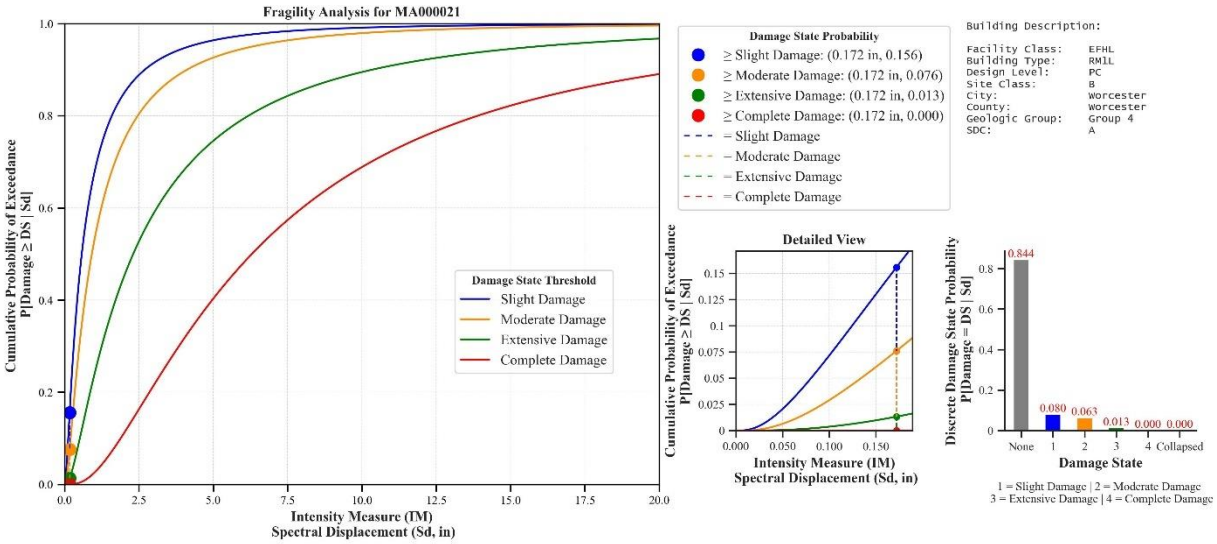
Fragility Analysis for MA000021
Cumulative Probability of Exceedance P[Damage ≥ DS | Sd]
Intensity Measure (IM) Spectral Displacement (Sd, in)
Damage State Threshold
Slight Damage
Moderate Damage
Extensive Damage
Complete Damage
Damage State Probability
≥ Slight Damage: (0.172 in, 0.156)
≥ Moderate Damage: (0.172 in, 0.076)
≥ Extensive Damage: (0.172 in, 0.013)
≥ Complete Damage: (0.172 in, 0.000)
= Slight Damage
= Moderate Damage
= Extensive Damage
= Complete Damage
Detailed View
Building Description:
Facility Class: EFHL
Building Type: RMLL
Design Level: PC
Site Class: B
City: Worcester
County: Worcester
Geologic Group: Group 4
SDC: A
Discrete Damage State Probability P[Damage = DS | Sd]
0.844
0.080
0.063
0.013
0.000
0.000
None
Collapsed
Damage State
1 = Slight Damage | 2 = Moderate Damage
3 = Extensive Damage | 4 = Complete Damage

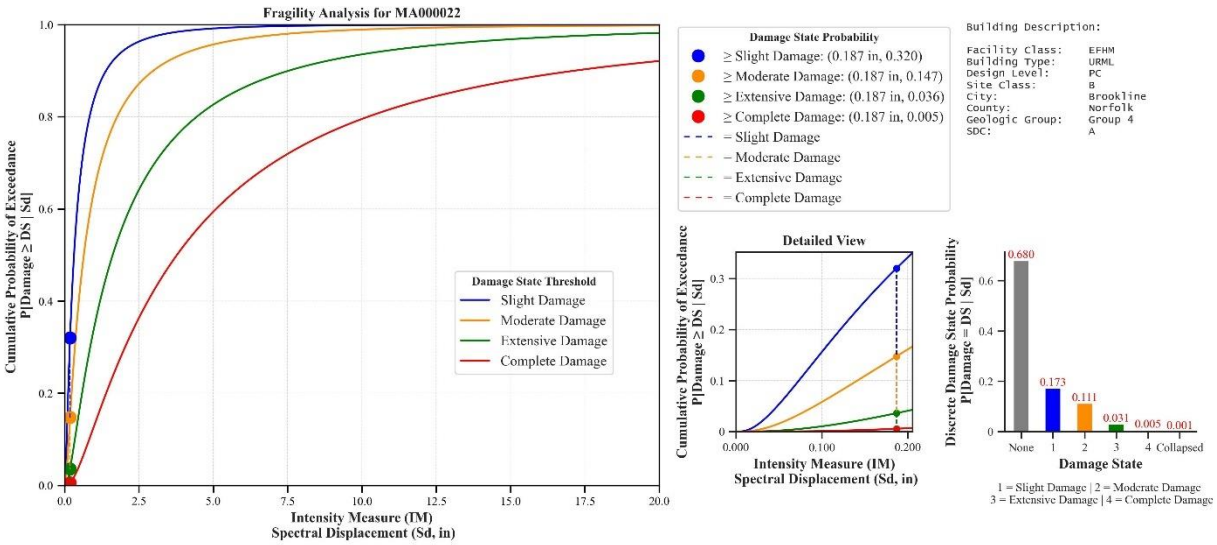
Fragility Analysis for MA000022
Cumulative Probability of Exceedance P[Damage ≥ DS | Sd]
Intensity Measure (IM) Spectral Displacement (Sd, in)
Damage State Threshold
Slight Damage
Moderate Damage
Extensive Damage
Complete Damage
Damage State Probability
≥ Slight Damage: (0.187 in, 0.320)
≥ Moderate Damage: (0.187 in, 0.147)
≥ Extensive Damage: (0.187 in, 0.036)
≥ Complete Damage: (0.187 in, 0.005)
= Slight Damage
= Moderate Damage
= Extensive Damage
= Complete Damage
Detailed View
Building Description:
Facility Class: EFHM
Building Type: URML
Design Level: PC
Site Class: B
City: Brookline
County: Norfolk
Geologic Group: Group 4
SDC: A
Discrete Damage State Probability P[Damage = DS | Sd]
0.680
0.173
0.111
0.031
0.005
0.001
None
Collapsed
Damage State
1 = Slight Damage | 2 = Moderate Damage
3 = Extensive Damage | 4 = Complete Damage

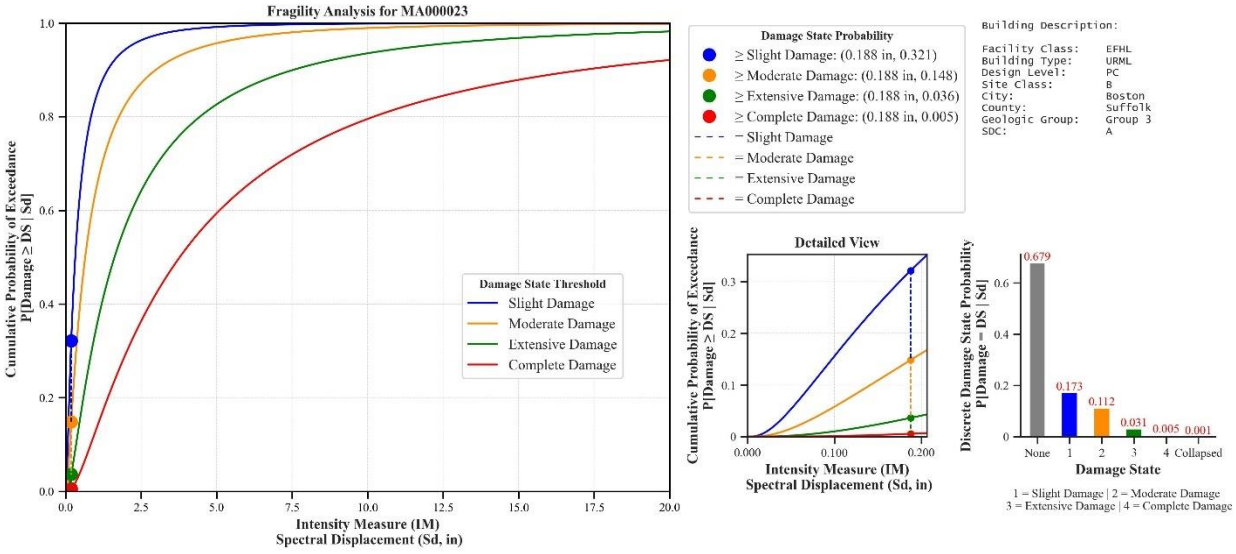
Fragility Analysis for MA000023
Cumulative Probability of Exceedance
P[Damage ≥ DS | Sd]
Intensity Measure (IM)
Spectral Displacement (Sd, in)
Damage State Threshold
Slight Damage
Moderate Damage
Extensive Damage
Complete Damage
Damage State Probability
≥ Slight Damage: (0.188 in, 0.321)
≥ Moderate Damage: (0.188 in, 0.148)
≥ Extensive Damage: (0.188 in, 0.036)
≥ Complete Damage: (0.188 in, 0.005)
= Slight Damage
= Moderate Damage
= Extensive Damage
= Complete Damage
Detailed View
Building Description:
Facility Class: EFHL
Building Type: URML
Design Level: PC
Site Class: B
City: Boston
County: Suffolk
Geologic Group: Group 3
SDC: A
Discrete Damage State Probability
P[Damage = DS | Sd]
0.679
0.173
0.112
0.031
0.005
0.001
None
1
2
3
4
Collapsed
Damage State
1 = Slight Damage | 2 = Moderate Damage
3 = Extensive Damage | 4 = Complete Damage

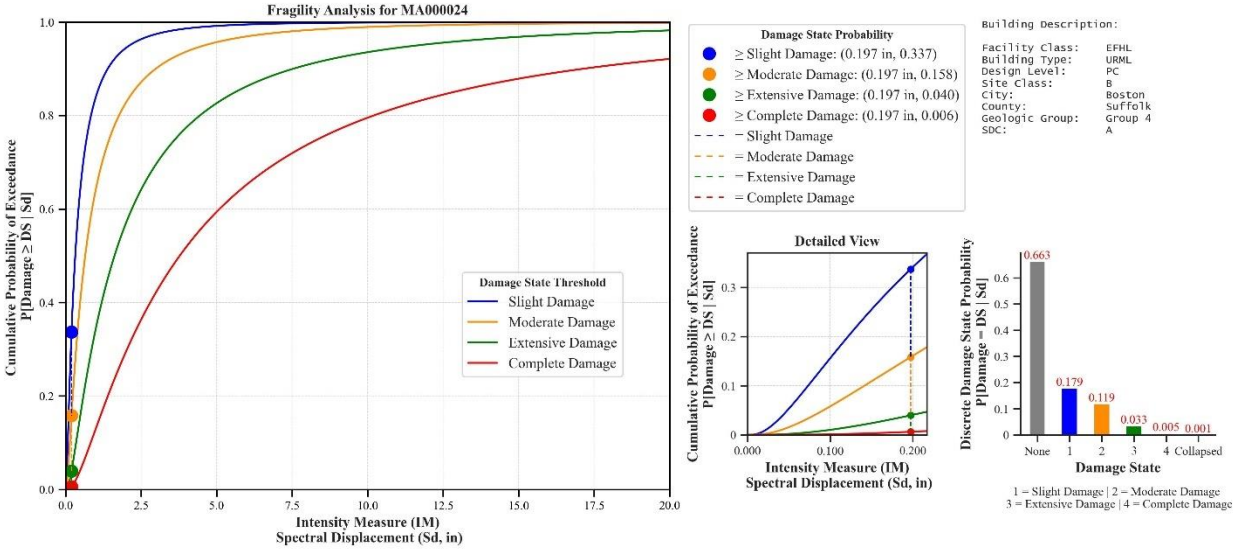
Fragility Analysis for MA000024
Cumulative Probability of Exceedance
P[Damage ≥ DS | Sd]
Intensity Measure (IM)
Spectral Displacement (Sd, in)
Damage State Threshold
Slight Damage
Moderate Damage
Extensive Damage
Complete Damage
Damage State Probability
≥ Slight Damage: (0.197 in, 0.337)
≥ Moderate Damage: (0.197 in, 0.158)
≥ Extensive Damage: (0.197 in, 0.040)
≥ Complete Damage: (0.197 in, 0.006)
= Slight Damage
= Moderate Damage
= Extensive Damage
= Complete Damage
Detailed View
Building Description:
Facility Class: EFHL
Building Type: URML
Design Level: PC
Site Class: B
City: Boston
County: Suffolk
Geologic Group: Group 4
SDC: A
Discrete Damage State Probability
P[Damage = DS | Sd]
0.663
0.179
0.119
0.033
0.005
0.001
None
1
2
3
4
Collapsed
Damage State
1 = Slight Damage | 2 = Moderate Damage
3 = Extensive Damage | 4 = Complete Damage

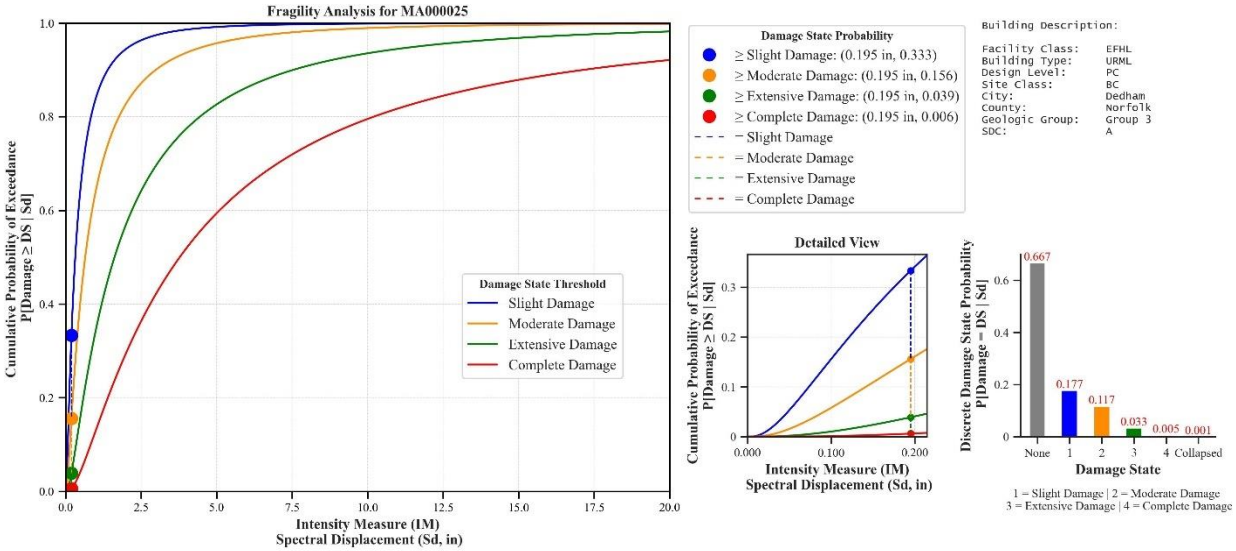
Fragility Analysis for MA000025
Cumulative Probability of Exceedance
P[Damage ≥ DS | Sd]
Intensity Measure (IM)
Spectral Displacement (Sd, in)
Damage State Threshold
Slight Damage
Moderate Damage
Extensive Damage
Complete Damage
Damage State Probability
≥ Slight Damage: (0.195 in, 0.333)
≥ Moderate Damage: (0.195 in, 0.156)
≥ Extensive Damage: (0.195 in, 0.039)
≥ Complete Damage: (0.195 in, 0.006)
= Slight Damage
= Moderate Damage
= Extensive Damage
= Complete Damage
Detailed View
Building Description:
Facility Class: EFHL
Building Type: URML
Design Level: PC
Site Class: BC
City: Dedham
County: Norfolk
Geologic Group: Group 3
SDC: A
Discrete Damage State Probability
P[Damage = DS | Sd]
0.667
0.177
0.117
0.033
0.005
0.001
None
1
2
3
4
Collapsed
Damage State
1 = Slight Damage | 2 = Moderate Damage
3 = Extensive Damage | 4 = Complete Damage

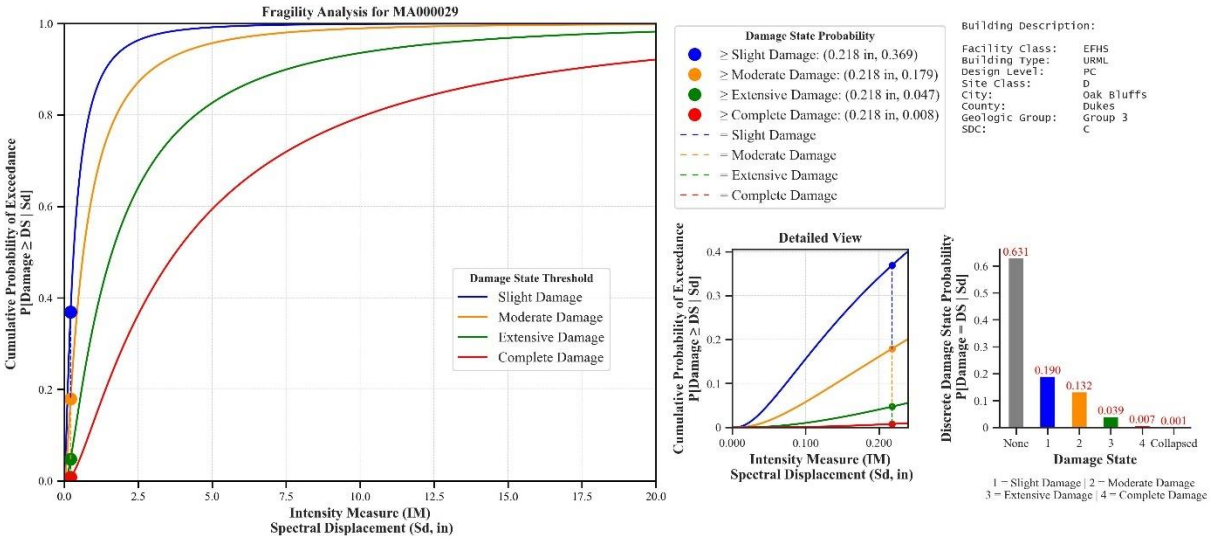
Fragility Analysis for MA000029
Cumulative Probability of Exceedance P[Damage ≥ DS | Sd]
Intensity Measure (IM) Spectral Displacement (Sd, in)
Damage State Threshold
Slight Damage
Moderate Damage
Extensive Damage
Complete Damage
Damage State Probability
≥ Slight Damage: (0.218 in, 0.369)
≥ Moderate Damage: (0.218 in, 0.179)
≥ Extensive Damage: (0.218 in, 0.047)
≥ Complete Damage: (0.218 in, 0.008)
Building Description:
Facility Class: EFHS
Building Type: URML
Design Level: PC
Site Class: D
City: Oak Bluffs
County: Dukes
Geologic Group: Group 3
SDC: C
Detailed View
Discrete Damage State Probability P[Damage = DS | Sd]
0.631
0.190
0.132
0.039
0.007
0.001
None
Collapsed
Damage State
1 = Slight Damage | 2 = Moderate Damage
3 = Extensive Damage | 4 = Complete Damage

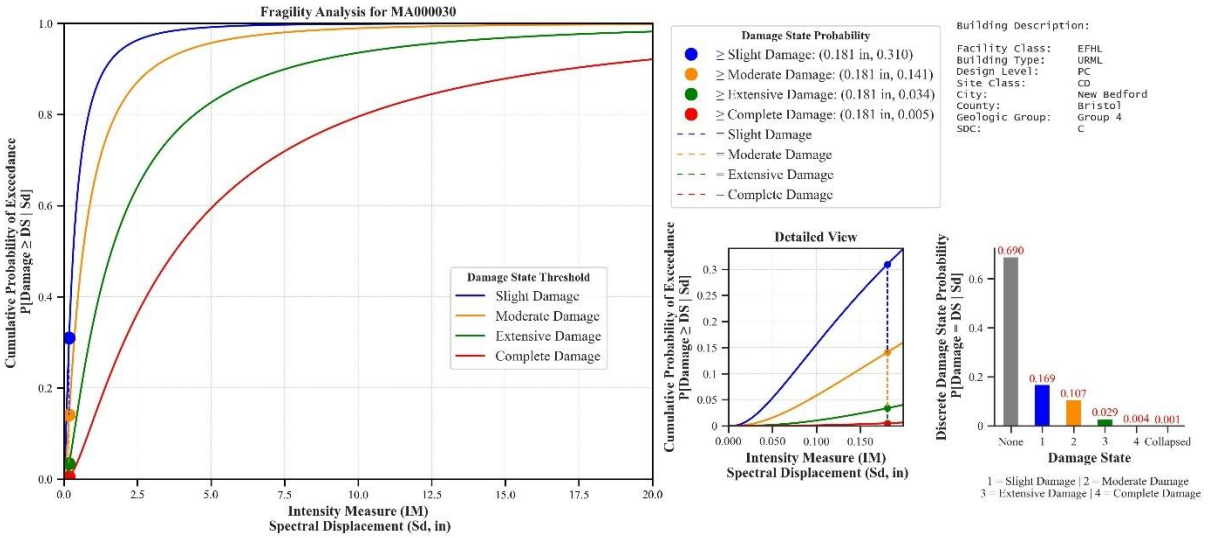
Fragility Analysis for MA000030
Cumulative Probability of Exceedance P[Damage ≥ DS | Sd]
Intensity Measure (IM) Spectral Displacement (Sd, in)
Damage State Threshold
Slight Damage
Moderate Damage
Extensive Damage
Complete Damage
Damage State Probability
≥ Slight Damage: (0.181 in, 0.310)
≥ Moderate Damage: (0.181 in, 0.141)
≥ Extensive Damage: (0.181 in, 0.034)
≥ Complete Damage: (0.181 in, 0.005)
Building Description:
Facility Class: EFHL
Building Type: URML
Design Level: PC
Site Class: CD
City: New Bedford
County: Bristol
Geologic Group: Group 4
SDC: C
Detailed View
Discrete Damage State Probability P[Damage = DS | Sd]
0.690
0.169
0.107
0.029
0.004
0.001
None
Collapsed
Damage State
1 = Slight Damage | 2 = Moderate Damage
3 = Extensive Damage | 4 = Complete Damage

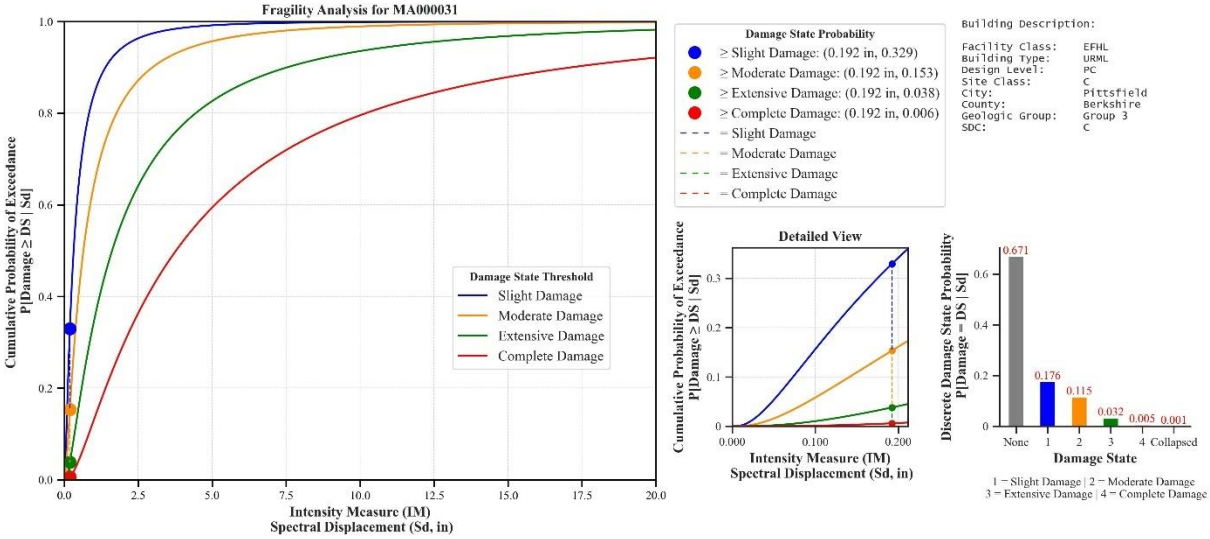
Fragility Analysis for MA000031
Cumulative Probability of Exceedance P[Damage ≥ DS | Sd]
Intensity Measure (IM) Spectral Displacement (Sd, in)
Damage State Threshold
Slight Damage
Moderate Damage
Extensive Damage
Complete Damage
Damage State Probability
≥ Slight Damage: (0.192 in, 0.329)
≥ Moderate Damage: (0.192 in, 0.153)
≥ Extensive Damage: (0.192 in, 0.038)
≥ Complete Damage: (0.192 in, 0.006)
Building Description:
Facility Class: EFHL
Building Type: URML
Design Level: PC
Site Class: C
City: Pittsfield
County: Berkshire
Geologic Group: Group 3
SDC: C
Detailed View
Discrete Damage State Probability P[Damage = DS | Sd]
0.671
0.176
0.115
0.032
0.005
0.001
None
Collapsed
Damage State
1 = Slight Damage | 2 = Moderate Damage
3 = Extensive Damage | 4 = Complete Damage

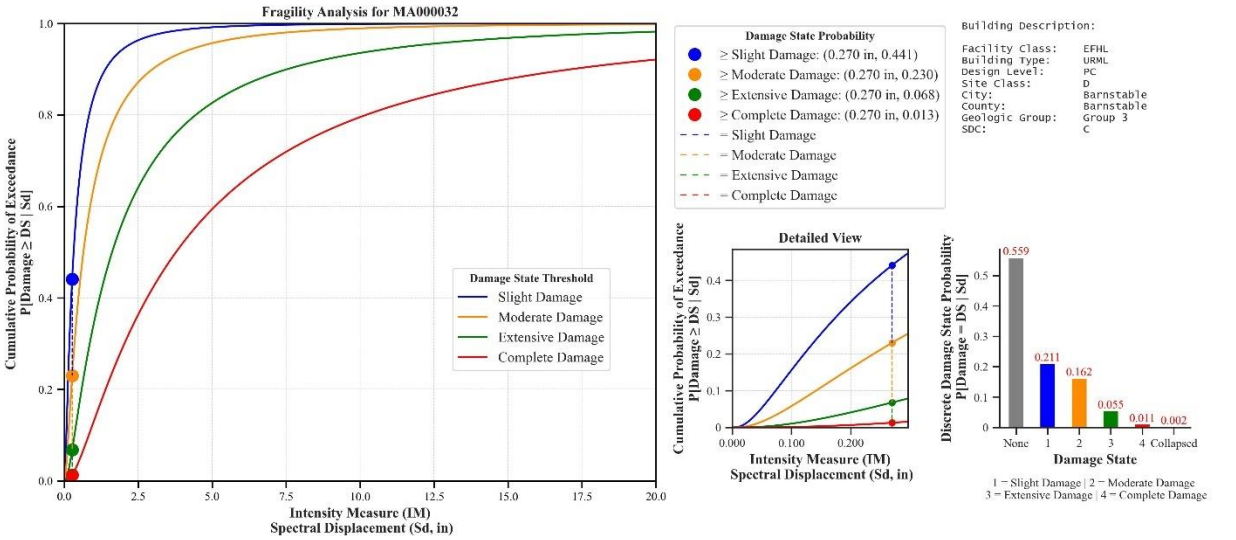
Fragility Analysis for MA000032
Cumulative Probability of Exceedance P[Damage ≥ DS | Sd]
Intensity Measure (IM) Spectral Displacement (Sd, in)
Damage State Threshold
Slight Damage
Moderate Damage
Extensive Damage
Complete Damage
Damage State Probability
≥ Slight Damage: (0.270 in, 0.441)
≥ Moderate Damage: (0.270 in, 0.230)
≥ Extensive Damage: (0.270 in, 0.068)
≥ Complete Damage: (0.270 in, 0.013)
Building Description:
Facility Class: EFHL
Building Type: URML
Design Level: PC
Site Class: D
City: Barnstable
County: Barnstable
Geologic Group: Group 3
SDC: C
Detailed View
Discrete Damage State Probability P[Damage = DS | Sd]
0.559
0.211
0.162
0.055
0.011
0.002
None
Collapsed
Damage State
1 = Slight Damage | 2 = Moderate Damage
3 = Extensive Damage | 4 = Complete Damage

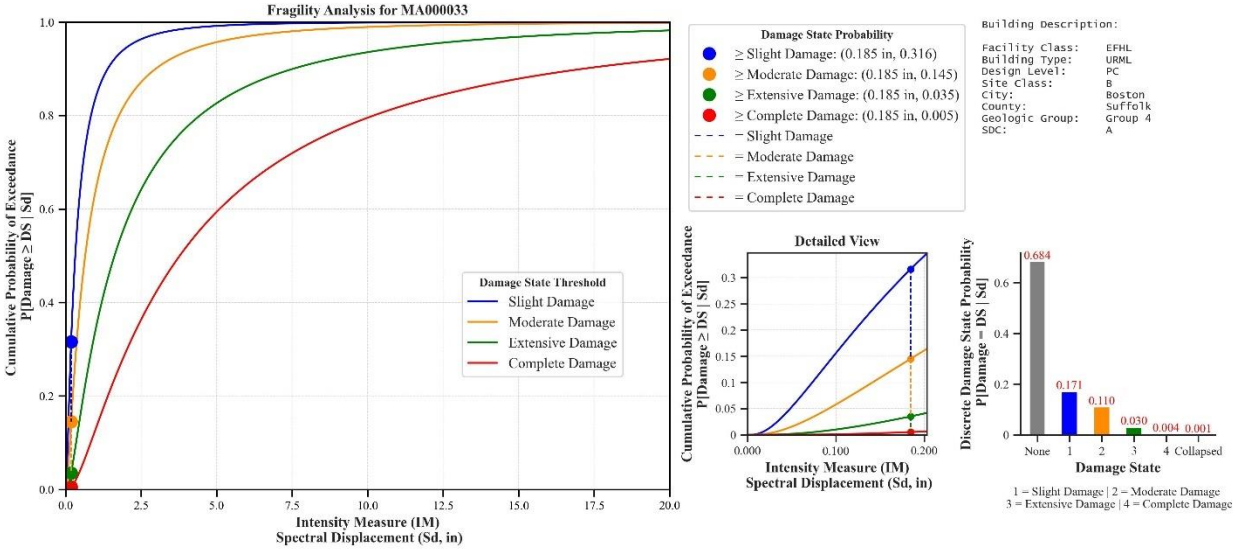
Fragility Analysis for MA000033
Cumulative Probability of Exceedance P[Damage ≥ DS | Sd]
Intensity Measure (IM) Spectral Displacement (Sd, in)
Damage State Threshold
Slight Damage
Moderate Damage
Extensive Damage
Complete Damage
Damage State Probability
≥ Slight Damage: (0.185 in, 0.316)
≥ Moderate Damage: (0.185 in, 0.145)
≥ Extensive Damage: (0.185 in, 0.035)
≥ Complete Damage: (0.185 in, 0.005)
Building Description:
Facility Class: EFHL
Building Type: URML
Design Level: PC
Site Class: B
City: Boston
County: Suffolk
Geologic Group: Group 4
SDC: A
Detailed View
Discrete Damage State Probability P[Damage = DS | Sd]
0.684
0.171
0.110
0.030
0.004
0.001
None
Collapsed
Damage State
1 = Slight Damage | 2 = Moderate Damage
3 = Extensive Damage | 4 = Complete Damage

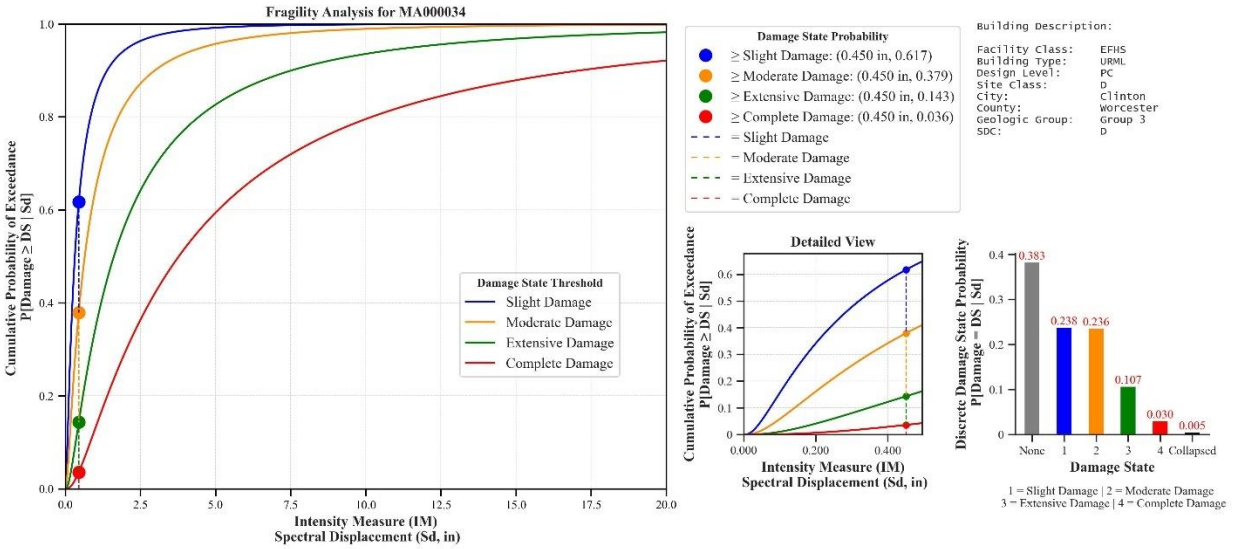
Fragility Analysis for MA000034
Cumulative Probability of Exceedance P[Damage ≥ DS | Sd]
Intensity Measure (IM) Spectral Displacement (Sd, in)
Damage State Threshold
Slight Damage
Moderate Damage
Extensive Damage
Complete Damage
Damage State Probability
≥ Slight Damage: (0.450 in, 0.617)
≥ Moderate Damage: (0.450 in, 0.379)
≥ Extensive Damage: (0.450 in, 0.143)
≥ Complete Damage: (0.450 in, 0.036)
Building Description:
Facility Class: EFHS
Building Type: URML
Design Level: PC
Site Class: D
City: Clinton
County: Worcester
Geologic Group: Group 3
SDC: D
Detailed View
Discrete Damage State Probability P[Damage = DS | Sd]
0.383
0.238
0.236
0.107
0.030
0.005
None
Collapsed
Damage State
1 = Slight Damage | 2 = Moderate Damage
3 = Extensive Damage | 4 = Complete Damage

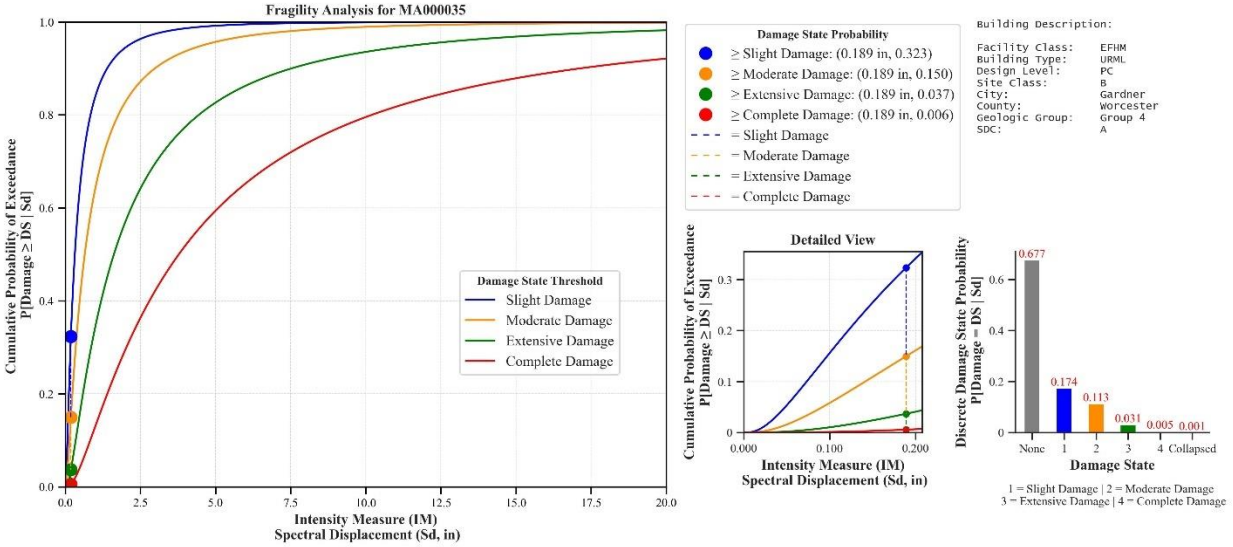
Fragility Analysis for MA000035
Cumulative Probability of Exceedance P[Damage ≥ DS | Sd]
Intensity Measure (IM) Spectral Displacement (Sd, in)
Damage State Threshold
Slight Damage
Moderate Damage
Extensive Damage
Complete Damage
Damage State Probability
≥ Slight Damage: (0.189 in, 0.323)
≥ Moderate Damage: (0.189 in, 0.150)
≥ Extensive Damage: (0.189 in, 0.037)
≥ Complete Damage: (0.189 in, 0.006)
Building Description:
Facility Class: EFHM
Building Type: URML
Design Level: PC
Site Class: B
City: Gardner
County: Worcester
Geologic Group: Group 4
SDC: A
Detailed View
Discrete Damage State Probability P[Damage = DS | Sd]
0.677
0.174
0.113
0.031
0.005
0.001
None
Collapsed
Damage State
1 = Slight Damage | 2 = Moderate Damage
3 = Extensive Damage | 4 = Complete Damage

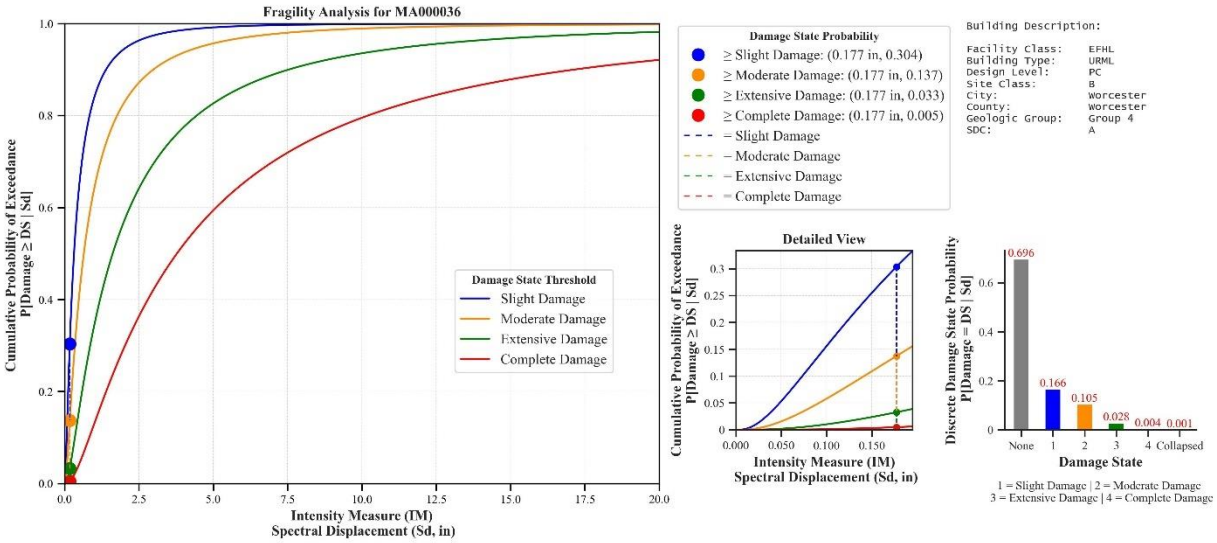
Fragility Analysis for MA000036
Cumulative Probability of Exceedance P[Damage ≥ DS | Sd]
Intensity Measure (IM) Spectral Displacement (Sd, in)
Damage State Threshold
Slight Damage
Moderate Damage
Extensive Damage
Complete Damage
Damage State Probability
≥ Slight Damage: (0.177 in, 0.304)
≥ Moderate Damage: (0.177 in, 0.137)
≥ Extensive Damage: (0.177 in, 0.033)
≥ Complete Damage: (0.177 in, 0.005)
Building Description:
Facility Class: EFHL
Building Type: URML
Design Level: PC
Site Class: B
City: Worcester
County: Worcester
Geologic Group: Group 4
SDC: A
Detailed View
Discrete Damage State Probability P[Damage = DS | Sd]
0.696
0.166
0.105
0.028
0.004
0.001
None
Collapsed
Damage State
1 = Slight Damage | 2 = Moderate Damage
3 = Extensive Damage | 4 = Complete Damage

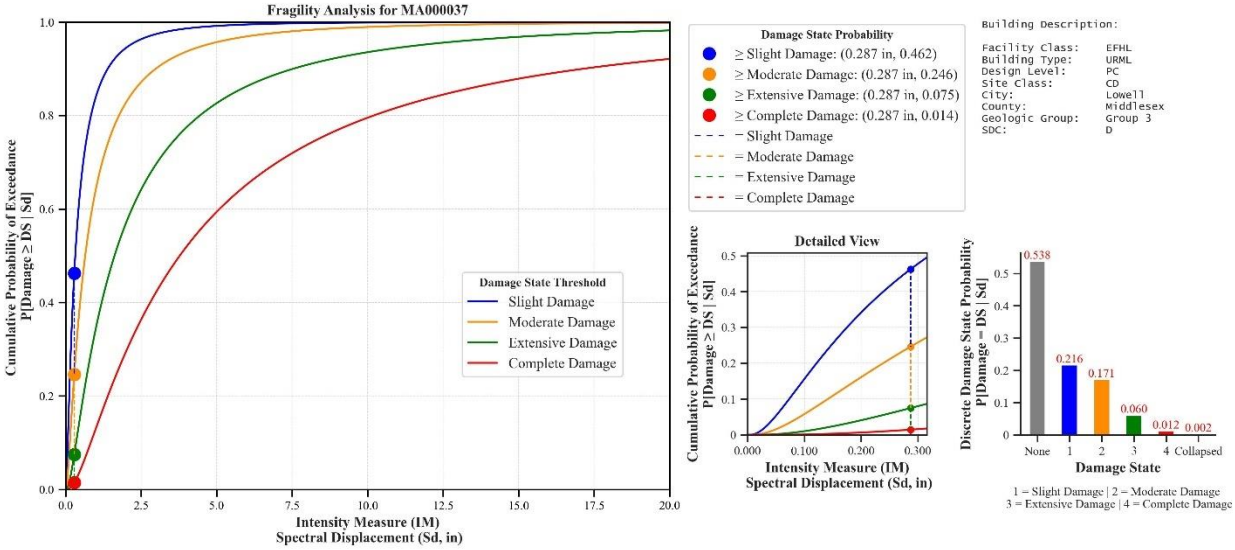
Fragility Analysis for MA000037
Cumulative Probability of Exceedance P[Damage ≥ DS | Sd]
Intensity Measure (IM) Spectral Displacement (Sd, in)
Damage State Threshold
Slight Damage
Moderate Damage
Extensive Damage
Complete Damage
Damage State Probability
≥ Slight Damage: (0.287 in, 0.462)
≥ Moderate Damage: (0.287 in, 0.246)
≥ Extensive Damage: (0.287 in, 0.075)
≥ Complete Damage: (0.287 in, 0.014)
Building Description:
Facility Class: EFHL
Building Type: URML
Design Level: PC
Site Class: CD
City: Lowell
County: Middlesex
Geologic Group: Group 3
SDC: D
Detailed View
Discrete Damage State Probability P[Damage = DS | Sd]
0.538
0.216
0.171
0.060
0.012
0.002
None
Collapsed
Damage State
1 = Slight Damage | 2 = Moderate Damage
3 = Extensive Damage | 4 = Complete Damage

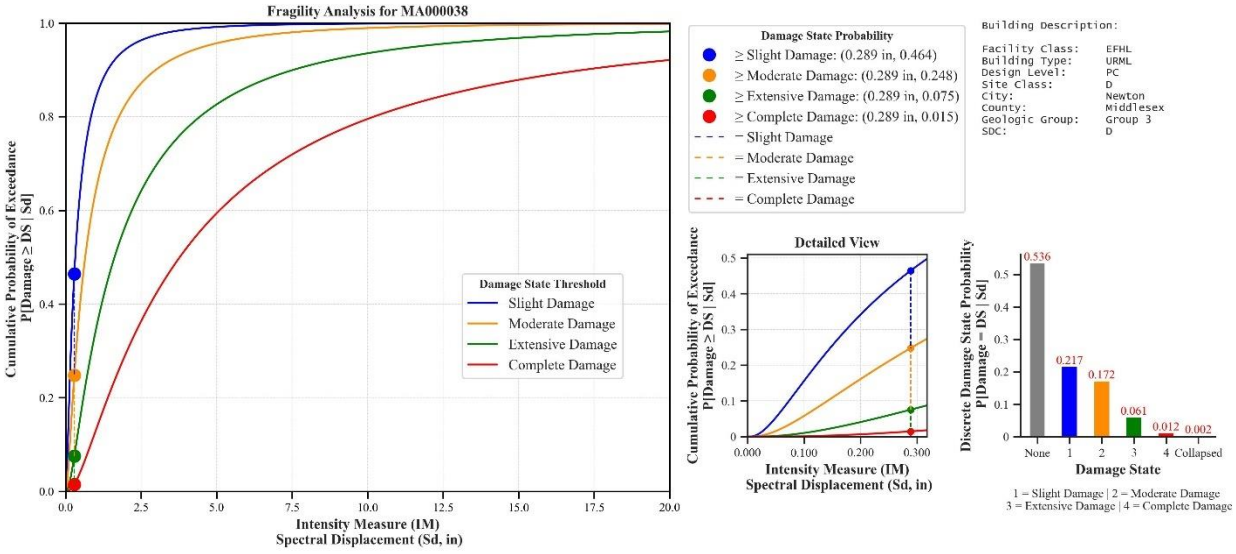
Fragility Analysis for MA000038
Cumulative Probability of Exceedance P[Damage ≥ DS | Sd]
Intensity Measure (IM) Spectral Displacement (Sd, in)
Damage State Threshold
Slight Damage
Moderate Damage
Extensive Damage
Complete Damage
Damage State Probability
≥ Slight Damage: (0.289 in, 0.464)
≥ Moderate Damage: (0.289 in, 0.248)
≥ Extensive Damage: (0.289 in, 0.075)
≥ Complete Damage: (0.289 in, 0.015)
Building Description:
Facility Class: EFHL
Building Type: URML
Design Level: PC
Site Class: D
City: Newton
County: Middlesex
Geologic Group: Group 3
SDC: D
Detailed View
Discrete Damage State Probability P[Damage = DS | Sd]
0.536
0.217
0.172
0.061
0.012
0.002
None
Collapsed
Damage State
1 = Slight Damage | 2 = Moderate Damage
3 = Extensive Damage | 4 = Complete Damage

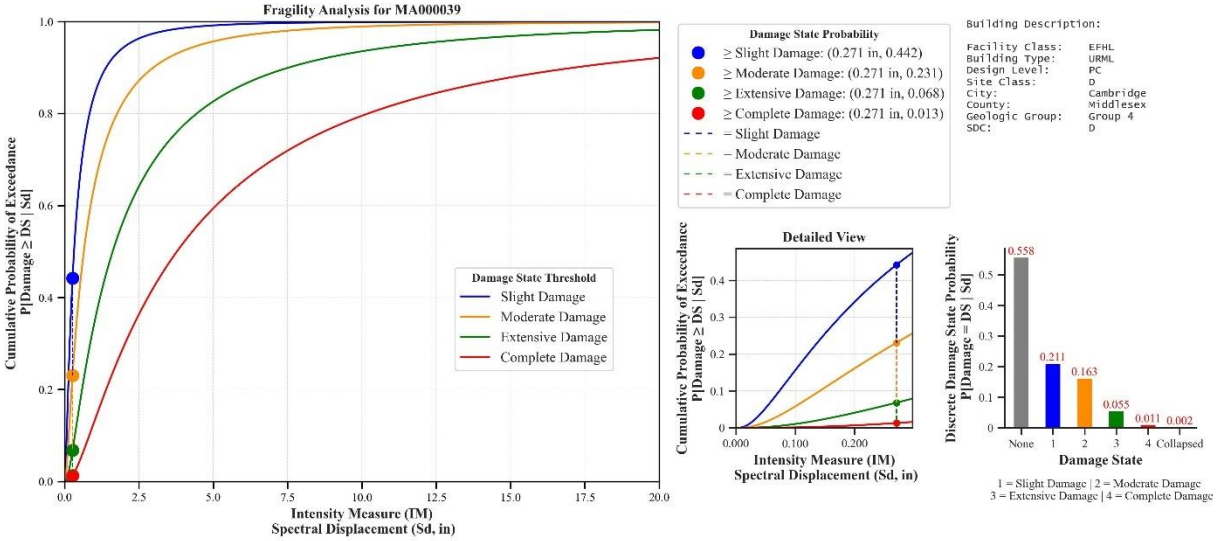
Fragility Analysis for MA000039
Cumulative Probability of Exceedance P[Damage ≥ DS | Sd]
Intensity Measure (IM) Spectral Displacement (Sd, in)
Damage State Threshold
Slight Damage
Moderate Damage
Extensive Damage
Complete Damage
Damage State Probability
≥ Slight Damage: (0.271 in, 0.442)
≥ Moderate Damage: (0.271 in, 0.231)
≥ Extensive Damage: (0.271 in, 0.068)
≥ Complete Damage: (0.271 in, 0.013)
Building Description:
Facility Class: EFHL
Building Type: URML
Design Level: PC
Site Class: D
City: Cambridge
County: Middlesex
Geologic Group: Group 4
SDC: D
Detailed View
Discrete Damage State Probability P[Damage = DS | Sd]
0.558
0.211
0.163
0.055
0.011
0.002
None
Collapsed
Damage State
1 = Slight Damage | 2 = Moderate Damage
3 = Extensive Damage | 4 = Complete Damage

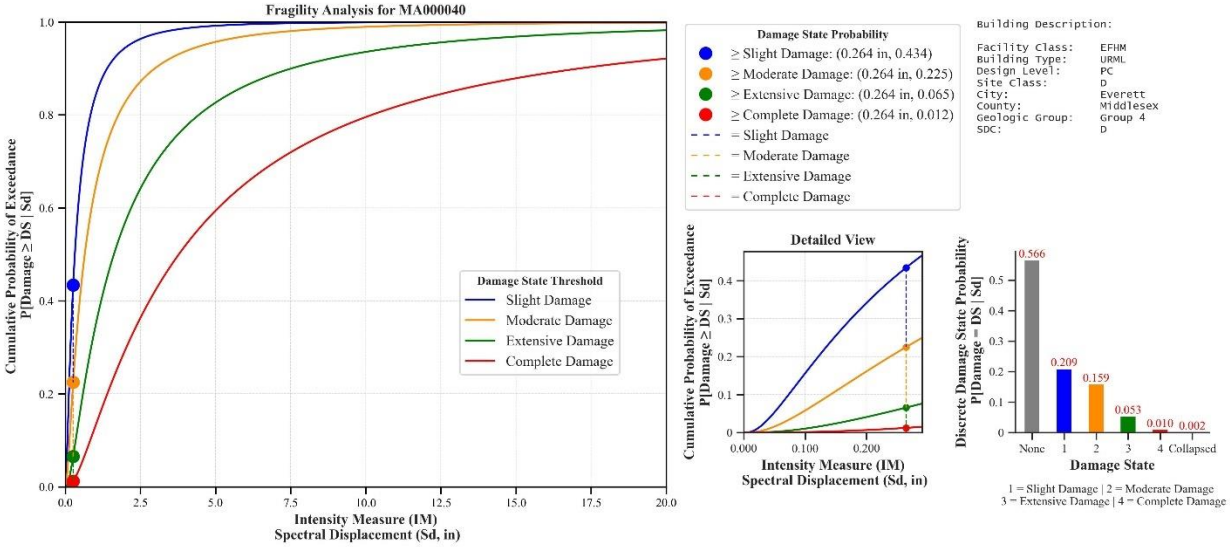
Fragility Analysis for MA000040
Cumulative Probability of Exceedance P[Damage ≥ DS | Sd]
Intensity Measure (IM) Spectral Displacement (Sd, in)
Damage State Threshold
Slight Damage
Moderate Damage
Extensive Damage
Complete Damage
Damage State Probability
≥ Slight Damage: (0.264 in, 0.434)
≥ Moderate Damage: (0.264 in, 0.225)
≥ Extensive Damage: (0.264 in, 0.065)
≥ Complete Damage: (0.264 in, 0.012)
Building Description:
Facility Class: EFHM
Building Type: URML
Design Level: PC
Site Class: D
City: Everett
County: Middlesex
Geologic Group: Group 4
SDC: D
Detailed View
Discrete Damage State Probability P[Damage = DS | Sd]
0.566
0.209
0.159
0.053
0.010
0.002
None
Collapsed
Damage State
1 = Slight Damage | 2 = Moderate Damage
3 = Extensive Damage | 4 = Complete Damage

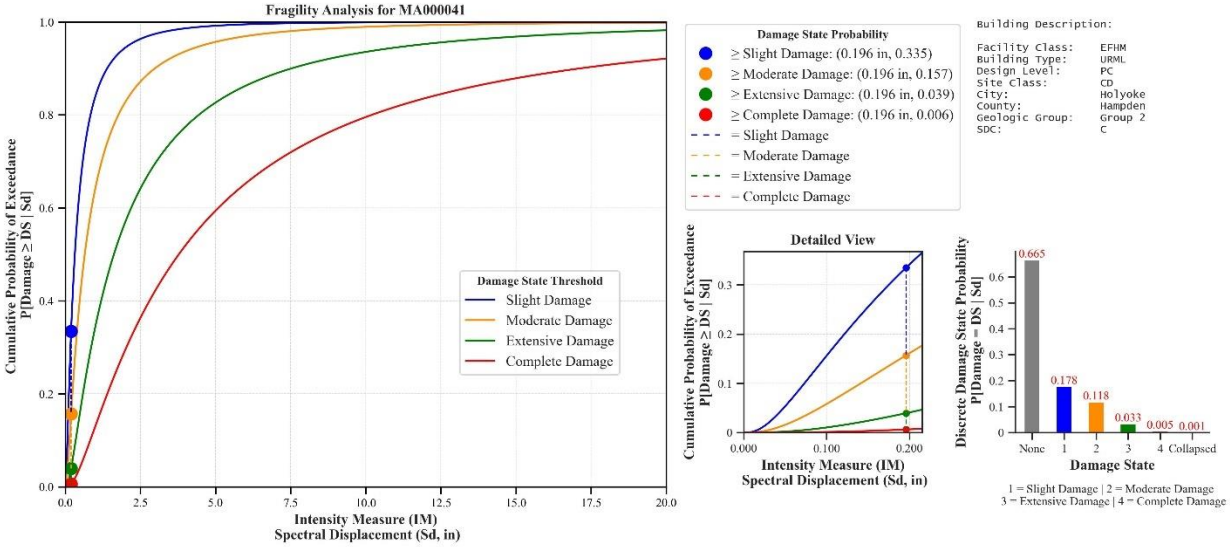
Fragility Analysis for MA000041
Cumulative Probability of Exceedance
P[Damage ≥ DS | Sd]
Intensity Measure (IM)
Spectral Displacement (Sd, in)
Damage State Threshold
Slight Damage
Moderate Damage
Extensive Damage
Complete Damage
Damage State Probability
≥ Slight Damage: (0.196 in, 0.335)
≥ Moderate Damage: (0.196 in, 0.157)
≥ Extensive Damage: (0.196 in, 0.039)
≥ Complete Damage: (0.196 in, 0.006)
Building Description:
Facility Class: EFHM
Building Type: URML
Design Level: PC
Site Class: CD
City: Holyoke
County: Hampden
Geologic Group: Group 2
SDC: C
Detailed View
Discrete Damage State Probability
P[Damage = DS | Sd]
0.665
0.178
0.118
0.033
0.005
0.001
None
Collapsed
Damage State
1 = Slight Damage | 2 = Moderate Damage
3 = Extensive Damage | 4 = Complete Damage

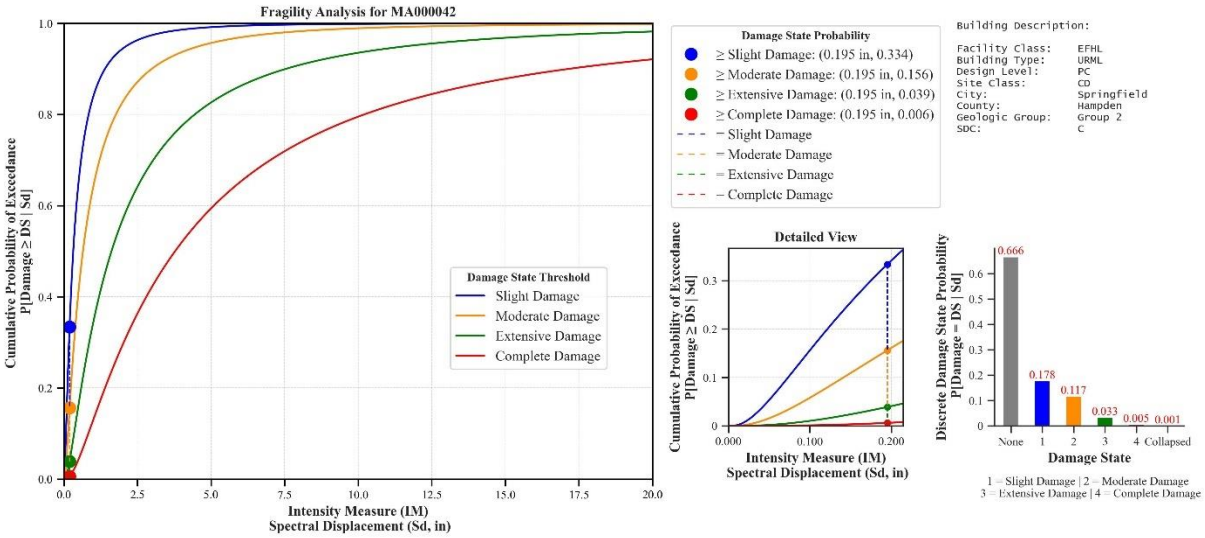
Fragility Analysis for MA000042
Cumulative Probability of Exceedance
P[Damage ≥ DS | Sd]
Intensity Measure (IM)
Spectral Displacement (Sd, in)
Damage State Threshold
Slight Damage
Moderate Damage
Extensive Damage
Complete Damage
Damage State Probability
≥ Slight Damage: (0.195 in, 0.334)
≥ Moderate Damage: (0.195 in, 0.156)
≥ Extensive Damage: (0.195 in, 0.039)
≥ Complete Damage: (0.195 in, 0.006)
Building Description:
Facility Class: EFHL
Building Type: URML
Design Level: PC
Site Class: CD
City: Springfield
County: Hampden
Geologic Group: Group 2
SDC: C
Detailed View
Discrete Damage State Probability
P[Damage = DS | Sd]
0.666
0.178
0.117
0.033
0.005
0.001
None
Collapsed
Damage State
1 = Slight Damage | 2 = Moderate Damage
3 = Extensive Damage | 4 = Complete Damage

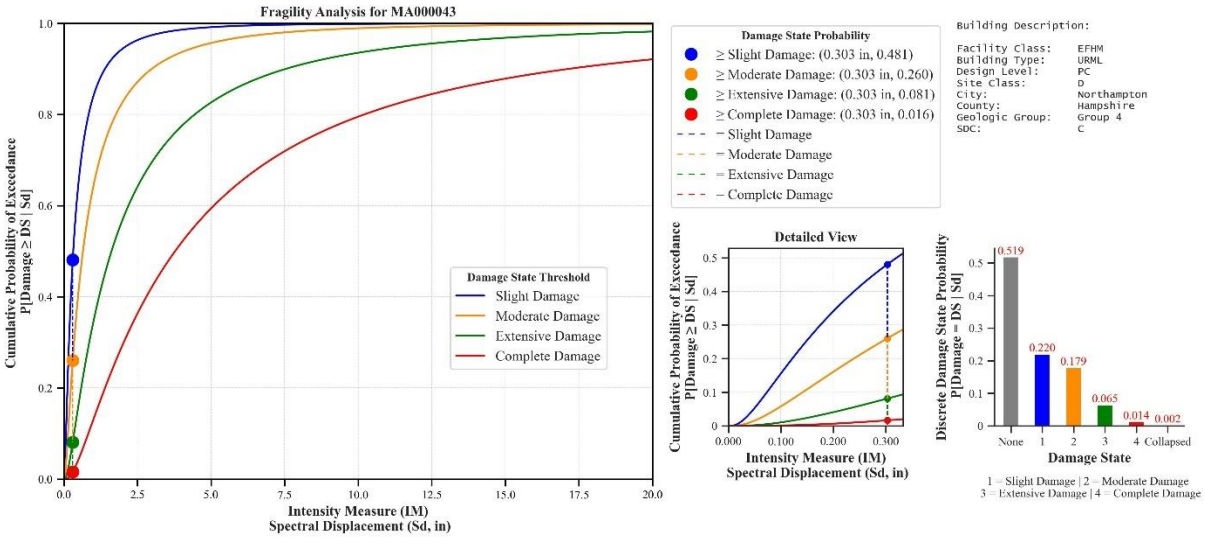
Fragility Analysis for MA000043
Cumulative Probability of Exceedance
P[Damage ≥ DS | Sd]
Intensity Measure (IM)
Spectral Displacement (Sd, in)
Damage State Threshold
Slight Damage
Moderate Damage
Extensive Damage
Complete Damage
Damage State Probability
≥ Slight Damage: (0.303 in, 0.481)
≥ Moderate Damage: (0.303 in, 0.260)
≥ Extensive Damage: (0.303 in, 0.081)
≥ Complete Damage: (0.303 in, 0.016)
Building Description:
Facility Class: EFHM
Building Type: URML
Design Level: PC
Site Class: D
City: Northampton
County: Hampshire
Geologic Group: Group 4
SDC: C
Detailed View
Discrete Damage State Probability
P[Damage = DS | Sd]
0.519
0.220
0.179
0.065
0.014
0.002
None
Collapsed
Damage State
1 = Slight Damage | 2 = Moderate Damage
3 = Extensive Damage | 4 = Complete Damage

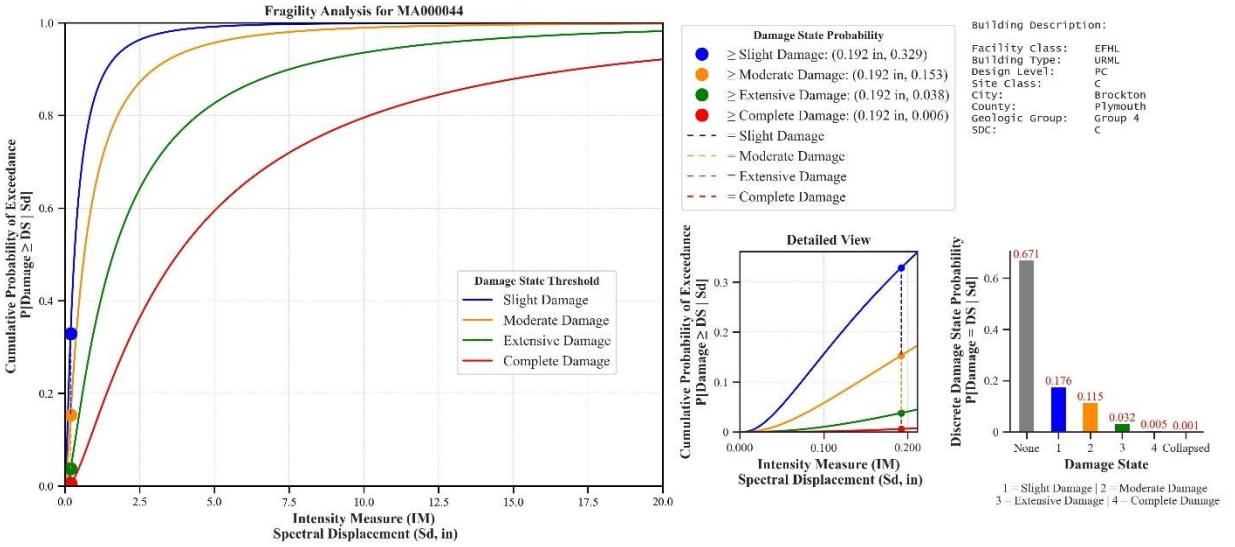
Fragility Analysis for MA000044
Cumulative Probability of Exceedance P[Damage ≥ DS | Sd]
Intensity Measure (IM) Spectral Displacement (Sd, in)
Damage State Threshold
Slight Damage
Moderate Damage
Extensive Damage
Complete Damage
Damage State Probability
≥ Slight Damage: (0.192 in, 0.329)
≥ Moderate Damage: (0.192 in, 0.153)
≥ Extensive Damage: (0.192 in, 0.038)
≥ Complete Damage: (0.192 in, 0.006)
= Slight Damage
= Moderate Damage
= Extensive Damage
= Complete Damage
Building Description:
Facility Class: EFHL
Building Type: URML
Design Level: PC
Site Class: C
City: Brockton
County: Plymouth
Geologic Group: Group 4
SDC: C
Detailed View
Discrete Damage State Probability P[Damage = DS | Sd]
0.671
0.176
0.115
0.032
0.005
0.001
None
1
2
3
4 Collapsed
Damage State
1 = Slight Damage | 2 = Moderate Damage
3 = Extensive Damage | 4 = Complete Damage

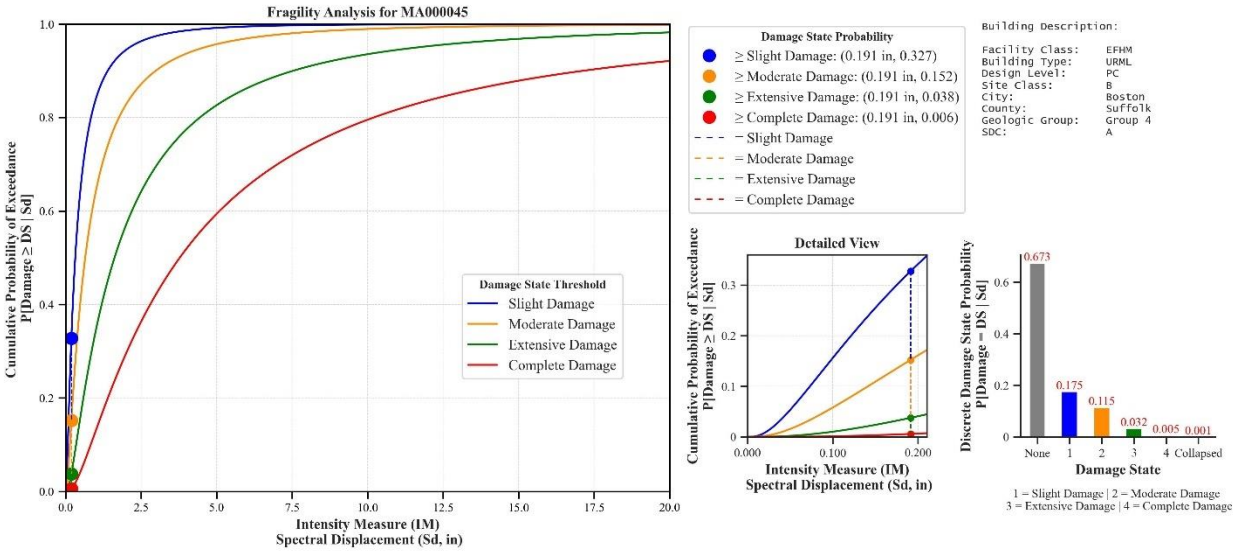
Fragility Analysis for MA000045
Cumulative Probability of Exceedance P[Damage ≥ DS | Sd]
Intensity Measure (IM) Spectral Displacement (Sd, in)
Damage State Threshold
Slight Damage
Moderate Damage
Extensive Damage
Complete Damage
Damage State Probability
≥ Slight Damage: (0.191 in, 0.327)
≥ Moderate Damage: (0.191 in, 0.152)
≥ Extensive Damage: (0.191 in, 0.038)
≥ Complete Damage: (0.191 in, 0.006)
= Slight Damage
= Moderate Damage
= Extensive Damage
= Complete Damage
Building Description:
Facility Class: EFHM
Building Type: URML
Design Level: PC
Site Class: B
City: Boston
County: Suffolk
Geologic Group: Group 4
SDC: A
Detailed View
Discrete Damage State Probability P[Damage = DS | Sd]
0.673
0.175
0.115
0.032
0.005
0.001
None
1
2
3
4 Collapsed
Damage State
1 = Slight Damage | 2 = Moderate Damage
3 = Extensive Damage | 4 = Complete Damage

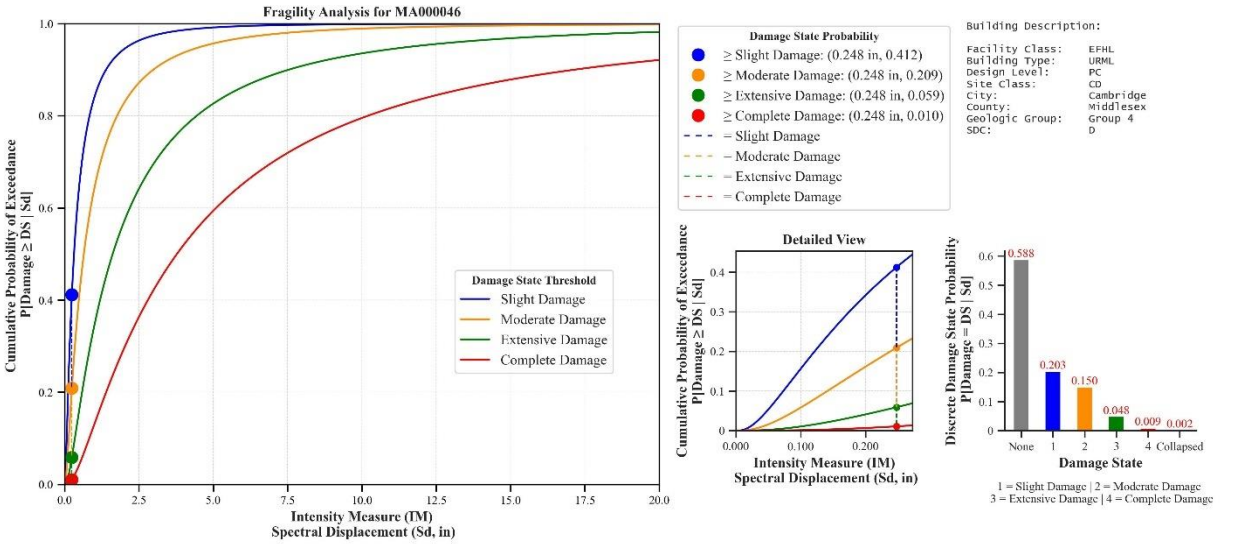
Fragility Analysis for MA000046
Cumulative Probability of Exceedance P[Damage ≥ DS | Sd]
Intensity Measure (IM) Spectral Displacement (Sd, in)
Damage State Threshold
Slight Damage
Moderate Damage
Extensive Damage
Complete Damage
Damage State Probability
≥ Slight Damage: (0.248 in, 0.412)
≥ Moderate Damage: (0.248 in, 0.209)
≥ Extensive Damage: (0.248 in, 0.059)
≥ Complete Damage: (0.248 in, 0.010)
= Slight Damage
= Moderate Damage
= Extensive Damage
= Complete Damage
Building Description:
Facility Class: EFHL
Building Type: URML
Design Level: PC
Site Class: CD
City: Cambridge
County: Middlesex
Geologic Group: Group 4
SDC: D
Detailed View
Discrete Damage State Probability P[Damage = DS | Sd]
0.588
0.203
0.150
0.048
0.009
0.002
None
1
2
3
4 Collapsed
Damage State
1 = Slight Damage | 2 = Moderate Damage
3 = Extensive Damage | 4 = Complete Damage

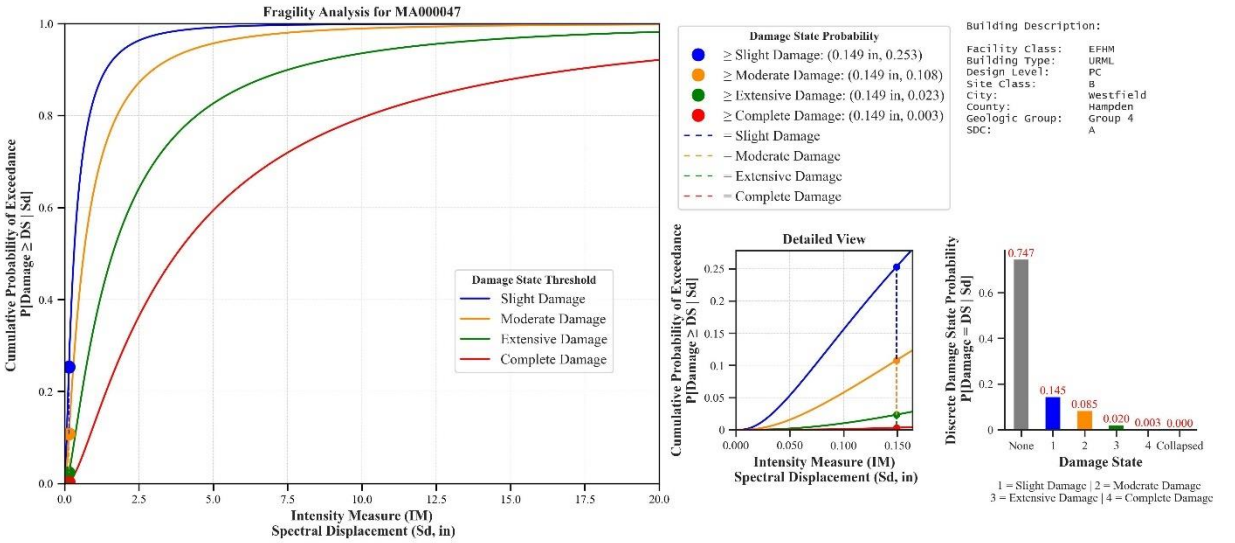
Fragility Analysis for MA000047
Cumulative Probability of Exceedance P[Damage ≥ DS | Sd]
Intensity Measure (IM) Spectral Displacement (Sd, in)
Damage State Threshold
Slight Damage
Moderate Damage
Extensive Damage
Complete Damage
Damage State Probability
≥ Slight Damage: (0.149 in, 0.253)
≥ Moderate Damage: (0.149 in, 0.108)
≥ Extensive Damage: (0.149 in, 0.023)
≥ Complete Damage: (0.149 in, 0.003)
Detailed View
Building Description:
Facility Class: EFHM
Building Type: URML
Design Level: PC
Site Class: B
City: Westfield
County: Hampden
Geologic Group: Group 4
SDC: A
Discrete Damage State Probability P[Damage = DS | Sd]
0.747
0.145
0.085
0.020
0.003
0.000
None 1 2 3 4 Collapsed
Damage State
1 = Slight Damage | 2 = Moderate Damage
3 = Extensive Damage | 4 = Complete Damage

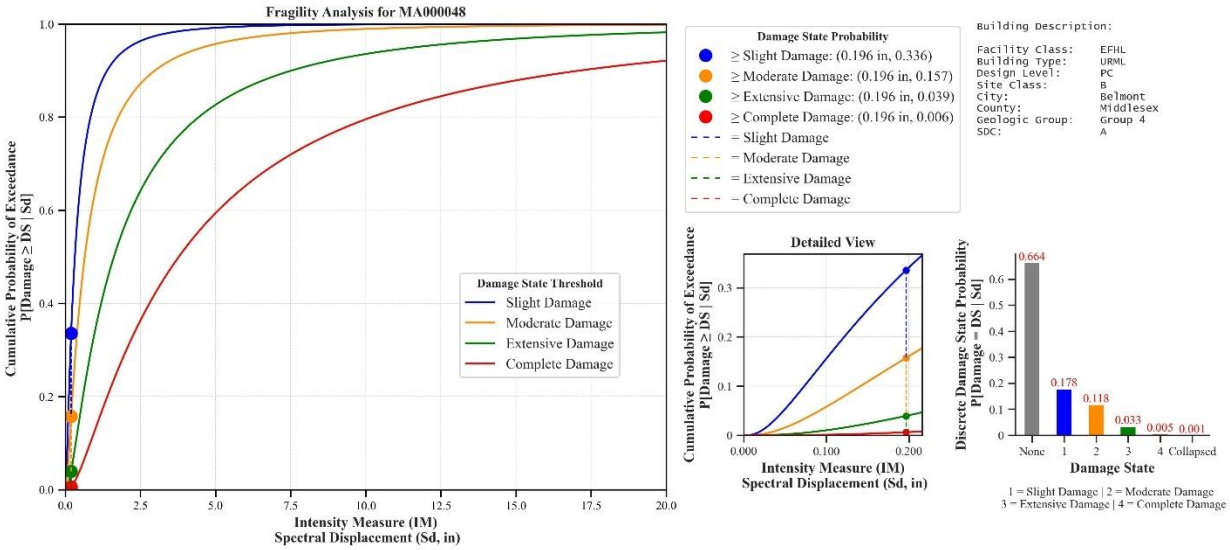
Fragility Analysis for MA000048
Cumulative Probability of Exceedance P[Damage ≥ DS | Sd]
Intensity Measure (IM) Spectral Displacement (Sd, in)
Damage State Threshold
Slight Damage
Moderate Damage
Extensive Damage
Complete Damage
Damage State Probability
≥ Slight Damage: (0.196 in, 0.336)
≥ Moderate Damage: (0.196 in, 0.157)
≥ Extensive Damage: (0.196 in, 0.039)
≥ Complete Damage: (0.196 in, 0.006)
Detailed View
Building Description:
Facility Class: EFHL
Building Type: URML
Design Level: PC
Site Class: B
City: Belmont
County: Middlesex
Geologic Group: Group 4
SDC: A
Discrete Damage State Probability P[Damage = DS | Sd]
0.664
0.178
0.118
0.033
0.005
0.001
None 1 2 3 4 Collapsed
Damage State
1 = Slight Damage | 2 = Moderate Damage
3 = Extensive Damage | 4 = Complete Damage

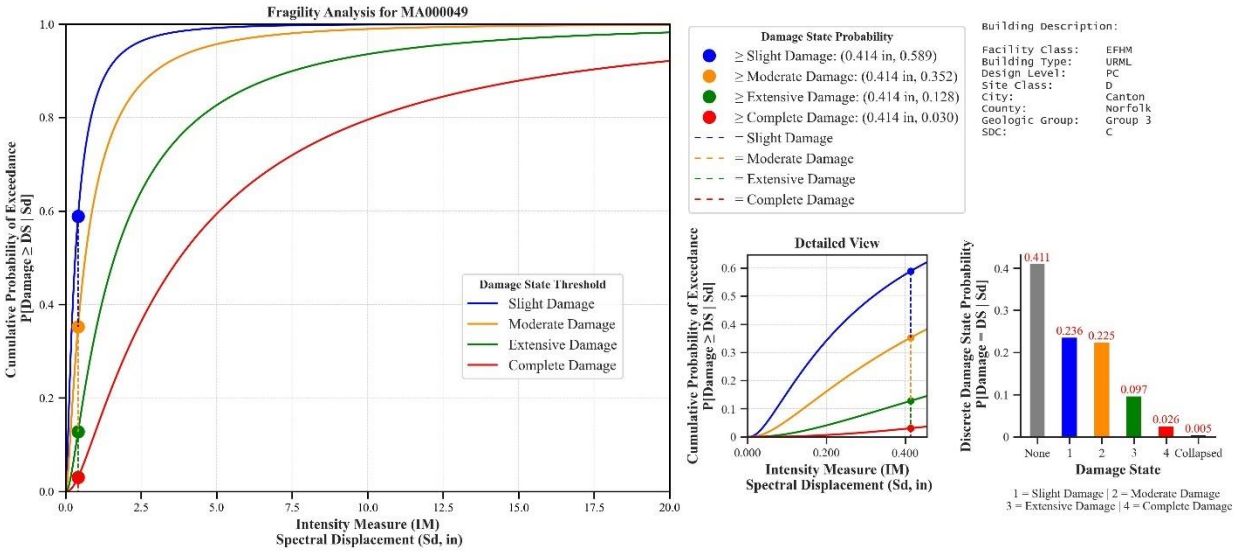
Fragility Analysis for MA000049
Cumulative Probability of Exceedance P[Damage ≥ DS | Sd]
Intensity Measure (IM) Spectral Displacement (Sd, in)
Damage State Threshold
Slight Damage
Moderate Damage
Extensive Damage
Complete Damage
Damage State Probability
≥ Slight Damage: (0.414 in, 0.589)
≥ Moderate Damage: (0.414 in, 0.352)
≥ Extensive Damage: (0.414 in, 0.128)
≥ Complete Damage: (0.414 in, 0.030)
Detailed View
Building Description:
Facility Class: EFHM
Building Type: URML
Design Level: PC
Site Class: D
City: Canton
County: Norfolk
Geologic Group: Group 3
SDC: C
Discrete Damage State Probability P[Damage = DS | Sd]
0.411
0.236
0.225
0.097
0.026
0.005
None 1 2 3 4 Collapsed
Damage State
1 = Slight Damage | 2 = Moderate Damage
3 = Extensive Damage | 4 = Complete Damage

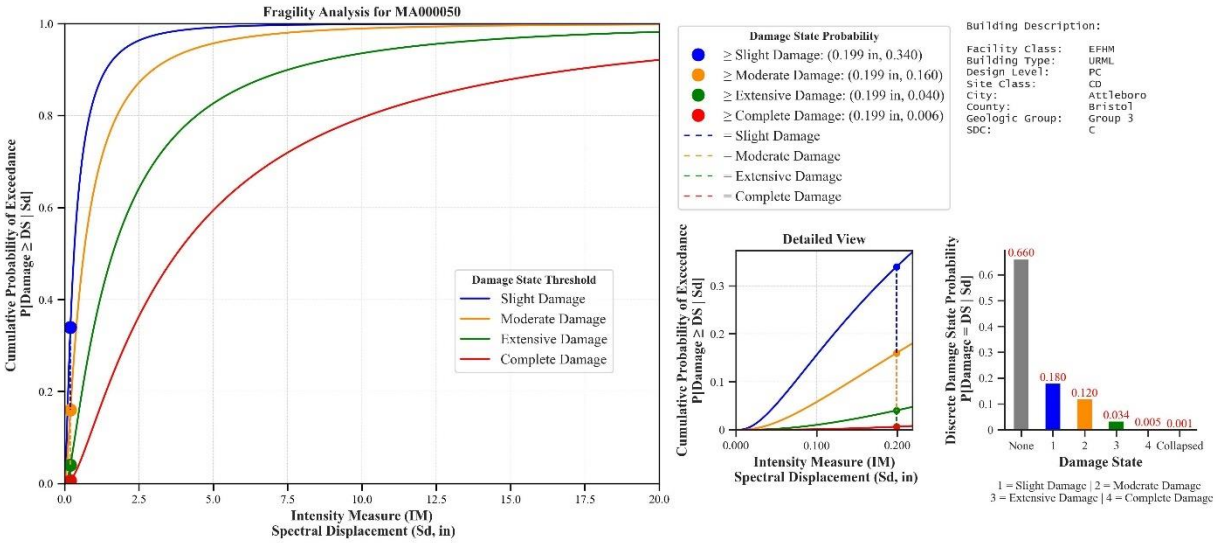
Fragility Analysis for MA000050
Cumulative Probability of Exceedance P[Damage ≥ DS | Sd]
Intensity Measure (IM) Spectral Displacement (Sd, in)
Damage State Threshold
Slight Damage
Moderate Damage
Extensive Damage
Complete Damage
Damage State Probability
≥ Slight Damage: (0.199 in, 0.340)
≥ Moderate Damage: (0.199 in, 0.160)
≥ Extensive Damage: (0.199 in, 0.040)
≥ Complete Damage: (0.199 in, 0.006)
= Slight Damage
= Moderate Damage
= Extensive Damage
= Complete Damage
Detailed View
Building Description:
Facility Class: EFHM
Building Type: URML
Design Level: PC
Site Class: CD
City: Attleboro
County: Bristol
Geologic Group: Group 3
SDC: C
Discrete Damage State Probability P[Damage = DS | Sd]
0.660
0.180
0.120
0.034
0.005
0.001
None
1
2
3
4 Collapsed
Damage State
1 = Slight Damage | 2 = Moderate Damage
3 = Extensive Damage | 4 = Complete Damage

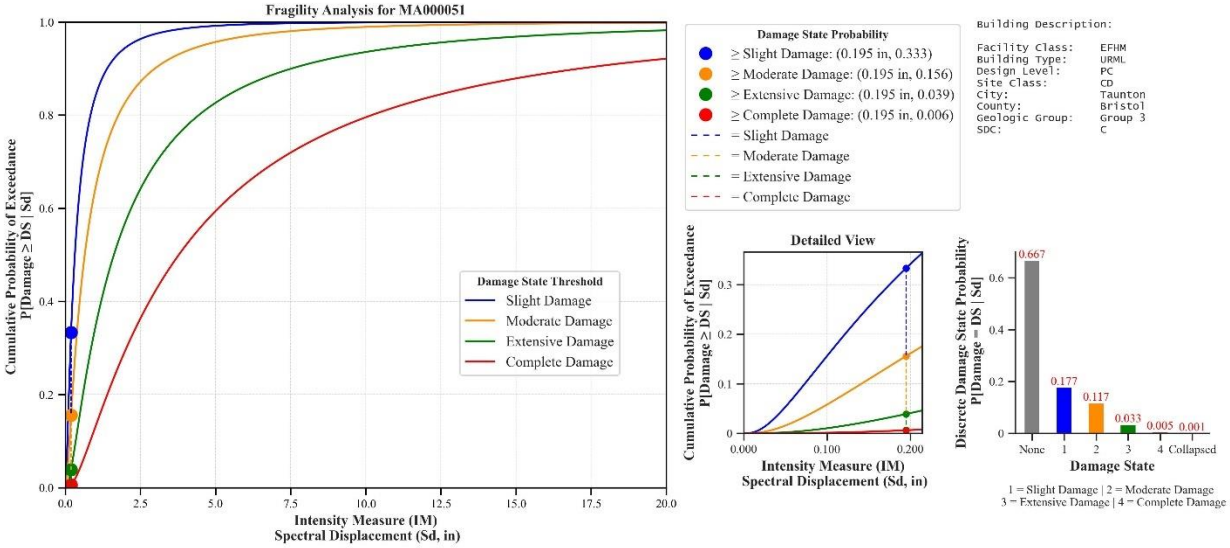
Fragility Analysis for MA000051
Cumulative Probability of Exceedance P[Damage ≥ DS | Sd]
Intensity Measure (IM) Spectral Displacement (Sd, in)
Damage State Threshold
Slight Damage
Moderate Damage
Extensive Damage
Complete Damage
Damage State Probability
≥ Slight Damage: (0.195 in, 0.333)
≥ Moderate Damage: (0.195 in, 0.156)
≥ Extensive Damage: (0.195 in, 0.039)
≥ Complete Damage: (0.195 in, 0.006)
= Slight Damage
= Moderate Damage
= Extensive Damage
= Complete Damage
Detailed View
Building Description:
Facility Class: EFHM
Building Type: URML
Design Level: PC
Site Class: CD
City: Taunton
County: Bristol
Geologic Group: Group 3
SDC: C
Discrete Damage State Probability P[Damage = DS | Sd]
0.667
0.177
0.117
0.033
0.005
0.001
None
1
2
3
4 Collapsed
Damage State
1 = Slight Damage | 2 = Moderate Damage
3 = Extensive Damage | 4 = Complete Damage

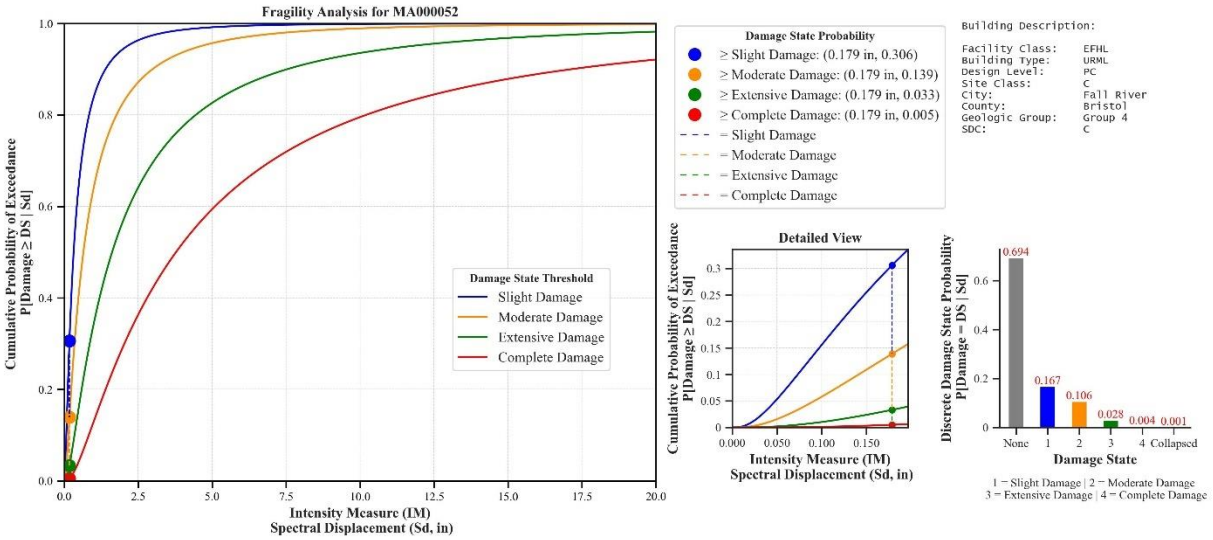
Fragility Analysis for MA000052
Cumulative Probability of Exceedance P[Damage ≥ DS | Sd]
Intensity Measure (IM) Spectral Displacement (Sd, in)
Damage State Threshold
Slight Damage
Moderate Damage
Extensive Damage
Complete Damage
Damage State Probability
≥ Slight Damage: (0.179 in, 0.306)
≥ Moderate Damage: (0.179 in, 0.139)
≥ Extensive Damage: (0.179 in, 0.033)
≥ Complete Damage: (0.179 in, 0.005)
= Slight Damage
= Moderate Damage
= Extensive Damage
= Complete Damage
Detailed View
Building Description:
Facility Class: EFHL
Building Type: URML
Design Level: PC
Site Class: C
City: Fall River
County: Bristol
Geologic Group: Group 4
SDC: C
Discrete Damage State Probability P[Damage = DS | Sd]
0.694
0.167
0.106
0.028
0.004
0.001
None
1
2
3
4 Collapsed
Damage State
1 = Slight Damage | 2 = Moderate Damage
3 = Extensive Damage | 4 = Complete Damage

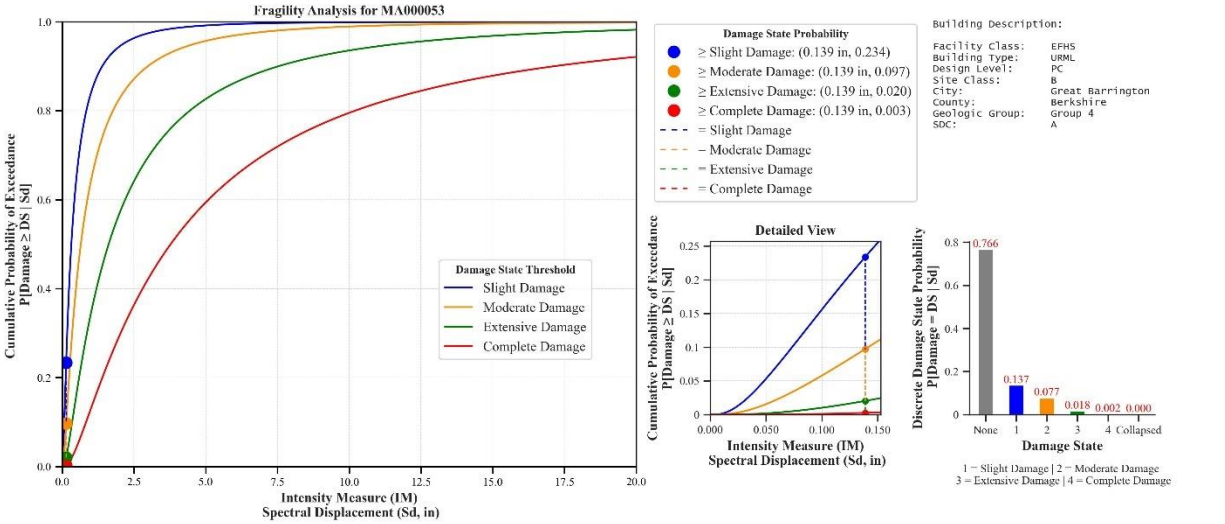
Fragility Analysis for MA000053
Cumulative Probability of Exceedance
P[Damage ≥ DS | Sd]
Intensity Measure (IM)
Spectral Displacement (Sd, in)
Damage State Threshold
Slight Damage
Moderate Damage
Extensive Damage
Complete Damage
Damage State Probability
≥ Slight Damage: (0.139 in, 0.234)
≥ Moderate Damage: (0.139 in, 0.097)
≥ Extensive Damage: (0.139 in, 0.020)
≥ Complete Damage: (0.139 in, 0.003)
= Slight Damage
= Moderate Damage
= Extensive Damage
= Complete Damage
Building Description:
Facility Class: EFHS
Building Type: URML
Design Level: PC
Site Class: B
City: Great Barrington
County: Berkshire
Geologic Group: Group 4
SDC: A
Detailed View
Discrete Damage State Probability
P[Damage = DS | Sd]
0.766
0.137
0.077
0.018
0.002
0.000
None
Collapsed
Damage State
1 = Slight Damage | 2 = Moderate Damage
3 = Extensive Damage | 4 = Complete Damage

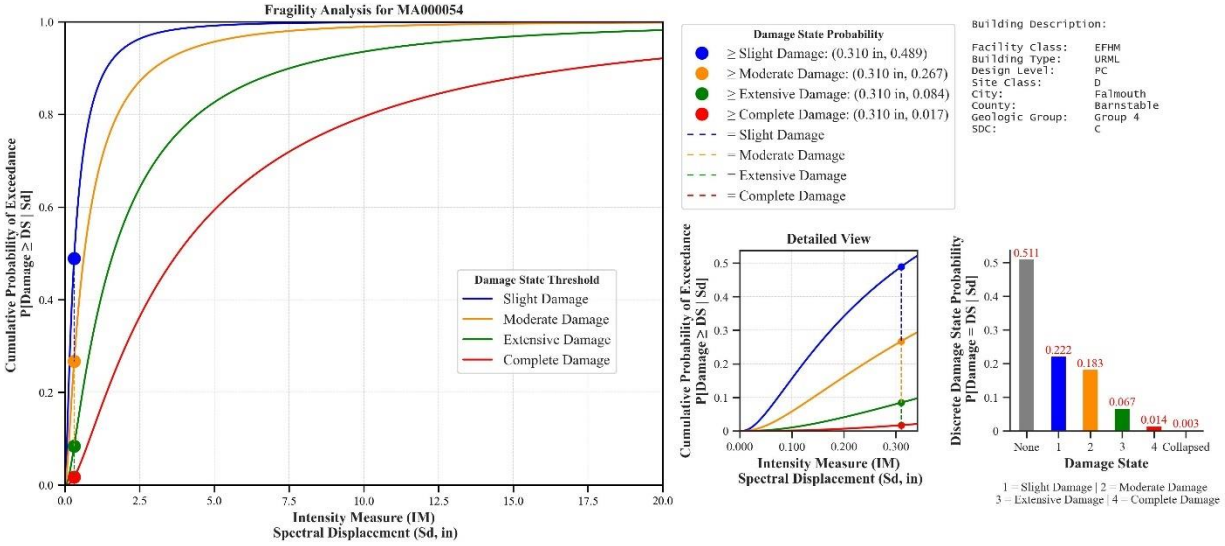
Fragility Analysis for MA000054
Cumulative Probability of Exceedance
P[Damage ≥ DS | Sd]
Intensity Measure (IM)
Spectral Displacement (Sd, in)
Damage State Threshold
Slight Damage
Moderate Damage
Extensive Damage
Complete Damage
Damage State Probability
≥ Slight Damage: (0.310 in, 0.489)
≥ Moderate Damage: (0.310 in, 0.267)
≥ Extensive Damage: (0.310 in, 0.084)
≥ Complete Damage: (0.310 in, 0.017)
= Slight Damage
= Moderate Damage
= Extensive Damage
= Complete Damage
Building Description:
Facility Class: EFHM
Building Type: URML
Design Level: PC
Site Class: D
City: Falmouth
County: Barnstable
Geologic Group: Group 4
SDC: C
Detailed View
Discrete Damage State Probability
P[Damage = DS | Sd]
0.511
0.222
0.183
0.067
0.014
0.003
None
Collapsed
Damage State
1 = Slight Damage | 2 = Moderate Damage
3 = Extensive Damage | 4 = Complete Damage

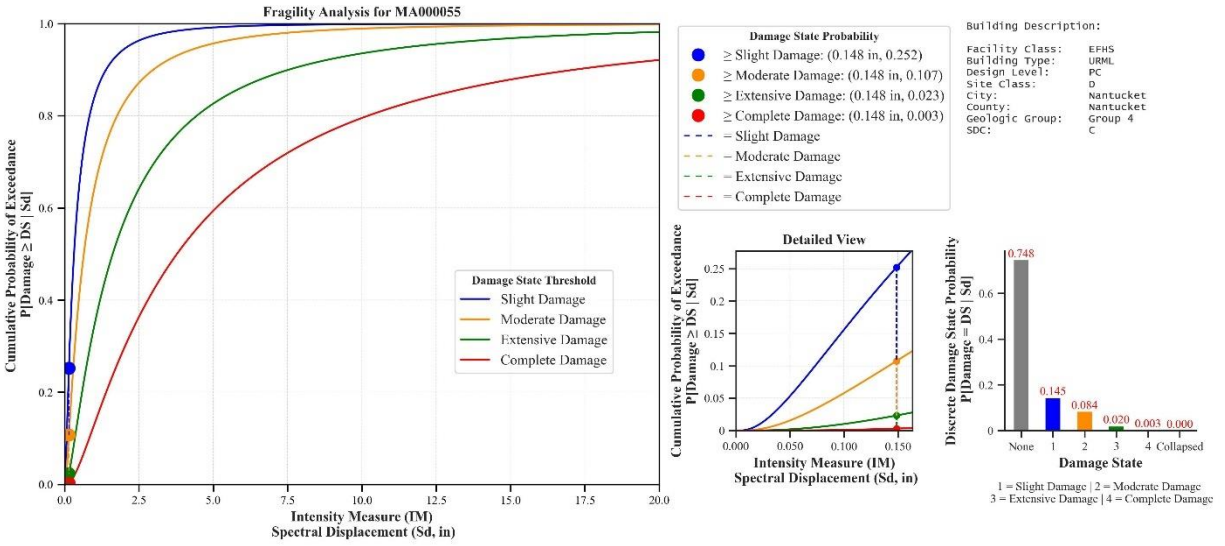
Fragility Analysis for MA000055
Cumulative Probability of Exceedance
P[Damage ≥ DS | Sd]
Intensity Measure (IM)
Spectral Displacement (Sd, in)
Damage State Threshold
Slight Damage
Moderate Damage
Extensive Damage
Complete Damage
Damage State Probability
≥ Slight Damage: (0.148 in, 0.252)
≥ Moderate Damage: (0.148 in, 0.107)
≥ Extensive Damage: (0.148 in, 0.023)
≥ Complete Damage: (0.148 in, 0.003)
= Slight Damage
= Moderate Damage
= Extensive Damage
= Complete Damage
Building Description:
Facility Class: EFHS
Building Type: URML
Design Level: PC
Site Class: D
City: Nantucket
County: Nantucket
Geologic Group: Group 4
SDC: C
Detailed View
Discrete Damage State Probability
P[Damage = DS | Sd]
0.748
0.145
0.084
0.020
0.003
0.000
None
Collapsed
Damage State
1 = Slight Damage | 2 = Moderate Damage
3 = Extensive Damage | 4 = Complete Damage

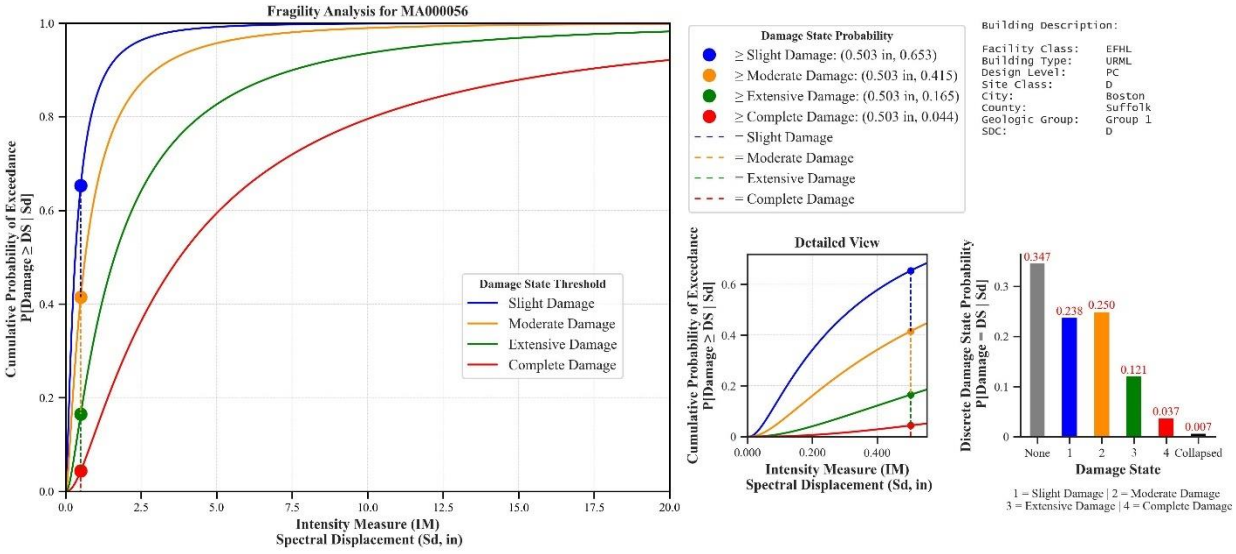
Fragility Analysis for MA000056
Cumulative Probability of Exceedance
P[Damage ≥ DS | Sd]
Intensity Measure (IM)
Spectral Displacement (Sd, in)
Damage State Threshold
Slight Damage
Moderate Damage
Extensive Damage
Complete Damage
Damage State Probability
≥ Slight Damage: (0.503 in, 0.653)
≥ Moderate Damage: (0.503 in, 0.415)
≥ Extensive Damage: (0.503 in, 0.165)
≥ Complete Damage: (0.503 in, 0.044)
Dctailed View
Discrete Damage State Probability
P[Damage = DS | Sd]
0.347
0.238
0.250
0.121
0.037
0.007
None
Collapsed
Damage State
1 = Slight Damage | 2 = Moderate Damage
3 = Extensive Damage | 4 = Complete Damage
Building Description:
Facility Class: EFHL
Building Type: URML
Design Level: PC
Site Class: D
City: Boston
County: Suffolk
Geologic Group: Group 1
SDC: D

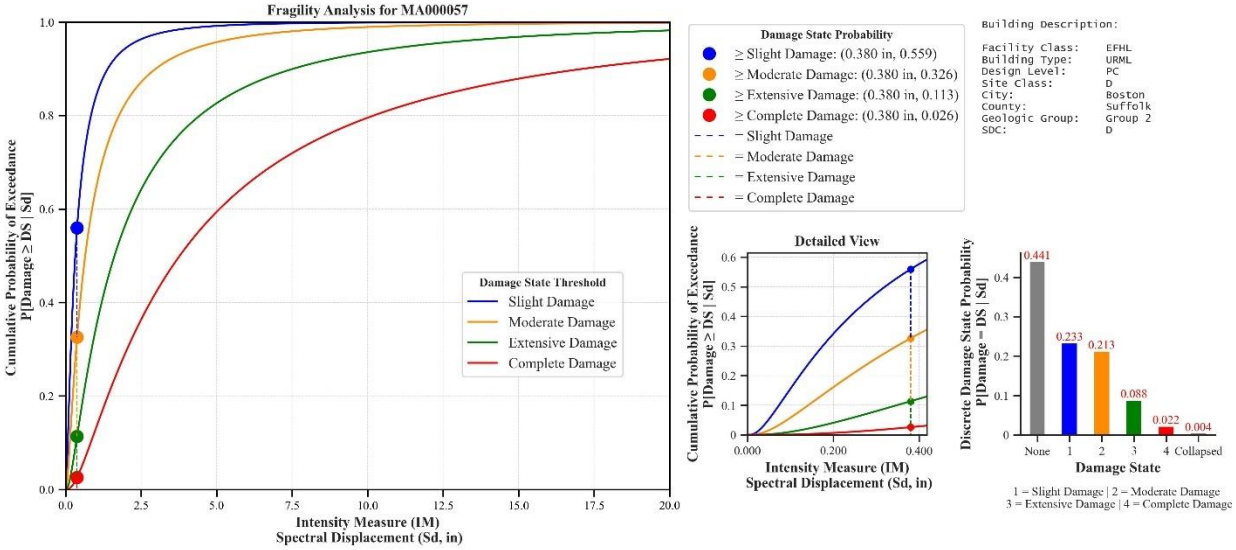
Fragility Analysis for MA000057
Cumulative Probability of Exceedance
P[Damage ≥ DS | Sd]
Intensity Measure (IM)
Spectral Displacement (Sd, in)
Damage State Threshold
Slight Damage
Moderate Damage
Extensive Damage
Complete Damage
Damage State Probability
≥ Slight Damage: (0.380 in, 0.559)
≥ Moderate Damage: (0.380 in, 0.326)
≥ Extensive Damage: (0.380 in, 0.113)
≥ Complete Damage: (0.380 in, 0.026)
Dctailed View
Discrete Damage State Probability
P[Damage = DS | Sd]
0.441
0.233
0.213
0.088
0.022
0.004
None
Collapsed
Damage State
1 = Slight Damage | 2 = Moderate Damage
3 = Extensive Damage | 4 = Complete Damage
Building Description:
Facility Class: EFHL
Building Type: URML
Design Level: PC
Site Class: D
City: Boston
County: Suffolk
Geologic Group: Group 2
SDC: D

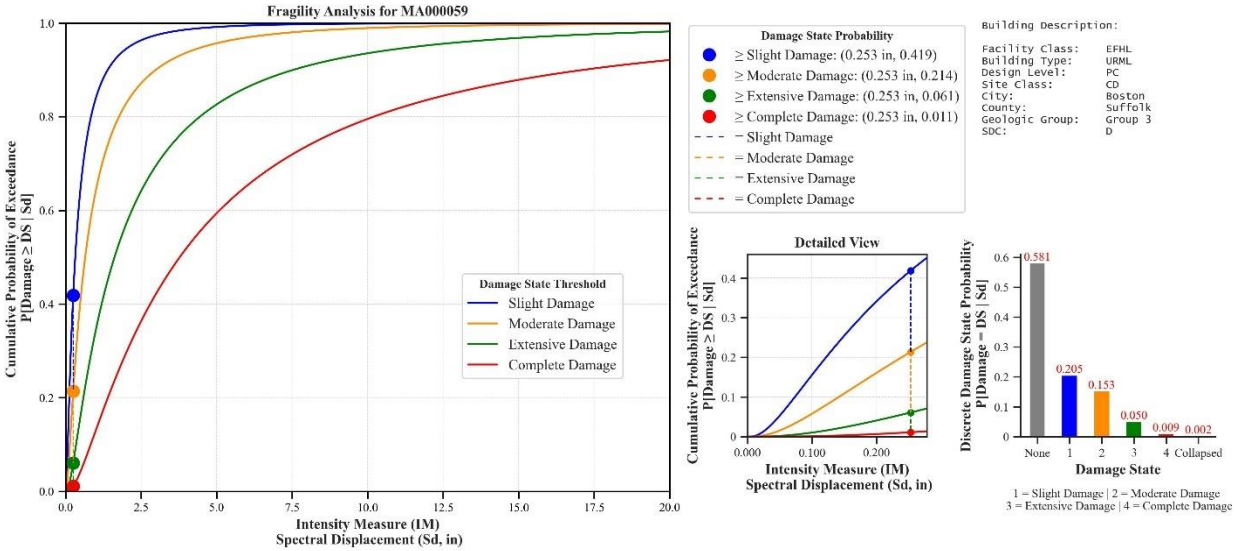
Fragility Analysis for MA000059
Cumulative Probability of Exceedance
P[Damage ≥ DS | Sd]
Intensity Measure (IM)
Spectral Displacement (Sd, in)
Damage State Threshold
Slight Damage
Moderate Damage
Extensive Damage
Complete Damage
Damage State Probability
≥ Slight Damage: (0.253 in, 0.419)
≥ Moderate Damage: (0.253 in, 0.214)
≥ Extensive Damage: (0.253 in, 0.061)
≥ Complete Damage: (0.253 in, 0.011)
Dctailed View
Discrete Damage State Probability
P[Damage = DS | Sd]
0.581
0.205
0.153
0.050
0.009
0.002
None
Collapsed
Damage State
1 = Slight Damage | 2 = Moderate Damage
3 = Extensive Damage | 4 = Complete Damage
Building Description:
Facility Class: EFHL
Building Type: URML
Design Level: PC
Site Class: CD
City: Boston
County: Suffolk
Geologic Group: Group 3
SDC: D

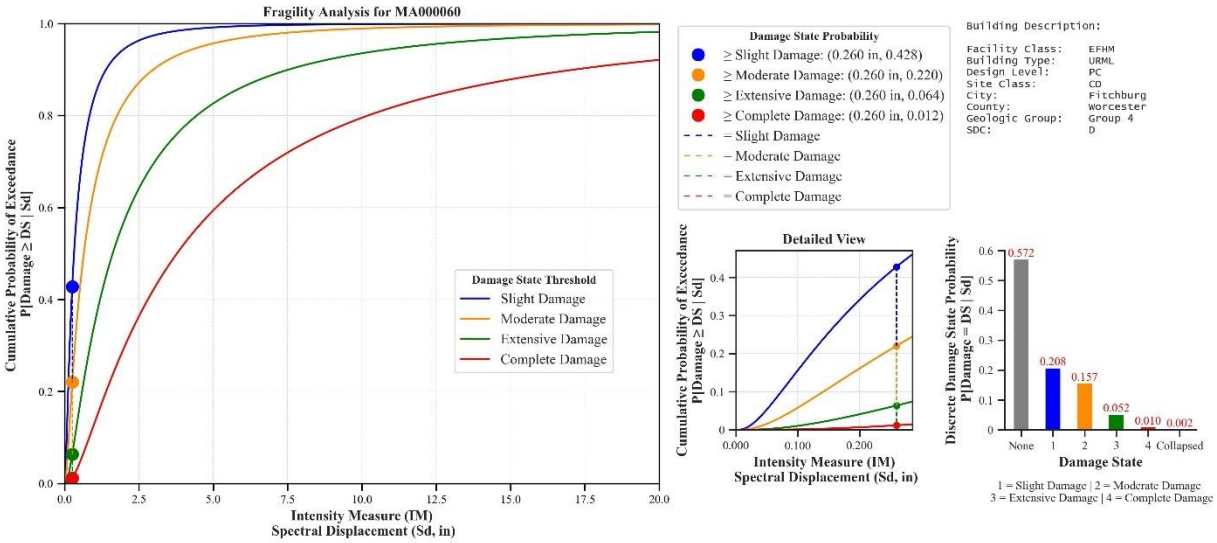
Fragility Analysis for MA000060
Cumulative Probability of Exceedance P[Damage ≥ DS | Sd]
Intensity Measure (IM) Spectral Displacement (Sd, in)
Damage State Threshold
Slight Damage
Moderate Damage
Extensive Damage
Complete Damage
Damage State Probability
≥ Slight Damage: (0.260 in, 0.428)
≥ Moderate Damage: (0.260 in, 0.220)
≥ Extensive Damage: (0.260 in, 0.064)
≥ Complete Damage: (0.260 in, 0.012)
Building Description:
Facility Class: EFHM
Building Type: URML
Design Level: PC
Site Class: CD
City: Fitchburg
County: Worcester
Geologic Group: Group 4
SDC: D
Detailed View
Discrete Damage State Probability P[Damage = DS | Sd]
0.572
0.208
0.157
0.052
0.010
0.002
None
Collapsed
Damage State
1 = Slight Damage | 2 = Moderate Damage
3 = Extensive Damage | 4 = Complete Damage

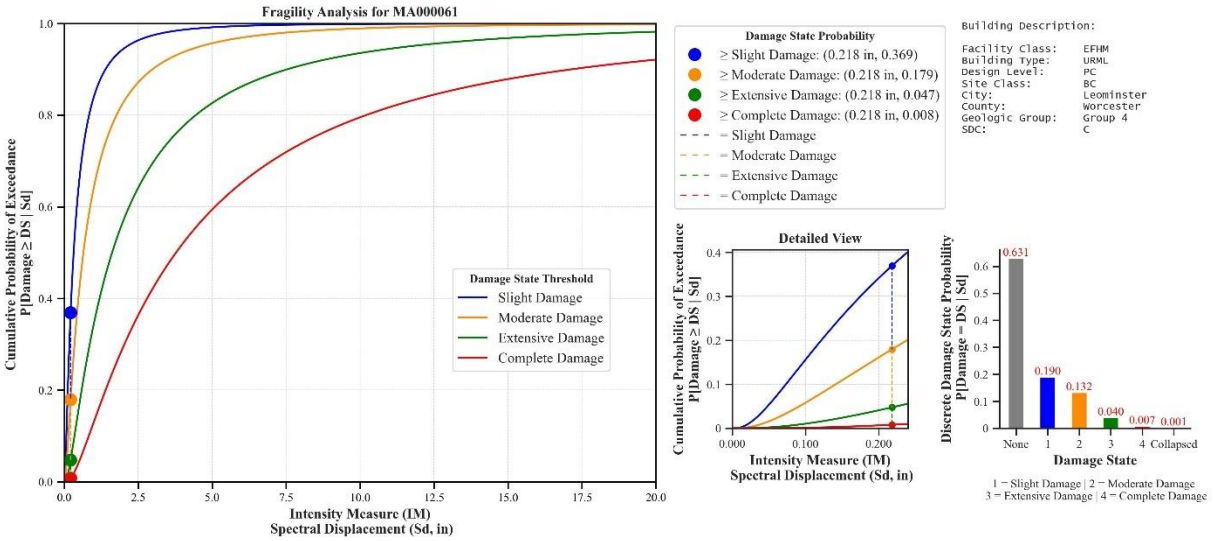
Fragility Analysis for MA000061
Cumulative Probability of Exceedance P[Damage ≥ DS | Sd]
Intensity Measure (IM) Spectral Displacement (Sd, in)
Damage State Threshold
Slight Damage
Moderate Damage
Extensive Damage
Complete Damage
Damage State Probability
≥ Slight Damage: (0.218 in, 0.369)
≥ Moderate Damage: (0.218 in, 0.179)
≥ Extensive Damage: (0.218 in, 0.047)
≥ Complete Damage: (0.218 in, 0.008)
Building Description:
Facility Class: EFHM
Building Type: URML
Design Level: PC
Site Class: BC
City: Leominster
County: Worcester
Geologic Group: Group 4
SDC: C
Detailed View
Discrete Damage State Probability P[Damage = DS | Sd]
0.631
0.190
0.132
0.040
0.007
0.001
None
Collapsed
Damage State
1 = Slight Damage | 2 = Moderate Damage
3 = Extensive Damage | 4 = Complete Damage

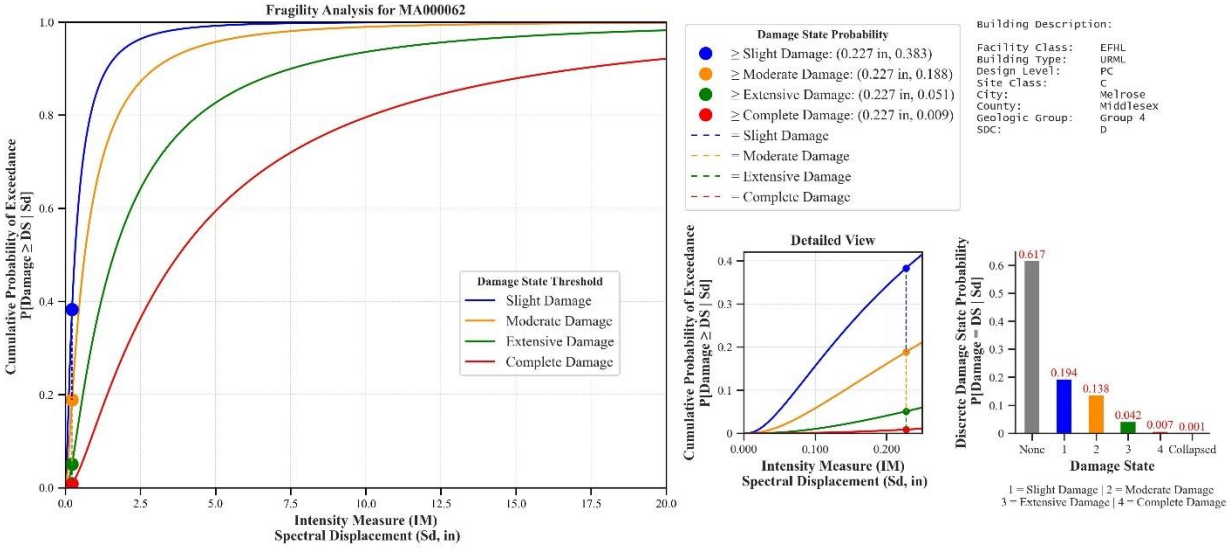
Fragility Analysis for MA000062
Cumulative Probability of Exceedance P[Damage ≥ DS | Sd]
Intensity Measure (IM) Spectral Displacement (Sd, in)
Damage State Threshold
Slight Damage
Moderate Damage
Extensive Damage
Complete Damage
Damage State Probability
≥ Slight Damage: (0.227 in, 0.383)
≥ Moderate Damage: (0.227 in, 0.188)
≥ Extensive Damage: (0.227 in, 0.051)
≥ Complete Damage: (0.227 in, 0.009)
Building Description:
Facility Class: EFHL
Building Type: URML
Design Level: PC
Site Class: C
City: Melrose
County: Middlesex
Geologic Group: Group 4
SDC: D
Detailed View
Discrete Damage State Probability P[Damage = DS | Sd]
0.617
0.194
0.138
0.042
0.007
0.001
None
Collapsed
Damage State
1 = Slight Damage | 2 = Moderate Damage
3 = Extensive Damage | 4 = Complete Damage

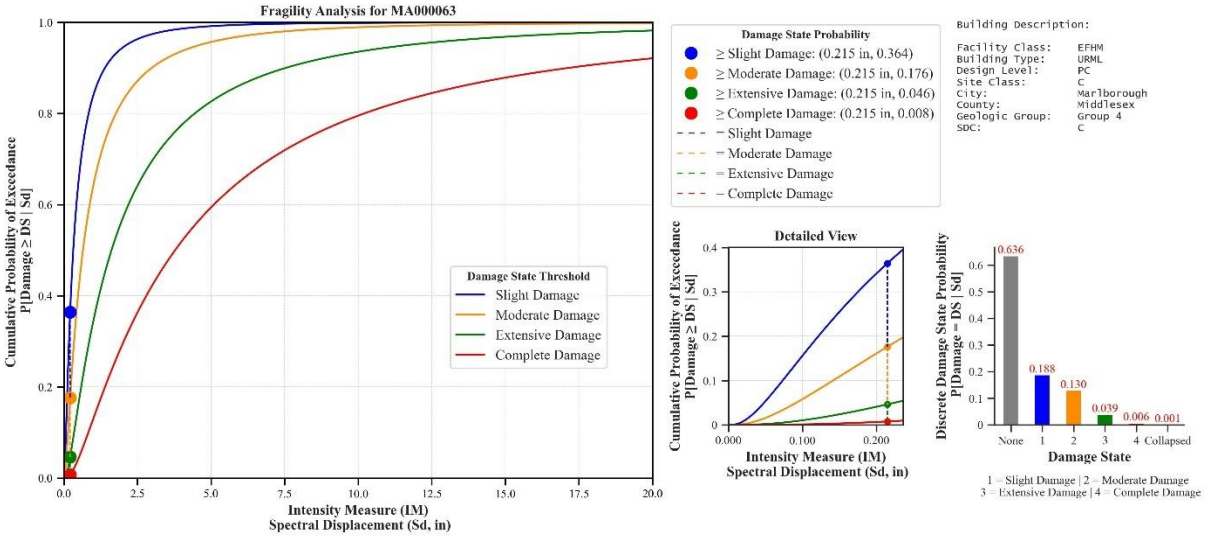
Fragility Analysis for MA000063
Cumulative Probability of Exceedance P[Damage ≥ DS | Sd]
Intensity Measure (IM) Spectral Displacement (Sd, in)
Damage State Threshold
Slight Damage
Moderate Damage
Extensive Damage
Complete Damage
Damage State Probability
≥ Slight Damage: (0.215 in, 0.364)
≥ Moderate Damage: (0.215 in, 0.176)
≥ Extensive Damage: (0.215 in, 0.046)
≥ Complete Damage: (0.215 in, 0.008)
Building Description:
Facility Class: EFHM
Building Type: URML
Design Level: PC
Site Class: C
City: Marlborough
County: Middlesex
Geologic Group: Group 4
SDC: C
Detailed View
Discrete Damage State Probability P[Damage = DS | Sd]
0.636
0.188
0.130
0.039
0.006
0.001
None
Collapsed
Damage State
1 – Slight Damage | 2 – Moderate Damage
3 – Extensive Damage | 4 – Complete Damage

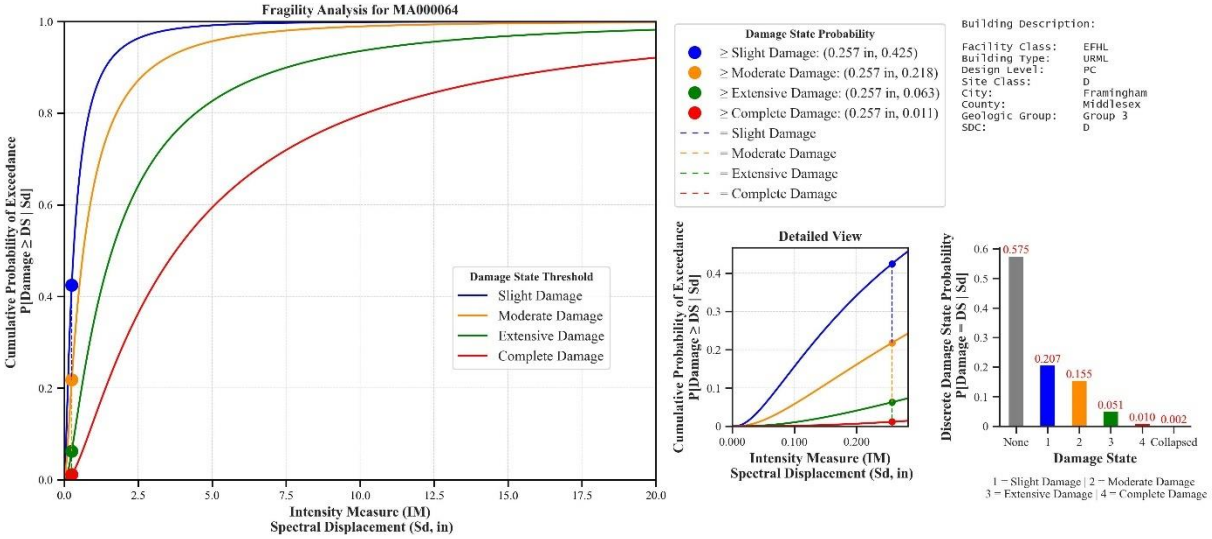
Fragility Analysis for MA000064
Cumulative Probability of Exceedance P[Damage ≥ DS | Sd]
Intensity Measure (IM) Spectral Displacement (Sd, in)
Damage State Threshold
Slight Damage
Moderate Damage
Extensive Damage
Complete Damage
Damage State Probability
≥ Slight Damage: (0.257 in, 0.425)
≥ Moderate Damage: (0.257 in, 0.218)
≥ Extensive Damage: (0.257 in, 0.063)
≥ Complete Damage: (0.257 in, 0.011)
Building Description:
Facility Class: EFHL
Building Type: URML
Design Level: PC
Site Class: D
City: Framingham
County: Middlesex
Geologic Group: Group 3
SDC: D
Detailed View
Discrete Damage State Probability P[Damage = DS | Sd]
0.575
0.207
0.155
0.051
0.010
0.002
None
Collapsed
Damage State
1 – Slight Damage | 2 – Moderate Damage
3 – Extensive Damage | 4 – Complete Damage

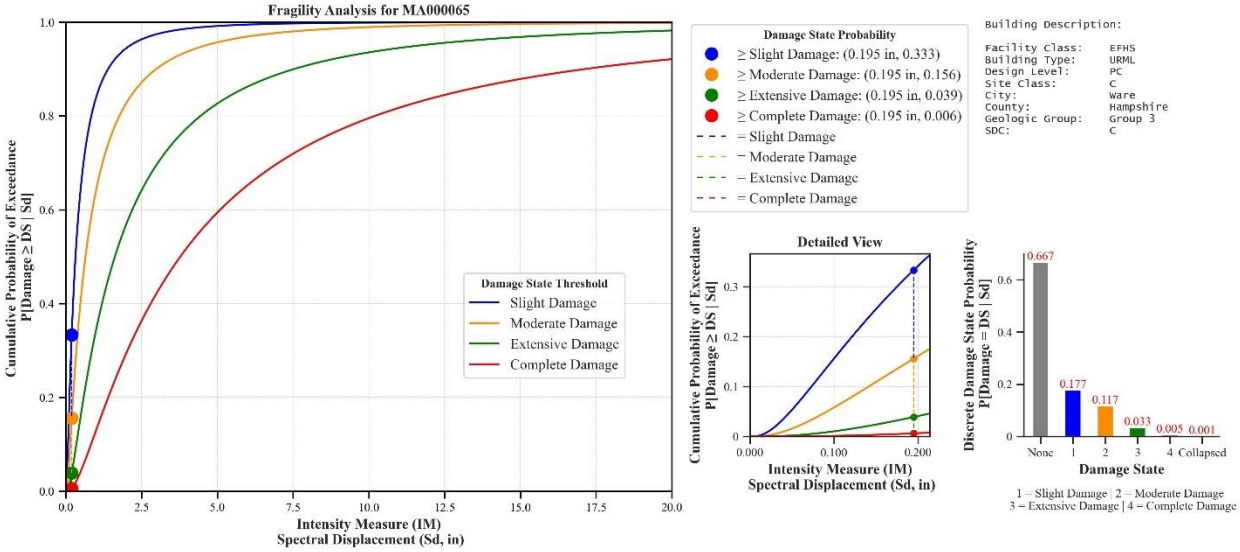
Fragility Analysis for MA000065
Cumulative Probability of Exceedance P[Damage ≥ DS | Sd]
Intensity Measure (IM) Spectral Displacement (Sd, in)
Damage State Threshold
Slight Damage
Moderate Damage
Extensive Damage
Complete Damage
Damage State Probability
≥ Slight Damage: (0.195 in, 0.333)
≥ Moderate Damage: (0.195 in, 0.156)
≥ Extensive Damage: (0.195 in, 0.039)
≥ Complete Damage: (0.195 in, 0.006)
Building Description:
Facility Class: EFHS
Building Type: URML
Design Level: PC
Site Class: C
City: Ware
County: Hampshire
Geologic Group: Group 3
SDC: C
Detailed View
Discrete Damage State Probability P[Damage = DS | Sd]
0.667
0.177
0.117
0.033
0.005
0.001
None
Collapsed
Damage State
1 – Slight Damage | 2 – Moderate Damage
3 – Extensive Damage | 4 – Complete Damage

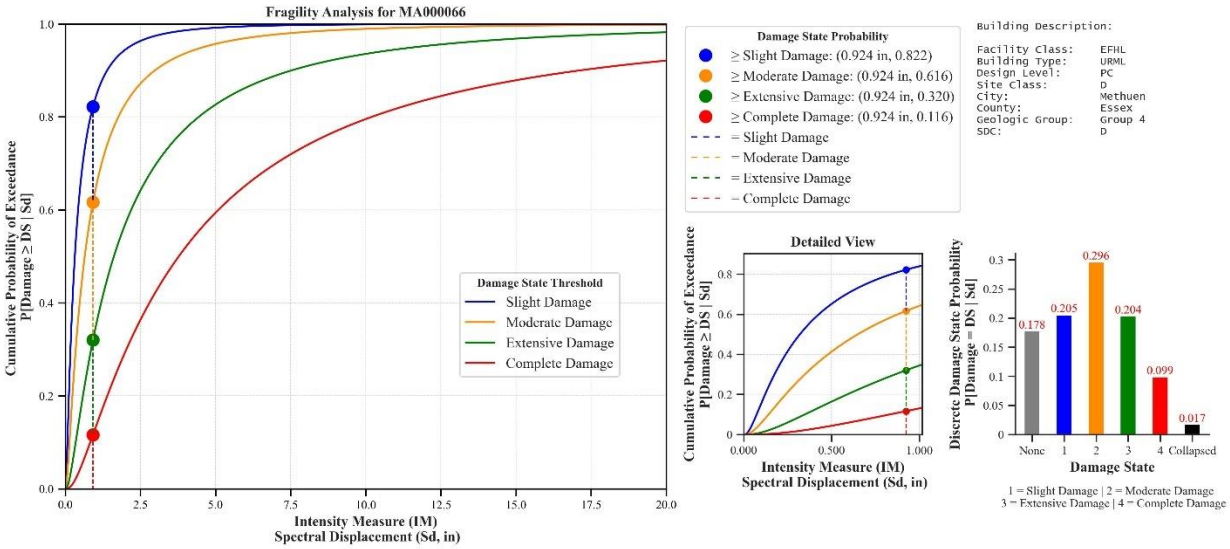
Fragility Analysis for MA000066
Cumulative Probability of Exceedance P[Damage ≥ DS | Sd]
Intensity Measure (IM) Spectral Displacement (Sd, in)
Damage State Threshold
Slight Damage
Moderate Damage
Extensive Damage
Complete Damage
Damage State Probability
≥ Slight Damage: (0.924 in, 0.822)
≥ Moderate Damage: (0.924 in, 0.616)
≥ Extensive Damage: (0.924 in, 0.320)
≥ Complete Damage: (0.924 in, 0.116)
Building Description:
Facility Class: EFHL
Building Type: URML
Design Level: PC
Site Class: D
City: Methuen
County: Essex
Geologic Group: Group 4
SDC: D
Detailed View
Discrete Damage State Probability P[Damage = DS | Sd]
0.178
0.205
0.296
0.204
0.099
0.017
None 1 2 3 4 Collapsed
Damage State
1 = Slight Damage | 2 = Moderate Damage
3 = Extensive Damage | 4 = Complete Damage

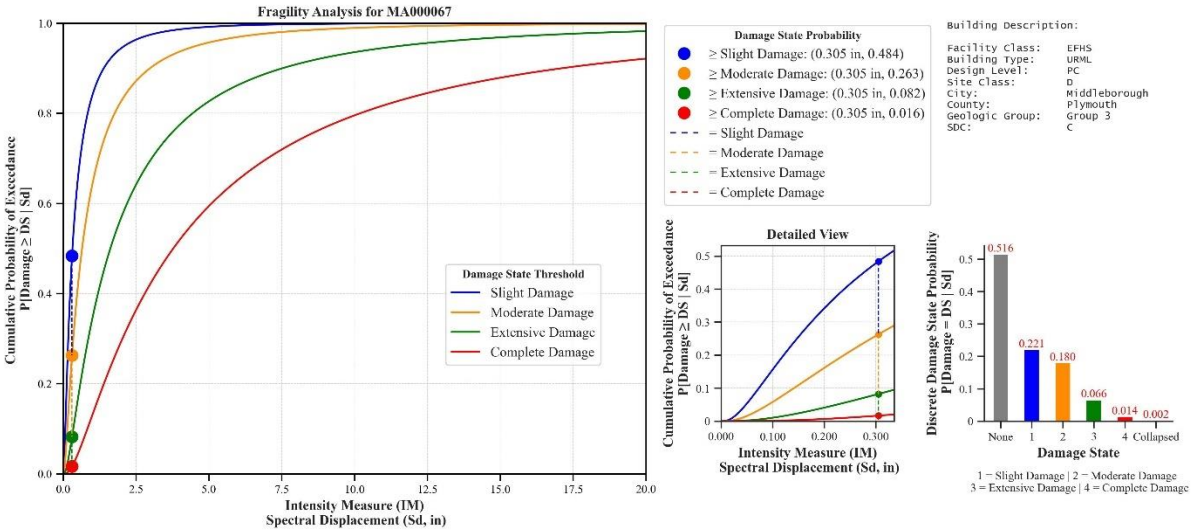
Fragility Analysis for MA000067
Cumulative Probability of Exceedance P[Damage ≥ DS | Sd]
Intensity Measure (IM) Spectral Displacement (Sd, in)
Damage State Threshold
Slight Damage
Moderate Damage
Extensive Damage
Complete Damage
Damage State Probability
≥ Slight Damage: (0.305 in, 0.484)
≥ Moderate Damage: (0.305 in, 0.263)
≥ Extensive Damage: (0.305 in, 0.082)
≥ Complete Damage: (0.305 in, 0.016)
Building Description:
Facility Class: EFHS
Building Type: URML
Design Level: PC
Site Class: D
City: Middleborough
County: Plymouth
Geologic Group: Group 3
SDC: C
Detailed View
Discrete Damage State Probability P[Damage = DS | Sd]
0.516
0.221
0.180
0.066
0.014
0.002
None 1 2 3 4 Collapsed
Damage State
1 = Slight Damage | 2 = Moderate Damage
3 = Extensive Damage | 4 = Complete Damage

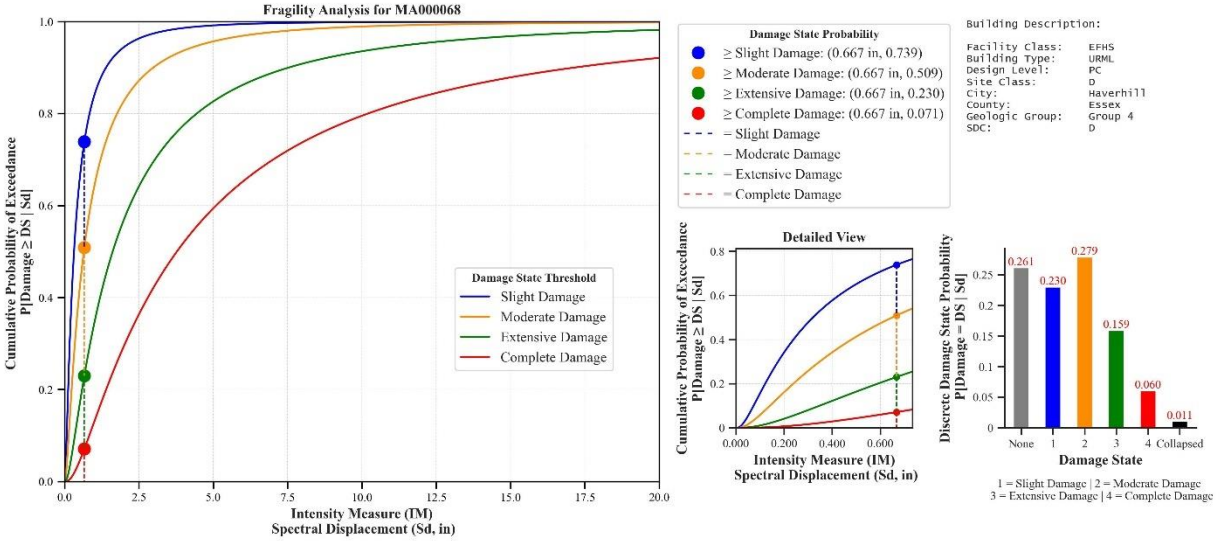
Fragility Analysis for MA000068
Cumulative Probability of Exceedance P[Damage ≥ DS | Sd]
Intensity Measure (IM) Spectral Displacement (Sd, in)
Damage State Threshold
Slight Damage
Moderate Damage
Extensive Damage
Complete Damage
Damage State Probability
≥ Slight Damage: (0.667 in, 0.739)
≥ Moderate Damage: (0.667 in, 0.509)
≥ Extensive Damage: (0.667 in, 0.230)
≥ Complete Damage: (0.667 in, 0.071)
Building Description:
Facility Class: EFHS
Building Type: URML
Design Level: PC
Site Class: D
City: Haverhill
County: Essex
Geologic Group: Group 4
SDC: D
Detailed View
Discrete Damage State Probability P[Damage = DS | Sd]
0.261
0.230
0.279
0.159
0.060
0.011
None 1 2 3 4 Collapsed
Damage State
1 = Slight Damage | 2 = Moderate Damage
3 = Extensive Damage | 4 = Complete Damage

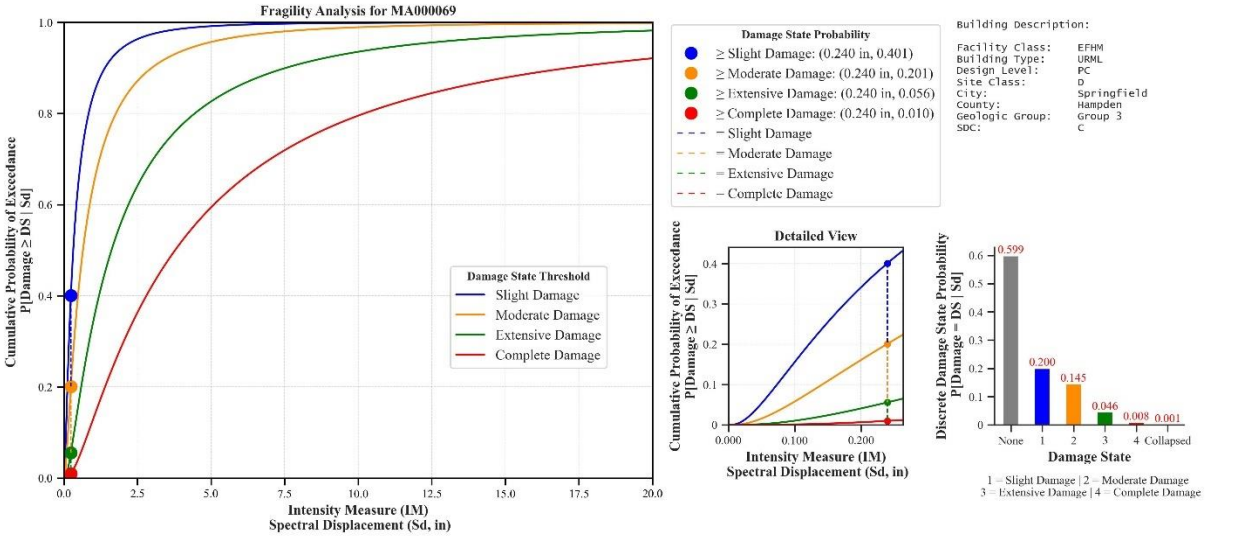
Fragility Analysis for MA000069
Cumulative Probability of Exceedance P[Damage ≥ DS | Sd]
Intensity Measure (IM) Spectral Displacement (Sd, in)
Damage State Threshold
Slight Damage
Moderate Damage
Extensive Damage
Complete Damage
Damage State Probability
≥ Slight Damage: (0.240 in, 0.401)
≥ Moderate Damage: (0.240 in, 0.201)
≥ Extensive Damage: (0.240 in, 0.056)
≥ Complete Damage: (0.240 in, 0.010)
Building Description:
Facility Class: EFHM
Building Type: URML
Design Level: PC
Site Class: D
City: Springfield
County: Hampden
Geologic Group: Group 3
SDC: C
Detailed View
Discrete Damage State Probability P[Damage = DS | Sd]
0.599
0.200
0.145
0.046
0.008
0.001
None 1 2 3 4 Collapsed
Damage State
1 = Slight Damage | 2 = Moderate Damage
3 = Extensive Damage | 4 = Complete Damage

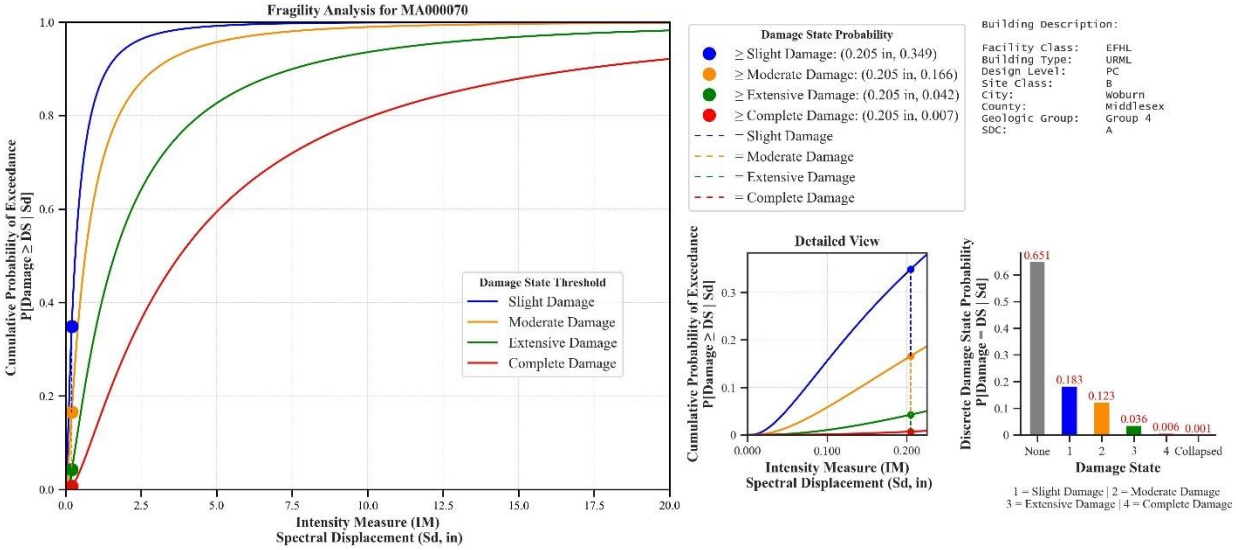
Fragility Analysis for MA000070
Cumulative Probability of Exceedance P[Damage ≥ DS | Sd]
Intensity Measure (IM) Spectral Displacement (Sd, in)
Damage State Threshold
Slight Damage
Moderate Damage
Extensive Damage
Complete Damage
Damage State Probability
≥ Slight Damage: (0.205 in, 0.349)
≥ Moderate Damage: (0.205 in, 0.166)
≥ Extensive Damage: (0.205 in, 0.042)
≥ Complete Damage: (0.205 in, 0.007)
Building Description:
Facility Class: EFHL
Building Type: URML
Design Level: PC
Site Class: B
City: Woburn
County: Middlesex
Geologic Group: Group 4
SDC: A
Detailed View
Discrete Damage State Probability P[Damage = DS | Sd]
0.651
0.183
0.123
0.036
0.006
0.001
None 1 2 3 4 Collapsed
Damage State
1 = Slight Damage | 2 = Moderate Damage
3 = Extensive Damage | 4 = Complete Damage

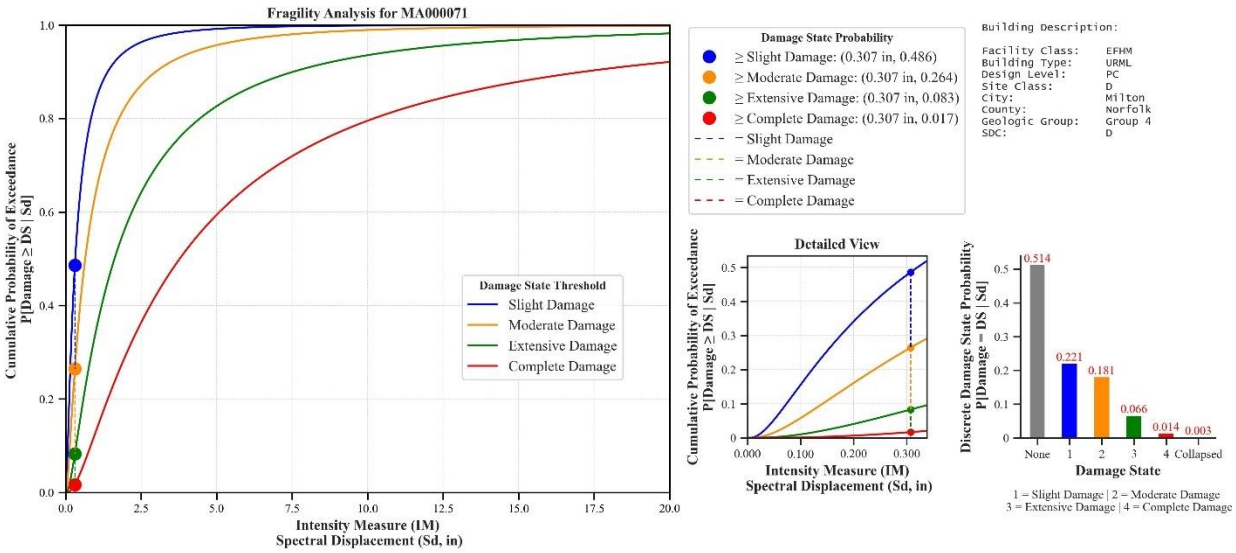
Fragility Analysis for MA000071
Cumulative Probability of Exceedance P[Damage ≥ DS | Sd]
Intensity Measure (IM) Spectral Displacement (Sd, in)
Damage State Threshold
Slight Damage
Moderate Damage
Extensive Damage
Complete Damage
Damage State Probability
≥ Slight Damage: (0.307 in, 0.486)
≥ Moderate Damage: (0.307 in, 0.264)
≥ Extensive Damage: (0.307 in, 0.083)
≥ Complete Damage: (0.307 in, 0.017)
Building Description:
Facility Class: EFHM
Building Type: URML
Design Level: PC
Site Class: D
City: Milton
County: Norfolk
Geologic Group: Group 4
SDC: D
Detailed View
Discrete Damage State Probability P[Damage = DS | Sd]
0.514
0.221
0.181
0.066
0.014
0.003
None 1 2 3 4 Collapsed
Damage State
1 = Slight Damage | 2 = Moderate Damage
3 = Extensive Damage | 4 = Complete Damage

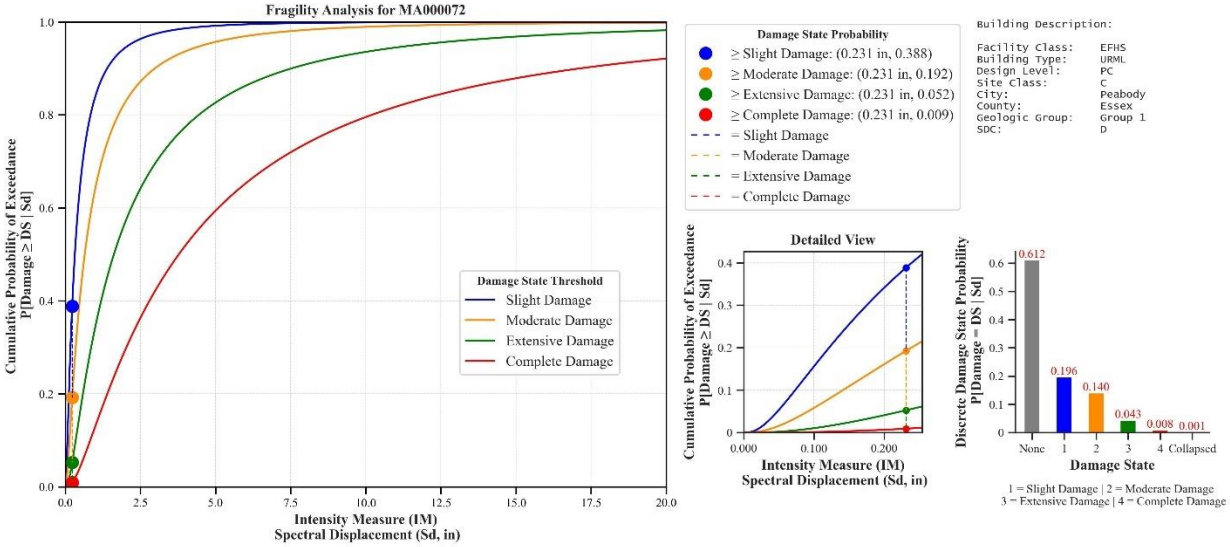
Fragility Analysis for MA000072
Cumulative Probability of Exceedance
P[Damage ≥ DS | Sd]
Intensity Measure (IM)
Spectral Displacement (Sd, in)
Damage State Threshold
Slight Damage
Moderate Damage
Extensive Damage
Complete Damage
Damage State Probability
≥ Slight Damage: (0.231 in, 0.388)
≥ Moderate Damage: (0.231 in, 0.192)
≥ Extensive Damage: (0.231 in, 0.052)
≥ Complete Damage: (0.231 in, 0.009)
Building Description:
Facility Class: EFHS
Building Type: URML
Design Level: PC
Site Class: C
City: Peabody
County: Essex
Geologic Group: Group 1
SDC: D
Detailed View
Discrete Damage State Probability
P[Damage = DS | Sd]
0.612
0.196
0.140
0.043
0.008
0.001
None
Collapsed
Damage State
1 = Slight Damage | 2 = Moderate Damage
3 = Extensive Damage | 4 = Complete Damage

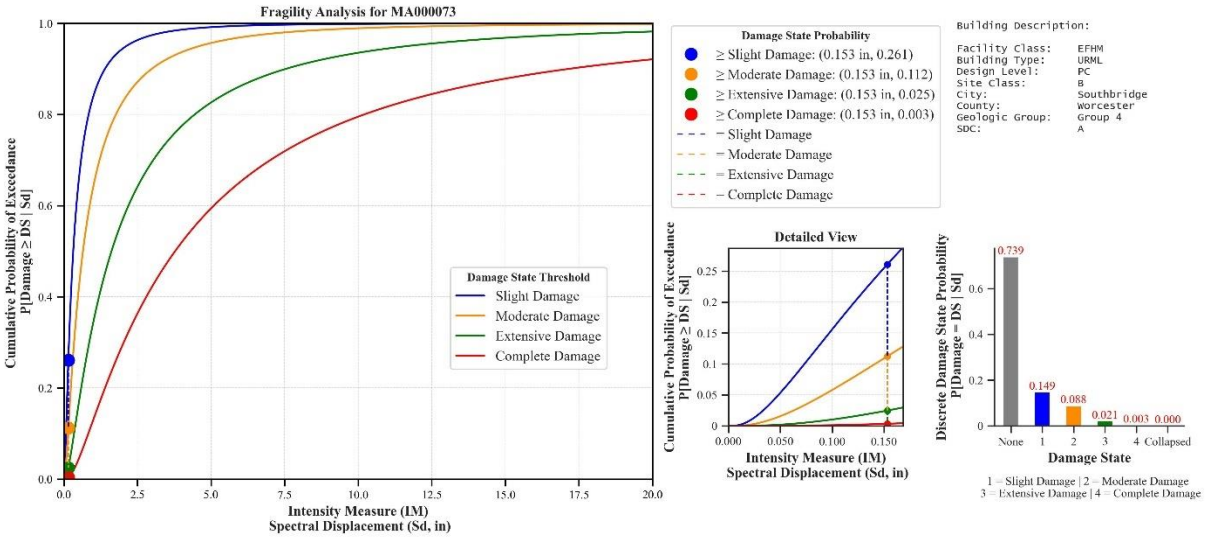
Fragility Analysis for MA000073
Cumulative Probability of Exceedance
P[Damage ≥ DS | Sd]
Intensity Measure (IM)
Spectral Displacement (Sd, in)
Damage State Threshold
Slight Damage
Moderate Damage
Extensive Damage
Complete Damage
Damage State Probability
≥ Slight Damage: (0.153 in, 0.261)
≥ Moderate Damage: (0.153 in, 0.112)
≥ Extensive Damage: (0.153 in, 0.025)
≥ Complete Damage: (0.153 in, 0.003)
Building Description:
Facility Class: EFHM
Building Type: URML
Design Level: PC
Site Class: B
City: Southbridge
County: Worcester
Geologic Group: Group 4
SDC: A
Detailed View
Discrete Damage State Probability
P[Damage = DS | Sd]
0.739
0.149
0.088
0.021
0.003
0.000
None
Collapsed
Damage State
1 = Slight Damage | 2 = Moderate Damage
3 = Extensive Damage | 4 = Complete Damage

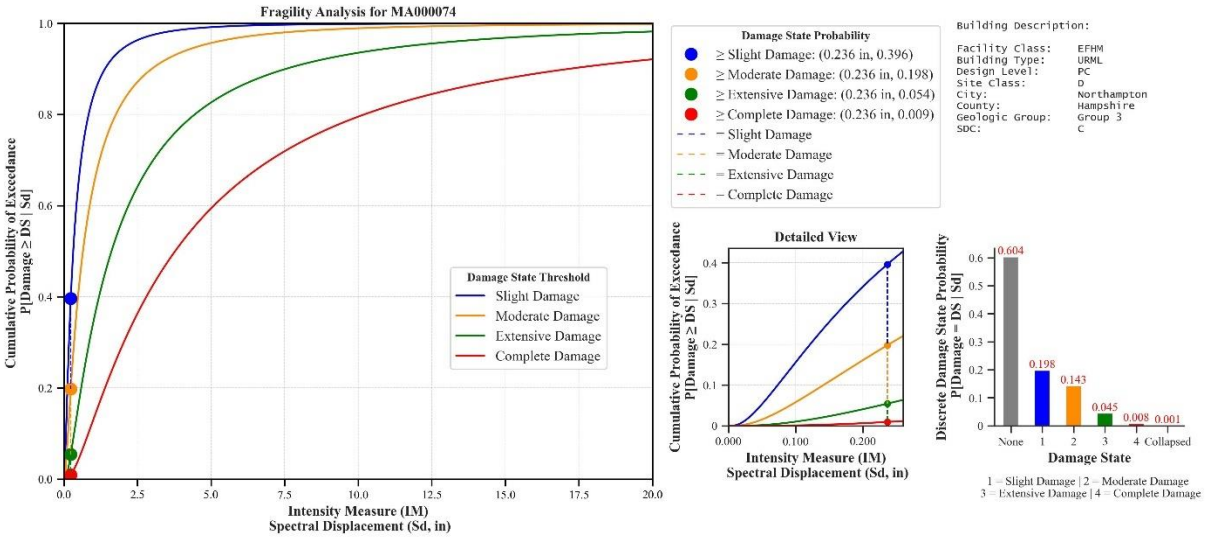
Fragility Analysis for MA000074
Cumulative Probability of Exceedance
P[Damage ≥ DS | Sd]
Intensity Measure (IM)
Spectral Displacement (Sd, in)
Damage State Threshold
Slight Damage
Moderate Damage
Extensive Damage
Complete Damage
Damage State Probability
≥ Slight Damage: (0.236 in, 0.396)
≥ Moderate Damage: (0.236 in, 0.198)
≥ Extensive Damage: (0.236 in, 0.054)
≥ Complete Damage: (0.236 in, 0.009)
Building Description:
Facility Class: EFHM
Building Type: URML
Design Level: PC
Site Class: D
City: Northampton
County: Hampshire
Geologic Group: Group 3
SDC: C
Detailed View
Discrete Damage State Probability
P[Damage = DS | Sd]
0.604
0.198
0.143
0.045
0.008
0.001
None
Collapsed
Damage State
1 = Slight Damage | 2 = Moderate Damage
3 = Extensive Damage | 4 = Complete Damage

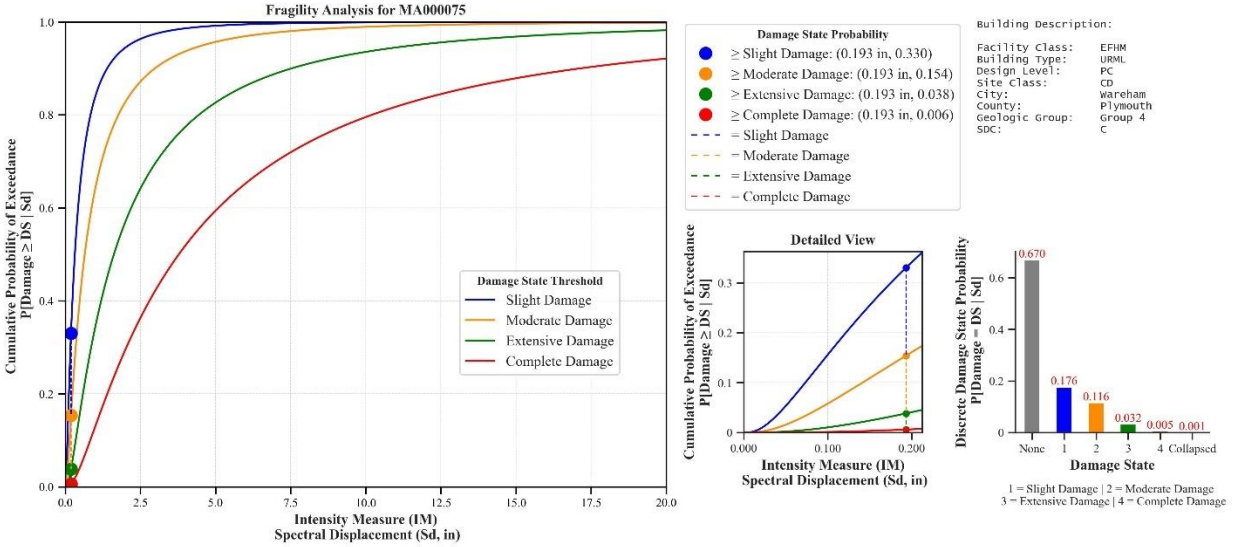
Fragility Analysis for MA000075
Cumulative Probability of Exceedance P[Damage ≥ DS | Sd]
Intensity Measure (IM) Spectral Displacement (Sd, in)
Damage State Threshold
Slight Damage
Moderate Damage
Extensive Damage
Complete Damage
Damage State Probability
≥ Slight Damage: (0.193 in, 0.330)
≥ Moderate Damage: (0.193 in, 0.154)
≥ Extensive Damage: (0.193 in, 0.038)
≥ Complete Damage: (0.193 in, 0.006)
= Slight Damage
= Moderate Damage
= Extensive Damage
= Complete Damage
Detailed View
Building Description:
Facility Class: EFHM
Building Type: URML
Design Level: PC
Site Class: CD
City: Wareham
County: Plymouth
Geologic Group: Group 4
SDC: C
Discrete Damage State Probability P[Damage = DS | Sd]
0.670
0.176
0.116
0.032
0.005
0.001
None
1
2
3
4 Collapsed
Damage State
1 = Slight Damage | 2 = Moderate Damage
3 = Extensive Damage | 4 = Complete Damage

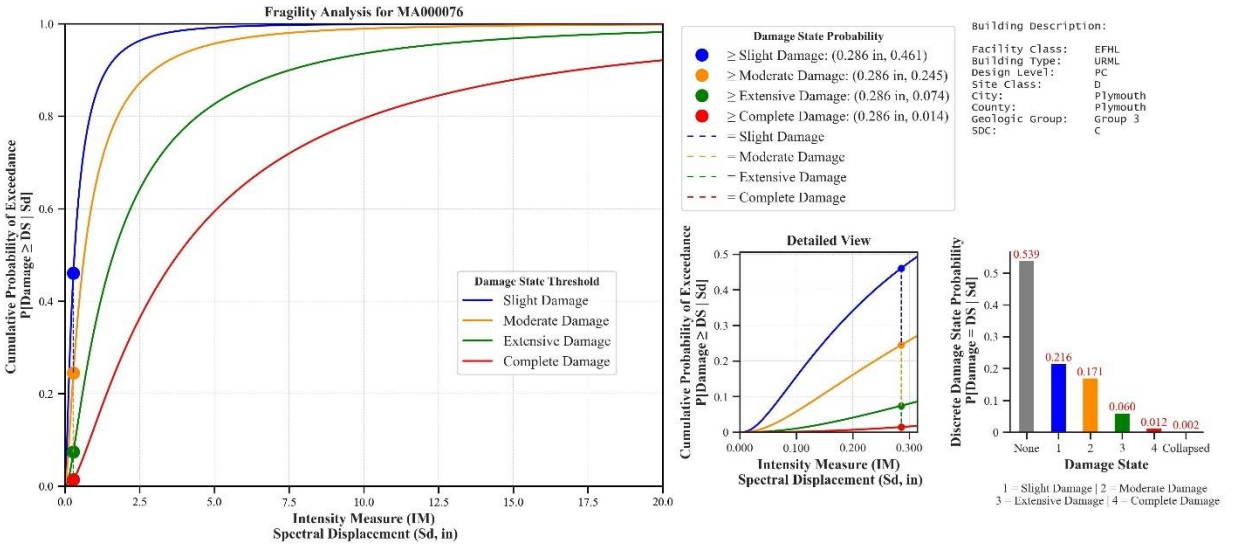
Fragility Analysis for MA000076
Cumulative Probability of Exceedance P[Damage ≥ DS | Sd]
Intensity Measure (IM) Spectral Displacement (Sd, in)
Damage State Threshold
Slight Damage
Moderate Damage
Extensive Damage
Complete Damage
Damage State Probability
≥ Slight Damage: (0.286 in, 0.461)
≥ Moderate Damage: (0.286 in, 0.245)
≥ Extensive Damage: (0.286 in, 0.074)
≥ Complete Damage: (0.286 in, 0.014)
= Slight Damage
= Moderate Damage
= Extensive Damage
= Complete Damage
Detailed View
Building Description:
Facility Class: EFHL
Building Type: URML
Design Level: PC
Site Class: D
City: Plymouth
County: Plymouth
Geologic Group: Group 3
SDC: C
Discrete Damage State Probability P[Damage = DS | Sd]
0.539
0.216
0.171
0.060
0.012
0.002
None
1
2
3
4 Collapsed
Damage State
1 = Slight Damage | 2 = Moderate Damage
3 = Extensive Damage | 4 = Complete Damage

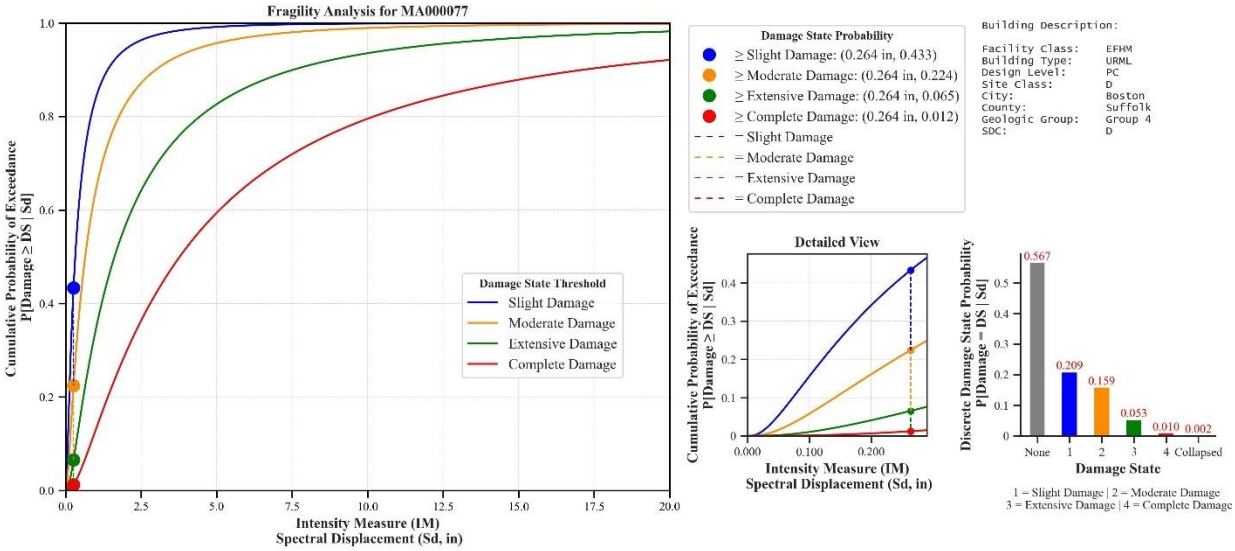
Fragility Analysis for MA000077
Cumulative Probability of Exceedance P[Damage ≥ DS | Sd]
Intensity Measure (IM) Spectral Displacement (Sd, in)
Damage State Threshold
Slight Damage
Moderate Damage
Extensive Damage
Complete Damage
Damage State Probability
≥ Slight Damage: (0.264 in, 0.433)
≥ Moderate Damage: (0.264 in, 0.224)
≥ Extensive Damage: (0.264 in, 0.065)
≥ Complete Damage: (0.264 in, 0.012)
= Slight Damage
= Moderate Damage
= Extensive Damage
= Complete Damage
Detailed View
Building Description:
Facility Class: EFHM
Building Type: URML
Design Level: PC
Site Class: D
City: Boston
County: Suffolk
Geologic Group: Group 4
SDC: D
Discrete Damage State Probability P[Damage = DS | Sd]
0.567
0.209
0.159
0.053
0.010
0.002
None
1
2
3
4 Collapsed
Damage State
1 = Slight Damage | 2 = Moderate Damage
3 = Extensive Damage | 4 = Complete Damage

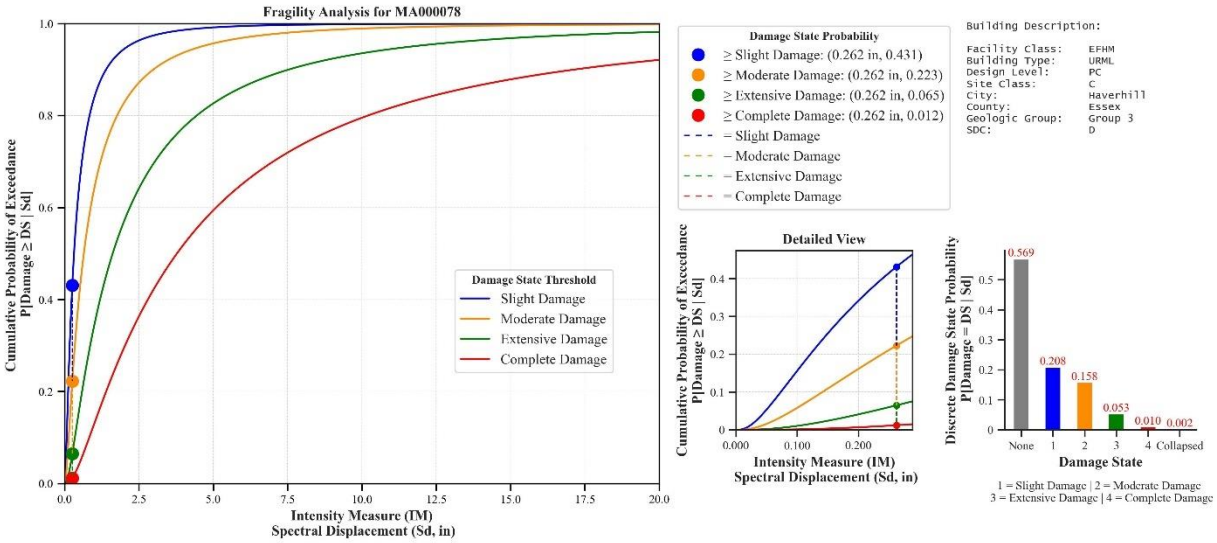
Fragility Analysis for MA000078
Cumulative Probability of Exceedance P[Damage ≥ DS | Sd]
Intensity Measure (IM) Spectral Displacement (Sd, in)
Damage State Threshold
Slight Damage
Moderate Damage
Extensive Damage
Complete Damage
Damage State Probability
≥ Slight Damage: (0.262 in, 0.431)
≥ Moderate Damage: (0.262 in, 0.223)
≥ Extensive Damage: (0.262 in, 0.065)
≥ Complete Damage: (0.262 in, 0.012)
= Slight Damage
= Moderate Damage
= Extensive Damage
= Complete Damage
Detailed View
Building Description:
Facility Class: EFHM
Building Type: URML
Design Level: PC
Site Class: C
City: Haverhill
County: Essex
Geologic Group: Group 3
SDC: D
Discrete Damage State Probability P[Damage = DS | Sd]
0.569
0.208
0.158
0.053
0.010
0.002
None
Collapsed
Damage State
1 = Slight Damage | 2 = Moderate Damage
3 = Extensive Damage | 4 = Complete Damage

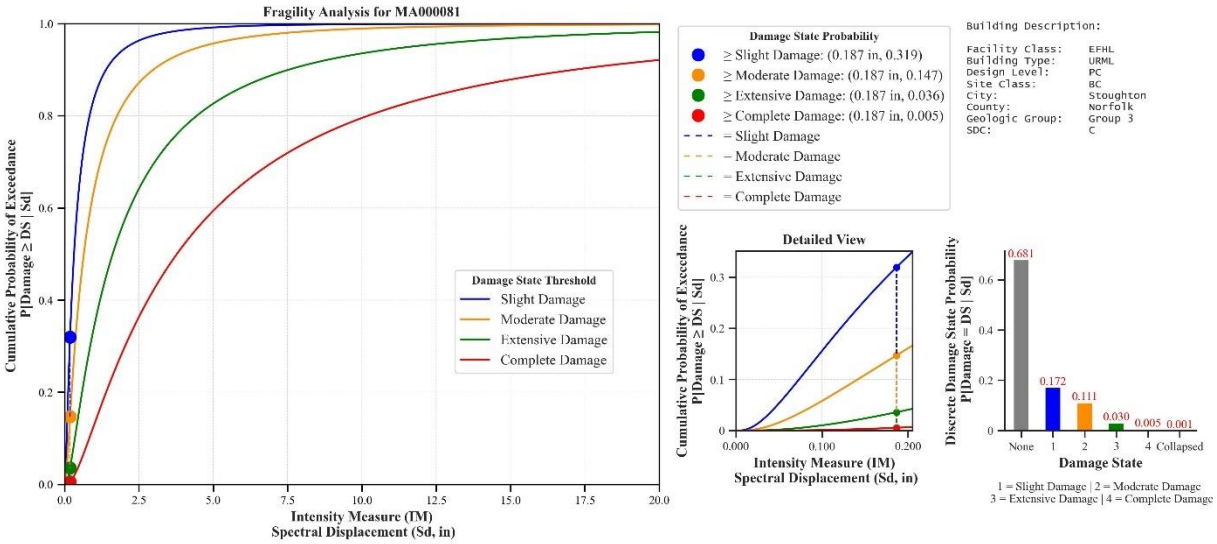
Fragility Analysis for MA000081
Cumulative Probability of Exceedance P[Damage ≥ DS | Sd]
Intensity Measure (IM) Spectral Displacement (Sd, in)
Damage State Threshold
Slight Damage
Moderate Damage
Extensive Damage
Complete Damage
Damage State Probability
≥ Slight Damage: (0.187 in, 0.319)
≥ Moderate Damage: (0.187 in, 0.147)
≥ Extensive Damage: (0.187 in, 0.036)
≥ Complete Damage: (0.187 in, 0.005)
= Slight Damage
= Moderate Damage
= Extensive Damage
= Complete Damage
Detailed View
Building Description:
Facility Class: EFHL
Building Type: URML
Design Level: PC
Site Class: BC
City: Stoughton
County: Norfolk
Geologic Group: Group 3
SDC: C
Discrete Damage State Probability P[Damage = DS | Sd]
0.681
0.172
0.111
0.030
0.005
0.001
None
Collapsed
Damage State
1 = Slight Damage | 2 = Moderate Damage
3 = Extensive Damage | 4 = Complete Damage

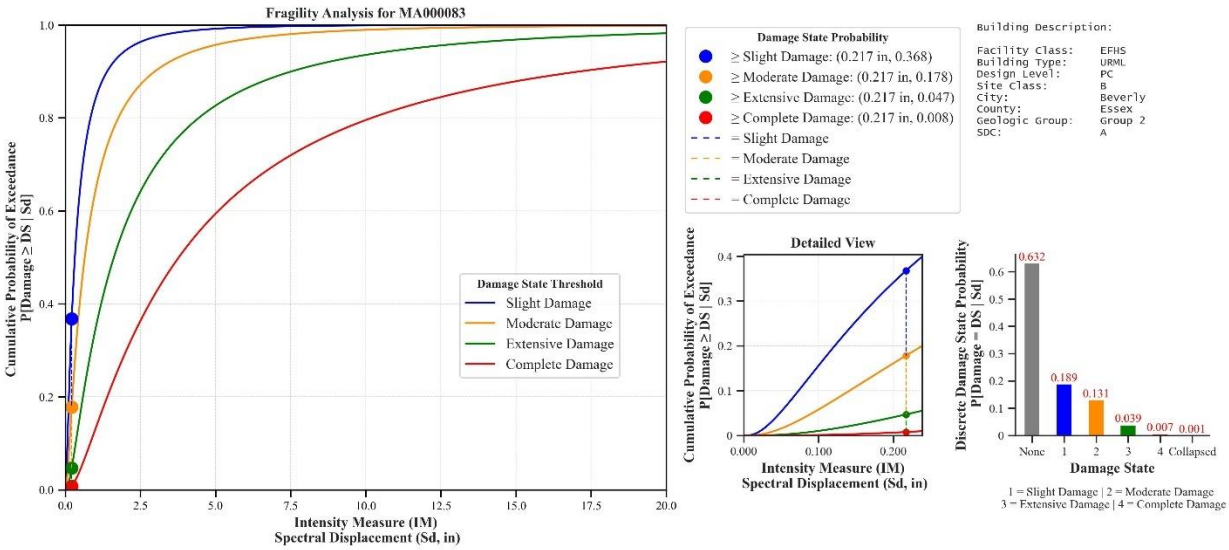
Fragility Analysis for MA000083
Cumulative Probability of Exceedance P[Damage ≥ DS | Sd]
Intensity Measure (IM) Spectral Displacement (Sd, in)
Damage State Threshold
Slight Damage
Moderate Damage
Extensive Damage
Complete Damage
Damage State Probability
≥ Slight Damage: (0.217 in, 0.368)
≥ Moderate Damage: (0.217 in, 0.178)
≥ Extensive Damage: (0.217 in, 0.047)
≥ Complete Damage: (0.217 in, 0.008)
= Slight Damage
= Moderate Damage
= Extensive Damage
= Complete Damage
Detailed View
Building Description:
Facility Class: EFHS
Building Type: URML
Design Level: PC
Site Class: B
City: Beverly
County: Essex
Geologic Group: Group 2
SDC: A
Discrete Damage State Probability P[Damage = DS | Sd]
0.632
0.189
0.131
0.039
0.007
0.001
None
Collapsed
Damage State
1 = Slight Damage | 2 = Moderate Damage
3 = Extensive Damage | 4 = Complete Damage

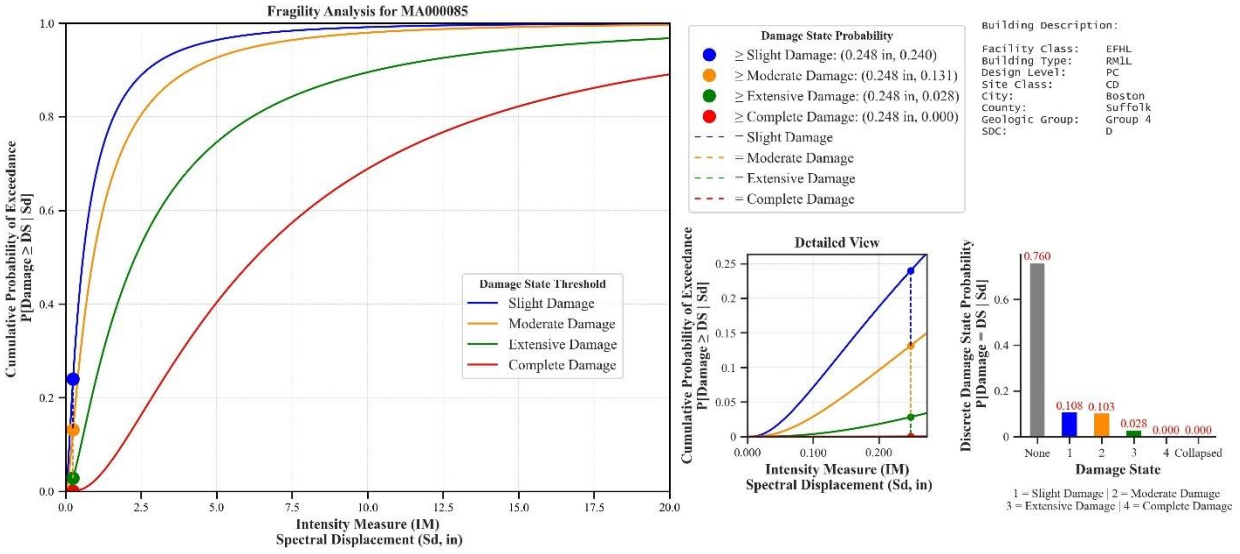
Fragility Analysis for MA000085
Cumulative Probability of Exceedance
P[Damage ≥ DS | Sd]
Intensity Measure (IM)
Spectral Displacement (Sd, in)
Damage State Threshold
Slight Damage
Moderate Damage
Extensive Damage
Complete Damage
Damage State Probability
≥ Slight Damage: (0.248 in, 0.240)
≥ Moderate Damage: (0.248 in, 0.131)
≥ Extensive Damage: (0.248 in, 0.028)
≥ Complete Damage: (0.248 in, 0.000)
= Slight Damage
= Moderate Damage
= Extensive Damage
= Complete Damage
Detailed View
Discrete Damage State Probability
P[Damage = DS | Sd]
0.760
0.108
0.103
0.028
0.000
0.000
None
1
2
3
4
Collapsed
Damage State
1 = Slight Damage | 2 = Moderate Damage
3 = Extensive Damage | 4 = Complete Damage
Building Description:
Facility Class: EFHL
Building Type: RM1L
Design Level: PC
Site Class: CD
City: Boston
County: Suffolk
Geologic Group: Group 4
SDC: D

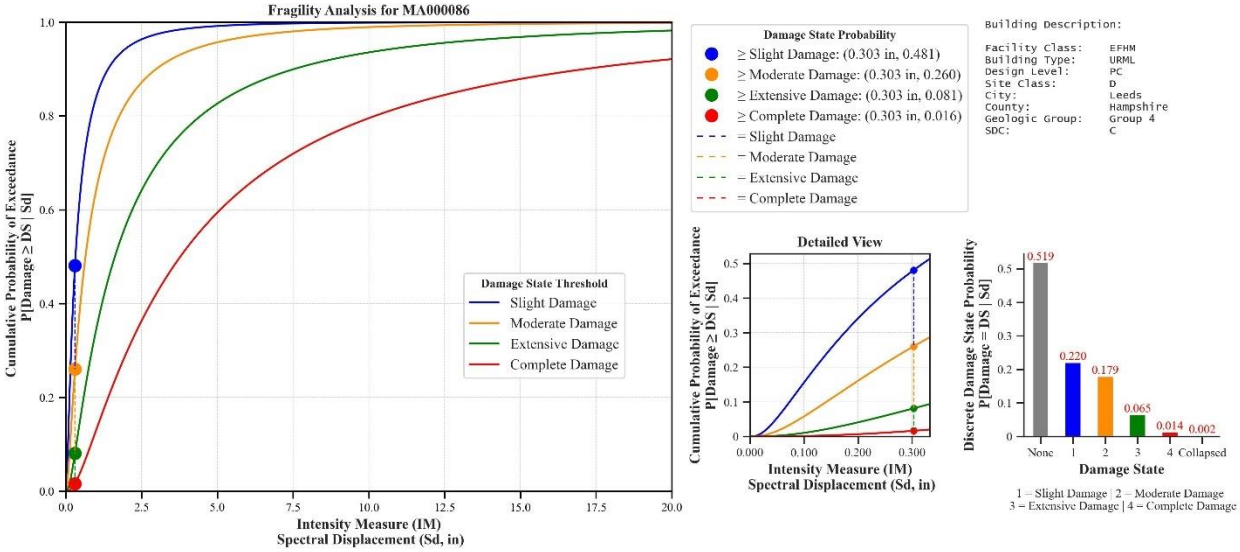
Fragility Analysis for MA000086
Cumulative Probability of Exceedance
P[Damage ≥ DS | Sd]
Intensity Measure (IM)
Spectral Displacement (Sd, in)
Damage State Threshold
Slight Damage
Moderate Damage
Extensive Damage
Complete Damage
Damage State Probability
≥ Slight Damage: (0.303 in, 0.481)
≥ Moderate Damage: (0.303 in, 0.260)
≥ Extensive Damage: (0.303 in, 0.081)
≥ Complete Damage: (0.303 in, 0.016)
= Slight Damage
= Moderate Damage
= Extensive Damage
= Complete Damage
Detailed View
Discrete Damage State Probability
P[Damage = DS | Sd]
0.519
0.220
0.179
0.065
0.014
0.002
None
1
2
3
4
Collapsed
Damage State
1 = Slight Damage | 2 = Moderate Damage
3 = Extensive Damage | 4 = Complete Damage
Building Description:
Facility Class: EFHM
Building Type: URML
Design Level: PC
Site Class: D
City: Leeds
County: Hampshire
Geologic Group: Group 4
SDC: C

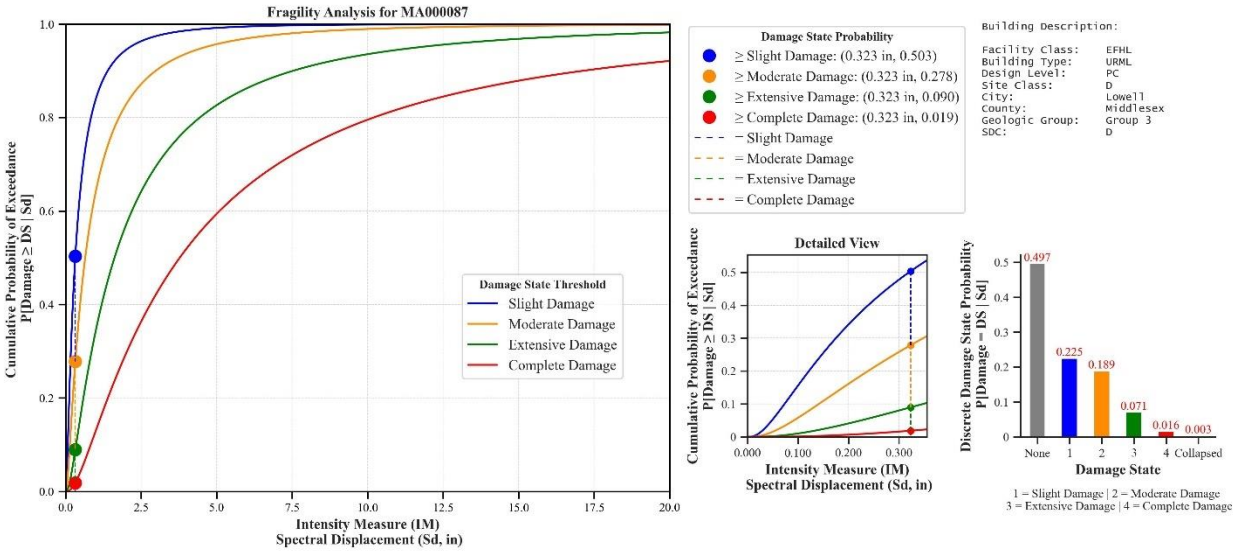
Fragility Analysis for MA000087
Cumulative Probability of Exceedance
P[Damage ≥ DS | Sd]
Intensity Measure (IM)
Spectral Displacement (Sd, in)
Damage State Threshold
Slight Damage
Moderate Damage
Extensive Damage
Complete Damage
Damage State Probability
≥ Slight Damage: (0.323 in, 0.503)
≥ Moderate Damage: (0.323 in, 0.278)
≥ Extensive Damage: (0.323 in, 0.090)
≥ Complete Damage: (0.323 in, 0.019)
= Slight Damage
= Moderate Damage
= Extensive Damage
= Complete Damage
Detailed View
Discrete Damage State Probability
P[Damage = DS | Sd]
0.497
0.225
0.189
0.071
0.016
0.003
None
1
2
3
4
Collapsed
Damage State
1 = Slight Damage | 2 = Moderate Damage
3 = Extensive Damage | 4 = Complete Damage
Building Description:
Facility Class: EFHL
Building Type: URML
Design Level: PC
Site Class: D
City: Lowell
County: Middlesex
Geologic Group: Group 3
SDC: D

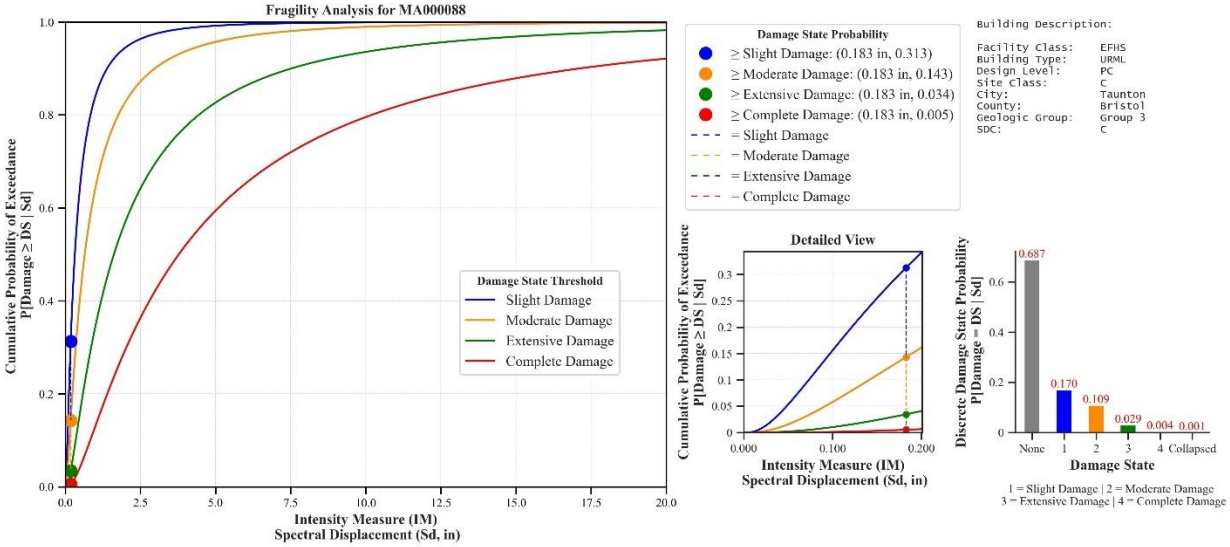
Fragility Analysis for MA000088
Cumulative Probability of Exceedance P[Damage ≥ DS | Sd]
Intensity Measure (IM) Spectral Displacement (Sd, in)
Damage State Threshold
Slight Damage
Moderate Damage
Extensive Damage
Complete Damage
Damage State Probability
≥ Slight Damage: (0.183 in, 0.313)
≥ Moderate Damage: (0.183 in, 0.143)
≥ Extensive Damage: (0.183 in, 0.034)
≥ Complete Damage: (0.183 in, 0.005)
= Slight Damage
= Moderate Damage
= Extensive Damage
= Complete Damage
Building Description:
Facility Class: EFHS
Building Type: URML
Design Level: PC
Site Class: C
City: Taunton
County: Bristol
Geologic Group: Group 3
SDC: C
Detailed View
Discrete Damage State Probability P[Damage = DS | Sd]
0.687
0.170
0.109
0.029
0.004
0.001
None
Collapsed
Damage State
1 = Slight Damage | 2 = Moderate Damage
3 = Extensive Damage | 4 = Complete Damage

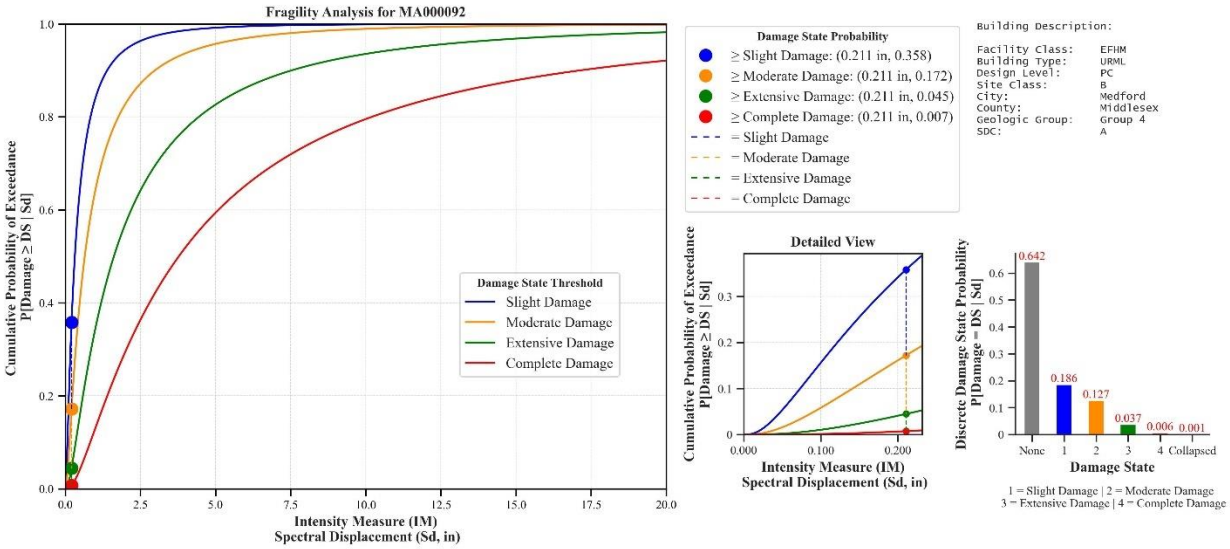
Fragility Analysis for MA000092
Cumulative Probability of Exceedance P[Damage ≥ DS | Sd]
Intensity Measure (IM) Spectral Displacement (Sd, in)
Damage State Threshold
Slight Damage
Moderate Damage
Extensive Damage
Complete Damage
Damage State Probability
≥ Slight Damage: (0.211 in, 0.358)
≥ Moderate Damage: (0.211 in, 0.172)
≥ Extensive Damage: (0.211 in, 0.045)
≥ Complete Damage: (0.211 in, 0.007)
= Slight Damage
= Moderate Damage
= Extensive Damage
= Complete Damage
Building Description:
Facility Class: EFHM
Building Type: URML
Design Level: PC
Site Class: B
City: Medford
County: Middlesex
Geologic Group: Group 4
SDC: A
Detailed View
Discrete Damage State Probability P[Damage = DS | Sd]
0.642
0.186
0.127
0.037
0.006
0.001
None
Collapsed
Damage State
1 = Slight Damage | 2 = Moderate Damage
3 = Extensive Damage | 4 = Complete Damage

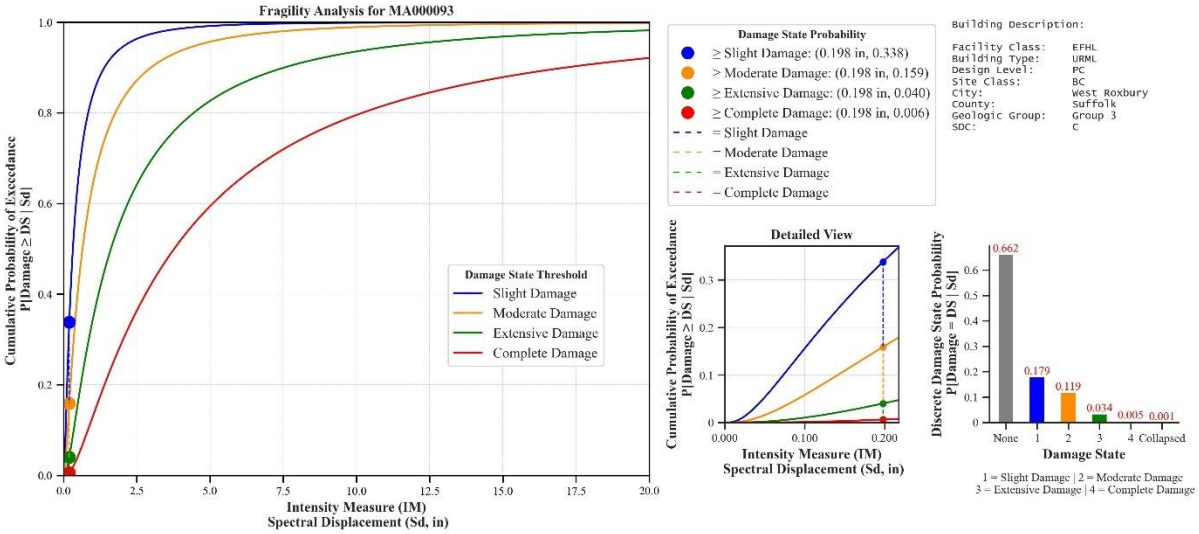
Fragility Analysis for MA000093
Cumulative Probability of Exceedance P[Damage ≥ DS | Sd]
Intensity Measure (IM) Spectral Displacement (Sd, in)
Damage State Threshold
Slight Damage
Moderate Damage
Extensive Damage
Complete Damage
Damage State Probability
≥ Slight Damage: (0.198 in, 0.338)
> Moderate Damage: (0.198 in, 0.159)
≥ Extensive Damage: (0.198 in, 0.040)
≥ Complete Damage: (0.198 in, 0.006)
= Slight Damage
= Moderate Damage
= Extensive Damage
= Complete Damage
Building Description:
Facility Class: EFHL
Building Type: URML
Design Level: PC
Site Class: BC
City: West Roxbury
County: Suffolk
Geologic Group: Group 3
SDC: C
Detailed View
Discrete Damage State Probability P[Damage = DS | Sd]
0.662
0.179
0.119
0.034
0.005
0.001
None
Collapsed
Damage State
1 = Slight Damage | 2 = Moderate Damage
3 = Extensive Damage | 4 = Complete Damage

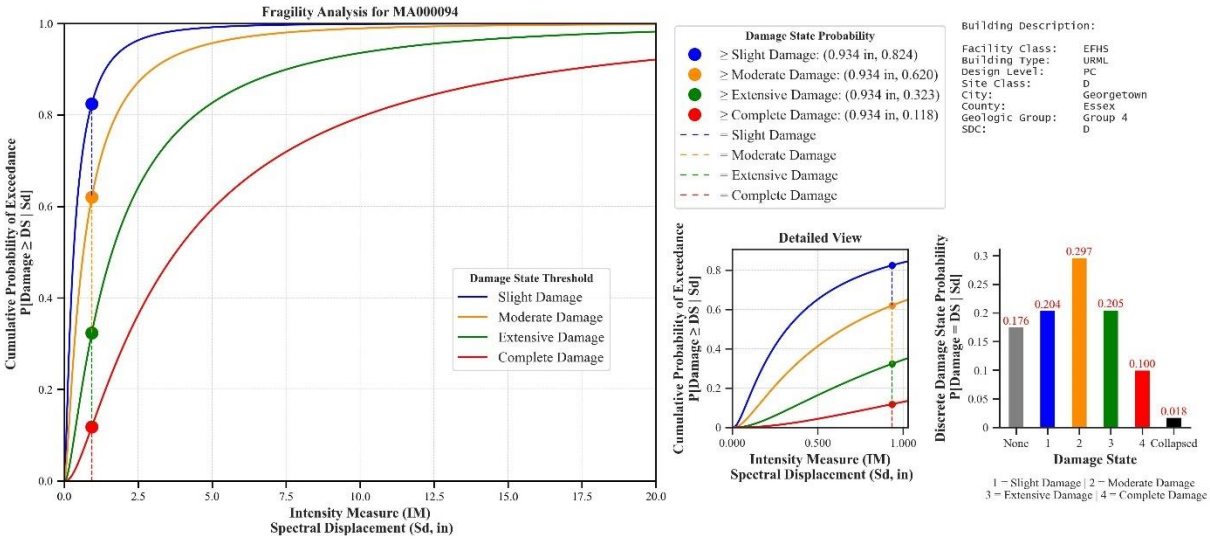
Fragility Analysis for MA000094
Cumulative Probability of Exceedance P[Damage ≥ DS | Sd]
Intensity Measure (IM) Spectral Displacement (Sd, in)
Damage State Threshold
Slight Damage
Moderate Damage
Extensive Damage
Complete Damage
Damage State Probability
≥ Slight Damage: (0.934 in, 0.824)
≥ Moderate Damage: (0.934 in, 0.620)
≥ Extensive Damage: (0.934 in, 0.323)
≥ Complete Damage: (0.934 in, 0.118)
Building Description:
Facility Class: EFHS
Building Type: URML
Design Level: PC
Site Class: D
City: Georgetown
County: Essex
Geologic Group: Group 4
SDC: D
Detailed View
Discrete Damage State Probability P[Damage = DS | Sd]
0.176
0.204
0.297
0.205
0.100
0.018
None 1 2 3 4 Collapsed
Damage State
1 = Slight Damage | 2 = Moderate Damage
3 = Extensive Damage | 4 = Complete Damage

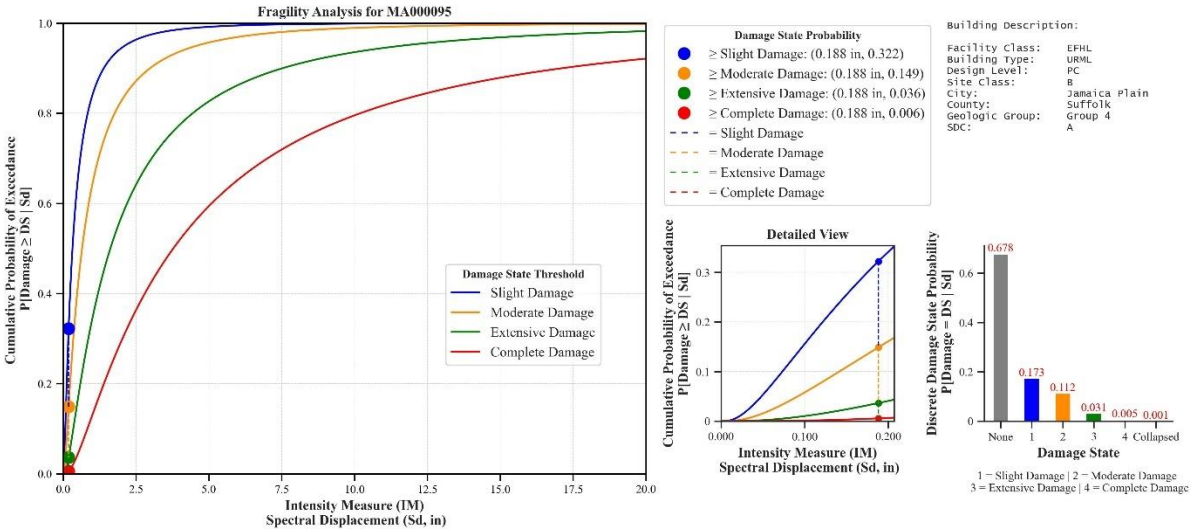
Fragility Analysis for MA000095
Cumulative Probability of Exceedance P[Damage ≥ DS | Sd]
Intensity Measure (IM) Spectral Displacement (Sd, in)
Damage State Threshold
Slight Damage
Moderate Damage
Extensive Damage
Complete Damage
Damage State Probability
≥ Slight Damage: (0.188 in, 0.322)
≥ Moderate Damage: (0.188 in, 0.149)
≥ Extensive Damage: (0.188 in, 0.036)
≥ Complete Damage: (0.188 in, 0.006)
Building Description:
Facility Class: EFHL
Building Type: URML
Design Level: PC
Site Class: B
City: Jamaica Plain
County: Suffolk
Geologic Group: Group 4
SDC: A
Detailed View
Discrete Damage State Probability P[Damage = DS | Sd]
0.678
0.173
0.112
0.031
0.005
0.001
None 1 2 3 4 Collapsed
Damage State
1 = Slight Damage | 2 = Moderate Damage
3 = Extensive Damage | 4 = Complete Damage

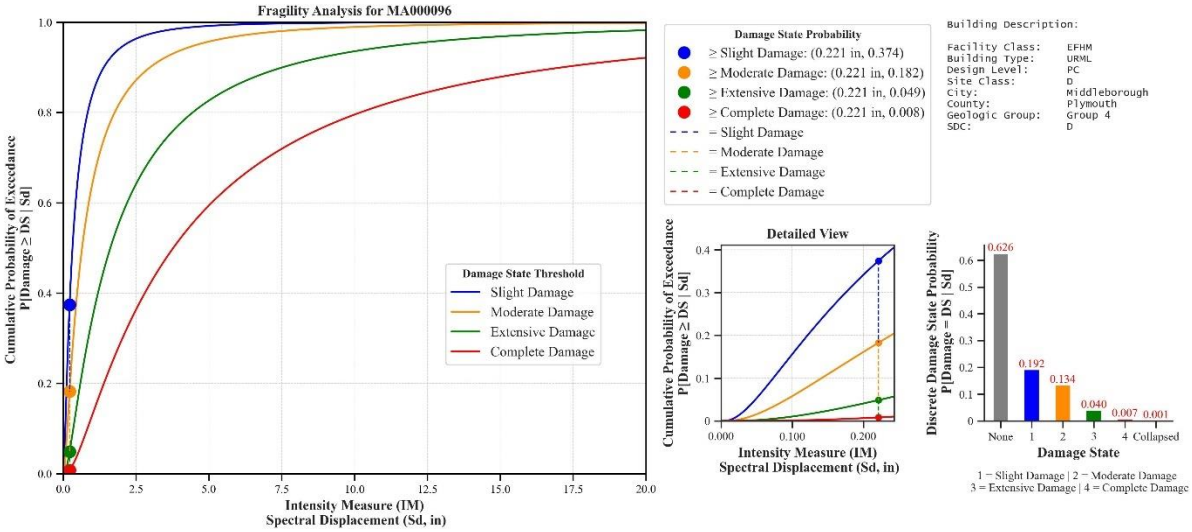
Fragility Analysis for MA000096
Cumulative Probability of Exceedance P[Damage ≥ DS | Sd]
Intensity Measure (IM) Spectral Displacement (Sd, in)
Damage State Threshold
Slight Damage
Moderate Damage
Extensive Damage
Complete Damage
Damage State Probability
≥ Slight Damage: (0.221 in, 0.374)
≥ Moderate Damage: (0.221 in, 0.182)
≥ Extensive Damage: (0.221 in, 0.049)
≥ Complete Damage: (0.221 in, 0.008)
Building Description:
Facility Class: EFHM
Building Type: URML
Design Level: PC
Site Class: D
City: Middleborough
County: Plymouth
Geologic Group: Group 4
SDC: D
Detailed View
Discrete Damage State Probability P[Damage = DS | Sd]
0.626
0.192
0.134
0.040
0.007
0.001
None 1 2 3 4 Collapsed
Damage State
1 = Slight Damage | 2 = Moderate Damage
3 = Extensive Damage | 4 = Complete Damage

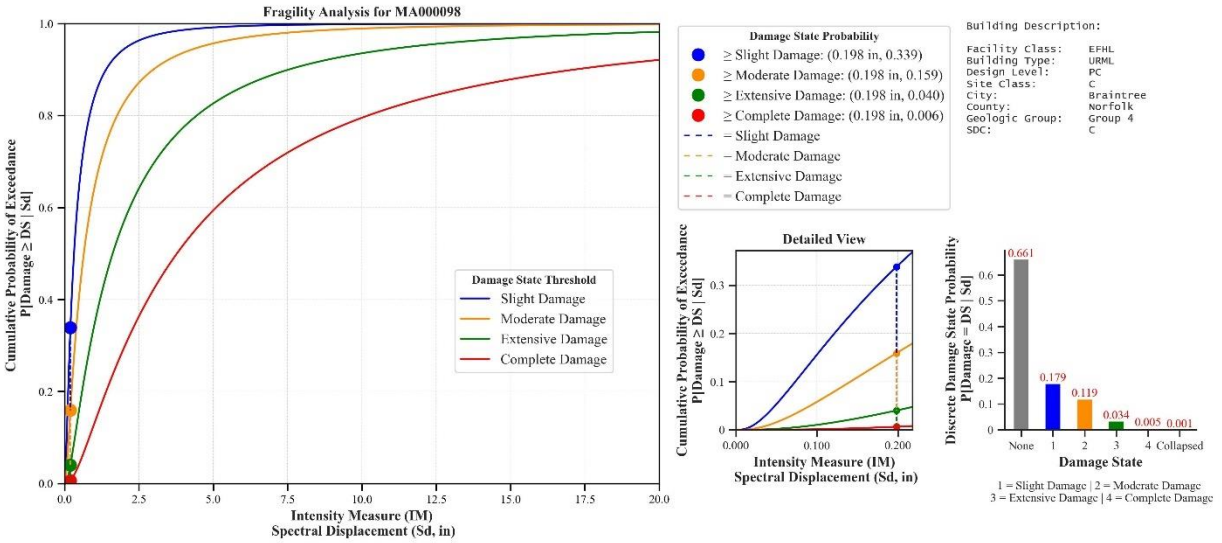
Fragility Analysis for MA000098
Cumulative Probability of Exceedance P[Damage ≥ DS | Sd]
Intensity Measure (IM) Spectral Displacement (Sd, in)
Damage State Threshold
Slight Damage
Moderate Damage
Extensive Damage
Complete Damage
Damage State Probability
≥ Slight Damage: (0.198 in, 0.339)
≥ Moderate Damage: (0.198 in, 0.159)
≥ Extensive Damage: (0.198 in, 0.040)
≥ Complete Damage: (0.198 in, 0.006)
Building Description:
Facility Class: EFHL
Building Type: URML
Design Level: PC
Site Class: C
City: Braintree
County: Norfolk
Geologic Group: Group 4
SDC: C
Detailed View
Discrete Damage State Probability P[Damage = DS | Sd]
0.661
0.179
0.119
0.034
0.005
0.001
None
Collapsed
Damage State
1 = Slight Damage | 2 = Moderate Damage
3 = Extensive Damage | 4 = Complete Damage

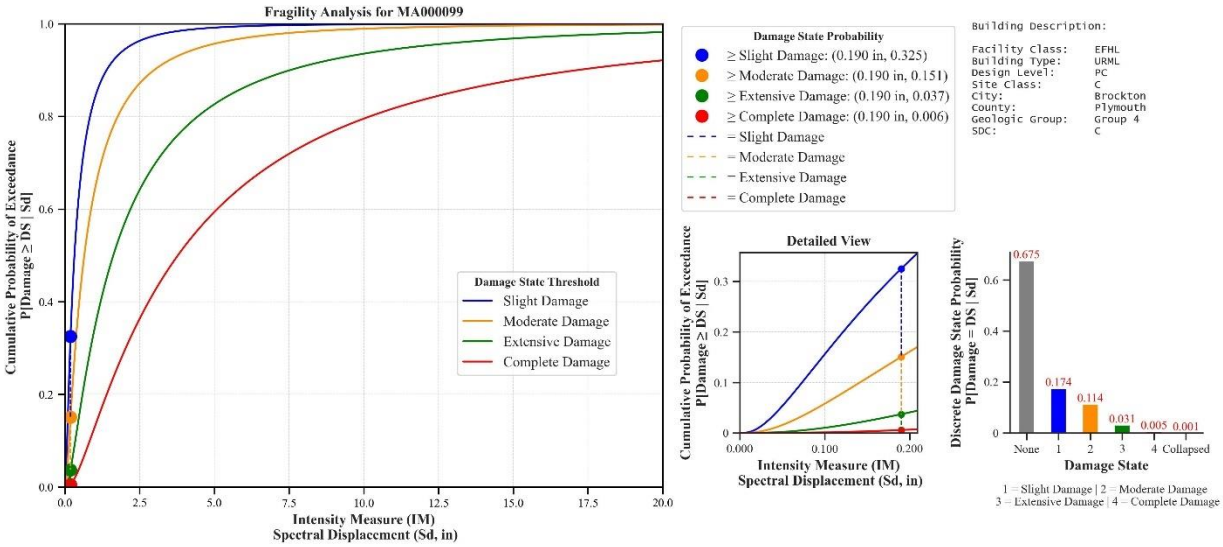
Fragility Analysis for MA000099
Cumulative Probability of Exceedance P[Damage ≥ DS | Sd]
Intensity Measure (IM) Spectral Displacement (Sd, in)
Damage State Threshold
Slight Damage
Moderate Damage
Extensive Damage
Complete Damage
Damage State Probability
≥ Slight Damage: (0.190 in, 0.325)
≥ Moderate Damage: (0.190 in, 0.151)
≥ Extensive Damage: (0.190 in, 0.037)
≥ Complete Damage: (0.190 in, 0.006)
Building Description:
Facility Class: EFHL
Building Type: URML
Design Level: PC
Site Class: C
City: Brockton
County: Plymouth
Geologic Group: Group 4
SDC: C
Detailed View
Discrete Damage State Probability P[Damage = DS | Sd]
0.675
0.174
0.114
0.031
0.005
0.001
None
Collapsed
Damage State
1 = Slight Damage | 2 = Moderate Damage
3 = Extensive Damage | 4 = Complete Damage

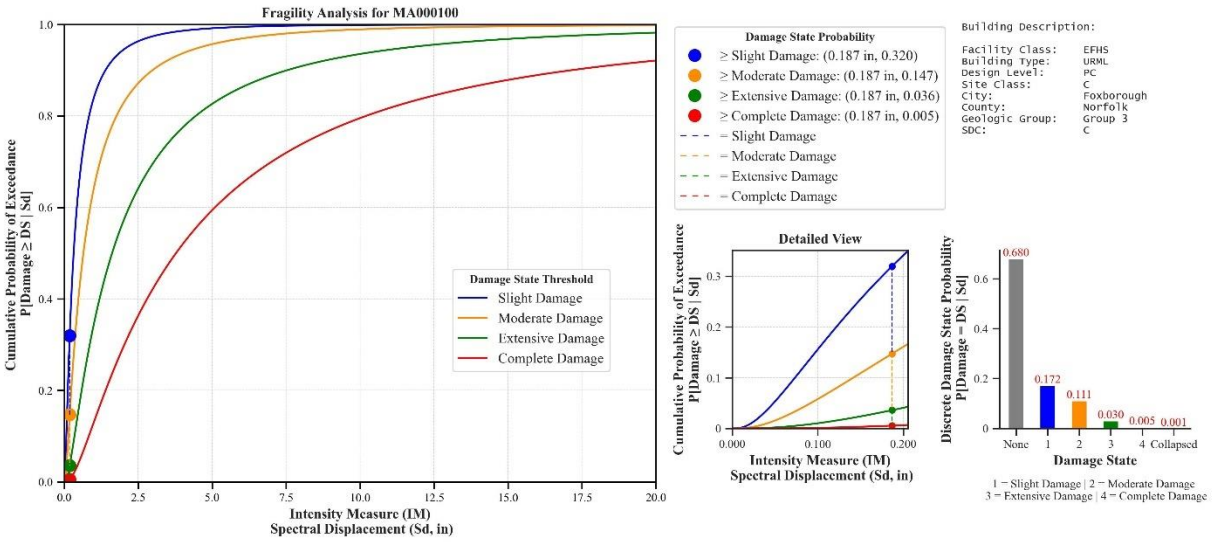
Fragility Analysis for MA000100
Cumulative Probability of Exceedance P[Damage ≥ DS | Sd]
Intensity Measure (IM) Spectral Displacement (Sd, in)
Damage State Threshold
Slight Damage
Moderate Damage
Extensive Damage
Complete Damage
Damage State Probability
≥ Slight Damage: (0.187 in, 0.320)
≥ Moderate Damage: (0.187 in, 0.147)
≥ Extensive Damage: (0.187 in, 0.036)
≥ Complete Damage: (0.187 in, 0.005)
Building Description:
Facility Class: EFHS
Building Type: URML
Design Level: PC
Site Class: C
City: Foxborough
County: Norfolk
Geologic Group: Group 3
SDC: C
Detailed View
Discrete Damage State Probability P[Damage = DS | Sd]
0.680
0.172
0.111
0.030
0.005
0.001
None
Collapsed
Damage State
1 = Slight Damage | 2 = Moderate Damage
3 = Extensive Damage | 4 = Complete Damage

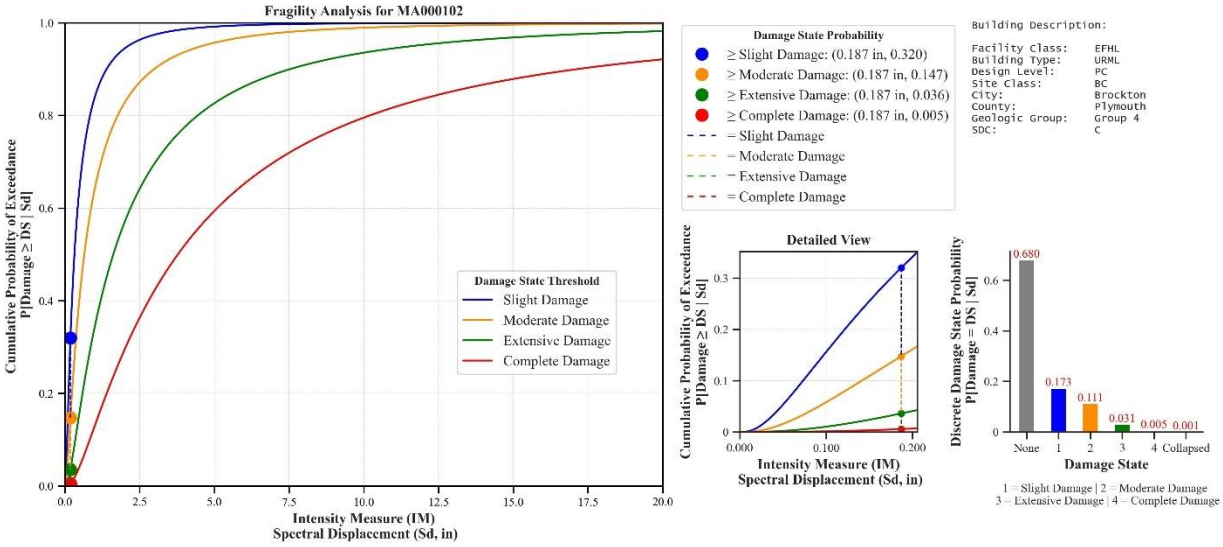
Fragility Analysis for MA000102
Cumulative Probability of Exceedance P[Damage ≥ DS | Sd]
Intensity Measure (IM) Spectral Displacement (Sd, in)
Damage State Threshold
Slight Damage
Moderate Damage
Extensive Damage
Complete Damage
Damage State Probability
≥ Slight Damage: (0.187 in, 0.320)
≥ Moderate Damage: (0.187 in, 0.147)
≥ Extensive Damage: (0.187 in, 0.036)
≥ Complete Damage: (0.187 in, 0.005)
= Slight Damage
= Moderate Damage
= Extensive Damage
= Complete Damage
Detailed View
Building Description:
Facility Class: EFHL
Building Type: URML
Design Level: PC
Site Class: BC
City: Brockton
County: Plymouth
Geologic Group: Group 4
SDC: C
Discrete Damage State Probability P[Damage = DS | Sd]
0.680
0.173
0.111
0.031
0.005
0.001
None
1
2
3
4 Collapsed
Damage State
1 = Slight Damage | 2 = Moderate Damage
3 = Extensive Damage | 4 = Complete Damage

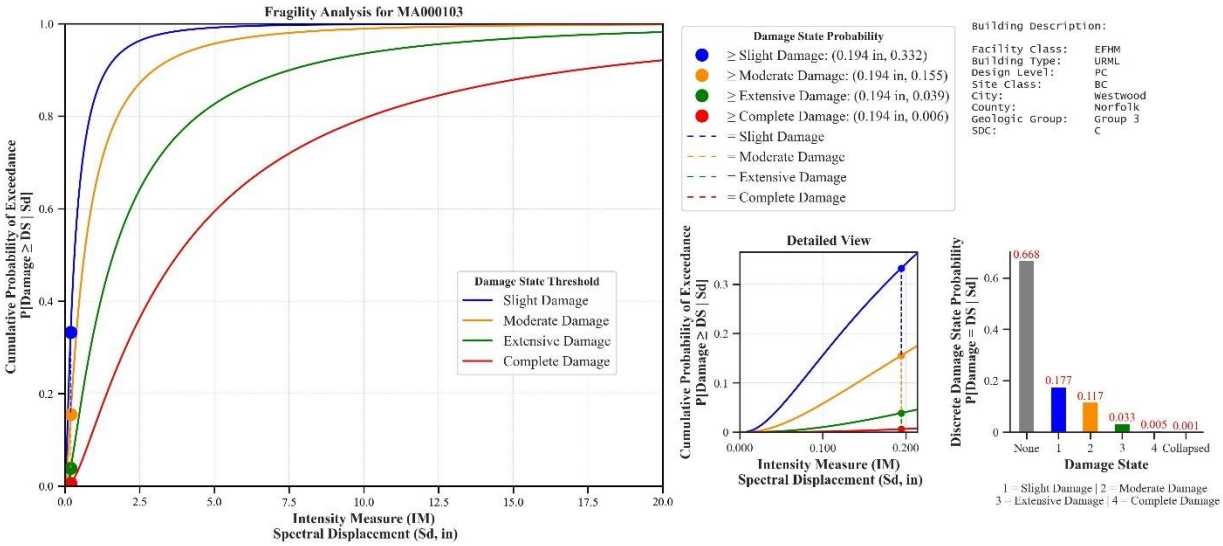
Fragility Analysis for MA000103
Cumulative Probability of Exceedance P[Damage ≥ DS | Sd]
Intensity Measure (IM) Spectral Displacement (Sd, in)
Damage State Threshold
Slight Damage
Moderate Damage
Extensive Damage
Complete Damage
Damage State Probability
≥ Slight Damage: (0.194 in, 0.332)
≥ Moderate Damage: (0.194 in, 0.155)
≥ Extensive Damage: (0.194 in, 0.039)
≥ Complete Damage: (0.194 in, 0.006)
= Slight Damage
= Moderate Damage
= Extensive Damage
= Complete Damage
Detailed View
Building Description:
Facility Class: EFHM
Building Type: URML
Design Level: PC
Site Class: BC
City: Westwood
County: Norfolk
Geologic Group: Group 3
SDC: C
Discrete Damage State Probability P[Damage = DS | Sd]
0.668
0.177
0.117
0.033
0.005
0.001
None
1
2
3
4 Collapsed
Damage State
1 = Slight Damage | 2 = Moderate Damage
3 = Extensive Damage | 4 = Complete Damage

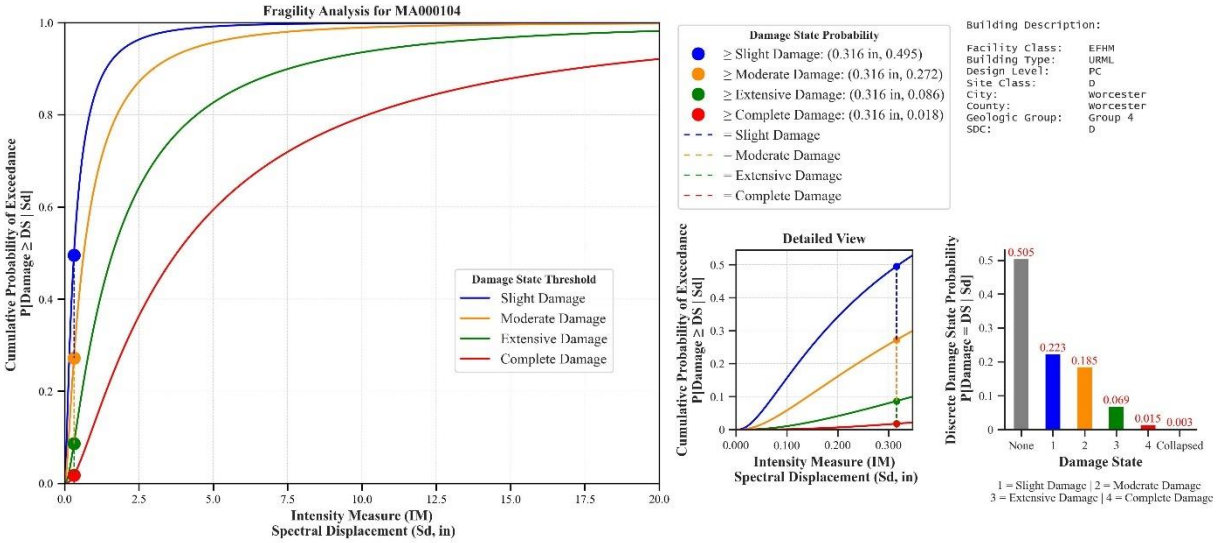
Fragility Analysis for MA000104
Cumulative Probability of Exceedance P[Damage ≥ DS | Sd]
Intensity Measure (IM) Spectral Displacement (Sd, in)
Damage State Threshold
Slight Damage
Moderate Damage
Extensive Damage
Complete Damage
Damage State Probability
≥ Slight Damage: (0.316 in, 0.495)
≥ Moderate Damage: (0.316 in, 0.272)
≥ Extensive Damage: (0.316 in, 0.086)
≥ Complete Damage: (0.316 in, 0.018)
= Slight Damage
= Moderate Damage
= Extensive Damage
= Complete Damage
Detailed View
Building Description:
Facility Class: EFHM
Building Type: URML
Design Level: PC
Site Class: D
City: Worcester
County: Worcester
Geologic Group: Group 4
SDC: D
Discrete Damage State Probability P[Damage = DS | Sd]
0.505
0.223
0.185
0.069
0.015
0.003
None
1
2
3
4 Collapsed
Damage State
1 = Slight Damage | 2 = Moderate Damage
3 = Extensive Damage | 4 = Complete Damage

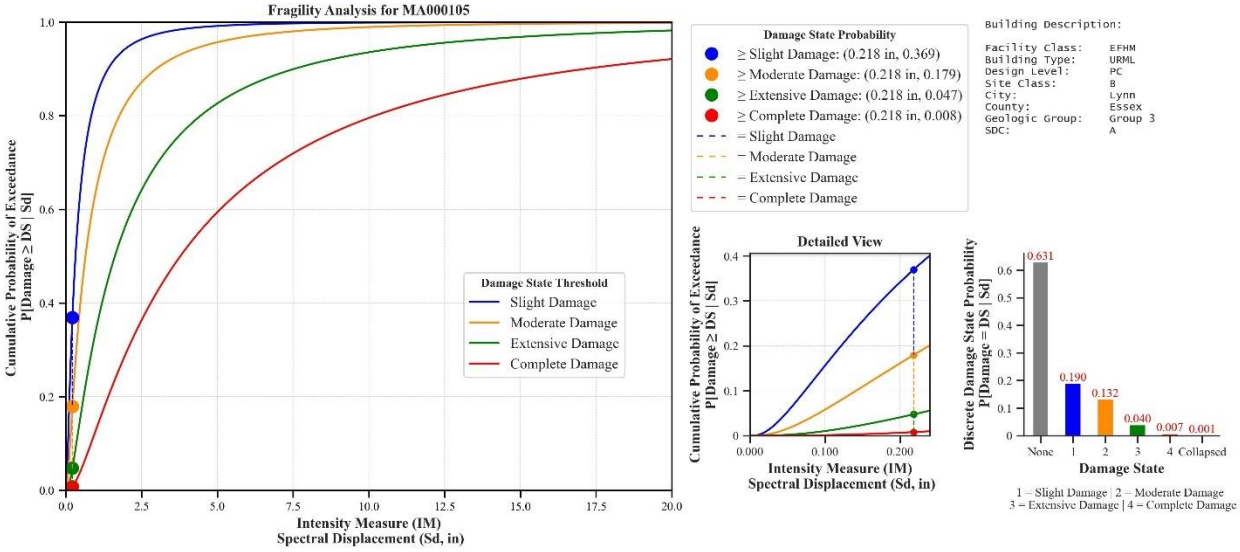
Fragility Analysis for MA000105
Cumulative Probability of Exceedance P[Damage ≥ DS | Sd]
Intensity Measure (IM) Spectral Displacement (Sd, in)
Damage State Threshold
Slight Damage
Moderate Damage
Extensive Damage
Complete Damage
Damage State Probability
≥ Slight Damage: (0.218 in, 0.369)
≥ Moderate Damage: (0.218 in, 0.179)
≥ Extensive Damage: (0.218 in, 0.047)
≥ Complete Damage: (0.218 in, 0.008)
= Slight Damage
= Moderate Damage
= Extensive Damage
= Complete Damage
Detailed View
Building Description:
Facility Class: EFHM
Building Type: URML
Design Level: PC
Site Class: B
City: Lynn
County: Essex
Geologic Group: Group 3
SDC: A
Discrete Damage State Probability P[Damage = DS | Sd]
0.631
0.190
0.132
0.040
0.007
0.001
None
Collapsed
Damage State
1 = Slight Damage | 2 = Moderate Damage
3 = Extensive Damage | 4 = Complete Damage

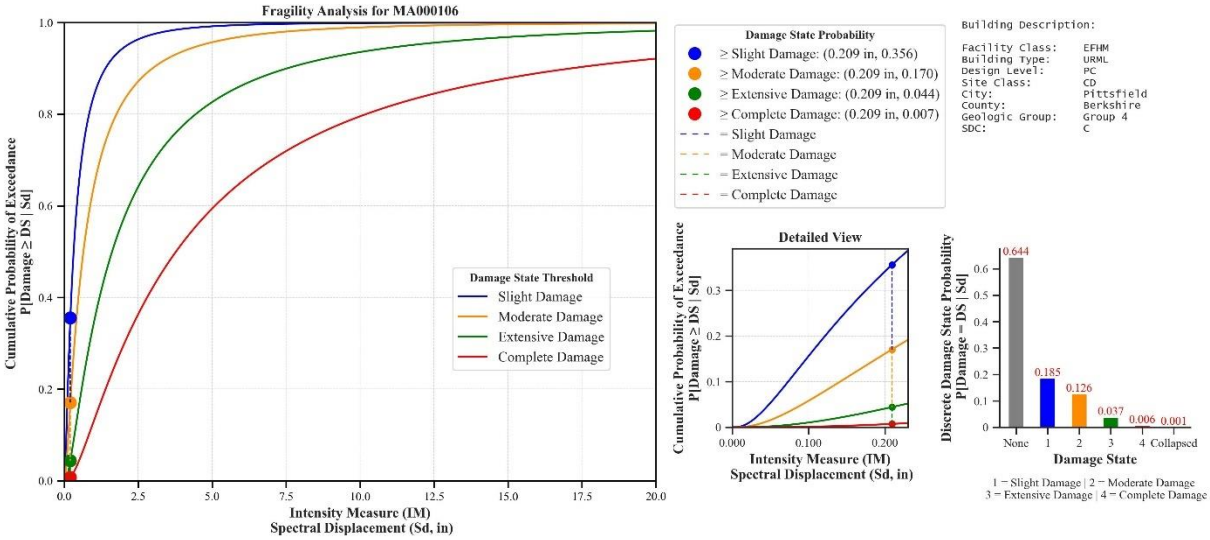
Fragility Analysis for MA000106
Cumulative Probability of Exceedance P[Damage ≥ DS | Sd]
Intensity Measure (IM) Spectral Displacement (Sd, in)
Damage State Threshold
Slight Damage
Moderate Damage
Extensive Damage
Complete Damage
Damage State Probability
≥ Slight Damage: (0.209 in, 0.356)
≥ Moderate Damage: (0.209 in, 0.170)
≥ Extensive Damage: (0.209 in, 0.044)
≥ Complete Damage: (0.209 in, 0.007)
= Slight Damage
= Moderate Damage
= Extensive Damage
= Complete Damage
Detailed View
Building Description:
Facility Class: EFHM
Building Type: URML
Design Level: PC
Site Class: CD
City: Pittsfield
County: Berkshire
Geologic Group: Group 4
SDC: C
Discrete Damage State Probability P[Damage = DS | Sd]
0.644
0.185
0.126
0.037
0.006
0.001
None
Collapsed
Damage State
1 = Slight Damage | 2 = Moderate Damage
3 = Extensive Damage | 4 = Complete Damage

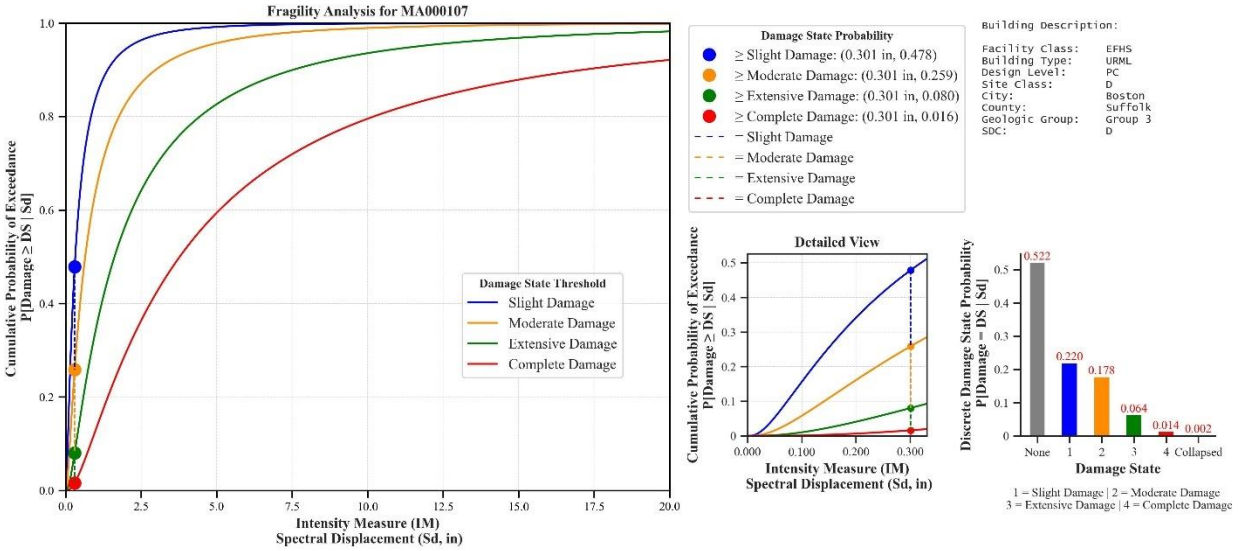
Fragility Analysis for MA000107
Cumulative Probability of Exceedance P[Damage ≥ DS | Sd]
Intensity Measure (IM) Spectral Displacement (Sd, in)
Damage State Threshold
Slight Damage
Moderate Damage
Extensive Damage
Complete Damage
Damage State Probability
≥ Slight Damage: (0.301 in, 0.478)
≥ Moderate Damage: (0.301 in, 0.259)
≥ Extensive Damage: (0.301 in, 0.080)
≥ Complete Damage: (0.301 in, 0.016)
= Slight Damage
= Moderate Damage
= Extensive Damage
= Complete Damage
Detailed View
Building Description:
Facility Class: EFHS
Building Type: URML
Design Level: PC
Site Class: D
City: Boston
County: Suffolk
Geologic Group: Group 3
SDC: D
Discrete Damage State Probability P[Damage = DS | Sd]
0.522
0.220
0.178
0.064
0.014
0.002
None
Collapsed
Damage State
1 = Slight Damage | 2 = Moderate Damage
3 = Extensive Damage | 4 = Complete Damage

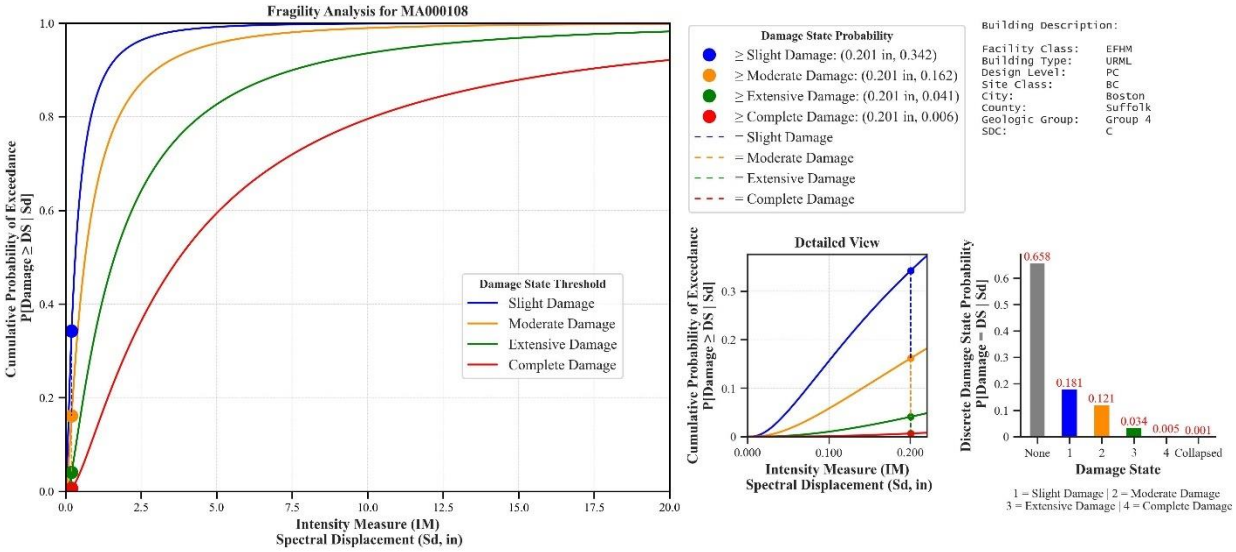
Fragility Analysis for MA000108
Cumulative Probability of Exceedance P[Damage ≥ DS | Sd]
Intensity Measure (IM) Spectral Displacement (Sd, in)
Damage State Threshold
Slight Damage
Moderate Damage
Extensive Damage
Complete Damage
Damage State Probability
≥ Slight Damage: (0.201 in, 0.342)
≥ Moderate Damage: (0.201 in, 0.162)
≥ Extensive Damage: (0.201 in, 0.041)
≥ Complete Damage: (0.201 in, 0.006)
= Slight Damage
= Moderate Damage
= Extensive Damage
= Complete Damage
Detailed View
Building Description:
Facility Class: EFHM
Building Type: URML
Design Level: PC
Site Class: BC
City: Boston
County: Suffolk
Geologic Group: Group 4
SDC: C
Discrete Damage State Probability P[Damage = DS | Sd]
0.658
0.181
0.121
0.034
0.005
0.001
None
Collapsed
Damage State
1 = Slight Damage | 2 = Moderate Damage
3 = Extensive Damage | 4 = Complete Damage

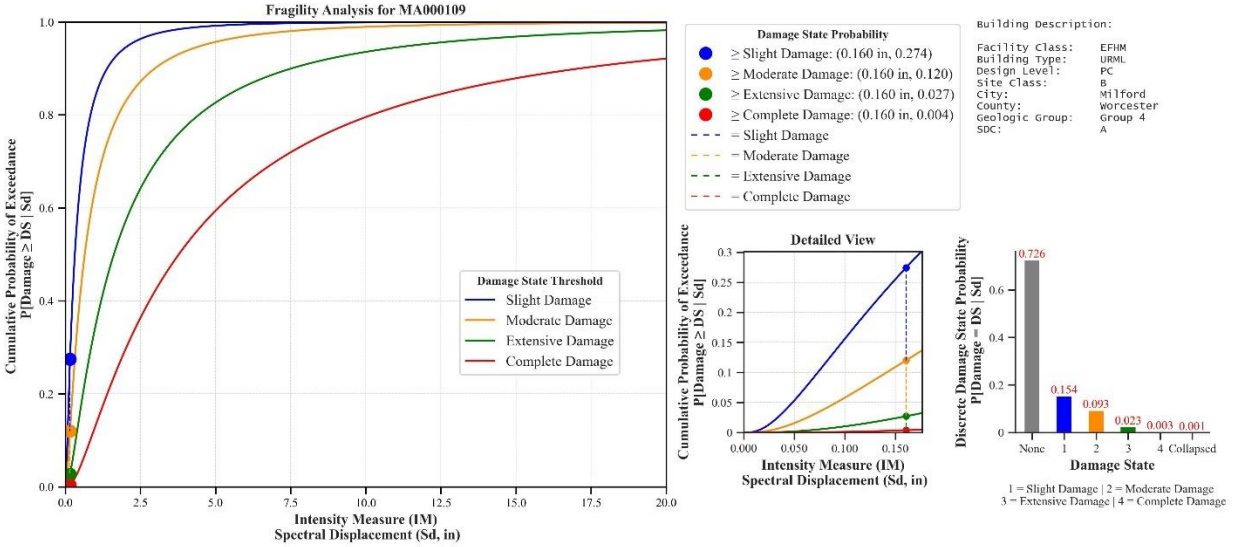
Fragility Analysis for MA000109
Cumulative Probability of Exceedance P[Damage ≥ DS | Sd]
Intensity Measure (IM) Spectral Displacement (Sd, in)
Damage State Threshold
Slight Damage
Moderate Damage
Extensive Damage
Complete Damage
Damage State Probability
≥ Slight Damage: (0.160 in, 0.274)
≥ Moderate Damage: (0.160 in, 0.120)
≥ Extensive Damage: (0.160 in, 0.027)
≥ Complete Damage: (0.160 in, 0.004)
= Slight Damage
= Moderate Damage
= Extensive Damage
= Complete Damage
Detailed View
Building Description:
Facility Class: EFHM
Building Type: URML
Design Level: PC
Site Class: B
City: Milford
County: Worcester
Geologic Group: Group 4
SDC: A
Discrete Damage State Probability P[Damage = DS | Sd]
0.726
0.154
0.093
0.023
0.003
0.001
None
Collapsed
Damage State
1 = Slight Damage | 2 = Moderate Damage
3 = Extensive Damage | 4 = Complete Damage

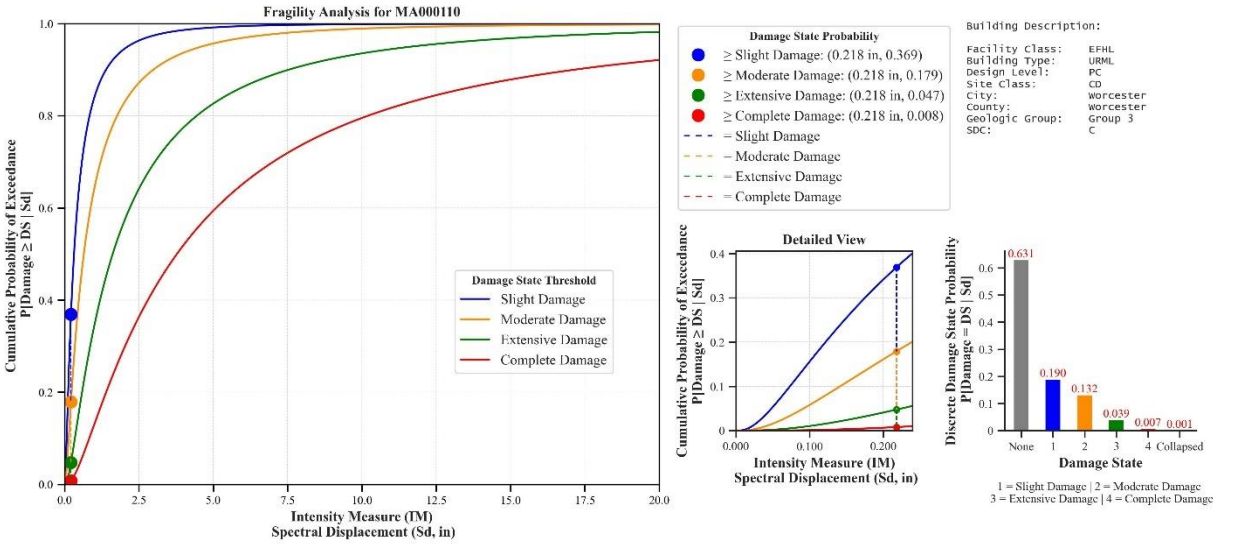
Fragility Analysis for MA000110
Cumulative Probability of Exceedance P[Damage ≥ DS | Sd]
Intensity Measure (IM) Spectral Displacement (Sd, in)
Damage State Threshold
Slight Damage
Moderate Damage
Extensive Damage
Complete Damage
Damage State Probability
≥ Slight Damage: (0.218 in, 0.369)
≥ Moderate Damage: (0.218 in, 0.179)
≥ Extensive Damage: (0.218 in, 0.047)
≥ Complete Damage: (0.218 in, 0.008)
= Slight Damage
= Moderate Damage
= Extensive Damage
= Complete Damage
Detailed View
Building Description:
Facility Class: EFHL
Building Type: URML
Design Level: PC
Site Class: CD
City: Worcester
County: Worcester
Geologic Group: Group 3
SDC: C
Discrete Damage State Probability P[Damage = DS | Sd]
0.631
0.190
0.132
0.039
0.007
0.001
None
Collapsed
Damage State
1 = Slight Damage | 2 = Moderate Damage
3 = Extensive Damage | 4 = Complete Damage

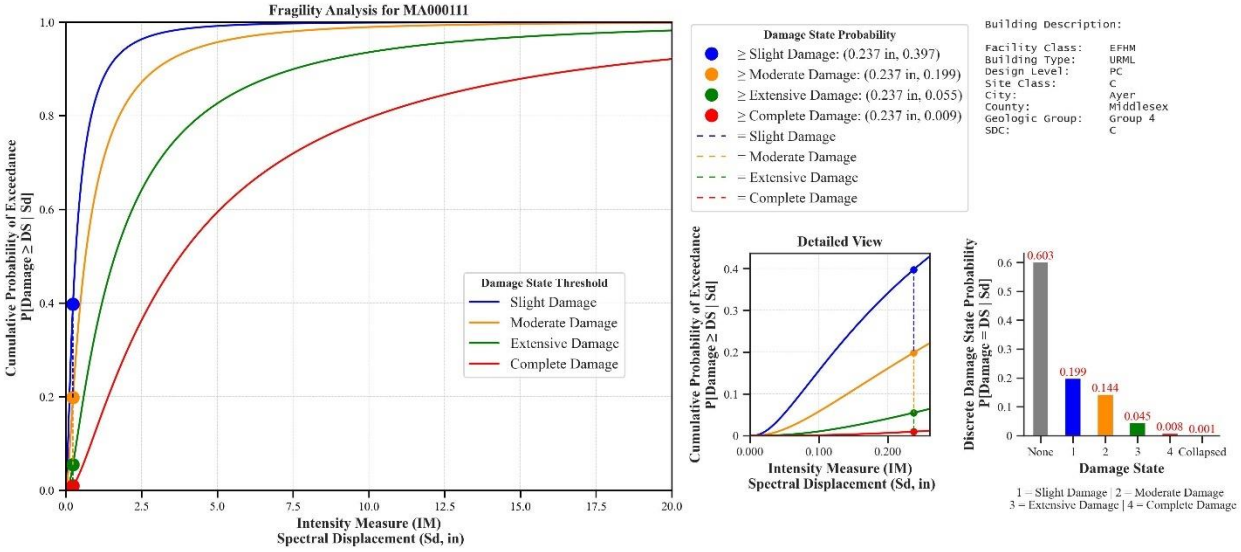
Fragility Analysis for MA000111
Cumulative Probability of Exceedance P[Damage ≥ DS | Sd]
Intensity Measure (IM) Spectral Displacement (Sd, in)
Damage State Threshold
Slight Damage
Moderate Damage
Extensive Damage
Complete Damage
Damage State Probability
≥ Slight Damage: (0.237 in, 0.397)
≥ Moderate Damage: (0.237 in, 0.199)
≥ Extensive Damage: (0.237 in, 0.055)
≥ Complete Damage: (0.237 in, 0.009)
= Slight Damage
= Moderate Damage
= Extensive Damage
= Complete Damage
Building Description:
Facility Class: EFHM
Building Type: URML
Design Level: PC
Site Class: C
City: Ayer
County: Middlesex
Geologic Group: Group 4
SDC: C
Detailed View
Discrete Damage State Probability P[Damage = DS | Sd]
0.603
0.199
0.144
0.045
0.008
0.001
None 1 2 3 4 Collapsed
Damage State
1 = Slight Damage | 2 = Moderate Damage
3 = Extensive Damage | 4 = Complete Damage

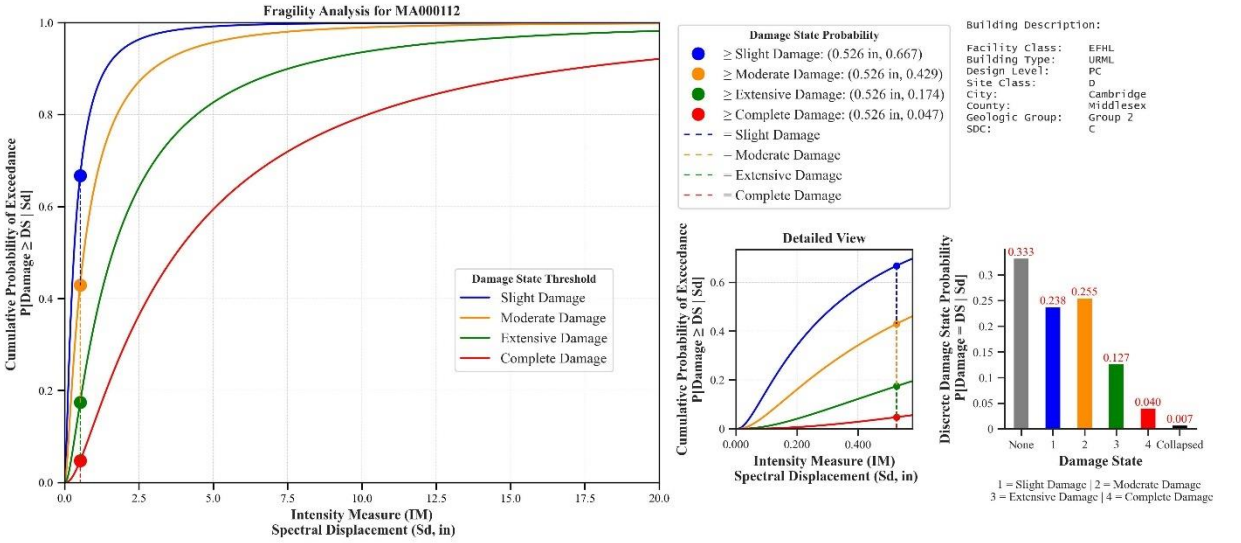
Fragility Analysis for MA000112
Cumulative Probability of Exceedance P[Damage ≥ DS | Sd]
Intensity Measure (IM) Spectral Displacement (Sd, in)
Damage State Threshold
Slight Damage
Moderate Damage
Extensive Damage
Complete Damage
Damage State Probability
≥ Slight Damage: (0.526 in, 0.667)
≥ Moderate Damage: (0.526 in, 0.429)
≥ Extensive Damage: (0.526 in, 0.174)
≥ Complete Damage: (0.526 in, 0.047)
= Slight Damage
= Moderate Damage
= Extensive Damage
= Complete Damage
Building Description:
Facility Class: EFHL
Building Type: URML
Design Level: PC
Site Class: D
City: Cambridge
County: Middlesex
Geologic Group: Group 2
SDC: C
Detailed View
Discrete Damage State Probability P[Damage = DS | Sd]
0.333
0.238
0.255
0.127
0.040
0.007
None 1 2 3 4 Collapsed
Damage State
1 = Slight Damage | 2 = Moderate Damage
3 = Extensive Damage | 4 = Complete Damage

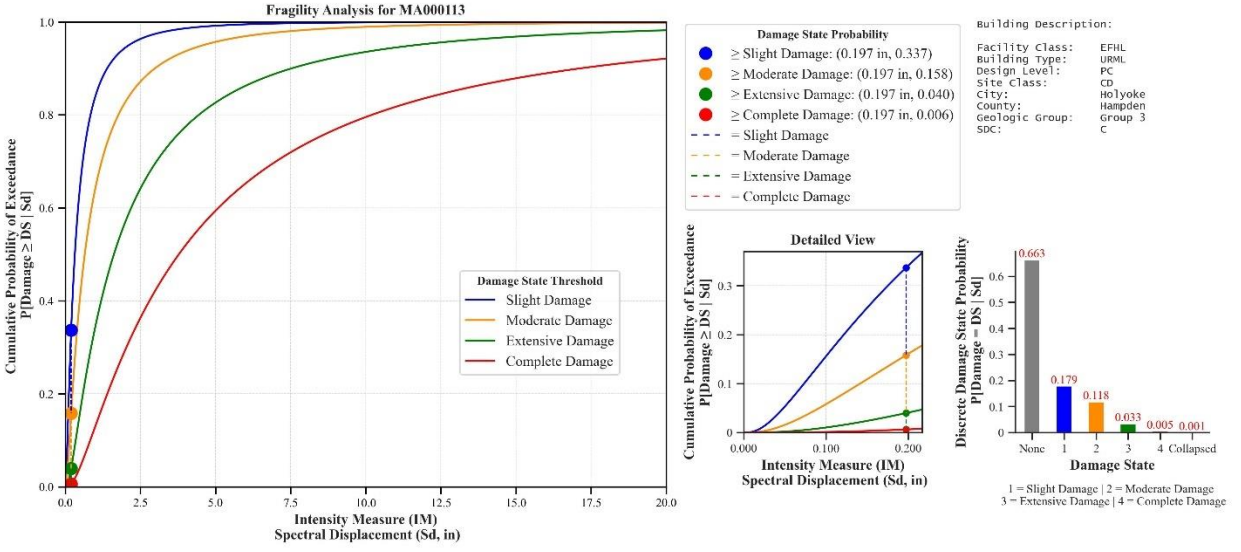
Fragility Analysis for MA000113
Cumulative Probability of Exceedance P[Damage ≥ DS | Sd]
Intensity Measure (IM) Spectral Displacement (Sd, in)
Damage State Threshold
Slight Damage
Moderate Damage
Extensive Damage
Complete Damage
Damage State Probability
≥ Slight Damage: (0.197 in, 0.337)
≥ Moderate Damage: (0.197 in, 0.158)
≥ Extensive Damage: (0.197 in, 0.040)
≥ Complete Damage: (0.197 in, 0.006)
= Slight Damage
= Moderate Damage
= Extensive Damage
= Complete Damage
Building Description:
Facility Class: EFHL
Building Type: URML
Design Level: PC
Site Class: CD
City: Holyoke
County: Hampden
Geologic Group: Group 3
SDC: C
Detailed View
Discrete Damage State Probability P[Damage = DS | Sd]
0.663
0.179
0.118
0.033
0.005
0.001
None 1 2 3 4 Collapsed
Damage State
1 = Slight Damage | 2 = Moderate Damage
3 = Extensive Damage | 4 = Complete Damage

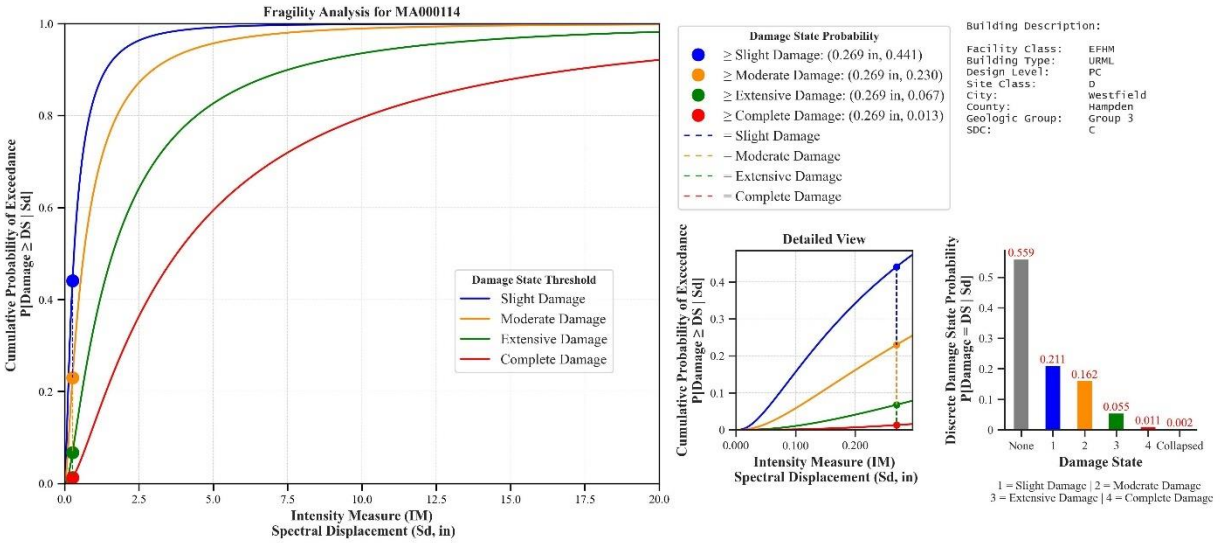
Fragility Analysis for MA000114
Cumulative Probability of Exceedance P[Damage ≥ DS | Sd]
Intensity Measure (IM) Spectral Displacement (Sd, in)
Damage State Threshold
Slight Damage
Moderate Damage
Extensive Damage
Complete Damage
Damage State Probability
≥ Slight Damage: (0.269 in, 0.441)
≥ Moderate Damage: (0.269 in, 0.230)
≥ Extensive Damage: (0.269 in, 0.067)
≥ Complete Damage: (0.269 in, 0.013)
Detailed View
Discrete Damage State Probability P[Damage = DS | Sd]
0.559
0.211
0.162
0.055
0.011
0.002
None
Collapsed
Damage State
1 = Slight Damage | 2 = Moderate Damage
3 = Extensive Damage | 4 = Complete Damage
Building Description:
Facility Class: EFHM
Building Type: URML
Design Level: PC
Site Class: D
City: Westfield
County: Hampden
Geologic Group: Group 3
SDC: C

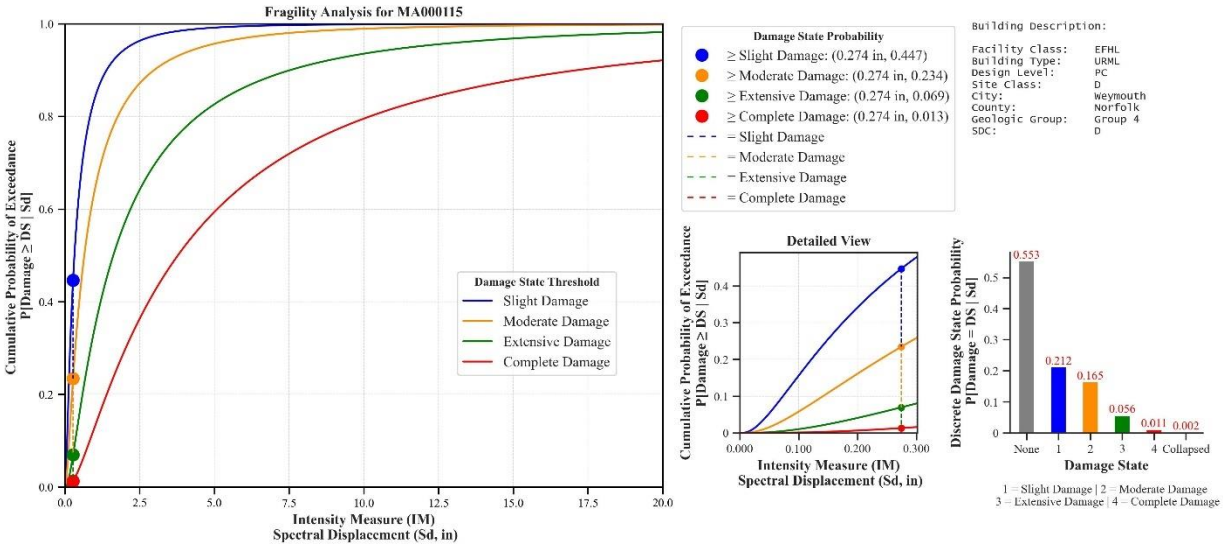
Fragility Analysis for MA000115
Cumulative Probability of Exceedance P[Damage ≥ DS | Sd]
Intensity Measure (IM) Spectral Displacement (Sd, in)
Damage State Threshold
Slight Damage
Moderate Damage
Extensive Damage
Complete Damage
Damage State Probability
≥ Slight Damage: (0.274 in, 0.447)
≥ Moderate Damage: (0.274 in, 0.234)
≥ Extensive Damage: (0.274 in, 0.069)
≥ Complete Damage: (0.274 in, 0.013)
Detailed View
Discrete Damage State Probability P[Damage = DS | Sd]
0.553
0.212
0.165
0.056
0.011
0.002
None
Collapsed
Damage State
1 = Slight Damage | 2 = Moderate Damage
3 = Extensive Damage | 4 = Complete Damage
Building Description:
Facility Class: EFHL
Building Type: URML
Design Level: PC
Site Class: D
City: Weymouth
County: Norfolk
Geologic Group: Group 4
SDC: D

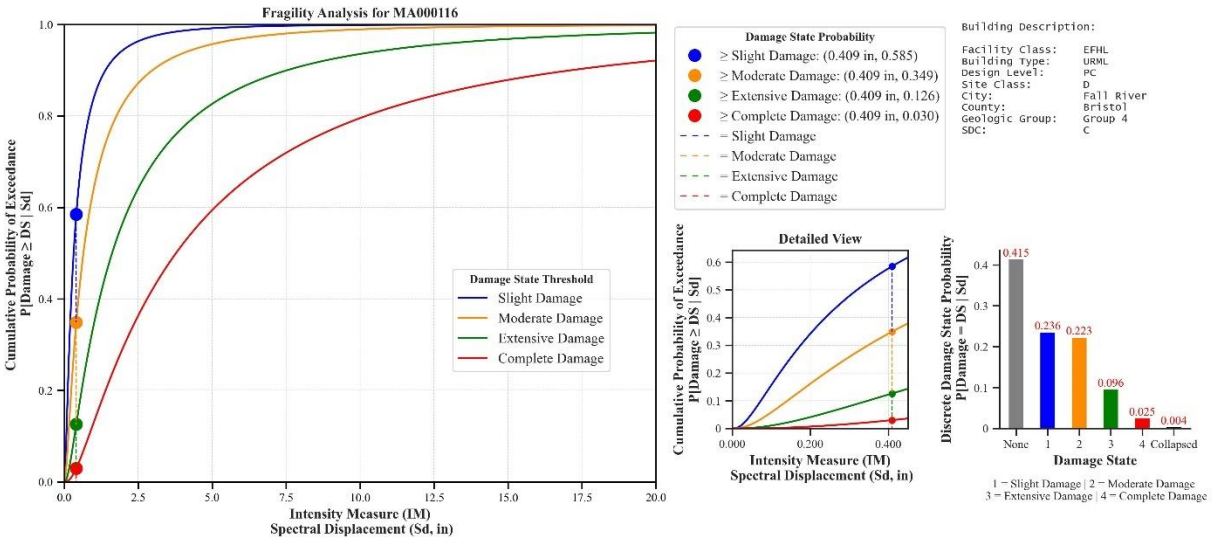
Fragility Analysis for MA000116
Cumulative Probability of Exceedance P[Damage ≥ DS | Sd]
Intensity Measure (IM) Spectral Displacement (Sd, in)
Damage State Threshold
Slight Damage
Moderate Damage
Extensive Damage
Complete Damage
Damage State Probability
≥ Slight Damage: (0.409 in, 0.585)
≥ Moderate Damage: (0.409 in, 0.349)
≥ Extensive Damage: (0.409 in, 0.126)
≥ Complete Damage: (0.409 in, 0.030)
Detailed View
Discrete Damage State Probability P[Damage = DS | Sd]
0.415
0.236
0.223
0.096
0.025
0.004
None
Collapsed
Damage State
1 = Slight Damage | 2 = Moderate Damage
3 = Extensive Damage | 4 = Complete Damage
Building Description:
Facility Class: EFHL
Building Type: URML
Design Level: PC
Site Class: D
City: Fall River
County: Bristol
Geologic Group: Group 4
SDC: C

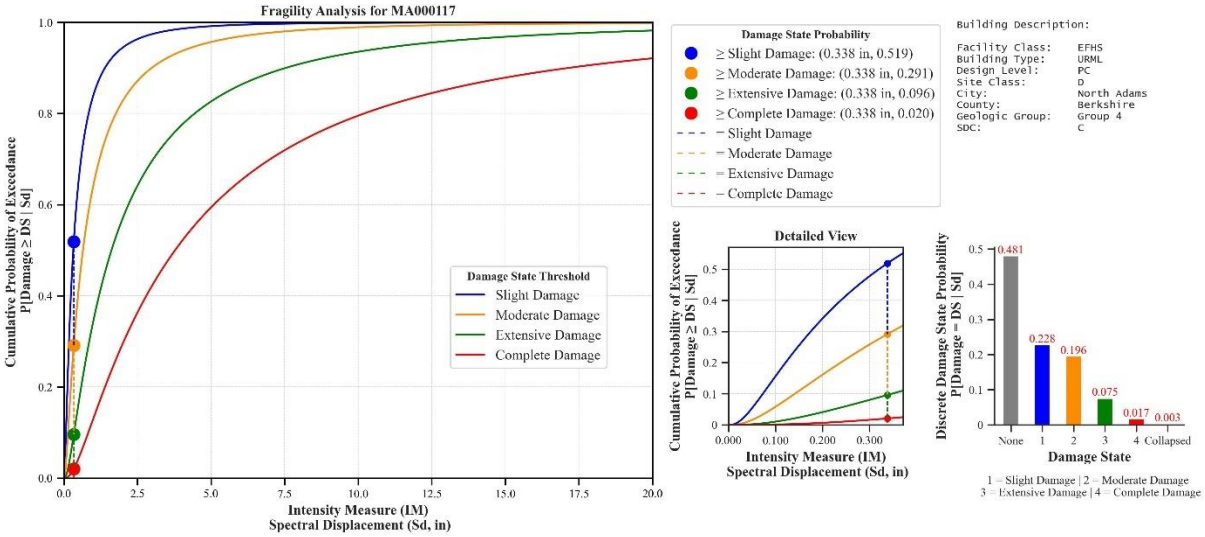
Fragility Analysis for MA000117
Cumulative Probability of Exceedance P[Damage ≥ DS | Sd]
Intensity Measure (IM) Spectral Displacement (Sd, in)
Damage State Threshold
Slight Damage
Moderate Damage
Extensive Damage
Complete Damage
Damage State Probability
≥ Slight Damage: (0.338 in, 0.519)
≥ Moderate Damage: (0.338 in, 0.291)
≥ Extensive Damage: (0.338 in, 0.096)
≥ Complete Damage: (0.338 in, 0.020)
= Slight Damage
= Moderate Damage
= Extensive Damage
= Complete Damage
Detailed View
Discrete Damage State Probability P[Damage = DS | Sd]
0.481
0.228
0.196
0.075
0.017
0.003
None 1 2 3 4 Collapsed
Damage State
1 = Slight Damage | 2 = Moderate Damage
3 = Extensive Damage | 4 = Complete Damage
Building Description:
Facility Class: EFHS
Building Type: URML
Design Level: PC
Site Class: D
City: North Adams
County: Berkshire
Geologic Group: Group 4
SDC: C

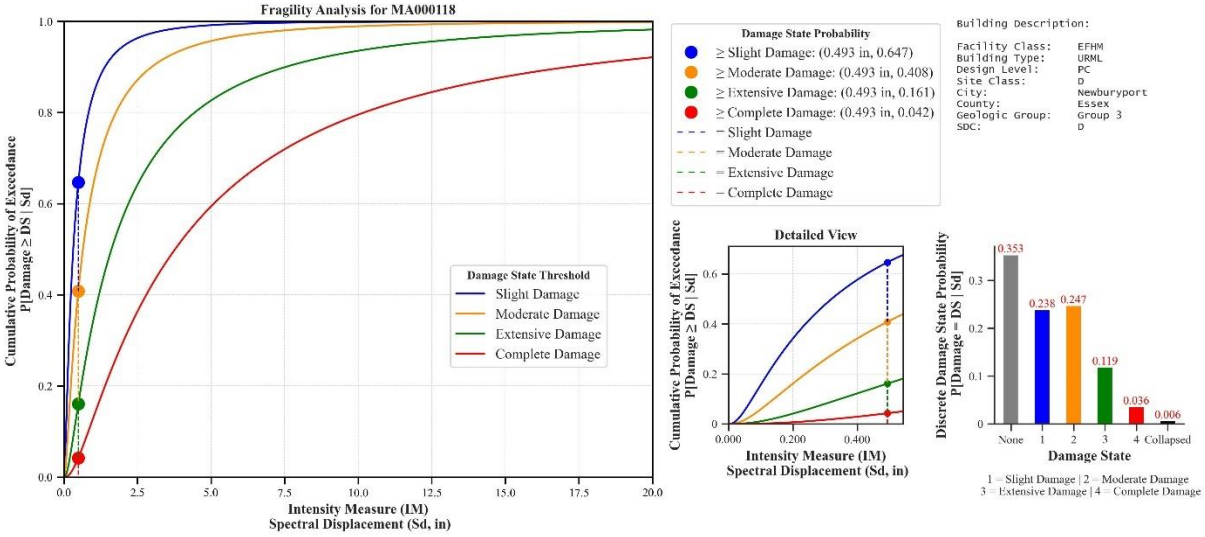
Fragility Analysis for MA000118
Cumulative Probability of Exceedance P[Damage ≥ DS | Sd]
Intensity Measure (IM) Spectral Displacement (Sd, in)
Damage State Threshold
Slight Damage
Moderate Damage
Extensive Damage
Complete Damage
Damage State Probability
≥ Slight Damage: (0.493 in, 0.647)
≥ Moderate Damage: (0.493 in, 0.408)
≥ Extensive Damage: (0.493 in, 0.161)
≥ Complete Damage: (0.493 in, 0.042)
= Slight Damage
= Moderate Damage
= Extensive Damage
= Complete Damage
Detailed View
Discrete Damage State Probability P[Damage = DS | Sd]
0.353
0.238
0.247
0.119
0.036
0.006
None 1 2 3 4 Collapsed
Damage State
1 = Slight Damage | 2 = Moderate Damage
3 = Extensive Damage | 4 = Complete Damage
Building Description:
Facility Class: EFHM
Building Type: URML
Design Level: PC
Site Class: D
City: Newburyport
County: Essex
Geologic Group: Group 3
SDC: D

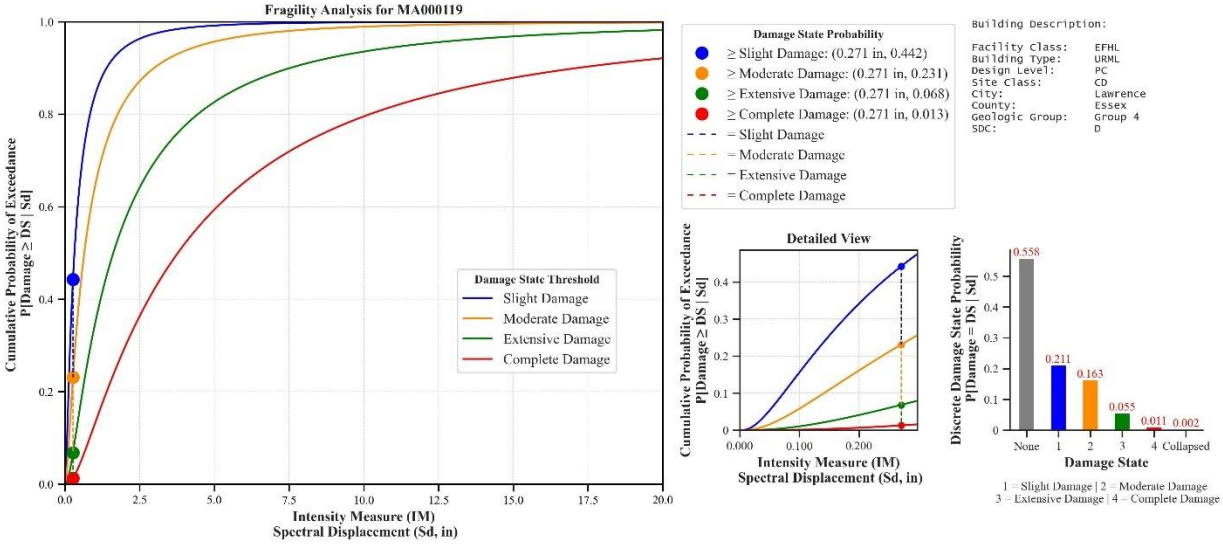
Fragility Analysis for MA000119
Cumulative Probability of Exceedance P[Damage ≥ DS | Sd]
Intensity Measure (IM) Spectral Displacement (Sd, in)
Damage State Threshold
Slight Damage
Moderate Damage
Extensive Damage
Complete Damage
Damage State Probability
≥ Slight Damage: (0.271 in, 0.442)
≥ Moderate Damage: (0.271 in, 0.231)
≥ Extensive Damage: (0.271 in, 0.068)
≥ Complete Damage: (0.271 in, 0.013)
= Slight Damage
= Moderate Damage
= Extensive Damage
= Complete Damage
Detailed View
Discrete Damage State Probability P[Damage = DS | Sd]
0.558
0.211
0.163
0.055
0.011
0.002
None 1 2 3 4 Collapsed
Damage State
1 = Slight Damage | 2 = Moderate Damage
3 = Extensive Damage | 4 = Complete Damage
Building Description:
Facility Class: EFHL
Building Type: URML
Design Level: PC
Site Class: CD
City: Lawrence
County: Essex
Geologic Group: Group 4
SDC: D

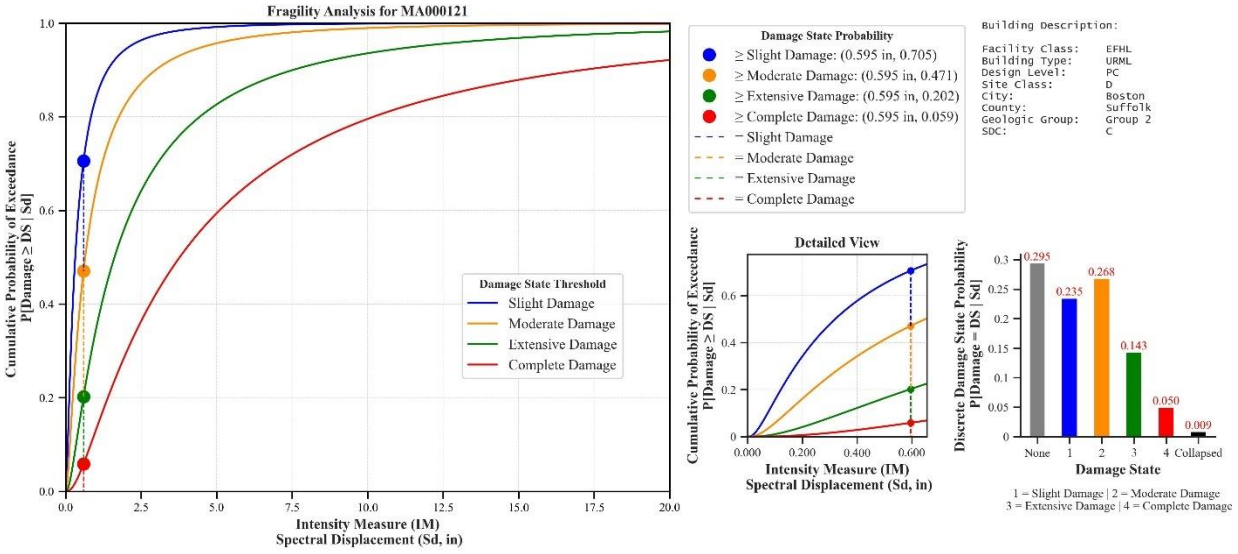
Fragility Analysis for MA000121
Cumulative Probability of Exceedance P[Damage ≥ DS | Sd]
Intensity Measure (IM) Spectral Displacement (Sd, in)
Damage State Threshold
Slight Damage
Moderate Damage
Extensive Damage
Complete Damage
Damage State Probability
≥ Slight Damage: (0.595 in, 0.705)
≥ Moderate Damage: (0.595 in, 0.471)
≥ Extensive Damage: (0.595 in, 0.202)
≥ Complete Damage: (0.595 in, 0.059)
Building Description:
Facility Class: EFHL
Building Type: URML
Design Level: PC
Site Class: D
City: Boston
County: Suffolk
Geologic Group: Group 2
SDC: C
Detailed View
Discrete Damage State Probability P[Damage = DS | Sd]
0.295
0.235
0.268
0.143
0.050
0.009
None 1 2 3 4 Collapsed
Damage State
1 = Slight Damage | 2 = Moderate Damage
3 = Extensive Damage | 4 = Complete Damage

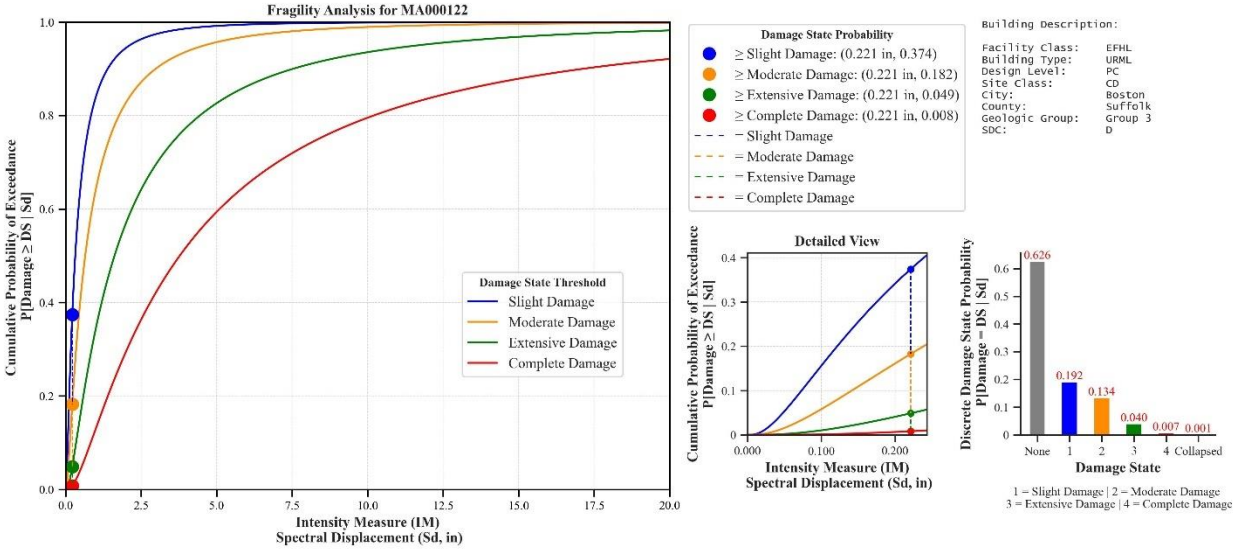
Fragility Analysis for MA000122
Cumulative Probability of Exceedance P[Damage ≥ DS | Sd]
Intensity Measure (IM) Spectral Displacement (Sd, in)
Damage State Threshold
Slight Damage
Moderate Damage
Extensive Damage
Complete Damage
Damage State Probability
≥ Slight Damage: (0.221 in, 0.374)
≥ Moderate Damage: (0.221 in, 0.182)
≥ Extensive Damage: (0.221 in, 0.049)
≥ Complete Damage: (0.221 in, 0.008)
Building Description:
Facility Class: EFHL
Building Type: URML
Design Level: PC
Site Class: CD
City: Boston
County: Suffolk
Geologic Group: Group 3
SDC: D
Detailed View
Discrete Damage State Probability P[Damage = DS | Sd]
0.626
0.192
0.134
0.040
0.007
0.001
None 1 2 3 4 Collapsed
Damage State
1 = Slight Damage | 2 = Moderate Damage
3 = Extensive Damage | 4 = Complete Damage

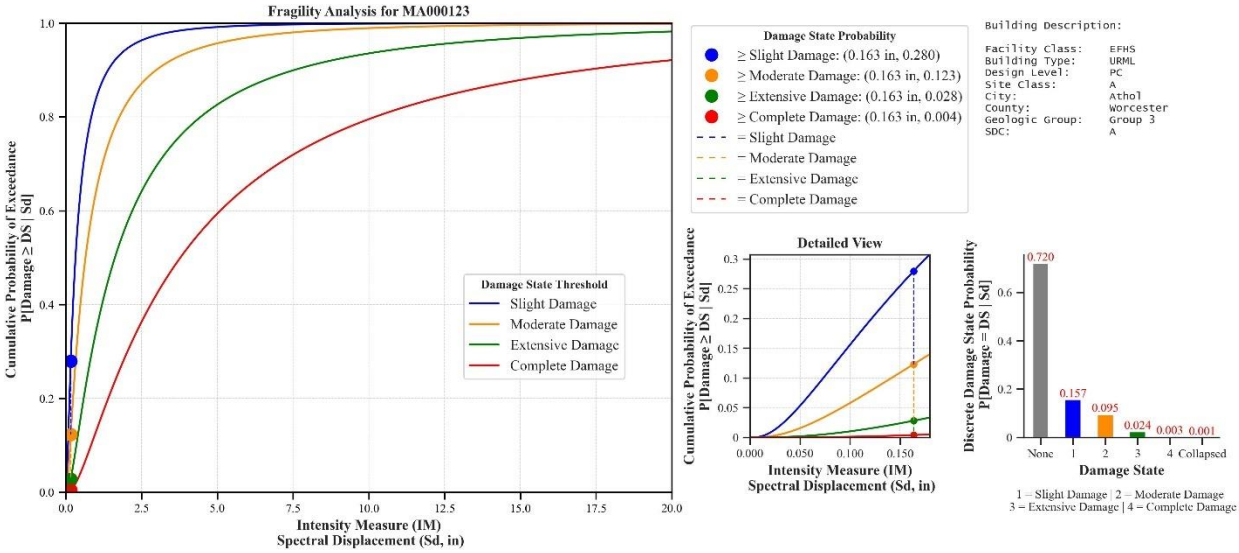
Fragility Analysis for MA000123
Cumulative Probability of Exceedance P[Damage ≥ DS | Sd]
Intensity Measure (IM) Spectral Displacement (Sd, in)
Damage State Threshold
Slight Damage
Moderate Damage
Extensive Damage
Complete Damage
Damage State Probability
≥ Slight Damage: (0.163 in, 0.280)
≥ Moderate Damage: (0.163 in, 0.123)
≥ Extensive Damage: (0.163 in, 0.028)
≥ Complete Damage: (0.163 in, 0.004)
Building Description:
Facility Class: EFHS
Building Type: URML
Design Level: PC
Site Class: A
City: Athol
County: Worcester
Geologic Group: Group 3
SDC: A
Detailed View
Discrete Damage State Probability P[Damage = DS | Sd]
0.720
0.157
0.095
0.024
0.003
0.001
None 1 2 3 4 Collapsed
Damage State
1 = Slight Damage | 2 = Moderate Damage
3 = Extensive Damage | 4 = Complete Damage

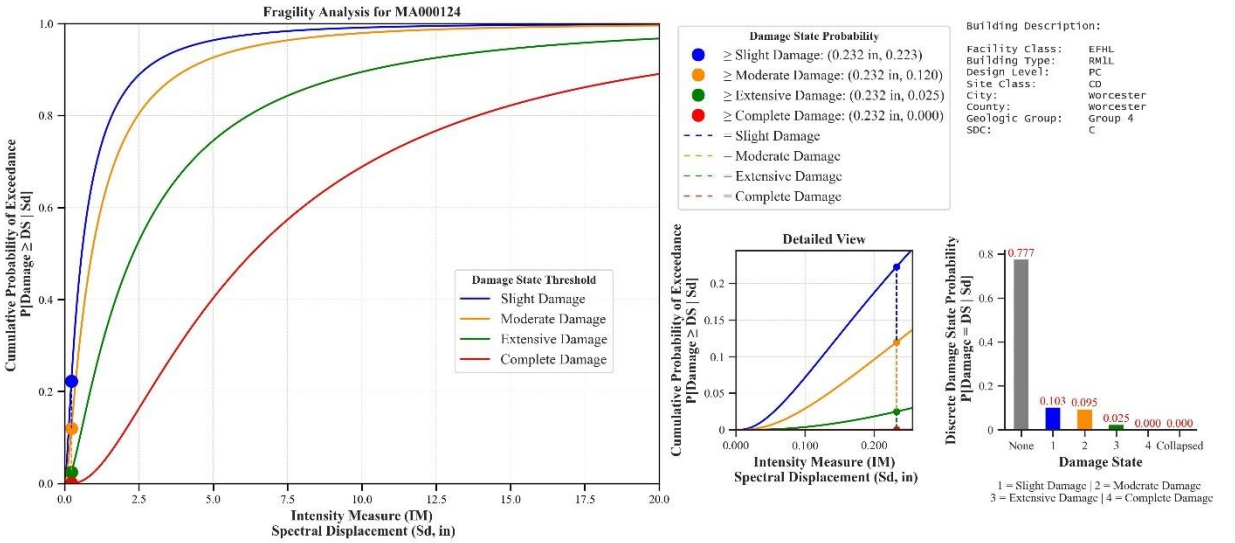
Fragility Analysis for MA000124
Cumulative Probability of Exceedance P[Damage ≥ DS | Sd]
Intensity Measure (IM) Spectral Displacement (Sd, in)
Damage State Threshold
Slight Damage
Moderate Damage
Extensive Damage
Complete Damage
Damage State Probability
≥ Slight Damage: (0.232 in, 0.223)
≥ Moderate Damage: (0.232 in, 0.120)
≥ Extensive Damage: (0.232 in, 0.025)
≥ Complete Damage: (0.232 in, 0.000)
Building Description:
Facility Class: EFHL
Building Type: RM1L
Design Level: PC
Site Class: CD
City: Worcester
County: Worcester
Geologic Group: Group 4
SDC: C
Detailed View
Discrete Damage State Probability P[Damage = DS | Sd]
0.777
0.103
0.095
0.025
0.000
0.000
None
Collapsed
Damage State
1 = Slight Damage | 2 = Moderate Damage
3 = Extensive Damage | 4 = Complete Damage

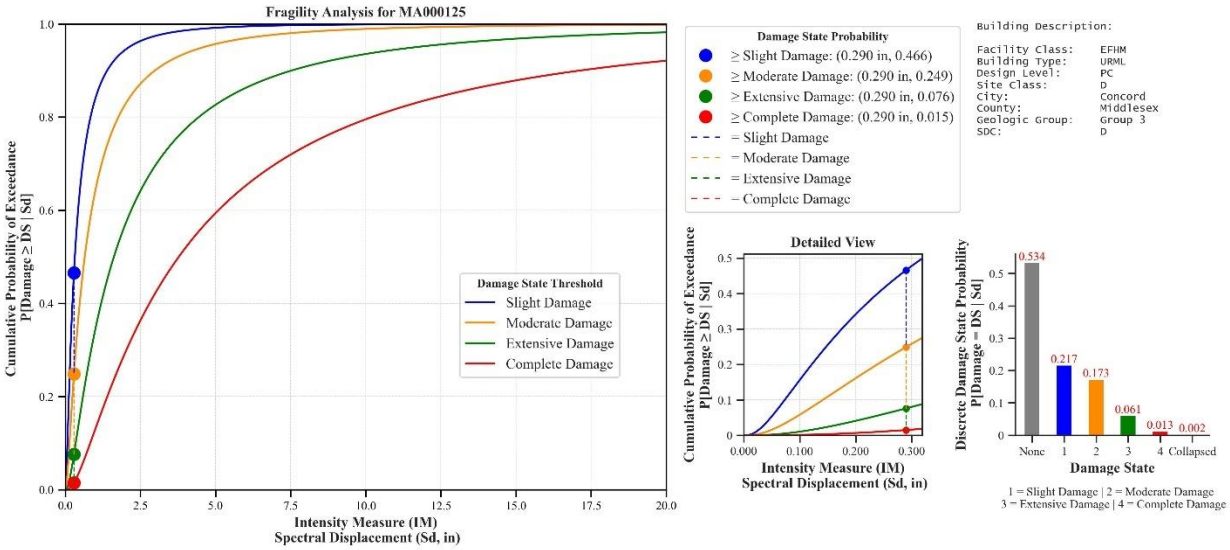
Fragility Analysis for MA000125
Cumulative Probability of Exceedance P[Damage ≥ DS | Sd]
Intensity Measure (IM) Spectral Displacement (Sd, in)
Damage State Threshold
Slight Damage
Moderate Damage
Extensive Damage
Complete Damage
Damage State Probability
≥ Slight Damage: (0.290 in, 0.466)
≥ Moderate Damage: (0.290 in, 0.249)
≥ Extensive Damage: (0.290 in, 0.076)
≥ Complete Damage: (0.290 in, 0.015)
Building Description:
Facility Class: EFHM
Building Type: URML
Design Level: PC
Site Class: D
City: Concord
County: Middlesex
Geologic Group: Group 3
SDC: D
Detailed View
Discrete Damage State Probability P[Damage = DS | Sd]
0.534
0.217
0.173
0.061
0.013
0.002
None
Collapsed
Damage State
1 = Slight Damage | 2 = Moderate Damage
3 = Extensive Damage | 4 = Complete Damage

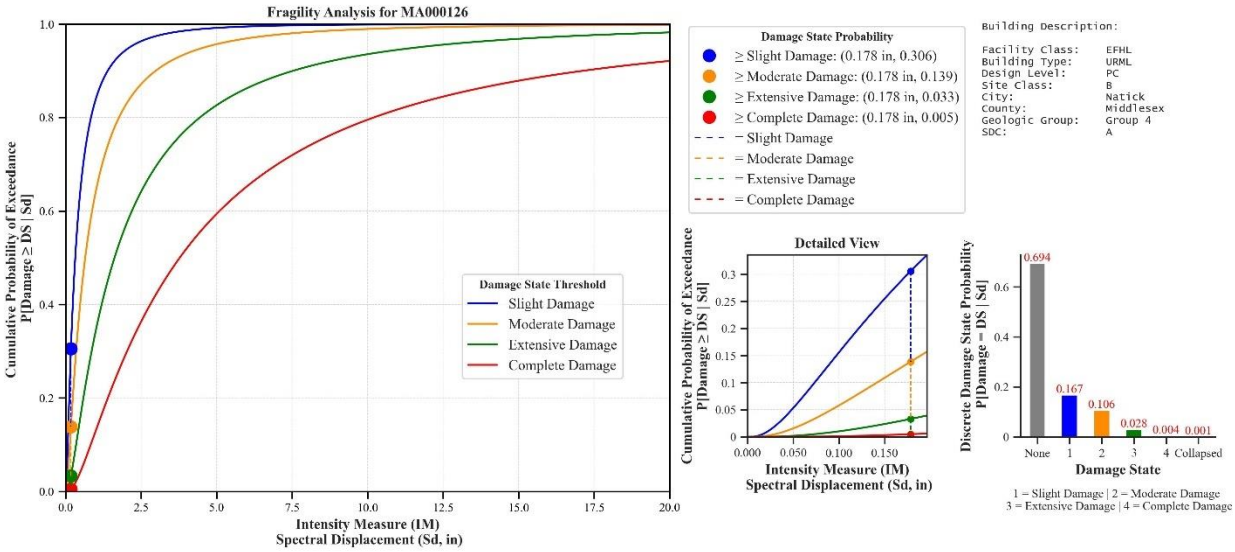
Fragility Analysis for MA000126
Cumulative Probability of Exceedance P[Damage ≥ DS | Sd]
Intensity Measure (IM) Spectral Displacement (Sd, in)
Damage State Threshold
Slight Damage
Moderate Damage
Extensive Damage
Complete Damage
Damage State Probability
≥ Slight Damage: (0.178 in, 0.306)
≥ Moderate Damage: (0.178 in, 0.139)
≥ Extensive Damage: (0.178 in, 0.033)
≥ Complete Damage: (0.178 in, 0.005)
Building Description:
Facility Class: EFHL
Building Type: URML
Design Level: PC
Site Class: B
City: Natick
County: Middlesex
Geologic Group: Group 4
SDC: A
Detailed View
Discrete Damage State Probability P[Damage = DS | Sd]
0.694
0.167
0.106
0.028
0.004
0.001
None
Collapsed
Damage State
1 = Slight Damage | 2 = Moderate Damage
3 = Extensive Damage | 4 = Complete Damage

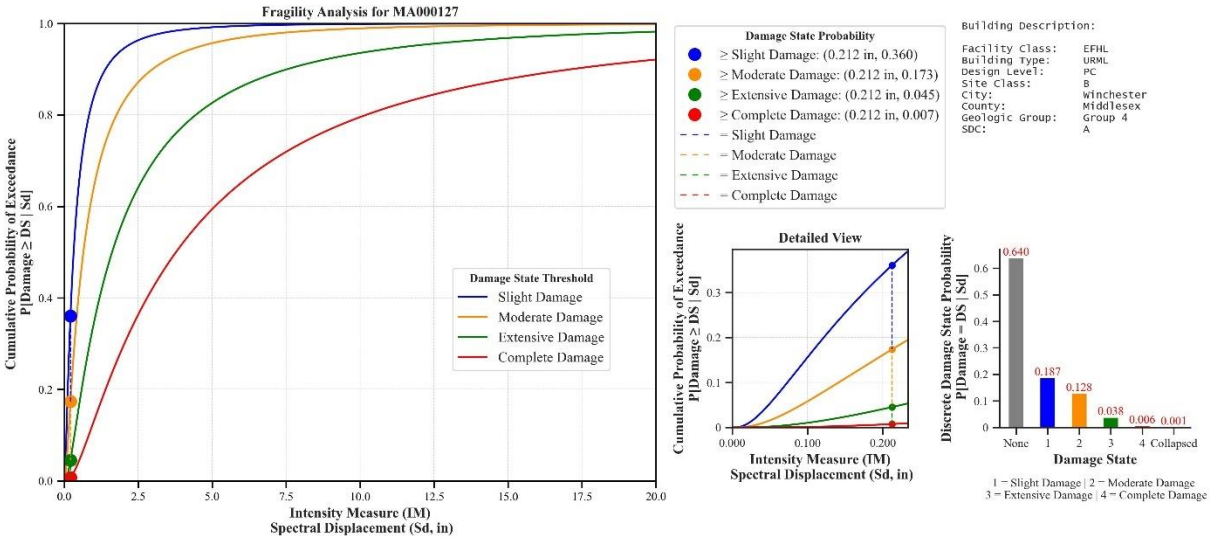
Fragility Analysis for MA000127
Cumulative Probability of Exceedance P[Damage ≥ DS | Sd]
Intensity Measure (IM) Spectral Displacement (Sd, in)
Damage State Threshold
Slight Damage
Moderate Damage
Extensive Damage
Complete Damage
Damage State Probability
≥ Slight Damage: (0.212 in, 0.360)
≥ Moderate Damage: (0.212 in, 0.173)
≥ Extensive Damage: (0.212 in, 0.045)
≥ Complete Damage: (0.212 in, 0.007)
Detailed View
Discrete Damage State Probability P[Damage = DS | Sd]
0.640
0.187
0.128
0.038
0.006
0.001
None
Collapsed
Damage State
1 = Slight Damage | 2 = Moderate Damage
3 = Extensive Damage | 4 = Complete Damage
Building Description:
Facility Class: EFHL
Building Type: URML
Design Level: PC
Site Class: B
City: Winchester
County: Middlesex
Geologic Group: Group 4
SDC: A

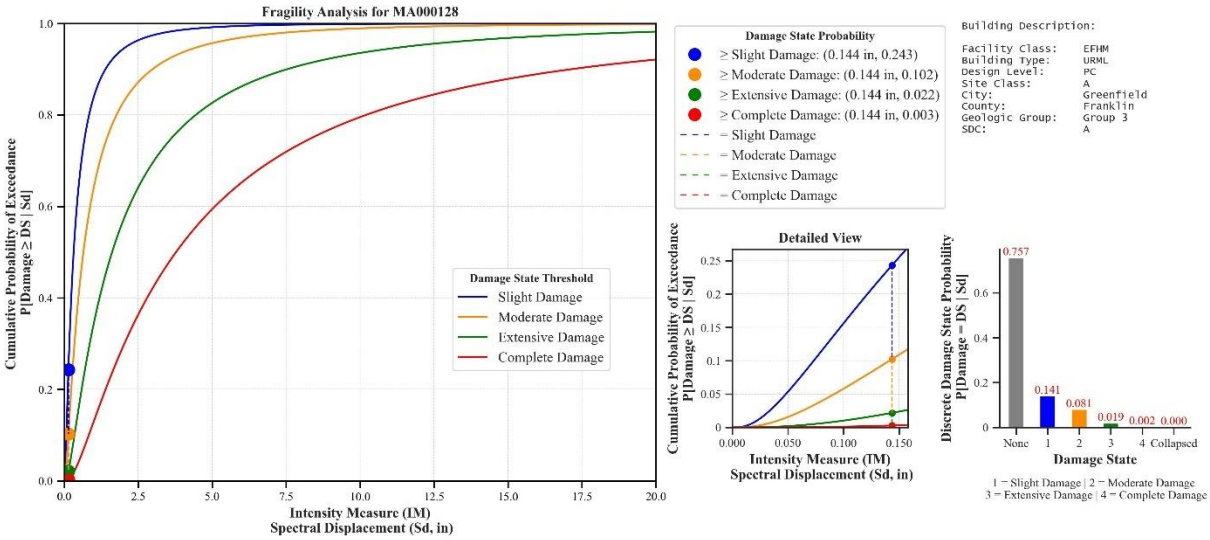
Fragility Analysis for MA000128
Cumulative Probability of Exceedance P[Damage ≥ DS | Sd]
Intensity Measure (IM) Spectral Displacement (Sd, in)
Damage State Threshold
Slight Damage
Moderate Damage
Extensive Damage
Complete Damage
Damage State Probability
≥ Slight Damage: (0.144 in, 0.243)
≥ Moderate Damage: (0.144 in, 0.102)
≥ Extensive Damage: (0.144 in, 0.022)
≥ Complete Damage: (0.144 in, 0.003)
Detailed View
Discrete Damage State Probability P[Damage = DS | Sd]
0.757
0.141
0.081
0.019
0.002
0.000
None
Collapsed
Damage State
1 = Slight Damage | 2 = Moderate Damage
3 = Extensive Damage | 4 = Complete Damage
Building Description:
Facility Class: EFHM
Building Type: URML
Design Level: PC
Site Class: A
City: Greenfield
County: Franklin
Geologic Group: Group 3
SDC: A

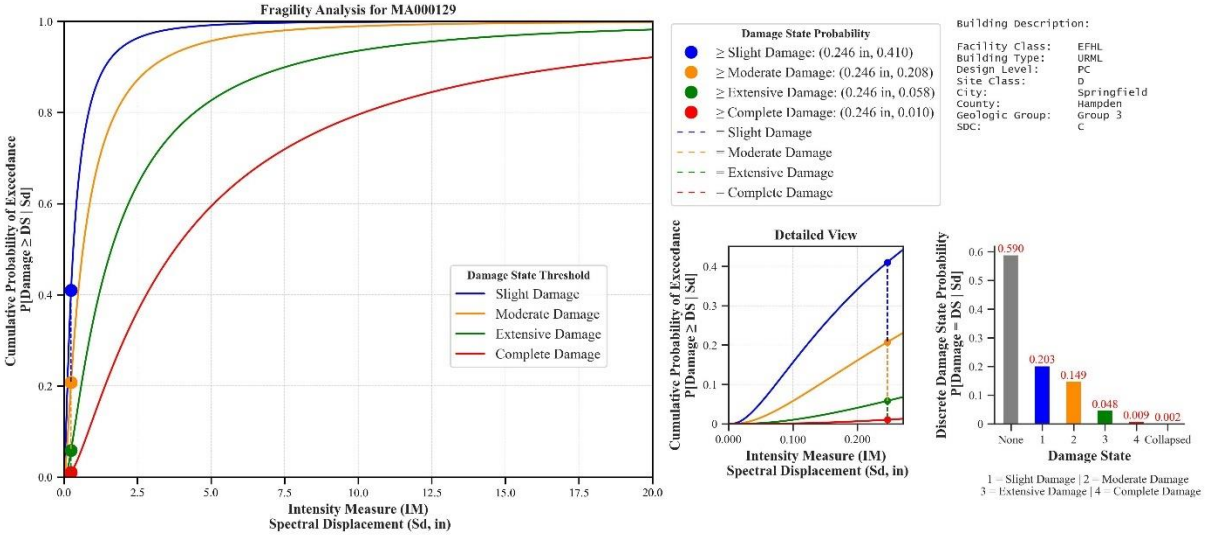
Fragility Analysis for MA000129
Cumulative Probability of Exceedance P[Damage ≥ DS | Sd]
Intensity Measure (IM) Spectral Displacement (Sd, in)
Damage State Threshold
Slight Damage
Moderate Damage
Extensive Damage
Complete Damage
Damage State Probability
≥ Slight Damage: (0.246 in, 0.410)
≥ Moderate Damage: (0.246 in, 0.208)
≥ Extensive Damage: (0.246 in, 0.058)
≥ Complete Damage: (0.246 in, 0.010)
Detailed View
Discrete Damage State Probability P[Damage = DS | Sd]
0.590
0.203
0.149
0.048
0.009
0.002
None
Collapsed
Damage State
1 = Slight Damage | 2 = Moderate Damage
3 = Extensive Damage | 4 = Complete Damage
Building Description:
Facility Class: EFHL
Building Type: URML
Design Level: PC
Site Class: D
City: Springfield
County: Hampden
Geologic Group: Group 3
SDC: C

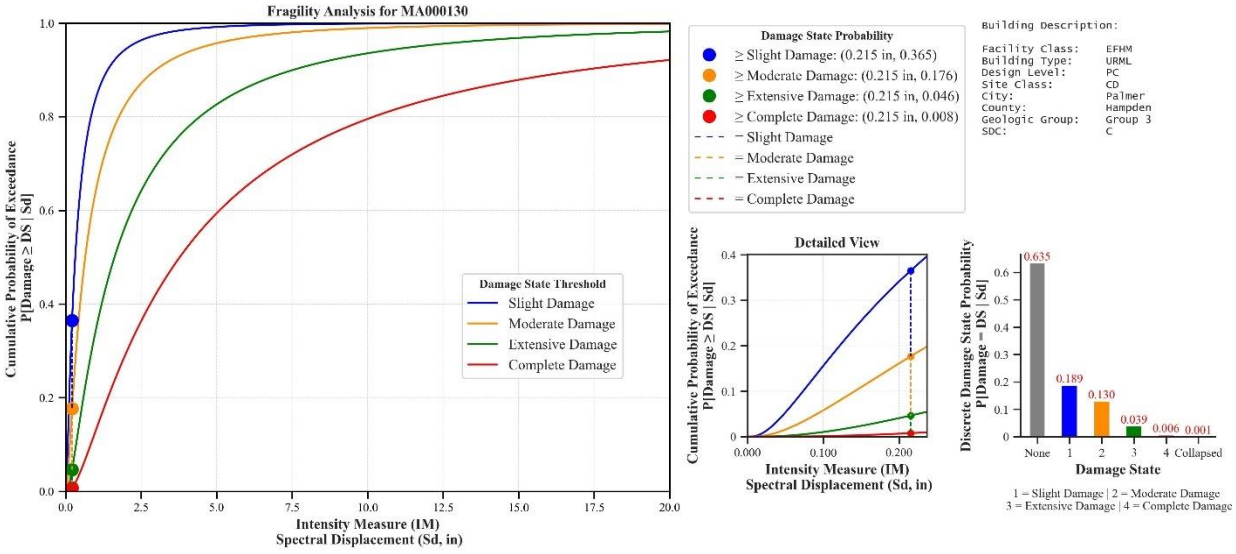
Fragility Analysis for MA000130
Cumulative Probability of Exceedance P[Damage ≥ DS | Sd]
Intensity Measure (IM) Spectral Displacement (Sd, in)
Damage State Threshold
Slight Damage
Moderate Damage
Extensive Damage
Complete Damage
Damage State Probability
≥ Slight Damage: (0.215 in, 0.365)
≥ Moderate Damage: (0.215 in, 0.176)
≥ Extensive Damage: (0.215 in, 0.046)
≥ Complete Damage: (0.215 in, 0.008)
Detailed View
Discrete Damage State Probability P[Damage = DS | Sd]
0.635
0.189
0.130
0.039
0.006
0.001
None
Collapsed
Damage State
1 = Slight Damage | 2 = Moderate Damage
3 = Extensive Damage | 4 = Complete Damage
Building Description:
Facility Class: EFHM
Building Type: URML
Design Level: PC
Site Class: CD
City: Palmer
County: Hampden
Geologic Group: Group 3
SDC: C

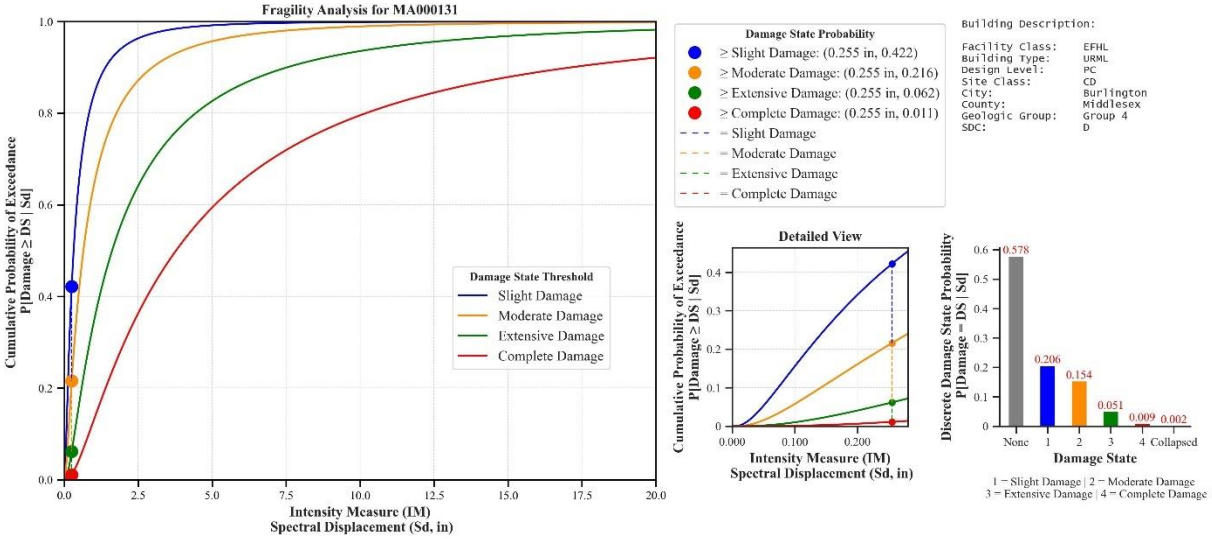
Fragility Analysis for MA000131
Cumulative Probability of Exceedance P[Damage ≥ DS | Sd]
Intensity Measure (IM) Spectral Displacement (Sd, in)
Damage State Threshold
Slight Damage
Moderate Damage
Extensive Damage
Complete Damage
Damage State Probability
≥ Slight Damage: (0.255 in, 0.422)
≥ Moderate Damage: (0.255 in, 0.216)
≥ Extensive Damage: (0.255 in, 0.062)
≥ Complete Damage: (0.255 in, 0.011)
Detailed View
Discrete Damage State Probability P[Damage = DS | Sd]
0.578
0.206
0.154
0.051
0.009
0.002
None
Collapsed
Damage State
1 = Slight Damage | 2 = Moderate Damage
3 = Extensive Damage | 4 = Complete Damage
Building Description:
Facility Class: EFHL
Building Type: URML
Design Level: PC
Site Class: CD
City: Burlington
County: Middlesex
Geologic Group: Group 4
SDC: D

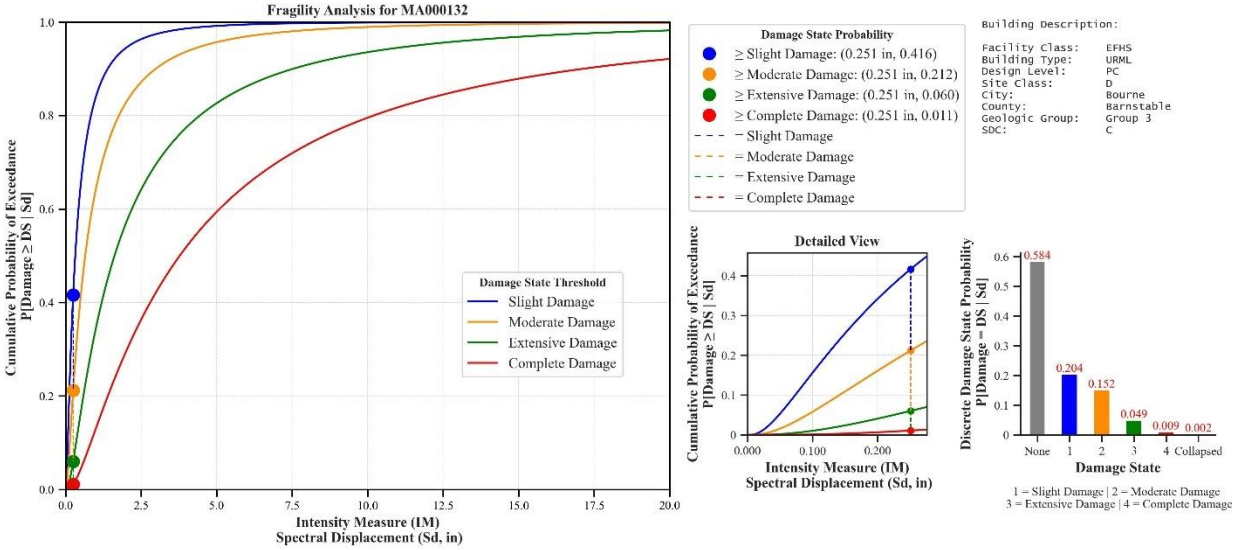
Fragility Analysis for MA000132
Cumulative Probability of Exceedance P[Damage ≥ DS | Sd]
Intensity Measure (IM) Spectral Displacement (Sd, in)
Damage State Threshold
Slight Damage
Moderate Damage
Extensive Damage
Complete Damage
Damage State Probability
≥ Slight Damage: (0.251 in, 0.416)
≥ Moderate Damage: (0.251 in, 0.212)
≥ Extensive Damage: (0.251 in, 0.060)
≥ Complete Damage: (0.251 in, 0.011)
Detailed View
Discrete Damage State Probability P[Damage = DS | Sd]
0.584
0.204
0.152
0.049
0.009
0.002
None
Collapsed
Damage State
1 = Slight Damage | 2 = Moderate Damage
3 = Extensive Damage | 4 = Complete Damage
Building Description:
Facility Class: EFHS
Building Type: URML
Design Level: PC
Site Class: D
City: Bourne
County: Barnstable
Geologic Group: Group 3
SDC: C

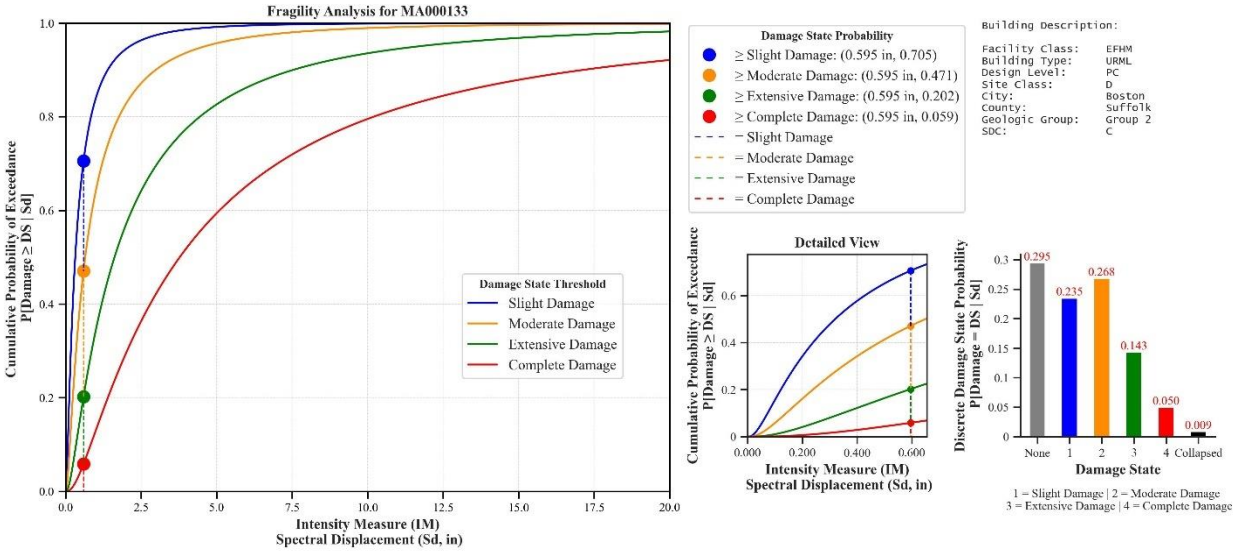
Fragility Analysis for MA000133
Cumulative Probability of Exceedance P[Damage ≥ DS | Sd]
Intensity Measure (IM) Spectral Displacement (Sd, in)
Damage State Threshold
Slight Damage
Moderate Damage
Extensive Damage
Complete Damage
Damage State Probability
≥ Slight Damage: (0.595 in, 0.705)
≥ Moderate Damage: (0.595 in, 0.471)
≥ Extensive Damage: (0.595 in, 0.202)
≥ Complete Damage: (0.595 in, 0.059)
Building Description:
Facility Class: EFHM
Building Type: URML
Design Level: PC
Site Class: D
City: Boston
County: Suffolk
Geologic Group: Group 2
SDC: C
Detailed View
Discrete Damage State Probability P[Damage = DS | Sd]
0.295
0.235
0.268
0.143
0.050
0.009
None 1 2 3 4 Collapsed
Damage State
1 = Slight Damage | 2 = Moderate Damage
3 = Extensive Damage | 4 = Complete Damage

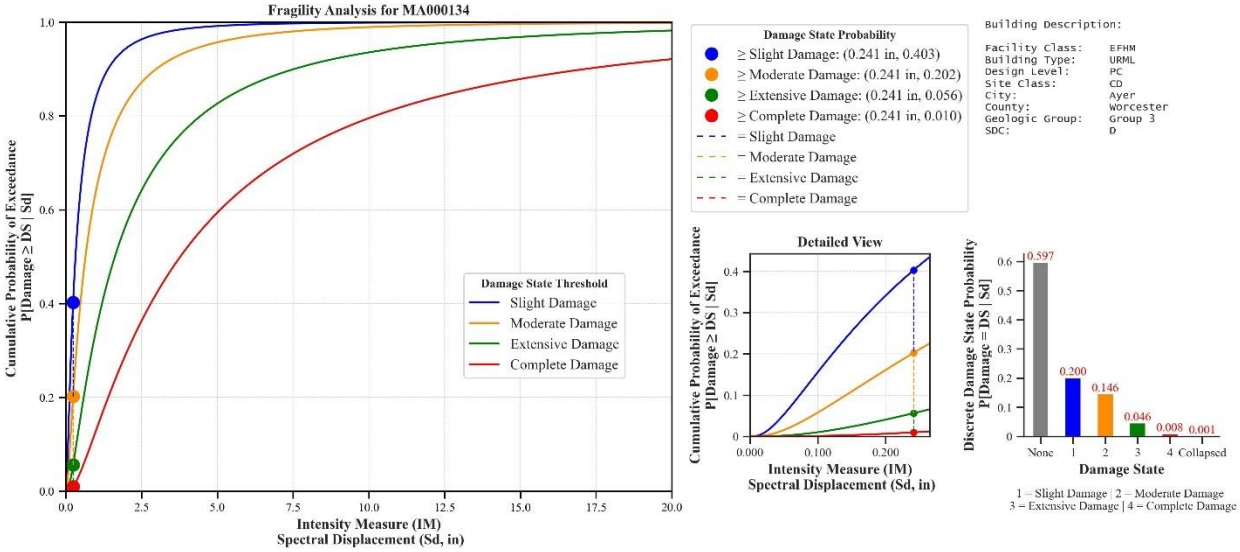
Fragility Analysis for MA000134
Cumulative Probability of Exceedance P[Damage ≥ DS | Sd]
Intensity Measure (IM) Spectral Displacement (Sd, in)
Damage State Threshold
Slight Damage
Moderate Damage
Extensive Damage
Complete Damage
Damage State Probability
≥ Slight Damage: (0.241 in, 0.403)
≥ Moderate Damage: (0.241 in, 0.202)
≥ Extensive Damage: (0.241 in, 0.056)
≥ Complete Damage: (0.241 in, 0.010)
Building Description:
Facility Class: EFHM
Building Type: URML
Design Level: PC
Site Class: CD
City: Ayer
County: Worcester
Geologic Group: Group 3
SDC: D
Detailed View
Discrete Damage State Probability P[Damage = DS | Sd]
0.597
0.200
0.146
0.046
0.008
0.001
None 1 2 3 4 Collapsed
Damage State
1 = Slight Damage | 2 = Moderate Damage
3 = Extensive Damage | 4 = Complete Damage

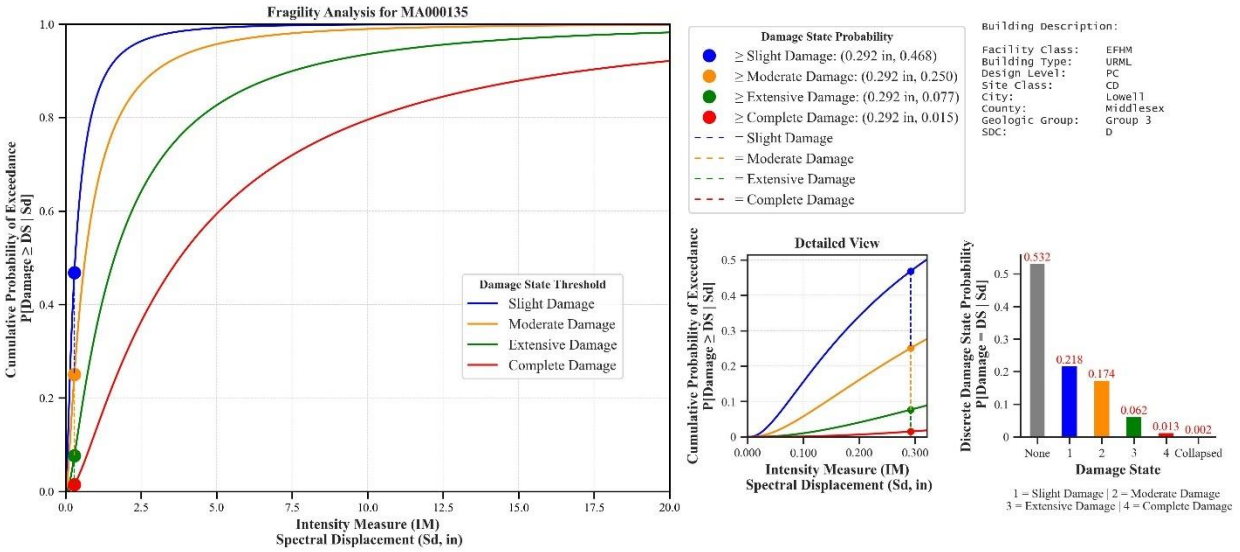
Fragility Analysis for MA000135
Cumulative Probability of Exceedance P[Damage ≥ DS | Sd]
Intensity Measure (IM) Spectral Displacement (Sd, in)
Damage State Threshold
Slight Damage
Moderate Damage
Extensive Damage
Complete Damage
Damage State Probability
≥ Slight Damage: (0.292 in, 0.468)
≥ Moderate Damage: (0.292 in, 0.250)
≥ Extensive Damage: (0.292 in, 0.077)
≥ Complete Damage: (0.292 in, 0.015)
Building Description:
Facility Class: EFHM
Building Type: URML
Design Level: PC
Site Class: CD
City: Lowell
County: Middlesex
Geologic Group: Group 3
SDC: D
Detailed View
Discrete Damage State Probability P[Damage = DS | Sd]
0.532
0.218
0.174
0.062
0.013
0.002
None 1 2 3 4 Collapsed
Damage State
1 = Slight Damage | 2 = Moderate Damage
3 = Extensive Damage | 4 = Complete Damage

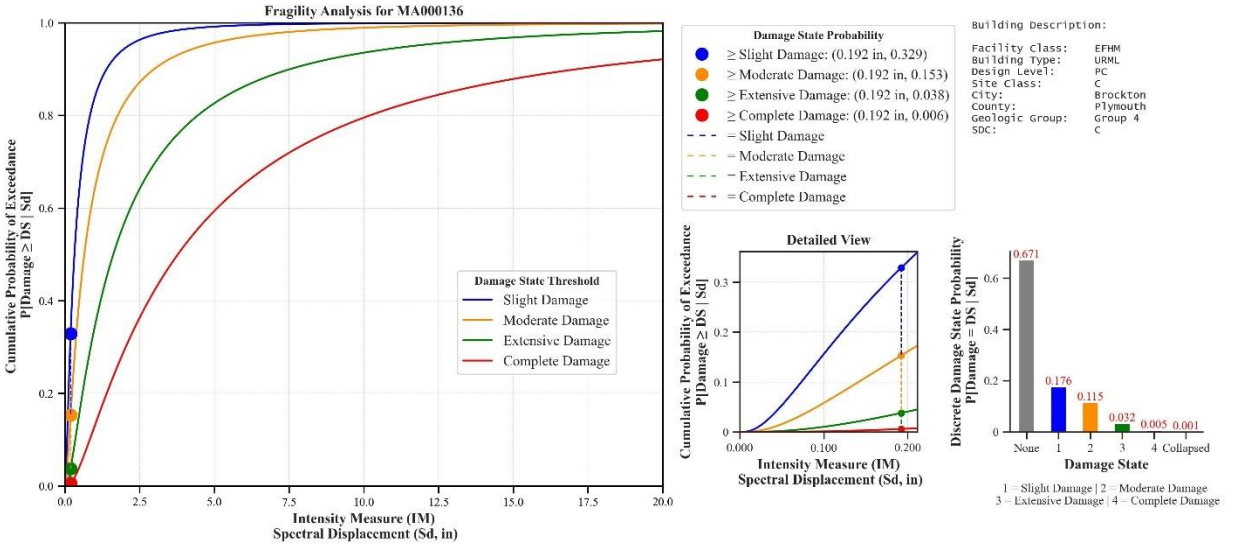
Fragility Analysis for MA000136
Cumulative Probability of Exceedance P[Damage ≥ DS | Sd]
Intensity Measure (IM) Spectral Displacement (Sd, in)
Damage State Threshold
Slight Damage
Moderate Damage
Extensive Damage
Complete Damage
Damage State Probability
≥ Slight Damage: (0.192 in, 0.329)
≥ Moderate Damage: (0.192 in, 0.153)
≥ Extensive Damage: (0.192 in, 0.038)
≥ Complete Damage: (0.192 in, 0.006)
= Slight Damage
= Moderate Damage
= Extensive Damage
= Complete Damage
Building Description:
Facility Class: EFHM
Building Type: URML
Design Level: PC
Site Class: C
City: Brockton
County: Plymouth
Geologic Group: Group 4
SDC: C
Detailed View
Discrete Damage State Probability P[Damage = DS | Sd]
0.671
0.176
0.115
0.032
0.005
0.001
None
1
2
3
4 Collapsed
Damage State
1 = Slight Damage | 2 = Moderate Damage
3 = Extensive Damage | 4 = Complete Damage

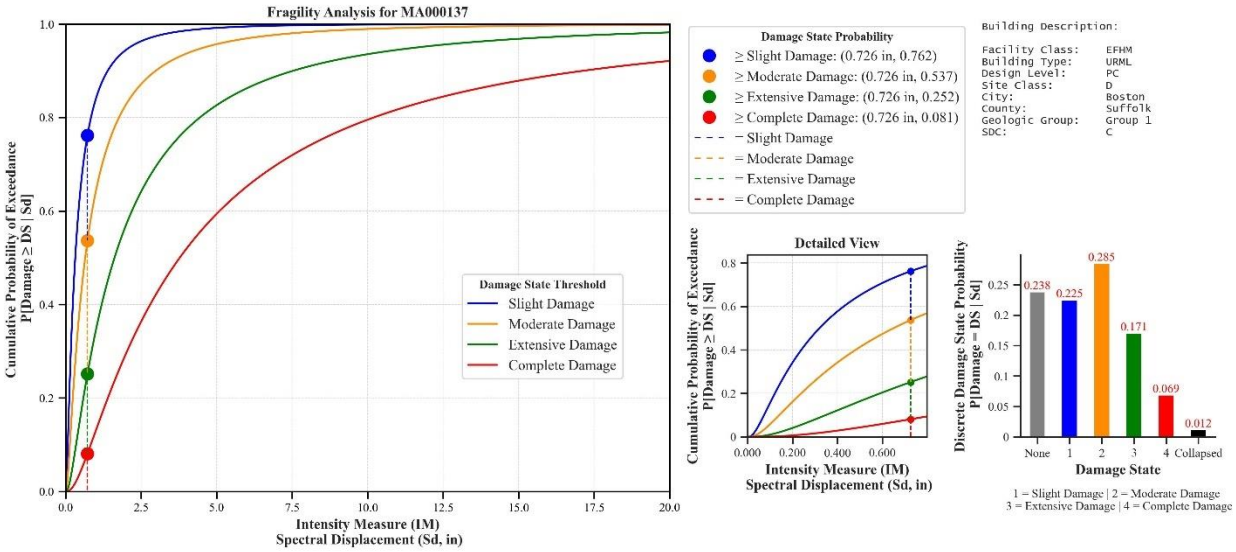
Fragility Analysis for MA000137
Cumulative Probability of Exceedance P[Damage ≥ DS | Sd]
Intensity Measure (IM) Spectral Displacement (Sd, in)
Damage State Threshold
Slight Damage
Moderate Damage
Extensive Damage
Complete Damage
Damage State Probability
≥ Slight Damage: (0.726 in, 0.762)
≥ Moderate Damage: (0.726 in, 0.537)
≥ Extensive Damage: (0.726 in, 0.252)
≥ Complete Damage: (0.726 in, 0.081)
= Slight Damage
= Moderate Damage
= Extensive Damage
= Complete Damage
Building Description:
Facility Class: EFHM
Building Type: URML
Design Level: PC
Site Class: D
City: Boston
County: Suffolk
Geologic Group: Group 1
SDC: C
Detailed View
Discrete Damage State Probability P[Damage = DS | Sd]
0.238
0.225
0.285
0.171
0.069
0.012
None
1
2
3
4 Collapsed
Damage State
1 = Slight Damage | 2 = Moderate Damage
3 = Extensive Damage | 4 = Complete Damage

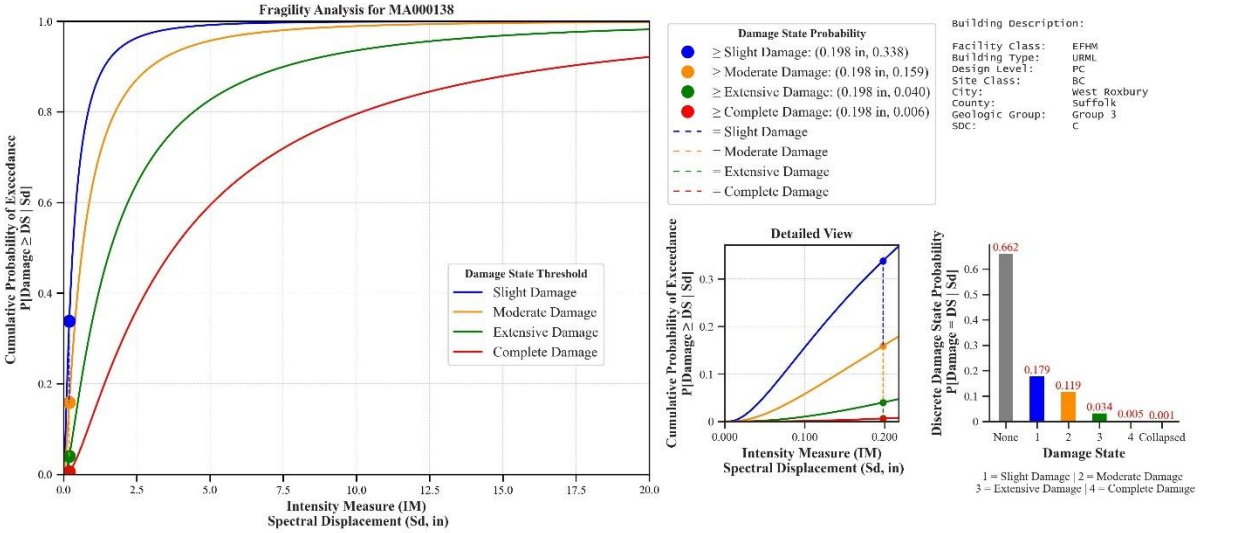
Fragility Analysis for MA000138
Cumulative Probability of Exceedance P[Damage ≥ DS | Sd]
Intensity Measure (IM) Spectral Displacement (Sd, in)
Damage State Threshold
Slight Damage
Moderate Damage
Extensive Damage
Complete Damage
Damage State Probability
≥ Slight Damage: (0.198 in, 0.338)
≥ Moderate Damage: (0.198 in, 0.159)
≥ Extensive Damage: (0.198 in, 0.040)
≥ Complete Damage: (0.198 in, 0.006)
= Slight Damage
= Moderate Damage
= Extensive Damage
= Complete Damage
Building Description:
Facility Class: EFHM
Building Type: URML
Design Level: PC
Site Class: BC
City: West Roxbury
County: Suffolk
Geologic Group: Group 3
SDC: C
Detailed View
Discrete Damage State Probability P[Damage = DS | Sd]
0.662
0.179
0.119
0.034
0.005
0.001
None
1
2
3
4 Collapsed
Damage State
1 = Slight Damage | 2 = Moderate Damage
3 = Extensive Damage | 4 = Complete Damage

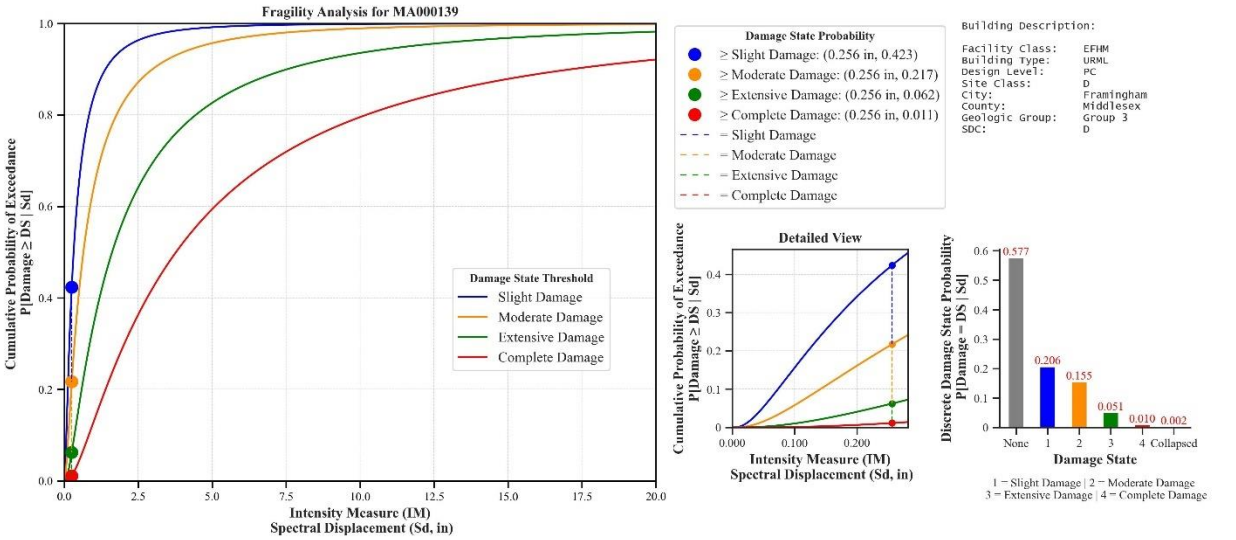
Fragility Analysis for MA000139
Cumulative Probability of Exceedance P[Damage ≥ DS | Sd]
Intensity Measure (IM) Spectral Displacement (Sd, in)
Damage State Threshold
Slight Damage
Moderate Damage
Extensive Damage
Complete Damage
Damage State Probability
≥ Slight Damage: (0.256 in, 0.423)
≥ Moderate Damage: (0.256 in, 0.217)
≥ Extensive Damage: (0.256 in, 0.062)
≥ Complete Damage: (0.256 in, 0.011)
Building Description:
Facility Class: EFHM
Building Type: URML
Design Level: PC
Site Class: D
City: Framingham
County: Middlesex
Geologic Group: Group 3
SDC: D
Detailed View
Discrete Damage State Probability P[Damage = DS | Sd]
0.577
0.206
0.155
0.051
0.010
0.002
None 1 2 3 4 Collapsed
Damage State
1 = Slight Damage | 2 = Moderate Damage
3 = Extensive Damage | 4 = Complete Damage

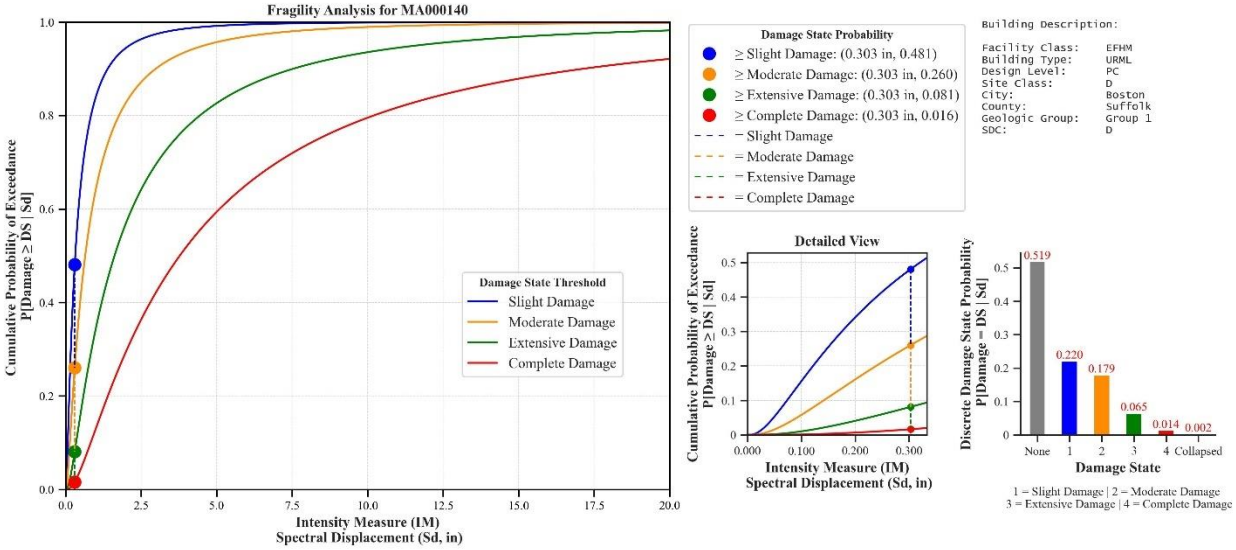
Fragility Analysis for MA000140
Cumulative Probability of Exceedance P[Damage ≥ DS | Sd]
Intensity Measure (IM) Spectral Displacement (Sd, in)
Damage State Threshold
Slight Damage
Moderate Damage
Extensive Damage
Complete Damage
Damage State Probability
≥ Slight Damage: (0.303 in, 0.481)
≥ Moderate Damage: (0.303 in, 0.260)
≥ Extensive Damage: (0.303 in, 0.081)
≥ Complete Damage: (0.303 in, 0.016)
Building Description:
Facility Class: EFHM
Building Type: URML
Design Level: PC
Site Class: D
City: Boston
County: Suffolk
Geologic Group: Group 1
SDC: D
Detailed View
Discrete Damage State Probability P[Damage = DS | Sd]
0.519
0.220
0.179
0.065
0.014
0.002
None 1 2 3 4 Collapsed
Damage State
1 = Slight Damage | 2 = Moderate Damage
3 = Extensive Damage | 4 = Complete Damage

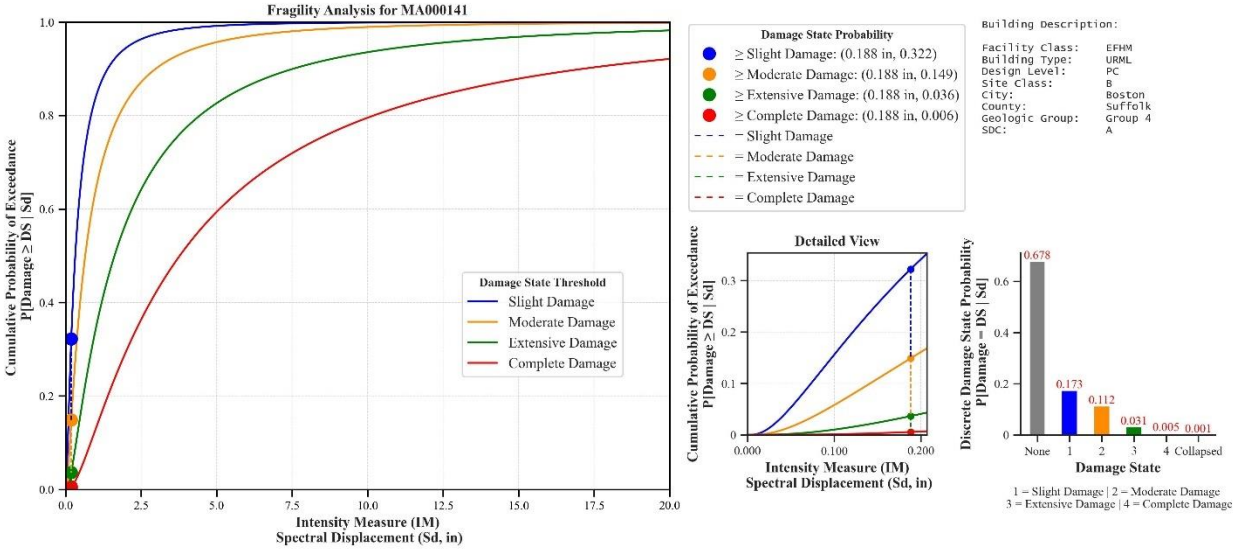
Fragility Analysis for MA000141
Cumulative Probability of Exceedance P[Damage ≥ DS | Sd]
Intensity Measure (IM) Spectral Displacement (Sd, in)
Damage State Threshold
Slight Damage
Moderate Damage
Extensive Damage
Complete Damage
Damage State Probability
≥ Slight Damage: (0.188 in, 0.322)
≥ Moderate Damage: (0.188 in, 0.149)
≥ Extensive Damage: (0.188 in, 0.036)
≥ Complete Damage: (0.188 in, 0.006)
Building Description:
Facility Class: EFHM
Building Type: URML
Design Level: PC
Site Class: B
City: Boston
County: Suffolk
Geologic Group: Group 4
SDC: A
Detailed View
Discrete Damage State Probability P[Damage = DS | Sd]
0.678
0.173
0.112
0.031
0.005
0.001
None 1 2 3 4 Collapsed
Damage State
1 = Slight Damage | 2 = Moderate Damage
3 = Extensive Damage | 4 = Complete Damage

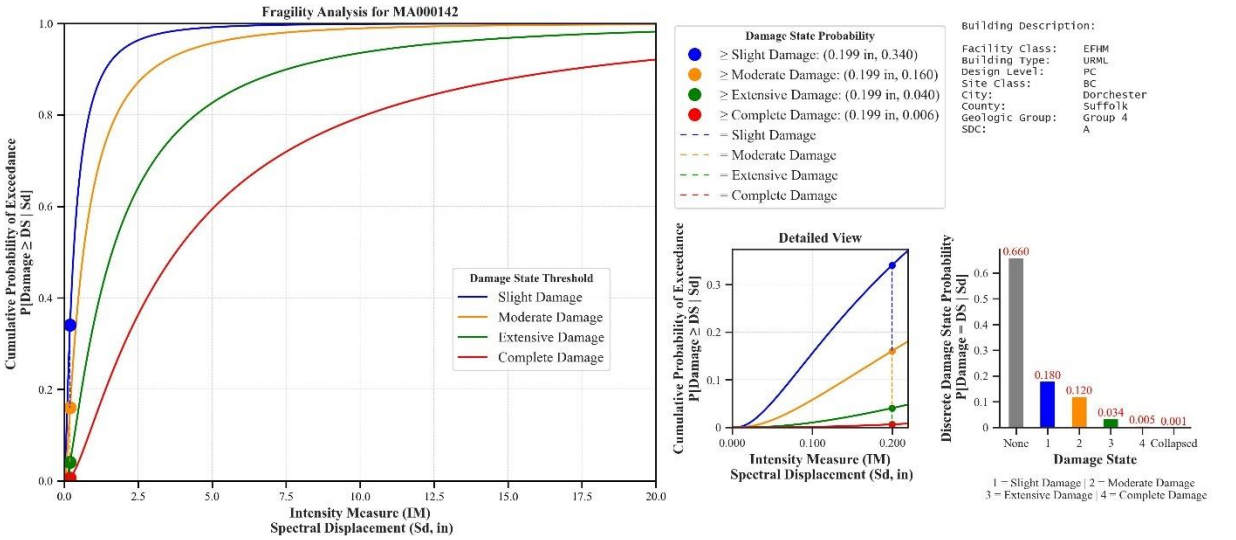
Fragility Analysis for MA000142
Cumulative Probability of Exceedance P[Damage ≥ DS | Sd]
Intensity Measure (IM) Spectral Displacement (Sd, in)
Damage State Threshold
Slight Damage
Moderate Damage
Extensive Damage
Complete Damage
Damage State Probability
≥ Slight Damage: (0.199 in, 0.340)
≥ Moderate Damage: (0.199 in, 0.160)
≥ Extensive Damage: (0.199 in, 0.040)
≥ Complete Damage: (0.199 in, 0.006)
Building Description:
Facility Class: EFHM
Building Type: URML
Design Level: PC
Site Class: BC
City: Dorchester
County: Suffolk
Geologic Group: Group 4
SDC: A
Detailed View
Discrete Damage State Probability P[Damage = DS | Sd]
0.660
0.180
0.120
0.034
0.005
0.001
None 1 2 3 4 Collapsed
Damage State
1 = Slight Damage | 2 = Moderate Damage
3 = Extensive Damage | 4 = Complete Damage

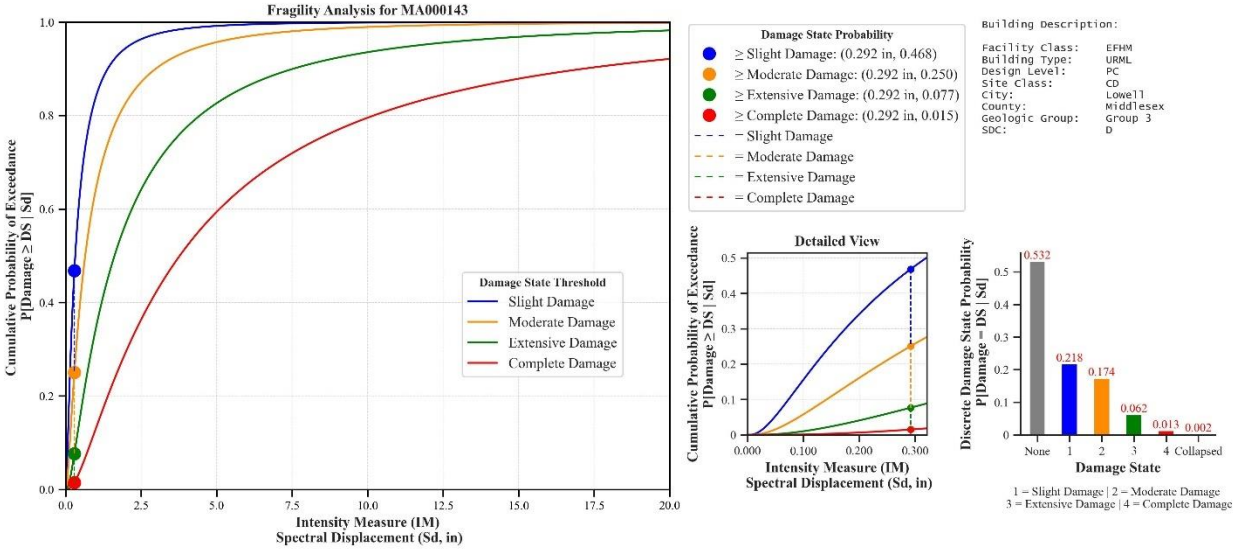
Fragility Analysis for MA000143
Cumulative Probability of Exceedance P[Damage ≥ DS | Sd]
Intensity Measure (IM) Spectral Displacement (Sd, in)
Damage State Threshold
Slight Damage
Moderate Damage
Extensive Damage
Complete Damage
Damage State Probability
≥ Slight Damage: (0.292 in, 0.468)
≥ Moderate Damage: (0.292 in, 0.250)
≥ Extensive Damage: (0.292 in, 0.077)
≥ Complete Damage: (0.292 in, 0.015)
Building Description:
Facility Class: EFHM
Building Type: URML
Design Level: PC
Site Class: CD
City: Lowell
County: Middlesex
Geologic Group: Group 3
SDC: D
Detailed View
Discrete Damage State Probability P[Damage = DS | Sd]
0.532
0.218
0.174
0.062
0.013
0.002
None 1 2 3 4 Collapsed
Damage State
1 = Slight Damage | 2 = Moderate Damage
3 = Extensive Damage | 4 = Complete Damage

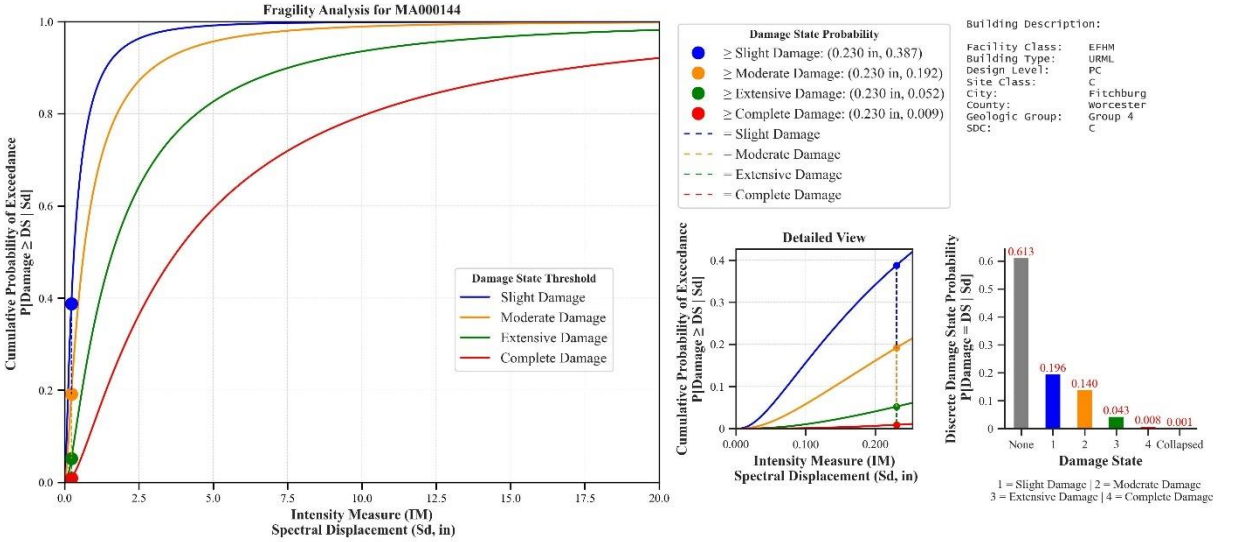
Fragility Analysis for MA000144
Cumulative Probability of Exceedance P[Damage ≥ DS | Sd]
Intensity Measure (IM) Spectral Displacement (Sd, in)
Damage State Threshold
Slight Damage
Moderate Damage
Extensive Damage
Complete Damage
Damage State Probability
≥ Slight Damage: (0.230 in, 0.387)
≥ Moderate Damage: (0.230 in, 0.192)
≥ Extensive Damage: (0.230 in, 0.052)
≥ Complete Damage: (0.230 in, 0.009)
Building Description:
Facility Class: EFHM
Building Type: URML
Design Level: PC
Site Class: C
City: Fitchburg
County: Worcester
Geologic Group: Group 4
SDC: C
Detailed View
Discrete Damage State Probability P[Damage = DS | Sd]
0.613
0.196
0.140
0.043
0.008
0.001
None 1 2 3 4 Collapsed
Damage State
1 = Slight Damage | 2 = Moderate Damage
3 = Extensive Damage | 4 = Complete Damage

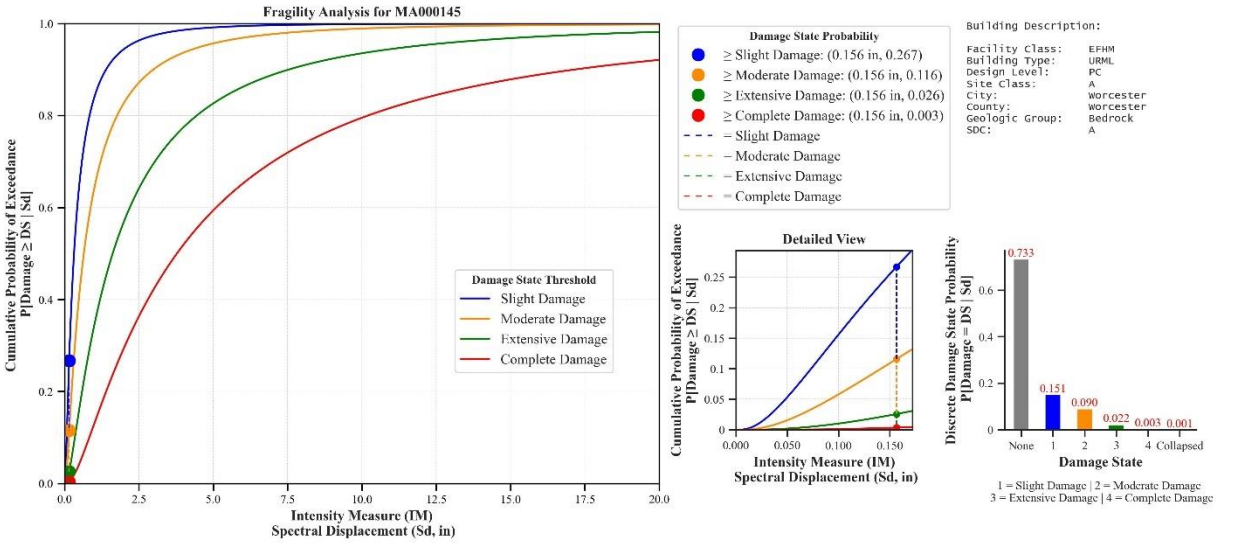
Fragility Analysis for MA000145
Cumulative Probability of Exceedance P[Damage ≥ DS | Sd]
Intensity Measure (IM) Spectral Displacement (Sd, in)
Damage State Threshold
Slight Damage
Moderate Damage
Extensive Damage
Complete Damage
Damage State Probability
≥ Slight Damage: (0.156 in, 0.267)
≥ Moderate Damage: (0.156 in, 0.116)
≥ Extensive Damage: (0.156 in, 0.026)
≥ Complete Damage: (0.156 in, 0.003)
Detailed View
Discrete Damage State Probability P[Damage = DS | Sd]
0.733
0.151
0.090
0.022
0.003
0.001
None
Collapsed
Damage State
1 = Slight Damage | 2 = Moderate Damage
3 = Extensive Damage | 4 = Complete Damage
Building Description:
Facility Class: EFHM
Building Type: URML
Design Level: PC
Site Class: A
City: Worcester
County: Worcester
Geologic Group: Bedrock
SDC: A

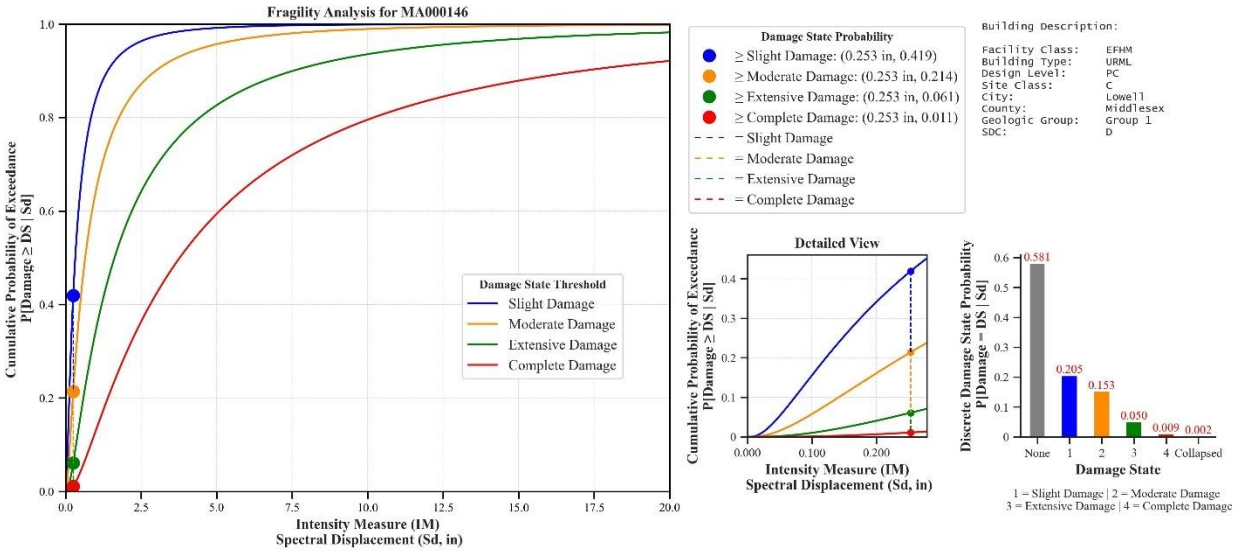
Fragility Analysis for MA000146
Cumulative Probability of Exceedance P[Damage ≥ DS | Sd]
Intensity Measure (IM) Spectral Displacement (Sd, in)
Damage State Threshold
Slight Damage
Moderate Damage
Extensive Damage
Complete Damage
Damage State Probability
≥ Slight Damage: (0.253 in, 0.419)
≥ Moderate Damage: (0.253 in, 0.214)
≥ Extensive Damage: (0.253 in, 0.061)
≥ Complete Damage: (0.253 in, 0.011)
Dctailed View
Discrete Damage State Probability P[Damage = DS | Sd]
0.581
0.205
0.153
0.050
0.009
0.002
None
Collapsed
Damage State
1 = Slight Damage | 2 = Moderate Damage
3 = Extensive Damage | 4 = Complete Damage
Building Description:
Facility Class: EFHM
Building Type: URML
Design Level: PC
Site Class: C
City: Lowell
County: Middlesex
Geologic Group: Group 1
SDC: D

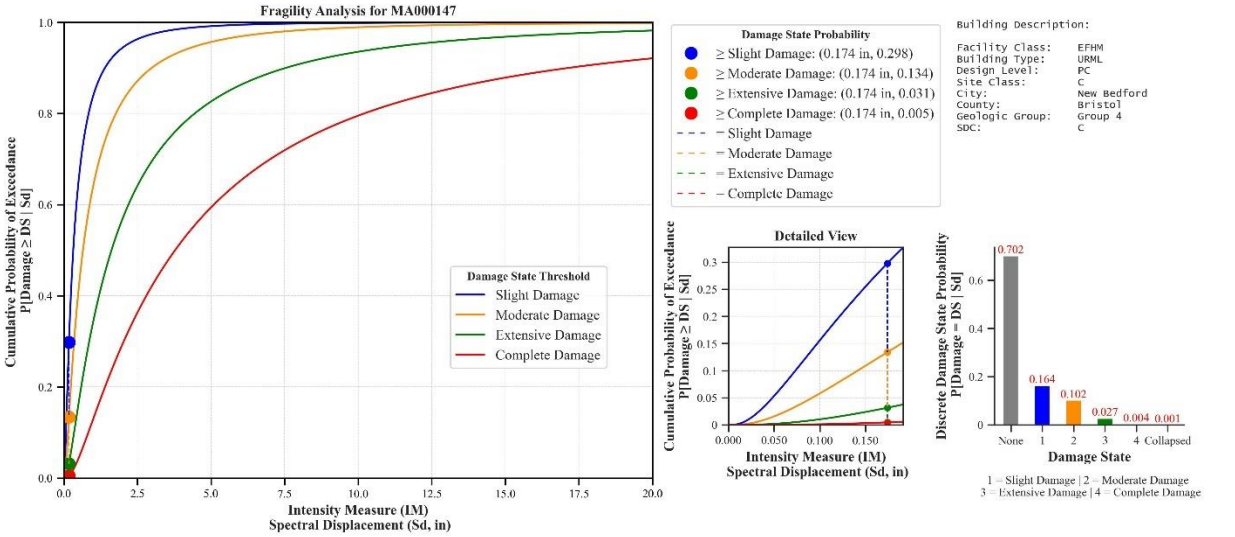
Fragility Analysis for MA000147
Cumulative Probability of Exceedance P[Damage ≥ DS | Sd]
Intensity Measure (IM) Spectral Displacement (Sd, in)
Damage State Threshold
Slight Damage
Moderate Damage
Extensive Damage
Complete Damage
Damage State Probability
≥ Slight Damage: (0.174 in, 0.298)
≥ Moderate Damage: (0.174 in, 0.134)
≥ Extensive Damage: (0.174 in, 0.031)
≥ Complete Damage: (0.174 in, 0.005)
Dctailed View
Discrete Damage State Probability P[Damage = DS | Sd]
0.702
0.164
0.102
0.027
0.004
0.001
None
Collapsed
Damage State
1 = Slight Damage | 2 = Moderate Damage
3 = Extensive Damage | 4 = Complete Damage
Building Description:
Facility Class: EFHM
Building Type: URML
Design Level: PC
Site Class: C
City: New Bedford
County: Bristol
Geologic Group: Group 4
SDC: C

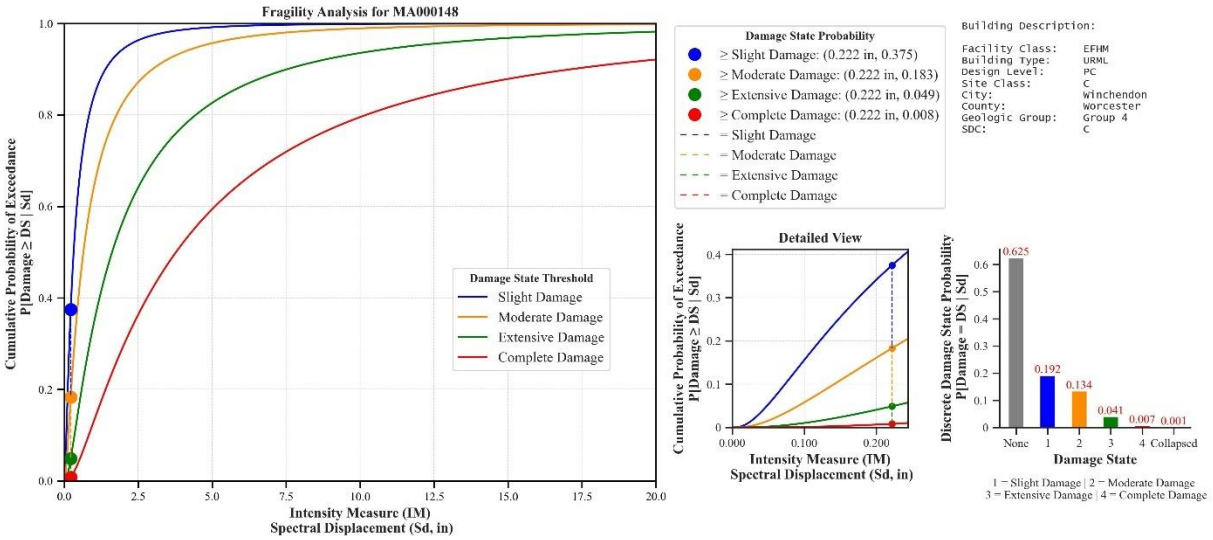
Fragility Analysis for MA000148
Cumulative Probability of Exceedance P[Damage ≥ DS | Sd]
Intensity Measure (IM) Spectral Displacement (Sd, in)
Damage State Threshold
Slight Damage
Moderate Damage
Extensive Damage
Complete Damage
Damage State Probability
≥ Slight Damage: (0.222 in, 0.375)
≥ Moderate Damage: (0.222 in, 0.183)
≥ Extensive Damage: (0.222 in, 0.049)
≥ Complete Damage: (0.222 in, 0.008)
Building Description:
Facility Class: EFHM
Building Type: URML
Design Level: PC
Site Class: C
City: Winchendon
County: Worcester
Geologic Group: Group 4
SDC: C
Detailed View
Discrete Damage State Probability P[Damage = DS | Sd]
0.625
0.192
0.134
0.041
0.007
0.001
None 1 2 3 4 Collapsed
Damage State
1 = Slight Damage | 2 = Moderate Damage
3 = Extensive Damage | 4 = Complete Damage

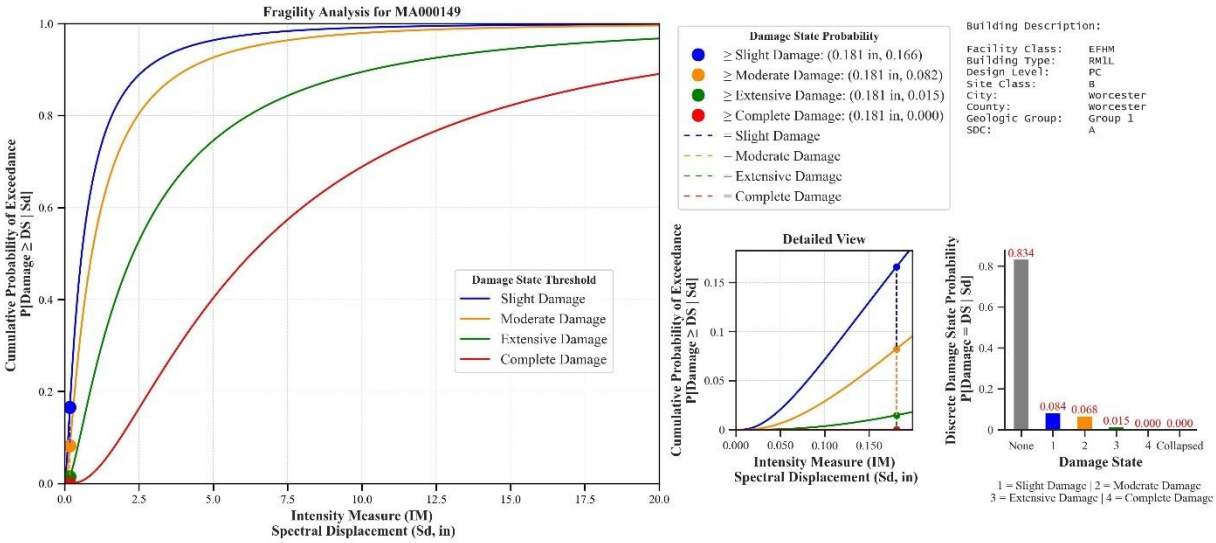
Fragility Analysis for MA000149
Cumulative Probability of Exceedance P[Damage ≥ DS | Sd]
Intensity Measure (IM) Spectral Displacement (Sd, in)
Damage State Threshold
Slight Damage
Moderate Damage
Extensive Damage
Complete Damage
Damage State Probability
≥ Slight Damage: (0.181 in, 0.166)
≥ Moderate Damage: (0.181 in, 0.082)
≥ Extensive Damage: (0.181 in, 0.015)
≥ Complete Damage: (0.181 in, 0.000)
Building Description:
Facility Class: EFHM
Building Type: RM1L
Design Level: PC
Site Class: B
City: Worcester
County: Worcester
Geologic Group: Group 1
SDC: A
Detailed View
Discrete Damage State Probability P[Damage = DS | Sd]
0.834
0.084
0.068
0.015
0.000
0.000
None 1 2 3 4 Collapsed
Damage State
1 = Slight Damage | 2 = Moderate Damage
3 = Extensive Damage | 4 = Complete Damage

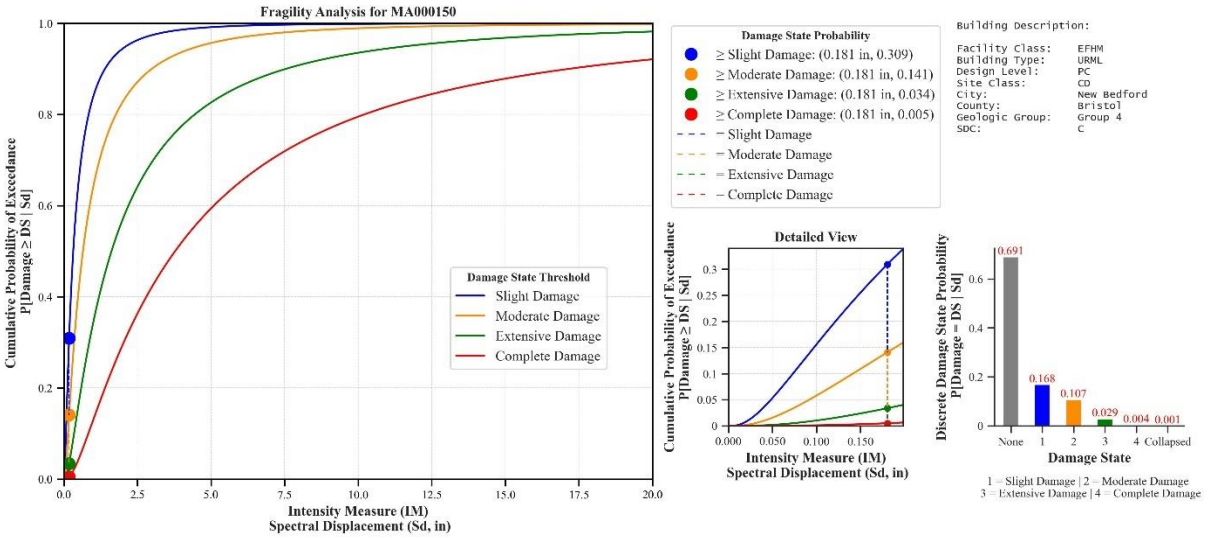
Fragility Analysis for MA000150
Cumulative Probability of Exceedance P[Damage ≥ DS | Sd]
Intensity Measure (IM) Spectral Displacement (Sd, in)
Damage State Threshold
Slight Damage
Moderate Damage
Extensive Damage
Complete Damage
Damage State Probability
≥ Slight Damage: (0.181 in, 0.309)
≥ Moderate Damage: (0.181 in, 0.141)
≥ Extensive Damage: (0.181 in, 0.034)
≥ Complete Damage: (0.181 in, 0.005)
Building Description:
Facility Class: EFHM
Building Type: URML
Design Level: PC
Site Class: CD
City: New Bedford
County: Bristol
Geologic Group: Group 4
SDC: C
Detailed View
Discrete Damage State Probability P[Damage = DS | Sd]
0.691
0.168
0.107
0.029
0.004
0.001
None 1 2 3 4 Collapsed
Damage State
1 = Slight Damage | 2 = Moderate Damage
3 = Extensive Damage | 4 = Complete Damage

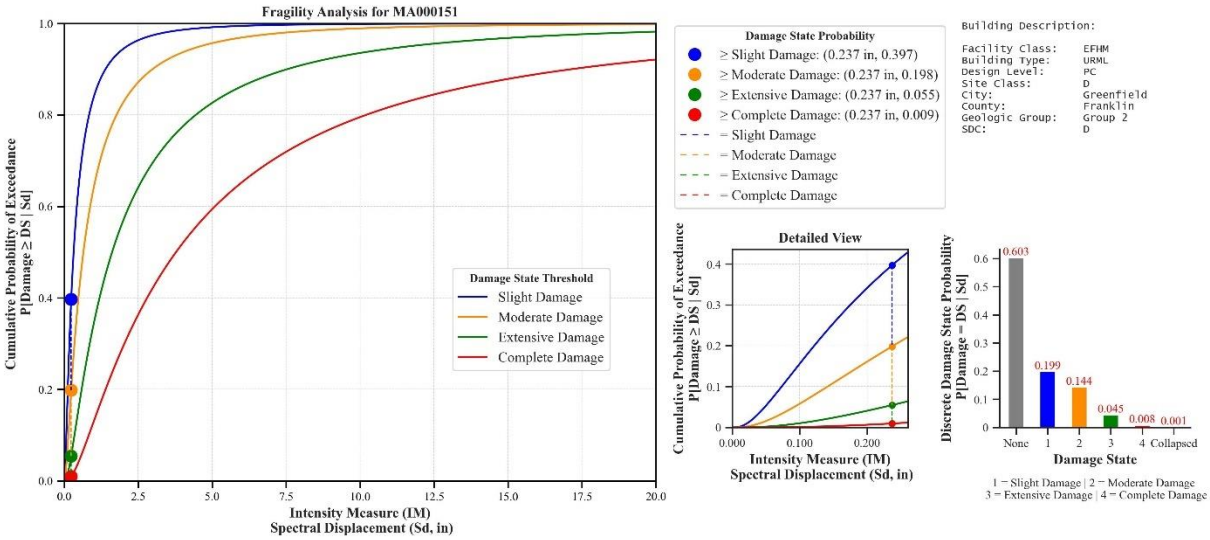
Fragility Analysis for MA000151
Cumulative Probability of Exceedance P[Damage ≥ DS | Sd]
Intensity Measure (IM) Spectral Displacement (Sd, in)
Damage State Threshold
Slight Damage
Moderate Damage
Extensive Damage
Complete Damage
Damage State Probability
≥ Slight Damage: (0.237 in, 0.397)
≥ Moderate Damage: (0.237 in, 0.198)
≥ Extensive Damage: (0.237 in, 0.055)
≥ Complete Damage: (0.237 in, 0.009)
Building Description:
Facility Class: EFHM
Building Type: URML
Design Level: PC
Site Class: D
City: Greenfield
County: Franklin
Geologic Group: Group 2
SDC: D
Detailed View
Discrete Damage State Probability P[Damage = DS | Sd]
0.603
0.199
0.144
0.045
0.008
0.001
None 1 2 3 4 Collapsed
Damage State
1 = Slight Damage | 2 = Moderate Damage
3 = Extensive Damage | 4 = Complete Damage

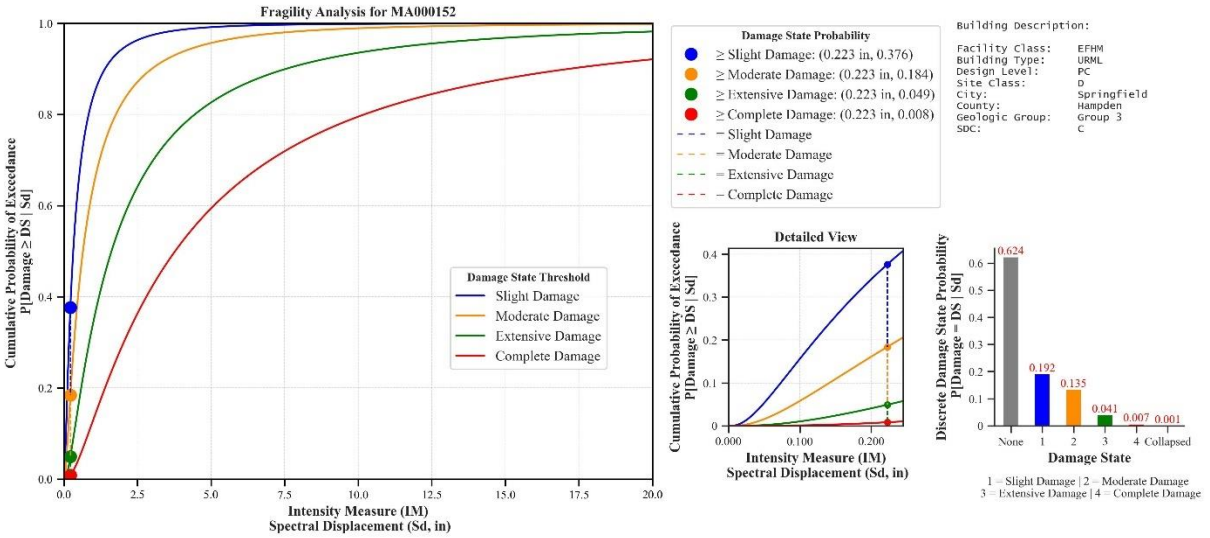
Fragility Analysis for MA000152
Cumulative Probability of Exceedance P[Damage ≥ DS | Sd]
Intensity Measure (IM) Spectral Displacement (Sd, in)
Damage State Threshold
Slight Damage
Moderate Damage
Extensive Damage
Complete Damage
Damage State Probability
≥ Slight Damage: (0.223 in, 0.376)
≥ Moderate Damage: (0.223 in, 0.184)
≥ Extensive Damage: (0.223 in, 0.049)
≥ Complete Damage: (0.223 in, 0.008)
Building Description:
Facility Class: EFHM
Building Type: URML
Design Level: PC
Site Class: D
City: Springfield
County: Hampden
Geologic Group: Group 3
SDC: C
Detailed View
Discrete Damage State Probability P[Damage = DS | Sd]
0.624
0.192
0.135
0.041
0.007
0.001
None 1 2 3 4 Collapsed
Damage State
1 = Slight Damage | 2 = Moderate Damage
3 = Extensive Damage | 4 = Complete Damage

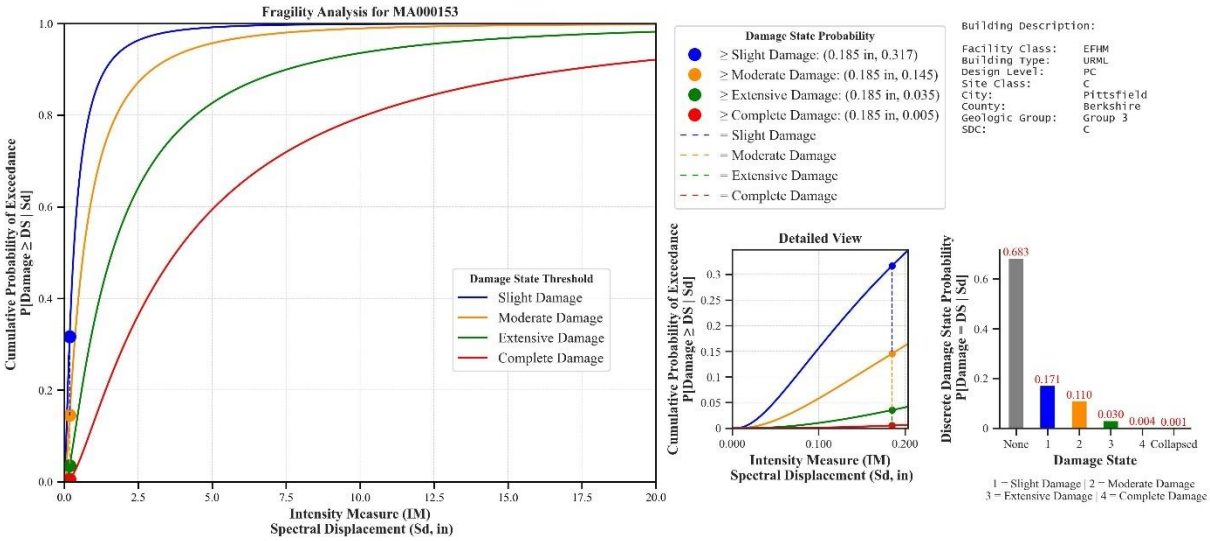
Fragility Analysis for MA000153
Cumulative Probability of Exceedance P[Damage ≥ DS | Sd]
Intensity Measure (IM) Spectral Displacement (Sd, in)
Damage State Threshold
Slight Damage
Moderate Damage
Extensive Damage
Complete Damage
Damage State Probability
≥ Slight Damage: (0.185 in, 0.317)
≥ Moderate Damage: (0.185 in, 0.145)
≥ Extensive Damage: (0.185 in, 0.035)
≥ Complete Damage: (0.185 in, 0.005)
Building Description:
Facility Class: EFHM
Building Type: URML
Design Level: PC
Site Class: C
City: Pittsfield
County: Berkshire
Geologic Group: Group 3
SDC: C
Detailed View
Discrete Damage State Probability P[Damage = DS | Sd]
0.683
0.171
0.110
0.030
0.004
0.001
None 1 2 3 4 Collapsed
Damage State
1 = Slight Damage | 2 = Moderate Damage
3 = Extensive Damage | 4 = Complete Damage

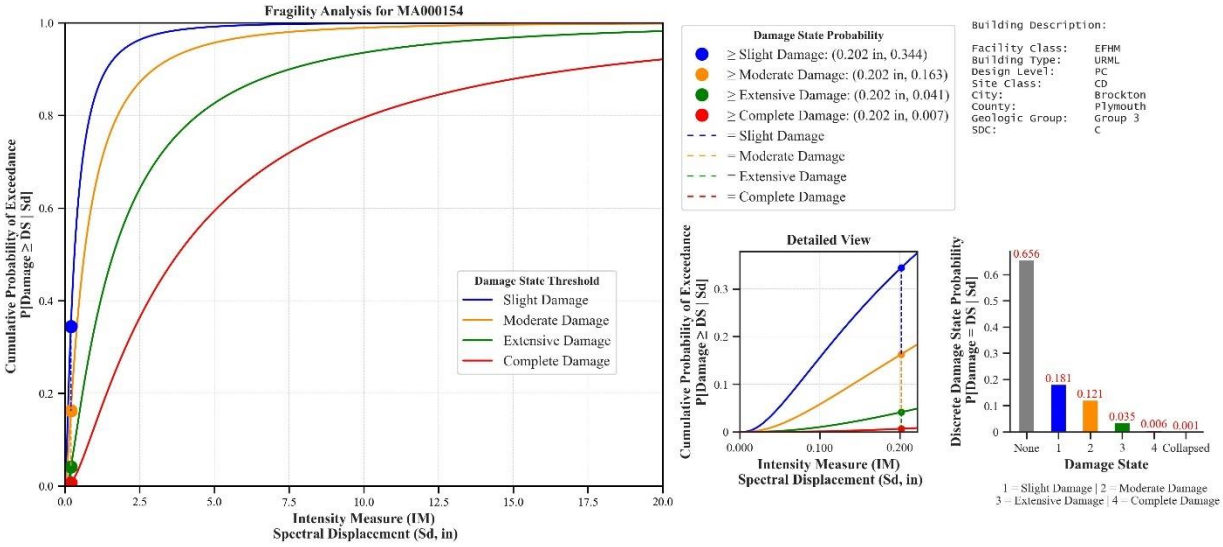
Fragility Analysis for MA000154
Cumulative Probability of Exceedance P[Damage ≥ DS | Sd]
Intensity Measure (IM) Spectral Displacement (Sd, in)
Damage State Threshold
Slight Damage
Moderate Damage
Extensive Damage
Complete Damage
Damage State Probability
≥ Slight Damage: (0.202 in, 0.344)
≥ Moderate Damage: (0.202 in, 0.163)
≥ Extensive Damage: (0.202 in, 0.041)
≥ Complete Damage: (0.202 in, 0.007)
Building Description:
Facility Class: EFHM
Building Type: URML
Design Level: PC
Site Class: CD
City: Brockton
County: Plymouth
Geologic Group: Group 3
SDC: C
Detailed View
Discrete Damage State Probability P[Damage = DS | Sd]
0.656
0.181
0.121
0.035
0.006
0.001
None
Collapsed
Damage State
1 = Slight Damage | 2 = Moderate Damage
3 = Extensive Damage | 4 = Complete Damage

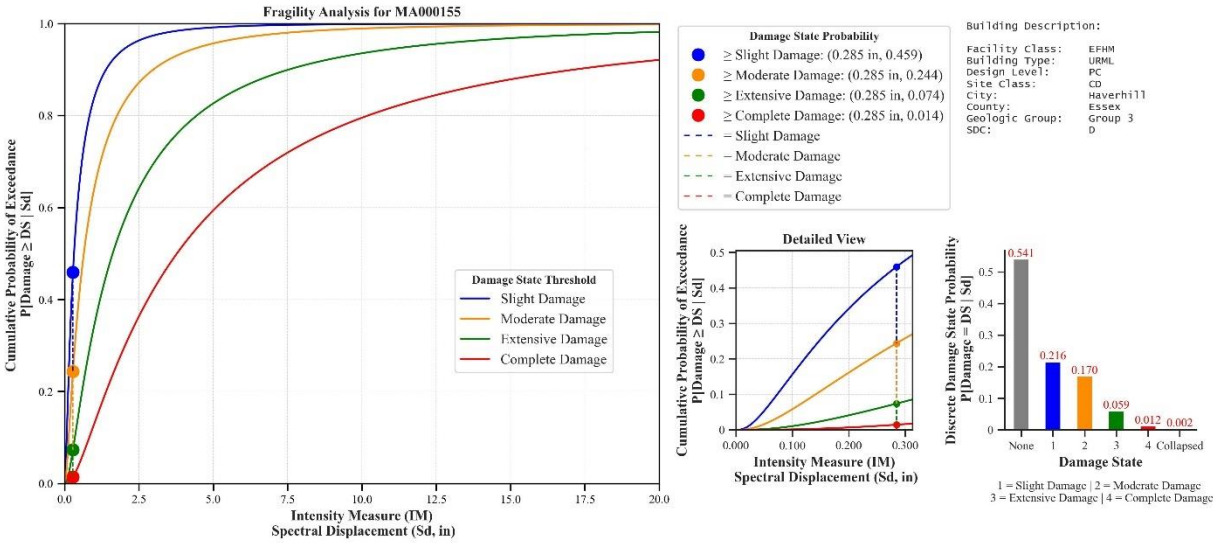
Fragility Analysis for MA000155
Cumulative Probability of Exceedance P[Damage ≥ DS | Sd]
Intensity Measure (IM) Spectral Displacement (Sd, in)
Damage State Threshold
Slight Damage
Moderate Damage
Extensive Damage
Complete Damage
Damage State Probability
≥ Slight Damage: (0.285 in, 0.459)
≥ Moderate Damage: (0.285 in, 0.244)
≥ Extensive Damage: (0.285 in, 0.074)
≥ Complete Damage: (0.285 in, 0.014)
Building Description:
Facility Class: EFHM
Building Type: URML
Design Level: PC
Site Class: CD
City: Haverhill
County: Essex
Geologic Group: Group 3
SDC: D
Detailed View
Discrete Damage State Probability P[Damage = DS | Sd]
0.541
0.216
0.170
0.059
0.012
0.002
None
Collapsed
Damage State
1 = Slight Damage | 2 = Moderate Damage
3 = Extensive Damage | 4 = Complete Damage

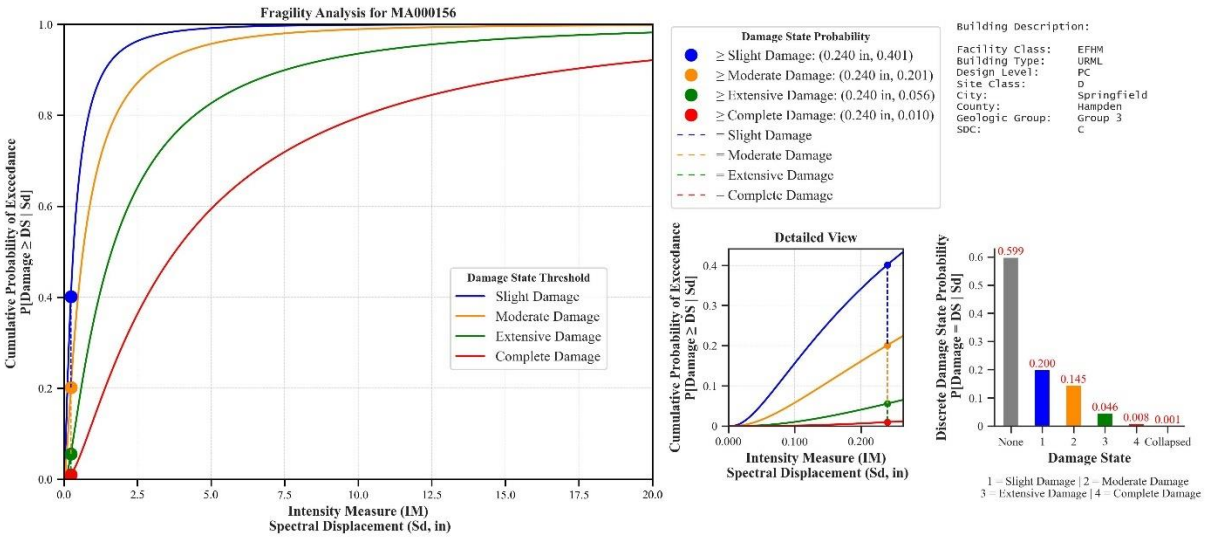
Fragility Analysis for MA000156
Cumulative Probability of Exceedance P[Damage ≥ DS | Sd]
Intensity Measure (IM) Spectral Displacement (Sd, in)
Damage State Threshold
Slight Damage
Moderate Damage
Extensive Damage
Complete Damage
Damage State Probability
≥ Slight Damage: (0.240 in, 0.401)
≥ Moderate Damage: (0.240 in, 0.201)
≥ Extensive Damage: (0.240 in, 0.056)
≥ Complete Damage: (0.240 in, 0.010)
Building Description:
Facility Class: EFHM
Building Type: URML
Design Level: PC
Site Class: D
City: Springfield
County: Hampden
Geologic Group: Group 3
SDC: C
Detailed View
Discrete Damage State Probability P[Damage = DS | Sd]
0.599
0.200
0.145
0.046
0.008
0.001
None
Collapsed
Damage State
1 = Slight Damage | 2 = Moderate Damage
3 = Extensive Damage | 4 = Complete Damage

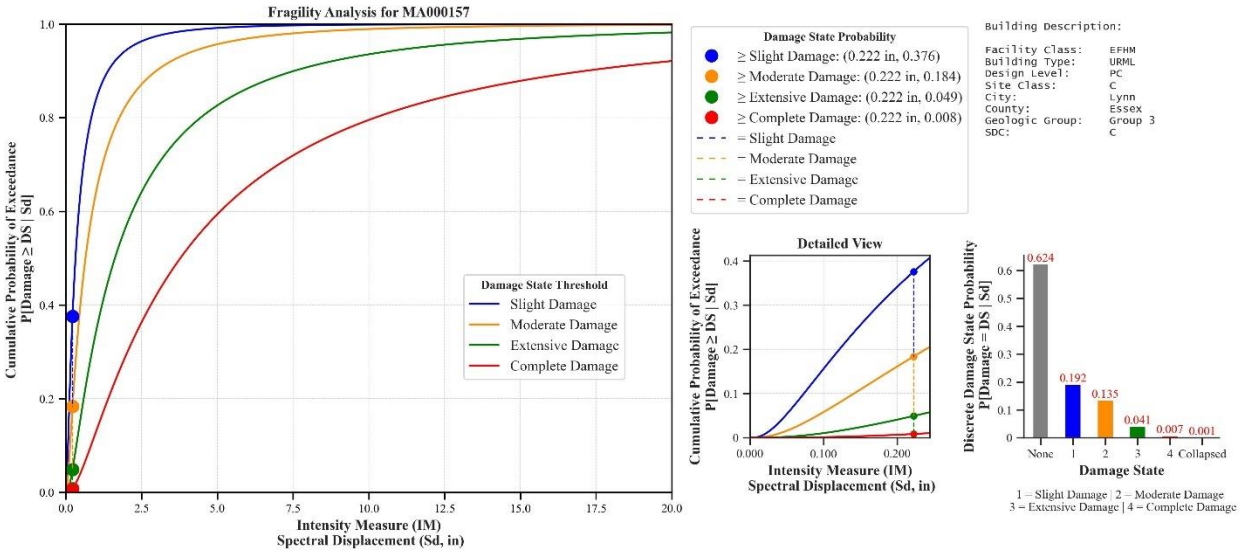
Fragility Analysis for MA000157
Cumulative Probability of Exceedance
P[Damage ≥ DS | Sd]
Intensity Measure (IM)
Spectral Displacement (Sd, in)
Damage State Threshold
Slight Damage
Moderate Damage
Extensive Damage
Complete Damage
Damage State Probability
≥ Slight Damage: (0.222 in, 0.376)
≥ Moderate Damage: (0.222 in, 0.184)
≥ Extensive Damage: (0.222 in, 0.049)
≥ Complete Damage: (0.222 in, 0.008)
= Slight Damage
= Moderate Damage
= Extensive Damage
= Complete Damage
Detailed View
Building Description:
Facility Class: EFHM
Building Type: URML
Design Level: PC
Site Class: C
City: Lynn
County: Essex
Geologic Group: Group 3
SDC: C
Discrete Damage State Probability
P[Damage = DS | Sd]
0.624
0.192
0.135
0.041
0.007
0.001
None
1
2
3
4 Collapsed
Damage State
1 – Slight Damage | 2 – Moderate Damage
3 – Extensive Damage | 4 – Complete Damage

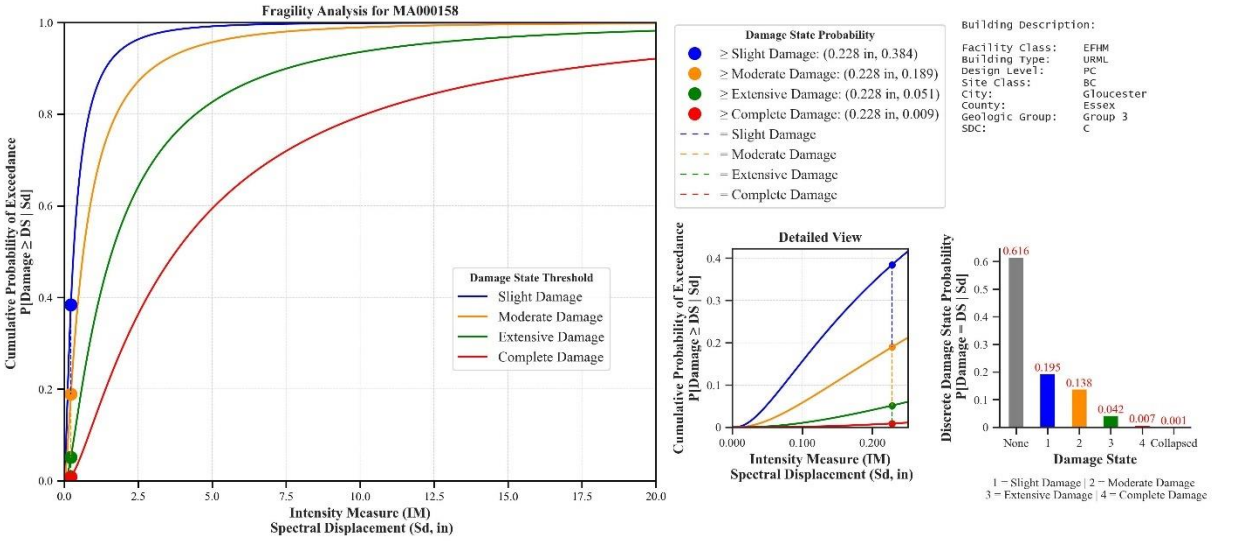
Fragility Analysis for MA000158
Cumulative Probability of Exceedance
P[Damage ≥ DS | Sd]
Intensity Measure (IM)
Spectral Displacement (Sd, in)
Damage State Threshold
Slight Damage
Moderate Damage
Extensive Damage
Complete Damage
Damage State Probability
≥ Slight Damage: (0.228 in, 0.384)
≥ Moderate Damage: (0.228 in, 0.189)
≥ Extensive Damage: (0.228 in, 0.051)
≥ Complete Damage: (0.228 in, 0.009)
= Slight Damage
= Moderate Damage
= Extensive Damage
= Complete Damage
Detailed View
Building Description:
Facility Class: EFHM
Building Type: URML
Design Level: PC
Site Class: BC
City: Gloucester
County: Essex
Geologic Group: Group 3
SDC: C
Discrete Damage State Probability
P[Damage = DS | Sd]
0.616
0.195
0.138
0.042
0.007
0.001
None
1
2
3
4 Collapsed
Damage State
1 – Slight Damage | 2 – Moderate Damage
3 – Extensive Damage | 4 – Complete Damage

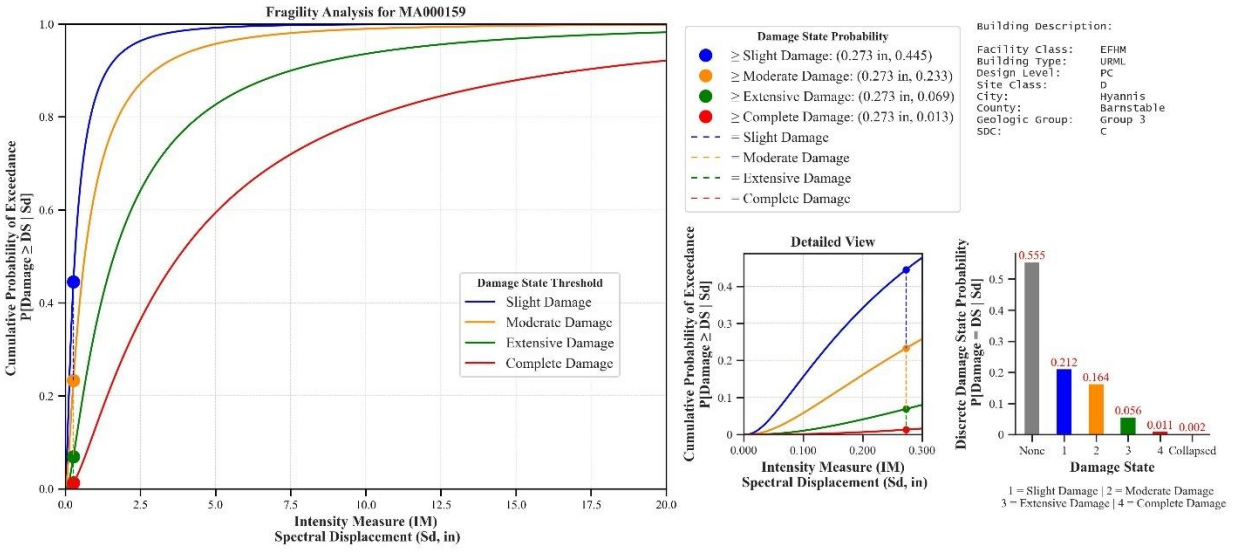
Fragility Analysis for MA000159
Cumulative Probability of Exceedance
P[Damage ≥ DS | Sd]
Intensity Measure (IM)
Spectral Displacement (Sd, in)
Damage State Threshold
Slight Damage
Moderate Damage
Extensive Damage
Complete Damage
Damage State Probability
≥ Slight Damage: (0.273 in, 0.445)
≥ Moderate Damage: (0.273 in, 0.233)
≥ Extensive Damage: (0.273 in, 0.069)
≥ Complete Damage: (0.273 in, 0.013)
= Slight Damage
= Moderate Damage
= Extensive Damage
= Complete Damage
Detailed View
Building Description:
Facility Class: EFHM
Building Type: URML
Design Level: PC
Site Class: D
City: Hyannis
County: Barnstable
Geologic Group: Group 3
SDC: C
Discrete Damage State Probability
P[Damage = DS | Sd]
0.555
0.212
0.164
0.056
0.011
0.002
None
Collapsed
Damage State
1 = Slight Damage | 2 = Moderate Damage
3 = Extensive Damage | 4 = Complete Damage

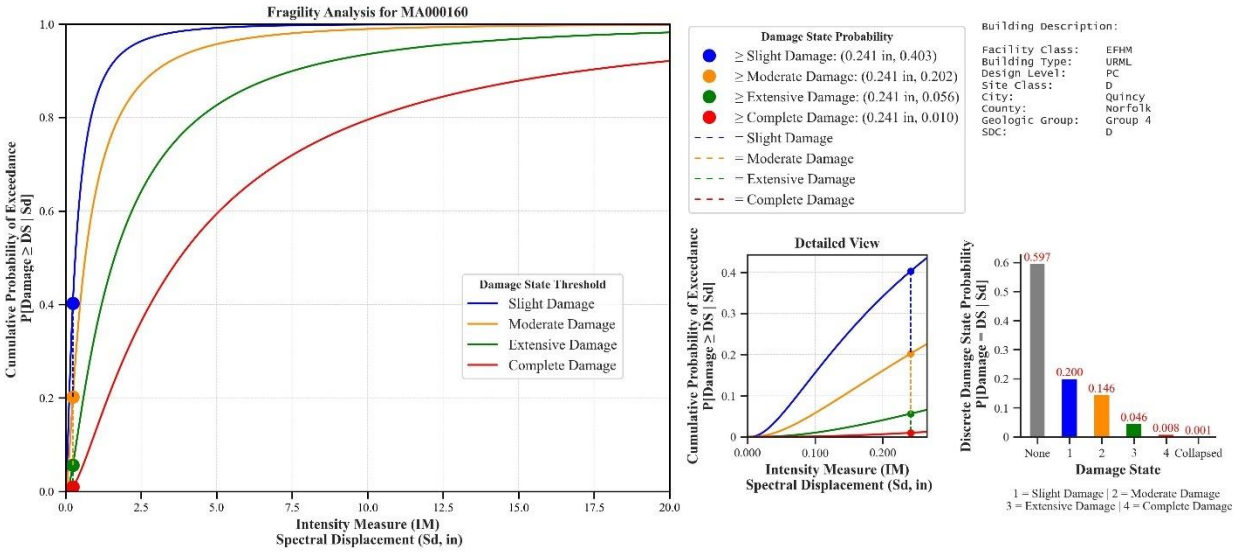
Fragility Analysis for MA000160
Cumulative Probability of Exceedance
P[Damage ≥ DS | Sd]
Intensity Measure (IM)
Spectral Displacement (Sd, in)
Damage State Threshold
Slight Damage
Moderate Damage
Extensive Damage
Complete Damage
Damage State Probability
≥ Slight Damage: (0.241 in, 0.403)
≥ Moderate Damage: (0.241 in, 0.202)
≥ Extensive Damage: (0.241 in, 0.056)
≥ Complete Damage: (0.241 in, 0.010)
= Slight Damage
= Moderate Damage
= Extensive Damage
= Complete Damage
Detailed View
Building Description:
Facility Class: EFHM
Building Type: URML
Design Level: PC
Site Class: D
City: Quincy
County: Norfolk
Geologic Group: Group 4
SDC: D
Discrete Damage State Probability
P[Damage = DS | Sd]
0.597
0.200
0.146
0.046
0.008
0.001
None
Collapsed
Damage State
1 = Slight Damage | 2 = Moderate Damage
3 = Extensive Damage | 4 = Complete Damage

Appendix G: HAZUS Vs_{30}-based Fragility Output – GBS Care Facilities

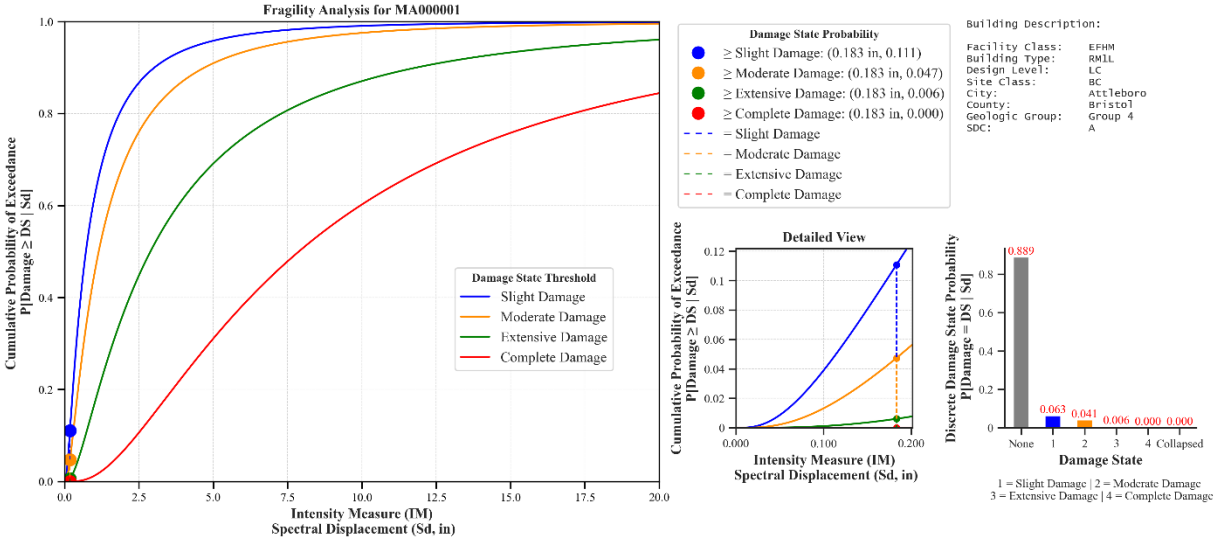

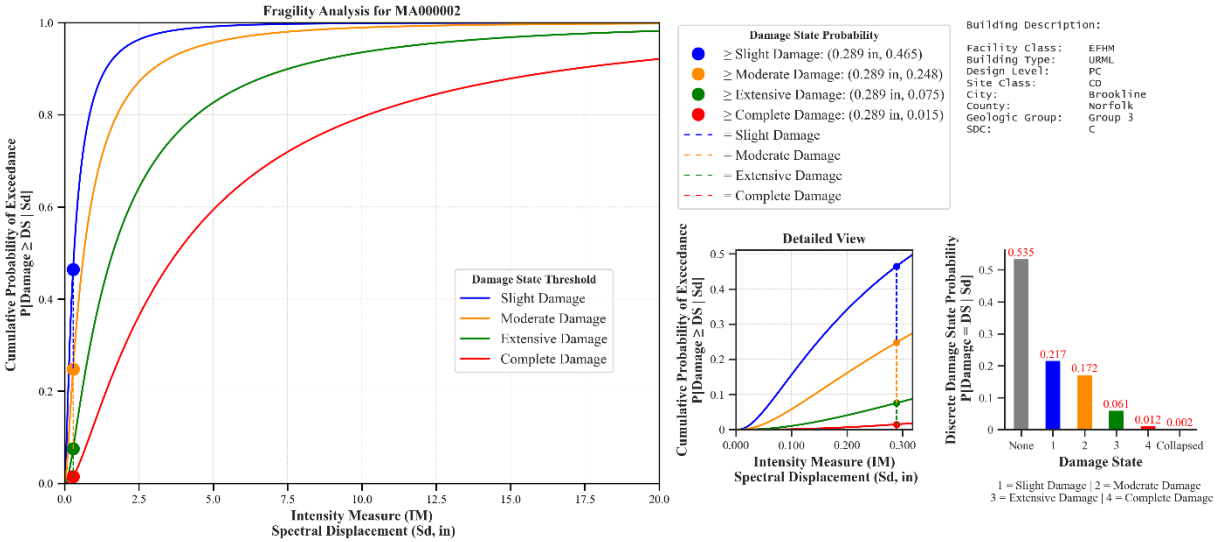

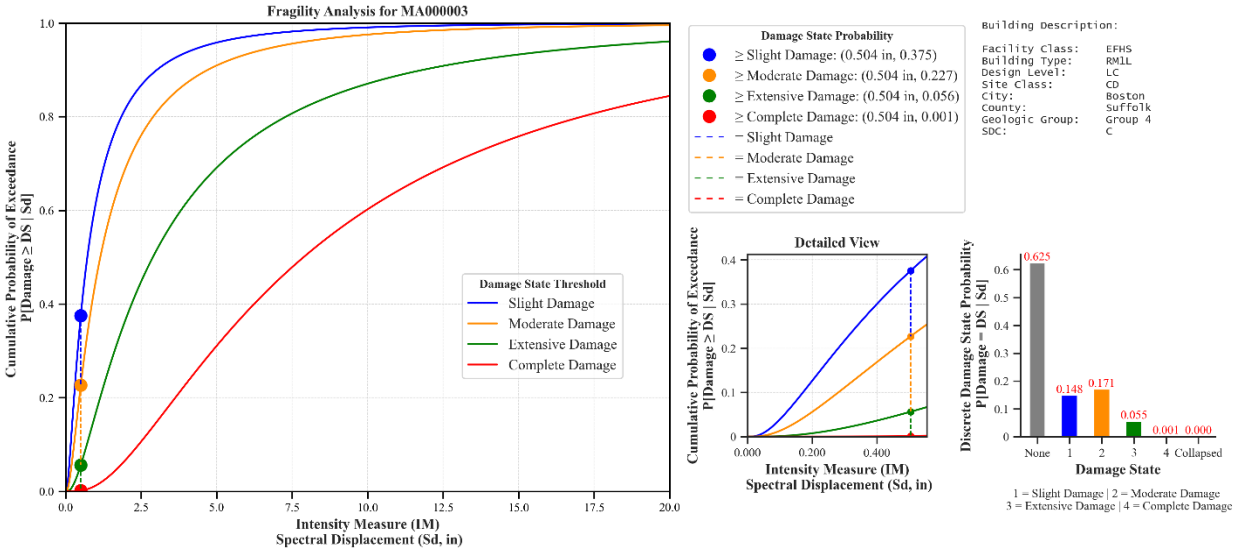
Fragility Analysis for MA000003
Cumulative Probability of Exceedance P[Damage ≥ DS | Sd]
Intensity Measure (IM) Spectral Displacement (Sd, in)
Damage State Threshold
Slight Damage
Moderate Damage
Extensive Damage
Complete Damage
Damage State Probability
≥ Slight Damage: (0.504 in, 0.375)
≥ Moderate Damage: (0.504 in, 0.227)
≥ Extensive Damage: (0.504 in, 0.056)
≥ Complete Damage: (0.504 in, 0.001)
= Slight Damage
= Moderate Damage
= Extensive Damage
= Complete Damage
Detailed View
Discrete Damage State Probability P[Damage = DS | Sd]
0.625
0.148
0.171
0.055
0.001
0.000
None
1
2
3
4
Collapsed
Damage State
1 = Slight Damage | 2 = Moderate Damage
3 = Extensive Damage | 4 = Complete Damage
Building Description:
Facility Class: EFHS
Building Type: RM1L
Design Level: LC
Site Class: CD
City: Boston
County: Suffolk
Geologic Group: Group 4
SDC: C

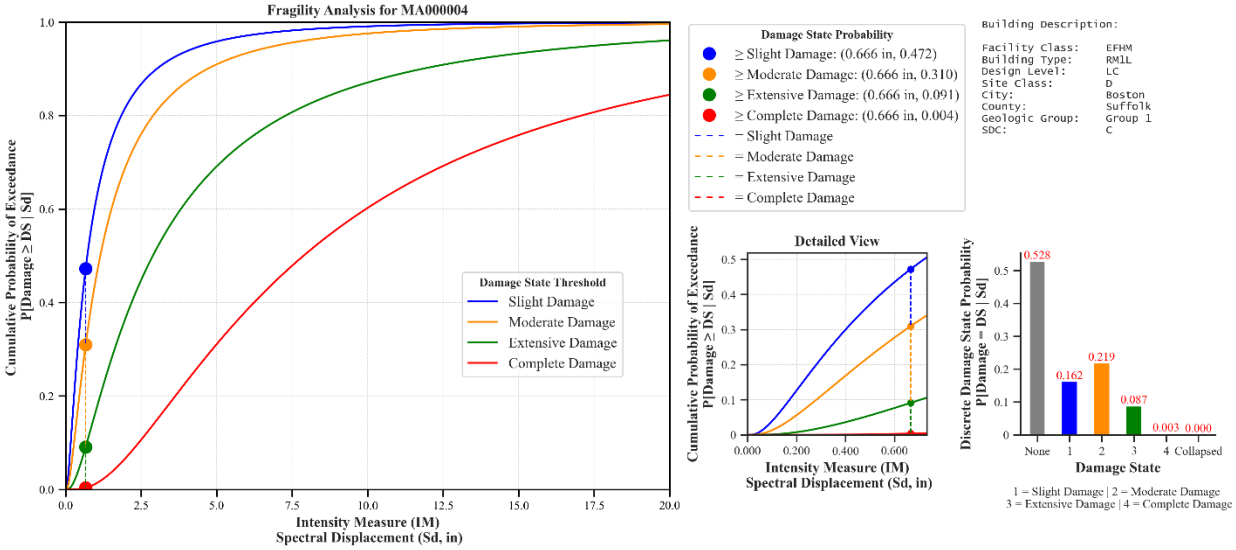
Fragility Analysis for MA000004
Cumulative Probability of Exceedance P[Damage ≥ DS | Sd]
Intensity Measure (IM) Spectral Displacement (Sd, in)
Damage State Threshold
Slight Damage
Moderate Damage
Extensive Damage
Complete Damage
Damage State Probability
≥ Slight Damage: (0.666 in, 0.472)
≥ Moderate Damage: (0.666 in, 0.310)
≥ Extensive Damage: (0.666 in, 0.091)
≥ Complete Damage: (0.666 in, 0.004)
= Slight Damage
= Moderate Damage
= Extensive Damage
= Complete Damage
Detailed View
Discrete Damage State Probability P[Damage = DS | Sd]
0.528
0.162
0.219
0.087
0.003
0.000
None
1
2
3
4
Collapsed
Damage State
1 = Slight Damage | 2 = Moderate Damage
3 = Extensive Damage | 4 = Complete Damage
Building Description:
Facility Class: EFHM
Building Type: RM1L
Design Level: LC
Site Class: D
City: Boston
County: Suffolk
Geologic Group: Group 1
SDC: C

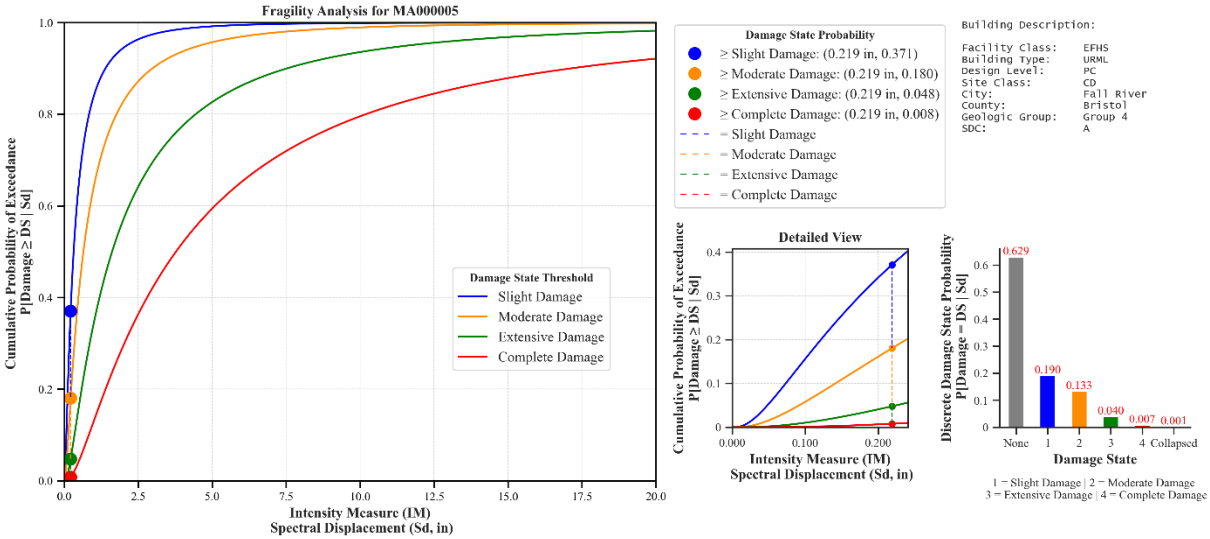
Fragility Analysis for MA000005
Cumulative Probability of Exceedance P[Damage ≥ DS | Sd]
Intensity Measure (IM) Spectral Displacement (Sd, in)
Damage State Threshold
Slight Damage
Moderate Damage
Extensive Damage
Complete Damage
Damage State Probability
≥ Slight Damage: (0.219 in, 0.371)
≥ Moderate Damage: (0.219 in, 0.180)
≥ Extensive Damage: (0.219 in, 0.048)
≥ Complete Damage: (0.219 in, 0.008)
= Slight Damage
= Moderate Damage
= Extensive Damage
= Complete Damage
Detailed View
Discrete Damage State Probability P[Damage = DS | Sd]
0.629
0.190
0.133
0.040
0.007
0.001
None
1
2
3
4
Collapsed
Damage State
1 = Slight Damage | 2 = Moderate Damage
3 = Extensive Damage | 4 = Complete Damage
Building Description:
Facility Class: EFHS
Building Type: URML
Design Level: PC
Site Class: CD
City: Fall River
County: Bristol
Geologic Group: Group 4
SDC: A

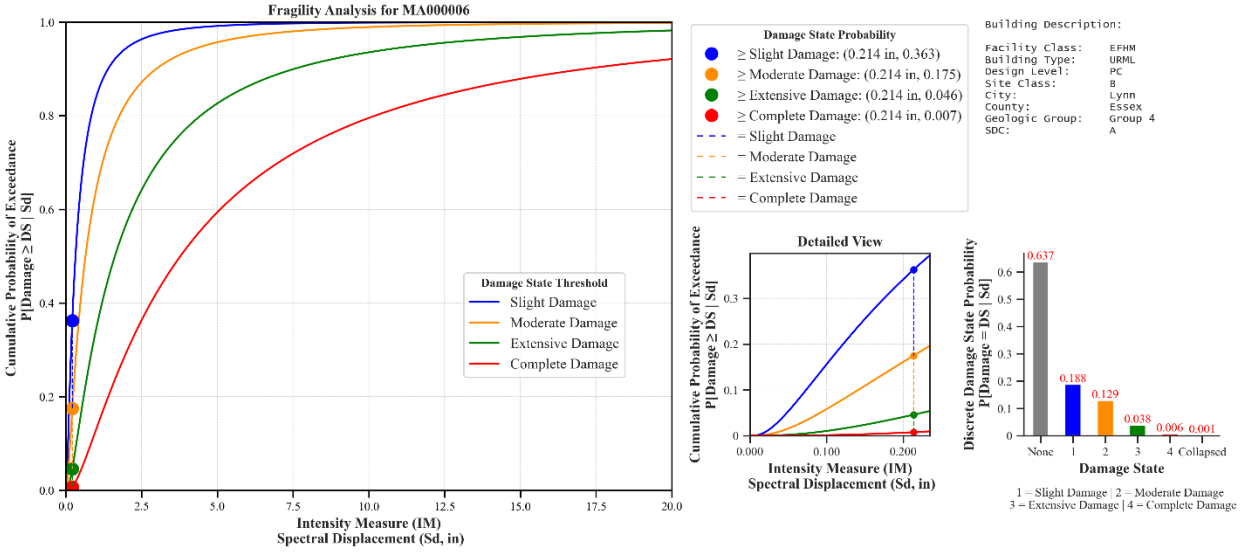
Fragility Analysis for MA000006
Cumulative Probability of Exceedance P[Damage ≥ DS | Sd]
Intensity Measure (IM) Spectral Displacement (Sd, in)
Damage State Threshold
Slight Damage
Moderate Damage
Extensive Damage
Complete Damage
Damage State Probability
≥ Slight Damage: (0.214 in, 0.363)
≥ Moderate Damage: (0.214 in, 0.175)
≥ Extensive Damage: (0.214 in, 0.046)
≥ Complete Damage: (0.214 in, 0.007)
= Slight Damage
= Moderate Damage
= Extensive Damage
= Complete Damage
Building Description:
Facility Class: EFHM
Building Type: URML
Design Level: PC
Site Class: B
City: Lynn
County: Essex
Geologic Group: Group 4
SDC: A
Detailed View
Discrete Damage State Probability P[Damage = DS | Sd]
0.637
0.188
0.129
0.038
0.006
0.001
None
1
2
3
4 Collapsed
Damage State
1 = Slight Damage | 2 = Moderate Damage
3 = Extensive Damage | 4 = Complete Damage

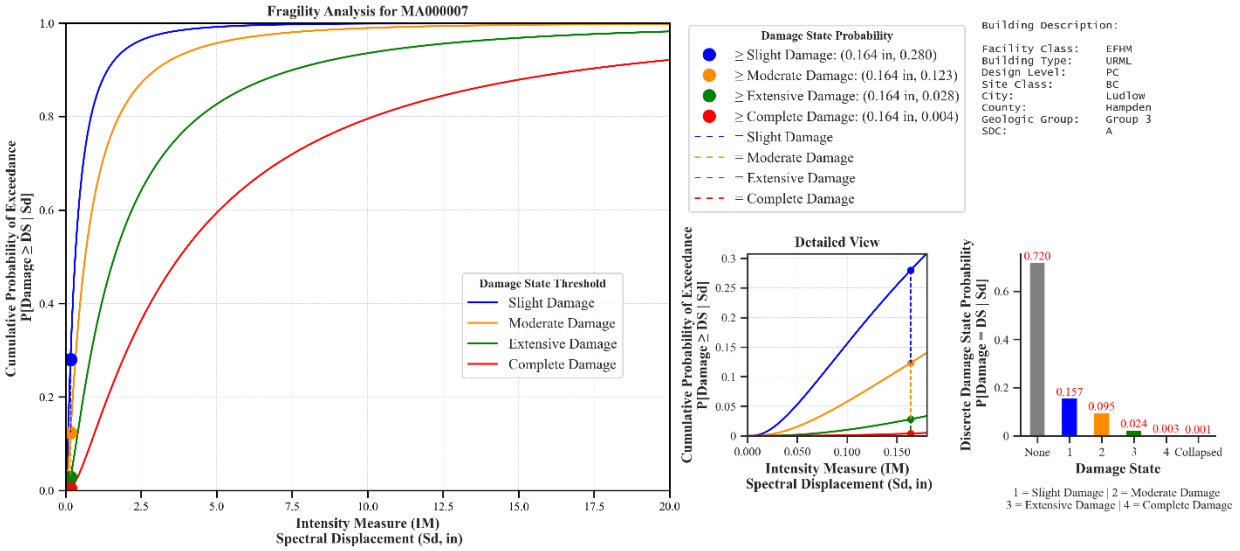
Fragility Analysis for MA000007
Cumulative Probability of Exceedance P[Damage ≥ DS | Sd]
Intensity Measure (IM) Spectral Displacement (Sd, in)
Damage State Threshold
Slight Damage
Moderate Damage
Extensive Damage
Complete Damage
Damage State Probability
≥ Slight Damage: (0.164 in, 0.280)
≥ Moderate Damage: (0.164 in, 0.123)
≥ Extensive Damage: (0.164 in, 0.028)
≥ Complete Damage: (0.164 in, 0.004)
= Slight Damage
= Moderate Damage
= Extensive Damage
= Complete Damage
Building Description:
Facility Class: EFHM
Building Type: URML
Design Level: PC
Site Class: BC
City: Ludlow
County: Hampden
Geologic Group: Group 3
SDC: A
Detailed View
Discrete Damage State Probability P[Damage = DS | Sd]
0.720
0.157
0.095
0.024
0.003
0.001
None
1
2
3
4 Collapsed
Damage State
1 = Slight Damage | 2 = Moderate Damage
3 = Extensive Damage | 4 = Complete Damage

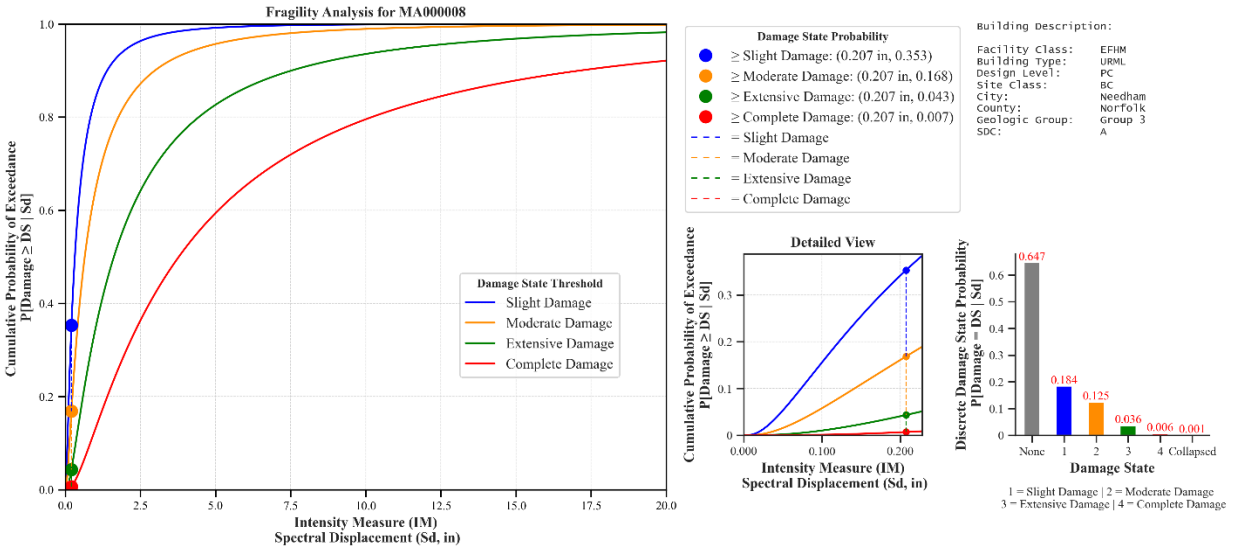
Fragility Analysis for MA000008
Cumulative Probability of Exceedance P[Damage ≥ DS | Sd]
Intensity Measure (IM) Spectral Displacement (Sd, in)
Damage State Threshold
Slight Damage
Moderate Damage
Extensive Damage
Complete Damage
Damage State Probability
≥ Slight Damage: (0.207 in, 0.353)
≥ Moderate Damage: (0.207 in, 0.168)
≥ Extensive Damage: (0.207 in, 0.043)
≥ Complete Damage: (0.207 in, 0.007)
= Slight Damage
= Moderate Damage
= Extensive Damage
= Complete Damage
Building Description:
Facility Class: EFHM
Building Type: URML
Design Level: PC
Site Class: BC
City: Needham
County: Norfolk
Geologic Group: Group 3
SDC: A
Detailed View
Discrete Damage State Probability P[Damage = DS | Sd]
0.647
0.184
0.125
0.036
0.006
0.001
None
1
2
3
4 Collapsed
Damage State
1 = Slight Damage | 2 = Moderate Damage
3 = Extensive Damage | 4 = Complete Damage

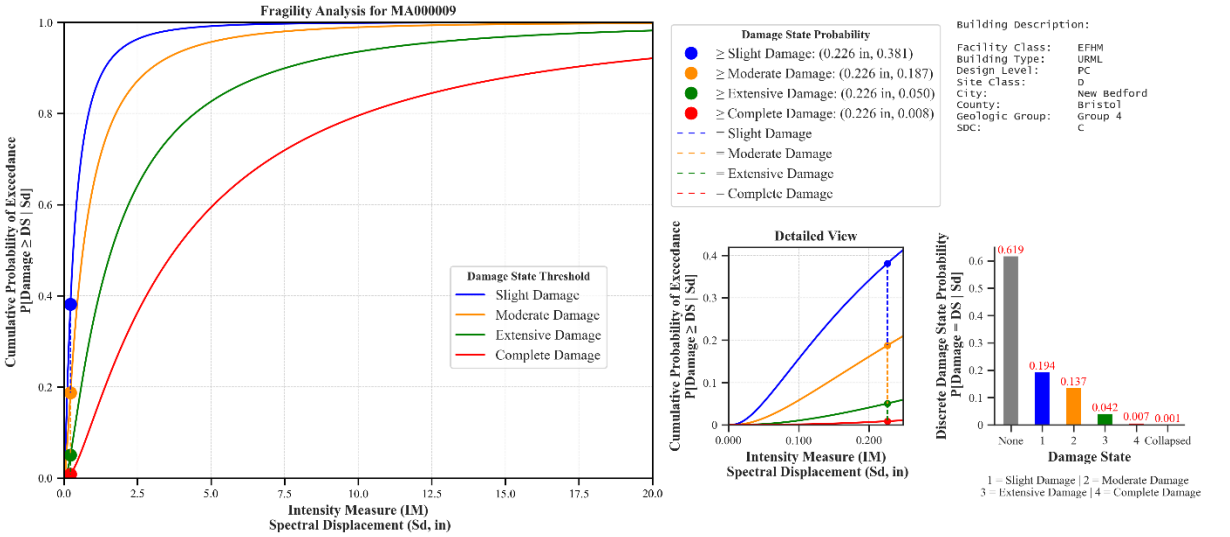
Fragility Analysis for MA000009
Cumulative Probability of Exceedance P[Damage ≥ DS | Sd]
Intensity Measure (IM) Spectral Displacement (Sd, in)
Damage State Threshold
Slight Damage
Moderate Damage
Extensive Damage
Complete Damage
Damage State Probability
≥ Slight Damage: (0.226 in, 0.381)
≥ Moderate Damage: (0.226 in, 0.187)
≥ Extensive Damage: (0.226 in, 0.050)
≥ Complete Damage: (0.226 in, 0.008)
Detailed View
Discrete Damage State Probability P[Damage = DS | Sd]
0.619
0.194
0.137
0.042
0.007
0.001
None
Collapsed
Damage State
1 = Slight Damage | 2 = Moderate Damage
3 = Extensive Damage | 4 = Complete Damage
Building Description:
Facility Class: EFHM
Building Type: URML
Design Level: PC
Site Class: D
City: New Bedford
County: Bristol
Geologic Group: Group 4
SDC: C

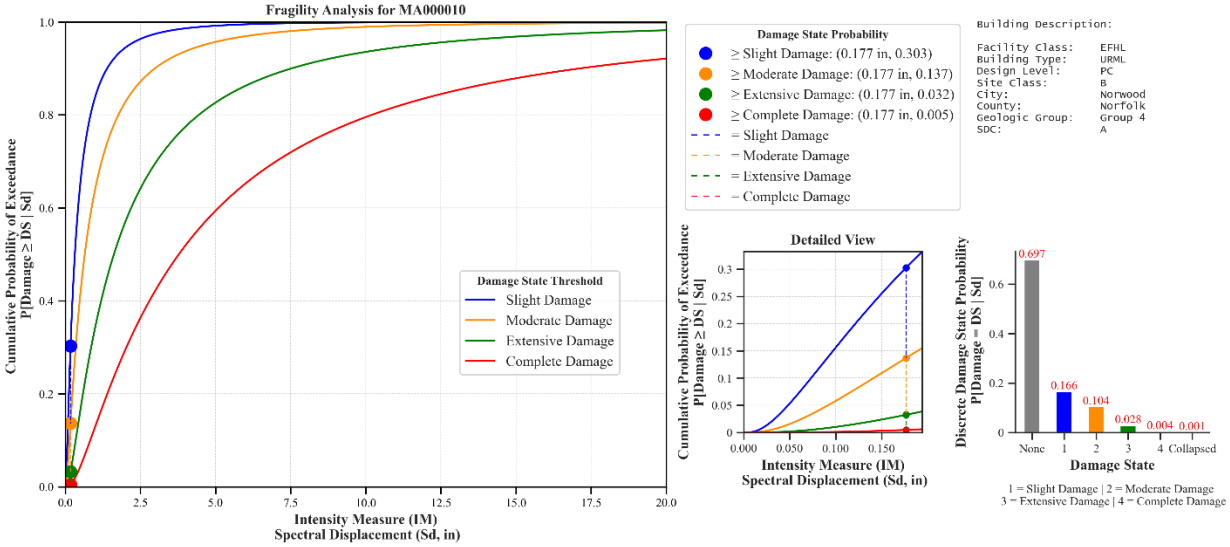
Fragility Analysis for MA000010
Cumulative Probability of Exceedance P[Damage ≥ DS | Sd]
Intensity Measure (IM) Spectral Displacement (Sd, in)
Damage State Threshold
Slight Damage
Moderate Damage
Extensive Damage
Complete Damage
Damage State Probability
≥ Slight Damage: (0.177 in, 0.303)
≥ Moderate Damage: (0.177 in, 0.137)
≥ Extensive Damage: (0.177 in, 0.032)
≥ Complete Damage: (0.177 in, 0.005)
Detailed View
Discrete Damage State Probability P[Damage = DS | Sd]
0.697
0.166
0.104
0.028
0.004
0.001
None
Collapsed
Damage State
1 = Slight Damage | 2 = Moderate Damage
3 = Extensive Damage | 4 = Complete Damage
Building Description:
Facility Class: EFHL
Building Type: URML
Design Level: PC
Site Class: B
City: Norwood
County: Norfolk
Geologic Group: Group 4
SDC: A

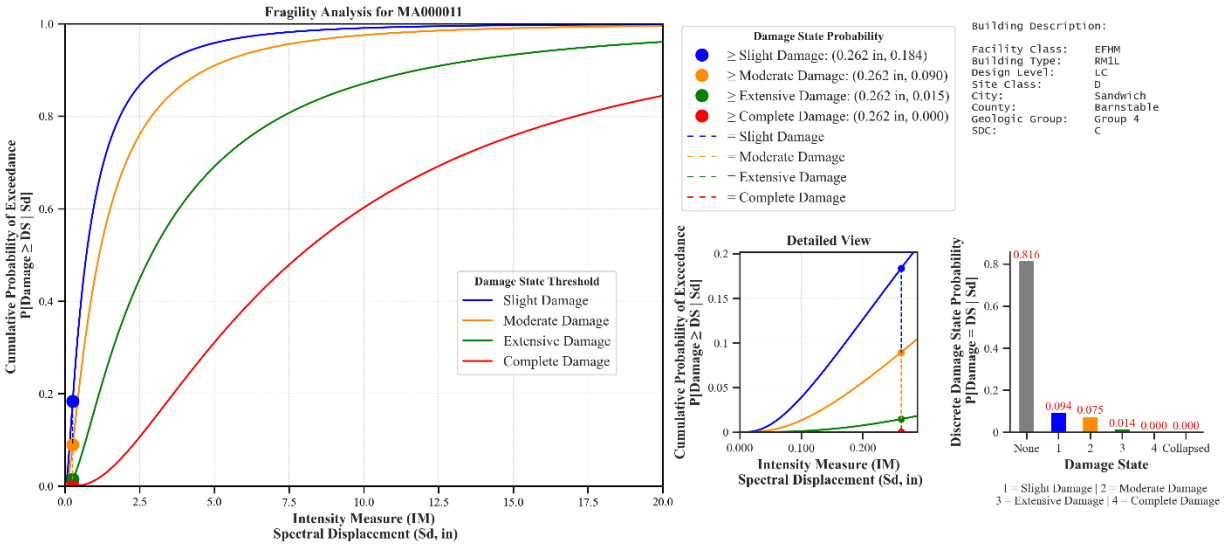
Fragility Analysis for MA000011
Cumulative Probability of Exceedance P[Damage ≥ DS | Sd]
Intensity Measure (IM) Spectral Displacement (Sd, in)
Damage State Threshold
Slight Damage
Moderate Damage
Extensive Damage
Complete Damage
Damage State Probability
≥ Slight Damage: (0.262 in, 0.184)
≥ Moderate Damage: (0.262 in, 0.090)
≥ Extensive Damage: (0.262 in, 0.015)
≥ Complete Damage: (0.262 in, 0.000)
Detailed View
Discrete Damage State Probability P[Damage = DS | Sd]
0.816
0.094
0.075
0.014
0.000
0.000
None
Collapsed
Damage State
1 = Slight Damage | 2 = Moderate Damage
3 = Extensive Damage | 4 = Complete Damage
Building Description:
Facility Class: EFHM
Building Type: RM1L
Design Level: LC
Site Class: D
City: Sandwich
County: Barnstable
Geologic Group: Group 4
SDC: C

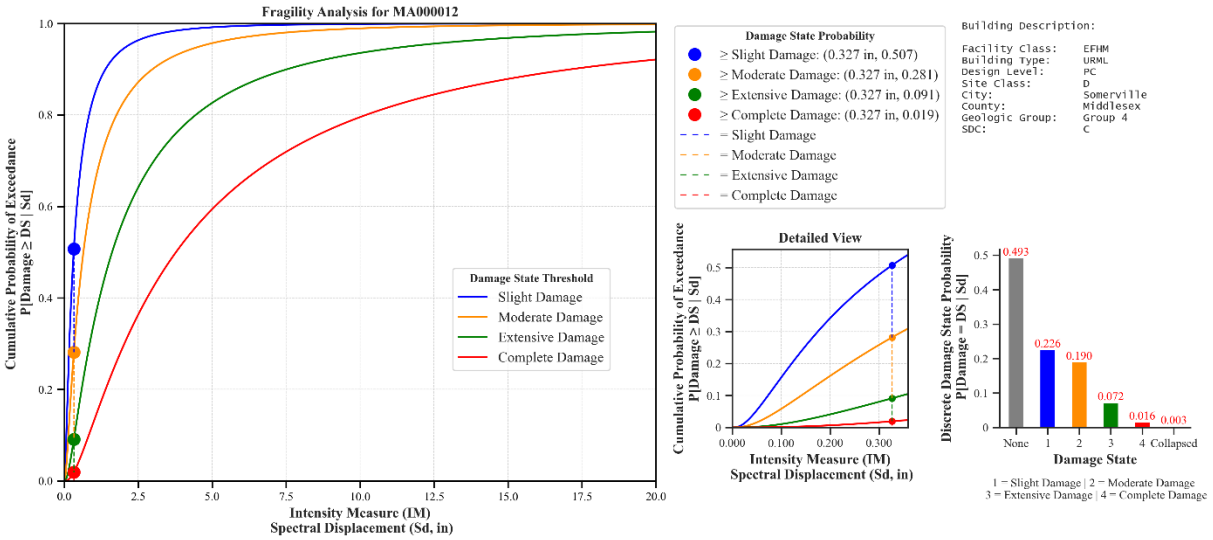
Fragility Analysis for MA000012
Cumulative Probability of Exceedance P[Damage ≥ DS | Sd]
Intensity Measure (IM) Spectral Displacement (Sd, in)
Damage State Threshold
Slight Damage
Moderate Damage
Extensive Damage
Complete Damage
Damage State Probability
≥ Slight Damage: (0.327 in, 0.507)
≥ Moderate Damage: (0.327 in, 0.281)
≥ Extensive Damage: (0.327 in, 0.091)
≥ Complete Damage: (0.327 in, 0.019)
Building Description:
Facility Class: EFHM
Building Type: URML
Design Level: PC
Site Class: D
City: Somerville
County: Middlesex
Geologic Group: Group 4
SDC: C
Detailed View
Discrete Damage State Probability P[Damage = DS | Sd]
0.493
0.226
0.190
0.072
0.016
0.003
None 1 2 3 4 Collapsed
Damage State
1 = Slight Damage | 2 = Moderate Damage
3 = Extensive Damage | 4 = Complete Damage

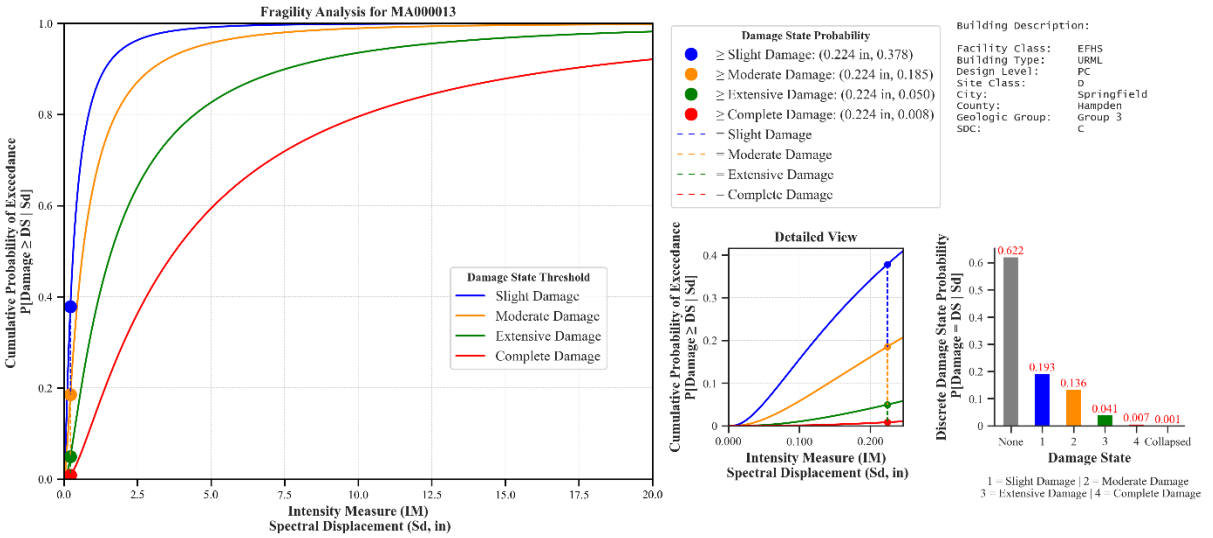
Fragility Analysis for MA000013
Cumulative Probability of Exceedance P[Damage ≥ DS | Sd]
Intensity Measure (IM) Spectral Displacement (Sd, in)
Damage State Threshold
Slight Damage
Moderate Damage
Extensive Damage
Complete Damage
Damage State Probability
≥ Slight Damage: (0.224 in, 0.378)
≥ Moderate Damage: (0.224 in, 0.185)
≥ Extensive Damage: (0.224 in, 0.050)
≥ Complete Damage: (0.224 in, 0.008)
Building Description:
Facility Class: EFHS
Building Type: URML
Design Level: PC
Site Class: D
City: Springfield
County: Hampden
Geologic Group: Group 3
SDC: C
Detailed View
Discrete Damage State Probability P[Damage = DS | Sd]
0.622
0.193
0.136
0.041
0.007
0.001
None 1 2 3 4 Collapsed
Damage State
1 = Slight Damage | 2 = Moderate Damage
3 = Extensive Damage | 4 = Complete Damage

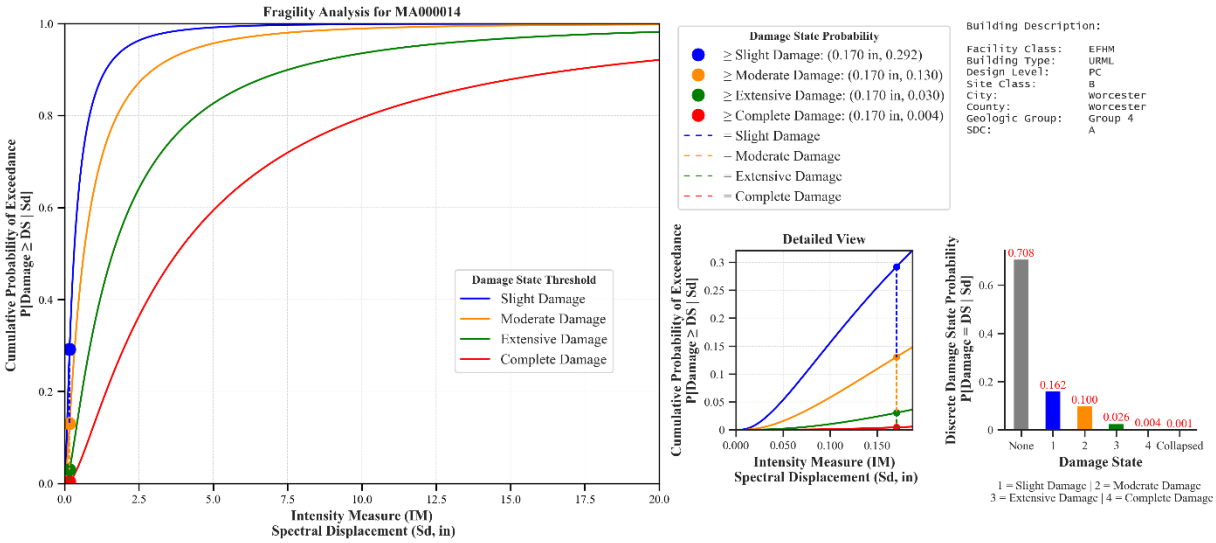
Fragility Analysis for MA000014
Cumulative Probability of Exceedance P[Damage ≥ DS | Sd]
Intensity Measure (IM) Spectral Displacement (Sd, in)
Damage State Threshold
Slight Damage
Moderate Damage
Extensive Damage
Complete Damage
Damage State Probability
≥ Slight Damage: (0.170 in, 0.292)
≥ Moderate Damage: (0.170 in, 0.130)
≥ Extensive Damage: (0.170 in, 0.030)
≥ Complete Damage: (0.170 in, 0.004)
Building Description:
Facility Class: EFHM
Building Type: URML
Design Level: PC
Site Class: B
City: Worcester
County: Worcester
Geologic Group: Group 4
SDC: A
Detailed View
Discrete Damage State Probability P[Damage = DS | Sd]
0.708
0.162
0.100
0.026
0.004
0.001
None 1 2 3 4 Collapsed
Damage State
1 = Slight Damage | 2 = Moderate Damage
3 = Extensive Damage | 4 = Complete Damage

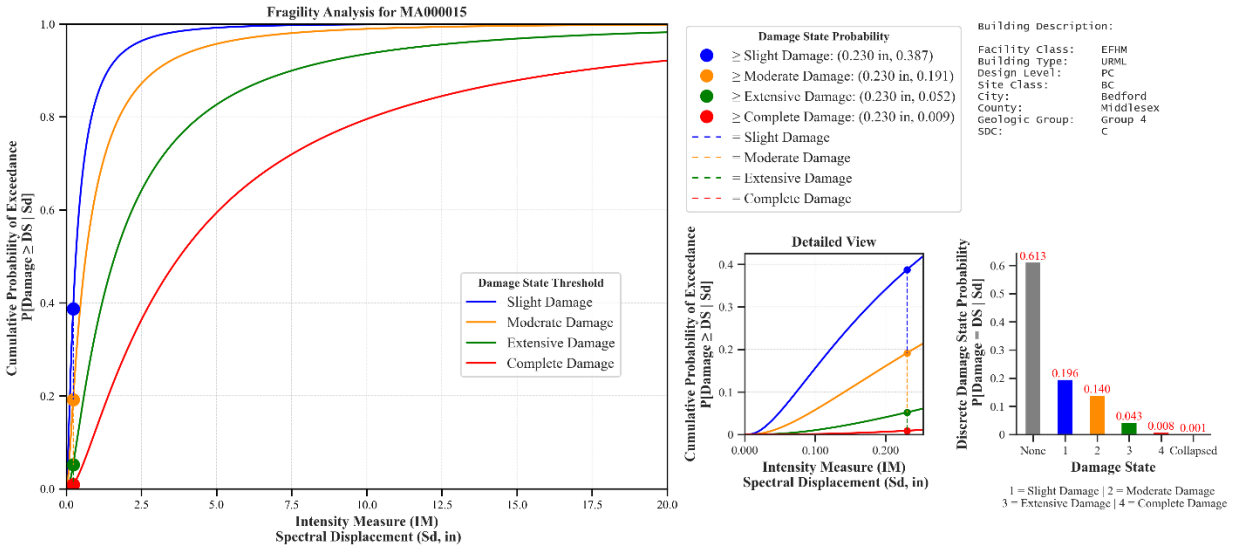
Fragility Analysis for MA000015
Cumulative Probability of Exceedance P[Damage ≥ DS | Sd]
Intensity Measure (IM) Spectral Displacement (Sd, in)
Damage State Threshold
Slight Damage
Moderate Damage
Extensive Damage
Complete Damage
Damage State Probability
≥ Slight Damage: (0.230 in, 0.387)
≥ Moderate Damage: (0.230 in, 0.191)
≥ Extensive Damage: (0.230 in, 0.052)
≥ Complete Damage: (0.230 in, 0.009)
= Slight Damage
= Moderate Damage
= Extensive Damage
= Complete Damage
Building Description:
Facility Class: EFHM
Building Type: URML
Design Level: PC
Site Class: BC
City: Bedford
County: Middlesex
Geologic Group: Group 4
SDC: C
Detailed View
Discrete Damage State Probability P[Damage = DS | Sd]
0.613
0.196
0.140
0.043
0.008
0.001
None
Collapsed
Damage State
1 = Slight Damage | 2 = Moderate Damage
3 = Extensive Damage | 4 = Complete Damage

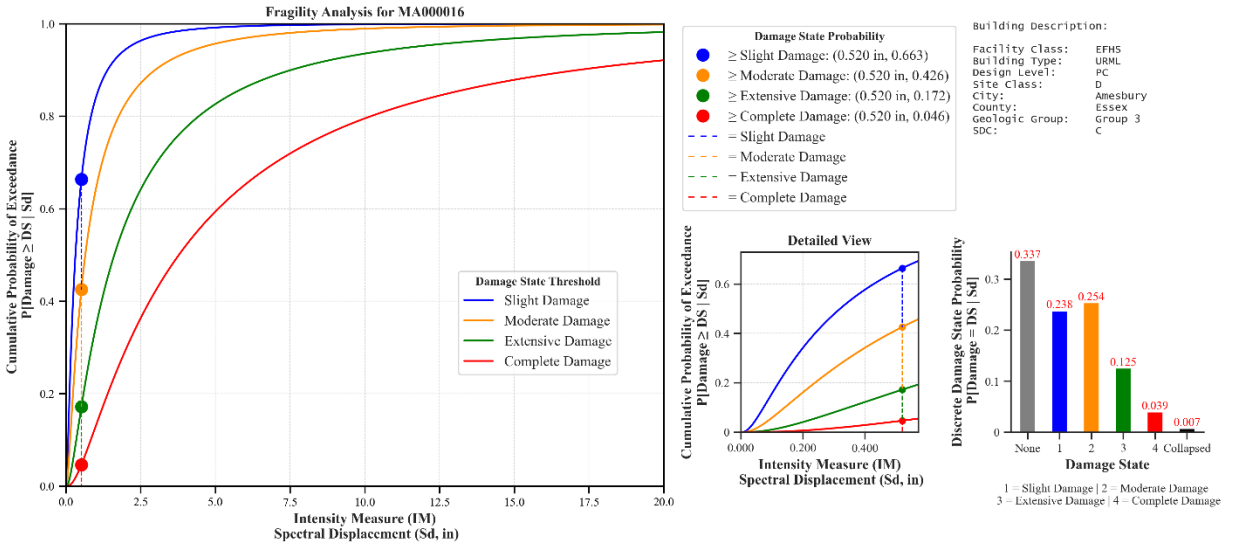
Fragility Analysis for MA000016
Cumulative Probability of Exceedance P[Damage ≥ DS | Sd]
Intensity Measure (IM) Spectral Displacement (Sd, in)
Damage State Threshold
Slight Damage
Moderate Damage
Extensive Damage
Complete Damage
Damage State Probability
≥ Slight Damage: (0.520 in, 0.663)
≥ Moderate Damage: (0.520 in, 0.426)
≥ Extensive Damage: (0.520 in, 0.172)
≥ Complete Damage: (0.520 in, 0.046)
= Slight Damage
= Moderate Damage
= Extensive Damage
= Complete Damage
Building Description:
Facility Class: EFHS
Building Type: URML
Design Level: PC
Site Class: D
City: Amesbury
County: Essex
Geologic Group: Group 3
SDC: C
Detailed View
Discrete Damage State Probability P[Damage = DS | Sd]
0.337
0.238
0.254
0.125
0.039
0.007
None
Collapsed
Damage State
1 = Slight Damage | 2 = Moderate Damage
3 = Extensive Damage | 4 = Complete Damage

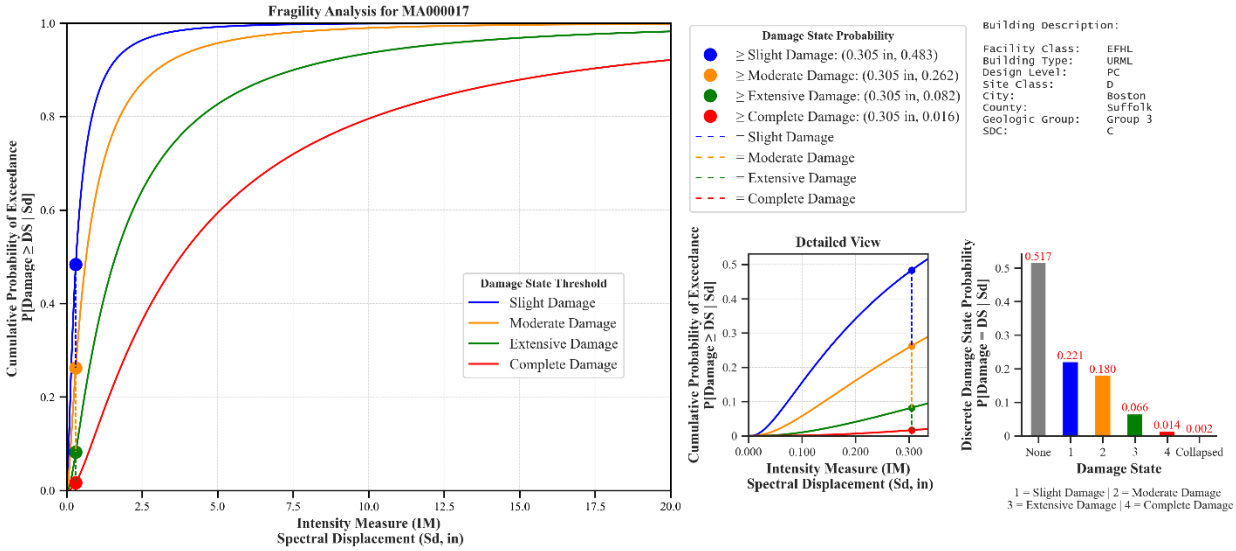
Fragility Analysis for MA000017
Cumulative Probability of Exceedance P[Damage ≥ DS | Sd]
Intensity Measure (IM) Spectral Displacement (Sd, in)
Damage State Threshold
Slight Damage
Moderate Damage
Extensive Damage
Complete Damage
Damage State Probability
≥ Slight Damage: (0.305 in, 0.483)
≥ Moderate Damage: (0.305 in, 0.262)
≥ Extensive Damage: (0.305 in, 0.082)
≥ Complete Damage: (0.305 in, 0.016)
= Slight Damage
= Moderate Damage
= Extensive Damage
= Complete Damage
Building Description:
Facility Class: EFHL
Building Type: URML
Design Level: PC
Site Class: D
City: Boston
County: Suffolk
Geologic Group: Group 3
SDC: C
Detailed View
Discrete Damage State Probability P[Damage = DS | Sd]
0.517
0.221
0.180
0.066
0.014
0.002
None
Collapsed
Damage State
1 = Slight Damage | 2 = Moderate Damage
3 = Extensive Damage | 4 = Complete Damage

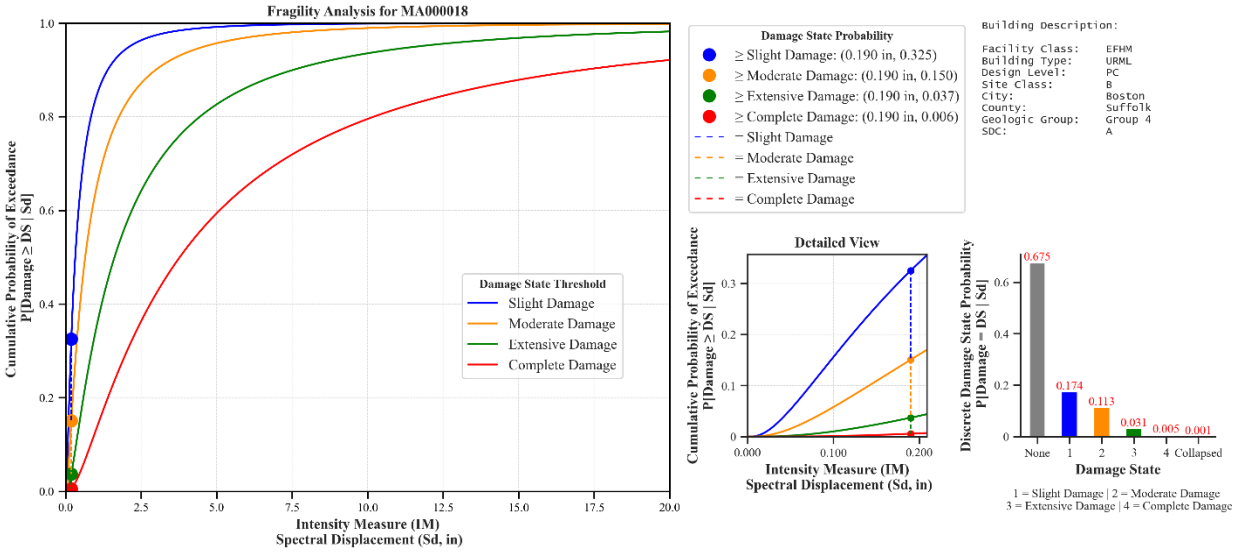
Fragility Analysis for MA000018
Damage State Threshold
Slight Damage
Moderate Damage
Extensive Damage
Complete Damage
Cumulative Probability of Exceedance
P[Damage ≥ DS | Sd]
Intensity Measure (IM)
Spectral Displacement (Sd, in)
Damage State Probability
≥ Slight Damage: (0.190 in, 0.325)
≥ Moderate Damage: (0.190 in, 0.150)
≥ Extensive Damage: (0.190 in, 0.037)
≥ Complete Damage: (0.190 in, 0.006)
= Slight Damage
= Moderate Damage
= Extensive Damage
= Complete Damage
Detailed View
Building Description:
Facility Class: EFHM
Building Type: URML
Design Level: PC
Site Class: B
City: Boston
County: Suffolk
Geologic Group: Group 4
SDC: A
Discrete Damage State Probability
P[Damage = DS | Sd]
0.675
0.174
0.113
0.031
0.005
0.001
None
Collapsed
Damage State
1 = Slight Damage | 2 = Moderate Damage
3 = Extensive Damage | 4 = Complete Damage

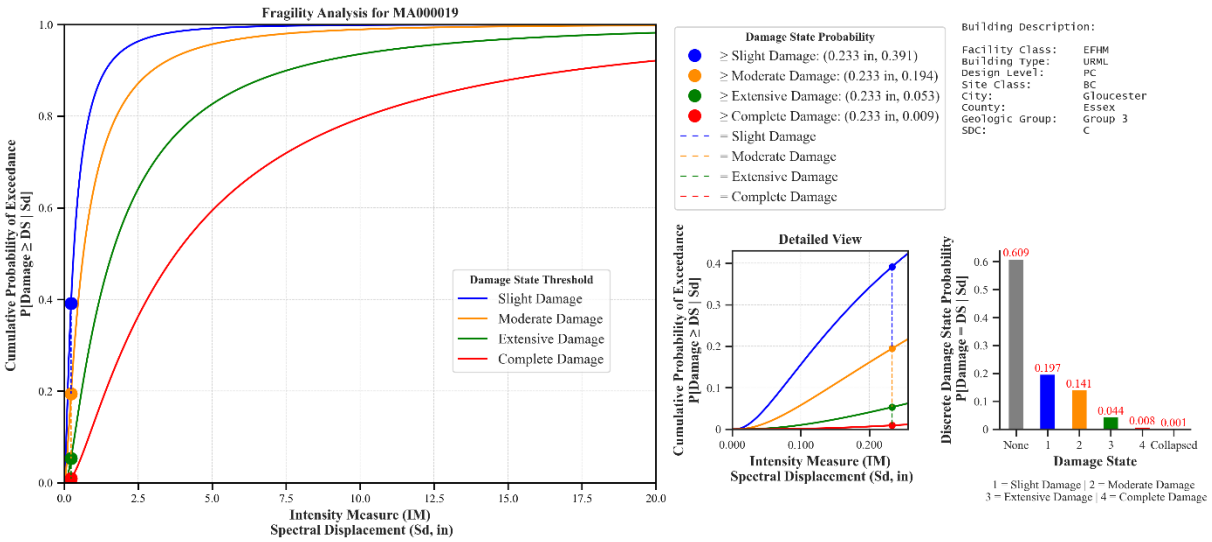
Fragility Analysis for MA000019
Damage State Threshold
Slight Damage
Moderate Damage
Extensive Damage
Complete Damage
Cumulative Probability of Exceedance
P[Damage ≥ DS | Sd]
Intensity Measure (IM)
Spectral Displacement (Sd, in)
Damage State Probability
≥ Slight Damage: (0.233 in, 0.391)
≥ Moderate Damage: (0.233 in, 0.194)
≥ Extensive Damage: (0.233 in, 0.053)
≥ Complete Damage: (0.233 in, 0.009)
= Slight Damage
= Moderate Damage
= Extensive Damage
= Complete Damage
Detailed View
Building Description:
Facility Class: EFHM
Building Type: URML
Design Level: PC
Site Class: BC
City: Gloucester
County: Essex
Geologic Group: Group 3
SDC: C
Discrete Damage State Probability
P[Damage = DS | Sd]
0.609
0.197
0.141
0.044
0.008
0.001
None
Collapsed
Damage State
1 = Slight Damage | 2 = Moderate Damage
3 = Extensive Damage | 4 = Complete Damage

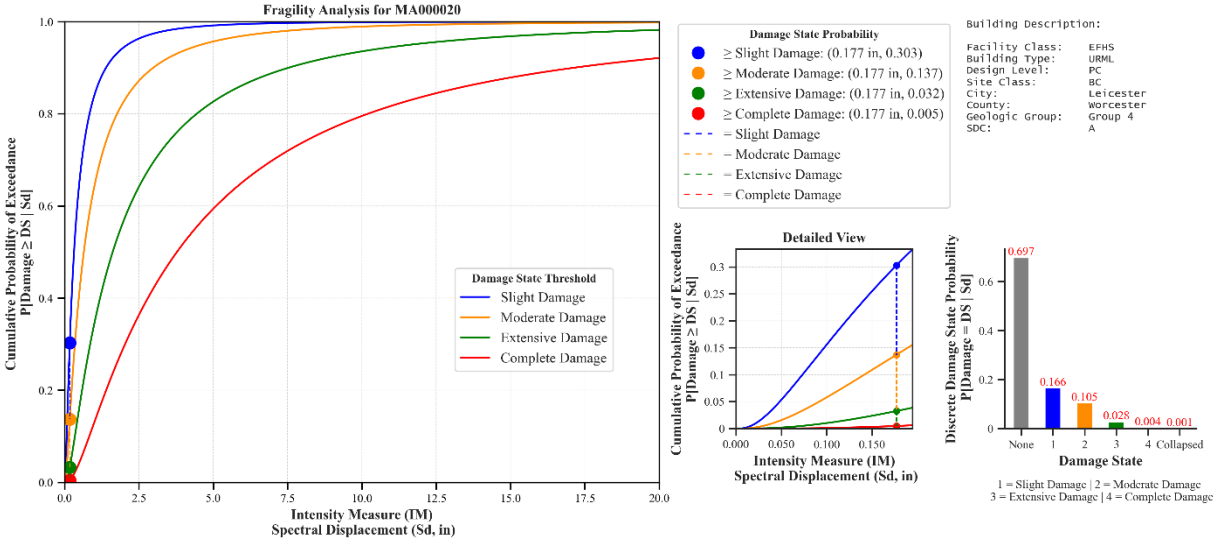
Fragility Analysis for MA000020
Damage State Threshold
Slight Damage
Moderate Damage
Extensive Damage
Complete Damage
Cumulative Probability of Exceedance
P[Damage ≥ DS | Sd]
Intensity Measure (IM)
Spectral Displacement (Sd, in)
Damage State Probability
≥ Slight Damage: (0.177 in, 0.303)
≥ Moderate Damage: (0.177 in, 0.137)
≥ Extensive Damage: (0.177 in, 0.032)
≥ Complete Damage: (0.177 in, 0.005)
= Slight Damage
= Moderate Damage
= Extensive Damage
= Complete Damage
Detailed View
Building Description:
Facility Class: EFHS
Building Type: URML
Design Level: PC
Site Class: BC
City: Leicester
County: Worcester
Geologic Group: Group 4
SDC: A
Discrete Damage State Probability
P[Damage = DS | Sd]
0.697
0.166
0.105
0.028
0.004
0.001
None
Collapsed
Damage State
1 = Slight Damage | 2 = Moderate Damage
3 = Extensive Damage | 4 = Complete Damage

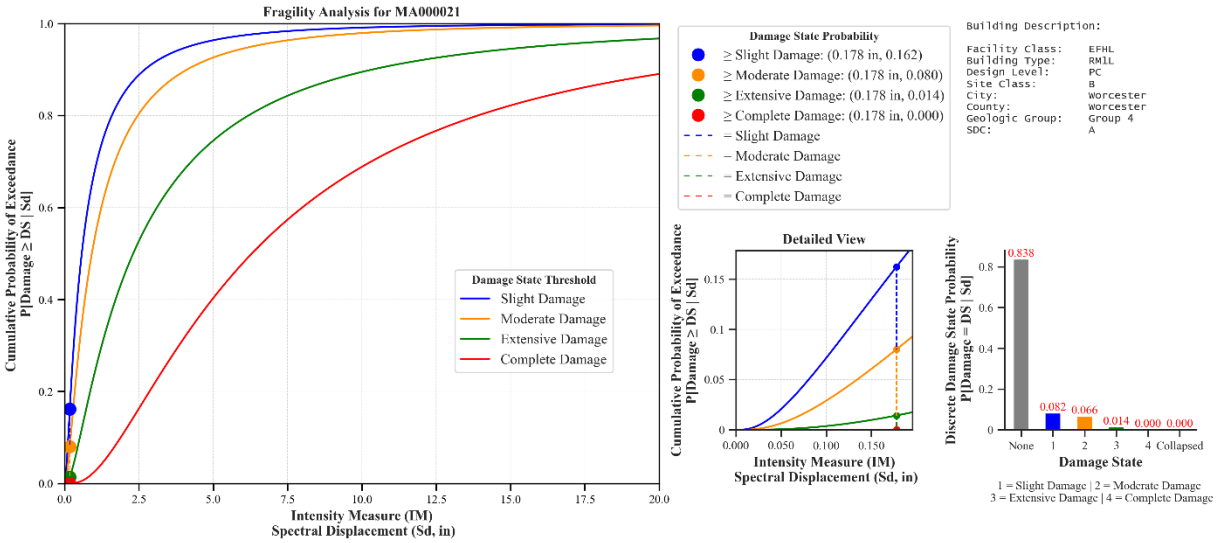
Fragility Analysis for MA000021
Cumulative Probability of Exceedance P[Damage ≥ DS | Sd]
Intensity Measure (IM) Spectral Displacement (Sd, in)
Damage State Threshold
Slight Damage
Moderate Damage
Extensive Damage
Complete Damage
Damage State Probability
≥ Slight Damage: (0.178 in, 0.162)
≥ Moderate Damage: (0.178 in, 0.080)
≥ Extensive Damage: (0.178 in, 0.014)
≥ Complete Damage: (0.178 in, 0.000)
Detailed View
Discrete Damage State Probability P[Damage = DS | Sd]
0.838
0.082
0.066
0.014
0.000
0.000
None
Collapsed
Damage State
1 = Slight Damage | 2 = Moderate Damage
3 = Extensive Damage | 4 = Complete Damage
Building Description:
Facility Class: EFHL
Building Type: RM1L
Design Level: PC
Site Class: B
City: Worcester
County: Worcester
Geologic Group: Group 4
SDC: A

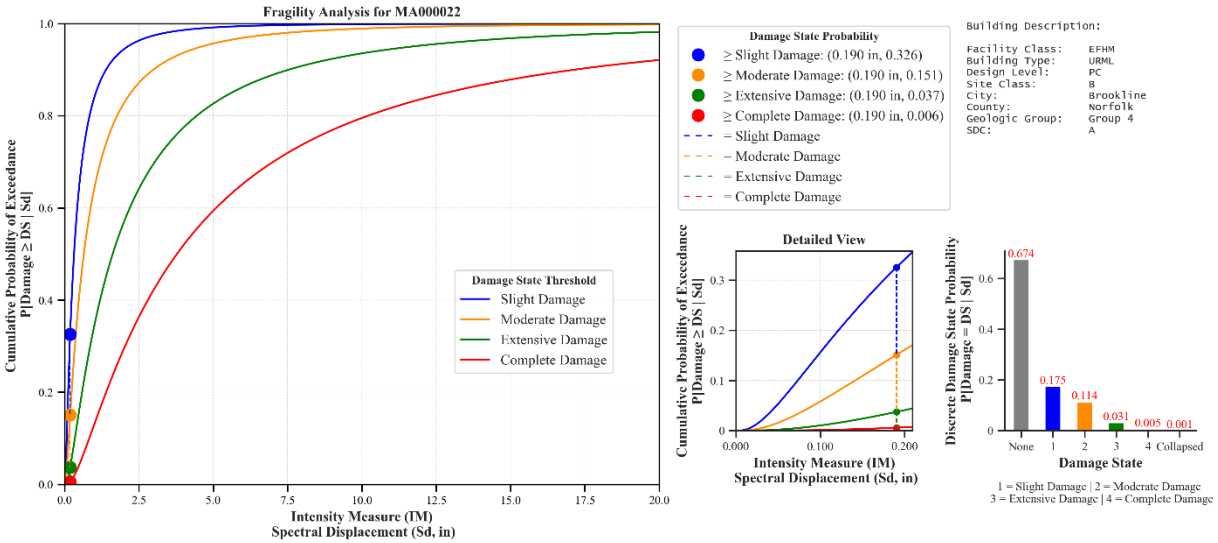
Fragility Analysis for MA000022
Cumulative Probability of Exceedance P[Damage ≥ DS | Sd]
Intensity Measure (IM) Spectral Displacement (Sd, in)
Damage State Threshold
Slight Damage
Moderate Damage
Extensive Damage
Complete Damage
Damage State Probability
≥ Slight Damage: (0.190 in, 0.326)
≥ Moderate Damage: (0.190 in, 0.151)
≥ Extensive Damage: (0.190 in, 0.037)
≥ Complete Damage: (0.190 in, 0.006)
Detailed View
Discrete Damage State Probability P[Damage = DS | Sd]
0.674
0.175
0.114
0.031
0.005
0.001
None
Collapsed
Damage State
1 = Slight Damage | 2 = Moderate Damage
3 = Extensive Damage | 4 = Complete Damage
Building Description:
Facility Class: EFHM
Building Type: URML
Design Level: PC
Site Class: B
City: Brookline
County: Norfolk
Geologic Group: Group 4
SDC: A

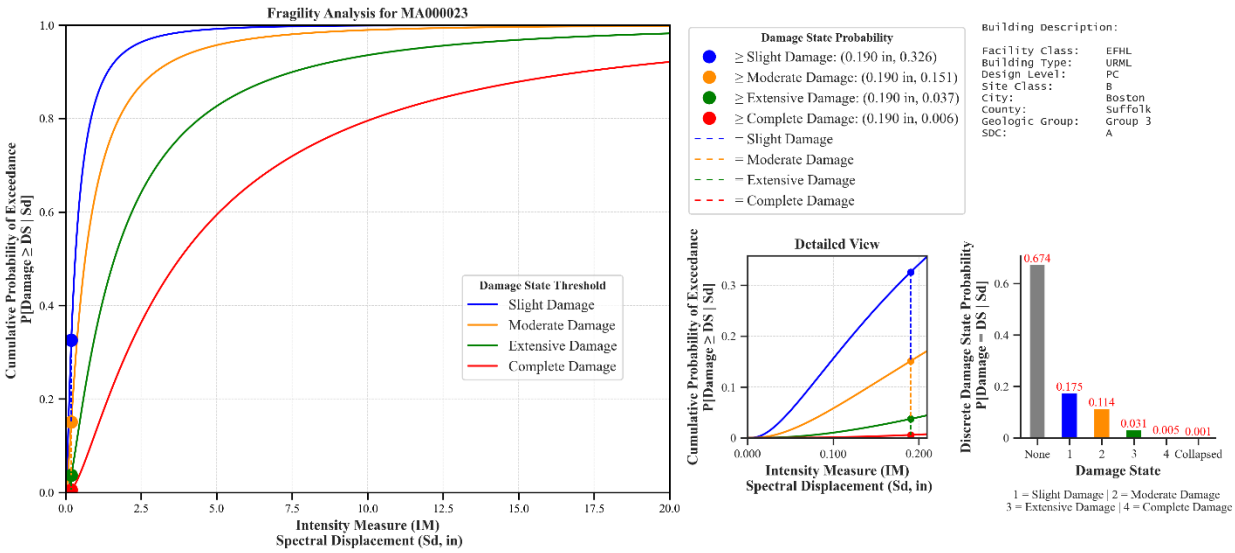
Fragility Analysis for MA000023
Cumulative Probability of Exceedance P[Damage ≥ DS | Sd]
Intensity Measure (IM) Spectral Displacement (Sd, in)
Damage State Threshold
Slight Damage
Moderate Damage
Extensive Damage
Complete Damage
Damage State Probability
≥ Slight Damage: (0.190 in, 0.326)
≥ Moderate Damage: (0.190 in, 0.151)
≥ Extensive Damage: (0.190 in, 0.037)
≥ Complete Damage: (0.190 in, 0.006)
Detailed View
Discrete Damage State Probability P[Damage = DS | Sd]
0.674
0.175
0.114
0.031
0.005
0.001
None
Collapsed
Damage State
1 = Slight Damage | 2 = Moderate Damage
3 = Extensive Damage | 4 = Complete Damage
Building Description:
Facility Class: EFHL
Building Type: URML
Design Level: PC
Site Class: B
City: Boston
County: Suffolk
Geologic Group: Group 3
SDC: A

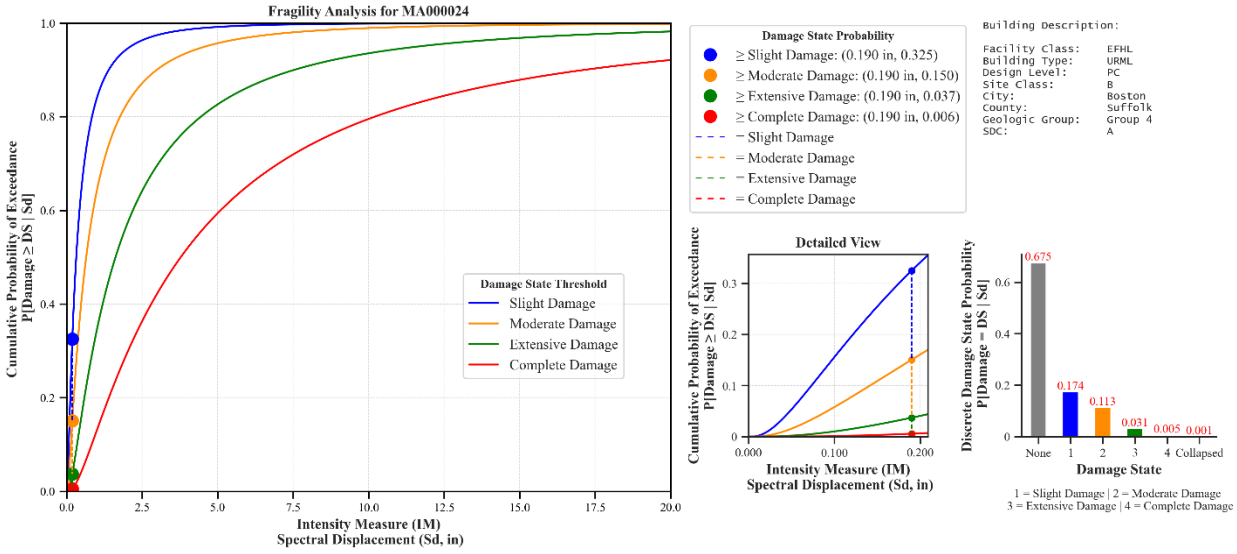
Fragility Analysis for MA000024
Cumulative Probability of Exceedance P[Damage ≥ DS | Sd]
Intensity Measure (IM) Spectral Displacement (Sd, in)
Damage State Threshold
Slight Damage
Moderate Damage
Extensive Damage
Complete Damage
Damage State Probability
≥ Slight Damage: (0.190 in, 0.325)
≥ Moderate Damage: (0.190 in, 0.150)
≥ Extensive Damage: (0.190 in, 0.037)
≥ Complete Damage: (0.190 in, 0.006)
= Slight Damage
= Moderate Damage
= Extensive Damage
= Complete Damage
Detailed View
Discrete Damage State Probability P[Damage = DS | Sd]
0.675
0.174
0.113
0.031
0.005
0.001
None
Collapsed
Damage State
1 = Slight Damage | 2 = Moderate Damage
3 = Extensive Damage | 4 = Complete Damage
Building Description:
Facility Class: EFHL
Building Type: URML
Design Level: PC
Site Class: B
City: Boston
County: Suffolk
Geologic Group: Group 4
SDC: A

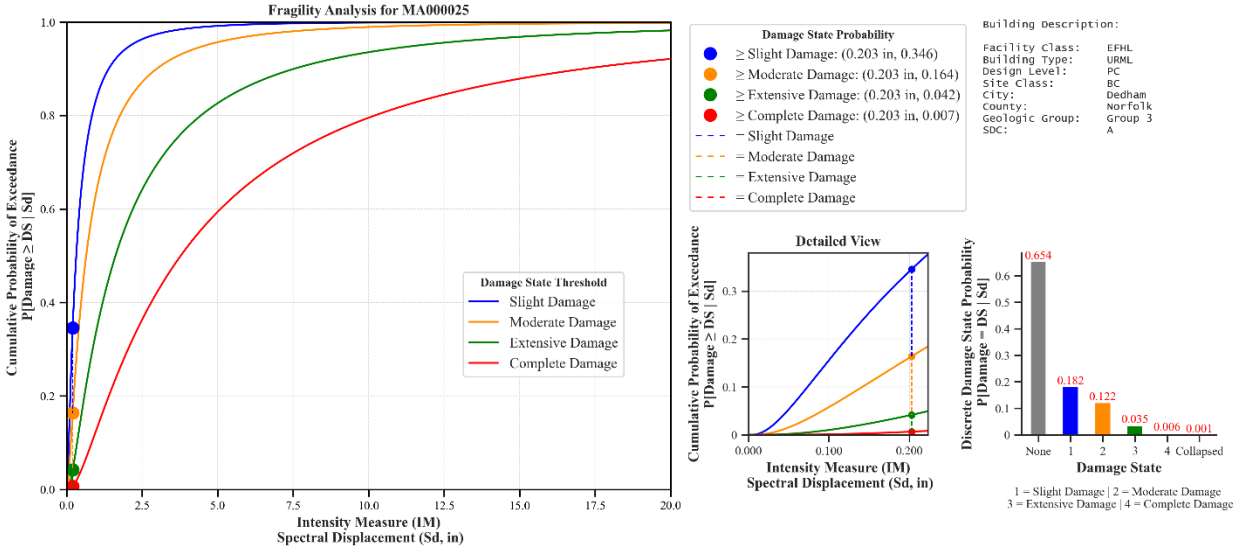
Fragility Analysis for MA000025
Cumulative Probability of Exceedance P[Damage ≥ DS | Sd]
Intensity Measure (IM) Spectral Displacement (Sd, in)
Damage State Threshold
Slight Damage
Moderate Damage
Extensive Damage
Complete Damage
Damage State Probability
≥ Slight Damage: (0.203 in, 0.346)
≥ Moderate Damage: (0.203 in, 0.164)
≥ Extensive Damage: (0.203 in, 0.042)
≥ Complete Damage: (0.203 in, 0.007)
= Slight Damage
= Moderate Damage
= Extensive Damage
= Complete Damage
Detailed View
Discrete Damage State Probability P[Damage = DS | Sd]
0.654
0.182
0.122
0.035
0.006
0.001
None
Collapsed
Damage State
1 = Slight Damage | 2 = Moderate Damage
3 = Extensive Damage | 4 = Complete Damage
Building Description:
Facility Class: EFHL
Building Type: URML
Design Level: PC
Site Class: BC
City: Dedham
County: Norfolk
Geologic Group: Group 3
SDC: A

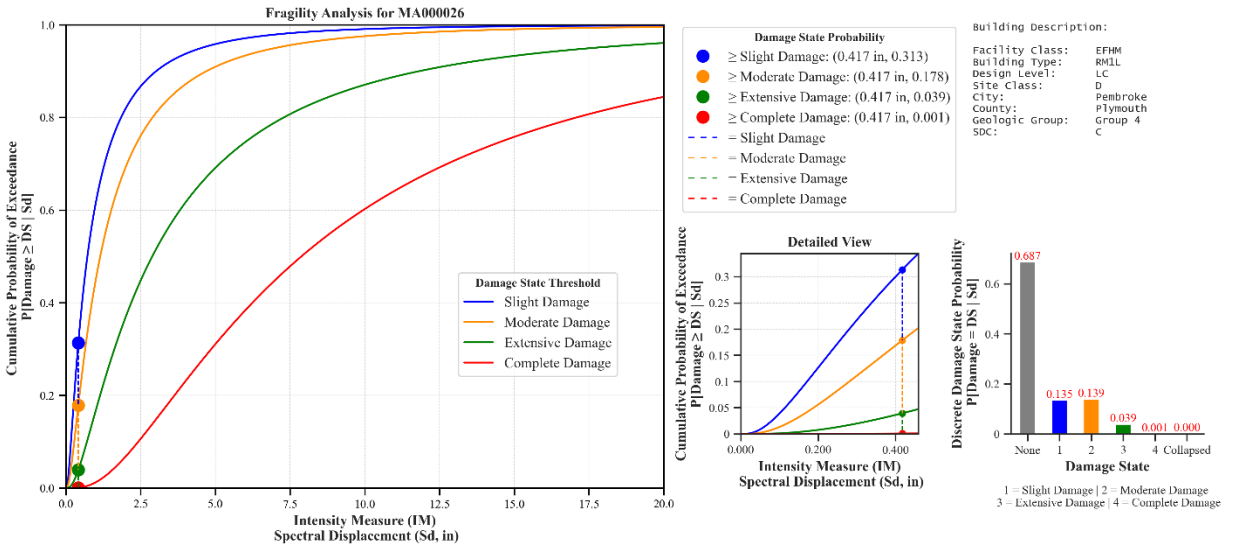
Fragility Analysis for MA000026
Cumulative Probability of Exceedance P[Damage ≥ DS | Sd]
Intensity Measure (IM) Spectral Displacement (Sd, in)
Damage State Threshold
Slight Damage
Moderate Damage
Extensive Damage
Complete Damage
Damage State Probability
≥ Slight Damage: (0.417 in, 0.313)
≥ Moderate Damage: (0.417 in, 0.178)
≥ Extensive Damage: (0.417 in, 0.039)
≥ Complete Damage: (0.417 in, 0.001)
= Slight Damage
= Moderate Damage
= Extensive Damage
= Complete Damage
Detailed View
Discrete Damage State Probability P[Damage = DS | Sd]
0.687
0.135
0.139
0.039
0.001
0.000
None
Collapsed
Damage State
1 = Slight Damage | 2 = Moderate Damage
3 = Extensive Damage | 4 = Complete Damage
Building Description:
Facility Class: EFHM
Building Type: RM1L
Design Level: LC
Site Class: D
City: Pembroke
County: Plymouth
Geologic Group: Group 4
SDC: C

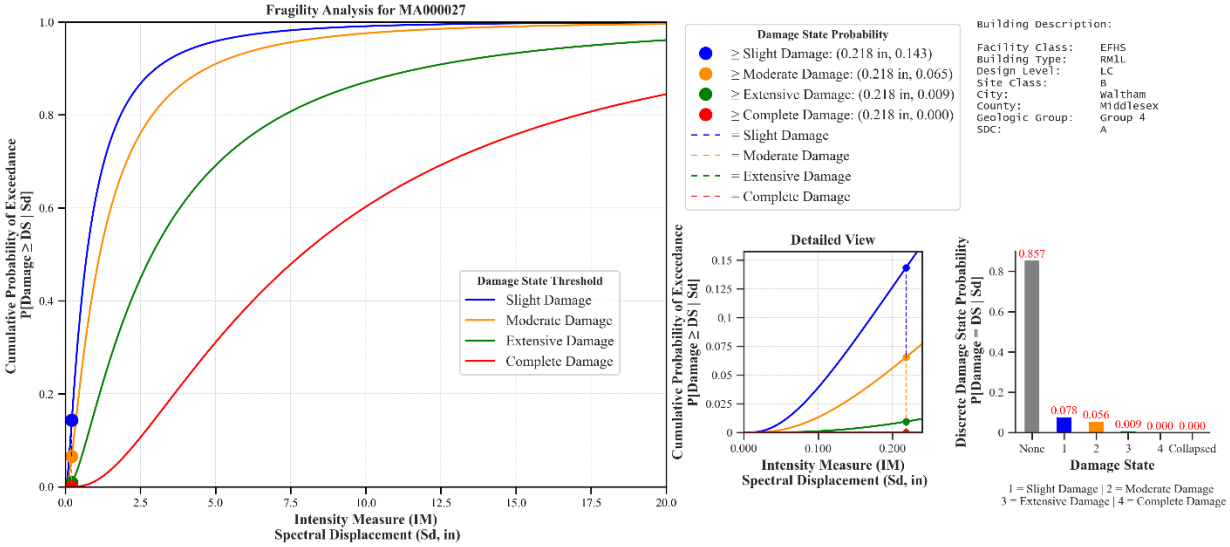
Fragility Analysis for MA000027
Damage State Threshold
Slight Damage
Moderate Damage
Extensive Damage
Complete Damage
Cumulative Probability of Exceedance P[Damage ≥ DS | Sd]
Intensity Measure (IM) Spectral Displacement (Sd, in)
Damage State Probability
≥ Slight Damage: (0.218 in, 0.143)
≥ Moderate Damage: (0.218 in, 0.065)
≥ Extensive Damage: (0.218 in, 0.009)
≥ Complete Damage: (0.218 in, 0.000)
= Slight Damage
= Moderate Damage
= Extensive Damage
= Complete Damage
Building Description:
Facility Class: EFHS
Building Type: RM1L
Design Level: LC
Site Class: B
City: Waltham
County: Middlesex
Geologic Group: Group 4
SDC: A
Detailed View
Discrete Damage State Probability P[Damage = DS | Sd]
0.857
0.078
0.056
0.009
0.000
0.000
None
1
2
3
4 Collapsed
Damage State
1 = Slight Damage | 2 = Moderate Damage
3 = Extensive Damage | 4 = Complete Damage

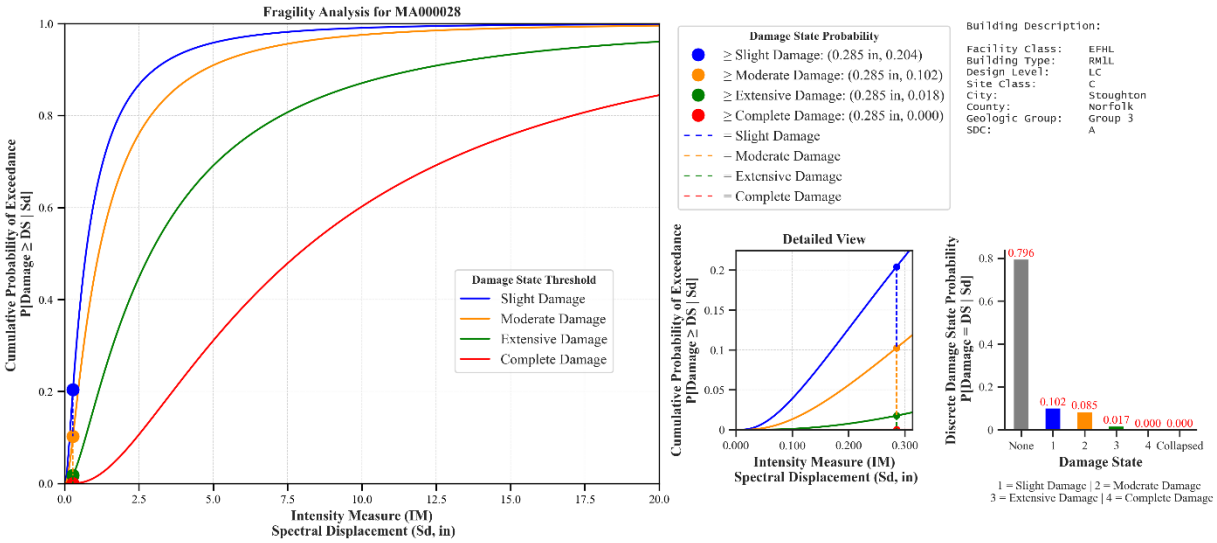
Fragility Analysis for MA000028
Damage State Threshold
Slight Damage
Moderate Damage
Extensive Damage
Complete Damage
Cumulative Probability of Exceedance P[Damage ≥ DS | Sd]
Intensity Measure (IM) Spectral Displacement (Sd, in)
Damage State Probability
≥ Slight Damage: (0.285 in, 0.204)
≥ Moderate Damage: (0.285 in, 0.102)
≥ Extensive Damage: (0.285 in, 0.018)
≥ Complete Damage: (0.285 in, 0.000)
= Slight Damage
= Moderate Damage
= Extensive Damage
= Complete Damage
Building Description:
Facility Class: EFHL
Building Type: RM1L
Design Level: LC
Site Class: C
City: Stoughton
County: Norfolk
Geologic Group: Group 3
SDC: A
Detailed View
Discrete Damage State Probability P[Damage = DS | Sd]
0.796
0.102
0.085
0.017
0.000
0.000
None
1
2
3
4 Collapsed
Damage State
1 = Slight Damage | 2 = Moderate Damage
3 = Extensive Damage | 4 = Complete Damage

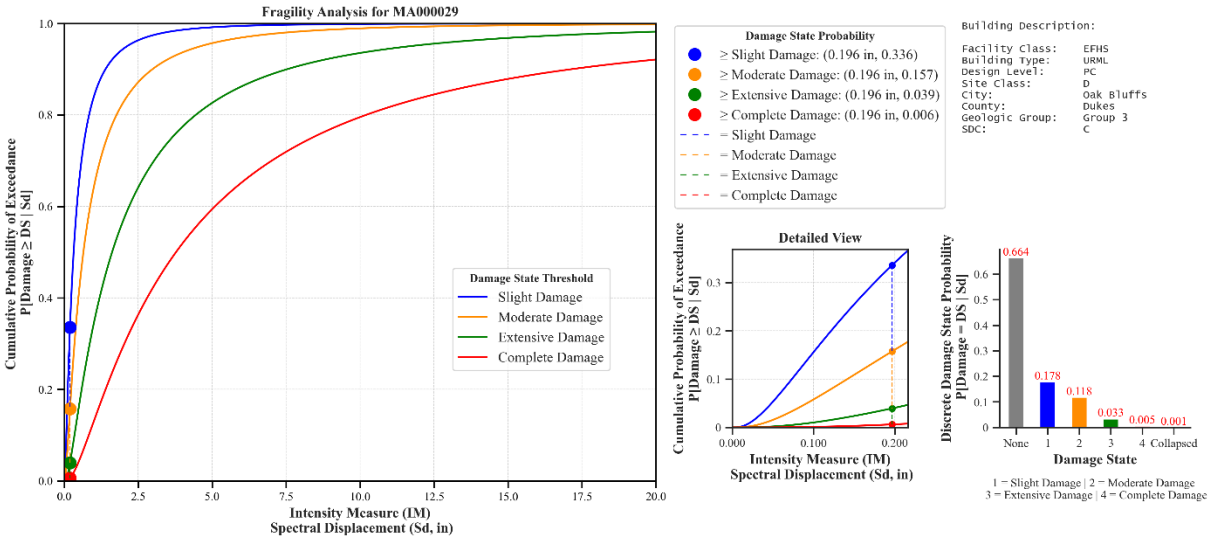
Fragility Analysis for MA000029
Damage State Threshold
Slight Damage
Moderate Damage
Extensive Damage
Complete Damage
Cumulative Probability of Exceedance P[Damage ≥ DS | Sd]
Intensity Measure (IM) Spectral Displacement (Sd, in)
Damage State Probability
≥ Slight Damage: (0.196 in, 0.336)
≥ Moderate Damage: (0.196 in, 0.157)
≥ Extensive Damage: (0.196 in, 0.039)
≥ Complete Damage: (0.196 in, 0.006)
= Slight Damage
= Moderate Damage
= Extensive Damage
= Complete Damage
Building Description:
Facility Class: EFHS
Building Type: URML
Design Level: PC
Site Class: D
City: Oak Bluffs
County: Dukes
Geologic Group: Group 3
SDC: C
Detailed View
Discrete Damage State Probability P[Damage = DS | Sd]
0.664
0.178
0.118
0.033
0.005
0.001
None
1
2
3
4 Collapsed
Damage State
1 = Slight Damage | 2 = Moderate Damage
3 = Extensive Damage | 4 = Complete Damage

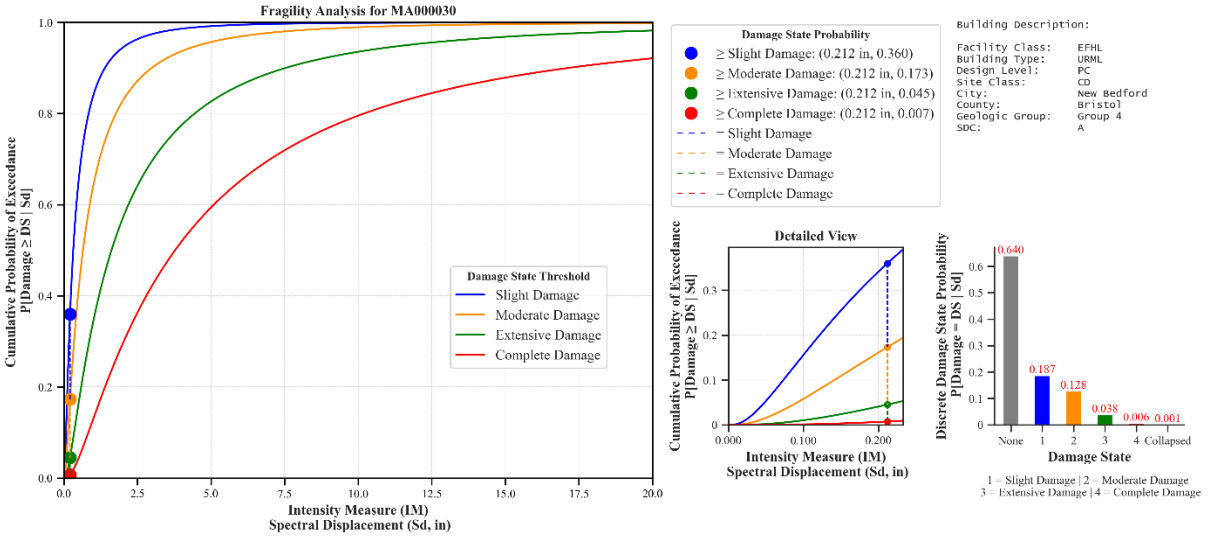
Fragility Analysis for MA000030
Cumulative Probability of Exceedance P[Damage ≥ DS | Sd]
Intensity Measure (IM) Spectral Displacement (Sd, in)
Damage State Threshold
Slight Damage
Moderate Damage
Extensive Damage
Complete Damage
Damage State Probability
≥ Slight Damage: (0.212 in, 0.360)
≥ Moderate Damage: (0.212 in, 0.173)
≥ Extensive Damage: (0.212 in, 0.045)
≥ Complete Damage: (0.212 in, 0.007)
Detailed View
Discrete Damage State Probability P[Damage = DS | Sd]
0.640
0.187
0.128
0.038
0.006
0.001
None
Collapsed
Damage State
1 = Slight Damage | 2 = Moderate Damage
3 = Extensive Damage | 4 = Complete Damage
Building Description:
Facility Class: EFHL
Building Type: URML
Design Level: PC
Site Class: CD
City: New Bedford
County: Bristol
Geologic Group: Group 4
SDC: A

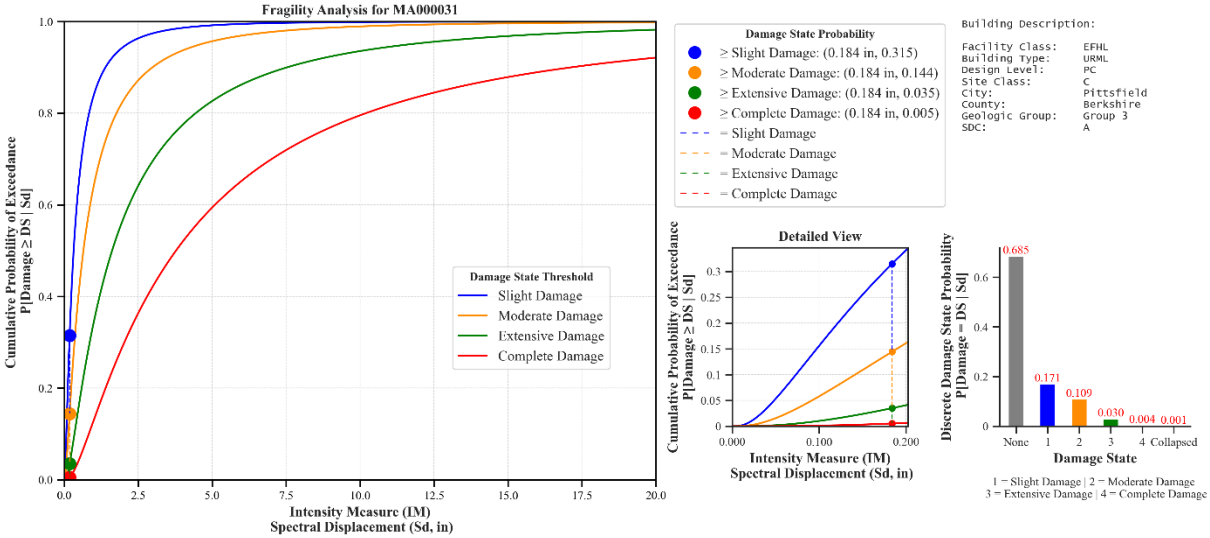
Fragility Analysis for MA000031
Cumulative Probability of Exceedance P[Damage ≥ DS | Sd]
Intensity Measure (IM) Spectral Displacement (Sd, in)
Damage State Threshold
Slight Damage
Moderate Damage
Extensive Damage
Complete Damage
Damage State Probability
≥ Slight Damage: (0.184 in, 0.315)
≥ Moderate Damage: (0.184 in, 0.144)
≥ Extensive Damage: (0.184 in, 0.035)
≥ Complete Damage: (0.184 in, 0.005)
Detailed View
Discrete Damage State Probability P[Damage = DS | Sd]
0.685
0.171
0.109
0.030
0.004
0.001
None
Collapsed
Damage State
1 = Slight Damage | 2 = Moderate Damage
3 = Extensive Damage | 4 = Complete Damage
Building Description:
Facility Class: EFHL
Building Type: URML
Design Level: PC
Site Class: C
City: Pittsfield
County: Berkshire
Geologic Group: Group 3
SDC: A

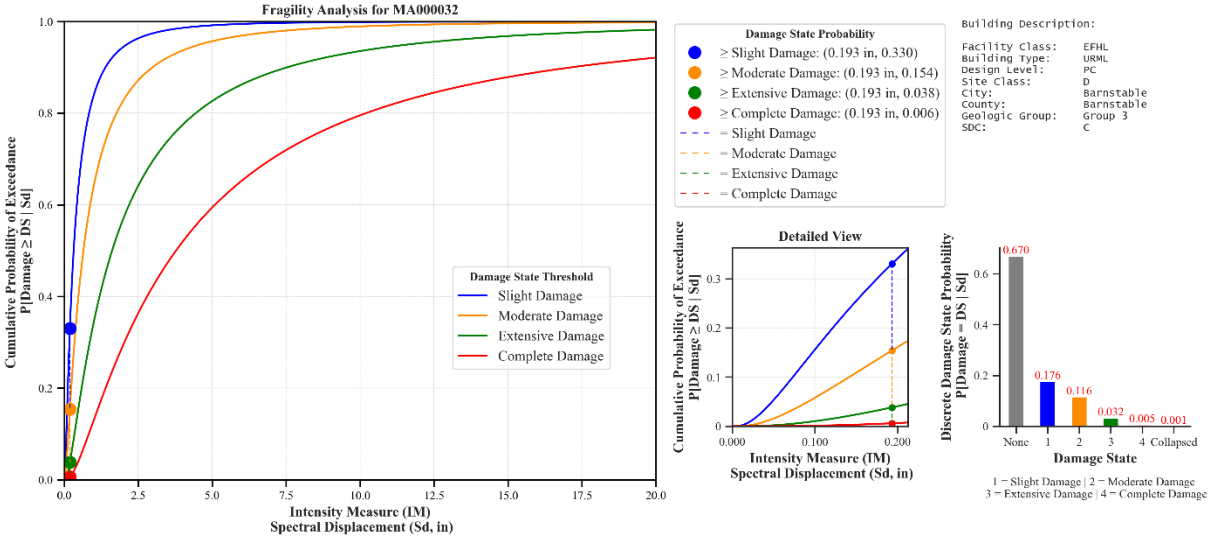
Fragility Analysis for MA000032
Cumulative Probability of Exceedance P[Damage ≥ DS | Sd]
Intensity Measure (IM) Spectral Displacement (Sd, in)
Damage State Threshold
Slight Damage
Moderate Damage
Extensive Damage
Complete Damage
Damage State Probability
≥ Slight Damage: (0.193 in, 0.330)
≥ Moderate Damage: (0.193 in, 0.154)
≥ Extensive Damage: (0.193 in, 0.038)
≥ Complete Damage: (0.193 in, 0.006)
Detailed View
Discrete Damage State Probability P[Damage = DS | Sd]
0.670
0.176
0.116
0.032
0.005
0.001
None
Collapsed
Damage State
1 = Slight Damage | 2 = Moderate Damage
3 = Extensive Damage | 4 = Complete Damage
Building Description:
Facility Class: EFHL
Building Type: URML
Design Level: PC
Site Class: D
City: Barnstable
County: Barnstable
Geologic Group: Group 3
SDC: C

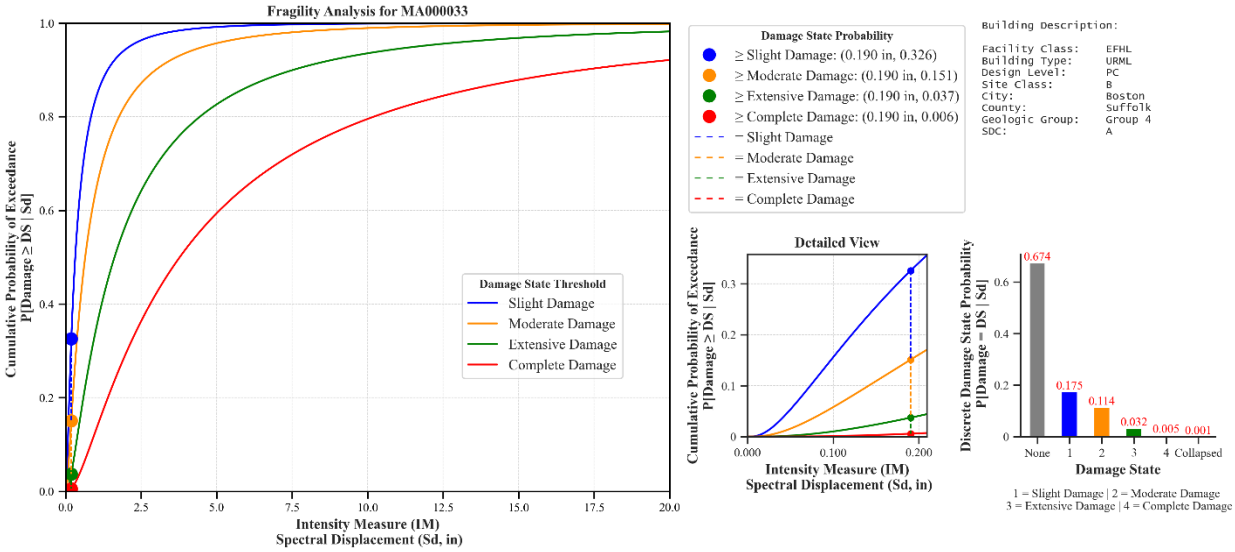
Fragility Analysis for MA000033
Cumulative Probability of Exceedance P[Damage ≥ DS | Sd]
Intensity Measure (IM) Spectral Displacement (Sd, in)
Damage State Threshold
Slight Damage
Moderate Damage
Extensive Damage
Complete Damage
Damage State Probability
≥ Slight Damage: (0.190 in, 0.326)
≥ Moderate Damage: (0.190 in, 0.151)
≥ Extensive Damage: (0.190 in, 0.037)
≥ Complete Damage: (0.190 in, 0.006)
= Slight Damage
= Moderate Damage
= Extensive Damage
= Complete Damage
Detailed View
Discrete Damage State Probability P[Damage = DS | Sd]
0.674
0.175
0.114
0.032
0.005
0.001
None
1
2
3
4 Collapsed
Damage State
1 = Slight Damage | 2 = Moderate Damage
3 = Extensive Damage | 4 = Complete Damage
Building Description:
Facility Class: EFHL
Building Type: URML
Design Level: PC
Site Class: B
City: Boston
County: Suffolk
Geologic Group: Group 4
SDC: A

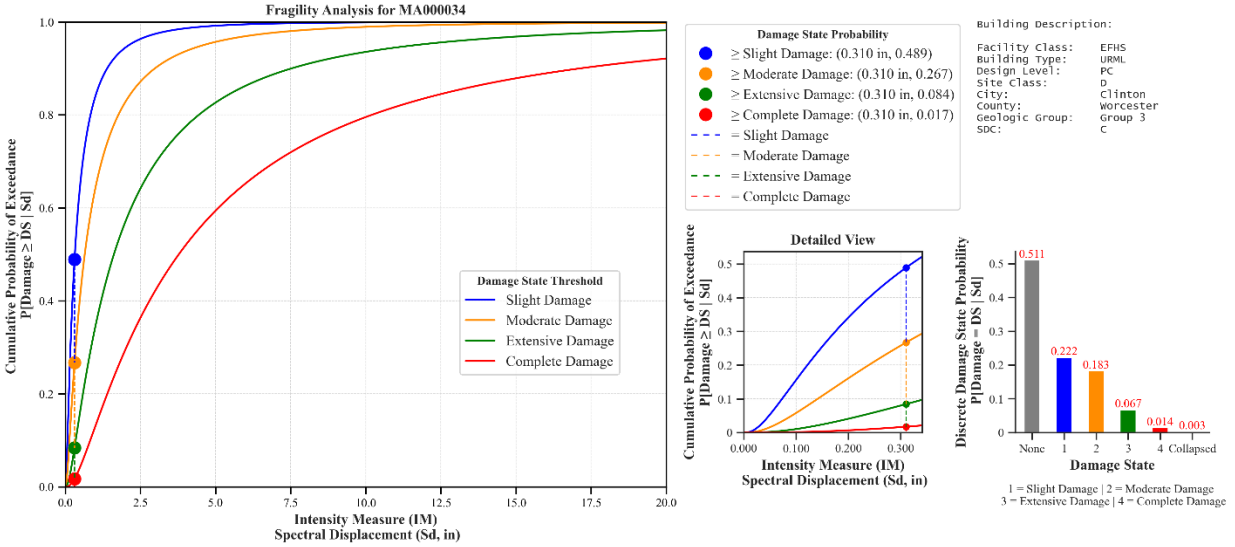
Fragility Analysis for MA000034
Cumulative Probability of Exceedance P[Damage ≥ DS | Sd]
Intensity Measure (IM) Spectral Displacement (Sd, in)
Damage State Threshold
Slight Damage
Moderate Damage
Extensive Damage
Complete Damage
Damage State Probability
≥ Slight Damage: (0.310 in, 0.489)
≥ Moderate Damage: (0.310 in, 0.267)
≥ Extensive Damage: (0.310 in, 0.084)
≥ Complete Damage: (0.310 in, 0.017)
= Slight Damage
= Moderate Damage
= Extensive Damage
= Complete Damage
Detailed View
Discrete Damage State Probability P[Damage = DS | Sd]
0.511
0.222
0.183
0.067
0.014
0.003
None
1
2
3
4 Collapsed
Damage State
1 = Slight Damage | 2 = Moderate Damage
3 = Extensive Damage | 4 = Complete Damage
Building Description:
Facility Class: EFHS
Building Type: URML
Design Level: PC
Site Class: D
City: Clinton
County: Worcester
Geologic Group: Group 3
SDC: C

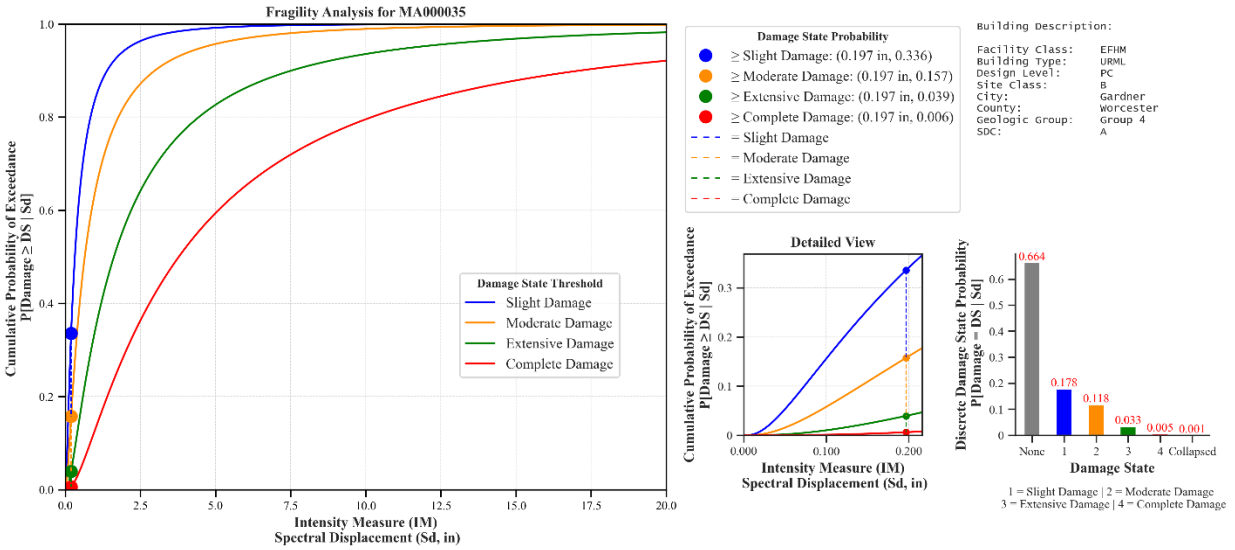
Fragility Analysis for MA000035
Cumulative Probability of Exceedance P[Damage ≥ DS | Sd]
Intensity Measure (IM) Spectral Displacement (Sd, in)
Damage State Threshold
Slight Damage
Moderate Damage
Extensive Damage
Complete Damage
Damage State Probability
≥ Slight Damage: (0.197 in, 0.336)
≥ Moderate Damage: (0.197 in, 0.157)
≥ Extensive Damage: (0.197 in, 0.039)
≥ Complete Damage: (0.197 in, 0.006)
= Slight Damage
= Moderate Damage
= Extensive Damage
= Complete Damage
Detailed View
Discrete Damage State Probability P[Damage = DS | Sd]
0.664
0.178
0.118
0.033
0.005
0.001
None
1
2
3
4 Collapsed
Damage State
1 = Slight Damage | 2 = Moderate Damage
3 = Extensive Damage | 4 = Complete Damage
Building Description:
Facility Class: EFHM
Building Type: URML
Design Level: PC
Site Class: B
City: Gardner
County: Worcester
Geologic Group: Group 4
SDC: A

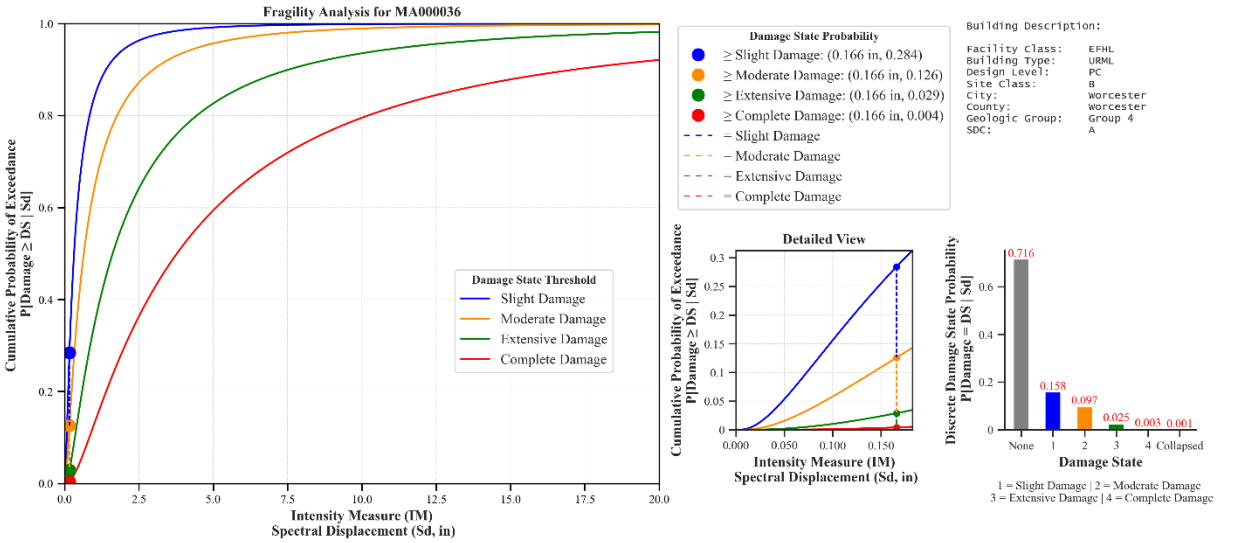
Fragility Analysis for MA000036
Cumulative Probability of Exceedance P[Damage ≥ DS | Sd]
Intensity Measure (IM) Spectral Displacement (Sd, in)
Damage State Threshold
Slight Damage
Moderate Damage
Extensive Damage
Complete Damage
Damage State Probability
≥ Slight Damage: (0.166 in, 0.284)
≥ Moderate Damage: (0.166 in, 0.126)
≥ Extensive Damage: (0.166 in, 0.029)
≥ Complete Damage: (0.166 in, 0.004)
Building Description:
Facility Class: EFHL
Building Type: URML
Design Level: PC
Site Class: B
City: Worcester
County: Worcester
Geologic Group: Group 4
SDC: A
Detailed View
Discrete Damage State Probability P[Damage = DS | Sd]
0.716
0.158
0.097
0.025
0.003
0.001
None 1 2 3 4 Collapsed
Damage State
1 = Slight Damage | 2 = Moderate Damage
3 = Extensive Damage | 4 = Complete Damage

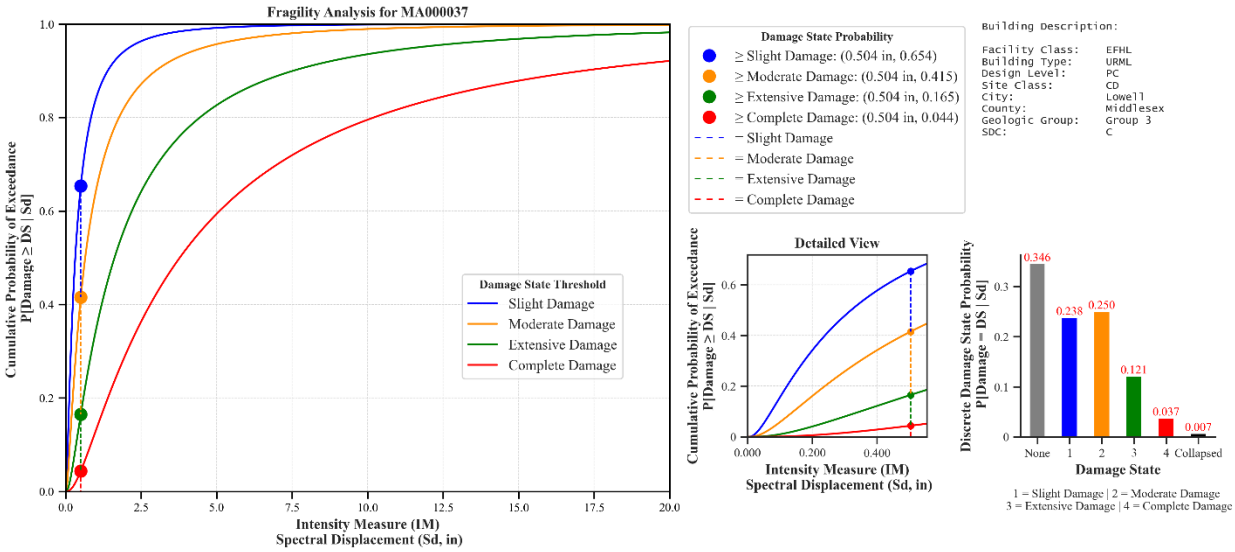
Fragility Analysis for MA000037
Cumulative Probability of Exceedance P[Damage ≥ DS | Sd]
Intensity Measure (IM) Spectral Displacement (Sd, in)
Damage State Threshold
Slight Damage
Moderate Damage
Extensive Damage
Complete Damage
Damage State Probability
≥ Slight Damage: (0.504 in, 0.654)
≥ Moderate Damage: (0.504 in, 0.415)
≥ Extensive Damage: (0.504 in, 0.165)
≥ Complete Damage: (0.504 in, 0.044)
Building Description:
Facility Class: EFHL
Building Type: URML
Design Level: PC
Site Class: CD
City: Lowell
County: Middlesex
Geologic Group: Group 3
SDC: C
Detailed View
Discrete Damage State Probability P[Damage = DS | Sd]
0.346
0.238
0.250
0.121
0.037
0.007
None 1 2 3 4 Collapsed
Damage State
1 = Slight Damage | 2 = Moderate Damage
3 = Extensive Damage | 4 = Complete Damage

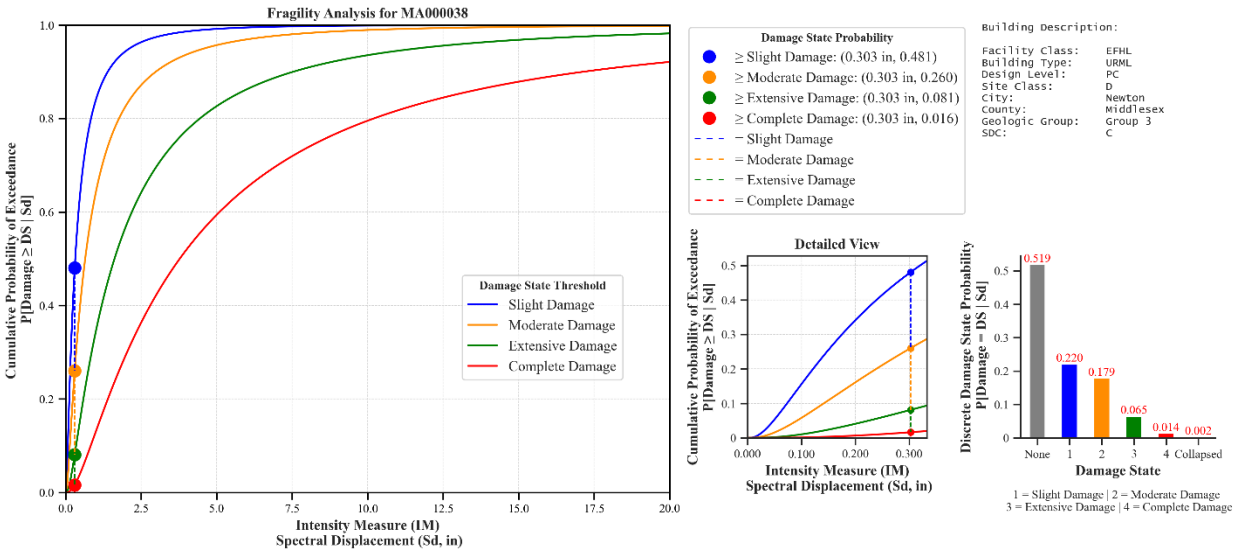
Fragility Analysis for MA000038
Cumulative Probability of Exceedance P[Damage ≥ DS | Sd]
Intensity Measure (IM) Spectral Displacement (Sd, in)
Damage State Threshold
Slight Damage
Moderate Damage
Extensive Damage
Complete Damage
Damage State Probability
≥ Slight Damage: (0.303 in, 0.481)
≥ Moderate Damage: (0.303 in, 0.260)
≥ Extensive Damage: (0.303 in, 0.081)
≥ Complete Damage: (0.303 in, 0.016)
Building Description:
Facility Class: EFHL
Building Type: URML
Design Level: PC
Site Class: D
City: Newton
County: Middlesex
Geologic Group: Group 3
SDC: C
Detailed View
Discrete Damage State Probability P[Damage = DS | Sd]
0.519
0.220
0.179
0.065
0.014
0.002
None 1 2 3 4 Collapsed
Damage State
1 = Slight Damage | 2 = Moderate Damage
3 = Extensive Damage | 4 = Complete Damage

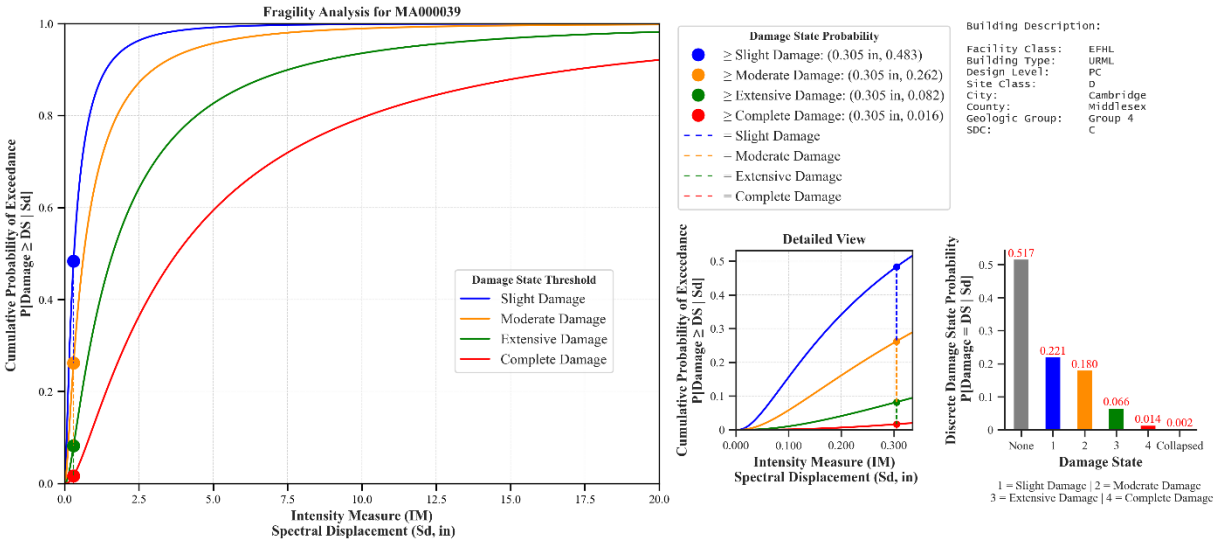
Fragility Analysis for MA000039
Cumulative Probability of Exceedance P[Damage ≥ DS | Sd]
Intensity Measure (IM) Spectral Displacement (Sd, in)
Damage State Threshold
Slight Damage
Moderate Damage
Extensive Damage
Complete Damage
Damage State Probability
≥ Slight Damage: (0.305 in, 0.483)
≥ Moderate Damage: (0.305 in, 0.262)
≥ Extensive Damage: (0.305 in, 0.082)
≥ Complete Damage: (0.305 in, 0.016)
Building Description:
Facility Class: EFHL
Building Type: URML
Design Level: PC
Site Class: D
City: Cambridge
County: Middlesex
Geologic Group: Group 4
SDC: C
Detailed View
Discrete Damage State Probability P[Damage = DS | Sd]
0.517
0.221
0.180
0.066
0.014
0.002
None
Collapsed
Damage State
1 = Slight Damage | 2 = Moderate Damage
3 = Extensive Damage | 4 = Complete Damage

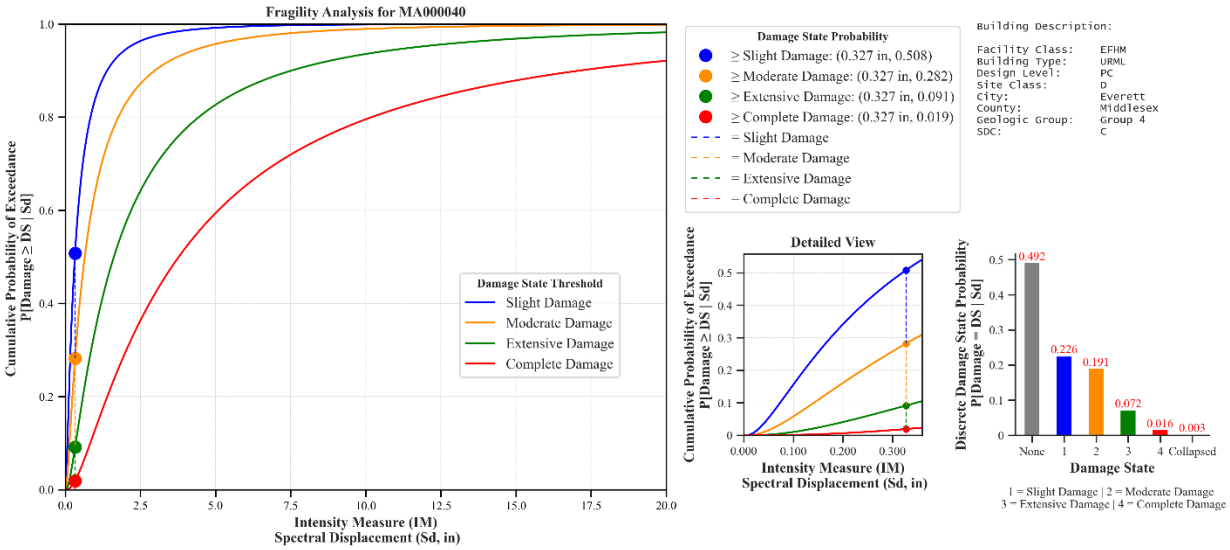
Fragility Analysis for MA000040
Cumulative Probability of Exceedance P[Damage ≥ DS | Sd]
Intensity Measure (IM) Spectral Displacement (Sd, in)
Damage State Threshold
Slight Damage
Moderate Damage
Extensive Damage
Complete Damage
Damage State Probability
≥ Slight Damage: (0.327 in, 0.508)
≥ Moderate Damage: (0.327 in, 0.282)
≥ Extensive Damage: (0.327 in, 0.091)
≥ Complete Damage: (0.327 in, 0.019)
Building Description:
Facility Class: EFHM
Building Type: URML
Design Level: PC
Site Class: D
City: Everett
County: Middlesex
Geologic Group: Group 4
SDC: C
Detailed View
Discrete Damage State Probability P[Damage = DS | Sd]
0.492
0.226
0.191
0.072
0.016
0.003
None
Collapsed
Damage State
1 = Slight Damage | 2 = Moderate Damage
3 = Extensive Damage | 4 = Complete Damage

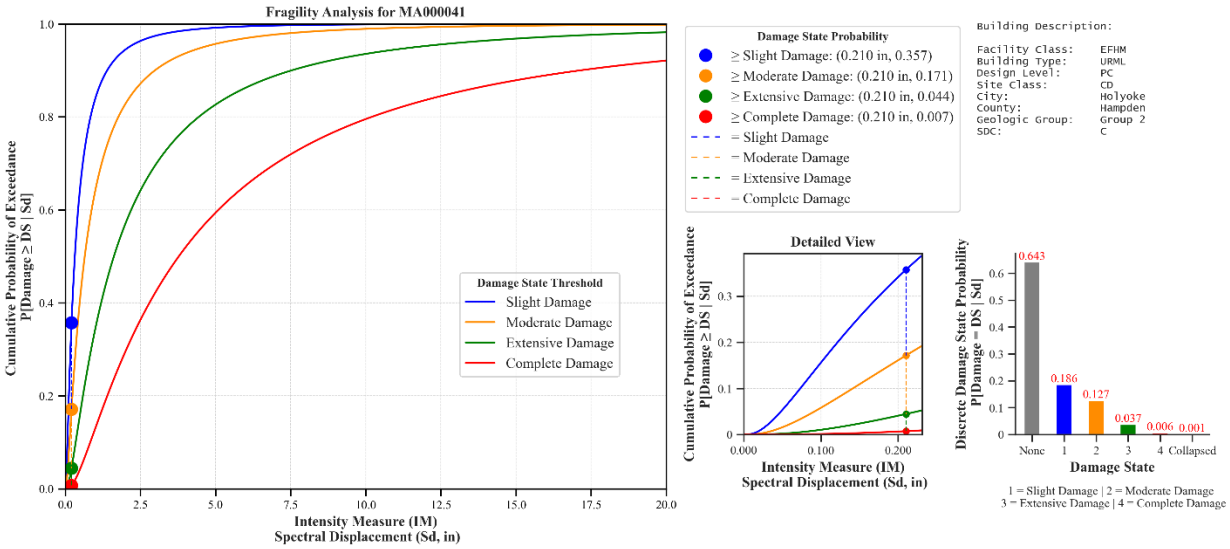
Fragility Analysis for MA000041
Cumulative Probability of Exceedance P[Damage ≥ DS | Sd]
Intensity Measure (IM) Spectral Displacement (Sd, in)
Damage State Threshold
Slight Damage
Moderate Damage
Extensive Damage
Complete Damage
Damage State Probability
≥ Slight Damage: (0.210 in, 0.357)
≥ Moderate Damage: (0.210 in, 0.171)
≥ Extensive Damage: (0.210 in, 0.044)
≥ Complete Damage: (0.210 in, 0.007)
Building Description:
Facility Class: EFHM
Building Type: URML
Design Level: PC
Site Class: CD
City: Holyoke
County: Hampden
Geologic Group: Group 2
SDC: C
Detailed View
Discrete Damage State Probability P[Damage = DS | Sd]
0.643
0.186
0.127
0.037
0.006
0.001
None
Collapsed
Damage State
1 = Slight Damage | 2 = Moderate Damage
3 = Extensive Damage | 4 = Complete Damage

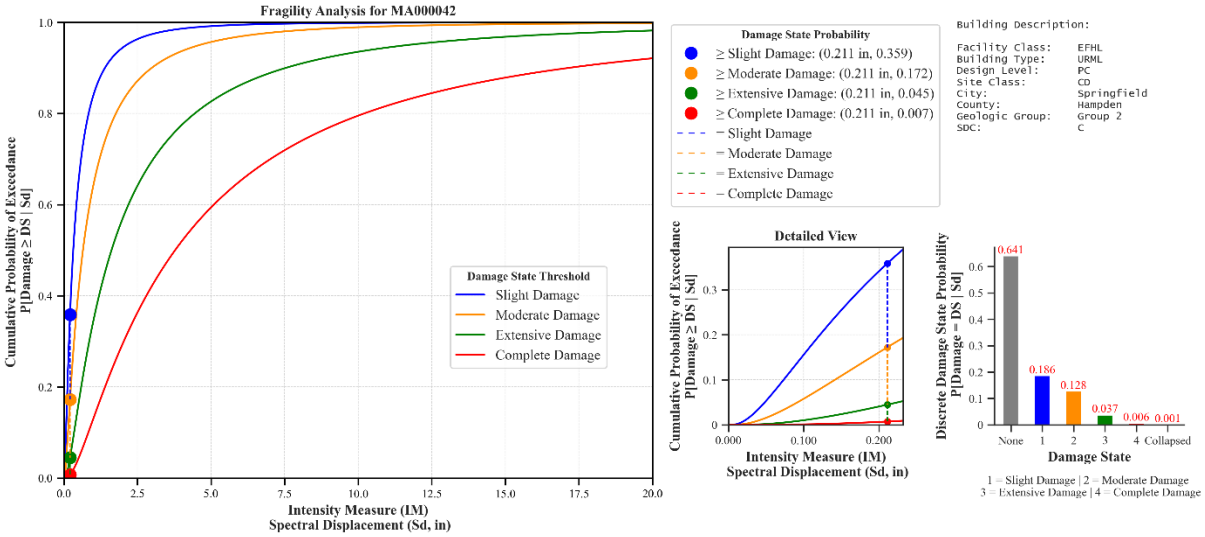
Fragility Analysis for MA000042
Cumulative Probability of Exceedance P[Damage ≥ DS | Sd]
Intensity Measure (IM) Spectral Displacement (Sd, in)
Damage State Threshold
Slight Damage
Moderate Damage
Extensive Damage
Complete Damage
Damage State Probability
≥ Slight Damage: (0.211 in, 0.359)
≥ Moderate Damage: (0.211 in, 0.172)
≥ Extensive Damage: (0.211 in, 0.045)
≥ Complete Damage: (0.211 in, 0.007)
Detailed View
Discrete Damage State Probability P[Damage = DS | Sd]
0.641
0.186
0.128
0.037
0.006
0.001
None
Collapsed
Damage State
1 = Slight Damage | 2 = Moderate Damage
3 = Extensive Damage | 4 = Complete Damage
Building Description:
Facility Class: EFHL
Building Type: URML
Design Level: PC
Site Class: CD
City: Springfield
County: Hampden
Geologic Group: Group 2
SDC: C

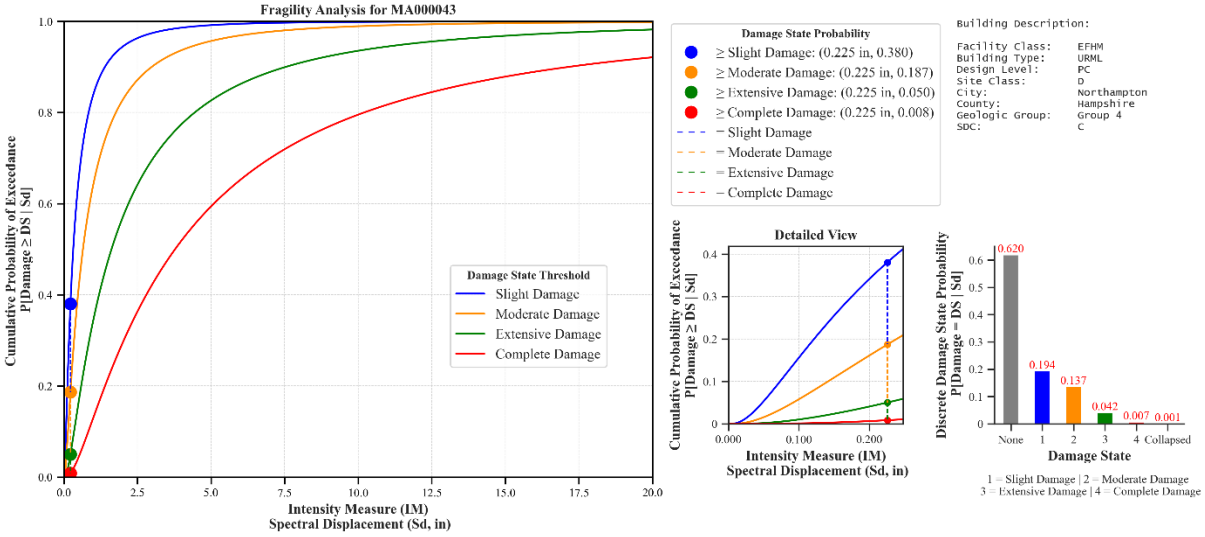
Fragility Analysis for MA000043
Cumulative Probability of Exceedance P[Damage ≥ DS | Sd]
Intensity Measure (IM) Spectral Displacement (Sd, in)
Damage State Threshold
Slight Damage
Moderate Damage
Extensive Damage
Complete Damage
Damage State Probability
≥ Slight Damage: (0.225 in, 0.380)
≥ Moderate Damage: (0.225 in, 0.187)
≥ Extensive Damage: (0.225 in, 0.050)
≥ Complete Damage: (0.225 in, 0.008)
Detailed View
Discrete Damage State Probability P[Damage = DS | Sd]
0.620
0.194
0.137
0.042
0.007
0.001
None
Collapsed
Damage State
1 = Slight Damage | 2 = Moderate Damage
3 = Extensive Damage | 4 = Complete Damage
Building Description:
Facility Class: EFHM
Building Type: URML
Design Level: PC
Site Class: D
City: Northampton
County: Hampshire
Geologic Group: Group 4
SDC: C

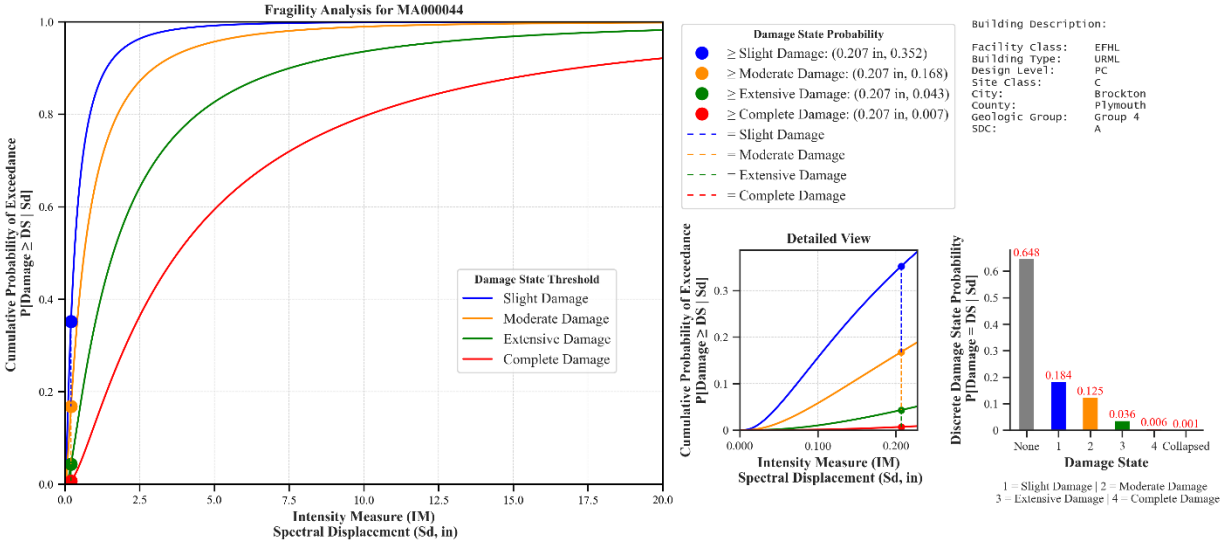
Fragility Analysis for MA000044
Cumulative Probability of Exceedance P[Damage ≥ DS | Sd]
Intensity Measure (IM) Spectral Displacement (Sd, in)
Damage State Threshold
Slight Damage
Moderate Damage
Extensive Damage
Complete Damage
Damage State Probability
≥ Slight Damage: (0.207 in, 0.352)
≥ Moderate Damage: (0.207 in, 0.168)
≥ Extensive Damage: (0.207 in, 0.043)
≥ Complete Damage: (0.207 in, 0.007)
Detailed View
Discrete Damage State Probability P[Damage = DS | Sd]
0.648
0.184
0.125
0.036
0.006
0.001
None
Collapsed
Damage State
1 = Slight Damage | 2 = Moderate Damage
3 = Extensive Damage | 4 = Complete Damage
Building Description:
Facility Class: EFHL
Building Type: URML
Design Level: PC
Site Class: C
City: Brockton
County: Plymouth
Geologic Group: Group 4
SDC: A

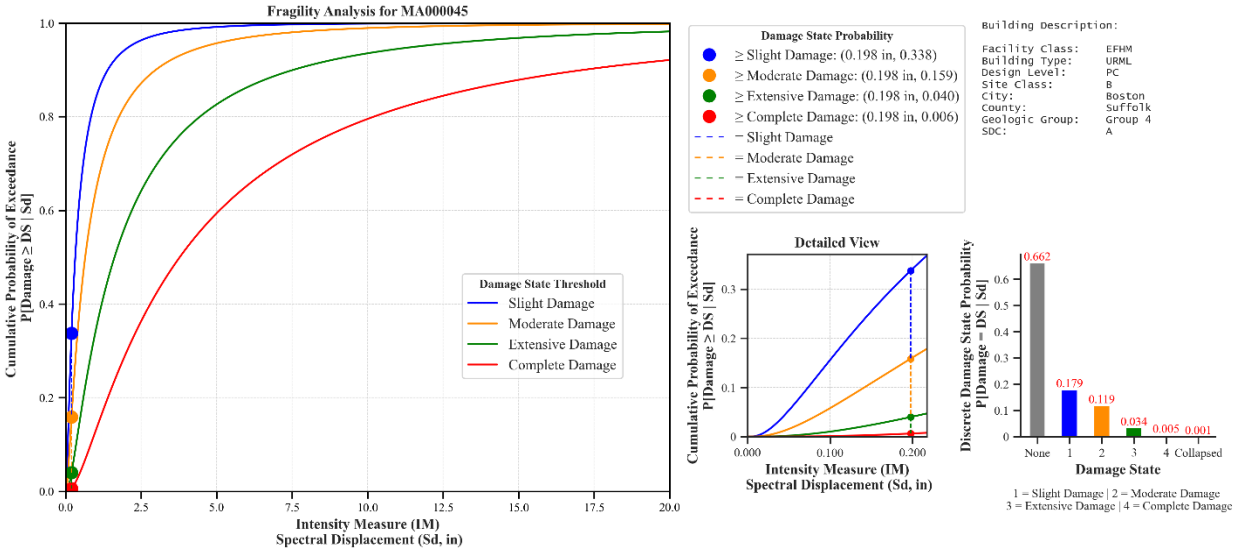
Fragility Analysis for MA000045
Cumulative Probability of Exceedance P[Damage ≥ DS | Sd]
Intensity Measure (IM) Spectral Displacement (Sd, in)
Damage State Threshold
Slight Damage
Moderate Damage
Extensive Damage
Complete Damage
Damage State Probability
≥ Slight Damage: (0.198 in, 0.338)
≥ Moderate Damage: (0.198 in, 0.159)
≥ Extensive Damage: (0.198 in, 0.040)
≥ Complete Damage: (0.198 in, 0.006)
Detailed View
Discrete Damage State Probability P[Damage = DS | Sd]
0.662
0.179
0.119
0.034
0.005
0.001
None 1 2 3 4 Collapsed
Damage State
1 = Slight Damage | 2 = Moderate Damage
3 = Extensive Damage | 4 = Complete Damage
Building Description:
Facility Class: EFHM
Building Type: URML
Design Level: PC
Site Class: B
City: Boston
County: Suffolk
Geologic Group: Group 4
SDC: A

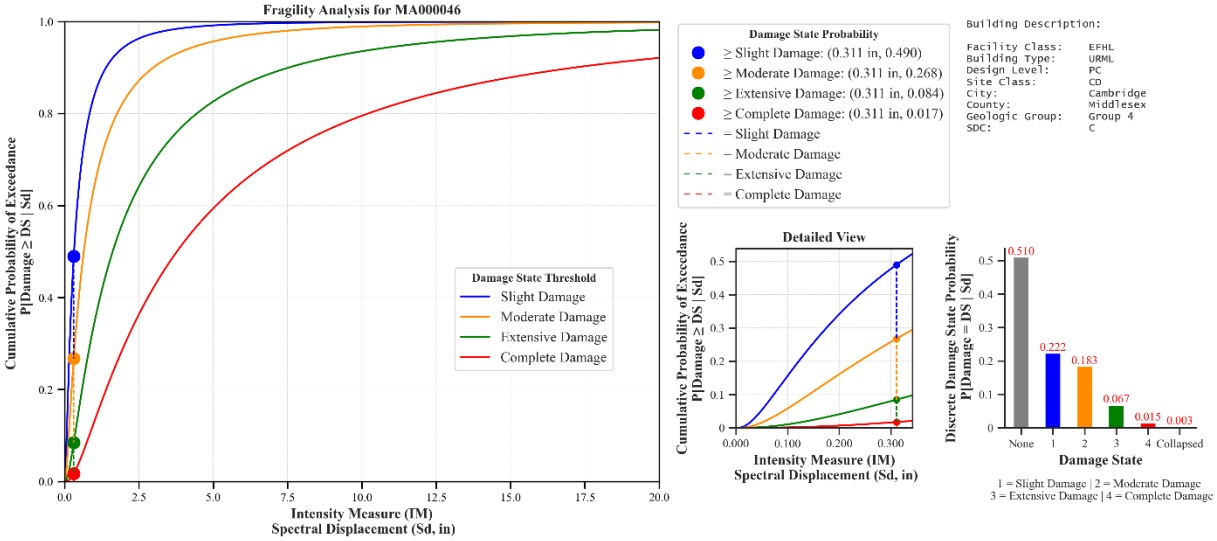
Fragility Analysis for MA000046
Cumulative Probability of Exceedance P[Damage ≥ DS | Sd]
Intensity Measure (IM) Spectral Displacement (Sd, in)
Damage State Threshold
Slight Damage
Moderate Damage
Extensive Damage
Complete Damage
Damage State Probability
≥ Slight Damage: (0.311 in, 0.490)
≥ Moderate Damage: (0.311 in, 0.268)
≥ Extensive Damage: (0.311 in, 0.084)
≥ Complete Damage: (0.311 in, 0.017)
Detailed View
Discrete Damage State Probability P[Damage = DS | Sd]
0.510
0.222
0.183
0.067
0.015
0.003
None 1 2 3 4 Collapsed
Damage State
1 = Slight Damage | 2 = Moderate Damage
3 = Extensive Damage | 4 = Complete Damage
Building Description:
Facility Class: EFHL
Building Type: URML
Design Level: PC
Site Class: CD
City: Cambridge
County: Middlesex
Geologic Group: Group 4
SDC: C

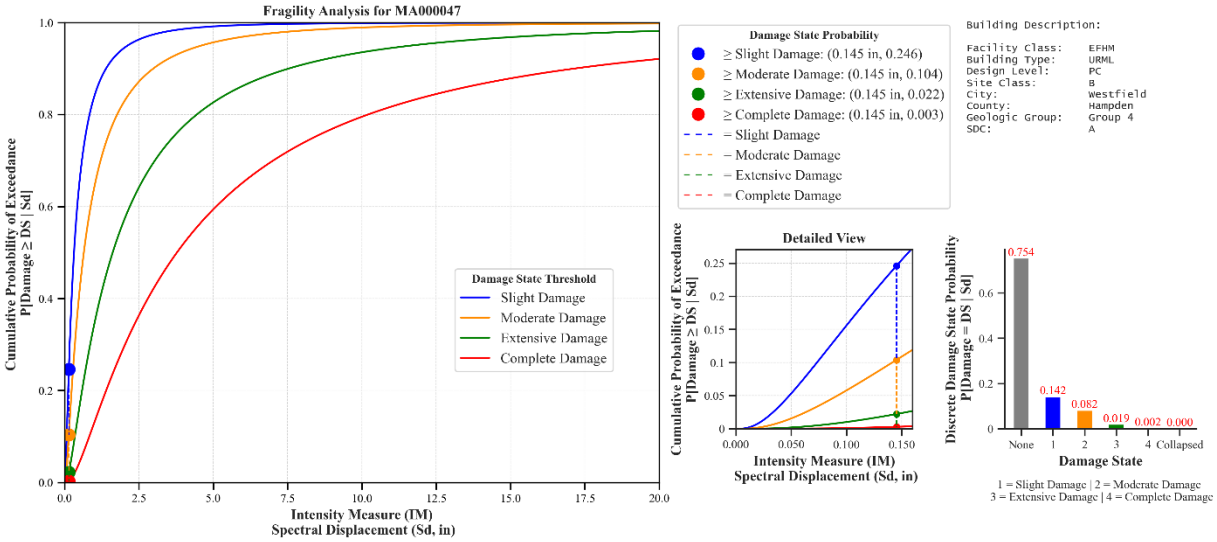
Fragility Analysis for MA000047
Cumulative Probability of Exceedance P[Damage ≥ DS | Sd]
Intensity Measure (IM) Spectral Displacement (Sd, in)
Damage State Threshold
Slight Damage
Moderate Damage
Extensive Damage
Complete Damage
Damage State Probability
≥ Slight Damage: (0.145 in, 0.246)
≥ Moderate Damage: (0.145 in, 0.104)
≥ Extensive Damage: (0.145 in, 0.022)
≥ Complete Damage: (0.145 in, 0.003)
Detailed View
Discrete Damage State Probability P[Damage = DS | Sd]
0.754
0.142
0.082
0.019
0.002
0.000
None 1 2 3 4 Collapsed
Damage State
1 = Slight Damage | 2 = Moderate Damage
3 = Extensive Damage | 4 = Complete Damage
Building Description:
Facility Class: EFHM
Building Type: URML
Design Level: PC
Site Class: B
City: Westfield
County: Hampden
Geologic Group: Group 4
SDC: A

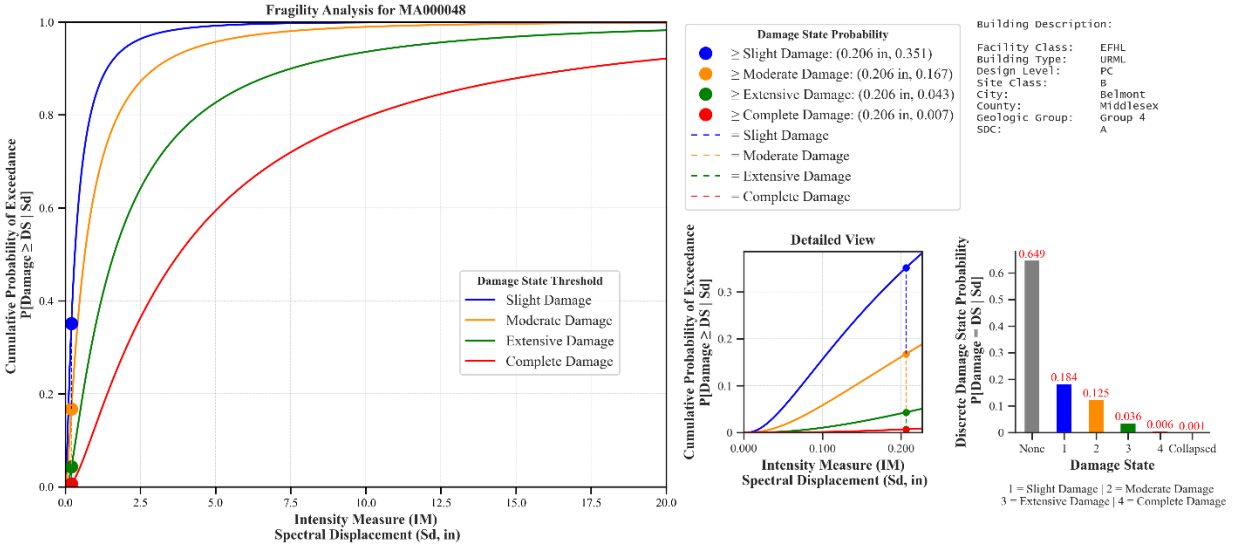
Fragility Analysis for MA000048
Cumulative Probability of Exceedance
P[Damage ≥ DS | Sd]
Intensity Measure (IM)
Spectral Displacement (Sd, in)
Damage State Threshold
Slight Damage
Moderate Damage
Extensive Damage
Complete Damage
Damage State Probability
≥ Slight Damage: (0.206 in, 0.351)
≥ Moderate Damage: (0.206 in, 0.167)
≥ Extensive Damage: (0.206 in, 0.043)
≥ Complete Damage: (0.206 in, 0.007)
Building Description:
Facility Class: EFHL
Building Type: URML
Design Level: PC
Site Class: B
City: Belmont
County: Middlesex
Geologic Group: Group 4
SDC: A
Detailed View
Discrete Damage State Probability
P[Damage = DS | Sd]
0.649
0.184
0.125
0.036
0.006
0.001
None
Collapsed
Damage State
1 = Slight Damage | 2 = Moderate Damage
3 = Extensive Damage | 4 = Complete Damage

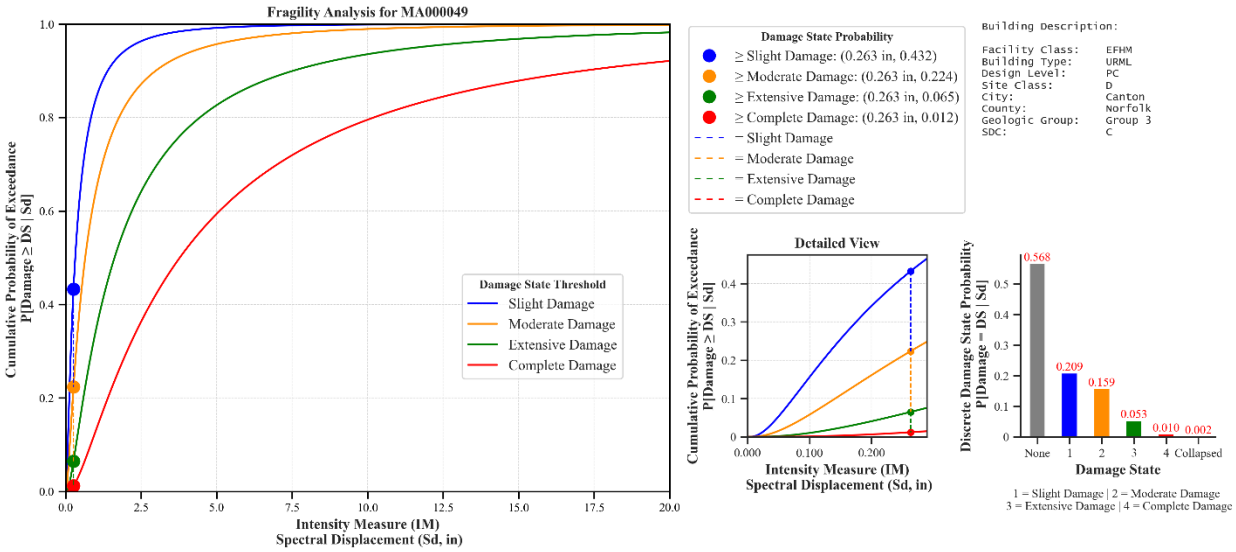
Fragility Analysis for MA000049
Cumulative Probability of Exceedance
P[Damage ≥ DS | Sd]
Intensity Measure (IM)
Spectral Displacement (Sd, in)
Damage State Threshold
Slight Damage
Moderate Damage
Extensive Damage
Complete Damage
Damage State Probability
≥ Slight Damage: (0.263 in, 0.432)
≥ Moderate Damage: (0.263 in, 0.224)
≥ Extensive Damage: (0.263 in, 0.065)
≥ Complete Damage: (0.263 in, 0.012)
Building Description:
Facility Class: EFHM
Building Type: URML
Design Level: PC
Site Class: D
City: Canton
County: Norfolk
Geologic Group: Group 3
SDC: C
Detailed View
Discrete Damage State Probability
P[Damage = DS | Sd]
0.568
0.209
0.159
0.053
0.010
0.002
None
Collapsed
Damage State
1 = Slight Damage | 2 = Moderate Damage
3 = Extensive Damage | 4 = Complete Damage

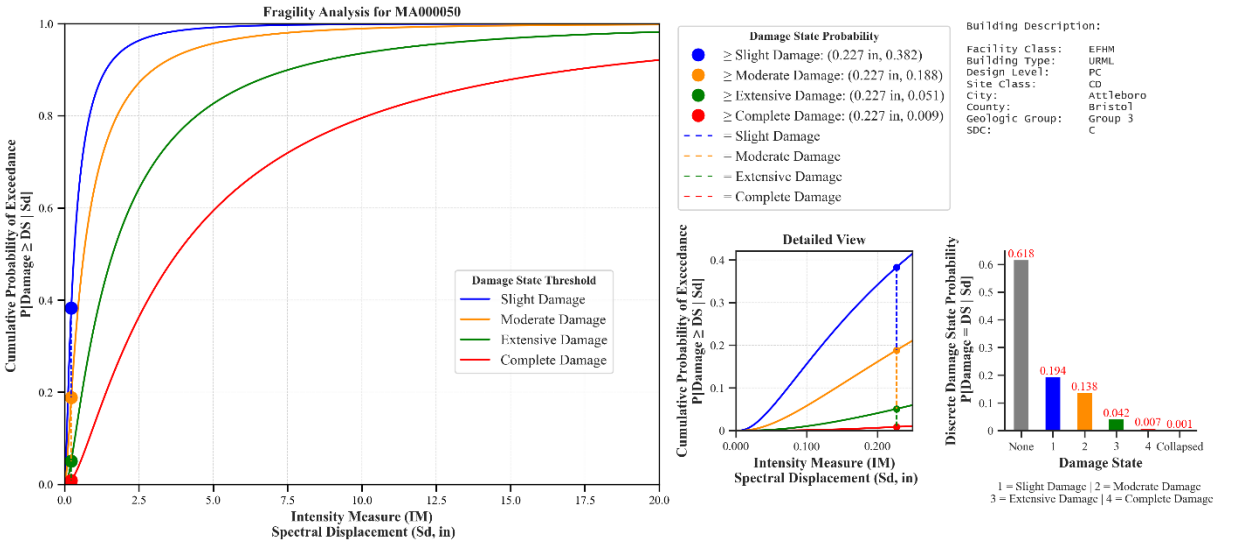
Fragility Analysis for MA000050
Cumulative Probability of Exceedance
P[Damage ≥ DS | Sd]
Intensity Measure (IM)
Spectral Displacement (Sd, in)
Damage State Threshold
Slight Damage
Moderate Damage
Extensive Damage
Complete Damage
Damage State Probability
≥ Slight Damage: (0.227 in, 0.382)
≥ Moderate Damage: (0.227 in, 0.188)
≥ Extensive Damage: (0.227 in, 0.051)
≥ Complete Damage: (0.227 in, 0.009)
Building Description:
Facility Class: EFHM
Building Type: URML
Design Level: PC
Site Class: CD
City: Attleboro
County: Bristol
Geologic Group: Group 3
SDC: C
Detailed View
Discrete Damage State Probability
P[Damage = DS | Sd]
0.618
0.194
0.138
0.042
0.007
0.001
None
Collapsed
Damage State
1 = Slight Damage | 2 = Moderate Damage
3 = Extensive Damage | 4 = Complete Damage

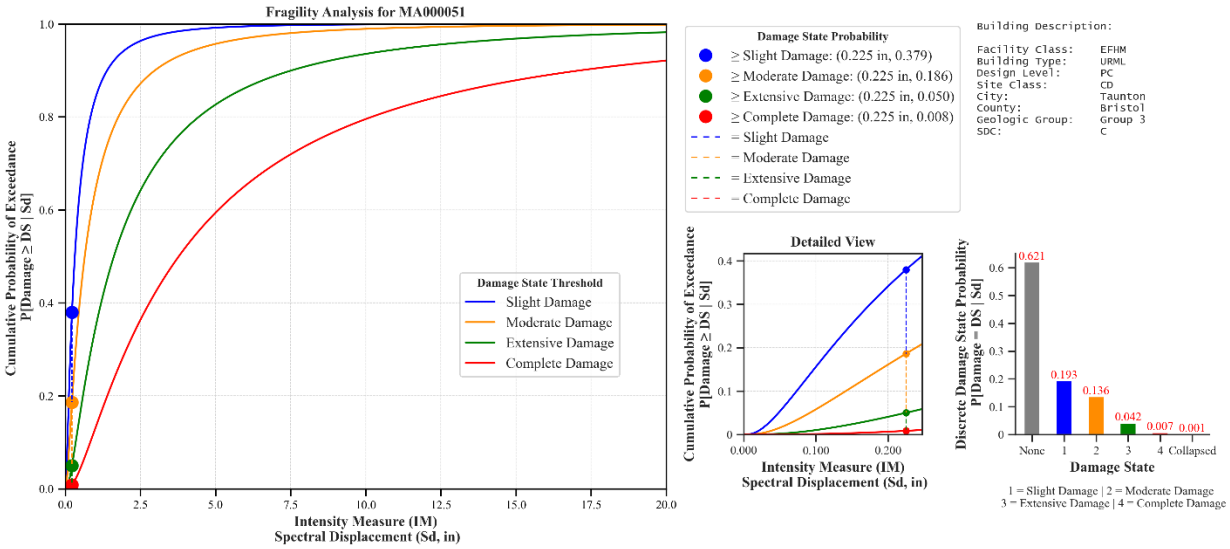
Fragility Analysis for MA000051
Cumulative Probability of Exceedance P[Damage ≥ DS | Sd]
Intensity Measure (IM) Spectral Displacement (Sd, in)
Damage State Threshold
Slight Damage
Moderate Damage
Extensive Damage
Complete Damage
Damage State Probability
≥ Slight Damage: (0.225 in, 0.379)
≥ Moderate Damage: (0.225 in, 0.186)
≥ Extensive Damage: (0.225 in, 0.050)
≥ Complete Damage: (0.225 in, 0.008)
= Slight Damage
= Moderate Damage
= Extensive Damage
= Complete Damage
Building Description:
Facility Class: EFHM
Building Type: URML
Design Level: PC
Site Class: CD
City: Taunton
County: Bristol
Geologic Group: Group 3
SDC: C
Detailed View
Discrete Damage State Probability P[Damage = DS | Sd]
0.621
0.193
0.136
0.042
0.007
0.001
None
1
2
3
4 Collapsed
Damage State
1 = Slight Damage | 2 = Moderate Damage
3 = Extensive Damage | 4 = Complete Damage

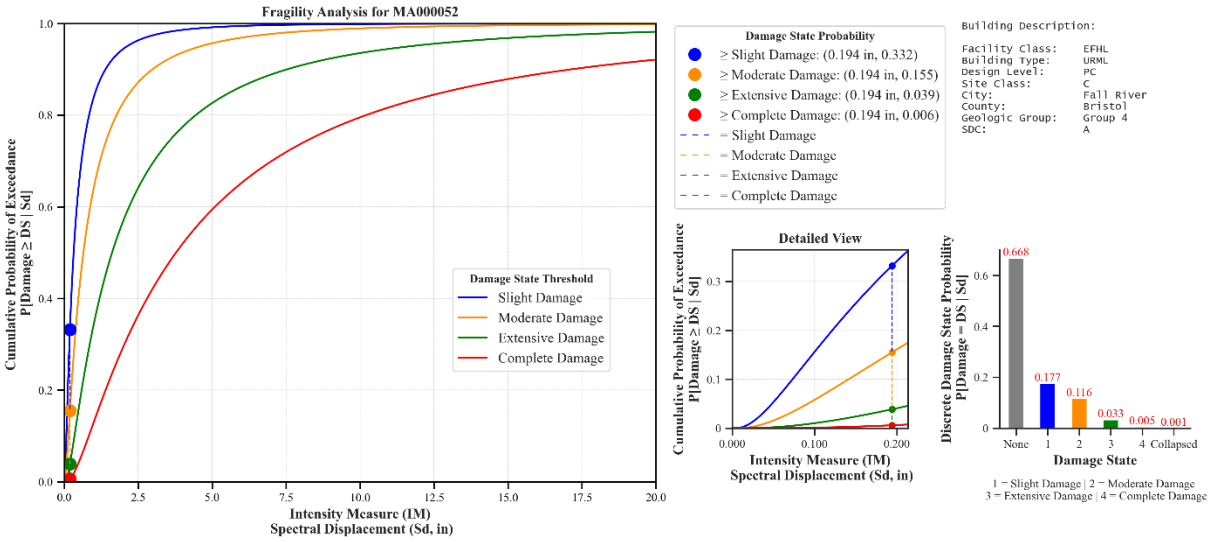
Fragility Analysis for MA000052
Cumulative Probability of Exceedance P[Damage ≥ DS | Sd]
Intensity Measure (IM) Spectral Displacement (Sd, in)
Damage State Threshold
Slight Damage
Moderate Damage
Extensive Damage
Complete Damage
Damage State Probability
≥ Slight Damage: (0.194 in, 0.332)
≥ Moderate Damage: (0.194 in, 0.155)
≥ Extensive Damage: (0.194 in, 0.039)
≥ Complete Damage: (0.194 in, 0.006)
= Slight Damage
= Moderate Damage
= Extensive Damage
= Complete Damage
Building Description:
Facility Class: EFHL
Building Type: URML
Design Level: PC
Site Class: C
City: Fall River
County: Bristol
Geologic Group: Group 4
SDC: A
Detailed View
Discrete Damage State Probability P[Damage = DS | Sd]
0.668
0.177
0.116
0.033
0.005
0.001
None
1
2
3
4 Collapsed
Damage State
1 = Slight Damage | 2 = Moderate Damage
3 = Extensive Damage | 4 = Complete Damage

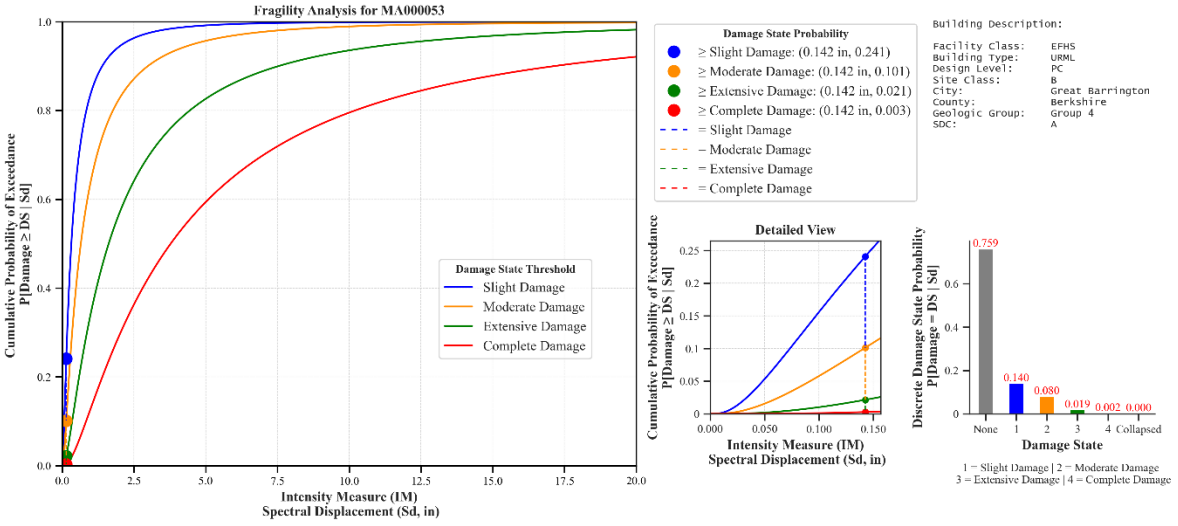
Fragility Analysis for MA000053
Cumulative Probability of Exceedance P[Damage ≥ DS | Sd]
Intensity Measure (IM) Spectral Displacement (Sd, in)
Damage State Threshold
Slight Damage
Moderate Damage
Extensive Damage
Complete Damage
Damage State Probability
≥ Slight Damage: (0.142 in, 0.241)
≥ Moderate Damage: (0.142 in, 0.101)
≥ Extensive Damage: (0.142 in, 0.021)
≥ Complete Damage: (0.142 in, 0.003)
= Slight Damage
= Moderate Damage
= Extensive Damage
= Complete Damage
Building Description:
Facility Class: EFHS
Building Type: URML
Design Level: PC
Site Class: B
City: Great Barrington
County: Berkshire
Geologic Group: Group 4
SDC: A
Detailed View
Discrete Damage State Probability P[Damage = DS | Sd]
0.759
0.140
0.080
0.019
0.002
0.000
None
1
2
3
4 Collapsed
Damage State
1 = Slight Damage | 2 = Moderate Damage
3 = Extensive Damage | 4 = Complete Damage

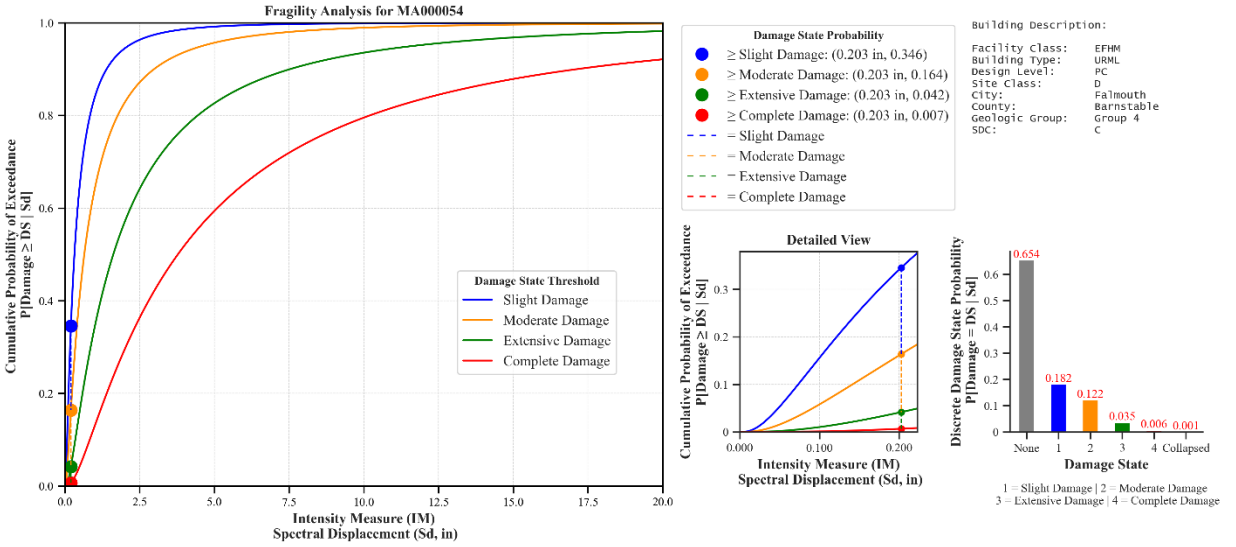
Fragility Analysis for MA000054
Cumulative Probability of Exceedance P[Damage ≥ DS | Sd]
Intensity Measure (IM) Spectral Displacement (Sd, in)
Damage State Threshold
Slight Damage
Moderate Damage
Extensive Damage
Complete Damage
Damage State Probability
≥ Slight Damage: (0.203 in, 0.346)
≥ Moderate Damage: (0.203 in, 0.164)
≥ Extensive Damage: (0.203 in, 0.042)
≥ Complete Damage: (0.203 in, 0.007)
Building Description:
Facility Class: EFHM
Building Type: URML
Design Level: PC
Site Class: D
City: Falmouth
County: Barnstable
Geologic Group: Group 4
SDC: C
Detailed View
Discrete Damage State Probability P[Damage = DS | Sd]
0.654
0.182
0.122
0.035
0.006
0.001
None
Collapsed
Damage State
1 = Slight Damage | 2 = Moderate Damage
3 = Extensive Damage | 4 = Complete Damage

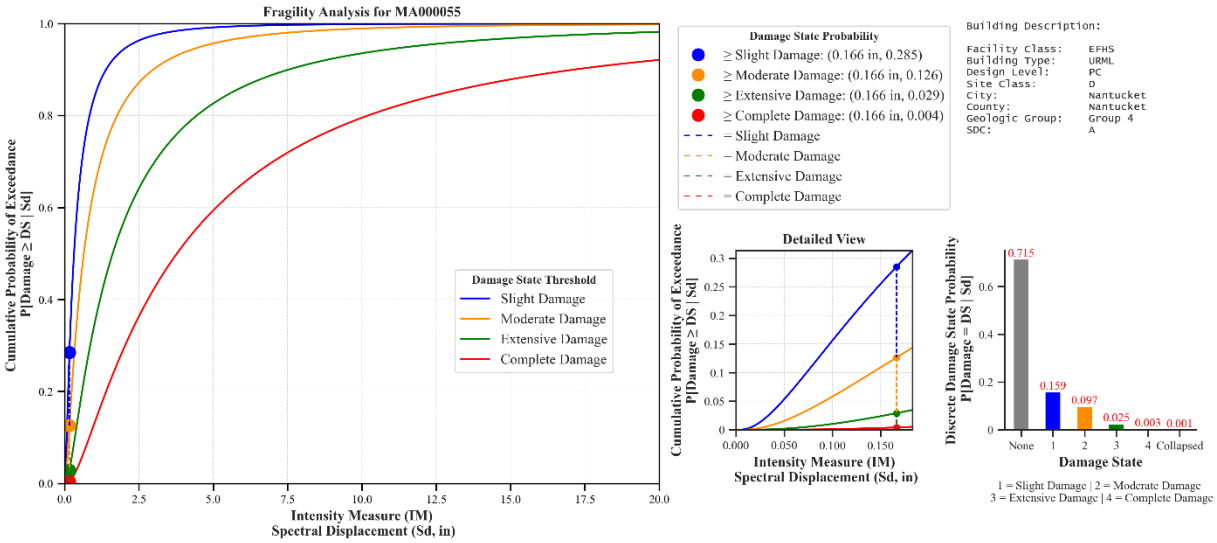
Fragility Analysis for MA000055
Cumulative Probability of Exceedance P[Damage ≥ DS | Sd]
Intensity Measure (IM) Spectral Displacement (Sd, in)
Damage State Threshold
Slight Damage
Moderate Damage
Extensive Damage
Complete Damage
Damage State Probability
≥ Slight Damage: (0.166 in, 0.285)
≥ Moderate Damage: (0.166 in, 0.126)
≥ Extensive Damage: (0.166 in, 0.029)
≥ Complete Damage: (0.166 in, 0.004)
Building Description:
Facility Class: EFHS
Building Type: URML
Design Level: PC
Site Class: D
City: Nantucket
County: Nantucket
Geologic Group: Group 4
SDC: A
Detailed View
Discrete Damage State Probability P[Damage = DS | Sd]
0.715
0.159
0.097
0.025
0.003
0.001
None
Collapsed
Damage State
1 = Slight Damage | 2 = Moderate Damage
3 = Extensive Damage | 4 = Complete Damage

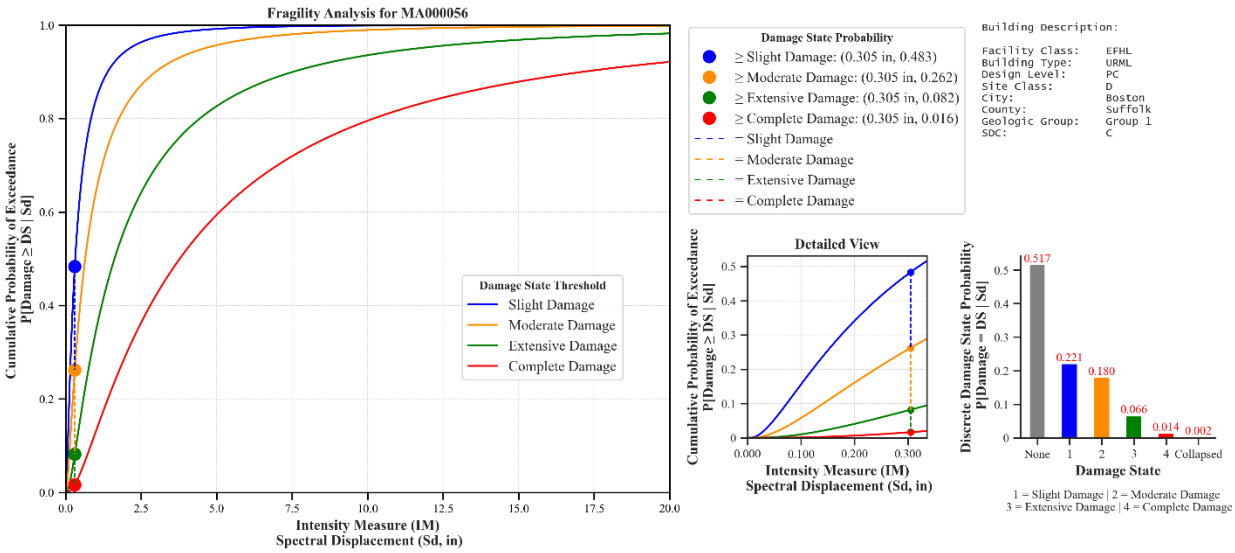
Fragility Analysis for MA000056
Cumulative Probability of Exceedance P[Damage ≥ DS | Sd]
Intensity Measure (IM) Spectral Displacement (Sd, in)
Damage State Threshold
Slight Damage
Moderate Damage
Extensive Damage
Complete Damage
Damage State Probability
≥ Slight Damage: (0.305 in, 0.483)
≥ Moderate Damage: (0.305 in, 0.262)
≥ Extensive Damage: (0.305 in, 0.082)
≥ Complete Damage: (0.305 in, 0.016)
Building Description:
Facility Class: EFHL
Building Type: URML
Design Level: PC
Site Class: D
City: Boston
County: Suffolk
Geologic Group: Group 1
SDC: C
Detailed View
Discrete Damage State Probability P[Damage = DS | Sd]
0.517
0.221
0.180
0.066
0.014
0.002
None
Collapsed
Damage State
1 = Slight Damage | 2 = Moderate Damage
3 = Extensive Damage | 4 = Complete Damage

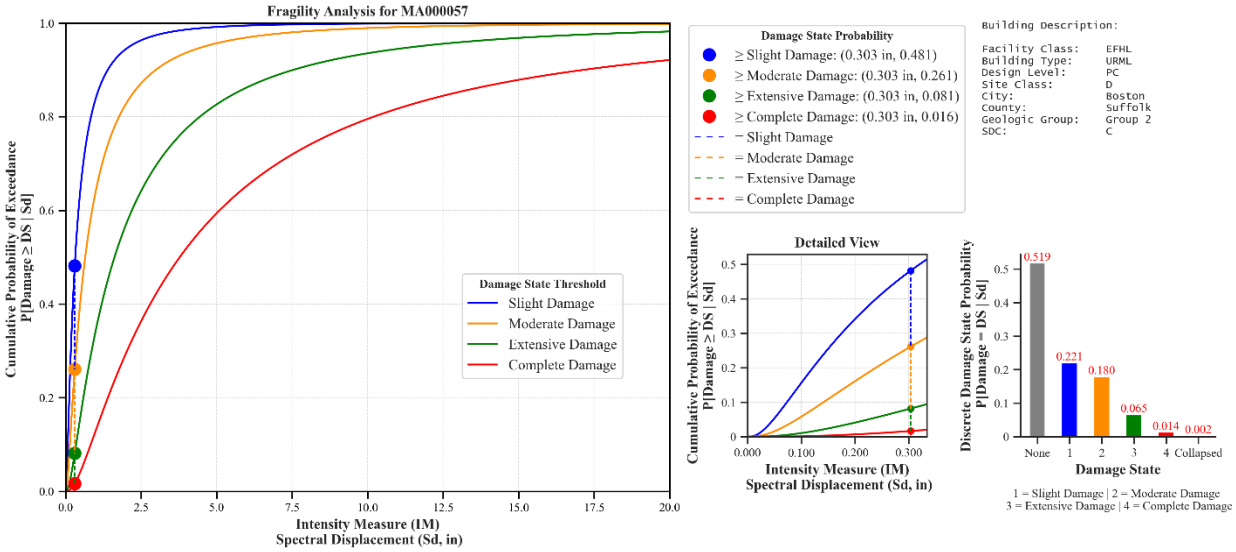
Fragility Analysis for MA000057
Cumulative Probability of Exceedance
P[Damage ≥ DS | Sd]
Intensity Measure (IM)
Spectral Displacement (Sd, in)
Damage State Threshold
Slight Damage
Moderate Damage
Extensive Damage
Complete Damage
Damage State Probability
≥ Slight Damage: (0.303 in, 0.481)
≥ Moderate Damage: (0.303 in, 0.261)
≥ Extensive Damage: (0.303 in, 0.081)
≥ Complete Damage: (0.303 in, 0.016)
Dctailed View
Discrete Damage State Probability
P[Damage = DS | Sd]
0.519
0.221
0.180
0.065
0.014
0.002
None
Collapsed
Damage State
1 = Slight Damage | 2 = Moderate Damage
3 = Extensive Damage | 4 = Complete Damage
Building Description:
Facility Class: EFHL
Building Type: URML
Design Level: PC
Site Class: D
City: Boston
County: Suffolk
Geologic Group: Group 2
SDC: C

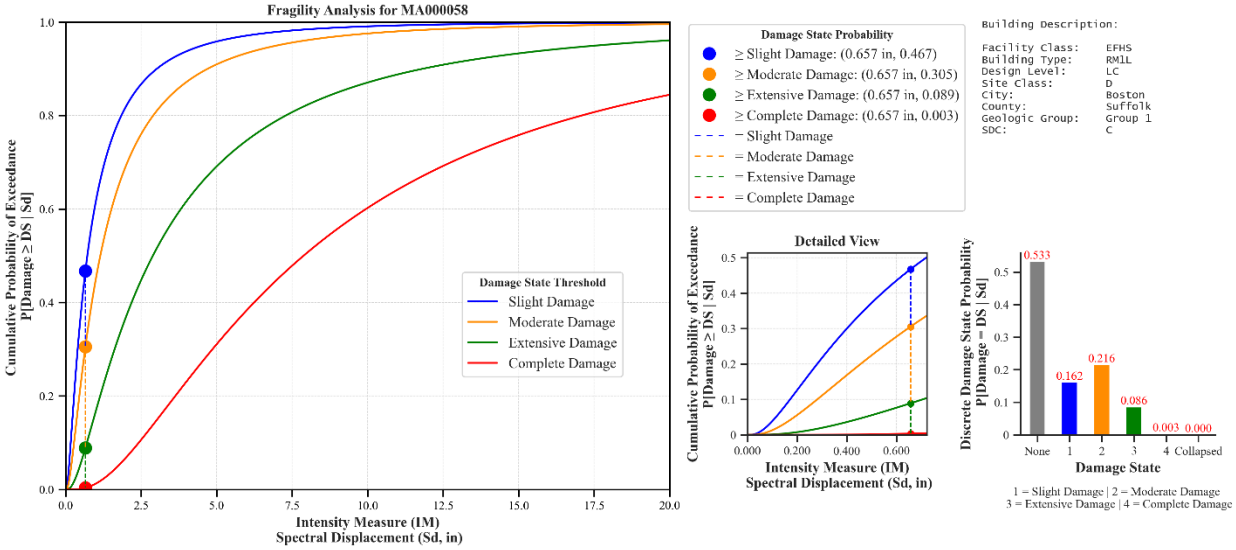
Fragility Analysis for MA000058
Cumulative Probability of Exceedance
P[Damage ≥ DS | Sd]
Intensity Measure (IM)
Spectral Displacement (Sd, in)
Damage State Threshold
Slight Damage
Moderate Damage
Extensive Damage
Complete Damage
Damage State Probability
≥ Slight Damage: (0.657 in, 0.467)
≥ Moderate Damage: (0.657 in, 0.305)
≥ Extensive Damage: (0.657 in, 0.089)
≥ Complete Damage: (0.657 in, 0.003)
Dctailed View
Discrete Damage State Probability
P[Damage = DS | Sd]
0.533
0.162
0.216
0.086
0.003
0.000
None
Collapsed
Damage State
1 = Slight Damage | 2 = Moderate Damage
3 = Extensive Damage | 4 = Complete Damage
Building Description:
Facility Class: EFHS
Building Type: RM1L
Design Level: LC
Site Class: D
City: Boston
County: Suffolk
Geologic Group: Group 1
SDC: C

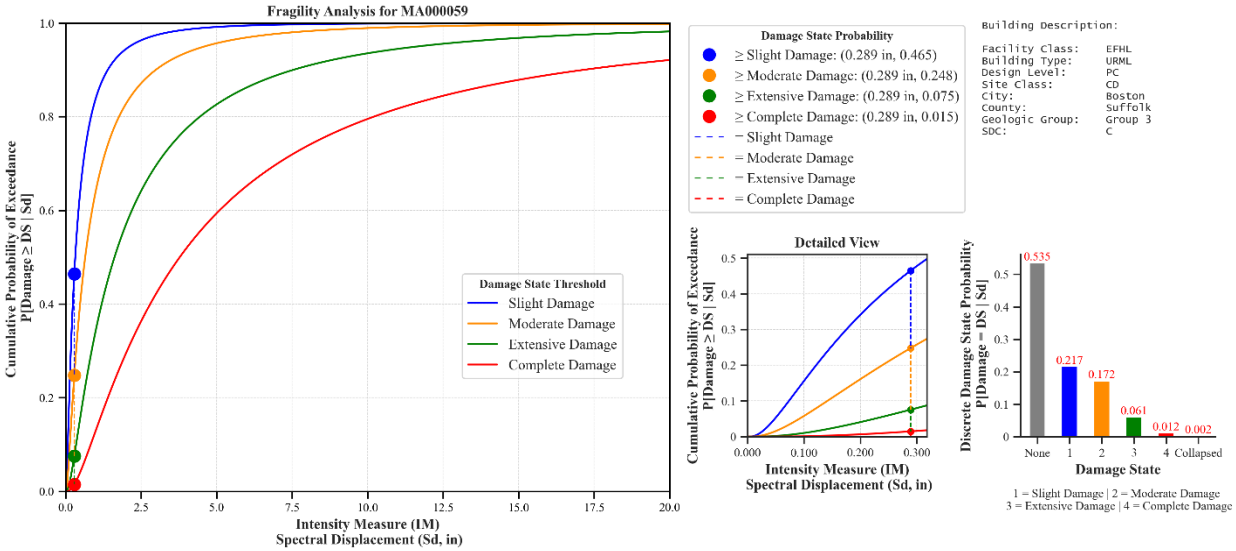
Fragility Analysis for MA000059
Cumulative Probability of Exceedance
P[Damage ≥ DS | Sd]
Intensity Measure (IM)
Spectral Displacement (Sd, in)
Damage State Threshold
Slight Damage
Moderate Damage
Extensive Damage
Complete Damage
Damage State Probability
≥ Slight Damage: (0.289 in, 0.465)
≥ Moderate Damage: (0.289 in, 0.248)
≥ Extensive Damage: (0.289 in, 0.075)
≥ Complete Damage: (0.289 in, 0.015)
Dctailed View
Discrete Damage State Probability
P[Damage = DS | Sd]
0.535
0.217
0.172
0.061
0.012
0.002
None
Collapsed
Damage State
1 = Slight Damage | 2 = Moderate Damage
3 = Extensive Damage | 4 = Complete Damage
Building Description:
Facility Class: EFHL
Building Type: URML
Design Level: PC
Site Class: CD
City: Boston
County: Suffolk
Geologic Group: Group 3
SDC: C

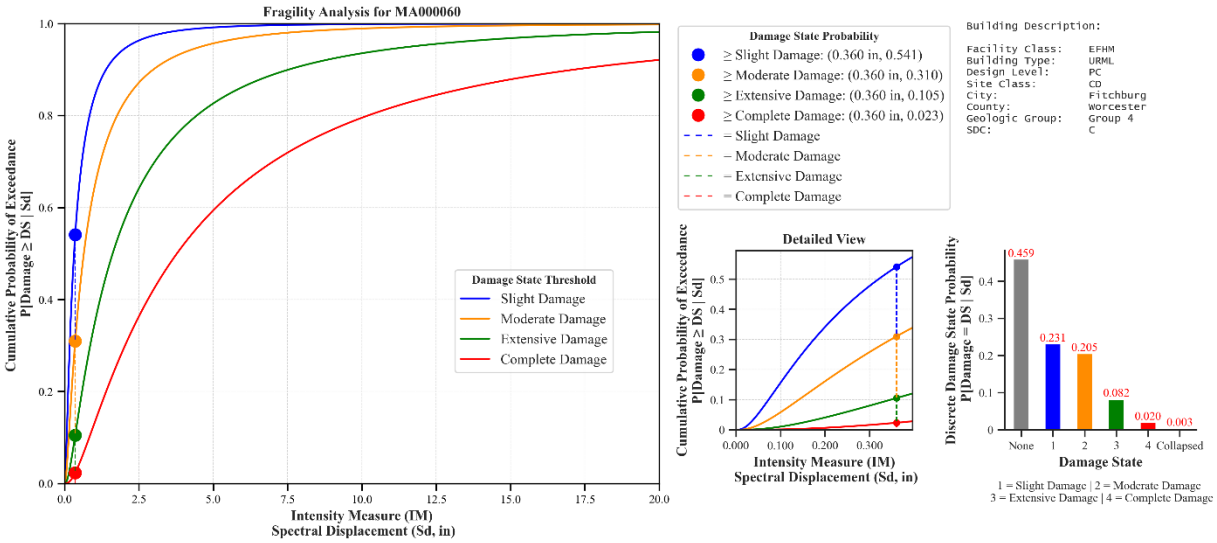
Fragility Analysis for MA000060
Cumulative Probability of Exceedance P[Damage ≥ DS | Sd]
Intensity Measure (IM) Spectral Displacement (Sd, in)
Damage State Threshold
Slight Damage
Moderate Damage
Extensive Damage
Complete Damage
Damage State Probability
≥ Slight Damage: (0.360 in, 0.541)
≥ Moderate Damage: (0.360 in, 0.310)
≥ Extensive Damage: (0.360 in, 0.105)
≥ Complete Damage: (0.360 in, 0.023)
Building Description:
Facility Class: EFHM
Building Type: URML
Design Level: PC
Site Class: CD
City: Fitchburg
County: Worcester
Geologic Group: Group 4
SDC: C
Detailed View
Discrete Damage State Probability P[Damage = DS | Sd]
0.459
0.231
0.205
0.082
0.020
0.003
None 1 2 3 4 Collapsed
Damage State
1 = Slight Damage | 2 = Moderate Damage
3 = Extensive Damage | 4 = Complete Damage

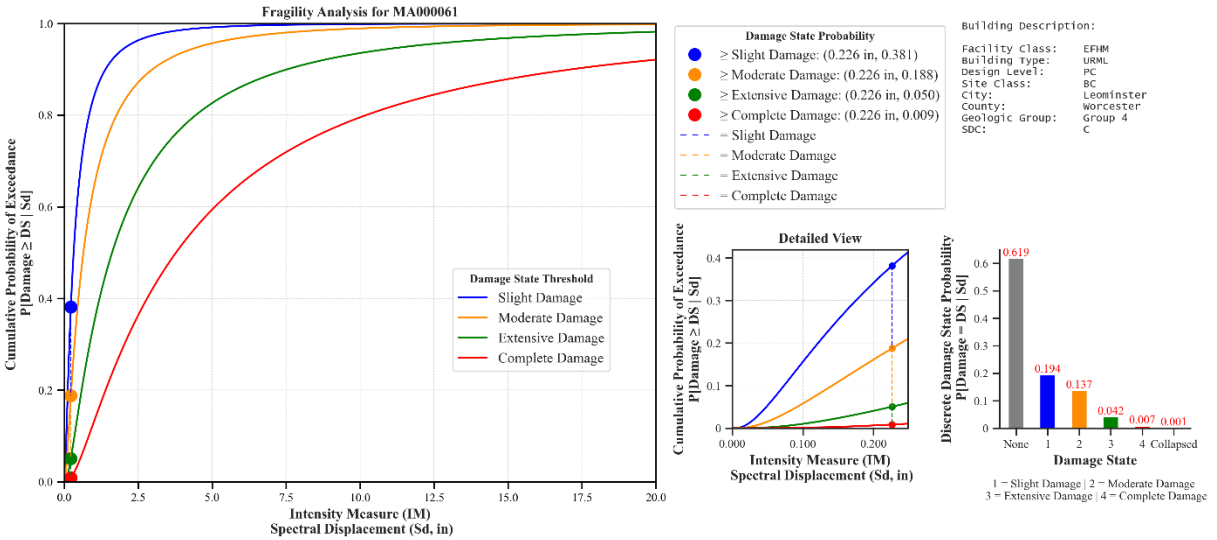
Fragility Analysis for MA000061
Cumulative Probability of Exceedance P[Damage ≥ DS | Sd]
Intensity Measure (IM) Spectral Displacement (Sd, in)
Damage State Threshold
Slight Damage
Moderate Damage
Extensive Damage
Complete Damage
Damage State Probability
≥ Slight Damage: (0.226 in, 0.381)
≥ Moderate Damage: (0.226 in, 0.188)
≥ Extensive Damage: (0.226 in, 0.050)
≥ Complete Damage: (0.226 in, 0.009)
Building Description:
Facility Class: EFHM
Building Type: URML
Design Level: PC
Site Class: BC
City: Leominster
County: Worcester
Geologic Group: Group 4
SDC: C
Detailed View
Discrete Damage State Probability P[Damage = DS | Sd]
0.619
0.194
0.137
0.042
0.007
0.001
None 1 2 3 4 Collapsed
Damage State
1 = Slight Damage | 2 = Moderate Damage
3 = Extensive Damage | 4 = Complete Damage

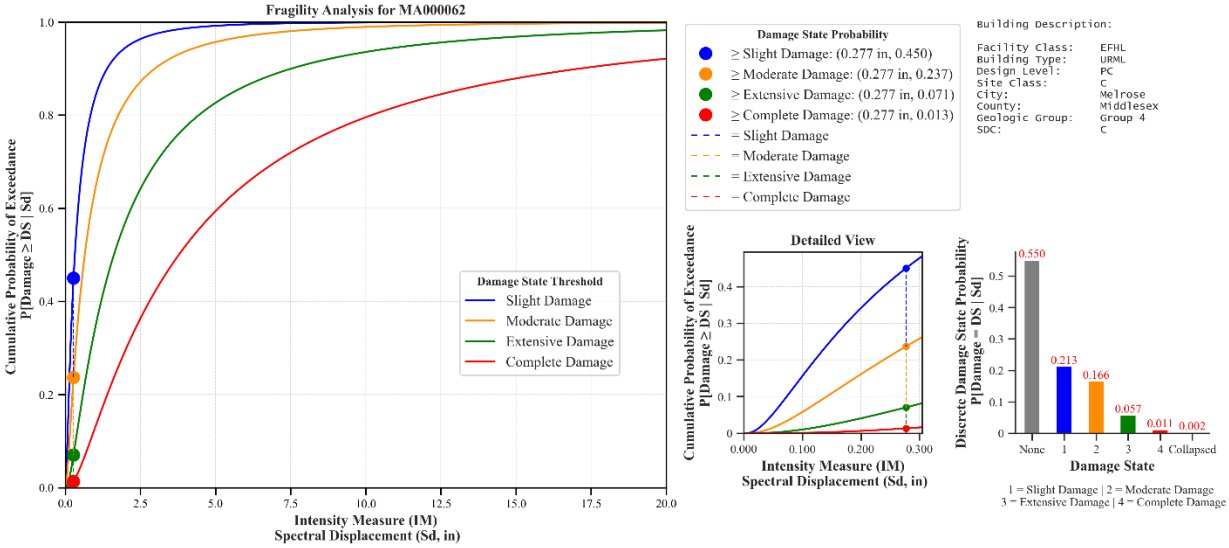
Fragility Analysis for MA000062
Cumulative Probability of Exceedance P[Damage ≥ DS | Sd]
Intensity Measure (IM) Spectral Displacement (Sd, in)
Damage State Threshold
Slight Damage
Moderate Damage
Extensive Damage
Complete Damage
Damage State Probability
≥ Slight Damage: (0.277 in, 0.450)
≥ Moderate Damage: (0.277 in, 0.237)
≥ Extensive Damage: (0.277 in, 0.071)
≥ Complete Damage: (0.277 in, 0.013)
Building Description:
Facility Class: EFHL
Building Type: URML
Design Level: PC
Site Class: C
City: Melrose
County: Middlesex
Geologic Group: Group 4
SDC: C
Detailed View
Discrete Damage State Probability P[Damage = DS | Sd]
0.550
0.213
0.166
0.057
0.011
0.002
None 1 2 3 4 Collapsed
Damage State
1 = Slight Damage | 2 = Moderate Damage
3 = Extensive Damage | 4 = Complete Damage

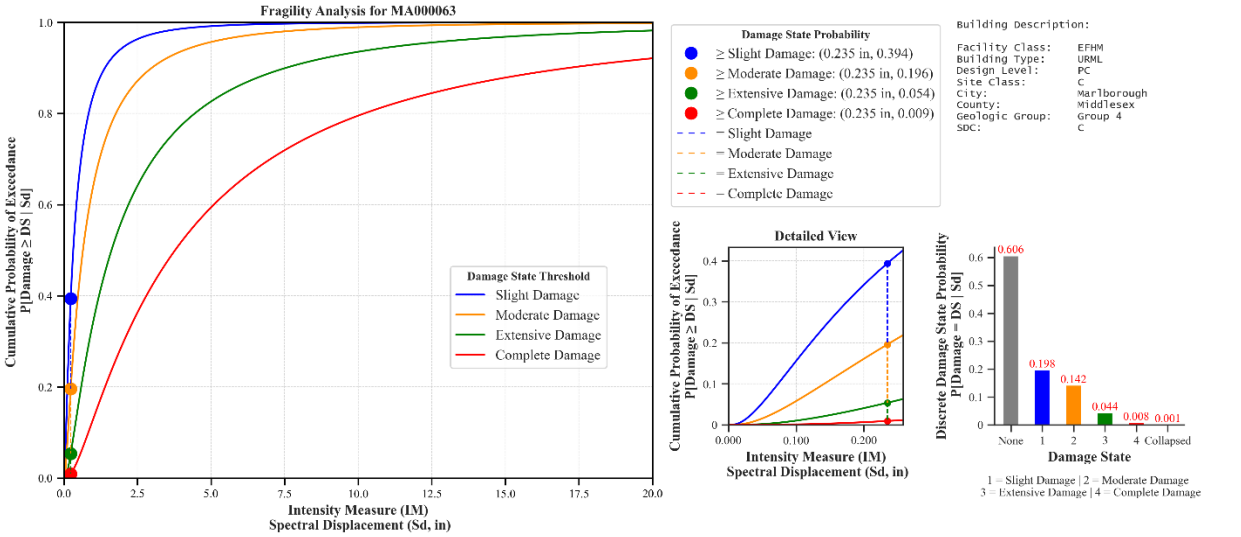
Fragility Analysis for MA000063
Cumulative Probability of Exceedance P[Damage ≥ DS | Sd]
Intensity Measure (IM) Spectral Displacement (Sd, in)
Damage State Threshold
Slight Damage
Moderate Damage
Extensive Damage
Complete Damage
Damage State Probability
≥ Slight Damage: (0.235 in, 0.394)
≥ Moderate Damage: (0.235 in, 0.196)
≥ Extensive Damage: (0.235 in, 0.054)
≥ Complete Damage: (0.235 in, 0.009)
= Slight Damage
= Moderate Damage
= Extensive Damage
= Complete Damage
Building Description:
Facility Class: EFHM
Building Type: URML
Design Level: PC
Site Class: C
City: Marlborough
County: Middlesex
Geologic Group: Group 4
SDC: C
Detailed View
Discrete Damage State Probability P[Damage = DS | Sd]
0.606
0.198
0.142
0.044
0.008
0.001
None
Collapsed
Damage State
1 = Slight Damage | 2 = Moderate Damage
3 = Extensive Damage | 4 = Complete Damage

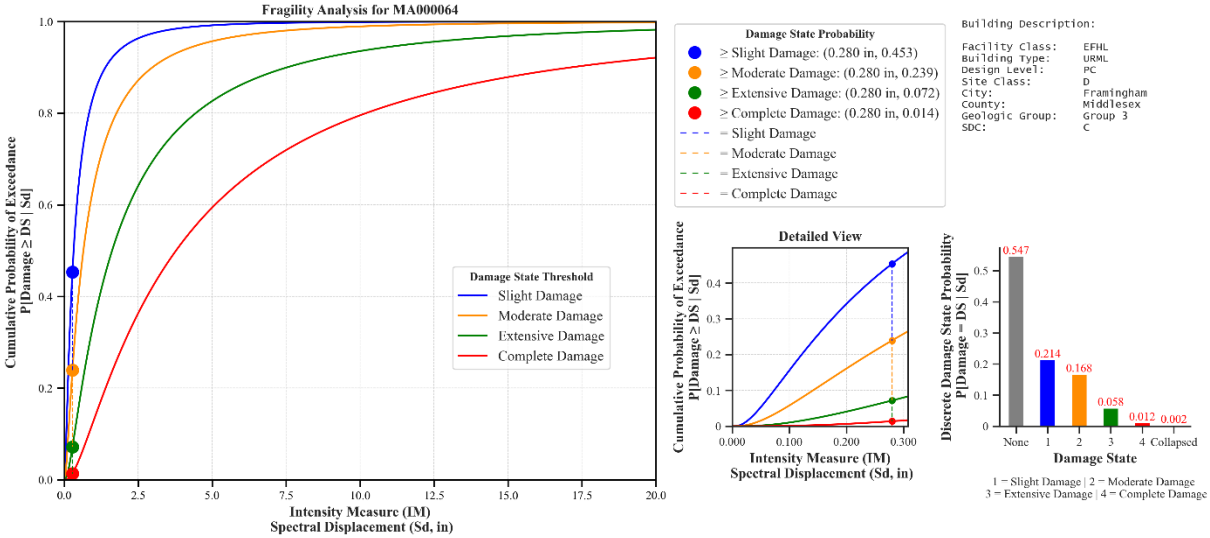
Fragility Analysis for MA000064
Cumulative Probability of Exceedance P[Damage ≥ DS | Sd]
Intensity Measure (IM) Spectral Displacement (Sd, in)
Damage State Threshold
Slight Damage
Moderate Damage
Extensive Damage
Complete Damage
Damage State Probability
≥ Slight Damage: (0.280 in, 0.453)
≥ Moderate Damage: (0.280 in, 0.239)
≥ Extensive Damage: (0.280 in, 0.072)
≥ Complete Damage: (0.280 in, 0.014)
= Slight Damage
= Moderate Damage
= Extensive Damage
= Complete Damage
Building Description:
Facility Class: EFHL
Building Type: URML
Design Level: PC
Site Class: D
City: Framingham
County: Middlesex
Geologic Group: Group 3
SDC: C
Detailed View
Discrete Damage State Probability P[Damage = DS | Sd]
0.547
0.214
0.168
0.058
0.012
0.002
None
Collapsed
Damage State
1 = Slight Damage | 2 = Moderate Damage
3 = Extensive Damage | 4 = Complete Damage

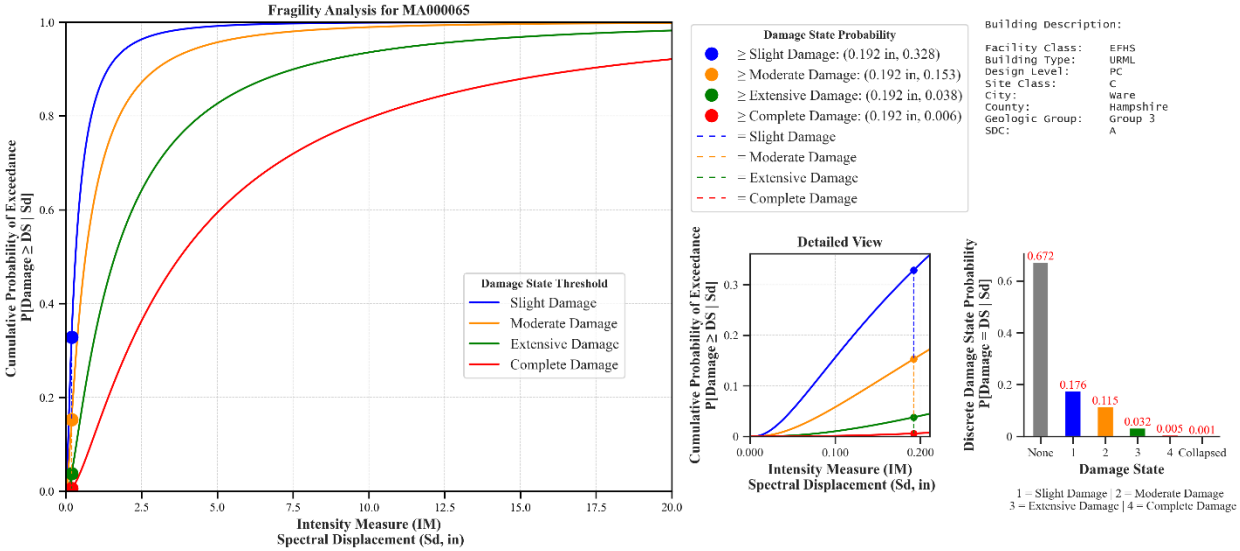
Fragility Analysis for MA000065
Cumulative Probability of Exceedance P[Damage ≥ DS | Sd]
Intensity Measure (IM) Spectral Displacement (Sd, in)
Damage State Threshold
Slight Damage
Moderate Damage
Extensive Damage
Complete Damage
Damage State Probability
≥ Slight Damage: (0.192 in, 0.328)
≥ Moderate Damage: (0.192 in, 0.153)
≥ Extensive Damage: (0.192 in, 0.038)
≥ Complete Damage: (0.192 in, 0.006)
= Slight Damage
= Moderate Damage
= Extensive Damage
= Complete Damage
Building Description:
Facility Class: EFHS
Building Type: URML
Design Level: PC
Site Class: C
City: Ware
County: Hampshire
Geologic Group: Group 3
SDC: A
Detailed View
Discrete Damage State Probability P[Damage = DS | Sd]
0.672
0.176
0.115
0.032
0.005
0.001
None
Collapsed
Damage State
1 = Slight Damage | 2 = Moderate Damage
3 = Extensive Damage | 4 = Complete Damage

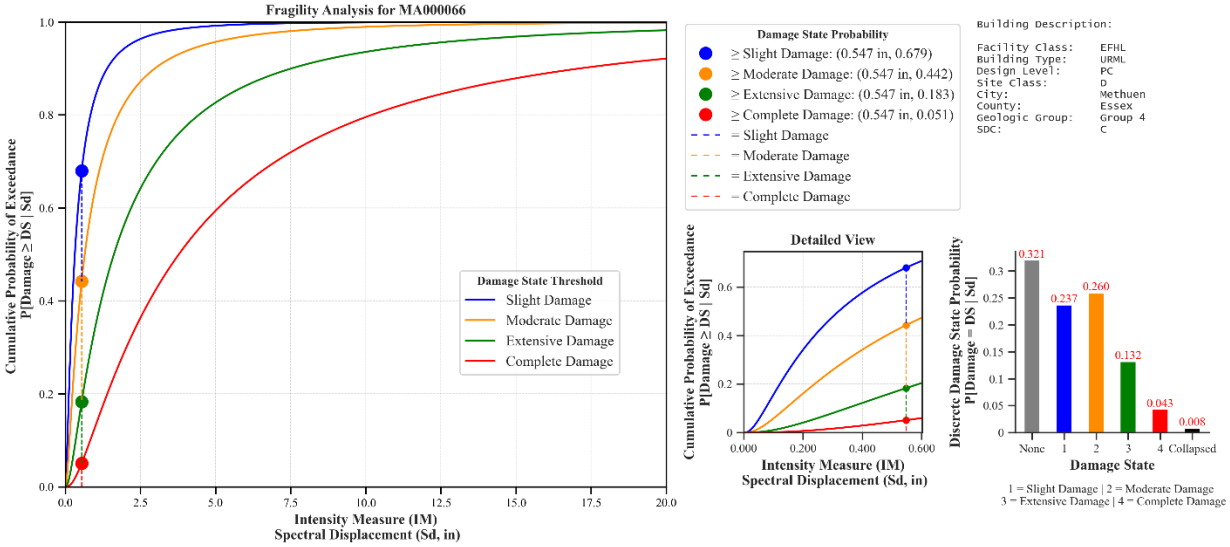
Fragility Analysis for MA000066
Cumulative Probability of Exceedance P[Damage ≥ DS | Sd]
Intensity Measure (IM) Spectral Displacement (Sd, in)
Damage State Threshold
Slight Damage
Moderate Damage
Extensive Damage
Complete Damage
Damage State Probability
≥ Slight Damage: (0.547 in, 0.679)
≥ Moderate Damage: (0.547 in, 0.442)
≥ Extensive Damage: (0.547 in, 0.183)
≥ Complete Damage: (0.547 in, 0.051)
Building Description:
Facility Class: EFHL
Building Type: URML
Design Level: PC
Site Class: D
City: Methuen
County: Essex
Geologic Group: Group 4
SDC: C
Detailed View
Discrete Damage State Probability P[Damage = DS | Sd]
0.321
0.237
0.260
0.132
0.043
0.008
None 1 2 3 4 Collapsed
Damage State
1 = Slight Damage | 2 = Moderate Damage
3 = Extensive Damage | 4 = Complete Damage

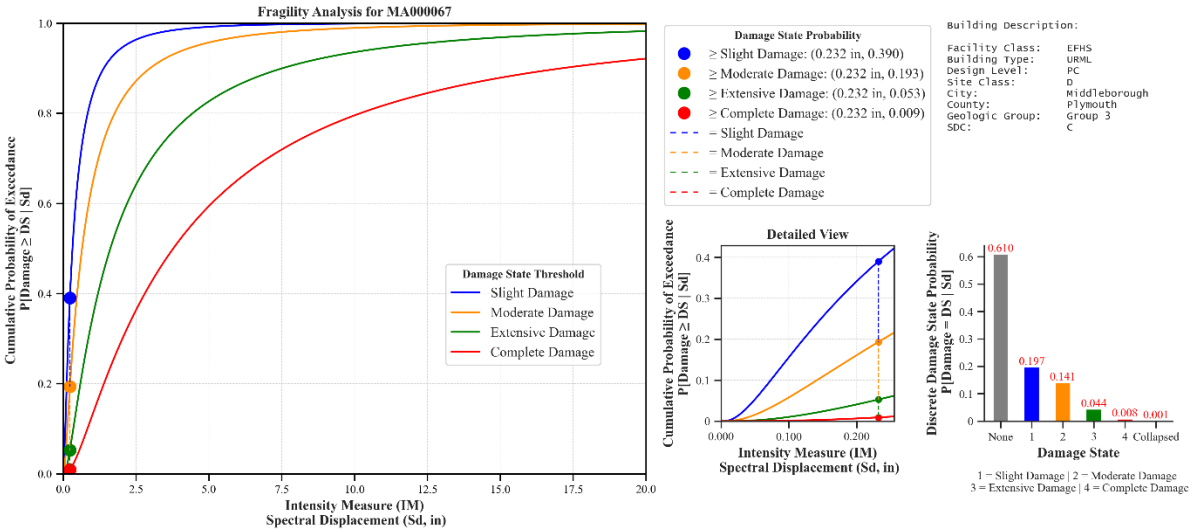
Fragility Analysis for MA000067
Cumulative Probability of Exceedance P[Damage ≥ DS | Sd]
Intensity Measure (IM) Spectral Displacement (Sd, in)
Damage State Threshold
Slight Damage
Moderate Damage
Extensive Damage
Complete Damage
Damage State Probability
≥ Slight Damage: (0.232 in, 0.390)
≥ Moderate Damage: (0.232 in, 0.193)
≥ Extensive Damage: (0.232 in, 0.053)
≥ Complete Damage: (0.232 in, 0.009)
Building Description:
Facility Class: EFHS
Building Type: URML
Design Level: PC
Site Class: D
City: Middleborough
County: Plymouth
Geologic Group: Group 3
SDC: C
Detailed View
Discrete Damage State Probability P[Damage = DS | Sd]
0.610
0.197
0.141
0.044
0.008
0.001
None 1 2 3 4 Collapsed
Damage State
1 = Slight Damage | 2 = Moderate Damage
3 = Extensive Damage | 4 = Complete Damage

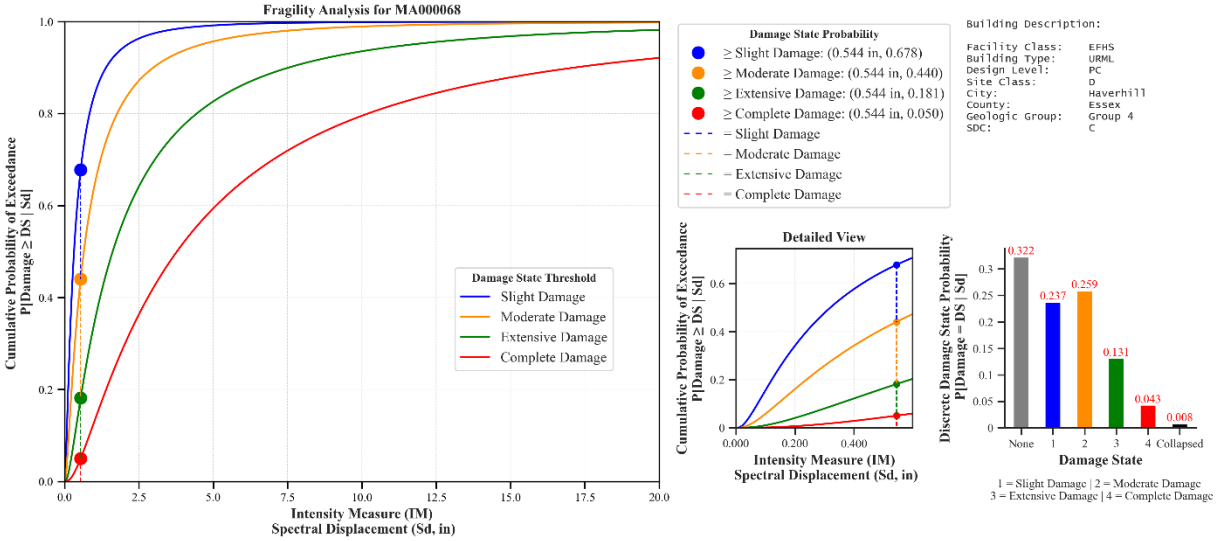
Fragility Analysis for MA000068
Cumulative Probability of Exceedance P[Damage ≥ DS | Sd]
Intensity Measure (IM) Spectral Displacement (Sd, in)
Damage State Threshold
Slight Damage
Moderate Damage
Extensive Damage
Complete Damage
Damage State Probability
≥ Slight Damage: (0.544 in, 0.678)
≥ Moderate Damage: (0.544 in, 0.440)
≥ Extensive Damage: (0.544 in, 0.181)
≥ Complete Damage: (0.544 in, 0.050)
Building Description:
Facility Class: EFHS
Building Type: URML
Design Level: PC
Site Class: D
City: Haverhill
County: Essex
Geologic Group: Group 4
SDC: C
Detailed View
Discrete Damage Stafe Probability P[Damage = DS | Sd]
0.322
0.237
0.259
0.131
0.043
0.008
None 1 2 3 4 Collapsed
Damage State
1 = Slight Damage | 2 = Moderate Damage
3 = Extensive Damage | 4 = Complete Damage

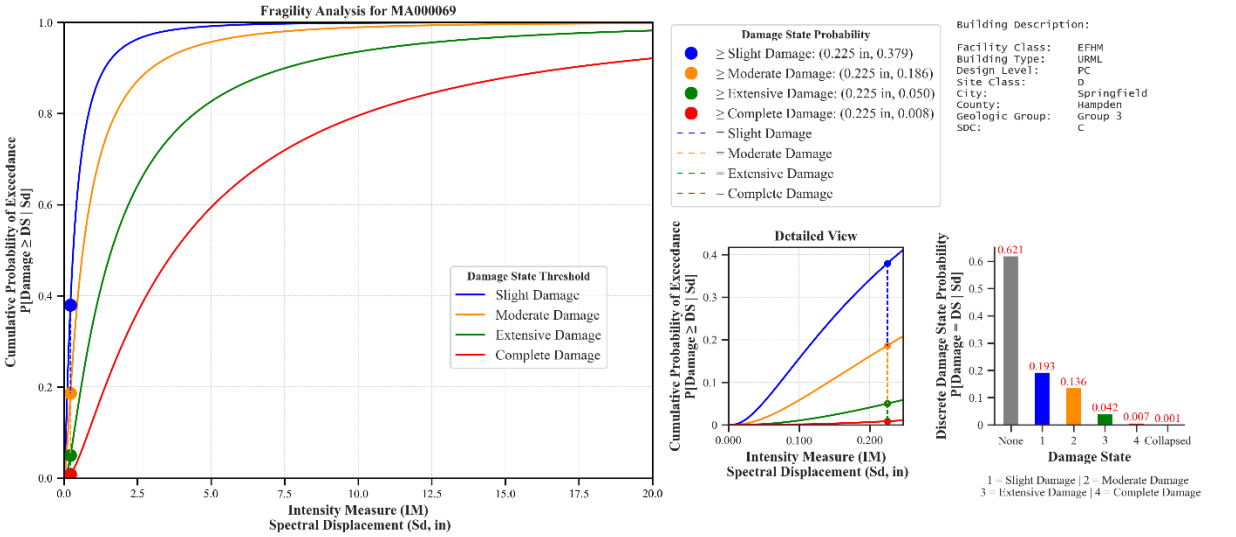
Fragility Analysis for MA000069
Cumulative Probability of Exceedance
P[Damage ≥ DS | Sd]
Intensity Measure (IM)
Spectral Displacement (Sd, in)
Damage State Threshold
Slight Damage
Moderate Damage
Extensive Damage
Complete Damage
Damage State Probability
≥ Slight Damage: (0.225 in, 0.379)
≥ Moderate Damage: (0.225 in, 0.186)
≥ Extensive Damage: (0.225 in, 0.050)
≥ Complete Damage: (0.225 in, 0.008)
– Slight Damage
– Moderate Damage
– Extensive Damage
– Complete Damage
Building Description:
Facility Class: EFHM
Building Type: URML
Design Level: PC
Site Class: D
City: Springfield
County: Hampden
Geologic Group: Group 3
SDC: C
Detailed View
Discrete Damage State Probability
P[Damage = DS | Sd]
0.621
0.193
0.136
0.042
0.007
0.001
None
1
2
3
4
Collapsed
Damage State
1 = Slight Damage | 2 = Moderate Damage
3 = Extensive Damage | 4 = Complete Damage

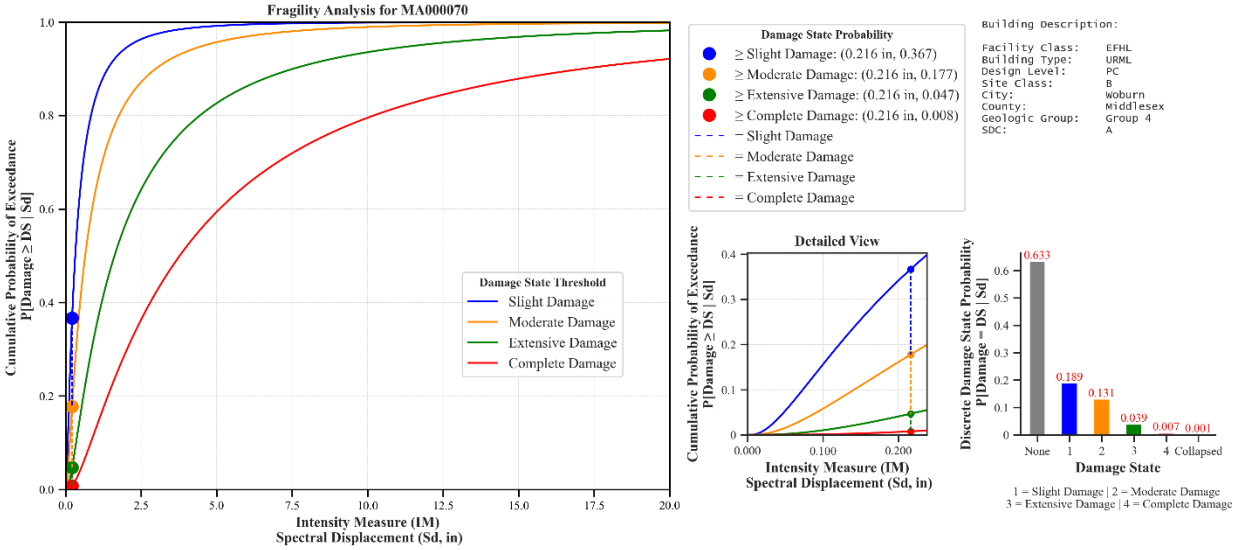
Fragility Analysis for MA000070
Cumulative Probability of Exceedance
P[Damage ≥ DS | Sd]
Intensity Measure (IM)
Spectral Displacement (Sd, in)
Damage State Threshold
Slight Damage
Moderate Damage
Extensive Damage
Complete Damage
Damage State Probability
≥ Slight Damage: (0.216 in, 0.367)
≥ Moderate Damage: (0.216 in, 0.177)
≥ Extensive Damage: (0.216 in, 0.047)
≥ Complete Damage: (0.216 in, 0.008)
– Slight Damage
– Moderate Damage
– Extensive Damage
– Complete Damage
Building Description:
Facility Class: EFHL
Building Type: URML
Design Level: PC
Site Class: B
City: Woburn
County: Middlesex
Geologic Group: Group 4
SDC: A
Detailed View
Discrete Damage State Probability
P[Damage = DS | Sd]
0.633
0.189
0.131
0.039
0.007
0.001
None
1
2
3
4
Collapsed
Damage State
1 = Slight Damage | 2 = Moderate Damage
3 = Extensive Damage | 4 = Complete Damage

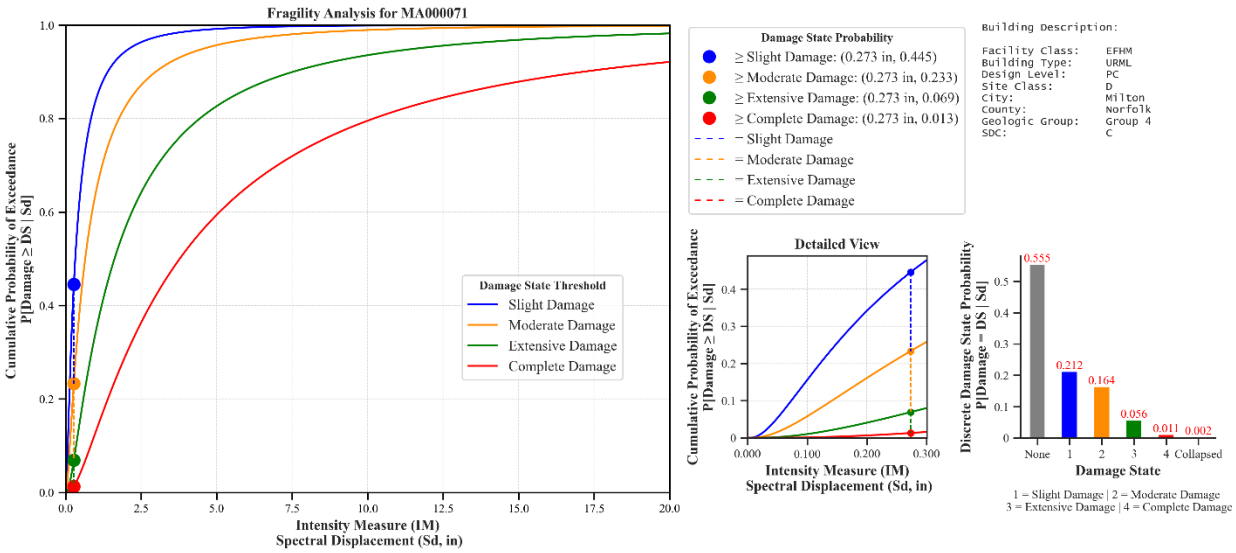
Fragility Analysis for MA000071
Cumulative Probability of Exceedance
P[Damage ≥ DS | Sd]
Intensity Measure (IM)
Spectral Displacement (Sd, in)
Damage State Threshold
Slight Damage
Moderate Damage
Extensive Damage
Complete Damage
Damage State Probability
≥ Slight Damage: (0.273 in, 0.445)
≥ Moderate Damage: (0.273 in, 0.233)
≥ Extensive Damage: (0.273 in, 0.069)
≥ Complete Damage: (0.273 in, 0.013)
– Slight Damage
– Moderate Damage
– Extensive Damage
– Complete Damage
Building Description:
Facility Class: EFHM
Building Type: URML
Design Level: PC
Site Class: D
City: Milton
County: Norfolk
Geologic Group: Group 4
SDC: C
Detailed View
Discrete Damage State Probability
P[Damage = DS | Sd]
0.555
0.212
0.164
0.056
0.011
0.002
None
1
2
3
4
Collapsed
Damage State
1 = Slight Damage | 2 = Moderate Damage
3 = Extensive Damage | 4 = Complete Damage

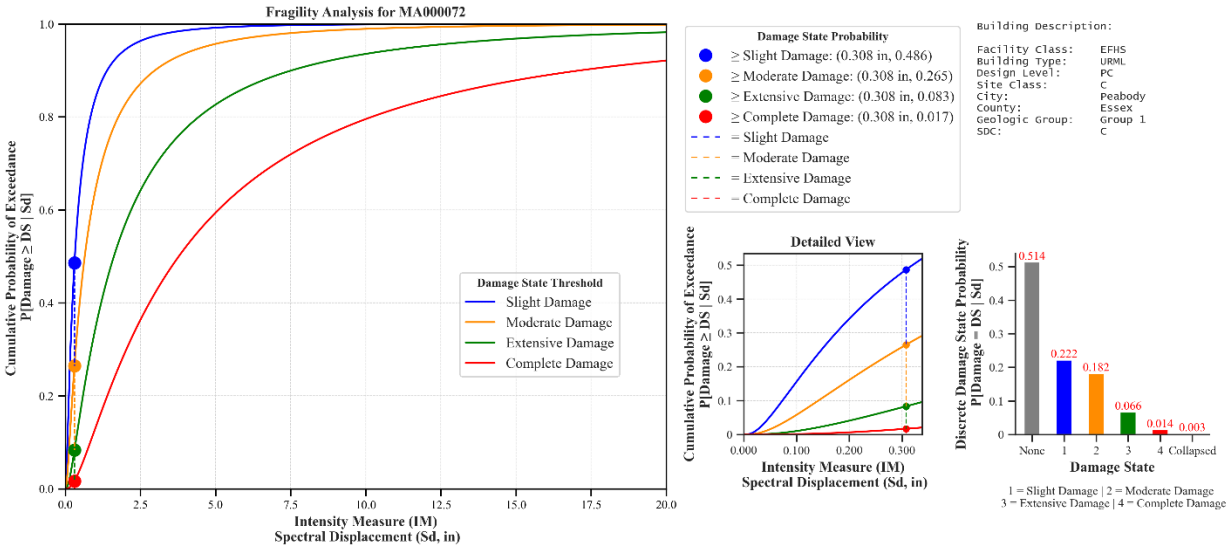
Fragility Analysis for MA000072
Cumulative Probability of Exceedance P[Damage ≥ DS | Sd]
Intensity Measure (IM) Spectral Displacement (Sd, in)
Damage State Threshold
Slight Damage
Moderate Damage
Extensive Damage
Complete Damage
Damage State Probability
≥ Slight Damage: (0.308 in, 0.486)
≥ Moderate Damage: (0.308 in, 0.265)
≥ Extensive Damage: (0.308 in, 0.083)
≥ Complete Damage: (0.308 in, 0.017)
Building Description:
Facility Class: EFHS
Building Type: URML
Design Level: PC
Site Class: C
City: Peabody
County: Essex
Geologic Group: Group 1
SDC: C
Detailed View
Discrete Damage State Probability P[Damage = DS | Sd]
0.514
0.222
0.182
0.066
0.014
0.003
None
Collapsed
Damage State
1 = Slight Damage | 2 = Moderate Damage
3 = Extensive Damage | 4 = Complete Damage

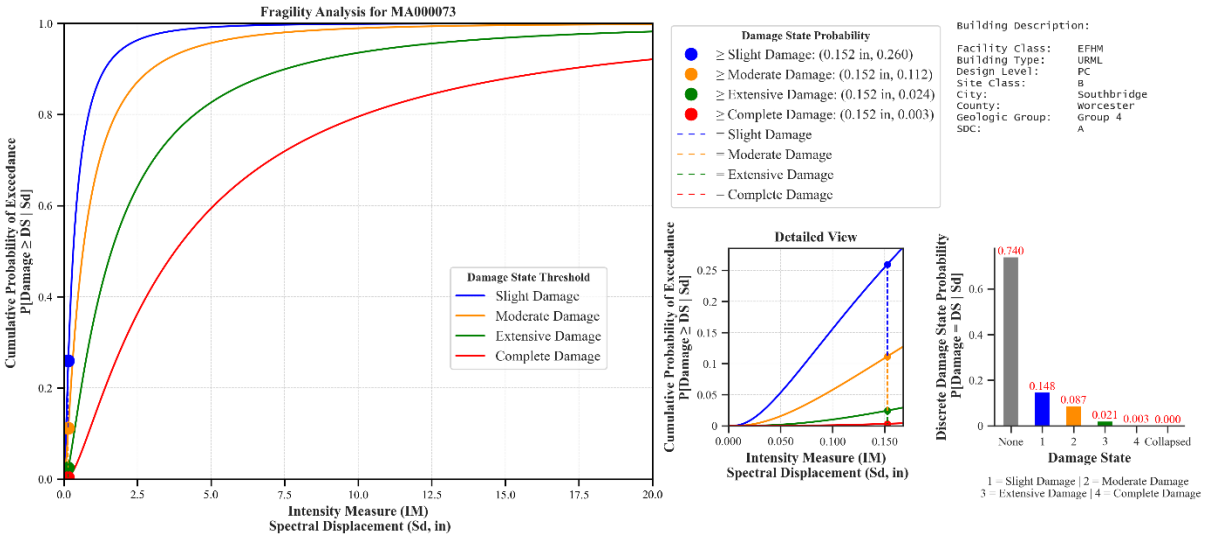
Fragility Analysis for MA000073
Cumulative Probability of Exceedance P[Damage ≥ DS | Sd]
Intensity Measure (IM) Spectral Displacement (Sd, in)
Damage State Threshold
Slight Damage
Moderate Damage
Extensive Damage
Complete Damage
Damage State Probability
≥ Slight Damage: (0.152 in, 0.260)
≥ Moderate Damage: (0.152 in, 0.112)
≥ Extensive Damage: (0.152 in, 0.024)
≥ Complete Damage: (0.152 in, 0.003)
Building Description:
Facility Class: EFHM
Building Type: URML
Design Level: PC
Site Class: B
City: Southbridge
County: Worcester
Geologic Group: Group 4
SDC: A
Detailed View
Discrete Damage State Probability P[Damage = DS | Sd]
0.740
0.148
0.087
0.021
0.003
0.000
None
Collapsed
Damage State
1 = Slight Damage | 2 = Moderate Damage
3 = Extensive Damage | 4 = Complete Damage

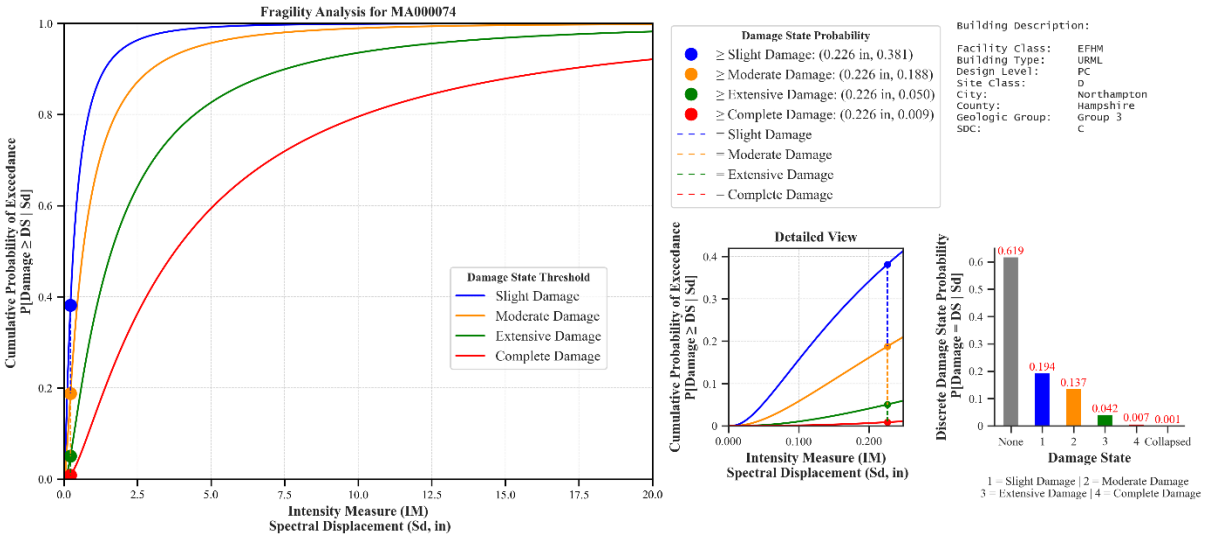
Fragility Analysis for MA000074
Cumulative Probability of Exceedance P[Damage ≥ DS | Sd]
Intensity Measure (IM) Spectral Displacement (Sd, in)
Damage State Threshold
Slight Damage
Moderate Damage
Extensive Damage
Complete Damage
Damage State Probability
≥ Slight Damage: (0.226 in, 0.381)
≥ Moderate Damage: (0.226 in, 0.188)
≥ Extensive Damage: (0.226 in, 0.050)
≥ Complete Damage: (0.226 in, 0.009)
Building Description:
Facility Class: EFHM
Building Type: URML
Design Level: PC
Site Class: D
City: Northampton
County: Hampshire
Geologic Group: Group 3
SDC: C
Detailed View
Discrete Damage State Probability P[Damage = DS | Sd]
0.619
0.194
0.137
0.042
0.007
0.001
None
Collapsed
Damage State
1 = Slight Damage | 2 = Moderate Damage
3 = Extensive Damage | 4 = Complete Damage

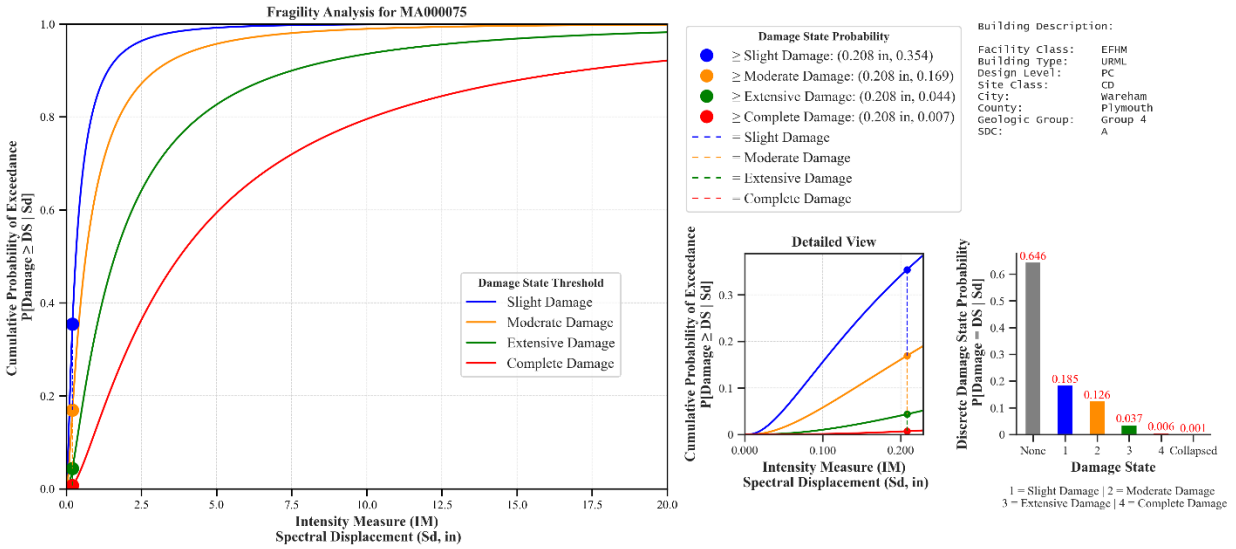
Fragility Analysis for MA000075
Cumulative Probability of Exceedance P[Damage ≥ DS | Sd]
Intensity Measure (IM) Spectral Displacement (Sd, in)
Damage State Threshold
Slight Damage
Moderate Damage
Extensive Damage
Complete Damage
Damage State Probability
≥ Slight Damage: (0.208 in, 0.354)
≥ Moderate Damage: (0.208 in, 0.169)
≥ Extensive Damage: (0.208 in, 0.044)
≥ Complete Damage: (0.208 in, 0.007)
Building Description:
Facility Class: EFHM
Building Type: URML
Design Level: PC
Site Class: CD
City: Wareham
County: Plymouth
Geologic Group: Group 4
SDC: A
Detailed View
Discrete Damage State Probability P[Damage = DS | Sd]
0.646
0.185
0.126
0.037
0.006
0.001
None
Collapsed
Damage State
1 = Slight Damage | 2 = Moderate Damage
3 = Extensive Damage | 4 = Complete Damage

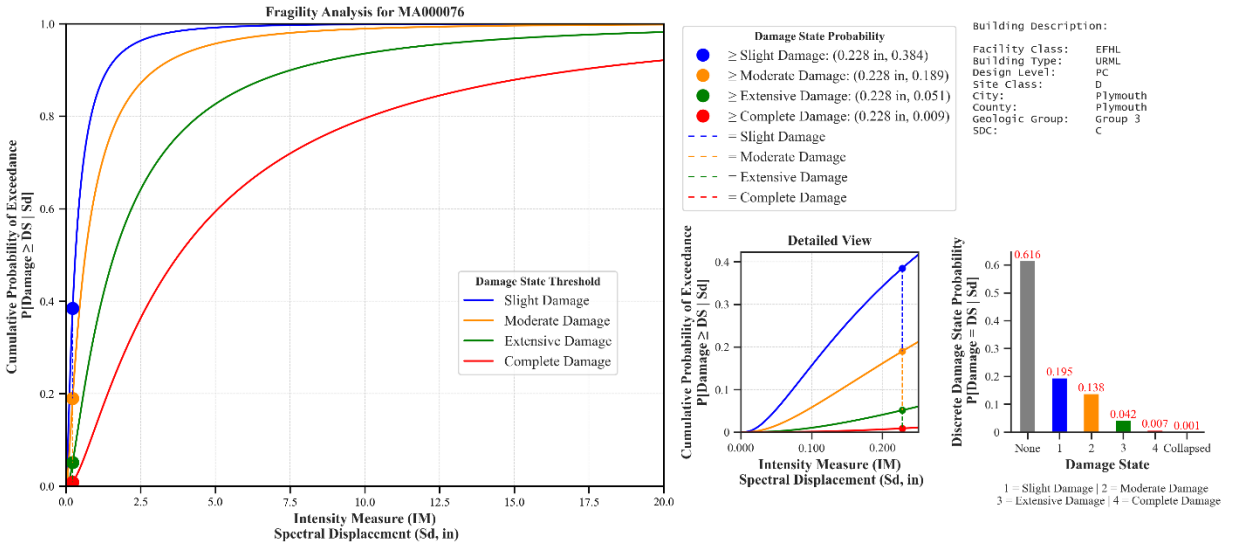
Fragility Analysis for MA000076
Cumulative Probability of Exceedance P[Damage ≥ DS | Sd]
Intensity Measure (IM) Spectral Displacement (Sd, in)
Damage State Threshold
Slight Damage
Moderate Damage
Extensive Damage
Complete Damage
Damage State Probability
≥ Slight Damage: (0.228 in, 0.384)
≥ Moderate Damage: (0.228 in, 0.189)
≥ Extensive Damage: (0.228 in, 0.051)
≥ Complete Damage: (0.228 in, 0.009)
Building Description:
Facility Class: EFHL
Building Type: URML
Design Level: PC
Site Class: D
City: Plymouth
County: Plymouth
Geologic Group: Group 3
SDC: C
Detailed View
Discrete Damage State Probability P[Damage = DS | Sd]
0.616
0.195
0.138
0.042
0.007
0.001
None
Collapsed
Damage State
1 = Slight Damage | 2 = Moderate Damage
3 = Extensive Damage | 4 = Complete Damage

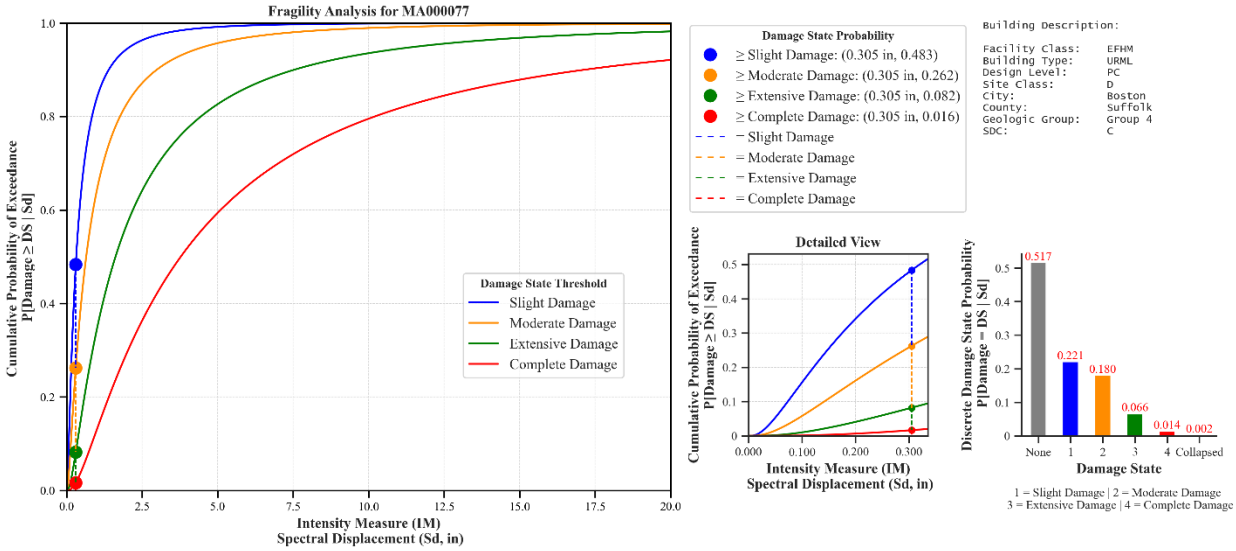
Fragility Analysis for MA000077
Cumulative Probability of Exceedance P[Damage ≥ DS | Sd]
Intensity Measure (IM) Spectral Displacement (Sd, in)
Damage State Threshold
Slight Damage
Moderate Damage
Extensive Damage
Complete Damage
Damage State Probability
≥ Slight Damage: (0.305 in, 0.483)
≥ Moderate Damage: (0.305 in, 0.262)
≥ Extensive Damage: (0.305 in, 0.082)
≥ Complete Damage: (0.305 in, 0.016)
Building Description:
Facility Class: EFHM
Building Type: URML
Design Level: PC
Site Class: D
City: Boston
County: Suffolk
Geologic Group: Group 4
SDC: C
Detailed View
Discrete Damage State Probability P[Damage = DS | Sd]
0.517
0.221
0.180
0.066
0.014
0.002
None
Collapsed
Damage State
1 = Slight Damage | 2 = Moderate Damage
3 = Extensive Damage | 4 = Complete Damage

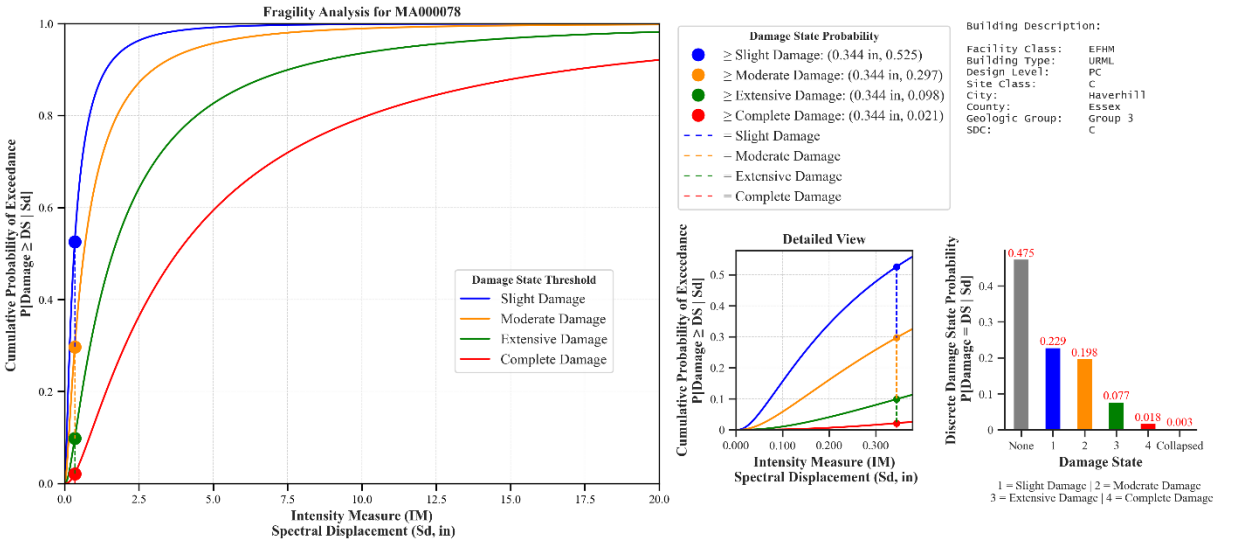
Fragility Analysis for MA000078
Cumulative Probability of Exceedance
P[Damage ≥ DS | Sd]
Intensity Measure (IM)
Spectral Displacement (Sd, in)
Damage State Threshold
Slight Damage
Moderate Damage
Extensive Damage
Complete Damage
Damage State Probability
≥ Slight Damage: (0.344 in, 0.525)
≥ Moderate Damage: (0.344 in, 0.297)
≥ Extensive Damage: (0.344 in, 0.098)
≥ Complete Damage: (0.344 in, 0.021)
Building Description:
Facility Class: EFHM
Building Type: URML
Design Level: PC
Site Class: C
City: Haverhill
County: Essex
Geologic Group: Group 3
SDC: C
Detailed View
Discrete Damage State Probability
P[Damage = DS | Sd]
0.475
0.229
0.198
0.077
0.018
0.003
None
Collapsed
Damage State
1 = Slight Damage | 2 = Moderate Damage
3 = Extensive Damage | 4 = Complete Damage

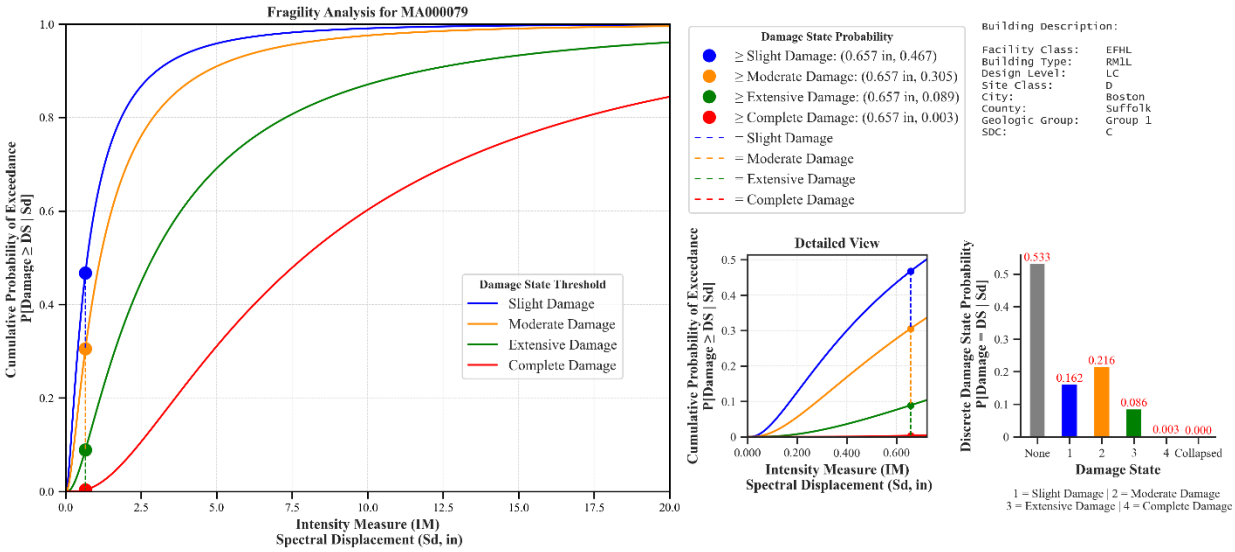
Fragility Analysis for MA000079
Cumulative Probability of Exceedance
P[Damage ≥ DS | Sd]
Intensity Measure (IM)
Spectral Displacement (Sd, in)
Damage State Threshold
Slight Damage
Moderate Damage
Extensive Damage
Complete Damage
Damage State Probability
≥ Slight Damage: (0.657 in, 0.467)
≥ Moderate Damage: (0.657 in, 0.305)
≥ Extensive Damage: (0.657 in, 0.089)
≥ Complete Damage: (0.657 in, 0.003)
Building Description:
Facility Class: EFHL
Building Type: RM1L
Design Level: LC
Site Class: D
City: Boston
County: Suffolk
Geologic Group: Group 1
SDC: C
Detailed View
Discrete Damage State Probability
P[Damage = DS | Sd]
0.533
0.162
0.216
0.086
0.003
0.000
None
Collapsed
Damage State
1 = Slight Damage | 2 = Moderate Damage
3 = Extensive Damage | 4 = Complete Damage

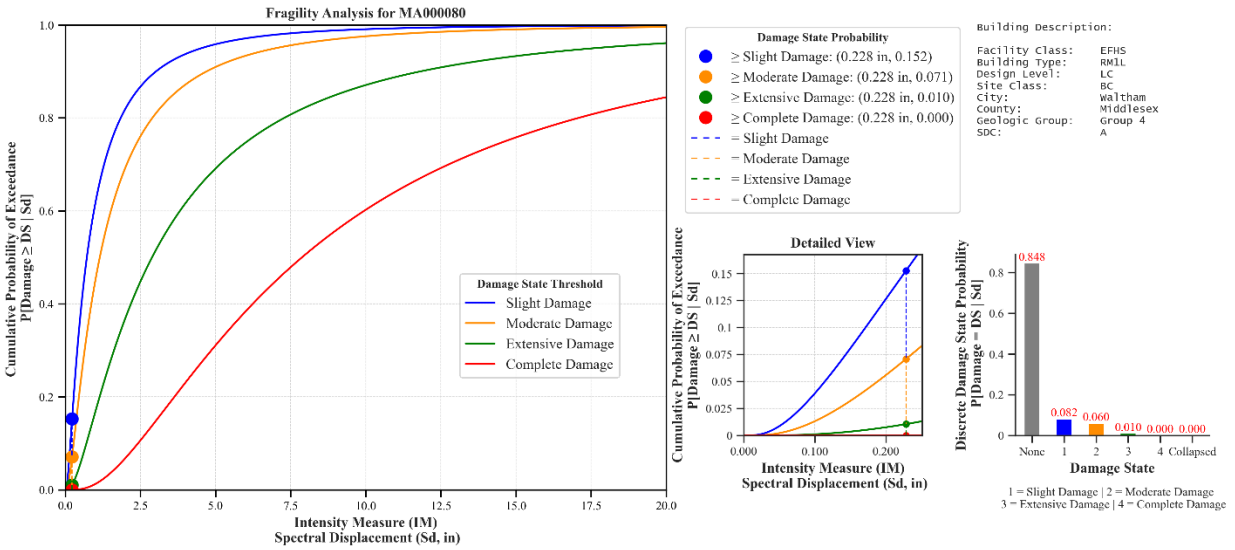
Fragility Analysis for MA000080
Cumulative Probability of Exceedance
P[Damage ≥ DS | Sd]
Intensity Measure (IM)
Spectral Displacement (Sd, in)
Damage State Threshold
Slight Damage
Moderate Damage
Extensive Damage
Complete Damage
Damage State Probability
≥ Slight Damage: (0.228 in, 0.152)
≥ Moderate Damage: (0.228 in, 0.071)
≥ Extensive Damage: (0.228 in, 0.010)
≥ Complete Damage: (0.228 in, 0.000)
Building Description:
Facility Class: EFHS
Building Type: RM1L
Design Level: LC
Site Class: BC
City: Waltham
County: Middlesex
Geologic Group: Group 4
SDC: A
Detailed View
Discrete Damage State Probability
P[Damage = DS | Sd]
0.848
0.082
0.060
0.010
0.000
0.000
None
Collapsed
Damage State
1 = Slight Damage | 2 = Moderate Damage
3 = Extensive Damage | 4 = Complete Damage

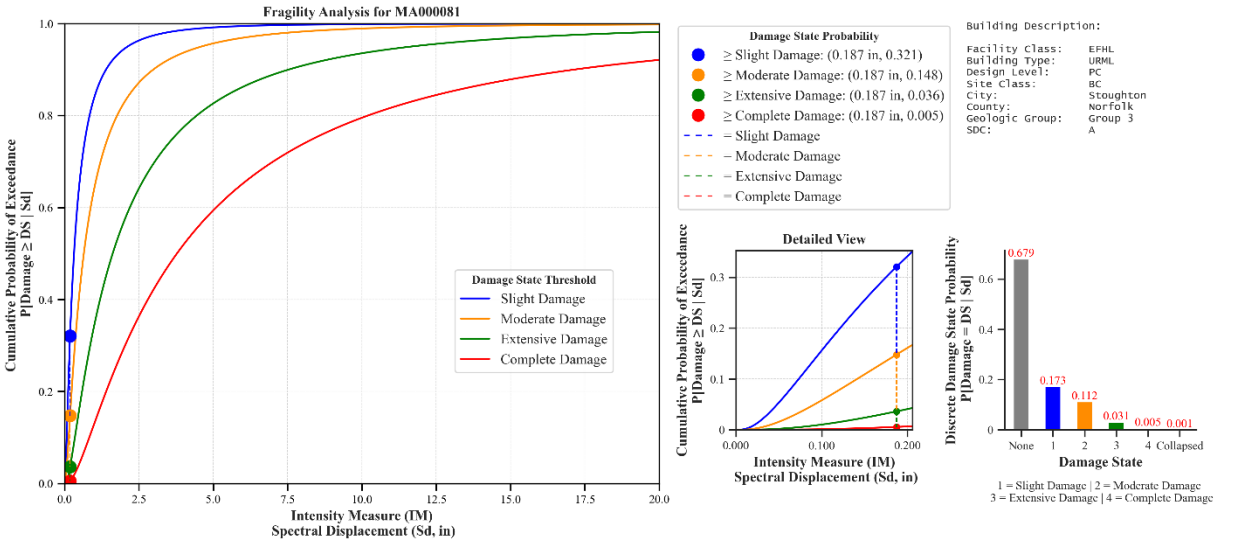
Fragility Analysis for MA000081
Cumulative Probability of Exceedance P[Damage ≥ DS | Sd]
Intensity Measure (IM) Spectral Displacement (Sd, in)
Damage State Threshold
Slight Damage
Moderate Damage
Extensive Damage
Complete Damage
Damage State Probability
≥ Slight Damage: (0.187 in, 0.321)
≥ Moderate Damage: (0.187 in, 0.148)
≥ Extensive Damage: (0.187 in, 0.036)
≥ Complete Damage: (0.187 in, 0.005)
Building Description:
Facility Class: EFHL
Building Type: URML
Design Level: PC
Site Class: BC
City: Stoughton
County: Norfolk
Geologic Group: Group 3
SDC: A
Detailed View
Discrete Damage State Probability P[Damage = DS | Sd]
0.679
0.173
0.112
0.031
0.005
0.001
None
Collapsed
Damage State
1 = Slight Damage | 2 = Moderate Damage
3 = Extensive Damage | 4 = Complete Damage

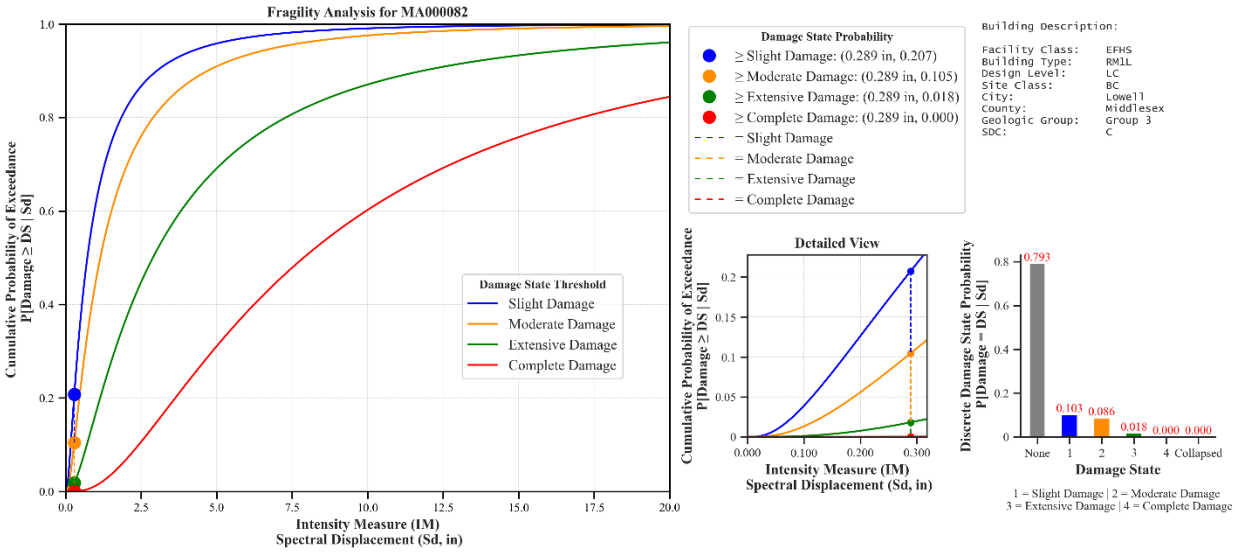
Fragility Analysis for MA000082
Cumulative Probability of Exceedance P[Damage ≥ DS | Sd]
Intensity Measure (IM) Spectral Displacement (Sd, in)
Damage State Threshold
Slight Damage
Moderate Damage
Extensive Damage
Complete Damage
Damage State Probability
≥ Slight Damage: (0.289 in, 0.207)
≥ Moderate Damage: (0.289 in, 0.105)
≥ Extensive Damage: (0.289 in, 0.018)
≥ Complete Damage: (0.289 in, 0.000)
Building Description:
Facility Class: EFHS
Building Type: RM1L
Design Level: LC
Site Class: BC
City: Lowell
County: Middlesex
Geologic Group: Group 3
SDC: C
Detailed View
Discrete Damage State Probability P[Damage = DS | Sd]
0.793
0.103
0.086
0.018
0.000
0.000
None
Collapsed
Damage State
1 = Slight Damage | 2 = Moderate Damage
3 = Extensive Damage | 4 = Complete Damage

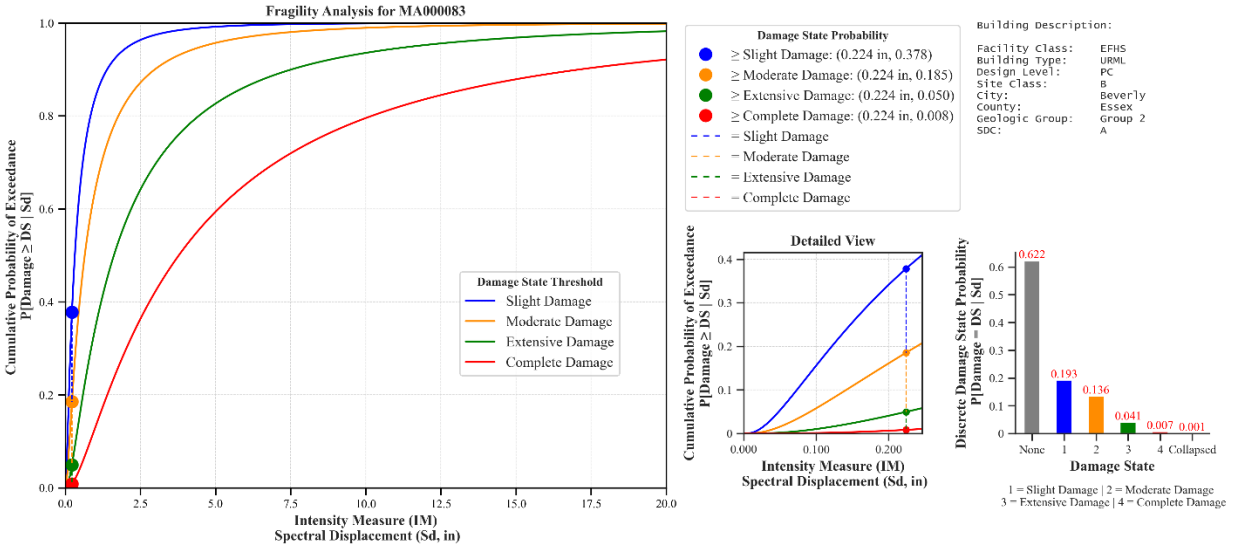
Fragility Analysis for MA000083
Cumulative Probability of Exceedance P[Damage ≥ DS | Sd]
Intensity Measure (IM) Spectral Displacement (Sd, in)
Damage State Threshold
Slight Damage
Moderate Damage
Extensive Damage
Complete Damage
Damage State Probability
≥ Slight Damage: (0.224 in, 0.378)
≥ Moderate Damage: (0.224 in, 0.185)
≥ Extensive Damage: (0.224 in, 0.050)
≥ Complete Damage: (0.224 in, 0.008)
Building Description:
Facility Class: EFHS
Building Type: URML
Design Level: PC
Site Class: B
City: Beverly
County: Essex
Geologic Group: Group 2
SDC: A
Detailed View
Discrete Damage State Probability P[Damage = DS | Sd]
0.622
0.193
0.136
0.041
0.007
0.001
None
Collapsed
Damage State
1 = Slight Damage | 2 = Moderate Damage
3 = Extensive Damage | 4 = Complete Damage

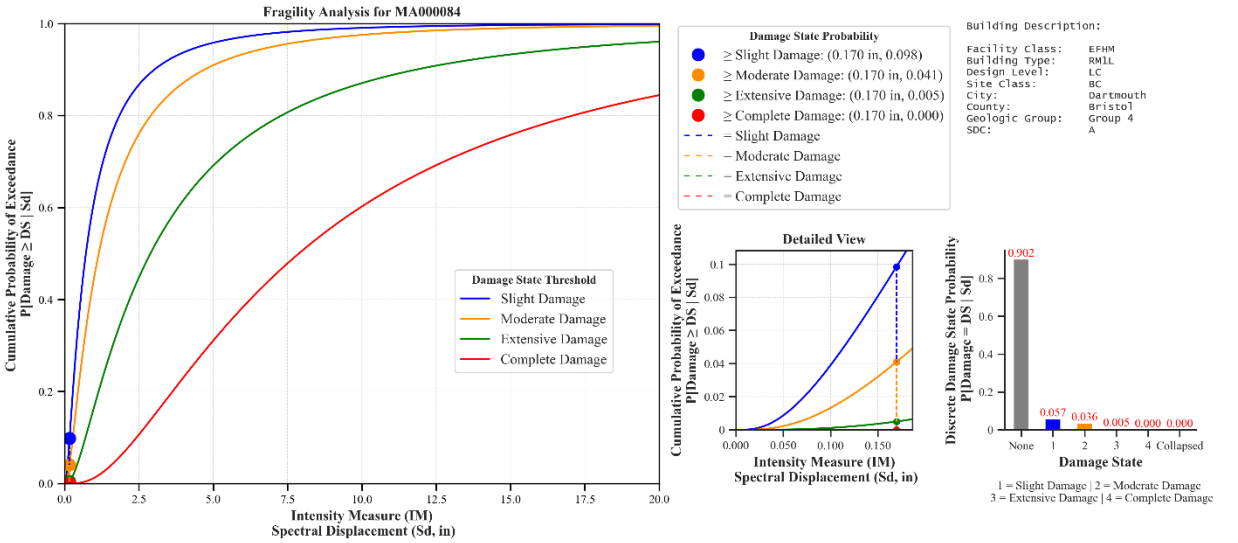
Fragility Analysis for MA000084
Cumulative Probability of Exceedance P[Damage ≥ DS | Sd]
Intensity Measure (IM) Spectral Displacement (Sd, in)
Damage State Threshold
Slight Damage
Moderate Damage
Extensive Damage
Complete Damage
Damage State Probability
≥ Slight Damage: (0.170 in, 0.098)
≥ Moderate Damage: (0.170 in, 0.041)
≥ Extensive Damage: (0.170 in, 0.005)
≥ Complete Damage: (0.170 in, 0.000)
Building Description:
Facility Class: EFHM
Building Type: RM1L
Design Level: LC
Site Class: BC
City: Dartmouth
County: Bristol
Geologic Group: Group 4
SDC: A
Detailed View
Discrete Damage State Probability P[Damage = DS | Sd]
0.902
0.057
0.036
0.005
0.000
0.000
None
Collapsed
Damage State
1 = Slight Damage | 2 = Moderate Damage
3 = Extensive Damage | 4 = Complete Damage

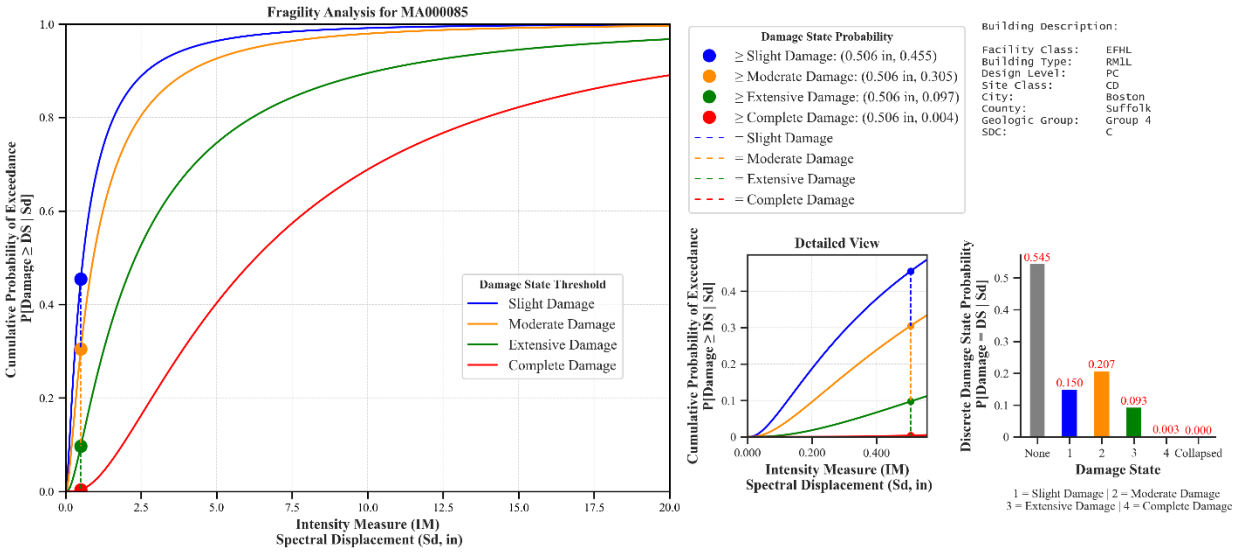
Fragility Analysis for MA000085
Cumulative Probability of Exceedance P[Damage ≥ DS | Sd]
Intensity Measure (IM) Spectral Displacement (Sd, in)
Damage State Threshold
Slight Damage
Moderate Damage
Extensive Damage
Complete Damage
Damage State Probability
≥ Slight Damage: (0.506 in, 0.455)
≥ Moderate Damage: (0.506 in, 0.305)
≥ Extensive Damage: (0.506 in, 0.097)
≥ Complete Damage: (0.506 in, 0.004)
Building Description:
Facility Class: EFHL
Building Type: RM1L
Design Level: PC
Site Class: CD
City: Boston
County: Suffolk
Geologic Group: Group 4
SDC: C
Detailed View
Discrete Damage State Probability P[Damage = DS | Sd]
0.545
0.150
0.207
0.093
0.003
0.000
None
Collapsed
Damage State
1 = Slight Damage | 2 = Moderate Damage
3 = Extensive Damage | 4 = Complete Damage

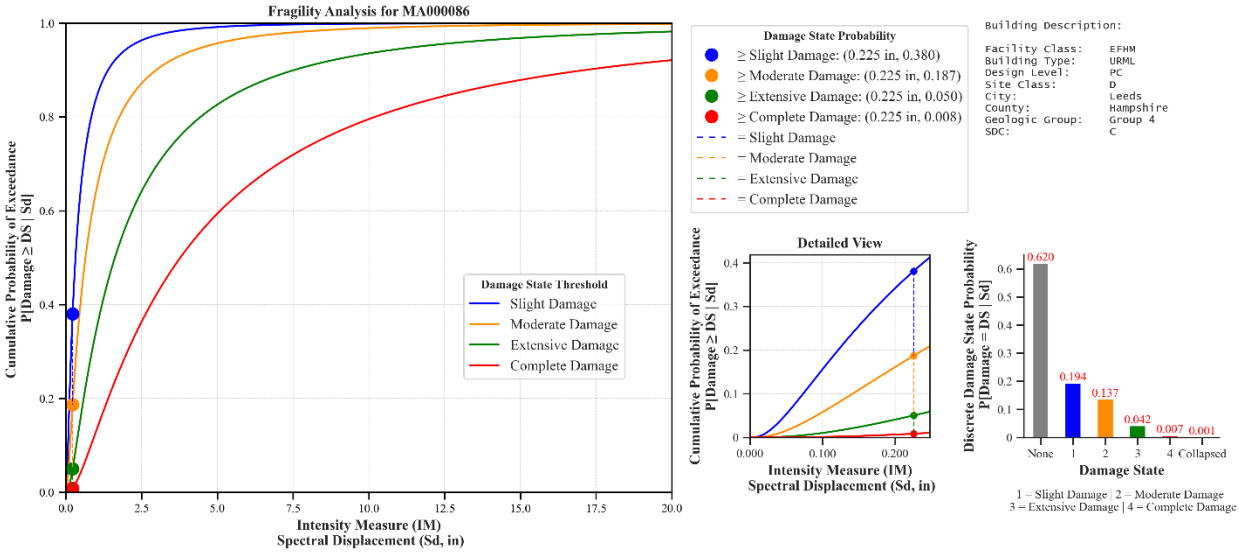
Fragility Analysis for MA000086
Cumulative Probability of Exceedance P[Damage ≥ DS | Sd]
Intensity Measure (IM) Spectral Displacement (Sd, in)
Damage State Threshold
Slight Damage
Moderate Damage
Extensive Damage
Complete Damage
Damage State Probability
≥ Slight Damage: (0.225 in, 0.380)
≥ Moderate Damage: (0.225 in, 0.187)
≥ Extensive Damage: (0.225 in, 0.050)
≥ Complete Damage: (0.225 in, 0.008)
Building Description:
Facility Class: EFHM
Building Type: URML
Design Level: PC
Site Class: D
City: Leeds
County: Hampshire
Geologic Group: Group 4
SDC: C
Detailed View
Discrete Damage State Probability P[Damage = DS | Sd]
0.620
0.194
0.137
0.042
0.007
0.001
None
Collapsed
Damage State
1 = Slight Damage | 2 = Moderate Damage
3 = Extensive Damage | 4 = Complete Damage

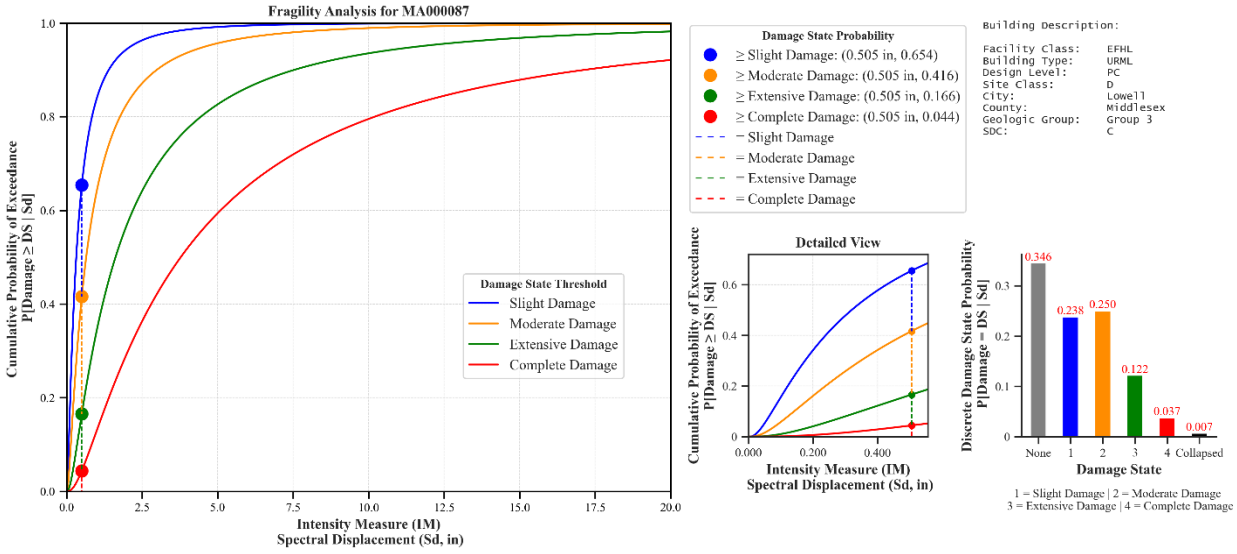
Fragility Analysis for MA000087
Cumulative Probability of Exceedance
P[Damage ≥ DS | Sd]
Intensity Measure (IM)
Spectral Displacement (Sd, in)
Damage State Threshold
Slight Damage
Moderate Damage
Extensive Damage
Complete Damage
Damage State Probability
≥ Slight Damage: (0.505 in, 0.654)
≥ Moderate Damage: (0.505 in, 0.416)
≥ Extensive Damage: (0.505 in, 0.166)
≥ Complete Damage: (0.505 in, 0.044)
= Slight Damage
= Moderate Damage
= Extensive Damage
= Complete Damage
Building Description:
Facility Class: EFHL
Building Type: URML
Design Level: PC
Site Class: D
City: Lowell
County: Middlesex
Geologic Group: Group 3
SDC: C
Detailed View
Discrete Damage State Probability
P[Damage = DS | Sd]
0.346
0.238
0.250
0.122
0.037
0.007
None
1
2
3
4 Collapsed
Damage State
1 = Slight Damage | 2 = Moderate Damage
3 = Extensive Damage | 4 = Complete Damage

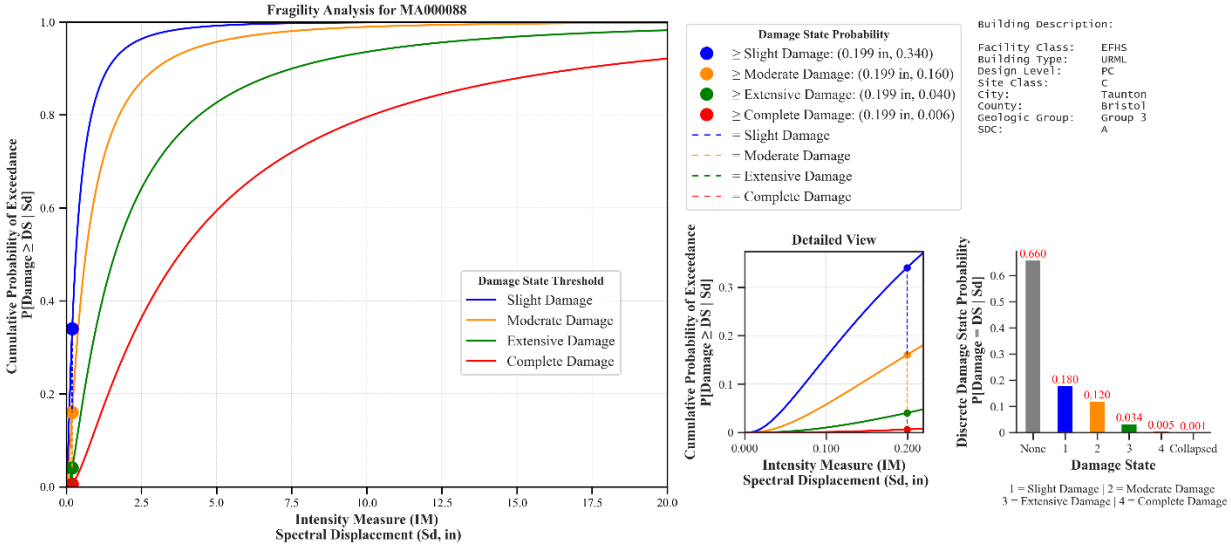
Fragility Analysis for MA000088
Cumulative Probability of Exceedance
P[Damage ≥ DS | Sd]
Intensity Measure (IM)
Spectral Displacement (Sd, in)
Damage State Threshold
Slight Damage
Moderate Damage
Extensive Damage
Complete Damage
Damage State Probability
≥ Slight Damage: (0.199 in, 0.340)
≥ Moderate Damage: (0.199 in, 0.160)
≥ Extensive Damage: (0.199 in, 0.040)
≥ Complete Damage: (0.199 in, 0.006)
= Slight Damage
= Moderate Damage
= Extensive Damage
= Complete Damage
Building Description:
Facility Class: EFHS
Building Type: URML
Design Level: PC
Site Class: C
City: Taunton
County: Bristol
Geologic Group: Group 3
SDC: A
Detailed View
Discrete Damage State Probability
P[Damage = DS | Sd]
0.660
0.180
0.120
0.034
0.005
0.001
None
1
2
3
4 Collapsed
Damage State
1 = Slight Damage | 2 = Moderate Damage
3 = Extensive Damage | 4 = Complete Damage

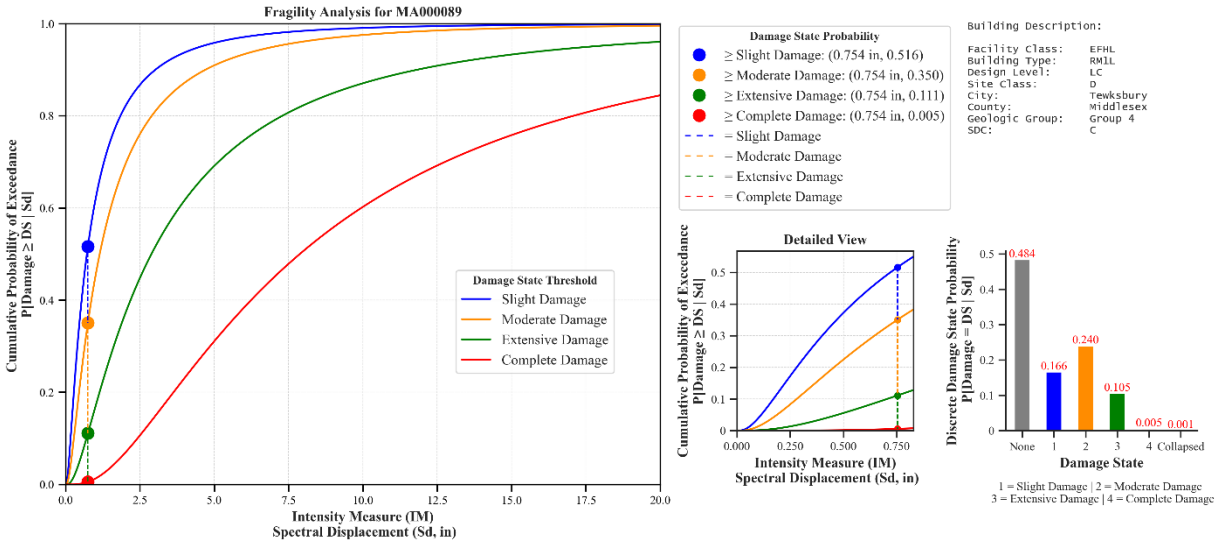
Fragility Analysis for MA000089
Cumulative Probability of Exceedance
P[Damage ≥ DS | Sd]
Intensity Measure (IM)
Spectral Displacement (Sd, in)
Damage State Threshold
Slight Damage
Moderate Damage
Extensive Damage
Complete Damage
Damage State Probability
≥ Slight Damage: (0.754 in, 0.516)
≥ Moderate Damage: (0.754 in, 0.350)
≥ Extensive Damage: (0.754 in, 0.111)
≥ Complete Damage: (0.754 in, 0.005)
= Slight Damage
= Moderate Damage
= Extensive Damage
= Complete Damage
Building Description:
Facility Class: EFHL
Building Type: RM1L
Design Level: LC
Site Class: D
City: Tewksbury
County: Middlesex
Geologic Group: Group 4
SDC: C
Detailed View
Discrete Damage State Probability
P[Damage = DS | Sd]
0.484
0.166
0.240
0.105
0.005
0.001
None
1
2
3
4 Collapsed
Damage State
1 = Slight Damage | 2 = Moderate Damage
3 = Extensive Damage | 4 = Complete Damage

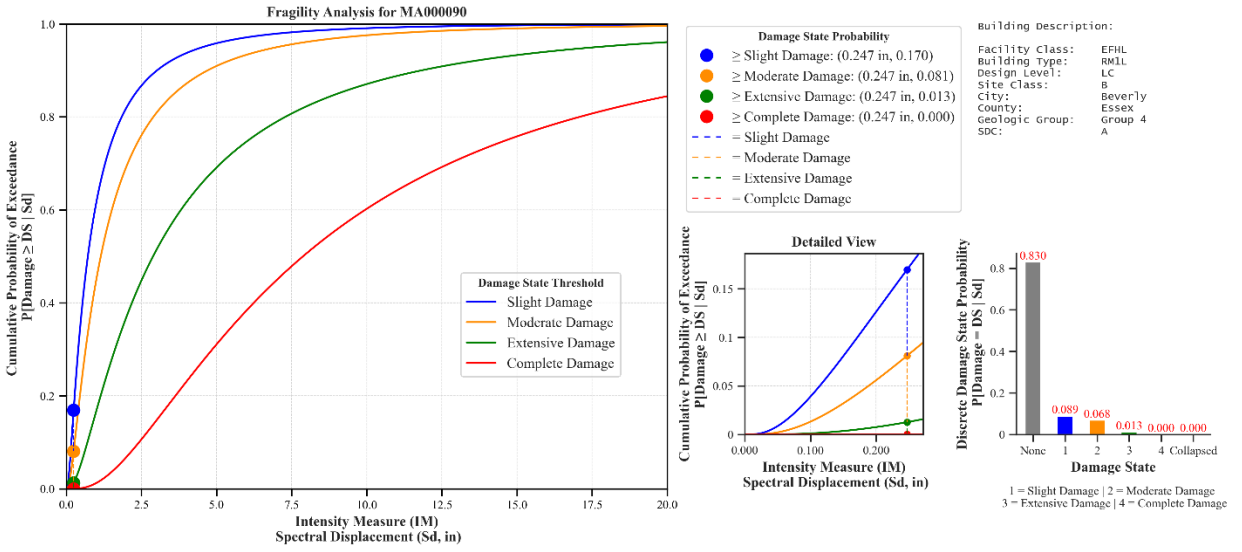
Fragility Analysis for MA000090
Cumulative Probability of Exceedance P[Damage ≥ DS | Sd]
Intensity Measure (IM) Spectral Displacement (Sd, in)
Damage State Threshold
Slight Damage
Moderate Damage
Extensive Damage
Complete Damage
Damage State Probability
≥ Slight Damage: (0.247 in, 0.170)
≥ Moderate Damage: (0.247 in, 0.081)
≥ Extensive Damage: (0.247 in, 0.013)
≥ Complete Damage: (0.247 in, 0.000)
Detailed View
Discrete Damage State Probability P[Damage = DS | Sd]
0.830
0.089
0.068
0.013
0.000
0.000
None
Collapsed
Damage State
1 = Slight Damage | 2 = Moderate Damage
3 = Extensive Damage | 4 = Complete Damage
Building Description:
Facility Class: EFHL
Building Type: RM1L
Design Level: LC
Site Class: B
City: Beverly
County: Essex
Geologic Group: Group 4
SDC: A

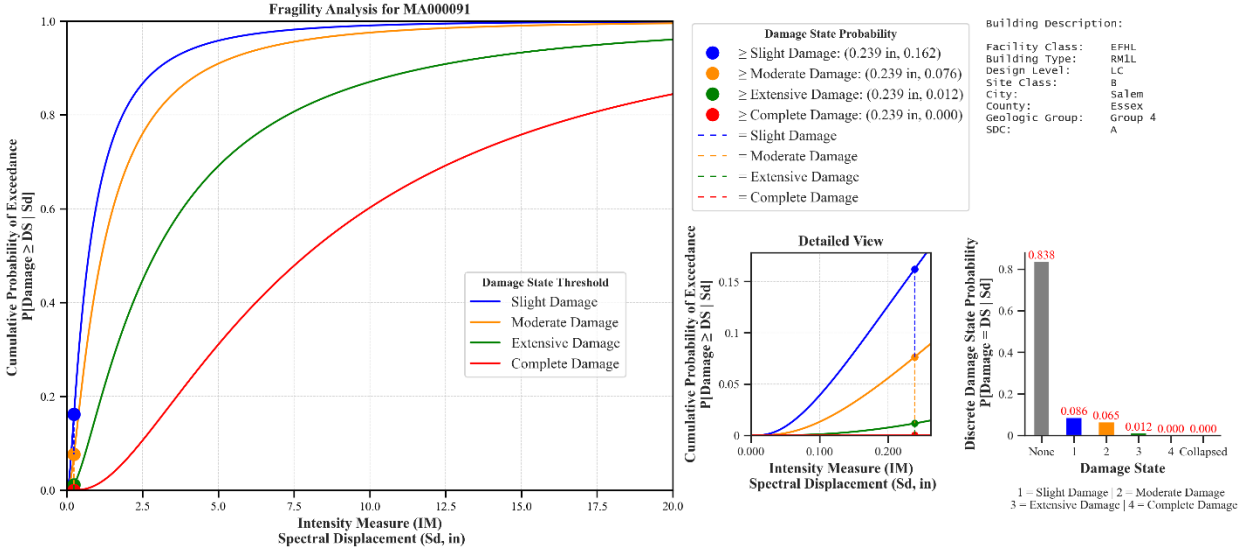
Fragility Analysis for MA000091
Cumulative Probability of Exceedance P[Damage ≥ DS | Sd]
Intensity Measure (IM) Spectral Displacement (Sd, in)
Damage State Threshold
Slight Damage
Moderate Damage
Extensive Damage
Complete Damage
Damage State Probability
≥ Slight Damage: (0.239 in, 0.162)
≥ Moderate Damage: (0.239 in, 0.076)
≥ Extensive Damage: (0.239 in, 0.012)
≥ Complete Damage: (0.239 in, 0.000)
Detailed View
Discrete Damage State Probability P[Damage = DS | Sd]
0.838
0.086
0.065
0.012
0.000
0.000
None
Collapsed
Damage State
1 = Slight Damage | 2 = Moderate Damage
3 = Extensive Damage | 4 = Complete Damage
Building Description:
Facility Class: EFHL
Building Type: RM1L
Design Level: LC
Site Class: B
City: Salem
County: Essex
Geologic Group: Group 4
SDC: A

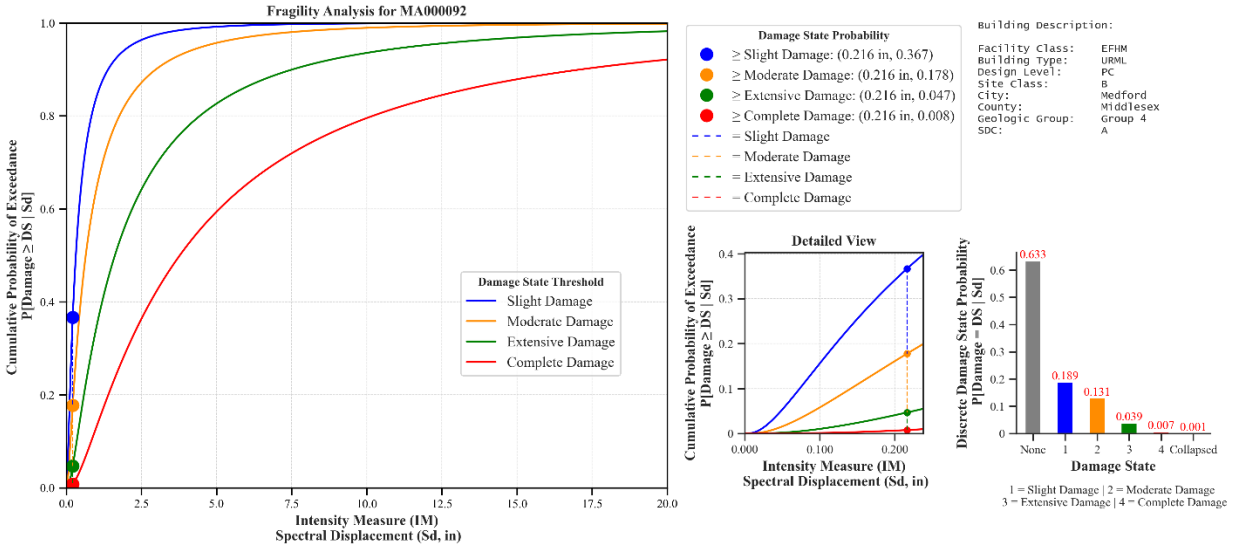
Fragility Analysis for MA000092
Cumulative Probability of Exceedance P[Damage ≥ DS | Sd]
Intensity Measure (IM) Spectral Displacement (Sd, in)
Damage State Threshold
Slight Damage
Moderate Damage
Extensive Damage
Complete Damage
Damage State Probability
≥ Slight Damage: (0.216 in, 0.367)
≥ Moderate Damage: (0.216 in, 0.178)
≥ Extensive Damage: (0.216 in, 0.047)
≥ Complete Damage: (0.216 in, 0.008)
Detailed View
Discrete Damage State Probability P[Damage = DS | Sd]
0.633
0.189
0.131
0.039
0.007
0.001
None
Collapsed
Damage State
1 = Slight Damage | 2 = Moderate Damage
3 = Extensive Damage | 4 = Complete Damage
Building Description:
Facility Class: EFHM
Building Type: URML
Design Level: PC
Site Class: B
City: Medford
County: Middlesex
Geologic Group: Group 4
SDC: A

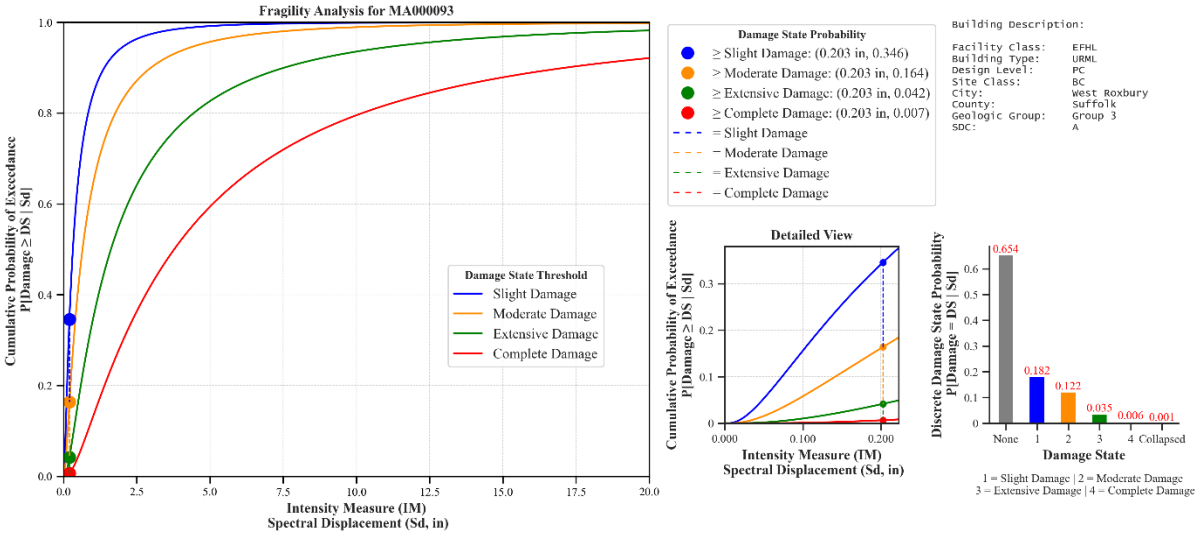
Fragility Analysis for MA000093
Cumulative Probability of Exceedance P[Damage ≥ DS | Sd]
Intensity Measure (IM) Spectral Displacement (Sd, in)
Damage State Threshold
Slight Damage
Moderate Damage
Extensive Damage
Complete Damage
Damage State Probability
≥ Slight Damage: (0.203 in, 0.346)
> Moderate Damage: (0.203 in, 0.164)
≥ Extensive Damage: (0.203 in, 0.042)
≥ Complete Damage: (0.203 in, 0.007)
= Slight Damage
= Moderate Damage
= Extensive Damage
= Complete Damage
Building Description:
Facility Class: EFHL
Building Type: URML
Design Level: PC
Site Class: BC
City: West Roxbury
County: Suffolk
Geologic Group: Group 3
SDC: A
Detailed View
Cumulative Probability of Exceedance P[Damage ≥ DS | Sd]
Intensity Measure (IM) Spectral Displacement (Sd, in)
Discrete Damage State Probability P[Damage = DS | Sd]
0.654
0.182
0.122
0.035
0.006
0.001
None
1
2
3
4 Collapsed
Damage State
1 = Slight Damage | 2 = Moderate Damage
3 = Extensive Damage | 4 = Complete Damage

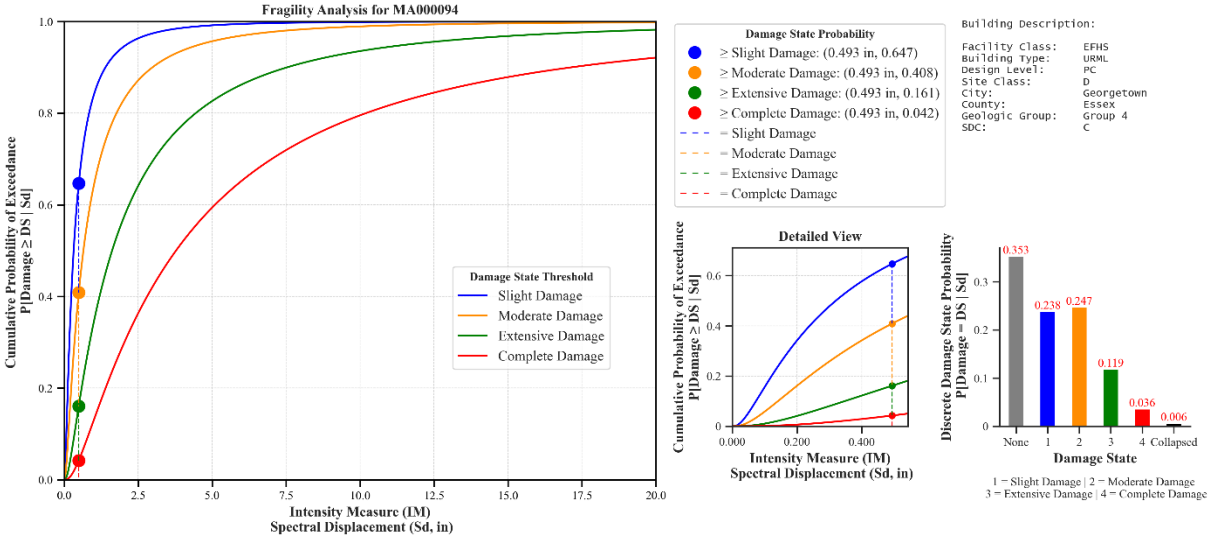
Fragility Analysis for MA000094
Cumulative Probability of Exceedance P[Damage ≥ DS | Sd]
Intensity Measure (IM) Spectral Displacement (Sd, in)
Damage State Threshold
Slight Damage
Moderate Damage
Extensive Damage
Complete Damage
Damage State Probability
≥ Slight Damage: (0.493 in, 0.647)
≥ Moderate Damage: (0.493 in, 0.408)
≥ Extensive Damage: (0.493 in, 0.161)
≥ Complete Damage: (0.493 in, 0.042)
= Slight Damage
= Moderate Damage
= Extensive Damage
= Complete Damage
Building Description:
Facility Class: EFHS
Building Type: URML
Design Level: PC
Site Class: D
City: Georgetown
County: Essex
Geologic Group: Group 4
SDC: C
Detailed View
Cumulative Probability of Exceedance P[Damage ≥ DS | Sd]
Intensity Measure (IM) Spectral Displacement (Sd, in)
Discrete Damage State Probability P[Damage = DS | Sd]
0.353
0.238
0.247
0.119
0.036
0.006
None
1
2
3
4 Collapsed
Damage State
1 = Slight Damage | 2 = Moderate Damage
3 = Extensive Damage | 4 = Complete Damage

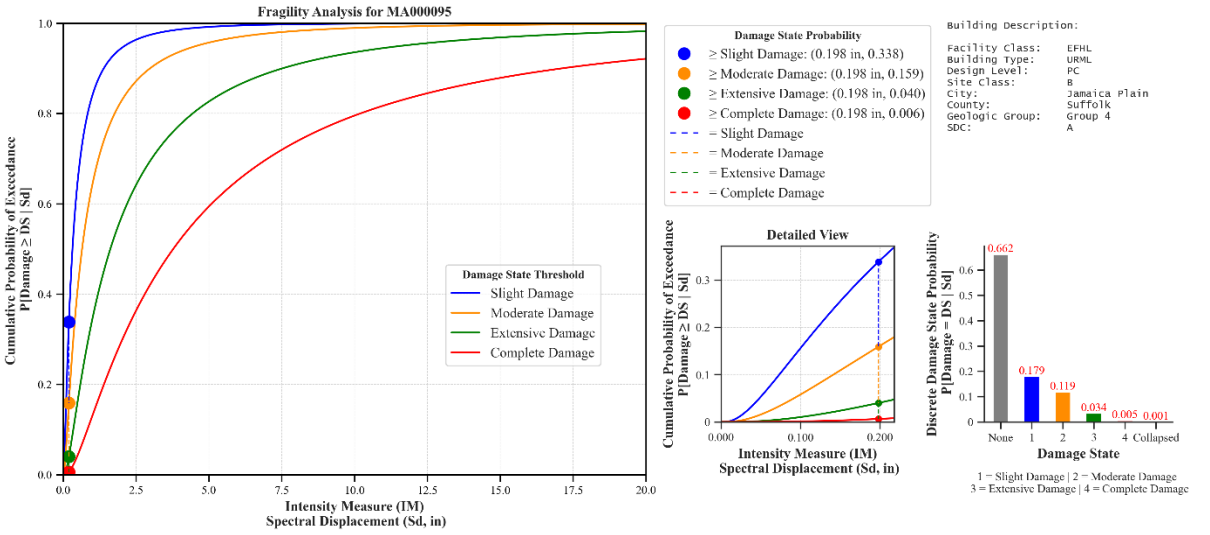
Fragility Analysis for MA000095
Cumulative Probability of Exceedance P[Damage ≥ DS | Sd]
Intensity Measure (IM) Spectral Displacement (Sd, in)
Damage State Threshold
Slight Damage
Moderate Damage
Extensive Damage
Complete Damage
Damage State Probability
≥ Slight Damage: (0.198 in, 0.338)
≥ Moderate Damage: (0.198 in, 0.159)
≥ Extensive Damage: (0.198 in, 0.040)
≥ Complete Damage: (0.198 in, 0.006)
= Slight Damage
= Moderate Damage
= Extensive Damage
= Complete Damage
Building Description:
Facility Class: EFHL
Building Type: URML
Design Level: PC
Site Class: B
City: Jamaica Plain
County: Suffolk
Geologic Group: Group 4
SDC: A
Detailed View
Cumulative Probability of Exceedance P[Damage ≥ DS | Sd]
Intensity Measure (IM) Spectral Displacement (Sd, in)
Discrete Damage State Probability P[Damage = DS | Sd]
0.662
0.179
0.119
0.034
0.005
0.001
None
1
2
3
4 Collapsed
Damage State
1 = Slight Damage | 2 = Moderate Damage
3 = Extensive Damage | 4 = Complete Damage

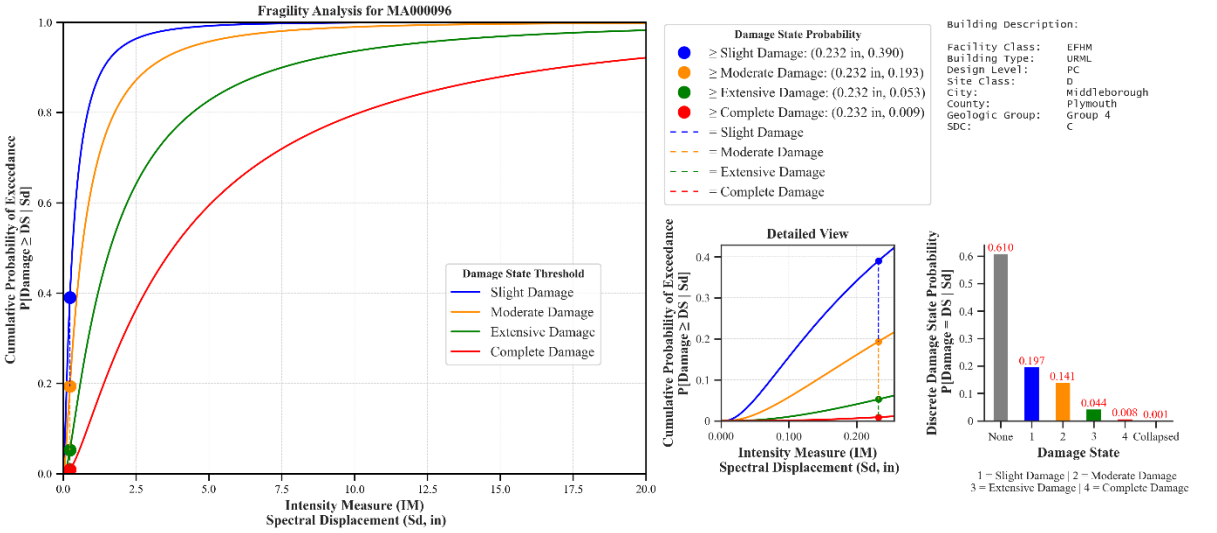
Fragility Analysis for MA000096
Cumulative Probability of Exceedance P[Damage ≥ DS | Sd]
Intensity Measure (IM) Spectral Displacement (Sd, in)
Damage State Threshold
Slight Damage
Moderate Damage
Extensive Damage
Complete Damage
Damage State Probability
≥ Slight Damage: (0.232 in, 0.390)
≥ Moderate Damage: (0.232 in, 0.193)
≥ Extensive Damage: (0.232 in, 0.053)
≥ Complete Damage: (0.232 in, 0.009)
Building Description:
Facility Class: EFHM
Building Type: URML
Design Level: PC
Site Class: D
City: Middleborough
County: Plymouth
Geologic Group: Group 4
SDC: C
Detailed View
Discrete Damage State Probability P[Damage = DS | Sd]
0.610
0.197
0.141
0.044
0.008
0.001
None
Collapsed
Damage State
1 = Slight Damage | 2 = Moderate Damage
3 = Extensive Damage | 4 = Complete Damage

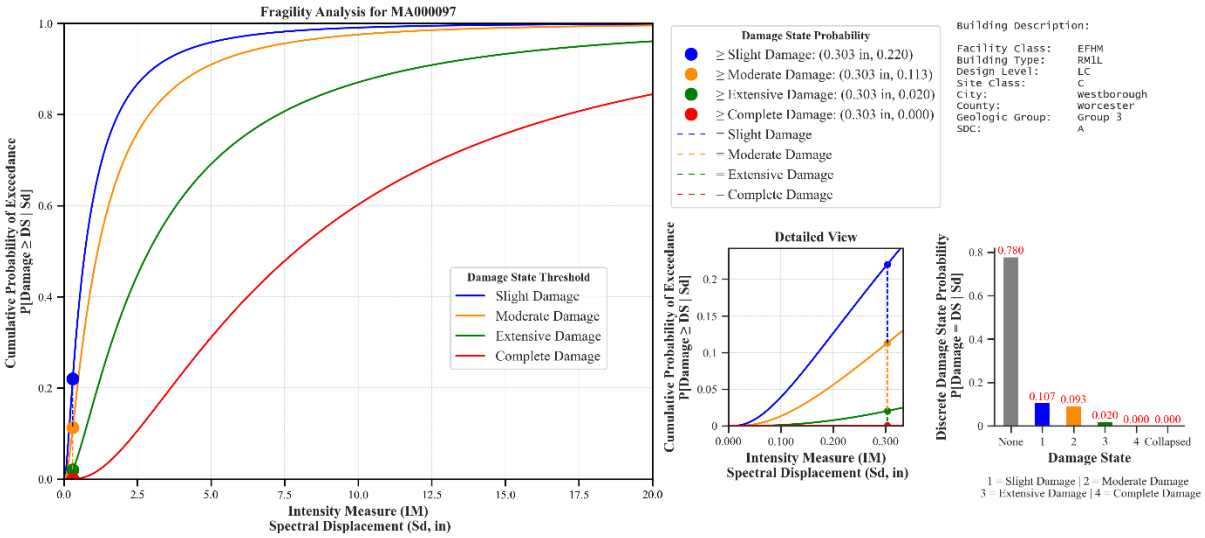
Fragility Analysis for MA000097
Cumulative Probability of Exceedance P[Damage ≥ DS | Sd]
Intensity Measure (IM) Spectral Displacement (Sd, in)
Damage State Threshold
Slight Damage
Moderate Damage
Extensive Damage
Complete Damage
Damage State Probability
≥ Slight Damage: (0.303 in, 0.220)
≥ Moderate Damage: (0.303 in, 0.113)
≥ Extensive Damage: (0.303 in, 0.020)
≥ Complete Damage: (0.303 in, 0.000)
Building Description:
Facility Class: EFHM
Building Type: RMLL
Design Level: LC
Site Class: C
City: Westborough
County: Worcester
Geologic Group: Group 3
SDC: A
Detailed View
Discrete Damage State Probability P[Damage = DS | Sd]
0.780
0.107
0.093
0.020
0.000
0.000
None
Collapsed
Damage State
1 = Slight Damage | 2 = Moderate Damage
3 = Extensive Damage | 4 = Complete Damage

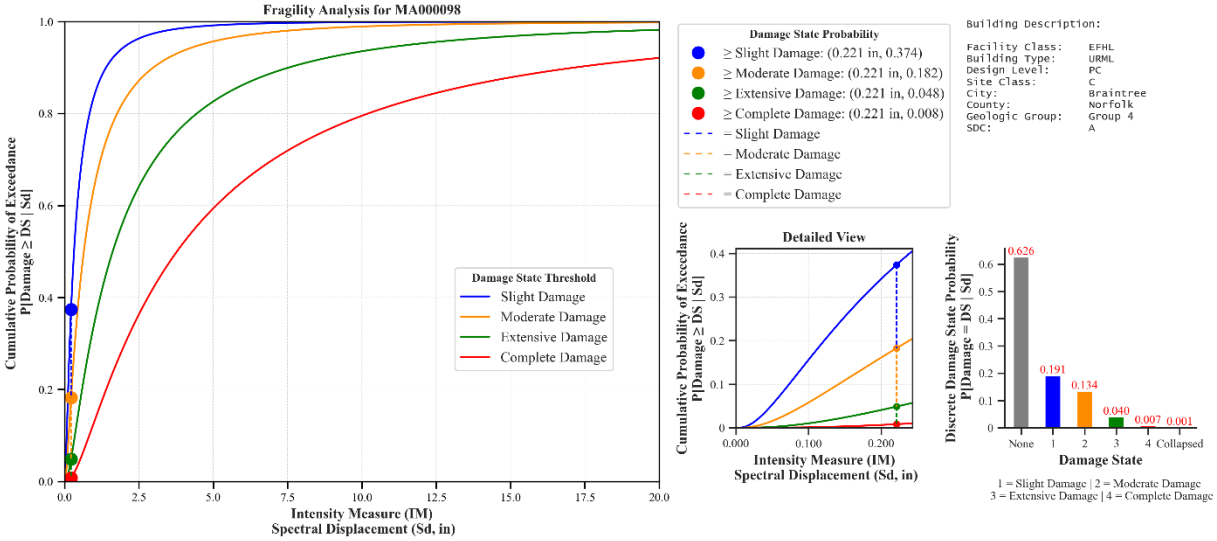
Fragility Analysis for MA000098
Cumulative Probability of Exceedance P[Damage ≥ DS | Sd]
Intensity Measure (IM) Spectral Displacement (Sd, in)
Damage State Threshold
Slight Damage
Moderate Damage
Extensive Damage
Complete Damage
Damage State Probability
≥ Slight Damage: (0.221 in, 0.374)
≥ Moderate Damage: (0.221 in, 0.182)
≥ Extensive Damage: (0.221 in, 0.048)
≥ Complete Damage: (0.221 in, 0.008)
Building Description:
Facility Class: EFHL
Building Type: URML
Design Level: PC
Site Class: C
City: Braintree
County: Norfolk
Geologic Group: Group 4
SDC: A
Detailed View
Discrete Damage State Probability P[Damage = DS | Sd]
0.626
0.191
0.134
0.040
0.007
0.001
None
Collapsed
Damage State
1 = Slight Damage | 2 = Moderate Damage
3 = Extensive Damage | 4 = Complete Damage

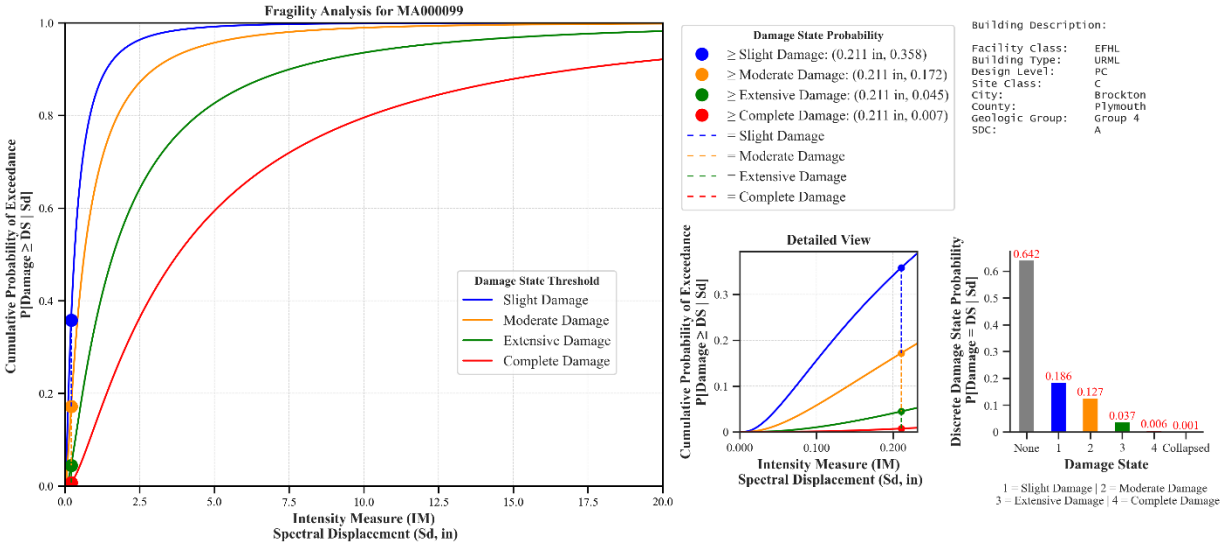
Fragility Analysis for MA000099
Cumulative Probability of Exceedance P[Damage ≥ DS | Sd]
Intensity Measure (IM) Spectral Displacement (Sd, in)
Damage State Threshold
Slight Damage
Moderate Damage
Extensive Damage
Complete Damage
Damage State Probability
≥ Slight Damage: (0.211 in, 0.358)
≥ Moderate Damage: (0.211 in, 0.172)
≥ Extensive Damage: (0.211 in, 0.045)
≥ Complete Damage: (0.211 in, 0.007)
= Slight Damage
= Moderate Damage
= Extensive Damage
= Complete Damage
Building Description:
Facility Class: EFHL
Building Type: URML
Design Level: PC
Site Class: C
City: Brockton
County: Plymouth
Geologic Group: Group 4
SDC: A
Detailed View
Discrete Damage State Probability P[Damage = DS | Sd]
0.642
0.186
0.127
0.037
0.006
0.001
None 1 2 3 4 Collapsed
Damage State
1 = Slight Damage | 2 = Moderate Damage
3 = Extensive Damage | 4 = Complete Damage

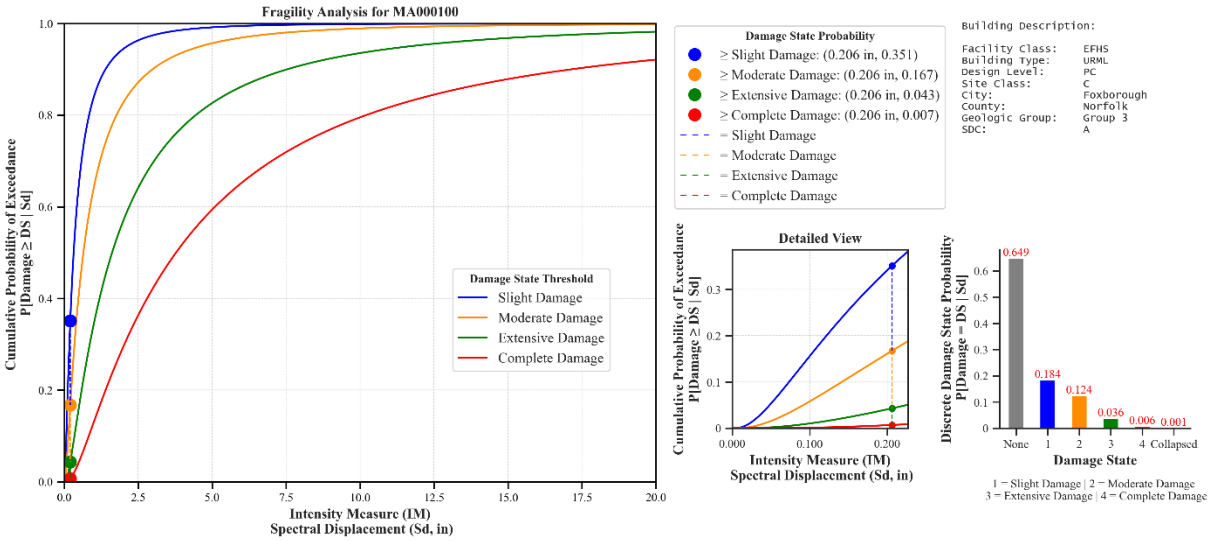
Fragility Analysis for MA000100
Cumulative Probability of Exceedance P[Damage ≥ DS | Sd]
Intensity Measure (IM) Spectral Displacement (Sd, in)
Damage State Threshold
Slight Damage
Moderate Damage
Extensive Damage
Complete Damage
Damage State Probability
≥ Slight Damage: (0.206 in, 0.351)
≥ Moderate Damage: (0.206 in, 0.167)
≥ Extensive Damage: (0.206 in, 0.043)
≥ Complete Damage: (0.206 in, 0.007)
= Slight Damage
= Moderate Damage
= Extensive Damage
= Complete Damage
Building Description:
Facility Class: EFHS
Building Type: URML
Design Level: PC
Site Class: C
City: Foxborough
County: Norfolk
Geologic Group: Group 3
SDC: A
Detailed View
Discrete Damage State Probability P[Damage = DS | Sd]
0.649
0.184
0.124
0.036
0.006
0.001
None 1 2 3 4 Collapsed
Damage State
1 = Slight Damage | 2 = Moderate Damage
3 = Extensive Damage | 4 = Complete Damage

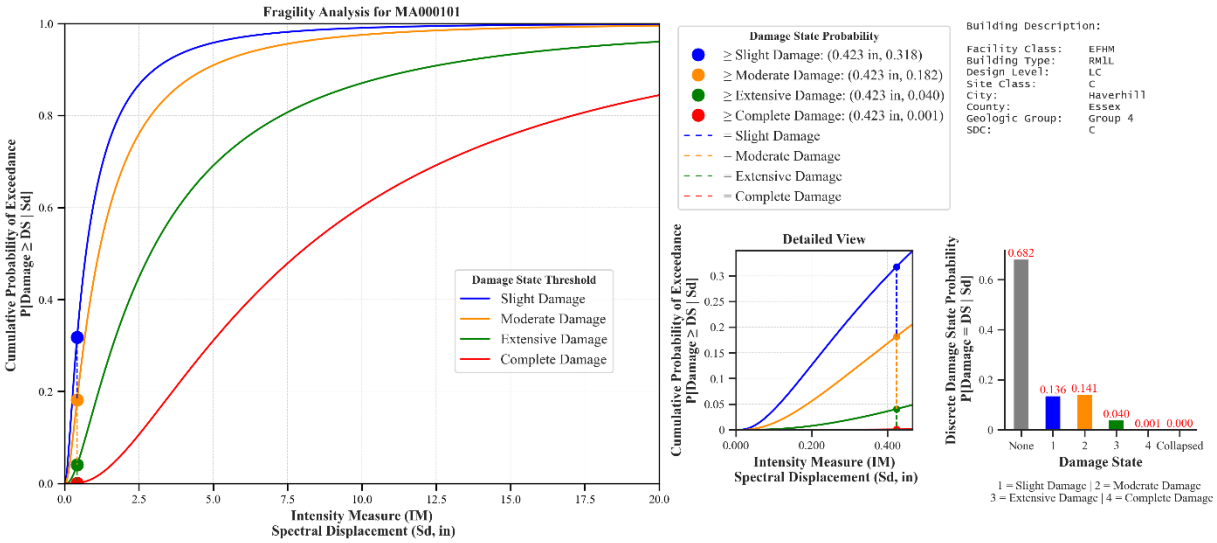
Fragility Analysis for MA000101
Cumulative Probability of Exceedance P[Damage ≥ DS | Sd]
Intensity Measure (IM) Spectral Displacement (Sd, in)
Damage State Threshold
Slight Damage
Moderate Damage
Extensive Damage
Complete Damage
Damage State Probability
≥ Slight Damage: (0.423 in, 0.318)
≥ Moderate Damage: (0.423 in, 0.182)
≥ Extensive Damage: (0.423 in, 0.040)
≥ Complete Damage: (0.423 in, 0.001)
= Slight Damage
= Moderate Damage
= Extensive Damage
= Complete Damage
Building Description:
Facility Class: EFHM
Building Type: RMLL
Design Level: LC
Site Class: C
City: Haverhill
County: Essex
Geologic Group: Group 4
SDC: C
Detailed View
Discrete Damage State Probability P[Damage = DS | Sd]
0.682
0.136
0.141
0.040
0.001
0.000
None 1 2 3 4 Collapsed
Damage State
1 = Slight Damage | 2 = Moderate Damage
3 = Extensive Damage | 4 = Complete Damage

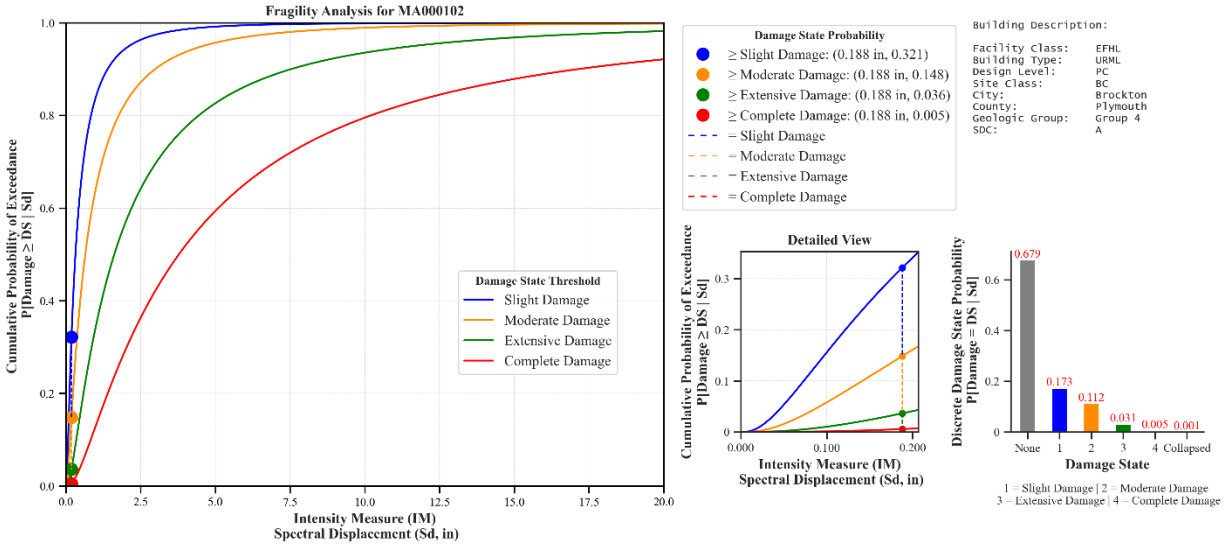
Fragility Analysis for MA000102
Cumulative Probability of Exceedance P[Damage ≥ DS | Sd]
Intensity Measure (IM) Spectral Displacement (Sd, in)
Damage State Threshold
Slight Damage
Moderate Damage
Extensive Damage
Complete Damage
Damage State Probability
≥ Slight Damage: (0.188 in, 0.321)
≥ Moderate Damage: (0.188 in, 0.148)
≥ Extensive Damage: (0.188 in, 0.036)
≥ Complete Damage: (0.188 in, 0.005)
= Slight Damage
= Moderate Damage
= Extensive Damage
= Complete Damage
Detailed View
Discrete Damage State Probability P[Damage = DS | Sd]
0.679
0.173
0.112
0.031
0.005
0.001
None
1
2
3
4 Collapsed
Damage State
1 = Slight Damage | 2 = Moderate Damage
3 = Extensive Damage | 4 = Complete Damage
Building Description:
Facility Class: EFHL
Building Type: URML
Design Level: PC
Site Class: BC
City: Brockton
County: Plymouth
Geologic Group: Group 4
SDC: A

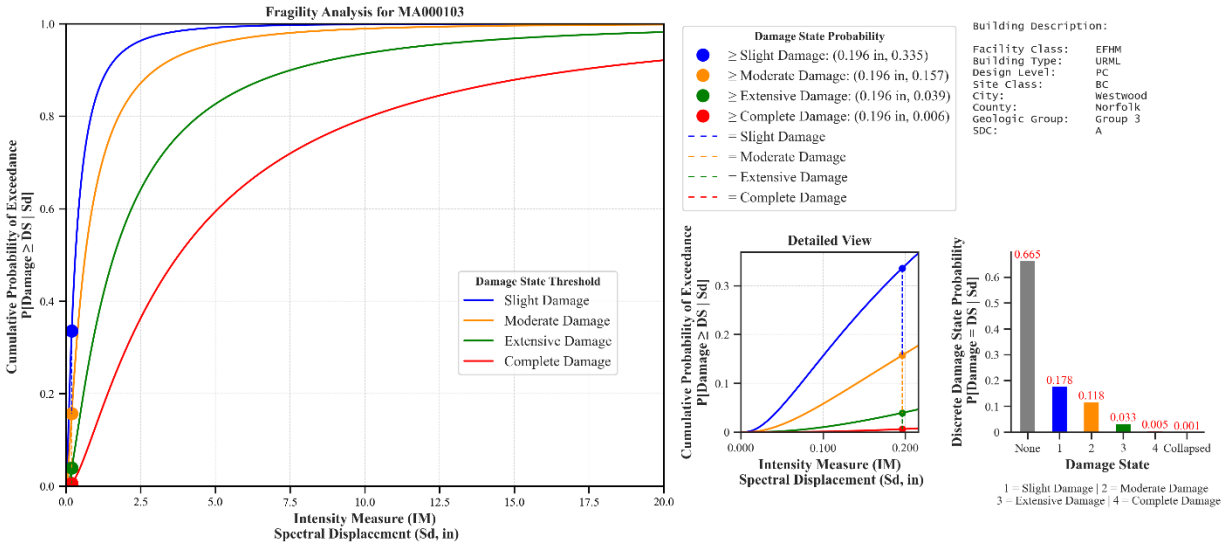
Fragility Analysis for MA000103
Cumulative Probability of Exceedance P[Damage ≥ DS | Sd]
Intensity Measure (IM) Spectral Displacement (Sd, in)
Damage State Threshold
Slight Damage
Moderate Damage
Extensive Damage
Complete Damage
Damage State Probability
≥ Slight Damage: (0.196 in, 0.335)
≥ Moderate Damage: (0.196 in, 0.157)
≥ Extensive Damage: (0.196 in, 0.039)
≥ Complete Damage: (0.196 in, 0.006)
= Slight Damage
= Moderate Damage
= Extensive Damage
= Complete Damage
Detailed View
Discrete Damage State Probability P[Damage = DS | Sd]
0.665
0.178
0.118
0.033
0.005
0.001
None
1
2
3
4 Collapsed
Damage State
1 = Slight Damage | 2 = Moderate Damage
3 = Extensive Damage | 4 = Complete Damage
Building Description:
Facility Class: EFHM
Building Type: URML
Design Level: PC
Site Class: BC
City: Westwood
County: Norfolk
Geologic Group: Group 3
SDC: A

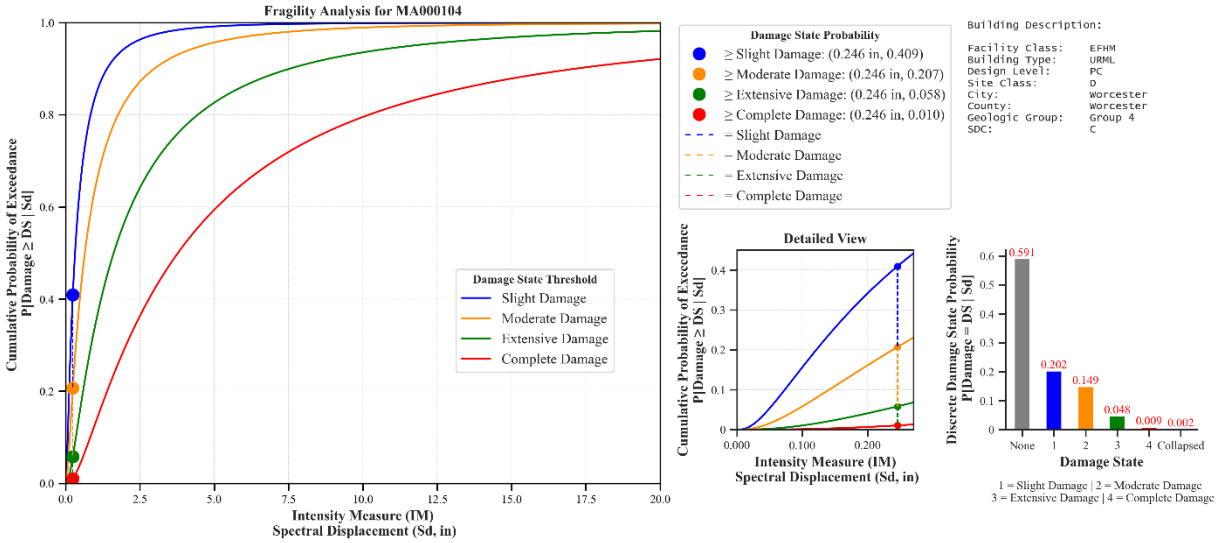
Fragility Analysis for MA000104
Cumulative Probability of Exceedance P[Damage ≥ DS | Sd]
Intensity Measure (IM) Spectral Displacement (Sd, in)
Damage State Threshold
Slight Damage
Moderate Damage
Extensive Damage
Complete Damage
Damage State Probability
≥ Slight Damage: (0.246 in, 0.409)
≥ Moderate Damage: (0.246 in, 0.207)
≥ Extensive Damage: (0.246 in, 0.058)
≥ Complete Damage: (0.246 in, 0.010)
= Slight Damage
= Moderate Damage
= Extensive Damage
= Complete Damage
Detailed View
Discrete Damage State Probability P[Damage = DS | Sd]
0.591
0.202
0.149
0.048
0.009
0.002
None
1
2
3
4 Collapsed
Damage State
1 = Slight Damage | 2 = Moderate Damage
3 = Extensive Damage | 4 = Complete Damage
Building Description:
Facility Class: EFHM
Building Type: URML
Design Level: PC
Site Class: D
City: Worcester
County: Worcester
Geologic Group: Group 4
SDC: C

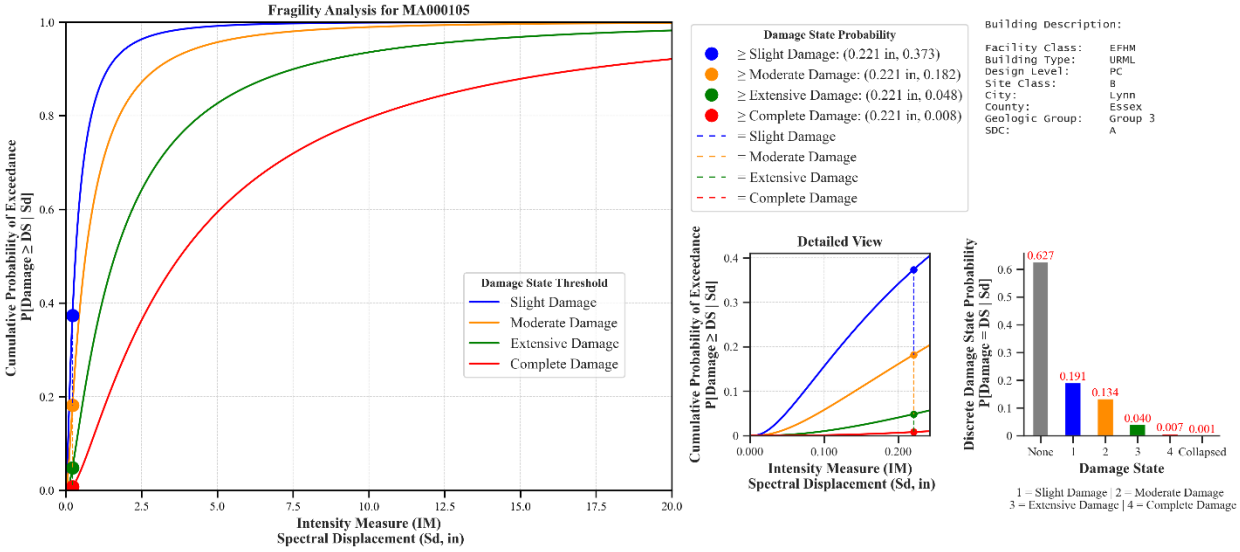
Fragility Analysis for MA000105
Cumulative Probability of Exceedance P[Damage ≥ DS | Sd]
Intensity Measure (IM) Spectral Displacement (Sd, in)
Damage State Threshold
Slight Damage
Moderate Damage
Extensive Damage
Complete Damage
Damage State Probability
≥ Slight Damage: (0.221 in, 0.373)
≥ Moderate Damage: (0.221 in, 0.182)
≥ Extensive Damage: (0.221 in, 0.048)
≥ Complete Damage: (0.221 in, 0.008)
= Slight Damage
= Moderate Damage
= Extensive Damage
= Complete Damage
Building Description:
Facility Class: EFHM
Building Type: URML
Design Level: PC
Site Class: B
City: Lynn
County: Essex
Geologic Group: Group 3
SDC: A
Detailed View
Discrete Damage State Probability P[Damage = DS | Sd]
0.627
0.191
0.134
0.040
0.007
0.001
None
Collapsed
Damage State
1 = Slight Damage | 2 = Moderate Damage
3 = Extensive Damage | 4 = Complete Damage

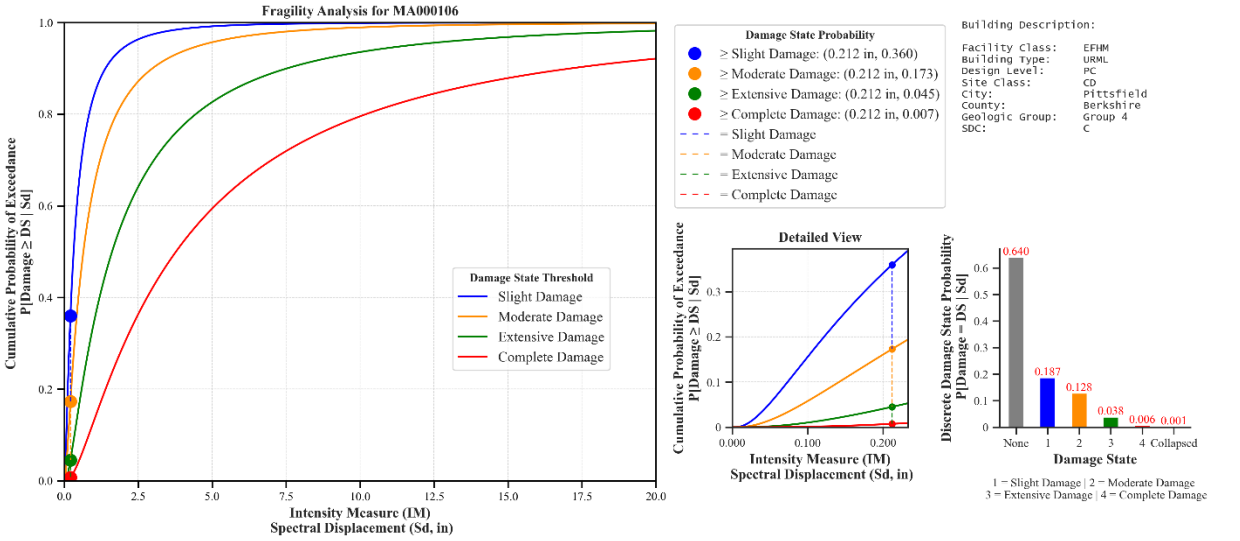
Fragility Analysis for MA000106
Cumulative Probability of Exceedance P[Damage ≥ DS | Sd]
Intensity Measure (IM) Spectral Displacement (Sd, in)
Damage State Threshold
Slight Damage
Moderate Damage
Extensive Damage
Complete Damage
Damage State Probability
≥ Slight Damage: (0.212 in, 0.360)
≥ Moderate Damage: (0.212 in, 0.173)
≥ Extensive Damage: (0.212 in, 0.045)
≥ Complete Damage: (0.212 in, 0.007)
= Slight Damage
= Moderate Damage
= Extensive Damage
= Complete Damage
Building Description:
Facility Class: EFHM
Building Type: URML
Design Level: PC
Site Class: CD
City: Pittsfield
County: Berkshire
Geologic Group: Group 4
SDC: C
Detailed View
Discrete Damage State Probability P[Damage = DS | Sd]
0.640
0.187
0.128
0.038
0.006
0.001
None
Collapsed
Damage State
1 = Slight Damage | 2 = Moderate Damage
3 = Extensive Damage | 4 = Complete Damage

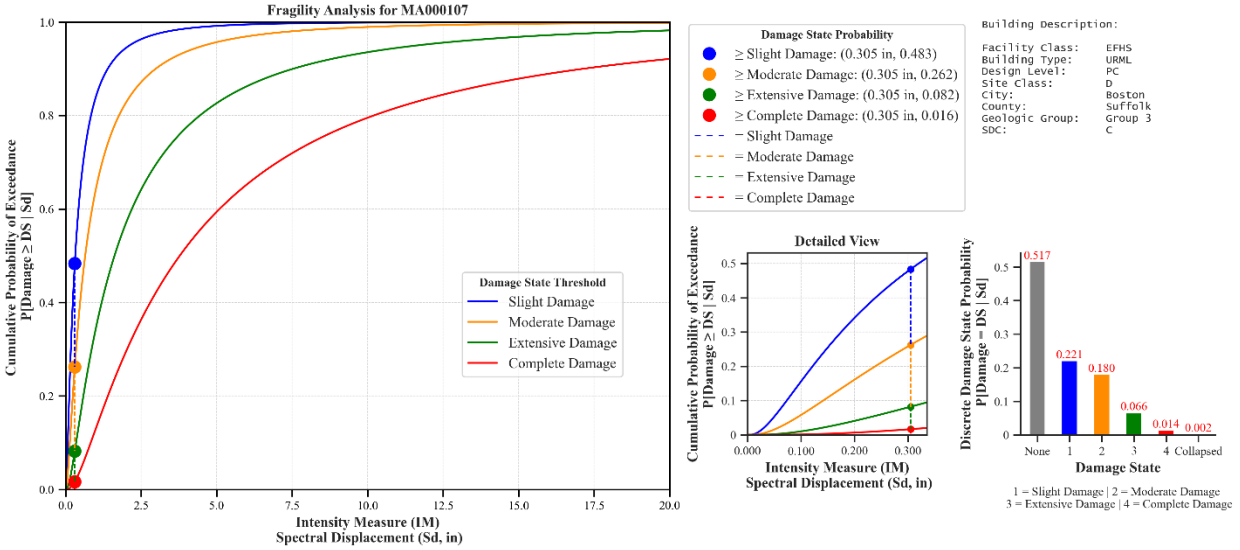
Fragility Analysis for MA000107
Cumulative Probability of Exceedance P[Damage ≥ DS | Sd]
Intensity Measure (IM) Spectral Displacement (Sd, in)
Damage State Threshold
Slight Damage
Moderate Damage
Extensive Damage
Complete Damage
Damage State Probability
≥ Slight Damage: (0.305 in, 0.483)
≥ Moderate Damage: (0.305 in, 0.262)
≥ Extensive Damage: (0.305 in, 0.082)
≥ Complete Damage: (0.305 in, 0.016)
= Slight Damage
= Moderate Damage
= Extensive Damage
= Complete Damage
Building Description:
Facility Class: EFHS
Building Type: URML
Design Level: PC
Site Class: D
City: Boston
County: Suffolk
Geologic Group: Group 3
SDC: C
Detailed View
Discrete Damage State Probability P[Damage = DS | Sd]
0.517
0.221
0.180
0.066
0.014
0.002
None
Collapsed
Damage State
1 = Slight Damage | 2 = Moderate Damage
3 = Extensive Damage | 4 = Complete Damage

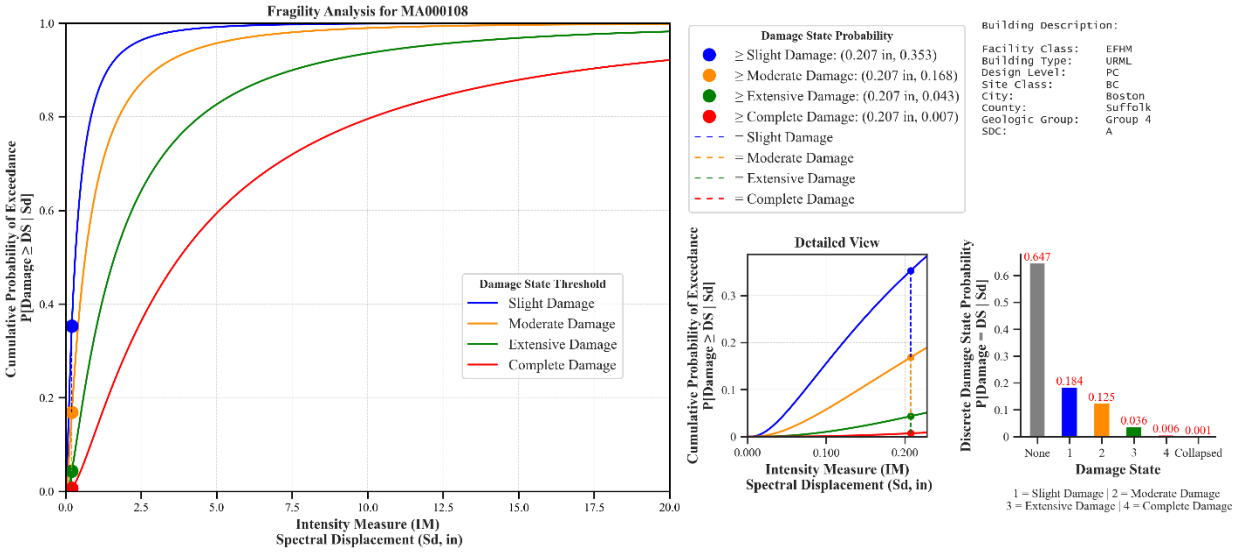
Fragility Analysis for MA000108
Cumulative Probability of Exceedance P[Damage ≥ DS | Sd]
Intensity Measure (IM) Spectral Displacement (Sd, in)
Damage State Threshold
Slight Damage
Moderate Damage
Extensive Damage
Complete Damage
Damage State Probability
≥ Slight Damage: (0.207 in, 0.353)
≥ Moderate Damage: (0.207 in, 0.168)
≥ Extensive Damage: (0.207 in, 0.043)
≥ Complete Damage: (0.207 in, 0.007)
= Slight Damage
= Moderate Damage
= Extensive Damage
= Complete Damage
Detailed View
Building Description:
Facility Class: EFHM
Building Type: URML
Design Level: PC
Site Class: BC
City: Boston
County: Suffolk
Geologic Group: Group 4
SDC: A
Discrete Damage State Probability P[Damage = DS | Sd]
0.647
0.184
0.125
0.036
0.006
0.001
None
Collapsed
Damage State
1 = Slight Damage | 2 = Moderate Damage
3 = Extensive Damage | 4 = Complete Damage

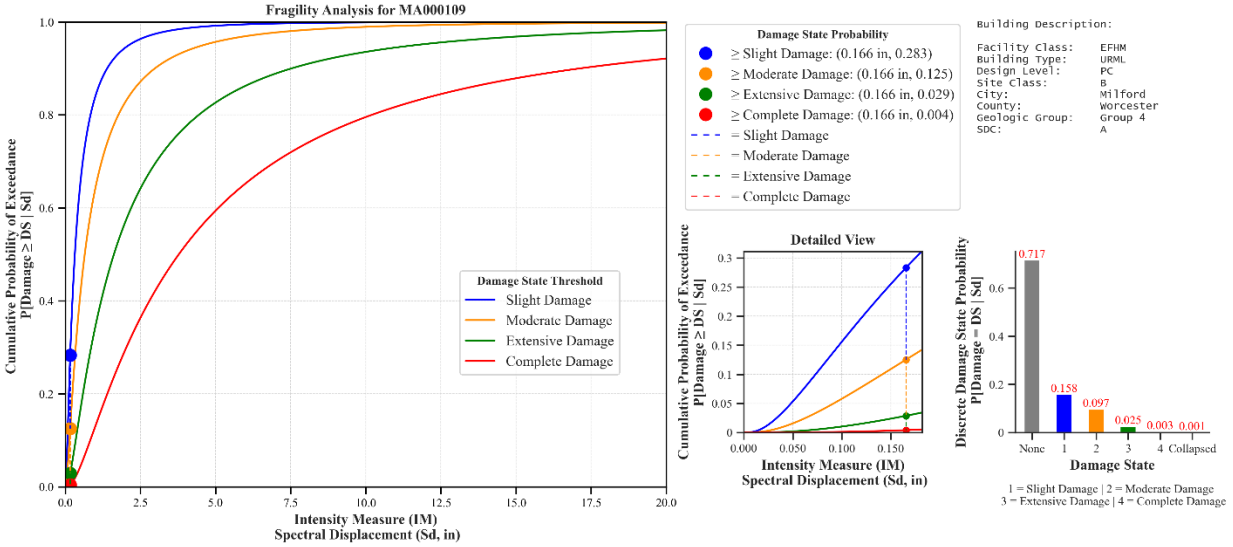
Fragility Analysis for MA000109
Cumulative Probability of Exceedance P[Damage ≥ DS | Sd]
Intensity Measure (IM) Spectral Displacement (Sd, in)
Damage State Threshold
Slight Damage
Moderate Damage
Extensive Damage
Complete Damage
Damage State Probability
≥ Slight Damage: (0.166 in, 0.283)
≥ Moderate Damage: (0.166 in, 0.125)
≥ Extensive Damage: (0.166 in, 0.029)
≥ Complete Damage: (0.166 in, 0.004)
= Slight Damage
= Moderate Damage
= Extensive Damage
= Complete Damage
Detailed View
Building Description:
Facility Class: EFHM
Building Type: URML
Design Level: PC
Site Class: B
City: Milford
County: Worcester
Geologic Group: Group 4
SDC: A
Discrete Damage State Probability P[Damage = DS | Sd]
0.717
0.158
0.097
0.025
0.003
0.001
None
Collapsed
Damage State
1 = Slight Damage | 2 = Moderate Damage
3 = Extensive Damage | 4 = Complete Damage

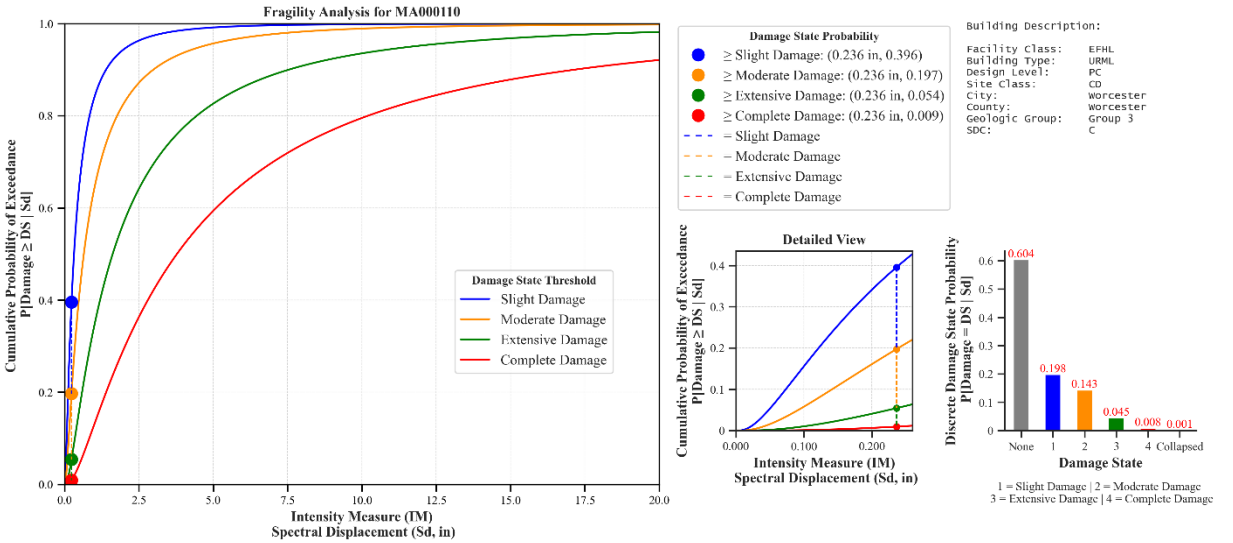
Fragility Analysis for MA000110
Cumulative Probability of Exceedance P[Damage ≥ DS | Sd]
Intensity Measure (IM) Spectral Displacement (Sd, in)
Damage State Threshold
Slight Damage
Moderate Damage
Extensive Damage
Complete Damage
Damage State Probability
≥ Slight Damage: (0.236 in, 0.396)
≥ Moderate Damage: (0.236 in, 0.197)
≥ Extensive Damage: (0.236 in, 0.054)
≥ Complete Damage: (0.236 in, 0.009)
= Slight Damage
= Moderate Damage
= Extensive Damage
= Complete Damage
Detailed View
Building Description:
Facility Class: EFHL
Building Type: URML
Design Level: PC
Site Class: CD
City: Worcester
County: Worcester
Geologic Group: Group 3
SDC: C
Discrete Damage State Probability P[Damage = DS | Sd]
0.604
0.198
0.143
0.045
0.008
0.001
None
Collapsed
Damage State
1 = Slight Damage | 2 = Moderate Damage
3 = Extensive Damage | 4 = Complete Damage

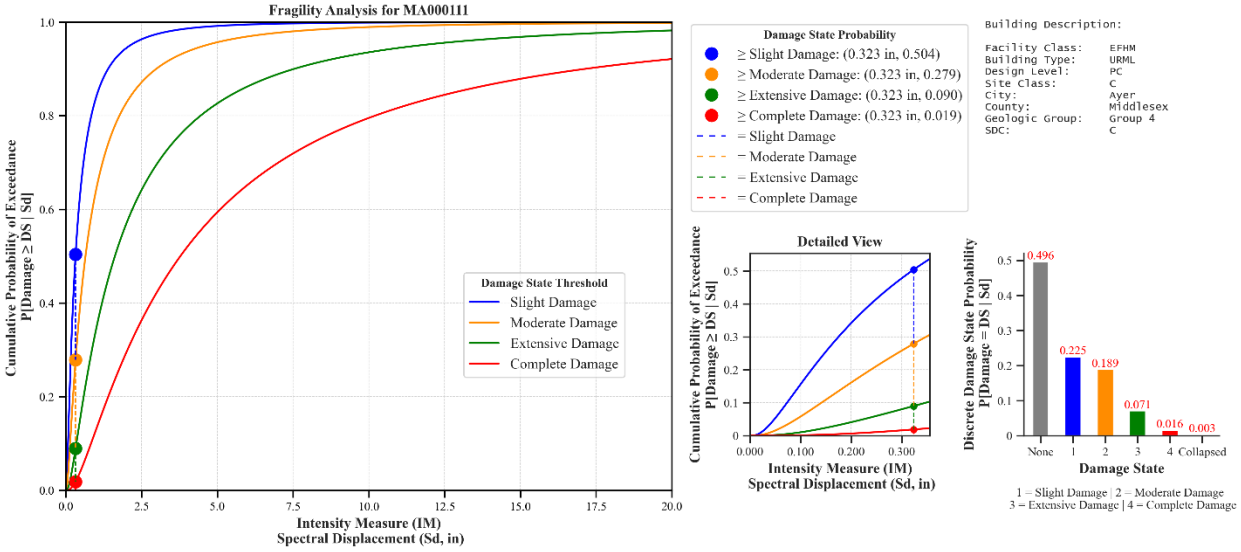
Fragility Analysis for MA000111
Cumulative Probability of Exceedance P[Damage ≥ DS | Sd]
Intensity Measure (IM) Spectral Displacement (Sd, in)
Damage State Threshold
Slight Damage
Moderate Damage
Extensive Damage
Complete Damage
Damage State Probability
≥ Slight Damage: (0.323 in, 0.504)
≥ Moderate Damage: (0.323 in, 0.279)
≥ Extensive Damage: (0.323 in, 0.090)
≥ Complete Damage: (0.323 in, 0.019)
= Slight Damage
= Moderate Damage
= Extensive Damage
= Complete Damage
Building Description:
Facility Class: EFHM
Building Type: URML
Design Level: PC
Site Class: C
City: Ayer
County: Middlesex
Geologic Group: Group 4
SDC: C
Detailed View
Discrete Damage State Probability P[Damage = DS | Sd]
0.496
0.225
0.189
0.071
0.016
0.003
None
1
2
3
4
Collapsed
Damage State
1 = Slight Damage | 2 = Moderate Damage
3 = Extensive Damage | 4 = Complete Damage

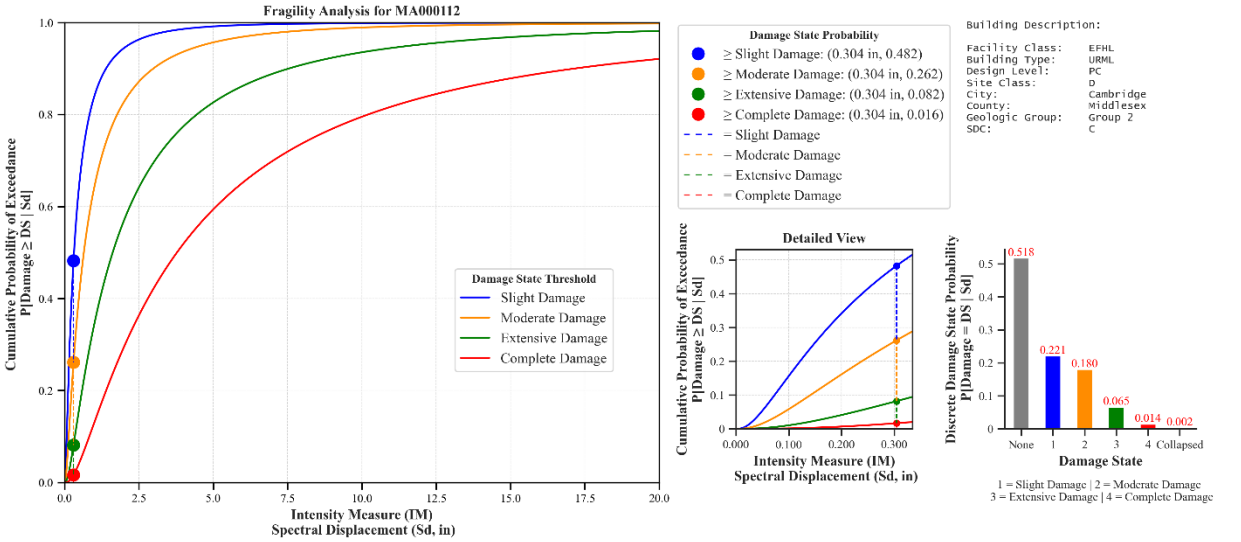
Fragility Analysis for MA000112
Cumulative Probability of Exceedance P[Damage ≥ DS | Sd]
Intensity Measure (IM) Spectral Displacement (Sd, in)
Damage State Threshold
Slight Damage
Moderate Damage
Extensive Damage
Complete Damage
Damage State Probability
≥ Slight Damage: (0.304 in, 0.482)
≥ Moderate Damage: (0.304 in, 0.262)
≥ Extensive Damage: (0.304 in, 0.082)
≥ Complete Damage: (0.304 in, 0.016)
= Slight Damage
= Moderate Damage
= Extensive Damage
= Complete Damage
Building Description:
Facility Class: EFHL
Building Type: URML
Design Level: PC
Site Class: D
City: Cambridge
County: Middlesex
Geologic Group: Group 2
SDC: C
Detailed View
Discrete Damage State Probability P[Damage = DS | Sd]
0.518
0.221
0.180
0.065
0.014
0.002
None
1
2
3
4
Collapsed
Damage State
1 = Slight Damage | 2 = Moderate Damage
3 = Extensive Damage | 4 = Complete Damage

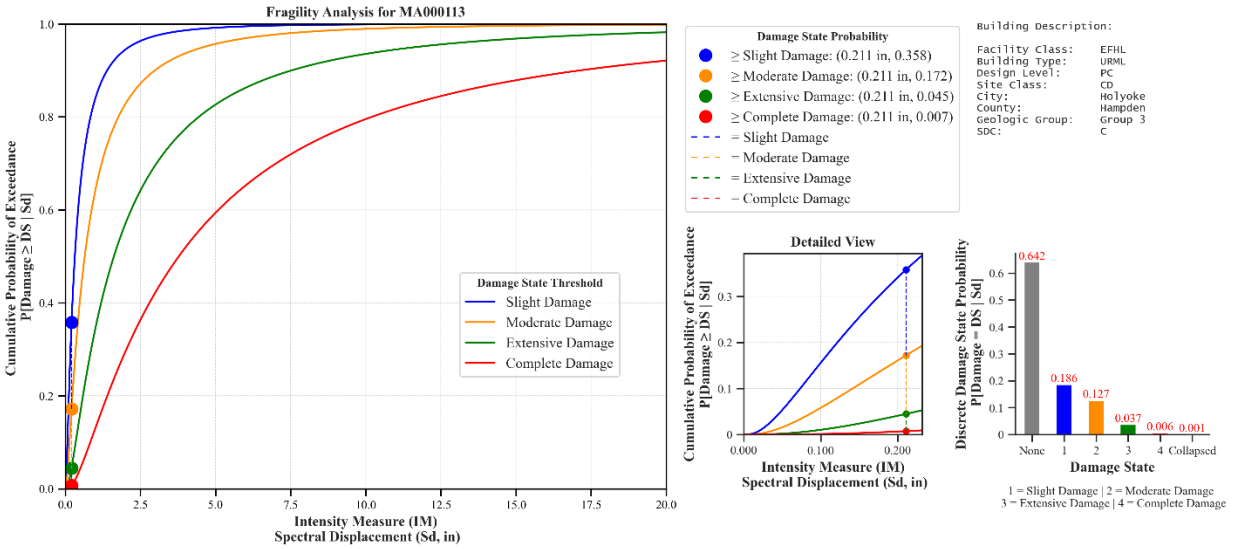
Fragility Analysis for MA000113
Cumulative Probability of Exceedance P[Damage ≥ DS | Sd]
Intensity Measure (IM) Spectral Displacement (Sd, in)
Damage State Threshold
Slight Damage
Moderate Damage
Extensive Damage
Complete Damage
Damage State Probability
≥ Slight Damage: (0.211 in, 0.358)
≥ Moderate Damage: (0.211 in, 0.172)
≥ Extensive Damage: (0.211 in, 0.045)
≥ Complete Damage: (0.211 in, 0.007)
= Slight Damage
= Moderate Damage
= Extensive Damage
= Complete Damage
Building Description:
Facility Class: EFHL
Building Type: URML
Design Level: PC
Site Class: CD
City: Holyoke
County: Hampden
Geologic Group: Group 3
SDC: C
Detailed View
Discrete Damage State Probability P[Damage = DS | Sd]
0.642
0.186
0.127
0.037
0.006
0.001
None
1
2
3
4
Collapsed
Damage State
1 = Slight Damage | 2 = Moderate Damage
3 = Extensive Damage | 4 = Complete Damage

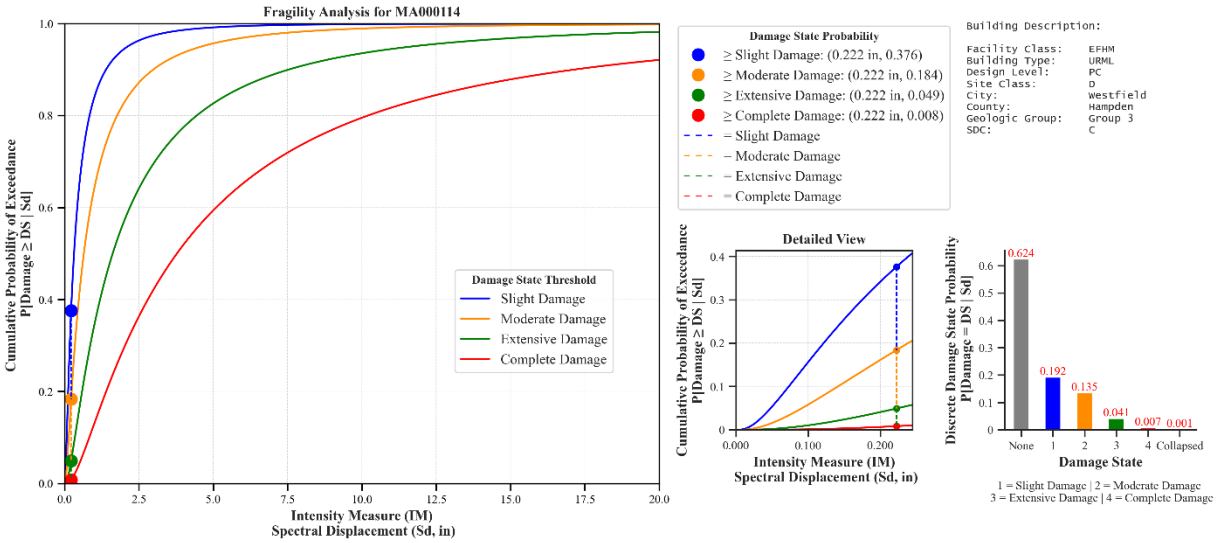
Fragility Analysis for MA000114
Cumulative Probability of Exceedance P[Damage ≥ DS | Sd]
Intensity Measure (IM) Spectral Displacement (Sd, in)
Damage State Threshold
Slight Damage
Moderate Damage
Extensive Damage
Complete Damage
Damage State Probability
≥ Slight Damage: (0.222 in, 0.376)
≥ Moderate Damage: (0.222 in, 0.184)
≥ Extensive Damage: (0.222 in, 0.049)
≥ Complete Damage: (0.222 in, 0.008)
Detailed View
Discrete Damage State Probability P[Damage = DS | Sd]
0.624
0.192
0.135
0.041
0.007
0.001
None
Collapsed
Damage State
1 = Slight Damage | 2 = Moderate Damage
3 = Extensive Damage | 4 = Complete Damage
Building Description:
Facility Class: EFHM
Building Type: URML
Design Level: PC
Site Class: D
City: Westfield
County: Hampden
Geologic Group: Group 3
SDC: C

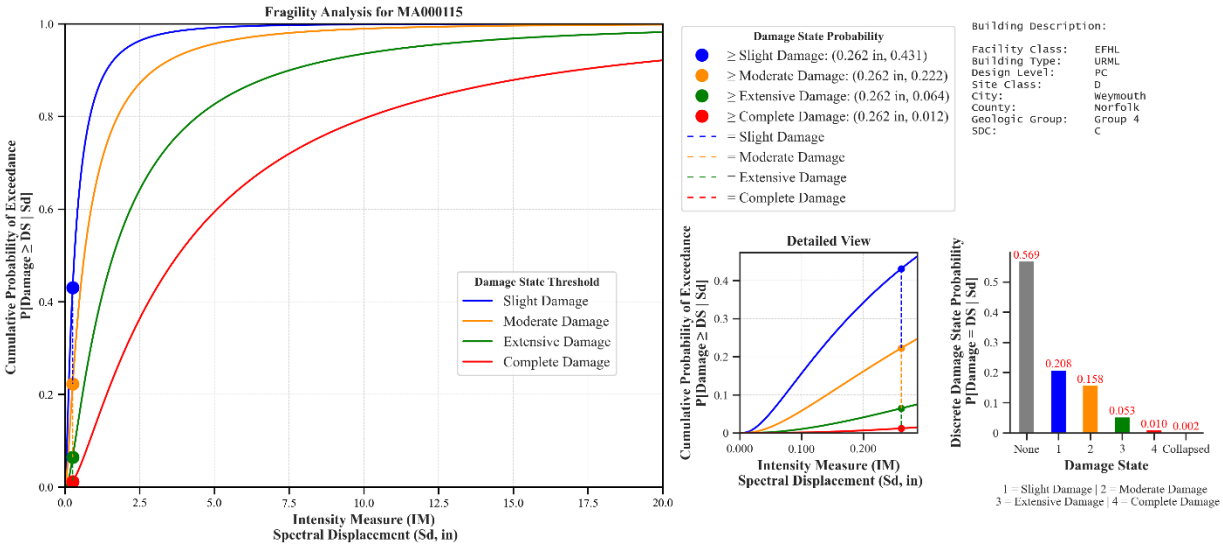
Fragility Analysis for MA000115
Cumulative Probability of Exceedance P[Damage ≥ DS | Sd]
Intensity Measure (IM) Spectral Displacement (Sd, in)
Damage State Threshold
Slight Damage
Moderate Damage
Extensive Damage
Complete Damage
Damage State Probability
≥ Slight Damage: (0.262 in, 0.431)
≥ Moderate Damage: (0.262 in, 0.222)
≥ Extensive Damage: (0.262 in, 0.064)
≥ Complete Damage: (0.262 in, 0.012)
Detailed View
Discrete Damage State Probability P[Damage = DS | Sd]
0.569
0.208
0.158
0.053
0.010
0.002
None
Collapsed
Damage State
1 = Slight Damage | 2 = Moderate Damage
3 = Extensive Damage | 4 = Complete Damage
Building Description:
Facility Class: EFHL
Building Type: URML
Design Level: PC
Site Class: D
City: Weymouth
County: Norfolk
Geologic Group: Group 4
SDC: C

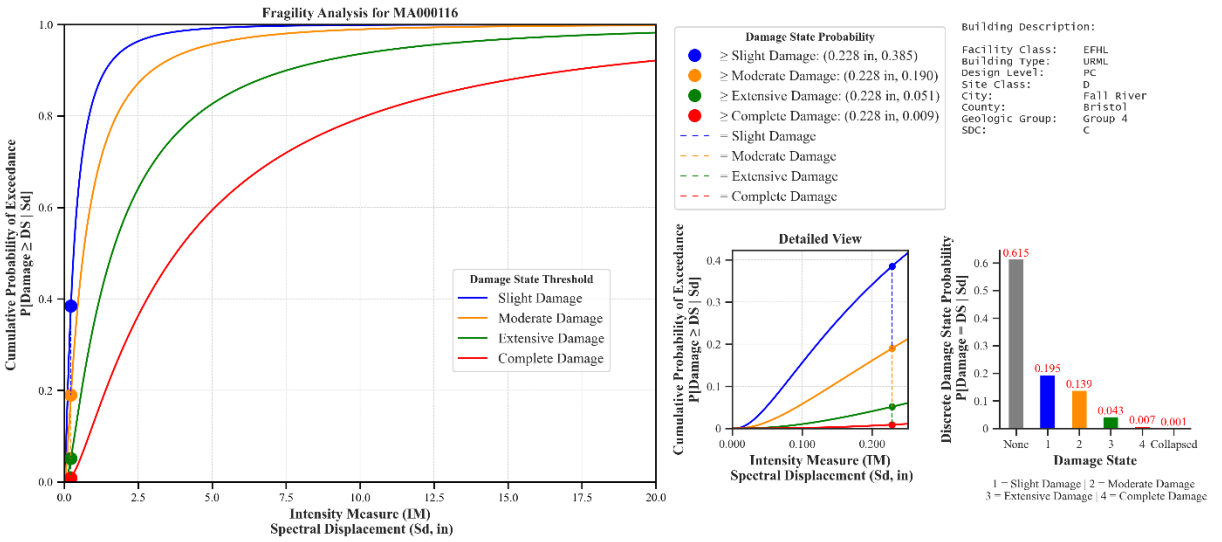
Fragility Analysis for MA000116
Cumulative Probability of Exceedance P[Damage ≥ DS | Sd]
Intensity Measure (IM) Spectral Displacement (Sd, in)
Damage State Threshold
Slight Damage
Moderate Damage
Extensive Damage
Complete Damage
Damage State Probability
≥ Slight Damage: (0.228 in, 0.385)
≥ Moderate Damage: (0.228 in, 0.190)
≥ Extensive Damage: (0.228 in, 0.051)
≥ Complete Damage: (0.228 in, 0.009)
Detailed View
Discrete Damage State Probability P[Damage = DS | Sd]
0.615
0.195
0.139
0.043
0.007
0.001
None
Collapsed
Damage State
1 = Slight Damage | 2 = Moderate Damage
3 = Extensive Damage | 4 = Complete Damage
Building Description:
Facility Class: EFHL
Building Type: URML
Design Level: PC
Site Class: D
City: Fall River
County: Bristol
Geologic Group: Group 4
SDC: C

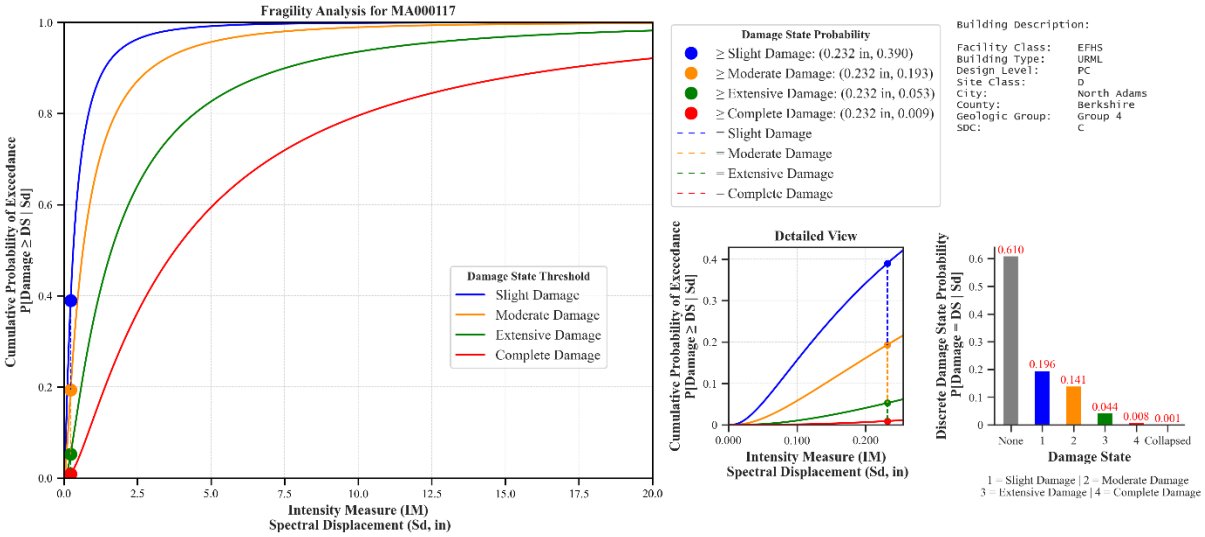
Fragility Analysis for MA000117
Cumulative Probability of Exceedance P[Damage ≥ DS | Sd]
Intensity Measure (IM) Spectral Displacement (Sd, in)
Damage State Threshold
Slight Damage
Moderate Damage
Extensive Damage
Complete Damage
Damage State Probability
≥ Slight Damage: (0.232 in, 0.390)
≥ Moderate Damage: (0.232 in, 0.193)
≥ Extensive Damage: (0.232 in, 0.053)
≥ Complete Damage: (0.232 in, 0.009)
Detailed View
Discrete Damage State Probability P[Damage = DS | Sd]
0.610
0.196
0.141
0.044
0.008
0.001
None 1 2 3 4 Collapsed
Damage State
1 = Slight Damage | 2 = Moderate Damage
3 = Extensive Damage | 4 = Complete Damage
Building Description:
Facility Class: EFHS
Building Type: URML
Design Level: PC
Site Class: D
City: North Adams
County: Berkshire
Geologic Group: Group 4
SDC: C

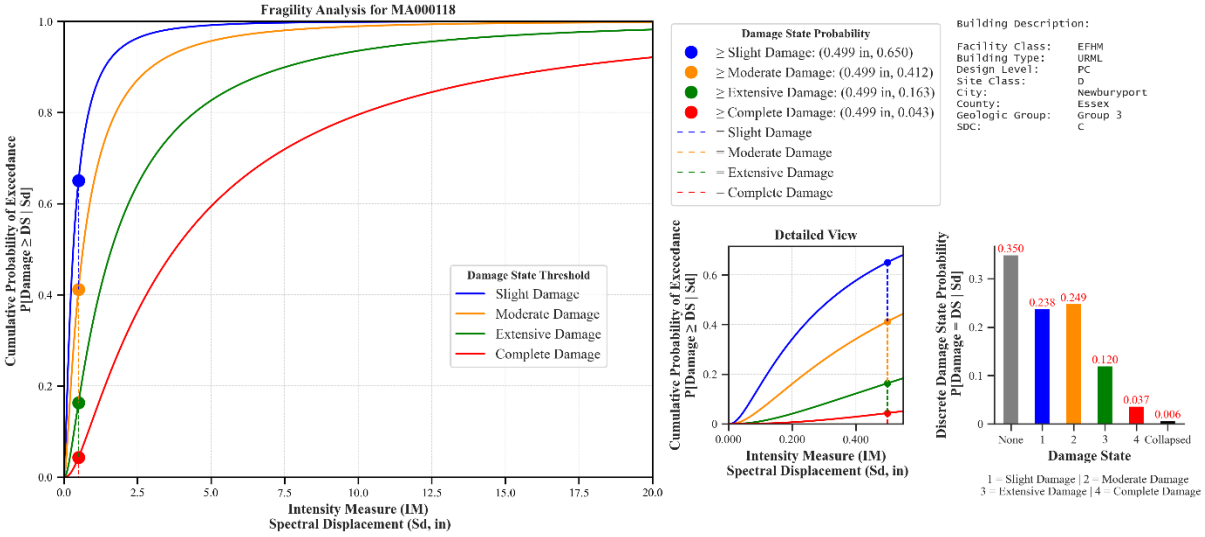
Fragility Analysis for MA000118
Cumulative Probability of Exceedance P[Damage ≥ DS | Sd]
Intensity Measure (IM) Spectral Displacement (Sd, in)
Damage State Threshold
Slight Damage
Moderate Damage
Extensive Damage
Complete Damage
Damage State Probability
≥ Slight Damage: (0.499 in, 0.650)
≥ Moderate Damage: (0.499 in, 0.412)
≥ Extensive Damage: (0.499 in, 0.163)
≥ Complete Damage: (0.499 in, 0.043)
Detailed View
Discrete Damage State Probability P[Damage = DS | Sd]
0.350
0.238
0.249
0.120
0.037
0.006
None 1 2 3 4 Collapsed
Damage State
1 = Slight Damage | 2 = Moderate Damage
3 = Extensive Damage | 4 = Complete Damage
Building Description:
Facility Class: EFHM
Building Type: URML
Design Level: PC
Site Class: D
City: Newburyport
County: Essex
Geologic Group: Group 3
SDC: C

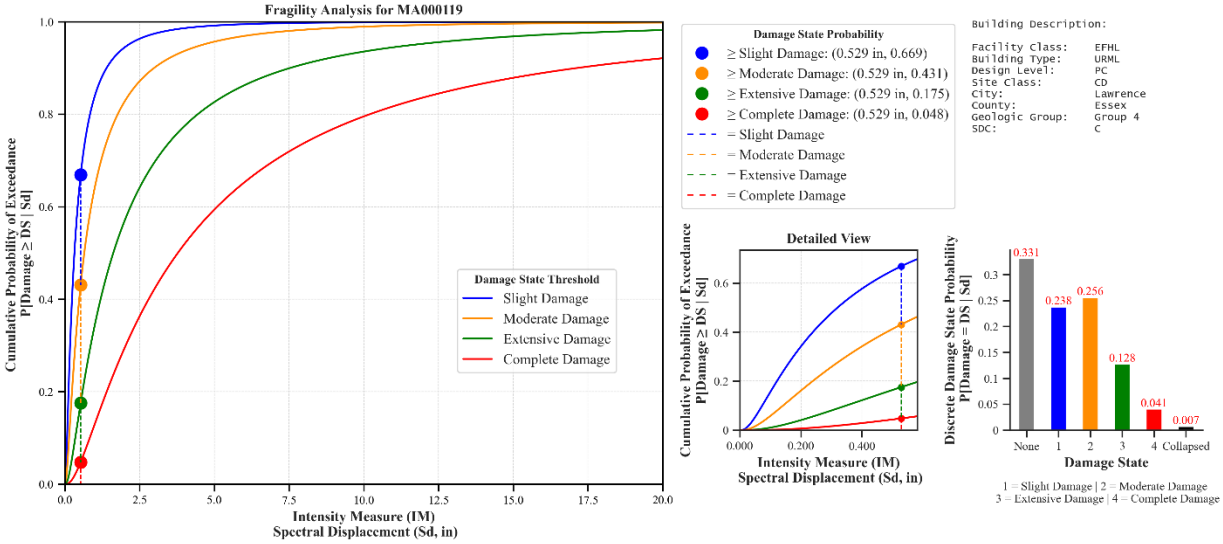
Fragility Analysis for MA000119
Cumulative Probability of Exceedance P[Damage ≥ DS | Sd]
Intensity Measure (IM) Spectral Displacement (Sd, in)
Damage State Threshold
Slight Damage
Moderate Damage
Extensive Damage
Complete Damage
Damage State Probability
≥ Slight Damage: (0.529 in, 0.669)
≥ Moderate Damage: (0.529 in, 0.431)
≥ Extensive Damage: (0.529 in, 0.175)
≥ Complete Damage: (0.529 in, 0.048)
Detailed View
Discrete Damage State Probability P[Damage = DS | Sd]
0.331
0.238
0.256
0.128
0.041
0.007
None 1 2 3 4 Collapsed
Damage State
1 = Slight Damage | 2 = Moderate Damage
3 = Extensive Damage | 4 = Complete Damage
Building Description:
Facility Class: EFHL
Building Type: URML
Design Level: PC
Site Class: CD
City: Lawrence
County: Essex
Geologic Group: Group 4
SDC: C

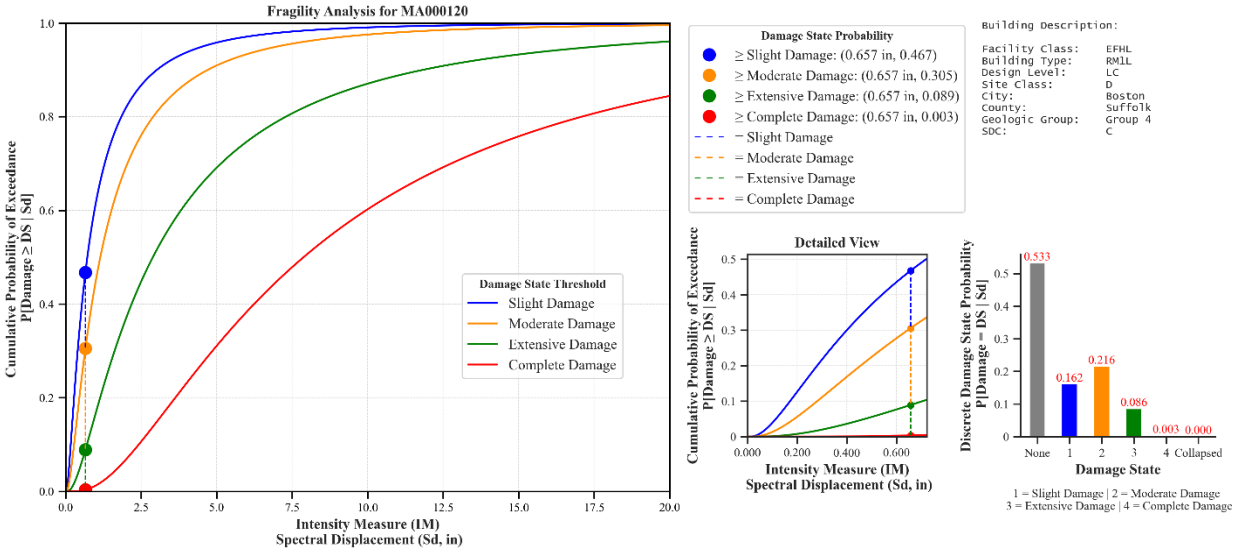
Fragility Analysis for MA000120
Cumulative Probability of Exceedance
P[Damage ≥ DS | Sd]
Intensity Measure (IM)
Spectral Displacement (Sd, in)
Damage State Threshold
Slight Damage
Moderate Damage
Extensive Damage
Complete Damage
Damage State Probability
≥ Slight Damage: (0.657 in, 0.467)
≥ Moderate Damage: (0.657 in, 0.305)
≥ Extensive Damage: (0.657 in, 0.089)
≥ Complete Damage: (0.657 in, 0.003)
= Slight Damage
= Moderate Damage
= Extensive Damage
= Complete Damage
Dctailed View
Discrete Damage State Probability
P[Damage = DS | Sd]
0.533
0.162
0.216
0.086
0.003
0.000
None
1
2
3
4
Collapsed
Damage State
1 = Slight Damage | 2 = Moderate Damage
3 = Extensive Damage | 4 = Complete Damage
Building Description:
Facility Class: EFHL
Building Type: RM1L
Design Level: LC
Site Class: D
City: Boston
County: Suffolk
Geologic Group: Group 4
SDC: C

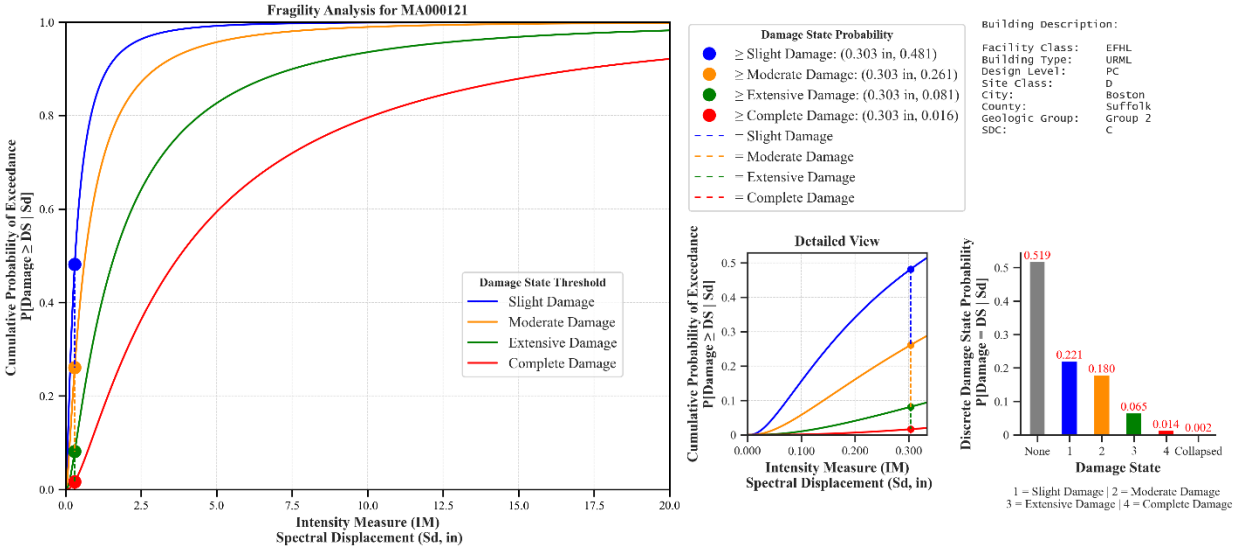
Fragility Analysis for MA000121
Cumulative Probability of Exceedance
P[Damage ≥ DS | Sd]
Intensity Measure (IM)
Spectral Displacement (Sd, in)
Damage State Threshold
Slight Damage
Moderate Damage
Extensive Damage
Complete Damage
Damage State Probability
≥ Slight Damage: (0.303 in, 0.481)
≥ Moderate Damage: (0.303 in, 0.261)
≥ Extensive Damage: (0.303 in, 0.081)
≥ Complete Damage: (0.303 in, 0.016)
= Slight Damage
= Moderate Damage
= Extensive Damage
= Complete Damage
Dctailed View
Discrete Damage State Probability
P[Damage = DS | Sd]
0.519
0.221
0.180
0.065
0.014
0.002
None
1
2
3
4
Collapsed
Damage State
1 = Slight Damage | 2 = Moderate Damage
3 = Extensive Damage | 4 = Complete Damage
Building Description:
Facility Class: EFHL
Building Type: URML
Design Level: PC
Site Class: D
City: Boston
County: Suffolk
Geologic Group: Group 2
SDC: C

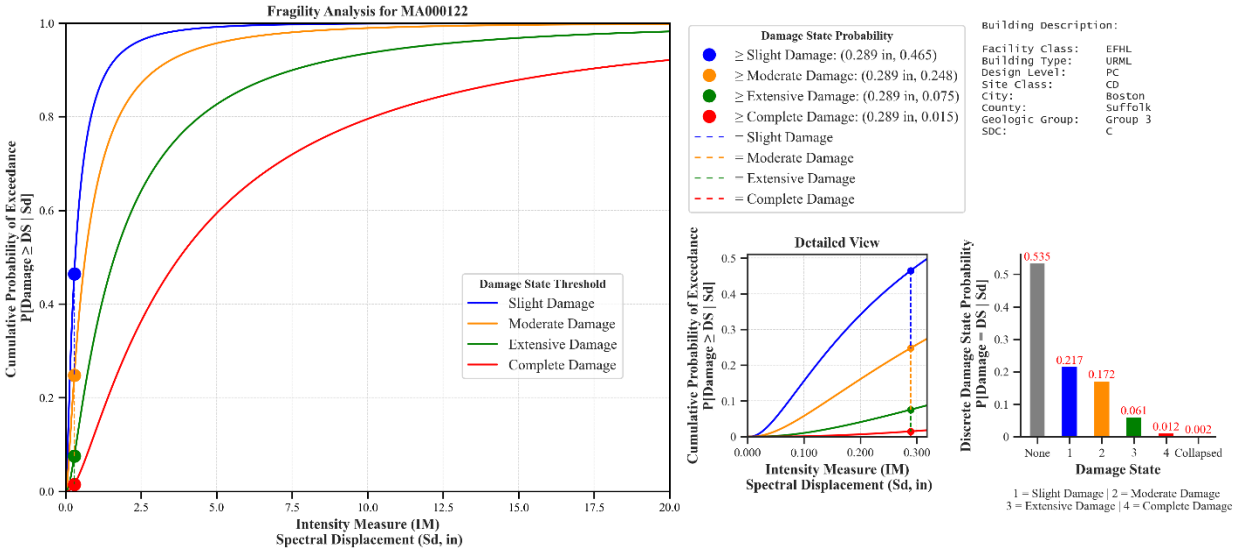
Fragility Analysis for MA000122
Cumulative Probability of Exceedance
P[Damage ≥ DS | Sd]
Intensity Measure (IM)
Spectral Displacement (Sd, in)
Damage State Threshold
Slight Damage
Moderate Damage
Extensive Damage
Complete Damage
Damage State Probability
≥ Slight Damage: (0.289 in, 0.465)
≥ Moderate Damage: (0.289 in, 0.248)
≥ Extensive Damage: (0.289 in, 0.075)
≥ Complete Damage: (0.289 in, 0.015)
= Slight Damage
= Moderate Damage
= Extensive Damage
= Complete Damage
Dctailed View
Discrete Damage State Probability
P[Damage = DS | Sd]
0.535
0.217
0.172
0.061
0.012
0.002
None
1
2
3
4
Collapsed
Damage State
1 = Slight Damage | 2 = Moderate Damage
3 = Extensive Damage | 4 = Complete Damage
Building Description:
Facility Class: EFHL
Building Type: URML
Design Level: PC
Site Class: CD
City: Boston
County: Suffolk
Geologic Group: Group 3
SDC: C

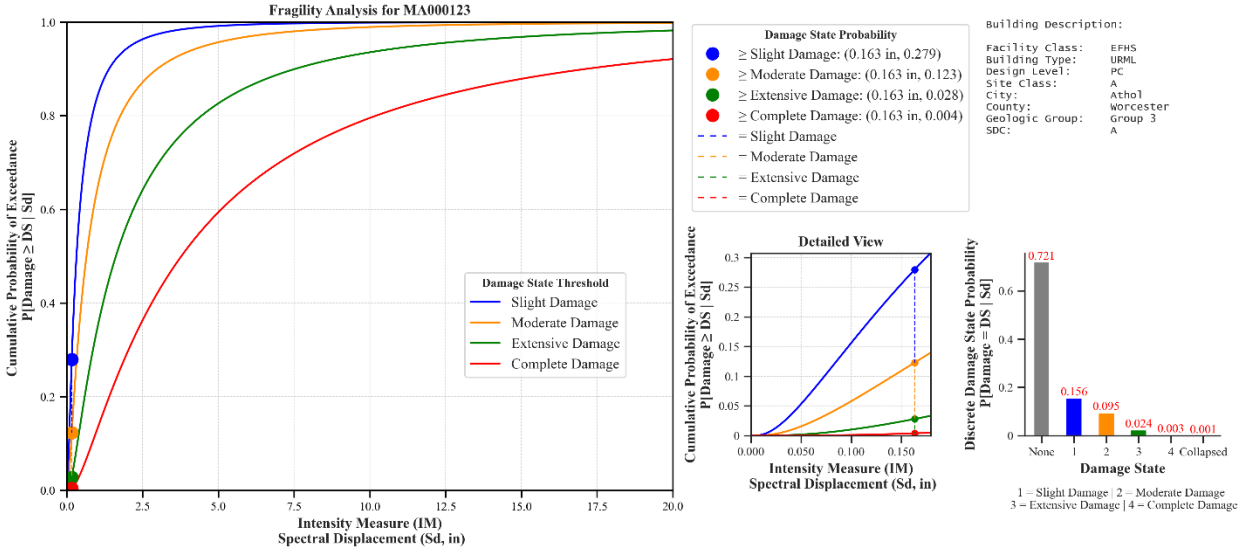
Fragility Analysis for MA000123
Cumulative Probability of Exceedance
P[Damage ≥ DS | Sd]
Intensity Measure (IM)
Spectral Displacement (Sd, in)
Damage State Threshold
Slight Damage
Moderate Damage
Extensive Damage
Complete Damage
Damage State Probability
≥ Slight Damage: (0.163 in, 0.279)
≥ Moderate Damage: (0.163 in, 0.123)
≥ Extensive Damage: (0.163 in, 0.028)
≥ Complete Damage: (0.163 in, 0.004)
= Slight Damage
= Moderate Damage
= Extensive Damage
= Complete Damage
Building Description:
Facility Class: EFHS
Building Type: URML
Design Level: PC
Site Class: A
City: Athol
County: Worcester
Geologic Group: Group 3
SDC: A
Detailed View
Discrete Damage State Probability
P[Damage = DS | Sd]
0.721
0.156
0.095
0.024
0.003
0.001
None
1
2
3
4
Collapsed
Damage State
1 = Slight Damage | 2 = Moderate Damage
3 = Extensive Damage | 4 = Complete Damage

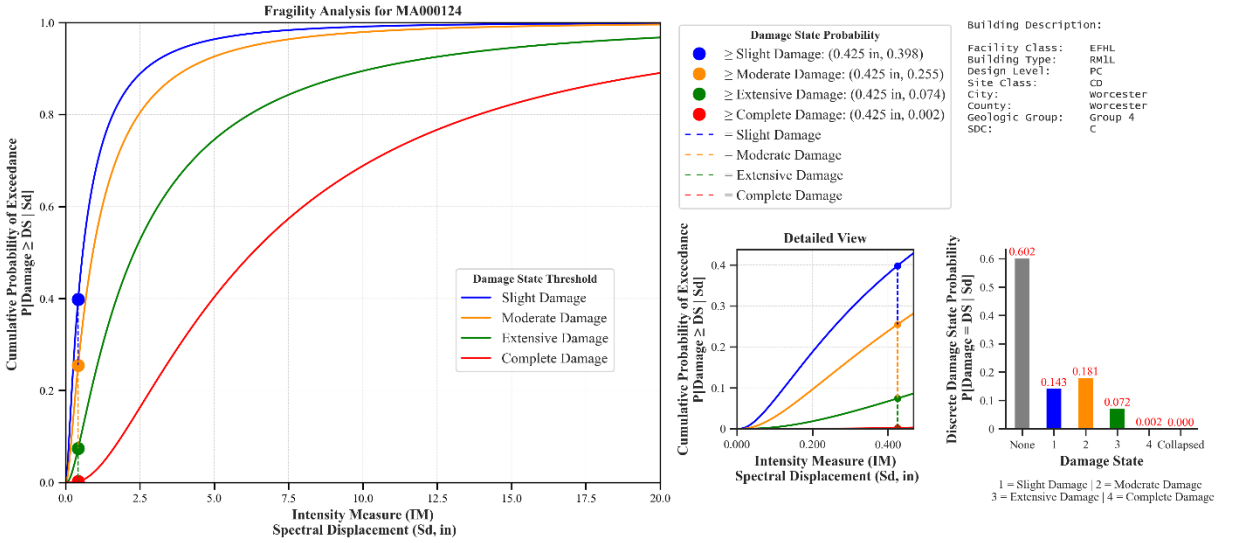
Fragility Analysis for MA000124
Cumulative Probability of Exceedance
P[Damage ≥ DS | Sd]
Intensity Measure (IM)
Spectral Displacement (Sd, in)
Damage State Threshold
Slight Damage
Moderate Damage
Extensive Damage
Complete Damage
Damage State Probability
≥ Slight Damage: (0.425 in, 0.398)
≥ Moderate Damage: (0.425 in, 0.255)
≥ Extensive Damage: (0.425 in, 0.074)
≥ Complete Damage: (0.425 in, 0.002)
= Slight Damage
= Moderate Damage
= Extensive Damage
= Complete Damage
Building Description:
Facility Class: EFHL
Building Type: RMLL
Design Level: PC
Site Class: CD
City: Worcester
County: Worcester
Geologic Group: Group 4
SDC: C
Detailed View
Discrete Damage State Probability
P[Damage = DS | Sd]
0.602
0.143
0.181
0.072
0.002
0.000
None
1
2
3
4
Collapsed
Damage State
1 = Slight Damage | 2 = Moderate Damage
3 = Extensive Damage | 4 = Complete Damage

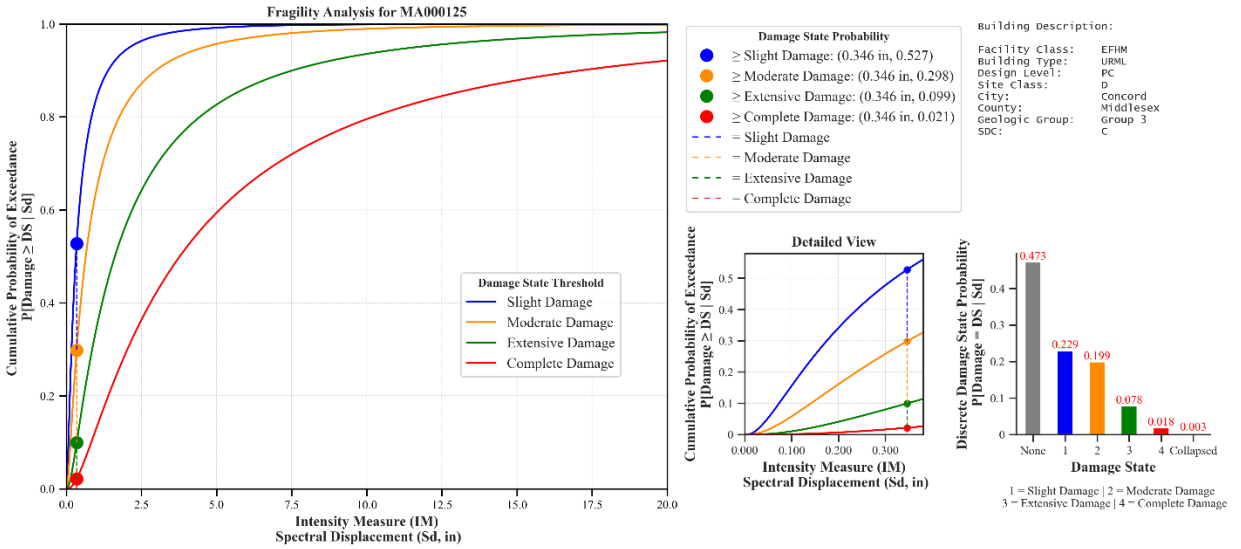
Fragility Analysis for MA000125
Cumulative Probability of Exceedance
P[Damage ≥ DS | Sd]
Intensity Measure (IM)
Spectral Displacement (Sd, in)
Damage State Threshold
Slight Damage
Moderate Damage
Extensive Damage
Complete Damage
Damage State Probability
≥ Slight Damage: (0.346 in, 0.527)
≥ Moderate Damage: (0.346 in, 0.298)
≥ Extensive Damage: (0.346 in, 0.099)
≥ Complete Damage: (0.346 in, 0.021)
= Slight Damage
= Moderate Damage
= Extensive Damage
= Complete Damage
Building Description:
Facility Class: EFHM
Building Type: URML
Design Level: PC
Site Class: D
City: Concord
County: Middlesex
Geologic Group: Group 3
SDC: C
Detailed View
Discrete Damage State Probability
P[Damage = DS | Sd]
0.473
0.229
0.199
0.078
0.018
0.003
None
1
2
3
4
Collapsed
Damage State
1 = Slight Damage | 2 = Moderate Damage
3 = Extensive Damage | 4 = Complete Damage

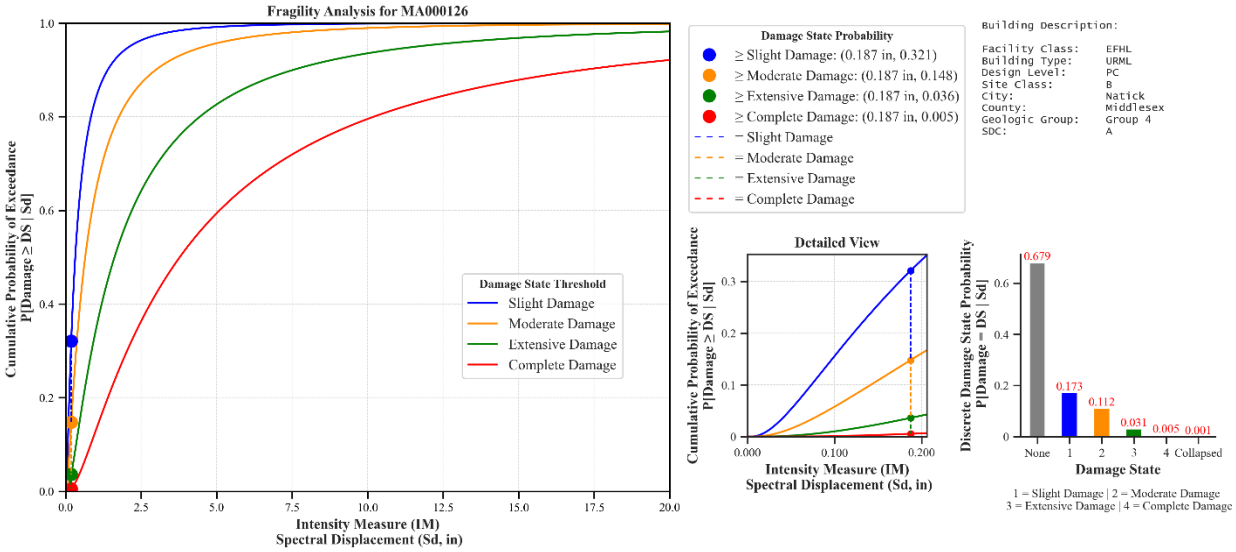
Fragility Analysis for MA000126
Cumulative Probability of Exceedance P[Damage ≥ DS | Sd]
Intensity Measure (IM) Spectral Displacement (Sd, in)
Damage State Threshold
Slight Damage
Moderate Damage
Extensive Damage
Complete Damage
Damage State Probability
≥ Slight Damage: (0.187 in, 0.321)
≥ Moderate Damage: (0.187 in, 0.148)
≥ Extensive Damage: (0.187 in, 0.036)
≥ Complete Damage: (0.187 in, 0.005)
= Slight Damage
= Moderate Damage
= Extensive Damage
= Complete Damage
Detailed View
Building Description:
Facility Class: EFHL
Building Type: URML
Design Level: PC
Site Class: B
City: Natick
County: Middlesex
Geologic Group: Group 4
SDC: A
Discrete Damage State Probability P[Damage = DS | Sd]
0.679
0.173
0.112
0.031
0.005
0.001
None
1
2
3
4 Collapsed
Damage State
1 = Slight Damage | 2 = Moderate Damage
3 = Extensive Damage | 4 = Complete Damage

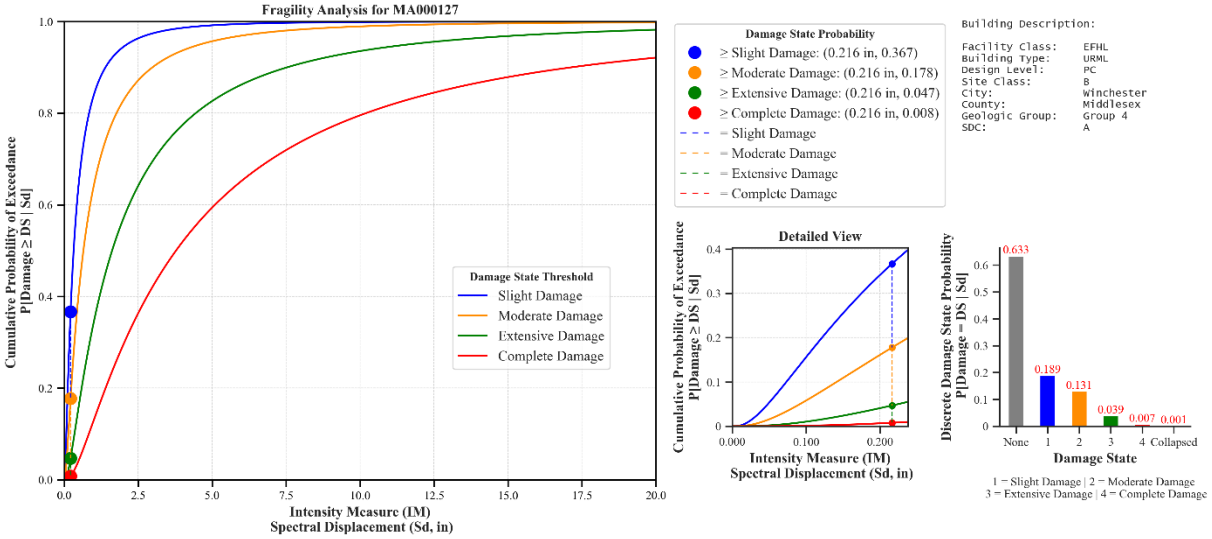
Fragility Analysis for MA000127
Cumulative Probability of Exceedance P[Damage ≥ DS | Sd]
Intensity Measure (IM) Spectral Displacement (Sd, in)
Damage State Threshold
Slight Damage
Moderate Damage
Extensive Damage
Complete Damage
Damage State Probability
≥ Slight Damage: (0.216 in, 0.367)
≥ Moderate Damage: (0.216 in, 0.178)
≥ Extensive Damage: (0.216 in, 0.047)
≥ Complete Damage: (0.216 in, 0.008)
= Slight Damage
= Moderate Damage
= Extensive Damage
= Complete Damage
Detailed View
Building Description:
Facility Class: EFHL
Building Type: URML
Design Level: PC
Site Class: B
City: Winchester
County: Middlesex
Geologic Group: Group 4
SDC: A
Discrete Damage State Probability P[Damage = DS | Sd]
0.633
0.189
0.131
0.039
0.007
0.001
None
1
2
3
4 Collapsed
Damage State
1 = Slight Damage | 2 = Moderate Damage
3 = Extensive Damage | 4 = Complete Damage

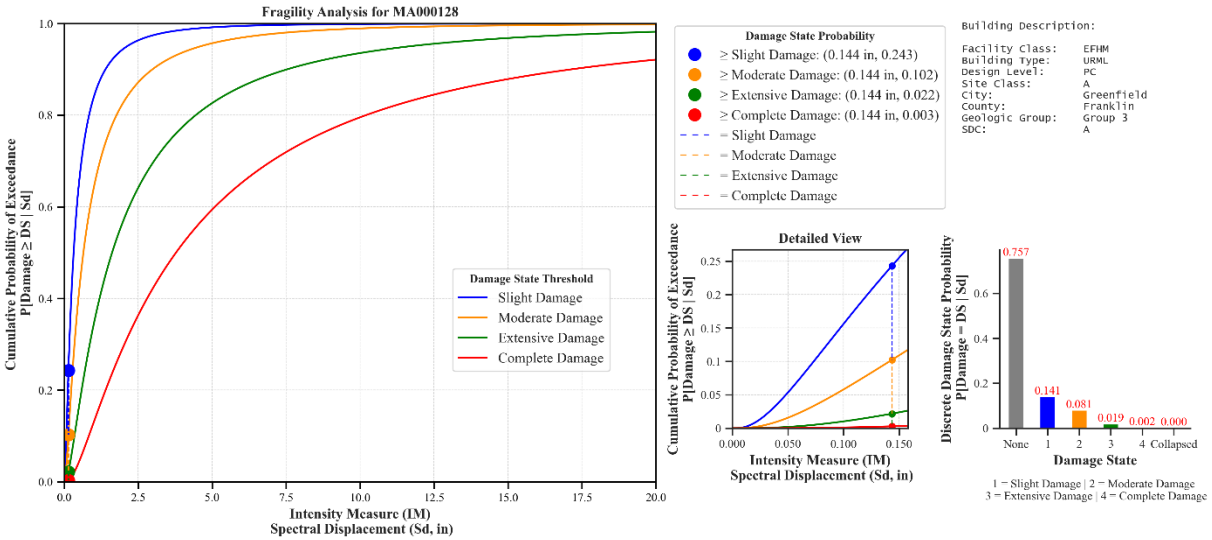
Fragility Analysis for MA000128
Cumulative Probability of Exceedance P[Damage ≥ DS | Sd]
Intensity Measure (IM) Spectral Displacement (Sd, in)
Damage State Threshold
Slight Damage
Moderate Damage
Extensive Damage
Complete Damage
Damage State Probability
≥ Slight Damage: (0.144 in, 0.243)
≥ Moderate Damage: (0.144 in, 0.102)
≥ Extensive Damage: (0.144 in, 0.022)
≥ Complete Damage: (0.144 in, 0.003)
= Slight Damage
= Moderate Damage
= Extensive Damage
= Complete Damage
Detailed View
Building Description:
Facility Class: EFHM
Building Type: URML
Design Level: PC
Site Class: A
City: Greenfield
County: Franklin
Geologic Group: Group 3
SDC: A
Discrete Damage State Probability P[Damage = DS | Sd]
0.757
0.141
0.081
0.019
0.002
0.000
None
1
2
3
4 Collapsed
Damage State
1 = Slight Damage | 2 = Moderate Damage
3 = Extensive Damage | 4 = Complete Damage

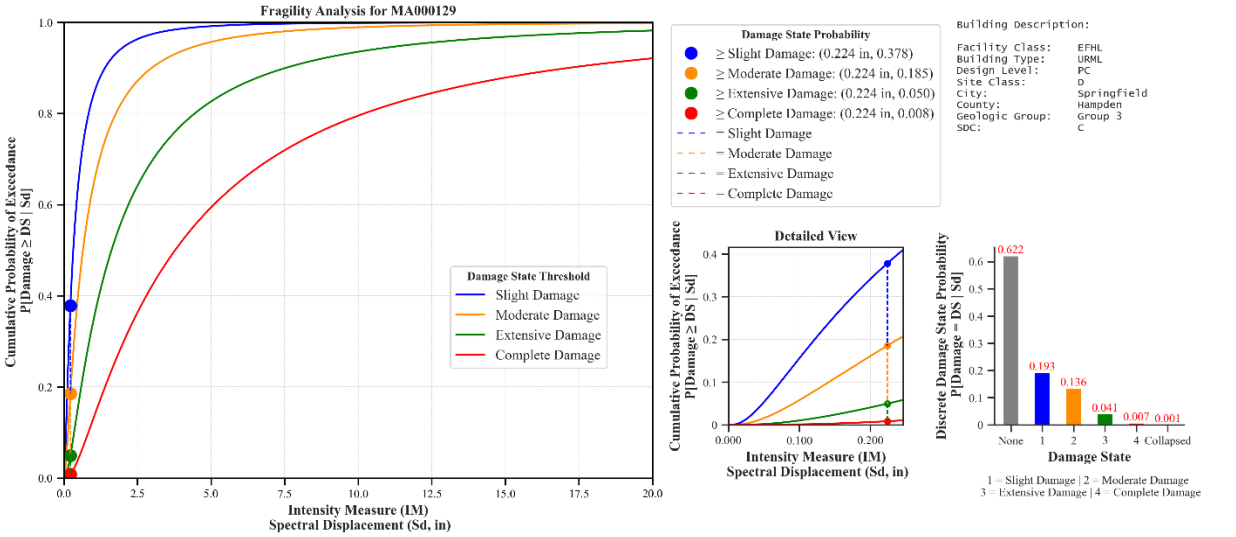
Fragility Analysis for MA000129
Cumulative Probability of Exceedance P[Damage ≥ DS | Sd]
Intensity Measure (IM) Spectral Displacement (Sd, in)
Damage State Threshold
Slight Damage
Moderate Damage
Extensive Damage
Complete Damage
Damage State Probability
≥ Slight Damage: (0.224 in, 0.378)
≥ Moderate Damage: (0.224 in, 0.185)
≥ Extensive Damage: (0.224 in, 0.050)
≥ Complete Damage: (0.224 in, 0.008)
Building Description:
Facility Class: EFHL
Building Type: URML
Design Level: PC
Site Class: D
City: Springfield
County: Hampden
Geologic Group: Group 3
SDC: C
Detailed View
Discrete Damage State Probability P[Damage = DS | Sd]
0.622
0.193
0.136
0.041
0.007
0.001
None
Collapsed
Damage State
1 = Slight Damage | 2 = Moderate Damage
3 = Extensive Damage | 4 = Complete Damage

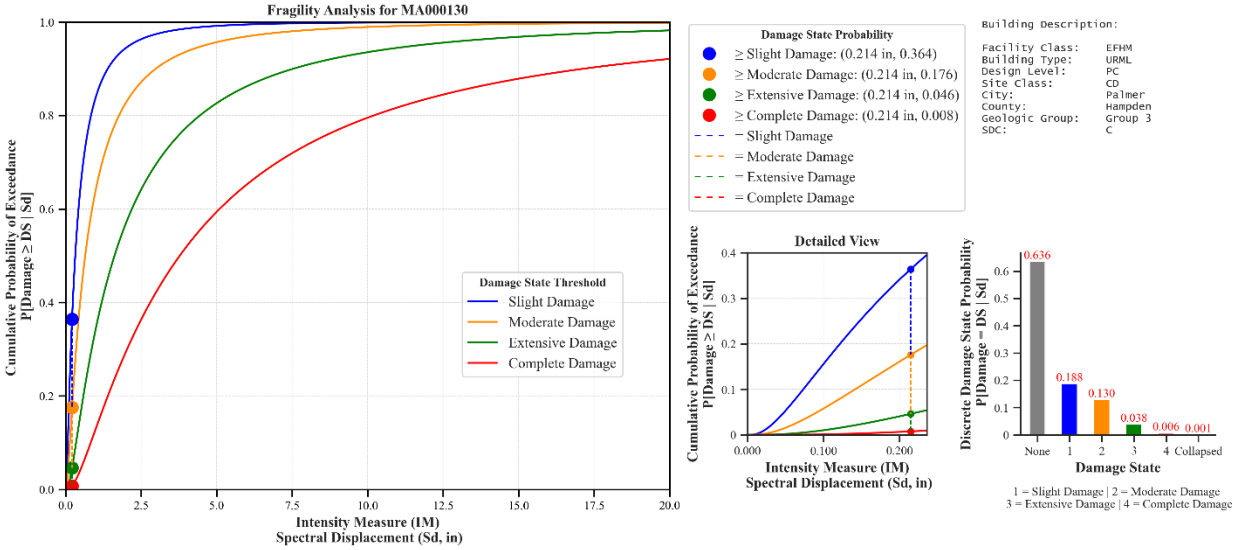
Fragility Analysis for MA000130
Cumulative Probability of Exceedance P[Damage ≥ DS | Sd]
Intensity Measure (IM) Spectral Displacement (Sd, in)
Damage State Threshold
Slight Damage
Moderate Damage
Extensive Damage
Complete Damage
Damage State Probability
≥ Slight Damage: (0.214 in, 0.364)
≥ Moderate Damage: (0.214 in, 0.176)
≥ Extensive Damage: (0.214 in, 0.046)
≥ Complete Damage: (0.214 in, 0.008)
Building Description:
Facility Class: EFHM
Building Type: URML
Design Level: PC
Site Class: CD
City: Palmer
County: Hampden
Geologic Group: Group 3
SDC: C
Detailed View
Discrete Damage State Probability P[Damage = DS | Sd]
0.636
0.188
0.130
0.038
0.006
0.001
None
Collapsed
Damage State
1 = Slight Damage | 2 = Moderate Damage
3 = Extensive Damage | 4 = Complete Damage

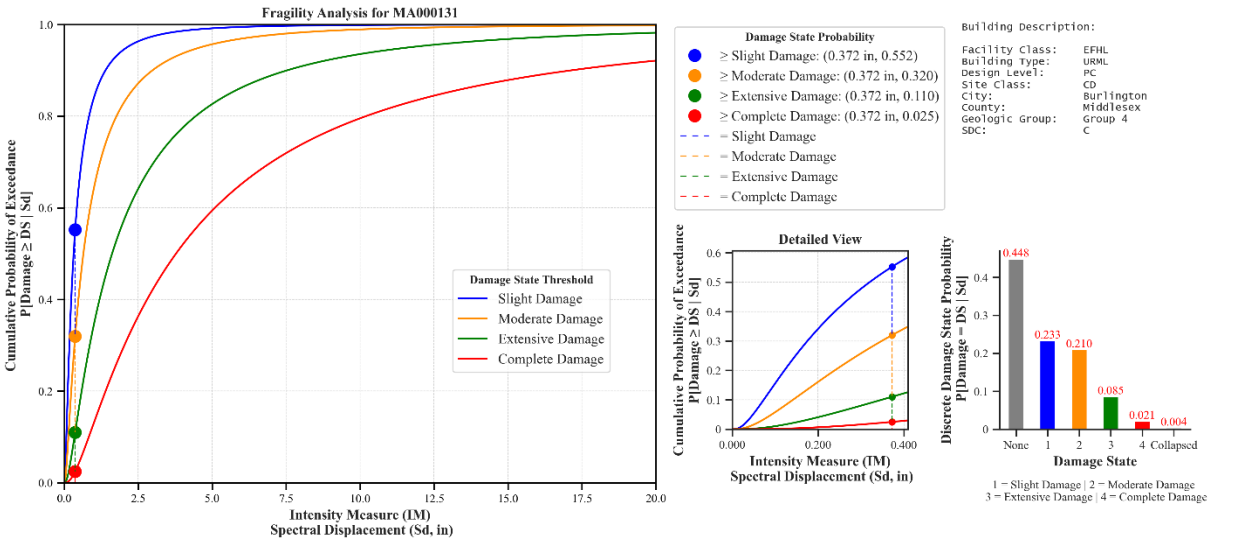
Fragility Analysis for MA000131
Cumulative Probability of Exceedance P[Damage ≥ DS | Sd]
Intensity Measure (IM) Spectral Displacement (Sd, in)
Damage State Threshold
Slight Damage
Moderate Damage
Extensive Damage
Complete Damage
Damage State Probability
≥ Slight Damage: (0.372 in, 0.552)
≥ Moderate Damage: (0.372 in, 0.320)
≥ Extensive Damage: (0.372 in, 0.110)
≥ Complete Damage: (0.372 in, 0.025)
Building Description:
Facility Class: EFHL
Building Type: URML
Design Level: PC
Site Class: CD
City: Burlington
County: Middlesex
Geologic Group: Group 4
SDC: C
Detailed View
Discrete Damage State Probability P[Damage = DS | Sd]
0.448
0.233
0.210
0.085
0.021
0.004
None
Collapsed
Damage State
1 = Slight Damage | 2 = Moderate Damage
3 = Extensive Damage | 4 = Complete Damage

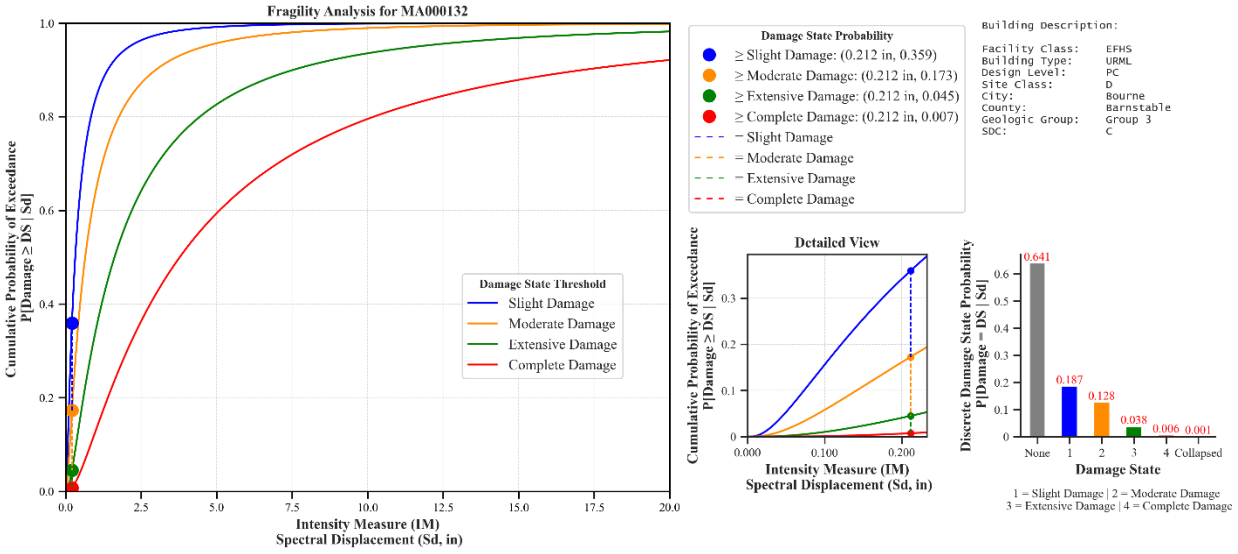
Fragility Analysis for MA000132
Cumulative Probability of Exceedance P[Damage ≥ DS | Sd]
Intensity Measure (IM) Spectral Displacement (Sd, in)
Damage State Threshold
Slight Damage
Moderate Damage
Extensive Damage
Complete Damage
Damage State Probability
≥ Slight Damage: (0.212 in, 0.359)
≥ Moderate Damage: (0.212 in, 0.173)
≥ Extensive Damage: (0.212 in, 0.045)
≥ Complete Damage: (0.212 in, 0.007)
= Slight Damage
= Moderate Damage
= Extensive Damage
= Complete Damage
Detailed View
Discrete Damage State Probability P[Damage = DS | Sd]
0.641
0.187
0.128
0.038
0.006
0.001
None
1
2
3
4
Collapsed
Damage State
1 = Slight Damage | 2 = Moderate Damage
3 = Extensive Damage | 4 = Complete Damage
Building Description:
Facility Class: EFHS
Building Type: URML
Design Level: PC
Site Class: D
City: Bourne
County: Barnstable
Geologic Group: Group 3
SDC: C

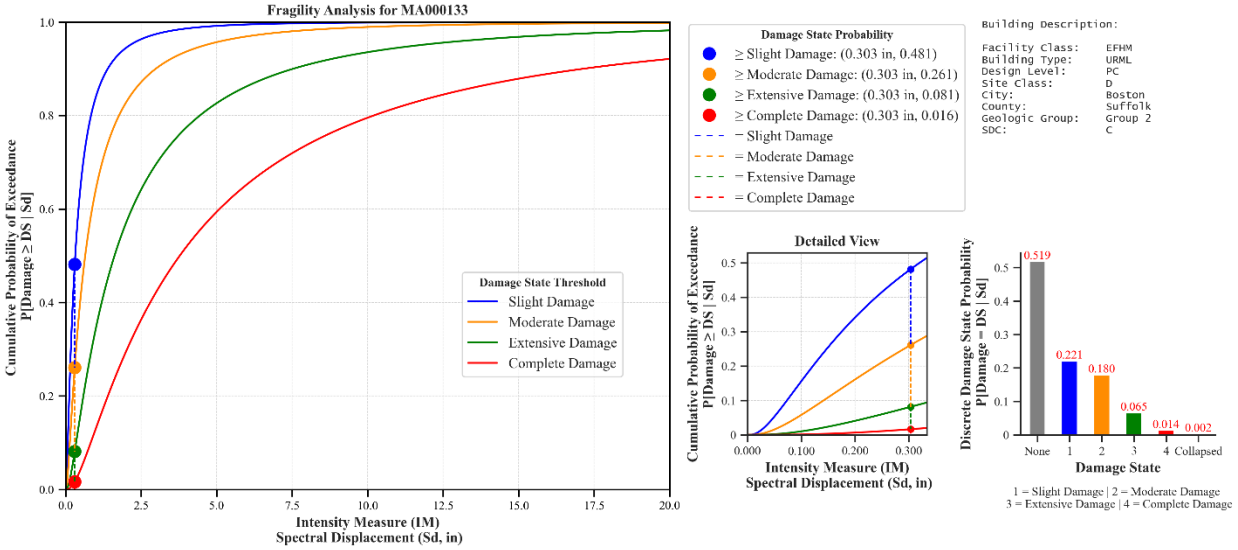
Fragility Analysis for MA000133
Cumulative Probability of Exceedance P[Damage ≥ DS | Sd]
Intensity Measure (IM) Spectral Displacement (Sd, in)
Damage State Threshold
Slight Damage
Moderate Damage
Extensive Damage
Complete Damage
Damage State Probability
≥ Slight Damage: (0.303 in, 0.481)
≥ Moderate Damage: (0.303 in, 0.261)
≥ Extensive Damage: (0.303 in, 0.081)
≥ Complete Damage: (0.303 in, 0.016)
= Slight Damage
= Moderate Damage
= Extensive Damage
= Complete Damage
Detailed View
Discrete Damage State Probability P[Damage = DS | Sd]
0.519
0.221
0.180
0.065
0.014
0.002
None
1
2
3
4
Collapsed
Damage State
1 = Slight Damage | 2 = Moderate Damage
3 = Extensive Damage | 4 = Complete Damage
Building Description:
Facility Class: EFHM
Building Type: URML
Design Level: PC
Site Class: D
City: Boston
County: Suffolk
Geologic Group: Group 2
SDC: C

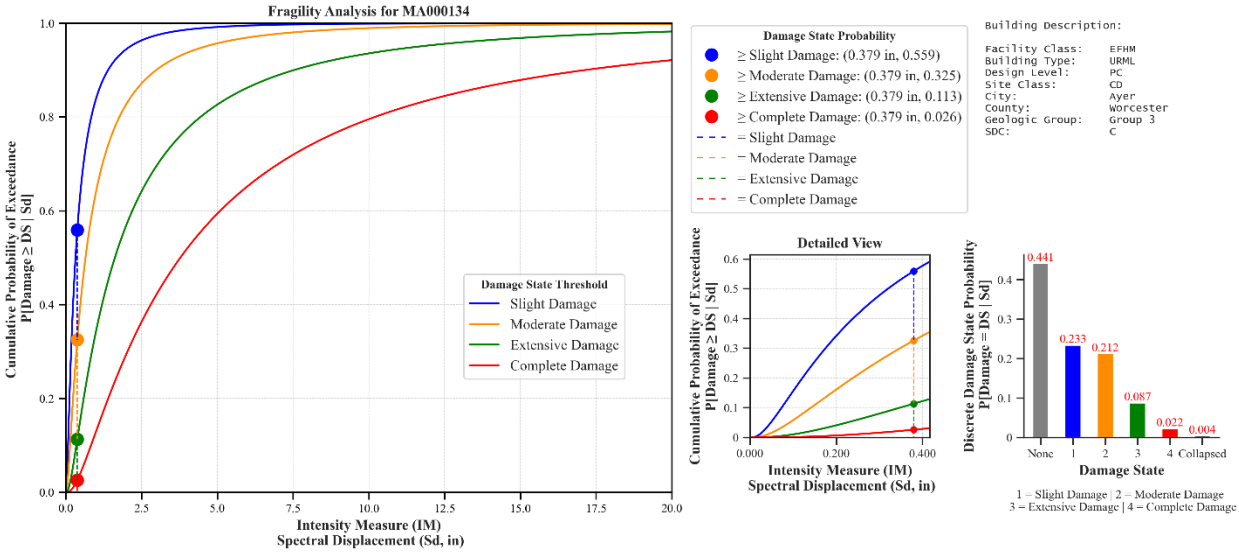
Fragility Analysis for MA000134
Cumulative Probability of Exceedance P[Damage ≥ DS | Sd]
Intensity Measure (IM) Spectral Displacement (Sd, in)
Damage State Threshold
Slight Damage
Moderate Damage
Extensive Damage
Complete Damage
Damage State Probability
≥ Slight Damage: (0.379 in, 0.559)
≥ Moderate Damage: (0.379 in, 0.325)
≥ Extensive Damage: (0.379 in, 0.113)
≥ Complete Damage: (0.379 in, 0.026)
= Slight Damage
= Moderate Damage
= Extensive Damage
= Complete Damage
Detailed View
Discrete Damage State Probability P[Damage = DS | Sd]
0.441
0.233
0.212
0.087
0.022
0.004
None
1
2
3
4
Collapsed
Damage State
1 = Slight Damage | 2 = Moderate Damage
3 = Extensive Damage | 4 = Complete Damage
Building Description:
Facility Class: EFHM
Building Type: URML
Design Level: PC
Site Class: CD
City: Ayer
County: Worcester
Geologic Group: Group 3
SDC: C

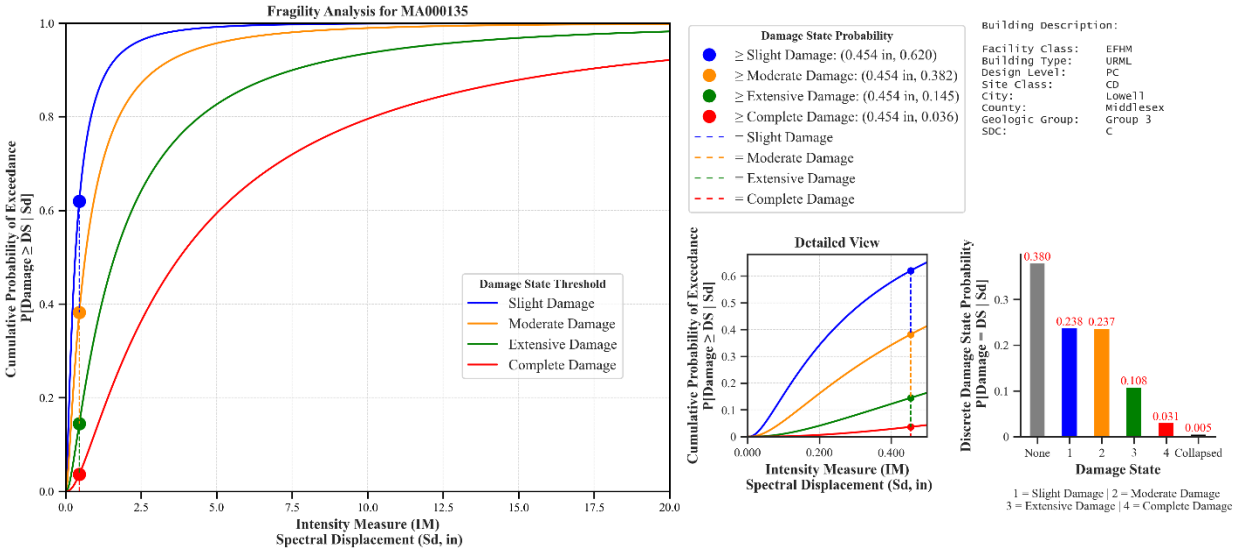
Fragility Analysis for MA000135
Cumulative Probability of Exceedance P[Damage ≥ DS | Sd]
Intensity Measure (IM) Spectral Displacement (Sd, in)
Damage State Threshold
Slight Damage
Moderate Damage
Extensive Damage
Complete Damage
Damage State Probability
≥ Slight Damage: (0.454 in, 0.620)
≥ Moderate Damage: (0.454 in, 0.382)
≥ Extensive Damage: (0.454 in, 0.145)
≥ Complete Damage: (0.454 in, 0.036)
Detailed View
Discrete Damage State Probability P[Damage = DS | Sd]
0.380
0.238
0.237
0.108
0.031
0.005
None
Collapsed
Damage State
1 = Slight Damage | 2 = Moderate Damage
3 = Extensive Damage | 4 = Complete Damage
Building Description:
Facility Class: EFHM
Building Type: URML
Design Level: PC
Site Class: CD
City: Lowell
County: Middlesex
Geologic Group: Group 3
SDC: C

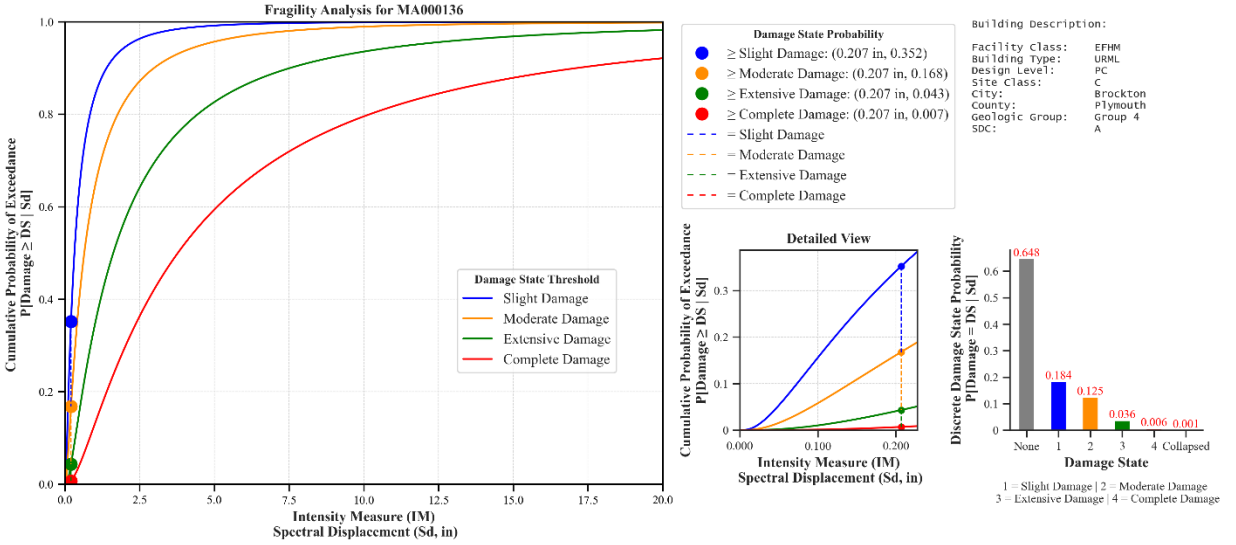
Fragility Analysis for MA000136
Cumulative Probability of Exceedance P[Damage ≥ DS | Sd]
Intensity Measure (IM) Spectral Displacement (Sd, in)
Damage State Threshold
Slight Damage
Moderate Damage
Extensive Damage
Complete Damage
Damage State Probability
≥ Slight Damage: (0.207 in, 0.352)
≥ Moderate Damage: (0.207 in, 0.168)
≥ Extensive Damage: (0.207 in, 0.043)
≥ Complete Damage: (0.207 in, 0.007)
Detailed View
Discrete Damage State Probability P[Damage = DS | Sd]
0.648
0.184
0.125
0.036
0.006
0.001
None
Collapsed
Damage State
1 = Slight Damage | 2 = Moderate Damage
3 = Extensive Damage | 4 = Complete Damage
Building Description:
Facility Class: EFHM
Building Type: URML
Design Level: PC
Site Class: C
City: Brockton
County: Plymouth
Geologic Group: Group 4
SDC: A

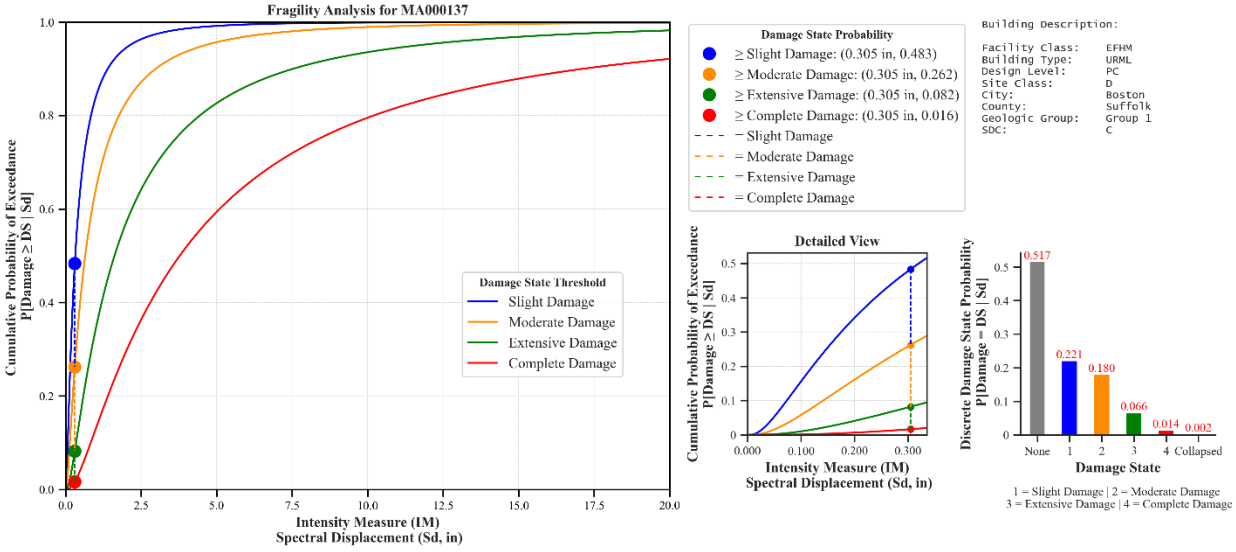
Fragility Analysis for MA000137
Cumulative Probability of Exceedance P[Damage ≥ DS | Sd]
Intensity Measure (IM) Spectral Displacement (Sd, in)
Damage State Threshold
Slight Damage
Moderate Damage
Extensive Damage
Complete Damage
Damage State Probability
≥ Slight Damage: (0.305 in, 0.483)
≥ Moderate Damage: (0.305 in, 0.262)
≥ Extensive Damage: (0.305 in, 0.082)
≥ Complete Damage: (0.305 in, 0.016)
Detailed View
Discrete Damage State Probability P[Damage = DS | Sd]
0.517
0.221
0.180
0.066
0.014
0.002
None
Collapsed
Damage State
1 = Slight Damage | 2 = Moderate Damage
3 = Extensive Damage | 4 = Complete Damage
Building Description:
Facility Class: EFHM
Building Type: URML
Design Level: PC
Site Class: D
City: Boston
County: Suffolk
Geologic Group: Group 1
SDC: C

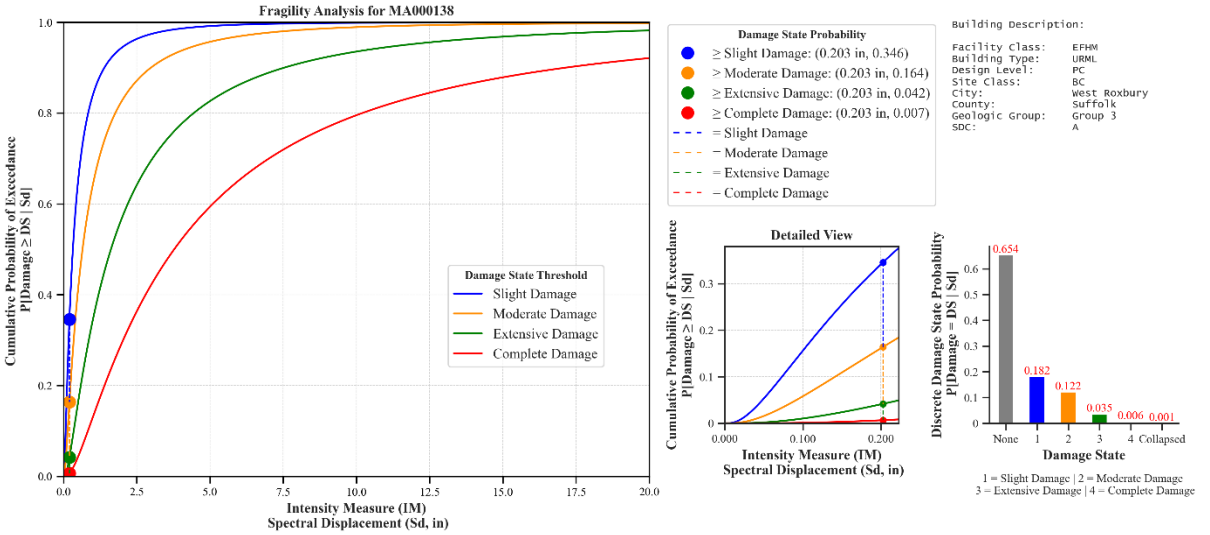
Fragility Analysis for MA000138
Cumulative Probability of Exceedance
P[Damage ≥ DS | Sd]
Intensity Measure (IM)
Spectral Displacement (Sd, in)
Damage State Threshold
Slight Damage
Moderate Damage
Extensive Damage
Complete Damage
Damage State Probability
≥ Slight Damage: (0.203 in, 0.346)
> Moderate Damage: (0.203 in, 0.164)
≥ Extensive Damage: (0.203 in, 0.042)
≥ Complete Damage: (0.203 in, 0.007)
= Slight Damage
= Moderate Damage
= Extensive Damage
= Complete Damage
Building Description:
Facility Class: EFHM
Building Type: URML
Design Level: PC
Site Class: BC
City: West Roxbury
County: Suffolk
Geologic Group: Group 3
SDC: A
Detailed View
Discrete Damage State Probability
P[Damage = DS | Sd]
0.654
0.182
0.122
0.035
0.006
0.001
None
1
2
3
4 Collapsed
Damage State
1 = Slight Damage | 2 = Moderate Damage
3 = Extensive Damage | 4 = Complete Damage

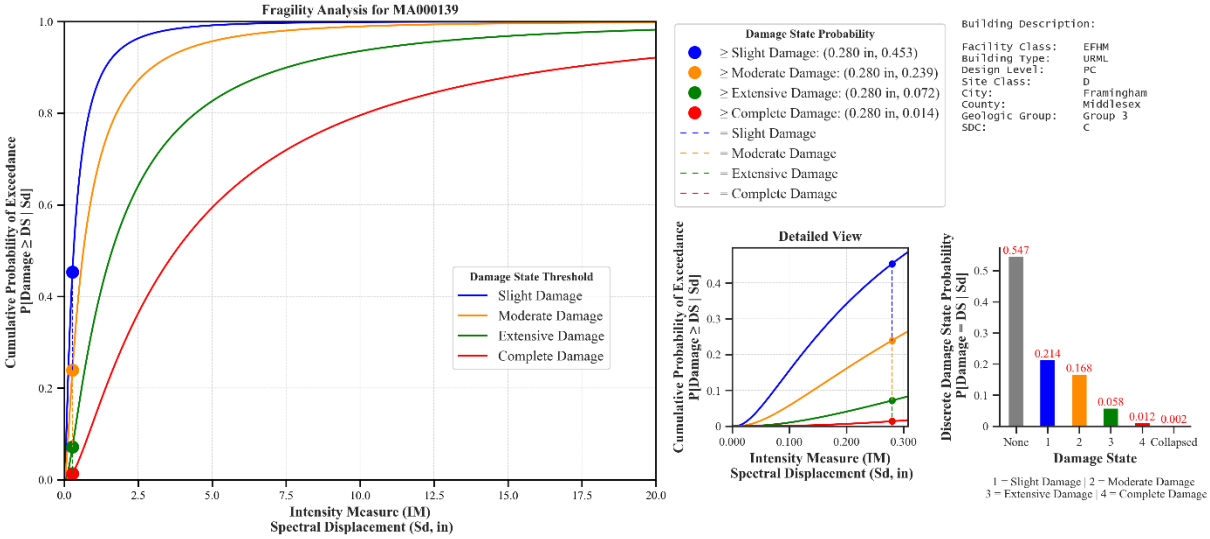
Fragility Analysis for MA000139
Cumulative Probability of Exceedance
P[Damage ≥ DS | Sd]
Intensity Measure (IM)
Spectral Displacement (Sd, in)
Damage State Threshold
Slight Damage
Moderate Damage
Extensive Damage
Complete Damage
Damage State Probability
≥ Slight Damage: (0.280 in, 0.453)
≥ Moderate Damage: (0.280 in, 0.239)
≥ Extensive Damage: (0.280 in, 0.072)
≥ Complete Damage: (0.280 in, 0.014)
= Slight Damage
= Moderate Damage
= Extensive Damage
= Complete Damage
Building Description:
Facility Class: EFHM
Building Type: URML
Design Level: PC
Site Class: D
City: Framingham
County: Middlesex
Geologic Group: Group 3
SDC: C
Detailed View
Discrete Damage State Probability
P[Damage = DS | Sd]
0.547
0.214
0.168
0.058
0.012
0.002
None
1
2
3
4 Collapsed
Damage State
1 = Slight Damage | 2 = Moderate Damage
3 = Extensive Damage | 4 = Complete Damage

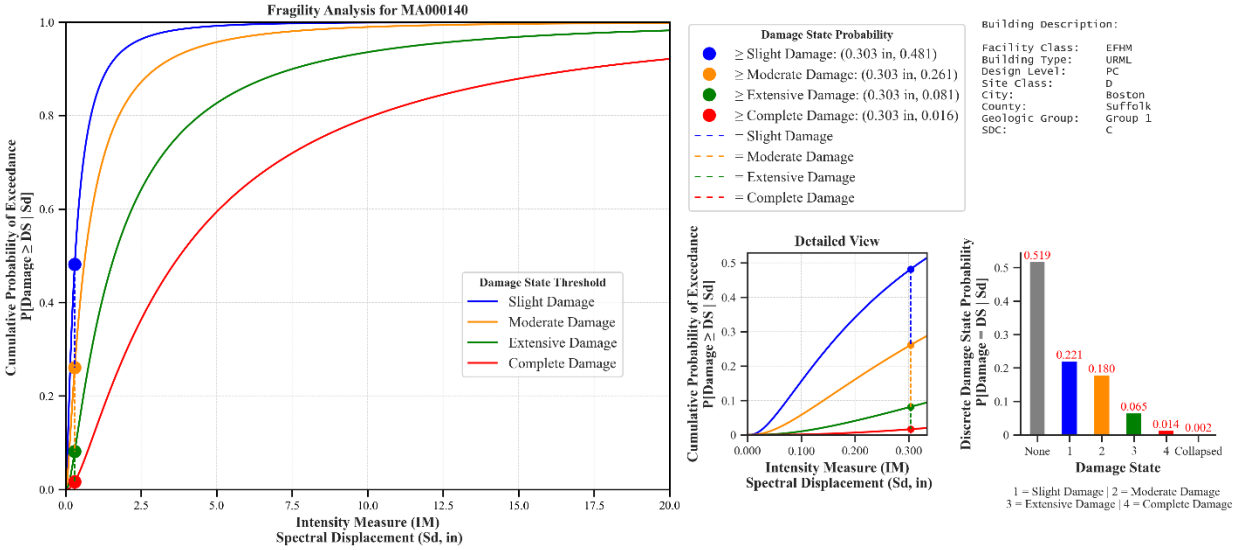
Fragility Analysis for MA000140
Cumulative Probability of Exceedance
P[Damage ≥ DS | Sd]
Intensity Measure (IM)
Spectral Displacement (Sd, in)
Damage State Threshold
Slight Damage
Moderate Damage
Extensive Damage
Complete Damage
Damage State Probability
≥ Slight Damage: (0.303 in, 0.481)
≥ Moderate Damage: (0.303 in, 0.261)
≥ Extensive Damage: (0.303 in, 0.081)
≥ Complete Damage: (0.303 in, 0.016)
= Slight Damage
= Moderate Damage
= Extensive Damage
= Complete Damage
Building Description:
Facility Class: EFHM
Building Type: URML
Design Level: PC
Site Class: D
City: Boston
County: Suffolk
Geologic Group: Group 1
SDC: C
Detailed View
Discrete Damage State Probability
P[Damage = DS | Sd]
0.519
0.221
0.180
0.065
0.014
0.002
None
1
2
3
4 Collapsed
Damage State
1 = Slight Damage | 2 = Moderate Damage
3 = Extensive Damage | 4 = Complete Damage

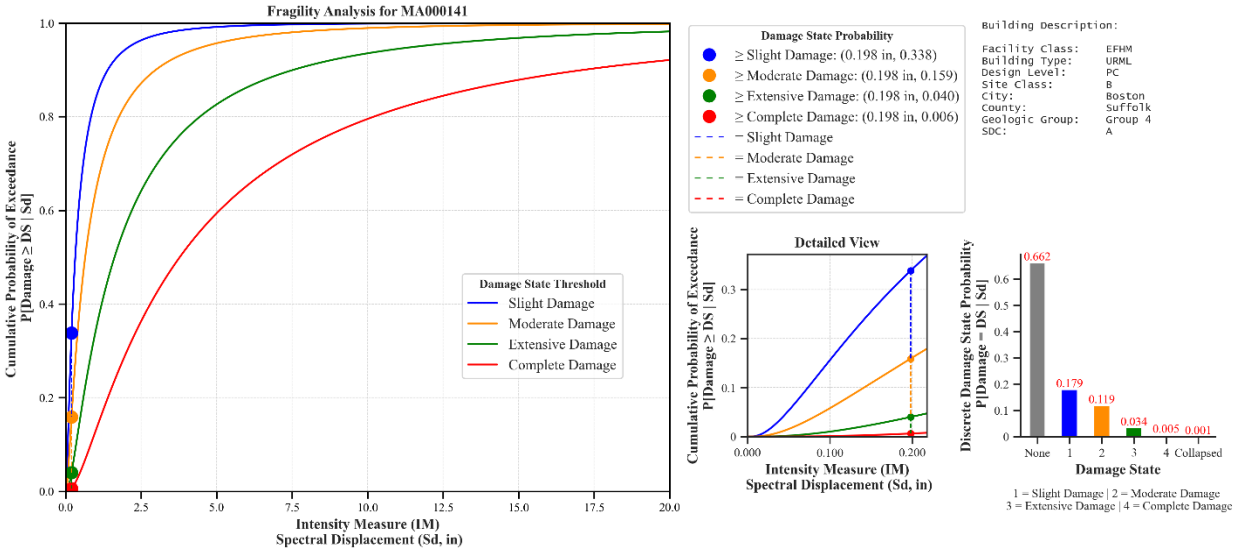
Fragility Analysis for MA000141
Cumulative Probability of Exceedance P[Damage ≥ DS | Sd]
Intensity Measure (IM) Spectral Displacement (Sd, in)
Damage State Threshold
Slight Damage
Moderate Damage
Extensive Damage
Complete Damage
Damage State Probability
≥ Slight Damage: (0.198 in, 0.338)
≥ Moderate Damage: (0.198 in, 0.159)
≥ Extensive Damage: (0.198 in, 0.040)
≥ Complete Damage: (0.198 in, 0.006)
Detailed View
Discrete Damage State Probability P[Damage = DS | Sd]
0.662
0.179
0.119
0.034
0.005
0.001
None 1 2 3 4 Collapsed
Damage State
1 = Slight Damage | 2 = Moderate Damage
3 = Extensive Damage | 4 = Complete Damage
Building Description:
Facility Class: EFHM
Building Type: URML
Design Level: PC
Site Class: B
City: Boston
County: Suffolk
Geologic Group: Group 4
SDC: A

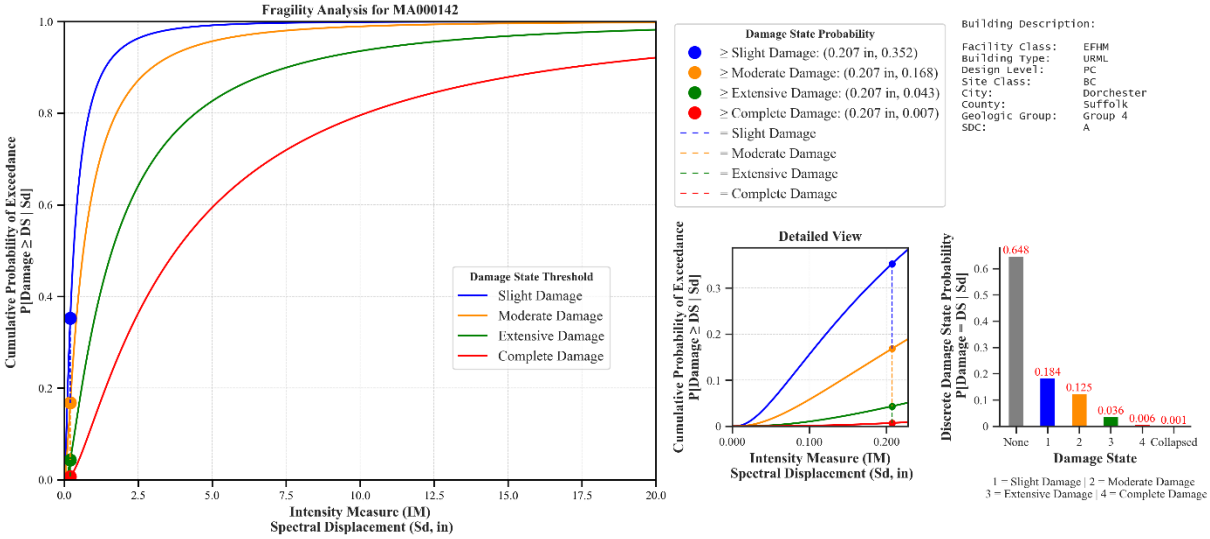
Fragility Analysis for MA000142
Cumulative Probability of Exceedance P[Damage ≥ DS | Sd]
Intensity Measure (IM) Spectral Displacement (Sd, in)
Damage State Threshold
Slight Damage
Moderate Damage
Extensive Damage
Complete Damage
Damage State Probability
≥ Slight Damage: (0.207 in, 0.352)
≥ Moderate Damage: (0.207 in, 0.168)
≥ Extensive Damage: (0.207 in, 0.043)
≥ Complete Damage: (0.207 in, 0.007)
Detailed View
Discrete Damage State Probability P[Damage = DS | Sd]
0.648
0.184
0.125
0.036
0.006
0.001
None 1 2 3 4 Collapsed
Damage State
1 = Slight Damage | 2 = Moderate Damage
3 = Extensive Damage | 4 = Complete Damage
Building Description:
Facility Class: EFHM
Building Type: URML
Design Level: PC
Site Class: BC
City: Dorchester
County: Suffolk
Geologic Group: Group 4
SDC: A

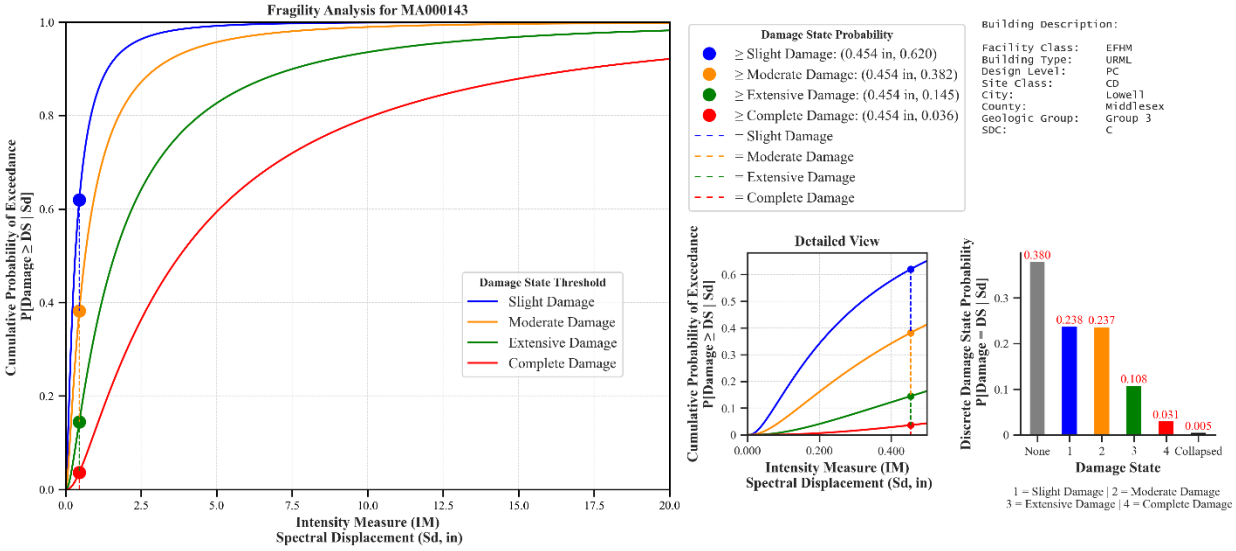
Fragility Analysis for MA000143
Cumulative Probability of Exceedance P[Damage ≥ DS | Sd]
Intensity Measure (IM) Spectral Displacement (Sd, in)
Damage State Threshold
Slight Damage
Moderate Damage
Extensive Damage
Complete Damage
Damage State Probability
≥ Slight Damage: (0.454 in, 0.620)
≥ Moderate Damage: (0.454 in, 0.382)
≥ Extensive Damage: (0.454 in, 0.145)
≥ Complete Damage: (0.454 in, 0.036)
Detailed View
Discrete Damage State Probability P[Damage = DS | Sd]
0.380
0.238
0.237
0.108
0.031
0.005
None 1 2 3 4 Collapsed
Damage State
1 = Slight Damage | 2 = Moderate Damage
3 = Extensive Damage | 4 = Complete Damage
Building Description:
Facility Class: EFHM
Building Type: URML
Design Level: PC
Site Class: CD
City: Lowell
County: Middlesex
Geologic Group: Group 3
SDC: C

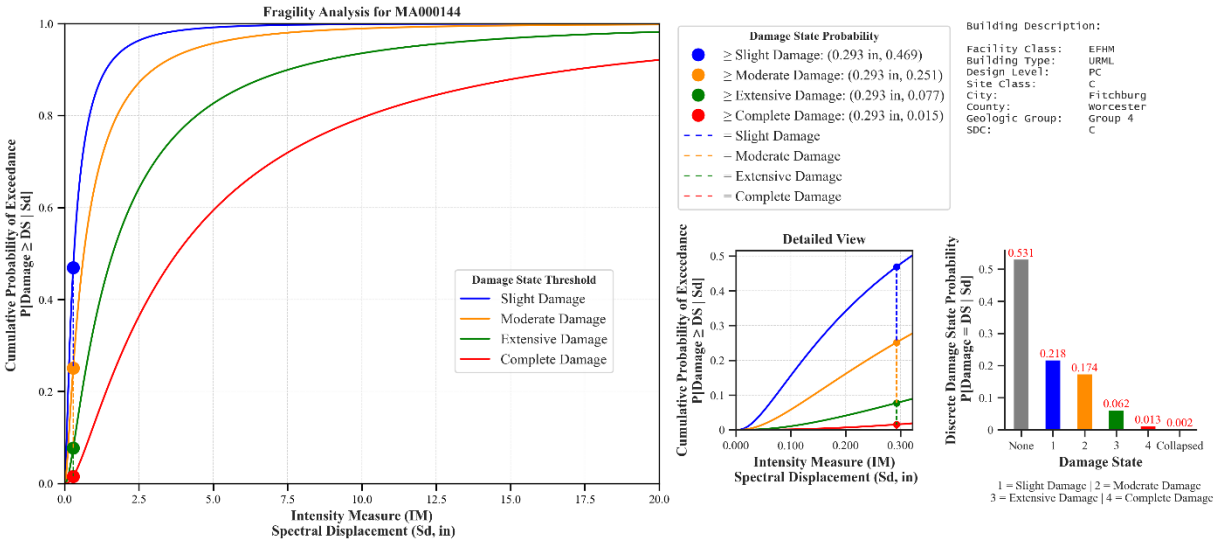
Fragility Analysis for MA000144
Cumulative Probability of Exceedance P[Damage ≥ DS | Sd]
Intensity Measure (IM) Spectral Displacement (Sd, in)
Damage State Threshold
Slight Damage
Moderate Damage
Extensive Damage
Complete Damage
Damage State Probability
≥ Slight Damage: (0.293 in, 0.469)
≥ Moderate Damage: (0.293 in, 0.251)
≥ Extensive Damage: (0.293 in, 0.077)
≥ Complete Damage: (0.293 in, 0.015)
Building Description:
Facility Class: EFHM
Building Type: URML
Design Level: PC
Site Class: C
City: Fitchburg
County: Worcester
Geologic Group: Group 4
SDC: C
Detailed View
Discrete Damage State Probability P[Damage = DS | Sd]
0.531
0.218
0.174
0.062
0.013
0.002
None
Collapsed
Damage State
1 = Slight Damage | 2 = Moderate Damage
3 = Extensive Damage | 4 = Complete Damage

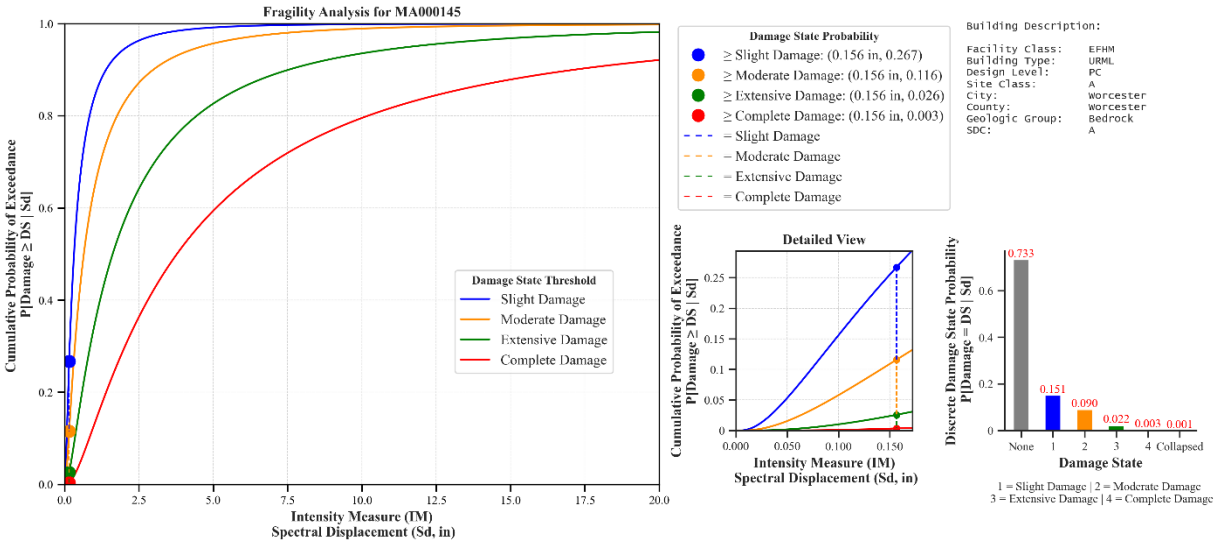
Fragility Analysis for MA000145
Cumulative Probability of Exceedance P[Damage ≥ DS | Sd]
Intensity Measure (IM) Spectral Displacement (Sd, in)
Damage State Threshold
Slight Damage
Moderate Damage
Extensive Damage
Complete Damage
Damage State Probability
≥ Slight Damage: (0.156 in, 0.267)
≥ Moderate Damage: (0.156 in, 0.116)
≥ Extensive Damage: (0.156 in, 0.026)
≥ Complete Damage: (0.156 in, 0.003)
Building Description:
Facility Class: EFHM
Building Type: URML
Design Level: PC
Site Class: A
City: Worcester
County: Worcester
Geologic Group: Bedrock
SDC: A
Detailed View
Discrete Damage State Probability P[Damage = DS | Sd]
0.733
0.151
0.090
0.022
0.003
0.001
None
Collapsed
Damage State
1 = Slight Damage | 2 = Moderate Damage
3 = Extensive Damage | 4 = Complete Damage

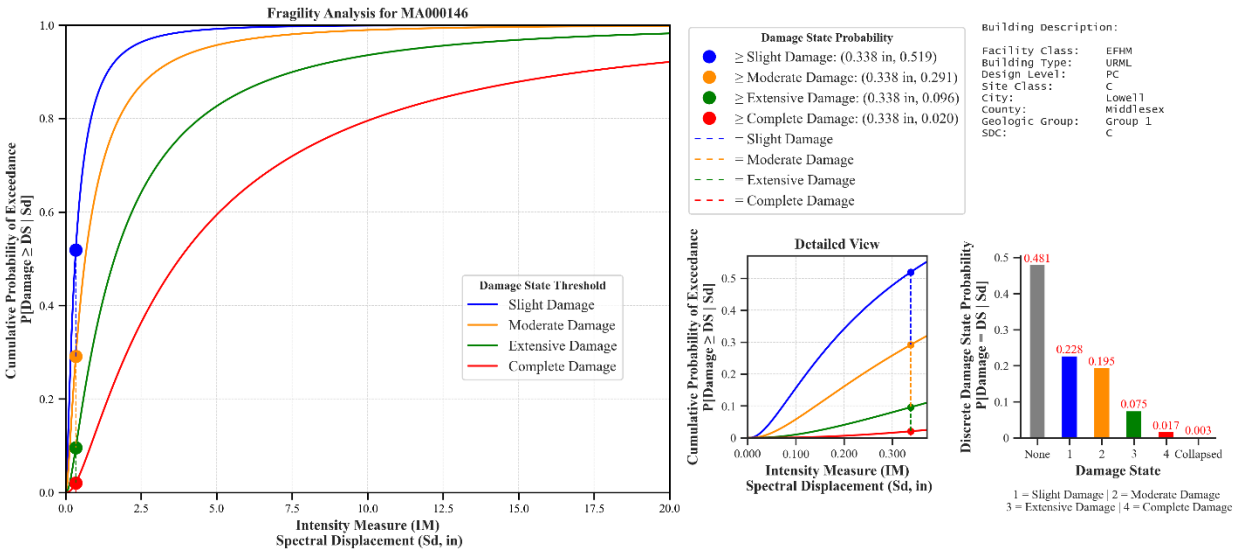
Fragility Analysis for MA000146
Cumulative Probability of Exceedance P[Damage ≥ DS | Sd]
Intensity Measure (IM) Spectral Displacement (Sd, in)
Damage State Threshold
Slight Damage
Moderate Damage
Extensive Damage
Complete Damage
Damage State Probability
≥ Slight Damage: (0.338 in, 0.519)
≥ Moderate Damage: (0.338 in, 0.291)
≥ Extensive Damage: (0.338 in, 0.096)
≥ Complete Damage: (0.338 in, 0.020)
Building Description:
Facility Class: EFHM
Building Type: URML
Design Level: PC
Site Class: C
City: Lowell
County: Middlesex
Geologic Group: Group 1
SDC: C
Detailed View
Discrete Damage State Probability P[Damage = DS | Sd]
0.481
0.228
0.195
0.075
0.017
0.003
None
Collapsed
Damage State
1 = Slight Damage | 2 = Moderate Damage
3 = Extensive Damage | 4 = Complete Damage

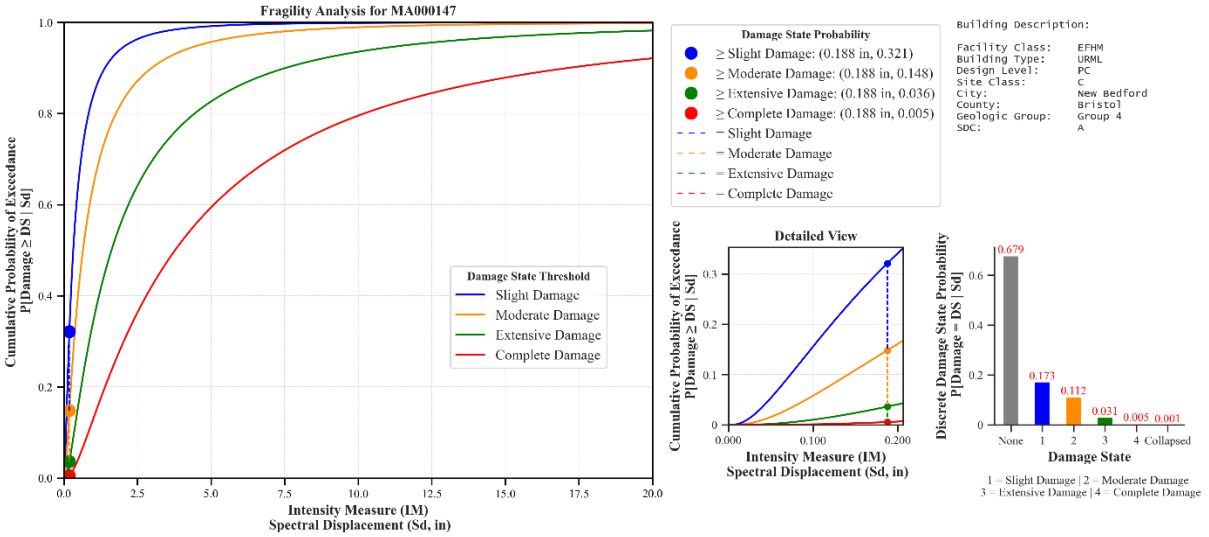
Fragility Analysis for MA000147
Cumulative Probability of Exceedance P[Damage ≥ DS | Sd]
Intensity Measure (IM) Spectral Displacement (Sd, in)
Damage State Threshold
Slight Damage
Moderate Damage
Extensive Damage
Complete Damage
Damage State Probability
≥ Slight Damage: (0.188 in, 0.321)
≥ Moderate Damage: (0.188 in, 0.148)
≥ Extensive Damage: (0.188 in, 0.036)
≥ Complete Damage: (0.188 in, 0.005)
Detailed View
Discrete Damage State Probability P[Damage = DS | Sd]
0.679
0.173
0.112
0.031
0.005
0.001
None 1 2 3 4 Collapsed
Damage State
1 = Slight Damage | 2 = Moderate Damage
3 = Extensive Damage | 4 = Complete Damage
Building Description:
Facility Class: EFHM
Building Type: URML
Design Level: PC
Site Class: C
City: New Bedford
County: Bristol
Geologic Group: Group 4
SDC: A

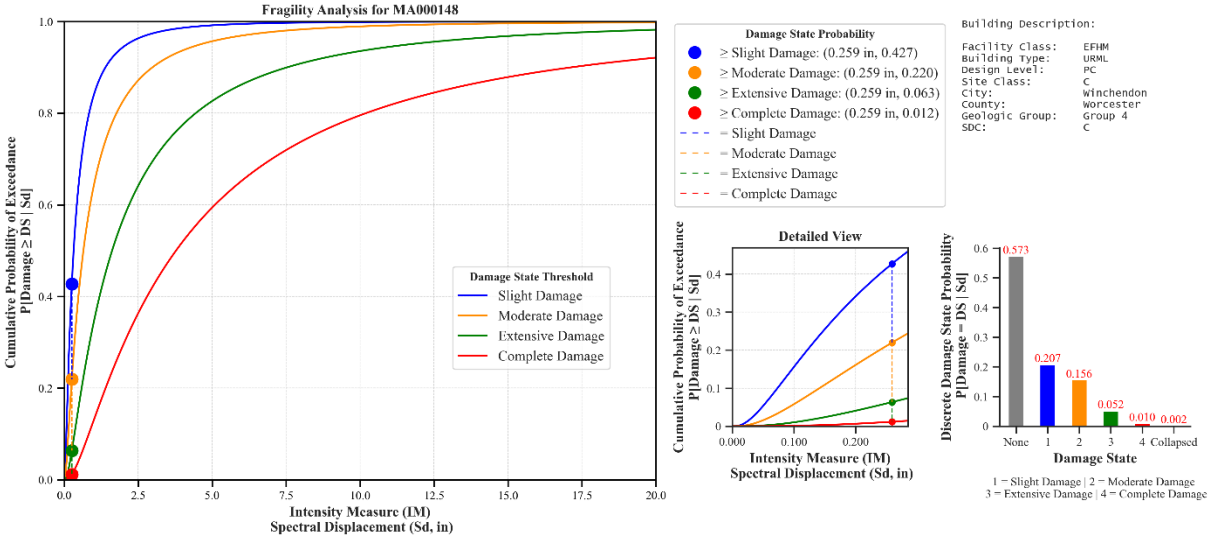
Fragility Analysis for MA000148
Cumulative Probability of Exceedance P[Damage ≥ DS | Sd]
Intensity Measure (IM) Spectral Displacement (Sd, in)
Damage State Threshold
Slight Damage
Moderate Damage
Extensive Damage
Complete Damage
Damage State Probability
≥ Slight Damage: (0.259 in, 0.427)
≥ Moderate Damage: (0.259 in, 0.220)
≥ Extensive Damage: (0.259 in, 0.063)
≥ Complete Damage: (0.259 in, 0.012)
Detailed View
Discrete Damage State Probability P[Damage = DS | Sd]
0.573
0.207
0.156
0.052
0.010
0.002
None 1 2 3 4 Collapsed
Damage State
1 = Slight Damage | 2 = Moderate Damage
3 = Extensive Damage | 4 = Complete Damage
Building Description:
Facility Class: EFHM
Building Type: URML
Design Level: PC
Site Class: C
City: Winchendon
County: Worcester
Geologic Group: Group 4
SDC: C

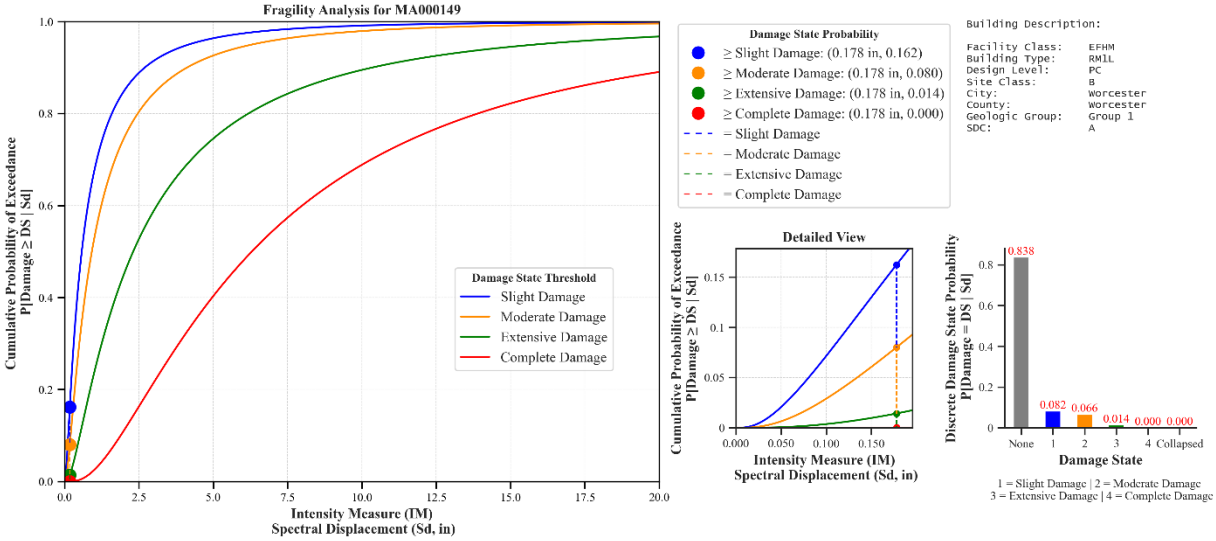
Fragility Analysis for MA000149
Cumulative Probability of Exceedance P[Damage ≥ DS | Sd]
Intensity Measure (IM) Spectral Displacement (Sd, in)
Damage State Threshold
Slight Damage
Moderate Damage
Extensive Damage
Complete Damage
Damage State Probability
≥ Slight Damage: (0.178 in, 0.162)
≥ Moderate Damage: (0.178 in, 0.080)
≥ Extensive Damage: (0.178 in, 0.014)
≥ Complete Damage: (0.178 in, 0.000)
Detailed View
Discrete Damage State Probability P[Damage = DS | Sd]
0.838
0.082
0.066
0.014
0.000
0.000
None 1 2 3 4 Collapsed
Damage State
1 = Slight Damage | 2 = Moderate Damage
3 = Extensive Damage | 4 = Complete Damage
Building Description:
Facility Class: EFHM
Building Type: RMLL
Design Level: PC
Site Class: B
City: Worcester
County: Worcester
Geologic Group: Group 1
SDC: A

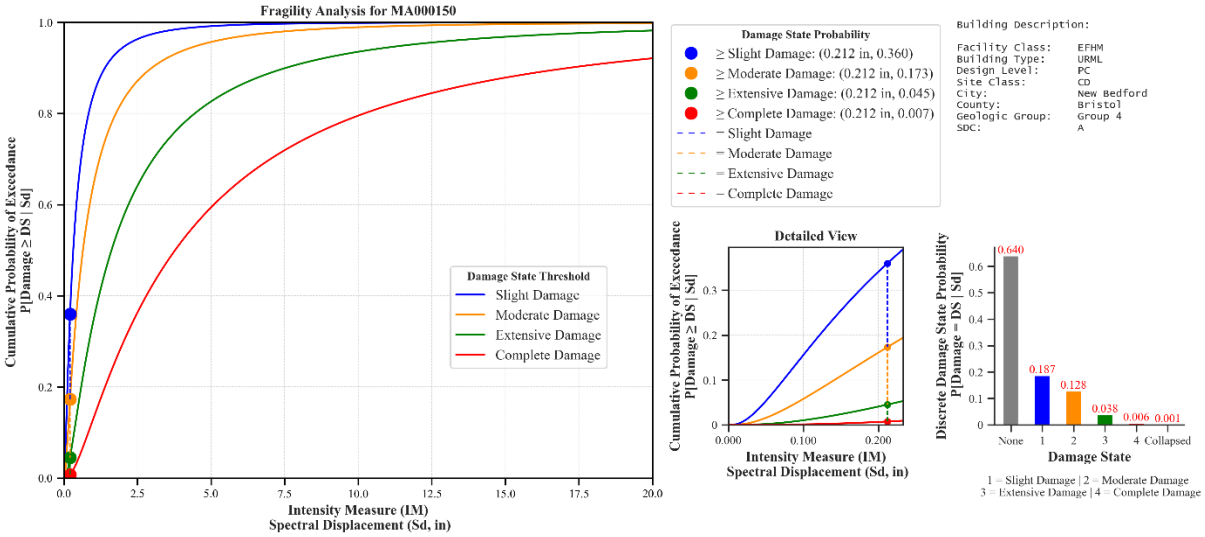
Fragility Analysis for MA000150
Cumulative Probability of Exceedance P[Damage ≥ DS | Sd]
Intensity Measure (IM) Spectral Displacement (Sd, in)
Damage State Threshold
Slight Damage
Moderate Damage
Extensive Damage
Complete Damage
Damage State Probability
≥ Slight Damage: (0.212 in, 0.360)
≥ Moderate Damage: (0.212 in, 0.173)
≥ Extensive Damage: (0.212 in, 0.045)
≥ Complete Damage: (0.212 in, 0.007)
Detailed View
Discrete Damage State Probability P[Damage = DS | Sd]
0.640
0.187
0.128
0.038
0.006
0.001
None 1 2 3 4 Collapsed
Damage State
1 = Slight Damage | 2 = Moderate Damage
3 = Extensive Damage | 4 = Complete Damage
Building Description:
Facility Class: EFHM
Building Type: URML
Design Level: PC
Site Class: CD
City: New Bedford
County: Bristol
Geologic Group: Group 4
SDC: A

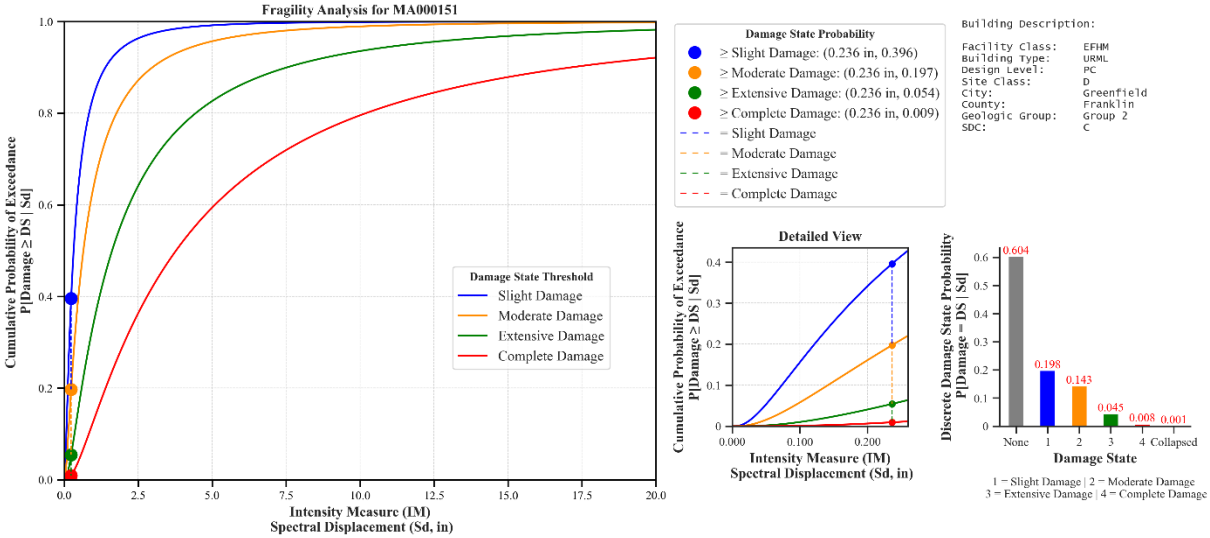
Fragility Analysis for MA000151
Cumulative Probability of Exceedance P[Damage ≥ DS | Sd]
Intensity Measure (IM) Spectral Displacement (Sd, in)
Damage State Threshold
Slight Damage
Moderate Damage
Extensive Damage
Complete Damage
Damage State Probability
≥ Slight Damage: (0.236 in, 0.396)
≥ Moderate Damage: (0.236 in, 0.197)
≥ Extensive Damage: (0.236 in, 0.054)
≥ Complete Damage: (0.236 in, 0.009)
Detailed View
Discrete Damage State Probability P[Damage = DS | Sd]
0.604
0.198
0.143
0.045
0.008
0.001
None 1 2 3 4 Collapsed
Damage State
1 = Slight Damage | 2 = Moderate Damage
3 = Extensive Damage | 4 = Complete Damage
Building Description:
Facility Class: EFHM
Building Type: URML
Design Level: PC
Site Class: D
City: Greenfield
County: Franklin
Geologic Group: Group 2
SDC: C

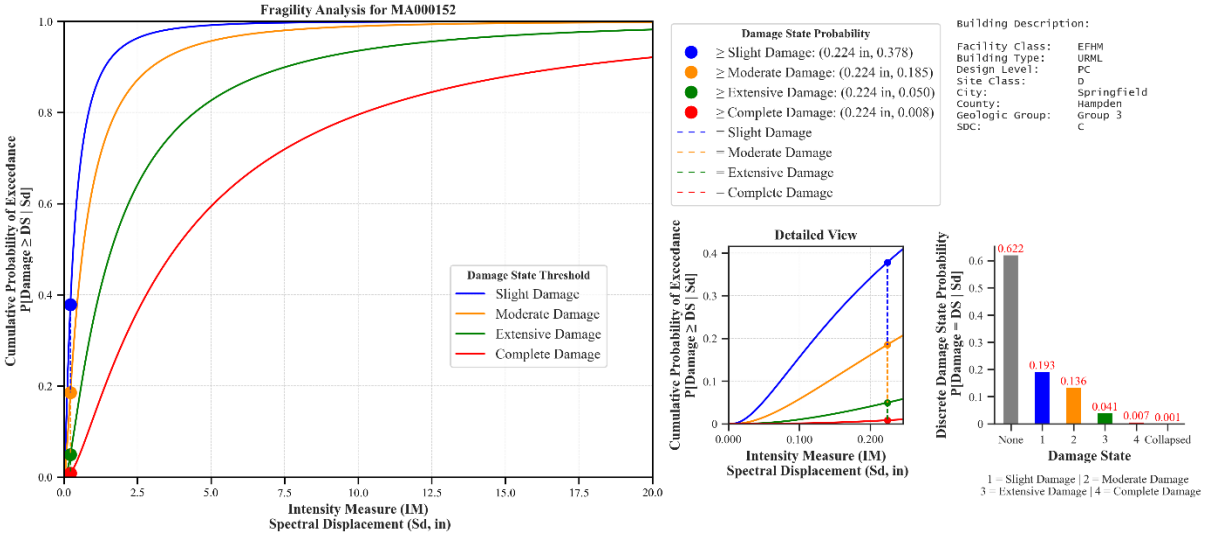
Fragility Analysis for MA000152
Cumulative Probability of Exceedance P[Damage ≥ DS | Sd]
Intensity Measure (IM) Spectral Displacement (Sd, in)
Damage State Threshold
Slight Damage
Moderate Damage
Extensive Damage
Complete Damage
Damage State Probability
≥ Slight Damage: (0.224 in, 0.378)
≥ Moderate Damage: (0.224 in, 0.185)
≥ Extensive Damage: (0.224 in, 0.050)
≥ Complete Damage: (0.224 in, 0.008)
Detailed View
Discrete Damage State Probability P[Damage = DS | Sd]
0.622
0.193
0.136
0.041
0.007
0.001
None 1 2 3 4 Collapsed
Damage State
1 = Slight Damage | 2 = Moderate Damage
3 = Extensive Damage | 4 = Complete Damage
Building Description:
Facility Class: EFHM
Building Type: URML
Design Level: PC
Site Class: D
City: Springfield
County: Hampden
Geologic Group: Group 3
SDC: C

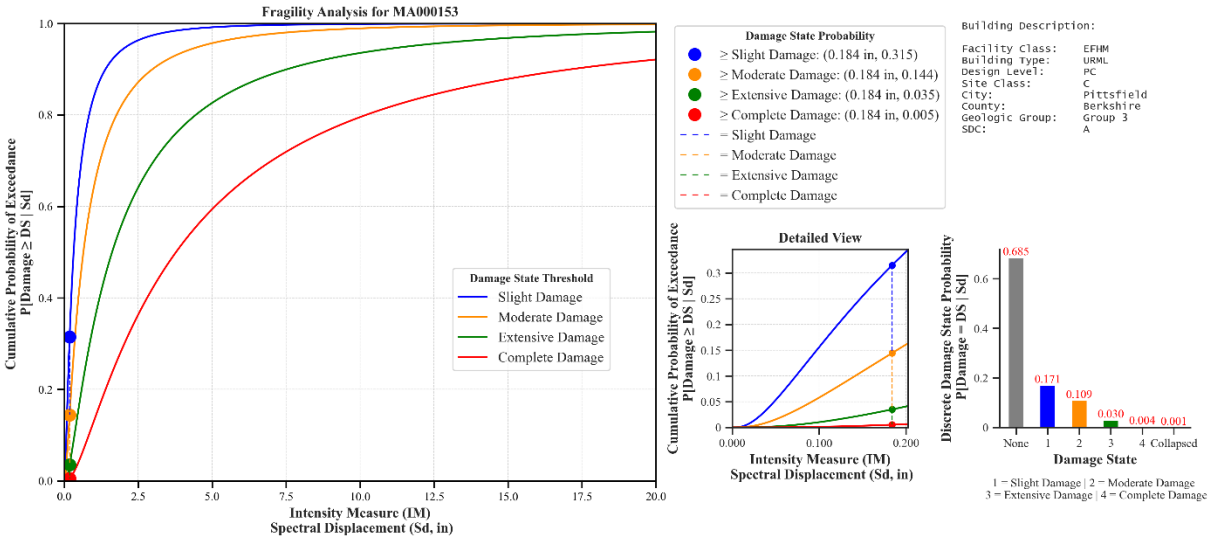
Fragility Analysis for MA000153
Cumulative Probability of Exceedance P[Damage ≥ DS | Sd]
Intensity Measure (IM) Spectral Displacement (Sd, in)
Damage State Threshold
Slight Damage
Moderate Damage
Extensive Damage
Complete Damage
Damage State Probability
≥ Slight Damage: (0.184 in, 0.315)
≥ Moderate Damage: (0.184 in, 0.144)
≥ Extensive Damage: (0.184 in, 0.035)
≥ Complete Damage: (0.184 in, 0.005)
= Slight Damage
= Moderate Damage
= Extensive Damage
= Complete Damage
Building Description:
Facility Class: EFHM
Building Type: URML
Design Level: PC
Site Class: C
City: Pittsfield
County: Berkshire
Geologic Group: Group 3
SDC: A
Detailed View
Discrete Damage State Probability P[Damage = DS | Sd]
0.685
0.171
0.109
0.030
0.004
0.001
None
Collapsed
Damage State
1 = Slight Damage | 2 = Moderate Damage
3 = Extensive Damage | 4 = Complete Damage

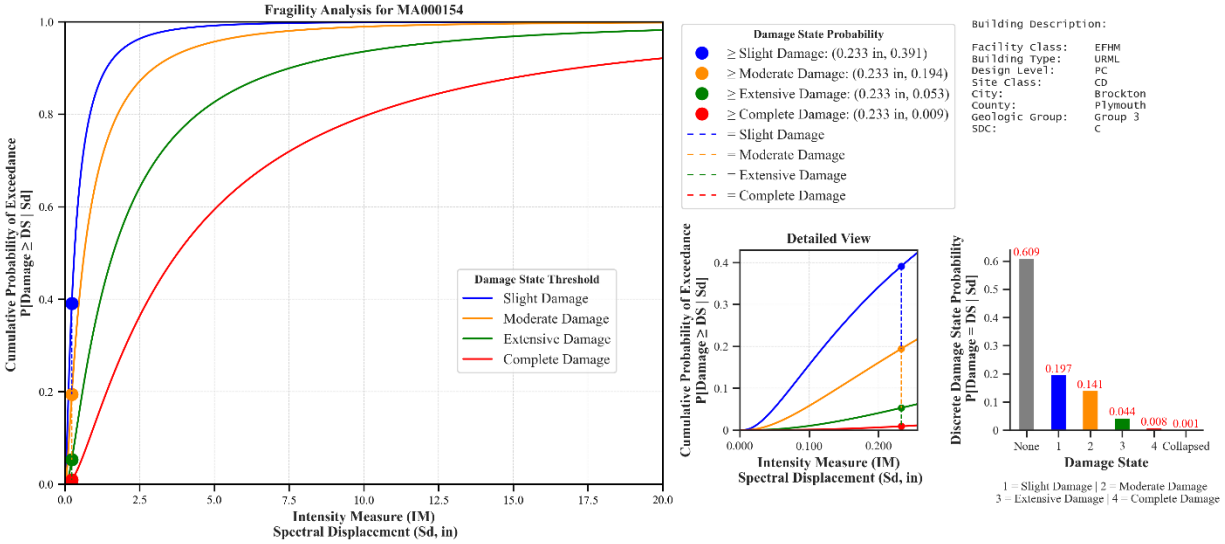
Fragility Analysis for MA000154
Cumulative Probability of Exceedance P[Damage ≥ DS | Sd]
Intensity Measure (IM) Spectral Displacement (Sd, in)
Damage State Threshold
Slight Damage
Moderate Damage
Extensive Damage
Complete Damage
Damage State Probability
≥ Slight Damage: (0.233 in, 0.391)
≥ Moderate Damage: (0.233 in, 0.194)
≥ Extensive Damage: (0.233 in, 0.053)
≥ Complete Damage: (0.233 in, 0.009)
= Slight Damage
= Moderate Damage
= Extensive Damage
= Complete Damage
Building Description:
Facility Class: EFHM
Building Type: URML
Design Level: PC
Site Class: CD
City: Brockton
County: Plymouth
Geologic Group: Group 3
SDC: C
Detailed View
Discrete Damage State Probability P[Damage = DS | Sd]
0.609
0.197
0.141
0.044
0.008
0.001
None
Collapsed
Damage State
1 = Slight Damage | 2 = Moderate Damage
3 = Extensive Damage | 4 = Complete Damage

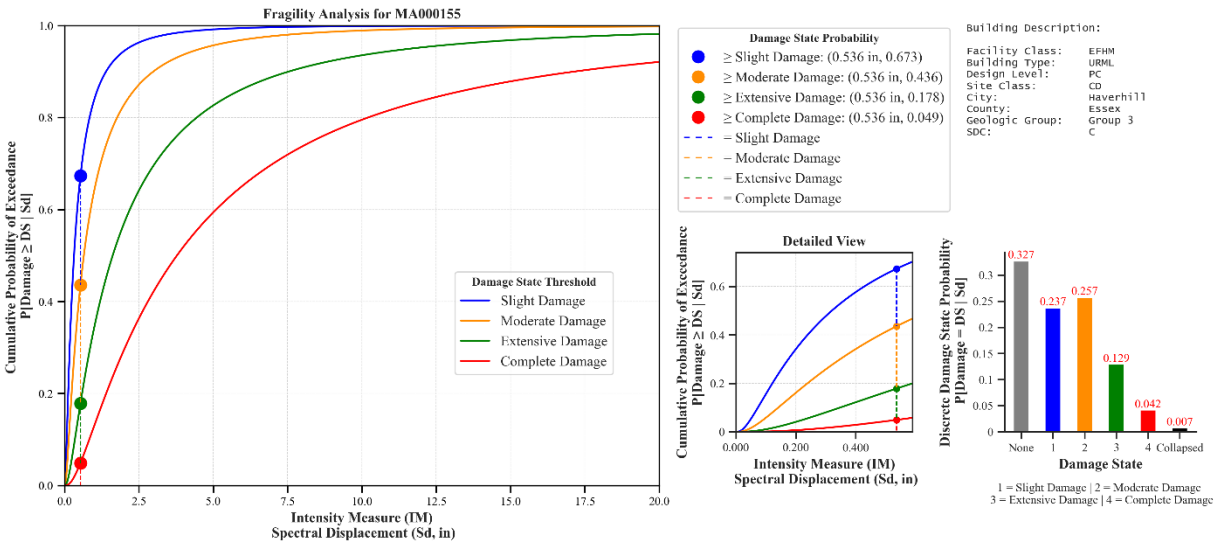
Fragility Analysis for MA000155
Cumulative Probability of Exceedance P[Damage ≥ DS | Sd]
Intensity Measure (IM) Spectral Displacement (Sd, in)
Damage State Threshold
Slight Damage
Moderate Damage
Extensive Damage
Complete Damage
Damage State Probability
≥ Slight Damage: (0.536 in, 0.673)
≥ Moderate Damage: (0.536 in, 0.436)
≥ Extensive Damage: (0.536 in, 0.178)
≥ Complete Damage: (0.536 in, 0.049)
= Slight Damage
= Moderate Damage
= Extensive Damage
= Complete Damage
Building Description:
Facility Class: EFHM
Building Type: URML
Design Level: PC
Site Class: CD
City: Haverhill
County: Essex
Geologic Group: Group 3
SDC: C
Detailed View
Discrete Damage State Probability P[Damage = DS | Sd]
0.327
0.237
0.257
0.129
0.042
0.007
None
Collapsed
Damage State
1 = Slight Damage | 2 = Moderate Damage
3 = Extensive Damage | 4 = Complete Damage

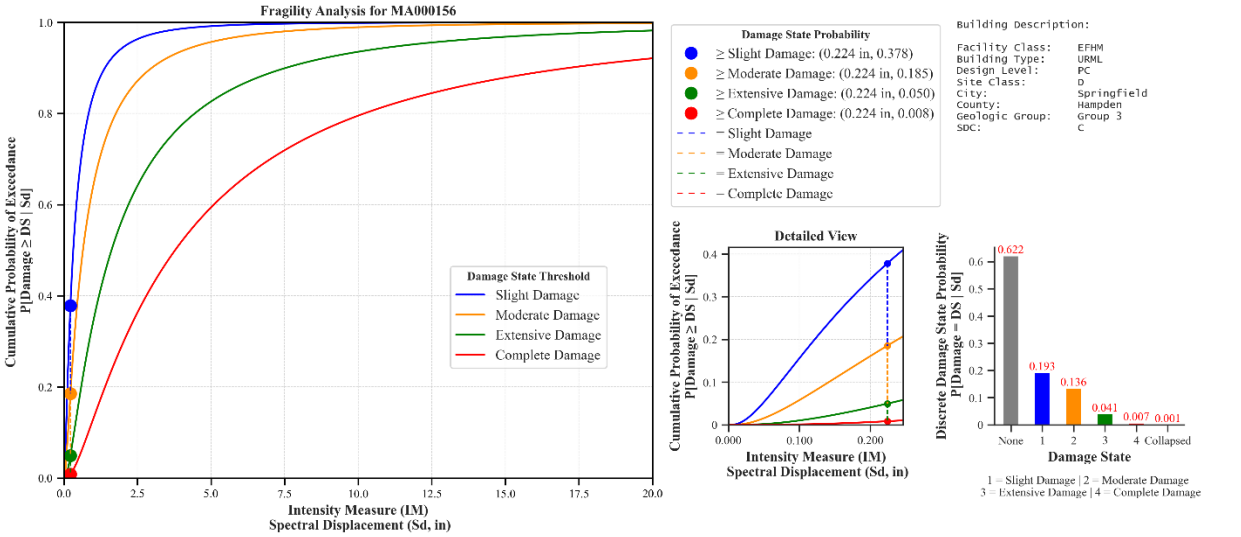
Fragility Analysis for MA000156
Cumulative Probability of Exceedance P[Damage ≥ DS | Sd]
Intensity Measure (IM) Spectral Displacement (Sd, in)
Damage State Threshold
Slight Damage
Moderate Damage
Extensive Damage
Complete Damage
Damage State Probability
≥ Slight Damage: (0.224 in, 0.378)
≥ Moderate Damage: (0.224 in, 0.185)
≥ Extensive Damage: (0.224 in, 0.050)
≥ Complete Damage: (0.224 in, 0.008)
= Slight Damage
= Moderate Damage
= Extensive Damage
= Complete Damage
Detailed View
Building Description:
Facility Class: EFHM
Building Type: URML
Design Level: PC
Site Class: D
City: Springfield
County: Hampden
Geologic Group: Group 3
SDC: C
Discrete Damage State Probability P[Damage = DS | Sd]
0.622
0.193
0.136
0.041
0.007
0.001
None 1 2 3 4 Collapsed
Damage State
1 = Slight Damage | 2 = Moderate Damage
3 = Extensive Damage | 4 = Complete Damage

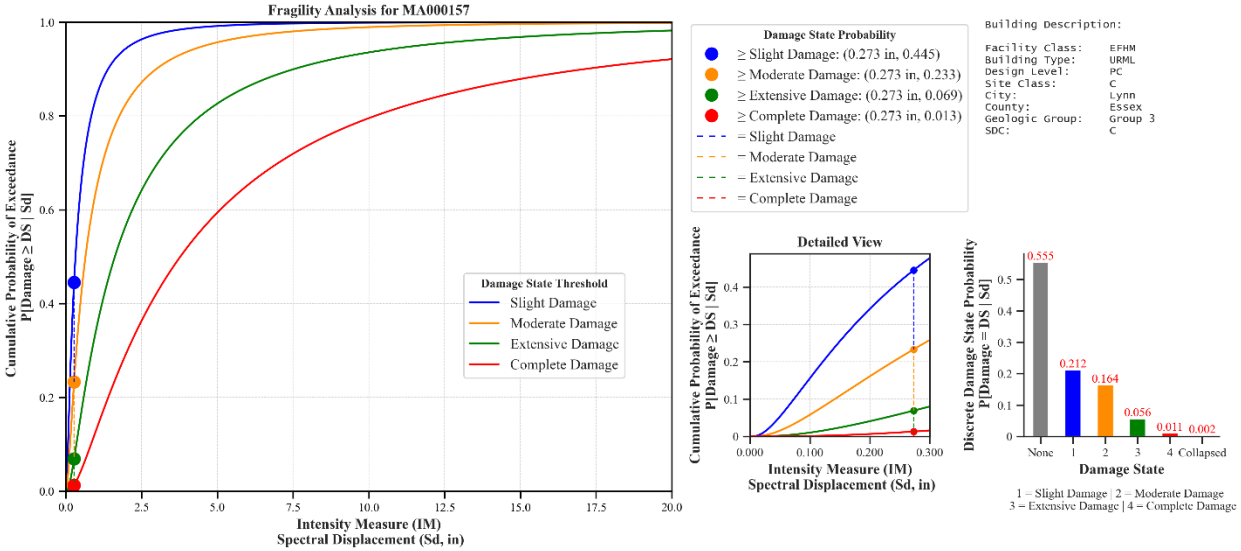
Fragility Analysis for MA000157
Cumulative Probability of Exceedance P[Damage ≥ DS | Sd]
Intensity Measure (IM) Spectral Displacement (Sd, in)
Damage State Threshold
Slight Damage
Moderate Damage
Extensive Damage
Complete Damage
Damage State Probability
≥ Slight Damage: (0.273 in, 0.445)
≥ Moderate Damage: (0.273 in, 0.233)
≥ Extensive Damage: (0.273 in, 0.069)
≥ Complete Damage: (0.273 in, 0.013)
= Slight Damage
= Moderate Damage
= Extensive Damage
= Complete Damage
Detailed View
Building Description:
Facility Class: EFHM
Building Type: URML
Design Level: PC
Site Class: C
City: Lynn
County: Essex
Geologic Group: Group 3
SDC: C
Discrete Damage State Probability P[Damage = DS | Sd]
0.555
0.212
0.164
0.056
0.011
0.002
None 1 2 3 4 Collapsed
Damage State
1 = Slight Damage | 2 = Moderate Damage
3 = Extensive Damage | 4 = Complete Damage

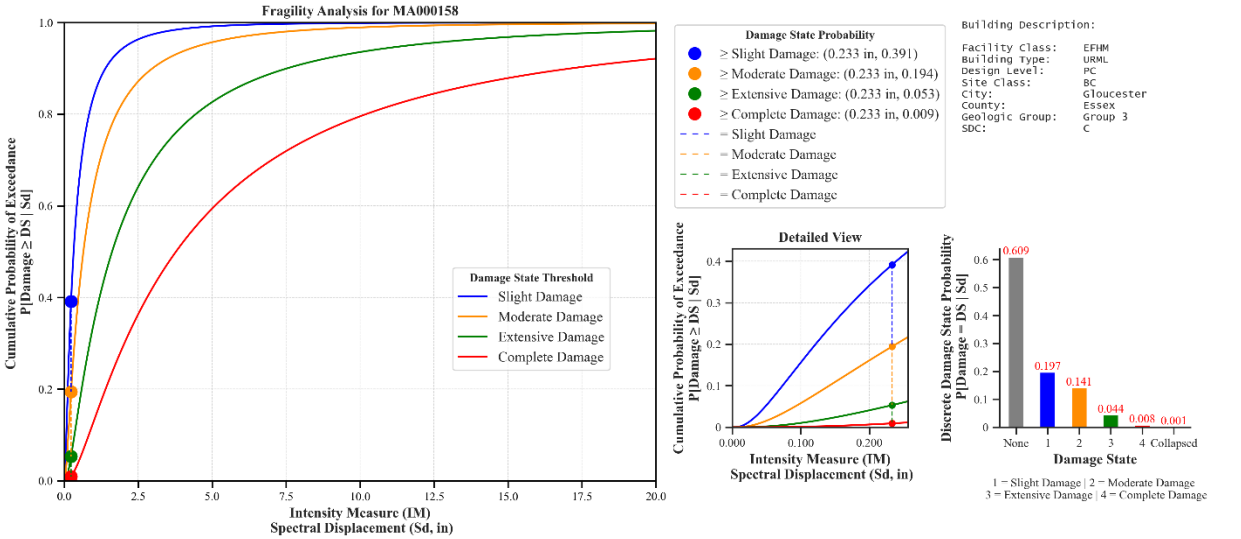
Fragility Analysis for MA000158
Cumulative Probability of Exceedance P[Damage ≥ DS | Sd]
Intensity Measure (IM) Spectral Displacement (Sd, in)
Damage State Threshold
Slight Damage
Moderate Damage
Extensive Damage
Complete Damage
Damage State Probability
≥ Slight Damage: (0.233 in, 0.391)
≥ Moderate Damage: (0.233 in, 0.194)
≥ Extensive Damage: (0.233 in, 0.053)
≥ Complete Damage: (0.233 in, 0.009)
= Slight Damage
= Moderate Damage
= Extensive Damage
= Complete Damage
Detailed View
Building Description:
Facility Class: EFHM
Building Type: URML
Design Level: PC
Site Class: BC
City: Gloucester
County: Essex
Geologic Group: Group 3
SDC: C
Discrete Damage State Probability P[Damage = DS | Sd]
0.609
0.197
0.141
0.044
0.008
0.001
None 1 2 3 4 Collapsed
Damage State
1 = Slight Damage | 2 = Moderate Damage
3 = Extensive Damage | 4 = Complete Damage

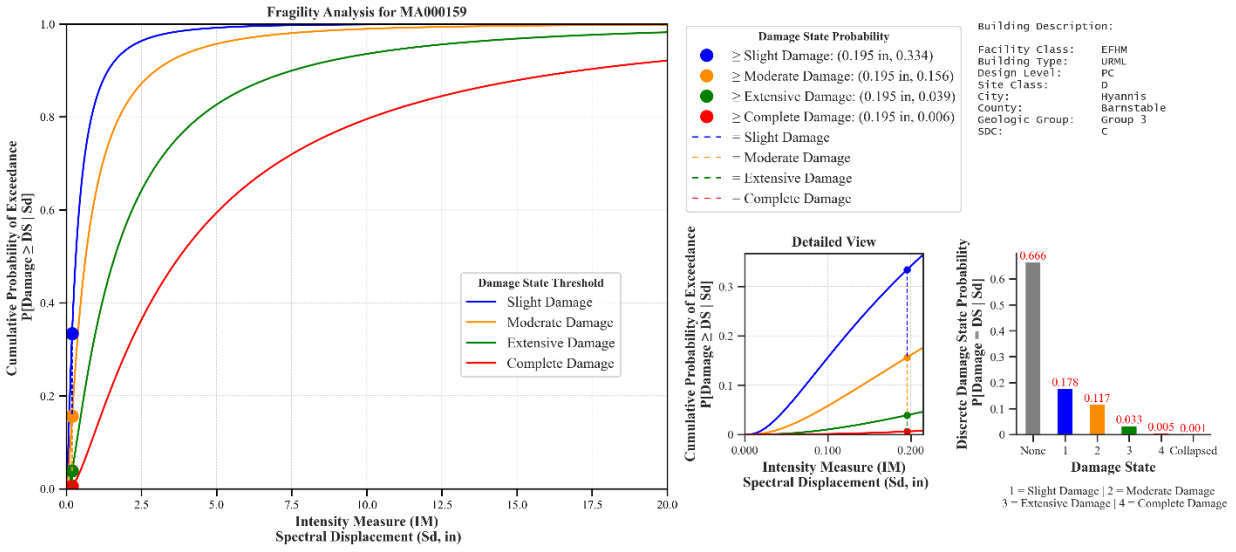
Fragility Analysis for MA000159
Cumulative Probability of Exceedance
P[Damage ≥ DS | Sd]
Intensity Measure (IM)
Spectral Displacement (Sd, in)
Damage State Threshold
Slight Damage
Moderate Damage
Extensive Damage
Complete Damage
Damage State Probability
≥ Slight Damage: (0.195 in, 0.334)
≥ Moderate Damage: (0.195 in, 0.156)
≥ Extensive Damage: (0.195 in, 0.039)
≥ Complete Damage: (0.195 in, 0.006)
= Slight Damage
= Moderate Damage
= Extensive Damage
= Complete Damage
Detailed View
Building Description:
Facility Class: EFHM
Building Type: URML
Design Level: PC
Site Class: D
City: Hyannis
County: Barnstable
Geologic Group: Group 3
SDC: C
Discrete Damage State Probability
P[Damage = DS | Sd]
0.666
0.178
0.117
0.033
0.005
0.001
None
1
2
3
4 Collapsed
Damage State
1 = Slight Damage | 2 = Moderate Damage
3 = Extensive Damage | 4 = Complete Damage

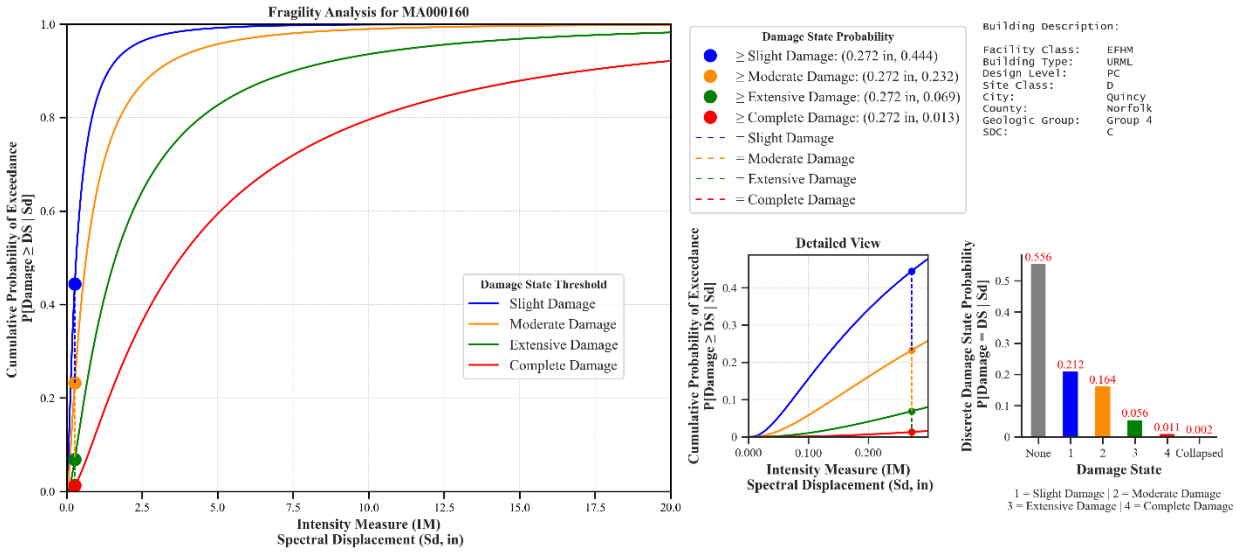
Fragility Analysis for MA000160
Cumulative Probability of Exceedance
P[Damage ≥ DS | Sd]
Intensity Measure (IM)
Spectral Displacement (Sd, in)
Damage State Threshold
Slight Damage
Moderate Damage
Extensive Damage
Complete Damage
Damage State Probability
≥ Slight Damage: (0.272 in, 0.444)
≥ Moderate Damage: (0.272 in, 0.232)
≥ Extensive Damage: (0.272 in, 0.069)
≥ Complete Damage: (0.272 in, 0.013)
= Slight Damage
= Moderate Damage
= Extensive Damage
= Complete Damage
Detailed View
Building Description:
Facility Class: EFHM
Building Type: URML
Design Level: PC
Site Class: D
City: Quincy
County: Norfolk
Geologic Group: Group 4
SDC: C
Discrete Damage State Probability
P[Damage = DS | Sd]
0.556
0.212
0.164
0.056
0.011
0.002
None
1
2
3
4 Collapsed
Damage State
1 = Slight Damage | 2 = Moderate Damage
3 = Extensive Damage | 4 = Complete Damage